

Towards a new 3Rs era in experimental research

Edited by

Christopher R. Cederroth, Marta L. Alves Da Silva, Annemarie Lang, Armand Mensen, Peter Bollen, Benjamin Victor Ineichen, Doris Wilflingseder, Jenny Stina-Maria Sandström and Serban Morosan

Published in

Frontiers in Veterinary Science
Frontiers in Behavioral Neuroscience
Frontiers in Oncology
Frontiers in Cell and Developmental Biology
Frontiers in Physiology
Frontiers for Young Minds
Frontiers in Immunology
Frontiers in Neuroscience
Frontiers in Pharmacology
Frontiers in Animal Science
Frontiers in Cellular and Infection Microbiology
Frontiers in Chemistry
Frontiers in Neurology



FRONTIERS EBOOK COPYRIGHT STATEMENT

The copyright in the text of individual articles in this ebook is the property of their respective authors or their respective institutions or funders. The copyright in graphics and images within each article may be subject to copyright of other parties. In both cases this is subject to a license granted to Frontiers.

The compilation of articles constituting this ebook is the property of Frontiers.

Each article within this ebook, and the ebook itself, are published under the most recent version of the Creative Commons CC-BY licence. The version current at the date of publication of this ebook is CC-BY 4.0. If the CC-BY licence is updated, the licence granted by Frontiers is automatically updated to the new version.

When exercising any right under the CC-BY licence, Frontiers must be attributed as the original publisher of the article or ebook, as applicable.

Authors have the responsibility of ensuring that any graphics or other materials which are the property of others may be included in the CC-BY licence, but this should be checked before relying on the CC-BY licence to reproduce those materials. Any copyright notices relating to those materials must be complied with.

Copyright and source acknowledgement notices may not be removed and must be displayed in any copy, derivative work or partial copy which includes the elements in question.

All copyright, and all rights therein, are protected by national and international copyright laws. The above represents a summary only. For further information please read Frontiers' Conditions for Website Use and Copyright Statement, and the applicable CC-BY licence.

ISSN 1664-8714
ISBN 978-2-8325-4834-9
DOI 10.3389/978-2-8325-4834-9

About Frontiers

Frontiers is more than just an open access publisher of scholarly articles: it is a pioneering approach to the world of academia, radically improving the way scholarly research is managed. The grand vision of Frontiers is a world where all people have an equal opportunity to seek, share and generate knowledge. Frontiers provides immediate and permanent online open access to all its publications, but this alone is not enough to realize our grand goals.

Frontiers journal series

The Frontiers journal series is a multi-tier and interdisciplinary set of open-access, online journals, promising a paradigm shift from the current review, selection and dissemination processes in academic publishing. All Frontiers journals are driven by researchers for researchers; therefore, they constitute a service to the scholarly community. At the same time, the *Frontiers journal series* operates on a revolutionary invention, the tiered publishing system, initially addressing specific communities of scholars, and gradually climbing up to broader public understanding, thus serving the interests of the lay society, too.

Dedication to quality

Each Frontiers article is a landmark of the highest quality, thanks to genuinely collaborative interactions between authors and review editors, who include some of the world's best academicians. Research must be certified by peers before entering a stream of knowledge that may eventually reach the public - and shape society; therefore, Frontiers only applies the most rigorous and unbiased reviews. Frontiers revolutionizes research publishing by freely delivering the most outstanding research, evaluated with no bias from both the academic and social point of view. By applying the most advanced information technologies, Frontiers is catapulting scholarly publishing into a new generation.

What are Frontiers Research Topics?

Frontiers Research Topics are very popular trademarks of the *Frontiers journals series*: they are collections of at least ten articles, all centered on a particular subject. With their unique mix of varied contributions from Original Research to Review Articles, Frontiers Research Topics unify the most influential researchers, the latest key findings and historical advances in a hot research area.

Find out more on how to host your own Frontiers Research Topic or contribute to one as an author by contacting the Frontiers editorial office: frontiersin.org/about/contact

Towards a new 3Rs era in experimental research

Topic editors

Christopher R. Cederroth — Swiss 3R Competence Centre, Switzerland
Marta L. Alves Da Silva — Universidade do Porto, Portugal
Annemarie Lang — University Hospital Carl Gustav Carus, Germany
Armand Mensen — Swiss 3R Competence Centre, Switzerland
Peter Bollen — University of Copenhagen, Denmark
Benjamin Victor Ineichen — University of Zurich, Switzerland
Doris Wilflingseder — Innsbruck Medical University, Austria
Jenny Stina-Maria Sandström — Swiss 3R Competence Centre, Switzerland
Serban Morosan — INSERM US28 Phénotypage du Petit Animal, France

Citation

Cederroth, C. R., Da Silva, M. L. A., Lang, A., Mensen, A., Bollen, P., Ineichen, B. V., Wilflingseder, D., Sandström, J. S.-M., Morosan, S., eds. (2024). *Towards a new 3Rs era in experimental research*. Lausanne: Frontiers Media SA. doi: 10.3389/978-2-8325-4834-9

Table of contents

- 07 **Editorial: Towards a new 3Rs era in experimental research**
Christopher R. Cederroth and Jenny Sandström
- 10 **Electrophysiological Analysis of Brain Organoids: Current Approaches and Advancements**
Austin P. Passaro and Steven L. Stice
- 23 **3D *in vivo* Magnetic Particle Imaging of Human Stem Cell-Derived Islet Organoid Transplantation Using a Machine Learning Algorithm**
Aixia Sun, Hasaan Hayat, Sihai Liu, Eliah Tull, Jack Owen Bishop, Bennett Francis Dwan, Mithil Gudi, Nazanin Talebloo, James Raynard Dizon, Wen Li, Jeffery Gaudet, Adam Alessio, Aitor Aguirre and Ping Wang
- 35 **The Development of Ovine Gastric and Intestinal Organoids for Studying Ruminant Host-Pathogen Interactions**
David Smith, Daniel R. G. Price, Alison Burrells, Marc N. Faber, Katie A. Hildersley, Cosmin Chintoan-Uta, Ambre F. Chapuis, Mark Stevens, Karen Stevenson, Stewart T. G. Burgess, Elisabeth A. Innes, Alasdair J. Nisbet and Tom N. McNeilly
- 53 **Patient-Derived Organoids in Precision Medicine: Drug Screening, Organoid-on-a-Chip and Living Organoid Biobank**
Zilong Zhou, Lele Cong and Xianling Cong
- 69 **The “WWHow” Concept for Prospective Categorization of Post-operative Severity Assessment in Mice and Rats**
Anke Tappe-Theodor, Claudia Pitzer, Lars Lewejohann, Paulin Jirkof, Katja Siegeler, Astra Segelcke, Natascha Drude, Bruno Pradier, Esther Pogatzki-Zahn, Britta Hollinderbäumer and Daniel Segelcke
- 82 **The zebrafish Multivariate Concentric Square Field: A Standardized Test for Behavioral Profiling of Zebrafish (*Danio rerio*)**
Laura E. Vossen, Ronja Brunberg, Pontus Rådén, Svante Winberg and Erika Roman
- 97 **Zebrafish as a Vertebrate Model for Studying Nodavirus Infections**
Raquel Lama, Patricia Pereiro, Antonio Figueras and Beatriz Novoa
- 114 ***Drosophila* as a Model to Study the Mechanism of Nociception**
Jianzheng He, Botong Li, Shuzhen Han, Yuan Zhang, Kai Liu, Simeng Yi, Yongqi Liu and Minghui Xiu
- 128 **Deep Metabolic Profiling Assessment of Tissue Extraction Protocols for Three Model Organisms**
Hagen M. Gegner, Nils Mechtel, Elena Heidenreich, Angela Wirth, Fabiola Garcia Cortizo, Katrin Bennewitz, Thomas Fleming, Carolin Andresen, Marc Freichel, Aurelio A. Telean, Jens Kroll, Rüdiger Hell and Gernot Poschet

- 139 **Gut Bacteria Regulate the Pathogenesis of Huntington's Disease in *Drosophila* Model**
Anjalika Chongtham, Jung Hyun Yoo, Theodore M. Chin, Ngozi D. Akingbesote, Ainul Huda, J. Lawrence Marsh and Ali Khoshnan
- 154 **New Enclosure for *in vivo* Medical Imaging of Zebrafish With Vital Signs Monitoring**
A. C. M. Magalhães, P. M. M. Correia, R. G. Oliveira, P. M. C. C. Encarnação, I. Domingues, J. F. C. A. Veloso and A. L. M. Silva
- 164 **Lung Organoids—The Ultimate Tool to Dissect Pulmonary Diseases?**
Veronika Bosáková, Marco De Zuani, Lucie Sládková, Zuzana Garlíková, Shyam Sushama Jose, Teresa Zelante, Marcela Hortová Kohoutková and Jan Frič
- 183 **Liver organoids: From fabrication to application in liver diseases**
Qianglin Liu, Anqi Zeng, Zibo Liu, Chunjie Wu and Linjiang Song
- 199 **Patient-Derived Organoid Facilitating Personalized Medicine in Gastrointestinal Stromal Tumor With Liver Metastasis: A Case Report**
Ying Cao, Xi Zhang, Qianyun Chen, Xi Rao, Enming Qiu, Gang Wu, Yu Lin, Ziqi Zeng, Bin Zheng, Zhou Li, Zhai Cai, Huaiming Wang and Shuai Han
- 207 **Bored at home?—A systematic review on the effect of environmental enrichment on the welfare of laboratory rats and mice**
Paul Mieske, Ute Hobbiesiefken, Carola Fischer-Tenhagen, Céline Heintz, Katharina Hohlbaum, Pia Kahnau, Jennifer Meier, Jenny Wilzopolski, Daniel Butzke, Juliane Rudeck, Lars Lewejohann and Kai Diederich
- 226 ***Drosophila* exercise, an emerging model bridging the fields of exercise and aging in human**
Meng Ding, Hongyu Li and Lan Zheng
- 237 **Replacing Animal Testing: How and When?**
Thomas Hartung
- 245 **Reducing the Number of Research Animals: How Imaging Technologies Can Help**
Jordi L. Tremoleda
- 253 **Refining Research to Improve the Lives of Laboratory Mice**
Paulin Jirkof
- 260 **Functional identification of the zebrafish Interleukin-1 receptor in an embryonic model of IL-1 β -induced systemic inflammation**
Dylan J. Sebo, Audrey R. Fetsko, Kallie K. Phipps and Michael R. Taylor

- 275 **Zebrafish as a platform to evaluate the potential of lipidic nanoemulsions for gene therapy in cancer**
María Cascallar, Pablo Hurtado, Saínza Lores, Alba Pensado-López, Ana Quelle-Regaldie, Laura Sánchez, Roberto Piñeiro and María de la Fuente
- 288 **RELSA—A multidimensional procedure for the comparative assessment of well-being and the quantitative determination of severity in experimental procedures**
Steven R. Talbot, Birgitta Struve, Laura Wassermann, Miriam Heider, Nora Weegh, Tilo Knape, Martine C. J. Hofmann, Andreas von Knethen, Paulin Jirkof, Christine Häger and André Bleich
- 304 **“Do not look at me like that”: Is the facial expression score reliable and accurate to evaluate pain in large domestic animals? A systematic review**
Carola Fischer-Tenhagen, Jennifer Meier and Alina Pohl
- 315 **Glucocorticoids in relation to behavior, morphology, and physiology as proxy indicators for the assessment of animal welfare. A systematic mapping review**
Inga Tiemann, Lisa B. Fijn, Marc Bagaria, Esther M. A. Langen, F. Josef van der Staay, Saskia S. Arndt, Cathalijn Leenaars and Vivian C. Goerlich
- 335 **A theoretical approach to improving interspecies welfare comparisons**
Leigh P. Gaffney, J. Michelle Lavery, Martina Schiestl, Anna Trevarthen, Jason Schukraft, Rachael Miller, Alexandra K. Schnell and Bob Fischer
- 347 **Progress of research on tumor organoids: A bibliometric analysis of relevant publications from 2011 to 2021**
Yin Shuoxin, Wang Shuping, Zhang Xinyue, Zhang Tao and Chen Yuanneng
- 360 **Norecopa: A global knowledge base of resources for improving animal research and testing**
Adrian J. Smith
- 366 **Decreased levels of discomfort in repeatedly handled mice during experimental procedures, assessed by facial expressions**
Julia Swan, Scott Boyer, Karolina Westlund, Camilla Bengtsson, Gunnar Nordahl and Elin Törnqvist
- 375 **The power of a touch: Regular touchscreen training but not its termination affects hormones and behavior in mice**
Sophia Marie Quante, Viktoria Siewert, Rupert Palme, Sylvia Kaiser, Norbert Sachser and S. Helene Richter
- 386 **Towards a New 3Rs Era in the construction of 3D cell culture models simulating tumor microenvironment**
Long Zhang, Weiqi Liao, Shimin Chen, Yukun Chen, Pengrui Cheng, Xinjun Lu and Yi Ma

- 399 **Neuroimaging findings in preclinical amyotrophic lateral sclerosis models—How well do they mimic the clinical phenotype? A systematic review**
Amelia Elaine Cannon, Wolfgang Emanuel Zürrer, Charlotte Zejlou, Zsolt Kulcsar, Sebastian Lewandowski, Fredrik Piehl, Tobias Granberg and Benjamin Victor Ineichen
- 407 **Advancing the 3Rs: innovation, implementation, ethics and society**
Herwig Grimm, Nikola Biller-Andorno, Thorsten Buch, Maik Dahlhoff, Gail Davies, Christopher R. Cederroth, Otto Maissen, Wilma Lukas, Elisa Passini, Elin Törnqvist, I. Anna S. Olsson and Jenny Sandström
- 420 **CIRS-LAS – a novel approach to increase transparency in laboratory animal science for improving animal welfare by reducing laboratory animal distress**
Astrid Enkelmann and Sabine J. Bischoff
- 427 **Magnetic resonance imaging and ultrasound elastography in the context of preclinical pharmacological research: significance for the 3R principles**
Michael Obrecht, Stefan Zurbrugg, Nathalie Accart, Christian Lambert, Arno Doelemeyer, Birgit Ledermann and Nicolau Beckmann
- 451 **Toward the use of novel alternative methods in epilepsy modeling and drug discovery**
Claudia Miguel Sanz, Miriam Martinez Navarro, Daniel Caballero Diaz, Gentzane Sanchez-Elexpuru and Vincenzo Di Donato
- 467 **Structural enrichment for laboratory mice: exploring the effects of novelty and complexity**
Lena Bohn, Louisa Bierbaum, Niklas Kästner, Vanessa Tabea von Kortzfleisch, Sylvia Kaiser, Norbert Sachser and S. Helene Richter



OPEN ACCESS

EDITED AND REVIEWED BY

Richard G. Hunter,
University of Massachusetts Boston,
United States

*CORRESPONDENCE

Jenny Sandström
✉ Jenny.Sandstrom@swiss3RCC.org

RECEIVED 20 March 2024

ACCEPTED 01 April 2024

PUBLISHED 15 April 2024

CITATION

Cederroth CR and Sandström J (2024)
Editorial: Towards a new 3Rs era in
experimental research.
Front. Behav. Neurosci. 18:1404294.
doi: 10.3389/fnbeh.2024.1404294

COPYRIGHT

© 2024 Cederroth and Sandström. This is an open-access article distributed under the terms of the [Creative Commons Attribution License \(CC BY\)](https://creativecommons.org/licenses/by/4.0/). The use, distribution or reproduction in other forums is permitted, provided the original author(s) and the copyright owner(s) are credited and that the original publication in this journal is cited, in accordance with accepted academic practice. No use, distribution or reproduction is permitted which does not comply with these terms.

Editorial: Towards a new 3Rs era in experimental research

Christopher R. Cederroth and Jenny Sandström*

Swiss 3R Competence Center, Bern, Switzerland

KEYWORDS

3Rs, replace, reduce, refine, ethics, animal welfare

Editorial on the Research Topic

Towards a new 3Rs era in experimental research

The last decade has seen a rise in the interest to apply the 3Rs principle in pre-clinical research. This 64 years old principle, formulated by Russell and Burch in 1959, has been incorporated in many animal welfare legislations to make research more responsible, more ethical and of better quality. Being at the crossroad of innovation, implementation, ethics and society, the advancement of 3Rs has never been more critical (Grimm et al.) and has been the focus of recent international networking initiatives,¹ funding incentives,² and the creation of 3R centers across Europe (Neuhaus et al., 2022a,b).

The aim of this Research Topic is to provide an inter- and multi-disciplinary view on the most advanced level of 3Rs research. This includes a broad range of research foci spanning from human disease models, 3D culture systems, organoid models, non-sentient invertebrates, computational modeling, imaging, animal welfare, education, and legislation. Furthermore, it shows that the coordination of multiple scientific disciplines including biomedical, veterinary, biostatistics, biotechnology, and computer sciences is required to tackle the future challenges for 3Rs. We also know that research alone will not suffice, but that educational, social, political, and ethical perspectives are crucial to shape 3Rs research and its implementation. Within this topic current knowledge on **replacement**, **reduction**, and **refinement** is reviewed, spanning 14 associated journals and attesting to the requirement for trans- and cross disciplinarity of 3Rs research to keep at pace with advancing 3Rs methodologies for ethical and humane research practices in the rapidly evolving fields of life sciences, where the 3Rs Principles remain at its core.

Statistics on this Research Topic: This Research Topic was open between the 29th of November 2022 and the 28th of February 2023. It received 37 submissions by 231 authors, of which 36 were finally accepted after a peer reviewing process and the topic has to date received over 207,000 views (20th of March 2024).

Overview of this Research Topic: This Frontiers Research Topic commences with three Frontiers Young Minds articles, which form part of a broader educational initiative by the Swiss 3Rs Competence Centre aimed at providing an overview of each of the 3Rs for the general public (Hartung; Tremoleda; Jirkof). Following these, Tappe et al. present a hypothesis on assessing post-operative severity in rodents. The first chapter focuses on **replacement**, exploring the validity of disease models in cellular systems and non-sentient invertebrates. The second chapter delves into **reduction** and the long-term monitoring of animals, while the third chapter discusses **refinement** and various methodologies for

1 <https://cost-improve.eu/>

2 <https://www.nfp79.ch/en>

assessing animal welfare. Concluding the topic are two **perspectives on animal welfare**. It's worth noting that some articles may overlap between replacement and reduction and there remains ongoing debate about whether organisms like zebrafish and fruit flies can truly replace rodents. Ethically, this debate hinges on whether these organisms are considered sentient beings, which can vary depending on legislation and perspective.

1 Replacement

Replacement are “*methods, which permit a given purpose to be achieved without conducting experiments or other scientific procedures on animals.*” In this Research Topic, [Zhou et al.](#) provide a review on how organoid biobanks may help in drug discovery and precision medicine. Other reviews covered the advancements in 3D cell culture to model tumors and their microenvironment ([Zhang et al.](#)), accompanied by a bibliometric analysis of tumor organoid research ([Shuoxin et al.](#)). Research on pulmonary or liver diseases using organoids is also reviewed ([Bosákov et al.](#); [Liu et al.](#)), and the challenges with brain organoids are discussed ([Passaro and Stice](#)). New organoids for replacing sheep in research on ruminant host-pathogen interactions are proposed ([Smith et al.](#)). Several articles present the fruit fly *Drosophila melanogaster* as an emerging model for studying exercise and aging ([Ding et al.](#)), nociception ([He et al.](#)), and Huntington's Disease ([Chongtham et al.](#)). In the same direction, the embryos of the zebrafish *Danio rerio* were suggested as models of nodavirus infection ([Lama et al.](#)), systemic inflammation ([Sebo et al.](#)), and cancer gene therapy ([Cascallar et al.](#)). Finally, and to our knowledge a first, tumor organoids derived from a patient with a gastrointestinal stromal tumor mimicked the patient's positive response to sunitinib, suggesting that patient-derived organoids may help predicting responses to drug interventions against cancer ([Cao et al.](#)).

2 Reduction

Reduction are “*methods for obtaining comparable levels of information from the use of fewer animals in scientific procedures, or for obtaining more information from the same number of animals.*” In this regard, technologies have made significant advances for instance in the monitoring of zebrafish behavior and health ([Magalhães et al.](#); [Vossen et al.](#)). New methods to optimize metabolomic assays across various model organisms (e.g., mouse, fruit fly and zebrafish) were proposed by [Gegner et al.](#). In a mouse model of diabetes, the transplantation of human-derived pancreatic islet organoids were labeled and tracked with magnetic particle imaging using mCT, enabling to track the progress of the transplant *in vivo* over a month ([Sun et al.](#)). Finally, a large systematic review covered animal and human evidence to demonstrate the benefits of using neuroimaging in pre-clinical models of amyotrophic lateral sclerosis ([Cannon et al.](#)).

3 Refinement

Refinement encompasses *methods aimed at alleviating or minimizing potential pain, suffering, and distress while enhancing*

animal wellbeing. Several articles in this area focus on improving welfare comparisons among different non-human species ([Gaffney et al.](#)) and enhancing transparency in laboratory animal science ([Enkelmann and Bischoff](#)). Additionally, two studies advocate for the use of facial expressions to monitor animal pain or distress ([Fischer-Tenhagen et al.](#); [Swan et al.](#)). The enrichment loss hypothesis posits that the deprivation of enrichment may lead to stress and anxiety. Interestingly, the touchscreen method, designed to reduce the impact of experimenters on animals, did not induce stress effects upon termination of training ([Quante et al.](#)). However, the authors urge caution and call for further research to evaluate the benefits and potential negative effects of touchscreen technology. Moreover, glucocorticoids have often been utilized as a surrogate marker for stress and animal welfare. [Tiemann et al.](#) conducted a systematic review and concluded that evidence supporting such a correlation is still lacking. In addressing this challenge, [Talbot et al.](#) developed RELSA (RELative Severity Assessment), a tool integrating various outcome measures to assess severity and welfare impact. Furthermore, environmental enrichment has garnered significant attention for refining laboratory animal procedures. [Mieske et al.](#) employed a systematic review approach to highlight the benefits of a stimulating environment on animal welfare. Here again, the assessment of animal welfare remains a topic of debate, with varying methodologies across studies, primarily relying on behavioral assessments.

4 Perspectives

Concluding this Research Topic, [Düpjan and Dawkins \(2022\)](#) provide evidence supporting the idea that good welfare can influence disease resistance. Following this, [Smith](#) introduces Norecopa, a website summarizing the steps in preparing animal studies, primarily based on the PREPARE guidelines, aimed at enhancing planning and reducing animal use in research.

5 Concluding remarks

This Research Topic explores interdisciplinary facets of the latest 3Rs research, covering advancement in replacement with 3D culture systems, organoids, and non-sentient invertebrates, as well as cutting-edge imaging techniques, impact reduction and refine animal procedures for better welfare.

The role of innovation in driving progress within the realm of 3Rs cannot be overstated. From pioneering techniques like organoids and on-a-chip systems, to sophisticated new approaches to assess animal wellbeing, each representing the vast range where technological innovation and advancement come to practical use in a 3Rs context. However, while these advancements showcase the potential of scientific innovation to revolutionize research practices, their true impact is contingent upon effective implementation and adoption across the scientific community.

In conclusion, this Research Topic attests to the multitude of disciplines that are involved in pushing the frontiers of 3Rs research forward and points to some of the challenges we are facing in better defining indicators for measuring successful implementation of 3Rs methodologies that can inform the pursuit of the most

impactful 3Rs research. It is also an acknowledgment to the robust engagement by the research community to advance 3Rs research and tackle the multidisciplinary challenges that 3Rs research and implementation entail.

Author contributions

CC: Conceptualization, Project administration, Writing – original draft, Writing – review & editing. JS: Funding acquisition, Resources, Writing – original draft, Writing – review & editing.

Funding

The author(s) declare that financial support was received for the research, authorship, and/or publication of this article. We acknowledge financial support from the Swiss 3R Competence Centre.

Acknowledgments

We extend our gratitude to all contributors to this Research Topic. A total of 231 authors contributed research and review articles. We express our appreciation to the reviewers for their

assistance in creating an engaging and high-quality Research Topic. Additionally, we are thankful to the numerous members of the Swiss 3R Competence Centre, collaborating institutions, and the working group for enabling the realization of this Research Topic. We trust that readers will derive as much enjoyment from reading this Research Topic as we have had in editing it.

Conflict of interest

CC was an employee of the Swiss 3RCC during the Research Topic management and JS is executive director of the Swiss 3RCC.

The author(s) declared that they were an editorial board member of Frontiers, at the time of submission. This had no impact on the peer review process and the final decision.

Publisher's note

All claims expressed in this article are solely those of the authors and do not necessarily represent those of their affiliated organizations, or those of the publisher, the editors and the reviewers. Any product that may be evaluated in this article, or claim that may be made by its manufacturer, is not guaranteed or endorsed by the publisher.

References

Düpján, S., and Dawkins, M., S. (2022). Animal Welfare and Resistance to Disease: Interaction of Affective States and the Immune System. *Front Vet Sci.* 9:929805. doi: 10.3389/fvets.2022.929805

Neuhaus, W., Reininger-Gutmann, B., Rinner, B., Plasenzotti, R., Willflingseder, D., De Kock, J., et al. (2022a). The rise of three Rs centres and platforms

in Europe. *Altern. Lab. Anim.* 50, 90–120. doi: 10.1177/02611929221099165

Neuhaus, W., Reininger-Gutmann, B., Rinner, B., Plasenzotti, R., Willflingseder, D., De Kock, J., et al. (2022b). The current status and work of three rs centres and platforms in Europe. *Altern. Lab. Anim.* 50, 381–413. doi: 10.1177/02611929221140909



Electrophysiological Analysis of Brain Organoids: Current Approaches and Advancements

Austin P. Passaro^{1,2} and Steven L. Stice^{1,2,3*}

¹ Regenerative Bioscience Center, University of Georgia, Athens, GA, United States, ² Division of Neuroscience, Biomedical & Health Sciences Institute, University of Georgia, Athens, GA, United States, ³ Department of Animal and Dairy Science, University of Georgia, Athens, GA, United States

OPEN ACCESS

Edited by:

Arti Ahluwalia,
University of Pisa, Italy

Reviewed by:

Vishalini Emmenegger,
ETH Zürich, Switzerland
Chiara Magliaro,
University of Pisa, Italy
Andrea Spanu,
University of Cagliari, Italy

*Correspondence:

Steven L. Stice
sstice@uga.edu

Specialty section:

This article was submitted to
Neural Technology,
a section of the journal
Frontiers in Neuroscience

Received: 27 October 2020

Accepted: 11 December 2020

Published: 12 January 2021

Citation:

Passaro AP and Stice SL (2021)
Electrophysiological Analysis of Brain
Organoids: Current Approaches
and Advancements.
Front. Neurosci. 14:622137.
doi: 10.3389/fnins.2020.622137

Brain organoids, or cerebral organoids, have become widely used to study the human brain *in vitro*. As pluripotent stem cell-derived structures capable of self-organization and recapitulation of physiological cell types and architecture, brain organoids bridge the gap between relatively simple two-dimensional human cell cultures and non-human animal models. This allows for high complexity and physiological relevance in a controlled *in vitro* setting, opening the door for a variety of applications including development and disease modeling and high-throughput screening. While technologies such as single cell sequencing have led to significant advances in brain organoid characterization and understanding, improved functional analysis (especially electrophysiology) is needed to realize the full potential of brain organoids. In this review, we highlight key technologies for brain organoid development and characterization, then discuss current electrophysiological methods for brain organoid analysis. While electrophysiological approaches have improved rapidly for two-dimensional cultures, only in the past several years have advances been made to overcome limitations posed by the three-dimensionality of brain organoids. Here, we review major advances in electrophysiological technologies and analytical methods with a focus on advances with applicability for brain organoid analysis.

Keywords: electrophysiology, multi-electrode array, brain organoids, optogenetics, electrophysiological analysis, neurological disease modeling

INTRODUCTION

Over the past few decades, advances in stem cell biology have provided significant insight into neural development and understanding neurological disorders (Kelava and Lancaster, 2016b). Human pluripotent stem cells (hPSCs), especially human induced PSCs (hiPSCs), have proven very useful for modeling neurological disorders *in vitro* and examining potential therapeutics (Ebert et al., 2012; Avior et al., 2016; Liu et al., 2018). Recently, these models have improved with the advent of brain, or cerebral, organoids—three-dimensional self-organized structures containing many cell types and cytoarchitectures typical of the human brain (Lancaster et al., 2013; Kelava and Lancaster, 2016a).

Brain organoids have advanced quickly in complexity, from relatively unpredictable heterogeneous spheroids to highly organized and controllable representations of specific brain regions. This increased complexity can be attributed largely to advances and the coalescence of various technologies from many fields, such as biomaterials and genetics. To develop organoids in three dimensions, extracellular matrices—both organic and synthetic—and other scaffolds are vital to ensuring organoids have support to organize properly (Yin et al., 2016). Additionally, these materials play important roles in cell signaling and providing appropriate biomechanical cues needed for development (Yin et al., 2016).

Improved genetic technologies and transcriptomics, such as single-cell RNA sequencing, have allowed for detailed characterization of cell types and developmental states within organoids (Quadrato et al., 2017; Fischer et al., 2019); however, functional analysis of brain organoids is limited (Schröter et al., 2018; Poli et al., 2019). Classical electrophysiological methods such as patch clamp allow for high temporal resolution of neural activity in organoids but offer little spatial resolution for assessment of whole-organoid activity (Pasca et al., 2015). Calcium imaging provides larger-scale activity information but sacrifices temporal resolution and is reliant on imaging capabilities (Lancaster et al., 2013). Finally, microelectrode arrays (MEAs), adopted over the past several years (Giandomenico et al., 2019), provide both network-scale and high temporal resolution but currently lack three-dimensionality needed to properly analyze brain organoid activity. These and other key technologies for brain organoids are highlighted in this review with the goal of discussing how brain organoids have evolved so quickly in recent years, where the field has been slower to evolve, and looking forward to cutting-edge technologies with potential to overcome these shortcomings, primarily in electrophysiology. Here we directly compare strengths and weaknesses of existing and new electrophysiological methods, as they relate to organoid analysis.

BRAIN ORGANOID APPLICATIONS

Early brain organoids consisted of relatively disorganized, spontaneously differentiated structures containing multiple cell types characteristic of the human brain (Lancaster et al., 2013; Lancaster and Knoblich, 2014). While these primitive organoids proved useful for studying early aspects of development, such as neural migration, a lack of controlled differentiation and organization hindered reproducibility and more complex applications (Kelava and Lancaster, 2016b; Kyrousi and Cappello, 2020). Since then, more mature and organized brain organoids have been developed, allowing for a wide variety of developmental studies (Qian et al., 2019). While early brain organoids contributed primarily to developmental studies regarding neural stem maintenance and differentiation and corticogenesis (Kadoshima et al., 2013; Lancaster et al., 2013; Lancaster and Knoblich, 2014; Camp et al., 2015), later brain region-specific organoids provided insight into specific regional development, including both general regions (i.e., forebrain,

midbrain) and highly specific regions and structures (i.e., hippocampus, cerebellum, retina) (Muguruma et al., 2015; Sakaguchi et al., 2015; Jo et al., 2016; Parfitt et al., 2016; Monzel et al., 2017; Muguruma, 2017). For a more comprehensive review of regional brain organoids, see Gopalakrishnan (2019).

The advent of brain region-specific organoids unlocked the potential for significantly improved neurological disease modeling (Jo et al., 2016; Monzel et al., 2017). The promise of stem cells, especially hiPSCs, for modeling neurodegenerative diseases has been acknowledged for years but somewhat hindered by traditional two-dimensional cell culture and difficult co-culture conditions. Two-dimensional cell culture does not allow for complex cellular interactions that occur in three dimensions *in vivo* and does not allow for analysis of certain disease phenotypes, such as extracellular protein aggregation in Alzheimer's disease (Raja et al., 2016). By allowing for physiologically accurate, three-dimensional recapitulation of specific brain regions, more relevant models can be developed to study and develop therapeutics for diseases such as Parkinson's disease and Alzheimer's using brain organoids (Raja et al., 2016; Smits et al., 2019). For example, brain organoids generated from hiPSCs from Parkinson's (Smits et al., 2019) and Alzheimer's (Raja et al., 2016) patients recapitulate hallmark disease phenotypes, most notably reduced dopaminergic neurons in Parkinson's organoids and amyloid beta aggregation and hyperphosphorylated tau protein in Alzheimer's organoids. Similarly, as organoids are developed from hiPSCs, they may be used for personalized medicine to develop custom therapies for the above-mentioned diseases and other disorders (Kyrousi and Cappello, 2020). As evidence of this potential, organoids developed from several Alzheimer's patients carrying different mutations (one line with a mutation in APP and two lines with different mutations in PSEN1) exhibited different phenotypes, particularly in Tau hyperphosphorylation, suggesting the capacity to model specific disease phenotypes from individual patients (Raja et al., 2016).

The need for improved *in vitro* models has been widely recognized for screening approaches, such as those used in drug development and toxicology (Frank et al., 2017; Bal-Price et al., 2018; Kim et al., 2019; Shafer et al., 2019). Drug development costs continue to rise, and it has long been reasoned that improved *in vitro* models of human physiology could lower these costs by improving preclinical studies and reducing failure rate of potential therapeutics in clinical trials (Begley and Ellis, 2012). Similarly, improved models would lead to increased detection sensitivity in toxicological screening assays, as these models would more accurately recapitulate physiology (Bal-Price et al., 2018; Kim et al., 2019). While microphysiological systems (e.g., engineered microfluidic devices, described in detail in the next section) have improved *in vitro* models and offer precise control over culture parameters, organoids provide macroscale architecture and organization that is difficult to recreate in traditional 3D culture systems (Bhatia and Ingber, 2014). As a tradeoff, organoid models sacrifice throughput—due to long culture times necessary for maturation—for this increased accuracy; however, researchers are implementing technological advances from more conventional systems, such as microfluidics

and synthetic scaffolds, to increase throughput and efficacy of organoid models (Esch et al., 2015; Skardal et al., 2015, 2016).

TECHNOLOGICAL ADVANCES FOR BRAIN ORGANOID DEVELOPMENT AND CHARACTERIZATION

Advances in brain organoid complexity have come as a result of advances and new applications of various technologies. One such technology includes microfluidics, which allow for “organoids-on-a-chip” (Wang et al., 2018; Kim et al., 2019; Park et al., 2019). Microfluidics have been used to control the cellular microenvironment and engineer organ-on-a-chip systems, which recapitulate specific physiological aspects of particular organs and tissues (Bhatia and Ingber, 2014). While traditionally considered at-odds with organoids due to fundamental differences in engineering approaches (Jackson and Lu, 2016) and control (Bhatia and Ingber, 2014)—top-down approach and assembly of organ-on-a-chip models versus bottom-up approach and self-organization of organoids—researchers have recently begun combining the two approaches (Skardal et al., 2016; Takebe et al., 2017; Park et al., 2019). Microfluidic systems for brain organoid culture provide additional control of signaling molecules required for differentiation (i.e., morphogens) (Demers et al., 2016) and oxygen diffusion (Berger et al., 2018), which has long been recognized as a hurdle for brain organoid development (Lancaster et al., 2017). Improved control of morphogen gradients can be used to study developmental stages and differentiation at highly precise levels, such as motor neuron differentiation in the developing neural tube (Demers et al., 2016). By increasing oxygen diffusion throughout brain organoids via microfluidics, midbrain organoids exhibited reduced necrotic cores and increased numbers of dopaminergic neurons, highlighting increased differentiation efficiency (Berger et al., 2018). Ultimately, microfluidic devices provide precise control of many organoid parameters, such as size/shape (Ao et al., 2020) and media perfusion rate (including nutrient and growth factor supply) (Wang et al., 2018), leading to increased reproducibility (Yin et al., 2016; Wang et al., 2018; Kim et al., 2019; Park et al., 2019). Additionally, many microfluidic platforms are compatible with common imaging setups, allowing for live organoid imaging and monitoring (Yin et al., 2016; Kim et al., 2019). A microfabricated system was used to image and analyze folding dynamics of brain organoids over several weeks of development (Karzbrun et al., 2018a,b) and an organoid-on-a-chip model using controlled perfusion enabled assessment of developmental effects of nicotine exposure (Wang et al., 2018). These platforms have allowed for live imaging over time and throughout brain organoid development, as well as precise microenvironment control, leading to increased reproducibility when studying early development or developmental diseases and toxicity (Berger et al., 2018; Karzbrun et al., 2018a; Wang et al., 2018).

Biomaterials advances over the past decade have also contributed to development of improved organoids. Extracellular matrices and scaffolds are vital to stem cell self-renewal and

differentiation, leading to the use of natural materials, such as Matrigel. However, Matrigel is not well-defined and can have considerable batch variation, prompting a need for defined scaffolds and materials (Yin et al., 2016). Defined biological materials have been widely used for neural tissue engineering (Boni et al., 2018; Kratochvil et al., 2019) and are beginning to show promise as scaffolds for brain organoid culture, as well. For example, brain organoids were generated in 10–14 days on composite hyaluronic acid-chitosan hydrogels in chemically defined media (Lindborg et al., 2016). These materials have many beneficial characteristics for brain organoid applications: they allow for simple and scalable organoid generation with high accessibility and applicability due to the lack of exogenous materials, they are widely available, they have a long history of neural biocompatibility, and they are amenable to growth factor loading and modification, if desired (Yang et al., 2015). In a similar strategy, hyaluronic acid-heparin hydrogels were shown to promote caudalization of brain organoids, demonstrating how various ECM components and factors can influence brain organoid development and function (Bejoy et al., 2018). In addition to biological materials, synthetic scaffolds and materials can be designed to mimic natural ECM mechanical properties and are tunable, providing precise control and mechanistic understanding of elements underlying neurogenesis and brain organoid development (Ranga et al., 2016). These scaffolds can also be loaded with various soluble factors to control signaling and the microenvironment, which contribute significantly to organoid development (Yin et al., 2016; Koo et al., 2019). Synthetic scaffolds that are chemically defined, scalable, and good manufacturing practices (GMP)-compliant—important for drug development and personalized medicine applications—have been specially designed to support 3D hPSC culture, allowing for expansion and simple passaging via thermoresponsive properties (Lei and Schaffer, 2013). Recently, similar synthetic, defined hydrogel scaffolds have been used to generate intestinal organoids comparable to those generated with Matrigel (Gjorevski et al., 2016; Cruz-Acuña et al., 2017; Gjorevski and Lutolf, 2017). These biomaterial advances—along with increased characterization of brain extracellular matrix and biomechanical properties—provide many capabilities to help design and engineer brain organoids.

In addition to bioengineering advances contributing to brain organoid development, considerable work has been done with genetic approaches to allow for precise genetic manipulation of organoids. Established genetic tools including adeno-associated viruses (AAVs), lentiviruses, electroporation, and CRISPR/Cas9 have been applied to brain organoids for a wide range of applications, from simple reporter expression to disease modeling (Fischer et al., 2019). This wide range of available tools can be utilized to obtain targeted spatiotemporal manipulation, for example, modifying all cells at an early stage or a specific subset of cells in a mature, developed organoid. These approaches have been used for various applications, from simple fluorescent labeling of neurons to study migration deficits in mutant organoids modeling lissencephaly (Bershteyn et al., 2017) to RNA knock-in or knockdown via electroporation to examine mechanisms of hypoplasia in microcephalic organoids

(Lancaster et al., 2013; Li et al., 2017). In addition to these transient applications, CRISPR/Cas9 has been used to stably modify stem cell populations prior to organoid generation (Bershteyn et al., 2017; Li et al., 2017; Karzbrun et al., 2018a) or at specific time points, such as to introduce an oncogene to study glioblastoma in 4-months-old brain organoids (Ogawa et al., 2018). These examples demonstrate the considerable utility of genetic modifications for studying precise aspects of brain development and disease modeling, and how genetic approaches will continue to be vital to both organoid development and design, as well as characterization and mechanistic understanding. For an excellent recent review on genetic manipulation of brain organoids, see Fischer et al. (2019).

Along with genetic tools allowing researchers to characterize brain organoids and explore various mechanisms, -omics approaches have provided a much greater understanding of brain organoid development, both in healthy and disease states. Early organoids were characterized using common immunohistological markers, but in-depth characterization was limited (Lancaster et al., 2013; Lancaster and Knoblich, 2014). Recently, single cell RNA-sequencing (sc-RNA-seq) has unveiled the considerable diversity of cell types comprising brain organoids (Quadrato et al., 2017). The ability to analyze single cells across organoids, along with improved analytical methods [i.e., t-distributed stochastic neighbor embedding (tSNE)], has allowed researchers to examine cellular diversity at much higher detail (e.g., whole transcriptome compared to individual markers), at different developmental time points within organoids, and among organoids (Quadrato et al., 2017). Understanding this variability is important for improved organoid development and characterization, especially for disease modeling applications.

While promising, early organoid characterization left much to be desired in terms of depth—without understanding the extent of neuronal maturity and subtypes, cellular and regional interactions, and functional maturation, it is difficult to determine the usefulness of brain organoids as truly physiological models of disease (Quadrato et al., 2016). For example, a midbrain organoid with a high proportion of dopaminergic neurons could be useful for modeling Parkinson's disease, but neuronal maturation and glia are also important components that may considerably affect degeneration and disease phenotype. To this end, sc-RNA-seq has begun to reveal the vast array of brain organoid cellular diversity and extent of maturation (e.g., dendritic spine formation) necessary for developing proper disease models (Quadrato et al., 2016, 2017).

Finally, a significant effort has been made to vascularize brain organoids in recent years. Without vascularization, significant cell death is observed in the inner regions of brain organoids, limiting proper development and analysis (Lancaster et al., 2013; Vargas-Valderrama et al., 2020). Several strategies have been employed to vascularize brain organoids. An initial strategy used implantation of brain organoids *in vivo*, resulting in host vascularization of the engrafted organoids, organoid maturation, and prolonged survival (Mansour et al., 2018). This approach has since been improved, incorporating endothelial cells to develop vascular structures *in vitro* prior to implantation, with implanted

organoids developing more complex vasculature and integrating with host vessels, resulting in long-term survival and functional maturation (Pham et al., 2018; Shi et al., 2020). Notably, patient-derived hiPSCs were used to generate brain organoids and endothelial cells, supporting this approach to generate patient-specific vascularized brain organoids (Pham et al., 2018). Lastly, neural and endothelial co-differentiation has been observed in hESC-derived organoids, induced by vascular endothelial growth factor (VEGF) (Ham et al., 2020) or expression of an endothelial transcription factor, ETV2 (Cakir et al., 2019) early in brain organoid differentiation. Both approaches generated vascularized brain organoids exhibiting blood-brain barrier characteristics, and ETV2 expression increased neuronal activity and maturation (Cakir et al., 2019), suggesting significant value in disease modeling.

ELECTROPHYSIOLOGICAL ANALYSIS OF BRAIN ORGANIDS

The hallmark of functional analysis for neural cells and tissues, including brain organoids, is electrophysiology. The ability to record neuronal function is essential for many brain organoid applications, especially disease modeling and drug development (Sakaguchi et al., 2019). Most traditional electrophysiology techniques have been applied to brain organoids and have unique advantages and disadvantages (Poli et al., 2019).

Patch clamping allows researchers to record individual neurons in a brain organoid at high temporal resolution, providing detailed analysis of specific neurons (Pasca et al., 2015; Di Lullo and Kriegstein, 2017; Li et al., 2017; Cakir et al., 2019). The high temporal resolution is particularly useful for determining responses to specific perturbations, such as pharmacological treatment or optogenetic stimulation; however, as only individual neurons can be analyzed, little-to-no information on network connectivity or dynamics important to regional or global organoid function. To increase spatial resolution and analyze network activity, calcium imaging has been utilized (Lancaster et al., 2013; Sakaguchi et al., 2019). Calcium imaging overcomes these limitations of patch clamping, allowing for live cell imaging of neural activity in small groups of neurons. This is useful for analyzing specific regions of brain organoids and attempting to analyze synaptic activity and neural circuits (Sakaguchi et al., 2019). As a tradeoff, some of the high temporal resolution of patch clamping is lost. Additionally, the three-dimensionality of organoids poses challenges to acquiring calcium imaging data, as neurons must be oriented closely in the z-dimension to capture them in close succession and analyze connectivity patterns. While this may be acceptable for specific small regions, it limits global functional analysis.

Microelectrode arrays (MEAs) have been increasingly adopted for screening applications and other studies due to the ability to combine the temporal resolution of patch clamping with the network resolution of calcium imaging (McConnell et al., 2012; Cotterill et al., 2016; Frank et al., 2017; Shafer et al., 2019). By analyzing extracellular potentials from a relatively large array of electrodes simultaneously, many parameters of

network connectivity can be assessed in real time. MEAs also offer significantly improved throughput compared to other recording techniques and many analytical tools have been developed for improved data analysis and interpretation (Egert et al., 2002; Pastore et al., 2016; Bridges et al., 2018). In organoids, this provides similar connectivity data as calcium imaging but on a much larger scale, allowing for entire region analysis or potential analysis of several organoid regions (Giandomenico et al., 2019). Recording across large portions of brain organoids has revealed strong connectivity between various regions within organoids, suggesting long-range neural circuits and inter-regional connectivity, instead of simply “nearest neighbor” connections (Giandomenico et al., 2019). As further evidence of these long-range circuits, brain organoids co-cultured with spinal cord explants were observed to project functional axon tracts toward the spinal cord explants that were able to stimulate muscle contraction (Giandomenico et al., 2019). As brain organoids become more complex and are used to model complex aspects of development and diseases, the ability to detect and analyze inter-regional connectivity and neural circuits across large distances becomes vital, and MEAs are useful tools to provide insight into these circuits. The large-scale recordings provided by MEAs are also amenable to combination with additional data sets or multiplexing with other assays. For example, correlation analysis of MEA activity throughout development with transcriptomics (sc-RNA-seq) and immunohistochemistry has provided mechanistic insight into developmental processes, such as simultaneous astrocyte population growth and neuronal maturation (Fair et al., 2020). Additionally, multiplexing MEA analysis with high content imaging can help offset concerns associated with brain organoid variability by increasing confidence in results reflected across modalities, supporting potential use for drug screening and other high-throughput approaches (Durens et al., 2020). Despite these advantages, however, MEAs are not without drawbacks. Most notably, the three-dimensionality of the organoids and planar electrode arrays typically limit recording to the outer edges of organoids, which may or may not be areas of significant interest. Recent advances to overcome this challenge are discussed in the next section.

Finally, optogenetics have been employed in conjunction with the above techniques to allow for precise stimulation and mechanistic studies (Shiri et al., 2019). Optogenetic manipulation has received widespread use in neuroscience and recent application in organoids to analyze and manipulate neural activity (Watanabe et al., 2017; Mansour et al., 2018). In particular, neuronal-specific channelrhodopsin expression in brain organoids was demonstrated (Watanabe et al., 2017), and optogenetic manipulation of implanted organoids in rodents was used to assess successful integration into the host brain, opening the door for vascularization strategies and disease modeling in a physiological microenvironment (Mansour et al., 2018). Despite relatively few applications in hiPSC-derived cells thus far, the potential for optogenetics to improve hiPSC and brain organoid models by allowing for deeper mechanistic analysis has been recognized (Chin and Goh, 2015; Su et al., 2015; Trujillo and Muotri, 2018). Relatively low transfection

efficiency in hiPSC-derived cells compared to somatic cells may be partially responsible for the slow adoption of optogenetics in brain organoids and other hiPSC-derived cells; however, recent advances and comparisons of transfection techniques may help increase these studies moving forward (Chin and Goh, 2015; Rapti et al., 2015; Lee et al., 2019). Indeed, a neuromuscular junction (NMJ) model implementing hiPSC-derived neurospheres and muscle tissue was recently used to assess functional deficits in amyotrophic lateral sclerosis (ALS) (Osaki et al., 2018). This study suggests similar utility for functional disease modeling via optogenetics and brain organoids in the near future.

RECENT ADVANCES IN ELECTROPHYSIOLOGY—APPLICABILITY TO BRAIN ORGANIDS

While the electrophysiological techniques discussed above have been effective in providing functional data on brain organoids, the drawbacks of each method are notable, ultimately hindering the extent of functional analysis that can be performed. There have been many recent advances in electrophysiology that may provide improvements over these traditional methods, though these technologies are in their infancy or have yet to be applied to brain organoids. Some key advances with clear applicability for brain organoids are highlighted below and in **Table 1**.

A recently developed technique, dubbed PatchSeq, combines patch clamp electrophysiological recordings with sc-RNA-seq, allowing functional correlation to gene expression (Bardy et al., 2016; Cadwell et al., 2016, 2017; Chen et al., 2016; Földy et al., 2016; Fuzik et al., 2016; van den Hurk and Bardy, 2019). While still limited in scale and throughput, the correlation to genetic and morphological analysis provides a new dimension of functional analysis and could be extremely useful when analyzing particular subsets of neurons in brain organoids (Bardy et al., 2016; van den Hurk and Bardy, 2019). The authors found strong correlations between neuronal activity/maturation and 45 genes, some with known neuronal function, including synaptic plasticity and voltage-gated sodium channels. Interestingly, most of these genes had not previously been associated with neuronal function, representing potential new biomarkers for neuronal activity and maturation (Bardy et al., 2016). While this study was performed in mixed hiPSC-derived neuron and astrocyte co-cultures, this approach could reveal similar discoveries and associations about neurons in brain organoids, and perhaps more physiologically relevant biomarkers, as brain organoids contain more cell types and important three-dimensional organization.

Optogenetics has proven to be a useful tool for manipulation of neural activity, both in monolayer cultures and organoids. Traditionally, optogenetics has been utilized to stimulate and/or inhibit neurons of interest. Recently, the development of all-optical electrophysiology has provided a method to both manipulate and record neural activity at high spatiotemporal resolution (Hochbaum et al., 2014; Werley et al., 2017;

TABLE 1 | Electrophysiological advances with applicability to brain organoids.

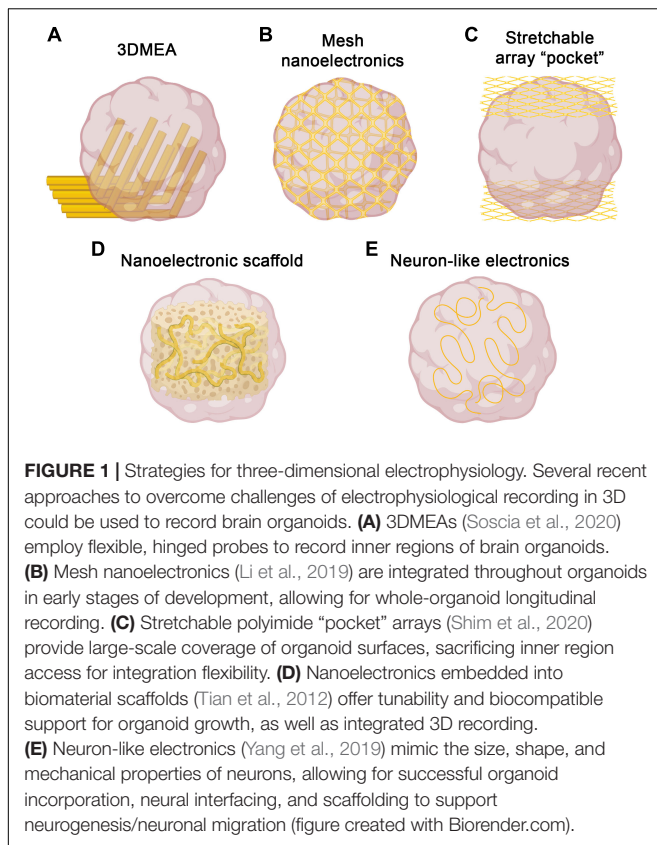
Technology	Major advantage	Cellular resolution	Global resolution	Temporal resolution	Throughput*	Cultures used for validation	References
PatchSeq	Combines transcriptomics and electrophysiology at single-cell resolution	High (single cell)	High (cells can be analyzed from different regions of entire organoid)	High (20 kHz)	Low (single cell)	Primary mouse neocortical cells hESC/hiPSC-derived neurons Primary mouse hippocampal neurons	Cadwell et al., 2016, 2017; Fuzik et al., 2016 Chen et al., 2016 Földy et al., 2016
All-optical electrophysiology	Combines advantages of patch clamp and calcium imaging	High (single cell)	Medium (cells in a general region/cluster can be analyzed simultaneously, but constrained by imaging field)	Medium (1–2 ms)	Medium (clusters of cells within single imaging field)	Primary rat hippocampal neurons, hiPSC-derived neurons (iCell) hiPSC-derived motor neurons (incl. SOD1-mutant)	Hochbaum et al., 2014 Kiskinis et al., 2018
3DMEA	Allows three-dimensional recording (e.g., inner regions of organoids) as opposed to planar recording	Low (cannot correlate signals to individual cells, but can identify signals in 3D space)	High (3D probes allow for recording of large, identifiable regions throughout organoid)	High (10 kHz)	Very high (large number of cells throughout organoid with 256 recording channels)	3D hiPSC-derived neuron + astrocyte co-cultures	Soscia et al., 2020
Mesh nanoelectronics	Whole-organoid electrode coverage throughout all stages of development	Very low (low electrode density and ability to correlate signals to individual cells)	Very high (electrode coverage across entire organoid, but difficult to spatially control and locate specific electrodes)	High (10 kHz)	High (cells across organoid, but only 16 channels in current design)	Cardiac organoids	Li et al., 2019

*Throughput defined as how many cells can be recorded simultaneously, especially relative to other recording techniques.

Kiskinis et al., 2018). This method consists of co-transfecting neurons with both a channelrhodopsin (CheRiff) allowing for optogenetic stimulation and a spectrally orthogonal fluorescent genetically encoded voltage indicator (GEVI) (QuasAr) allowing for simultaneous recording of neural activity. Being able to stimulate and record simultaneously via this all-optical setup allows for network level recordings of neural circuits while maintaining both single-cell and high temporal resolution. Despite this promise, adoption began slowly due to relatively low construct expression levels and highly complex data analysis. More recently, however, improved analytical algorithms were developed to better extract activity and morphology data using this system and applied it to analyze human iPSC-derived motor neurons in a model of ALS (Kiskinis et al., 2018). There were clear differences between control and ALS cells, demonstrating its usefulness for both hiPSCs and disease modeling, which could be adapted to brain organoids. Particularly, ALS cells were hyperexcitable when unstimulated, as previously reported (Wainger et al., 2014), but the single-cell resolution afforded by optical electrophysiology showed hypoexcitability in response to strong stimulus. This highlights a key advantage of single-cell electrophysiology on larger populations of neurons, which would not be feasible with traditional patch clamping (Kiskinis et al., 2018). Ultimately, while it is still slightly less precise than patch clamping (1–2 ms vs. submillisecond temporal resolution), optical electrophysiology maintains much of the resolution

afforded by patch clamping while significantly increasing throughput, which is important for the large-scale analysis needed for brain organoids.

The two-dimensionality of traditional MEAs is not an issue for typical monolayer cell culture; however, the three-dimensionality of brain organoids significantly limits accessibility to the majority of cells in the organoid. MEAs have still been useful to date, but recordings must be performed in a single plane, usually at the edge of the organoid. To overcome this, three-dimensional MEAs (3DMEAs) are currently being developed (Soscia et al., 2020; **Figure 1A**). By incorporating electrodes into flexible, hinged probes, extracellular recordings can be taken from 3D neural networks, such as those found in organoids. Importantly, these devices are compatible with many existing readily accessible recording setups, thus facilitating rapid adoption by brain organoid researchers. 3D hiPSC-derived neural cultures were recorded over 38 days *in vitro* (DIV), observing similar activity as other recording methods, suggesting viability and long-term biocompatibility without sacrificing recording ability or resolution. The culture analyzed was a mixed neuron-astrocyte co-culture suspended in hydrogel, which—while less complex than organoids—demonstrates the ability to record from similar 3D cultures and neural networks, as well as to spatially map neural activity in three dimensions. A high-density 3DMEA platform may allow for more precise spatial mapping of active neurons (Yuan et al., 2020). Indeed, another high density MEA



platform was recently used to assess activity in retinal organoids, demonstrating applicability to organoid cultures (Georgiou et al., 2020). This same MEA platform was also used in a similar manner to compare differentiation protocols for retinal organoid development (Mellough et al., 2019), further demonstrating utility for quick, simple quantification of organoid activity. Traditional MEA systems provide network-level information at the cost of single cell-resolution due to relatively low electrode density, making it difficult, if not impossible, to correlate specific signals with individual neurons. With increased electrode density, single-cell activity analysis can be performed, providing both network dynamics and changes in individual cells, allowing for neural circuit mapping and analysis of how circuit connectivity changes over time (Yuan et al., 2020). This detailed connectivity analysis in brain organoids could reveal developmental insights (i.e., regional interconnectivity) or insight into neurodegeneration or synaptic rearrangement typical of diseases such as ALS or Alzheimer’s disease. These applications to organoids should be feasible, providing an avenue to record the inner regions of brain organoids, which has to date been elusive.

An alternative approach to obtain three-dimensional recordings of brain organoids is the use of electrodes embedded into a stretchable mesh. These “mesh nanoelectronics” can be integrated with cell monolayers in the early stages of organoid development, after which they have the ability to stretch as the organoids develop into three-dimensional structures,

essentially taking the shape of the entire organoid (Li et al., 2019; **Figure 1B**). The unique advantage of this approach is that by the time the organoid finishes developing, it consists of evenly spaced electrodes across the entire structure. Additionally, this provides the ability to record from the organoid across all stages of development, assessing neural ontogeny and the onset of activity. The researchers demonstrated this ability, as well as long-term biocompatibility, via integration into cardiac organoids. By recording throughout organogenesis, researchers were able to determine organoid maturation state by measuring synchronized bursting patterns, which would be difficult or impossible to measure with traditional recording techniques. Combined with no observable changes in marker expression throughout development, this suggests device implantation does not interfere with typical developmental processes, including sarcomere assembly. A similar approach was recently reported, in which stretchable polyimide arrays were sandwiched around brain organoids, creating a stretched “pocket” capable of conforming to the organoids (Shim et al., 2020; **Figure 1C**). This approach is more limited to the outside surface of the organoid, but may provide more flexibility with timing and application, as it does not need to be integrated from the beginning of organoid development. As with the 3DMEAs, electrode density can be improved, but the potential for whole-organoid recordings, especially throughout development, represents a significant improvement over traditional electrophysiological methods.

While the above approaches address challenges associated with recording 3D brain organoids, considerable improvements are also being made regarding materials and electrode designs to enhance both recording capabilities and biocompatibility (Didier et al., 2020). Recent advances in bioprinting have been utilized to demonstrate proof-of-concept for patterning and printing MEAs on soft material substrates with mechanical properties similar to brain tissue, assisting with biocompatibility (Adly et al., 2018; Borda et al., 2020). To improve electrode properties (i.e., biocompatibility, impedance, structural integrity, transparency), many new materials have been used for design and coating, such as indium tin oxide, gold, titanium nitride, and ruthenium oxide, among others (Jahnke et al., 2019; Koklu et al., 2019; Ryyänen et al., 2019, 2020; Atmaramani et al., 2020). The continued development of MEAs incorporating these and other materials, as well as improved incorporation methods, may help improve signal-to-noise ratios and fidelity for brain organoid recordings.

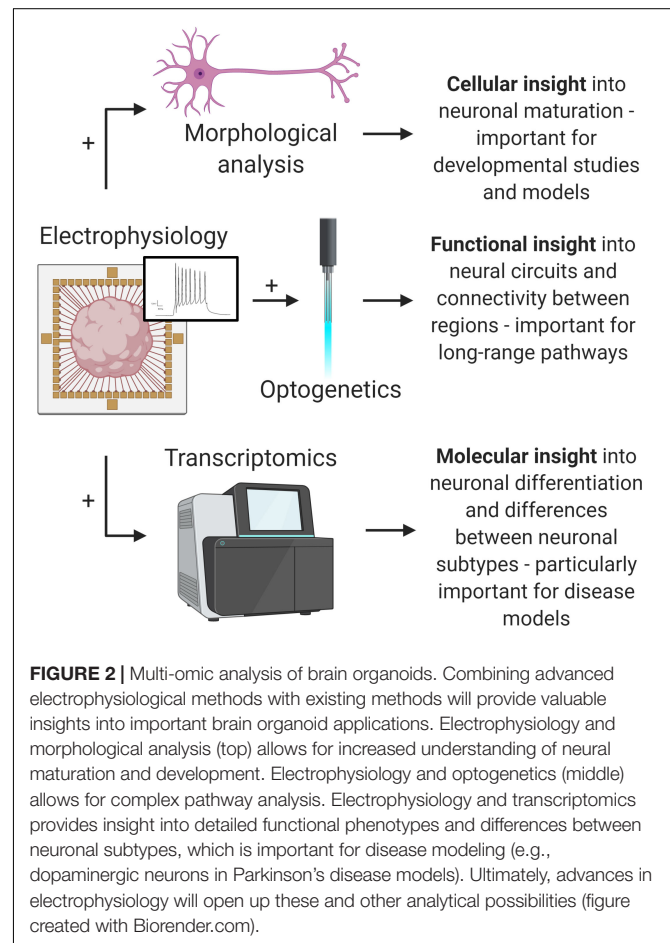
Bioinspired electrodes and scaffolds also have significant potential to improve recording capabilities in brain organoids (Li et al., 2020). By integrating nanoelectronics into biomaterials, nanoelectronic scaffolds (nanoES) were created and used to support 3D neural cultures (Tian et al., 2012; **Figure 1D**). These nanoES have macroporous structures, mimicking natural extracellular matrices and allowing for unimpeded neurite outgrowth and integration, as well as good biocompatibility. By modifying this approach with various biomaterials and synthetic scaffolds, nanoES are tunable, increasing the potential for incorporation into brain organoids. Another bioinspired approach was the recent design of neuron-like electronics (NeuE)—neural probes that mimic the size, shape, and

mechanical properties of neurons for high resolution and integration into neural tissues (Yang et al., 2019; **Figure 1E**). The mechanical properties of these neurite-diameter probes allow for significantly reduced stiffness compared to most other flexible electrodes, supporting neuronal interfacing. These interfaces are stable over time, allowing for chronic recording, and easily able to be multiplexed with 3D imaging. Notably, NeuE implanted into mouse brains also enhanced endogenous neural progenitor cell migration, providing similar scaffolding properties as radial glia cells, suggesting the potential to enhance neural development in brain organoids while also providing high resolution electrophysiological recording.

Finally, in addition to the physical limitations of recording brain organoids in three dimensions, there are also challenges associated with data processing and analysis. Traditional electrophysiological data processing is typically carried out in a similar fashion, regardless of recording method. For action potential (spike) and burst analysis, recorded signals are high pass filtered, followed by spike detection and sorting, and finally parameter calculation from the analyzed spike patterns (Robinette et al., 2011; Latchoumane et al., 2018). Many labs perform these steps with custom scripts, but there is also a litany of commercial and open source software solutions available (Egert et al., 2002; Pastore et al., 2016; Bridges et al., 2018; Unakafova and Gail, 2019), which may be useful when adapting these analyses to 3D recordings, especially for researchers without a strong background in electrophysiology that may be analyzing brain organoids. Spike detection is typically threshold-based to detect spikes over baseline noise, and spike sorting often consists of cluster analysis to separate spikes based on waveform shape corresponding to individual neurons detected by the same electrode (Hilgen et al., 2017). This is a crucial technique for three-dimensional analysis, especially when high spatial resolution and individual neuronal signal isolation is necessary (e.g., connectivity mapping, spike timing analysis) (Regalia et al., 2016; Hilgen et al., 2017; Yger et al., 2018). Spike sorting can be computationally intensive for 2D analysis and may be much more difficult in 3D, as increased channels and spiking events increases computation exponentially (Hilgen et al., 2017). Additionally, with more electrodes in the vicinity of each other due to the third dimension, more electrodes must be considered when attempting to distinguish spikes across multiple electrodes (Yger et al., 2018). To address these issues, solutions have been developed implementing improved spike detection, dimensionality reduction, and pre-defined templates to achieve lower error rates—and thus, reduced necessity for manual oversight which becomes impossible with high-density arrays (Lefebvre et al., 2016; Hilgen et al., 2017)—as well as template-matching, where spikes are assumed to adhere to pre-defined “template” waveforms, reducing computational cost (Marre et al., 2012). Another promising approach involves utilizing probe geometry and knowledge of the spatial relationship between electrodes to optimize analysis (Rossant et al., 2016), which would be useful in 3D arrays with relatively determinable electrode locations within a brain organoid (e.g., the 3DMEAs highlighted above).

OUTLOOK

Brain organoids present enormous potential for disease modeling and understanding the human brain and represent a culmination of many advancements in stem cell biology. To improve the applicability of brain organoids, knowledge can also be taken from advances realized in other organoid models. For example, improved characterization approaches have been applied to other organoid models, such as single molecule fluorescent in situ hybridization (smFISH). This technique provides single-cell analysis while preserving spatial information, as it is performed in situ without disrupting the three-dimensional architecture of the organoids (Omerzu et al., 2019). While fewer transcripts can be analyzed at once, the spatial information can provide insight and context into the activity of individual cells in specific organoid regions. This has recently been applied to colon organoids to assess Wnt signaling pathway alterations across entire organoids and regional transcription differences between crypt structures and the main organoid body (Omerzu et al., 2019); this could prove highly useful for analyzing cell signaling throughout developmental stages in brain organoids, especially development and integration of multiple regions. smFISH was also used to analyze post-transcriptional regulation in whole *Drosophila* brains, demonstrating its utility for detailed



mechanistic analysis not feasible with immunohistochemistry (Yang et al., 2017).

Despite the significant advances and rapid evolution in brain organoid generation and engineering in recent years, reliable functional output and analysis is vital for brain organoid applications, especially disease modeling, and has lagged behind other organoid characterization, such as immunohistochemistry and transcriptomics (Wang, 2018; Poli et al., 2019). Just as *in vivo* models typically require overt behavioral phenotypes relevant to the diseases they are modeling, brain organoids cannot truly be considered representative of the human brain without physiologically relevant function—in this case, neural activity.

Electrophysiological advances for *in vivo* recording, such as Neuropixels (Jun et al., 2017; Steinmetz et al., 2018), and human medicine (e.g., neuroimaging) (Lau-Zhu et al., 2019) are opening the door to analyze highly specific populations of neurons and brain regions at high spatiotemporal resolution. For example, Neuropixels probes have the capability to record entire pathways consisting of several brain regions *in vivo* simultaneously, such as the primary motor cortex and striatum (Steinmetz et al., 2018). The 3DMEAs highlighted in this review present similar opportunities for *in vitro* analysis of brain organoids, such as the potential to record, say, dopaminergic neurons in both a substantia nigra-like region and ventral tegmental area-like region of a midbrain organoid to study Parkinson's disease. These areas are differentially affected in Parkinson's disease (Smits and Schwamborn, 2020), representing a clear application for brain organoid modeling.

Advances over the past several decades in stem cell biology, synthetic biology, and bioengineering have coalesced into a large umbrella of multi-cellular engineered living systems (M-CELS) (Kamm et al., 2018). M-CELS, including organoids, microphysiological systems, and “biobots”—machines consisting of biological material as building blocks and actuators—is a quickly developing field that could benefit significantly from advances in brain organoid analysis. One example of a potential M-CELS therapeutic is a biological pump, consisting of an endothelial vessel surrounded by muscle, which is innervated and controlled by a brain organoid (Kamm et al., 2018). This pump could be used for *in vitro* models of cardiovascular function or potentially implanted for regenerative medicine applications. While M-CELS as a whole is still in its infancy, rapid advances in underlying fields and technologies (including many of those described here) are enabling the realization of many of these systems. Improvements in brain organoid analysis and control, such as the electrophysiological advances described in this review, could help design M-CELS with the ability to sense and process

their surroundings, leading to autonomous function via neural logic and computation.

Improved recording also introduces analytical considerations. While each of these methods presents promise for brain organoid analysis, each method also presents new analytical challenges. All-optical electrophysiology requires complex image analysis, electrophysiological parameter extraction, and statistical analysis, hindering early adoption (Kiskinis et al., 2018). 3DMEAs will likely require similar changes to existing analytical pipelines to account for the increased spatial information during processing (e.g., spike sorting). “Big data” has become a common challenge in neuroscience as technologies improve (including the ones mentioned above, sc-RNA-seq, and others), large multi-institutional projects are launched (e.g., the Brain Research through Advancing Innovative Neurotechnologies (BRAIN) Initiative), and researchers have access to high-performance computing (Chen et al., 2019; Qu et al., 2019). These advances, combined with continued dimensionality reduction, deep learning, and other “big data” approaches to traditional methods will help facilitate adaptability and utility of these methods.

Ultimately, the approaches highlighted here represent a new wave of brain organoid functional analysis. By incorporating these with existing organoid technologies, such as optogenetics and sc-RNA-seq, researchers can extract more valuable information from brain organoids (Figure 2). The rapid development and evolution of these technologies continues to move closer to the goal of comprehensive organoid characterization—correlation of both identity and function of individual cells comprising brain organoids. These approaches will hopefully help unlock the full potential of brain organoids for developmental studies, disease modeling, and drug discovery applications.

AUTHOR CONTRIBUTIONS

AP and SS designed, wrote, and edited the manuscript and have approved it for publication. Both authors contributed to the article and approved the submitted version.

FUNDING

This work was funded by the National Science Foundation Science and Technology Center for Emergent Behaviors of Integrated Cellular Systems, Grant No. 0939511.

REFERENCES

- Adly, N., Weidlich, S., Seyock, S., Brings, F., Yakushenko, A., Offenhäusser, A., et al. (2018). Printed microelectrode arrays on soft materials: from PDMS to hydrogels. *NPJ Flex. Electron.* 2:15. doi: 10.1038/s41528-018-0027-z
- Ao, Z., Cai, H., Havert, D. J., Wu, Z., Gong, Z., Beggs, J. M., et al. (2020). One-Stop Microfluidic Assembly of Human Brain Organoids to Model Prenatal Cannabis Exposure. *Anal. Chem.* 92, 4630–4638. doi: 10.1021/acs.analchem.0c00205
- Atmaramani, R., Chakraborty, B., Rihani, R. T., Usoro, J., Hammack, A., Abbott, J., et al. (2020). Ruthenium oxide based microelectrode arrays for *in vitro* and *in vivo* neural recording and stimulation. *Acta Biomater.* 101, 565–574. doi: 10.1016/j.actbio.2019.10.040
- Avior, Y., Sagi, I., and Benvenisty, N. (2016). Pluripotent stem cells in disease modelling and drug discovery. *Nat. Rev. Mol. Cell Biol.* 17, 170–182. doi: 10.1038/nrm.2015.27
- Bal-Price, A., Pistollato, F., Sachana, M., Bopp, S. K., Munn, S., and Worth, A. (2018). Strategies to improve the regulatory assessment of developmental

- neurotoxicity (DNT) using in vitro methods. *Toxicol. Appl. Pharmacol.* 354, 7–18. doi: 10.1016/j.taap.2018.02.008
- Bardy, C., Van Den Hurk, M., Kakaradov, B., Erwin, J. A., Jaeger, B. N., Hernandez, R. V., et al. (2016). Predicting the functional states of human iPSC-derived neurons with single-cell RNA-seq and electrophysiology. *Mol. Psych.* 21, 1573–1588. doi: 10.1038/mp.2016.158
- Begley, C. G., and Ellis, L. M. (2012). Raise standards for preclinical cancer research. *Nature* 483, 531–533. doi: 10.1038/483531a
- Bejoy, J., Wang, Z., Bijonowski, B., Yang, M., Ma, T., Sang, Q. X., et al. (2018). Differential Effects of Heparin and Hyaluronic Acid on Neural Patterning of Human Induced Pluripotent Stem Cells. *ACS Biomater. Sci. Eng.* 4, 4354–4366. doi: 10.1021/acsbomaterials.8b01142
- Berger, E., Magliaro, C., Paczia, N., Monzel, A. S., Antony, P., Linster, C. L., et al. (2018). Millifluidic culture improves human midbrain organoid vitality and differentiation. *Lab. Chip.* 18, 3172–3183. doi: 10.1039/c8lc00206a
- Bershteyn, M., Nowakowski, T. J., Pollen, A. A., Di Lullo, E., Nene, A., Wynshaw-Boris, A., et al. (2017). Human iPSC-Derived Cerebral Organoids Model Cellular Features of Lissencephaly and Reveal Prolonged Mitosis of Outer Radial Glia. *Cell Stem Cell.* 20, 435–449. doi: 10.1016/j.stem.2016.12.007
- Bhatia, S. N., and Ingber, D. E. (2014). Microfluidic organs-on-chips. *Nat. Biotechnol.* 32, 760–772. doi: 10.1038/nbt.2989
- Boni, R., Ali, A., Shavandi, A., and Clarkson, A. N. (2018). Current and novel polymeric biomaterials for neural tissue engineering. *J. Biomed. Sci.* 25, 1–21. doi: 10.1186/s12929-018-0491-8
- Borda, E., Ferlauto, L., Schleuniger, J., Mustaccio, A., Lütolf, F., Lücke, A., et al. (2020). All-Printed ElectroCorticography Array for In Vivo Neural Recordings. *Adv. Eng. Mater.* 22:1901403. doi: 10.1002/adem.201901403
- Bridges, D. C., Tovar, K. R., Wu, B., Hansma, P. K., and Kosik, K. S. (2018). MEA Viewer: A high-performance interactive application for visualizing electrophysiological data. *PLoS One* 13:e0192477. doi: 10.1371/journal.pone.0192477
- Cadwell, C. R., Palasantza, A., Jiang, X., Berens, P., Deng, Q., Yilmaz, M., et al. (2016). Electrophysiological, transcriptomic and morphologic profiling of single neurons using Patch-seq. *Nat. Biotechnol.* 34, 199–203. doi: 10.1038/nbt.3445
- Cadwell, C. R., Scala, F., Li, S., Livrizzi, G., Shen, S., Sandberg, R., et al. (2017). Multimodal profiling of single-cell morphology, electrophysiology, and gene expression using Patch-seq. *Nat. Protoc.* 12, 2531–2553. doi: 10.1038/nprot.2017.120
- Cakir, B., Xiang, Y., Tanaka, Y., Kural, M. H., Parent, M., Kang, Y. J., et al. (2019). Engineering of human brain organoids with a functional vascular-like system. *Nat. Methods* 16, 1169–1175. doi: 10.1038/s41592-019-0586-5
- Camp, J. G., Badsha, F., Florio, M., Kanton, S., Gerber, T., Wilsch-Bräuninger, M., et al. (2015). Human cerebral organoids recapitulate gene expression programs of fetal neocortex development. *Proc. Natl. Acad. Sci. U. S. A.* 112, 15672–15677. doi: 10.1073/pnas.1520760112
- Chen, S., He, Z., Han, X., He, X., Li, R., Zhu, H., et al. (2019). How Big Data and High-performance Computing Drive Brain Science. *Genom. Proteom. Bioinforma.* 17, 381–392. doi: 10.1016/j.gpb.2019.09.003
- Chen, X., Zhang, K., Zhou, L., Gao, X., Wang, J., Yao, Y., et al. (2016). Coupled electrophysiological recording and single cell transcriptome analyses revealed molecular mechanisms underlying neuronal maturation. *Protein Cell* 7, 175–186. doi: 10.1007/s13238-016-0247-8
- Chin, E. W. M., and Goh, E. L. K. (2015). Studying neurological disorders using induced pluripotent stem cells and optogenetics. *Neural. Regen. Res.* 10, 1720–1722. doi: 10.4103/1673-5374.169607
- Cotterill, E., Hall, D., Wallace, K., Mundy, W. R., Eglen, S. J., and Shafer, T. J. (2016). Characterization of early cortical neural network development in multiwell microelectrode array plates. *J. Biomol. Screen* 21, 510–519. doi: 10.1177/1087057116640520
- Cruz-Acuña, R., Quirós, M., Farkas, A. E., Dedhia, P. H., Huang, S., Siuda, D., et al. (2017). Synthetic hydrogels for human intestinal organoid generation and colonic wound repair. *Nat. Cell Biol.* 19, 1326–1335. doi: 10.1038/ncb3632
- Demers, C. J., Soundararajan, P., Chennampally, P., Cox, G. A., Briscoe, J., Collins, S. D., et al. (2016). Development-on-chip: In vitro neural tube patterning with a microfluidic device. *Dev* 143, 1884–1892. doi: 10.1242/dev.126847
- Di Lullo, E., and Kriegstein, A. R. (2017). The use of brain organoids to investigate neural development and disease. *Nat. Rev. Neurosci.* 18, 573–584. doi: 10.1038/nrn.2017.107
- Didier, C. M., Kundu, A., Deroo, D., and Rajaraman, S. (2020). Development of in vitro 2D and 3D microelectrode arrays and their role in advancing biomedical research. *J. Micromech. Microengin.* 30:103001. doi: 10.1088/1361-6439/ab8e91
- Durens, M., Nestor, J., Williams, M., Herold, K., Niescier, R. F., Lunden, J. W., et al. (2020). High-throughput screening of human induced pluripotent stem cell-derived brain organoids. *J. Neurosci. Methods* 335:108627. doi: 10.1016/j.jneumeth.2020.108627
- Ebert, A. D., Liang, P., and Wu, J. C. (2012). Induced pluripotent stem cells as a disease modeling and drug screening platform. *J. Cardiovasc. Pharmacol.* 60, 408–416. doi: 10.1097/FJC.0b013e318247f642
- Egert, U., Knott, T., Schwarz, C., Nawrot, M., Brandt, A., Rotter, S., et al. (2002). MEA-Tools: An open source toolbox for the analysis of multi-electrode data with MATLAB. *J. Neurosci. Methods* 117, 33–42. doi: 10.1016/S0165-0270(02)00045-6
- Esch, E. W., Bahinski, A., and Huh, D. (2015). Organs-on-chips at the frontiers of drug discovery. *Nat. Rev. Drug Discov.* 14, 248–260. doi: 10.1038/nrd4539
- Fair, S. R., Julian, D., Hartlaub, A. M., Pusuluri, S. T., Malik, G., Summerfield, T. L., et al. (2020). Electrophysiological Maturation of Cerebral Organoids Correlates with Dynamic Morphological and Cellular Development. *Stem Cell Rep.* 15, 855–868. doi: 10.1016/j.stemcr.2020.08.017
- Fischer, J., Heide, M., and Huttner, W. B. (2019). Genetic Modification of Brain Organoids. *Front. Cell. Neurosci.* 13:558. doi: 10.3389/fncel.2019.00558
- Földy, C., Darmanis, S., Aoto, J., Malenka, R. C., Quake, S. R., and Südhof, T. C. (2016). Single-cell RNAseq reveals cell adhesion molecule profiles in electrophysiologically defined neurons. *Proc. Natl. Acad. Sci. U. S. A.* 113, E5222–E5231. doi: 10.1073/pnas.1610155113
- Frank, C. L., Brown, J. P., Wallace, K., Mundy, W. R., and Shafer, T. J. (2017). From the Cover: Developmental Neurotoxicants Disrupt Activity in Cortical Networks on Microelectrode Arrays: Results of Screening 86 Compounds During Neural Network Formation. *Toxicol. Sci.* 160, 121–135. doi: 10.1093/toxsci/kfx169
- Fuzik, J., Zeisel, A., Mate, Z., Calvigioni, D., Yanagawa, Y., Szabo, G., et al. (2016). Integration of electrophysiological recordings with single-cell RNA-seq data identifies neuronal subtypes. *Nat. Biotechnol.* 34, 175–183. doi: 10.1038/nbt.3443
- Georgiou, M., Chichagova, V., Hilgen, G., Dorgau, B., Sernagor, E., Armstrong, L., et al. (2020). Room temperature shipment does not affect the biological activity of pluripotent stem cell-derived retinal organoids. *PLoS One* 15:e0233860. doi: 10.1371/journal.pone.0233860
- Giandomenico, S. L., Mierau, S. B., Gibbons, G. M., Wenger, L. M. D., Masullo, L., Sit, T., et al. (2019). Cerebral organoids at the air-liquid interface generate diverse nerve tracts with functional output. *Nat. Neurosci.* 22, 669–679. doi: 10.1038/s41593-019-0350-2
- Gjorevski, N., and Lutolf, M. P. (2017). Synthesis and characterization of well-defined hydrogel matrices and their application to intestinal stem cell and organoid culture. *Nat. Protoc.* 12, 2263–2274. doi: 10.1038/nprot.2017.095
- Gjorevski, N., Sachs, N., Manfrin, A., Giger, S., Bragina, M. E., Ordóñez-Morán, P., et al. (2016). Designer matrices for intestinal stem cell and organoid culture. *Nature* 539, 560–564. doi: 10.1038/nature20168
- Gopalakrishnan, J. (2019). The Emergence of Stem Cell-Based Brain Organoids: Trends and Challenges. *BioEssays* 41:1900011. doi: 10.1002/bies.201900011
- Ham, O., Jin, Y. B., Kim, J., and Lee, M. O. (2020). Blood vessel formation in cerebral organoids formed from human embryonic stem cells. *Biochem. Biophys. Res. Commun.* 521, 84–90. doi: 10.1016/j.bbrc.2019.10.079
- Hilgen, G., Sorbaro, M., Zanacchi, F. C., Sernagor, E., Hennig, M. H., Pirmoradian, S., et al. (2017). Unsupervised Spike Sorting for Large-Scale, High-Density Multielectrode Arrays. *Cell Rep.* 18, 2521–2532. doi: 10.1016/j.celrep.2017.02.038
- Hochbaum, D. R., Zhao, Y., Farhi, S. L., Klapoetke, N., Werley, C. A., Kapoor, V., et al. (2014). All-optical electrophysiology in mammalian neurons using engineered microbial rhodopsins. *Nat. Methods* 11, 825–833. doi: 10.1038/NMETH.3000
- Jackson, E. L., and Lu, H. (2016). Three-dimensional models for studying development and disease: Moving on from organisms to organs-on-a-chip and organoids. *Integr. Biol.* 8, 672–683. doi: 10.1039/c6ib00039h
- Jahnke, H. G., Schmidt, S., Frank, R., Weigel, W., Prönncke, C., and Robitzki, A. A. (2019). FEM-based design of optical transparent indium tin oxide

- multielectrode arrays for multiparametric, high sensitive cell based assays. *Biosens. Bioelectron.* 129, 208–215. doi: 10.1016/j.bios.2018.09.095
- Jo, J., Xiao, Y., Sun, A. X., Cukuroglu, E., Tran, H. D., Göke, J., et al. (2016). Midbrain-like Organoids from Human Pluripotent Stem Cells Contain Functional Dopaminergic and Neuromelanin-Producing Neurons. *Cell Stem Cell* 19, 248–257. doi: 10.1016/j.stem.2016.07.005
- Jun, J. J., Steinmetz, N. A., Siegle, J. H., Denman, D. J., Bauza, M., Barbarits, B., et al. (2017). Fully integrated silicon probes for high-density recording of neural activity. *Nature* 551, 232–236. doi: 10.1038/nature24636
- Kadoshima, T., Sakaguchi, H., Nakano, T., Soen, M., Ando, S., Eiraku, M., et al. (2013). Self-organization of axial polarity, inside-out layer pattern, and species-specific progenitor dynamics in human ES cell-derived neocortex. *Proc. Natl. Acad. Sci. U. S. A.* 110, 20284–20289. doi: 10.1073/pnas.1315710110
- Kamm, R. D., Bashir, R., Arora, N., Dar, R. D., Gillette, M. U., Griffith, L. G., et al. (2018). Perspective: The promise of multi-cellular engineered living systems. *APL Bioeng.* 2:040901. doi: 10.1063/1.5038337
- Karzbrun, E., Kshirsagar, A., Cohen, S. R., Hanna, J. H., and Reiner, O. (2018a). Human brain organoids on a chip reveal the physics of folding. *Nat. Phys.* 14, 515–522. doi: 10.1038/s41567-018-0046-7
- Karzbrun, E., Tshuva, R. Y., and Reiner, O. (2018b). An On-Chip Method for Long-Term Growth and Real-Time Imaging of Brain Organoids. *Curr. Protoc. Cell Biol.* 81, 1–17. doi: 10.1002/cpcb.62
- Kelava, I., and Lancaster, M. A. (2016a). Dishing out mini-brains: Current progress and future prospects in brain organoid research. *Dev. Biol.* 420, 199–209. doi: 10.1016/j.ydbio.2016.06.037
- Kelava, I., and Lancaster, M. A. (2016b). Stem Cell Models of Human Brain Development. *Cell Stem Cell* 18, 736–748. doi: 10.1016/j.stem.2016.05.022
- Kim, J. A., Hong, S., and Rhee, W. J. (2019). Microfluidic three-dimensional cell culture of stem cells for high-throughput analysis. *World J. Stem Cells* 11, 803–816. doi: 10.4252/wjsc.v11.i10.803
- Kiskinis, E., Kralj, J. M., Zou, P., Weinstein, E. N., Zhang, H., Tsioras, K., et al. (2018). All-Optical Electrophysiology for High-Throughput Functional Characterization of a Human iPSC-Derived Motor Neuron Model of ALS. *Stem Cell Rep.* 10, 1991–2004. doi: 10.1016/j.stemcr.2018.04.020
- Koklu, A., Atmaramani, R., Hammack, A., Beskok, A., Pancrazio, J. J., Gnade, B. E., et al. (2019). Gold nanostructure microelectrode arrays for in vitro recording and stimulation from neuronal networks. *Nanotechnology* 101, 565–574. doi: 10.1088/1361-6528/ab07cd
- Koo, B., Choi, B., Park, H., and Yoon, K. J. (2019). Past, Present, and Future of Brain Organoid Technology. *Mol. Cells* 42, 617–627. doi: 10.14348/molcells.2019.0162
- Kratochvil, M. J., Seymour, A. J., Li, T. L., Paşca, S. P., Kuo, C. J., and Heilshorn, S. C. (2019). Engineered materials for organoid systems. *Nat. Rev. Mater.* 4, 606–622. doi: 10.1038/s41578-019-0129-9
- Kyrousi, C., and Cappello, S. (2020). Using brain organoids to study human neurodevelopment, evolution and disease. *Wiley Interdisc. Rev. Dev. Biol.* 9, 1–19. doi: 10.1002/wdev.347
- Lancaster, M. A., and Knoblich, J. A. (2014). Generation of cerebral organoids from human pluripotent stem cells. *Nat. Protoc.* 9, 2329–2340. doi: 10.1038/nprot.2014.158
- Lancaster, M. A., Renner, M., Martin, C.-A., Wenzel, D., Bicknell, L. S., Hurler, M. E., et al. (2013). Cerebral organoids model human brain development and microcephaly. *Nature* 501, 373–379. doi: 10.1038/nature12517
- Lancaster, M., Takebe, T., and Lancaster, M. (2017). Advances in Organoid Technology: Hans Clevers, Madeline Lancaster, and Takanori Takebe. *Cell Stem Cell* 20, 759–762. doi: 10.1016/j.stem.2017.05.014
- Latchoumane, C.-F. V., Jackson, L., Sendi, M. S. E., Tehrani, K. F., Mortensen, L. J., Stice, S. L., et al. (2018). Chronic Electrical Stimulation Promotes the Excitability and Plasticity of ESC-derived Neurons following Glutamate-induced Inhibition In vitro. *Sci. Rep.* 8:10957. doi: 10.1038/s41598-018-29069-3
- Lau-Zhu, A., Lau, M. P. H., and McLoughlin, G. (2019). Mobile EEG in research on neurodevelopmental disorders: Opportunities and challenges. *Dev. Cogn. Neurosci.* 36:100635. doi: 10.1016/j.dcn.2019.100635
- Lee, S. Y., George, J. H., Nagel, D. A., Ye, H., Kueberuwa, G., and Seymour, L. W. (2019). Optogenetic control of iPS cell-derived neurons in 2D and 3D culture systems using channelrhodopsin-2 expression driven by the synapsin-1 and calcium-calmodulin kinase II promoters. *J. Tissue Eng. Regen. Med.* 13, 369–384. doi: 10.1002/term.2786
- Lefebvre, B., Yger, P., and Marre, O. (2016). Recent progress in multi-electrode spike sorting methods. *J. Physiol. Paris* 110, 327–335. doi: 10.1016/j.jphysparis.2017.02.005
- Lei, Y., and Schaffer, D. V. (2013). A fully defined and scalable 3D culture system for human pluripotent stem cell expansion and differentiation. *Proc. Natl. Acad. Sci. U. S. A.* 110, E5039–E5048. doi: 10.1073/pnas.1309408110
- Li, H., Wang, J., and Fang, Y. (2020). Bioinspired flexible electronics for seamless neural interfacing and chronic recording. *Nanoscale Adv.* 2, 3095–3102. doi: 10.1039/d0na00323a
- Li, Q., Nan, K., Le Floch, P., Lin, Z., Sheng, H., Blum, T. S., et al. (2019). Cyborg Organoids: Implantation of Nanoelectronics via Organogenesis for Tissue-Wide Electrophysiology. *Nano Lett.* 19, 5781–5789. doi: 10.1021/acs.nanolett.9b02512
- Li, R., Sun, L., Fang, A., Li, P., Wu, Q., and Wang, X. (2017). Recapitulating cortical development with organoid culture in vitro and modeling abnormal spindle-like (ASPM related primary) microcephaly disease. *Protein Cell* 8, 823–833. doi: 10.1007/s13238-017-0479-2
- Lindborg, B. A., Brekke, J. H., Vegoe, A. L., Ulrich, C. B., Haider, K. T., Subramaniam, S., et al. (2016). Rapid Induction of Cerebral Organoids From Human Induced Pluripotent Stem Cells Using a Chemically Defined Hydrogel and Defined Cell Culture Medium. *Stem Cells Transl. Med.* 5, 970–979. doi: 10.5966/sctm.2015-0305
- Liu, C., Oikonomopoulos, A., Sayed, N., and Wu, J. C. (2018). Modeling human diseases with induced pluripotent stem cells: From 2D to 3D and beyond. *Dev* 145:dev156166. doi: 10.1242/dev.156166
- Mansour, A. A., Gonçalves, J. T., Bloyd, C. W., Li, H., Fernandes, S., Quang, D., et al. (2018). An in vivo model of functional and vascularized human brain organoids. *Nat. Biotechnol.* 36, 432–441. doi: 10.1038/nbt.4127
- Marre, O., Amodei, D., Deshmukh, N., Sadeghi, K., Soo, F., Holy, T. E., et al. (2012). Mapping a complete neural population in the retina. *J. Neurosci.* 32, 14859–14873. doi: 10.1523/JNEUROSCI.0723-12.2012
- McConnell, E. R., McClain, M. A., Ross, J., LeFevre, W. R., and Shafer, T. J. (2012). Evaluation of multi-well microelectrode arrays for neurotoxicity screening using a chemical training set. *Neurotoxicology* 33, 1048–1057. doi: 10.1016/j.neuro.2012.05.001
- Mellough, C. B., Collin, J., Queen, R., Hilgen, G., Dorgau, B., Zerti, D., et al. (2019). Systematic Comparison of Retinal Organoid Differentiation from Human Pluripotent Stem Cells Reveals Stage Specific, Cell Line, and Methodological Differences. *Stem Cells Transl. Med.* 8, 694–706. doi: 10.1002/sctm.18-0267
- Monzel, A. S., Smits, L. M., Hemmer, K., Hachi, S., Moreno, E. L., van Wullen, T., et al. (2017). Derivation of Human Midbrain-Specific Organoids from Neuroepithelial Stem Cells. *Stem Cell Rep.* 8, 1144–1154. doi: 10.1016/j.stemcr.2017.03.010
- Muguruma, K. (2017). 3D culture for self-formation of the cerebellum from human pluripotent stem cells through induction of the isthmus organizer. *Methods Mole. Biol.* 1597, 31–41. doi: 10.1007/978-1-4939-6949-4_3
- Muguruma, K., Nishiyama, A., Kawakami, H., Hashimoto, K., and Sasai, Y. (2015). Self-organization of polarized cerebellar tissue in 3D culture of human pluripotent stem cells. *Cell Rep.* 10, 537–550. doi: 10.1016/j.celrep.2014.12.051
- Ogawa, J., Pao, G. M., Shokhirev, M. N., and Verma, I. M. (2018). Glioblastoma Model Using Human Cerebral Organoids. *Cell Rep.* 23, 1220–1229. doi: 10.1016/j.celrep.2018.03.105
- Omerzu, M., Fenderico, N., De Barbanson, B., Sprangers, J., De Ridder, J., and Maurice, M. M. (2019). Three-dimensional analysis of single molecule FISH in human colon organoids. *Biol. Open* 8:bio042812. doi: 10.1242/bio.042812
- Osaki, T., Uzel, S. G. M., and Kamm, R. D. (2018). Microphysiological 3D model of amyotrophic lateral sclerosis (ALS) from human iPSC-derived muscle cells and optogenetic motor neurons. *Sci. Adv.* 4:5847. doi: 10.1126/sciadv.aat5847
- Parfitt, D. A., Lane, A., Ramsden, C. M., Carr, A. J. F., Munro, P. M., Jovanovic, K., et al. (2016). Identification and Correction of Mechanisms Underlying Inherited Blindness in Human iPSC-Derived Optic Cups. *Cell Stem Cell* 18, 769–781. doi: 10.1016/j.stem.2016.03.021
- Park, S. E., Georgescu, A., and Huh, D. (2019). Organoids-on-a-chip. *Science* 364, 960–965. doi: 10.1126/science.aaw7894
- Pasca, A. M., Sloan, S. A., Clarke, L. E., Tian, Y., Makinson, C. D., Huber, N., et al. (2015). Functional cortical neurons and astrocytes from human pluripotent stem cells in 3D culture. *Nat. Methods* 12, 671–678. doi: 10.1038/nmeth.3415

- Pastore, V. P., Poli, D., Godjoski, A., Martinoia, S., and Massobrio, P. (2016). ToolConnect: A functional connectivity toolbox for In vitro networks. *Front. Neuroinform.* 10:13. doi: 10.3389/fninf.2016.00013
- Pham, M. T., Pollock, K. M., Rose, M. D., Cary, W. A., Stewart, H. R., Zhou, P., et al. (2018). Generation of human vascularized brain organoids. *Neuroreport* 29, 588–593. doi: 10.1097/WNR.0000000000001014
- Poli, D., Magliaro, C., and Ahluwalia, A. (2019). Experimental and Computational Methods for the Study of Cerebral Organoids: A Review. *Front. Neurosci.* 13:162. doi: 10.3389/fnins.2019.00162
- Qian, X., Song, H., and Ming, G. L. (2019). Brain organoids: Advances, applications and challenges. *Dev* 146:dev166074. doi: 10.1242/dev.166074
- Qu, H., Lei, H., and Fang, X. (2019). Big Data and the Brain: Peeking at the Future. *Genom. Proteom. Bioinforma.* 17, 333–336. doi: 10.1016/j.gpb.2019.11.003
- Quadrato, G., Brown, J., and Arlotta, P. (2016). The promises and challenges of human brain organoids as models of neuropsychiatric disease. *Nat. Med.* 22, 1220–1228. doi: 10.1038/nm.4214
- Quadrato, G., Nguyen, T., Macosko, E. Z., Sherwood, J. L., Yang, S. M., Berger, D. R., et al. (2017). Cell diversity and network dynamics in photosensitive human brain organoids. *Nature* 545, 48–53. doi: 10.1038/nature22047
- Raja, W. K., Mungenast, A. E., Lin, Y. T., Ko, T., Abdurrob, F., Seo, J., et al. (2016). Self-organizing 3D human neural tissue derived from induced pluripotent stem cells recapitulate Alzheimer's disease phenotypes. *PLoS One* 11:e0161969. doi: 10.1371/journal.pone.0161969
- Ranga, A., Girgin, M., Meinhardt, A., Eberle, D., Caiazzo, M., Tanaka, E. M., et al. (2016). Neural tube morphogenesis in synthetic 3D microenvironments. *Proc. Natl. Acad. Sci. U. S. A.* 113, E6831–E6839. doi: 10.1073/pnas.1603529113
- Rapti, K., Stilitano, F., Karakikes, I., Nonnenmacher, M., Weber, T., Hulot, J. S., et al. (2015). Effectiveness of gene delivery systems for pluripotent and differentiated cells. *Mol. Ther. Methods Clin. Dev.* 2:14067. doi: 10.1038/mtm.2014.67
- Regalia, G., Coelli, S., Biffi, E., Ferrigno, G., and Pedrocchi, A. (2016). A framework for the comparative assessment of neuronal spike sorting algorithms towards more accurate off-line and on-line microelectrode arrays data analysis. *Comput. Intell. Neurosci.* 2016:8416237. doi: 10.1155/2016/8416237
- Robinette, B. L., Harrill, J. A., Mundy, W. R., and Shafer, T. J. (2011). In vitro assessment of developmental neurotoxicity: Use of microelectrode arrays to measure functional changes in neuronal network ontogeny. *Front. Neuroeng* 4:1. doi: 10.3389/fneng.2011.00001
- Rossant, C., Kadir, S. N., Goodman, D. F. M., Schulman, J., Hunter, M. L. D., Saleem, A. B., et al. (2016). Spike sorting for large, dense electrode arrays. *Nat. Neurosci.* 19, 634–641. doi: 10.1038/nn.4268
- Ryynänen, T., Mzezewa, R., Meriläinen, E., Hyvärinen, T., Lekkala, J., Narkilahti, S., et al. (2020). Transparent microelectrode arrays fabricated by ion beam assisted deposition for neuronal cell in vitro recordings. *Micromachines* 11:497. doi: 10.3390/M111050497
- Ryynänen, T., Pelkonen, A., Grigoras, K., Ylivaara, O. M. E., Hyvärinen, T., Ahopelto, J., et al. (2019). Microelectrode Array With Transparent ALD TiN Electrodes. *Front. Neurosci.* 13:226. doi: 10.3389/fnins.2019.00226
- Sakaguchi, H., Kadoshima, T., Soen, M., Narii, N., Ishida, Y., Ohgushi, M., et al. (2015). Generation of functional hippocampal neurons from self-organizing human embryonic stem cell-derived dorsomedial telencephalic tissue. *Nat. Commun.* 6, 1–11. doi: 10.1038/ncomms9896
- Sakaguchi, H., Ozaki, Y., Ashida, T., Matsubara, T., Oishi, N., Kihara, S., et al. (2019). Self-Organized Synchronous Calcium Transients in a Cultured Human Neural Network Derived from Cerebral Organoids. *Stem Cell Rep.* 13, 458–473. doi: 10.1016/j.stemcr.2019.05.029
- Schröter, M., Girr, M., Boos, J., Renner, M., Gazorpak, M., Gong, W., et al. (2018). Mapping neuronal network dynamics in developing cerebral organoids. *Front. Cell. Neurosci.* 12:66. doi: 10.3389/conf.fncl.2018.38.00066
- Shafer, T. J., Brown, J. P., Lynch, B., Davila-Montero, S., Wallace, K., and Friedman, K. P. (2019). Evaluation of Chemical Effects on Network Formation in Cortical Neurons Grown on Microelectrode Arrays. *Toxicol. Sci.* 169, 436–455. doi: 10.1093/toxsci/kfz052
- Shi, Y., Sun, L., Wang, M., Liu, J., Zhong, S., Li, R., et al. (2020). Vascularized human cortical organoids (vOrganoids) model cortical development in vivo. *PLoS Biol.* 18:e3000705. doi: 10.1371/journal.pbio.3000705
- Shim, C., Jo, Y., Cha, H. K., Kim, M. K., Kim, H., Kook, G., et al. (2020). Highly Stretchable Microelectrode Array for Free-form 3D Neuronal Tissue. in *Proceedings of the IEEE International Conference on Micro Electro Mechanical Systems (MEMS)*. New York: Institute of Electrical and Electronics Engineers Inc, 380–383. doi: 10.1109/MEMS46641.2020.9056250
- Shiri, Z., Simorgh, S., Naderi, S., and Baharvand, H. (2019). Optogenetics in the Era of Cerebral Organoids. *Trends Biotechnol.* 37, 1282–1294. doi: 10.1016/j.tibtech.2019.05.009
- Skardal, A., Devarasetty, M., Soker, S., and Hall, A. R. (2015). In situ patterned micro 3D liver constructs for parallel toxicology testing in a fluidic device. *Biofabrication* 7:031001. doi: 10.1088/1758-5090/7/3/031001
- Skardal, A., Shupe, T., and Atala, A. (2016). Organoid-on-a-chip and body-on-a-chip systems for drug screening and disease modeling. *Drug Discov. Today* 21, 1399–1411. doi: 10.1016/j.drudis.2016.07.003
- Smits, L. M., and Schwamborn, J. C. (2020). Midbrain Organoids: A New Tool to Investigate Parkinson's Disease. *Front. Cell Dev. Biol.* 8:359. doi: 10.3389/fcell.2020.00359
- Smits, L. M., Reinhardt, L., Reinhardt, P., Glatza, M., Monzel, A. S., Stanslowsky, N., et al. (2019). Modeling Parkinson's disease in midbrain-like organoids. *npj Park. Dis* 5:5. doi: 10.1038/s41531-019-0078-4
- Soscia, D. A., Lam, D., Tooker, A. C., Enright, H. A., Triplett, M., Karande, P., et al. (2020). A flexible 3-dimensional microelectrode array for: In vitro brain models. *Lab. Chip* 20, 901–911. doi: 10.1039/c9lc01148j
- Steinmetz, N. A., Koch, C., Harris, K. D., and Carandini, M. (2018). Challenges and opportunities for large-scale electrophysiology with Neuropixels probes. *Curr. Opin. Neurobiol.* 50, 92–100. doi: 10.1016/j.conb.2018.01.009
- Su, C. T. E., Yoon, S. I., Marcy, G., Chin, E. W. M., Augustine, G. J., and Goh, E. L. K. (2015). An optogenetic approach for assessing formation of neuronal connections in a co-culture system. *J. Vis. Exp.* 96:52408. doi: 10.3791/52408
- Takebe, T., Zhang, B., and Radisic, M. (2017). Synergistic Engineering: Organoids Meet Organs-on-a-Chip. *Cell Stem Cell* 21, 297–300. doi: 10.1016/j.stem.2017.08.016
- Tian, B., Liu, J., Dvir, T., Jin, L., Tsui, J. H., Qing, Q., et al. (2012). Macroporous nanowire nanoelectronic scaffolds for synthetic tissues. *Nat. Mater.* 11, 986–994. doi: 10.1038/nmat3404
- Trujillo, C. A., and Muotri, A. R. (2018). Brain Organoids and the Study of Neurodevelopment. *Trends Mol. Med.* 24, 982–990. doi: 10.1016/j.molmed.2018.09.005
- Unakafova, V. A., and Gail, A. (2019). Comparing Open-Source Toolboxes for Processing and Analysis of Spike and Local Field Potentials Data. *Front. Neuroinform.* 13:57. doi: 10.3389/fninf.2019.00057
- van den Hurk, M., and Bardy, C. (2019). Single-cell multimodal transcriptomics to study neuronal diversity in human stem cell-derived brain tissue and organoid models. *J. Neurosci. Methods* 325:108350. doi: 10.1016/j.jneumeth.2019.10.8350
- Vargas-Valderrama, A., Messina, A., Mitjavila-Garcia, M. T., and Guenou, H. (2020). The endothelium, a key actor in organ development and hPSC-derived organoid vascularization. *J. Biomed. Sci.* 27:661. doi: 10.1186/s12929-020-00661-y
- Wainger, B. J., Kiskinis, E., Mellin, C., Wiskow, O., Han, S. S. W., Sandoe, J., et al. (2014). Intrinsic membrane hyperexcitability of amyotrophic lateral sclerosis patient-derived motor neurons. *Cell Rep.* 7, 1–11. doi: 10.1016/j.celrep.2014.03.019
- Wang, H. (2018). Modeling Neurological Diseases With Human Brain Organoids. *Front. Synaptic Neurosci.* 10:15. doi: 10.3389/fnsyn.2018.00015
- Wang, Y., Wang, L., Zhu, Y., and Qin, J. (2018). Human brain organoid-on-a-chip to model prenatal nicotine exposure. *Lab. Chip* 18, 851–860. doi: 10.1039/c7lc01084b
- Watanabe, M., Buth, J. E., Vishlaghi, N., de la Torre-Ubieta, L., Taxisidis, J., Khakh, B. S., et al. (2017). Self-Organized Cerebral Organoids with Human-Specific Features Predict Effective Drugs to Combat Zika Virus Infection. *Cell Rep.* 21, 517–532. doi: 10.1016/j.celrep.2017.09.047
- Werley, C. A., Brookings, T., Upadhyay, H., Williams, L. A., McManus, O. B., and Dempsey, G. T. (2017). All-optical electrophysiology for disease modeling and pharmacological characterization of neurons. *Curr. Protoc. Pharmacol.* 2017, 1–11. doi: 10.1002/cpph.25
- Yang, L., Titlow, J., Ennis, D., Smith, C., Mitchell, J., Young, F. L., et al. (2017). Single molecule fluorescence in situ hybridisation for quantitating post-transcriptional regulation in Drosophila brains. *Methods* 126, 166–176. doi: 10.1016/j.ymeth.2017.06.025

- Yang, X., Zhou, T., Zwang, T. J., Hong, G., Zhao, Y., Viveros, R. D., et al. (2019). Bioinspired neuron-like electronics. *Nat. Mater.* 18, 510–517. doi: 10.1038/s41563-019-0292-9
- Yang, Z., Zhang, A., Duan, H., Zhang, S., Hao, P., Ye, K., et al. (2015). NT3-chitosan elicits robust endogenous neurogenesis to enable functional recovery after spinal cord injury. *Proc. Natl. Acad. Sci. U. S. A.* 112, 13354–13359. doi: 10.1073/pnas.1510194112
- Yger, P., Spampinato, G. L. B., Esposito, E., Lefebvre, B., Deny, S., Gardella, C., et al. (2018). A spike sorting toolbox for up to thousands of electrodes validated with ground truth recordings in vitro and in vivo. *Elife* 7:e34518. doi: 10.7554/eLife.34518
- Yin, X., Mead, B. E., Safaei, H., Langer, R., Karp, J. M., and Levy, O. (2016). Engineering Stem Cell Organoids. *Cell Stem Cell* 18, 25–38. doi: 10.1016/j.stem.2015.12.005
- Yuan, X., Schröter, M., Obien, M. E. J., Fiscella, M., Gong, W., Kikuchi, T., et al. (2020). Versatile live-cell activity analysis platform for characterization of neuronal dynamics at single-cell and network level. *Nat. Commun.* 11, 1–14.
- Conflict of Interest:** The authors declare that the research was conducted in the absence of any commercial or financial relationships that could be construed as a potential conflict of interest.
- Copyright © 2021 Passaro and Stice. This is an open-access article distributed under the terms of the Creative Commons Attribution License (CC BY). The use, distribution or reproduction in other forums is permitted, provided the original author(s) and the copyright owner(s) are credited and that the original publication in this journal is cited, in accordance with accepted academic practice. No use, distribution or reproduction is permitted which does not comply with these terms.



3D *in vivo* Magnetic Particle Imaging of Human Stem Cell-Derived Islet Organoid Transplantation Using a Machine Learning Algorithm

Aixia Sun^{1,2†}, Hasaan Hayat^{1,3†}, Sihai Liu^{1,2,4}, Eliah Tull⁵, Jack Owen Bishop^{1,6}, Bennett Francis Dwan^{1,7}, Mithil Gudi^{1,3}, Nazanin Talebloo^{1,8}, James Raynard Dizon⁹, Wen Li^{10,11}, Jeffery Gaudet^{11,12}, Adam Alessio^{11,13}, Aitor Aguirre¹¹ and Ping Wang^{1,2*}

¹ Precision Health Program, Michigan State University, East Lansing, MI, United States, ² Department of Radiology, College of Human Medicine, Michigan State University, East Lansing, MI, United States, ³ Lyman Briggs College, Michigan State University, East Lansing, MI, United States, ⁴ Department of Orthopedics, Beijing Charity Hospital, Capital Medical University, Beijing, China, ⁵ Medgar Evers College, City University of New York, Brooklyn, NY, United States, ⁶ Department of Neuroscience, College of Natural Science, Michigan State University, East Lansing, MI, United States, ⁷ College of Natural Science, Michigan State University, East Lansing, MI, United States, ⁸ Department of Chemistry, College of Natural Science, Michigan State University, East Lansing, MI, United States, ⁹ Department of Radiology, UT Southwestern Medical Center, Dallas, TX, United States, ¹⁰ Department of Electrical and Computer Engineering, College of Engineering, Michigan State University, East Lansing, MI, United States, ¹¹ Institute for Quantitative Health Science and Engineering (IQ), Department of Biomedical Engineering, Michigan State University, East Lansing, MI, United States, ¹² Magnetic Insight Inc., Alameda, CA, United States, ¹³ Department of Computational Mathematics, Science and Engineering, College of Engineering, Michigan State University, East Lansing, MI, United States

OPEN ACCESS

Edited by:

Ming Li,
Osaka University, Japan

Reviewed by:

Aileen King,
King's College London,
United Kingdom
Luiza Ghila,
University of Bergen, Norway
Reihaneh Safavisohi,
Michigan State University,
United States

*Correspondence:

Ping Wang
wangpin4@msu.edu

† These authors have contributed
equally to this work and share first
authorship

Specialty section:

This article was submitted to
Stem Cell Research,
a section of the journal
Frontiers in Cell and Developmental
Biology

Received: 03 May 2021

Accepted: 15 July 2021

Published: 12 August 2021

Citation:

Sun A, Hayat H, Liu S, Tull E,
Bishop JO, Dwan BF, Gudi M,
Talebloo N, Dizon JR, Li W, Gaudet J,
Alessio A, Aguirre A and Wang P
(2021) 3D *in vivo* Magnetic Particle
Imaging of Human Stem Cell-Derived
Islet Organoid Transplantation Using
a Machine Learning Algorithm.
Front. Cell Dev. Biol. 9:704483.
doi: 10.3389/fcell.2021.704483

Stem cell-derived islet organoids constitute a promising treatment of type 1 diabetes. A major hurdle in the field is the lack of appropriate *in vivo* method to determine graft outcome. Here, we investigate the feasibility of *in vivo* tracking of transplanted stem cell-derived islet organoids using magnetic particle imaging (MPI) in a mouse model. Human induced pluripotent stem cells-L1 were differentiated to islet organoids and labeled with superparamagnetic iron oxide nanoparticles. The phantoms comprising of different numbers of labeled islet organoids were imaged using an MPI system. Labeled islet organoids were transplanted into NOD/scid mice under the left kidney capsule and were then scanned using 3D MPI at 1, 7, and 28 days post transplantation. Quantitative assessment of the islet organoids was performed using the *K-means++* algorithm analysis of 3D MPI. The left kidney was collected and processed for immunofluorescence staining of C-peptide and dextran. Islet organoids expressed islet cell markers including insulin and glucagon. Image analysis of labeled islet organoids phantoms revealed a direct linear correlation between the iron content and the number of islet organoids. The *K-means++* algorithm showed that during the course of the study the signal from labeled islet organoids under the left kidney capsule decreased. Immunofluorescence staining of the kidney sections showed the presence of islet organoid grafts as confirmed by double staining for dextran and C-peptide. This study demonstrates that MPI with machine learning algorithm analysis can monitor islet organoids grafts labeled with super-paramagnetic iron oxide nanoparticles and provide quantitative information of their presence *in vivo*.

Keywords: artificial intelligence, unsupervised machine learning, magnetic particle imaging, stem cell tracking, diabetes

INTRODUCTION

Type 1 diabetes (T1D) is characterized by an absolute deficiency of insulin secretion with hyperglycemia as a consequence. Transplantation of exogenous pancreatic islets to replace dead or dysfunctional endogenous beta cells is a strategy for controlling blood glucose levels in T1D patients. Severe shortage of cadaveric organ donors, requirement for lifelong immunosuppression, and reverting to using insulin after transplantation, however, largely hampers its application. In recent years advances in stem cell research, such as the derivation of human induced pluripotent stem cells (hiPSCs) and the emergence of organoid technologies, have enabled the creation of highly sophisticated human tissues and organ-like structures *in vitro*. These tissues could be used for isogenic or allogenic transplantation in the clinical setting to treat a diverse number of conditions, including T1D. *In vitro* created pancreatic islet organoids can be readily generated from hiPSCs matching the patient, thus providing an alternative similar to cadaveric donor islets that bypasses immune rejection concerns. Additionally, the number of pancreatic islet organoids that can be potentially produced is unlimited. A significant hurdle, however, is monitoring integration and survival of the pancreatic islet organoid after transplantation, and the lack of suitable non-invasive imaging techniques allowing us to determine the longer-term graft outcome (Rizzo et al., 2017; Wang and Aguirre, 2018).

Stem cell replacement therapy needs a technique that can quantitatively evaluate the fate of cells *in vivo* with high specificity and sensitivity. There are several techniques that have been used for imaging of islet or stem cell transplantation, including: optical imaging, magnetic resonance imaging (MRI) and positron emission tomography (PET). Optical imaging methods, both bioluminescence and fluorescence imaging, have the limitation of penetration depth preventing linear quantification and clinical translation. PET has excellent tracer sensitivity and depth penetration but cannot assess cell fate due to the limited tracer half-life. The evaluation of islet transplantation efficacy in the clinic relies on destructive analytical methods like histology or functional improvements that can take months to manifest. Most studies of cell tracking have used super-paramagnetic iron oxide nanoparticles (SPIONs) labeled cells, because SPIONs-based methods have few effects on cell viability, proliferation, and differentiation (Crabbe et al., 2010; Wang and Moore, 2012; Janowski et al., 2014; Bulte and Daldrup-Link, 2018), along with excellent depth penetration and *in vivo* persistence on the order of months. The primary challenge for MRI-based SPIONs cell tracking, however, is that SPIONs induced MRI signal dropouts that are difficult to distinguish from tissues with naturally low MRI signal (e.g., bones, tendon, lungs, bleeding, or any tissues near air). Moreover, MRI methods with positive contrast suffer from toxicity and sensitivity challenges (Magnitsky et al., 2017).

Magnetic particle imaging (MPI) is a novel imaging modality that directly detects the SPIONs, and is specific, sensitive, and linearly quantitative (Talebloo et al., 2020). MPI has been used for a wide range of biomedical applications such as tumors (Yu et al., 2017; Wu et al., 2019), vascular imaging (Khandhar et al., 2017), drug delivery (Wang et al., 2019), and *in vivo* tracking of labeled cells (Bulte et al., 2011; Zheng et al., 2015, 2016). Previously, our

group demonstrated MPI could be used for *in vivo* tracking of transplanted pancreatic islets in a mouse model (Wang et al., 2018). Furthermore, we have developed an unsupervised machine learning (ML) algorithm for monitoring *in vivo* 2D MPI data of islet grafts (Hayat et al., 2020). Such algorithms are required for standardized, high-throughput monitoring of transplanted organoids *in vivo* due to the highly variable nature of a region of interest (ROI) between MPI data. Often, it is difficult for human raters to maintain consistency regarding the threshold of cutoff for the true MPI signal from background. Therefore, applying a ML algorithm for segmenting of the desired ROIs from an MPI scan provides a reliable and standardized method of image quantification. So far, there are no reports on using MPI for imaging stem cell-derived islet organoids and it is critical to advance our algorithm to a 3D setting for more accurate and reliable signal quantification. Herein, we demonstrate the feasibility to develop and use the *K-means++* clustering-based, unsupervised ML algorithm to provide a novel method/tool for 3D image segmentation and quantification in the MPI domain, using SPIONs labeled stem cell differentiated islet organoids in a mouse model. We then used the segmentation output from the *K-means++* algorithm to generate a standard curve using fiducial markers in order to estimate the total iron value (TIV) of segmented ROIs. This provides information on the SPIONs accumulation within the labeled islet organoids and permits longitudinal evaluation of TIV of the ROI in the mice (Figure 1).

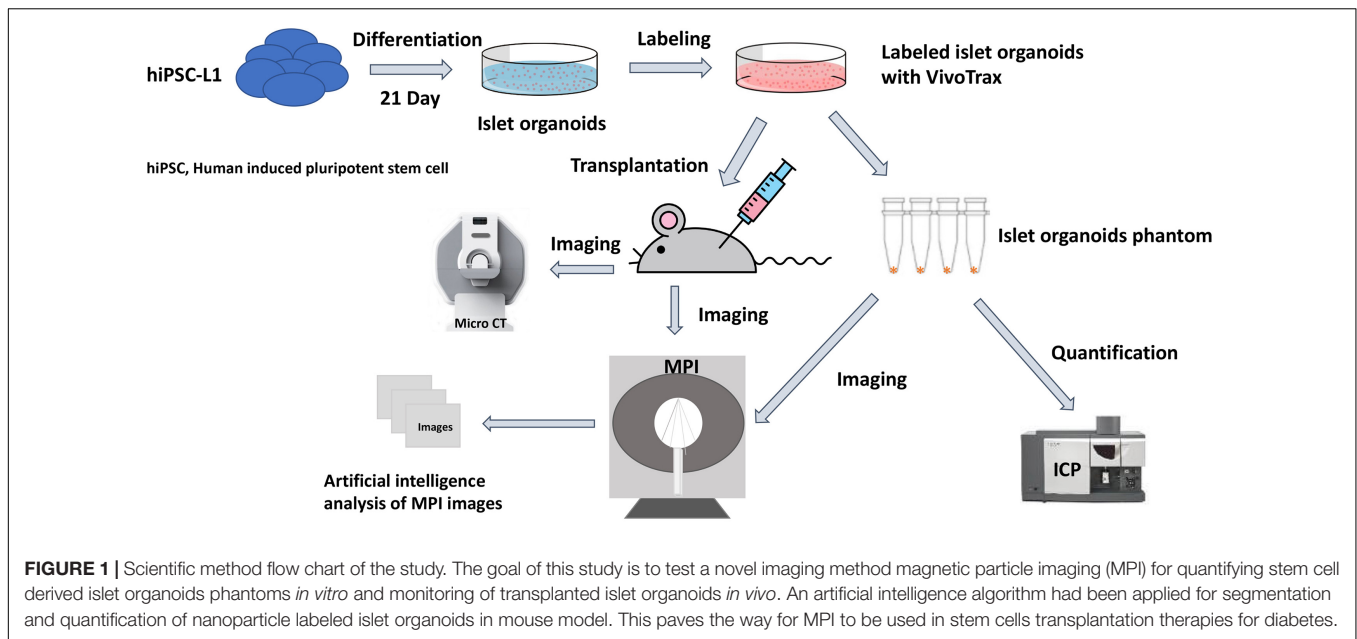
MATERIALS AND METHODS

Stem Cell Culture and Pancreatic Islet Organoid Differentiation

All hiPSC lines were validated for pluripotency and genomic integrity. hiPSC-L1 were cultured in Essential 8 Flex medium (Thermo Fisher Scientific, MA, United States) containing 1% penicillin/streptomycin (Gibco, Thermo Fisher Scientific, MA, United States) on six-well plates coated with growth factor-reduced Matrigel (Corning, NY, United States) in an incubator at 37°C, 5% CO₂, until 60–80% confluency was reached, at which point cells were split into new wells using ReLeSR passaging reagent (STEMCELL Technologies, Vancouver, BC, Canada).

To generate embryonic bodies, the confluent cultures were dissociated into small cluster suspension by incubation with accutase (Innovative Cell Technologies, Inc., San Diego, CA, United States). Cells were counted and each well of six-well low-adherence plates (Corning, NY, United States) were seeded with 5.5×10^6 cells in 5.5 ml Essential 8 Flex Medium supplemented with 10 ng/ml Activin A protein (Activin A, R&D Systems, MN, United States) and 10 ng/ml heregulin-beta-1 (PeproTech, NJ, United States). Plates were placed on an orbital shaker at 100 rpm to induce embryonic bodies.

To generate islet organoids, cell differentiation underwent five stages (21 days) was performed as described before (Russ et al., 2015). Briefly, to initiate differentiation, embryonic body was suspended into a low-adherence six-well plate in 5.5 ml d1 media [RPMI (Gibco) containing 0.2% FBS, 1:5,000 insulin-transferrin-selenium (ITS) supplement (Gibco), 100 ng/ml activin A, and



50 ng/ml WNT3a (R&D Systems)]. Media thereafter were changed daily, by removing either 4.5 ml media (at the end of d1) or 5.5 ml media the following days and adding back 5.5 ml fresh media until day 9. After day 9, only 5 ml of media was removed and added daily (Russ et al., 2015). Media in this differentiation protocol consist of the following: d2: RPMI containing 0.2% FBS, 1:2,000 ITS, and 100 ng/ml activin A; d3: RPMI containing 0.2% FBS, 1:1,000 ITS, 2.5 μ M TGF-beta Inhibitor IV (Calbiochem, MA, United States), and 25 ng/ml KGF (R&D Systems); d4–5: RPMI containing 0.4% FBS, 1:1,000 ITS, and 25 ng/ml KGF; d6–7: DMEM (Gibco) with 25 mM glucose containing 1:100 B27 (Gibco), 3 nM TTNBP (Sigma); d8: DMEM with 25 mM glucose containing 1:100 B27, 3 nM TTNBP, and 50 ng/ml EGF (R&D Systems); d9: DMEM with 25 mM glucose containing 1:100 B27, 50 ng/ml EGF, and 50 ng/ml KGF; d10–14: DMEM with 25 mM glucose containing 1:100 B27, 500 nM LDN–193189 (Stemgent, MD), 30 nM TPB (Millipore Sigma, MA, United States), 1,000 nM ALKi II (Axxora), and 25 ng/ml KGF; and d15–21: DMEM with 2.8 mM glucose containing 1:100 Glutamax (Gibco) and 1:100 non-essential amino acids solution (Gibco) (Russ et al., 2015).

Immunofluorescence Confocal Microscopy Imaging

Human islet organoids were transferred to microcentrifuge tubes (Eppendorf) using a cut 1000- μ L pipette tip to avoid disruption to the islet organoids and fixed in 4% paraformaldehyde solution for 15 min at room temperature. Fixation was followed by three washes in PBS and incubation in blocking solution (10% goat normal serum in PBS) on a thermal mixer (Thermo Scientific) at 300 RPM at 4°C overnight. Islet organoids were then incubated with anti-insulin primary antibody (Abcam, Cambridge, MA, United States) and anti-glucagon antibody (Abcam, Cambridge, MA, United States) in Antibody Solution

(10% goat normal serum and 0.5% bovine serum albumin in PBS) on a thermal mixer at 300 RPM at 4°C for 24 h. Primary antibody exposure was followed by three washes in PBS and incubation with FITC-labeled goat anti-mouse secondary IgG (Abcam, Cambridge, MA, United States) and Texas red conjugated goat anti-rabbit secondary IgG (Santa Cruz Biotechnology, Santa Cruz, CA, United States) in Antibody Solution on a thermal mixer at 300 RPM at room temperature for 1 h in the dark. The stained islet organoids were washed three times in PBS before being mounted on glass microscope slides (Fisher Scientific) using mounting medium containing DAPI (Vectashield; Vector Laboratories). Ninety micrometers Polybead Microspheres (Polysciences, Inc.) were placed between the slide and the coverslip (No. 1.5) to preserve some of the 3D structure of the organoids while accommodating the penetration capacity of the confocal microscope. Samples were imaged using an Olympus FluoView 1000 Filter-based laser scanning confocal microscope. Immunofluorescence images of islet organoids were semi-quantitatively analyzed using Fiji.¹ Briefly multi-color fluorescent images were split into single channels and converted to grayscale images. The area of interests was selected using selection tools in Fiji. The insulin and glucagon positive cells percentages of islet organoids were calculated.

Glucose-Stimulated Insulin Secretion Assay

One Hundred islet organoids (between 28 and 30 days of differentiation) were pre-incubated in 1 ml of low (2.8 mM) glucose Krebs buffer (KRB) and washed twice with KRB to remove residual insulin, then islet organoids were incubated in 1 ml of 2.8 mM glucose KRB for 30 min in a 37°C cell culture incubator, and the supernatant was collected. After they were

¹<https://imagej.net/Fiji>

washed twice with 2.8 mM glucose KRB, the islet organoids were incubated in 1 ml of high (28 mM) glucose Krebs buffer for 30 min, and the supernatant was collected. Human insulin was measured using the Insulin Human ELISA kit (Abcam, ab100578). Human insulin measurements were normalized by cell counts that were acquired by dispersing islet organoids into single cells with Accutase (Innovative Cell Technologies, Inc.) and counted using a cell counter.

Cell Labeling and *in vitro* Characterization of Labeled Cells

Islet organoids were feed with the concentration of 560 µg/ml VivoTrax (Magnetic Insight Inc., Alameda, CA, United States) in CMRL media with 5% FBS and incubated for 48 h at 37°C with 5% CO₂ (Wang et al., 2018; Hayat et al., 2020). VivoTrax is a dextran coated SPION with core size of 4.2 nm and a mean hydrodynamic diameter of 62 nm. Cell labeling efficiency was tested using immunofluorescence staining for dextran coating with anti-dextran antibody (STEMCELL Technologies, Vancouver, BC, Canada), followed by an FITC-labeled goat anti-mouse secondary IgG (Abcam, Cambridge, MA, United States), mounted with a mounting medium containing DAPI and analyzed using fluorescence microscopy. Islet organoids viability was tested after labeling by colorimetric [3-(4,5-dimethylthiazol-2-yl)-2,5-diphenyltetrazolium bromide] assay according to the manufacturer's protocol (Promega, Madison, WI, United States) (Wang et al., 2011, 2012).

Cell function of secreted C-peptide was also tested using immunofluorescence staining with anti-C-peptide primary antibody (Abcam, Cambridge, MA, United States) and anti-dextran antibody (STEMCELL Technologies, Vancouver, BC, Canada), followed by an FITC-labeled goat anti-mouse secondary IgG (Abcam, Cambridge, MA, United States) and Texas red conjugated goat anti-rabbit secondary IgG (Santa Cruz Biotechnology, Santa Cruz, CA, United States).

Imaging of Islet Organoid Phantoms

In vitro phantoms comprising of different numbers of VivoTrax labeled islet organoids (0, 25, 50, 100, 200, and 400) in PBS were imaged using an MPI scanner (MOMENTUM MPI, Magnetic Insight Inc., Alameda, CA, United States) with the fiducial markers. Each 2D MPI images were acquired with parameters of a field-of-view (FOV) of 6 cm × 12 cm, a 5.7 T/m selection field gradient, a drive field strength of 20 mT peak amplitude and a 45.0 kHz drive frequency. Images were reconstructed using x-space reconstruction. Quantification of the islet organoids phantoms was performed using the 2D MPI image intensity calibrated against a fiducial marker of known iron content (2.2 µg of iron) using VivoQuant imaging software (Invicro, Boston, MA, United States).

Inductively Coupled Plasma Optical Emission Spectroscopy

Iron content of labeled islet organoids were determined using inductively coupled plasma optical emission spectroscopy (ICP-OES). Different numbers of labeled islet organoids were digested

with concentrated nitric acid (Sigma-Aldrich, St. Louis, MO, United States). Digested samples were diluted and the total iron content of the samples were determined using an Agilent 710-ES ICP-OES (Agilent Technologies, Santa Clara, CA, United States). For the measurement of the iron content with ICP-OES, a calibration line was generated by six standard samples containing 0, 0.125, 0.25, 0.5, 1, 2, 3, and 4 ppm Fe. All iron standards were prepared from a stock certified standard reference material (FeCl₃, Iron Standard for ICP, 1000 ± 2 mg/l Fe in 2% nitric acid, Sigma-Aldrich, St. Louis, MO, United States). An eight-point calibration curve was performed prior to sample analysis. The total iron content of samples was calculated, accounting for the number of islet organoids provided as well as dilution factors, as the mean value for analysis.

Cell Transplantation Under Kidney Capsule in a Mouse Model

All animal experiments were performed in compliance with institutional guidelines and were approved by the Institutional Animal Care and Use Committee (IACUC) at the Michigan State University. Labeled islet organoids were collected 1 h before transplantation. Female NOD/scid immunodeficient mice ($n = 5$, 10 weeks old, Jackson Laboratory, Bar Harbor, ME, United States) were anesthetized with 2% isoflurane. An incision made to expose the left kidney of the mouse, a catheter needle inserted underneath the kidney capsule and 800 islet organoids VivoTrax labeled were transplanted. Then the incision was closed, mice were monitored after transplantation.

MPI Tracking of Transplanted Islet Organoids Under Kidney Capsule of Mice

Under anesthesia with 2% isoflurane, mice were imaged using 3D MPI at 1, 7, and 28-day post-transplantation ($n = 3$) with operating parameters, a FOV of 6 cm × 6 cm × 12 cm, acquisition time of 10 s per projection (total 55 projections) plus 30 s for automatic set up of the magnets, with an approximate total time of 35 min including for image reconstruction. Anatomic CT reference images were acquired by the whole-body model of Perkin Elmer QuantumGX microCT. MPI images were co-registered to CT with fiducial markers using VivoQuant Imaging Software (Invicro, Boston, MA, United States). Control animals did not receive islet organoids ($n = 2$).

3D *K-means++* Unsupervised Machine Learning Algorithm

In order to segment the ROI from the MPI, we used the previously established *k-means++* algorithm for ROI segmentation and a standard curve model for prediction of the TIV of the cells (Hayat et al., 2020). This TIV correlates linearly to increasing ROI intensity and size (Hayat et al., 2020). Hence, here we apply the *k-means++* algorithm to a 3D MPI Image sequence through layer-by-layer segmentation of the individual ROIs and TIV estimations from 32 to 36 layers per scan, and these values are summed to provide a TIV for the entire 3D structure. As determined in our previous study by the elbow method, the *k*-value for number of centroids in this study

was 4 (Hayat et al., 2020). The concentrations of the fiducial markers (1 μ l) used to generate the standard curve were 10, 20, and 40% of VivoTrax solution (5.5 mg/ml iron). For all MPI image scans, placement of fiducial markers was kept in the same location in order to provide optimal data for *k-means++* segmentation of the ROI and subsequent TIV estimation *via* the generated standard curve.

Intraclass Correlation Coefficient Validation

In order to measure accuracy of the algorithm and determine its validity, its TIV prediction was compared to that of a manual rater, in this case a board-certified radiologist. The rater segmented the ROI manually on 15 images using the VivoQuant Imaging Software (Invicro, Boston, MA, United States), and total pixel sum values were extracted for TIV analysis from the ROIs using a ratio method with reference to a singular fiducial marker for TIV prediction (Makela et al., 2020), calibrated against a 40% fiducial marker of known iron concentration (2.2 μ g of iron). For statistical analysis, SPSS statistical software (IBM, Armonk, NY, United States) was used to calculate intraclass correlation coefficient (ICC), which provides a measure of the inter-rater reliability between the rater and algorithm. A two-way mixed model with a confidence interval of 95% was selected, and a measure of absolute agreement was calculated with the ICC. A higher ICC score indicates greater reliability of algorithm performance due to the high degree of agreement between the rater and algorithm.

Ex vivo Immunohistochemistry

After the last round of MPI, animals were sacrificed and left kidneys were removed, fixed in 4% paraformaldehyde solution for 16 h at 4°C, and embedded in paraffin. Paraffin sections of grafts under the left kidney capsule were incubated with anti-C-peptide primary antibody (Abcam, Cambridge, MA, United States) and anti-dextran antibody (STEMCELL Technologies, Vancouver, BC, Canada) at 4°C for 16 h, followed by an FITC-labeled goat anti-mouse secondary IgG (Abcam, Cambridge, MA, United States) and Texas red conjugated goat anti-rabbit secondary IgG (1:100 dilution, Santa Cruz Biotechnology, Santa Cruz, CA, United States) at room temperature for 1 h. All sections were mounted with a mounting medium containing DAPI (Vectashield; Vector Laboratories) and analyzed using fluorescence microscopy (Eclipse 50i; Nikon Metrology, Brighton, MI, United States) (Pomposelli et al., 2020; Wang et al., 2020).

Statistical Analysis

Data are presented as mean \pm SD. Statistical comparisons between two groups were evaluated by Student *t*-test and corrected by one-way ANOVA for multiple comparisons using GraphPad Prism 5 (GraphPad Software, Inc., La Jolla, CA, United States). A two-way repeated measures ANOVA was performed for evaluating TIV predictions as the independent variable for different imaging days. Correlation and linear regression analysis between measured iron content in the

phantoms and the number of labeled islets was assessed using GraphPad Prism 5 and SPSS statistical software (IBM, Armonk, NY, United States) as well. A value of $p < 0.05$ was considered to be statistically significant.

RESULTS

Characterization of Differentiated Islet Organoids

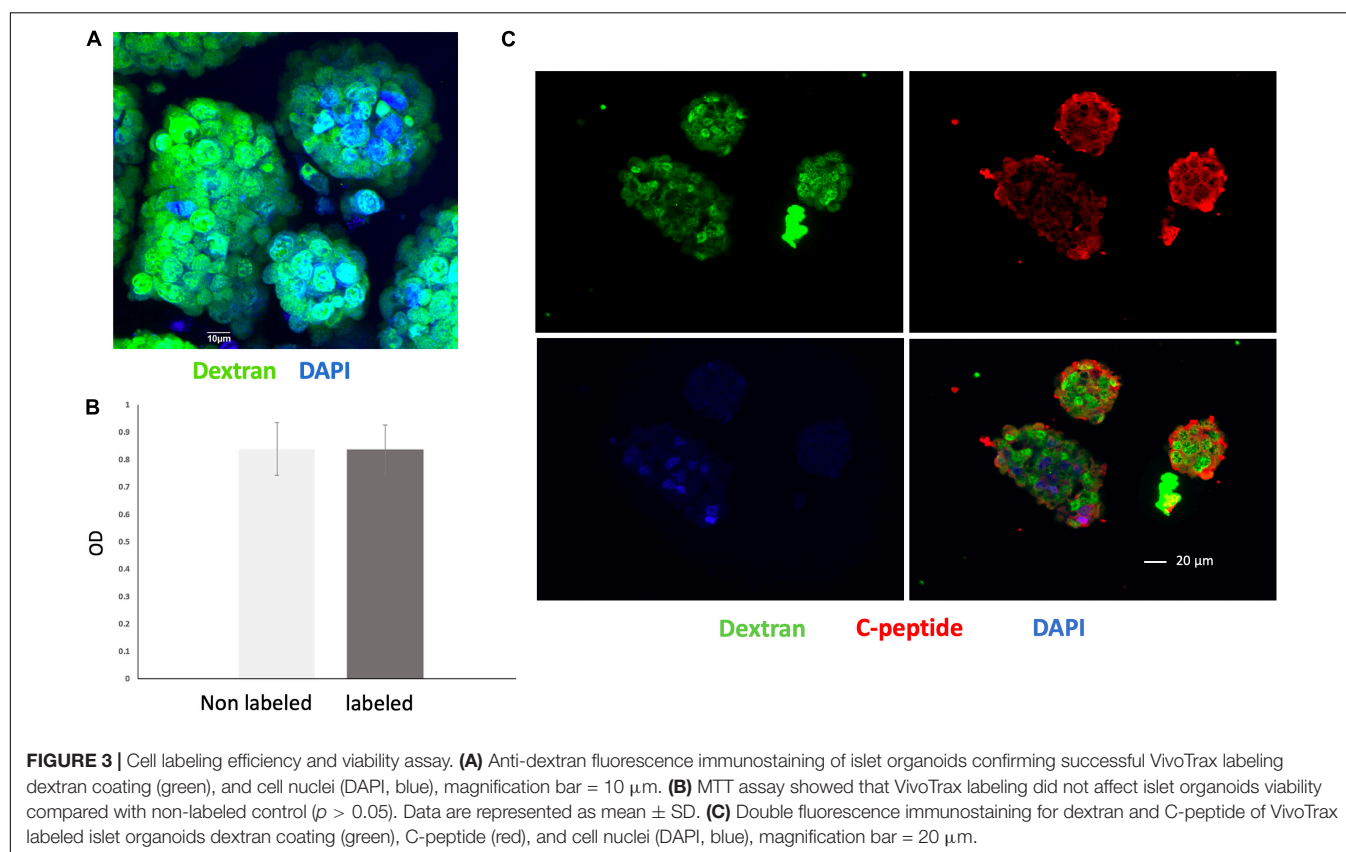
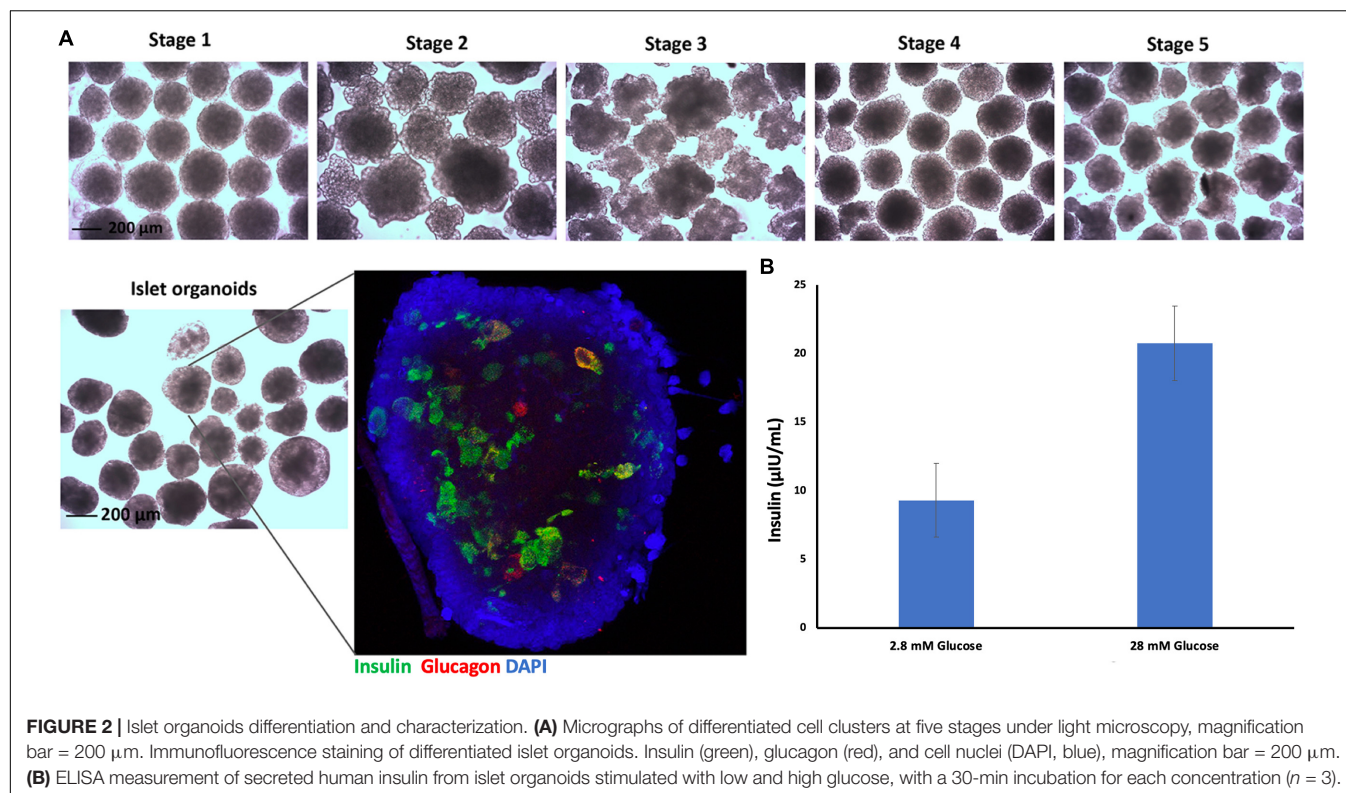
Embryoid bodies derived from hiPSC-L1 cells were produced in 3D-suspension culture to generate pancreatic islet organoids using already described protocols. After 21 days differentiated islet organoids were stained for immunofluorescence and confocal imaging to determine expression of insulin ($24 \pm 4\%$) and glucagon ($9 \pm 3\%$) in the differentiated islet organoids (Figure 2A and Supplementary Video 1). Functional test glucose-stimulated insulin secretion (GSIS) assay demonstrated the differentiated islet organoids reacted to glucose stimulation and secrete human insulin (Figure 2B). We further analyzed the expression of hormone genes in islet organoids including insulin and glucagon. Quantitative RT-PCR analysis showed high levels of insulin and glucagon gene transcripts in stage 5 cell clusters and islet organoids (Supplementary Figure 1), which was consistent with the immunofluorescence analysis.

Assessment of Labeling Efficacy and Viability of VivoTrax Labeled Islet Organoids

Nearly all of the cells within the islet organoids were labeled with VivoTrax as confirmed by anti-dextran antibody staining (Figure 3A). MTT assay showed that compared with non-labeled islet organoids, VivoTrax labeling treatment did not have significant effect on islet organoid viability (Figure 3B; $p > 0.05$). Double stained islet organoids with C-peptide (in green) and dextran showed that the VivoTrax labeled islet organoids expressed C-peptide, which demonstrated the labeling treatment did not affect insulin biosynthesis in differentiated islet organoids (Figure 3C).

Imaging of Islet Organoids Phantoms *in vitro*

In vitro MPI showed the signal intensity of phantoms increased with increasing number of islet organoids (Figure 4A). The iron content was inferred from the MPI signal by quantitative analysis of the hand-drawn ROIs of MPI intensity using VivoQuant, calibrated against a 40% fiducial marker of known iron content (2.2 μ g of iron). A linear correlation was revealed between the number of islet organoids and the MPI signal ($R^2 = 0.997$, $p < 0.0001$) (Figure 4B). In equivalent control cell populations without VivoTrax labeling, no MPI signal was detected. Likewise, ICP-OES results showed that a linear correlation was found between the number of islet organoids and the iron content ($R^2 = 0.977$, $p < 0.0001$) (Figure 4B), further confirmed the MPI quantification results.



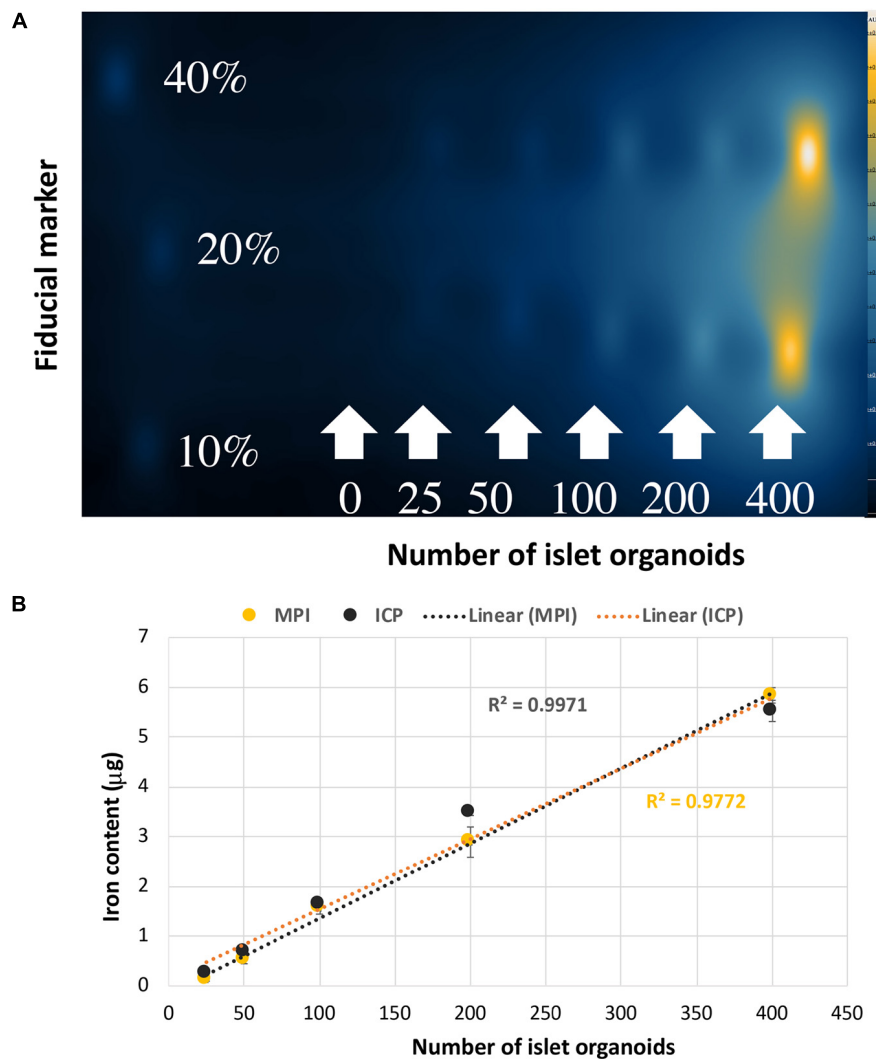


FIGURE 4 | Islet organoids phantoms imaging and iron content quantification. **(A)** MPI of the different number of SPIO labeling islet organoids phantom. **(B)** Iron content of the islet organoids phantoms measured by MPI ($R^2 = 0.9971$) and ICP-OES ($R^2 = 0.9772$) both correlated with the number of labeled islet organoids. Data are represented as mean \pm SD.

In vivo MPI K-means++ Algorithm Analysis and ICC Validation

Strong MPI signals representing labeled islet organoids were detected under the left kidney capsule from 3D images on the first day post-transplantation in all recipients (**Figure 5A** and **Supplementary Video 2**). *K-means++* algorithm was applied for the 3D segmentations and TIV estimations on the ROIs from *in vivo* MPI (**Figure 5B**). Since MPI signal is not detectable in the absence of iron oxide nanoparticles, we did not observe any signal in control animals that did not receive the labeled graft (**Supplementary Video 3**).

3D MPI were followed up at 7, and 28-day post-transplantation for these recipient mice (**Figure 6A**). **Figure 6B** depicts the output results from the single *k-means++* segmentation of the ROI from longitudinal MPI scans of mice which received islet organoid transplants. **Figure 6C** and

Supplementary Video 4 showed the 3D output of the signal *k-means++* segmentation of the ROIs from an MPI scan of a recipient mouse. As is evidenced by the eventual loss of iron over the course of 28 days, which is visible both visually and through quantification *via* TIV estimation, the algorithm is able to trace the necessary ROI from the MPI image scans of mice and predict the TIVs which portray a linear trend in correlation with increasing total pixel sum of the ROI (**Figure 6D**, $p < 0.05$). An initial increase was observed in the MPI ROI size from day 1 to 7, with a decrease in overall ROI size by day 28 (**Figures 6D,E**, $p < 0.05$). Statistical evaluation *via* two-way repeated measures ANNOVA indicated significant difference between the predicted TIV from different days. These findings are reflected in the TIV prediction of the mice from different days in which there is an increase in TIV (and ROI size) from day 1 to 7 followed by a decrease from day 7 to 28. These results were fortified by ICC

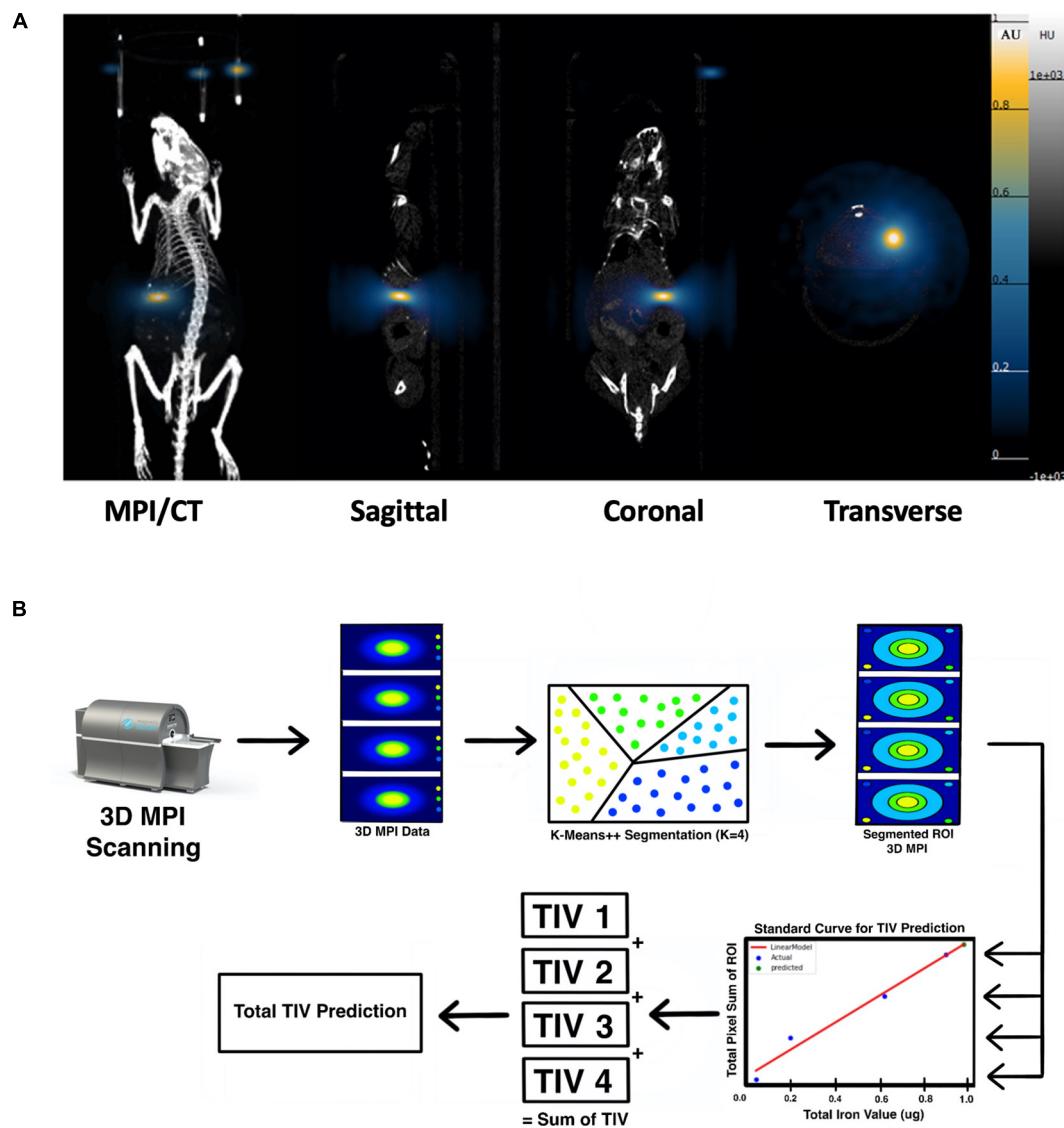


FIGURE 5 | (A) 3D reconstructed MPI co-registered with microCT imaging of VivoTrax labeled islet organoids under the left kidney capsule of mouse on day 1 post-transplantation, all animals were placed in the prone position for both MPI and CT scanning. **(B)** Overview of the *K-means++* algorithm for segmentation and TIV prediction.

validation of the algorithm's performance in comparison to a board-certified imaging specialist. A near-excellent and excellent ICC score of 0.898 and 0.927 for single and average measures, respectively, was determined through ICC validation (Table 1, $p < 0.05$). This indicated a high degree of agreement between TIV prediction of the algorithm and the imaging specialist.

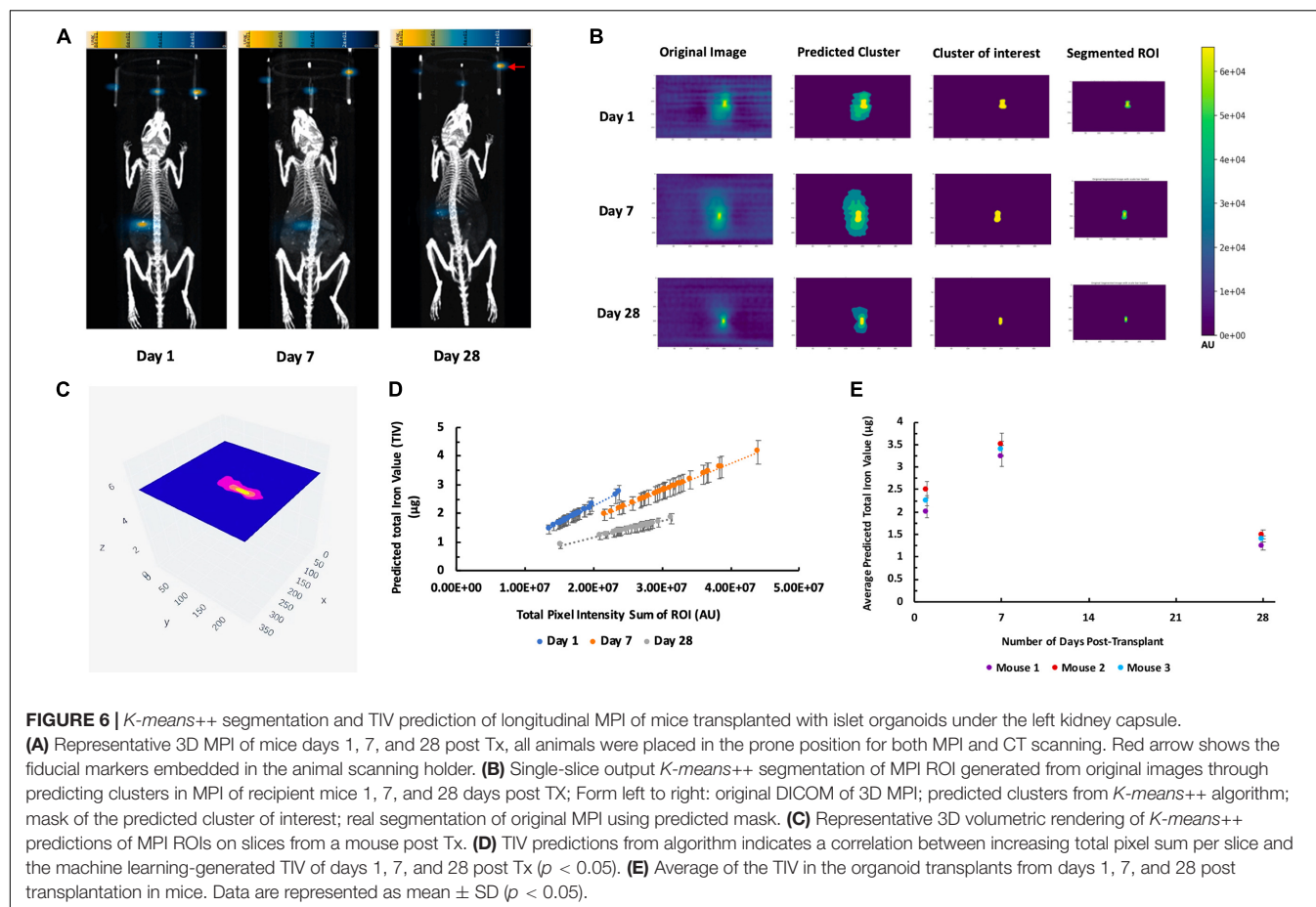
Ex vivo Immunohistochemistry

Immunofluorescence staining of the left kidney sections showed the presence of islet organoid grafts as confirmed by double staining for dextran and C-peptide 1-week post transplantation (Figure 7). Dextran expression was visible in these graft cells, which indicated that VivoTrax were retained in these transplanted cells (Figure 7). With the double immunostaining,

these graft cells also expressed C-peptide, which demonstrated insulin biosynthesis in the graft organoids (Figure 7). This *ex vivo* data, consistent with *in vivo* MPI results, attest to the feasibility of labeling islet organoids using SPIONs and monitoring these functional islet organoids by MPI after transplantation.

DISCUSSION

Stem cell replacement therapy is a promising approach for the treatment of T1D. Studies demonstrated that hiPSC can become an unlimited, relatively safe (autologous-derived cells, thus devoid of rejection risk), and an efficient alternative source to generate insulin-producing islet organoids



(Soejitno and Prayudi, 2011; Li et al., 2014; Maxwell et al., 2020). Methods to track islet organoids outcome after transplantation, however, are needed. MPI is an emerging tomographic technique that directly detects iron oxide nanoparticle tracers. These tracers are safe, non-toxic tracer, biocompatible and not normally found in the body, thus MPI images have exceptional contrast and high sensitivity. MPI imaging of these tracers provided an approach to track islet organoids and longitudinally monitor islet organoids *in vivo*. In this study, we successfully differentiated hiPSC-L1 into islet organoids and labeled islet organoids with SPIONs. Labeled islet organoids were highly effective at accumulation of SPIONs, immunostaining demonstrated nearly all of the cells within the islet organoids were labeled with SPIONs. MPI has

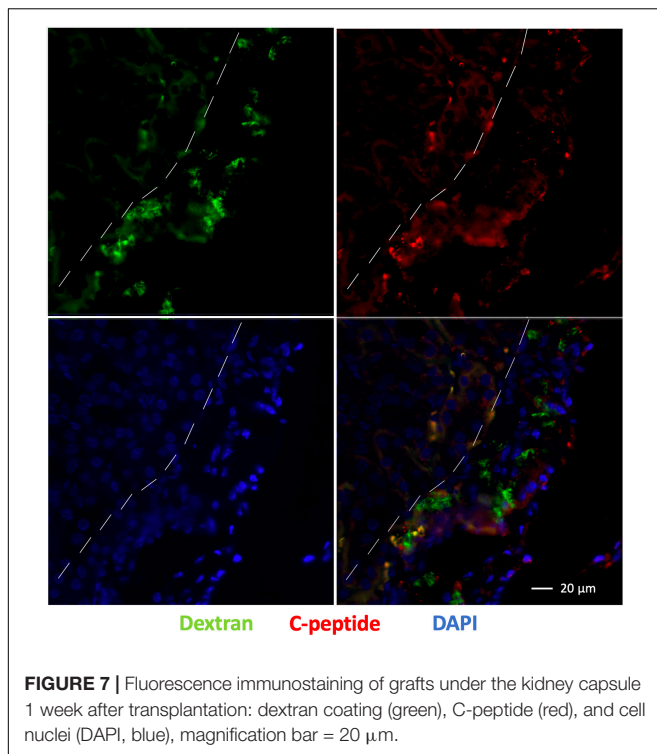
a detection sensitivity of as few as 25 islet organoids *in vitro*. The quantification demonstrates a linear correlation between MPI signal intensity and the number of labeled islet organoids. We further found that the estimated iron content from the MPI image was consistent with the iron content measured by ICP. This demonstrates that MPI is able to quantify SPIONs-labeled islet organoids *in vitro*, which provides evidence that MPI may be able to track and quantify islet organoids *in vivo*. We used 800 labeled islet organoids per transplant to establish the feasibility of MPI detection *in vivo*. MPI 3D images with a co-registered CT show strong signals were detected under the left kidney capsule on the first day in all recipients that represented labeled islet organoids.

TABLE 1 | Intraclass correlation coefficient (ICC) validation of ROI segmentation and TIV prediction of the *K-means++* based algorithm in comparison to an imaging specialist.

Type	Interclass correlation	95% Confidence interval: lower bound	95% Confidence interval: upper bound	F-test with true value 0: df	F-test with true value 0: sig.
Single measures	0.898	0.621	0.979	14	0.001
Average measures	0.927	0.546	0.973	14	0.001

Top row: data for single measures.

Bottom row: data for average measures.



To monitor reproducibly the transplanted islet organoids longitudinally and analyze the ROIs from the MPI scans of mice, the canonical unsupervised ML algorithm of *k-means++* was employed in conjunction with a linear regression based standard curve model. This algorithm is different from that which we applied previously to 2D MPI scans of transplanted islets, because it applies the algorithm to multiple layers of a 3D MPI scan (Hayat et al., 2020). This signal is indicative of the current nanoparticle content inside the mice which is evidence of the islet organoid cell content at the time of MPI scanning. Through segmentation and TIV prediction on the MPI data of the mice from days 1, 7, and 28, the algorithm was able to monitor the transplanted islet organoids longitudinally with indications on total iron content within subjects in a 3D manner.

The reasons why we chose VivoTrax for this study was because this tracer has been widely used for MPI. There are other SPIONs available, Feraheme (ferumoxytol) is another SPIONs product that is clinically used for iron anemia/deficiency and may have potential for MPI, although likely with less sensitivity due to its smaller size (Bulte, 2019). It was unexpected that there would be an increase in TIV (and ROI size) of the labeled transplants from day 1 to 7. The possible explanations for this finding include environmental induced degradation of the dextran coating of the VivoTrax, which may increase the total signal intensity, decreasing the peak signal intensity. Dynamic light scattering (DLS) studies have demonstrated that an increase in the nanoparticle size of degraded VivoTrax from 75 to 330 nm, which suggests the removal of the dextran coating resulted aggregation of the nanocrystal core *in vitro* (Guzy et al., 2020). Another factor that may contribute to this signal increase

could be cell division triggered aggregation and releasing of the iron oxides nanostructure from encapsulated VivoTrax in the proliferating stem cell differentiated islet organoids. Possible explanation for the increase in TIV and ROI size might also be in relation with restructuration of the graft upon transplantation: the cell cluster break down and migrate to occupy the space under the kidney capsule, allowing vascularization and innervation of the grafts. Davalli et al. (1996) investigated syngeneic islets transplantation under the kidney capsule in a murine model. Grafts were harvested 1, 3, 7, and 14 days after transplantation and analyzed for morphology and insulin content. Their results showed that substantial damage in islet grafts was found on days 1 and 3 with apoptotic nuclei and necrotic cores; Tissue remodeling occurred with stable graft appearance on day 14; Graft insulin content decreased on day 1 and fell even further on days 3 and 7. We do agree that there are differences between *in vivo* imaging and histological evaluations, hence, we want to emphasize this is the first study on MPI of stem cell differentiated islet organoids transplantation, which is similar but still different from islet transplantation. In addition, measurement of labeled islet organoids in our study relies on imaging of the aforementioned nanoparticles, whereas Davalli et al. (1996) evaluated and quantified graft loss based on factors such as *ex vivo* morphology and insulin content/mRNA expression. This initial observation, irrespective of underlying mechanism, demonstrates the power of our data analysis algorithm for *in vivo* MPI.

Our method faces limitations as it cannot be applied to MPI scans that do not have the reference fiducial markers in the proper spatial orientation. Furthermore, it only takes into account three concentrations of fiducial markers in order to generate the standard curve with which the TIV is predicted. Future studies involving deep learning can potentially resolve these limitations by training on known TIV of diverse phantoms and their associated ICP values in order to predict the unknown TIV of a new ROI (Hayat and Wang, 2020). Nonetheless, the current algorithm provides a standardized, automated method for TIV analysis of transplanted organoids *in vivo*. This has implications for future studies in which the therapeutic effect of the transplanted islet organoids can be observed in diabetic mice, and such ML algorithms will be employed to accurately monitor the labeled iron signals from the organoid cell clusters longitudinally. This also has other implications in applying AI to monitor different cell-based therapies such as pancreatic islet transplantation, chimeric antigen receptor (CAR), T-Cell therapy, and other cellular approaches to treating diseases.

CONCLUSION

In this study, we demonstrated the feasibility of longitudinal *in vivo* tracking and quantifying implanted islet organoids grafts for 28 days using MPI and ML algorithm. We believe that MPI could play an important role in monitoring the grafts, by directly imaging of the graft itself. In future studies, we plan to transplant islet organoids in a diabetic mouse model and verify and improve the *K-mean++* algorithm for unbiased quantification of *in vivo* MPI.

DATA AVAILABILITY STATEMENT

The original contributions presented in the study are included in the article/**Supplementary Material**, further inquiries can be directed to the corresponding author/s.

ETHICS STATEMENT

The animal study was reviewed and approved by Institutional Animal Care and Use Committee (IACUC) at the Michigan State University.

AUTHOR CONTRIBUTIONS

AS, HH, SL, JB, BD, MG, NT, and JD researched the data. HH and AS led the data analysis. ET, JB, BD, MG, and JG participated in data analysis. AS, HH, WL, AAL, and AAG participated in drafting the manuscript. PW conceived the idea, designed the study, drafted the manuscript and is the guarantor of this work and, as such, had full access to all the data in the study and take responsibility for the integrity of the data and the accuracy of the data analysis. All authors contributed to the article and approved the submitted version.

REFERENCES

- Bulte, J. W., Walczak, P., Gleich, B., Weizenecker, J., Markov, D. E., Aerts, H. C., et al. (2011). MPI Cell Tracking: what Can We Learn from MRI? *Proc. SPIE Int. Soc. Opt. Eng.* 7965:79650z. doi: 10.1117/12.879844
- Bulte, J. W. M. (2019). Superparamagnetic iron oxides as MPI tracers: a primer and review of early applications. *Adv. Drug Deliv. Rev.* 138, 293–301. doi: 10.1016/j.addr.2018.12.007
- Bulte, J. W. M., and Daldrup-Link, H. E. (2018). Clinical Tracking of Cell Transfer and Cell Transplantation: trials and Tribulations. *Radiology* 289, 604–615. doi: 10.1148/radiol.2018180449
- Crabbe, A., Vandeputte, C., Dresselaers, T., Sacido, A. A., Verdugo, J. M., Eyckmans, J., et al. (2010). Effects of MRI contrast agents on the stem cell phenotype. *Cell Transplant* 19, 919–936. doi: 10.3727/096368910X494623
- Davalli, A. M., Scaglia, L., Zangen, D. H., Hollister, J., Bonner-Weir, S., and Weir, G. C. (1996). Vulnerability of islets in the immediate posttransplantation period: Dynamic changes in structure and function. *Diabetes* 45, 1161–1167. doi: 10.2337/diab.45.9.1161
- Guzy, J., Chakravarty, S., Buchanan, F., Chen, H., Gaudet, J., Hix, J., et al. (2020). Complex Relationship between Iron Oxide Nanoparticle Degradation and the Signal Intensity in Magnetic Particle Imaging. *ACS Appl. Nano Mater.* 3, 3991–3999. doi: 10.1021/acsanm.0c00779
- Hayat, H., Sun, A., Hayat, H., Liu, S., Talebloo, N., Pinger, C., et al. (2020). Artificial Intelligence Analysis of Magnetic Particle Imaging for Islet Transplantation in a Mouse Model. *Mol. Imaging Biol.* 23, 18–29. doi: 10.1007/s11307-020-01533-5
- Hayat, H., and Wang, P. (2020). The application of artificial intelligence in biomedical imaging. *Am. J. Biomed. Sci. Res.* 8, 228–231. doi: 10.34297/ajbsr.2020.08.001279
- Janowski, M., Walczak, P., Kropiwnicki, T., Jurkiewicz, E., Domanska-Janik, K., Bulte, J. W., et al. (2014). Long-term MRI cell tracking after intraventricular delivery in a patient with global cerebral ischemia and prospects for magnetic navigation of stem cells within the CSF. *PLoS One* 9:e97631. doi: 10.1371/journal.pone.0097631
- Khandhar, A. P., Keselman, P., Kemp, S. J., Ferguson, R. M., Goodwill, P. W., Conolly, S. M., et al. (2017). Evaluation of PEG-coated iron oxide nanoparticles

FUNDING

The project was partly funded by the 1R03EB028349 from NIH/NIBIB to PW.

ACKNOWLEDGMENTS

We would like to thank L. Karl Olson (Department of Physiology, College of Natural Science, Michigan State University), Ripla Arora (The Institute for Quantitative Health Science and Engineering, Department of Obstetrics, Gynecology and Reproductive Biology, College of Human Medicine, Michigan State University), Christopher H. Contag (The Institute for Quantitative Health Science and Engineering, Department of Biomedical Engineering, College of Engineering, Michigan State University), and Anna Moore (Precision Health Program, Michigan State University) for their great discussions and support.

SUPPLEMENTARY MATERIAL

The Supplementary Material for this article can be found online at: <https://www.frontiersin.org/articles/10.3389/fcell.2021.704483/full#supplementary-material>

- as blood pool tracers for preclinical magnetic particle imaging. *Nanoscale* 9, 1299–1306. doi: 10.1039/c6nr08468k
- Li, J., Song, W., Pan, G., and Zhou, J. (2014). Advances in understanding the cell types and approaches used for generating induced pluripotent stem cells. *J. Hematol. Oncol.* 7:50. doi: 10.1186/s13045-014-0050-z
- Magnitsky, S., Zhang, J., Idiyatullin, D., Mohan, G., Garwood, M., Lane, N. E., et al. (2017). Positive contrast from cells labeled with iron oxide nanoparticles: quantitation of imaging data. *Magn. Reson. Med.* 78, 1900–1910. doi: 10.1002/mrm.26585
- Makela, A. V., Gaudet, J. M., Schott, M. A., Sehl, O. C., Contag, C. H., and Foster, P. J. (2020). Magnetic Particle Imaging of Macrophages Associated with Cancer: filling the Voids Left by Iron-Based Magnetic Resonance Imaging. *Mol. Imaging Biol.* 22, 958–968. doi: 10.1007/s11307-020-01473-0
- Maxwell, K. G., Augsornworawat, P., Velazco-Cruz, L., Kim, M. H., Asada, R., Hogrebe, N. J., et al. (2020). Gene-edited human stem cell-derived beta cells from a patient with monogenic diabetes reverse preexisting diabetes in mice. *Sci. Transl. Med.* 12, eaax9106. doi: 10.1126/scitranslmed.aax9106
- Pomposelli, T., Wang, P., Takeuchi, K., Miyake, K., Ariyoshi, Y., Watanabe, H., et al. (2020). Protection of Pancreatic Islets Using Theranostic Silencing Nanoparticles in a Baboon Model of Islet Transplantation. *Diabetes* 69, 2414–2422. doi: 10.2337/db20-0517
- Rizzo, S., Petrella, F., Politi, L. S., and Wang, P. (2017). Molecular Imaging of Stems Cells: in Vivo Tracking and Clinical Translation. *Stem Cells Int.* 2017:1783841. doi: 10.1155/2017/1783841
- Russ, H. A., Parent, A. V., Ringler, J. J., Hennings, T. G., Nair, G. G., Shveygert, M., et al. (2015). Controlled induction of human pancreatic progenitors produces functional beta-like cells in vitro. *EMBO J.* 34, 1759–1772. doi: 10.15252/embj.201591058
- Soejitno, A., and Prayudi, P. K. (2011). The prospect of induced pluripotent stem cells for diabetes mellitus treatment. *Ther. Adv. Endocrinol. Metab.* 2, 197–210. doi: 10.1177/2042018811420198
- Talebloo, N., Gudi, M., Robertson, N., and Wang, P. (2020). Magnetic Particle Imaging: current Applications in Biomedical Research. *J. Magn. Reson. Imaging* 51, 1659–1668. doi: 10.1002/jmri.26875

- Wang, L., Song, Y., Parikh, A., Joyce, P., Chung, R., Liu, L., et al. (2019). Doxorubicin-Loaded Delta Inulin Conjugates for Controlled and Targeted Drug Delivery: development, Characterization, and In Vitro Evaluation. *Pharmaceutics* 11:581. doi: 10.3390/pharmaceutics11110581
- Wang, P., and Aguirre, A. (2018). New Strategies and In Vivo Monitoring Methods for Stem Cell-Based Anticancer Therapies. *Stem Cells Int.* 2018:7315218. doi: 10.1155/2018/7315218
- Wang, P., Goodwill, P. W., Pandit, P., Gaudet, J., Ross, A., Wang, J., et al. (2018). Magnetic particle imaging of islet transplantation in the liver and under the kidney capsule in mouse models. *Quant. Imaging Med. Surg.* 8, 114–122. doi: 10.21037/qims.2018.02.06
- Wang, P., Liu, Q., Zhao, H., Bishop, J. O., Zhou, G., Olson, L. K., et al. (2020). miR-216a-targeting theranostic nanoparticles promote proliferation of insulin-secreting cells in type 1 diabetes animal model. *Sci. Rep.* 10:5302. doi: 10.1038/s41598-020-62269-4
- Wang, P., and Moore, A. (2012). Molecular imaging of stem cell transplantation for neurodegenerative diseases. *Curr. Pharm. Des.* 18, 4426–4440. doi: 10.2174/138161212802481255
- Wang, P., Yigit, M. V., Medarova, Z., Wei, L., Dai, G., Schuetz, C., et al. (2011). Combined small interfering RNA therapy and in vivo magnetic resonance imaging in islet transplantation. *Diabetes* 60, 565–571. doi: 10.2337/db10-1400
- Wang, P., Yigit, M. V., Ran, C., Ross, A., Wei, L., Dai, G., et al. (2012). A theranostic small interfering RNA nanoprobe protects pancreatic islet grafts from adoptively transferred immune rejection. *Diabetes* 61, 3247–3254. doi: 10.2337/db12-0441
- Wu, L. C., Zhang, Y., Steinberg, G., Qu, H., Huang, S., Cheng, M., et al. (2019). A Review of Magnetic Particle Imaging and Perspectives on Neuroimaging. *AJNR Am. J. Neuroradiol.* 40, 206–212. doi: 10.3174/ajnr.A5896
- Yu, E. Y., Bishop, M., Zheng, B., Ferguson, R. M., Khandhar, A. P., Kemp, S. J., et al. (2017). Magnetic Particle Imaging: a Novel in Vivo Imaging Platform for Cancer Detection. *Nano Lett.* 17, 1648–1654. doi: 10.1021/acs.nanolett.6b04865
- Zheng, B., Vazin, T., Goodwill, P. W., Conway, A., Verma, A., Saritas, E. U., et al. (2015). Magnetic Particle Imaging tracks the long-term fate of in vivo neural cell implants with high image contrast. *Sci. Rep.* 5:14055. doi: 10.1038/srep14055
- Zheng, B., von See, M. P., Yu, E., Gunel, B., Lu, K., Vazin, T., et al. (2016). Quantitative Magnetic Particle Imaging Monitors the Transplantation, Biodistribution, and Clearance of Stem Cells In Vivo. *Theranostics* 6, 291–301. doi: 10.7150/thno.13728

Conflict of Interest: JG was employed by company Magnetic Insight Inc.

The remaining authors declare that the research was conducted in the absence of any commercial or financial relationships that could be construed as a potential conflict of interest.

The reviewer RS declared a shared affiliation with the authors to the handling editor at the time of review.

Publisher's Note: All claims expressed in this article are solely those of the authors and do not necessarily represent those of their affiliated organizations, or those of the publisher, the editors and the reviewers. Any product that may be evaluated in this article, or claim that may be made by its manufacturer, is not guaranteed or endorsed by the publisher.

Copyright © 2021 Sun, Hayat, Liu, Tull, Bishop, Dwan, Gudi, Talebloo, Dizon, Li, Gaudet, Alessio, Aguirre and Wang. This is an open-access article distributed under the terms of the Creative Commons Attribution License (CC BY). The use, distribution or reproduction in other forums is permitted, provided the original author(s) and the copyright owner(s) are credited and that the original publication in this journal is cited, in accordance with accepted academic practice. No use, distribution or reproduction is permitted which does not comply with these terms.



The Development of Ovine Gastric and Intestinal Organoids for Studying Ruminant Host-Pathogen Interactions

David Smith^{1†}, Daniel R. G. Price^{2†}, Alison Burrells¹, Marc N. Faber¹, Katie A. Hildersley^{1,3}, Cosmin Chintoan-Uta⁴, Ambre F. Chapuis^{2,4}, Mark Stevens⁴, Karen Stevenson², Stewart T. G. Burgess², Elisabeth A. Innes¹, Alasdair J. Nisbet² and Tom N. McNeilly¹

OPEN ACCESS

Edited by:

Tiago W. P. Mineo,
Federal University of Uberlandia, Brazil

Reviewed by:

Constance Finney,
University of Calgary, Canada
Camila Coelho,
La Jolla Institute for Immunology (LJI),
United States

*Correspondence:

David Smith
d.smith@moredun.ac.uk

[†]These authors share first authorship

Specialty section:

This article was submitted to
Parasite and Host,
a section of the journal
Frontiers in Cellular and
Infection Microbiology

Received: 30 June 2021

Accepted: 13 August 2021

Published: 08 September 2021

Citation:

Smith D, Price DRG, Burrells A, Faber MN, Hildersley KA, Chintoan-Uta C, Chapuis AF, Stevens M, Stevenson K, Burgess STG, Innes EA, Nisbet AJ and McNeilly TN (2021) The Development of Ovine Gastric and Intestinal Organoids for Studying Ruminant Host-Pathogen Interactions. *Front. Cell. Infect. Microbiol.* 11:733811. doi: 10.3389/fcimb.2021.733811

¹ Department of Disease Control, Moredun Research Institute, Midlothian, United Kingdom, ² Department of Vaccines and Diagnostics, Moredun Research Institute, Midlothian, United Kingdom, ³ Institute of Biodiversity, Animal Health and Comparative Medicine, University of Glasgow, Glasgow, United Kingdom, ⁴ The Roslin Institute, University of Edinburgh, Midlothian, United Kingdom

Gastrointestinal (GI) infections in sheep have significant implications for animal health, welfare and productivity, as well as being a source of zoonotic pathogens. Interactions between pathogens and epithelial cells at the mucosal surface play a key role in determining the outcome of GI infections; however, the inaccessibility of the GI tract *in vivo* significantly limits the ability to study such interactions in detail. We therefore developed ovine epithelial organoids representing physiologically important gastric and intestinal sites of infection, specifically the abomasum (analogous to the stomach in monogastrics) and ileum. We show that both abomasal and ileal organoids form self-organising three-dimensional structures with a single epithelial layer and a central lumen that are stable in culture over serial passage. We performed RNA-seq analysis on abomasal and ileal tissue from multiple animals and on organoids across multiple passages and show the transcript profile of both abomasal and ileal organoids cultured under identical conditions are reflective of the tissue from which they were derived and that the transcript profile in organoids is stable over at least five serial passages. In addition, we demonstrate that the organoids can be successfully cryopreserved and resuscitated, allowing long-term storage of organoid lines, thereby reducing the number of animals required as a source of tissue. We also report the first published observations of a helminth infecting gastric and intestinal organoids by challenge with the sheep parasitic nematode *Teladorsagia circumcincta*, demonstrating the utility of these organoids for pathogen co-culture experiments. Finally, the polarity in the abomasal and ileal organoids can be inverted to make the apical surface directly accessible to pathogens or their products, here shown by infection of apical-out organoids with the zoonotic enteric bacterial pathogen *Salmonella enterica* serovar Typhimurium. In summary, we report a simple and reliable *in vitro* culture system for generation and maintenance of

small ruminant intestinal and gastric organoids. In line with 3Rs principals, use of such organoids will reduce and replace animals in host-pathogen research.

Keywords: mini-guts, three-dimensional (3D) organoids, host-pathogen interactions, *in vitro* culture systems, stem cells, crypts, sheep, gastrointestinal

INTRODUCTION

The mammalian gastrointestinal (GI) tract is the site of digestion and nutrient absorption, as well as a predilection site for many infectious pathogens, including bacteria, viruses and parasites. Understanding how pathogens attach and invade cells in the GI tract will help determine mechanisms of host infection, disease pathogenesis and enable strategies to prevent and control infectious disease. Both the gastric stomach and intestine share a number of common features, including a single luminal layer of epithelial cells sealed by tight junctions which is renewed approximately every 3 – 5 days. In both organs, this huge regenerative capacity is mediated by proliferation and differentiation of tissue resident adult stem cells (ASCs) (Barker et al., 2007; Sato et al., 2009; Barker et al., 2010; Xiao and Zhou, 2020). In intestinal tissues, pockets of leucine-rich repeat-containing G protein-coupled receptor 5 (LGR5)-expressing ASCs reside in the base of the crypts of Lieberkühn and can differentiate into all five epithelial cell types of the intestine: enterocytes, goblet cells, enteroendocrine cells, tuft cells, and Paneth cells (Barker et al., 2007; Sato et al., 2009). In the stomach the epithelia is arranged into multiple gastric units, which comprise of the gastric pit, isthmus, neck and base with proliferative stem cells located in the isthmus (Barker et al., 2010; Xiao and Zhou, 2020). The ASCs of the gastric gland can differentiate into all five epithelial cell types of the gastric stomach: surface neck mucus cells, parietal cells, chief cells, enteroendocrine cells (including G cells, D cells, and enterochromaffin-like cells) and tuft cells (Barker et al., 2010; Xiao and Zhou, 2020).

The huge regenerative capacity of GI tract and the ability of ASCs to differentiate into epithelial cell types present in the GI tract has been exploited to develop GI organoids or “mini-guts” that reflect the cellular diversity and physiology of the organ from which they were derived (Sato et al., 2009; Barker et al., 2010). Organoid models of the GI tract were first developed from mouse stomach and intestine tissues. To achieve this, researchers isolated mouse LGR5⁺ adult stem cells from these organs and cultured them in a laminin rich extracellular matrix extracted from the Engelbreth-Holm-Swarm (EHS) mouse sarcoma, with appropriate growth factors (including Wnt3a, epidermal growth factor, Noggin and R-spondin 1). The resulting organoids consisted of organ-specific tissue (gastric or intestinal epithelia) that self-organised into spherical three-dimensional (3D) structures with a single epithelial layer and a central lumen (Sato et al., 2009; Barker et al., 2010). Since this initial discovery, organoids have been derived from a large number of different tissue types and from numerous mammalian species using similar ASC isolation and tissue culture techniques.

The development of *in vitro* organoid culture systems has transformed biomedical research as they provide a reproducible cell culture system that closely represents the physiology of the host. As the majority of infectious agents enter the body or reside at mucosal surfaces, organoids derived from mucosal sites such as the gastro-intestinal, respiratory and urogenital tracts promise to transform research into host-pathogen interactions as they allow detailed studies of early infection processes that are difficult to address using animal models.

Gastrointestinal (GI) disease in small ruminants has significant implications for animal health and welfare as well as substantial economic losses because of decreased production efficiency. In sheep, gastrointestinal nematodes (GIN) have major economic and welfare impacts worldwide, with the principal GIN of sheep including: *Haemonchus contortus*; *Nematodirus battus*; *Teladorsagia circumcincta* and *Trichostrongylus* spp. (including *T. colubriformis* and *T. vitrinus*) (Nieuwhof and Bishop, 2005; Roeber et al., 2013). These parasites are transmitted by the faecal-oral route where infective stage larvae develop in either the small intestine or abomasum (which is analogous to the gastric stomach) causing significant mucosal damage associated with host inflammatory immune responses (Stear et al., 2003; Roeber et al., 2013). In addition, sheep are natural reservoirs for enteric zoonotic pathogens of worldwide significance, such as Shiga toxin producing *Escherichia coli* (STEC) and *Salmonella enterica* (Heredia and García, 2018). The obvious challenge with studying interactions between the ovine host and GI pathogens is the lack of accessibility to the site of infection, making detailed studies particularly challenging. With the current lack of physiologically relevant *in vitro* cell culture systems to study ovine-GI pathogen interactions, research has relied heavily on use of sheep infection models, which have led to important insights into host immune responses against pathogens, immune evasion by pathogens and pathogen transmission (Stear et al., 1995; McSorley et al., 2013; Ellis et al., 2014). Despite these successes, animal experiments are often complex, costly and have ethical implications.

The use of stem-cell derived GI organoids or “mini-guts” for farmed livestock species, including ruminants, is an exciting recent development that promises to provide a physiologically relevant and host-specific *in vitro* cell culture system to interrogate host-pathogen interactions (Beaumont et al., 2021; Kar et al., 2021). A recent study has demonstrated the feasibility of generating organoids from bovine ileum tissue with the derived organoids expressing genes associated with intestinal epithelia cell types (Hamilton et al., 2018). However, no ruminant gastric organoid model has been previously reported. In this current study, in line with 3Rs principles to reduce and replace the use of animals in experiments, we develop ovine ileum and abomasum organoids as physiologically relevant *in vitro* culture systems to

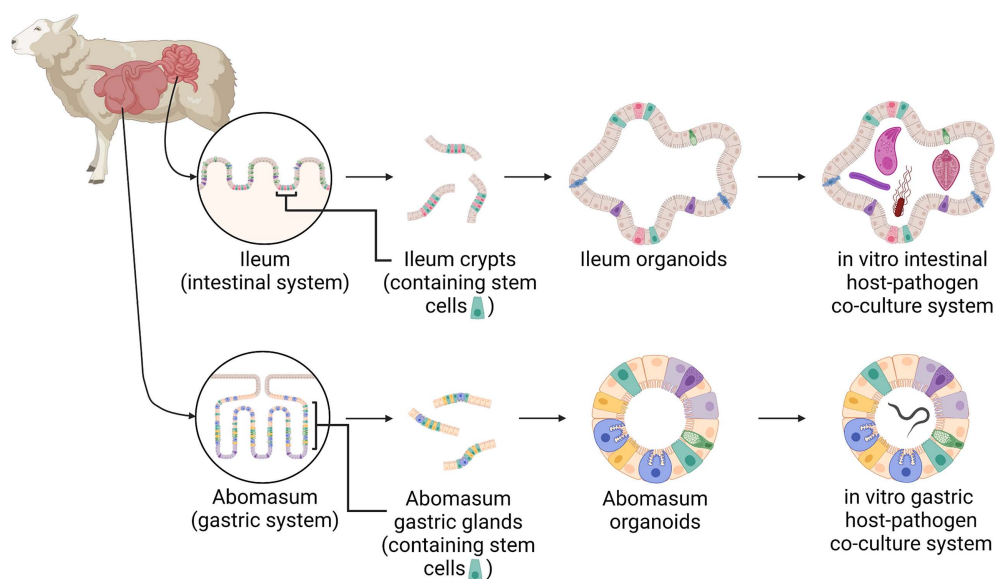


FIGURE 1 | A schematic of the development of ovine gastric and intestinal organoids for studying host-pathogen interactions. Stem cells isolated from sheep ileum crypts and abomasum gastric glands can be cultivated into tissue-specific organoids when grown in a three-dimensional culture system. Gastric and intestinal organoids can be co-cultured with pathogens to model host-parasite interactions in physiologically and biologically-relevant *in vitro* culture systems. Created with BioRender.com.

investigate ovine GI infection and disease (**Figure 1**). Using RNA-seq of both tissue and derived organoids we demonstrate that the expression profile of abomasum and ileum organoids are representative of the tissue from which they were derived. In addition, we demonstrate the utility of these *in vitro* organoid systems to study host-pathogen interactions by performing challenge studies with the abomasal parasite *T. circumcincta* and enteric bacteria *Salmonella enterica* serovar Typhimurium.

MATERIALS AND METHODS

Animals

All ovine abomasum and ileum tissues used in this study were derived from 7-8-month old helminth-free Texel cross male lambs (*Ovis aries*). The presented research was performed in line with 3Rs principles, particularly regarding the reduction and replacement of animals for use in scientific research. Therefore, the animal tissue used for developing organoids in this study was derived post-mortem from healthy control animals used in separate research trials, thereby reducing the number of animals necessary for research. Due to the timing of the study, we were limited to tissue derived from male lambs.

Isolation of Gastric Glands and Intestinal Crypts

Tissues were removed from sheep at post-mortem. Approximately 10 cm² sections of fundic gastric fold were collected from the abomasum and approximately 10 cm sections of ileal tissue were collected from a region ~ 30 cm distal to the ileocecal junction. Tissues were removed using a sterile scalpel and forceps and

placed into sterile ice-cold Hank's buffered saline solution (HBSS) containing 25 µg/ml gentamicin (G1397-10ML; Sigma-Aldrich) and 100 U/ml penicillin/streptomycin. To expose the epithelial surfaces, the abomasum was opened along the greater curvature and the ileum opened longitudinally using dissection scissors. The luminal surfaces were rinsed with tap water to remove digesta and then placed onto sterile Petri dishes. The majority of the mucus layer was gently removed using a glass slide, after which the surface mucosal tissue (containing the gastric glands or intestinal crypts) was collected by firm scraping with a fresh glass slide. Mucosal tissue was then transferred to a Falcon tube containing 50 ml of HBSS containing 25 µg/ml gentamicin and 100 U/ml penicillin/streptomycin. Samples were centrifuged at 400 x g for 2 min, resulting in a tissue pellet with a mucus layer on top. The supernatant and top forming mucus layer were aspirated and discarded and the tissue was re-suspended in 50 ml of HBSS containing 25 µg/ml gentamicin and 100 U/ml penicillin/streptomycin. This process of centrifugation, aspiration and resuspension was repeated until a mucus layer was no longer visible above the pellet. To release gastric glands and intestinal crypts from tissue, pellets were re-suspended in 25 ml of digestion medium (Dulbecco's Modified Eagle Medium [DMEM] high glucose, (11574486; Gibco) 1% FBS, 20 µg/ml dispase (4942086001; Roche), 75 U/ml collagenase (C2674; Sigma-Aldrich) 25 µg/ml gentamicin and 100 U/ml penicillin/streptomycin) and incubated horizontally in a shaking incubator at 80 rpm for 40 minutes at 37°C. Following digestion, the tube was gently shaken to loosen the cells and then left briefly at room temperature to allow large tissue debris to settle. The supernatant was transferred to a sterile 50 ml Falcon tube and gland/crypt integrity within the supernatant was assessed by light microscopy.

Samples were then centrifuged at 400 x g for 2 minutes, with the resulting supernatant containing released glands or crypts. The gland/crypt-containing supernatant was washed by centrifugation at 400 x g for 2 minutes and the glands/crypts re-suspended in 1-2 ml advanced DMEM/F12 (12634-010; Gibco) containing 1X B27 supplement minus vitamin A (12587-010; Gibco), 25 µg/ml gentamicin and 100 U/ml penicillin/streptomycin.

Organoid Culture

Two-hundred to one-thousand gastric glands or intestinal crypts were re-suspended in 100 µl advanced DMEM/F12 medium (containing 1X B27 supplement minus vitamin A, 25 µg/ml gentamicin and 100 U/ml penicillin/streptomycin) and were then added to 150 µl of BD Growth Factor Reduced Matrigel Matrix (356230; BD Biosciences). Fifty microliter droplets were added to consecutive wells of a 24-well tissue culture plate (3524, Corning). Plates were incubated at 37°C, 5% CO₂ for 15-20 minutes to allow the Matrigel to polymerize and then 550 µl of pre-warmed complete IntestiCult Growth Medium (mouse) (6005; STEMCELL Technologies) containing 500 nM Y-27632 (10005583; Cambridge Bioscience), 10 µM LY2157299 (15312; Cambridge Bioscience), 10 µM SB202190 (ALX-270-268-M001; Enzo Life Sciences) and gentamicin (50 µg/ml) were added to each well. Plates were incubated at 37°C, 5% CO₂ to allow organoids to develop, replacing complete IntestiCult medium every 2-3 days. Organoids were typically cultured for 7-14 days prior to passaging. Phase contrast microscopy was used to image organoids over the course of 14 days of *in vitro* growth.

Organoid Passage

IntestiCult media was removed from the cultured organoids and the Matrigel matrix was dissolved by replacement with 1 ml ice-cold advanced DMEM/F12. The re-suspended organoids were transferred to a 15 ml Falcon tube and the total volume of advanced DMEM/F12 was increased to 10 ml. Samples were left on ice for 5 minutes to allow organoids to settle and the supernatant was removed. The organoids were re-suspended in 200 µl advanced DMEM/F12 medium (containing 1X B27 supplement minus vitamin A, 25 µg/ml gentamicin and 100 U/ml penicillin/streptomycin) and then mechanically disrupted by repeatedly pipetting (approximately fifty times) using a 200 µl pipette tip bent at a 90° angle. The number of organoid fragments were counted by light microscopy and samples diluted to 200-1000 crypts per 100 µl. One-hundred microliters of fragments were then combined with Matrigel and plated into 24-well tissue culture plates as described in section 2.4. Phase contrast microscopy was used to image organoids from passage one to passage five, following seven days of *in vitro* growth at each passage.

Organoid Cryopreservation

IntestiCult media was removed from the cultured organoids and the Matrigel matrix was dissolved by replacement with 1 ml ice-cold advanced DMEM/F12. The re-suspended organoids were transferred to a microcentrifuge tube and pelleted by centrifugation at 290 x g for 5 minutes at 4°C. Following centrifugation, the supernatant was removed and organoid pellets were re-suspended in Cryostor CS10

cryopreservation medium (STEMCELL Technologies) at approximately 500-1000 organoids/ml before being transferred to a cryovial. Cryovials were stored in a cryogenic freezing container for 2 hours at -80°C and subsequently transferred to -196°C for long-term storage.

Cryopreserved organoids were resuscitated by thawing cryovials in a water bath at 37°C and then rapidly transferring the organoids into a 15 ml Falcon tube containing 8 ml of advanced DMEM/F12 medium (containing 1X B27 supplement minus vitamin A, 25 µg/ml gentamicin and 100 U/ml penicillin/streptomycin). The cryovial was washed with a further 1 ml of media and added to the Falcon tube. Samples were pelleted by centrifugation at 290 x g for 5 minutes at 4°C and then re-suspended in 200 µl of fresh advanced DMEM/F12 medium (containing 1X B27 supplement minus vitamin A, 25 µg/ml gentamicin and 100 U/ml penicillin/streptomycin). Re-suspended organoids were added to Matrigel and cultivated as described in Section 2.4. Organoids were imaged by phase contrast microscopy following seven days of *in vitro* growth prior to cryopreservation and post-cryopreservation.

Total RNA Extraction

Total RNA was extracted from gastric and intestinal organoids after multiple serial passages that included passage 0 (P0) through to passage 4 (P4). Ovine gastric and intestinal organoids were prepared as described above; organoids that were formed from animal tissue-derived crypts were designated P0 and these were cultured by serial passage until P4. Each passage was cultured in triplicate wells of a 24-well tissue culture plate and allowed to mature for seven days before collecting for total RNA extraction. For total RNA extraction, IntestiCult media was removed from wells and replaced with 1 ml of ice-cold advanced DMEM/F12. The resulting suspension containing dissolved Matrigel and organoids was transferred to 15 ml sterile Falcon tubes and brought up to 10 ml with ice-cold advanced DMEM/F12. Organoids were gently pelleted by centrifugation at 200 x g for 5 min and the supernatant removed. Organoid pellets were re-suspended in 350 µl RLT buffer (Qiagen) containing β-mercaptoethanol, according to manufacturer's guidelines and stored at -70°C. Total RNA was isolated from each sample using a RNeasy mini kit (Qiagen) with the optional on-column DNase digest and total RNA eluted in 30 µl nuclease-free water, according to the manufacturers protocol. Total RNA from each extraction was quantified using a NanoDropTM One spectrophotometer and integrity analysed using a Bioanalyzer (Agilent) with the total RNA 6000 Nano kit. Purified total RNA was stored at -70°C until RNA-seq analysis.

Total RNA was also extracted from ovine abomasum and ileum tissue harvested at post-mortem from five individual 6-month old helminth-free Texel cross lambs and stored in RNAlater (ThermoFisher). Specifically, samples were taken from the same tissue regions stated above for crypt isolation. For total RNA isolation, approx. 30 mg of tissue was homogenized in 600 µl of RLT buffer containing β-mercaptoethanol using a Precellys[®] Tissue Homogenizer with CK28 tubes using x3 10s pulses at 5500 rpm with 5 min on ice between each pulse (Bertin InstrumentsTM). Total RNA

was isolated and quantified as described previously, except the total RNA was eluted in 50 μ l nuclease-free water. Purified total RNA was stored at -70°C until RNA-seq analysis.

RNA-Seq Analysis

For each sample, 1 μ g of total RNA was used for RNA-seq analysis. All library synthesis and sequencing were conducted at The University of Liverpool, Centre for Genomic Research (CGR). In brief, dual-indexed, strand-specific RNA-seq libraries were constructed from submitted total RNA sample using the NEBNext[®] Poly(A) mRNA Magnetic Isolation Module (NEB #E7490) and NEBNext Ultra II Directional RNA Library Prep Kit for Illumina (NEB #E7760). A total of 20 libraries were constructed [including: ovine abomasum organoid P0-P4 (triplicate pooled wells for each passage); ovine ileum organoid P0-P4 (triplicate pooled wells for each passage); ovine abomasum tissues ($n = 5$); ovine ileum tissues ($n = 5$)]. The barcoded individual libraries were pooled and sequenced on a single lane of an Illumina NovaSeq flowcell using S1 chemistry (Paired-end, 2x150 bp sequencing, generating an estimated 650 million clusters per lane). Following sequencing adaptors were trimmed using Cutadapt version 1.2.1 (Martin, 2011) and reads were further trimmed using Sickle version 1.200 (Joshi and Fass, 2011) with a minimum window quality score of 20. Reads shorter than 15 bp after trimming were removed. Sequence reads were checked for quality using FastQC v0.11.7. Reads were pseudo-aligned to the *Ovis aries* transcriptome (Oar_v3.1 GCA_000298735.1) using Kallisto v0.46.2 with default settings (Bray et al., 2016) and read abundance calculated as transcripts per million (TPM). Gene expression data was analysed by principal component analysis (PCA) using pcaExplorer version 2.12.0 R/Bioconductor package (Marini and Binder, 2019). Specific genes were also manually retrieved from our transcriptomic dataset and their TPM values \log_2 transformed for presenting in heat maps, which were generated using GraphPad Prism software (v8.0).

Immunohistochemistry

Abomasum and ileum organoids were cultivated in Matrigel for 7 days in 8-well chamber slides (354118; Falcon) as described in section 2.4. To make organoids accessible to immunohistochemistry reagents, the culture medium was removed and replaced with ice-cold 4% paraformaldehyde. For fixation, samples were kept at 4°C for 20 minutes to also dissolve the Matrigel and prevent it from re-solidifying. Organoids were washed twice with IF buffer (0.1% Tween20 in PBS) and then permeabilised with 0.1% TritonX-100 in PBS for 20 minutes at room temperature. Samples were washed three times with IF buffer and then blocked for 30 minutes with 1% BSA in IF buffer at room temperature. Next, primary antibodies diluted in blocking solution were added to the organoids and samples were left overnight at 4°C . Primary antibodies used included polyclonal rabbit α -Ki67 (ab15580, abcam, used at a 1:500 dilution), polyclonal rabbit α -EPCAM (orb10618, Biorbyt, used at a 1:600 dilution), monoclonal mouse α -villin (sc-58897, Santa Cruz Biotechnology, used at a 1:200 dilution) and monoclonal mouse α -pan cytokeratin (used at a 1:100 dilution). For isotype controls, mouse or rabbit IgG were used in place of the specific primary antibodies and were diluted at 1:100 or 1:500 for mouse

and rabbit IgG respectively. The next day, samples were washed three times with IF buffer and then secondary antibodies added (diluted at 1:500 in blocking buffer) and incubated at room temperature for 1 hour. Secondary antibodies used were goat α -mouse Alexa Fluor 488 (ab150117, abcam) and goat α -rabbit Alexa Fluor 488 (ab150081, abcam). Phalloidin-iFluor 555 reagent (ab176756, abcam, used at a 1:1000 dilution) was also added during the secondary antibody step to label F-actin. Samples were washed three times with IF buffer and then Hoechst 33258 solution diluted 1:200 in IF buffer was added to label nuclei (94403, Sigma-Aldrich). Samples were incubated for a further 5 minutes at room temperature before three washes with IF buffer. Finally, slides were mounted using ProLong Gold antifade mountant (P10144, ThermoFisher Scientific) and imaged by confocal microscopy using a Zeiss LSM 710 Inverted Confocal Microscope and Zeiss Zen Black operating software.

Exsheathment of *Teladorsagia circumcincta* Third Stage Larvae (L3)

T. circumcincta L3 (Moredun isolate MTci2, CVL) were exsheathed and labelled using modified protocols previously published (Dinh et al., 2014; Bekelaar et al., 2019). Nine millilitres of Earle's balanced salts solution (EBSS) buffer in a 15 ml Falcon tube was preheated in a water bath to 37°C and CO_2 -saturated over 1 hour using an incubator tube connected to a CO_2 tank. Approximately 5×10^4 *T. circumcincta* L3 in 1 ml of tap water were added to the CO_2 -saturated EBSS and the sample continued to be saturated for a further 15 minutes. The Falcon tube was then sealed with Parafilm[®] M and inverted 6 times before being placed horizontally into an incubator at 37°C , 5% CO_2 for 4 hours. Following incubation, the whole sample was transferred into a 25 cm^2 vented cap flask and incubated overnight at 37°C /5% CO_2 , to allow L3s to continue exsheathing. Exsheathment was validated the following morning by light microscopy. The larvae were then washed 4 times by repeated centrifugation at $330 \times g$ for 2 minutes and re-suspension in 50 ml of distilled water (pre-warmed to 37°C). After the final wash, the L3 larvae were re-suspended in 1 ml distilled water and transferred to a microcentrifuge tube. Exsheathed L3 (exL3) were fluorescently labelled by the addition of 2 μ l PKH26 dye (1 mM stock concentration) from the MINI26 PKH26 Red Fluorescent Cell Linker Kit (Sigma-Aldrich) and mixed by pipetting. Parasites were incubated with the dye for 15 minutes at room temperature, protected from light. Excess dye was removed by washing the larvae five times with distilled water as described above before finally re-suspending them in 1 ml of complete IntestiCult organoid growth medium.

Teladorsagia circumcincta L3-Organoid Co-Culture

Abomasum and ileum organoids were cultivated in Matrigel for 7 days in 8-well chamber slides (354118; Falcon) as described in section 2.4. Immediately prior to organoid-*T. circumcincta* co-culture, complete IntestiCult media was removed from the cultured organoids and replaced with 250 μ l of fresh pre-warmed complete IntestiCult. Twenty to 50 PKH26 labelled *T. circumcincta* exL3 in 50 μ l complete IntestiCult media were added to each well of organoids and organoid-larval cultures incubated at 37°C , 5% CO_2 . Note that organoids were not

removed from their Matrigel domes prior to the addition of *T. circumcincta* L3. Upon observation of multiple organoids containing *T. circumcincta* L3 within their lumen (after ~24–48 hours of organoid-*T. circumcincta* co-culture) the samples were fixed with 4% PFA for 30 min, followed by 3 washes with PBS, and stored at 4°C until fluorescence staining. Organoids were permeabilized, blocked and probed with Phalloidin-488 and Hoechst 33258 as described for organoid immunohistochemistry above. Images were captured using a Zeiss LSM 710 Inverted Confocal Microscope and Zeiss Zen Black operating software.

Generation of Apical-Out Organoids

Epithelial polarity was inverted in gastric and intestinal ovine organoids by following a previously published method for reverse polarity in human intestinal organoids (Co et al., 2019). Briefly, gastric and intestinal organoids were grown in Matrigel as described above for 7 days. Matrigel domes containing developed organoids were gently dissolved by the addition of 500 µl ice-cold 5 mM EDTA in PBS, taking care not to rupture the organoids. The resulting suspension was transferred to a 15 ml Falcon tube that was subsequently filled with 14 ml of 5 mM EDTA in PBS. Samples were placed on a rocker and mixed gently for 1 hour at 4°C. Organoids were pelleted by centrifugation at 200 × g for 3 min at 4°C and the supernatant was removed. Pellets were re-suspended in complete IntestiCult growth media (containing 500 nM Y-27632, 10 µM LY2157299, 10 µM SB202190 and gentamicin (50 µg/ml), with the addition of 10% advanced DMEM/F12 medium (containing 1X B27 supplement minus vitamin A, 25 µg/ml gentamicin and 100 U/ml penicillin/streptomycin). Re-suspended organoids were transferred to the wells of 8-well glass chamber slides and incubated at 37°C, 5% CO₂ for a period of 72 hours, prior to being fixed and stained with Phalloidin-iFluor 555 reagent and Hoechst 33258, as described in section 2.9. Confocal imaging was performed as described in section 2.9.

Infection of Apical-Out Organoids With *Salmonella enterica* Serovar Typhimurium

The polarity of gastric and intestinal organoids was inverted as described above. *Salmonella* Typhimurium strain ST4/74 was chosen for this experiment as its full genome sequence is available (Richardson et al., 2011) and it has been shown to efficiently invade the ovine ileal mucosa and elicit inflammatory responses in an ovine ligated ileal loop model (Uzzau et al., 2001). To aid visualization of the bacteria in organoids, the strain was electroporated with plasmid pFPV25.1 which carries *gfpmut3A* under the control of the *rpsM* promoter resulting in the constitutive synthesis of green fluorescent protein (Valdivia and Falkow, 1996). Stability of the plasmid in the absence of antibiotic selection during *Salmonella* infection has been confirmed (Vohra et al., 2019). The bacteria were grown on Luria Bertani (LB) agar supplemented with 100 µg/ml ampicillin at 37°C overnight. Single colonies were transferred to LB broth supplemented with the same antibiotic and grown for 20 hours shaking at 180 rpm at 37°C. The liquid cultures were diluted to 3.3 × 10⁶ CFU/ml in complete IntestiCult growth medium, described above, and 300 µl of the dilution was added to half of the wells, which

already contained organoids that had already been maintained in conditions for generating apical-out organoids for 72 hours. The other half of the wells acted as negative controls, with organoids being re-suspended in 300 µl of complete IntestiCult growth medium alone (no bacteria). After 30 minutes of incubation another 300 µl of complete IntestiCult growth medium with 200 µg/ml gentamycin was added to kill extracellular bacteria. The slides were incubated at 37°C, 5% CO₂ for a total of 6 hours. At the end of the incubation period the entire volume of the liquid from each well, including the organoids, were transferred to separate 15ml Falcon tubes (Corning, UK). All centrifugations for organoid collection during washing were done at 200 rpm for 5 minutes. The supernatant was removed and the organoids were washed twice in PBS, and then re-suspended in 4% PFA for 30 minutes for fixation. The organoids were processed for immunohistochemistry as described in section 2.9 and stained with Phalloidin-iFluor 555 reagent, prior to mounting with ProLong Diamond antifade mountant (P36961, ThermoFisher Scientific). Confocal imaging was performed as described in section 2.9.

RESULTS

Growth of Ovine Gastrointestinal Organoids *In Vitro*

Fragmented gastric glands and intestinal crypts isolated from the abomasum fundic fold and the ileum of 7 to 8-month old Texel cross lambs were embedded in Matrigel and grown in complete IntestiCult organoid growth medium. Under identical growth conditions, epithelial stem cells from these two different organ tissues were able to develop into organoids *in vitro* (Figure 2A). By 24 hours, sealed spherical structures containing a central lumen had formed in both the abomasum and ileum organoids. However, while the ileum organoids became branched after 5–7 days of *in vitro* culture, the vast majority of abomasum organoids retained a spherical structure that persisted for the duration of a culture passage (Figures 2A, B).

Abomasum and ileum organoids could be serially passaged by removal from Matrigel, fragmentation by pipetting and re-embedding in Matrigel. At each passage, ileum organoids continued to form into branched structures, while the abomasum organoids persistently formed spherical structures. (Figure 2B). Organoids that were cryopreserved in liquid nitrogen after 7 days of *in vitro* culture could be thawed and re-cultured, demonstrating the potential to store organoids long-term and to resuscitate when required. Furthermore, we found that the cryopreserved organoids can be resuscitated after at least 18 months of storage in liquid nitrogen. Abomasum and ileum organoids retained their spherical and branched structures, respectively, following resuscitation and 7 days of *in vitro* culture (Figure 2C).

Epithelial Cell Markers Associated With Ovine Gastric and Intestinal Organoids

Immunohistochemistry was performed to identify key structural features associated with both abomasum and ileum organoids.

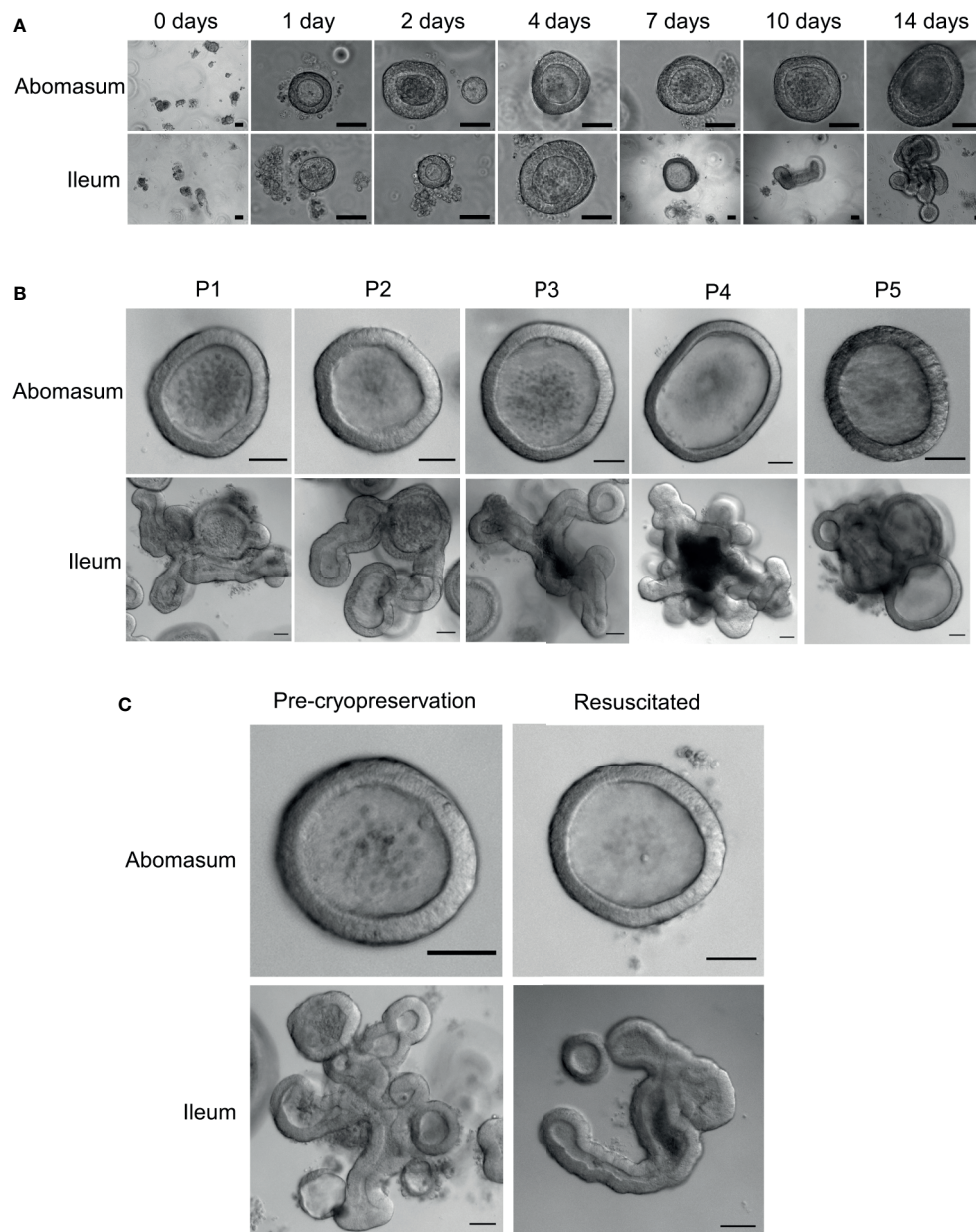


FIGURE 2 | *In vitro* growth of ovine abomasum and ileum organoids. **(A)** Representative images of abomasum and ileum organoids grown over 14 days in the same culture conditions. **(B)** Representative images showing the growth and development of mature abomasum and ileum organoids across multiple consecutive passages (P1 - P5) at seven days of *in vitro* culture. **(C)** Representative images of abomasum and ileum organoids grown for seven days, both pre-cryopreservation and after resuscitation. Scale bars = 10 μ m.

Individual Z-stack images of organoids stained with phalloidin to label F-actin clearly demonstrated that the apical surface of the epithelium is present on the interior of the organoid, for both abomasum and ileum organoids, indicated by the presence of a solid F-actin-positive boundary (**Figures 3A, 4A**). This imaging also confirmed the presence of a hollow lumen within the organoids (**Figures 3A, 4A**).

The proliferation marker Ki67 was detectable in both the abomasum and ileum organoids, indicating that cell division

continued to take place at 7 days of *in vitro* culture (**Figures 3B, 4B**). The epithelial cell markers EpCAM (epithelium cell adherence molecule), villin (epithelium-specific actin-binding protein) and cytokeratin (epithelial cell cytoskeleton filament protein) were each detectable in abomasum and ileum organoids at seven days of *in vitro* culture (**Figures 3B, 4B**), confirming the differentiation of stem cells into epithelium cell-containing organoids. Control samples of organoids probed with mouse and rabbit serum IgG

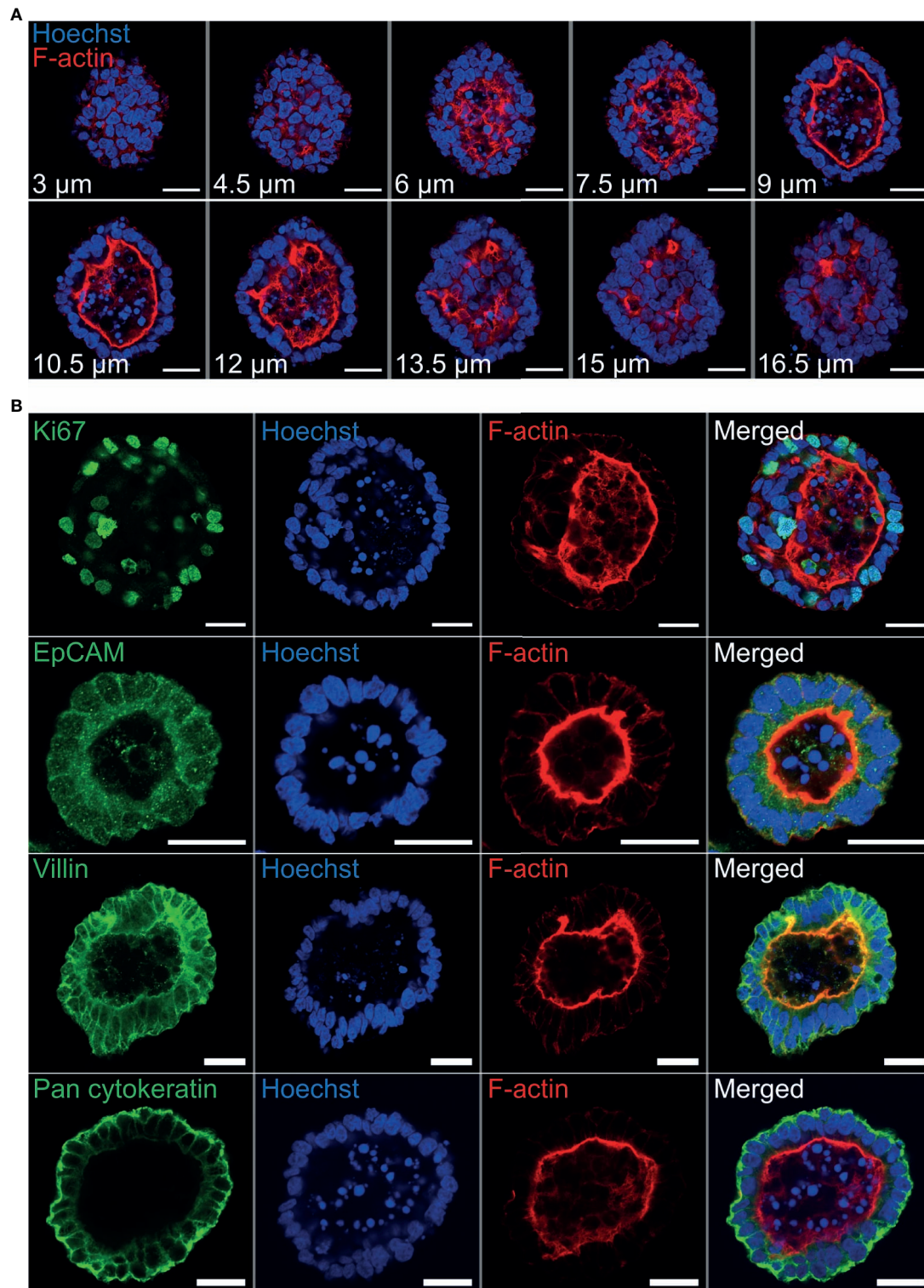


FIGURE 3 | Characterisation of ovine abomasum organoids by immunofluorescence confocal microscopy at seven days of *in vitro* culture. **(A)** Representative Z-stack images of an individual abomasum organoid with a closed luminal space and an internal F-actin-expressing brush border. Red = F-actin and blue = Hoechst (nuclei). **(B)** Representative images of abomasum organoids probed for either the cell proliferation marker Ki67, or the epithelial cell markers EpCAM, villin and pan-cytokeratin (all green). F-actin (red) and Hoechst (blue). Scale bars = 10 μm .

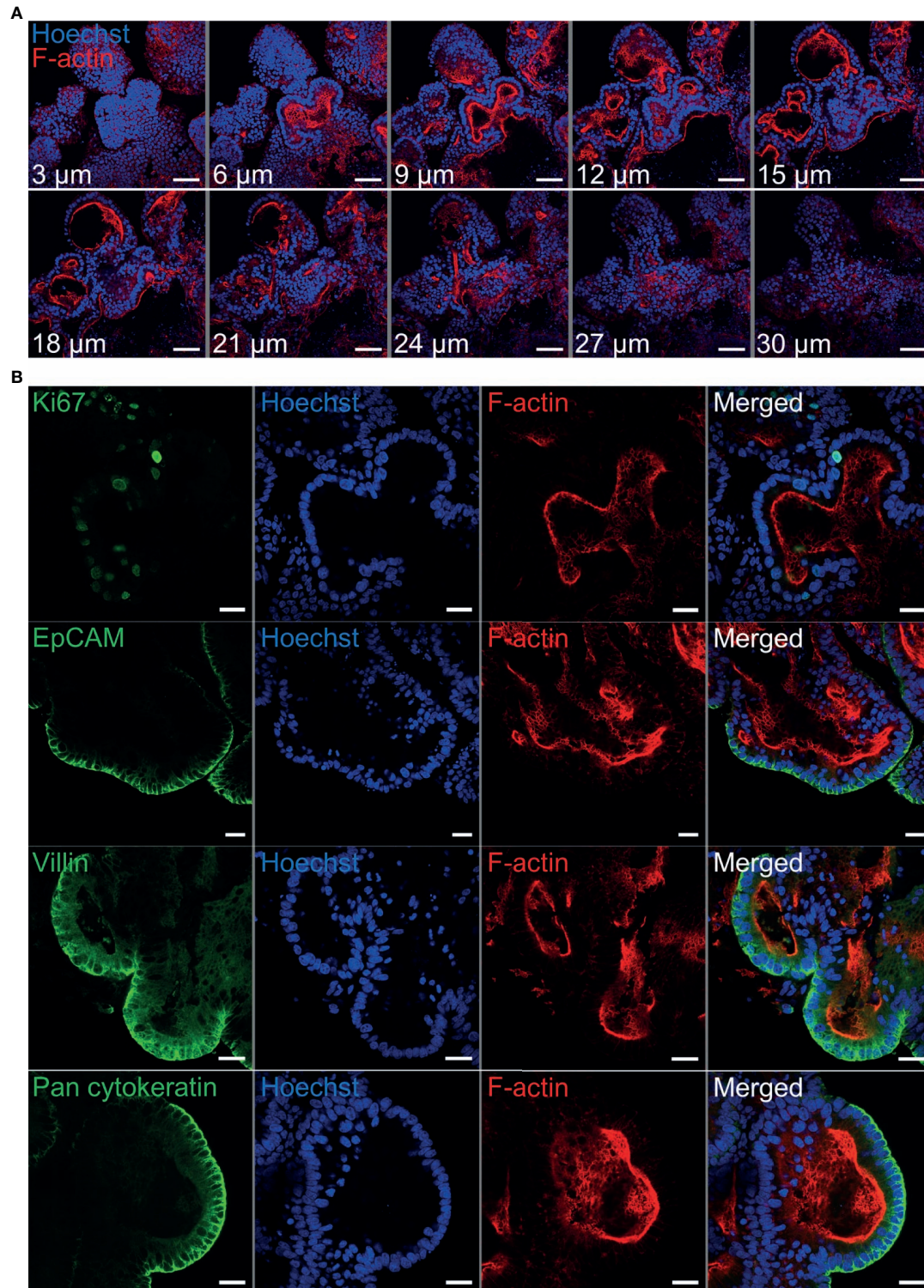


FIGURE 4 | Characterisation of ovine ileum organoids by immunofluorescence confocal microscopy at seven days of *in vitro* culture. **(A)** Representative Z-stack images of part of an individual branched ileum organoid with a closed luminal space and an internal F-actin-expressing brush border. Red = F-actin and blue = Hoechst (nuclei). **(B)** Representative images of abomasum organoids probed for either the cell proliferation marker Ki67, or the epithelial cell markers EpCAM, villin and pan-cytokeratin (all green). F-actin (red) and Hoechst (blue). Scale bars = 10 µm.

did not label positive for any of the epithelial cell markers, confirming the specificity of the epithelial cell labelling (Supplemental Figures 1, 2).

Transcriptional Analysis of Abomasum and Ileum Organoids and Tissue

Gene expression profiles from: ovine ileum organoids (P0 – P4); ovine abomasum organoids (P0 – P4); ovine ileum tissue (n = 5) and ovine abomasum tissue (n = 5) were compared by RNA-seq analysis. The global gene expression profiles of the complete dataset, consisting of 20 individual samples, were initially compared by principal component analysis (PCA) (Figure 5). The PCA analysis resulted in four statistically significant clusters (95% confidence intervals), with each cluster representing a sample type (i.e. ileum organoids; abomasum organoids; ileum tissue; or abomasum tissue). This demonstrates that the global transcriptome profile of ovine abomasum tissue (n = 5) and ovine ileum tissue (n = 5) are different (Figure 5). Based on global gene expression profiles, organoids also grouped by the tissue type from which they derived, with ileum and abomasum organoids forming separate statistically significant clusters (95% confidence intervals) in the PCA analysis (Figure 5). Importantly, for both ileum and abomasum organoids, each passage (P0 – P4) is represented in each cluster, showing that there was no global change in the transcriptome profile following serial passage (Figure 5).

The expression profiles of the top 40 most variable genes (of genes ranked by inter-sample variation) were compared from ileum and abomasum organoids from serial passages (P0 – P4) and ileum and abomasum tissue derived from five lambs (n = 5) (Figure 6). This analysis broadly identified three categories of genes, including genes with: i) abomasum (tissue and organoid) specific expression; ii) ileum (tissue and organoid) specific expression and iii) ileum and abomasum (tissue only) expression.

Based on gene expression profiles, genes that were highly expressed in abomasum tissue and abomasum organoids, but

absent in all ileum samples, included genes of known gastric function, such as: *claudin-18*; *gastrokinase*; *gastric lysozyme* and *pepsin*. Similarly, ileum specific genes were detected in both ileum tissue and ileum organoid samples, but absent from all abomasum samples included: *galectin*; *lingual antimicrobial peptide*; *guanylin* (a 15 amino acid peptide secreted from goblet cells). Interestingly, genes shared by ileum tissue and abomasum tissue, but largely absent from organoid cultures, were predominantly immune related genes (such as: C-C motif chemokine 5, regakine-1-like and various immunoglobulin chains) and likely reflect the presence of immune cells in ileal and abomasal mucosal tissue samples, which were not represented in ASC derived ileum and abomasum organoids. In summary, based on transcriptional profiles, abomasum and ileum organoids are broadly representative of the tissues they were derived from and appear to be transcriptionally stable over multiple passages.

Expression of Cell- and Tissue-Specific Genes in Abomasum and Ileum Organoids and Tissues

The ovine gastrointestinal transcriptomic database generated here was manually searched for genes that are representative of specific cell and tissue markers. A total of 151 genes were searched in this way and their expression in abomasum and ileum organoids and tissue was presented in heat maps. A number of cell junction markers were consistently expressed in both organoids and tissue, including genes encoding proteins related to tight junctions, gap junctions, adherens junctions and desmosomes (Supplemental Figure 3).

We identified genes associated with particular epithelial cell subpopulations that were consistently expressed in abomasum and ileum organoids across multiple passages (P0-P4), as well as in ileum and abomasum tissue samples from five individual animals. These include numerous markers associated with stem cells, enterocytes, secretory and mucus-producing cells and Paneth cells (Figure 7). In particular, expression of the stem cell marker *LGR5* was higher in both abomasum and ileum organoids compared to the respective tissue samples, indicating the presence of a relatively higher stem cell subpopulation in the organoids compared to tissues (Figure 6). Three enterocyte genes associated with ileum tissue were not detected in ileum organoids, namely *ALPI*, *APOA4* and *APOC3* (Figure 7). These enterocyte markers were not detected in abomasum organoids or abomasum tissue from any of the five individual animals. Expression of several genes associated with homeostasis in gastrointestinal cells was conserved between tissue samples and organoids, for both abomasum and ileum samples. This included *HES1*, *ADAM10*, *ADAM17*, *FGF20* and *SHH* (Figure 7).

A number of genes associated with specific epithelial cell subpopulations were differentially expressed in ileum and abomasum tissue. For example, the early enterocyte precursor-associated gene *REG3G*, the Paneth cell marker *DEFB1*, the enteroendocrine cell marker *REG4* and the enteroendocrine cell-derived hormone *GCG* were expressed in ileum tissue and not in abomasum tissue (Figure 7). These genes were also

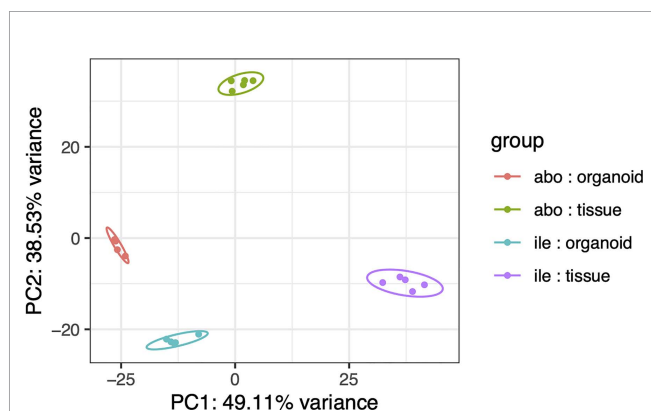


FIGURE 5 | Principal component analysis (PCA) of RNA-seq expression of the top 500 most variant genes (of genes ranked by inter-sample variance) in ovine abomasum and ileum organoid and tissue samples. Sample type is indicated in the key and includes: abomasum organoid (red); abomasum tissue (green); ileum organoid (blue); ileum tissue (purple). Ellipses indicates 95% confidence intervals for each cluster.

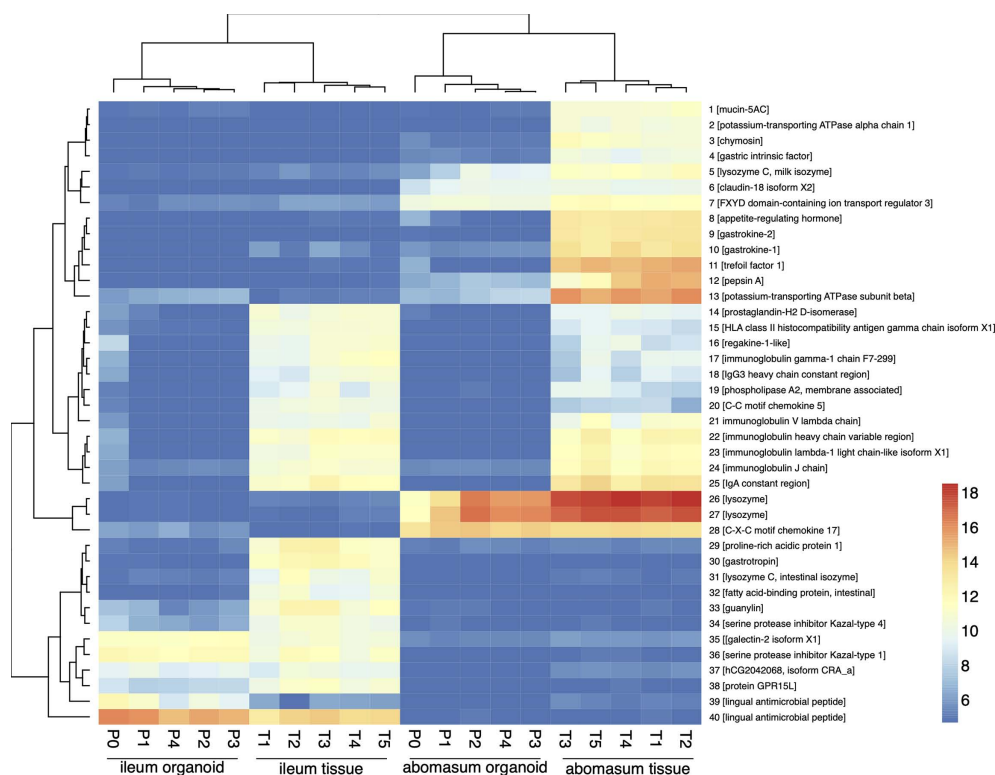


FIGURE 6 | Heat map showing expression level of top 40 most variant genes (of genes ranked by inter-sample variance) from ileum (ile) and abomasum (abo) organoids from serial passages (P0 – P4) and ileum (ile) and abomasum (abo) tissue derived from five lambs (T1 – T5). Colours indicate level of expression from low (blue) to high (red). The dendrograms indicate similarity between samples. Details of genes included in the heat map, including ENSOART sequence identifiers, are shown in **Supplemental File 1**.

expressed in intestinal organoids and not abomasum organoids, indicating the conservation of tissue-specific differences in the cell subpopulations of the two different types of organoids.

Various genes were found to be specific for the abomasum, being expressed in both abomasal tissue and abomasum organoids but not in ileal tissue or ileum organoids. These included *PGA5*, *CCKBR* and *CBLIF* (*GIF*) (**Figure 8**). We also found that some genes specifically expressed in abomasal tissue were not expressed in abomasum organoids, including *SLC5A5*, *DUOX2*, *MCT9*, *PGC*, *ATP4A*, *AQP4*, and *HDC* (**Figure 8**).

The expression of immune-related genes, including toll-like receptors (TLRs), c-type lectin receptors (CLRs), chemokines, cytokines and antimicrobials were examined in abomasum and ileum tissue and organoids. The TLRs – *TLR3*, *TLR5* and *TLR6*, and CLR *Dectin-1* were expressed in abomasum and ileum organoids and their respective tissues (**Supplemental Figure 4**). A number of chemokines were expressed in abomasum organoids and abomasal tissue, including *CXCL16*, *CCL20*, *CCL24* and *ACKR3*. Interestingly, the chemokine *CCL17* was up-regulated in abomasum and ileum organoids compared to the respective tissue samples (**Supplemental Figure 4**). The expression of cytokine associated genes *IL18BP*, *IL27RA*, *IL4I1*, *IL13RA1* and *IFNGR1* was detected in abomasum and ileum organoids (**Supplemental Figure 4**). Of note, the antimicrobial gene *SBD2*

was found to be highly expressed in ileum and ileal tissue, but was not expressed in either abomasum organoids nor abomasal tissue (**Figures 6** and **Supplemental Figure 4**).

Organoid Co-Culture With the Helminth *Teladorsagia circumcincta*

In order to use gastrointestinal organoids to study host-pathogen interactions *in vitro*, it is important to be able to challenge organoids with the pathogen-of-interest. Here, we co-cultured abomasum and ileum organoids with larvae of the important ruminant helminth parasite *T. circumcincta*. Infective, third stage larvae (L3) were ex-sheathed *in vitro* and labelled with the lipophilic dye PKH26. Labelled larvae were added directly to the well of a 24-well tissue culture plate containing abomasum or ileum organoids embedded in Matrigel and complete IntestiCult growth media. A number of *T. circumcincta* L3 penetrated the Matrigel, of which approximately 50% subsequently burrowed into central lumen of the organoids by 24 hours post-incubation, with some individual L3 invading the organoids as early as 2 hours. This indicated that it was possible to infect the organoids with the parasite in the correct orientation (i.e. with the parasite residing at the luminal surface of the organoid) without having to mechanically disrupt the organoids to allow access to the central lumen. *T. circumcincta* L3 were equally

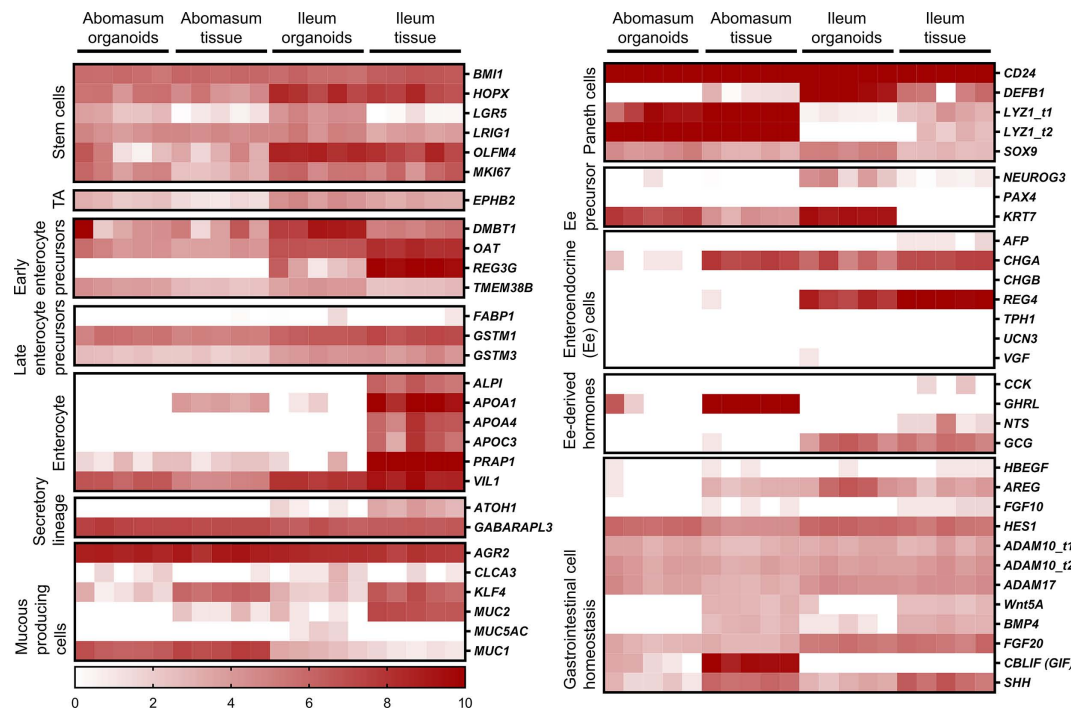


FIGURE 7 | Heat map showing the expression of genes associated with gastrointestinal epithelia in abomasum and ileum tissue and organoids. RNA-seq analysis was performed to compare gene expression in abomasal and ileal tissue derived from five lambs and abomasum and ileum organoids across multiple passages. Squares from left to right under “abomasum tissue” and “ileum tissue” represent lambs T1-T5. Squares from left to right under abomasum organoids and ileum organoids represent passages P0-P4. Scale = \log_2 transcripts per million reads. Ee: enteroendocrine. Details of genes included in the heat map, including ENSOART sequence identifiers, are shown in **Supplemental File 2**.

effective at infecting both abomasum and ileum organoids and motile larvae were still present after 14 days of co-culture. While we mainly observed abomasum organoids containing single larvae (**Figure 9A**), we found multiple larvae residing in the lumen of the larger ileum organoids (**Figure 9B**). Z-stack analysis on fixed samples showed worms were present within the lumen of the organoids and demonstrated L3 larvae burrowing directly through the epithelium of abomasum and ileum organoids to access the central lumen (**Figure 9C**).

Generation of Apical-Out Organoids and Infection With *Salmonella typhimurium*

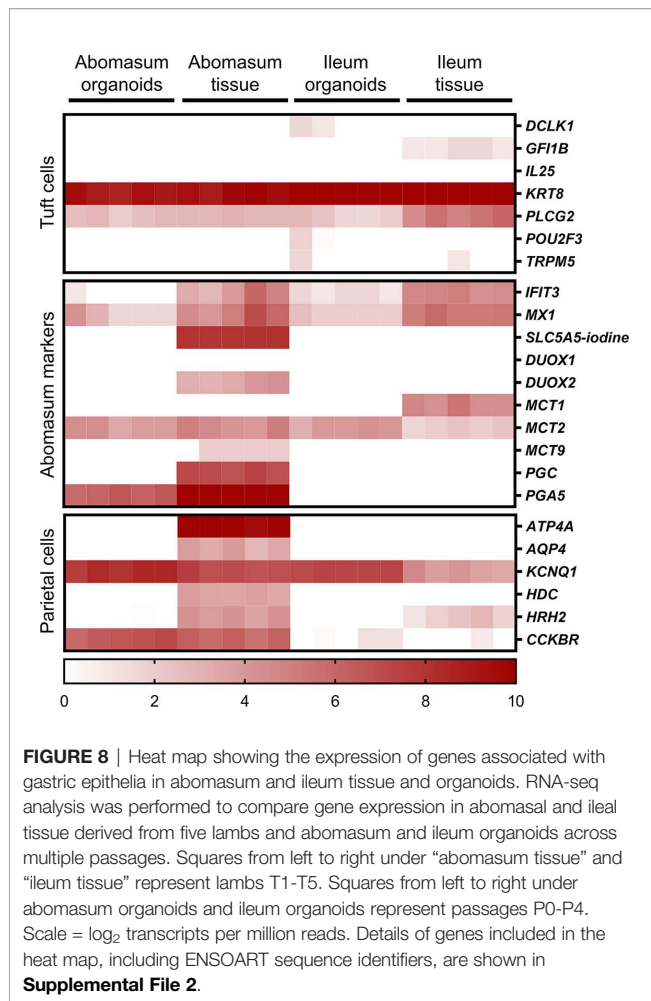
It is necessary to expose the apical surface of the organoid epithelia in order to have a working co-culture system for some pathogens. A recently published protocol (Co et al., 2019) described a method to invert the basal-out orientation of the abomasum and intestinal organoids. When the organoids were removed from Matrigel and incubated in 5 mM EDTA for 1 hour, the polarity of both the abomasum and intestinal organoids was reversed following 72 hours' incubation in complete IntestiCult growth medium. F-actin staining of fixed organoid samples clearly highlighted the apical surface of the epithelium, which is initially internally located in basal-out abomasum and ileum organoids; however, after removing the extra cellular matrix from the organoids, the apical surface became positioned on the exterior surface of the organoids,

with a microvilli brush edge apparent by confocal microscopy (**Figures 10A, B**).

To demonstrate the utility of apical-out ovine gastric and intestinal organoids as an *in vitro* model for host-pathogen interactions, the apical-out organoids were exposed to the bacterial pathogen *Salmonella enterica* serovar Typhimurium, which is known to invade the epithelium *via* the apical surface (Finlay and Falkow, 1990). After 6 hours of organoid-bacteria co-culture freely suspended in complete IntestiCult growth medium, GFP-expressing *S. Typhimurium* were identifiable attached to the apical surface and within epithelial cells of the organoids by confocal microscopy. Although *S. Typhimurium* is an intestinal pathogen, here we observed GFP-expressing bacteria attached to both abomasum and ileum apical-out organoids (**Figure 10C**).

DISCUSSION

Ruminants are key food-producing animals worldwide, providing a nutrient source to billions of people. Furthermore, dependency upon ruminants as a food source continues to increase in order to meet growing global dietary requirements. Gastrointestinal disease in ruminants is a major concern and accounts for significant economic losses and reduction in production efficiency. It is therefore important that ruminant health and



welfare is improved through prevention and control of disease in order to meet ethical, economic and nutrient demands (Sargison, 2020).

An obvious challenge with studying gastrointestinal host-pathogen interactions *in vivo* is the internal nature of infections and the physical barriers associated with directly observing them. Therefore, a useful advancement for studying such infections is the development of a physiologically relevant *in vitro* model systems that allows experimental interrogation of host and pathogen interactions in fine detail. Stem cell-derived organoids have become a prominent feature of modern cell and tissue biology in recent years, representing *in vitro* cell cultures that retain structural and functional properties of the *in vivo* organ/tissue they represent (Clevers, 2016). To date, organoid cultivation has been achieved for numerous and diverse organs and tissues from different host species. In particular, organoids derived from gastrointestinal tissue have been generated for numerous livestock species, including cattle (Hamilton et al., 2018; Beaumont et al., 2021). However, the vast majority of these have been organoids representing the intestinal tract. Here, we demonstrated the ability to cultivate organoids from gastric and intestinal tissues of a small ruminant host and, to our

knowledge, this is the first demonstration of organoids representing the gastric system of a ruminant.

Following the same protocol and using the same *in vitro* culture conditions, we report the ability to cultivate tissue-specific gastric and intestinal organoids from sheep. By comparing gene expression profiles between tissue and organoids, we found that when grown in identical conditions *in vitro*, stem cells from gastric glands developed into organoids that retained key characteristics associated with abomasum tissue. Stem cells from ileal crypts, on the other hand, developed into organoids which conserved important gene expression profiles associated with the ileum. It is important to note that there are differences in the global transcriptome between organoids and the tissue from which they are derived. This is largely due to the complexity associated with *ex vivo* tissue which contains immune cells, fibroblasts, a microbiome, as well as digested material at the point of collection and this will influence overall gene expression. By contrast, the organoids characterized here specifically represent the epithelium layer of the organ from which they were derived, resulting in a less complex gene expression profile than that associated with their respective whole tissue. Despite this, the cell diversity, self-organising properties and the conserved expression of tissue-specific gene markers associated with organoids makes them the most physiologically representative *in vitro* cell culture systems developed to date.

Ruminants, including cattle, sheep and goats are polygastric, in that they have a four-chambered gastric system. The fourth chamber, the abomasum, is most closely akin to the stomach of monogastric animals. An important differentiating characteristic between abomasum and ileum tissue is the expression of the digestive stomach enzyme pepsinogen in the abomasum (Mostofa et al., 1990). Another digestive protease associated with the abomasum in ruminants is lysozyme, which is highly expressed in this compartment (Stevens and Hume, 1998). Importantly, we found that both pepsinogen and lysozyme are expressed in abomasum organoids and not in ileum organoids. We also found evidence of parietal cells specifically present in abomasum organoids and not ileum organoids. This was indicated by the detection of *CCKBR* mRNA only in abomasum organoids and tissue following transcriptomic analysis. *CCKBR* is a cholecystokinin receptor expressed in the gastric and central nervous systems and more specifically it is associated with parietal cells in the stomach (Kulaksiz et al., 2000; Schmitz et al., 2001; Engevik et al., 2019). Conversely, we also identified genes whose expression was specific to ileum tissue that were also expressed in ileum organoids and not in abomasum organoids. For example, *REG4*, a marker of enteroendocrine cells (specifically enterochromaffin cells) in intestinal epithelia (Gehart et al., 2019) and *SBD2*, an antimicrobial sheep beta-defensin associated with the mucosal surface of small intestinal crypts (Meyerholz et al., 2004) were found to be specifically and abundantly expressed in ileum tissue and organoids and not abomasum. Specific expression of *SBD2* in the intestinal samples indicates this gene plays a role in antimicrobial defence of intestinal crypts, but not in gastric glands. Collectively, these

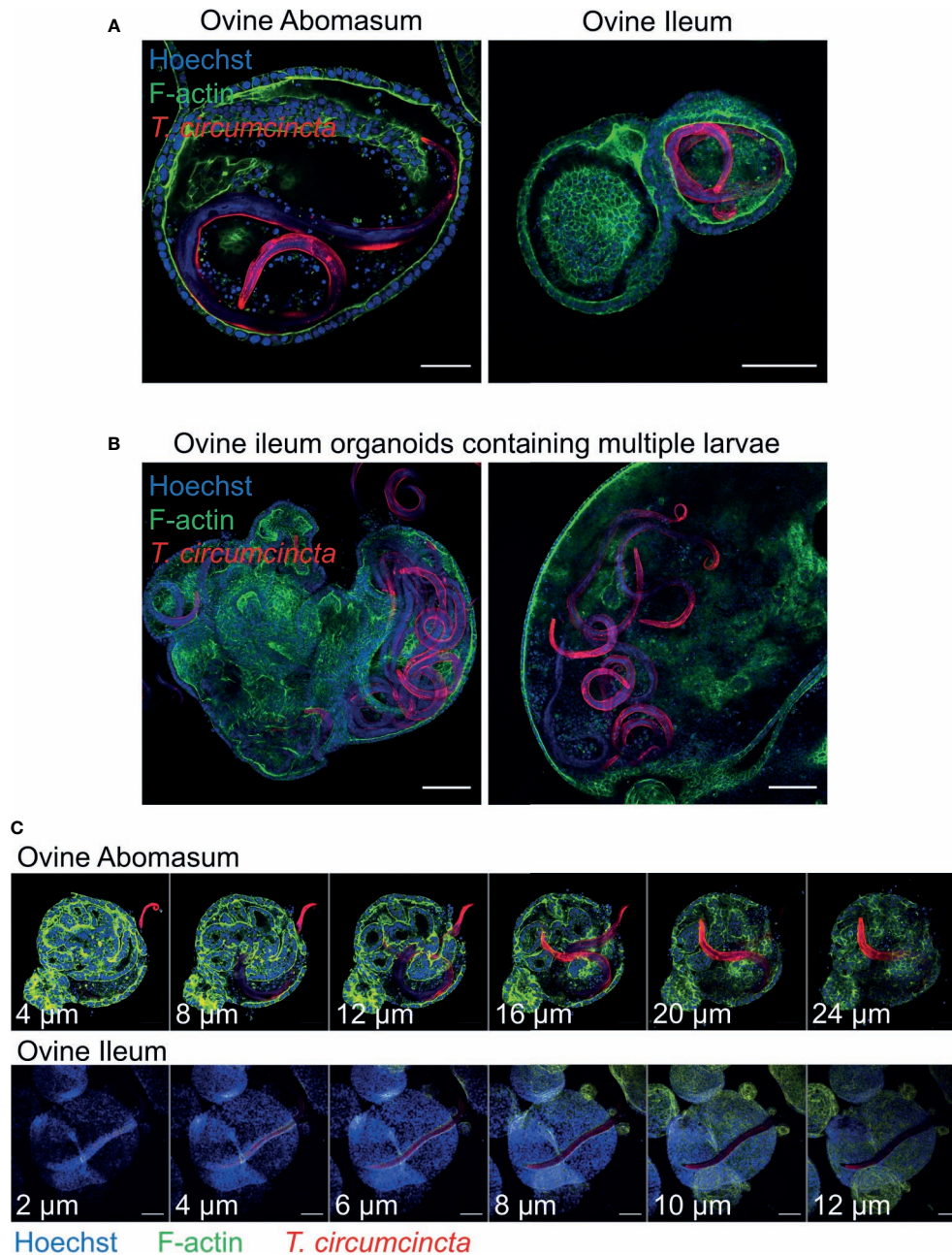


FIGURE 9 | Ovine gastric and intestinal organoids modelling a helminth infection. **(A)** Representative images of ovine abomasum and ileum organoids challenged with the helminth parasite *Teladorsagia circumcincta*. Following 24 hours of co-culture, L3 stage *T. circumcincta* (red) are visible within the lumen of abomasum and ileum organoids. **(B)** Representative images of individual ileum organoids presenting an enlarged lumen containing multiple worms (red). **(C)** Representative Z-stack images showing L3 stage *T. circumcincta* (red) migrating through the epithelial layer in abomasum and ileum organoids. F-actin (green) and Hoescht (blue). Scale bars = 10 μm.

key differences in gene expression indicates that the two different types of organoid are tissue-specific and representative of the tissue from which the stem cells are derived. Intriguingly, we noted that while certain mucin genes are expressed in the organoids, the expression of particular mucins is lower than in their respective tissue. For example, *muc2* shows lower expression in ovine ileum organoids than in ileum tissue. However, *muc2*

expression in ovine ileum organoids is similar to that previously reported for bovine ileum organoids (Hamilton et al., 2018), albeit there was no direct comparison of gene expression in tissue for the bovine ileum organoids. We predict that this lower expression of certain mucin genes in the organoids is due to the sterile system in which they were cultured that does not contain a microbiome, pathogens or food within or passing through the lumen and it

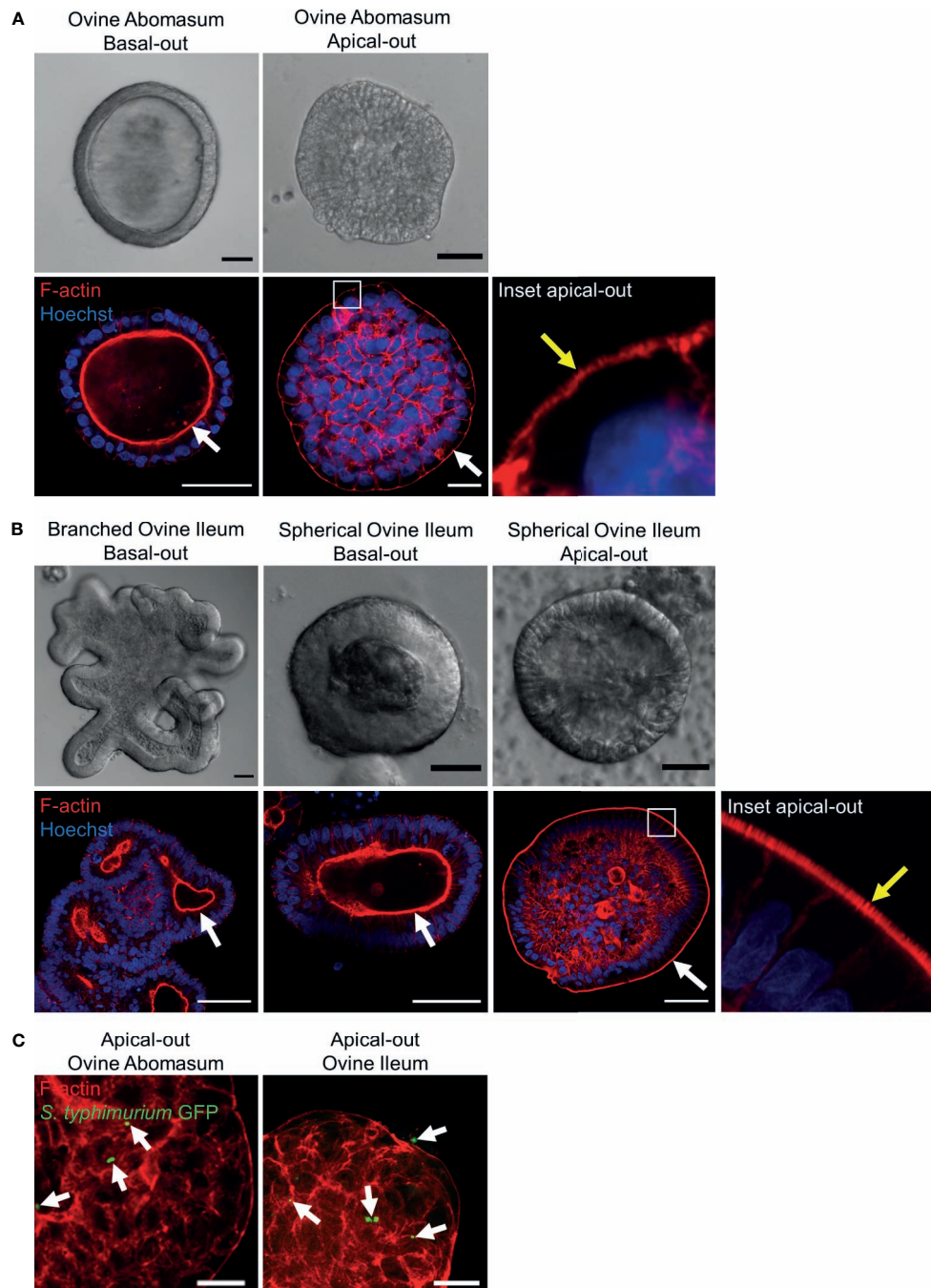


FIGURE 10 | Reverse polarisation of ovine gastric and intestinal organoids for modelling host-pathogen interactions across the apical surface. Basal-out and apical-out abomasum (**A**) and ileum (**B**) organoids imaged by differential interference contrast (top) and confocal immunofluorescence microscopy (bottom). White arrows indicate the F-actin-expressing brush border associated with the apical surface of the epithelia. Yellow arrow in the inset panel indicates microvilli at the externally located brush border in apical-out organoids. (**C**) Cross sections of apical-out abomasum and ileum organoids imaged by confocal microscopy. GFP-expressing *Salmonella enterica* Typhimurium (green), indicated by white arrows, are detectable on the surface of and within epithelial cells. F-actin (red) and Hoechst (blue). Scale bars = 10 μ m.

would be interesting to see if mucin gene expression is increased in ruminant gut organoids in response to these stimuli in future studies. Interestingly, the relatively high *muc1* gene expression associated with abomasum tissue was maintained in

the abomasum organoids, which could be a necessary response to protect the epithelium against secreted host enzymes such as pepsin and lysozyme. We also found that a number of genes used in previous studies as gastrointestinal epithelial markers

(Hamilton et al., 2018) were not detected in our transcriptomic analysis of ileal or abomasal tissue from five individual animals, suggesting these genes are not reliable markers of gastrointestinal epithelia in sheep.

A necessary feature of an organoid cell line is the conservation of gene expression profiles across multiple passages. Transcriptomic analysis of abomasum and ileum organoid samples collected across five consecutive passages revealed that gene expression profiles were consistent. Further analysis of the expression of specific cell markers indicated that the diversity of epithelial cell types was also maintained across multiple passages. That the different organoid types maintain their tissue specificity and cell diversity, as well as the ability to cryopreserve them makes them a robust model that will ensure reproducibility across experiments, as well as reducing the reliance on deriving material from animals and thereby reducing the number of animals used in associated research.

To demonstrate the effectiveness of ovine gastric and intestinal organoids for modelling pathogen infections *in vitro*, we exposed abomasum and ileum organoids to different pathogens and showed they could invade them. It has been recognized that gastrointestinal organoids could represent useful *in vitro* models for studying helminth infections (Duque-Correa et al., 2020). However, to-date this has been limited to applying worm excretory and secretory products to organoids, or growing organoids from helminth-infected mice, as opposed to live host-parasite co-cultures (Eichenberger et al., 2018a; Eichenberger et al., 2018b; Nusse et al., 2018; Luo et al., 2019; Duque-Correa et al., 2020). Here, we applied a very simple method of adding ex-sheathed *T. circumcincta* L3 directly to the growth media of organoids that were embedded in Matrigel. We found that after 24 hours, worms had burrowed through the Matrigel dome and into the lumen of individual organoids. We were also able to capture direct *T. circumcincta* invasion through the epithelium in both abomasum and ileum organoids. Furthermore, motile worms were observed at least 14 days following organoid invasion, demonstrating the potential to prolong parasite survival *in vitro* and to perform more long-term studies on the parasite compared to worms cultured under previous *in vitro* methods (*pers comms*). While invasion across the epithelium, particularly from the basal side, is not necessarily a behaviour associated with *T. circumcincta* larvae, the homing capacity of larvae to migrate to the organoid lumen and interact with the apical surface of the epithelium provides a suitable *in vitro* system for studying host-pathogen interactions between host and helminth. Furthermore, the ability of worms to invade the organoids themselves allows organoids to be infected with the worms following a minimally disruptive method.

Gastrointestinal pathogens that invade the epithelial mucosa commonly interact with the apical surface of epithelial cells. However, the innate polarity of mammalian gastrointestinal organoids grown in Matrigel is with the apical surface on the inside of the organoid. Various approaches have previously been used to expose pathogens to the apical surface of the epithelium, including microinjection directly into the lumen of the organoid, fragmentation of organoids and open-format 2D monolayers. A recent publication also demonstrated the ability to reverse the polarity of human ileum organoids by the removal of Matrigel

and extracellular matrix proteins (Co et al., 2019). This has since been replicated in porcine ileum organoids (Beaumont et al., 2021) and here, we showed that ruminant ileum organoids can also have the polarity reversed following the same method. We also demonstrated that the polarity of gastric organoids can be reversed to an apical-out conformation. The ability to expose the apical surface of gastric and intestinal organoids to the culture supernatant facilitates direct interaction of the organoids with microbes, as we showed here by infecting apical-out organoids with *S. Typhimurium*. Since this method does not require the use of specialist equipment to administer pathogens into a central organoid lumen, this makes modelling host-pathogen infections *in vitro* significantly more practical.

In summary, the results from this study demonstrate the ability to isolate stem cells from gastric glands and crypts of the sheep abomasum and intestine, respectively and show that they differentiate into tissue-specific organoids when grown under identical conditions. The robustness of both gastric and intestinal organoids from sheep was demonstrated by showing that tissue-specific gene expression is maintained across multiple passages. Finally, both gastric and intestinal sheep organoids can be invaded by important bacterial and parasitic pathogens and they therefore represent a useful tool for modelling host-pathogen interactions.

DATA AVAILABILITY STATEMENT

The transcriptomic datasets presented here are available at the NCBI database accession number PRJNA736945. The web link for the database is <https://www.ncbi.nlm.nih.gov/sra/?term=PRJNA736945>.

ETHICS STATEMENT

Ethical review and approval was not required for the animal study because no animal was killed for the purposes of this study and all animal material was derived from animals post-mortem, from animals used in separate trials. No procedures were performed on live animals for the purposes of this study.

AUTHOR CONTRIBUTIONS

DS, DP, EI and TM conceived the study. All authors designed the research. DS, DP, AB, KH, MF, AC and CC-U performed research. DS, DP and SB analysed data. DS and DP wrote the paper with contributions from all authors. All authors contributed to the article and approved the submitted version.

FUNDING

The work was supported in part by Moredun Foundation Research fellowships awarded to DP and DS. AB was supported by funding from the Moredun Innovation fund. KS, SB, EI, AN and TM gratefully receive funding from the Scottish Government

Rural and Environment Science and Analytical Services (RESAS). KH is supported by an Industrial Partnership PhD studentship funded by the University of Glasgow, Moredun Foundation and Pentlands Science Park, UK. MS and CC-U acknowledge funding from the Biotechnology & Biological Sciences Research Council via the Institute Strategic Programme on Control of Infectious Diseases (BB/P013740/1) and its constituent project BBS/E/D/20002173.

ACKNOWLEDGMENTS

We would like to thank Leigh Andrews, Alison Morrison and Dave Bartley, Moredun Research Institute, UK, for their help and in the provision of parasite material and the Bioservices Unit, Moredun Research Institute, for expert care of the animals. We would also like to express our gratitude to Dr Prerna Vohra at the University of Edinburgh for their advice on the experimental infection of organoids with *S. Typhimurium* and for generation of the ST4/74 pFPV25.1 strain in a prior study.

SUPPLEMENTARY MATERIAL

The Supplementary Material for this article can be found online at: <https://www.frontiersin.org/articles/10.3389/fcimb.2021.733811/full#supplementary-material>

REFERENCES

- Barker, N., Huch, M., Kujala, P., van de Wetering, M., Snippert, H. J., van Es, J. H., et al. (2010). Lgr5(+ve) Stem Cells Drive Self-Renewal in the Stomach and Build Long-Lived Gastric Units *In Vitro*. *Cell Stem Cell* 6, 25–36. doi: 10.1016/j.stem.2009.11.013
- Barker, N., van Es, J. H., Kuipers, J., Kujala, P., van den Born, M., Cozijnsen, M., et al. (2007). Identification of Stem Cells in Small Intestine and Colon by Marker Gene Lgr5. *Nature* 449, 1003–1007. doi: 10.1038/nature06196
- Beaumont, M., Blanc, F., Cherbuy, C., Egidy, G., Giuffra, E., Lacroix-Lamandé, S., et al. (2021). Intestinal Organoids in Farm Animals. *Vet. Res.* 52, 33. doi: 10.1186/s13567-021-00909-x
- Bekelaar, K., Waghorn, T., Tavendale, M., McKenzie, C., and Leathwick, D. (2019). Abomasal Nematode Species Differ in Their *In Vitro* Response to Exsheathment Triggers. *Parasitol. Res.* 118, 707–710. doi: 10.1007/s00436-018-6183-1
- Bray, N. L., Pimentel, H., Melsted, P., and Pachter, L. (2016). Near-Optimal Probabilistic RNA-Seq Quantification. *Nat. Biotechnol.* 34, 525–527. doi: 10.1038/nbt.3519
- Clevers, H. (2016). Modeling Development and Disease With Organoids. *Cell* 165, 1586–1597. doi: 10.1016/j.cell.2016.05.082
- Co, J. Y., Margalef-Català, M., Li, X., Mah, A. T., Kuo, C. J., Monack, D. M., et al. (2019). Controlling Epithelial Polarity: A Human Enteroid Model for Host-Pathogen Interactions. *Cell Rep.* 26, 2509–2520.e4. doi: 10.1016/j.celrep.2019.01.108
- Dinh, P. T. Y., Knoblauch, M., and Elling, A. A. (2014). Nondestructive Imaging of Plant-Parasitic Nematode Development and Host Response to Nematode Pathogenesis. *Phytopathology* 104, 497–506. doi: 10.1094/PHYTO-08-13-0240-R
- Duque-Correa, M. A., Maizels, R. M., Grencis, R. K., and Berriman, M. (2020). Organoids – New Models for Host–Helminth Interactions. *Trends Parasitol.* 36, 170–181. doi: 10.1016/j.pt.2019.10.013
- Eichenberger, R. M., Ryan, S., Jones, L., Buitrago, G., Polster, R., Montes de Oca, M., et al. (2018a). Hookworm Secreted Extracellular Vesicles Interact With Host Cells and Prevent Inducible Colitis in Mice. *Front. Immunol.* 9, 850. doi: 10.3389/fimmu.2018.00850
- Eichenberger, R. M., Talukder, M. H., Field, M. A., Wangchuk, P., Giacomini, P., Loukas, A., et al. (2018b). Characterization of Trichuris Muris Secreted Proteins and Extracellular Vesicles Provides New Insights Into Host–Parasite Communication. *J. Extracell. Vesicles* 7, 1428004. doi: 10.1080/20013078.2018.1428004
- Ellis, S., Matthews, J. B., Shaw, D. J., Paterson, S., McWilliam, H. E. G., Inglis, N. F., et al. (2014). Ovine IgA-Reactive Proteins From Teladorsagia Circumcincta Infective Larvae. *Int. J. Parasitol.* 44, 743–750. doi: 10.1016/j.ijpara.2014.05.007
- Engelvik, A. C., Kaji, I., and Goldenring, J. R. (2019). The Physiology of the Gastric Parietal Cell. *Physiol. Rev.* 100, 573–602. doi: 10.1152/physrev.00016.2019
- Finlay, B. B., and Falkow, S. (1990). Salmonella Interactions With Polarized Human Intestinal Caco-2 Epithelial Cells. *J. Infect. Dis.* 162, 1096–1106. doi: 10.1093/infdis/162.5.1096
- Gehart, H., van Es, J. H., Hamer, K., Beumer, J., Kretzschmar, K., Dekkers, J. F., et al. (2019). Identification of Enterendocrine Regulators by Real-Time Single-Cell Differentiation Mapping. *Cell* 176, 1158–1173.e16. doi: 10.1016/j.cell.2018.12.029
- Hamilton, C. A., Young, R., Jayaraman, S., Sehgal, A., Paxton, E., Thomson, S., et al. (2018). Development of *In Vitro* Enteroids Derived From Bovine Small Intestinal Crypts. *Vet. Res.* 49, 54. doi: 10.1186/s13567-018-0547-5
- Heredia, N., and García, S. (2018). Animals as Sources of Food-Borne Pathogens: A Review. *Anim. Nutr.* 4, 250–255. doi: 10.1016/j.aninu.2018.04.006
- Joshi, N. A., and Fass, J. N. (2011). Sickle: A Sliding-Window, Adaptive, Quality-Based Trimming Tool for FastQ Files (Version 1.33). Available at: <https://github.com/najoshi/sickle>.
- Kar, S. K., Wells, J. M., Ellen, E. D., te Pas, M. F. W., Madsen, O., Groenen, M. A. M., et al. (2021). Organoids: A Promising New *In Vitro* Platform in Livestock and Veterinary Research. *Vet. Res.* 52, 43. doi: 10.1186/s13567-021-00904-2
- Kulaksiz, H., Arnold, R., Göke, B., Maronde, E., Meyer, M., Fahrenholz, F., et al. (2000). Expression and Cell-Specific Localization of the Cholecystokinin B/gastrin Receptor in the Human Stomach. *Cell Tissue Res.* 299, 289–298. doi: 10.1007/s004410050027

- Luo, X.-C., Chen, Z.-H., Xue, J.-B., Zhao, D.-X., Lu, C., Li, Y.-H., et al. (2019). Infection by the Parasitic Helminth *Trichinella Spiralis* Activates a Tas2r-Mediated Signaling Pathway in Intestinal Tuft Cells. *Proc. Natl. Acad. Sci. U. S. A.* 116, 5564–5569. doi: 10.1073/pnas.1812901116
- Marini, F., and Binder, H. (2019). Pcaexplorer: An R/Bioconductor Package for Interacting With RNA-Seq Principal Components. *BMC Bioinf.* 20, 331. doi: 10.1186/s12859-019-2879-1
- Martin, M. (2011). Cutadapt Removes Adapter Sequences From High-Throughput Sequencing Reads. *EMBnet. J.* 17, 10–12. doi: 10.14806/ej.17.1.200
- McSorley, H. J., Hewitson, J. P., and Maizels, R. M. (2013). Immunomodulation by Helminth Parasites: Defining Mechanisms and Mediators. *Int. J. Parasitol.* 43, 301–310. doi: 10.1016/j.ijpara.2012.11.011
- Meyerholz, D. K., Gallup, J. M., Grubor, B. M., Evans, R. B., Tack, B. F., McCray, P. B. Jr., et al. (2004). Developmental Expression and Distribution of Sheep β -Defensin-2. *Dev. Comp. Immunol.* 28, 171–178. doi: 10.1016/S0145-305X(03)00105-8
- Mostofa, M., McKELLAR, Q. A., and Eckersall, P. D. (1990). Comparison of Pepsinogen Forms in Cattle, Sheep and Goats. *Res. Vet. Sci.* 48, 33–37. doi: 10.1016/S0034-5288(18)31505-4
- Nieuwhof, G. J., and Bishop, S. C. (2005). Costs of the Major Endemic Diseases of Sheep in Great Britain and the Potential Benefits of Reduction in Disease Impact. *Anim. Sci.* 81, 23–29. doi: 10.1079/ASC41010023
- Nusse, Y. M., Savage, A. K., Marangoni, P., Rosendahl-Huber, A. K. M., Landman, T. A., de Sauvage, F. J., et al. (2018). Parasitic Helminths Induce Fetal-Like Reversion in the Intestinal Stem Cell Niche. *Nature* 559, 109–113. doi: 10.1038/s41586-018-0257-1
- Richardson, E. J., Limaye, B., Inamdar, H., Datta, A., Manjari, K. S., Pullinger, G. D., et al. (2011). Genome Sequences of *Salmonella* Enterica Serovar Typhimurium, Choleraesuis, Dublin, and Gallinarum Strains of Well-Defined Virulence in Food-Producing Animals. *J. Bacteriol.* 193, 3162–3163. doi: 10.1128/JB.00394-11
- Roeber, F., Jex, A. R., and Gasser, R. B. (2013). Impact of Gastrointestinal Parasitic Nematodes of Sheep, and the Role of Advanced Molecular Tools for Exploring Epidemiology and Drug Resistance - An Australian Perspective. *Parasit. Vectors* 6, 153. doi: 10.1186/1756-3305-6-153
- Sargison, N. D. (2020). The Critical Importance of Planned Small Ruminant Livestock Health and Production in Addressing Global Challenges Surrounding Food Production and Poverty Alleviation. *New Z. Vet. J.* 68, 136–144. doi: 10.1080/00480169.2020.1719373
- Sato, T., Vries, R. G., Snippert, H. J., van de Wetering, M., Barker, N., Stange, D. E., et al. (2009). Single Lgr5 Stem Cells Build Crypt-Villus Structures *In Vitro* Without a Mesenchymal Niche. *Nature* 459, 262–265. doi: 10.1038/nature07935
- Schmitz, F., Göke, M. N., Otte, J.-M., Schrader, H., Reimann, B., Kruse, M.-L., et al. (2001). Cellular Expression of CCK-A and CCK-B/gastrin Receptors in Human Gastric Mucosa. *Regul. Peptides* 102, 101–110. doi: 10.1016/S0167-0115(01)00307-X
- Stear, M. J., Bishop, S. C., Doligalska, M., Duncan, J. L., Holmes, P. H., Irvine, J., et al. (1995). Regulation of Egg Production, Worm Burden, Worm Length and Worm Fecundity by Host Responses in Sheep Infected With *Ostertagia Circumcincta*. *Parasite Immunol.* 17, 643–652. doi: 10.1111/j.1365-3024.1995.tb01010.x
- Stear, M. J., Bishop, S. C., Henderson, N. G., and Scott, I. (2003). A Key Mechanism of Pathogenesis in Sheep Infected With the Nematode *Teladorsagia Circumcincta*. *Anim. Health Res. Rev.* 4, 45–52. doi: 10.1079/ahrr200351
- Stevens, C. E., and Hume, I. D. (1998). Contributions of Microbes in Vertebrate Gastrointestinal Tract to Production and Conservation of Nutrients. *Physiol. Rev.* 78, 393–427. doi: 10.1152/physrev.1998.78.2.393
- Uzzau, S., Leori, G. S., Petrucci, V., Watson, P. R., Schianchi, G., Bacciu, D., et al. (2001). *Salmonella* Enterica Serovar-Host Specificity Does Not Correlate With the Magnitude of Intestinal Invasion in Sheep. *Infect. Immun.* 69, 3092–3099. doi: 10.1128/IAI.69.5.3092-3099.2001
- Valdivia, R. H., and Falkow, S. (1996). Bacterial Genetics by Flow Cytometry: Rapid Isolation of *Salmonella* Typhimurium Acid-Inducible Promoters by Differential Fluorescence Induction. *Mol. Microbiol.* 22, 367–378. doi: 10.1046/j.1365-2958.1996.00120.x
- Vohra, P., Vrettou, C., Hope, J. C., Hopkins, J., and Stevens, M. P. (2019). Nature and Consequences of Interactions Between *Salmonella* Enterica Serovar Dublin and Host Cells in Cattle. *Vet. Res.* 50, 99. doi: 10.1186/s13567-019-0720-5
- Xiao, S., and Zhou, L. (2020). Gastric Stem Cells: Physiological and Pathological Perspectives. *Front. Cell Dev. Biol.* 8, 571536. doi: 10.3389/fcell.2020.571536

Conflict of Interest: The authors declare that the research was conducted in the absence of any commercial or financial relationships that could be construed as a potential conflict of interest.

Publisher's Note: All claims expressed in this article are solely those of the authors and do not necessarily represent those of their affiliated organizations, or those of the publisher, the editors and the reviewers. Any product that may be evaluated in this article, or claim that may be made by its manufacturer, is not guaranteed or endorsed by the publisher.

Copyright © 2021 Smith, Price, Burrells, Faber, Hildersley, Chintoan-Uta, Chapuis, Stevens, Stevenson, Burgess, Innes, Nisbet and McNeilly. This is an open-access article distributed under the terms of the Creative Commons Attribution License (CC BY). The use, distribution or reproduction in other forums is permitted, provided the original author(s) and the copyright owner(s) are credited and that the original publication in this journal is cited, in accordance with accepted academic practice. No use, distribution or reproduction is permitted which does not comply with these terms.



Patient-Derived Organoids in Precision Medicine: Drug Screening, Organoid-on-a-Chip and Living Organoid Biobank

Zilong Zhou¹, Lele Cong^{2*} and Xianling Cong^{2*}

¹ Biobank, China-Japan Union Hospital of Jilin University, Changchun, China, ² Department of Dermatology, China-Japan Union Hospital of Jilin University, Changchun, China

OPEN ACCESS

Edited by:

Daniel P. Bezerra,
Oswaldo Cruz Foundation (FIOCRUZ),
Brazil

Reviewed by:

Eliane Gouvêa Oliveira-Barros,
Juiz de Fora Federal University, Brazil
Federico La Manna,
University of Bern, Switzerland
Lejia Sun,
Nanjing Medical University, China

*Correspondence:

Xianling Cong
congxl@jlu.edu.cn
Lele Cong
congl18@mails.jlu.edu.cn

Specialty section:

This article was submitted to
Molecular and Cellular Oncology,
a section of the journal
Frontiers in Oncology

Received: 21 August 2021

Accepted: 13 December 2021

Published: 30 December 2021

Citation:

Zhou Z, Cong L and Cong X
(2021) Patient-Derived Organoids
in Precision Medicine: Drug
Screening, Organoid-on-a-Chip
and Living Organoid Biobank.
Front. Oncol. 11:762184.
doi: 10.3389/fonc.2021.762184

Organoids are *in vitro* self-assembling, organ-like, three-dimensional cellular structures that stably retain key characteristics of the respective organs. Organoids can be generated from healthy or pathological tissues derived from patients. Cancer organoid culture platforms have several advantages, including conservation of the cellular composition that captures the heterogeneity and pharmacotypic signatures of the parental tumor. This platform has provided new opportunities to fill the gap between cancer research and clinical outcomes. Clinical trials have been performed using patient-derived organoids (PDO) as a tool for personalized medical decisions to predict patients' responses to therapeutic regimens and potentially improve treatment outcomes. Living organoid biobanks encompassing several cancer types have been established, providing a representative collection of well-characterized models that will facilitate drug development. In this review, we highlight recent developments in the generation of organoid cultures and PDO biobanks, in preclinical drug discovery, and methods to design a functional organoid-on-a-chip combined with microfluidic. In addition, we discuss the advantages as well as limitations of human organoids in patient-specific therapy and highlight possible future directions.

Keywords: organoids, patient-derived organoid, living biobanks, microfluidics, drug screening, organoids-on-a-chip

INTRODUCTION

Cancer is a heterogeneous disease that includes a complex ecosystem of diverse cell types. Apart from neoplastic cells, tumors include cancer-associated stromal cells, growth factors and metabolites in the microenvironment, which have profound effects on tumor cell growth, invasion ability, and drug response (1). Therefore, these microenvironmental elements are critical in the development of pathologically relevant culture models to study cancer progression. For decades, preclinical cancer research has relied on cell lines as *in vitro* representations of tumor heterogeneity. Traditional drug development is carried out *via* two-dimensional (2D) tumor cell line cultures and transplantation of patient-derived tumor xenografts in animals (2). However, there are several drawbacks in these

approaches. For instance, 2D cell line cultures poorly reflect the native microenvironment of tumor tissue, and after many passages in culture, cancer cell lines lose the genetic heterogeneity of parental tumors because of clonal selection (3, 4). This contributes to the low success rate of newly developed drugs in clinical trials (5, 6). Organoids are self-organizing, three-dimensional (3D) structures that are grown *in vitro* from stem cells, and resemble the organ from which the cells were derived (2, 7). The starting cells could be adult stem cells, cancer stem cell, or cancer tissue-derived spheroids. Organoids preserve many structural and functional features such as cell composition and tissue architecture of their corresponding *in vivo* organs.

Clevers et al. developed crypt-villus organoids from a single Lgr5⁺ stem cell using the WENR (Wnt3a+EGF+Noggin+R-spondin-1) protocol that allowed long-term culture and differentiation of primary epithelial cells isolated from intestinal tissue (7–9). The key components of the culture medium included the ligand of LGR5 R-spondin-1, the Wnt pathway agonist, epidermal growth factor (EGF), and bone morphogenetic protein pathway inhibitor Noggin. In addition, the anokis antagonist Rho-kinase inhibitor Y-27632 is a key factor for improving the success rate of organoid culture. The genotype and genetics of organoids derived from adult stem cells are consistent with those of their parental tissues and remain stable for a long time (10, 11). Another strategy involving the use of pluripotent stem cells (PSCs) has been applied to generate organoids resembling the brain (12), intestine (13), kidney (14, 15) and retina (16, 17).

From 2009 to 2021, use of organoid technology has been rapidly increasing in cancer research, especially for therapeutic screening and precision medicine (18–20). 3D organoid culture systems provide efficient preclinical cancer models of patient-derived organoids (PDOs), can better mimic the components of a tumor tissue, and can be efficiently established from patient specimens (18, 21, 22). The intratumor diversity in PDOs captures tumor heterogeneity at the single cell level and provides a valuable resource for cancer research. PDO cultures can be used to expanded over time while still retaining the mutational profiles of the parental tumors (23). On the contrary, traditional long-term 2D cultures have very high genomic instability. The highly conserved genomic landscape of PDOs is crucial to perform genotype-phenotype correlation analysis and to assess patient's sensitivity to treatment. Although 2D culture is cheaper and relatively easy to maintain, the success rate of drug screening using 2D cultured tumor cells is very low, and the results are often conflicting. This may be because the 2D model cannot accurately reflect and maintain the tumor characteristics and complex cell-extracellular matrix interactions. Newly developed organoid culture platforms enable routine primary culture of resected human tumor tissues (24, 25). Numerous PDOs have been established from tissues derived from patients' tumors, including colon (9), liver (25), gastric (26), lung (27), bladder (28), breast (29), and pancreatic cancers (30, 31) and head and neck squamous cell carcinoma (32). PDOs can be used to generate a well-annotated living cancer biobank as a resource for drug discovery and

personalized therapy (33, 34). Although there are established PDOs generated from epithelial tissues, PDOs generated from non-epithelial cells are still rare. Sarcomas, malignant neoplasms originating from mesenchymal cells, have a high level of histopathological heterogeneity (35). Currently, several 3D sarcoma models with or without scaffold have been established from osteosarcoma, chondrosarcoma, Ewing sarcoma and soft tissue sarcoma (36–38). However, a standard protocol to generate sarcoma-derived organoid models has not yet been established. Therefore, we expect more advanced innovations to break through the bottleneck of developing sarcoma organoid culture and applications in the future, such as capturing the biological characteristics of native sarcomas in drug screening.

The tumor microenvironment (TME) includes vascular structures, extracellular matrix, and immune cell components, including lymphocytes, macrophages, myeloid-derived suppressor cells, dendritic cells, and natural killer cells (24). Cellular interactions in TME often determine drug response and the fate of the tumor. Functionally, the TME provides conditions for tumor progression and metastasis (39, 40). The recently developed PDO cultures provide an outstanding system to model patient-specific tumor-immune interactions. For instance, the co-culture of patient-derived cancer-associated fibroblasts and peripheral blood lymphocytes with pancreatic cancer organoids has been used to assess lymphocyte migration towards organoids in Matrigel and the activation status of myofibroblast-like cancer-associated fibroblasts (41). Co-culture of non-small-cell lung cancer and colorectal cancer organoids with autologous peripheral blood lymphocytes generates tumor-reactive T cells, and these T cells have the ability to kill tumor cells derived from the parental tumor tissue (20). In addition, culturing patient-derived organotypic tumor spheroids in microfluidic devices preserve endogenous immune cells, and this approach can model the tumor's response to PD-1 blockade.

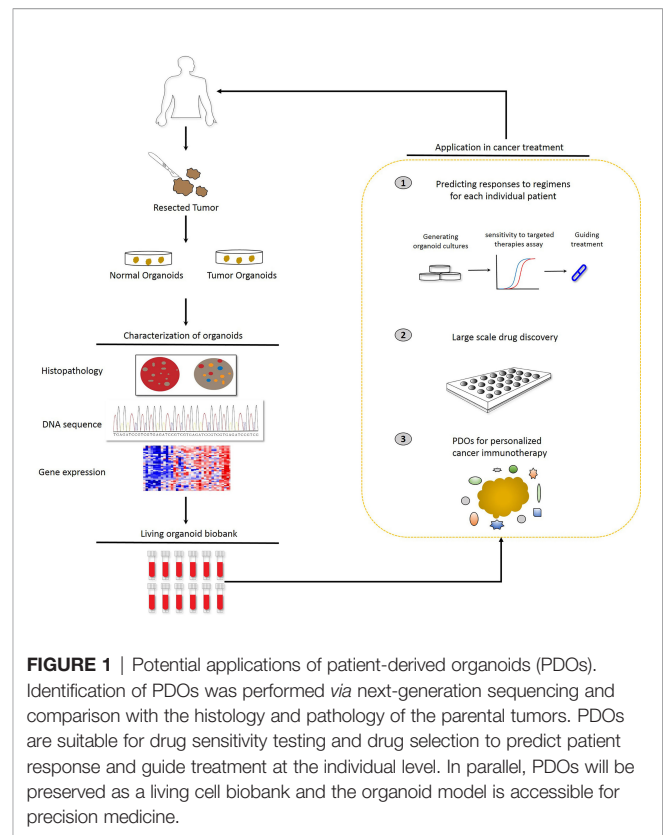
With the advancement of technology, many highly reproducible and controllable approaches have been developed to generate the microenvironment of human cancer bioengineered 3D organoid platforms that closely mimic *in vivo* tumor conditions (42). These platforms, such as organ-on-a-chip, can offer individual empirical data to better determine a patient's drug response (43). Organ-on-a-chip is a multi-channel microfluidic cell culture device that includes multiple cell types to model the structure and function of the parental tissue (42, 44). Organoids develop from self-organizing stem cells to recapitulate the key physiological and pathological characteristics of their parental tissues. By integrating living human self-organizing organoids with organ-on-a-chip engineering, physiologically relevant microenvironments can be generated, and the resulting organoids-on-a-chip platform can combine the best features of both approaches to provide a model truly representing the complex characteristics of cancer progression (45). As a strategic integration, organoid-on-a-chip technology provides a superior *in vitro* platform for preclinical screening of chemotherapy drugs and predicting outcomes of radiotherapy and chemotherapy regimens.

In this review, we introduce the experimental approach of deriving organoids from adult stem cells, which can be generated directly from the epithelium of organs and explore how organoid cultures serve as a basis for developing a variety of microfluidic organ-on-a-chip platforms for clinical applications. In addition, we focus on patient-derived tumor organoids (PDTOs) in individualized cancer treatment and illustrate the advantages and limitations of PDTO biobanks as a resource for preclinical models and in enabling precision medicine (**Figure 1**).

FRONTIER APPLICATION OF PDOs

PDOs in Precision Medicine

Currently, patients with similar cancer types receive cognate treatments, but these treatments do not always achieve a uniform outcome across patient populations. Moreover, regardless of whether patients have undergone neoadjuvant chemoradiation or surgical treatment, individual drug response cannot be tested prior to treatment. In addition, recurring tumors may differ from the initial surgically resected tumors. Despite obvious interpatient heterogeneity, most clinical drugs are not developed using molecular biomarkers, except for some that target specific pathway mutations. To personalize cancer treatment, individual drug sensitivity assays with PDOs are progressively improving by recapitulating more physiological and pathological characteristics of tumors. Therefore, PDOs should be applied to drug screening and guide clinical treatment to improve prognosis. Traditionally, precision therapies have been performed by using mutational biomarkers; however, these biomarkers often lack a considerable tumor mass due to intratumor heterogeneity. As a result, treatments targeting these markers do not always elicit desirable patient responses. PDO models have been utilized in drug discovery (21) to explore the cytotoxicity of therapeutic candidates (46–49) and to enable personalized cancer treatments (18, 50). Recent studies on the generation and use of PDOs are summarized in **Table 1** (18, 21, 27–29, 33, 51–62). Using 19 colorectal cancer organoid lines, Van de Wetering et al. screened 83 drugs, including targeted inhibitors (18). Ooft et al. used PDOs to predict the response to chemotherapy in patients with metastatic colorectal cancer, and these results offer a chance to assess the reproducibility and applicability of organoid-based drug screening (63). Sachs et al. tested the response of six drugs targeting the human EGF receptor signaling pathway in 28 organoid lines and confirmed that breast cancer organoids serve as a superior physiologically relevant model for *in vitro* drug screening (29). Similarly, Yan et al. performed large-scale drug sensitivity screening using 37 anticancer compounds in nine gastric cancer organoids derived from seven patients (33). Vlachogiannis et al. applied patient-derived cancer organoids to predict the clinical outcomes of gastrointestinal cancer patients undergoing chemotherapy, targeted drug therapy and immunotherapy (64). By comparative analysis of the drug sensitivity of patients with metastatic gastrointestinal cancers and that of corresponding PDO models, they showed that the PDO model had a very high accuracy in predicting drug



responses (64). Lee et al. screened 50 drugs in organoid models of bladder cancer, expressing the fibroblast growth factor (FGF) receptor, mitogen-activated protein kinase, and the mechanistic target of rapamycin inhibitors (28). Using 27 liver cancer organoid lines from five patients, Li et al. screened 129 cancer drugs and demonstrated that a subset of drugs induced a uniform toxic response across patient samples while the response to other drugs was heterogeneous (60). Pauli et al. performed a complete genomic analysis of four patients and high-throughput screening of 160 drugs using cancer organoids, and showed that 3D cultures are better than 2D cultures in identifying suitable individual or combination drugs for individual patients (21). These cancer organoids were derived from patients with metastatic and primary tumors, including prostate, bladder/ureter, kidney, colon/rectum, brain, pancreas, breast, stomach and esophagus, soft tissue, small intestine, lung, liver, adrenal gland, uterus, ovary, appendix and thyroid cancer. Brandenburg et al. reported an automated high-throughput screening system based on organoid cultures that could analyze thousands of individual gastrointestinal organoids within a polymer-hydrogel substrate (65). This 3D culture system significantly reduced the consumption of expansion reagents and was suitable for large-scale drug screening. Kim et al. reported an effective method for generating a living biobank of 80 lung cancer organoids (27). The drug responses of these organoid lines were consistent with interpatient and intratumor heterogeneity, indicating that cancer organoids are physiologically relevant drug screening platforms. Yao et al. established a living

TABLE 1 | Application of drug screening with organoid culture platforms.

Cancer Type	Organoid Type	Library	Compounds Tested	Cases Tested	Assay Conditions	Refs
Bladder	CSC-derived	Target-known inhibitors + chemotherapy drugs	50	11	Matrigel	(28)
Breast	CSC-derived	EGFR/AKT/mTORC pathway inhibitors	6	28	BME	(29)
Breast	CSC-derived	CDK4/6 and BCL2 signaling pathway inhibitors	3	3	BME	(51)
Breast	CSC-derived	Docetaxel, Doxorubicin P4HA inhibitor	3	1	BME	(52)
Colorectal	CSC-derived	Target-known inhibitors + chemotherapy drugs	83	19	BME	(18)
Colorectal	CSC-derived	Target-know inhibitor + chemotherapy drugs	8	19	Matrigel	(53)
Colorectal	CTOS	Target-known inhibitors	71	1	W/O Matrix	(54)
Colorectal	CTOS	Target-known inhibitors + FDA-approved drugs	2427	2	W/O Matrix	(55)
Endometrium	CTOS organoids	Target-known inhibitors	79	5	W/O Matrix	(56)
Endometrium	CSC-derived	Menin-MLL complex inhibitor	1/276	4	Matrigel	(57)
Gastric	CSC-derived	Approved anti-cancer drugs	37	7	Matrigel	(33)
Glioblastoma	CSC-derived	EGFR/PDGFR/Topoisomerase-II inhibitors and p53 pathway activator	4	3	Collagen-hyaluronic acid bioink	(58)
Glioblastoma	CSC-derived	Target-known inhibitors	64	2	Matrigel	(59)
Liver	CSC-derived	NCI-Approved Oncology Drugs Set VII	129	5	Matrigel	(60)
Liver	CSC-derived	Target-know inhibitor + chemotherapy drugs	29	5	BME	(61)
Lung	CSC-derived	PARP /c-Met /EGFR inhibitor + Docetaxel	4	6	Matrigel	(27)
Ovarian	CSC-derived	Target-known inhibitors + chemotherapy drugs	22	10	Matrigel	(62)
Various	CSC-derived	chemotherapy drugs and targeted agents under clinical development	160 + 120	4	Matrigel	(21)

CSC, cancer stem cell; CTOS, cancer tissue-originated spheroid; BME, basement membrane extract. Chemo drugs; W/O, Water/Oil.

organoid biobank of locally advanced rectal cancer and showed that PDOs could predict chemoradiation responses in patients (66). Wang et al. reported a blinded study that found a PDTO model to be accurate in predicting chemotherapy responses in stage IV colorectal cancer (67).

Monoclonal antibodies that target immune checkpoints, such as anti-CTLA4 and anti-PD-1, have been used to enhance anti-tumor T cell responses, increasing the overall survival rate in patients. Nigris et al. reported that PDOs were able to predict the patient's response to PD-1/PD-L1 inhibitor therapy in primary chordoma (68). Jenkins et al. established a microfluidic culture of an organoid tumor spheroid platform to test the response of patient-derived tumors to immune checkpoint blockade treatment (69). Using a PDO/immune cell co-culture model, Zavros et al. demonstrated that rapamycin blocked the transcriptional regulation of PD-L1 by GLI1 and GLI2, and concluded that it is a valid model to assess immunosuppressive myeloid-derived suppressor cell function (70). These results show that gastric cancer organoids and immune cell co-culture systems can be used to predict patient response to immune checkpoint blockade and CAR-T cell infusion.

A search of ClinicalTrials.gov database from May 2015 to June 2021 revealed organoid-related clinical trials with the purpose of evaluating the probability of PDTO models to accurately predict patients' responses or resistance to existing chemotherapeutic agents (Table 2). These clinical trials mainly focused on the individualized treatment of patients with various tumors and showed numerous advantages of using PDOs in precisely testing the corresponding patient's sensitivity to chemotherapy and targeted therapy. In addition, an increasing number of PDO-based clinical trials in recent years suggests a trend towards an increasing reliance on PDOs for clinical

decision making in personalized medicine. Nevertheless, clinical trials based on PDO models are still focused on tumors with relatively high morbidity and mortality, such as colorectal cancer, lung cancer, glioma, breast cancer, liver cancer, and pancreatic cancer. Moreover, PDOs are mainly derived from epithelial cells, and organoid culture techniques of non-epithelial cells are relatively immature and cannot be used in clinical trials.

Organoid culture can partially reveal interpatient heterogeneity in terms of sensitivity to anti-cancer drugs (71). Thus, it is critical to develop an organoid model system to predict drug sensitivity to estimate diversification in drug responses and reduce misguided selection of remedies in clinical trials. In addition, PDOs can be generated from various cancer patients and exhibit the intratumoral heterogeneity of the parental tumors. Herein, we have emphasized that organoid culture systems, especially PDOs, are suitable for precision medicine, including drug screening and prediction of individual patient's response. As described above, colorectal cancer, breast cancer, gastric cancer, bladder cancer, liver cancer, and lung cancer organoids have been reported for drug screening and sensitivity. However, the application of conventional PDO models in precision medicine has numerous challenges. Although most tumor PDOs recapitulate the genetic composition of the parental tumor at early passages, the extent of genetic drift or the proportion of genetically stable cells in organoids at later passages has not been fully characterized (21). In addition, the lack of endogenous tumor-associated stromal components remains another key limitation of current organoid methods. Thus, the current PDO model is still unable to reflect all the characteristics of an organ. Although we have many urgent challenges to overcome, the continued development of PDOs incorporating immune and other stromal components may ultimately help actualize the promise of precision cancer therapies.

TABLE 2 | Summary of Clinical Trials of drug sensitivity with organoid methods.

Tissue Type	Source of Organoids	Aim of study	Estimated Enrollment	First Posted	Sponsors/ Collaborators	ClinicalTrials.gov Identifier/Status
Astrocytoma	iPSC from patients' peripheral blood mononuclear cell	To demonstrate that brain organoids can be used to test the impact of genetic mutants.	20	June 3, 2019	Sponsors and Collaborators: Assistance Publique Hopitaux De Marseille	NCT03971812/ Unknown
Breast cancer	breast cancer organ platform	Sensitivity Detection and Drug Resistance Mechanism (29 compounds)	300	April 24, 2019	Sponsor and Collaborators: Xijing Hospital, Xi'an, China	NCT03925233/ Enrolling by invitation
Breast cancer	Biopsy of primary or metastatic tumors	Drug Sensitivity Verification or Prediction (Paclitaxel)	50	June 1, 2018	Sponsors and Collaborators: Peking Union Medical College, Beijing, China	NCT03544047/ Unknown
Biliary Tract Cancer	Tumor resection	Multi-Platform Profiling with Organoid Drug Sensitivity Screening and ctDNA Monitoring	20	September 23, 2020	Sponsor: University of Washington Collaborators: Natera, Inc. SEngine Precision Medicine, Inc.	NCT04561453/ Recruiting
Colon Cancer	biopsy of RAS/RAF wild-type metastatic right colon cancer tumor lesion	Test the sensitivity and clinical consistency of cetuximab.	80	May 28, 2021	Sponsor: Danwang Medical Technology (Shanghai) Co., Ltd, China Collaborator: Fudan University, China	NCT04906733/ Recruiting
Cholangitis/ Cholangiocarcinoma	Cholecystectomy (gallbladder removal); bile and biliary brushings	Characterization of Biliary Cell-derived Organoids	300	February 15, 2021	Sponsors and Collaborators: Mayo Clinic; National Institute of Diabetes and Digestive and Kidney Diseases (NIDDK)	NCT04753996/ Recruiting
Cystic Fibrosis	Rectal Biopsy and Suction biopsy or forceps biopsy (CF and R334W mutation)	Investigate the response to ivacaftor/tezacaftor in patients with CF and a R334W mutation.	30	February 5, 2020	Sponsor: Universitaire Ziekenhuizen Leuven; Collaborators: Vertex Pharmaceuticals Incorporated KU Leuven University of Lisbon	NCT04254705/ Not yet recruiting
Esophageal Cancer	Biopsy by diagnostic EUS	Prospective evaluation of chemoradioresistance	100	September 14, 2017	Sponsors and Collaborators: University Medical Center Groningen, Netherlands	NCT03283527/ Unknown
Familial adenomatous polyposis, Crohn and ulcerative colitis	intestinal biopsies (From Inflammatory Bowel Disease and Intestinal Polyposis Patients)	ISC and organoid characterization	120	August 22, 2016	Sponsors and Collaborators: University Hospital, Toulouse, France	NCT02874365/ Recruiting
Glioblastoma	Tumor biopsy ('left-over' tumor tissue)	Explore Resistance Mechanisms	60	April 30, 2021	Sponsor and Collaborators: Maastricht Radiation Oncology, Netherlands	NCT04868396/ Active, not recruiting
Glioma	Tumor resection and blood sampling	Establishing living biobank	50	April 29, 2021	Sponsor: Maastricht Radiation Oncology Collaborators: Maastricht University Medical Center Zuyderland Medisch Centrum Ziekenhuis Oost-Limburg	NCT04865315/ Active, not recruiting

(Continued)

TABLE 2 | Continued

Tissue Type	Source of Organoids	Aim of study	Estimated Enrollment	First Posted	Sponsors/ Collaborators	ClinicalTrials.gov Identifier/Status
Gut	Biopsy specimens (patients with and without hypertension who routinely undergo colonoscopy)	Determine if there are fundamental differences in the gut epithelium in hypertension compared to normotension.	50	August 4, 2020	Sponsor: University of Florida, United State Collaborator: National Heart, Lung, and Blood Institute (NHLBI)	NCT04497727/ Not yet recruiting
Human Gut Sensory Epithelial Cells	Endoscopic and colonoscopic biopsies	Study the biology of innervated sensory epithelial cells	50	September 5, 2016	Sponsor and Collaborators: Duke University	NCT02888587/ Recruiting
Head and Neck Cancer	Constitution of tumor and blood samples	Predicting the response to patients' treatments	98	February 7, 2020	Sponsors and Collaborators: Centre Francois Baclesse, France	NCT04261192/ Recruiting
Intestine	Small intestinal biopsies (A. healthy controls; B. patients with Food intolerances or Food allergy, patients with inflammatory bowel disease, irritable bowel disease, gluten sensitivity, short bowel syndrome)	The effect of nutrient antigens or therapeutic agents	375	August 22, 2017	Sponsors and Collaborators: University of Erlangen-Nürnberg Medical School, Germany	NCT03256266/ Recruiting
Kidney Cancer	Tumor resection, Blood and Urine sample	Establish a reliable and effective method to cultivate kidney cancer cells	20	April 13, 2020	Sponsors and Collaborators: Chinese University of Hong Kong	NCT04342286/ Recruiting
Lung Cancer	Surgical specimens	Establish long term culturing and bio-banking conditions, and Predict Treatment Response	30	April 26, 2021	Sponsors and Collaborators: Maastricht Radiation Oncology, Netherlands	NCT04859166/ Recruiting
Lung cancer	Resection of tumor tissue	Drug response testing	50	June 7, 2019	Sponsors and Collaborators: University Hospital, Geneva, Switzerland	NCT03979170/ Recruiting
Lung Neoplasm	Lung Tumor Resection and Circulating Tumor Cells	Creation a living biobank of PDOs from Stage I-IV lung cancer patients; Treatment Response of Organoids	150	August 31, 2018	Sponsors and Collaborators: The University of Texas Health Science Center at San Antonio, United States	NCT03655015/ Recruiting
Liver and Pancreatic Cancer	Tumor resection	Develop <i>in Vitro</i> Models of Liver, Biliary and Pancreatic Cancer	75	May 7, 2015	Sponsor: Cambridge University Hospitals NHS Foundation Trust Collaborators: The Gurdon Institute Ann McLaren Laboratory of Regenerative Medicine, UK	NCT02436564/ Unknown
Meningioma	Surgical specimens	Establishment and Characterization of Meningioma PDOs	30	July 21, 2020	Sponsors and Collaborators: Chinese University of Hong Kong	NCT04478877/ Recruiting
Multiple Myeloma	Marrow aspirates	Test chemosensitivity in relapsed multiple myeloma	70	March 26, 2019	Sponsor: Wake Forest University Health Sciences Collaborator: National Cancer Institute (NCI), United States	NCT03890614/ Recruiting
NSCLC	Surgical specimens and whole blood	High Throughput Screening Device Based on 3D Nano-matrices and 3D Tumors With Functional Vascularization	100	April 1, 2021	Sponsors and Collaborators: University Hospital, Strasbourg, France	NCT04826913/ Not yet recruiting

(Continued)

TABLE 2 | Continued

Tissue Type	Source of Organoids	Aim of study	Estimated Enrollment	First Posted	Sponsors/ Collaborators	ClinicalTrials.gov Identifier/Status
NSCLC	Resection tissue or biopsy tissue of NSCLC	Drug Sensitivity Correlation Between PDO Model and Clinical Response	100	March 5, 2018	K2 Oncology, Inc, China	NCT03453307/ Recruiting
NSCLC	Surgical specimens	Drug sensitivity test	100	March 5, 2018	Sponsors and Collaborators: K2 Oncology, Inc., China	NCT03453307/ Recruiting
Neuroendocrine neoplasm	Biopsy/surgical fresh tissue of gastroenteropancreatic neuroendocrine neoplasms and pancreatic ductal adenocarcinoma.	To use single-cell sequencing technology to explore neuroendocrine neoplasm molecular biological characteristics, tumor heterogeneity and cell subtypes.	200	June 16, 2021	Sponsors and Collaborators: Fudan University, China	NCT04927611/ Not yet recruiting
Ovarian Cancer	Operative specimens	Drug sensitivity (standard regimens: chemotherapies and targeted agents)	30	February 24, 2021	Sponsors and Collaborators: Chongqing University Cancer Hospital	NCT04768270/ Recruiting
Ovarian Cancer	Tumor biopsy	Drug response testing	48	September 18, 2020	Sponsors and Collaborators: Fondazione Policlinico Universitario Agostino Gemelli IRCCS, Italy	NCT04555473/ Recruiting
Pancreatic Cancer	EUS-FNA and EUS-FNB within the pancreatic cancer diagnostic process; Surgical specimens after neoadjuvant chemotherapy	Check for the reactivity to anti-cancer drugs used as neoadjuvant chemotherapy	300	March 2, 2021	Sponsors and Collaborators: Samsung Medical Center, Korea	NCT04777604/ Not yet recruiting
Pancreatic Cancer	FNA and FNB	Evaluation and Comparison of the Growth Rate of Pancreatic Cancer Patient-derived Organoids to improve diagnostics and therapeutics	50	June 19, 2019	Sponsors and Collaborators: Technische Universität München	NCT04736043/ Recruiting
Pancreatic Cancer	EUS-FNA	Assess the responses of FDA-approved anti-cancer drugs	50	June 1, 2018	Sponsors and Collaborators: Ying Lv, China	NCT03990675/ Recruiting
Pancreatic adenocarcinoma	Biopsies of metastases or primary tumour tissue of pancreatic cancer	Establishing organoids	30	April 17, 2018	Sponsor: AMC-UvA Collaborator: Erasmus Medical Center	NCT03544255/ Recruiting
Prostate Cancer	Extended biopsy (metastatic prostate cancer)	Development of the organoid culture technique from metastases from patients with advanced form of prostate cancer	20	May 16, 2019	Sponsor: Centre Antoine Lacassagne, France Collaborator: Centre Méditerranéen de Médecine Moléculaire UMR_S-1065	NCT03500068/ Recruiting
Rectal Cancer	Tumor biopsies	Establish a biospecimen collection protocol	20	May 1, 2020	Sponsor: Centre Antoine Lacassagne, France Collaborator: Centre Méditerranéen de Médecine Moléculaire UMR_S-1065	NCT03952793/ Recruiting
Rectal cancer	Pre-treatment biopsies	Predicting neoadjuvant chemoradiation sensitivity	80	July 5, 2018	Sponsors and Collaborators: Duke University	NCT04371198/ Recruiting
Refractory Solid Tumours	Biopsy of HNSCC, Epithelial Ovarian, colorectal, breast cancer.	15-drug panel screening	35	May 29, 2019	Sponsors and Collaborators: Zhen Zhang, Fudan University, China	NCT03577808/ Unknown
Vaginal Cancer/ Cervical Dysplasia/ Cervical Cancer	Vaginal Biopsy	Primary Organoid Models for Anti-HPV Treatments	50	February 20, 2020	Sponsors and Collaborators: National University Hospital, Singapore	NCT04279509/ Recruiting
					Sponsor: Centre Hospitalier Régional d'Orléans Collaborators: CNRS - Pr Chantal PICHON	NCT04278326/ Recruiting

NSCLC, Non-Small Cell Lung Cancer; HNSCC, Head and neck squamous cell carcinoma; PDOs, Patient-Derived Organoids; EUS, endoscopic ultrasound; AMC-UvA, Academisch Medisch Centrum - Universiteit van Amsterdam; UMCG, University Medical Center Groningen; EUS-FNA, EUS-guided fine-needle aspiration; EUS-FNB, EUS-guided fine-needle biopsy; iPSC, Induced-Pluripotent Stem Cells; FAP, familial adenomatous polyposis.

Combination of PDOs and CRISPR/Cas9 Gene Editing

CRISPR/Cas9 genome editing in PDOs is used to establish transformation models, and eventually, for drug testing in the future. The use of CRISPR/Cas9 gene editing in PDOs has contributed to uncovering the functional basis of diverse oncogene mutations while also helping to correct the causing mutation in human cancers. Kuo et al. established the first human forward genetic modeling of a commonly mutated tumor suppressor gene, ARID1A, using CRISPR/Cas9 genome editing (72). Using this model, they obtained insights into early transformation mechanisms of ARID1A-deficient gastric cancers. Visvader et al. knocked out breast cancer-associated tumor suppressor genes using CRISPR/Cas9 editing to generate PDO model, and showed that the breast cancer organoid can be used for long-term growth (73). Meltzer et al. generated a novel PDO model to recapitulate aberrantly activated Wnt signaling by combining organoids and CRISPR/Cas9 genome editing (74). Using this model, they investigated the effect of an individual signaling alteration to human Barrett epithelial neoplastic transformation. Their research showed that the application of CRISPR/Cas9 genome editing creates an ideal Barrett epithelial PDO model to study 'driver' pathway alterations and improve our understanding of human tumorigenesis.

ORGANOIDS-ON-A-CHIP AND 3D BIOPRINTING

Microfluidic Engineering Organoid Culture System

Recent studies of organoids have applied microfluidics and organ-on-a-chip technology in drug screening (75), in an attempt to overcome the shortcomings of organoid culture. Microfluidic cell culture technology has generated 3D culture devices that are now adapted to spheroid-based organotypic cultures and have been used to model organ microenvironments *in vitro* (76). This technology provides the possibility of precisely controlling the microscale to model physiological conditions and high-throughput approaches. Patient-derived organotypic tumor spheroids can be generated and evaluated within one to two weeks (69, 77, 78). Li et al. reported that the application of an air-liquid interface (ALI) provides sufficient oxygen supply to sustain organoid growth, which supports the generation of epithelial/mesenchymal hybrids without supplementation of exogenous growth factors (79, 80). The long-term 3D culture is a collagen-based ALI tumor organoid culture system that enables to expand the primary gastrointestinal cells as organoids for months (80). The ALI organoid method has been exploited to culture PDOs from normal and tumor specimens, including melanoma, renal cell carcinoma and non-small cell lung cancer (24). ALI PDOs preserves the heterogeneity of the parental tumor as well as the complex cellular network of the TME. Pavesi et al. developed a microfluidic device that could measure the changes in the antitumor efficacy of adoptive T cells in a 3D collagen

microenvironment (81). Jung et al. devised a clinically relevant microphysiological microfluidic-based platform for drug sensitivity testing that could form tumor organoids with preserved morphological and genetic characteristics of the primary lung cancer (82). Torabi et al. designed micropatterned surfaces that integrated 3D cell culture with microfluidics through a hydrogel solution (83). Using the Cassie-Baxter mode, they created a diffusion and transfer pathway between the hydrogel and bulk fluid, providing an excellent option for PDO culture. The microfluidic 3D culture device could help PDOs retain the parenchyma and stroma, and enabled further assessment of new therapeutic modalities and elucidated the mechanism of chemotherapy resistance (24, 82, 84). Nikolaev et al. established a biomaterial microfluidic platform using tissue engineering and cell self-organizing approaches, which induced intestinal stem cells to establish a tube-shaped epithelium. Moreover, they demonstrated that this device could achieve a spatial arrangement similar to the crypt- and villus-like domains of the intestine *in vivo* (75). Interestingly, the mini-intestine specialized cell type, which is rarely found in conventional organoids and the luminal capability of the bioengineered system was sufficient to maintain long-term host-microorganism symbiosis (Figure 2A).

The combination of microfluidics and cell biology has led to the development of the organ-on-a-chip platform, which is a miniaturized biomimetic system that represents many physiological characteristics of living tissue, such as the 3D microarchitecture composed of multiple tissue types, dynamic mechanical and biomechanical forces, and functional multiple tissue integrations. Microfluidic organ-on-a-chip technology provides the possibility of easily controlling spatiotemporal flow thereby recreating a microenvironment for developing and maintaining the organoid model. Additionally, nutrient supply, shear stress and geometry can be easily controlled in an organ-on-a-chip platform, so that it is important to choose a critical function for this platform which can be achieved by designing a constructible simplified version of the real system. Achberger et al. presented a novel microphysiological model of the human retina, retina-on-a-chip, which included at least seven different essential retinal cell types derived from hiPSCs (85). The platform provided vasculature-like perfusion by microflow control technology and recapitulated the interaction of mature photoreceptor segments *in vitro*. In addition, they applied the anti-malaria drug chloroquine and the antibiotic gentamicin to reproduce retinopathic side effects and demonstrated the potential of retina-on-a-chip in drug development. Skardal et al. established a single and integrated multi-organoid body-on-a-chip system with a single recirculating perfusion system to maintain the viability and function of organoids derived from human tissue (86). These integrated systems could support six distinct tissue organoid types for at least 28 days, including the liver, cardiac, vascular, lung, testis, and either colon or brain. Interestingly, the six-organoid integrated platform was used to screen the toxicity of drug compounds at clinically relevant doses, and it was demonstrated that the functionality of one organoid influences the response of other organoids (Figure 2B).

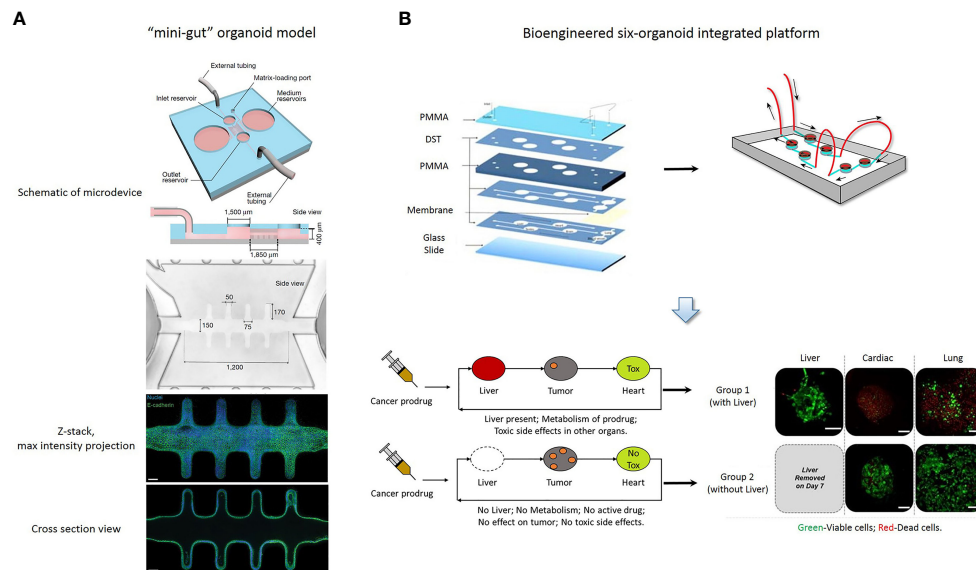


FIGURE 2 | (A) A "mini-gut" organoid model is established in a microdevice containing 3D hydrogel. This microdevice guides self-organizing intestinal stem cells into functional organoids-on-a-chip. [Cited from (75)]. **(B)** A bioengineered six-organoid integrated platform is generated by microfluidically linked chambers, each containing liver, cardiac, lung, endothelial, testis, and brain organoids. Capecitabine treatment of a system containing liver, results in cytotoxicity in cardiac and lung organoids. Expectedly, this platform without liver organoids does not show significant toxicity. Green, Calcein AM-stained viable cells; Red, Ethidium homodimer-stained dead cells. PMMA, poly (methyl methacrylate); DST, double sided tape. Scale bars, 100 µm. [Adapted from (86)].

Kasendra et al. established a human duodenum intestine chip using organoids and organ-on-chips technology that mimicked intestinal tissue structure and functions and could be used for preclinical drug evaluation (87).

3D Bioprinting of PDOs

The construction of organoids still faces several challenges, including incorporation of vascular structures and immune system, precise architecture in space, and breakthrough in scale size. These vascular structures and immune systems can affect PDOs to predict the response of drug. The advantages of 3D bioprinting in biological reconstruction accelerates the process of organoid construction. Daly et al. developed a bioprinting approach to transfer spheroids into self-healing support hydrogels at high resolution, which achieves the precise manipulation of single spheroids and organoids (88). Ayan et al. discovered an "aspiration-assisted bioprinting" approach to improve the precise of biofabrication and bioprinted different biologics, including tissue spheroids, tissue strands, or single cells (89). In addition, Brassard et al. pursued an approach by printing organoid-forming stem cells to form centimeter-scale tissues that comprise self-organized features (90). The combination of 3D bioprinting and PDOs has successfully recapitulated part of the real structure and function of organoids, and achieved long-term expansion and improved drug testing. Kinsella et al. established bioprinting tumor models to maintain PDO sphere culture of gastric adenocarcinoma using hydrogels with alginate and gelatin (91). Bioprinted brain PDOs can be used for individual drug screening in neurological diseases. Using embedded 3D

bioprinting and photocrosslinkable bioink, Shin et al. exploited a 3D brain-like co-culture construct that was composed of heterogeneous neural populations with neurospheroids and glia (92). The study showed that the engineered brain organoid exhibited the capability to differentiate into neuronal cells, and the platform may be used to model neurological disease and drug discovery. The use of 3D bioprinting platforms to generate and culture organoids can improve reproducibility to a certain extent and promote the standardization of protocols. Although 3D bioprinting has been used in many organoid platforms, it still has numerous challenges, such as precise construction, printing speed, and suitable biomaterials. First, there is a gap in scale between organoids and actual organs: organoids are only up to a few cubic millimeters in size, which is a million times smaller than actual organs. Second, the long duration of the current manufacturing process may lead to hypoxia related damage by interrupting the continuous supply of nutrients and oxygen levels in the culture system. In addition, a single vasculature is insufficient for organoid development in the later stages of 3D printing organoid culture. Third, although bioprinting technology can effectively control the precise arrangement of cells, a precise construct is still difficult to achieve. Although challenges remain in the bioprinting organoid field, printable bioink and bioprinting strategies will be further developed in the future. Biomaterials, cell and matrix components of organoids, and the scale of organoids is the same as that of an organ. With breakthroughs in bioprinting organoid technologies and microfluidic culture systems, these challenges will be overcome and 3D organ bioprinting will eventually be realized.

ORGANOID BIOBANKING AND ETHICAL CONCERNS

Living Organoid Biobanks

For individualized cancer treatment, a bridge between clinical practice and translational research is urgently needed. Personalized therapies are based on the molecular and histopathological features of each patient's tumor. In addition to traditional tissue and biomolecular-based biobanks, the establishment of a "living organism biobank" is receiving increasing attention, and one of its representatives is organoid biobanks. PDOs can be passaged and cryopreserved, providing a chance to establish living biobanks with higher clinical relevance to the patients. PDO libraries allow in-depth investigation of tumor characteristics *in vitro*. Organoid biobanks, combined with drug sensitivity testing and next-generation sequencing, now support clinical decision-making and clinical trial performance analysis (Figure 3). Van de Wetering et al. first established a living colorectal cancer organoid biobank and described that the organoid culture platform can be exploited for genomic and functional research at the level of the individual patient (18). They provided detailed characterizations of a colorectal cancer biobank, including whole-exome sequencing, copy number analysis, histology and drug screening. Meanwhile, Geurts et al. described a cystic fibrosis intestinal organoid biobank, representing 664 patients (93). In addition, Fujii et al. generated a colorectal cancer organoid biobank that included 52 tumor subtypes and discovered that several organoids obtained new genetic mutations during passage, indicating that current research has not completely avoided the genetic instability of cancer organoids during long-term passage (94). These experimental results show the enormous potential of large-scale PDO biobanks

that represent hereditary diseases. Sachs et al. established a living biobank of over 100 breast cancer organoid lines from a wide variety of primary and metastatic tumors (29). Moreover, they analyzed breast cancer organoids to characterize various profiles by large-scale sequencing and drug screening and generated a well-defined living biobank. These analyses ensured that the characteristics of breast cancer organoids were consistent with those of normal and tumor tissues from patients. These results indicated that PDO biobanks are more suitable for rare human cancer subtypes that are difficult to establish as immortalized cell lines. Yan et al. generated a gastric cancer organoid biobank derived from normal, dysplastic, cancer, and lymph node metastatic patients, and it retained different molecular subtypes (33). This biobank preserved features such as paired tumor tissue germline DNA information, which is critical for future reference and prediction of patient responsiveness and sensitivity to anti-tumor treatments. Amieva et al. proposed a protocol to rapidly establish apical-out polarity and maintain the integrity and secretory function of epithelium (95). This protocol provides a tool for establishing a living gastrointestinal organoid biobank that can be used to study the impact of host-microbe interactions on epithelial function. Beato et al. established a living biobank of organoids from 15 patients with intraductal papillary mucinous neoplasms (IPMN) of the pancreas (96). These PDOs recapitulated the molecular and histopathological characteristics of the parental IPMN tumors, and the success rates for organoid generation from IPMN tumors and normal pancreatic tissues were similar to those of previous reports wherein the success rates were up to 80% and 87%, respectively (30, 31, 97–99). Jacob et al. reported the generation of patient-derived glioblastoma organoids that were suitable for constructing a biobank and modeling immunotherapy responses. With the complexity of cancer types dictates the outcome, the key

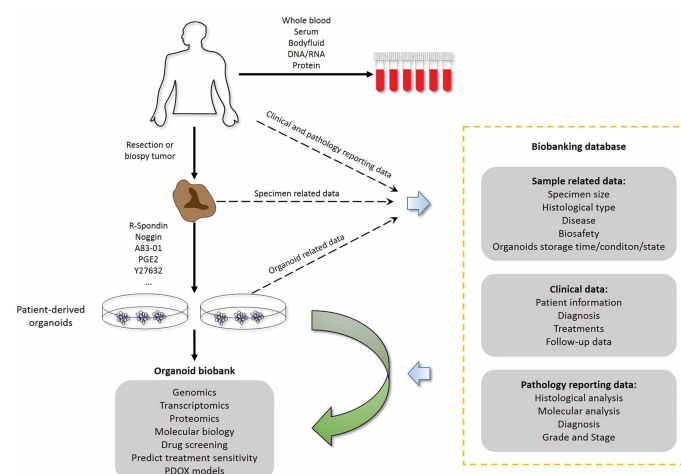


FIGURE 3 | Combination of living organoid biobank and databases improves cancer research and precision medicine. Patient-related data are available through the hospital information system and contain sensitive patient information that external researchers cannot access. Researchers who have obtained ethics committee approval can collect sample-related anonymous information from the biobank data management system, and obtain the organoid model and fresh frozen tissue from the biobanking infrastructure. Therefore, researchers can use organoid models for drug screening and testing chemotherapy response at the individual patient level. PDOX models, Patient-derived organoid xenograft models.

advantage of these biobanks is that they provide cancer organoid cultures representing the complexity of different tumor subtypes. These cancer and normal organoids accurately reflect patient's sensitivity to drugs and their tolerance to drug toxicity. An increasing number of cancer biobanks has been reported, but most of the existing organoid culture protocols are only suitable for epithelial carcinomas.

As we have described, only a few living tumor biobanks have been established by PDO technology, including colorectal cancer, breast cancer, gastric cancer and glioblastoma. In addition, fewer non-epithelial cancer-derived organoids have been established, such as glioblastoma (100) and childhood kidney cancers (34). Therefore, the generation of more organoid cultures from non-epithelial cancers should be promoted in the future. Based on the current status, more exploration should be performed to obtain living biobanks of rare tumor organoids. In addition, standardization of organoid production is needed to control the quality of PDOs, to improve the reproducibility and scalability, and to avoid the diversity of organoids. Based on the current research status, PDOs cannot fully recapitulate the natural characteristic of the parental tumor, which results in many uncertainties for the promotion of innovative clinical applications of living biobanks in the future.

Ethical Concerns of PDO Research

Although advances in 3D models allow for more complex products to be generated from human tissues, the progress of human organoids may be hindered by ethical concerns. Vasiliki Mollaki analyzed several serious challenges posed by organoid use and biobanking and provided many unique and profound insights to promote the healthy development of organoid research and application (101). He provided an in-depth discussion on ethical challenges in organoid use, which includes the source of stem cells, informed consent of cell donors, issues specific to brain organoids and multi-organoid complexes, gene editing, creation of chimeras, organoid transplantation, commercialization of organoids, patentability of organoids, treatment costs, issues of equity, misuse and dual use of organoids, and organoid biobanking (101). His main suggestion is the four-step approach to help increase the biomedical and social benefits of organoids: the first is related to existing regulations and guidelines, the second is related to special regulatory provisions, the third is public engagement and the fourth is continuous monitoring of rapid advancements.

Organoid biobanking and issues specific to brain organoids are our main concerns. As mentioned above, living organoid biobanking provides an important source for promoting the development of translational research. PDOs have an inevitable connection with the donor's body, identity, and privacy, among others, which involves human rights issues of the donor, and should differ from the tissues and organs directly derived from the human body. However, there are no binding principles or legal norms defining the rights and duties of donors and biobankers. Organoids are also a technology and a tool; hence, with the increasing commercialization of human organoid-related products, more and more ethical challenges have begun

to emerge, especially in drug development, preclinical prediction of patient drug responses, and toxicology testing (102). The conventional frameworks are inapt to capture the practical and ethical complexity of human organoid products. Lensink et al. indicates that commercialization of PDO biobanks raise challenges associated with commercial involvement, trust, and ownership (103). By conducting 21 semi-structured qualitative interviews, they indicated that academia, clinical care, biobanks and industry stakeholders do not belong to distinct domains, and suggest that participants should be regarded as "partner" rather than passive tissue or service providers. These efforts are aimed at establishing an ecosystem that maintains a sound balance between ongoing cooperation and a feasible and sustainable research climate, while making governance more responsible and fair. In addition, living organoid samples can be stored for a long time after being collected and cultivated, even longer than the lifespan of the donor, and follow-up research often fails to provide informed consent. At the current stage of organoid biobanking, there are no standardized and individualized informed consents that can cover all the specific concerns of donors, such as personal values and beliefs. Therefore, opt-out options should be available to allow donors to object to certain uses. In any case, the consent procedure is the central tenet of organoid biobank management to ensure the implementation of the principle of a voluntary and well-informed donation (101).

The ethical issues of special living biobank samples, such as brain organoids, should also draw our attention. The human brain organoid system has already been applied to modeling neurological diseases, including microcephaly, macrocephaly, autism, Miller-Dieker syndrome, Rett syndrome, Sandhoff disease, prenatal drug exposure, ZIKA virus infection, and neurodegenerative diseases (104). Trujillo et al. developed human cortical organoids to model early human brain network development and achieved complex oscillatory waves (105). Reardon et al. discussed the sentient states of brain organoids, and pointed out that a conscious brain should display a much more complex, unpredictable electrical activity than an unconscious one, which responds in simple and regular patterns (106, 107). Although brain organoids do not have neurological functions, these miniature organs constitute neural entities of human origin. Currently, most scientists and ethicists agree that consciousness has not been created; however, with the continuous advance of technologies, brain organoids may be induced to develop consciousness, sensation, and cognition, thus possessing characteristics related to human morality. Therefore, ethical stakes are much more complex than those of other organs. Hyun et al. provided their opinions on the ethics of brain organoids (108). They indicated that brain organoids lack the sensory inputs and a complex network structure and, thus, declared that peoples' concerns about the moral status might be excessive. At the current stage of development, the degree at which brain organoids exhibit human consciousness is difficult to determine, and neuroscientists have not reached a consensus on the definition and measurement of consciousness. However, if the brain organoids could feel pain, the principles of animal welfare

would be imposed at least. In addition, the informed consent still should be modified to prepare for the day when brain organoids will be conscious, because the existing informed consent does not reflect all possible connections between the cell donor and brain organoids. Boers et al. proposed a “consent for governance” model that includes privacy by design, participant engagement, benefit sharing and ethical oversight, which contributes to responsible innovation and clinical translation (102). Overall, conventional bioethical frames are inept in addressing the practical and ethical complexities of PDOs. Therefore, it is essential to develop binding legal norms that overcome most of the ethical dilemmas in this exciting field.

DISCUSSION

Models of 3D tumor spheroids preserve cell-cell contact and cell-matrix interaction, present a more clinically relevant resistome and improve the success rate of drug screening (109). Studies have shown that the gene expression profiles of 3D cancer spheroids are different from 2D cultures, recapitulating various features in genes associated with proliferation, survival and drug sensitivity (110). Tumor spheroids embedded in ECM preserve most characteristics of cell biology associated with cell-matrix interrelations, including interaction with basement membranes and interstitial matrix (111, 112). Therefore, despite higher cost compared to 2D cell culture models, 3D tumor spheroids are popular for drug screening and response testing. Current 3D culture tumor models include organotypic multicellular spheroids (from tumor tissues), tumor-derived organoids (from dissociated tumor tissues) and multicellular tumor spheroids (from cancer cell lines) (113). Traditional spheroid culture models involve supplementation with B27, EGF, and FGFs. Organoid culture supplements depend on the type of tissue, and major supplements include the Wnt pathway agonist, RSPO1, nicotinamide, N-acetylcysteine, FGFs, noggin and molecule inhibitors (9, 66, 114–116). PDOs recapitulate the intercellular interactions and the characterizations of histology and enable long-term cultivation and stable passage (117). Therefore, PDOs mimic the genotype and phenotype of parental tumor and effectively retain patient-specific tumor heterogeneity, which make them superior to traditional spheroid models for drug screening. However, there are several disadvantages with PDO models that need to be overcome, including high cost and the potential effect of matrix on therapeutic responses. In addition, one main concern in cancer treatment is intra- and intertumor heterogeneity (118), which can result in inaccurate decision-making and partial treatment benefits. Organoids derived from a portion of a tumor just match the genomic portrait of that particular tumor region, and may not represent the genome map of the entire tumor. Therefore, organoid assays of tumors *in vitro* should take the spatial tumor heterogeneity into consideration. In addition, owing to patient diversity and varying spheroid culture protocols, the outcome may vary by the laboratory. Culture protocols should be formulated that are specific and standardized for organoids derived from individual organs.

Although PDO models mimic some key aspects of human tumorigenesis, they cannot fully recapitulate the complicated

structure of the TME. Tumorigenesis and drug resistance are not only driven by gene alterations in the tumor cells but are also affected by the components of the TME, such as blood vessels, neurons, fibroblasts and immune cells. First, immune system could be polarized to contribute to tumor development during progressive growth phase. Therefore, effort has been made to rejuvenate the anti-tumor immune response in organoid culture systems. Intestinal epithelial organoids have been co-cultured with lymphocytes and macrophages, and showed a significant dynamic movement and continued proliferation activity (75, 119).

As presented in the previous section, PDOs can predict the response of cancer patients to chemotherapy. However, these studies have several limitations. First, owing to the lack of an integral microenvironment, organoid models cannot mimic immunotherapy and antiangiogenic therapy. Second major limitation of the current protocols for organoid culture is the inability to part with animal-derived Matrigel or collagens. These extracellular matrices contain undetermined extracellular components, which may unexpectedly modify biological cell behavior. Third, organ-on-a-chip organoids are suitable for studying the mechanism of tumor metastasis. However, multiorgan metastasis has not yet been achieved in organoid models. Additionally, current cancer organoid cultures do not replicate accurate mechanical control and physical manipulations that occur *in vivo*. Engineered extracellular matrix has been reported, which, however, still cannot meet the requirements of fully functional organoids (120).

Organoids are less expensive than mouse models, but they are relatively expensive compared to traditional cell line models. The time required to establish an organoid model is a few weeks which is less than that in animal models but is still longer than in cell line models. High-throughput assays are required to decrease the time and cost of organoid generation as well as the input material needed to establish the culture. In this regard, microfluidic 3D culture has generated spheroid-based organotypic culture devices. Organoid-on-a-chip is also a microfabricated microfluidic culture platform that combines extracellular matrix and microstructures to simulate one part of the cytoarchitecture and tissue function (42). However, the microfluidic system cannot replicate the interactions between the tumor and the immune network that occurs *in situ* and is required for an accurate prediction of immunotherapy response *ex vivo*. Moreover, although intestinal organoid fragments on hydrogel have been applied to manufacture organoid arrays (65, 121, 122), they are not adequate to provide fully automated organoid culture for high-throughput assays. Finally, the generation of organoids and other human tissue products leads to ethical challenges, including gift versus market systems especially during the commercialized exchange of organoids, and the awakening of consciousness in brain organoids.

CONCLUSION

Despite the remaining challenges, PDOs have a higher physiological and pathological relevance than traditional models, and human cancer organoid assays have great

potential in guiding personalized therapies. Meanwhile, PDTOs allow to reliably preserve the molecular, cellular, and histopathological phenotypes of parental tumors and retain patient-specific tumor heterogeneity. Furthermore, organ-on-a-chip has been applied to organoids to accomplish physiological or pathological model systems that are closer to the state of the tissue *in vivo*. Future advancements in organoid technologies are anticipated to achieve a comprehensive cancer model system that recapitulates physiological conditions by integrating tumor parenchyma cells, vascular and immune cellular networks, and non-cellular TME. This robust model will provide a powerful tool for biomarker research, drug screening, and a more accurate prediction of therapeutic efficacy and eventually improve human health.

REFERENCES

- Elia I, Haigis MC. Metabolites and the Tumour Microenvironment: From Cellular Mechanisms to Systemic Metabolism. *Science* (2021) 3:1:21–32. doi: 10.1038/s42255-020-00317-z
- Tuveson D, Clevers H. Cancer Modeling Meets Human Organoid Technology. *Science* (2019) 364(6444):952–5. doi: 10.1126/science.aaw6985
- Birgersdotter A, Sandberg R, Ernberg I. Gene Expression Perturbation *In Vitro*—A Growing Case for Three-Dimensional (3D) Culture Systems. *Semin Cancer Biol* (2005) 15(5):405–12. doi: 10.1016/j.semcancer.2005.06.009
- Lee J, Kotliarova S, Kotliarov Y, Li A, Su Q, Donin NM, et al. Tumor Stem Cells Derived From Glioblastomas Cultured in bFGF and EGF More Closely Mirror the Phenotype and Genotype of Primary Tumors Than Do Serum-Cultured Cell Lines. *Cancer Cell* (2006) 9(5):391–403. doi: 10.1016/j.ccr.2006.03.030
- Kamb A. What's Wrong With Our Cancer Models? *Nat Rev Drug Discovery* (2005) 4(2):161–5. doi: 10.1038/nrd1635
- Caponigro G, Sellers WR. Advances in the Preclinical Testing of Cancer Therapeutic Hypotheses. *Nat Rev Drug Discov* (2011) 10(3):179–87. doi: 10.1038/nrd3385
- Sato T, Vries RG, Snippert HJ, van de Wetering M, Barker N, Stange DE, et al. Single Lgr5 Stem Cells Build Crypt-Villus Structures *In Vitro* Without a Mesenchymal Niche. *Nature* (2009) 459(7244):262–5. doi: 10.1038/nature07935
- Sato T, van Es JH, Snippert HJ, Stange DE, Vries RG, van den Born M, et al. Paneth Cells Constitute the Niche for Lgr5 Stem Cells in Intestinal Crypts. *Nature* (2011) 469(7330):415–8. doi: 10.1038/nature09637
- Sato T, Stange DE, Ferrante M, Vries RGJ, van Es JH, van den Brink S, et al. Long-Term Expansion of Epithelial Organoids From Human Colon, Adenoma, Adenocarcinoma, and Barrett's Epithelium. *Gastroenterology* (2011) 141(5):1762–72. doi: 10.1053/j.gastro.2011.07.050
- Blokzijl F, de Ligt J, Jager M, Sasselli V, Roerink S, Sasaki N, et al. Tissue-Specific Mutation Accumulation in Human Adult Stem Cells During Life. *Nature* (2016) 538(7624):260–4. doi: 10.1038/nature19768
- Serra D, Mayr U, Boni A, Lukonin I, Rempfler M, Challet Meylan L, et al. Self-Organization and Symmetry Breaking in Intestinal Organoid Development. *Nature* (2019) 569(7754):66–72. doi: 10.1038/s41586-019-1146-y
- Lancaster MA, Renner M, Martin CA, Wenzel D, Bicknell LS, Hurles ME, et al. Cerebral Organoids Model Human Brain Development and Microcephaly. *Nature* (2013) 501(7467):373–9. doi: 10.1038/nature12517
- Spence JR, Mayhew CN, Rankin SA, Kuhar MF, Vallance JE, Tolle K, et al. Directed Differentiation of Human Pluripotent Stem Cells Into Intestinal Tissue *In Vitro*. *Nature* (2011) 470(7332):105–9. doi: 10.1038/nature09691
- Taguchi A, Kaku Y, Ohmori T, Sharmin S, Ogawa M, Sasaki H, et al. Redefining the *In Vivo* Origin of Metanephric Nephron Progenitors Enables

AUTHOR CONTRIBUTIONS

The concept of the manuscript was originated by ZZ and XC. The original manuscript was written by ZZ, with additions to the manuscript provided by LC. All authors contributed to the article and approved the submitted version.

FUNDING

This study was supported by the Science and Technology Development Project of Jilin Province (20210402030GH, 20200601010JC, 2021C017, 20210204150YY).

- Generation of Complex Kidney Structures From Pluripotent Stem Cells. *Cell Stem Cell* (2014) 14(1):53–67. doi: 10.1016/j.stem.2013.11.010
- Takasato M, Er PX, Becroft M, Vanslambrouck JM, Stanley EG, Elefanty AG, et al. Directing Human Embryonic Stem Cell Differentiation Towards a Renal Lineage Generates a Self-Organizing Kidney. *Nat Cell Biol* (2014) 16(1):118–26. doi: 10.1038/ncb2894
- Eiraku M, Takata N, Ishibashi H, Kawada M, Sakakura E, Okuda S, et al. Self-Organizing Optic-Cup Morphogenesis in Three-Dimensional Culture. *Nature* (2011) 472(7341):51–6. doi: 10.1038/nature09941
- Nakano T, Ando S, Takata N, Kawada M, Muguruma K, Sekiguchi K, et al. Self-Formation of Optic Cups and Storable Stratified Neural Retina From Human ESCs. *Cell Stem Cell* (2012) 10(6):771–85. doi: 10.1016/j.stem.2012.05.009
- van de Wetering M, Francies HE, Francis JM, Bounova G, Iorio F, Pronk A, et al. Prospective Derivation of a Living Organoid Biobank of Colorectal Cancer Patients. *Cell* (2015) 161(4):933–45. doi: 10.1016/j.cell.2015.03.053
- Drost J, Clevers H. Organoids in Cancer Research. *Nat Rev Cancer* (2018) 18(7):407–18. doi: 10.1038/s41568-018-0007-6
- Dijkstra KK, Cattaneo CM, Weeber F, Chalabi M, van de Haar J, Fanchi LF, et al. Generation of Tumor-Reactive T Cells by Co-Culture of Peripheral Blood Lymphocytes and Tumor Organoids. *Cell* (2018) 174(6):1586–98.e12. doi: 10.1016/j.cell.2018.07.009
- Pauli C, Hopkins BD, Prandi D, Shaw R, Fedrizzi T, Shoner A, et al. Personalized *In Vitro* and *In Vivo* Cancer Models to Guide Precision Medicine. *Cancer Discov* (2017) 7(5):462–77. doi: 10.1158/2159-8290.cd-16-1154
- Schutgens F, Clevers H. Human Organoids: Tools for Understanding Biology and Treating Diseases. *Annu Rev Pathol* (2020) 15:211–34. doi: 10.1146/annurev-pathmechdis-012419-032611
- Artegiani B, Clevers H. Use and Application of 3D-Organoid Technology. *Hum Mol Genet* (2018) 27(R2):R99–r107. doi: 10.1093/hmg/ddy187
- Neal JT, Li X, Zhu J, Giangarra V, Grzeskowiak CL, Ju J, et al. Organoid Modeling of the Tumor Immune Microenvironment. *Cell* (2018) 175(7):1972–88.e16. doi: 10.1016/j.cell.2018.11.021
- Nuciforo S, Fofana I, Matter MS, Blumer T, Calabrese D, Boldanova T, et al. Organoid Models of Human Liver Cancers Derived From Tumor Needle Biopsies. *Cell Rep* (2018) 24(5):1363–76. doi: 10.1016/j.celrep.2018.07.001
- Wang K, Yuen ST, Xu J, Lee SP, Yan HH, Shi ST, et al. Whole-Genome Sequencing and Comprehensive Molecular Profiling Identify New Driver Mutations in Gastric Cancer. *Nat Genet* (2014) 46(6):573–82. doi: 10.1038/ng.2983
- Kim M, Mun H, Sung CO, Cho EJ. Patient-Derived Lung Cancer Organoids as *In Vitro* Cancer Models for Therapeutic Screening. *Nat Commun* (2019) 10(1):3991. doi: 10.1038/s41467-019-11867-6
- Lee SH, Hu W, Matulay JT, Silva MV, Owczarek TB, Kim K, et al. Tumor Evolution and Drug Response in Patient-Derived Organoid Models of Bladder Cancer. *Cell* (2018) 173(2):515–28.e17. doi: 10.1016/j.cell.2018.03.017

29. Sachs N, de Ligt J, Kopper O, Gogola E, Bounova G, Weeber F, et al. A Living Biobank of Breast Cancer Organoids Captures Disease Heterogeneity. *Cell* (2018) 172(1-2):373–86.e10. doi: 10.1016/j.cell.2017.11.010
30. Huang L, Holtzinger A, Jagan I, BeGora M, Lohse I, Ngai N, et al. Ductal Pancreatic Cancer Modeling and Drug Screening Using Human Pluripotent Stem Cell- and Patient-Derived Tumor Organoids. *Nat Med* (2015) 21(11):1364–71. doi: 10.1038/nm.3973
31. Boj SF, Hwang C-I, Baker LA, Chio IIC, Engle DD, Corbo V, et al. Organoid Models of Human and Mouse Ductal Pancreatic Cancer. *Cell* (2015) 160(1-2):324–38. doi: 10.1016/j.cell.2014.12.021
32. Driehuis E, Kolders S, Spelier S, Löhmußaar K, Willems SM, Devriese LA, et al. Oral Mucosal Organoids as a Potential Platform for Personalized Cancer Therapy. *Cancer Discov* (2019) 9(7):852–71. doi: 10.1158/2159-8290.cd-18-1522
33. Yan HHN, Siu HC, Law S, Ho SL, Yue SSK, Tsui WY, et al. A Comprehensive Human Gastric Cancer Organoid Biobank Captures Tumor Subtype Heterogeneity and Enables Therapeutic Screening. *Cell Stem Cell* (2018) 23(6):882–97.e11. doi: 10.1016/j.stem.2018.09.016
34. Calandrini C, Schutgens F, Oka R. An Organoid Biobank for Childhood Kidney Cancers That Captures Disease and Tissue Heterogeneity. *Nat Commun* (2020) 11(1):1310. doi: 10.1038/s41467-020-15155-6
35. Kondo T. Current Status and Future Outlook for Patient-Derived Cancer Models From a Rare Cancer Research Perspective. *Cancer Sci* (2021) 112(3):953–61. doi: 10.1111/cas.14669
36. Colella G, Fazioli F, Gallo M, De Chiara A, Apice G, Ruosi C, et al. Sarcoma Spheroids and Organoids-Promising Tools in the Era of Personalized Medicine. *Int J Mol Sci* (2018) 19(2):615. doi: 10.3390/ijms19020615
37. Zannoni M, Cortesi M, Zamagni A, Arienti C, Pignatta S, Tesi A. Modeling Neoplastic Disease With Spheroids and Organoids. *J Hematol Oncol* (2020) 13(1):97. doi: 10.1186/s13045-020-00931-0
38. Gaebler M, Silvestri A, Haybaeck J, Reichardt P, Lowery CD, Stancato LF, et al. Three-Dimensional Patient-Derived *In Vitro* Sarcoma Models: Promising Tools for Improving Clinical Tumor Management. *Front Oncol* (2017) 7:203. doi: 10.3389/fonc.2017.00203
39. Jin MZ, Jin WL. The Updated Landscape of Tumor Microenvironment and Drug Repurposing. *Signal Transduct Targ Ther* (2020) 5(1):166. doi: 10.1038/s41392-020-00280-x
40. Deepak KKG, Vempati R, Nagaraju GP, Dasari VR. S NTumor Microenvironment: Challenges and Opportunities in Targeting Metastasis of Triple Negative Breast Cancer. *Pharmacol Res* (2020) 153:104683. doi: 10.1016/j.phrs.2020.104683
41. Tsai S, McOlash L, Palen K, Johnson B, Duris C, Yang Q, et al. Development of Primary Human Pancreatic Cancer Organoids, Matched Stromal and Immune Cells and 3D Tumor Microenvironment Models. *BMC Cancer* (2018) 18(1):335. doi: 10.1186/s12885-018-4238-4
42. Park SE, Georgescu A. Organoids-On-a-Chip. *Science* (2019) 364(6444):960–5. doi: 10.1126/science.aaw7894
43. Ma C, Peng Y, Li H, Chen W. Organ-On-a-Chip: A New Paradigm for Drug Development. *Trends Pharmacol Sci* (2021) 42(2):119–33. doi: 10.1016/j.tips.2020.11.009
44. Bein A, Shin W, Jalili-Firoozinezhad S, Park MH, Sontheimer-Phelps A, Tovaglieri A, et al. Microfluidic Organ-On-a-Chip Models of Human Intestine. *Cell Mol Gastroenterol Hepatol* (2018) 5(4):659–68. doi: 10.1016/j.jcmgh.2017.12.010
45. Takebe T, Zhang B, Radisic M. Synergistic Engineering: Organoids Meet Organs-On-a-Chip. *Cell Stem Cell* (2017) 21(3):297–300. doi: 10.1016/j.stem.2017.08.016
46. Astashkina A, Grainger DW. Critical Analysis of 3-D Organoid *In Vitro* Cell Culture Models for High-Throughput Drug Candidate Toxicity Assessments. *Adv Drug Deliv Rev* (2014) 69:70:1–18. doi: 10.1016/j.addr.2014.02.008
47. Katsuda T, Kawamata M, Hagiwara K, Takahashi RU, Yamamoto Y, Camargo FD, et al. Conversion of Terminally Committed Hepatocytes to Culturable Bipotent Progenitor Cells With Regenerative Capacity. *Cell Stem Cell* (2017) 20(1):41–55. doi: 10.1016/j.stem.2016.10.007
48. Eder A, Vollert I, Hansen A, Eschenhagen T. Human Engineered Heart Tissue as a Model System for Drug Testing. *Adv Drug Deliv Rev* (2016) 96:214–24. doi: 10.1016/j.addr.2015.05.010
49. Voges HK, Mills RJ, Elliott DA, Parton RG, Porrello ER, Hudson JE. Development of a Human Cardiac Organoid Injury Model Reveals Innate Regenerative Potential. *Development* (2017) 144(6):1118–27. doi: 10.1242/dev.143966
50. Verissimo CS, Overmeer RM, Ponsioen B, Drost J, Mertens S, Verlaan-Klink I, et al. Targeting Mutant RAS in Patient-Derived Colorectal Cancer Organoids by Combinatorial Drug Screening. *eLife* (2016) 5:e18489. doi: 10.7554/eLife.18489
51. Whittle JR, Vaillant F. Dual Targeting of CDK4/6 and BCL2 Pathways Augments Tumor Response in Estrogen Receptor-Positive Breast Cancer. *Clin Cancer Res* (2020) 26(15):4120–34. doi: 10.1158/1078-0432.ccr-19-1872
52. Xiong G, Stewart RL. Collagen Prolyl 4-Hydroxylase 1 Is Essential for HIF-1 α Stabilization and TNBC Chemoresistance. *Nat Commun* (2018) 9(1):4456. doi: 10.1038/s41467-018-06893-9
53. Schütte M, Risch T, Abdavi-Azar N, Boehnke K, Schumacher D, Keil M, et al. Molecular Dissection of Colorectal Cancer in Pre-Clinical Models Identifies Biomarkers Predicting Sensitivity to EGFR Inhibitors. *Nat Commun* (2017) 8:14262. doi: 10.1038/ncomms14262
54. Tashiro T, Okuyama H, Endo H, Kawada K, Ashida Y, Ohue M, et al. *In Vivo* and *Ex Vivo* Cetuximab Sensitivity Assay Using Three-Dimensional Primary Culture System to Stratify KRAS Mutant Colorectal Cancer. *PloS One* (2017) 12(3):e0174151. doi: 10.1371/journal.pone.0174151
55. Kondo J, Ekawa T, Endo H, Yamazaki K, Tanaka N, Kukita Y, et al. High-Throughput Screening in Colorectal Cancer Tissue-Originated Spheroids. *Cancer Sci* (2019) 110(1):345–55. doi: 10.1111/cas.13843
56. Kiyohara Y, Yoshino K, Kubota S, Okuyama H, Endo H, Ueda Y, et al. Drug Screening and Grouping by Sensitivity With a Panel of Primary Cultured Cancer Spheroids Derived From Endometrial Cancer. *Cancer Sci* (2016) 107(4):452–60. doi: 10.1111/cas.12898
57. Chen J, Zhao L, Peng H, Dai S, Quan Y, Wang M, et al. An Organoid-Based Drug Screening Identified a Menin-MLL Inhibitor for Endometrial Cancer Through Regulating the HIF Pathway. *Cancer Gene Ther* (2021) 28(1-2):112–25. doi: 10.1038/s41417-020-0190-y
58. Maloney E, Clark C, Sivakumar H, Yoo K, Aleman J, Rajan SAP, et al. Immersion Bioprinting of Tumor Organoids in Multi-Well Plates for Increasing Chemotherapy Screening Throughput. *Micromachines* (2020) 11(2):208. doi: 10.3390/mi11020208
59. Lenin S, Ponthier E, Scheer KG. A Drug Screening Pipeline Using 2D and 3D Patient-Derived *In Vitro* Models for Pre-Clinical Analysis of Therapy Response in Glioblastoma. *Int J Mol Sci* (2021) 22(9):4322. doi: 10.3390/ijms22094322
60. Li L, Knutsdottir H, Hui K, Weiss MJ, He J, Philosophe B, et al. Human Primary Liver Cancer Organoids Reveal Intratumor and Interpatient Drug Response Heterogeneity. *JCI Insight* (2019) 4(2). doi: 10.1172/jci.insight.121490
61. Broutier L, Mastrogianni G, Verstegen MM, Francies HE, Gavarró LM, Bradshaw CR, et al. Human Primary Liver Cancer-Derived Organoid Cultures for Disease Modeling and Drug Screening. *Nat Med* (2017) 23(12):1424–35. doi: 10.1038/nm.4438
62. Jabs J, Zickgraf FM. Screening Drug Effects in Patient-Derived Cancer Cells Links Organoid Responses to Genome Alterations. *Mol Syst Biol* (2017) 13(11):955. doi: 10.15252/msb.20177697
63. Ooft SN, Weeber F. Patient-Derived Organoids can Predict Response to Chemotherapy in Metastatic Colorectal Cancer Patients. *Sci Transl Med* (2019) 11(513). doi: 10.1126/scitranslmed.aay2574
64. Vlachogiannis G, Hedayat S. Patient-Derived Organoids Model Treatment Response of Metastatic Gastrointestinal Cancers. *Science* (2018) 359(6378):920–6. doi: 10.1126/science.aao2774
65. Brandenburg N, Hoehnel S, Kuttler F. High-Throughput Automated Organoid Culture via Stem-Cell Aggregation in Microcavity Arrays. *Nat Biomed Eng* (2020) 4(9):863–74. doi: 10.1038/s41551-020-0565-2
66. Yao Y, Xu X, Yang L, Zhu J, Wan J, Shen L, et al. Patient-Derived Organoids Predict Chemoradiation Responses of Locally Advanced Rectal Cancer. *Cell Stem Cell* (2020) 26(1):17–26.e6. doi: 10.1016/j.stem.2019.10.010
67. Wang T, Pan W, Zheng H, Zheng H, Wang Z, Li JJ, et al. Accuracy of Using a Patient-Derived Tumor Organoid Culture Model to Predict the Response to Chemotherapy Regimens In Stage IV Colorectal Cancer: A Blinded

- Study. *Dis Colon Rectum* (2021) 64(7):833–50. doi: 10.1097/dcr.0000000000001971
68. Scognamiglio G, De Chiara A, Parafioriti A, Armiraglio E, Fazioli F, Gallo M, et al. Patient-Derived Organoids as a Potential Model to Predict Response to PD-1/PD-L1 Checkpoint Inhibitors. *Br J Cancer* (2019) 121(11):979–82. doi: 10.1038/s41416-019-0616-1
 69. Aref AR, Campisi M, Ivanova E, Portell A, Larios D, Piel BP, et al. 3D Microfluidic *Ex Vivo* Culture of Organotypic Tumor Spheroids to Model Immune Checkpoint Blockade. *Lab Chip* (2018) 18(20):3129–43. doi: 10.1039/c8lc00322j
 70. Koh V, Chakrabarti J, Torvund M, Steele N, Hawkins JA, Ito Y, et al. Hedgehog Transcriptional Effector GLI Mediates mTOR-Induced PD-L1 Expression in Gastric Cancer Organoids. *Cancer Lett* (2021) 518:59–71. doi: 10.1016/j.canlet.2021.06.007
 71. Dugger SA, Platt A, Goldstein DB. Drug Development in the Era of Precision Medicine. *Nat Rev Drug Discov* (2018) 17(3):183–96. doi: 10.1038/nrd.2017.226
 72. Lo YH, Kolahi KS. A CRISPR/Cas9-Engineered ARID1A-Deficient Human Gastric Cancer Organoid Model Reveals Essential and Nonessential Modes of Oncogenic Transformation. *Cancer Discov* (2021) 11(6):1562–81. doi: 10.1158/2159-8290.cd-20-1109
 73. Dekkers JF, Whittle JR, Vaillant F, Chen HR, Dawson C, Liu K, et al. Modeling Breast Cancer Using CRISPR-Cas9-Mediated Engineering of Human Breast Organoids. *J Natl Cancer Instit* (2020) 112(5):540–4. doi: 10.1093/jnci/djz196
 74. Liu X, Cheng Y, Abraham JM, Wang Z, Wang Z, Ke X, et al. Modeling Wnt Signaling by CRISPR-Cas9 Genome Editing Recapitulates Neoplasia in Human Barrett Epithelial Organoids. *Cancer Lett* (2018) 436:109–18. doi: 10.1016/j.canlet.2018.08.017
 75. Nikolaev M, Mitrofanova O. Homeostatic Mini-Intestines Through Scaffold-Guided Organoid Morphogenesis. *Nature* (2020) 585(7826):574–8. doi: 10.1038/s41586-020-2724-8
 76. Sontheimer-Phelps A, Hassell BA, Ingber DE. Modelling Cancer in Microfluidic Human Organs-on-Chips. *Nat Rev Cancer* (2019) 19(2):65–81. doi: 10.1038/s41568-018-0104-6
 77. Jenkins RW, Aref AR, Lizotte PH, Ivanova E, Stinson S, Zhou CW, et al. *Ex Vivo* Profiling of PD-1 Blockade Using Organotypic Tumor Spheroids. *Cancer Discov* (2018) 8(2):196–215. doi: 10.1158/2159-8290.CD-17-0833
 78. Deng J, Wang ES, Jenkins RW, Li S, Dries R, Yates K, et al. CDK4/6 Inhibition Augments Antitumor Immunity by Enhancing T-Cell Activation. *Cancer Discov* (2018) 8(2):216–33. doi: 10.1158/2159-8290.cd-17-0915
 79. Li X, Nadauld L, Ootani A, Corney DC, Pai RK, Gevaert O, et al. Oncogenic Transformation of Diverse Gastrointestinal Tissues in Primary Organoid Culture. *Nat Med* (2014) 20(7):769–77. doi: 10.1038/nm.3585
 80. Li X, Ootani A, Kuo C. An Air-Liquid Interface Culture System for 3D Organoid Culture of Diverse Primary Gastrointestinal Tissues. *Methods Mol Biol* (2016) 1422:33–40. doi: 10.1007/978-1-4939-3603-8_4
 81. Pavesi A, Tan AT, Koh S, Chia A, Colombo M, Antonicchia E, et al. A 3D Microfluidic Model for Preclinical Evaluation of TCR-Engineered T Cells Against Solid Tumors. *JCI Insight* (2017) 2(12). doi: 10.1172/jci.insight.89762
 82. Jung DJ, Shin TH, Kim M, Sung CO, Jang SJ, Jeong GS. A One-Stop Microfluidic-Based Lung Cancer Organoid Culture Platform for Testing Drug Sensitivity. *Lab on a Chip* (2019) 19(17):2854–65. doi: 10.1039/c9lc00496c
 83. Torabi S, Li L, Grabau J, Sands M, Berron BJ, Xu R, et al. Cassie-Baxter Surfaces for Reversible, Barrier-Free Integration of Microfluidics and 3D Cell Culture. *Langmuir ACS J Surfaces Colloids* (2019) 35(32):10299–308. doi: 10.1021/acs.langmuir.9b01163
 84. Niu Y, Bai J, Kamm RD, Wang Y, Wang C. Validating Antimetastatic Effects of Natural Products in an Engineered Microfluidic Platform Mimicking Tumor Microenvironment. *Mol Pharmaceutics* (2014) 11(7):2022–9. doi: 10.1021/mp500054h
 85. Achberger K, Probst C. Merging Organoid and Organ-on-a-Chip Technology to Generate Complex Multi-Layer Tissue Models in a Human Retina-on-a-Chip Platform. *eLife* (2019) 8:e46188. doi: 10.7554/eLife.46188
 86. Skardal A, Aleman J, Forsythe S, Rajan S, Murphy S, Devarasetty M, et al. Drug Compound Screening in Single and Integrated Multi-Organoid Body-on-a-Chip Systems. *Biofabrication* (2020) 12(2):025017. doi: 10.1088/1758-5090/ab6d36
 87. Kasendra M, Luc R, Yin J, Manatakis DV, Kulkarni G, Lucchesi C, et al. Duodenum Intestine-Chip for Preclinical Drug Assessment in a Human Relevant Model. *eLife* (2020) 9:e50135. doi: 10.7554/eLife.50135
 88. Daly AC, Davidson MD, Burdick JA. 3D Bioprinting of High Cell-Density Heterogeneous Tissue Models Through Spheroid Fusion Within Self-Healing Hydrogels. *Nat Commun* (2021) 12(1):753. doi: 10.1038/s41467-021-21029-2
 89. Ayan B, Heo DN. Aspiration-Assisted Bioprinting for Precise Positioning of Biologics. *Sci Adv* (2020) 6: (10):eaaw5111. doi: 10.1126/sciadv.aaw5111
 90. Brassard JA, Nikolaev M. Recapitulating Macro-Scale Tissue Self-Organization Through Organoid Bioprinting. *Nat Mater* (2021) 20(1):22–9. doi: 10.1038/s41563-020-00803-5
 91. Flores-Torres S, Peza-Chavez O. Alginate-Gelatin-Matrigel Hydrogels Enable the Development and Multigenerational Passaging of Patient-Derived 3D Bioprinted Cancer Spheroid Models. *Biofabrication* (2021) 13(2):025001. doi: 10.1088/1758-5090/abdb87
 92. Li YC, Jodat YA. Toward a Neurospheroid Niche Model: Optimizing Embedded 3D Bioprinting for Fabrication of Neurospheroid Brain-Like Co-Culture Constructs. *Biofabrication* (2020) 13(1):015014. doi: 10.1088/1758-5090/abc1be
 93. Geurts MH, de Poel E, Amatngalim GD, Oka R, Meijers FM, Kruisselbrink E, et al. CRISPR-Based Adenine Editors Correct Nonsense Mutations in a Cystic Fibrosis Organoid Biobank. *Cell Stem Cell* (2020) 26(4):503–10.e7. doi: 10.1016/j.stem.2020.01.019
 94. Fujii M, Shimokawa M, Date S, Takano A, Matano M, Nanki K, et al. A Colorectal Tumor Organoid Library Demonstrates Progressive Loss of Niche Factor Requirements During Tumorigenesis. *Cell Stem Cell* (2016) 18(6):827–38. doi: 10.1016/j.stem.2016.04.003
 95. Co JY, Margalef-Català M, Monack DM, Amieva MR. Controlling the Polarity of Human Gastrointestinal Organoids to Investigate Epithelial Biology and Infectious Diseases. *Nat Protoc* (2021) 16(11):5171–92. doi: 10.1038/s41596-021-00607-0
 96. Beato F, Reverón D, Dezi KB, Ortiz A, Johnson JO, Chen DT, et al. Establishing a Living Biobank of Patient-Derived Organoids of Intraductal Papillary Mucinous Neoplasms of the Pancreas. *Lab Invest* (2021) 101(2):204–17. doi: 10.1038/s41374-020-00494-1
 97. Tiriach H, Belleau P, Engle DD. Organoid Profiling Identifies Common Responders to Chemotherapy in Pancreatic Cancer. *Cancer Discovery* (2018) 8: (9):1112–29. doi: 10.1158/2159-8290.cd-18-0349
 98. Tiriach H, Bucobo JC, Tzimas D, Grewel S, Lacombe JF, Rowehl LM, et al. Successful Creation of Pancreatic Cancer Organoids by Means of EUS-Guided Fine-Needle Biopsy Sampling for Personalized Cancer Treatment. *Gastrointest Endosc* (2018) 87(6):1474–80. doi: 10.1016/j.gie.2017.12.032
 99. Baker LA, Tiriach H, Tuveson DA. Generation and Culture of Human Pancreatic Ductal Adenocarcinoma Organoids From Resected Tumor Specimens. *Methods Mol Biol* (2019) 1882:97–115. doi: 10.1007/978-1-4939-8879-2_9
 100. Jacob F, Salinas RD, Zhang DY, Nguyen PTT, Schnoll JG, Wong SZH, et al. A Patient-Derived Glioblastoma Organoid Model and Biobank Recapitulates Inter- and Intra-Tumoral Heterogeneity. *Cell* (2020) 180(1):188–204.e22. doi: 10.1016/j.cell.2019.11.036
 101. Mollaki V. Ethical Challenges in Organoid Use. *BioTech* (2021) 10(3):12. doi: 10.3390/biotech10030012
 102. Boers SN, van Delden JJM, Bredenoord AL. Organoids as Hybrids: Ethical Implications for the Exchange of Human Tissues. *J Med Ethics* (2019) 45(2):131–9. doi: 10.1136/medethics-2018-104846
 103. Lensink MA, Boers SN, Jongsma KR, Carter SE, van der Ent CK, Bredenoord AL. Organoids for Personalized Treatment of Cystic Fibrosis: Professional Perspectives on the Ethics and Governance of Organoid Biobanking. *J Cystic Fibrosis Off J Eur Cystic Fibrosis Soc* (2021) 20(3):443–51. doi: 10.1016/j.jcf.2020.11.015
 104. Wang H. Modeling Neurological Diseases With Human Brain Organoids. *Front Synaptic Neurosci* (2018) 10:15. doi: 10.3389/fnsyn.2018.00015
 105. Trujillo CA, Gao R, Negraes PD, Gu J, Buchanan J, Preissl S, et al. Complex Oscillatory Waves Emerging From Cortical Organoids Model Early Human

- Brain Network Development. *Cell Stem Cell* (2019) 25(4):558–69.e7. doi: 10.1016/j.stem.2019.08.002
106. Reardon S. Can Lab-Grown Brains Become Conscious? *Nature* (2020) 586(7831):658–61. doi: 10.1038/d41586-020-02986-y
 107. Paşca SP. The Rise of Three-Dimensional Human Brain Cultures. *Nature* (2018) 553(7689):437–45. doi: 10.1038/nature25032
 108. Hyun I, Scharf-Deering JC, Lunshof JE. Ethical Issues Related to Brain Organoid Research. *Brain Res* (2020) 1732:146653. doi: 10.1016/j.brainres.2020.146653
 109. Dickreuter E, Cordes N. The Cancer Cell Adhesion Resistome: Mechanisms, Targeting and Translational Approaches. *Biol Chem* (2017) 398(7):721–35. doi: 10.1515/hsz-2016-0326
 110. Fang Y, Eglén RM. Three-Dimensional Cell Cultures in Drug Discovery and Development. *SLAS Discov Advancing Life Sci R D* (2017) 22(5):456–72. doi: 10.1177/1087057117696795
 111. Katt ME, Placone AL, Wong AD, Xu ZS, Searson PC. *In Vitro* Tumor Models: Advantages, Disadvantages, Variables, and Selecting the Right Platform. *Front Bioeng Biotechnol* (2016) 4:12. doi: 10.3389/fbioe.2016.00012
 112. Fennema E, Rivron N, Rouwkema J, van Blitterswijk C, de Boer J. Spheroid Culture as a Tool for Creating 3D Complex Tissues. *Trends Biotechnol* (2013) 31(2):108–15. doi: 10.1016/j.tibtech.2012.12.003
 113. Ishiguro T, Ohata H, Sato A, Yamawaki K, Enomoto T, Okamoto K. Tumor-Derived Spheroids: Relevance to Cancer Stem Cells and Clinical Applications. *Cancer Sci* (2017) 108(3):283–9. doi: 10.1111/cas.13155
 114. Xu H, Lyu X, Yi M, Zhao W, Song Y, Wu K. Organoid Technology and Applications in Cancer Research. *J Hematol Oncol* (2018) 11(1):116. doi: 10.1186/s13045-018-0662-9
 115. Fiorini E, Veghini L, Corbo V. Modeling Cell Communication in Cancer With Organoids: Making the Complex Simple. *Front Cell Dev Biol* (2020) 8:166. doi: 10.3389/fcell.2020.00166
 116. Nunes AS, Barros AS, Costa EC, Moreira AF, Correia JJ. 3D Tumor Spheroids as *In Vitro* Models to Mimic *In Vivo* Human Solid Tumors Resistance to Therapeutic Drugs. *Biotechnol Bioeng* (2019) 116: (1):206–26. doi: 10.1002/bit.26845
 117. Gilazieva Z, Ponomarev A, Rutland C. Promising Applications of Tumor Spheroids and Organoids for Personalized Medicine. *Cancers* (2020) 12(10):2727. doi: 10.3390/cancers12102727
 118. Gerlinger M, Rowan AJ, Horswell S, Math M, Larkin J, Endesfelder D, et al. Intratumor Heterogeneity and Branched Evolution Revealed by Multiregion Sequencing. *N Engl J Med* (2012) 366(10):883–92. doi: 10.1056/NEJMoa1113205
 119. Nozaki K, Mochizuki W, Matsumoto Y, Matsumoto T, Fukuda M, Mizutani T, et al. Co-Culture With Intestinal Epithelial Organoids Allows Efficient Expansion and Motility Analysis of Intraepithelial Lymphocytes. *J Gastroenterol* (2016) 51(3):206–13. doi: 10.1007/s00535-016-1170-8
 120. DiMarco RL, Dewi RE, Bernal G, Kuo C, Heilshorn SC. Protein-Engineered Scaffolds for *In Vitro* 3D Culture of Primary Adult Intestinal Organoids. *Biomater Sci* (2015) 3(10):1376–85. doi: 10.1039/c5bm00108k
 121. Gunasekara DB, DiSalvo M, Wang Y, Nguyen DL, Reed MI, Speer J, et al. Development of Arrayed Colonic Organoids for Screening of Secretagogues Associated With Enterotoxins. *Anal Chem* (2018) 90(3):1941–50. doi: 10.1021/acs.analchem.7b04032
 122. Francies HE, Barthorpe A, McLaren-Douglas A, Barendt WJ, Garnett MJ. Drug Sensitivity Assays of Human Cancer Organoid Cultures. *Methods Mol Biol* (2019) 1576:339–51. doi: 10.1007/7651_2016_10

Conflict of Interest: The authors declare that the research was conducted in the absence of any commercial or financial relationships that could be construed as a potential conflict of interest.

Publisher's Note: All claims expressed in this article are solely those of the authors and do not necessarily represent those of their affiliated organizations, or those of the publisher, the editors and the reviewers. Any product that may be evaluated in this article, or claim that may be made by its manufacturer, is not guaranteed or endorsed by the publisher.

Copyright © 2021 Zhou, Cong and Cong. This is an open-access article distributed under the terms of the Creative Commons Attribution License (CC BY). The use, distribution or reproduction in other forums is permitted, provided the original author(s) and the copyright owner(s) are credited and that the original publication in this journal is cited, in accordance with accepted academic practice. No use, distribution or reproduction is permitted which does not comply with these terms.



The “WWHow” Concept for Prospective Categorization of Post-operative Severity Assessment in Mice and Rats

Anke Tappe-Theodor¹, Claudia Pitzer², Lars Lewejohann^{3,4}, Paulin Jirkof⁵, Katja Siegeler⁶, Astra Segelcke⁷, Natascha Drude⁸, Bruno Pradier⁹, Esther Pogatzki-Zahn⁹, Britta Hollinderbäumer¹⁰ and Daniel Segelcke^{9*}

¹ Institute of Pharmacology, University of Heidelberg, Heidelberg, Germany, ² Interdisciplinary Neurobehavioral Core, University of Heidelberg, Heidelberg, Germany, ³ Institute of Animal Welfare, Animal Behavior and Laboratory Animal Science, Freie Universität Berlin, Berlin, Germany, ⁴ German Federal Institute for Risk Assessment (BfR), German Center for the Protection of Laboratory Animals (Bf3R), Berlin, Germany, ⁵ Office for Animal Welfare and 3Rs, University of Zurich, Zurich, Switzerland, ⁶ Department of Work and Environmental Protection, Westphalian Wilhelms University Muenster, Münster, Germany, ⁷ Independent Researcher, Herne, Germany, ⁸ Berlin Institute of Health (BIH) at Charité, QUEST Center for Responsible Research, Berlin, Germany, ⁹ Department of Anesthesiology, Intensive Care and Pain Medicine, University Hospital Muenster, Münster, Germany, ¹⁰ Member of Working Group for Animal Welfare, BÜNDNIS 90/DIE GRÜNEN, Düsseldorf, Germany

OPEN ACCESS

Edited by:

Marta L. Alves Da Silva,
Universidade do Porto, Portugal

Reviewed by:

Vera Baumans,
Utrecht University, Netherlands
Penny Hawkins,
Royal Society for the Prevention of
Cruelty to Animals, United Kingdom

*Correspondence:

Daniel Segelcke
Segelcke@anit.uni-muenster.de

Specialty section:

This article was submitted to
Animal Behavior and Welfare,
a section of the journal
Frontiers in Veterinary Science

Received: 22 December 2021

Accepted: 09 February 2022

Published: 15 March 2022

Citation:

Tappe-Theodor A, Pitzer C,
Lewejohann L, Jirkof P, Siegeler K,
Segelcke A, Drude N, Pradier B,
Pogatzki-Zahn E, Hollinderbäumer B
and Segelcke D (2022) The “WWHow”
Concept for Prospective
Categorization of Post-operative
Severity Assessment in Mice and
Rats. *Front. Vet. Sci.* 9:841431.
doi: 10.3389/fvets.2022.841431

The prospective severity assessment in animal experiments in the categories’ non-recovery, mild, moderate, and severe is part of each approval process and serves to estimate the harm/benefit. Harms are essential for evaluating ethical justifiability, and on the other hand, they may represent confounders and effect modifiers within an experiment. Catalogs and guidelines provide a way to assess the experimental severity prospectively but are limited in adaptation due to their nature of representing particular examples without clear explanations of the assessment strategies. To provide more flexibility for current and future practices, we developed the modular Where-What-How (WWHow) concept, which applies findings from pre-clinical studies using surgical-induced pain models in mice and rats to provide a prospective severity assessment. The WWHow concept integrates intra-operative characteristics for predicting the maximum expected severity of surgical procedures. The assessed severity categorization is mainly congruent with examples in established catalogs; however, because the WWHow concept is based on anatomical location, detailed analysis of the tissue trauma and other intra-operative characteristics, it enables refinement actions, provides the basis for a fact-based dialogue with authority officials and other stakeholders, and helps to identify confounder factors of study findings.

Keywords: postoperative, surgery surgical procedures, severity assessment, rodents, prospective, mice, rats

INTRODUCTION

Pre-clinical animal research constitutes an essential part of several avenues to understand mechanisms and develop novel treatment options and strategies in diverse research fields. Although intense efforts are being made to replace and reduce animal experiments, they are not yet entirely dispensable. Depending on the research question, animal experimentation can be associated with

harm, including pain, suffering, and distress for the animal. According to the Directive 2010/63/EU on the protection of animals used for scientific purposes, part of each application is the prospective evaluation of the severity assessment of each animal experiment in the categories of non-recovery, mild, moderate, or severe, allowing ethical consideration with respect to points weighting the likely harms to the animals against potential benefits of the planned experiments (harm/benefit analysis) (1). Therefore, researchers are required to classify the severity of every single intervention (e.g., surgical procedure, behavior test) and provide an ethical classification of the entire experiment. However, suitable categorization tools are still lacking. Besides a few reports addressing the severity classification (2, 3), three catalogs are available and widely accepted in Europe. The Berlin Animal Welfare officer catalog, named “Berlin catalog”, the EU Directive 2010/63/EU Annex VIII, called the “EU catalog” and the Swiss Federal office catalog named the “Swiss catalog” from here on (4–6). While catalogs are valuable for established interventions for which severity has been carefully evaluated in the past, they are of limited use for experiments with unknown/novel, unevaluated procedures. They can provide only rough indications of severity for comparable interventions. Furthermore, it is often not apparent which variables were used to classify individual interventions, and finally, the “nature of pain” is not sufficiently described. Nevertheless, the explicit description of the “nature of pain” is a requirement of the EU directive. Thus, a basic set of tools is needed for a prospective, transparent and objective severity assessment.

These much-needed tools should integrate the anatomical, physiological, and ethological (including evolutionary) traits of the animal species used and incorporate the specific intervention, enabling a precise, individualized prospective categorization.

The severity classification for weighing up an animal experiment is essential in many aspects. First, it allows the definition of humane endpoints and interventions to minimize the animal burden within the experiment. Second, it is of utmost importance for the experimenter to accurately predict the severity to identify direct and indirect consequences that may affect the scientific work. For example, inadequately treated pain has divergent effects, such as alterations in metabolism, hormonal imbalances (7) and psychological distress, which might also cause physiological coping mechanisms and, therefore potential confounders. Knowledge of the potential harms affects experimental design and study results. Finally, it helps to implement actions that directly or indirectly reduce the severity, maintain animal health and welfare, and minimize factors (e.g., confounder, effect modifier) related to the well-being of the individual animal, consequently increasing the quality of research.

Pain, suffering, and distress to the animal are difficult to objectify and have many different causes. The characterization of morphological tissue damage in combination with ethological parameters and methodological aspects can serve to objectify pain and suffering in surgical procedures to some extent, as they are quantifiable and interpretable parameters. For objective quantifiability, the required parameters must not be obtained

purely by analogy to humans but from pre-clinical, experimental animal pain models. Over the past 25 years, several surgical pain models—primarily in rodents (rats and mice)—have been published to reveal underlying mechanisms of post-operative pain in humans (8, 9). The findings of these studies can be applied to improve clinical treatment options but also bidirectionally in animal welfare science. In our opinion, accurate knowledge of the possible pain modalities, their time courses, intensity, and localization, as well as the underlying mechanisms based on studies with pain models, can be used to provide a prospective severity assessment of surgical procedures in rodents used for scientific purposes.

Surgical interventions are ubiquitously used in rodent biomedical research for generating disease states, sampling tissue, implanting, or testing medical devices. However, it is worth pointing out that there is a specific manifestation of post-operative pain-related behavior in intensity and time dependence on the surgical characteristics (10–12).

We aimed to provide an easy-to-use concept based on intra-operative features, being orientated and adapted from different rodent models for surgically induced pain. The integration of intra-operative characteristics related to the surgical site (Where), tissue trauma (What), and methodological aspects (How) result in a method that is ready to understand, transparent in the approach, transferable to any laboratory, and applicable for any rodent surgical intervention. Thereby, the Where, What, and How (WWHow) concept enables an objective and customized prospective severity assessment of surgical interventions according to the EU directive (1).

METHODOLOGIES FOR THE WWHOW CONCEPT

A multidisciplinary and interprofessional group developed this concept with diverse interests and expertise in animal welfare research. These include medical professionals (veterinary and human), biologists, pre-clinical scientists, animal welfare-associated experts, and politicians (see individual affiliations). The WWHow concept is based on ordinal scales to integrate multidimensional variables into a score with an unknown interval property and relative rank of variables. Score summation for the categories “Where”, “What” and “How” gives the total score, which forms the trichotomous outcome with an ordering to the categories into mild, moderate, or severe, as suggested by the current EU directive (1). The categorization is according to the intra-operative characteristics of surgical interventions; therefore, an obvious prerequisite is to know the exact procedure.

We have chosen a score from 1 to 5 for the “Where” part and 1–9 for the “What” and “How” parts. These numbers are not mathematically consecutive; the scoring increases with the importance of the region, the size of the intervention and the duration of the surgical procedure, but not in calculative numbers, which means that a value of four does not mean double of two. The parameters considered in the establishment of the score are explained below. According to our definition, total scores between 4 and 9 points lead to a mild severity, 10–16

points belong to the moderate, and 17–23 points indicate a severe category. However, it should be borne in mind that the proposed concept is not a set of rules fixed for all time but should always be seen as a process of further development. In this context, the transition from numerical to the ordinal scale indicated here may well be modified based on future scientific results. Significantly, this categorization concept is based on one and not multiple surgical injury regions. Noteworthy, our concept is designed for mice and rats and should be adapted for other rodents.

Intra-Operative Characteristics

Anatomical Localization of the Surgical Procedure (“Where”)

The rodent body surface was divided into 11 general regions, spanning the dorsal and ventral bodyside, including three shared regions (tail, front and hind legs) (**Figure 1**). The classification was based on rats’ and mice’s general anatomy and myology (13–16). Scoring of each body region was based on two variables, (1) biomechanical functioning and (2) its involvement in rodent-specific *maintenance* and *general* behavior. *Maintenance* behaviors include necessary behaviors for preserving the body and social homeostases, such as *drinking*, *feeding*, *grooming*, *social interaction*, and *nest building*. In contrast, *general* behaviors refer to other movement-related activities, such as exploratory or miscellaneous activities (e.g., climbing, rearing). Therefore, *maintenance* behaviors are directly linked to animal survival and are more important than *general* activity when evaluating body regions.

All extremities are involved in *movement* behaviors, including *locomotion*, *balancing*, *rearing*, *grooming*, and *scratching*. However, movement is usually not substantially restricted because rodents are quadrupeds and can compensate for the impairment, especially for an injury to the hind legs (16, 17). In contrast, unilateral injury to a front extremity leads to a more significant restriction. Here, the *food intake* and thus indirectly the *maintenance behavior* is affected. Therefore, on an ordinal scale, the hind legs are rated 1 and the front legs 2 because of their different effects on *maintenance behavior*.

The tail, neck, flanks, back, thorax, and abdomen are essential for general *body stability in rest* and *under movement*, including *locomotion*, *grooming*, and *scratching*. However, the proportion of these body regions in their function is to be weighed separately; thus, the tail, the neck, and the flanks are rated with a score of 2 because they are essential for the body’s stability and posture, but they are not (or less) necessary for *maintenance* behavior. The back and the abdomen are rated 3. This is due to the fact that the back and the associated muscles are involved in the body’s stability and *movement* behavior. The abdomen is also necessary for this behavior and forms the body cavity for various inner organs (13, 17). The thorax, scored with 4, is particularly important because it is essential for *maintenance* (breathing) and *general* behaviors. Respiration leads to a continuous thorax movement without compensation and/or avoidance opportunities for the rodent. Rodent ears and nose (including vibrissae/whiskers) detect sounds and olfactory cues to perceive environmental changes and provide essential social communication and orientation. Therefore, the ears are rated

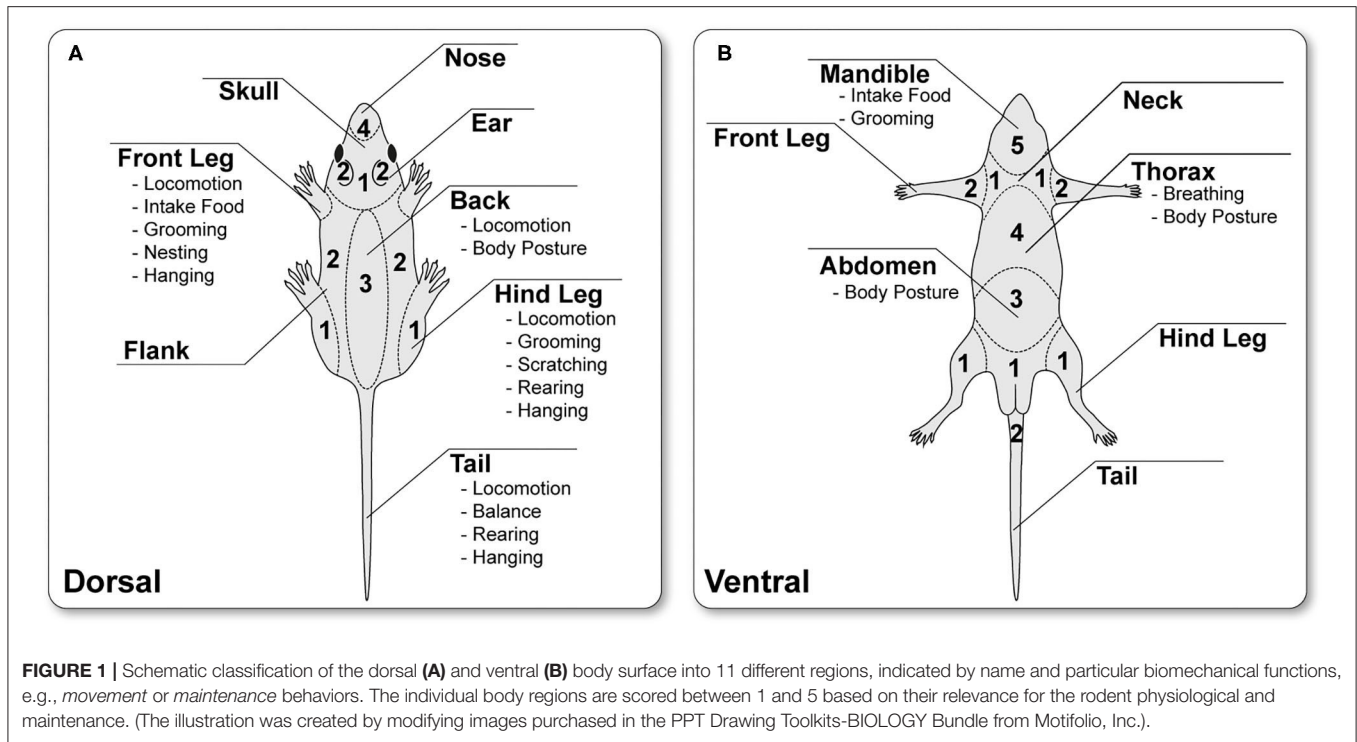
2, and the nose/whisker region 3. For *maintenance* behavior and ensuring survival, water and food intake are necessary. For this, the ventral part of the skull is essential for water and food ingestion and is, therefore, to be rated with a score of 5. In contrast, the dorsal cranial and genital regions are rated with 1 because surgical interventions in these regions have less impact on rodent behaviors.

Tissue Trauma (“What”) Caused by Surgical Procedure (“How”)

Based on findings from surgical-induced pain models in rodents, the “What” of tissue trauma and the “How” in the form of surgical techniques, i.e., size of the injury, total surgery duration, and retraction duration, may influence the type, intensity, and time course of post-operative pain and, thus, the overall severity. Therefore, these different variables of the post-operative period were integrated to form another ordinal scale for the two remaining categories. In addition, mechanistic, anatomical, and morphological data were considered. The following describes the respective variables and their potential impact in detail.

Every surgical intervention causes typical tissue trauma, which must be described as detailed as possible when assessing post-operative severity. The correlation between tissue trauma characteristics and post-operative pain-related symptoms in well-characterized procedures can help to allow a more accurate prospective assessment of surgical severity in terms of pain modalities in future procedures. One of the most critical factors for the prospective estimation of surgical-induced severity in rodents is pain, which is measurable as non-evoked or evoked pain-related behavior to different modalities (18). In addition, pain modalities are measured in pre-clinical surgical rodent pain models over time (11, 19). These evidence-based trajectories provide another essential basis for a prospective severity assessment while also identifying mechanisms that underlie different pain modalities. For example, physiological changes, e.g., in sleep behavior or stress hormone levels, are caused by pain. However, these changes are assessed sporadically in pre-clinical animal pain research so that the concept is based exclusively on the observed post-operative pain behavior, which determines the score. Overall, detailed knowledge about different pain modalities is of enormous importance for further post-operative treatment recommendations.

Most surgical procedures start with a localized skin incision. Rodent skin is thin (25 μ m) with 2 or 3 layers and loose (20, 21). Cutaneous incision injury directly activates peripheral nociceptive fibers (high-threshold) and causes hemorrhage and cell debris (22). Incisions of skin tissue during surgery represent a primary wound (23). In contrast to other types of wounds (secondary or tertiary), they are characterized by fresh, aseptic injuries that have smooth edges and are closed by suturing (23). The inflammatory processes are diverse and trigger a prolonged hypersensitivity to evoked mechanical and heat but not to cold stimuli (24), directly around the incision injury (primary area of hypersensitivity). The primary hypersensitivity reaches a maximum shortly after awakening from anesthesia and is steadily reduced in the course of primary wound healing (depending on incision dimension) (10, 11).



In contrast to primary hypersensitivity, driven by peripheral processes mainly in the injured tissue, secondary hypersensitivity is a central product only to mechanical stimuli in a larger area around the incisional wound (22, 25). Peripheral sensitized nociceptors contribute to the sensitization of spinal dorsal horn neurons, expanding their receptive fields and modulating their responsiveness (22, 26). These symptoms after skin incision may manifest in avoidance/guarding behavior (27). Generally, a pure skin incision is rated 1. The type and severity of behavioral changes depend on the surgical injury location (see “Where”) as well as on the size of the injury (see “How”). Avoidance behavior is characterized by reduced weight-bearing (protective behavior) of the affected area and possibly an altered gait pattern if body regions are injured that are important for *movement* (see “Where”) (19, 28, 29). If the traumatized region is not essential for *rearing*, *grooming*, *scratching*, or *locomotion*, observations to estimate severity are hampered and can usually only be assessed by specific behavioral tests or by interpolation of mechanistic data from rodents.

Furthermore, the incised skin, most surgical procedures involve manipulating the underlying muscles, such as creating subcutaneous cavities for implantation of mini-pumps, displaying blood vessels or nerves, or providing access to internal organs (see examples in the results part). Manipulation of the muscle layer ranges from blunt dissection or displacement (30) to muscle incision (31). Unlike displacement and blunt preparations, incision always results in hemorrhage, direct activation of nociceptive fibers, and a distinct inflammatory response triggered by hemorrhage and cellular debris. These processes lead to the release of diverse damage-associated mediators, reactive oxygen species, pro-inflammatory mediators,

activate residents, and facilitate the migration of immune cells, thereby altering the local tissue pH and further signaling cascades, including nociceptor sensitization (10, 32). Compared to skin-only incision, these effects are massive and, thus, have a more pronounced influence on pain behavior (31), especially during muscle contraction for *movement* (33). In contrast, blunt dissection and displacement of the muscle layers are associated with a lower degree of hemorrhage or cells debris. In addition, temporary hypoxia and mechanical stretching of the muscle play an essential role, especially in a time-dependent manner. Here, too, an inflammatory process is initiated postoperatively and is less severe and shorter than in the case of muscle injury by incision (30). Due to different degrees of inflammatory responses caused by manipulation characteristics of muscle, displacing the muscle and/or blunt dissection is rated as 1 and the muscle incision as 2.

In addition to skin and muscle trauma, sensory nerve fiber tracts are often displaced, crushed, ligated, or lesioned in some surgical procedures (9, 34–36). Injuries of small cutaneous nerves play a minor role, whereas large nerve fiber tracts, such as the sciatic, femoral, intercostal, radial, or ulnar nerves with their direct branches (e.g., first branches of the sciatic nerve: tibial, peroneal, and sural nerve, see **Figure 2**) are more relevant. The grade of nerve injury can significantly affect the post-operative severity. Therefore, to assess the potential severity, it is essential to know whether and how nerve fibers tracts are injured, where and in which body regions the neuropathic pain symptoms can be expected. Nerve trauma during surgeries mainly involves partial damage to peripheral axons through blunt trauma, including crush, stretching, perineural inflammation, compression, and scar formation, with entrapment of sensory fibers and/or

neuroma formation. In general, partial damage to sensory axons during surgery results in spontaneous activity, a lower activation threshold, and an enhanced response to a stimulus (37). Hyperesthesia can be ascribed to enhanced sensitivity of non-interrupted but injured axons associated with spontaneous ectopic discharges by increased ion channel expression along the axon. In addition, the inflammatory response may alter gene expression in the dorsal root ganglion, which increases the synthesis of peripheral receptors that sensitize nociceptors (38).

The displacement of nerve tracts within the soft tissue results in minor pathological consequences and is rated as 1. However, inadequate anatomical knowledge, abnormalities, or surgical techniques that may result in a lesion during surgery are rated as 3. In this case, neuroplastic changes in the entire neuroaxis of pain are expected, resulting in possible nerve degeneration and thus an increased transition from acute to persistent post-surgical pain. Nerve ligation is graded lower than the lesion itself and therefore rated as 2.

Other scientific questions require surgical interventions involving mechanical distortion of bones. Mechanical bone distortion can range from craniotomy over laminectomy to experimental bone fractures. In addition, consideration must be given to which part of the skeleton is injured and to what extent is essential for *maintenance behavior*. Disturbing periosteum, cortical bone, or bone marrow can induce bone pain, depending on different pathological processes. This suggests that nociceptive fibers innervate all bone structural compartments (39–41). The periosteum has the highest density of fibers arranged as a mesh network, allowing detection of mechanical distortion (e.g., stretching of periosteum). Mechanical distortion, such as a fracture or drilling a hole, directly activates nociceptive fibers, but this depends on the surgical trauma extent. These traumas may be associated with a short-lasting sensation of sharp and localized pain experienced in the immediate recovery phase after anesthesia, followed by a more long-lasting dull, deep pain. Hours after bone trauma, osteoclasts, osteoblasts, and immune cells release pro-inflammatory mediators, creating an inflammatory environment close to the trauma, contributing to the peripheral sensitization processes. A distinction must be made regarding the stability of the bone injury. While removal of bone tissue (drilling a hole) and partial replacement (cranial window) represent stable injury, a fracture can be unstable. Due to the uniform nociceptive fiber bone distribution, the dimension of the bone injury is directly related to the activation. Since no direct studies address this question, we used the size of the bone damage as a parameter to generate a score. Bone trepanation is rated 1 (minimum), a craniotomy for implantation of a cranial window or a laminectomy is rated 2 (medium), and fractures are rated 3 (maximum) (**Figure 2**).

Characteristics of Surgical Intervention (“How”)

Surgical interventions contain various factors that can considerably influence the outcome and, consequently, the severity. In contrast to humans, only a few studies in surgical models exist on how intra-operative factors affect the severity in rodents. In total, three intra-operative factors have been identified for post-operative severity assessment in rodents; the

size of the incision, the duration of the surgery, and the time of tissue retraction.

The dimension of the skin incision is directly related to the activation of cutaneous nociceptive fibers and resident immune cells, such as mast cells or δ T cells (20, 21). Based on data from various surgical-induced pain models, a skin incision <5 mm is categorized as a 1, between 6 and 10 mm as a 2, and >10 mm as a 3. However, there are no specific data from animal studies describing the effect of incision size on pain behavior, especially since this information is given little or not at all in publication. Therefore, the data are taken from the description of the standardized post-operative pain models in rodents (8, 42, 43).

It is known from human studies that minimally invasive procedures reduce cutaneous hypersensitivity but do not contribute significantly to the overall reduction of post-operative pain (44, 45). This may be due to the minimally invasive procedure limiting the surgeon's vision and leading to additional tissue trauma (e.g., surgical neuropathy by nerve injury), directly impacting severity. Therefore, skin incision should be kept to a minimum, allowing the best performance of further surgical stages (17).

The second factor is the duration of a surgical procedure, which is related to the duration of the anesthesia, the resulting physiological changes, such as the local lack of oxygen in the injured tissue, loss of body temperature, and the inflammatory processes. Prolonged surgical duration is mainly associated with a more extensive or complex intervention. Therefore, three-time intervals were defined: Short interventions under 10 min [e.g., plantar incision models (43)] are rated 1, medium-length between 11 and 60 min (e.g., muscle retraction model, (30) are rated 2, and long duration surgeries over 60 min (e.g., thoracotomy models, (46) are rated 3.

The third factor is tissue retraction using surgical tools (forceps or retractors), which damage the tissue in several ways. Retraction of superficial tissues such as skin and muscles leads to oxygen deficiency, accompanied by tissue damage and even destruction (47). Also, nerve tracts can be displaced or lesioned with tissue retraction, resulting in increased inflammatory response (30). Potential manipulation of nerve tracts and undersupply by the retraction process are potentially time-dependent. Therefore, based on the characteristics of different surgical models in rodents, three-time intervals were defined, which differed in terms of post-operative outcomes and mechanisms. Retraction time from 1 to 10 min is rated 1, 11 to 60 min is rated 2, and over 60 min is rated 3 (see for examples “duration of surgery”).

Other intra-operative parameters have not yet been directly investigated in rodents. However, studies with surgical patients show that other interoperative factors like anesthetic technique, the surgical unit's experience, or open vs. laparoscopic are known (48).

EXEMPLARY APPLICATION OF THE WWHOW CONCEPT

Several exemplary surgical interventions are presented here to demonstrate the categorization according to the WWHOW

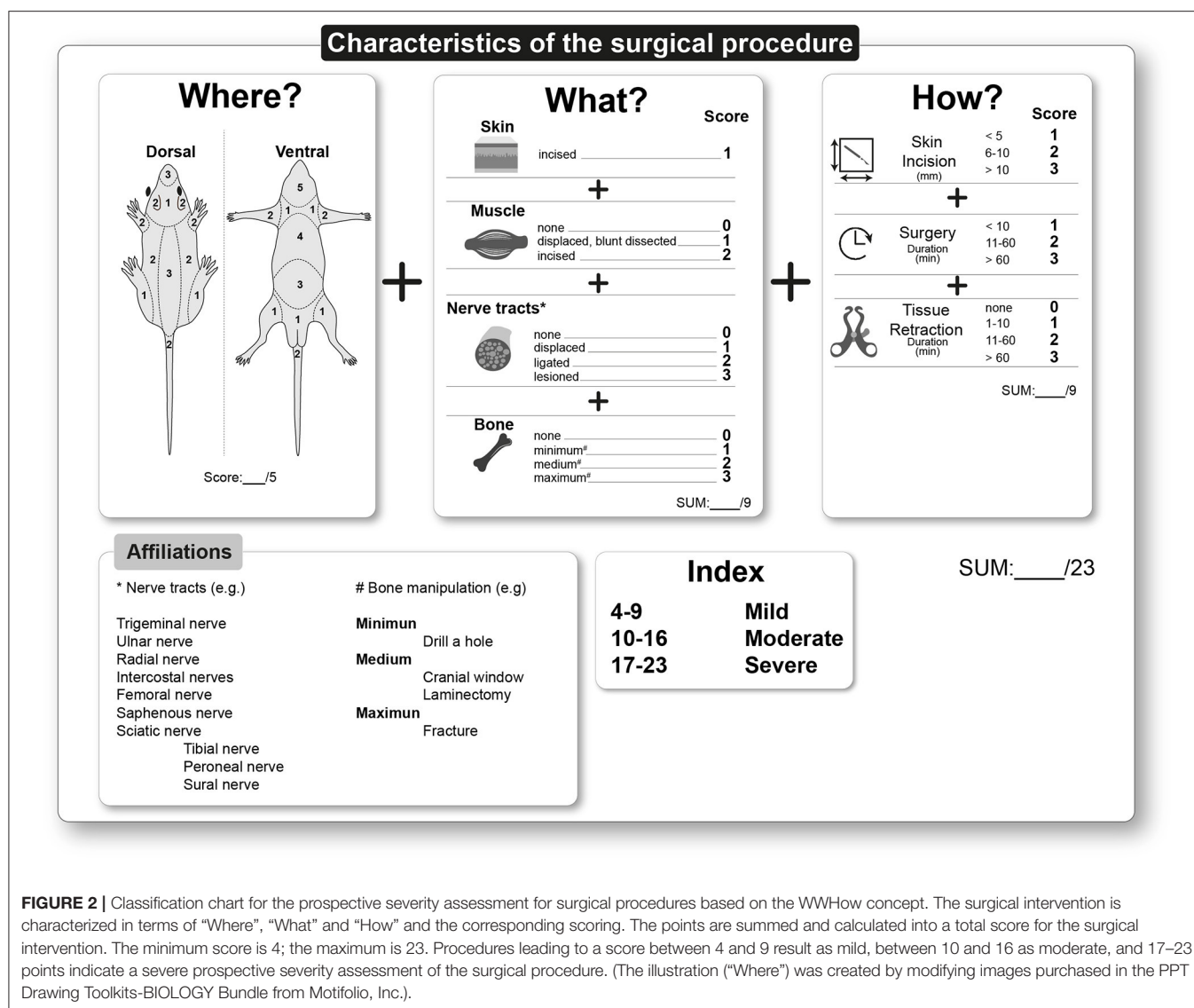


FIGURE 2 | Classification chart for the prospective severity assessment for surgical procedures based on the WWHow concept. The surgical intervention is characterized in terms of “Where”, “What” and “How” and the corresponding scoring. The points are summed and calculated into a total score for the surgical intervention. The minimum score is 4; the maximum is 23. Procedures leading to a score between 4 and 9 result as mild, between 10 and 16 as moderate, and 17–23 points indicate a severe prospective severity assessment of the surgical procedure. (The illustration (“Where”) was created by modifying images purchased in the PPT Drawing Toolkits-BIOLOGY Bundle from Motifolio, Inc.).

concept. The resulting prospective severity scores are explained in detail for each intervention. It is important to note that the data and values, e.g., for the incision size or the surgery duration, are based on published studies/protocols and may vary depending on the individual protocol. In addition, all surgical interventions described herein generally require adequate personal training for performance, aseptic techniques, potential ventilation, and intra-operative monitoring. Finally, all surgical interventions are performed under general anesthesia, potential analgetic regime, sterile, and in some cases, ventilated conditions (17).

First, we describe representative surgically-induced pain models in rodents, which address different intra-operative characteristics according to the WWHow concept. The pain-related behavior of these models performed without analgesia treatment is the subject of many studies in the pain field and thus represents a basis (“worst-case scenario”) necessary to predict the possible severity outcome of a surgical procedure. Next, common exemplary surgical interventions

widely employed in biomedical research will be explained, categorized, and when available, the severity assessment of relevant catalogs is mentioned.

Surgical Models in Rodents

Incision Models

Skin incision is an intra-operative component of many surgical procedures. Accordingly, various models in rodents address this injury. These models differ mainly in the localization and dimension of the skin incision. The plantar incision model was established in the rat in 1996 and in the mouse in 2003 to study post-operative pain mechanistically (42, 43). The incision is made unilaterally on a hind paw, causing evoked pain-related behavior represented by hypersensitivity to mechanical and heat stimuli. In this model, a 1 cm longitudinal incision in rats, or a 0.5 cm in mice, of the glabrous skin and fascia in the plantar aspect of the hind paw under general anesthesia and sterile conditions is performed with a scalpel (no 11). Compresses stop the bleeding caused by the skin incision. The skin is closed with a mattress

suture. The duration of the entire intervention is <10 min. Thus, after applying the WWHow concept for the category “Where”, 1 point, for “What” 1 point, and for “How” 3 points in rats, and 2 in mice because the different incision dimension (for the detailed calculation, see **Figure 3** and **Supplementary Figure 1A**). This surgical intervention results in a total score of 5 points in rats and 4 points in mice, leading to the mild severity level categorization. Even if the incision size is different between mice and rats, this does not lead to a higher categorization (robustness to individual procedures) but may also depend on the animal’s overall size.

Changes in the intra-operative characteristics, e.g., incision dimension in “knee skin incision model” (49), enhanced the score (**Figure 3**). Skin-only incision as a procedure is not clearly categorized in any of the severity catalogs. By comparing the tissue trauma (from pre-clinical models), these are comparable to incisional wounds, skin, and ear biopsies. This type of injury is categorized as mild in all catalogs, but without considering the injury’s location.

A change in the incised body region affects the total score, as in the “back hairy model” (50), although the tissue trauma is equal. Based on the available data, which have explicitly investigated post-operative pain behavior leads to medium persistence evoked pain-related behavior, which is represented by hypersensitivity to mechanical and heat stimuli around the incision wound.

Postoperatively, animals exhibit pain avoidance behavior, e.g., guarding the incised paw, limping (antalgic gait) during locomotion (19, 29, 31, 62), or spontaneous pain behavior [e.g., foot lifting (63), grimacing (64, 65)]. Additional manipulation of the underlying muscle tissue, whether by blunt dissection or incision, results in hemorrhage and exacerbates guarding behavior (31).

Surgical Nerve Injury Models

Nerve injury can be an intentional or unintentional element of a surgical procedure. Therefore, it is essential to distinguish which nerve was damaged and how. To what extent the manipulation of epidermal cutaneous nerve fibers influences the severity of surgical intervention has been poorly studied so far. Therefore, we will focus on manipulating nerve tracts because models exist for this purpose. For over three decades, rodent surgical-induced nerve injury models have been developed to study neuropathic pain’s molecular, cellular, and circuit mechanisms (9, 34, 35). Typical neuropathic pain models manipulate the sciatic nerve and its three branches; the tibial, peroneal, and sural nerve. Skin incision and blunt preparation of the underlying biceps femoris muscle are necessary to display the sciatic nerve with their trifurcation and ligate or lesion it according to the particular model.

A concrete example is the spared nerve injury (SNI) model (54). In the SNI model, two of the three branches of the sciatic nerve are ligated and lesioned, leaving the sural nerve intact. The intervention has an approximate total duration of 15 min. Overall, the post-operative severity is categorized as moderate based on the total score of 12. (“Where”, 1 point, “What” 5 points, “How” 6 points, in total 12 points (for the detailed calculation, see **Figure 3** and **Supplementary Figure 1B**). Pain symptoms in this model are evolving mechanical and cold hypersensitivity in

the lateral area of the paw, which is innervated by the spared sural nerve. Axotomy denervates tibial and peroneal dermatomes of the hind paw, resulting in total loss of sensory perception (hypoaesthesia) motion control. Around the skin incision above the biceps femoris muscle develops primary hypersensitivity to mechanical and heat stimuli (comparable to skin incision models). In addition, guarding behavior and an antalgic gait can be observed due to the mechanical stimuli caused by the injury in the musculus biceps femoris in the acute post-operative period. Only the swiss catalog explicitly categorizes this model and other surgical nerve injury models as severe. Other surgical nerve injury models have equally moderate severity (52, 53). Other severity catalogs categorize these interventions only indirectly or not at all (**Figure 3**).

Next to manipulating the sciatic nerve, there are other possibilities in which nerve tracts can be damaged or injured. As in the “skin/muscle incision and retraction” model (30), displacing nerve tracts by soft tissue retraction does not result in direct nerve injury, but a prolonged pain-related behavior is presented. In addition, direct nerve damage can occur when nerves are mechanically compressed against rigid structures such as the bone. An example of this is the “thoracotomy with rib retraction (TRR)” model (46). Thoracotomies are necessary for various models to, e.g., study myocardial diseases, such as myocardial infarction or heart insufficiency. Practically, a relative to the body size of the rodent, large incision between the 4 and 5th ribs around 3–4 cm skin and an ~1.5 cm muscle and pleura incision are performed in the TRR rat model. The incision is likely to cause hemorrhage of both the skin and the muscle layer. A small self-retaining retractor opened the intercostal space for possible inner body interventions of 60 min. Because of retraction, intercostal nerves are lesioned by compression to rigid structures, here the ribs. The intervention has an approximate total duration of 90 min. Overall, the severity after awakening from anesthesia is categorized as severe based on the total score of 18 (“Where”, 4 points, “What” 6 points, and “How” 8 points, for the detailed calculation, see **Figure 3** and **Supplementary Figure 1A**). The typical post-operative pain symptoms are similar to other surgical models involving nerve injury, especially non-evoked pain in the territory of the intercostal nerves. It has been shown that significant intraindividual differences exist in the intensity of pain-related behavior that is not due to the extent of nerve injury but to the complexity of the surgical intervention itself. The extent of post-operative rodent-specific and observable behaviors change after awakening from anesthesia has not yet been studied systematically and requires further investigation. Based on the findings from other pain models, it can be interpolated that the animals have restrictions in *movement behavior* (climbing, rearing, walking), which is caused by the surgical wound at the thorax region. The severe severity assessment by the WWHow-concept is in line with other severity catalogs (**Figure 3**).

Bone Injuries

In many biomedical experiments, manipulation of the skeletal system is a component, such as implanting catheters or optical fibers in spinal and supraspinal structures or generating a disease



FIGURE 3 | Detailed presentation of the scoring according to the WWHow concept of different pain models (A) and exemplary surgical interventions in biomedical research (B). The corresponding scoring is presented for each intra-operative parameter according to the WWHow concept. The individual factors are displayed pictographically for the “What” (blue shades) and “How” (magenta shades) categories according to the scoring. The total score is illustrated for each surgical intervention without any analgesia treatment and categorized into “mild” (green color, score 4–9), “moderate” (orange color, score 10–16), and “severe” (red color, score 17–23). On the right part of the figure, the severity assessment according to three widely used catalogs, namely the Swiss (Swiss symbol), the EU (EU symbol), and Berlin animal welfare (Brandenburger Tor symbol), are labeled in the corresponding colors if the interventions are listed there. The grading was represented by striped colors if a similar intervention was found. If no corresponding intervention was found in the catalogs, this position is white. ¹Pogatzki and Raja (42); ²Buvanendran et al. (49); ³Duarte et al. (50); ⁴Brennan et al. (43); ⁵Kendall et al. (51); ⁶Flatters (30); ⁷Ho Kim and Mo Chung (52); ⁸Bennett and Xie (53); ⁹Decosterd and Woolf (54); ¹⁰Buvanendran et al. (46); ¹¹Jimenez-Andrade et al. (55); ¹²Lu et al. (56); ¹³Ren et al. (57); ¹⁴Awsare et al. (58); ¹⁵Zięgłowski et al. (59); ¹⁶Llovera et al. (60); ¹⁷Kyweriga et al. (61).

state. Orthopedic and fracture pain models are particularly worth mentioning here, as various have been developed and established recently (41).

Skull Trepanation and Craniotomies

Skull trepanation represents an essential technique in neuroscience to directly access the brain, whether for injection or implantation of optical fiber or infusion devices. Craniotomies are more invasive than trepanation and are necessary, for example, to implant a cranial window or multifiber devices into the brain. As an example, here, we determine the severity

of a skull trepanation (60): The scalp is incised by scalpel dorsally between 0.5 and 1.5 cm, exposing the bregma and the relevant skull region. Muscles or nerve tracts are not present there. A hole is drilled into the skull; all bone layers are injured. However, the underlying dura mater is not traumatized. Stereotactic micro-injection is performed with a thin needle or glass capillary (usually 30G or smaller) through the dura mater after a scalp suture. A surgery duration from 10 to 60 min is plausible depending on the injection location, volume and injection speed, and reagent to be injected. Tissue retraction is not necessary or feasible. Thus, after applying the WWHow

concept for the category “Where”, 1 point, for “What” 2 points, and for “How” 4 points (for the detailed calculation, **Figure 3** and **Supplementary Figure 1B**). This surgical intervention results in a total score of 7 points (**Figure 3**), leading to the mild severity level categorization. Cutaneous mechanical and heat hypersensitivity is expected postoperatively (compared to plantar incision model), associated with localized bone pain around the trepanation. Because the dorsal side of the skull is not subjected to any other direct external mechanical stimulation, e.g., movement; bone pain, and the associated severity is relatively short and anatomically less relevant for the rodent and will decrease with healing (up to 2 days). Severity catalogs also classify skull trepanation as mild (**Figure 3**). Compared to trepanation, craniotomies usually do not differ in severity assessment, but the bone defect is larger (61). The extent to which such interventions impact severity has not yet been established. This increases the “What” score to 2 or 3, but the overall scoring (8–9) does not change the mild score.

Various models have been developed to mimic orthopedic surgery and bone fractures to study the consequences of skeletal surgery in a patient-oriented approach. Contrary to procedures on the skull, these are mainly performed on the bony locomotor apparatus and are associated with more significant bone trauma. For example, a 1 cm skin incision is prepared over the patella tendon in rats. The tendon is disengaged from the fascia, and, using a diamond drill, a 1.4 mm diameter and 0.5 mm deep hole with a total surgery duration of 5 min is performed (49). Applying the WWHow concept for the category “Where”, 1 point, for “What” 3 points, and for “How” 4 points are given (**Figure 3**). This surgical intervention results in a total score of 7 points (**Figure 3**), which leads to the categorization in the mild severity level. Cutaneous mechanical and heat hypersensitivity is expected postoperatively (compared to the plantar incision model), associated with localized bone pain around the holes. Changes in rodent-specific behavior, such as rearing and ambulation, are observed up to 3 days postoperatively. Swiss and the EU catalogs assign moderate to similar surgical interventions.

Laparotomic Interventions

Laparotomies are conducted to perform implantations, visceral organ harvesting, manipulating, or ectomies. A male mouse vasectomy (58) is described here as an example of a laparotomy procedure: The abdomen’s left and right inguinal region is opened with an incision (<0.5 cm) underlying muscle layer. Next, the spermatic duct is ligated twice and dissected between the sutures. Finally, the muscle layer is closed by sutures, and the skin is restored with staples or sutured. Depending on the exact surgical procedure, such a procedure lasts <10 min with minimal tissue retraction using a small metal retractor. Thus, after applying the WWHow concept for the category “Where”, 3 points, for “What” 3 points, and for “How” 3 points (**Figure 3** and **Supplementary Figure 1B**), resulting in a total score of 9 points, which leads to categorization in the mild severity level. This categorization is in line with the Swiss catalog.

In contrast, an experimental model for laparotomy (51) totals in a score of 13 and would thus have a moderate severity score because of a larger skin and muscle incision (2 cm) (**Figure 3**

and **Supplementary Figure 1A**). Again, hemorrhage of both the skin and muscle layer must be expected. Cutaneous mechanical and heat hypersensitivity are expected postoperatively, directly around the suture up to 72 h. Rodent-specific behaviors, such as grooming and nesting, are reduced by laparotomy in the acute post-operative period (up to 36 h) because the abdominal muscles necessary for these behaviors are injured (66). Here is a difference in severity between the plantar incision and the experimental laparotomy model. The characteristics of the tissue trauma are similar. However, incision localization, size, and the prolonged surgery duration categorize the experimental laparotomy (13/23 p), in contrast to the planar incision (6/23 p), in the moderate severity category. A moderate severity level was also suggested in other severity catalogs (**Figure 3**).

DISCUSSION

The prospective severity assessment of an animal experiment is a significant component of experimental planning. It is mandatory to evaluate an experiment’s ethical justifiability and knowledge gain (harm-benefit analysis) as stipulated in the Directive 2010/63/EU. Three main catalogs are available in the EU for prospective severity assessment and can provide rough guidance (4–6). However, in many cases, classifications in these catalogs are mainly expert and experience-based and only partly evidence-based. Furthermore, these catalogs are primarily lexicon-like, without giving the possibility of adaptation to the particular experiment. Consequently, we aimed to provide a conceptual framework, termed “WWHow-concept”, based on data from surgical-induced pain models in rodents and allows the determination of the severity categories (minor, medium, and severe) in a prospective, adaptable, and transparent manner.

Animal Welfare Science With the Help of Pain Models in Rodents?

In patient-oriented pain research, animal pain models are used to investigate the mechanisms of pain diseases or pain symptomatology. The most commonly used species to study pain are rats and mice (11, 35, 67). Using established rodent pain models provides a framework to objectively describe the “worst-case scenario” of animal well-being changes resulting from tissue damage and other interventions (8, 9, 12). This scenario can assist in defining a generally valid zero point for critically reviewing peri-operative refinement actions in terms of their impact. Notably, the available models address a wide range of different pain entities, ranging from acute substance irritation-related pain to tumor-related pain or inflammatory pain, to name a few (8, 34, 35). Behavioral tests are applied to measure the intensity and quality of the pain directly. Pain-related behavior tests in rodents are primarily performed without analgesia treatment. The underlying mechanisms of pain, or the developments of new analgesic compounds, are the scientific question of many studies in this field (34, 35). Notably, the thorough investigation of diverse aspects of the pain-related behavior in the different models (68–70) provides an essential prerequisite for the development and characterization of new

analgesic targets. The available results simulate a worst-case scenario in which the direct effect of various pain modalities on the rodent is documented in a time-dependent manner under standardized laboratory conditions. Our approach did not require any additional animal experiments.

The WWHow Concept—A Chance for Prospective Severity Assessment?

We propose a categorized, easily understandable, and applicable, transparent approach for a prospective severity assessment of rodent surgical interventions, which relates to the specific anatomy and behavior and biomechanical properties. The localization of surgical intervention and the associated influence on pain nature and well-being are enormous (66, 67). This has been shown in many rodent studies with surgically-induced pain models and the investigation of rodent-specific behaviors, such as grooming (66), burrowing (71) or nest building (72, 73). Based on the surgical intervention site, specific tissue traumas are associated with developing different pain natures, their intensity, and duration. The underlying mechanisms are reported in many studies, depending on the respective tissue trauma, and, thus, provide the basis to prospectively name the occurring types of pain in terms of duration, intensity, and localization in an evidence-based manner (10). Knowledge about the effects of surgical interventions in rodents will help avoid scientifically incorrect and potentially fatal analogies from humans to rodents.

Comparison With Severity Catalogs

This approach has several advantages compared to the most commonly used severity catalogs (Figure 3). Catalogs list and describe surgical interventions with varying levels of detail and simply categorize the severity assessment without further explanation. It is, therefore, challenging to extrapolate individual or non-listed models based on the catalog considerations. The WWHow severity categorization is transparent, adaptable, and based on considerations (Where, What, How), not represented in other guidelines or catalogs.

Severity catalogs provide a valuable resource for the researcher and the regulatory/ permitting agency to categorize the severity. This is in a first step, a prospective process. Catalogs can only be considered a collection of different interventions and, thus, represent a first rough orientation aid, which must be supplemented in each case by an individual assessment, which is also required in the EU directive. The score presented here with the WWHow concept represents a module, based on intra-operative characteristics, estimates the maximum severity without analgesic treatment to be expected prospectively.

Moreover, in contrast to the catalogs, transparency is highly increased. It was possible to directly compare several interventions with severity catalogs and the WWHow concept. Critically, except for the EU catalog, it is not apparent whether or which analgesia regime was or was not considered in the other two catalogs. For laparotomy procedures, as well as for thoracotomy, the same categorization could be found. There were differences in the stable femur fracture,

whereby an exact comparison between the surgical model and the description from the catalog was only possible to a limited extent. In addition, vasectomy was classified as moderate by both the Swiss and Berlin catalogs, whereas the application of the WWHow concept prospectively predicts mild severity. Additionally, empirical findings from, e.g., score sheet evaluation (59) and/or behavioral testing, home cage monitoring (74) show that the prospective severity score may be overestimated from a retrospective point of view, but this could be case dependent and not generalized. Corresponding detailed prospective and retrospective studies would enable clearer evidence.

It should be noted that vasectomy, according to the WWHow concept, can also be classified as moderate if other surgical protocols are used. This fact underlines the potential of the modular construction of this severity assessment using the WWHow concept, which is the separate consideration of each intervention as required by the EU Directive. Differences between the WWHow concept and the catalogs were in the surgical-induced neuropathic pain models, which are concretely assessed only in the Swiss catalog. In the other catalogs, no corresponding interventions could be indexed. All three neuropathic pain models (Figure 3) are classified as moderate by the WWHow concept.

In contrast, the Swiss catalog classifies them as severe. The classification with the WWHow concept shows that the severity is mainly determined by the nerve injury, which is distinct across the models. While in the “spinal nerve ligation” and “chronic constriction injury” models, there is ligation of the entire sciatic nerve, in the “spared nerve injury” model, there is a transaction of two sciatic nerve branches. Both procedures cause different (location and duration) pain symptoms, reflected by the WWHow concept. The Swiss catalog does not differentiate here, and the user cannot understand the classification due to a lack of transparency. However, knowing what tissue trauma looks like and how it occurs is needed to address prospective refinement actions that can potentially minimize severity directly. In addition, this knowledge can contribute to a fact-based dialogue with authority officials and other stakeholders. Importantly, future publications, harboring surgical interventions, should consider the WWHow concept for validation thereby not only confirming the scoring concept but also allowing the expansion of methods in this technically fast growing scientific century.

Limitations

This concept is based on surgical interventions—the procedure itself. The influence of the rodent strain, genetic manipulation effects, potential sex or age differences are not considered (27). Similarly, preoperative factors as particular treatments or behavioral-test induced stress or housing factors are not considered (11). Therefore, it is essential to strengthening the fact that the WWHow concept is applicable solely for surgical interventions as one part of a whole experimental procedure. Other experimental parts like behavioral tests, particular pre-treatments, and post-operative investigations must be considered separately to categorize an entire animal experiment.

Outlook

The WWHow concept may serve as a core module and should be included in future prospective studies. Moreover, the concept constitutes a basis for further categorization attempts to enable the transparent, adaptable, and prospective categorization of various animal experimental procedures and thereby enable their refinement. In the future, it would be helpful to establish concepts for classifying animal tests that include behavioral tests as such and in combination with specific treatment options. Moreover, due to the existing knowledge gaps mentioned in the limitations, the scoring system presented here is initially a first conceptional framework that should be regularly updated and expanded. In addition, the WWHow concept provides the basis for the development of recommendations for anesthetic and analgesic management and the preparation of experiment-related score sheets to evaluate actual severity concerning peri-operative characteristics. Thereby, our concept not only constitutes an accessible and broadly usable scoring system, it also presents a system with potential for refinement strategies.

DATA AVAILABILITY STATEMENT

The original contributions presented in the study are included in the article/**Supplementary Material**, further inquiries can be directed to the corresponding author/s.

ETHICS STATEMENT

Ethical review and approval was not required for the animal study because retrospective results of published studies were evaluated. No animals were used for this study.

REFERENCES

1. Directive 2010/63/EU, The European Parliament and the Council of the European Union. *Directive 2010/63/EU* (2010). Available online at: <https://eur-lex.europa.eu/LexUriServ/LexUriServ.do?uri=OJ:L:2010:276:0033:0079:en:PDF>
2. Smith D, Anderson D, Degryse A-D, Bol C, Criado A, Ferrara A, et al. Classification and reporting of severity experienced by animals used in scientific procedures: FELASA/ECLAM/ESLAV Working Group report. *Lab Anim.* (2018) 52:5–57. doi: 10.1177/0023677217744587
3. Zintzsch A, Noe E, Reißmann M, Ullmann K, Krämer S, Jerchow B, et al. Guidelines on severity assessment and classification of genetically altered mouse and rat lines. *Lab Anim.* (2017) 51:573–82. doi: 10.1177/0023677217718863
4. Swiss Federal Office for Food Safety and Veterinary Office. *Technical Information Animal Testing* (2018). Available online at: <https://www.blv.admin.ch/dam/blv/de/dokumente/tiere/publikationen-und-f> (accessed January 9, 2020).
5. Berlin Animal Welfare Officers. *Guidance of the Working Group of Berlin Animal Welfare Officers on the Classification into Degrees of Severity for Animal Experiments Subject to Approval*. (2017). Available at: https://cdn.web-site-editor.net/ff1c046715cb4085a12acde03e951ffa/files/uploaded/170501_Guidelines%2520severity%2520classification%2520GAA.PDF
6. Directive 2010/63/EU Annex VIII. The European Parliament and the Council of the European Union. *Directive 2010/63/EU Annex VIII* (2010).

AUTHOR CONTRIBUTIONS

AT-T, CP, and DS developed the score initially, finalized it with all other authors, and designed the figures. DS implemented the designed figures. AT-T and DS wrote the manuscript. The manuscript and its results were discussed with all authors. All authors listed have made a substantial and intellectual contribution to the work and approved it for publication.

ACKNOWLEDGMENTS

The authors acknowledge scientists in the Collaborative Research Center 1158 (SFB1158) in Heidelberg/Mannheim for valuable discussions on this topic and recognize funding in the form of an SFB1158 grant (project S01) from the Deutsche Forschungsgemeinschaft (DFG) to AT-T. Literature search and data extraction strategies were partially funded by the German Federal Ministry of Education and Research (BMBF, 01KC1903) to EP-Z. In addition, the authors also like to thank many members of Münster University Hospital and the Westphalian Wilhelms University of Münster, especially Dr. Martin Lücke, Dr. Sandra Stöppeler, and Dr. Jens Ehmcke, for the lively discussion on this topic.

SUPPLEMENTARY MATERIAL

The Supplementary Material for this article can be found online at: <https://www.frontiersin.org/articles/10.3389/fvets.2022.841431/full#supplementary-material>

Supplementary Figure 1 | Exemplary detailed scoring for different surgical interventions in rats (A) and mice (B) according to the WWHow concept, showing the respective scoring points of the “Where”, “What” and “How” categories and the total score from which the severity is determined.

Available online at: <https://eur-lex.europa.eu/LexUriServ/LexUriServ.do?uri=OJ:L:2010:276:0033:0079:en:PDF>

7. Foley PL, Kendall LV, Turner PV. Clinical Management of Pain in Rodents. *Comp Med.* (2019) 69:468–89. doi: 10.30802/AALAS-CM-19-000048
8. Pogatzki-Zahn E, Segelcke D, Zahn P. Mechanisms of acute and chronic pain after surgery: Update from findings in experimental animal models. *Curr Opin Anaesthesiol.* (2018). doi: 10.1097/ACO.0000000000000646
9. Burma NE, Leduc-Pessah H, Fan CY, Trang T. Animal models of chronic pain: Advances and challenges for clinical translation. *J Neurosci Res.* (2017) 95:1242–56. doi: 10.1002/jnr.23768
10. Segelcke D, Pogatzki-Zahn EM. Pathophysiology of postoperative pain. In: *The Senses: A Comprehensive Reference*. Netherlands: Elsevier (2020). p. 604–27. doi: 10.1016/B978-0-12-809324-5.24249-1
11. Segelcke D, Pradier B, Pogatzki-Zahn E. Advances in assessment of pain behaviors and mechanisms of post-operative pain models. *Curr Opin Physiol.* (2019) 11:85–92. doi: 10.1016/j.cophys.2019.07.002
12. Campbell JN, Meyer RA. Mechanisms of neuropathic pain. *Neuron.* (2006) 52:77–92. doi: 10.1016/j.neuron.2006.09.021
13. Hebel R, Stromberg MW. *Anatomy and Embryology of the Laboratory Rat*. Wörthsee: BioMed Verl. (1986). 271 p.
14. Margaret J. Cook. *Anatomy of the Laboratory Mouse*. Cambridge: Academic Press Inc. (1965).
15. Ruberte Paris J, Carretero Romay A, Navarro Beltrán M. *Morphological Mouse Phenotyping: Anatomy, Histology and Imaging*. Amsterdam, Heidelberg: Academic Press (2017). 585 p.

16. Hedrich H. *The Laboratory Mouse*. San Diego: Elsevier Science & Technology. (2012). 869 p.
17. Committee for the Update of the Guide for the Care and Use of Laboratory. *Guide for the Care and Use of Laboratory Animals*. Washington: National Academies Press (2011). 247 p.
18. Mouraux A, Bannister K, Becker S, Finn DP, Pickering G, Pogatzki-Zahn E, et al. Challenges and opportunities in translational pain research—An opinion paper of the working group on translational pain research of the European pain federation. (*EFIC Eur J Pain*. (2021) 25:731–56. doi: 10.1002/ejp.1730
19. Segelcke D, Pradier B, Reichl S, Schäfer LC, Pogatzki-Zahn EM. Investigating the role of Ly6G+ neutrophils in incisional and inflammatory pain by multidimensional pain-related behavioral assessments: Bridging the translational gap. *Front Pain Res*. (2021). doi: 10.3389/fpain.2021.735838
20. Zomer HD, Trentin AG. Skin wound healing in humans and mice: Challenges in translational research. *J Dermatol Sci*. (2018) 90:3–12. doi: 10.1016/j.jdermsci.2017.12.009
21. Treuting PM. *Comparative Anatomy and Histology: A Mouse, Rat, and Human Atlas*. Saint Louis: Elsevier Science (2017). 573 p.
22. Eisenach JC, Brennan TJ. Pain after surgery. *Pain*. (2018) 159:1010–1. doi: 10.1097/j.pain.0000000000001223
23. Velnar T, Bailey T, Smrkolj V. The wound healing process: an overview of the cellular and molecular mechanisms. *J Int Med Res*. (2009) 37:1528–42. doi: 10.1177/147323000903700531
24. Scherer M, Reichl SU, Augustin M, Pogatzki-Zahn EM, Zahn PK. The assessment of cold hyperalgesia after an incision. *Anesth Analg*. (2010) 110:222–7. doi: 10.1213/ANE.0b013e3181c0725f
25. Zahn PK, Brennan TJ. Primary and secondary hyperalgesia in a rat model for human postoperative pain. *Anesthesiology*. (1999) 90:863–72. doi: 10.1097/0000542-199903000-00030
26. Zahn PK, Brennan TJ. Incision-induced changes in receptive field properties of rat dorsal horn neurons. *Anesthesiology*. (1999) 91:772–85. doi: 10.1097/0000542-199909000-00030
27. Banik RK, Woo YC, Park SS, Brennan TJ. Strain and sex influence on pain sensitivity after plantar incision in the mouse. *Anesthesiology*. (2006) 105:1246–53. doi: 10.1097/0000542-200612000-00025
28. Feehan AK, Zadina JE. Morphine immunomodulation prolongs inflammatory and postoperative pain while the novel analgesic ZH853 accelerates recovery and protects against latent sensitization. *J Neuroinflammation*. (2019) 16:100. doi: 10.1186/s12974-019-1480-x
29. Sahbaie P, Li X, Shi X, Clark JD. Roles of Gr-1+ leukocytes in postincisional nociceptive sensitization and inflammation. *Anesthesiology*. (2012) 117:602–12. doi: 10.1097/ALN.0b013e3182655f9f
30. Flatters SJ. Characterization of a model of persistent postoperative pain evoked by skin/muscle incision and retraction. (*SMIR Pain*. (2008) 135:119–30. doi: 10.1016/j.pain.2007.05.013
31. Xu J, Brennan TJ. Guarding pain and spontaneous activity of nociceptors after skin versus skin plus deep tissue incision. *Anesthesiology*. (2010) 112:153–64. doi: 10.1097/ALN.0b013e3181c2952e
32. Kang S, Brennan TJ. Mechanisms of postoperative pain. *Anesth Pain Med*. (2016) 11:236–48. doi: 10.17085/apm.2016.11.3.236
33. Gu H, Sugiyama D, Kang S, Brennan TJ. Deep tissue incision enhances spinal dorsal horn neuron activity during static isometric muscle contraction in rats. *J Pain*. (2019) 20:301–14. doi: 10.1016/j.jpain.2018.09.012
34. Gregory NS, Harris AL, Robinson CR, Dougherty PM, Fuchs PN, Sluka KA. An overview of animal models of pain: disease models and outcome measures. *J Pain*. (2013) 14:1255–69. doi: 10.1016/j.jpain.2013.06.008
35. Mogil JS. Animal models of pain: progress and challenges. *Nat Rev Neurosci*. (2009) 10:283–94. doi: 10.1038/nrn2606
36. Burma A-NL, Skou ST, Nielsen TA, Petersen KK. Animal models of chronic pain: advances and challenges for clinical translation. *J Neurosci Res*. (2015) 13:225–34. doi: 10.1007/s11914-015-0276-x
37. Borsook D, Kussman BD, George E, Becerra LR, Burke DW. Surgically induced neuropathic pain: understanding the perioperative process. *Ann Surg*. (2013) 257:403–12. doi: 10.1097/SLA.0b013e3182701a7b
38. Hubbard CS, Khan SA, Xu S, Cha M, Masri R, Seminowicz DA. Behavioral, metabolic and functional brain changes in a rat model of chronic neuropathic pain: a longitudinal MRI study. *Neuroimage*. (2015) 107:333–44. doi: 10.1016/j.neuroimage.2014.12.024
39. Nencini S, Ivanusic JJ. The Physiology of Bone Pain. How Much Do We Really Know? *Front Physiol*. (2016) 7:157. doi: 10.3389/fphys.2016.00157
40. Mantyh PW. The neurobiology of skeletal pain. *Eur J Neurosci*. (2014) 39:508–19. doi: 10.1111/ejn.12462
41. Thompson AL, Largent-Milnes TM, Vanderah TW. Animal models for the study of bone-derived pain. *Methods Mol Biol*. (2019) 1914:391–407. doi: 10.1007/978-1-4939-8997-3_23
42. Pogatzki EM, Raja SN, A. mouse model of incisional pain. *Anesthesiology*. (2003) 99:1023–7. doi: 10.1097/0000542-200310000-00041
43. Brennan TJ, Vandermeulen EP, Gebhart GF. Characterization of a rat model of incisional pain. *Pain*. (1996) 64:493–502. doi: 10.1016/0304-3959(95)01441-1
44. Pogatzki-Zahn EM, Segelcke D, Schug SA. Postoperative pain-from mechanisms to treatment. *Pain Reports*. (2017) 2:e588. doi: 10.1097/PR9.0000000000000588
45. Cruz JJ, Kather A, Nicolaus K, Rengsberger M, Mothes AR, Schleussner E, et al. Acute postoperative pain in 23 procedures of gynaecological surgery analysed in a prospective open registry study on risk factors and consequences for the patient. *Sci Rep*. (2021) 11:22148. doi: 10.1038/s41598-021-01597-5
46. Buvanendran A, Kroin JS, Kerns JM, Nagalla SN, Tuman KJ. Characterization of a new animal model for evaluation of persistent postthoracotomy pain. *Anesth Analg*. (2004) 99:1453–60. doi: 10.1213/01.ANE.0000134806.61887.0D
47. Xu J, Brennan TJ. The pathophysiology of acute pain: animal models. *Curr Opin Anaesthesiol*. (2011) 24:508–14. doi: 10.1097/ACO.0b013e32834a50d8
48. Chapman CR, Vierck CJ. The transition of acute postoperative pain to chronic pain: an integrative overview of research on mechanisms. *J Pain*. (2017) 18:359.e1–38. doi: 10.1016/j.jpain.2016.11.004
49. Buvanendran A, Kroin JS, Kari MR, Tuman KJ, A. new knee surgery model in rats to evaluate functional measures of postoperative pain. *Anesth Analg*. (2008) 107:300–8. doi: 10.1213/ane.0b013e3181732f21
50. Duarte AM, Pospisilova E, Reilly E, Mujenda F, Hamaya Y, Strichartz GR. Reduction of postincisional allodynia by subcutaneous bupivacaine: findings with a new model in the hairy skin of the rat. *Anesthesiology*. (2005) 103:113–25. doi: 10.1097/0000542-200507000-00018
51. Kendall LV, Wegenast DJ, Smith BJ, Dorsey KM, Kang S, Lee NY, et al. Efficacy of sustained-release buprenorphine in an experimental laparotomy model in female mice. *J Am Assoc Lab Anim Sci*. (2016) 55:66–73.
52. Ho Kim S, Mo Chung J. An experimental model for peripheral neuropathy produced by segmental spinal nerve ligation in the rat. *Pain*. (1992) 50:355–63. doi: 10.1016/0304-3959(92)90041-9
53. Bennett GJ, Xie Y-K, A. peripheral mononeuropathy in rat that produces disorders of pain sensation like those seen in man. *Pain*. (1988) 33:87–107. doi: 10.1016/0304-3959(88)90209-6
54. Decosterd I, Woolf CJ. Spared nerve injury: an animal model of persistent peripheral neuropathic pain. *Pain*. (2000) 87:149–58. doi: 10.1016/S0304-3959(00)00276-1
55. Jimenez-Andrade JM, Bloom AP, Mantyh WG, Koewler NJ, Freeman KT, Delong D, et al. Capsaicin-sensitive sensory nerve fibers contribute to the generation and maintenance of skeletal fracture pain. *Neuroscience*. (2009) 162:1244–54. doi: 10.1016/j.neuroscience.2009.05.065
56. Lu H, Howatt DA, Balakrishnan A, Moorleghe JJ, Rateri DL, Cassis LA, et al. Subcutaneous Angiotensin II Infusion using Osmotic Pumps Induces Aortic Aneurysms in Mice. *J Vis Exp*. (2015) 103:53191. doi: 10.3791/53191
57. Ren S, Chang S, Tran A, Mandelli A, Wang Y, Wang JJ. Implantation of an Isoproterenol Mini-Pump to Induce Heart Failure in Mice. *Journal Vis Exp*. (2019) 103:53191. doi: 10.3791/59646
58. Awsare NS, Krishnan J, Boustead GB, Hanbury DC, McNicholas TA. Complications of vasectomy. *Ann R Coll Surg Engl*. (2005) 87:406–10. doi: 10.1308/003588405X71054
59. Ziegowski L, Kümmecke A, Ernst L, Schulz M, Talbot SR, Palme R, et al. Severity assessment using three common behavioral or locomotor tests after laparotomy in rats: a pilot study. *Lab Anim*. (2020) 54:525–35. doi: 10.1177/0023677220911680
60. Llovera G, Roth S, Plesnila N, Veltkamp R, Liesz A. Modeling stroke in mice: permanent coagulation of the distal middle cerebral artery. *J Vis Exp*. (2014) e51729. doi: 10.3791/51729

61. Kyweriga M, Sun J, Wang S, Kline R, Mohajerani MH. A large lateral craniotomy procedure for mesoscale wide-field optical imaging of brain activity. *J Vis Exp.* (2017). doi: 10.3791/52642
62. Pogatzki-Zahn EM, Gomez-Varela D, Erdmann G, Kaschube K, Segelcke D, Schmidt M, et al. proteome signature for acute incisional pain in dorsal root ganglia of mice. *Pain.* (2021) 162:2070–86. doi: 10.1097/j.pain.0000000000002207
63. Kabadi R, Kouya F, Cohen HW, Banik RK. Spontaneous pain-like behaviors are more sensitive to morphine and buprenorphine than mechanically evoked behaviors in a rat model of acute postoperative pain. *Anesth Analg.* (2015) 120:472–8. doi: 10.1213/ANE.0000000000000571
64. Miller AL, Leach MC, Samal SK. The Mouse Grimace Scale: A Clinically Useful Tool? *PLoS ONE.* (2015) 10:e0136000. doi: 10.1371/journal.pone.0136000
65. Langford DJ, Bailey AL, Chanda ML, Clarke SE, Drummond TE, Echols S, et al. Coding of facial expressions of pain in the laboratory mouse. *Nat Methods.* (2010) 7:447–9. doi: 10.1038/nmeth.1455
66. Oliver VL, Thurston SE, Lofgren JL. Using Cageside Measures to Evaluate Analgesic Efficacy in Mice (*Mus musculus*) after Surgery. *J Am Assoc Lab Anim Sci.* (2018) 57:186–201.
67. Turner PV, Pang DS, Lofgren JL, A. Review of pain assessment methods in laboratory rodents. *Comp Med.* (2019) 69:451–67. doi: 10.30802/AALAS-CM-19-000042
68. Mogil JS. The measurement of pain in the laboratory rodent. In: Wood JN, Mogil JS, editors. *The Oxford Handbook of the Neurobiology of Pain.* Oxford, UK: Oxford University Press (2020). p. 27–60. doi: 10.1093/oxfordhb/9780190860509.013.21
69. Deuis JR, Dvorakova LS, Vetter I. Methods used to evaluate pain behaviors in rodents. *Front Mol Neurosci.* (2017) 10:284. doi: 10.3389/fnfmol.2017.00284
70. Zhang H, Lecker I, Collymore C, Dokova A, Pham MC, Rosen SE, et al. Cage-lid hanging behavior as a translationally relevant measure of pain in mice. *Dan Med J.* (2021) 162:1416–25. doi: 10.1097/j.pain.0000000000002127
71. Jirkof P, Cesarovic N, Rettich A, Nicholls S, Seifert B, Arras M. Burrowing behavior as an indicator of post-laparotomy pain in mice. *Front Behav Neurosci.* (2010) 4:165. doi: 10.3389/fnbeh.2010.00165
72. Arras M, Rettich A, Cinelli P, Kasermann HP, Burki K. Assessment of post-laparotomy pain in laboratory mice by telemetric recording of heart rate and heart rate variability. *BMC Vet Res.* (2007) 3:16. doi: 10.1186/1746-6148-3-16
73. Deacon RM. Assessing nest building in mice. *Nat Protoc.* (2006) 1:1117–9. doi: 10.1038/nprot.2006.170
74. Pitzer C, Kuner R, Tappe-Theodor A. EXPRESS: voluntary and evoked behavioral correlates in neuropathic pain states under different housing conditions. *Mol Pain.* (2016) 12:1744806916656635. doi: 10.1177/1744806916656635

Conflict of Interest: ND is an external consultant and animal welfare officer at Medizinisches Kompetenzzentrum |c/o HCx Consulting GmbH | Ulmenstraße 12 | 15864 Wendisch Rietz During the last 5 years, EP-Z received financial support from Mundipharma GmbH and Grunenthal for research activities and from Grunenthal, MSD Sharp & DOHME GmbH, Mundipharma GmbH, Mundipharma International, Janssen-Cilag GmbH, Fresenius Kabi, and AcclRx for advisory board activities and/or lecture fees.

The remaining authors declare that the research was conducted in the absence of any commercial or financial relationships that could be construed as a potential conflict of interest.

Publisher's Note: All claims expressed in this article are solely those of the authors and do not necessarily represent those of their affiliated organizations, or those of the publisher, the editors and the reviewers. Any product that may be evaluated in this article, or claim that may be made by its manufacturer, is not guaranteed or endorsed by the publisher.

Copyright © 2022 Tappe-Theodor, Pitzer, Lewejohann, Jirkof, Siegeler, Segelcke, Drude, Pradier, Pogatzki-Zahn, Hollinderbäumer and Segelcke. This is an open-access article distributed under the terms of the Creative Commons Attribution License (CC BY). The use, distribution or reproduction in other forums is permitted, provided the original author(s) and the copyright owner(s) are credited and that the original publication in this journal is cited, in accordance with accepted academic practice. No use, distribution or reproduction is permitted which does not comply with these terms.



The zebrafish Multivariate Concentric Square Field: A Standardized Test for Behavioral Profiling of Zebrafish (*Danio rerio*)

Laura E. Vossen^{1*†}, Ronja Brunberg², Pontus Rådén², Svante Winberg^{3,4†} and Erika Roman^{1,2†}

OPEN ACCESS

Edited by:

Rui F. Oliveira,
University Institute of Psychological,
Social and Life Sciences (ISPA),
Portugal

Reviewed by:

Merid Negash Getahun,
International Centre of Insect
Physiology and Ecology (ICIPE),
Kenya
Magda C. Teles,
Gulbenkian Institute of Science (IGC),
Portugal

*Correspondence:

Laura E. Vossen
laura.vossen@slu.se

†ORCID:

Laura E. Vossen
orcid.org/0000-0001-5778-9530
Svante Winberg
orcid.org/0000-0003-4252-3144
Erika Roman
orcid.org/0000-0001-5418-8289

Specialty section:

This article was submitted to
Individual and Social Behaviors,
a section of the journal
Frontiers in Behavioral Neuroscience

Received: 20 July 2021

Accepted: 31 January 2022

Published: 17 March 2022

Citation:

Vossen LE, Brunberg R, Rådén P,
Winberg S and Roman E (2022) The
zebrafish Multivariate Concentric
Square Field: A Standardized Test
for Behavioral Profiling of Zebrafish
(*Danio rerio*).
Front. Behav. Neurosci. 16:744533.
doi: 10.3389/fnbeh.2022.744533

¹ Division of Anatomy and Physiology, Department of Anatomy, Physiology and Biochemistry, Swedish University of Agricultural Sciences, Uppsala, Sweden, ² Neuropharmacology, Addiction and Behavior, Department of Pharmaceutical Biosciences, Uppsala University, Uppsala, Sweden, ³ Behavioral Neuroendocrinology, Department of Neuroscience, Uppsala University, Uppsala, Sweden, ⁴ Behavioral Neuroendocrinology, Department of Medical Cell Biology, Uppsala University, Uppsala, Sweden

The zebrafish (*Danio rerio*) is an important model organism in the study of the neurobiological basis of human mental disorders. Yet the utility of this species is limited by the quality of the phenotypical characterization tools available. Here, we present a complex testing environment for the quantification of explorative behavior in adult zebrafish, the zebrafish Multivariate Concentric Square Field™ (zMCSF), adapted from the rodent equivalent that has been used in > 40 studies. The apparatus consists of a central open area which is surrounded by a dark corner with a roof (DCR), corridors, and an inclined ramp. These areas differ in illumination, water depth, and are sheltered or exposed to different degrees. We quantified behavior of male and female wild-caught and AB strain zebrafish in the zMCSF (day 1) and cross-validated these results using the novel tank diving test (NTDT) (day 2). To assess the effect of repeated testing, AB zebrafish we tested a second time in both tests 1 week later (on days 7 and 8). We detected strong differences between the strains, with wild zebrafish swimming faster and spending more time in the corridors and on the ramp, while they avoided the open area in the center. AB zebrafish were less hesitant to enter the center but avoided the ramp, and often left one or more zones unexplored. No major sex differences in exploratory behavior were detected in either strain, except for a slightly higher velocity of AB males which has been reported before. Importantly, the zMCSF was largely resilient to repeated testing. The diving test revealed only one difference confined to one sex; wild females paid more visits to the top third than AB females. In isolation, this finding could lead to the conclusion that wild zebrafish are more risk-taking, which is incorrect given this strain's avoidance of open areas. To conclude, our results suggest that the zMCSF presents a sophisticated behavioral tool that can distinguish between different magnitudes and types of risk, allowing the user to create an intricate behavioral profile of individual adult zebrafish.

Keywords: anxiety-related behavior, behavioral test, explorative behavior, locomotory activity, novel tank diving test, risk-taking

INTRODUCTION

Knowledge of the local environment can entail important advantages for animals, both in terms of survival and reproduction. When placed in an unfamiliar environment, animals strategically explore their novel surroundings to locate food, water and hiding places, and to assess whether conspecific competitors or predators are present (Winkler and Leisler, 1999). In many species ranging from rats to ants, exploratory behavior is structured around a familiar “home base,” a location (often close to a wall or corner) in which the animal spends a disproportional amount of time and from which it makes round trips in different directions (Eilam and Golani, 1989; Collett and Zeil, 2018). If the animal encounters novel objects or structures these may be investigated, manipulated or avoided (Belzung and Lepape, 1994). Defensive behaviors such as hiding and freezing (Walsh and Cummins, 1976) and scanning head movements (Dingemans et al., 2002) occur more readily in a novel environment.

Certain aspects of exploratory behavior can be measured using classical behavioral tests (Hanell and Marklund, 2014; Stewart et al., 2014), including home base behavior (Eilam and Golani, 1989; Stewart et al., 2010) and avoidance of brightly illuminated open spaces or elevated platforms (Rodgers, 1997). Other aspects remain concealed by the simplicity of the apparatus’ design. First, limited physical structure means that the whole apparatus can be overseen from one or more positions, which reduces the appropriateness of flight and risk assessment behaviors such as scanning head movements or “corner runs” [fast movement from one shelter to the next through an exposed space (Blanchard and Blanchard, 1989)]. In such an environment there is furthermore less novelty, which is rewarding in itself (Kakade and Dayan, 2002) and provides an incentive for exploration. Second, in classical tests the decision between safety and exploration is often binary (e.g., wall vs. center, open vs. closed arm), and the animal’s choice away from safety automatically assumes a choice for exploration. This while shelter seeking, roaming around in an area of relative safety, and actively seeking novelty may be considered different choices. Indeed, classical tests often represent only one type of risk (Hanell and Marklund, 2014; Stewart et al., 2014), whereas in nature the animal may need to balance risks of different kind and magnitude against each other. A final drawback of many classical tests is that animals often habituate to the novelty offered in the same test (Rodgers, 1997) and even generalize experiences from one test to another in a test battery (McIlwain et al., 2001; Blokland et al., 2012). Therefore, classical tests are less suitable for experimental designs that involve repeated testing of the same individuals. Taken together, the above considerations led to

the development of a novel test apparatus for rodents, the Multivariate Concentric Square FieldTM (MCSF; Meyerson et al., 2006; Roman and Colombo, 2009).

The zebrafish (*Danio rerio*) continues to increase in popularity as a model organism (Kalueff et al., 2014; Gerlai, 2020). Classical behavioral tests have already been translated to this species, including the open field (Stewart et al., 2012), light/dark (Maximino et al., 2010), and plus maze (Varga et al., 2018) tests, in addition to the highly used novel tank diving test (NTDT) (Levin et al., 2007). In the current study we adapted the standardized MCSF arena for rodent behavioral profiling, the MCSF, to zebrafish (zMCSF) (Bikovski et al., 2020). The apparatus consists of a central open area which is surrounded by a dark corner with a roof (DCR), corridors, and an inclined ramp. These areas differ in illumination and water depth, are sheltered or exposed to different degrees, and the arena cannot be overseen from any of these areas. This design offers the fish a free choice between several alternative locations of different quality in terms of risk and safety, while also providing an incentive for exploration. This generates a comprehensive and detailed behavioral profile of an individual zebrafish within a single behavioral test (Bikovski et al., 2020), while avoiding carry-over effects common to many test batteries (McIlwain et al., 2001).

In rodents, the sheltered dark corner room (DCR) is considered a safe and the elevated and illuminated bridge a risky area, based on the observations from pup retrieval, food hoarding and shelter seeking behaviors (Meyerson et al., 2006). The most central area of the MCSF, i.e., the central circle, is avoided by rats and they pass it at greater speed than neighboring areas (Meyerson et al., 2006). Moreover, administration of the benzodiazepine diazepam or alcohol increases the duration of visits to the MCSF center (Meyerson et al., 2013; Karlsson and Roman, 2016), suggesting that also this area is perceived as relatively risky, similar to the center of an open field (Momeni et al., 2014). In areas leading up to the elevated and illuminated bridge (slope and bridge entrance) stretched attend postures are most often observed (Augustsson and Meyerson, 2004; Meyerson et al., 2013), therefore these areas have been suggested as areas for risk assessment (Macintosh and Grant, 1963; Rodgers et al., 1999). Finally, the corridors act as semi-sheltered transit zones for entering the different areas of the arena (Augustsson and Meyerson, 2004; Roman and Colombo, 2009). In several rodent studies published so far, the MCSF has been used alongside classical tests such as the open field or elevated plus maze. This has not only provided important cross-validation, the MCSF has also repeatedly picked up on effects that were not registered by traditional tests (Birgner et al., 2010; Roman et al., 2012), such as the effect of low doses of the benzodiazepine diazepam not detected in the elevated plus maze (Meyerson et al., 2013).

The zMCSF has previously been optimized regarding the dimensions of the arena (Roman et al., 2016, 2018; Bikovski et al., 2020). Herein we optimized the zone settings and highlight strain differences between AB and wild zebrafish, test for sex differences within strains and report the effect of repeated testing in AB zebrafish. We also tested the same individuals in the NTDT, which gives further clues to the interpretation of the zones in the zMCSF. We compare exploratory behavior in the

Abbreviations: CENT, Center zone of the zMCSF; CIRC, Central circle zone of the zMCSF; CORN, Corner zone of the zMCSF; CORR1, Corridor 1 zone of the zMCSF; CORR2, Corridor 2 zone of the zMCSF; CORRS, Corridor 1, corner and corridor 2 of the zMCSF; DCR, Dark corner roof zone of the zMCSF; MCSF, Multivariate Concentric Square FieldTM; NTDT, Novel tank Diving Test; PCA, Principal Component Analysis; RAMP, Inclined ramp of the zMCSF; REST, The part of the zMCSF not designated to any other zone; START, Start zone of the zMCSF; zMCSF, zebrafish Multivariate Concentric Square FieldTM.

zMCSF to published studies that used classical tests to measure the effects of repeated testing, strain and sex. Finally, we evaluate similarities and differences between how zebrafish, mice and rat behave in the MCSF, and ask whether laboratory animals of these species show similar differences in explorative behavior and behavioral profiles.

MATERIALS AND METHODS

Animals and Housing

Experiments took place at the Department of Neuroscience, located at the Biomedical Center, Uppsala University in Sweden in September and October 2017. Ethical approval for the use of animals was given by the Uppsala Regional Animal Ethical Committee (permit C55/13), following the guidelines of the Swedish Legislation on Animal Experimentation (Animal Welfare Act SFS1998:56) and the European Union Directive on the Protection of Animals Used for Scientific Purposes (Directive 2010/63/EU).

In the current study, a total of 73 zebrafish were involved in behavioral testing; 13 females and 17 males of the AB strain, and 21 females and 22 males of the “wild” strain, i.e., offspring of wild-caught fish. Adult AB zebrafish (d.o.b. October 2015) were obtained from SciLifeLab (Evolutionary Biology Centre, Uppsala University) and transferred to the Department of Neuroscience. The wild-caught strain was collected from the river Ichamati (approximately 70 km from Calcutta), bred in ponds, and the resulting offspring were transferred as adults to the Department of Neuroscience where they were kept in two large, aerated aquaria (200 L). The lab-raised F1 offspring (d.o.b. April 2016) from the wild-caught individuals were included in this experiment, and will hereafter be referred to as “wild zebrafish.” Hence all animals were adults at the time of testing; the AB zebrafish were 23 months and the wild strain was 18 months of age.

Experimental animals were kept in 9.5L tanks in a stand-alone rack system (Aquaneering, San Diego, United States) that was maintained at $27 \pm 1.5^\circ\text{C}$ with a photoperiod of 14L:10D (lights on at 07:00 AM). The aquarium system contained a particular filter pad (exchanged weekly), a fluidized bed biological filter, carbon filters and an ultraviolet sterilizer. Fish tanks were supplied with recirculating copper-free Uppsala municipal tap water of which 10% was exchanged daily. Alkalinity ($66\text{--}119$, median 87 mmol L^{-1}), conductivity ($34\text{--}48$, median 40 mS m^{-1}) and pH ($8.2\text{--}8.5$, median 8.4) were monitored daily. Animals were fed twice daily with flakes (tropical energy food, Aquatic Nature, Roeslare, Belgium) and *Artemia* brine shrimp (Argentemia Platinum Grade 0, Argent Aquaculture, Redmond, United States).

Visual Implant Elastomer Tagging

Two weeks prior to the first behavioral test, AB zebrafish were anesthetized with tricaine (Sigma-Aldrich, Sweden) and injected with a visual implant elastomer (VIE) tag (Northwest Marine Technology, Anacortes, United States) using two colors at four possible tagging positions (Hohn and Petrie-Hanson, 2013). After

recovery from the anesthetic, animals were placed in same sex groups of 6–12 individuals in 2.8 L tanks, allowing for unique tags within each tank and creating smaller groups that could be tested within one session. The wild zebrafish were not tagged but were also placed in small same sex groups.

Behavioral Test Procedures

AB zebrafish were tested twice in the zMCSF test (on experimental days 1 and 7; Run 1 and 2, respectively), and twice in the NTDT (on days 2 and 8; Run 1 and 2, respectively). Wild zebrafish were tested once in each test (zMCSF on day 1 and NTDT on day 2). The morning feed was provided at least 30 min before behavioral tests were performed. None of the zebrafish used in this experiment had any previous experience of behavioral testing. All behavioral tests took place in a separate room located inside the aquarium room. The experimenter was not present or visible during video recordings. Male groups were tested before female groups, to minimize confounding effects of pheromones from ovulating females. Between trials, testing arenas were sprayed with ethanol (96%), rinsed twice with water and refilled.

The zebrafish Multivariate Concentric Square Field Test

The zMCSF consisted of a square aquarium ($30 \times 30 \times 25.8\text{ cm}$, water depth 10 cm) filled with 8 L pre-heated copper-free Uppsala municipal tap water ($23 \pm 2^\circ\text{C}$) and containing three objects; a roof, a corridor and a ramp, which were placed around the walls thereby surrounding a central open area (Figure 1A, blueprints provided in Supplementary Figure 1). These objects created 12 zones (Figure 1B): a dark corner with a roof (DCR), a semi-sheltered area consisting of two corridors (CORR1 and CORR2) and a corner (CORN), an inclined ramp leading from high to low water depth (RAMP1-4), a central square consisting of an central circle (CIRC) and the remnant of the central square (CENT) and finally the remaining floor area that did not belong to any of the other zones (REST). An infrared backlight (Noldus, Wageningen, the Netherlands) was placed under the zMCSF arena and an infrared camera (JVC SuperLoLux, Yokohama, Japan) on the ceiling to record the movement of the fish in the arena. The aquarium was made out of 7.5 mm thick transparent Perspex while the ramp consisted of 2 mm transparent perspex. The roof and corridors were composed of infrared transparent plastic, which appears untransparent to the fish but enables infrared video recording of the animal in these areas. Stainless steel pillars kept the DCR and corridors in place. Two photographic lights (Walimex daylight 1000, the Hague, the Netherlands) provided ambient lighting of 0.46 Lux (Lux meter, Fisher Scientific Ltd., Uppsala, Sweden).

Zebrafish were netted out of their 2.8 L housing tank, transferred in a 500 mL beaker, and released in the zMCSF arena at the START zone (Figure 1B). Videos were recorded with Ethovision XT12 (Noldus, Wageningen, the Netherlands), with recording starting 2 s after the fish was detected in the arena and lasting for 30 min. Thereafter, the fish was transferred to a 1.8 L tank where it was kept until all fish from its home tank were tested, and the group was reunited in the home tank.

Using Ethovision XT15 (Noldus, Wageningen, the Netherlands) we manually assessed all tracks for any tracking errors caused by reflections and extracted six variables from the videos. For the whole arena we extracted duration in arena (only used to check data integrity), total distance moved (cm) and average velocity (cm s^{-1}). For each zone, we extracted the cumulative duration (s) in zone, frequency of zone visits and latency (s) until first entry into zone. For the REST zone only the duration (s) in this zone could be extracted. From these variables, we derived five more ethologically relevant variables, following analyses of MCSF tests in rodents (Augustsson and Meyerson, 2004; Meyerson et al., 2013). Total activity (abbreviated as “Totact”) was calculated as the sum of all zone frequencies (entries). Average duration per visit (s) was calculated as the total duration in zone divided by the frequency of visits to that zone. Frequency (%), the percentage of visits to a zone, was computed as the frequency of visits to that zone divided by total activity. The zone in which the fish spent the longest cumulative duration was defined as the individual’s home base (Eilam and Golani, 1989). Using the latency (s) variable, we derived the number of zones entered by the fish, and if the fish had explored all zones (“fully explored,” a binary variable). Finally, these same variables were extracted from Ethovision in “minute bins,” allowing for analyses over time.

The Novel Tank Diving Test

We followed the original description of the NTDT (Levin et al., 2007), with minor modifications. Video recordings were made using the same equipment as outlined in section “The zebrafish Multivariate Concentric Square Field Test,” now placing the infrared light board behind the arena and filming the arenas from the side. We used a 1.8 L zebrafish housing system tank as an arena ($\text{LxWxD } 26 \times 5 \times 12 \text{ cm}$; ZT180, Aquaneering, San Diego, United States) filled with 1.75 L pre-heated copper-free Uppsala municipal tap water ($23 \pm 2^\circ\text{C}$). The arena was horizontally divided into three zones of equal height (4 cm): the bottom (BOT), middle (MID), and top zone (TOP). An open shelving system (IVAR, IKEA, Sweden) allowed for simultaneous recording of up to eight arenas. The short sides of each tank were covered with white plastic film to prevent the fish from seeing into the neighboring tank. Each NTDT trial lasted 15 min, after which the fish was placed back in its home tank. We extracted the same variables from the video tracking software as described for the zMCSF (see section “The zebrafish Multivariate Concentric Square Field Test”).

Statistical Analyses

All statistical analyses were carried out in R statistical computing software version 4.0.2 (R_Core_Team, 2020) with added packages “lmer” (Bates et al., 2015), “emmeans” (Lenth, 2020), “bestNormalize” (Peterson and Cavanaugh, 2019), “ggplot2” (Wickham, 2016), “pals” (Wright, 2019) and “ggalluvial” (Brunson and Read, 2020). The data was split up into two datasets, since the experimental design was not fully factorial (i.e., there was no Run 2 for the wild zebrafish). The “retested dataset” contained the data from all tests on the AB zebrafish, while the “strain dataset” contained the data from both strains on

the first testing occasion. We first explored the data by conducting a principal component analysis (PCA) on each dataset, using the “prcomp” function with scaling and centering of variables.

Strain and Sex Differences

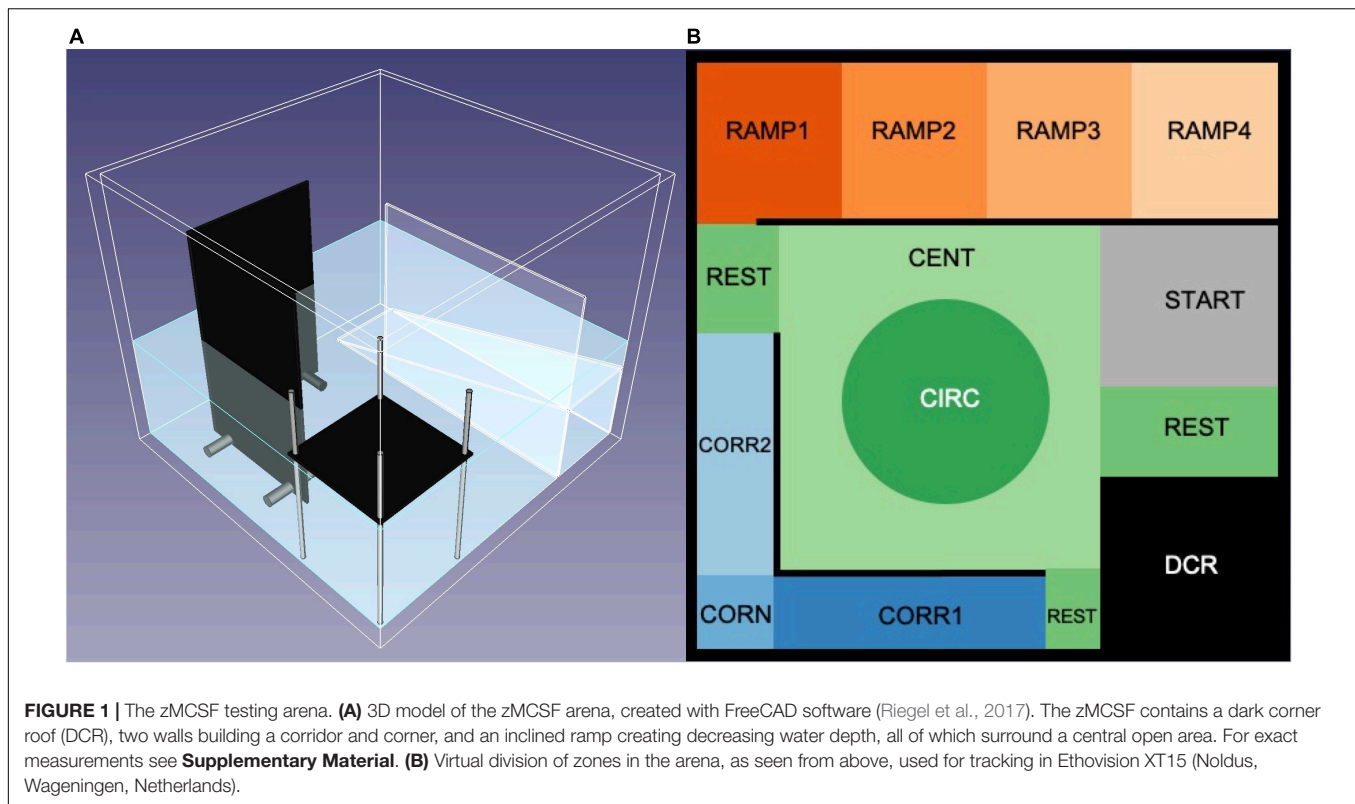
To evaluate the effect of Strain and Sex on total distance moved (cm) and mean velocity (cm s^{-1}), we computed two-way ANOVAs with main effects of Strain (AB or wild) and Sex plus the interaction effect. Total activity was modeled with a generalized linear model (GLM) with a negative binomial error distribution, using the same explanatory variables. For zone specific variables total duration (s), average duration per visit (s) and latency (s) a linear mixed-effects model (LMM) was constructed with fixed effects of Zone, Strain, Run and Sex and their interactions and a random intercept of Individual. Latency was transformed using an ordered quantile normalization (“orderNorm” function), a rank-based procedure, suggested by the “bestNormalize” function (both functions are part of the “bestNormalize” package). For count variables frequency and frequency (%) we computed a negative binomial generalized linear mixed-effects model (GLMM), with the same fixed and random effects, after a Poisson GLMM proved to suffer from overdispersion. For all models, *post hoc* pairwise comparisons with Bonferroni correction for multiple testing were computed using the “emmeans” function.

To evaluate the home base behavior of AB vs. wild zebrafish, we constructed a Poisson GLM with the number of zones explored as a response variable and Strain, Sex and their interaction as explanatory variables. In addition, a binomial GLM with the same explanatory variables was performed on the binary variable indicating whether all zones had been visited.

Effect of Repeated Testing

For arena wide variables total distance moved (cm) and mean velocity (cm s^{-1}) in the retesting dataset, we constructed two linear mixed effects models (LMM) with fixed effects of Run (1 or 2) and Sex (female or male) and their interaction, and a random intercept of Individual. Total activity was modeled using a GLMM with negative binomial error distribution with the same explanatory variables. To test for an effect of retesting on zone specific variables total duration (s), average duration per visit (s), frequency, frequency (%) and latency (s) we constructed similar (G)LMMs as described in section “Strain and Sex Differences,” but the fixed effect of Strain was exchanged for a fixed effect of Run.

We calculated consistency repeatability between Run 1 and 2 as the intraclass Pearson’s correlation coefficient (ICC) per zone, variable and group (Sokal and Rohlf, 1995; Nakagawa and Schielzeth, 2010) using the “cor.test” function. Total duration (s) and average duration per visit (s) were log transformed while for variable latency (s) an ordered quantile normalizing transformation was applied (orderNorm’ function). To assess the relationships between zones (e.g., did individuals that spent more time in the DCR also spent less time in the RAMP?), we created five correlation matrices per Strain and Run (i.e., AB Run 1, AB Run 2 or wild zebrafish), one for each of the five zone-related variables,



using the “chart.Correlation” function from the package “PerformanceAnalytics” with logarithmic transformations of the same variables as for the repeatability correlations.

To assess whether more zones were explored in the second run, we constructed a generalized linear model with Poisson error distribution (Poisson GLM) using the number of zones explored as a response variable and Run, Sex and their interaction as explanatory variables. Finally, a binomial GLM with the same explanatory variables was performed on the fully explored variable (binary variable).

Behavior in the Novel Tank Diving Test

The NTDT variables were assessed for effects of Strain, Sex and Run in the same fashion as the zMCSF variables, as described in sections “Strain and Sex Differences” and “Effect of Repeated Testing” Home base behavior was not assessed in the NTDT, since most animals spent the longest duration in the bottom zone.

RESULTS

Principal Component Analysis

Our initial PCA on the variables from the zMCSF revealed largely overlapping distributions of the two sexes within the same strain, while AB fish only partially overlapped with the wild strain (**Figure 2A**). The loading plot showed a clear separation of test variables (**Figure 2B**). The DCR, the CENT/CIRC and the RAMP variables all fell on the PC1 axis yet at distinct values, suggesting that these represent different magnitudes of exploration/avoidance. The corridor variables

(CORR1-CORN-CORR2, hereafter CORRS) were located at a distinct position on the PC2 axis, which appeared to be related to locomotory activity.

Behavior of Female and Male AB and Wild Zebrafish in the zebrafish Multivariate Concentric Square Field

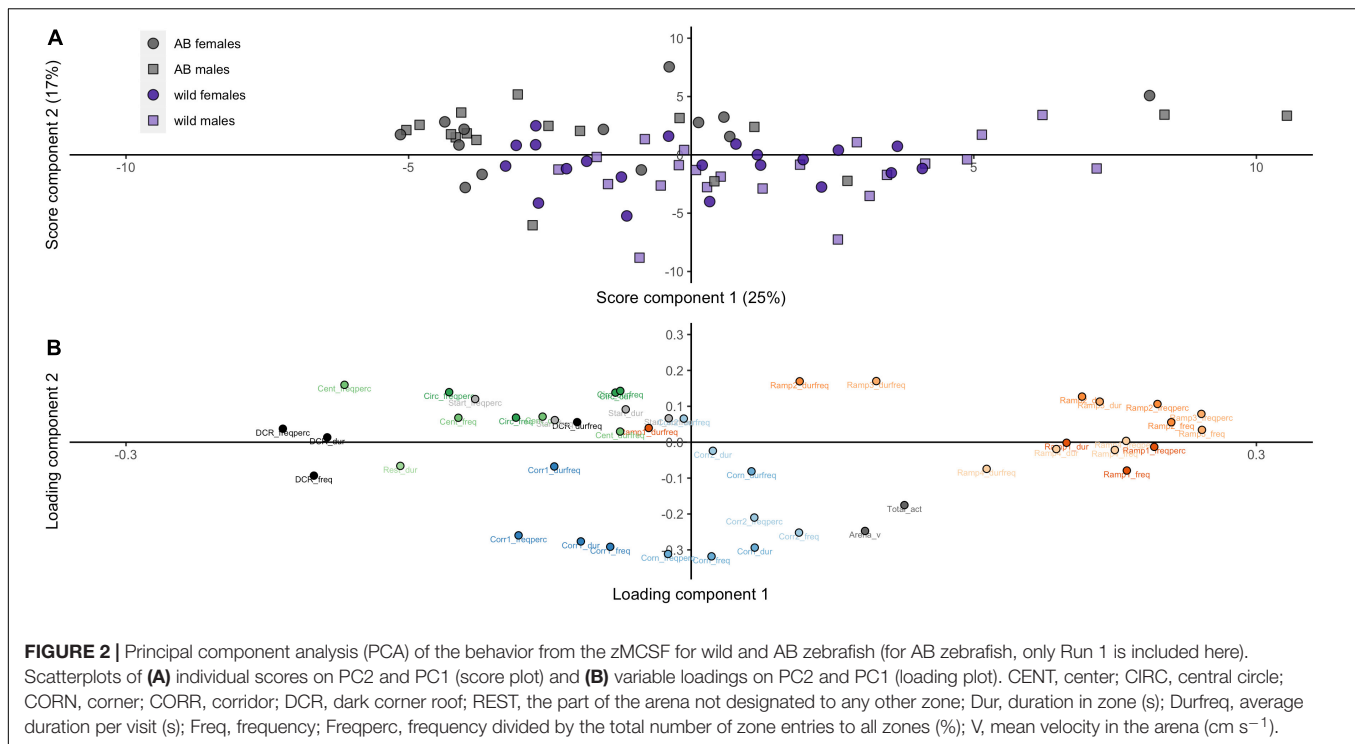
Locomotory Activity in the zebrafish Multivariate Concentric Square Field

Wild zebrafish moved longer distances than AB [LMM, $F_{(1, 69)} = 13.263$, $p < 0.001$; **Table 1**, **Supplementary Tables 1, 2**, and **Figure 3A**], at higher velocity [ANOVA, $F_{(1, 69)} = 14.010$, $p < 0.001$; **Figure 3B**] while the number of zone entries (total activity) was equal between the strains [Negative binomial GLM, $\chi^2_{(1, 69)} = 1.326$, $p = 0.250$; **Figure 3C**]. There was a tendency for a main effect of Sex on distance moved, with males of both strains moving marginally longer distances than females [LMM, $F_{(1, 69)} = 3.226$, $p = 0.077$; **Table 1**, **Supplementary Table 1**, and **Figure 3A**].

The PCA was unable to separate the data from the repeated runs of testing for the AB strain zebrafish (**Supplementary Figure 2A**). Nevertheless, the loading plot showed a clear separation of the zones (**Supplementary Figure 2B**), highly similar to the PCA on the data from both strains (**Figure 2B**).

Explorative Behavior in the zebrafish Multivariate Concentric Square Field

There were significant differences between the zones of the zMCSF in duration, duration per visit, frequency,



relative frequency and latency to visit (main effect of Zone, **Supplementary Table 1**). Wild zebrafish spent the longest duration in the DCR and shortest in the CIRC, in the order: DCR = RAMP1 = REST = CORN = CORR2 = CORR1 = START = RAMP2 = CENT = RAMP3 = RAMP4 > CIRC (**Supplementary Table 2** and **Figure 3D**). AB zebrafish also spent the longest duration in the DCR, but the zone visited for the shortest duration was RAMP4, in the order DCR > RAMP1 = REST > RAMP2 = START = CENT = CORR1 = CORR2 = CIRC = RAMP3 = CORN > RAMP4 (**Supplementary Table 2** and **Figure 3D**).

There was a significant main effect of Strain for response variables duration, frequency and latency, and a significant Zone by Strain interaction for all zone-related response variables (**Supplementary Table 1**), indicating that the strains allocated their time differently across the zMCSF zones. The pair-wise differences between the strain/sex groups are summarized in **Table 1**, **Supplementary Table 2** and **Figure 3A–I**. Compared to AB, wild zebrafish spent more time in CORR1, CORN and CORR2 [LMM contrasts, $t_{(11, 622)} = -3.220$, $p = 0.001$; $t_{(11, 622)} = -6.663$, $p < 0.001$; $t_{(11, 622)} = -5.348$, $p < 0.001$; **Figure 3D**] and in RAMP1, 3, and 4 [$t_{(11, 622)} = -3.238$, $p = 0.001$; $t_{(11, 622)} = -2.588$, $p = 0.010$; $t_{(11, 622)} = -6.654$, $p < 0.001$; **Figure 3D**]. By contrast, wild zebrafish spent a shorter duration in CIRC [$t_{(11, 622)} = -3.513$, $p = 0.001$; **Figure 3D**] and a shorter average duration per visit in the DCR [$t_{(11, 654)} = -2.463$, $p = 0.001$; **Figure 3G**]. The differences between the strains were always in the same direction for both sexes, but in some cases were only detected in one sex (**Supplementary Table 2**). A greater number of strain differences was detected in males compared to females (**Table 1** and **Supplementary Table 2**). Notably, compared to AB

males, wild males paid more visits to RAMP4 and fewer visits to CIRC and CENT, while this strain difference was absent in females (**Table 1** and **Supplementary Table 2**).

Time series plots (**Supplementary Figure 3**) suggested that AB explored the arena during the first 10 min, spending more time in the RAMP zones early on, only to reside in the DCR for the remaining 20 min. Wild zebrafish divided their activity and time more equally over the different zones and spent less time in DCR, especially later in the test (**Supplementary Figure 3**).

AB zebrafish had a more pronounced preference for the DCR as a home base (53% of fish), while in wild zebrafish 35% of fish preferred the DCR and 30% the RAMP1 as a home base, a strain difference that was borderline significant [Poisson GLM, $\chi^2_{(1, 23)} = 18.373$, $p = 0.073$; **Figure 3I**]. No sex differences were detected in the number of zones visited within either strain [Poisson GLM contrast, AB: $z_{1,69} = 0.368$, $p = 1.000$; Wild: $z_{(1, 69)} = 0.045$, $p = 1.000$]. While AB zebrafish often left one or more zones unexplored (**Figures 4B,E**), wild zebrafish explored all zones [Binomial GLM, $\chi^2_{(1, 72)} = 28.443$, $p < 0.001$], the only exception being one wild male that never entered CIRC (**Figures 4A,D**).

Functional Areas of the zebrafish Multivariate Concentric Square Field

Correlations between zones revealed that there were six areas in the arena, consisting of zones that were positively intercorrelated in terms of the duration of time spent in these zones. For AB zebrafish these areas were START, DCR, CORRS, RAMP1-4 (hereafter RAMP), CENT-CIRC and REST (**Supplementary Table 3A**). More active animals (high velocity and total activity) spent more time in the CORRS, RAMP and CIRC and less

time in the DCR. Individuals that spent more time in the DCR spent less time on the RAMP and more time in CORR1, CORN and REST zones. CORRS and CIRC, CENT and REST zones were positively correlated. However, REST was negatively correlated with RAMP, differentiating it from the CIRC-CENT area (**Supplementary Table 3A**).

The same six areas of intercorrelated zones could be differentiated in wild zebrafish, with minor modifications (**Supplementary Table 3B**). In wild zebrafish, duration in CORR2 was not correlated with CORR1 and CORN ($p = 0.138$ and $p = 0.263$, respectively). Moreover, only duration in RAMP1-2 but not in RAMP3-4 was negatively correlated with DCR (**Supplementary Table 3B**). In AB, the REST zone was negatively correlated with RAMP (**Supplementary Table 3A**), while in wild zebrafish the CENT and RAMP zones were negatively correlated (**Supplementary Table 3B**).

Effect of Repeated Testing in the zebrafish Multivariate Concentric Square Field

There was a tendency for increased locomotory activity from Run 1 to 2, although this effect only reached statistical significance for total activity [GLMM, $F_{(1, 28)} = 6.648$, $p = 0.011$; **Supplementary Table 4**]. The sex difference in locomotory activity became more pronounced after taking into account both runs, with AB males traveling longer distances [LMM, $F_{(1, 28)} = 7.452$, $p = 0.011$] at higher speed [LMM, $F_{(1, 28)} = 7.466$, $p = 0.011$] and exhibiting higher total activity [GLMM, $F_{(1, 28)} = 5.098$, $p = 0.024$; **Supplementary Table 4**].

On the second testing occasion, AB zebrafish again spent the longest duration in the DCR and shortest in RAMP4, in the order: DCR > RAMP1 > REST = CENT = START = CORR1 > CORN = CORR2 > RAMP2 = CIRC > RAMP3 > RAMP4 (LMM, $F_{(11, 308)} = 10.516$, $p < 0.001$; **Supplementary Table 2** and **Figure 3D**). For duration and frequency in zone, there was a main effect of Run [LMM, $F_{(1, 644)} = 22.866$, $p < 0.001$ and $F_{(1, 512)} = 8.150$, $p = 0.006$, respectively; **Supplementary Table 4**]. However, the lack of a Zone by Run interaction for all zone-related variables indicated that AB zebrafish did not allocate their time differently over zones on the second testing occasion (**Supplementary Table 4**). Only a single pairwise comparison between the runs was statistically significant: AB males had a shorter average duration per visit to DCR in Run 2 compared to Run 1 [LMM contrast, $t_{(10, 505)} = 3.215$, $p = 0.008$; **Supplementary Table 2**].

The six areas of correlated zones outlined in section “Behavior of Female and Male AB and Wild Zebrafish in the zebrafish Multivariate Concentric Square Field” could also be distinguished in the second run, but some relationships between areas changed (**Supplementary Table 3A**). Upon repeated testing, activity was no longer related to duration in RAMP and CIRC zones. Animals that stayed longer in the DCR now spent less time in the CORN and CORR2 zones. Also, the negative correlation between the REST and RAMP zones was no longer present (**Supplementary Table 3A**).

TABLE 1 | Pairwise comparisons between strains and sexes in the zones of the zMCSF in AB and wild (W) zebrafish, separating males and females.

Sex	Zone	Duration (s)	Duration per visit (s)	Frequency (%)	Frequency (%)	Latency (s)
Females	START					
	DCR					
	CORN					
	CORN	W > AB***				W < AB*
	CORN	W > AB*				
	RAMP1					
	RAMP2					
	RAMP3					
	RAMP4	W > AB***				W < AB**
	CIRC		W < AB*			
	CENT					
	REST					
Males	START					W < AB*
	DCR					
	CORN	W > AB*				
	CORN	W > AB***		W > AB**	W > AB***	W < AB**
	CORN	W > AB***		W > AB**	W > AB**	
	RAMP1	W > AB*				
	RAMP2					
	RAMP3					
	RAMP4	W > AB***		W > AB***	W > AB**	W < AB*
	CIRC			W < AB**	W < AB***	
	CENT			W < AB*	W < AB***	
	REST					

Texts in cells indicate which of the experimental groups had a significantly higher or lower value of the measured zone-related variable. * $p < 0.05$, ** $p < 0.01$, *** $p < 0.001$ comparing AB and wild within sex. CENT, center; CIRC, central circle; CORN, corner; CORR, corridor; DCR, dark corner roof; REST, the part of the arena not designated to any other zone.

Consistency repeatability was significant for distance moved and velocity ($r = 0.432$, $p = 0.014$ and $r = 0.446$, $p = 0.013$, respectively; **Supplementary Table 5**). RAMP1 had high repeatability both in terms of duration ($r = 0.508$, $p = 0.038$), frequency ($r = 0.376$, $p = 0.041$) and frequency (%) ($r = 0.533$, $p = 0.002$; **Supplementary Table 5**). Significant repeatabilities were also seen for the neighboring zones, average duration per visit to CORR2 ($r = 0.556$, $p = 0.001$) and frequency (%) of entering RAMP2 ($r = 0.379$, $p = 0.039$). Finally, the frequency of visits to the DCR was repeatable ($r = 0.497$, $p = 0.005$) and the repeatability of frequency to CIRC was approaching the significance level ($r = 0.326$, $p = 0.079$; **Supplementary Table 5**).

In the first run, the DCR was the home base for 60% of AB zebrafish (**Figure 3I**) and this preference was not altered by repeated testing [Poisson GLM, $\chi^2_{(1, 57)} = 0.000$, $p = 1.000$]. There was no significant effect of Run, Sex or their interaction on the number of zones explored [Poisson GLM, Run: $\chi^2_{(1, 58)} = 2.251$, $p = 0.134$; Sex: $\chi^2_{(1, 57)} = 0.041$, $p = 0.840$; Run by Sex: $\chi^2_{(1, 56)} = 0.100$, $p = 0.752$], nor whether or not all zones had been entered [Binomial GLM, Run: $\chi^2_{(1, 58)} = 0.000$, $p = 1.000$; Sex: $\chi^2_{(1, 58)} = 1.248$, $p = 0.264$; Run by Sex: $\chi^2_{(1, 58)} = 0.000$,

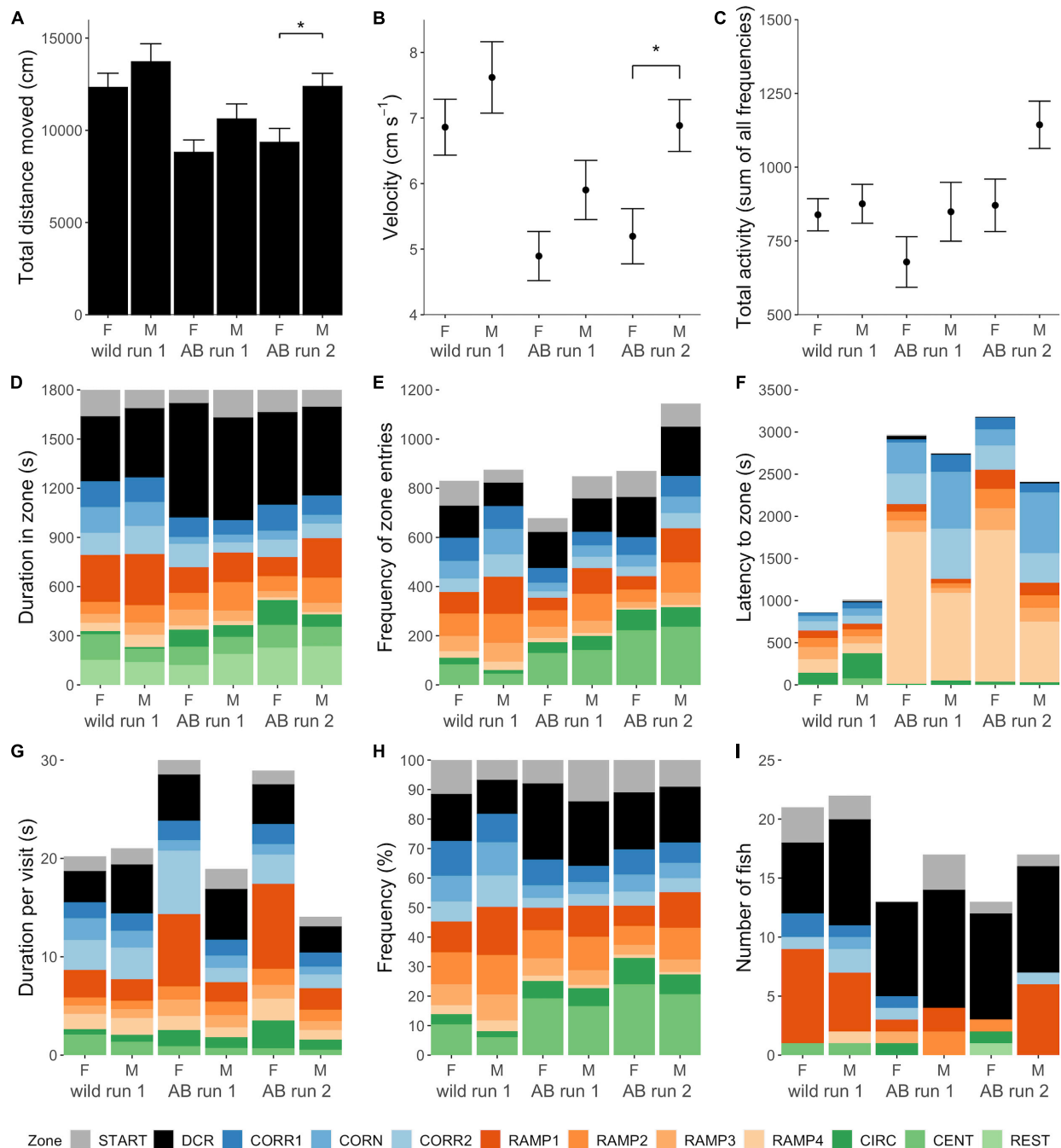


FIGURE 3 | Behavior in the zMCSP test. Locomotory activity variables (A) total distance moved (cm), (B) average velocity (cm s⁻¹) and (C) total activity (sum of all zone entries) per experimental group calculated for the whole arena. In (A–C), the height of the bars or points represents the mean \pm SEM per group. Brackets with stars (*) indicate statistically significant differences ($p < 0.05$) between experimental groups; main effects of Strain, Sex, and Run are shown in **Supplementary Table 1**. (D–I) Present zone related variables (D) duration (s) in zone, (E) frequency of zone entries, (F) Latency (s) to zone, (G) average duration per visit (s), (H) percentage of zone entries, and (I) the number of fish that had a certain zone as its home base. For example, the majority of AB females in run 1 had the DCR as their home base, so the DCR was zone that the fish spent the longest cumulative duration in. In (D–I), the height of each colored bar represents the mean per zone except for (F), where these represent median latency (the more accurate summarizing statistic for this variable). For the REST zone, only duration could be quantified. Note that this figure combines the “strain” and “retested” datasets which were analyzed in two separate models per response variable, see methods section “Statistical Analyses.” CENT, center; CIRC, central circle; CORN, corner; CORR, corridor; DCR, dark corner roof; REST, the part of the arena not designated to any other zone; F, female; M, male.

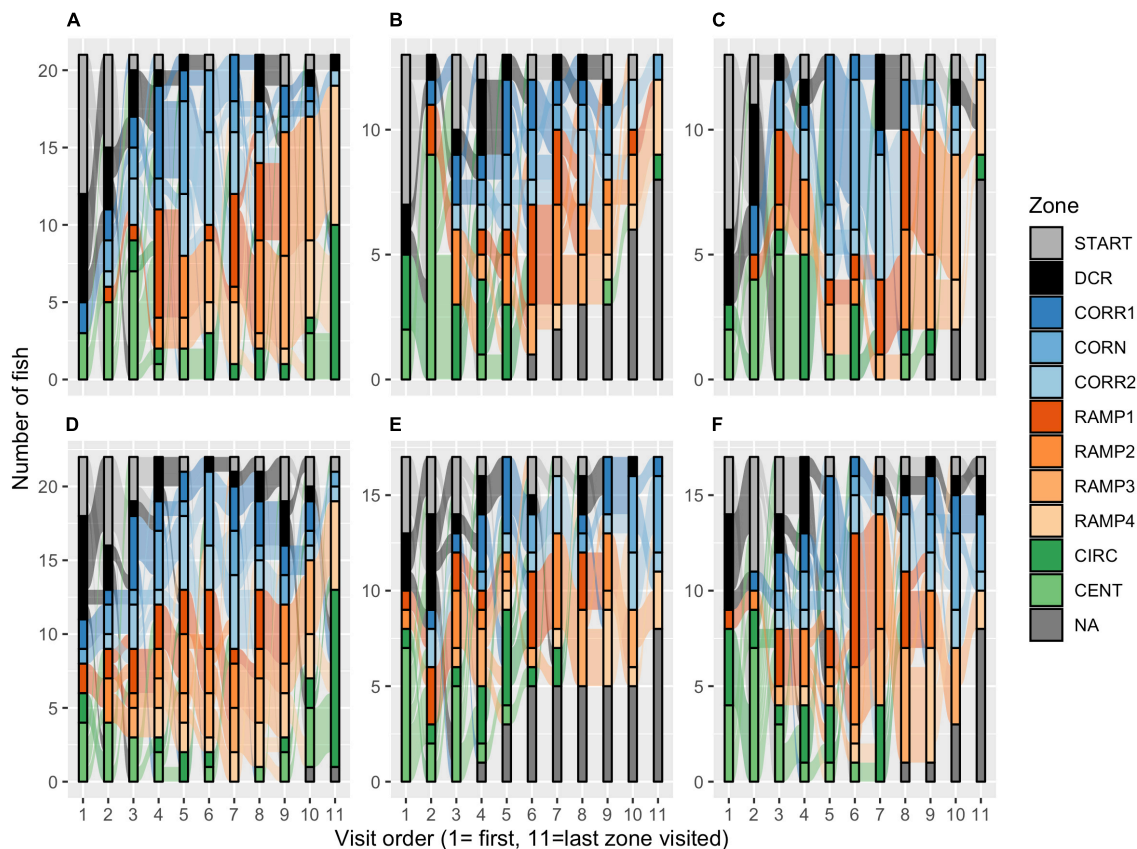


FIGURE 4 | Sankey diagrams of explorative strategies in the zMCSF test. The diagrams represent the order in which the zones were visited for **(A)** wild females, **(B)** AB females run 1, **(C)** AB females run 2, **(D)** wild males, **(E)** AB males run 1, and **(F)** AB males run 2. The height of each colored bar represents the number of fish that visited a particular zone as the n th novel zone they visited. The flows between the bars describe the number of individuals that moved from one zone to the next novel zone. The gray bars ("NA") represent the number of fish that did not have an n th zone, i.e., they did not explore more than $n-1$ zones. Example: in **(A)**, seven wild females were first detected in DCR; 5 of those fish then went on to the START zone while the other two moved to CORR1. CENT, center; CIRC, central circle; CORN, corner; CORR, corridor; DCR, dark corner roof; REST, the part of the arena not designated to any other zone; F, female; M, male.

$p = 1.000$]. In both runs, 8 AB females and 8 AB males (53%) left one or more zones unexplored (Figure 4).

Behavior of Female and Male AB and Wild Zebrafish in the Novel Tank Diving Test

In the NTDT, there was a main effect of Strain on all activity variables and a main effect of Sex on distance moved and velocity (Supplementary Table 1). Wild zebrafish had higher locomotory activity than AB as indicated by a longer distance moved [ANOVA, $F_{(1, 69)} = 53.091$, $p < 0.001$; Table 2 and Supplementary Table 6], higher velocity [ANOVA, $F_{(1, 69)} = 18.563$, $p < 0.001$; Figure 5A] and higher total activity [GLM, $\chi^2_{(1, 71)} = 11.422$, $p < 0.001$; Supplementary Table 6]. In both strains, females moved longer distances [ANOVA, $F_{(1, 69)} = 9.501$, $p < 0.003$] and at higher speed than males [ANOVA, $F_{(1, 69)} = 4.214$, $p = 0.044$], although there was no sex difference in total activity [GLM, $\chi^2_{(1, 70)} = 0.446$, $p = 0.504$; Supplementary Table 6].

Both zebrafish strains spent most time in the bottom and least time in the top third of the NTDT [LMM contrast, AB TOP vs. BOT, $t_{(2, 179)} = -4.053$, $p = 0.001$; wild Top vs. Bottom, $t_{(2, 179)} = -7.066$, $p < 0.001$; Supplementary Table 6 and Figure 5B]. There was a main effect of Strain and a Zone by Strain interaction for some zone-related variables (Supplementary Table 1), indicating that there were some differences in how much time each strain spent in the top, middle and bottom third of the arena. *Post-hoc* tests showed that wild females entered the top and middle third more often than AB females [GLMM contrast, $z_{(1, 205)} = -4.830$, $p < 0.001$; $z_{(1, 205)} = -3.805$, $p < 0.001$], while wild and AB males did not differ [GLMM contrast, $z_{(1, 205)} = -0.628$, $p = 1.000$; $z_{(1, 205)} = -2.005$, $p = 0.270$; Table 2 and Figure 5C].

Repetition of the NTDT for AB fish one week later revealed a tendency for an increase in velocity [LMM, $F_{(1, 28)} = 3.791$, $p = 0.061$] and total activity from Run 1 to 2 [GLMM, $F_{(1, 28)} = 3.311$, $p = 0.096$, Supplementary Tables 4, 6]. We did not detect a main effect of Run nor a Zone by Run interaction for any of the zone-related response variables (Supplementary Table 4).

Comparison of Behavior of AB Zebrafish in zebrafish Multivariate Concentric Square Field and Novel Tank Diving Test

In AB, correlations between duration spent in each zone of the zMCSF and NTDT revealed that in Run 2, duration in bottom of the NTDT correlated negatively with duration in RAMP2, 3, and 4 and duration in the top correlated positively with RAMP 2 and 3 (**Supplementary Table 3A**). Furthermore, duration in bottom correlated positively with DCR (**Supplementary Table 3A**).

DISCUSSION

Behavioral tests continue to play an important role for the discovery of novel neuroactive compounds and in the development of zebrafish models of neurological and neuropsychiatric disease. Classical tests, such as the open field, shelter, light/dark, elevated plus maze and NTDT, are still widely used since they enable comparisons with previous studies and generally translate well to other study species (in particular rodents). To ensure a broad behavioral screening, many studies make use of a sequence of classical tests (a “test battery”), but evidence is accumulating that animals habituate to the novelty offered in the same test (Rodgers, 1997) and even generalize experiences between tests (McIlwain et al., 2001; Blokland et al., 2012). Herein, we have developed a complex testing environment for the quantification of explorative behavior in adult zebrafish, the zebrafish Multivariate Concentric Square Field (zMCSF), that combines elements of classical tests in a single arena and greatly reduces the number of tests performed.

We previously optimized the dimensions of the zMCSF arena (Roman et al., 2016, 2018; Bikovski et al., 2020). Here, we further optimized the division of the arena into zones as compared to the previous version (Roman et al., 2018) by minimizing the area designated as the REST zone, by dividing the central square into the central circle (CIRC) and the surrounding area (CENT) and by dividing the inclined ramp into four rather than two zones. Although a formal comparison between the zone division settings is outside of the scope of the current study, we would like to emphasize that the current zone division further refined the study of explorative strategies and their behavioral interpretation as compared to previous versions (Roman et al., 2018). The division of the central square into an outer and central zone provided a closer comparison to the classical open field test, and the subdivision of the ramp enabled a more detailed study of risk-taking behavior.

Behavior of AB and Wild Zebrafish in the zebrafish Multivariate Concentric Square Field

We detected considerable differences in explorative behavior between laboratory and wild zebrafish. Notably, wild zebrafish swam faster and explored all zones, while AB zebrafish often left one or more zones unexplored. Wild zebrafish showed stronger avoidance of the open area in the center, but entered the shallowest zone in the arena, RAMP4, earlier. The strains

TABLE 2 | Pairwise comparisons between strains and sexes in the zones of the novel tank diving test (NTDT) in AB and wild (W) zebrafish, separating males and females.

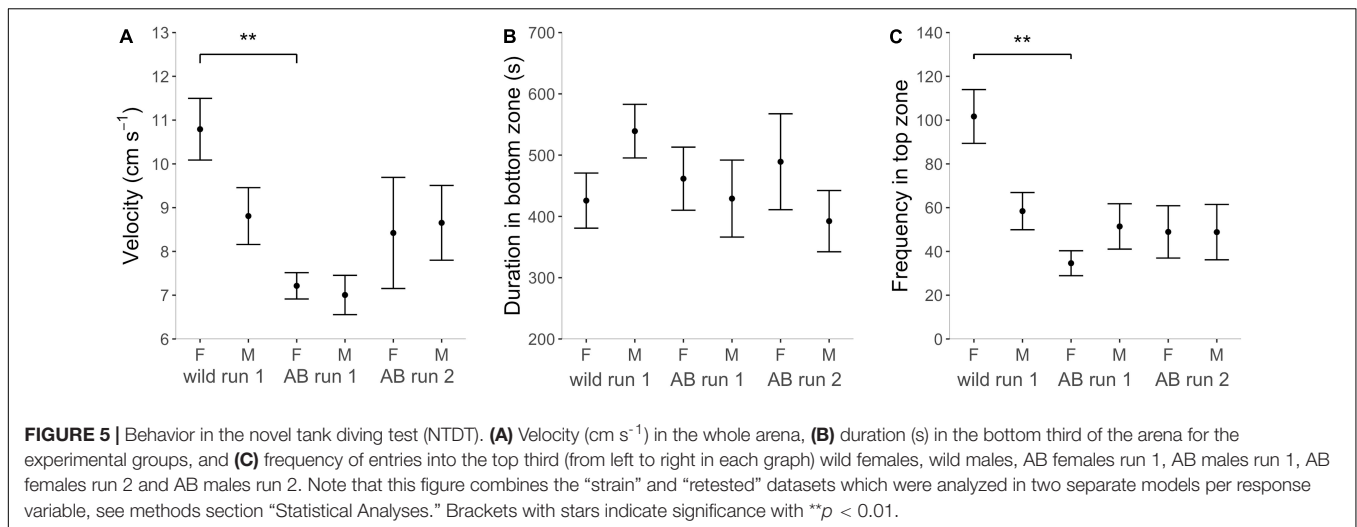
Sex	Zone	Duration (s)	Duration per visit (s)	Frequency (%)	Frequency (%)	Latency (s)
Females	TOP			W > AB***		
	MID			W > AB***		
	BOT					
Males	TOP					
	MID					
	BOT					

*Texts in cells indicate which of the experimental groups had a significantly higher or lower value of the measured zone-related variable. ***p < 0.001.*

did not differ in the time spent in the sheltered area (DCR). In nature, open areas are associated with increased predation risk for individual prey fish (Ruxton and Johnsen, 2016) and wild zebrafish occur in small vegetated streams feeding on insects, moving into shallow flooded areas for spawning at the start of the rainy season (Engeszer et al., 2007; Sundin et al., 2019). By contrast, the environment of laboratory zebrafish has for many generations consisted of deep tanks with no shallow areas and no vegetation cover (Sessa et al., 2008). It is possible that laboratory zebrafish over generations have become less selective with regards to the exact housing conditions, while in nature selection pressures for avoiding open water and exploring shallow water continued to act. This could explain the greater avoidance of the center zone and greater exploration of the shallow zones of the ramp by the wild strain. Indeed, the strain differences detected in the zMCSF imply that the behavioral adaption to the laboratory environment is characterized by relaxed aversion to risky areas with no potential gain (open area) and reduced exploration of risky areas with potential gain (the inclined ramp), while attraction to safe areas seems to be unaltered. These findings are congruent with the idea that domesticated animals are characterized by a low propensity to perform active behaviors (Van Reenen et al., 2005), and low stress reactivity, in other words, are “docile” rather than “shy” (Koolhaas et al., 2010; Koolhaas and Van Reenen, 2016; Rauw et al., 2017)."

The results from the zMCSF correspond well to the behavior of zebrafish in classical tests. The lower velocity and avoidance of the center of an open field by domesticated zebrafish has been reported before (Baker et al., 2018) and extends to other anti-predator behaviors, including reduced diving responses and altered responses to conspecific alarm pheromone (Mustafa et al., 2019; Vossen et al., 2020b). Moreover, the absence of large strain differences in DCR duration is in line with the absence of a strain difference in the shelter test in the same population of wild zebrafish (Mustafa et al., 2019). Thus, the strain differences we observed in the zMCSF appear to be comparable to those reported using single tests. However, the zMCSF adds the advantage of reducing the need for repeated testing, which makes the zMCSF more time-efficient, reduces handling stress and minimizes possible carry-over effects.

Comparing these results to wild and inbred lines of laboratory mice, it becomes apparent that the strong avoidance of the



central zone in wild animals is a particular consistent finding across species (Augustsson and Meyerson, 2004; Augustsson et al., 2005). A higher duration and frequency of visits to the slope (corresponding to RAMP1) has also been observed in wild mice in comparison to the BALB/c laboratory line, although no differences were observed with regard to the bridge (Augustsson and Meyerson, 2004; Augustsson et al., 2005). Similar to zebrafish, the duration in DCR was not different across wild and laboratory lines of mice (Augustsson and Meyerson, 2004; Augustsson et al., 2005). Hence, actively seeking shelter does not appear to be a major factor differentiating wild and laboratory bred animals, at least not in the current test environment in which animals can freely choose where to reside. It should be noted, however, that some wild zebrafish may have considered the RAMP1 zone an (additional) home base, in which case wild zebrafish may have spent more time in the safety of their home base than AB zebrafish. We found only one discrepancy in MCSF behavior between the species; wild zebrafish showed an increased duration in the corridors, while wild mice showed a lower use of this area compared to the laboratory lines. The corridors present a semi-sheltered area where movement is possible (Roman and Colombo, 2009), therefore we suggest that this difference is driven by the higher velocity of wild zebrafish. Wild mice did not have a higher velocity than the laboratory lines, explaining the absence of a difference in the corridor duration for this species. Mice and zebrafish may indeed differ at the species level in the propensity to respond reactively (freeze) or proactively (swimming) when entering a novel environment.

Sex Differences in the zebrafish Multivariate Concentric Square Field

We found no major differences between females and males of each strain. Locomotory activity was similar in the sexes in run 1. Studies using classical tests often report that AB males had a higher velocity than females (Vossen et al., 2016; Vossen et al., 2020b; Mustafa et al., 2019). In the zMCSF the sex difference in velocity was only marginally significant in the first run. This may be explained by the larger size and/or presence

of physical structure in the zMCSF, which limits repetitive movement along the walls. Indeed, upon inclusion of the second run of the zMCSF, velocity of AB males was higher than AB females (see section “Effect of Repeated Testing in the zebrafish Multivariate Concentric Square Field”), suggesting that the effect on locomotion is smaller in the zMCSF but can be still detected for larger samples.

The sexes did not show any major difference in the duration of time spent in and number of visits to any of the zMCSF zones. Previous studies have reported sex effects on risk-taking behaviors in different directions. Wild females exhibited increased shelter seeking and thigmotaxis (Dahlbom et al., 2011), and a stronger diving response to conspecific alarm pheromone (Vossen et al., 2020b), while another study on wild zebrafish reported no sex differences in shelter seeking and bottom dwelling (Mustafa et al., 2019). A recent study reported an opposite effect of a pharmaceutical (scopolamine) on anxiety-like behavior in males and females of the short-fin strain (Dos Santos et al., 2021). Although studies of “wild-caught” zebrafish are complicated by the different origin of the fish and should therefore be interpreted with caution, there does seem to be a disparity between studies in the direction and magnitude of sex differences reported. This may be because sex differences are few and/or of small effect. Alternatively, the differences between the zMCSF and classical tests may reflect the design of the test arena. Their higher activity may “drive” males into the center of the open field, the top zone of the NTDT, or the white compartment of the light/dark test, simply because there are no other zones to move in. In the zMCSF, the shelter and the risky areas only comprise a small part of the arena, therefore a move into this area may be interpreted as a more active choice for exploration. Hence the zMCSF may allow for a clearer separation between locomotion and explorative behavior.

Finally, it is worth mentioning that some of the strain differences were more pronounced in males than in females. Compared to AB males, wild males paid more visits to the corridors and RAMP4, and less visits to the central area, whilst these effects did not reach statistical significance for

the comparison between AB and wild females. This may imply that (the response to) selection for the domesticated environment is stronger in zebrafish males compared to females.

Effect of Repeated Testing in the zebrafish Multivariate Concentric Square Field

Overall, we found only minor changes in explorative behavior when the AB zebrafish were tested in the zMCSF 1 week later, and the few differences we found were confined to males. AB males were more active than females in the second run, an effect that has also been reported for the open field using the same interest interval (Thomson et al., 2020). In rodents, activity during the second test occasion is dependent on developmental stage. Adult rats were less active in the MCSF upon retesting (Meyerson et al., 2006; Momeni and Roman, 2014), while adolescent rats increased the total number of visits to zones (Lundberg et al., 2019).

Male zebrafish decreased their visit duration to the DCR, an effect that has been reported in rats by some studies (Momeni and Roman, 2014; Lundberg et al., 2019), whereas others found no effect (Meyerson et al., 2006; Roman and Colombo, 2009). A consistent finding in rats is a decrease in duration and/or frequency of visits to the hurdle, slope and bridge in the second trial (Meyerson et al., 2006; Roman and Colombo, 2009; Momeni and Roman, 2014; Lundberg et al., 2019), and in most of these studies, an increase in visits to the corridors. We did not detect these same effects in zebrafish, which may reflect underlying differences in episodic/spatial memory between the zebrafish and rodents. Zebrafish can be taught to associate a color with a mild electric shock within a single training session but fail to show avoidance of this color when tested again 1 week later (Vossen et al., 2020). By contrast, rats can spatially locate exposure to an aversive stimulus when repeatedly tested 2 weeks later (Karlsson et al., 2009).

Significant repeatabilities of $r \sim 0.5$ were found for activity variables as well as for the DCR and RAMP1 zones, which is considered to be a high repeatability (Bell et al., 2009). High consistency of velocity has also been reported for zebrafish repeatedly tested in the open field (Toms and Echevarria, 2014; Baker et al., 2018; Fangmeier et al., 2018; Thomson et al., 2020). Regarding responses to novelty, high consistency of inspection duration has also been reported for zebrafish repeatedly tested in the mirror (Toms and Echevarria, 2014), novel object and predator tests (Toms and Echevarria, 2014; Fangmeier et al., 2018). The high consistency of RAMP1 is interesting since rodents frequently display stretched attend posture in this zone (the slope in the rodent MCSF), which is a key part of risk assessment behavior (Macintosh and Grant, 1963; Rodgers et al., 1999; Augustsson and Meyerson, 2004). Under the assumption that the RAMP1 (zMCSF) and the slope (rodent MCSF) are homologous, this would imply that zebrafish show equal risk assessment in repeated testing while risk taking differs.

Comparison to the Novel Tank Diving Test

In line with the usual pattern reported for the NTDT (Levin et al., 2007), both AB and wild zebrafish avoided the top zone. However, wild zebrafish paid more visits to the middle and top third of the tank compared to AB zebrafish. High levels of bottom dwelling in the AB strain have been reported before (Gerlai et al., 2008), although it is not clear whether this accurately reflects increased anxiety-like behavior of this strain (Vossen et al., 2020b). The positive correlation between duration in bottom (NTDT) and DCR (zMCSF) suggests that these zones contain elements of safety. The positive correlation between the number of visits to the TOP (NTDT) and RAMP (zMCSF) was expected, since both zones are located close to the water surface, an area associated with a risk for avian predation (Levin et al., 2007).

At a first glance, the overall conclusions from the zMCSF and NTDT seem to agree that the strongest differences were those between the strains and no or minor effects were seen between the sexes and between repetitions of the zMCSF. The differences between the strains were furthermore in the same direction in both tests, with wild zebrafish exhibiting higher activity than AB and moving more in shallow water. However, upon a closer look it becomes apparent that a much smaller number of effects was detected in the NTDT, even after correcting for the lower number of zones in this arena. Apart from the strain difference in activity, the NTDT revealed only two differences (wild females paid more visits to the middle and top), whereas in the zMCSF 21 strain differences were detected (17 in males and 4 in females), related to 7 zones. Indeed, this suggests that the zMCSF, like the rodent MCSF, constitutes a more nuanced behavioral test.

Yet the distinction between the zMCSF and NTDT goes deeper than just a quantitative difference in the number of effects detected. The zMCSF was able to distinguish between two independent risk-related behaviors, which are intertwined in the NTDT. Paradoxically, in the zMCSF the wild strain displayed more elaborate exploration and entered the shallowest zone more readily, while it simultaneously avoided the open areas more than AB zebrafish. In the NTDT, only a reduced diving response of wild zebrafish was detected, which (when viewed in isolation) could lead to the erroneous conclusion that wild zebrafish “showed reduced anxiety-like behavior” or “were more bold/risk taking,” which is only one side of the coin. Taking into account both tests, it rather seems that while wild zebrafish are more active explorers that avoid shallow areas less, they also display more elaborate risk assessment and are more sensitive to certain kinds of risk (i.e., open areas). Indeed, the results from the zMCSF suggest that risk taking should be considered in relation to the nature of the challenge.

Interpretation of the zebrafish Multivariate Concentric Square Field Areas in Terms of Risk and Safety

Our findings indicate that the interpretation of the MCSF areas in terms of risk and safety is largely conserved between rodents and zebrafish. The DCR may be considered the safest zone of the zMCSF, since it often was the zone that was visited first, with the

longest cumulative duration, indicative of a home base (Eilam and Golani, 1989; Stewart et al., 2010). The NTDT provided cross-validation for this interpretation since the duration in the DCR was positively correlated with the duration in the bottom zone. We suggest that the corridors (CORR1, CORN, CORR2) also contains aspects of safety, but in contrast to the DCR the fish can swim larger distances in this relatively sheltered area. In the corridors motor restlessness can be expressed without affecting measures of active exploration, which has also been reported for rats (Roman and Colombo, 2009). The RAMP is an area of gradually decreasing water depth, zebrafish spent little time here and were most hesitant to enter this area (especially the shallowest part, RAMP4), AB more so than wild zebrafish. The RAMP has an inverse relationship to the DCR especially in AB zebrafish, providing further evidence for an interpretation as a high-risk zone. Also the center of the arena (CIRC and CENT) may be a high-risk zone, which in particular wild zebrafish are hesitant to enter and spend little time in, while AB zebrafish more readily move through it much like movement in the corridors, suggesting the interpretation of this area is more strain dependent. Hence the RAMP and arena center may each reflect different “qualities” in terms of risk assessment and risk taking (Roman et al., 2012; Meyerson et al., 2013). Further experiments using pharmacological pre-treatments with for instance anxiolytic substances such as benzodiazepines (Bencan et al., 2009) are needed to further validate the here proposed interpretation of the zMCSF zones.

CONCLUSION

The zMCSF constitutes a multifaceted test environment to quantify zebrafish explorative behavior and behavioral profiles, containing zones associated with different kinds and magnitudes of risk and safety. We here report that exploratory behavior in the zMCSF was qualitatively different between laboratory and wild zebrafish, while sex differences within strains were small and most pronounced in the AB strain. Our results suggest that the zMCSF is a more precise behavioral tool, able to detect small differences between the zebrafish strains and sexes that were not picked up in the more reductionistic NTDT. Simultaneously, the zMCSF provides a wider, more comprehensive perspective on exploration and risk-taking. An added benefit is the apparent high repeatability and low habituation to the zMCSF, as assessed from the single repetition described here. Additional pharmacological validation and cross-validation of the zMCSF with other classical tests (e.g., open field, shelter test, plus maze) may further substantiate the interpretation of behavior in the zMCSF.

REFERENCES

- Augustsson, H., Dahlborn, K., and Meyerson, B. J. (2005). Exploration and risk assessment in female wild house mice (*Mus musculus musculus*) and two laboratory strains. *Physiol. Behav.* 84, 265–277. doi: 10.1016/j.physbeh.2004.12.002
- Augustsson, H., and Meyerson, B. J. (2004). Exploration and risk assessment: a comparative study of male house mice (*Mus musculus musculus*) and

DATA AVAILABILITY STATEMENT

The datasets generated for this study can be found on figshare with the identifier <https://doi.org/10.6084/m9.figshare.15022482>.

ETHICS STATEMENT

The animal study was reviewed and approved by the Uppsala Regional Animal Ethical Committee (permit C55/13), following the guidelines of the Swedish Legislation on Animal Experimentation (Animal Welfare Act SFS1998:56) and the European Union Directive on the Protection of Animals Used for Scientific Purposes (Directive 2010/63/EU).

AUTHOR CONTRIBUTIONS

ER conceptualized, designed the study, and supervised RB and PR. SW provided supervision and resources. RB and PR performed the experiments. LV validated, curated, visualized the data, conducted the statistical analyses, and wrote the first draft of the manuscript. All authors contributed to manuscript revision, read, and approved the submitted version.

FUNDING

This work was supported by grants from the Torvald and Britta Gahlins Foundation (to ER), the Carl Tryggers Foundation (CTS 20:352 to ER), and the Facias Foundation (to ER).

ACKNOWLEDGMENTS

We thank Nikita Tjernström, Arshi Mustafa, and the staff of the Technical Service at BMC and the Uppsala University Behavioral Facility (UUBF), Disciplinary Domain of Medicine and Pharmacy, Uppsala University.

SUPPLEMENTARY MATERIAL

The Supplementary Material for this article can be found online at: <https://www.frontiersin.org/articles/10.3389/fnbeh.2022.744533/full#supplementary-material>

two laboratory strains. *Physiol. Behav.* 81, 685–698. doi: 10.1016/j.physbeh.2004.03.014

Baker, M. R., Goodman, A. C., Santo, J. B., and Wong, R. Y. (2018). Repeatability and reliability of exploratory behavior in proactive and reactive zebrafish, *Danio rerio*. *Sci. Rep.* 8:12114. doi: 10.1038/s41598-018-30630-3

Bates, D., Mächler, M., Bolker, B., and Walker, S. (2015). Fitting linear mixed-effects models using lme4. *J. Stat. Softw.* 67, 1–48.

- Bell, A. M., Hankison, S. J., and Laskowski, K. L. (2009). The repeatability of behaviour: a meta-analysis. *Anim. Behav.* 77, 771–783. doi: 10.1016/j.anbehav.2008.12.022
- Belzung, C., and Lepape, G. (1994). Comparison of different behavioral-test situations used in psychopharmacology for measurement of anxiety. *Physiol. Behav.* 56, 623–628. doi: 10.1016/0031-9384(94)90311-5
- Bencan, Z., Sledge, D., and Levin, E. D. (2009). Buspirone, chlordiazepoxide and diazepam effects in a zebrafish model of anxiety. *Pharmacol. Biochem. Behav.* 94, 75–80. doi: 10.1016/j.pbb.2009.07.009
- Bikovski, L., Robinson, L., Konradsson-Geuken, A., Kullander, K., Viereckel, T., Winberg, S., et al. (2020). Lessons, insights and newly developed tools emerging from behavioral phenotyping core facilities. *J. Neurosci. Methods* 334:108597. doi: 10.1016/j.jneumeth.2020.108597
- Birgner, C., Nordenankar, K., Lundblad, M., Mendez, J. A., and Smith, C. (2010). VGLUT2 in dopamine neurons is required for psychostimulant-induced behavioral activation. *Proc. Natl. Acad. Sci. U.S.A.* 107, 389–394. doi: 10.1073/pnas.0910986107
- Blanchard, R. J., and Blanchard, D. C. (1989). Antipredator Defensive Behaviors in a Visible Burrow System. *J. Comparative Psychol.* 103, 70–82. doi: 10.1037/0735-7036.103.1.70
- Blokland, A., Ten Oever, S., van Gorp, D., van Draanen, M., Schmidt, T., and Nguyen, E. (2012). The use of a test battery assessing affective behavior in rats: order effects. *Behav. Brain Res.* 228, 16–21. doi: 10.1016/j.bbr.2011.11.042
- Brunson, J. C., and Read, Q. D. (2020). *ggalluvial: Alluvial Plots in 'ggplot2'*. Available online at <http://corybrunson.github.io/ggalluvial/> (accessed on Feb 2, 2022)
- Collett, T. S., and Zeil, J. (2018). Insect learning flights and walks. *Curr. Biol.* 28, R984–R988. doi: 10.1016/j.cub.2018.04.050
- Dahlbom, S. J., Lagman, D., Lundstedt-Enkel, K., Sundstrom, L. F., and Winberg, S. (2011). Boldness predicts social status in zebrafish (*Danio rerio*). *PLoS One* 6:e23565. doi: 10.1371/journal.pone.0023565
- Dingemans, N. J., Both, C., Drent, P. J., van Oers, K., and van Noordwijk, A. J. (2002). Repeatability and heritability of exploratory behaviour in great tits from the wild. *Anim. Behav.* 64, 929–938. doi: 10.1006/anbe.2002.2006
- Dos Santos, B. E., Giacomini, A., Marcon, L., Demin, K. A., Strekalova, T., de Abreu, M. S., et al. (2021). Sex differences shape zebrafish performance in a battery of anxiety tests and in response to acute scopolamine treatment. *Neurosci. Lett.* 759:135993. doi: 10.1016/j.neulet.2021.135993
- Eilam, D., and Golani, I. (1989). Home base behavior of rats (*Rattus norvegicus*) exploring a novel environment. *Behav. Brain Res.* 34, 199–211. doi: 10.1016/S0166-4328(89)80102-0
- Engeszer, R. E., Patterson, L. B., Rao, A. A., and Parichy, D. M. (2007). Zebrafish in the wild: a review of natural history and new notes from the field. *Zebrafish* 4, 21–40. doi: 10.1089/zeb.2006.9997
- Fangmeier, M. L., Noble, D. W. A., O'Dea, R. E., Usui, T., Lagisz, M., Hesselson, D., et al. (2018). Computer Animation Technology in Behavioral Sciences: a Sequential, Automatic, and High-Throughput Approach to Quantifying Personality in Zebrafish (*Danio rerio*). *Zebrafish* 15, 206–210. doi: 10.1089/zeb.2017.1532
- Gerlai, R. (2020). Evolutionary conservation, translational relevance and cognitive function: the future of zebrafish in behavioral neuroscience. *Neurosci. Biobehav. Rev.* 116, 426–435. doi: 10.1016/j.neubiorev.2020.07.009
- Gerlai, R., Ahmad, F., and Prajapati, S. (2008). Differences in acute alcohol-induced behavioral responses among zebrafish populations. *Alcohol. Clin. Exp. Res.* 32, 1763–1773. doi: 10.1111/j.1530-0277.2008.00761.x
- Hanell, A., and Marklund, N. (2014). Structured evaluation of rodent behavioral tests used in drug discovery research. *Front. Behav. Neurosci.* 8:252. doi: 10.3389/fnbeh.2014.00252
- Hohn, C., and Petrie-Hanson, L. (2013). Evaluation of visible implant elastomer tags in zebrafish (*Danio rerio*). *Biol. Open* 2, 1397–1401. doi: 10.1242/bio.20136460
- Kakade, S., and Dayan, P. (2002). Dopamine: generalization and bonuses. *Neural Networks* 15, 549–559.
- Kalueff, A. V., Stewart, A. M., and Gerlai, R. (2014). Zebrafish as an emerging model for studying complex brain disorders. *Trends Pharmacol. Sci.* 35, 63–75. doi: 10.1016/j.tips.2013.12.002
- Karlsson, O., and Roman, E. (2016). Dose-dependent effects of alcohol administration on behavioral profiles in the MCSF test. *Alcohol* 50, 51–56. doi: 10.1016/j.alcohol.2015.10.003
- Karlsson, O., Roman, E., and Brittebo, E. B. (2009). Long-term Cognitive Impairments in Adult Rats Treated Neonatally with beta-N-Methylamino-L-Alanine. *Toxicol. Sci.* 112, 185–195. doi: 10.1093/toxsci/kfp196
- Koolhaas, J. M., de Boer, S. F., Coppens, C. M., and Buwalda, B. (2010). Neuroendocrinology of coping styles: towards understanding the biology of individual variation. *Front. Neuroendocrinol.* 31:307–321. doi: 10.1016/j.yfrne.2010.04.001
- Koolhaas, J. M., and Van Reenen, C. G. (2016). ANIMAL BEHAVIOR AND WELL-BEING SYMPOSIUM: interaction between coping style/personality, stress, and welfare: relevance for domestic farm animals. *J. Anim. Sci.* 94, 2284–2296. doi: 10.2527/jas.2015-0125
- Lenth, R. (2020). *Estimated Marginal Means, aka Least-Squares Means*. Available online at <https://github.com/rvnlenth/emmeans> (accessed on Jan 4, 2022).
- Levin, E. D., Bencan, Z., and Cerutti, D. T. (2007). Anxiolytic effects of nicotine in zebrafish. *Physiol. Behav.* 90, 54–58.
- Lundberg, S., Hogman, C., and Roman, E. (2019). Adolescent Exploratory Strategies and Behavioral Types in the Multivariate Concentric Square Field(TM) Test. *Front. Behav. Neurosci.* 13:41. doi: 10.3389/fnbeh.2019.00041
- Macintosh, J. H., and Grant, E. C. (1963). A comparison of the social postures of some common laboratory rodents. *Behaviour* 21, 246–259.
- Maximino, C., Marques de Brito, T., Dias, C. A., Gouveia, A. Jr., and Morato, S. (2010). Scototaxis as anxiety-like behavior in fish. *Nat. Protoc.* 5, 209–216. doi: 10.1038/nprot.2009.225
- McIlwain, K. L., Merriweather, M. Y., Yuva-Paylor, A., and Paylor, R. (2001). The use of behavioral test batteries: effects of training history. *Physiol. Behav.* 73, 705–717. doi: 10.1016/S0031-9384(01)00528-5
- Meyerson, B. J., Augustsson, H., Berg, M., and Roman, E. (2006). The Concentric Square Field: a multivariate test arena for analysis of explorative strategies. *Behav. Brain Res.* 168, 100–113. doi: 10.1016/j.bbr.2005.10.020
- Meyerson, B. J., Jurek, B., Roman, E., and Rank-Order Procedure, A. (2013). Applied to an Ethoexperimental Behavior Model—The Multivariate Concentric Square Field (MCSF) Test. *J. Behav. Brain Sci.* 03, 350–361. doi: 10.4236/jbbs.2013.34035
- Momeni, S., and Roman, E. (2014). Subgroup-dependent effects of voluntary alcohol intake on behavioral profiles in outbred Wistar rats. *Behav. Brain Res.* 275, 288–296. doi: 10.1016/j.bbr.2014.08.058
- Momeni, S., Sharif, M., Agren, G., and Roman, E. (2014). Individual differences in risk-related behaviors and voluntary alcohol intake in outbred Wistar rats. *Behav. Pharmacol.* 25, 206–215. doi: 10.1097/FBP.0000000000000036
- Mustafa, A., Roman, E., and Winberg, S. (2019). Boldness in Male and Female Zebrafish (*Danio rerio*) Is Dependent on Strain and Test. *Front. Behav. Neurosci.* 13:248. doi: 10.3389/fnbeh.2019.00248
- Nakagawa, S., and Schielzeth, H. (2010). Repeatability for Gaussian and non-Gaussian data: a practical guide for biologists. *Biol. Rev. Camb. Philos. Soc.* 85, 935–956. doi: 10.1111/j.1469-185X.2010.00141.x
- Peterson, R. A., and Cavanaugh, J. E. (2019). Ordered quantile normalization: a semiparametric transformation built for the cross-validation era. *J. Appl. Stat.* 47, 2312–2327. doi: 10.1080/02664763.2019.1630372
- Rauw, W. M., Johnson, A. K., Gomez-Raya, L., Dekkers, J. C. M., and Hypothesis, A. (2017). A Hypothesis and Review of the Relationship between Selection for Improved Production Efficiency, Coping Behavior, and Domestication. *Front. Genet.* 8:134. doi: 10.3389/fgene.2017.00134
- Riegel, J., Mayer, W., and van Havre, Y. (2017). *FreeCAD*. Available online at <https://www.freecadweb.org/> (accessed on Nov 1, 2019)
- Rodgers, R. J. (1997). Animal models of 'anxiety': where next? *Behav. Pharmacol.* 8, 477–496. doi: 10.1097/00008877-199711000-00003
- Rodgers, R. J., Haller, J., Holmes, A., Halasz, J., Walton, T. J., and Brain, P. F. (1999). Corticosterone response to the plus-maze: high correlation with risk assessment in rats and mice. *Physiol. Behav.* 68, 47–53. doi: 10.1016/S0031-9384(99)00140-7
- Roman, E., Brunberg, R., Mustafa, A., Thörnqvist, P. O., and Winberg, S. (2018). "Behavioral Profiling using a Modified Version of the Zebrafish Multivariate Concentric Square FieldTM (zMCSF) Test," in *Proceedings of Measuring Behavior*, eds R. Grant, T. Allen, T. Spink, and M. Sullivan (Manchester: Manchester Metropolitan University), 27–29.

- Roman, E., and Colombo, G. (2009). Lower risk taking and exploratory behavior in alcohol-preferring sP rats than in alcohol non-preferring sNP rats in the multivariate concentric square field (TM) (MCSF) test. *Behav. Brain Res.* 205, 249–258. doi: 10.1016/j.bbr.2009.08.020
- Roman, E., Stewart, R. B., Bertholomey, M. L., Jensen, M. L., Colombo, G., Hyttia, P., et al. (2012). Behavioral profiling of multiple pairs of rats selectively bred for high and low alcohol intake using the MCSF test. *Addict. Biol.* 17, 33–46. doi: 10.1111/j.1369-1600.2011.00327.x
- Roman, E., Tjernström, N., and Winberg, S. (2016). “Description of a multivariate behavioral test arena for zebrafish – the zebrafish multivariate concentric square field test,” in *Proceedings of Measuring Behavior 2016*, eds A. J. Spink, G. Riedel, L. Zhou, L. E. A. Teekens, R. Alatal, and C. Gurrin (Dublin: Dublin City University), 4–6.
- Ruxton, G. D., and Johnsen, S. (2016). The effect of aggregation on visibility in open water. *Proc. Biol. Sci.* 283:1098. doi: 10.1098/rspb.2016.1463
- R Core Team (2020). *A Language and Environment for Statistical Computing*. Vienna: R Foundation for Statistical Computing.
- Sessa, A. K., White, R., Houvras, Y., Burke, C., Pugach, E., Baker, B., et al. (2008). The Effect of a Depth Gradient on the Mating Behavior, Oviposition Site Preference, and Embryo Production in the Zebrafish, *Danio rerio*. *Zebrafish* 5, 335–339. doi: 10.1089/zeb.2008.0535
- Sokal, R. R., and Rohlf, F. J. (1995). *Biometry: The Principles and Practice of Statistics in Biological Research*. New York, NY: W.H. Freeman and Company.
- Stewart, A., Cachat, J., Wong, K., Gaikwad, S., Gilder, T., DiLeo, J., et al. (2010). Homebase behavior of zebrafish in novelty-based paradigms. *Behav. Proc.* 85, 198–203. doi: 10.1016/j.beproc.2010.07.009
- Stewart, A. M., Braubach, O., Spitsbergen, J., Gerlai, R., and Kalueff, A. V. (2014). Zebrafish models for translational neuroscience research: from tank to bedside. *Trends Neurosci.* 37, 264–278. doi: 10.1016/j.tins.2014.02.011
- Stewart, A. M., Gaikwad, S., Kyzar, E., and Kalueff, A. V. (2012). Understanding spatio-temporal strategies of adult zebrafish exploration in the open field test. *Brain Res.* 1451, 44–52. doi: 10.1016/j.brainres.2012.02.064
- Sundin, J., Morgan, R., Finnoen, M. H., Dey, A., Sarkar, K., and Jutfelt, F. (2019). On the Observation of Wild Zebrafish (*Danio rerio*) in India. *Zebrafish* 16, 546–553. doi: 10.1089/zeb.2019.1778
- Thomson, H. R., Lamb, S. D., Besson, A. A., Johnson, S. L., and Wright, J. (2020). Long-term repeatability of behaviours in zebrafish (*Danio rerio*). *Ethology* 126, 803–811.
- Toms, C. N., and Echevarria, D. J. (2014). Back to basics: searching for a comprehensive framework for exploring individual differences in zebrafish (*Danio rerio*) behavior. *Zebrafish* 11, 325–340. doi: 10.1089/zeb.2013.0952
- Van Reenen, C. G., O’Connell, N. E., Van der Werf, J. T., Korte, S. M., Hopster, H., Jones, R. B., et al. (2005). Responses of calves to acute stress: individual consistency and relations between behavioral and physiological measures. *Physiol. Behav.* 85, 557–570. doi: 10.1016/j.physbeh.2005.06.015
- Varga, Z. K., Zsigmond, A., Pejtsik, D., Varga, M., Demeter, K., Mikics, E., et al. (2018). The swimming plus-maze test: a novel high-throughput model for assessment of anxiety-related behaviour in larval and juvenile zebrafish (*Danio rerio*). *Sci. Rep.* 8:16590. doi: 10.1038/s41598-018-34989-1
- Vossen, L. E., Cervený, D., Osterkrans, M., Thornqvist, P. O., Jutfelt, F., Fick, J., et al. (2020). Chronic Exposure to Oxazepam Pollution Produces Tolerance to Anxiolytic Effects in Zebrafish (*Danio rerio*). *Environ. Sci. Technol.* 54, 1760–1769. doi: 10.1021/acs.est.9b06052
- Vossen, L. E., Cervený, D., Sen Sarma, O., Thornqvist, P. O., Jutfelt, F., Fick, J., et al. (2020b). Low concentrations of the benzodiazepine drug oxazepam induce anxiolytic effects in wild-caught but not in laboratory zebrafish. *Sci. Total Environ.* 703:134701. doi: 10.1016/j.scitotenv.2019.134701
- Vossen, L. E., Jutfelt, F., Cocco, A., Thornqvist, P. O., and Winberg, S. (2016). Zebrafish (*Danio rerio*) behaviour is largely unaffected by elevated pCO₂. *Conserv. Physiol.* 4:cow065. doi: 10.1093/conphys/cow065
- Walsh, R. N., and Cummins, R. A. (1976). The Open-Field Test: a Critical Review. *Psychol. Bull.* 83, 482–504.
- Wickham, H. (2016). *ggplot2: Elegant Graphics for Data Analysis*. New York, NY: Springer-Verlag.
- Winkler, H., and Leisler, B. (1999). “Exploration and curiosity in birds: Functions and mechanisms,” in *International Ornithological Congress, Durban*, eds N. J. Adams and R. J. Slotow (Johannesburg: BirdLife South Africa), 915–932.
- Wright, K. (2019). *pals: Color Palettes, Colormaps, and Tools to Evaluate Them*. Available online at <https://kwstat.github.io/pals> (accessed on Feb 2, 2022).

Conflict of Interest: The authors declare that the research was conducted in the absence of any commercial or financial relationships that could be construed as a potential conflict of interest.

Publisher’s Note: All claims expressed in this article are solely those of the authors and do not necessarily represent those of their affiliated organizations, or those of the publisher, the editors and the reviewers. Any product that may be evaluated in this article, or claim that may be made by its manufacturer, is not guaranteed or endorsed by the publisher.

Copyright © 2022 Vossen, Brunberg, Rådén, Winberg and Roman. This is an open-access article distributed under the terms of the Creative Commons Attribution License (CC BY). The use, distribution or reproduction in other forums is permitted, provided the original author(s) and the copyright owner(s) are credited and that the original publication in this journal is cited, in accordance with accepted academic practice. No use, distribution or reproduction is permitted which does not comply with these terms.



Zebrafish as a Vertebrate Model for Studying Nodavirus Infections

Raquel Lama, Patricia Pereiro, Antonio Figueras and Beatriz Novoa*

Instituto de Investigaciones Marinas (IIM), Consejo Superior de Investigaciones Científicas (CSIC), Vigo, Spain

OPEN ACCESS

Edited by:

Ming Xian Chang,
Institute of Hydrobiology (CAS), China

Reviewed by:

Evdokia Karagouni,
Pasteur Hellenic Institute, Greece
Jiang-Feng Lan,
Shandong Agricultural University,
China

Kuntong Jia,
Sun Yat-sen University, China

*Correspondence:

Beatriz Novoa
beatriznovoa@iim.csic.es

Specialty section:

This article was submitted to
Comparative Immunology,
a section of the journal
Frontiers in Immunology

Received: 26 January 2022

Accepted: 02 March 2022

Published: 24 March 2022

Citation:

Lama R, Pereiro P, Figueras A
and Novoa B (2022) Zebrafish
as a Vertebrate Model for
Studying Nodavirus Infections.
Front. Immunol. 13:863096.
doi: 10.3389/fimmu.2022.863096

Nervous necrosis virus (NNV) is a neurotropic pathogenic virus affecting a multitude of marine and freshwater fish species that has a high economic impact on aquaculture farms worldwide. Therefore, the development of new tools and strategies aimed at reducing the mortality caused by this virus is a pivotal need. Although zebrafish is not considered a natural host for NNV, the numerous experimental advantages of this species make zebrafish an attractive model for studying different aspects of the disease caused by NNV, viral encephalopathy and retinopathy (VER). In this work, we established the best way and age to infect zebrafish larvae with NNV, obtaining significant mortalities in 3-day-postfertilization larvae when the virus was inoculated directly into the brain or by intramuscular microinjection. As occurs in naturally susceptible fish species, we confirmed that after intramuscular injection the virus was able to migrate to the central nervous system (CNS). As expected, due to the severe damage that this virus causes to the CNS, alterations in the swimming behavior of the zebrafish larvae were also observed. Taking advantage of the existence of transgenic fluorescent zebrafish lines, we were able to track the migration of different innate immune cells, mainly neutrophils, to the site of infection with NNV via the brain. However, we did not observe colocalization between the viral particles and neutrophils. RNA-Seq analysis of NNV-infected and uninfected larvae at 1, 3 and 5 days postinfection (dpi) revealed a powerful modulation of the antiviral immune response, especially at 5 dpi. We found that this response was dominated by, though not restricted to, the type I interferon system, the major defence mechanism in the innate immune response against viral pathogens. Therefore, as zebrafish larvae are able to develop the main characteristic of NNV infection and respond with an efficient immune arsenal, we confirmed the suitability of zebrafish larvae for modelling VER disease and studying different aspects of NNV pathogenesis, immune response and screening of antiviral drugs.

Keywords: nodavirus, viral encephalopathy and retinopathy (VER), zebrafish, immune response, RNA-Seq

1 INTRODUCTION

Zebrafish (*Danio rerio*) are a very versatile animal model widely used in the study of a multitude of processes and disciplines. Among them, zebrafish are an excellent tool for understanding host-pathogen interactions during the course of infectious diseases (1, 2). Zebrafish possess innate and adaptive immunity resembling that of mammals and other higher vertebrates. However, in the early

stages, the larvae rely exclusively on their innate immune system, as the cells responsible for the adaptive responses are not functionally mature until 4 or 6 weeks postfertilization (3). This fact makes zebrafish larvae a very attractive model for studying the first line of defence against a pathogen, such as the action of primary immune cells, macrophages (4) and neutrophils (5) and the role of the main cytokines involved in the immune response, without interference from the adaptive response. In addition, other advantages of using early stages of zebrafish larvae are the large numbers of offspring, a short generation time, tolerance to anaesthesia, a small body size, and transparency, which allows easy visualization of the whole body by live imaging (6–8). At the genetic level, the zebrafish genome sequence has been extensively revised and refined, enabling the rapid accumulation of loss- or gain-of-function mutants and the generation of transgenic lines that allow traceability of different cell types.

Although no viruses, with some exceptions, are typically known to naturally infect zebrafish and cause massive mortality episodes (9, 10), several viruses (including those infecting humans) have been studied using zebrafish as a model of infection. In the case of fish, the main diseases caused by viruses have been reproduced in zebrafish: rhabdoviruses such as spring viremia of carp virus (SVCV) (11–15), snakehead rhabdovirus (SHRV) (16), viral haemorrhagic septicemia virus (VHSV) (17), and infectious haematopoietic necrosis virus (IHNV) (7); birnaviruses such as infectious pancreatic necrosis virus (IPNV) (18, 19); iridoviruses such as infectious spleen and kidney necrosis virus (ISKNV) (20, 21) or European sheatfish virus (ESV) (22); and nodaviruses such as nervous necrosis virus (NNV) (23, 24). Interestingly, two publications reported that zebrafish can be naturally infected by different nodaviruses (25, 26); this can probably occur as a consequence of increases in temperature and crowding (27). In both cases, extensive vacuolations were seen in the brain and retina (25, 26), and erratic swimming behavior and mortality episodes were reported by Binesh (25).

Viral encephalopathy and retinopathy (VER) disease, caused by NNV, is one of the most devastating diseases affecting commercial fish species around the world, such as European sea bass (*Dicentrarchus labrax*), Atlantic cod (*Gadus morhua*) or grouper (*Epinephelus* spp.), among others. This icosahedral naked positive-sense single-stranded RNA virus has a neurotropic nature and replicates in the nervous system (e.g., brain, retina and spinal cord) (28), causing a very characteristic abnormal and erratic swimming behavior in susceptible fish species, accompanied by other less specific signs (exophthalmia, swim bladder hyperinflation, skin darkening, anorexia or lethargy) (29). Despite the relevance of this disease and the high economic impact caused by NNV and although many studies have been conducted in commercial species to analyse different aspects of NNV infection (30–39), few studies have leveraged the benefits of zebrafish to investigate NNV infection. Furusawa et al. (40) tried to establish experimental infections in adult zebrafish but without success. Later, Lu et al. (23) were able to reproduce NNV infection in both

adult zebrafish and larvae, and relevant mortalities were observed in larvae microinjected with the virus, which was subsequently confirmed by Morick et al. (24) after bath exposure. The susceptibility of zebrafish larvae to NNV creates an opportunity to easily screen anti-NNV compounds in an *in vivo* model, as was performed with the antiviral drug ribavirin (41). Although the immune response to NNV in this fish species seems to indicate the relevance of the type I interferon (IFN) system (23, 42–44), a complete transcriptome response to NNV has not been previously determined in zebrafish.

In this work, we sought to improve the knowledge of VER disease through the use of zebrafish larvae as an NNV infection model, leveraging different imaging methods and transgenic fish lines, and by analysing their transcriptome response after challenge with the virus. We confirmed that zebrafish larvae are susceptible to NNV when they are challenged at 3 days postfertilization (dpf), especially when infections are conducted *via* the brain or intramuscularly. Indeed, NNV particles were detected by immunofluorescence in the heads of larvae infected by intramuscular injection, confirming the migration of the virus to nervous tissues. Moreover, as occurs in commercial fish species susceptible to the virus, the infection altered the swimming behavior of the larvae, reflecting their suitability as a good model for studying different aspects of the infection. An efficient immune response against NNV is mounted in the larvae, with a significant migration of neutrophils to the brain, although these cells were not found to colocalize with the virus. At the transcriptome level, a time-increasing immune response is mounted against the virus, which is mainly characterized by a large overexpression of those genes belonging to the type I IFN system but also with a vast representation of other immune processes.

2 MATERIALS AND METHODS

2.1 Fish

The embryos and larvae used in this study were obtained from our experimental facilities, where the animals were cultured using established protocols (45, 46). Different fish lines were used: wild-type (WT) zebrafish, AB wild-type line (AB), Tübingen wild-type line (TU), and the transgenic lines Tg(*mpx:GFP*), Tg(*mpeg:mCherry*) and Tg(*lyz:DsRed2*), with neutrophils, macrophages and lysozyme-expressing cells, respectively. The eggs were obtained according to protocols described in The Zebrafish Book (45) and maintained at 28°C in E3 egg water (5 mM NaCl, 0.17 mM KCl, 0.33 mM CaCl₂, 0.33 mM MgSO₄, and 0.00005% methylene blue). All experimental procedures were reviewed and approved by the CSIC National Committee of Bioethics under approval number ES3605702020012020/13/FUN.01/INM06/BNG.

2.2 Virus

The nodavirus red-spotted grouper nervous necrosis virus (RGNNV) (strain 475-9/99) was kindly provided by the Institute Zooprofilattico delle Venezie (Italy) after isolation from diseased sea bass (47). The virus was propagated in the

snakehead-fish cell line SSN-1 (ECACC 96082808) cultured in L-15 medium (Gibco) supplemented with 2 mM L-glutamine (Gibco), 2% FBS (Gibco), and 1% penicillin/streptomycin solution (Invitrogen) and incubated at 25°C. The viral stock was titrated into 96-well plates using the Reed-Müench method (48), and aliquots were stored at -80°C until use.

2.3 Mortality Assays in Zebrafish Larvae Infected With NNV

To determine the most efficient route and age of infection with NNV, WT zebrafish larvae were infected at 3 and 14 dpf through 4 different routes: a) *via* the brain by microinjecting the virus directly into the area of the head between the eyes to reach the brain, b) *via* the duct of Cuvier (DC) to produce a systemic infection, c) by intramuscular (IM) injection by microinjecting into the muscle in the middle of the back, and d) by bath by immersing the larvae in a viral suspension (Figure 1A).

Larvae were anaesthetized in zebrafish water containing 160 µg/mL MS-222 (Sigma-Aldrich), placed on an agarose plate and individually microinjected with a glass microneedle using a Narishige MN-151 micromanipulator and a FemtoJet 4x microinjector (Eppendorf). NNV was diluted at an appropriate concentration (10^6 TCDI₅₀/mL) in L15 medium with 0.1% phenol red (a coloured marker to easily visualize the correct injection of the solution into the larvae) just before microinjection of 2 nL of viral suspension to the larvae or 2 nL of L15+0.1% phenol red to the control larvae. Larvae were infected through microinjection into the brain or DC or intramuscularly and by immersion in water containing 10^6 TCDI₅₀/mL NNV. Then, larvae were maintained in Petri dishes at 28°C on a 12 h light-dark cycle. Mortality was recorded daily during the next 10 days in the three biological replicates (10 larvae/replicate) obtained for each condition. The experiments were repeated three times. Additionally, to confirm

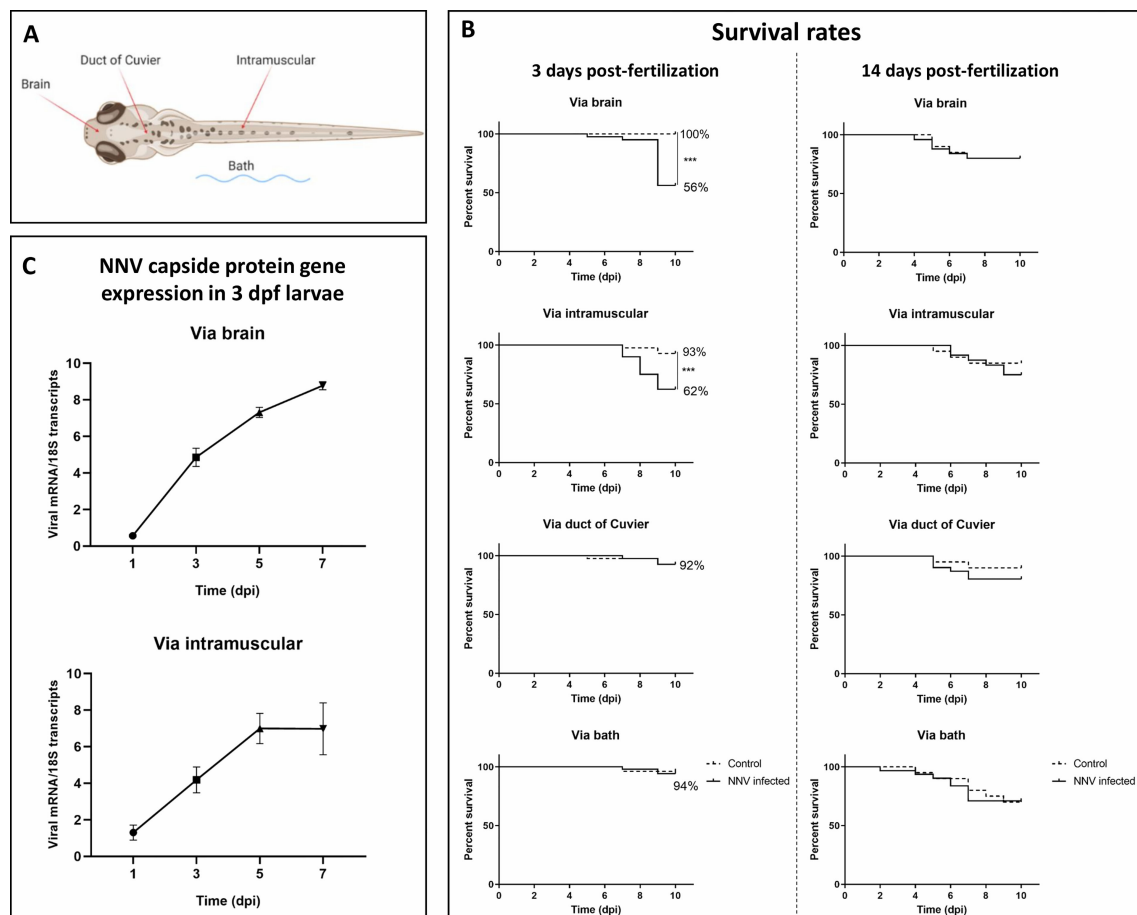


FIGURE 1 | Survival rates of zebrafish larvae challenged with NNV through different infection routes and NNV replication. **(A)** Schematic representation of the different infection routes used to determine the susceptibility of zebrafish larvae to NNV. **(B)** Kaplan-Meier survival curves of NNV-infected and uninfected larvae in 3- and 14-dpf larvae. Mortality was registered during the next 10 dpi. **(C)** Quantification of NNV capsid protein gene expression in 3-dpf larvae infected *via* the brain or intramuscularly at different sampling points through qPCR; data are presented as the mean ± SEM of biological replicates. Statistically significant differences are displayed as follows: ***, 0.0001 > p value > 0.001.

the mortality caused by the microinjection of the virus *via* the brain, AB and TU larvae (3 dpf) were also infected.

2.4 Evaluation of NNV Replication and Gene Expression of Immune Cell Markers in Zebrafish Larvae by Quantitative PCR (qPCR)

To evaluate the progress of NNV infection, larvae (3 dpf) were infected *via* the brain or intramuscularly, and samples were collected at 1, 3, 5 and 7 days postinfection (dpi). Whole larvae were harvested under RNase-free conditions in pools of 4 larvae each (3 biological replicates/4 larvae per replicate). Total RNA was isolated using the Maxwell[®] RSC simplyRNA Tissue kit (Promega) in accordance with the manufacturer's instructions. cDNA synthesis was performed with the NZY First-Strand cDNA Synthesis Kit (NZYtech) using 0.2 µg of total RNA. The qPCRs were performed using specific primers designed with Primer 3 software (49), and their efficiencies were previously tested according to the protocol described by Pfaffl (50). Individual qPCRs were conducted in 25-µl reaction volumes using 12.5 µL of SYBR GREEN PCR Master Mix (Applied Biosystems), 10.5 µL of ultrapure water (Sigma-Aldrich), 0.5 µL of each specific primer (10 µM) and 1 µL of cDNA template. All reactions were performed using technical triplicates in a 7300 Real-Time PCR System thermocycler (Applied Biosystems) with an initial denaturation step (95°C, 10 min), followed by 40 cycles of a denaturation step (95°C, 15 s) and one hybridization-elongation step (60°C, 1 min). Viral replication was detected by the relative gene expression of the NNV capsid protein gene (RNA2) (51). For larvae microinjected in the brain, the gene expression of the neutrophil marker *myeloperoxidase* (*mpx*) and the macrophage marker *macrophage receptor with a collagenous domain* (*marco*) was also evaluated; *mpx* and *marco* primers were previously confirmed to specifically amplify the myeloid zebrafish population (52). The relative expression levels of the different genes were normalized using the Pfaffl method (50) and *18S ribosomal RNA* (*18S*) as a reference gene. The primers used are listed in **Supplementary Table S1**.

2.5 Fluorescence Microscopy Images

Whole-mount immunofluorescence assays in zebrafish larvae were performed as follows. WT larvae (3 dpf) were infected *via* IM injection for 2, 6, 24 and 48 h. Then, larvae were fixed overnight (O/N) at 4°C in 4% paraformaldehyde (PFA) diluted in phosphate-buffered saline containing 0.1% Tween-20 (PBST). Larvae were washed twice in PBST, dehydrated in a graded series of methanol/PBST solutions (25% for 5 min, 50% for 10 min and 75% for 5 min), and stored in 100% methanol O/N at -20°C. For immunofluorescence processing, larvae were rehydrated in a graded series of methanol/PBST solutions (75% for 5 min, 50% for 10 min and 25% for 5 min) and washed 4 times for 5 min with PBST. Larvae were bleached by incubating them in bleaching solution (0.8 mL of KOH 10%, 0.3 mL of H₂O₂ 30%, 0.1 mL of Tween-80 and 8.8 mL of distilled water) for 5 min, and then they were washed twice for 5 min in PBST. Permeabilization was achieved by incubation with proteinase K at 10 µg/mL. After 2 h

at 37°C, larvae were washed twice in PBST and incubated in 2% Tween-20 in PBS for 24 h at room temperature (RT). Larvae were washed and blocked in 1% Tween-20/PBS and 10% lamb serum O/N at RT. Anti-sea bass encephalitis virus (anti-DIEV, 1:4,000) (53) was diluted in antibody solution (0.2% Tween-20/PBS and 10% lamb serum) and incubated with the larvae for 3 days at 4°C. Larvae were washed O/N and then incubated for 2 days with Alexa Fluor 546 goat anti-rabbit secondary antibody (Invitrogen) diluted in antibody solution (1:500). After this, larvae were washed O/N in PBST and stained with DAPI for 1 h at RT. After 3 washes with PBS, larvae were stored at 4°C until microscopy examination. Confocal images of fixed larvae were taken using a TSC SPE confocal microscope (Leica). The images were processed using the LAS-AF (Leica Application Suite Advanced Fluorescence) program. The same procedure was conducted for Tg(*mpx*:GFP) larvae (3 dpf) infected *via* the brain with NNV for 24 h. For the WT larvae, samples were also taken at the four sampling points for RNA isolation and qPCR analysis of NNV replication (5 samples of 5 larvae/sample).

Tg(*mpx*:GFP), Tg(*mpeg*:mCherry) and Tg(*lyz*:DsRed2) transgenic larvae (3 dpf) were infected by 4 different routes as explained in Section 2.3, and after 1, 2 and 3 dpi, images of whole larvae were taken using a Nikon AZ100 fluorescence microscope. Larvae were anaesthetized with a 0.01% MS-222 solution. The different immune cells labelled in the transgenic lines were counted using a macro of ImageJ (54) to calculate the percentage of cells that migrated to the brain during infection.

2.6 Video Recording of the Swimming Behavior

To analyse the swimming behavior of the fish larvae, two Petri dishes of 10 larvae each, inoculated by the same route (via brain or IM), one containing infected larvae and the other uninfected control larvae, were placed in the same plane of a video recording for 2 consecutive minutes. Recordings of 3- and 14-dpf larvae were made at 3, 6 and 10 dpi with a Leica camera of 48 Mpx, and the images were processed with Photoshop and ImageJ (54) using the Chemotaxis and Migration Tool plugin. The data obtained allowed us to reconstruct the larval movements to calculate the velocity, the accumulated and Euclidean distances and the directionality, parameters that were used to compare the swimming behavior between infected and uninfected control larvae.

2.7 High-Throughput Transcriptome Sequencing

To analyse the transcriptome response to NNV in zebrafish larvae infected *via* the brain, the samples collected in Section 2.4 and corresponding to sampling points 1, 3 and 5 dpi were used for high-throughput transcriptome sequencing. The RNA concentration and purity were measured with a Nanodrop ND-1000 spectrophotometer (Nanodrop Technologies Inc., USA), and RNA integrity was analysed in an Agilent 2100 Bioanalyzer (Agilent Technologies Inc., USA) according to the manufacturer's instructions. All samples showed an RNA integrity number (RIN) over 8.0 and were used for Illumina

library preparation. Double-stranded cDNA libraries were constructed using the TruSeq Stranded mRNA Kit Sample Prep Kit (Illumina, USA), and sequencing was performed using Illumina NovaSeq 6000 technology at Macrogen Inc., Korea (Republic of Korea). The raw read sequences were deposited in the Sequence Read Archive (SRA) (<http://www.ncbi.nlm.nih.gov/sra>) under the BioProject accession number PRJNA799765.

2.8 Raw Data Cleaning, Mapping, RNA-Seq and Differential Expression Analysis

CLC Genomics Workbench v. 20.0.4 (CLC Bio, Denmark) was used to filter and trim reads, map the high-quality reads against the last version of the zebrafish genome (GRCz11) and perform the differential expression analyses. Raw reads were trimmed to remove the adaptor sequences and low-quality reads. RNA-Seq analyses were conducted with the following parameters: length fraction = 0.8, similarity fraction = 0.8, mismatch cost = 2, insertion cost = 3 and deletion cost = 3. The expression values were set as transcripts per million (TPM). Finally, a differential expression analysis test was used to compare gene expression levels and to identify differentially expressed genes (DEGs). Transcripts with fold change (FC) values $> |2|$ and false discovery rate (FDR) values < 0.05 were retained for further analyses. To identify and quantify the directions of variability in the data, a principal component analysis (PCA) plot was constructed using the original expression values. Using the TPM values of the selected DEGs, heatmaps for each sampling point were constructed using the complete linkage method with Euclidean distance. Both PCA and heatmaps were constructed using the web tool Clustvis (55) (<https://biit.cs.ut.ee/clustvis/>), and a Venn diagram was constructed with the InteractiVenn web tool (56) (<http://www.interactivenn.net/>).

2.9 Gene Ontology (GO) Enrichment and Kyoto Encyclopedia of Genes and Genomes (KEGG) Pathway Analysis

For the DEGs between NNV-infected and noninfected zebrafish larvae, we conducted a GO enrichment analysis of biological processes and a KEGG pathway analysis using the functional annotation tool DAVID v. 6.8 (57, 58) (<https://david.ncifcrf.gov/summary.jsp>). For the GO and KEGG analyses, a p value < 0.05 was employed.

2.10 qPCR Validation of RNA-Seq Data

The RNA-Seq results were validated by qPCR analysis of five immune genes significantly modulated by NNV infection (*ifnphi1*, *il1b*, *mxe*, *tnfa* and *marco*), as mentioned above for NNV detection (Section 2.4). The primers used are listed in **Supplementary Table S1**. The correlation between the fold changes obtained by RNA-Seq and qPCR was calculated using Pearson's correlation coefficient.

2.11 Statistical Analysis

Kaplan–Meier survival curves were analysed with a log-rank (Mantel–Cox) test. For the remaining experiments, the results

were represented graphically as the mean \pm standard error of the mean (SEM), and significant differences were obtained using Student's t test and displayed as **** (< 0.0001), *** ($0.0001 < p < 0.001$), ** ($0.001 < p < 0.01$) or * ($0.01 < p < 0.05$).

3 RESULTS

3.1 Assessment of Susceptibility to NNV in Zebrafish Larvae Through Different Infection Routes and Larval Developmental Stages

Our results showed that the most effective route of infection with NNV in 3-dpf larvae was *via* the brain, with the survival of the larvae being 56%, whereas their corresponding uninfected controls showed a survival of 100% (**Figure 1B**). Infection *via* IM microinjection also showed significant differences between NN-infected and uninfected larvae, with a survival of 62% for the infected larvae and 93% for the control larvae (**Figure 1B**). Infections *via* DC or by bath did not show significantly different survival rates compared with their corresponding uninfected controls (**Figure 1B**). The lower survival of the 3-dpf WT larvae infected with NNV *via* the brain was also confirmed in the AB and TU zebrafish strains (**Supplementary Figure S1**). However, when the larvae were inoculated under the same conditions but at 14 dpf, the survival rates of the infected larvae were not significantly different from those of the uninfected controls (**Figure 1B**).

As significant mortalities after NNV challenge were observed in 3-dpf larvae infected *via* the brain and intramuscularly, we wanted to assess the replication of the virus in these larvae over time. In larvae inoculated both directly into the brain and through IM microinjection, time-increasing detection of the capsid protein gene was observed; however, in the case of IM microinjection, viral replication seemed to be stable between 5 and 7 dpi (**Figure 1C**).

3.2 Kinetic Analysis of Swimming Behavior by a Video Tracking System

Because alterations in swimming behavior are commonly observed in fish naturally susceptible to NNV, we wanted to investigate this fact in 3- and 14-dpf zebrafish larvae infected with NNV *via* the brain or intramuscularly. For this, a video tracking analysis was used to determine if the infection produced changes in their behavioral pattern by analysing certain measurable parameters of the larvae, such as velocity (mm/sec), accumulated distance (mm) of larval path, Euclidean distance (mm) (length of the straight line between the starting point and endpoint of the larvae), and directionality (calculated by comparing the Euclidean distance to the accumulated distance, which represents a measurement of the directness of larval trajectories). Data are represented as the fold change (FC) of infected larvae compared with their uninfected controls (FC = 1, dotted lines).

As shown in **Figure 2A**, in 3-dpf larvae infected *via* the brain, the velocity, directionality and Euclidean distance were found to

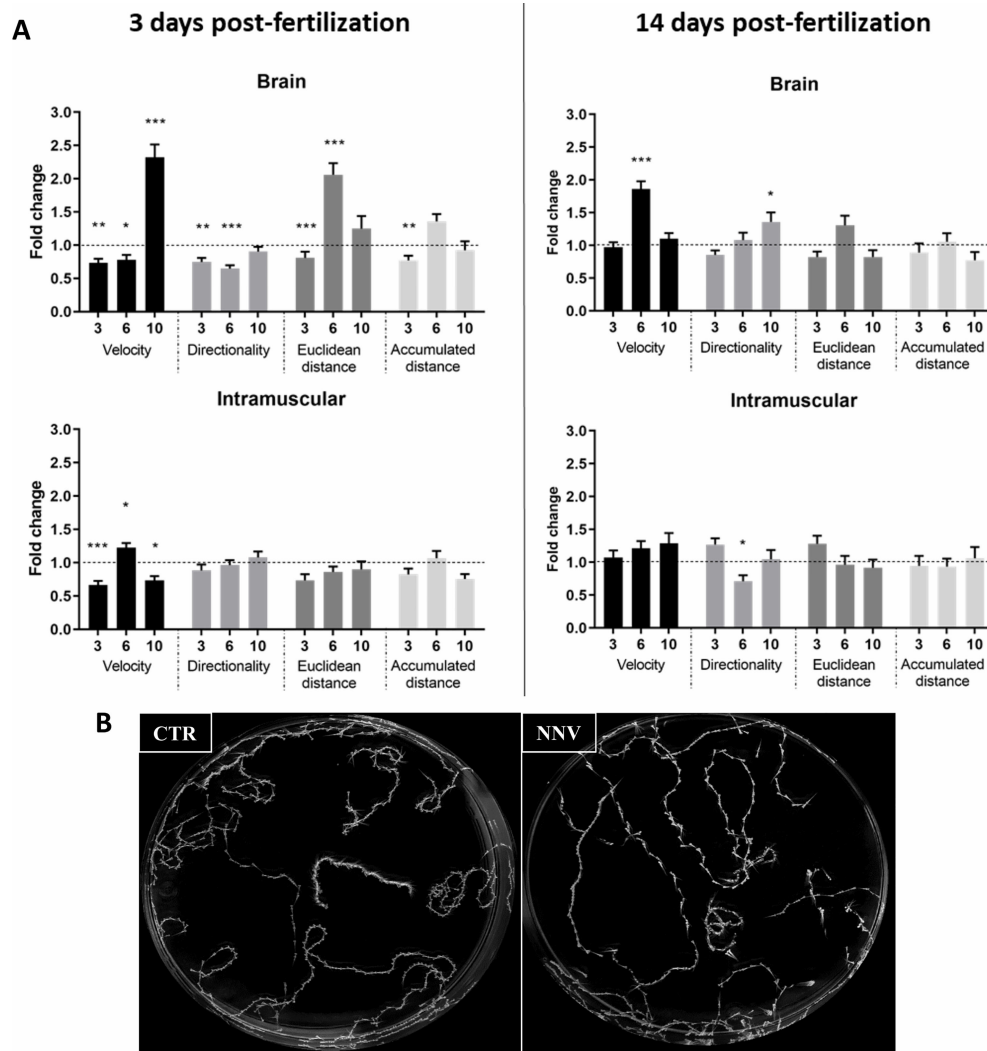


FIGURE 2 | Image analysis of the swimming behavior of zebrafish larvae (3 and 14 dpf) infected with NNV *via* brain or IM. **(A)** Comparison of velocity, directionality, accumulated distance and Euclidean distance parameters between NNV-infected and the corresponding uninfected control larvae. Video tracking of zebrafish larvae was conducted at different times postinfection (3, 6, and 10 dpi). The fold change (FC) of infected larvae compared with their uninfected control (Control FC = 1, dotted lines) was calculated. The graphs represent the mean \pm SEM of the biological replicates. Statistically significant differences are displayed as follows: ***, $0.0001 > p \text{ value} > 0.001$; **, $0.001 > p \text{ value} > 0.01$; *, $0.01 > p \text{ value} > 0.05$. **(B)** Example of maximal projection of the video recorded for 3-dpf larvae infected *via* brain and the corresponding controls at 6 dpi.

be significantly different between infected and uninfected larvae at least at one of the analysed times. On the other hand, IM microinjection in 3-dpf larvae produced only significant alterations in velocity. As expected, due to the absence of significantly different mortalities at 14 dpf between infected and uninfected larvae, alterations in these parameters were lower at this age, with only certain significant effects on velocity and directionality in those larvae inoculated *via* the brain and directionality in the larvae inoculated intramuscularly (**Figure 2A**). **Figure 2B** presents an example of the maximum projections used for the analysis of the videos.

3.3 Distribution of NNV Virions in Zebrafish Larvae

One of the powerful advantages provided by the use of zebrafish larvae as a working model is the possibility of performing whole-mount immunofluorescence staining, as it allows antigen-antibody interactions to be located without preparing sections of the larvae. Thus, using the anti-DIEV antibody, we were able to locate NNV inside the larvae and confirm that the virus can migrate to the cephalic region after IM infection (**Figure 3**). The virus was not detected until 24 h postinfection (data at 2 and 6 hours postinfection (hpi) not shown), but NNV particles were

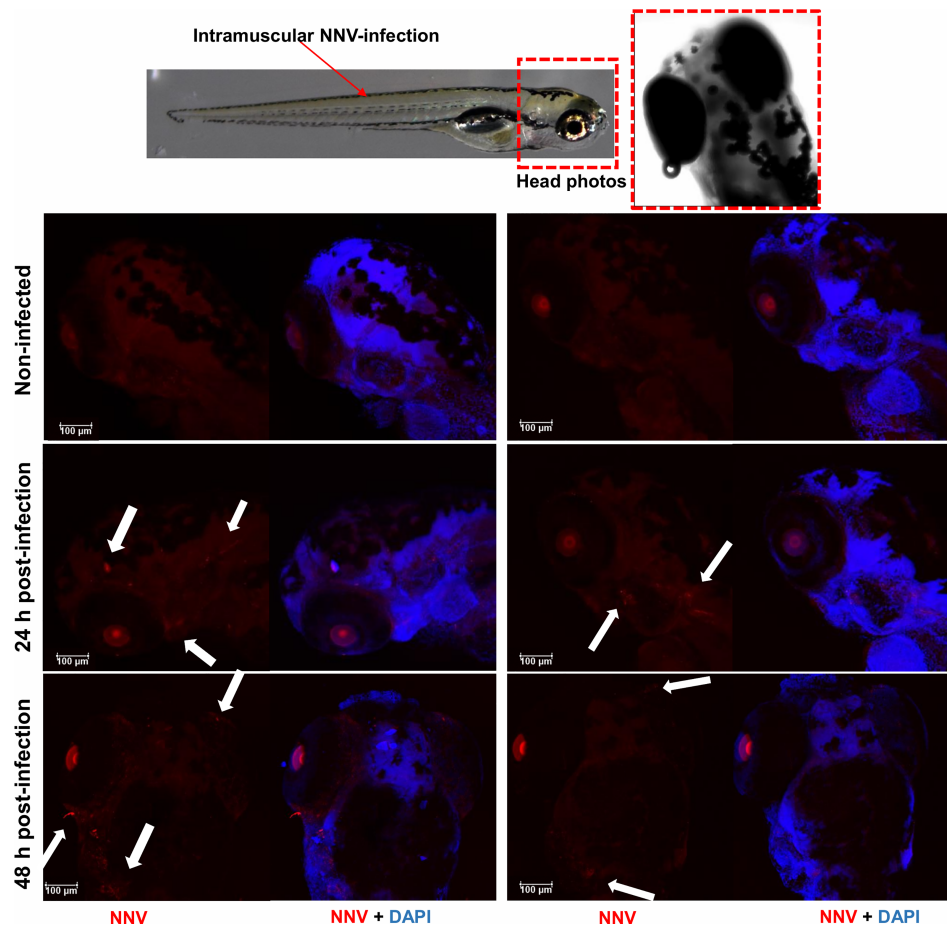


FIGURE 3 | Whole-mount immunofluorescence of zebrafish larvae infected by intramuscular microinjection with NNV. Confocal images of the head from uninfected and NNV-infected larvae at 24 and 48 hpi. NNV particles are stained red, and cell nuclei are stained blue (DAPI). White arrows denote the position of NNV-infected cells.

already observed after 24 h in different locations of the head, and at 48 hpi the virus was also detected in the eye area (**Figure 3**). According to this, the virus was practically undetectable by qPCR at 2 and 6 hpi, whereas a time-increasing detection was observed at 24 and 48 hpi (**Supplementary Figure S2**).

3.4 Effects of NNV Challenge on Innate Immune Cells

The existence of transgenic lines in zebrafish provides an easy-to-use working tool that gives us very useful information. To study the immune response of zebrafish to NNV infection, different transgenic lines were used. The transgenic line Tg(*lyz*:DsRed2) was used to detect cells expressing the *lysozyme c* gene (*lyz*) corresponding to myeloid precursors with lysozyme activity. The transgenic line Tg(*mpx*:GFP) was used to detect cells expressing the *myeloperoxidase* gene (*mpx*), a specific marker of differentiated neutrophils. On the other hand, the transgenic line Tg(*mpeg*:mCherry) was used to detect cells expressing *macrophage-expressed gene* (*mpeg*) (macrophages). The larvae were infected by 4 different infection routes, and these cell types

were counted at 1, 2 and 3 dpi in the cephalic region. The number of cells that migrated to the head after infection was determined.

The data represent the differences in the number of cells in infected larvae compared with the uninfected control larvae (control FC = 1 in the dotted line). *Lyz*⁺ cells showed significantly higher migration to the head at 48 and 72 hpi when the infection was carried out *via* the brain, whereas no differences were observed for the other infection routes (**Figure 4A**). A similar tendency was observed for neutrophils (*Mpx*⁺), which showed significant migration to the head at 24 and 48 hpi in larvae infected *via* the brain, and no effects were observed for the other infections (**Figure 4B**). Although a significant migration of neutrophils to the brain was observed in the larvae inoculated *via* the brain, confocal microscopy analysis showed that these cells did not colocalize with the virus (**Figure 4D**). Finally, no macrophage (*Mpeg*⁺) migration to the brain was observed by any route of infection (**Figure 4C**). Interestingly, the expression of the macrophage marker gene *marco* significantly increased after NNV infection in a time-

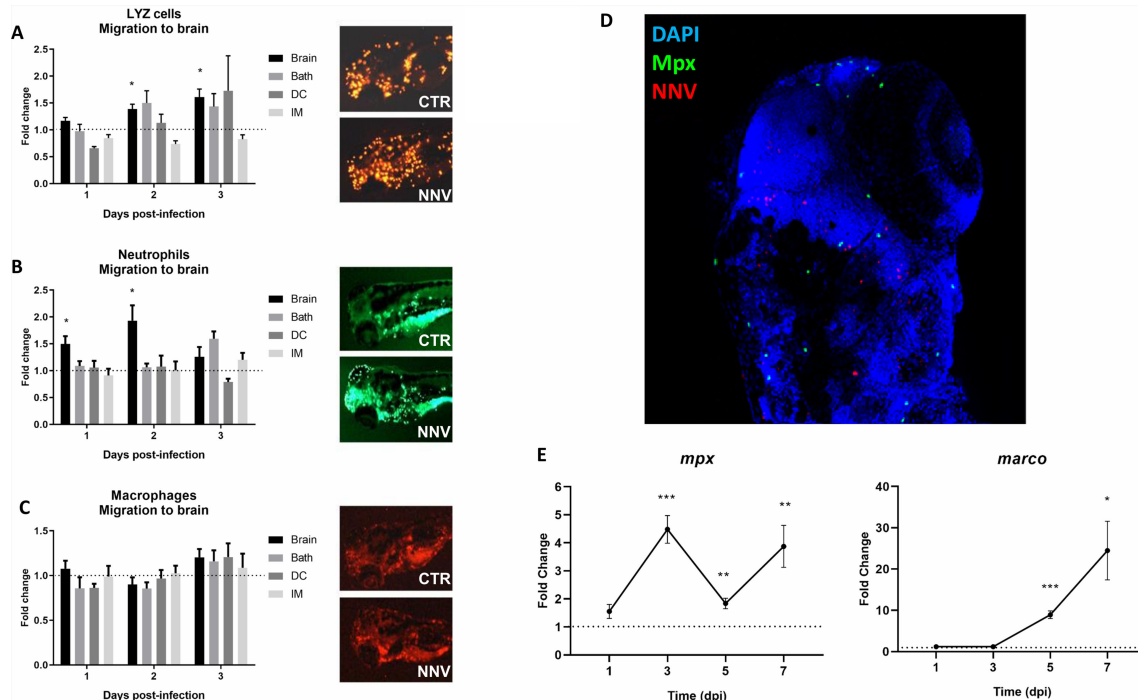


FIGURE 4 | Visualization and analysis of innate immune cell migration to the head of 3 dpf larvae infected through different routes. The transgenic zebrafish lines (A) Tg(*lyz*:DsRed2), (B) Tg(*mpx*:GFP) and (C) Tg(*mpeg*:mCherry) were used to analyse the migration of myeloid precursors with lysozyme activity, neutrophils and macrophages, respectively, to the cephalic region. Larvae were infected through the 4 infection routes analysed in this study, and the cells were counted at 1, 2 and 3 dpi. Fluorescent immune cells were counted using ImageJ, and the graphs represent the difference in fold change of the number of cells located in the head from infected larvae compared to their corresponding uninfected control larvae (control FC = 1 in the dotted line). Representative images of the three transgenic lines at 2 dpi were included. (D) Whole-mount immunofluorescence of Tg(*mpx*:GFP) transgenic larvae infected via the brain with NNV at 1 dpi; neutrophils are displayed in green, NNV are displayed in red, and nuclei are displayed in blue. No colocalization between NNV particles and neutrophils was observed. (E) Expression analysis of marker genes of the two major innate immune cells (*mpx* – neutrophils, *marco* – macrophages) in NNV-infected and uninfected larvae at different times postinfection. Each sample (5 biological replicates, pools of 4 larvae each) was normalized to the *18S* gene. The normalized expression values were standardized against their respective controls (Control FC = 1, dotted lines). For (A–C, E), the graphs represent the mean \pm SEM of the biological replicates. Statistically significant differences are displayed as follows: ***, 0.0001 > p value > 0.001; **, 0.001 > p value > 0.01; *, 0.01 > p value > 0.05.

dependent manner, with more marked increases than those observed for the neutrophil marker gene *mpx* (Figure 4E).

3.5 High-Throughput Sequencing, Mapping Information and PCA Distribution

To better elucidate the immune response generated in the larvae after challenge with NNV, high-throughput transcriptome sequencing and RNA-Seq analyses were conducted. Samples of 3-dpf larvae infected *via* the brain with NNV or the corresponding control larvae were collected at 1, 3 and 5 dpi for transcriptome sequencing (Figure 5A). A parallel assay of mortality was carried out to confirm the success of NNV infection (Figure 5B). A total of 541,547,936 reads were obtained from the 18 sequenced samples, with an average value of 30,085,996 reads per sample; of the total raw reads, 99.99% successfully passed the quality control. From these high-quality reads, 97.27% successfully mapped to the zebrafish genome. Therefore, only 2.71% of the reads remained unmapped.

Using the TPM values obtained from RNA-Seq analyses, PCA was performed to determine the sample distribution and to identify the presence of outliers. The PCA plot clearly showed

that the NNV-infected samples became more differentiated from the control samples in terms of the overall transcriptome as the postinfection time increased (Figure 5C). An evident influence of age on the sample distribution is also observed.

3.6 Differentially Expressed Genes, GO Enrichment and KEGG Pathway Analysis

RNA-Seq analyses were conducted to evaluate transcriptome modulation in zebrafish larvae during infection with NNV. Using the obtained data, differentially expressed genes (DEGs) between NNV-infected and uninfected larvae were identified for each sampling point (FC > |2| and FDR value < 0.05) (Supplementary Files S1–S3). The number of DEGs increased according to the progression of the infection, with 125 DEGs at 1 dpi, 305 DEGs at 3 dpi, and 1,388 DEGs at 5 dpi. The representation of these DEGs in stacked column charts subdividing the number of genes according to the intensity (FC) and direction of regulation (up or down) revealed that most of the genes affected by the infection showed positive regulation (Figure 6B). Indeed, the heatmaps representing the TPM values of these DEGs across the different samples also

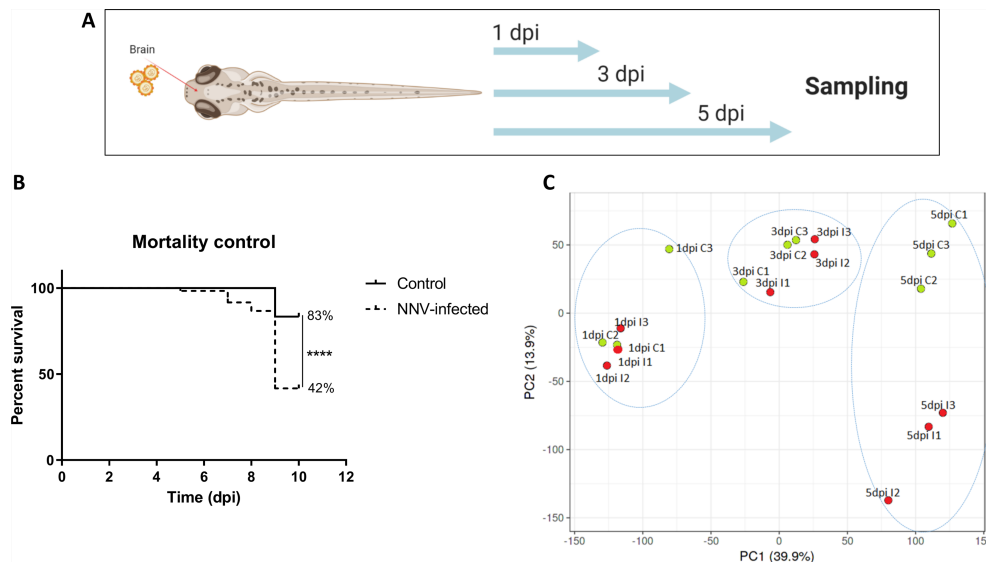


FIGURE 5 | Transcriptome analysis of 3-dpf zebrafish larvae infected with NNV *via* the brain. **(A)** RNA-Seq experimental design: Zebrafish larvae were microinjected *via* the brain, and three pools of infected and uninfected larvae were sampled at 1, 3, and 5 days postinfection for RNA isolation and Illumina sequencing. **(B)** Kaplan-Meier survival curves of NNV-infected and uninfected larvae conducted in parallel to RNA-Seq sampling. Statistically significant differences are displayed as follows: ****, p value < 0.0001. **(C)** Principal component analysis (PCA) of the samples.

revealed this pattern, with the exception of Replicate 3 from NNV-infected larvae at 1 dpi, whose TMP values of the DEGs at this sampling point were more similar to those observed in the uninfected controls (**Figure 6A**). These differential expression analyses were validated by qPCR amplification of 5 immune genes differentially modulated between NNV-infected and uninfected larvae; a Pearson's correlation coefficient (r) of 0.9755 was obtained for both data groups (**Supplementary Figure S3**).

A Venn diagram was constructed to illustrate the number of genes that were commonly regulated along the three sample points (**Figure 6C**); a total of 93 genes were found to be affected at the three times, which corresponded to genes mainly involved in immune response processes. Indeed, when GO enrichment analyses were conducted to explore the biological processes enriched during NNV infection, we observed that more than 60% of the significantly enriched terms were linked to immunity and antiviral response (viral process, response to virus, defence response to other organisms, innate immune response, etc.) (**Figure 7A**). The analysis of the KEGG pathways enriched during NNV infection resulted in a total of six pathways enriched at 1 dpi, eight at 3 dpi, and fifteen at 5 dpi (p value < 0.05) (**Figure 7B**). Four KEGG pathways were modulated throughout the 3 sampling points, and they corresponded to "herpes simplex infection", "RIG-I-like receptor signalling pathway", "Toll-like receptor signalling pathway", and "Jak-STAT signalling pathway", and the number of pathways related to immunity increased over time. The representation of the TPM values of the DEGs belonging to these pathways in heatmaps clearly demonstrated that the number of genes

induced by NNV challenge increased substantially over time (**Supplementary Figure S4**).

3.7 Expression Analysis of the Main Gene Groups Linked to Innate Immune Response

Different heatmaps were constructed to easily visualize the expression pattern of some of the main groups of immune genes regulated in zebrafish larvae during infection with NNV. As type I IFNs are the main regulators of the antiviral immune response in vertebrates, a heatmap was constructed with those DEGs directly linked to this antiviral mechanism and modulated at least at one of the sampling points by infection with NNV. For this, both interferon regulatory factors (IRFs), the type I IFNs themselves and a multitude of interferon-stimulated genes (ISGs) were considered. As expected, based on the time-increasing replication of NNV, some of these genes were already affected at 1 dpi, but the number of DEGs modulated substantially increased with time as the infection progressed (**Figure 8**). Due to the pivotal role of type I IFNs in the defence against viruses, these cytokines were considered separately from the other types of cytokines (chemokines, interleukins, colony-stimulating factors and tumour necrosis factors). A heatmap representing these other differentially expressed cytokines also reflected a strong overexpression of a multitude of them during the course of infection, with the exception of *chemokine (C-C motif) ligand 34b, duplicate 1 (ccl34b.1)*, which was significantly inhibited at 5 dpi by NNV (**Figure 9A**).

All of these cytokines mentioned above are induced after the recognition of pathogen-associated molecular patterns (PAMPs)

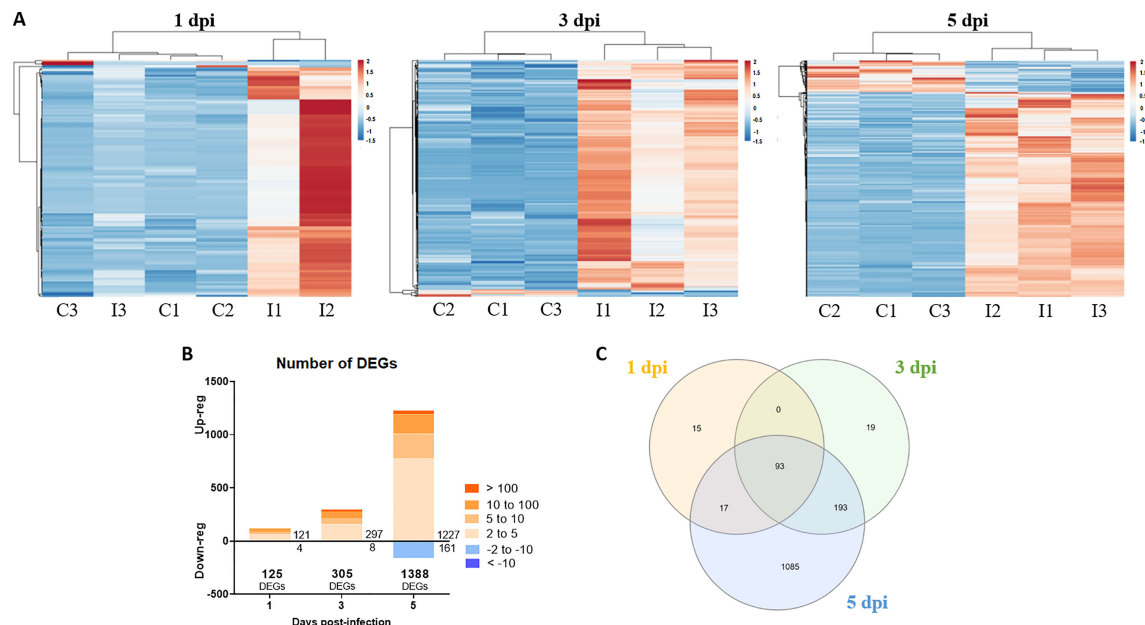


FIGURE 6 | Differentially expressed genes in zebrafish larvae infected with NNV. **(A)** Heatmaps representing the TPM expression values of the DEGs ($FC > |2|$; $FDR < 0.05$) modulated at 1, 3 and 5 dpi. Expression levels are represented as row-normalized values on a blue–red colour scale. **(B)** Stacked column chart reflecting the number and intensity (in FC value) of the DEGs identified at the 3 sampling points. **(C)** Venn diagram reflecting the common and exclusive DEGs at each sampling point.

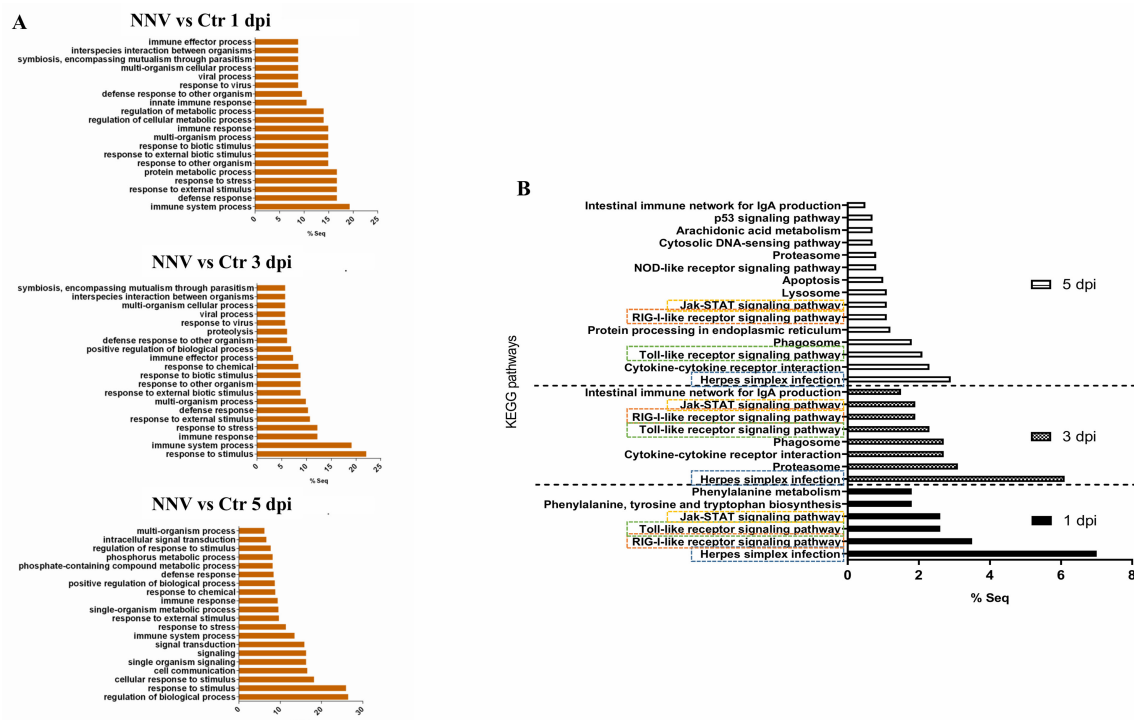
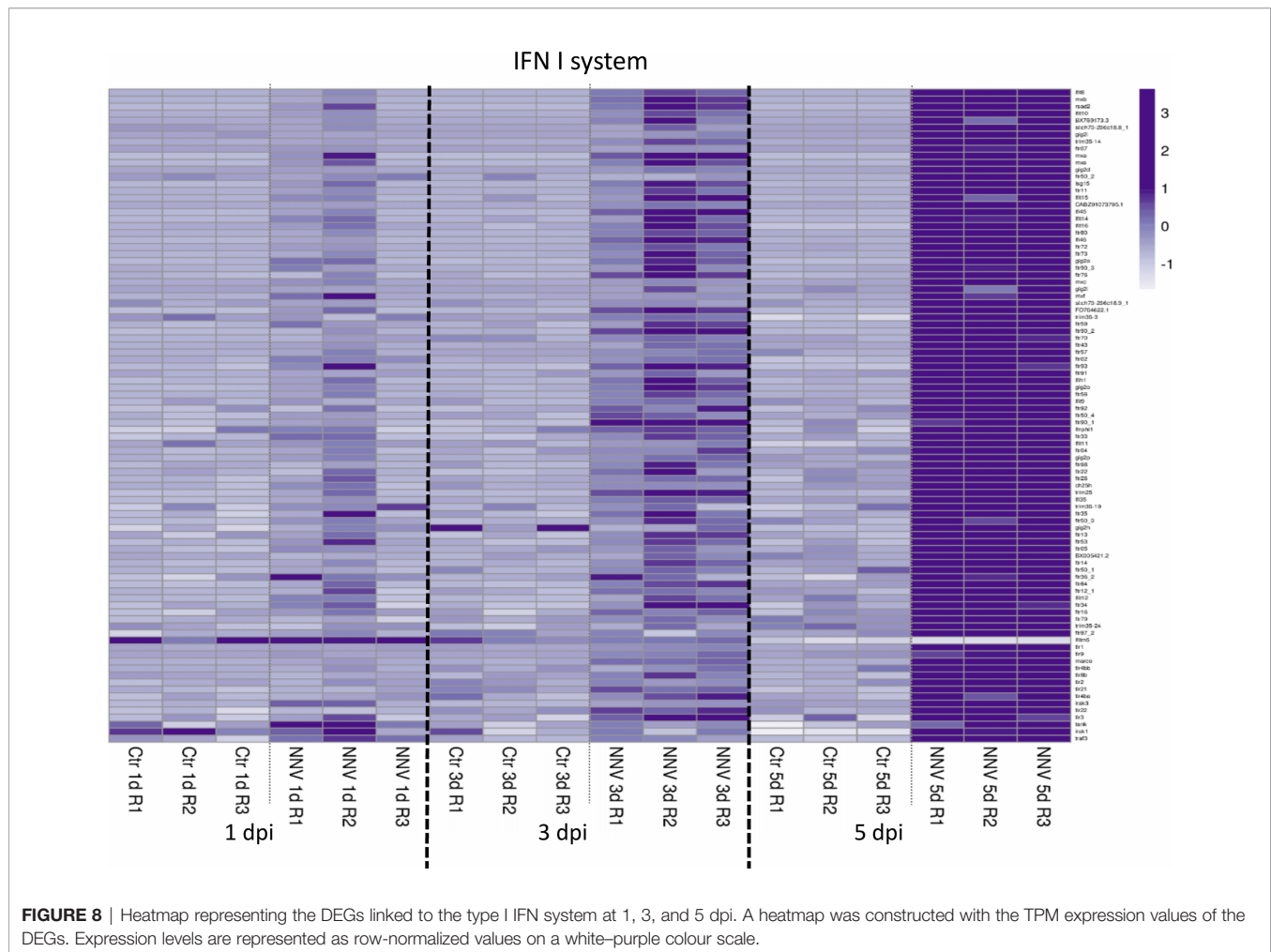


FIGURE 7 | GO terms and KEGG pathways enriched during NNV infection of zebrafish larvae. **(A)** GO biological process terms significantly enriched at 1, 3, and 5 dpi. **(B)** KEGG pathways enriched at 1, 3, and 5 dpi; the four common pathways significantly enriched over time are boxed.



by different pattern recognition receptors (PRRs). As mentioned above, the KEGG pathway enrichment analysis showed that two PRR pathways, the “RIG-I-like receptor signalling pathway” and the “Toll-like receptor signalling pathway”, were highly modulated by the virus at the three sampling points, and the “NOD-like receptor signalling pathway” was also enriched at 5 dpi. Therefore, we wanted to analyse in a more detailed way how the different differentially expressed PRRs were affected by the virus. As expected, numerous PRRs (*tlr1*, *tlr2*, *tlr3*, *tlr4ba*, *tlr4bb*, *tlr8b*, *tlr9*, *tlr21*, *tlr22*, *nod1*, and *marco*) and downstream signalling components (*irak1*, *irak3*, *tank*, and *traf3*) were also upregulated in a time-increasing manner (Figure 9B). Similar results were observed for different members of the complement system (Figure 9C) and the galectin family (Figure 9D).

4 DISCUSSION

VER disease has an important economic impact on marine aquaculture worldwide, although natural outbreaks have also been detected in several freshwater species (59). While considerable advances in the knowledge of the disease and

genetic variability of NNV have been conducted in recent years (59), host–virus interaction mechanisms need to be further studied to help develop effective antiviral strategies.

Zebrafish are a model organism widely used for biomedical research (60) and for studying different concerns linked to fish aquaculture production, such as skeletal malformations (61), pigmentation abnormalities (62), adaptation to prevalent stressful conditions in the aquaculture industry (63), nutrition (64) and infectious diseases (65). It is well known that zebrafish provide significant advantages for understanding host–pathogen interactions in the context of a complete vertebrate. For that reason, zebrafish have been increasingly used for modelling infectious diseases, including those caused by viruses (10), although their use in studying NNV infection remains poorly explored.

Although Furusawa et al. (40) reported that zebrafish were not susceptible to NNV, a year later, Lu et al. (23) were able to reproduce nodavirus infection in this fish species after intraperitoneal injection. They observed a time-increasing viral replication in the brain that peaked at 3 dpi, and histological studies of this tissue revealed lesions similar to those observed for naturally susceptible species (23). Moreover, zebrafish larvae

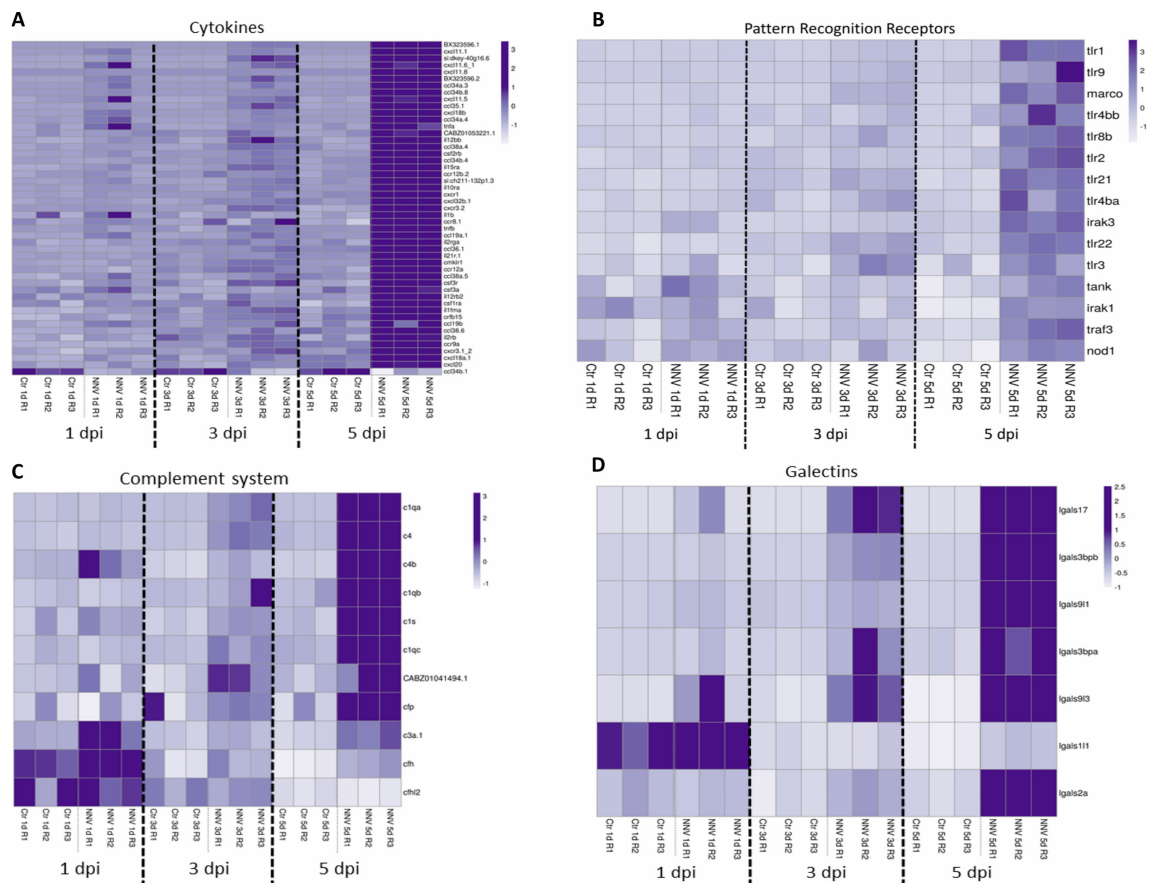


FIGURE 9 | Heatmaps representing the DEGs belonging to different immune categories at 1, 3 and 5 dpi: **(A)** cytokines; **(B)** pattern recognition receptors; **(C)** complement system; and **(D)** galectins. Heatmaps were constructed with the TPM expression values of the DEGs. Expression levels are represented as row-normalized values on a white-purple colour scale.

microinjected with NNV showed a high mortality rate at 24 hpi (98%) compared with the mock-injected larvae (24%), although the age of the larvae and route of microinjection were not specified by the authors (23). In that work, the pivotal role of the type I IFN system in protection against NNV was also demonstrated, as the treatment of zebrafish larvae with recombinant IFN conferred protection against viral infection (23). Afterwards, Morick et al. (24) described the infection of zebrafish larvae by bath challenge and the protection conferred by ribavirin treatment (41). However, these works did not fully use all of the advantages that this model species offers to us. In this study, we wanted to propose the use of zebrafish as a model species for this disease and to use techniques that allow us a deeper understanding of what happens during this viral disease.

First, we aimed to determine the most effective route and age of infection for zebrafish larvae to conduct further studies. After the infection of 3-dpf larvae *via* the brain, *via* the duct of Cuvier (DC), intramuscularly (IM) and by bath challenge, we found that the route that offered a significantly lower percentage of survival against NNV was microinjection *via* the brain followed by

microinjection IM. However, DC and bath challenges did not cause significant mortality to the larvae compared with the uninfected control larvae. This contrasts with the data published by Morick et al. (24), who found that 4-dpf larvae were highly susceptible to NNV by bath challenge, although the mortality significantly decreased in 6- and 8-dpf larvae. Based on this, we wanted to determine whether the age of the larvae influenced the susceptibility to the virus; therefore, larvae at 14 dpi were infected under the same conditions as the 3-dpf larvae, and no significant mortalities were observed for any of the infection routes. In agreement with Morick et al. (24), older larvae are more resistant to the virus, which could be due to a more developed immune system.

Therefore, 3-4-dpf larvae would be optimal for studying NNV-zebrafish larvae interactions not only for their higher susceptibility but also for their transparency, enabling the use of different imaging techniques. Among them, whole-mount immunofluorescence allowed us to confirm that, as occurs in naturally susceptible species, after IM infection, NNV can migrate to the brain and ocular region. Although different

natural routes of infection have been proposed for NNV (epithelial cells, gills, and nasal and oral cavity) (59), the process of viral migration from the muscle to the central nervous system (CNS) was largely confirmed, and due to the higher infective efficiency of the IM route (66), it is the most extensively used route for experimental infection in farmed fish species (32, 34, 38, 67, 68). The spread of infection from the muscle to the CNS may occur through nerve axonal transport (29, 69). As a consequence of the damage caused by NNV in the CNS, one of the main characteristic symptoms of VER disease is the erratic swimming of infected fish. The small size of the zebrafish larvae allows us to better control the experimental conditions *in vivo*, as very large spaces are not required; therefore, certain variables, such as the temperature, are more controlled. When the swimming behavior of 3- and 14-dpf NNV-infected larvae was compared with that of uninfected larvae, changes in velocity, directionality, and Euclidean and accumulated distance were specifically observed in 3-dpf larvae infected *via* the brain, which is probably due to the faster and higher replication of the virus in these larvae.

However, as expected, zebrafish larvae are already able to respond to the virus at early stages of development. The use of zebrafish transgenic lines to analyse the migration of innate immune cell types to the brain after NNV infection through this route revealed a significant migration of neutrophils (Mpx+ cells) and myeloid precursors with lysozyme activity (Lyz+) but not macrophages (Mpeg+). Although the *lyz* gene is expressed in both granulocytes and macrophages, its expression is considerably higher in granulocytes (70), which was also determined in mammals (71). Therefore, the similar migratory trend observed for the Mpx+ and Lyz+ cells is because, in both cases, these cells most likely correspond exclusively to neutrophils. Neutrophils are the first immune cells recruited to sites of infection, where they play important protective functions, including the phagocytosis of infectious agents (72). Nevertheless, although certain viruses have been detected inside neutrophils, it is not clear whether that is a consequence of the active infection and propagation of these specific viruses within neutrophils (72). Neuroinvasion is a rare phenomenon, but certain neuronal viruses, such as NNV, have the ability to colonize the CNS. Among the strategies to reach the brain, a highly protected organ, is the so-called ‘Trojan horse’ strategy, consisting of the camouflage of the pathogen inside immune cells, such as neutrophils and macrophages (72). However, immunofluorescence analysis showed that NNV and Mpx+ cells do not colocalize; consequently, neutrophils do not appear to phagocytose NNV particles as a protection strategy, but they are not used as ‘Trojan horses’ either.

Interestingly, although we did not observe migration of macrophages to the site of injection, the expression of the macrophage marker gene *marco* significantly increased during the course of the infection, reaching higher fold-change values than that observed for the *mpx* gene. It is possible that macrophages migrate to the brain at later infection stages, as cell migration was evaluated until 3 dpi; at this sampling point, the expression of *marco* was not affected by the infection,

reaching significant overexpression at 5 and 7 dpi. In contrast, the *mpx* gene showed higher overexpression at 3 dpi. Because both specific markers are already present in 2-dpf larvae (73, 74), these results could suggest a similar pattern to that observed in mammals: resident low immunoreactive macrophages recognize the pathogens and produce neutrophil chemoattractants and, after a rapid influx of neutrophils to the site of infection, they release chemoattracting factors involved in the recruitment of other immune cells, in particular inflammatory macrophages (75). However, more investigation will be needed to elucidate neutrophil–macrophage interactions after NNV infection.

To shed more light on the immune response of zebrafish larvae to NNV, we conducted RNA-Seq analyses of NNV-infected and control larvae at 1, 3 and 5 dpi. As expected, due to the time-increasing replication of the virus, the number of DEGs also increased with time, with most of them being overexpressed in the infected larvae compared with the controls. The GO terms and KEGG pathway enrichment analyses revealed a strong enrichment in immune processes. Among the KEGG pathways, the signalling cascades of the three main types of PRRs (Toll-like, RIG-I-like and NOD-like) were enriched, and a heatmap representing the DEG PRRs and downstream signalling molecules revealed a strong overexpression of a multitude of them at 5 dpi, especially different TLRs. A variety of TLRs were also found to be induced by NNV infection in European sea bass leucocytes (76) and brain DLB-1 cell line (77), although this intense TLR response was not observed in other RNA-Seq studies of fish or fish cells infected with NNV (38, 39, 68, 78–81). Although endosomal TLRs (TLR3, TLR7/8 and TLR9) are typically considered the antiviral TLRs, since they are specialized in the recognition of viral nucleic acids, certain TLRs anchored to the cellular membrane, such as TLR2 and TLR4, are able to recognize viral proteins (82). Ours results suggest the induction of TLRs involved in both nucleic acid and protein recognition. Interestingly, although RIG-I-like receptors have been described as pivotal PRRs in response to NNV infection (42, 43), we did not observe the induction of this type of receptors in our results.

The interaction of viral PAMPs with different PRRs initiates the recruitment of adapters and the activation of downstream transcription factors that express a multitude of cytokines, including type I IFNs (83). The expression of type I IFNs, the main cytokines orchestrating antiviral defence, mediates their protective effects through the induction of numerous ISGs (84). The relevance of the type I IFN response was well documented in fish after NNV infection, including zebrafish (23, 42–44). However, how the complete repertoire of members of the type I IFN system responds to NNV challenge in zebrafish remains unexplored. As expected, we found a powerful modulation of a multitude of genes involved in this pathway, which indicates a highly efficient response of zebrafish larvae to the virus. Interestingly, contrary to that observed by Chen et al. in the zebrafish cell line ZF4 (42), we did not observe induction in the expression of the different type I IFNs (*ifnphi1*, *ifnphi2*, *ifnphi3*, *ifnphi4*). This fact is probably due to the fast overexpression of

these interferons after NNV infection, returning to basal levels at 24 hpi. Nevertheless, the high representation of ISGs highlights the relevance of the type I IFN system. This contrasts with the total absence of a type I IFN response observed in European sea bass brain and head kidney samples at 24 and 72 hpi, which is mainly characterized by activation of the hypothalamic–pituitary–interrenal axis (stress response axis) (38). More investigation will be needed to elucidate whether the high susceptibility of European sea bass to NNV is a consequence of an impaired antiviral response to this virus. Indeed, when the expression of ISG *mx* was analysed in brain samples from European sea bass and in gilthead seabream (*Sparus aurata*), a fish species classically considered resistant to NNV, the induction of *mx* expression was substantially lower in European sea bass than in gilthead seabream (32).

In addition to the type I IFNs, a multitude of other cytokines were induced, reflecting a powerful inflammatory response to NNV, which is probably mediated in the first instance by neutrophils and then by neutrophils and macrophages (75). Indeed, the early migration of neutrophils to the cephalic region of zebrafish larvae after challenge with the virus could be triggered through the production of a multitude of chemokines and the infiltration of more neutrophils and macrophages. Increases in proinflammatory cytokines have also been observed in different organisms infected with NNV, such as Atlantic halibut (85), European sea bass and gilthead seabream (32), turbot (34), zebrafish (24), or different species of grouper (81, 86). Interestingly, the expression of *tumour necrosis factor alpha* (*tnfa*) was previously suggested to be substantially higher in species susceptible to NNV, such as European sea bass, compared with its expression in species resistant to NNV, such as gilthead seabream, which could indicate that this proinflammatory cytokine may be responsible for a large inflammatory reaction in the areas of infection of this virus, such as the brain, retina and spinal cord, producing a neurodegenerative process that the fish cannot overcome (32). However, this result contrasts with the total absence of overexpression of proinflammatory genes observed after an RNA-Seq analysis of brain samples from European sea bass infected with NNV (38), which could be a consequence of different degrees of disease severity or different evolution patterns as a consequence of a multitude of experimental factors (age and size of the animals, virulence of the NNV stock, temperature, etc.).

The complement system has the ability to recognize viruses and virus-infected cells and trigger effector pathways aimed at neutralizing viruses or killing infected cells (87). The strong induction of a multitude of components of the complement system also evidenced the importance of this immune mechanism in the defence against NNV. The overexpression of different complement members after infection with this virus was already observed in brain (38) or liver (88) samples from European sea bass or in leucocytes infected *in vitro* (76). Moreover, increases in the complement haemolytic activity of serum samples from NNV-infected gilthead seabream were

observed at 24 hpi, although this activity was not significantly affected in European sea bass (88), which could also contribute to the different susceptibilities to the virus. Indeed, some viruses are able to develop complement evasion strategies (87), and this ability could vary depending on the fish species. However, whether members of the *Nodaviridae* family are able to destabilize the complement response remains to be elucidated.

Finally, the other group of genes standing out from the DEGs in zebrafish larvae were galectins. These β -galactose-binding lectins, which could also be considered PRRs, are expressed in a multitude of cell types and play major roles in defence against pathogens (89). However, little is known about the role of galectins in viral infections, and although they clearly have a function in viral infections, their mode of action is not completely understood (89). Indeed, some investigations have reported antiviral activity of galectins against certain viruses, but other works attributed a proviral role to certain galectins (88). The recurrent overexpression of different galectin genes in different fish species challenged with NNV (67, 68, 76, 90) also evidence a function of these lectins in the response to this virus. Indeed, zebrafish galectin family members showed antiviral activity against the fish virus infectious haematopoietic necrosis virus (IHNV) through direct interaction with the viral glycoprotein, resulting in reduced viral adhesion to the cells (91, 92). Recombinant *Paralichthys olivaceus* Galectin 1 also showed the ability to neutralize lymphocystis disease virus (LCDV) and exert anti-inflammatory activity during infection with LCDV, but the lower expression of proinflammatory genes could be a consequence of lower viral replication in fish treated with the recombinant protein (93). Similar results were observed for the recombinant European sea bass Galectin 1 against NNV, with a significant reduction in the inflammatory response, although the concrete antiviral mechanism mediated by this galectin remains to be elucidated. Moreover, the overexpression of 7 different zebrafish galectin members after NNV observed in this work could indicate nonredundant and complementary roles in the fight against NNV.

While the numerous advantages of zebrafish as a model organism in biomedical and aquaculture research have been extensively noted in recent years, this work reaffirms the foundations of zebrafish larvae to be considered a model of infection, not only for NNV but also for many other viruses. The experimental challenge of zebrafish larvae can reproduce the disease and mimic the course of the infection, as occurs in other NNV hosts. Zebrafish larvae showed susceptibility to this virus, with significant mortalities after intramuscular microinjection or by directly inoculating the virus into the brain. As in the farmed fish species susceptible to NNV, the virus was able to migrate to the brain after an intramuscular infection, and alterations in swimming behavior were observed during infection, suggesting CNS damage. Larvae were also able to mount an efficient antiviral response at both the cellular and humoral levels. Based on these results, different aspects of NNV pathogenesis, immune response and screening of antiviral drugs could be easily studied in zebrafish larvae.

DATA AVAILABILITY STATEMENT

The datasets presented in this study can be found in online repositories. The names of the repository/repositories and accession number(s) can be found below: <http://www.ncbi.nlm.nih.gov/sra>, PRJNA799765.

ETHICS STATEMENT

The animal study was reviewed and approved by CSIC National Committee of Bioethics under approval number ES3605702020012020/13/FUN.01/INM06/BNG.

AUTHOR CONTRIBUTIONS

RL conducted the main experimental assays. RL and PP analysed the data, prepared the figures and wrote the manuscript. AF performed the RNA-Seq analyses. AF and BN conceived and supervised the study and edited and reviewed the manuscript. All authors contributed to the article and approved the submitted version.

REFERENCES

- Kanther M, Rawls JF. Host-Microbe Interactions in the Developing Zebrafish. *Curr Opin Immunol* (2010) 22:10–9. doi: 10.1016/j.coi.2010.01.006
- Novoa B, Figueras A. Zebrafish: Model for the Study of Inflammation and the Innate Immune Response to Infectious Diseases. *Adv Exp Med Biol* (2012) 946:253–75. doi: 10.1007/978-1-4614-0106-3_15
- Lam S, Chua H, Gong Z, Lam T, Sin Y. Development and Maturation of the Immune System in Zebrafish, *Danio Rerio*: A Gene Expression Profiling, *in Situ* Hybridization and Immunological Study. *Dev Comp Immunol* (2004) 28:9–28. doi: 10.1016/s0145-305x(03)00103-4
- Herbomel P, Thisse B, Thisse C. Ontogeny and Behaviour of Early Macrophages in the Zebrafish Embryo. *Development* (1999) 126:3735–45. doi: 10.1242/dev.126.17.3735
- Le Guyader D, Redd MJ, Colucci-Guyon E, Murayama E, Kissa K, Biolat V, et al. Origins and Unconventional Behavior of Neutrophils in Developing Zebrafish. *Blood* (2008) 111:132–41. doi: 10.1182/blood-2007-06-095398
- Cui C, Bernard EL, Kanwal Z, Stockhammer OW, van der Vaart M, Zakrzewska A, et al. Infectious Disease Modeling and Innate Immune Function in Zebrafish Embryos. *Methods Cell Biol* (2011) 105:273307. doi: 10.1016/B978-0-12-381320-6.00012-6
- Ludwig M, Palha N, Torhy C, Briolat V, Colucci-Guyon E, Brémont M, et al. Whole-Body Analysis of a Viral Infection: Vascular Endothelium Is a Primary Target of Infectious Hematopoietic Necrosis Virus in Zebrafish Larvae. *PLoS Pathog* (2011) 7:e1001269. doi: 10.1371/journal.ppat.1001269
- Levraud JP, Palha N, Langevin C, Boudinot P. Through the Looking Glass: Witnessing Host-Virus Interplay in Zebrafish. *Trends Microbiol* (2014) 22:490–7. doi: 10.1016/j.tim.2014.04.014
- Crim MJ, Riley LK. Viral Diseases in Zebrafish: What is Known and Unknown. *ILAR J* (2012) 53:135–43. doi: 10.1093/ilar.53.2.135
- Varela M, Figueras A, Novoa B. Modelling Viral Infections Using Zebrafish: Innate Immune Response and Antiviral Research. *Antiviral Res* (2017) 139:59–68. doi: 10.1016/j.antiviral.2016.12.013
- Sanders G, Batts W, Winton J. Susceptibility of Zebrafish (*Danio Rerio*) to a Model Pathogen, Spring Viremia of Carp Virus. *Comp Med* (2003) 53:514–21.

FUNDING

Our laboratory is funded by projects PID2020-119532RB-I00 from the Ministerio de Ciencia e Innovación, 0474_BLUEBIOLAB from EU FEDER Programa Interreg España-Portugal and IN607B 2019/01 from Consellería de Economía, Emprego e Industria (GAIN), Xunta de Galicia. RL and PP wish to thank the Axencia Galega de Innovación (GAIN, Xunta de Galicia) for their predoctoral ((IN606A-2017/011) and postdoctoral contracts (IN606B-2018/010), respectively. We acknowledge support of the publication fee by the CSIC Open Access Publication Support Initiative through its Unit of Information Resources for Research (URICI).

ACKNOWLEDGMENTS

We want to thank Judit Castro, Lucía Sánchez and the aquarium staff for their technical assistance.

SUPPLEMENTARY MATERIAL

The Supplementary Material for this article can be found online at: <https://www.frontiersin.org/articles/10.3389/fimmu.2022.863096/full#supplementary-material>

- Levraud JP, Boudinot P, Colin I, Benmansour A, Peyrieras N, Herbomel P, et al. Identification of the Zebrafish IFN Receptor: Implications for the Origin of the Vertebrate IFN System. *J Immunol* (2007) 178:4385–94. doi: 10.4049/jimmunol.178.7.4385
- López-Muñoz A, Roca FJ, Sepulcre MP, Meseguer J, Mulero V. Zebrafish Larvae are Unable to Mount a Protective Antiviral Response Against Waterborne Infection by Spring Viremia of Carp Virus. *Dev Comp Immunol* (2010) 34:546–52. doi: 10.1016/j.dci.2009.12.015
- Varela M, Díaz-Rosales P, Pereiro P, Forn-Cuní G, Costa MM, Dios S, et al. Interferon-Induced Genes of the Expanded IFIT Family Show Conserved Antiviral Activities in Non-Mammalian Species. *PLoS One* (2014) 9:e100015. doi: 10.1371/journal.pone.0100015
- Varela M, Romero A, Dios S, van der Vaart M, Figueras A, Meijer AH, et al. Cellular Visualization of Macrophage Pyroptosis and Interleukin-1 β Release in a Viral Hemorrhagic Infection in Zebrafish Larvae. *J Virol* (2014) 88:12026–40. doi: 10.1128/JVI.02056-14
- Phelan P, Pressley M, Witten P, Mellon M, Blake S, Kim CH. Characterization of Snakehead Rhabdovirus Infection in Zebrafish (*Danio Rerio*). *J Virol* (2005) 79:1842–52. doi: 10.1128/JVI.79.3.1842-1852.2005
- Novoa B, Romero A, Mulero V, Rodriguez I, Fernandez I, Figueras A. Zebrafish (*Danio Rerio*) as a Model for the Study of Vaccination Against Viral Haemorrhagic Septicemia Virus (VHSV). *Vaccine* (2006) 24:3924–31. doi: 10.1016/j.vaccine.2006.05.015
- LaPatra SE, Barone L, Jones GR, Zon LI. Effects of Infectious Hematopoietic Necrosis Virus and Infectious Pancreatic Necrosis Virus Infection on Hematopoietic Precursors of Zebrafish. *Blood Cells Mol Dis* (2000) 26:256–9. doi: 10.1006/bcmd.2000.0320
- Garner JN, Joshi B, Jagus R. Characterization of Rainbow Trout and Zebrafish Eukaryotic Initiation Factor 2 α and its Response to Endoplasmic Reticulum Stress and IPNV Infection. *Dev Comp Immunol* (2003) 27:217–31. doi: 10.1016/s0145-305x(02)00096-4
- Xu X, Zhang L, Weng S, Huang Z, Lu J, Lan D, et al. A Zebrafish (*Danio Rerio*) Model of Infectious Spleen and Kidney Necrosis Virus (ISKNV) Infection. *Virology* (2008) 376:1–12. doi: 10.1016/j.virol.2007.12.026
- Wang ZL, Xu XP, He BL, Weng SP, Xiao J, Wang L, et al. Infectious Spleen and Kidney Necrosis Virus OFR48R Functions as a New Viral Vascular

- Endothelial Growth Factor. *J Virol* (2008) 82:4371–83. doi: 10.1128/JVI.02027-07
22. Martín V, Mavian C, López Bueno A, Molina A, Díaz E, Andrés G, et al. Establishment of a Zebrafish Infection Model for the Study of Wild-Type and Recombinant European Sheatfish Virus. *J Virol* (2015) 89:10702–6. doi: 10.1128/JVI.01580-15
 23. Lu MW, Chao YM, Guo TC, Santi N, Evensen O, Kasani SK, et al. The Interferon Response is Involved in Nervous Necrosis Virus Acute and Persistent Infection in Zebrafish Infection Model. *Mol Immunol* (2008) 45:1146–52. doi: 10.1016/j.molimm.2007.07.018
 24. Morick D, Figenbaum O, Smirnov M, Fellig Y, Inbal A, Kotler M. Mortality Caused by Bath Exposure of Zebrafish (*Danio Rerio*) Larvae to Nervous Necrosis Virus Is Limited to the Fourth Day Postfertilization. *Appl Environ Microbiol* (2015) 81:3280–7. doi: 10.1128/AEM.04175-14
 25. Binesh CP. Mortality Due to Viral Nervous Necrosis in Zebrafish *Danio Rerio* and Goldfish *Carassius Auratus*. *Dis Aquat Organ* (2013) 104:257–60. doi: 10.3354/dao02605
 26. Wang C, Liu S, Tang KFJ, Zhang Q. Natural Infection of Covert Mortality Nodavirus Affects Zebrafish (*Danio Rerio*). *J Fish Dis* (2021) 44:1315–24. doi: 10.1111/jfd.13390
 27. Binesh CP. Elevation of Temperature and Crowding Trigger Acute Viral Nervous Necrosis in Zebrafish, *Brachydanio Rerio* (Hamilton-Buchanan), Subclinically Infected With Betanodavirus. *J Fish Dis* (2014) 37:279–82. doi: 10.1111/jfd.12080
 28. Munday BL, Kwang J, Moody N. Betanodavirus Infections of Teleost Fish: A Review. *J Fish Dis* (2002) 25:127–42. doi: 10.1046/j.1365-2761.2002.00350.x
 29. Costa JZ, Thompson KD. Understanding the Interaction Between Betanodavirus and Its Host for the Development of Prophylactic Measures for Viral Encephalopathy and Retinopathy. *Fish Shellfish Immunol* (2016) 53:35–49. doi: 10.1016/j.fsi.2016.03.033
 30. Chen YM, Su YL, Lin JHY, Yang HL, Chen TY. Cloning of an Orange-Spotted Grouper (*Epinephelus Coioides*) Mx cDNA and Characterisation of its Expression in Response to Nodavirus. *Fish Shellfish Immunol* (2006) 20:58–71. doi: 10.1016/j.fsi.2005.04.001
 31. Wu YC, Chi SC. Cloning and Analysis of Antiviral Activity of a Barramundi (*Lates Calcarifer*) Mx Gene. *Fish Shellfish Immunol* (2007) 23:97–108. doi: 10.1016/j.fsi.2006.09.008
 32. Poisa-Beiro L, Dios S, Montes A, Aranguren R, Figueras A, Novoa B. Nodavirus Increases the Expression of Mx and Inflammatory Cytokines in Fish Brain. *Mol Immunol* (2008) 45:218–25. doi: 10.1016/j.molimm.2007.04.016
 33. Park KC, Osborne JA, Montes A, Dios S, Nerland AH, Novoa B, et al. Immunological Responses of Turbot (*Psetta Maxima*) to Nodavirus Infection or Polyriboinosinic Acid (pIC) Stimulation, Using Expressed Sequences Tags (ESTs) Analysis and cDNA Microarrays. *Fish Shellfish Immunol* (2009) 26:91–108. doi: 10.1016/j.fsi.2008.03.010
 34. Montes A, Figueras A, Novoa B. Nodavirus Encephalopathy in Turbot (*Scophthalmus Maximus*): Inflammation, Nitric Oxide Production and Effect of Anti-Inflammatory Compounds. *Fish Shellfish Immunol* (2010) 28:281–8. doi: 10.1016/j.fsi.2009.11.002
 35. Scapigliati G, Buonocore F, Randelli E, Casani D, Meloni S, Zarletti G, et al. Cellular and Molecular Immune Responses of the Sea Bass (*Dicentrarchus Labrax*) Experimentally Infected With Betanodavirus. *Fish Shellfish Immunol* (2010) 28:303–11. doi: 10.1016/j.fsi.2009.11.008
 36. Krasnov A, Kileng Ø, Skugor S, Jørgensen SM, Afanasyev S, Timmerhaus G, et al. Genomic Analysis of the Host Response to Nervous Necrosis Virus in Atlantic Cod (*Gadus Morhua*) Brain. *Mol Immunol* (2013) 54:443–52. doi: 10.1016/j.molimm.2013.01.010
 37. Toffan A, Pascoli F, Pretto T, Panzarin V, Abbadi M, Buratin A, et al. Viral Nervous Necrosis in Gilthead Sea Bream (*Sparus Aurata*) Caused by Reassortant Betanodavirus RGNNV/SJNNV: An Emerging Threat for Mediterranean Aquaculture. *Sci Rep* (2017) 7:46755. doi: 10.1038/srep46755
 38. Lama R, Pereiro P, Valenzuela-Muñoz V, Gallardo-Escárate C, Tort L, Figueras A, et al. RNA-Seq Analysis of European Sea Bass (*Dicentrarchus Labrax* L.) Infected With Nodavirus Reveals Powerful Modulation of the Stress Response. *Vet Res* (2020) 51:64. doi: 10.1186/s13567-020-00784-y
 39. Wang Q, Peng C, Yang M, Huang F, Duan X, Wang S, et al. Single-Cell RNA-Seq Landscape Midbrain Cell Responses to Red Spotted Grouper Nervous Necrosis Virus Infection. *PloS Pathog* (2021) 17:e1009665. doi: 10.1371/journal.ppat.1009665
 40. Furusawa R, Okinaka Y, Uematsu K, Nakai T. Screening of Freshwater Fish Species for Their Susceptibility to a Betanodavirus. *Dis Aquat Organ* (2007) 77:119–25. doi: 10.3354/dao01841
 41. Morick D, Saragovi A. Inhibition of Nervous Necrosis Virus by Ribavirin in a Zebrafish Larvae Model. *Fish Shellfish Immunol* (2017) 60:537–44. doi: 10.1016/j.fsi.2016.11.015
 42. Chen HY, Liu W, Wu SY, Chiou PP, Li YH, Chen YC, et al. RIG-I Specifically Mediates Group II Type I IFN Activation in Nervous Necrosis Virus Infected Zebrafish Cells. *Fish Shellfish Immunol* (2015) 43:427–35. doi: 10.1016/j.fsi.2015.01.012
 43. Jin Y, Jia K, Zhang W, Xiang Y, Jia P, Liu W, et al. Zebrafish TRIM25 Promotes Innate Immune Response to RGNNV Infection by Targeting 2CARD and RD Regions of RIG-I for K63-Linked Ubiquitination. *Front Immunol* (2019) 10:2805. doi: 10.3389/fimmu.2019.02805
 44. Liu W, Jin Y, Zhang W, Xiang Y, Jia P, Yi M, et al. MiR-202-5p Inhibits RIG-I-Dependent Innate Immune Responses to RGNNV Infection by Targeting TRIM25 to Mediate RIG-I Ubiquitination. *Viruses* (2020) 12:261. doi: 10.3390/v12030261
 45. Westerfield M. *The Zebrafish Book. A Guide for the Laboratory Use of Zebrafish (Danio Rerio)*. Eugene, OR: University of Oregon Press (2000).
 46. Nüsslein-Volhard C, Dahm R. *Zebrafish: A Practical Approach*. 1st ed. New York NY: Oxford Univ Press (2002).
 47. Bovo G, Nishizawa T, Maltese C, Borghesan F, Mutinelli F, Montesi F, et al. Viral Encephalopathy and Retinopathy of Farmed Marine Fish Species in Italy. *Virus Res* (1999) 63:143–6. doi: 10.1016/s0168-1702(99)00068-4
 48. Reed LJ, Muench H. A Simple Method of Estimating Fifty Percent Endpoints. *Am J Epidemiol* (1938) 27:493–7. doi: 10.1093/oxfordjournals.aje.a118408
 49. Rozen S, Skaletsky H. Primer3 on the WWW for General Users and for Biologist Programmers. *Methods Mol Biol* (2000) 132:365–86. doi: 10.1385/1-59259-192-2:365
 50. Pfaffl MW. A New Mathematical Model for Relative Quantification in Real-Time RT-PCR. *Nucleic Acids Res* (2001) 29:e45. doi: 10.1093/nar/29.9.e45
 51. Kuo HC, Wang TY, Chen PP, Chen YM, Chuang HC, Chen TY. Real-Time Quantitative PCR Assay for Monitoring of Nervous Necrosis Virus Infection in Grouper Aquaculture. *J Clin Microbiol* (2011) 49:1090–6. doi: 10.1128/JCM.01016-10
 52. Pereiro P, Varela M, Diaz-Rosales P, Romero A, Dios S, Figueras A, et al. Zebrafish Nk-Lysins: First Insights About Their Cellular and Functional Diversification. *Dev Comp Immunol* (2015) 51:148–59. doi: 10.1016/j.dci.2015.03.009
 53. Aranguren R, Tafalla C, Novoa B, Figueras A. Experimental Transmission of Encephalopathy and Retinopathy Induced by Nodavirus to Sea Bream, *Sparus Aurata* L., Using Different Infection Models. *J Fish Dis* (2022) 25:317–24. doi: 10.1046/j.1365-2761.2002.00368.x
 54. Schneider CA, Rasband WS, Eliceiri KW. NIH Image to ImageJ: 25 Years of Image Analysis. *Nat Methods* (2012) 9:671–5. doi: 10.1038/nmeth.2089
 55. Metsalu T, Vilo J. ClustVis: A Web Tool for Visualizing Clustering of Multivariate Data Using Principal Component Analysis and Heatmap. *Nucleic Acids Res* (2015) 43:W566–70. doi: 10.1093/nar/gkv468
 56. Heberle H, Meirles GV, da Silva FR, Telles GP, Minghim R. InteractiVenn: A Web-Based Tool for the Analysis of Sets Through Venn Diagrams. *BMC Bioinf* (2015) 16:169. doi: 10.1186/s12859-015-0611-3
 57. Huang DW, Sherman BT, Lempicki RA. Systematic and Integrative Analysis of Large Gene Lists Using DAVID Bioinformatics Resources. *Nat Protoc* (2009) 4:44–57. doi: 10.1038/nprot.2008.211
 58. Huang DW, Sherman BT, Lempicki RA. Bioinformatics Enrichment Tools: Paths Toward the Comprehensive Functional Analysis of Large Gene Lists. *Nucleic Acids Res* (2009) 37:1–13. doi: 10.1093/nar/gkn923
 59. Bandín I, Souto S. Betanodavirus and VER Disease: A 30-Year Research Review. *Pathogens* (2020) 9:106. doi: 10.3390/pathogens9020106
 60. Lin CY, Chiang CY, Tsai HJ. Zebrafish and Medaka: New Model Organisms for Modern Biomedical Research. *J BioMed Sci* (2016) 23:19. doi: 10.1186/s12929-016-0236-5
 61. Harris MP, Henke K, Hawkins MB, Witten PE. Fish is Fish: The Use of Experimental Model Species to Reveal Causes of Skeletal Diversity in Evolution and Disease. *J Appl Ichthyol* (2014) 30:616–29. doi: 10.1111/jai.12533
 62. Cal L, Suarez-Bregua P, Moran P, Cerdá-Reverter JM, Rotllant J. Fish Pigmentation. A Key Issue for the Sustainable Development of Fish

- Farming. In: M Yúfera, editor. *Emerging Issues in Fish Larvae Research*. Cham, Switzerland: Springer (2018). p. 229–52. doi: 10.1007/978-3-319-73244-2_8
63. Abdollahpour H, Falahatkar B, Jafari N, Lawrence C. Effect of Stress Severity on Zebrafish (*Danio Rerio*) Growth, Gonadal Development and Reproductive Performance: Do Females and Males Respond Differently? *Aquaculture* (2020) 522:735099. doi: 10.1016/j.aquaculture.2020.735099
 64. Ulloa PE, Medrano JF, Feijoo CG. Zebrafish as Animal Model for Aquaculture Nutrition Research. *Front Genet* (2014) 5:313. doi: 10.3389/fgene.2014.00313
 65. Jørgensen LVG. Zebrafish as a Model for Fish Diseases in Aquaculture. *Pathogens* (2020) 9:609. doi: 10.3390/pathogens9080609
 66. Péducasse S, Castric J, Thiéry R, Jeffroy J, Le Ven A, Baudin Laurencin F. Comparative Study of Viral Encephalopathy and Retinopathy in Juvenile Sea Bass *Dicentrarchus Labrax* Infected in Different Ways. *Dis Aquat Organ* (1999) 36:11–20. doi: 10.3354/dao036011
 67. Kim JO, Kim JO, Kim WS, Oh MJ. Characterization of the Transcriptome and Gene Expression of Brain Tissue in Sevenband Grouper (*Hyporhamphus septemfasciatus*) in Response to NNV Infection. *Genes* (2017) 8:31. doi: 10.3390/genes8010031
 68. Labella AM, Garcia-Rosado E, Bandin I, Dopazo CP, Castro D, Alonso MC, et al. Transcriptomic Profiles of Senegalese Sole Infected With Nervous Necrosis Virus Reassortants Presenting Different Degree of Virulence. *Front Immunol* (2018) 9:1626. doi: 10.3389/fimmu.2018.01626
 69. Ikenaga T, Tateoka Y, Nakai T, Uematsu K. Betanodavirus as a Novel Transneuronal Tracer for Fish. *Neurosci Lett* (2002) 331:55–9. doi: 10.1016/s0304-3940(02)00831-5
 70. Su F, Juarez M, Cooke CL, LaPointe L, Shavit JA, Yamaoka JS, et al. Differential Regulation of Primitive Myelopoiesis in the Zebrafish by Spi-1/Pu.1 and C/EBP1. *Zebrafish* (2007) 4:187–99. doi: 10.1089/zeb.2007.0505
 71. Faust N, Varas F, Kelly LM, Heck S, Graf T. Insertion of Enhanced Green Fluorescent Protein Into the Lysozyme Gene Creates Mice With Green Fluorescent Granulocytes and Macrophages. *Blood* (2000) 96:719–26. doi: 10.1182/blood.V96.2.719.014k29_719_726
 72. Galani IE, Andreakos E. Neutrophils in Viral Infections: Current Concepts and Caveats. *J Leukoc Biol* (2015) 98:557–64. doi: 10.1189/jlb.4VMR1114-555R
 73. Elomaa O, Kangas M, Sahlberg C, Tuukkanen J, Sormunen R, Liakka A, et al. Cloning of a Novel Bacteria-Binding Receptor Structurally Related to Scavenger Receptors and Expressed in a Subset of Macrophages. *Cell* (1995) 80:603–9. doi: 10.1016/0092-8674(95)90514-6
 74. Lieschke GJ, Oates AC, Crowhurst MO, Ward AC, Layton JE. Morphologic and Functional Characterization of Granulocytes and Macrophages in Embryonic and Adult Zebrafish. *Blood* (2001) 98:3087–96. doi: 10.1182/blood.v98.10.3087
 75. Prame Kumar K, Nicholls AJ, Wong CHY. Partners in Crime: Neutrophils and Monocytes/Macrophages in Inflammation and Disease. *Cell Tissue Res* (2018) 371:551–65. doi: 10.1007/s00441-017-2753-2
 76. Chaves-Pozo E, Valero Y, Esteve-Codina A, Gómez-Garrido J, Dabad M, Alioto T, et al. Innate Cell-Mediated Cytotoxic Activity of European Sea Bass Leucocytes Against Nodavirus-Infected Cells: A Functional and RNA-Seq Study. *Sci Rep* (2017) 7:15396. doi: 10.1038/s41598-017-15629-6
 77. Chaves-Pozo E, Bandin I, Oliveira JG, Esteve-Codina A, Gómez-Garrido J, Dabad M, et al. European Sea Bass Brain DLB-1 Cell Line is Susceptible to Nodavirus: A Transcriptomic Study. *Fish Shellfish Immunol* (2019) 1:14–24. doi: 10.1038/s41598-017-15629-6
 78. Liu P, Wang L, Kwang J, Yue GH, Wong SM. Transcriptome Analysis of Genes Responding to NNV Infection in Asian Seabass Epithelial Cells. *Fish Shellfish Immunol* (2016) 54:342–52. doi: 10.1016/j.fsi.2016.04.029
 79. Chen W, Yi L, Feng S, Liu X, Asim M, Zhou Y, et al. Transcriptomic Profiles of Striped Snakehead Fish Cells (SSN-1) Infected With Red-Spotted Grouper Nervous Necrosis Virus (RGNNV) With an Emphasis on Apoptosis Pathway. *Fish Shellfish Immunol* (2017) 60:346–54. doi: 10.1016/j.fsi.2016.11.059
 80. Tso CH, Lu MW. Transcriptome Profiling Analysis of Grouper During Nervous Necrosis Virus Persistent Infection. *Fish Shellfish Immunol* (2018) 76:224–32. doi: 10.1016/j.fsi.2018.03.009
 81. Wang L, Tian Y, Cheng M, Li Z, Li S, Wu Y, et al. Transcriptome Comparative Analysis of Immune Tissues From Asymptomatic and Diseased *Epinephelus Moara* Naturally Infected With Nervous Necrosis Virus. *Fish Shellfish Immunol* (2019) 93:99–107. doi: 10.1016/j.fsi.2019.07.020
 82. Lester SN, Li K. Toll-Like Receptors in Antiviral Innate Immunity. *J Mol Biol* (2014) 426:1246–64. doi: 10.1016/j.jmb.2013.11.024
 83. Mogensen TH. Pathogen Recognition and Inflammatory Signaling in Innate Immune Defenses. *Clin Microbiol Rev* (2009) 22:240–73. doi: 10.1128/CMR.00046-08
 84. Schneider WM, Chevillotte MD, Rice CM. Interferon-Stimulated Genes: A Complex Web of Host Defenses. *Annu Rev Immunol* (2014) 32:513–45. doi: 10.1146/annurev-immunol-032713-120231
 85. Overgard AC, Nerland AH, Fiksdal IU, Patel S. Atlantic Halibut Experimentally Infected With Nodavirus Shows Increased Levels of T-Cell Marker and Ifn γ Transcripts. *Dev Comp Immunol* (2012) 37:139–50. doi: 10.1016/j.dci.2011.10.003
 86. Huang Y, Yu Y, Yang Y, Yang M, Zhou L, Huang X, et al. Antiviral Function of Grouper MDA5 Against Iridovirus and Nodavirus. *Fish Shellfish Immunol* (2016) 54:188–96. doi: 10.1016/j.fsi.2016.04.001
 87. Agrawal P, Nawadkar R, Ojha H, Kumar J, Sahu A. Complement Evasion Strategies of Viruses: An Overview. *Front Microbiol* (2017) 8:1117. doi: 10.3389/fmicb.2017.01117
 88. Mauri I, Romero A, Acerete L, Mackenzie S, Roher N, Callol A, et al. Changes in Complement Responses in Gilthead Seabream (*Sparus Aurata*) and European Seabass (*Dicentrarchus Labrax*) Under Crowding Stress, Plus Viral and Bacterial Challenges. *Fish Shellfish Immunol* (2011) 30:182–8. doi: 10.1016/j.fsi.2010.10.006
 89. Wang WH, Lin CY, Chang MR, Urbina AN, Assavalapsakul W, Thitithanyanont A, et al. The Role of Galectins in Virus Infection - A Systemic Literature Review. *J Microbiol Immunol Infect* (2020) 53:925–35. doi: 10.1016/j.jmii.2019.09.005
 90. Poisa-Beiro L, Dios S, Ahmed H, Vasta GR, Martínez-López A, Estepa A, et al. Nodavirus Infection of Sea Bass (*Dicentrarchus Labrax*) Induces Up-Regulation of Galectin-1 Expression With Potential Anti-Inflammatory Activity. *J Immunol* (2009) 183:6600–11. doi: 10.4049/jimmunol.0801726
 91. Nita-Lazar M, Mancini J, Feng C, González-Montalbán N, Ravindran C, Jackson S, et al. The Zebrafish Galectins Drgal1-L2 and Drgal3-L1 Bind *In Vitro* to the Infectious Hematopoietic Necrosis Virus (IHNV) Glycoprotein and Reduce Viral Adhesion to Fish Epithelial Cells. *Dev Comp Immunol* (2016) 55:241–52. doi: 10.1016/j.dci.2015.09.007
 92. Ghosh A, Banerjee A, Amzel LM, Vasta GR, Bianchet MA. Structure of the Zebrafish Galectin-1-L2 and Model of its Interaction With the Infectious Hematopoietic Necrosis Virus (IHNV) Envelope Glycoprotein. *Glycobiology* (2019) 29:419–30. doi: 10.1093/glycob/cwz015
 93. Liu S, Hu G, Sun C, Zhang S. Anti-Viral Activity of Galectin-1 From Flounder *Paralichthys Olivaceus*. *Fish Shellfish Immunol* (2013) 34:1463–9. doi: 10.1016/j.fsi.2013.03.354

Conflict of Interest: The authors declare that the research was conducted in the absence of any commercial or financial relationships that could be construed as a potential conflict of interest.

Publisher's Note: All claims expressed in this article are solely those of the authors and do not necessarily represent those of their affiliated organizations, or those of the publisher, the editors and the reviewers. Any product that may be evaluated in this article, or claim that may be made by its manufacturer, is not guaranteed or endorsed by the publisher.

Copyright © 2022 Lama, Pereiro, Figueras and Novoa. This is an open-access article distributed under the terms of the Creative Commons Attribution License (CC BY). The use, distribution or reproduction in other forums is permitted, provided the original author(s) and the copyright owner(s) are credited and that the original publication in this journal is cited, in accordance with accepted academic practice. No use, distribution or reproduction is permitted which does not comply with these terms.



Drosophila as a Model to Study the Mechanism of Nociception

Jianzheng He^{1,2,3†}, Botong Li^{1,2†}, Shuzhen Han^{1,2}, Yuan Zhang^{1,2}, Kai Liu⁴, Simeng Yi⁵, Yongqi Liu^{1,3*} and Minghui Xiu^{1,3,6*}

¹ Provincial-Level Key Laboratory for Molecular Medicine of Major Diseases and the Prevention and Treatment with Traditional Chinese Medicine Research in Gansu Colleges and University, Gansu University of Chinese Medicine, Lanzhou, China, ² College of Basic Medicine, Gansu University of Chinese Medicine, Lanzhou, China, ³ Key Laboratory for Transfer of Dunhuang Medicine at the Provincial and Ministerial Level, Gansu University of Chinese Medicine, Lanzhou, China, ⁴ College of Integrated Traditional Chinese and Western Medicine, Gansu University of Chinese Medicine, Lanzhou, China, ⁵ State Key Laboratory of Animal Nutrition, College of Animal Science and Technology, China Agricultural University, Beijing, China, ⁶ College of Public Health, Gansu University of Chinese Medicine, Lanzhou, China

OPEN ACCESS

Edited by:

Susumu Ohya,
Nagoya City University, Japan

Reviewed by:

Yong Fang Zhu,
McMaster University, Canada
Francisco J. Taberner,
Institute of Neurosciences (CSIC),
Spain

*Correspondence:

Yongqi Liu
liuyongqi73@163.com
Minghui Xiu
xiuminghui87@163.com

[†] These authors have contributed
equally to this work

Specialty section:

This article was submitted to
Cell Physiology,
a section of the journal
Frontiers in Physiology

Received: 13 January 2022

Accepted: 28 February 2022

Published: 28 March 2022

Citation:

He J, Li B, Han S, Zhang Y, Liu K,
Yi S, Liu Y and Xiu M (2022)
Drosophila as a Model to Study
the Mechanism of Nociception.
Front. Physiol. 13:854124.
doi: 10.3389/fphys.2022.854124

Nociception refers to the process of encoding and processing noxious stimuli, which allow animals to detect and avoid potentially harmful stimuli. Several types of stimuli can trigger nociceptive sensory transduction, including thermal, noxious chemicals, and harsh mechanical stimulation that depend on the corresponding nociceptors. In view of the high evolutionary conservation of the mechanisms that govern nociception from *Drosophila melanogaster* to mammals, investigation in the fruit fly *Drosophila* help us understand how the sensory nervous system works and what happen in nociception. Here, we present an overview of currently identified conserved genetics of nociception, the nociceptive sensory neurons responsible for detecting noxious stimuli, and various assays for evaluating different nociception. Finally, we cover development of anti-pain drug using fly model. These comparisons illustrate the value of using *Drosophila* as model for uncovering nociception mechanisms, which are essential for identifying new treatment goals and developing novel analgesics that are applicable to human health.

Keywords: nociception, conserved genetics, nociceptive sensory neurons, behavioral assay, *Drosophila melanogaster*

INTRODUCTION

Pain is an “unpleasant sensory and emotional experience associated with actual or potential tissue damage”—as defined by the International Association for the Study of Pain¹, it is an indispensable and rich sensory experience which can help people promote the healing and improvement of the injured or diseased parts of the body (Young et al., 2012). Pain can be classified into nociception, inflammatory and pathological pain according to the pathological mechanism (Costigan et al., 2009; Woolf, 2010; Haanpaa et al., 2011), and acute, chronic, and occasional pain according to the duration (Turk, 2001; Glare et al., 2019). Pain is a subjective experience, and nociception is an objective neural process that encodes and processes harmful stimuli. It is an evolutionary conservative mechanism that reminds organisms of potential tissue damage and is vital to survival (Neely et al., 2010; Khuong and Neely, 2013). For living organisms, the rapid response to harmful stimuli and the ability to react and avoid them (pain/nociception) is crucial (Milinkeviciute et al., 2012).

¹ <http://www.iasp-pain.org>

Most of the research objects on nociception are model animals, such as monkey (Lee et al., 2007), mice (Luo et al., 2019), zebrafish (Malafoglia et al., 2013), *Drosophila melanogaster* (Leung et al., 2013), *C. elegans* (Nkambeu et al., 2020) and so on. As a bridge between disease research and human beings, model animals play an important role in modern medical research. Extensive modeling has been performed in mammals, however, these models are expensive, and have ethical implications. In contrast, *Drosophila* has its unique advantages as a model animal for pain research, small size and relatively short lifecycle allows it could be produced in large numbers and easy to work with. Most importantly, fruit flies show a high degree of homology with humans at the organ and gene level, with flies sharing functional counterparts for most organ systems (Fortini et al., 2000; Chien et al., 2002). It has been estimated that 75% of human disease genes have conserved homologs in *Drosophila*, making this fly a model organism of great potential (Bier, 2005). Using fruit flies as human disease model would avoid the ethical controversy. At present flies has been used extensively as a model for human disease already, for example, to study cancer, Alzheimer's disease, nociception, obesity and diabetes and so on (Milinkeviciute et al., 2012; Enomoto et al., 2018; Tsuda and Lim, 2018; Warr et al., 2018).

As previously mentioned, there are conserved physiological mechanisms underlying the nociceptive system between human and flies (Sneddon, 2018). The nociceptors in the primary afferent nerve fibers are stimulated by thermal, mechanical and chemical stimulation, converted into electrical signals, and then transmitted to the central nervous system such as the spinal cord, and finally felt the pain (Julius, 2013; Bourne et al., 2014; Dai, 2016; Sneddon, 2018; St, 2018). These nerve fibers quickly transmit the perceived harmful information to the central nervous system through action potentials. In this process, ion channels play a vital role. These ion channels are specifically expressed in the above-mentioned nerve fibers (Julius, 2013; Dai, 2016; Yam et al., 2018). TRP, Piezo and other ion channels have been identified as key pain receptors (Hwang and Oh, 2007; Volkers et al., 2015). Among these channels, TRPV1, TRPA1, Piezo1 and Piezo2 are expressed in nociceptors (Liedtke, 2007; Flood et al., 2013; Volkers et al., 2015; Himmel and Cox, 2017; Boonen et al., 2021). They serve as detectors and sensors for cold, heat, chemical and mechanical stimuli in nociceptors. These conserved genes in *Drosophila* well prove the potential of flies as a nociceptive model animal. The purpose of this review is to present the aggregate findings of the pain-related genes in order to discuss the possibilities for *Drosophila* as model animal in nociception research, and provide a comprehensive evaluation for future human nociception studies.

THE ROLE OF PAIN-RELATED GENES IN REGULATING NOCICEPTION/PAIN

Transient Receptor Potential Channels

Transient receptor potential (TRP) channels are a large family of ion channels, and most of them are conserved from *Drosophila* to humans. It has more than 50 subtypes, divided into 7 subfamilies

according to their amino acid sequence homology, which includes vanilloid (TRPV1-6), canonical or classic (TRPC1-7), melastatin (TRPM1-8), non-mechanoreceptor potential C (NOMP-like, TRPN1), long TRP ankyrin (TRPA1), polycystins (TRPP1-5) and mucolipins (TRPML1-3) (Clapham et al., 2001; Nilius et al., 2005, 2012; Wu et al., 2010; Li, 2017; Bamps et al., 2021). TRP channels allow an inward cation current to regulate cell function, and have a variety of activation modes by mechanical, thermal and chemical stimuli (Nilius et al., 2007; Nilius and Owsianik, 2011). Therefore, the TRP family has a variety of physiological functions, including vision, hearing, taste, thermosensation and response to different environmental stimuli (Gees et al., 2012). The TRP channels are probably best known for its role in nociceptive perception, it is the largest group of noxious ion channels involved in pain. Among the sub-families, TRPA1, TRPV1, and TRPM2 have been shown to be related to nociception (Table 1; Flood et al., 2013; Himmel and Cox, 2017; Maiese, 2017; Logashina et al., 2019).

TRPA1 is a channel with non-selective permeability to calcium, sodium and potassium, while its permeability to calcium is higher than that of other TRPs (Kwan and Corey, 2009). It acts as a sensor for cell damage signals and is involved in inflammation and immune response (Bandell et al., 2004; Kwan et al., 2006; Kwan and Corey, 2009; Neely et al., 2011; Zygmunt and Hogestatt, 2014; Laursen et al., 2015; Viana, 2016). Mostly, TRPA1 is crucial in mediating long-term hypersensitivity to thermal, cold, chemical, and mechanical stimuli detected in nociceptive, inflammatory, and neuropathic pain models (Story et al., 2003; Corey et al., 2004; Kwan et al., 2006; Karashima et al., 2009; Del et al., 2010). TRPA1 has been proposed to function as a temperature-insensitive detrimental heat sensor and a detrimental cold sensor (Laursen et al., 2015). TRPA1 promotes excitatory effects of bradykinin through the PLC/calcium signaling pathway (Bandell et al., 2004), so it is an important downstream target for inducing pain receptor hypersensitivity (Bautista et al., 2006). In inflammatory pain, the role of TRPA1 channels is two sides. On the one hand, pro-inflammatory factors activate nociceptors through TRPA1. On the other hand, TRPA1 stimulation is usually related to the release of pro-inflammatory neuropeptides (Nassini et al., 2014).

TRPV1 is a cation permeable channel and shows important influence in feeling nociceptive stimuli and producing pain in primary afferent nociceptors (Immke and Gavva, 2006). As an ion channel, it can be activated by specific activators, such as vanillin, capsaicin, sorbamide, etc., (Gees et al., 2012; Julius, 2013; Dai, 2016; Li, 2017; Hung and Tan, 2018). TRPV1 is now considered to be a molecular integration factor of pain stimuli, and drug target. In animals, the sensitization and activation of peripheral nociceptors can cause TRPV1 to transmit nociceptive signals to the central nervous system, thereby producing unpleasant and painful sensations, warning the body of potential harmful threats (Hung and Tan, 2018). TRPV1 not only plays a vital role in nociception, but also leads to the generation of action potentials during inflammation, which in turn leads to the generation of pathological pain, such as thermal hyperalgesia, spontaneous pain and mechanical hypersensitivity (Caterina et al., 2000; Ma and Quirion, 2007). TRPV1 knockout mice

TABLE 1 | Genes that regulate pain in humans and *Drosophila*.

Human genes	Regulated types of pain	References	Drosophila genes	Regulated types of pain	References
TRPA1	Neuropathic pain, nociception, allodynia, cold hyperalgesia	Yu et al., 2010; Fowler and Montell, 2013; Hehlert et al., 2021	dTRPA1	Thermal nociception	Kolisek et al., 2005; Zhong et al., 2010; Khuong and Neely, 2013; Glare et al., 2019
			Painless	Thermal and mechanical nociception	Lee et al., 2005; Kwan and Corey, 2009; Zhong et al., 2010
			Pyrexia	Thermal nociception	Liedtke, 2007; Zhong et al., 2010
TRPM2	Thermosensation and nociception inflammatory, neuropathic and chronic pain	Hwang and Oh, 2007; Honjo et al., 2012; Zygmunt and Hogestatt, 2014			
Piezo1	Promotes mechanical response	Ma and Quirion, 2007; Maiese, 2017	DmPiezo	Mechanical nociception	McClung and Hirsh, 1998; Mauthner et al., 2014; Luo et al., 2019; Massingham et al., 2021
Piezo2	Feel gentle touch, proprioception, and abnormal tactile pain	Manev et al., 2003; Manev and Dimitrijevic, 2004; Malafoglia et al., 2013; Mandel et al., 2018	piezo-like	Crawling pattern and body gesture control	McParland et al., 2021
ASIC3	pain caused by acid	Merritt and Whittington, 1995; Milinkeviciute et al., 2012; Luo et al., 2017	Pickpocket1	Mechanical nociception	Minke et al., 1975; Neely et al., 2010; Nassini et al., 2014; Murthy et al., 2018
			Pickpocket26	Mechanical nociception	Neely et al., 2010, 2011
			Pickpocket30	Mechanical nociception	Nichols et al., 2002

have a significant reduction in thermal hypersensitivity after tissue injury, which clearly proves that TRPV1 is involved in the development of inflammatory pain (Caterina et al., 2000; Davis et al., 2000). TRPM2 as a calcium ion-permeable non-selective cation channel is expressed in the peripheral nervous system and immune system, which is activated by oxidative stress, moderate temperature and intracellular adenosine diphosphate ribose (ADPR) in various types of cells (Kolisek et al., 2005; Togashi et al., 2006). TRPM2 is of great importance in the pathogenesis of inflammation and neuropathic pain (Eisfeld and Luckhoff, 2007; Faouzi and Penner, 2014). A study showed that in carrageenan-induced inflammatory pain and sciatic nerve injury-induced neuropathic pain models, TRPM2 knockout mice have alleviated mechanical hyperalgesia and thermal hyperalgesia (Di Meglio et al., 2004).

The first evidence for the existence of TRP channels were found in *Drosophila* flies. Cosens and Manning used electroretinogram (ERG) measurements to analyze a spontaneous mutant in *Drosophila* that exhibited a temporary rather than a continuous response under long-term bright light (Cosens and Manning, 1969). It is firstly named a “type A” mutation. Later, it was found that this mutant had defects in light transmission, and had a representative name: “transient receptor potential” or Trp (Minke et al., 1975). TRP channels are diverse in structure and can modulate transduction of thermal, mechanical, and chemical stimuli and also can regulate cell growth, cell differentiation, and vascular physiology in flies (Pazienza et al., 2014; Maiese, 2017). The *Drosophila* genome contains genes encoding 13 TRP channels, and encodes four TRPA homologs: *dTRPA1*, *painless*, *pyrexia*, and *water witch* (Fowler and Montell, 2013). TRPA channels have been the most widely studied for their roles in temperature-sensing behavior in

flies (Goodman, 2003; Xu et al., 2006; Neely et al., 2011; Bellemer, 2015) and also play important roles in chemical and mechanical sensing (Mandel et al., 2018; Boonen et al., 2021). TRPA1 has been implicated as a mammal noxious cold receptor, which is activated by extremely cold temperatures (below < 15°C) (Kwan and Corey, 2009). However, the TRPA1 homologs *dTRPA1*, *painless*, *pyrexia* in flies have no function in regulation of cold avoidance. The temperature-sensitive diversity of TRPA1 channels in flies and mammals makes researchers more cautious when dissecting the role of TRPA1 in thermal stimulation and screening anti-pain drug using *D. melanogaster*.

dTRPA1 was first identified as a heat-activated channel in flies (Rosenzweig et al., 2005; Kwon et al., 2008). It is 32% identical and 54% similar to its mammalian orthology by amino acid identity, and is activated in response to high temperature, reactive chemicals and downstream of intracellular signaling pathways (Neely et al., 2011; Bellemer, 2015; Boonen et al., 2021). The dTRPA1 channel is expressed in the multiple groups of central neurons and several classes of peripheral sensory neurons (Hamada et al., 2008; Kang et al., 2010; Kim et al., 2010). dTRPA1 participates not only in the thermal pain of adults, but also in the thermal pain of larvae (Neely et al., 2011; Luo et al., 2017). Control adults flies respond very quickly to harmful heat at 46°C, but dTRPA1 mutants respond slowly to harmful heat, and their thermal pain ability was significantly reduced (Neely et al., 2011). Fly larvae trigger noxious rolling behavior when the temperature is below 40°C, and the frequency of this behavior increases rapidly as the temperature rises until 33°C. The above-mentioned nociceptive behaviors all depend on the dTRPA1 channel, the activity of which responds to the rate of temperature change (Luo et al., 2017). In addition to participating in the response to harmful temperature stimuli, dTRPA1 has also been detected

in chemical stimuli (Tracey et al., 2003; Im and Galko, 2012). Boonen et al. (2021) found that wild-type flies avoid citronellal and menthol in olfactory tests, while dTRPA1 mutant flies have reduced this behavior. dTRPA1 channel mediates chemical avoidance in gustatory receptor neurons (GRNs), in which knockdown of *dTRPA1* in GRNs significantly reduced the aversive response to aristolochic acid (Kim et al., 2010).

Painless as a member of the TRPA family channel was discovered and identified as an important gene for thermal and mechanical nociception in *Drosophila* flies (Tracey et al., 2003; Xu et al., 2006). It is expressed in the larval peripheral nervous system (Tracey et al., 2003), and various regions of the adult brain, such as mushroom body, a region important for learning and memory (Busto et al., 2010) ellipsoid body of the central complex (Sakai et al., 2012, 2014); olfactory projection neurons in antennal lobes (Wang et al., 2011); and the pars intercerebralis including insulin-producing cells (Sakai et al., 2012, 2014). *Painless* is a molecular sensor for noxious thermal stimuli in larvae and adult flies (Goodman, 2003). Studies have confirmed that wild-type larvae exhibit typical “rolling behavior” within 1 s of being contacted by the heated probe above 40°C, and this activity is absent in the *painless* mutant (Goodman, 2003). When the heating temperature exceeds 38°C, the firing of the multidendritic sensory neurons increases, but this increase is not seen in the *painless* mutant (Xu et al., 2006; Sokabe and Tominaga, 2009). In the hot plate assay, *painless* mutant adults exhibited a behavioral defect and could not jump quickly to escape from a hot plate, which can be rescued by a transformed *painless* gene, indicating that *painless* is required for thermal nociception in adult flies (Xu et al., 2006). *Painless* requires Ca^{2+} as a co-agonist for heat-evoked activation. *Painless* failed to respond to heat in the absence of intracellular and extracellular Ca^{2+} (Liu et al., 2003). *Painless* is also required for chemical and mechanical nociception (Tracey et al., 2003; Al-Anzi et al., 2006; Mandel et al., 2018). Mandel et al. (2018) found that allyl isothiocyanate (AITC) remarkably reduce the proboscis extension reflex frequencies in wild-type genotypes but did not in *painless* mutant, and AITC evoked calcium changes in *painless* expressing neurons. Expression of *painless* was also detected in mechanically-sensitive Johnston's organ, while *painless* could be activated by mechanical stimuli (Tracey et al., 2003). Additionally, *painless* is involved in a variety of neural processes in flies including negative geotaxis (Sun et al., 2009), larval social behavior (Xu et al., 2008) and sexual receptivity of virgin females (Sakai et al., 2014).

Pyrexia (*pyx*) gene is a heat-sensitive TRPA channel and protects flies from high temperature stress (Lee et al., 2005; Xu et al., 2006; Hamada et al., 2008). It is ubiquitously expressed along the dendrites of a subset of peripheral nervous system neurons and is more permeable to K^+ than to Na^+ (Lee et al., 2005). 60% of *pyx* null flies were paralyzed within 3 min after exposure to 40°C, while applying the same stimulation to wild-type fruit flies, the number of paralysis was only 9% (Lee et al., 2005). *pyx* is also responsible for the response of temperature-sensitive anterior cell (AC) brain neurons, which regulate the temperature preference behavior of adult flies (Hamada et al., 2008; Tang et al., 2013). *pyx* is involved in temperature synchronization of circadian clocks, in which *pyx*

mutants fail to synchronize their behavior to temperature cycles between “night” and “day” (Wolfgang et al., 2013).

Piezo Channel

Mechanical transduction is the process of converting mechanical force into biological signals, which plays a key role in various physiological processes of animals (Volkers et al., 2015). It is through the mechanically sensitive cation channel converts the mechanical stimulus received by the animal body into various activities, and plays an important role in the regulation of touch, hearing and blood pressure (Bagriantsev et al., 2014). Piezo channel is a type of mechanical-sensitive ion channel, which is necessary for cells to respond to mechanical stimuli (Coste et al., 2010). In vertebrates, Piezo channel proteins mainly include Piezo1 and Piezo2 proteins, which are encoded by the genes *Piezo1/FAM38A* and *Piezo2/FAM38B*, respectively (Coste et al., 2010, 2012; Bagriantsev et al., 2014). Piezo1 channels are characterized by slower kinetics, and can react to more persistent activation (Lewis et al., 2017). After silencing Piezo1 expression in chondrocytes, the number of chondrocytes responding to mechanical stimulation decreased, while activating Piezo1 significantly promotes mechanical response in chondrocytes (Servin-Vences et al., 2017). Piezo2 as a faster kinetics are more specified for detection of transient mechanical forces (Ranade et al., 2014; Woo et al., 2015; Szczot et al., 2018). Recent studies have shown that Piezo2 is essential for mediating abnormal tactile pain in mice (Murthy et al., 2018; Szczot et al., 2018), and it has been confirmed that Piezo2 is also necessary for humans to feel gentle touch, proprioception, and abnormal tactile pain (Szczot et al., 2018).

Only one single Piezo protein was found in lower organisms, such as nematodes and fruit flies (Hamada et al., 2008). In the *Drosophila melanogaster*, there is only one copy of the force-gated ion channel, *DmPiezo*, a Ca^{2+} permeable non-selective cation channel, similar to its mammalian homolog (Coste et al., 2012). *DmPiezo* is 24% identical to mammalian piezos, with sequence conservation throughout the length of the proteins (Coste et al., 2012). Studies have shown that the expression of *DmPiezo* is detected in all types of sensory neurons and some non-neural tissues of flies, including multimodal nociceptors of larvae. Among these neurons, *Dmpiezo* has a special contribution to mechanical pain (Kim et al., 2012). The researchers found that *Dmpiezo* expression in human cells induces mechanically activated currents, similar to its mammalian counterpart (Coste et al., 2012). In *Dmpiezo* knockout larvae, the behavioral response to harmful mechanical stimuli is severely reduced, while the response to another harmful stimulus or touch is not affected. Knockdown of *Dmpiezo* in sensory neurons that mediate nociception is sufficient to weaken the response to harmful mechanical stimuli. *Dmpiezo* and Pickpocket (*ppk*) are involved in the parallel pathways of *ppk*-positive cells, while their absence results in mechanical nociception elimination (Kim et al., 2012). Loss of *DmPiezo* renders class IV sensory neurons unresponsive to harsh touch (Kim et al., 2012) and makes mechanosensitive visceral neurons, which sit in the fly's brain and innervate the gut, mechanosensitive (Wang et al., 2020). *DmPiezo* also regulate axon regeneration in flies (Song et al., 2019), in which

DmPiezo activation during axon regeneration induces local Ca^{2+} transients at the growth cone, leading to activation of nitric oxide synthase and the downstream cGMP kinase foraging or PKG to restrict axon regrowth, while loss of DmPiezo increases axon regeneration of sensory neurons. A second *Drosophila* piezo family member, piezo-like (pzl; CG45783) shares similarity with that of Dmpiezo and its mammalian homologs Piezo1 and Piezo2 (Hu et al., 2019). Pzl gene expressed in larval chordotonal neurons is required for locomotion of *Drosophila* larvae. The pzl mutant showed severe defects in crawling pattern and body gesture control, which could be rescued by expressing human or mouse Piezo1, suggesting a conserved role the Piezo-family proteins in locomotion (Hu et al., 2019).

DEG/ENaC Family Channels

Acid-sensitive ion channels (ASICs) are a group of proton-gated ion channels that belong to the degenerin/epithelial sodium channel (DEG/ENaC) family. The channel can be activated when the extracellular pH drops below 7.0, or with aprotic ligands at physiological pH levels. The activation of ASICs mainly triggers Na^+ influx (Waldmann et al., 1997; Yu et al., 2010). ASIC was found to be a major player in human pain caused by acid (Luo et al., 2017). Increasing evidence further indicates that ASIC3 is a molecular determinant of pain-related tissue acidosis in rodent models. Members of the DEG/ENaC family also play a role in nociception, and have been shown to be essential mechanical transduction molecules in *Drosophila* flies (Luo et al., 2019). *Pickpocket1* (*Ppk1*) encodes an ion channel subunit of the DEG/ENaC family and is responsible for mechanical nociception responses in flies (Adams et al., 1998; Zhong et al., 2010). It is widely expressed in nociceptive and class IV multidendritic neurons (Zhong et al., 2010). Another ion channel subunits *balboa* (also known as *ppk26*) is highly enriched in nociceptive neurons and could bind to PPK to regulate mechanical nociception behaviors in *Drosophila* larvae (Guo et al., 2014; Mauthner et al., 2014). *Ppk26* mutant showed severe behavioral defects in a mechanical nociception behavioral test but responded to noxious heat stimuli compared to wild-type larvae (Guo et al., 2014). *Ppk1* and *ppk26* have the same signaling pathway to regulate mechanical nociception, and they do not have functional response to thermal stimulus (Gorczyca et al., 2014). *Ppk30* as a member of the *Drosophila* Ppk family is detected by class IV multidendritic neurons, and has a role in mechanosensation, but not in thermosensation (Jang et al., 2019).

DROSOPHILA MODELS OF NOCICEPTION/PAIN

Drosophila fly has high homology with human disease genes (75%), reproduces rapidly on its own, and the cost of establishing and maintaining a sufficient number of *drosophila* is much lower than that of the same number of vertebral model animals. These advantages make fly become a tool for studying the conservative genetics of pain (Tracey et al., 2003; Bier, 2005). The fly nociceptors are similar to vertebrates in morphology and

function, and they have unique naked nerve endings. The end of the nerve dendrites of *Drosophila* cover the entire epidermis without overlapping, allowing them to quickly perceive tissue damage. This characteristic proves the potential of *Drosophila* as a model animal for noxious research (Grueber et al., 2003, 2007; Hwang and Oh, 2007).

Nociceptive Sensory Neurons in Flies

Nociception refers to the sensation of harmful stimuli that can cause tissue damage. Nociceptive sensory neurons in *Drosophila* have one axon and one or several dendrites each (Hehlert et al., 2021). Fly larvae have two main peripheral sensory neurons located below the barrier epidermis: type I and type II, according to dendrite number and anatomy (Kernan, 2007). The type I neurons are related to bristle type and chordotonal sensory organs and have a single ciliated dendrites (Hwang et al., 2007). The type I neurons are more involved in mechanical sensory functions, such as light touch (Kernan et al., 1994). The type II neurons have many dendritic extensions that project to nearly every epidermal cell of the larval barrier epidermis, thus the type II neurons are also called multidendritic (md) sensory neurons or dendritic arborization (DA) (Grueber et al., 2002). They are structurally similar to mammalian nociceptors (Gao et al., 1999; Grueber et al., 2002). Larvae with gene-silenced md neurons are completely insensitive to harmful stimuli and cannot produce noxious responses. This underlying evidence suggests that md sensory neurons function as nociceptors (Williams and Truman, 2005; Grueber et al., 2007). The TRP channel mentioned above is necessary for nociception, and it has been confirmed that it is expressed in md neurons, which further shows that the status of md neurons in nociception is crucial (Tracey et al., 2003; Rosenzweig et al., 2005). Morphological studies on type II neurons show that these neurons are not a unified cell population. On the contrary, at least four subtypes have been identified (Grueber et al., 2002).

According to the complexity of dendrites and other morphological characteristics, these neurons are named class I-IV neurons that tile the larval body wall (Merritt and Whittington, 1995; Schrader and Merritt, 2000; Grueber et al., 2007). The dendrites of class I neurons are the simplest, while class IV neurons are the most complex (Grueber et al., 2002). Class I and Class II dendritic domains are relatively sparse and compact, while Class III and Class IV neurons have more complex branching patterns, wider coverage, and no branch overlap (Grueber et al., 2002, 2003). Class I neurons project to the motor nerve stacks of the ventral dorsal ganglia and are thought to provide feedback to the motor neurons. However, class II, class III, and class IV neurons all project to the ventral nerve pile, and by analogy with other insects, they are predicted to have somatosensory functions (Hwang et al., 2007; Yoshino et al., 2017; Burgos et al., 2018). Class I neurons are important for coordinating the appropriate timing of peristaltic locomotion (Cheng et al., 2010). Class II and Class III are both related to light contact reactions, of which type III takes the leading role (Tsubouchi et al., 2012; Yan et al., 2013). Class III neurons also mediate the mechanical nociception and cold nociception (Tsubouchi et al., 2012; Yan et al., 2013; Turner et al., 2016). Class

IV neurons appear like mammalian nociceptors morphologically (Tracey et al., 2003) and have polymodal sensitivity to a variety of sensory stimuli (Ohyama et al., 2013). Ablation or silencing class IV neurons significantly eliminates larval responses to noxious stimuli, while activation of class IV neurons is sufficient to stimulate corkscrew-like rolling behavior that is similar as larvae receive noxious stimuli (Tracey et al., 2003; Hwang et al., 2012; Ohyama et al., 2013). These neurons in the peripheral nervous system are responsible for perception of multiple nociceptive modalities, including mechanical force, harmful heat, low-wavelength light, and chemical stimuli, through distinct receptors (Tracey et al., 2003; Kang et al., 2010; Xiang et al., 2010; Hwang et al., 2012; Ohyama et al., 2013). Diverse ion channel are expressed in class IV neurons to evoke depolarization in response to corresponding noxious stimuli (Tracey et al., 2003; Lee et al., 2007; Zhong et al., 2010; Hwang et al., 2012; Kim et al., 2012).

Much of the current research on pain in *Drosophila* flies has focused on nociception, which is similar to acute pain in mammals. When flies suffer from noxious stimuli, multiple pathways are activated in md neurons. This includes the dTRPA1 (Mandel et al., 2018), painless (Tracey et al., 2003) and Pyrexia (Lee et al., 2005) that sense thermal pain; the DmPiezo (Song et al., 2019), painless (Tracey et al., 2003) and Pickpocket families (Zhong et al., 2010) that sense mechanical pain. After acute pain perception occurs, it is often accompanied by prolonged allodynia and hyperalgesia. Multiple pathways related to allodynia and hyperalgesia are also found in md neurons. Hedgehog (Hh) signaling is involved in allodynia and hyperalgesia when *Drosophila* larvae are exposed to UV light (Babcock et al., 2011). Meanwhile, Hh signaling acts in parallel with tumor necrosis factor (TNF) signaling to mediate allodynia (Babcock et al., 2009), and several TRP channels described above mediate allodynia and hyperalgesia downstream of these pathways. Painless is required for the development of Hh- or TNF-induced thermal hyperalgesia, whereas dTRPA1 is required for Hh-induced thermal hyperalgesia (Babcock et al., 2011). The BMP pathway is also expressed in md neurons during allodynia and hyperalgesia, and it is located downstream of the Hh signaling pathway (Honjo and Tracey, 2018). Decapentaplegic (Dpp, mammalian bone morphogenetic protein 2/4 ortholog) and its downstream signaling pathways in *Drosophila* md neurons have also been shown to be required to induce allodynia (Gjelsvik et al., 2018). The above studies show that when pain occurs, related pain signaling pathways in *Drosophila* md neurons are co-expressed to participate in acute nociception and subsequent chronic pain (allodynia and hyperalgesia).

Different Stimulation of Acute Nociception

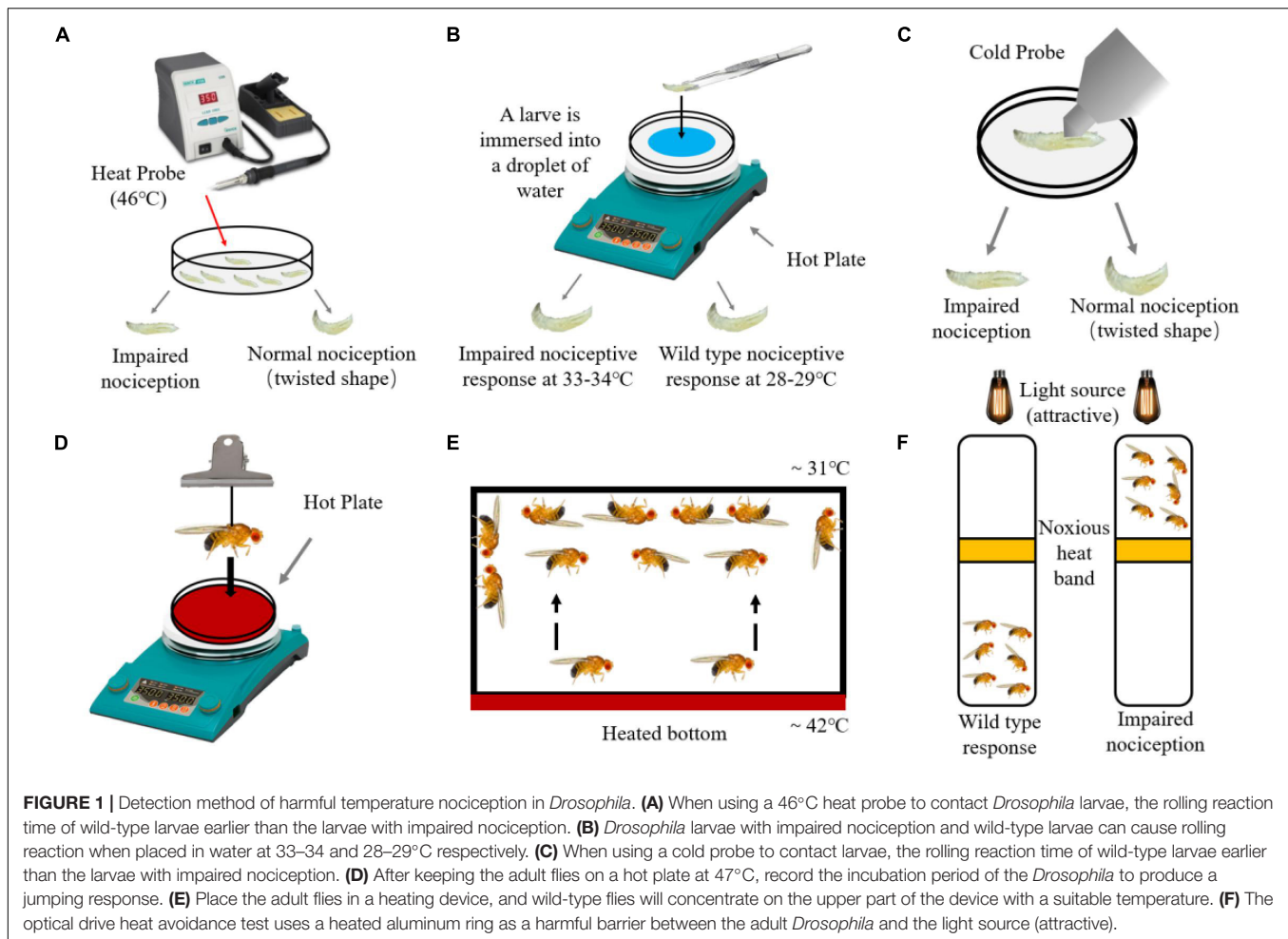
Currently, the method of nociceptive research using *Drosophila* fly as a model animal focuses on thermal, cold, chemical and mechanical stimulation of acute nociception.

Regarding the experimental example of thermal nociception, fly larvae and adults have different methods. One of the most classic experimental examples is to collect fly larvae and place

them in a petri dish, touch it with a soldering iron heated to 46°C, then the wild-type larvae would make a rolling response in a very short time (Tracey et al., 2003; Petersen et al., 2018; **Figure 1A**). TRPA1 mutants or painless mutants will exhibit a markedly slow response to temperature. The above experimental model has opened the door to the study of nociception or pain in *Drosophila* (Tracey et al., 2003; Manev and Dimitrijevic, 2004; Babcock et al., 2009; Aldrich et al., 2010; Coste et al., 2010). Another way to study the heat damage of larvae is to pour water on a petri dish filled with agar to form a water film so that the larvae can roll freely, put the larvae in the petri dish, and then put the petri dish on the heating plate. Record the length of time for the rolling response of larvae at different temperatures (Oswald et al., 2011; **Figure 1B**). Flies cannot be exposed to low temperatures for a long time, and their behavior prefers warmer temperatures, but the mechanism by which they perceive and avoid cold stimuli has not been studied until recently. The method of measuring the cold nociception of *Drosophila* larvae is to place the cold probe at a 45° angle to the back of the larva, and apply enough pressure downward to make the surface of the larva slightly concave while allowing it to move forward or backward (Turner et al., 2017). Keep the cold probe still for 10 s until the cold-induced response of the *Drosophila* larvae is observed, which is the response latency period (**Figure 1C**). The response latency period is simply the reaction time to cold stimuli. The shorter the latency period, the more sensitive the flies to cold stimuli. The response latency period of wild-type flies is shorter than that of mutant flies' in the revised manuscript.

The detection of typhoid fever on adult *Drosophila* is time-consuming and laborious. Firstly, researchers developed a method to model the "jumping" reflections that flies exhibit when exposed to noxious heat (**Figure 1D**), in which flies is suspended on an electric heating plate (47°C) using a nylon rope, then is dropped to get in touch with heating plate, and waiting time for flies to jump is recorded (Xu et al., 2006). Secondly, the adult flies are placed in an incubator with a heating function at the bottom, and the bottom of the box is heated to 46°C (**Figure 1E**). Wild-type flies will avoid that surface and rest at the upper part of 31°C (Neely et al., 2010). The group should be used as the nociception detection unit, and it is required to be simple and effective. Researchers can use this device to identify genes related to thermal nociception. The third method is to combine the light preference response of adult flies with harmful heat avoidance (**Figure 1F**). Flies are placed in a vertical transparent device, and a heating aluminum ring and a lamp are placed on the middle and top of the device. Wild-type flies with normal receptors are not attracted by light, while flies with knockdown of *painless* are attracted by light and pass through the heated aluminum ring (Benzer, 1967; Aldrich et al., 2010).

The way to study the chemical stimulation of fruit flies is to add nociceptor activators, such as capsaicin, menthol, allicin, isothiocyanate, etc., to food, which cause flies to resist food (Al-Anzi et al., 2006; Kim et al., 2010; Li et al., 2020; **Figure 2A**). Briefly, third-instar larvae are placed in a petri dish, use a pipette to add the above-mentioned chemical stimulus solution under and around the flies, and record the incubation period of the fruit flies (the time between the addition and the tumbling behavior)

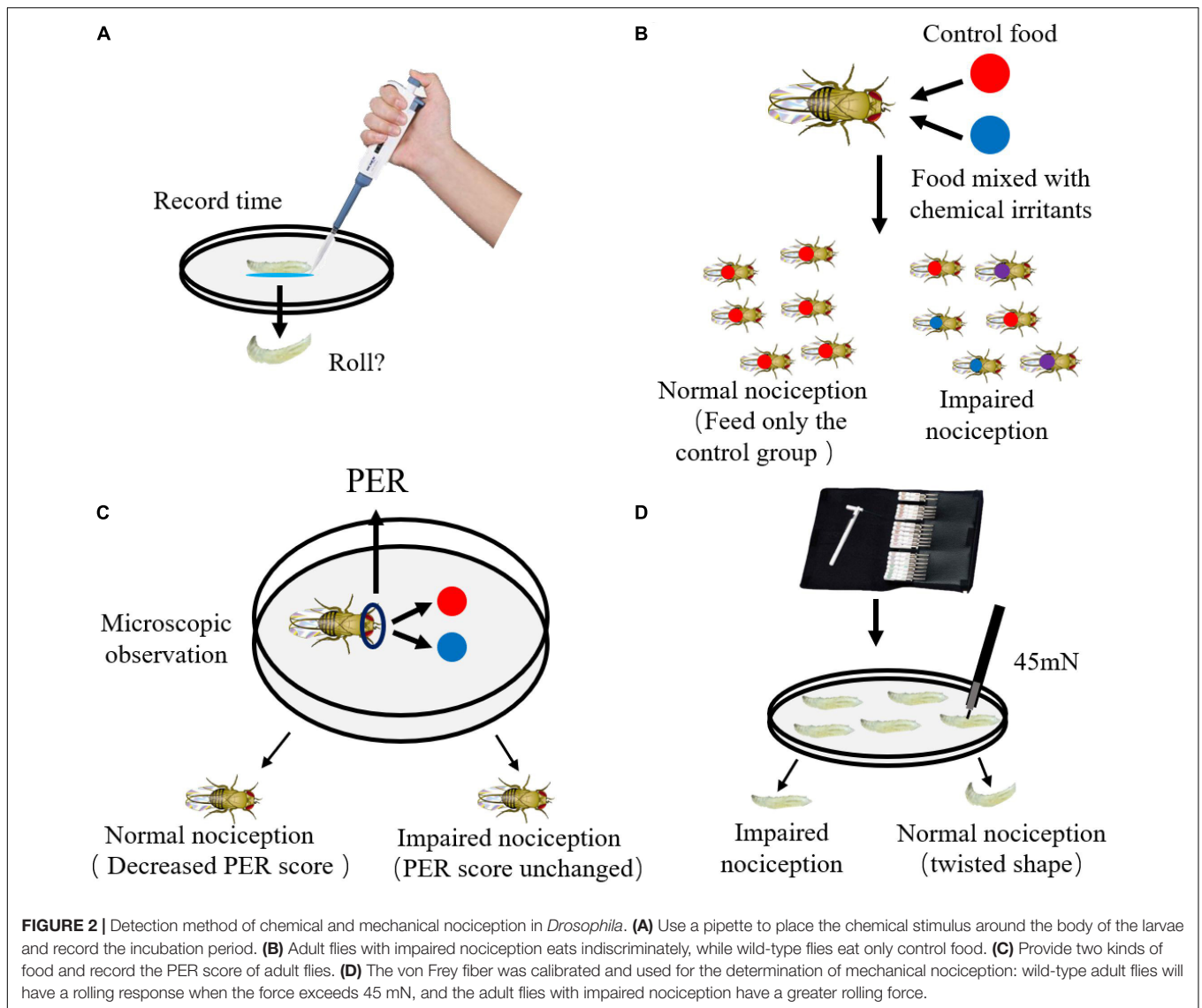


(Lopez-Bellido et al., 2019). As the concentration of the solution increases, the incubation period will become shorter and shorter. Another way to determine chemical stimulation is to test food choice, flies can make choice between control food and food with chemical irritants at the same time, and the chemical irritants can be increased in dose (Figure 2B). The control food is marked with red dye, and the food with chemical stimulus is marked with blue dye. The abdomen of wild-type flies will show a single red color, while the abdomen of mutant flies will show three colors, red, blue, and purple (two groups of food eat at the same time) (Al-Anzi et al., 2006). A method similar to the above method is to use the *Drosophila*'s proboscis extension response (PER) as an indicator of whether flies eat (Figure 2C). PER is judged based on the reaction of the nose of hungry flies when they eat normal food. Adding chemical stimulants to food will reduce the PER score of wild-type flies (Al-Anzi et al., 2006; Kang et al., 2010).

The noxious rolling response of fruit flies to harmful mechanical damage is produced by stimulating von Frey fibers in a petri dish (Figure 2D; Tracey et al., 2003). The mechanical stimulation is provided by the calibrated von Frey fiber, the larvae are less active, and the noxious response is easy to evaluate, so this method is not easy to be applied to the adult mechanical damage study. First, pour clean water into a petri dish with agar so that

the animals can crawl and perform rolling behaviors freely. The larvae will pause their normal feeding behavior when touched. Normal larvae elicit a rigid rolling response when subjected to a force of 45 mN von Frey fibers (Tracey et al., 2003; Hoyer et al., 2018), and painless mutant larvae appeared only spiral coiling until the stimulation increased to 100 mN (Tracey et al., 2003). This method has been improved recently. The von Frey fiber is replaced with a custom-made metal Nitinol (Nitinol) wire probe that detects mechanical damage (Hoyer et al., 2018).

Optogenetics is a powerful tool that enables spatiotemporal control of neuronal activity and circuits in behaving animals. Optogenetic nociception assay is widely used in *Drosophila* fly larvae (Hwang et al., 2007; Honjo et al., 2012; Dannhauser et al., 2020). The optogenetic technique with ChR2::YFP is developed and used to demonstrate the md neurons are nociceptive sensory neurons whose activation is sufficient to trigger larval nocifensive escape locomotion (Hwang et al., 2007; Honjo et al., 2012). Briefly, virgin female flies of the GAL4 driver strain that target md neurons are crossed to male flies of the UAS-ChR2::YFP strain. The larval progeny are allowed to develop and feed on the yeast paste (either atr+ or atr-) for 4 days. For behavioral analysis, the larvae are transferred to plastic Petri dishes and then stimulated



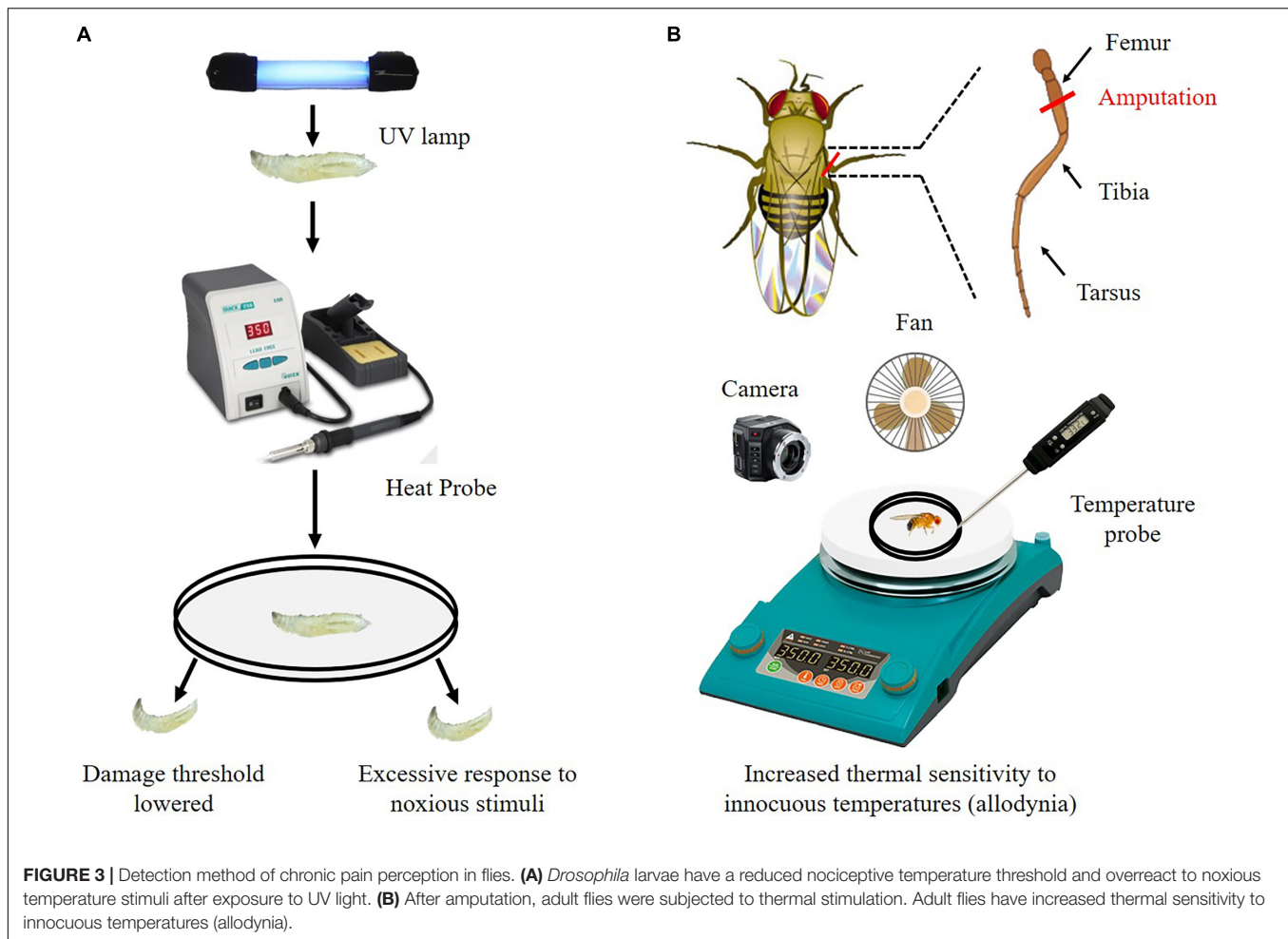
with blue light (460–500 nm). Blue light pulses are manually controlled and lasted for several seconds. Nocifensive roll and nocifensive escape locomotion are videotaped and analyzed. This model can be used to dissect the molecular mechanisms that sensitize responses of nociceptors and nociception behaviors (Honjo and Tracey, 2018).

Chronic Pain Perception in Flies

The above mentioned methods are mainly used to study acute nociception. Acute nociception is often caused by noxious stimuli, which usually protect the animal body from possible harm (Bell, 2018). Chronic pain results from maladaptive changes to this nociceptive system and persists even after the healing process is complete (Voscopoulos and Lema, 2010). Much of what is currently involved in the study of chronic pain in *Drosophila* flies is caused by nerve damage and inflammation following noxious stimuli, which can lead to hyperalgesia (increased sensitivity

to noxious stimuli) and allodynia (perceives innocuous stimuli as noxious) (Hamoudi et al., 2018; Khuong et al., 2019).

The chronic pain perception has been explored in larvae for several years. The researchers used ultraviolet (UV) light to induce tissue damage in fruit fly larvae, and then used thermal probes to demonstrate that the tissue-damaged fruit fly larvae developed allodynia and hyperalgesia (Figure 3A; Babcock et al., 2009). Briefly, the 3rd instar larvae are anesthetized with diethyl ether. Anesthetized larvae are then placed dorsal side up on a microscope slide using two-sided tape and subjected to (mJ/cm²) of UV irradiation. After UV exposure, larvae are gently rinsed and placed in a vial containing fly food for 24 h at 25°C. Then larvae are stimulated using a thermal probe. The temperature of thermal probe is set to 41°C to measure for allodynia, and 45°C to detect normal nociception. Withdrawal latency is recorded. After exposure to UV light, injured larvae exhibit heightened behavioral responses to both sub-noxious and noxious stimuli,



which suggest that this model serves to effectively investigate both allodynia and hyperalgesia (Babcock et al., 2009; McParland et al., 2021). Using this model, the Hedgehog (Hh), Bone Morphogenetic Protein (BMP), Tumor Necrosis Factor alpha (TNF- α), and Tackysin (Tk) signaling pathway are found to regulate nociceptive sensitization in response to injury in flies (Babcock et al., 2009; Im et al., 2015; McParland et al., 2021).

A novel adult fly model is developed for a chronic pain analysis process that adult flies show an increase response to a normally threshold temperature (allodynia) after they underwent a leg amputation surgery (Khuong et al., 2019; Massingham et al., 2021). Briefly, the right middle leg of adult fly is amputated at the femur segment using vannas scissors. After amputation, adult flies are fed individually in the vial containing fly food for 7 days. Then, flies are allowed to acclimate to the test chamber on a heating plate. The temperature of the heating plate is raised from 25 to 50°C over 3 min. A video recording camera positioned above the apparatus is used to record observations of flies. Jumping behavior and speed of movement are calculated according to the recorded videos (Figure 3B). This method allows for individualized analysis of allodynia and hyperalgesia.

In general, the current methods used to study the nociception of *Drosophila* flies are simple and easy to operate, and the equipment is extremely accessible. This makes it easier for researchers to investigate the genetics of acute and chronic pain in human using these tools and assays.

DEVELOPMENT OF ANTI-PAIN DRUG USING *DROSOPHILA* MODELS

Drosophila melanogaster are typically used for genetic studies but they also could be employed for drug discovery process (Lee and Min, 2019). The advantages of *D. melanogaster* qualified for drugs screening include the low cost of maintenance, the high reproductive capacity of propagation, and the rapidity of screening studies in the fly compared with traditional rat-based models. It places a high value on investigating new analgesics, especially, with evaluated conserved pain genes, responses and nature of nociception in parallel to human (Manev et al., 2003). Drugs can be delivered to the fruit fly by the following ways such as presented as a vapor (e.g., ethanol and cocaine) (McClung and Hirsh, 1998); either in the food or in the form of a filter

paper from sucrose/drug-saturated (Nichols et al., 2002); drug can also be injected or dropped directly onto the exposed nerve cord of flies, of which have been decapitated (Torres and Horowitz, 1998); drugs injected into the abdomen where it quickly diffuses throughout the whole organism can also be available for a valid alternative (Dzitoyeva et al., 2003). In addition, the ability to perform high-throughput screening in flies through random mutation or targeted RNAi-mediated knockdown can further facilitate the identification of new drugs or drug targets (Bell et al., 2009).

Thus, the *Drosophila* fly model for screening putative analgesics appears to be beneficial for the discovery of new drugs. Currently, more and more researchers use fruit flies for pharmacological pain research. Discussions of pain in animals inevitably lead to anthropomorphic references. From a practical standpoint, the animal's response to noxious stimuli and the ability of drug therapy to attenuate this response are important aspects of pain research. Excitation of gamma-aminobutyric acid B (GABA_B) receptors by injecting agonist 3-aminopropyl-(methyl) phosphinic acid (3-APMPA) significantly prolong latency to heat response in adult flies, and the threshold for heat avoidance enhanced as the injected 3-APMPA concentration increase (Dzitoyeva et al., 2003; Manev and Dimitrijevic, 2004). The peptide Tv1 from *Terebra variegata* has an antinociceptive effect in adult flies, in which injection of Tv1 significantly reduces fly sensitivity to noxious heat (Eriksson et al., 2018). Three analogs of anesthetics (enflurane, isoflurane, and desflurane) can act at a same target as halothane, and decrease the sensitivity to avoid heat in flies that exposed to the heating induced by an intense beam of light (Campbell and Nash, 1994). Paclitaxel as a common chemotherapeutics against cancer can lead to chronic nociception. Consistently, paclitaxel exposure on the fruit fly larval nociception system result in a robust and dose-dependent increase in aversive escape response during a noxious thermal stimulus (Hamoudi et al., 2018). Paclitaxel has also been reported to be toxic in somatic cells, and causes loss of axons in peripheral nerves in *Drosophila* flies (Cunha et al., 2001).

REFERENCES

- Adams, C. M., Anderson, M. G., Motto, D. G., Price, M. P., Johnson, W. A., and Welsh, M. J. (1998). Ripped pocket and pickpocket, novel *Drosophila* DEG/ENAC subunits expressed in early development and in mechanosensory neurons. *J. Cell Biol.* 140, 143–152. doi: 10.1083/jcb.140.1.143
- Al-Anzi, B., Tracey, W. J., and Benzer, S. (2006). Response of *Drosophila* to wasabi is mediated by painless, the fly homolog of mammalian TRPA1/ANKTM1. *Curr. Biol.* 16, 1034–1040. doi: 10.1016/j.cub.2006.04.002
- Aldrich, B. T., Kasuya, J., Faron, M., Ishimoto, H., and Kitamoto, T. (2010). The amnesiac gene is involved in the regulation of thermal nociception in *Drosophila melanogaster*. *J. Neurogenet.* 24, 33–41. doi: 10.1019/01677060903419751
- Babcock, D. T., Landry, C., and Galko, M. J. (2009). Cytokine signaling mediates UV-induced nociceptive sensitization in *Drosophila* larvae. *Curr. Biol.* 19, 799–806. doi: 10.1016/j.cub.2009.03.062
- Babcock, D. T., Shi, S., Jo, J., Shaw, M., Gutstein, H. B., and Galko, M. J. (2011). Hedgehog signaling regulates nociceptive sensitization. *Curr. Biol.* 21, 1525–1533. doi: 10.1016/j.cub.2011.08.020

CONCLUDING THOUGHTS

As briefly addressed above, there have been several published work in which the fly have been displayed key features that an alternate option biology and physiology, even functional pain genes are well conserved from the fly to humans. The fruit fly applied for pain genomics and pharmacogenomics are devoted in the validation of primary small molecule, the research of the target discovery and the selection of high-throughput screening. However, many factors may participate in pain processes including change of extracellular microenvironment and break of balance in extracellular matrix metabolism, which are never discussed in flies. Pain-like emotions generated by motivational mechanisms are impossible to answer conclusively in flies. As for studies of painkillers in fly, the pharmacological action, the side effects and the best drug-delivery way have not been discussed as to whether they work as well in humans. Although the status of *Drosophila* as a pain research model is still somewhat different from that of mammals, its potential as a pain research model is being further explored, and its entry into the field of pain research may help reduce the pressure on mammals *in vivo*.

AUTHOR CONTRIBUTIONS

JH, BL, SH, YZ, and KL: writing. MX and YL: manuscript editing. All authors contributed to the article and approved the submitted version.

FUNDING

This work received financial support from the National Natural Science Foundation of China (Nos. 82104562 and 82004228), “Double First Class” Scientific Research Key Project in Gansu (No. GSSYLXM-05), and Gansu Planning Projects on Science and Technology (No. 20JR10RA332).

- Bagriantsev, S. N., Gracheva, E. O., and Gallagher, P. G. (2014). Piezo proteins: regulators of mechanosensation and other cellular processes. *J. Biol. Chem.* 289, 31673–31681. doi: 10.1074/jbc.R114.612697
- Bamps, D., Vriens, J., de Hoon, J., and Voets, T. (2021). TRP channel cooperation for nociception: therapeutic opportunities. *Annu. Rev. Pharmacol. Toxicol.* 61, 655–677. doi: 10.1146/annurev-pharmtox-010919-023238
- Bandell, M., Story, G. M., Hwang, S. W., Viswanath, V., Eid, S. R., Petrus, M. J., et al. (2004). Noxious cold ion channel TRPA1 is activated by pungent compounds and bradykinin. *Neuron* 41, 849–857. doi: 10.1016/s0896-6273(04)00150-3
- Bautista, D. M., Jordt, S. E., Nikai, T., Tsuruda, P. R., Read, A. J., Poblete, J., et al. (2006). TRPA1 mediates the inflammatory actions of environmental irritants and proalgesic agents. *Cell* 124, 1269–1282. doi: 10.1016/j.cell.2006.02.023
- Bell, A. (2018). The neurobiology of acute pain. *Vet. J.* 237, 55–62. doi: 10.1016/j.tvjl.2018.05.004
- Bell, A. J., McBride, S. M. J., and Dockendorff, T. C. (2009). Flies as the ointment *Drosophila* modeling to enhance drug discovery. *Fly* 3, 39–49. doi: 10.4161/fly.3.1.7774
- Bellemer, A. (2015). Thermotaxis, circadian rhythms, and TRP channels in *Drosophila*. *Temperature (Austin)* 2, 227–243. doi: 10.1080/23328940.2015.1004972

- Benzer, S. (1967). Behavioral mutants of *Drosophila* isolated by countercurrent distribution. *Proc. Natl. Acad. Sci. U.S.A.* 58, 1112–1119. doi: 10.1073/pnas.58.3.1112
- Bier, E. (2005). *Drosophila*, the golden bug, emerges as a tool for human genetics. *Nat. Rev. Genet.* 6, 9–23. doi: 10.1038/nrg1503
- Boonen, B., Startek, J. B., Milici, A., Lopez-Requena, A., Beelen, M., Callaerts, P., et al. (2021). Activation of *Drosophila melanogaster* TRPA1 Isoforms by citronellal and menthol. *Int. J. Mol. Sci.* 22:10997. doi: 10.3390/ijms222010997
- Bourne, S., Machado, A. G., and Nagel, S. J. (2014). Basic anatomy and physiology of pain pathways. *Neurosurg. Clin. N. Am.* 25, 629–638. doi: 10.1016/j.nec.2014.06.001
- Burgos, A., Honjo, K., Ohyama, T., Qian, C. S., Shin, G. J., Gohl, D. M., et al. (2018). Nociceptive interneurons control modular motor pathways to promote escape behavior in *Drosophila*. *eLife* 7:e26016. doi: 10.7554/eLife.26016
- Busto, G. U., Cervantes-Sandoval, I., and Davis, R. L. (2010). Olfactory learning in *Drosophila*. *Physiology (Bethesda)* 25, 338–346. doi: 10.1152/physiol.00026.2010
- Campbell, D. B., and Nash, H. A. (1994). Use of *Drosophila* mutants to distinguish among volatile general anesthetics. *Proc. Natl. Acad. Sci. U.S.A.* 91, 2135–2139. doi: 10.1073/pnas.91.6.2135
- Caterina, M. J., Leffler, A., Malmberg, A. B., Martin, W. J., Trafton, J., Petersen-Zeit, K. R., et al. (2000). Impaired nociception and pain sensation in mice lacking the capsaicin receptor. *Science* 288, 306–313. doi: 10.1126/science.288.5464.306
- Cheng, L. E., Song, W., Looger, L. L., Jan, L. Y., and Jan, Y. N. (2010). The role of the TRP channel NompC in *Drosophila larval* and adult locomotion. *Neuron* 67, 373–380. doi: 10.1016/j.neuron.2010.07.004
- Chien, S., Reiter, L. T., Bier, E., and Gribskov, M. (2002). Homophila: human disease gene cognates in *Drosophila*. *Nucleic Acids Res.* 30, 149–151. doi: 10.1093/nar/30.1.149
- Clapham, D. E., Runnels, L. W., and Strubing, C. (2001). The TRP ion channel family. *Nat. Rev. Neurosci.* 2, 387–396. doi: 10.1038/35077544
- Corey, D. P., Garcia-Anoveros, J., Holt, J. R., Kwan, K. Y., Lin, S. Y., Vollrath, M. A., et al. (2004). TRPA1 is a candidate for the mechanosensitive transduction channel of vertebrate hair cells. *Nature* 432, 723–730. doi: 10.1038/nature03066
- Cosens, D. J., and Manning, A. (1969). Abnormal electroretinogram from a *Drosophila* mutant. *Nature* 224, 285–287. doi: 10.1038/224285a0
- Coste, B., Mathur, J., Schmidt, M., Earley, T. J., Ranade, S., Petrus, M. J., et al. (2010). Piezo1 and Piezo2 are essential components of distinct mechanically activated cation channels. *Science* 330, 55–60. doi: 10.1126/science.1193270
- Coste, B., Xiao, B., Santos, J. S., Syeda, R., Grandl, J., Spencer, K. S., et al. (2012). Piezo proteins are pore-forming subunits of mechanically activated channels. *Nature* 483, 176–181. doi: 10.1038/nature10812
- Costigan, M., Scholz, J., and Woolf, C. J. (2009). Neuropathic pain: a maladaptive response of the nervous system to damage. *Annu. Rev. Neurosci.* 32, 1–32. doi: 10.1146/annurev.neuro.051508.135531
- Cunha, K. S., Reguly, M. L., Graf, U., and de Andrade, H. (2001). Taxanes: the genetic toxicity of paclitaxel and docetaxel in somatic cells of *Drosophila melanogaster*. *Mutagenesis* 16, 79–84. doi: 10.1093/mutage/16.1.79
- Dai, Y. (2016). TRPs and pain. *Semin. Immunopathol.* 38, 277–291. doi: 10.1007/s00281-015-0526-0
- Dannhauser, S., Lux, T. J., Hu, C., Selcho, M., Chen, J. T., Ehmann, N., et al. (2020). Antinociceptive modulation by the adhesion GPCR C1RL promotes mechanosensory signal discrimination. *eLife* 9:e56738. doi: 10.7554/eLife.56738
- Davis, J. B., Gray, J., Gunthorpe, M. J., Hatcher, J. P., Davey, P. T., Overend, P., et al. (2000). Vanilloid receptor-1 is essential for inflammatory thermal hyperalgesia. *Nature* 405, 183–187. doi: 10.1038/35012076
- Del, C. D., Murphy, S., Heiry, M., Barrett, L. B., Earley, T. J., Cook, C. A., et al. (2010). TRPA1 contributes to cold hypersensitivity. *J. Neurosci.* 30, 15165–15174. doi: 10.1523/JNEUROSCI.2580-10.2010
- Di Meglio, S., Tramontano, F., Cimmino, G., Jones, R., and Quesada, P. (2004). Dual role for poly(ADP-ribose)polymerase-1 and -2 and poly(ADP-ribose)glycohydrolase as DNA-repair and pro-apoptotic factors in rat germinal cells exposed to nitric oxide donors. *Biochim. Biophys. Acta* 1692, 35–44. doi: 10.1016/j.bbamcr.2004.04.002
- Dzitoyeva, S., Dimitrijevic, N., and Manev, H. (2003). Gamma-aminobutyric acid B receptor 1 mediates behavior-impairing actions of alcohol in *Drosophila*: adult RNA interference and pharmacological evidence. *Proc. Natl. Acad. Sci. U.S.A.* 100, 5485–5490. doi: 10.1073/pnas.0830111100
- Eisfeld, J., and Luckhoff, A. (2007). Trpm2. *Handb. Exp. Pharmacol.* 179, 237–252. doi: 10.1007/978-3-540-34891-7_14
- Enomoto, M., Siow, C., and Igaki, T. (2018). *Drosophila* as a cancer model. *Adv. Exp. Med. Biol.* 1076, 173–194. doi: 10.1007/978-981-13-0529-0_10
- Eriksson, A., Anand, P., Gorson, J., Griju, C., Hadelia, E., Stewart, J. C., et al. (2018). Using *Drosophila* behavioral assays to characterize terebrid venom-peptide bioactivity. *Sci. Rep.* 8:15276. doi: 10.1038/s41598-018-33215-2
- Faouzi, M., and Penner, R. (2014). Trpm2. *Handb. Exp. Pharmacol.* 222, 403–426. doi: 10.1007/978-3-642-54215-2_16
- Flood, T. F., Gorczyca, M., White, B. H., Ito, K., and Yoshihara, M. (2013). A large-scale behavioral screen to identify neurons controlling motor programs in the *Drosophila* brain. *G3 (Bethesda)* 3, 1629–1637. doi: 10.1534/g3.113.006205
- Fortini, M. E., Skupski, M. P., Boguski, M. S., and Hariharan, I. K. (2000). A survey of human disease gene counterparts in the *Drosophila* genome. *J. Cell Biol.* 150, F23–F30. doi: 10.1083/jcb.150.2.f23
- Fowler, M. A., and Montell, C. (2013). *Drosophila* TRP channels and animal behavior. *Life Sci.* 92, 394–403. doi: 10.1016/j.lfs.2012.07.029
- Gao, F. B., Brenman, J. E., Jan, L. Y., and Jan, Y. N. (1999). Genes regulating dendritic outgrowth, branching, and routing in *Drosophila*. *Genes Dev.* 13, 2549–2561. doi: 10.1101/gad.13.19.2549
- Gees, M., Owsianik, G., Nilius, B., and Voets, T. (2012). TRP channels. *Compr. Physiol.* 2, 563–608. doi: 10.1002/cphy.c110026
- Gjelsvik, K. J., Follansbee, T. L., and Ganter, G. K. (2018). Bone Morphogenetic Protein Glass Bottom Boat (BMP5/6/7/8) and its receptor Wishful Thinking (BMPRII) are required for injury-induced allodynia in *Drosophila*. *Mol. Pain* 14:2070360817. doi: 10.1177/1744806918802703
- Glare, P., Aubrey, K. R., and Myles, P. S. (2019). Transition from acute to chronic pain after surgery. *Lancet* 393, 1537–1546. doi: 10.1016/S0140-6736(19)30352-6
- Goodman, M. B. (2003). Sensation is painless. *Trends Neurosci.* 26, 643–645. doi: 10.1016/j.tins.2003.09.013
- Gorczyca, D. A., Younger, S., Meltzer, S., Kim, S. E., Cheng, L., Song, W., et al. (2014). Identification of ppk26, a DEG/ENAC channel functioning with ppk1 in a mutually dependent manner to guide locomotion behavior in *Drosophila*. *Cell Rep.* 9, 1446–1458. doi: 10.1016/j.celrep.2014.10.034
- Grueber, W. B., Jan, L. Y., and Jan, Y. N. (2002). Tiling of the *Drosophila* epidermis by multidendritic sensory neurons. *Development* 129, 2867–2878. doi: 10.1242/dev.129.12.2867
- Grueber, W. B., Ye, B., Moore, A. W., Jan, L. Y., and Jan, Y. N. (2003). Dendrites of distinct classes of *Drosophila* sensory neurons show different capacities for homotypic repulsion. *Curr. Biol.* 13, 618–626. doi: 10.1016/s0960-9822(03)00207-0
- Grueber, W. B., Ye, B., Yang, C. H., Younger, S., Borden, K., Jan, L. Y., et al. (2007). Projections of *Drosophila* multidendritic neurons in the central nervous system: links with peripheral dendrite morphology. *Development* 134, 55–64. doi: 10.1242/dev.02666
- Guo, Y., Wang, Y., Wang, Q., and Wang, Z. (2014). The role of PPK26 in *Drosophila larval* mechanical nociception. *Cell Rep.* 9, 1183–1190. doi: 10.1016/j.celrep.2014.10.020
- Haanpää, M., Attal, N., Backonja, M., Baron, R., Bennett, M., Bouhassira, D., et al. (2011). NeuPSIG guidelines on neuropathic pain assessment. *Pain* 152, 14–27. doi: 10.1016/j.pain.2010.07.031
- Hamada, F. N., Rosenzweig, M., Kang, K., Pulver, S. R., Ghezzi, A., Jegla, T. J., et al. (2008). An internal thermal sensor controlling temperature preference in *Drosophila*. *Nature* 454, 217–220. doi: 10.1038/nature07001
- Hamoudi, Z., Khuong, T. M., Cole, T., and Neely, G. G. (2018). A fruit fly model for studying paclitaxel-induced peripheral neuropathy and hyperalgesia. *F1000Res* 7:99. doi: 10.12688/f1000research.13581.2
- Hehlert, P., Zhang, W., and Gopfert, M. C. (2021). *Drosophila* mechanosensory transduction. *Trends Neurosci.* 44, 323–335. doi: 10.1016/j.tins.2020.11.001
- Himmel, N. J., and Cox, D. N. (2017). Sensing the cold: TRP channels in thermal nociception. *Channels (Austin)* 11, 370–372. doi: 10.1080/19336950.2017.1336401
- Honjo, K., Hwang, R. Y., and Tracey, W. J. (2012). Optogenetic manipulation of neural circuits and behavior in *Drosophila larvae*. *Nat. Protoc.* 7, 1470–1478. doi: 10.1038/nprot.2012.079

- Honjo, K., and Tracey, W. J. (2018). BMP signaling downstream of the Highwire E3 ligase sensitizes nociceptors. *PLoS Genet.* 14:e1007464. doi: 10.1371/journal.pgen.1007464
- Hoyer, N., Petersen, M., Tenedini, F., and Soba, P. (2018). Assaying mechanonociceptive behavior in *Drosophila* larvae. *Bio Protoc.* 8, e2736. doi: 10.21769/BioProtoc.2736
- Hu, Y., Wang, Z., Liu, T., and Zhang, W. (2019). Piezo-like gene regulates locomotion in *Drosophila* larvae. *Cell Rep.* 26, 1369–1377. doi: 10.1016/j.celrep.2019.01.055
- Hung, C. Y., and Tan, C. H. (2018). TRP channels in nociception and pathological pain. *Adv. Exp. Med. Biol.* 1099, 13–27. doi: 10.1007/978-981-13-1756-9_2
- Hwang, R. Y., Stearns, N. A., and Tracey, W. D. (2012). The ankyrin repeat domain of the TRPA protein painless is important for thermal nociception but not mechanical nociception. *PLoS One* 7:e30090. doi: 10.1371/journal.pone.0030090
- Hwang, R. Y., Zhong, L., Xu, Y., Johnson, T., Zhang, F., Deisseroth, K., et al. (2007). Nociceptive neurons protect *Drosophila* larvae from parasitoid wasps. *Curr. Biol.* 17, 2105–2116. doi: 10.1016/j.cub.2007.11.029
- Hwang, S. W., and Oh, U. (2007). Current concepts of nociception: nociceptive molecular sensors in sensory neurons. *Curr. Opin. Anaesthesiol.* 20, 427–434. doi: 10.1097/ACO.0b013e3282eff91c
- Im, S. H., Takle, K., Jo, J., Babcock, D. T., Ma, Z., Xiang, Y., et al. (2015). Tachykinin acts upstream of autocrine Hedgehog signaling during nociceptive sensitization in *Drosophila*. *eLife* 4:e10735. doi: 10.7554/eLife.10735
- Im, S. H., and Galko, M. J. (2012). Pokes, sunburn, and hot sauce: *Drosophila* as an emerging model for the biology of nociception. *Dev. Dyn.* 241, 16–26. doi: 10.1002/dvdy.22737
- Immke, D. C., and Gava, N. R. (2006). The TRPV1 receptor and nociception. *Semin. Cell Dev. Biol.* 17, 582–591. doi: 10.1016/j.semcdb.2006.09.004
- Jang, W., Lee, S., Choi, S. I., Chae, H. S., Han, J., Jo, H., et al. (2019). Impairment of proprioceptive movement and mechanical nociception in *Drosophila melanogaster* larvae lacking Ppk30, a *Drosophila* member of the Degenerin/Epithelial Sodium Channel family. *Genes Brain Behav.* 18:e12545. doi: 10.1111/gbb.12545
- Julius, D. (2013). TRP channels and pain. *Annu. Rev. Cell Dev. Biol.* 29, 355–384. doi: 10.1146/annurev-cellbio-101011-155833
- Kang, K., Pulver, S. R., Panzano, V. C., Chang, E. C., Griffith, L. C., Theobald, D. L., et al. (2010). Analysis of *Drosophila* TRPA1 reveals an ancient origin for human chemical nociception. *Nature* 464, 597–600. doi: 10.1038/nature08848
- Karashima, Y., Talavera, K., Everaerts, W., Janssens, A., Kwan, K. Y., Vennekens, R., et al. (2009). TRPA1 acts as a cold sensor *in vitro* and *in vivo*. *Proc. Natl. Acad. Sci. U.S.A.* 106, 1273–1278. doi: 10.1073/pnas.0808487106
- Kernan, M., Cowan, D., and Zuker, C. (1994). Genetic dissection of mechanosensory transduction: mechanoreception-defective mutations of *Drosophila*. *Neuron* 12, 1195–1206. doi: 10.1016/0896-6273(94)90437-5
- Kernan, M. J. (2007). Mechanotransduction and auditory transduction in *Drosophila*. *Pflügers Arch.* 454, 703–720. doi: 10.1007/s00424-007-0263-x
- Khuong, T. M., Wang, Q. P., Manion, J., Oyston, L. J., Lau, M. T., Towler, H., et al. (2019). Nerve injury drives a heightened state of vigilance and neuropathic sensitization in *Drosophila*. *Sci. Adv.* 5:e4099. doi: 10.1126/sciadv.aaw4099
- Khuong, T. M., and Neely, G. G. (2013). Conserved systems and functional genomic assessment of nociception. *FEBS J.* 280, 5298–5306. doi: 10.1111/febs.12464
- Kim, S. E., Coste, B., Chadha, A., Cook, B., and Patapoutian, A. (2012). The role of *Drosophila* Piezo in mechanical nociception. *Nature* 483, 209–212. doi: 10.1038/nature10801
- Kim, S. H., Lee, Y., Akitake, B., Woodward, O. M., Guggino, W. B., and Montell, C. (2010). *Drosophila* TRPA1 channel mediates chemical avoidance in gustatory receptor neurons. *Proc. Natl. Acad. Sci. U.S.A.* 107, 8440–8445. doi: 10.1073/pnas.1001425107
- Kolisek, M., Beck, A., Fleig, A., and Penner, R. (2005). Cyclic ADP-ribose and hydrogen peroxide synergize with ADP-ribose in the activation of TRPM2 channels. *Mol. Cell* 18, 61–69. doi: 10.1016/j.molcel.2005.02.033
- Kwan, K. Y., Allchorne, A. J., Vollrath, M. A., Christensen, A. P., Zhang, D. S., Woolf, C. J., et al. (2006). TRPA1 contributes to cold, mechanical, and chemical nociception but is not essential for hair-cell transduction. *Neuron* 50, 277–289. doi: 10.1016/j.neuron.2006.03.042
- Kwan, K. Y., and Corey, D. P. (2009). Burning cold: involvement of TRPA1 in noxious cold sensation. *J. Gen. Physiol.* 133, 251–256. doi: 10.1085/jgp.200810146
- Kwon, Y., Shim, H. S., Wang, X., and Montell, C. (2008). Control of thermotactic behavior via coupling of a TRP channel to a phospholipase C signaling cascade. *Nat. Neurosci.* 11, 871–873. doi: 10.1038/nn.2170
- Laursen, W. J., Anderson, E. O., Hoffstaetter, L. J., Bagriantsev, S. N., and Gracheva, E. O. (2015). Species-specific temperature sensitivity of TRPA1. *Temperature (Austin)* 2, 214–226. doi: 10.1080/23328940.2014.1000702
- Lee, H., Naughton, N. N., Woods, J. H., and Ko, M. C. (2007). Effects of butorphanol on morphine-induced itch and analgesia in primates. *Anesthesiology* 107, 478–485. doi: 10.1097/01.anes.0000278876.20263.a7
- Lee, S., and Min, K. (2019). *Drosophila melanogaster* as a model system in the study of pharmacological interventions in aging. *Transl. Med. Aging* 3, 98–103. doi: 10.1016/j.tma.2019.09.004
- Lee, Y., Lee, Y., Lee, J., Bang, S., Hyun, S., Kang, J., et al. (2005). Pyrexia is a new thermal transient receptor potential channel endowing tolerance to high temperatures in *Drosophila melanogaster*. *Nat. Genet.* 37, 305–310. doi: 10.1038/ng1513
- Leung, C., Wilson, Y., Khuong, T. M., and Neely, G. G. (2013). Fruit flies as a powerful model to drive or validate pain genomics efforts. *Pharmacogenomics* 14, 1879–1887. doi: 10.2217/pgs.13.196
- Lewis, A. H., Cui, A. F., McDonald, M. F., and Grandl, J. (2017). Transduction of repetitive mechanical stimuli by piezo1 and piezo2 ion channels. *Cell Rep.* 19, 2572–2585. doi: 10.1016/j.celrep.2017.05.079
- Li, H. (2017). TRP channel classification. *Adv. Exp. Med. Biol.* 976, 1–8. doi: 10.1007/978-94-024-1088-4_1
- Li, Y., Bai, P., Wei, L., Kang, R., Chen, L., Zhang, M., et al. (2020). Capsaicin functions as *Drosophila* ovipositional repellent and causes intestinal dysplasia. *Sci. Rep.* 10:9963. doi: 10.1038/s41598-020-66900-2
- Liedtke, W. (2007). TRPV channels' role in osmotransduction and mechanotransduction. *Handb. Exp. Pharmacol.* 179, 473–487. doi: 10.1007/978-3-540-34891-7_28
- Liu, L., Yermolaeva, O., Johnson, W. A., Abboud, F. M., and Welsh, M. J. (2003). Identification and function of thermosensory neurons in *Drosophila* larvae. *Nat. Neurosci.* 6, 267–273. doi: 10.1038/nn1009
- Logashina, Y. A., Korolkova, Y. V., Kozlov, S. A., and Andreev, Y. A. (2019). TRPA1 channel as a regulator of neurogenic inflammation and pain: structure, function, role in pathophysiology, and therapeutic potential of ligands. *Biochemistry (Mosc)* 84, 101–118. doi: 10.1134/S0006297919020020
- Lopez-Bellido, R., Himmel, N. J., Gutstein, H. B., Cox, D. N., and Galko, M. J. (2019). An assay for chemical nociception in *Drosophila* larvae. *Philos. Trans. R. Soc. Lond. B Biol. Sci.* 374:20190282. doi: 10.1098/rstb.2019.0282
- Luo, J., Shen, W. L., and Montell, C. (2017). TRPA1 mediates sensation of the rate of temperature change in *Drosophila* larvae. *Nat. Neurosci.* 20, 34–41. doi: 10.1038/nn.4416
- Luo, X., Huh, Y., Bang, S., He, Q., Zhang, L., Matsuda, M., et al. (2019). Macrophage toll-like receptor 9 contributes to Chemotherapy-Induced neuropathic pain in male mice. *J. Neurosci.* 39, 6848–6864. doi: 10.1523/JNEUROSCI.3257-18.2019
- Ma, W., and Quirion, R. (2007). Inflammatory mediators modulating the transient receptor potential vanilloid 1 receptor: therapeutic targets to treat inflammatory and neuropathic pain. *Expert Opin. Ther. Targets* 11, 307–320. doi: 10.1517/14728222.11.3.307
- Maiese, K. (2017). Warming up to new possibilities with the capsaicin receptor TRPV1: MTOR, AMPK, and erythropoietin. *Curr. Neurovasc. Res.* 14, 184–189. doi: 10.2174/1567202614666170313105337
- Malafoglia, V., Bryant, B., Raffaelli, W., Giordano, A., and Bellipanni, G. (2013). The zebrafish as a model for nociception studies. *J. Cell Physiol.* 228, 1956–1966. doi: 10.1002/jcp.24379
- Mandel, S. J., Shoaf, M. L., Braco, J. T., Silver, W. L., and Johnson, E. C. (2018). Behavioral aversion to AITC requires both painless and dTRPA1 in *Drosophila*. *Front. Neural Circuits* 12:45. doi: 10.3389/fncir.2018.00045
- Manev, H., Dimitrijevic, N., and Dzitoyeva, S. (2003). Techniques: fruit flies as models for neuropharmacological research. *Trends Pharmacol. Sci.* 24, 41–43. doi: 10.1016/S0165-6147(02)00004-4

- Manev, H., and Dimitrijevic, N. (2004). *Drosophila* model for *in vivo* pharmacological analgesia research. *Eur. J. Pharmacol.* 491, 207–208. doi: 10.1016/j.ejphar.2004.03.030
- Massingham, J. N., Baron, O., and Neely, G. G. (2021). Evaluating baseline and sensitised heat nociception in adult *Drosophila*. *Bio Protoc.* 11:e4079. doi: 10.21769/BioProtoc.4079
- Mauthner, S. E., Hwang, R. Y., Lewis, A. H., Xiao, Q., Tsubouchi, A., Wang, Y., et al. (2014). Balboa binds to pickpocket *in vivo* and is required for mechanical nociception in *Drosophila* larvae. *Curr. Biol.* 24, 2920–2925. doi: 10.1016/j.cub.2014.10.038
- McClung, C., and Hirsh, J. (1998). Stereotypic behavioral responses to free-base cocaine and the development of behavioral sensitization in *Drosophila*. *Curr. Biol.* 8, 109–112. doi: 10.1016/s0960-9822(98)70041-7
- McParland, A., Moulton, J., Brann, C., Hale, C., Otis, Y., and Ganter, G. (2021). The brinker repressor system regulates injury-induced nociceptive sensitization in *Drosophila melanogaster*. *Mol. Pain* 17:794238681. doi: 10.1177/17448069211037401
- Merritt, D. J., and Whittington, P. M. (1995). Central projections of sensory neurons in the *Drosophila* embryo correlate with sensory modality, soma position, and proneural gene function. *J. Neurosci.* 15, 1755–1767. doi: 10.1523/JNEUROSCI.15-03-01755.1995
- Milinkeviciute, G., Gentile, C., and Neely, G. G. (2012). *Drosophila* as a tool for studying the conserved genetics of pain. *Clin Genet* 82, 359–366. doi: 10.1111/j.1399-0004.2012.01941.x
- Minke, B., Wu, C., and Pak, W. L. (1975). Induction of photoreceptor voltage noise in the dark in *Drosophila* mutant. *Nature* 258, 84–87. doi: 10.1038/258084a0
- Murthy, S. E., Loud, M. C., Dao, I., Marshall, K. L., Schwaller, F., Kühnemund, J., et al. (2018). The mechanosensitive ion channel Piezo2 mediates sensitivity to mechanical pain in mice. *Sci. Transl. Med.* 10:eaa9897. doi: 10.1126/scitranslmed.aat9897
- Nassini, R., Materazzi, S., Benemei, S., and Geppetti, P. (2014). The TRPA1 channel in inflammatory and neuropathic pain and migraine. *Rev. Physiol. Biochem. Pharmacol.* 167, 1–43. doi: 10.1007/112_2014_18
- Neely, G. G., Hess, A., Costigan, M., Keene, A. C., Goulas, S., Langeslag, M., et al. (2010). A genome-wide *Drosophila* screen for heat nociception identifies alpha2delta3 as an evolutionarily conserved pain gene. *Cell* 143, 628–638. doi: 10.1016/j.cell.2010.09.047
- Neely, G. G., Keene, A. C., Duchek, P., Chang, E. C., Wang, Q. P., Aksoy, Y. A., et al. (2011). TrpA1 regulates thermal nociception in *Drosophila*. *PLoS One* 6:e24343. doi: 10.1371/journal.pone.0024343
- Nichols, C. D., Ronesi, J., Pratt, W., and Sanders-Bush, E. (2002). Hallucinogens and *Drosophila*: linking serotonin receptor activation to behavior. *Neuroscience* 115, 979–984. doi: 10.1016/s0306-4522(02)00354-8
- Nilius, B., Appendino, G., and Owsianik, G. (2012). The transient receptor potential channel TRPA1: from gene to pathophysiology. *Pflugers Arch.* 464, 425–458. doi: 10.1007/s00424-012-1158-z
- Nilius, B., Owsianik, G., Voets, T., and Peters, J. A. (2007). Transient receptor potential cation channels in disease. *Physiol. Rev.* 87, 165–217. doi: 10.1152/physrev.00021.2006
- Nilius, B., Voets, T., and Peters, J. (2005). TRP channels in disease. *Sci. Stke* 2005:e8. doi: 10.1126/stke.2952005re8
- Nilius, B., and Owsianik, G. (2011). The transient receptor potential family of ion channels. *Genome Biol.* 12:218. doi: 10.1186/gb-2011-12-3-218
- Nkambeu, B., Salem, J. B., and Beaudry, F. (2020). Capsaicin and its analogues impede nocifensive response of *Caenorhabditis elegans* to noxious heat. *Neurochem. Res.* 45, 1851–1859. doi: 10.1007/s11064-020-03049-4
- Ohyama, T., Jovanic, T., Denisov, G., Dang, T. C., Hoffmann, D., Kerr, R. A., et al. (2013). High-throughput analysis of stimulus-evoked behaviors in *Drosophila* larva reveals multiple modality-specific escape strategies. *PLoS One* 8:e71706. doi: 10.1371/journal.pone.0071706
- Oswald, M., Rymarczyk, B., Chatters, A., and Sweeney, S. T. (2011). A novel thermosensitive escape behavior in *Drosophila* larvae. *Fly (Austin)* 5, 304–306. doi: 10.4161/fly.5.4.17810
- Pazienza, V., Pomara, C., Cappello, F., Calogero, R., Carrara, M., Mazzoccoli, G., et al. (2014). The TRPA1 channel is a cardiac target of mIGF-1/SIRT1 signaling. *Am. J. Physiol. Heart Circ. Physiol.* 307, H939–H944. doi: 10.1152/ajpheart.00150.2014
- Petersen, M., Tenedini, F., Hoyer, N., Kutschera, F., and Soba, P. (2018). Assaying thermo-nociceptive behavior in *Drosophila* larvae. *Biol. Protoc.* 8:e2737. doi: 10.21769/BioProtoc.2737
- Ranade, S. S., Woo, S. H., Dubin, A. E., Moshourab, R. A., Wetzel, C., Petrus, M., et al. (2014). Piezo2 is the major transducer of mechanical forces for touch sensation in mice. *Nature* 516, 121–125. doi: 10.1038/nature13980
- Rosenzweig, M., Brennan, K. M., Tayler, T. D., Phelps, P. O., Patapoutian, A., and Garrity, P. A. (2005). The *Drosophila* ortholog of vertebrate TRPA1 regulates thermotaxis. *Genes Dev.* 19, 419–424. doi: 10.1101/gad.1278205
- Sakai, T., Sato, S., Ishimoto, H., and Kitamoto, T. (2012). Significance of the centrally expressed TRP channel painless in *Drosophila* courtship memory. *Learn. Mem.* 20, 34–40. doi: 10.1101/lm.029041.112
- Sakai, T., Watanabe, K., Ohashi, H., Sato, S., Inami, S., Shimada, N., et al. (2014). Insulin-producing cells regulate the sexual receptivity through the painless TRP channel in *Drosophila* virgin females. *PLoS One* 9:e88175. doi: 10.1371/journal.pone.0088175
- Schrader, S., and Merritt, D. J. (2000). Central projections of *Drosophila* sensory neurons in the transition from embryo to larva. *J. Comp. Neurol.* 425, 34–44. doi: 10.1002/1096-9861(20000911)425:1<34::aid-cne4>3.0.co;2-g
- Servin-Vences, M. R., Moroni, M., Lewin, G. R., and Poole, K. (2017). Direct measurement of TRPV4 and PIEZO1 activity reveals multiple mechanotransduction pathways in chondrocytes. *eLife* 6:e21074. doi: 10.7554/eLife.21074
- Sneddon, L. U. (2018). Comparative physiology of nociception and pain. *Physiology (Bethesda)* 33, 63–73. doi: 10.1152/physiol.00022.2017
- Sokabe, T., and Tominaga, M. (2009). A temperature-sensitive TRP ion channel, Painless, functions as a noxious heat sensor in fruit flies. *Commun. Integr. Biol.* 2, 170–173. doi: 10.4161/cib.7708
- Song, Y., Li, D., Farrelly, O., Miles, L., Li, F., Kim, S. E., et al. (2019). The mechanosensitive ion channel piezo inhibits axon regeneration. *Neuron* 102, 373–389. doi: 10.1016/j.neuron.2019.01.050
- St, J. S. E. (2018). Advances in understanding nociception and neuropathic pain. *J. Neurol.* 265, 231–238. doi: 10.1007/s00415-017-8641-6
- Story, G. M., Peier, A. M., Reeve, A. J., Eid, S. R., Mosbacher, J., Hricik, T. R., et al. (2003). ANKTM1, a TRP-like channel expressed in nociceptive neurons, is activated by cold temperatures. *Cell* 112, 819–829. doi: 10.1016/s0092-8674(03)00158-2
- Sun, Y., Liu, L., Ben-Shahar, Y., Jacobs, J. S., Eberl, D. F., and Welsh, M. J. (2009). TRPA channels distinguish gravity sensing from hearing in Johnston's organ. *Proc. Natl. Acad. Sci. U.S.A.* 106, 13606–13611. doi: 10.1073/pnas.0906377106
- Szczot, M., Liljencrantz, J., Ghitani, N., Barik, A., Lam, R., Thompson, J. H., et al. (2018). PIEZO2 mediates injury-induced tactile pain in mice and humans. *Sci. Transl. Med.* 10:eaa9892. doi: 10.1126/scitranslmed.aat9892
- Tang, X., Platt, M. D., Lagnese, C. M., Leslie, J. R., and Hamada, F. N. (2013). Temperature integration at the AC thermosensory neurons in *Drosophila*. *J. Neurosci.* 33, 894–901. doi: 10.1523/JNEUROSCI.1894-12.2013
- Togashi, K., Hara, Y., Tominaga, T., Higashi, T., Konishi, Y., Mori, Y., et al. (2006). TRPM2 activation by cyclic ADP-ribose at body temperature is involved in insulin secretion. *EMBO J.* 25, 1804–1815. doi: 10.1038/sj.emboj.7601083
- Torres, G., and Horowitz, J. M. (1998). Activating properties of cocaine and cocaethylene in a behavioral preparation of *Drosophila melanogaster*. *Synapse* 29, 148–161. doi: 10.1002/(SICI)1098-2396(199806)29:2<148::AID-SYN6>gt;3.0.CO;2-7
- Tracey, W. J., Wilson, R. I., Laurent, G., and Benzer, S. (2003). Painless, a *Drosophila* gene essential for nociception. *Cell* 113, 261–273. doi: 10.1016/s0092-8674(03)00272-1
- Tsubouchi, A., Caldwell, J. C., and Tracey, W. D. (2012). Dendritic filopodia, Ripped Pocket, NompC, and NMDARs contribute to the sense of touch in *Drosophila* larvae. *Curr. Biol.* 22, 2124–2134. doi: 10.1016/j.cub.2012.09.019
- Tsuda, L., and Lim, Y. M. (2018). Alzheimer's disease model system using *drosophila*. *Adv. Exp. Med. Biol.* 1076, 25–40. doi: 10.1007/978-981-13-0529-0_3
- Turk, D. C. (2001). Management of pain: best of times, worst of times? *Clin. J. Pain* 17, 107–109. doi: 10.1097/00002508-200106000-00001
- Turner, H. N., Armengol, K., Patel, A. A., Himmel, N. J., Sullivan, L., Iyer, S. C., et al. (2016). The TRP channels pkd2, NompC, and trpm act in Cold-Sensing

- neurons to mediate unique aversive behaviors to noxious cold in *Drosophila*. *Curr. Biol.* 26, 3116–3128. doi: 10.1016/j.cub.2016.09.038
- Turner, H. N., Landry, C., and Galko, M. J. (2017). Novel assay for cold nociception in *Drosophila larvae*. *J. Vis. Exp.* 3:55568. doi: 10.3791/55568
- Viana, F. (2016). TRPA1 channels: molecular sentinels of cellular stress and tissue damage. *J. Physiol.* 594, 4151–4169. doi: 10.1113/JP270935
- Volkers, L., Mechoukhi, Y., and Coste, B. (2015). Piezo channels: from structure to function. *Pflugers Arch.* 467, 95–99. doi: 10.1007/s00424-014-1578-z
- Voscopoulos, C., and Lema, M. (2010). When does acute pain become chronic? *Br. J. Anaesth.* 105(Suppl 1), i69–i85. doi: 10.1093/bja/aeq323
- Waldmann, R., Champigny, G., Bassilana, F., Heurteaux, C., and Lazdunski, M. (1997). A proton-gated cation channel involved in acid-sensing. *Nature* 386, 173–177. doi: 10.1038/386173a0
- Wang, K., Guo, Y., Wang, F., and Wang, Z. (2011). *Drosophila* TRPA channel painless inhibits male-male courtship behavior through modulating olfactory sensation. *PLoS One* 6:e25890. doi: 10.1371/journal.pone.0025890
- Wang, P., Jia, Y., Liu, T., Jan, Y. N., and Zhang, W. (2020). Visceral mechanosensing neurons control *Drosophila* feeding by using piezo as a sensor. *Neuron* 108, 640–650. doi: 10.1016/j.neuron.2020.08.017
- Warr, C. G., Shaw, K. H., Azim, A., Piper, M., and Parsons, L. M. (2018). Using mouse and *Drosophila* models to investigate the mechanistic links between diet, obesity, type II diabetes, and cancer. *Int. J. Mol. Sci.* 19:4110. doi: 10.3390/ijms19124110
- Williams, D. W., and Truman, J. W. (2005). Cellular mechanisms of dendrite pruning in *Drosophila*: insights from *in vivo* time-lapse of remodeling dendritic arborizing sensory neurons. *Development* 132, 3631–3642. doi: 10.1242/dev.01928
- Wolfgang, W., Simoni, A., Gentile, C., and Stanewsky, R. (2013). The Pyrexia transient receptor potential channel mediates circadian clock synchronization to low temperature cycles in *Drosophila melanogaster*. *Proc. Biol. Sci.* 280:20130959. doi: 10.1098/rspb.2013.0959
- Woo, S. H., Lukacs, V., de Nooij, J. C., Zaytseva, D., Criddle, C. R., Francisco, A., et al. (2015). Piezo2 is the principal mechanotransduction channel for proprioception. *Nat. Neurosci.* 18, 1756–1762. doi: 10.1038/nn.4162
- Woolf, C. J. (2010). What is this thing called pain? *J. Clin. Invest.* 120, 3742–3744. doi: 10.1172/JCI45178
- Wu, L. J., Sweet, T. B., and Clapham, D. E. (2010). International Union of Basic and Clinical Pharmacology. LXXVI. Current progress in the mammalian TRP ion channel family. *Pharmacol. Rev.* 62, 381–404. doi: 10.1124/pr.110.002725
- Xiang, Y., Yuan, Q., Vogt, N., Looger, L. L., Jan, L. Y., and Jan, Y. N. (2010). Light-avoidance-mediating photoreceptors tile the *Drosophila* larval body wall. *Nature* 468, 921–926. doi: 10.1038/nature09576
- Xu, J., Sornborger, A. T., Lee, J. K., and Shen, P. (2008). *Drosophila* TRPA channel modulates sugar-stimulated neural excitation, avoidance and social response. *Nat. Neurosci.* 11, 676–682. doi: 10.1038/nn.2119
- Xu, S. Y., Cang, C. L., Liu, X. F., Peng, Y. Q., Ye, Y. Z., Zhao, Z. Q., et al. (2006). Thermal nociception in adult *Drosophila*: behavioral characterization and the role of the painless gene. *Genes Brain Behav.* 5, 602–613. doi: 10.1111/j.1601-183X.2006.00213.x
- Yam, M. F., Loh, Y. C., Tan, C. S., Khadijah, A. S., Abdul, M. N., and Basir, R. (2018). General pathways of pain sensation and the major neurotransmitters involved in pain regulation. *Int. J. Mol. Sci.* 19:2164. doi: 10.3390/ijms19082164
- Yan, Z., Zhang, W., He, Y., Gorczyca, D., Xiang, Y., Cheng, L. E., et al. (2013). *Drosophila* NOMPC is a mechanotransduction channel subunit for gentle-touch sensation. *Nature* 493, 221–225. doi: 10.1038/nature11685
- Yoshino, J., Morikawa, R. K., Hasegawa, E., and Emoto, K. (2017). Neural circuitry that evokes escape behavior upon activation of nociceptive sensory neurons in *drosophila larvae*. *Curr. Biol.* 27, 2499–2504. doi: 10.1016/j.cub.2017.06.068
- Young, E. E., Lariviere, W. R., and Belfer, I. (2012). Genetic basis of pain variability: recent advances. *J. Med. Genet.* 49, 1–9. doi: 10.1136/jmedgenet-2011-100386
- Yu, Y., Chen, Z., Li, W. G., Cao, H., Feng, E. G., Yu, F., et al. (2010). A nonproton ligand sensor in the acid-sensing ion channel. *Neuron* 68, 61–72. doi: 10.1016/j.neuron.2010.09.001
- Zhong, L., Hwang, R. Y., and Tracey, W. D. (2010). Pickpocket is a DEG/ENaC protein required for mechanical nociception in *Drosophila larvae*. *Curr. Biol.* 20, 429–434. doi: 10.1016/j.cub.2009.12.057
- Zygmunt, P. M., and Hogestatt, E. D. (2014). Trpa1. *Handb. Exp. Pharmacol.* 222, 583–630. doi: 10.1007/978-3-642-54215-2_23

Conflict of Interest: The authors declare that the research was conducted in the absence of any commercial or financial relationships that could be construed as a potential conflict of interest.

Publisher's Note: All claims expressed in this article are solely those of the authors and do not necessarily represent those of their affiliated organizations, or those of the publisher, the editors and the reviewers. Any product that may be evaluated in this article, or claim that may be made by its manufacturer, is not guaranteed or endorsed by the publisher.

Copyright © 2022 He, Li, Han, Zhang, Liu, Yi, Liu and Xiu. This is an open-access article distributed under the terms of the Creative Commons Attribution License (CC BY). The use, distribution or reproduction in other forums is permitted, provided the original author(s) and the copyright owner(s) are credited and that the original publication in this journal is cited, in accordance with accepted academic practice. No use, distribution or reproduction is permitted which does not comply with these terms.



Deep Metabolic Profiling Assessment of Tissue Extraction Protocols for Three Model Organisms

Hagen M. Gegner^{1†}, Nils Mechtel^{1†}, Elena Heidenreich¹, Angela Wirth², Fabiola Garcia Cortizo³, Katrin Bennewitz⁴, Thomas Fleming⁵, Carolin Andresen^{6,7,8}, Marc Freichel², Aurelio A. Teleman³, Jens Kroll⁴, Rüdiger Hell¹ and Gernot Poschet^{1*}

¹Metabolomics Core Technology Platform, Centre for Organismal Studies (COS), Heidelberg University, Heidelberg, Germany, ²Institute of Pharmacology, Heidelberg University, Heidelberg, Germany, ³Division of Signal Transduction in Cancer and Metabolism, German Cancer Research Center (DKFZ), Heidelberg, Germany, ⁴European Center for Angioscience (ECAS), Department of Vascular Biology and Tumor Angiogenesis, Medical Faculty Mannheim, Heidelberg University, Mannheim, Germany, ⁵Department of Internal Medicine I and Clinical Chemistry, Heidelberg University Hospital, Heidelberg, Germany, ⁶Heidelberg Institute for Stem Cell Technology and Experimental Medicine (HI-STEM GGmbH), Heidelberg, Germany, ⁷Division of Stem Cells and Cancer, Deutsches Krebsforschungszentrum (DKFZ) and DKFZ-ZMBH Alliance, Heidelberg, Germany, ⁸Faculty of Biosciences, Heidelberg University, Heidelberg, Germany

OPEN ACCESS

Edited by:

Roberto Romero González,
University of Almería, Spain

Reviewed by:

Claudio Luchinat,
University of Florence, Italy
Osmar Prestes,
Federal University of Santa Maria,
Brazil

*Correspondence:

Gernot Poschet
gernot.poschet@cos.
uni-heidelberg.de

[†]These authors have contributed
equally to this work

Specialty section:

This article was submitted to
Analytical Chemistry,
a section of the journal
Frontiers in Chemistry

Received: 04 February 2022

Accepted: 05 April 2022

Published: 25 April 2022

Citation:

Gegner HM, Mechtel N, Heidenreich E, Wirth A, Cortizo FG, Bennewitz K, Fleming T, Andresen C, Freichel M, Teleman AA, Kroll J, Hell R and Poschet G (2022) Deep Metabolic Profiling Assessment of Tissue Extraction Protocols for Three Model Organisms. *Front. Chem.* 10:869732. doi: 10.3389/fchem.2022.869732

Metabolic profiling harbors the potential to better understand various disease entities such as cancer, diabetes, Alzheimer's, Parkinson's disease or COVID-19. To better understand such diseases and their intricate metabolic pathways in human studies, model animals are regularly used. There, standardized rearing conditions and uniform sampling strategies are prerequisites towards a successful metabolomic study that can be achieved through model organisms. Although metabolomic approaches have been employed on model organisms before, no systematic assessment of different conditions to optimize metabolite extraction across several organisms and sample types has been conducted. We address this issue using a highly standardized metabolic profiling assay analyzing 630 metabolites across three commonly used model organisms (*Drosophila*, mouse, and zebrafish) to find an optimal extraction protocol for various matrices. Focusing on parameters such as metabolite coverage, concentration and variance between replicates we compared seven extraction protocols. We found that the application of a combination of 75% ethanol and methyl tertiary-butyl ether (MTBE), while not producing the broadest coverage and highest concentrations, was the most reproducible extraction protocol. We were able to determine up to 530 metabolites in mouse kidney samples, 509 in mouse liver, 422 in zebrafish and 388 in *Drosophila* and discovered a core overlap of 261 metabolites in these four matrices. To enable other scientists to search for the most suitable extraction protocol in their experimental context and interact with this comprehensive data, we have integrated our data set in the open-source shiny app "MetaboExtract". Hereby, scientists can search for

Abbreviations: LC-MS/MS, Liquid chromatography tandem mass spectrometry; FIA-MS/MS, Flow injection analysis and tandem mass spectrometry; ESI, Electrospray ionization; MRM, Multiple reaction monitoring; EtOH, Ethanol; MeOH, Methanol; MTBE, Methyl tert-butyl ether; ACN, Acetonitrile; IPA, Isopropanol; FA, Formic acid; PITC, Phenylisothiocyanate (or Edman's Reagent); LN₂, Liquid nitrogen; LOD, Limit of detection; LOQ, Limit of quantification; CV%, Coefficient of variation in percentage; ANOVA, Analysis of variance; MAD, Median absolute deviation.

metabolites or compound classes of interest, compare them across the different tested extraction protocols and sample types as well as find reference concentration values.

Keywords: metabolomics, LC-MS/MS, extraction protocol, model organisms, drosophila, mouse, zebrafish, MxP Quant 500

INTRODUCTION

Metabolomics, defined as the separation and subsequent measurement of small molecules in either a qualitative or quantitative way, enables the generation of metabolic profiles of any sample of interest. While genomics and transcriptomics are analyzed within the framework of a single organism and understood by the blueprint of genes or transcripts of the respective species, metabolomics encompasses all compounds that may be metabolized by an organism or its microbiome, or that are introduced by the environment (“exposome”) at a given time. Therefore, the metabolome incorporates the environmental influence as well as interactions with other organisms (Johnson et al., 2012). It can serve as a bridge between the organism, its interactions and any disease, e.g., between diet, the gut microbiome and metabolic disease (Pallister et al., 2017). While the complexity and dynamic nature of the metabolome is daunting from an analytical perspective, metabolomics harbors the potential to better understand as well as diagnose various disease entities such as diabetes (Arneith et al., 2019), kidney disease (Abbiss et al., 2019), Parkinson’s (Shao and Le, 2019), Alzheimer’s disease (Wilkins and Trushina, 2018) and most recently, COVID-19 (Sindelar et al., 2021).

The potential to understand the metabolic signatures of any given disease entity is tremendous, however, deciphering the intricate underpinnings of those in a human study requires costly, as well as time and work extensive population-wide association studies with several hundred participants per group (Nicholson et al., 2008). These broad studies may be successful in the discovery of new associations between a respective disease and the measured metabolites, i.e., biomarkers, but they are limited in their mechanistic explanations despite all efforts. While the dynamic nature of the metabolome provides incredibly powerful insights, it also highlights the challenges of metabolome analyses — its variability and associated pitfalls.

Variation and noise that are biologically inherent or are introduced at some point to the sample are complicating metabolic analyses, impairing the quality of the findings, limiting their validity and may even overshadow the effect size of the research question itself. Factors that introduce such variability range from intrinsic ones derived from the study organism (age or sex) (Brennan and Gibbons, 2020; Bell et al., 2021), to extrinsic factors (diet, lifestyle or medication) (Mellert et al., 2011; Adamski, 2016). Additionally, other factors, such as pre-analytical ones during sample collection (Yin et al., 2015; Lippi et al., 2020), or analytical factors deriving from the sample preparation, the extraction protocols or analytical approach used to conduct the measurement (Lin et al., 2007; Erben et al., 2021) are also influential and need to be accounted for.

Model organisms that are reared under controlled laboratory conditions and manipulated genetically to analyze a certain genotype address several of the challenges mentioned above. Combining the standardized rearing conditions and stringent sampling protocols with the already extensive knowledge accumulated from other “-omics” in models such as mice, *Drosophila* or zebrafish enhances the explanatory power of metabolomic studies tremendously while simultaneously reducing the number of samples needed to generate meaningful results. To ensure that the analytical phase, i.e., the extraction and measurement of metabolites, does not introduce biases and variability, an in-depth evaluation of such aspects is necessary.

Standardized metabolomic analyses are commercially available by companies such as Metabolon (www.metabolon.com) or Biocrates (www.biocrates.com). The latter has developed standardized and robust LC-MS/MS based kits which enable the absolute quantification of specific compound classes or more broadly, up to 630 metabolites in the case of the MxP Quant 500 kit (Biocrates). Within these 630 metabolites, the MxP Quant 500 kit covers 14 small molecule and 9 different lipid classes. Due to its standardized nature and compatibility with a multitude of LC-MS/MS platforms, data generated via such a kit-based approach enables inter- and intra-laboratory comparability (Siskos et al., 2017), as well as its integration from different experiments. Although these kits were initially developed for human biofluids, i.e., plasma and serum, they may be used for tissue samples (Zukunft et al., 2018) and other sample types such as cultured cells (Andresen et al., 2021) or supernatants likewise. However, there is no consensus on the optimal metabolite extraction procedure amongst the metabolomic community for the investigation of polar and non-polar metabolites covering that many chemical classes across different model organisms within one analysis.

In this study, this open question was addressed using the highly standardized targeted metabolomics kit (Biocrates MxP Quant 500) to evaluate seven extraction protocols designed to extract both, polar and non-polar metabolites, differing in their solvent composition and extraction mode (mono/biphasic) as well as handling complexity (**Figure 1**). We compared the metabolite coverage, concentration and robustness, i.e., the coefficient of variance (CV%) across three commonly used model organisms (mouse, zebrafish and *Drosophila*), focusing on either whole organisms as sample type (*Drosophila*) or specific organs (liver and kidney) of the respective model organism. Lastly, we integrated our data in the Shiny app “MetaboExtract” (Andresen et al., 2021) to provide a useful source of metabolite concentrations across model organisms and enable other scientists to search for an optimal extraction procedure for their metabolite or metabolite class of interest.

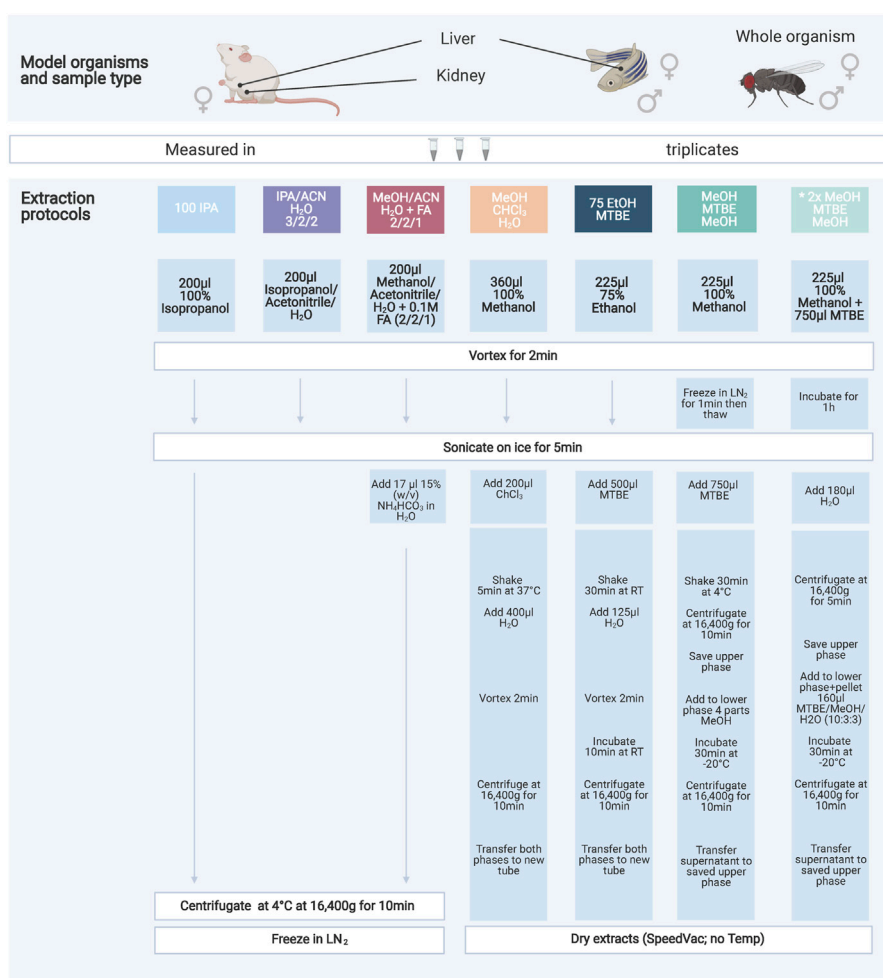


FIGURE 1 | Overview of the seven extraction protocols used as well as the model organisms and sample types investigated. The protocols increase in handling effort and complexity from left to right. The color code indicates similarities amongst the protocols either through solvents or chemicals used. All extraction products were stored at -80°C until further processing. A list of abbreviations can be found above.

MATERIALS AND METHODS

Chemicals

Chemicals were bought from Sigma-Aldrich (Germany). All solvents used for sample extractions and LC- or FIA-MS/MS analyses were of UHPLC-MS quality.

MODEL ORGANISM GROWTH/CULTURING CONDITIONS

Mouse—*Mus musculus*

Nine-week-old C57Bl6N wildtype mice (Charles River, Germany) were anesthetized with isoflurane and blood was taken to generate EDTA-Plasma. Without regaining consciousness mice were killed by cervical dislocation. Livers and kidneys were excised rapidly and shortly rinsed in ice-cold 0.9% NaCl. Excess liquid was removed before whole

organ weight was determined for later normalization and tissue was snap-frozen in liquid nitrogen. All procedures were approved by the Animal Care and Use Committee at the Regierungspräsidium Karlsruhe, Germany (T-40/20).

Fly - *Drosophila melanogaster*

W1118 *Drosophila* were acquired from Bloomington *Drosophila* Stock Center. For all metabolic measurements, *Drosophila* were grown under controlled conditions: *Drosophila* were allowed to lay eggs on apple plates for 12 h. First instar larvae hatching within a 4- or 6-h window were picked and seeded at a density of 60 animals per vial. Adult *Drosophila* of all genotypes enclosing within a 24-h time-window were separated by gender in groups of 30 *Drosophila* and aged for 10 days. *Drosophila* were grown and maintained on food consisting of the following ingredients for 30 L of food: 480 g agar, 660 g sugar syrup, 2400 g malt, 2400 g corn meal, 300 g soymeal, 540 g yeast, 72 g nipagin, 187 ml propionic acid and 18.7 ml phosphoric acid.

At sample collection, *Drosophila* were pooled and snap-frozen for metabolic profiling.

Zebrafish - *Danio rerio*

Adult zebrafish were kept under a 13-h light/11-h dark cycle and feeding of zebrafish took place twice a day, freshly hatched *Artemia salina* in the morning and fish flake food in the afternoon. All experimental interventions on animals were approved by the local government authority, Regierungspräsidium Karlsruhe and by Medical Faculty Mannheim (I-19/02) and carried out in accordance with the approved guidelines. Age of adult male zebrafish was 9 months and both sexes were included. Zebrafish were sacrificed in ice water and livers were immediately dissected and frozen in liquid nitrogen and subsequently stored at -80°C . 7–10 mg of livers were used for further analysis.

SAMPLE PREPARATION

To ensure sufficient input material across the model organisms 30 pooled *Drosophila* (w1118), 7–10 mg of zebrafish liver or 20–22 mg of mouse (C57Bl6N) liver and kidney pooled from three individuals respectively were used. All tissue samples were pulverized using a ball mill (MM400, Retsch) with precooled beakers and stainless-steel balls for 30 s at the highest frequency (30 Hz). The exact weight was determined for normalization of all measurements.

METABOLITE EXTRACTION PROTOCOLS

Here we evaluated six different extraction protocols that are described in **Figure 1**. We developed these protocols based on own preliminary experience and reviewing of general metabolomics literature addressing similar questions (Lisec et al., 2006; Rabinowitz and Kimball, 2007; Ivanisevic et al., 2013; Weir et al., 2013; Zukunft et al., 2018). The protocol “*MeOH/MTBE*”, noted with an asterisk, was applied twice with slight variations in mouse samples only. We are including this variation as an additional method (*2xMeOH/MTBE*) when we are referring to the seven extraction protocols.

Briefly, pulverized and frozen samples were extracted using the indicated solvents and subsequent steps of the respective protocol (**Figure 1**). After a final centrifugation step the solvent extract of the protocols 100IPA, IPA/ACN and *MeOH/ACN* were transferred into a new 1.5 ml tube (Eppendorf) and snap-frozen until kit preparation. The remaining protocols were dried using an Eppendorf Concentrator Plus set to no heat, stored at -80°C and reconstituted in 60 μL isopropanol (30 μL of 100% isopropanol, followed by 30 μL of 30% isopropanol in water) before the measurement.

STANDARDIZED TARGETED METABOLIC PROFILING

After conducting the described seven extraction protocols, tissue extracts were processed following the manufacturer's protocol of

the MxP® Quant 500 kit (Biocrates). Briefly, 10 μL of the samples or blanks were pipetted on the 96 well-plate based kit containing calibrators and internal standards using an automated liquid handling station (epMotion 5075, Eppendorf) and subsequently dried under a nitrogen stream using a positive pressure manifold (Waters). Afterwards, 50 μL phenyl isothiocyanate 5% (PITC) was added to each well to derivatize amino acids and biogenic amines. After 1 h incubation time at room temperature, the plate was dried again. To resolve all extracted metabolites 300 μL of 5 mM ammonium acetate in methanol were pipetted to each filter and incubated for 30 min. The extract was eluted into a new 96-well plate using positive pressure. For the LC-MS/MS analyses 150 μL of the extract was diluted with an equal volume of water. Similarly, for the FIA-MS/MS analyses 10 μL extract was diluted with 490 μL of FIA solvent (provided by Biocrates). After dilution, LC-MS/MS and FIA-MS/MS measurements were performed in positive and negative mode. For chromatographic separation an UPLC I-class PLUS (Waters) system was used coupled to a SCIEX QTRAP 6500 + mass spectrometry system in electrospray ionization (ESI) mode. LC gradient composition and specific 50×2.1 mm column are provided by Biocrates. Data was recorded using the Analyst (Version 1.7.2 Sciex) software suite and further processed via MetIDQ software (Oxygen-DB110-3005). All metabolites were identified using isotopically labeled internal standards and multiple reaction monitoring (MRM) using optimized MS conditions as provided by Biocrates. For quantification either a seven-point calibration curve or one-point calibration was used depending on the metabolite class.

DATA PROCESSING AND ANALYSES

Validation and Filtering

Data validation and quantification was performed using MetIDQ (Oxygen-DB110-3005). Here, metabolites were further categorized based on their quantitation ranges. Additional filtering per metabolite was based on the limit of detection (LOD), limit of quantification (LOQ) and concentration within the quantitative range (valid). To remove metabolites that were not present in any model organism and sample type, we considered a metabolite as detectable when at least 2 out of 3 replicates within a tested protocol were above LOD (see **Figure 2**). These metabolites are also visualized as Venn diagrams in **Figure 5** for the extraction protocol EtOH/MTBE and for the remaining extraction protocols in **Supplementary Figure S5**. An overview of the LOD, LOQ and valid metabolite proportions are shown in **Supplementary Figure S1**. For all detectable metabolites, the coefficient of variation (CV) in percentage was calculated as well as the median absolute deviation (MAD) based on the concentrations.

Statistical Analysis

To find the optimal protocol per model organism and sample type, we analyzed the concentration per metabolite achieved across the extraction protocols. For this comparison, missing values and zero values were imputed per metabolite with 20% of

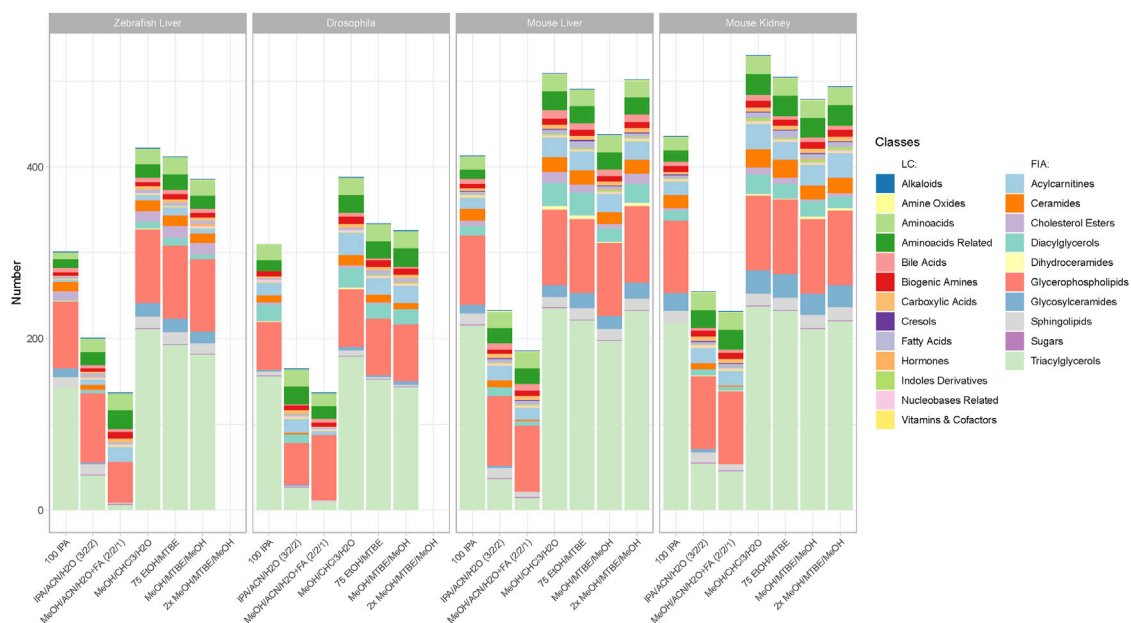


FIGURE 2 | Metabolite coverage per extraction protocol across all sample types and model organisms. Indicated by color are the different metabolite classes measured. A metabolite was counted as detectable when at least 2 out of 3 replicates were >LOD within a given extraction protocol. The legend is categorized between compound classes measured via LC-MS/MS or FIA-MS/MS. Ordering from left to right follows the level of complexity and required time per extraction.

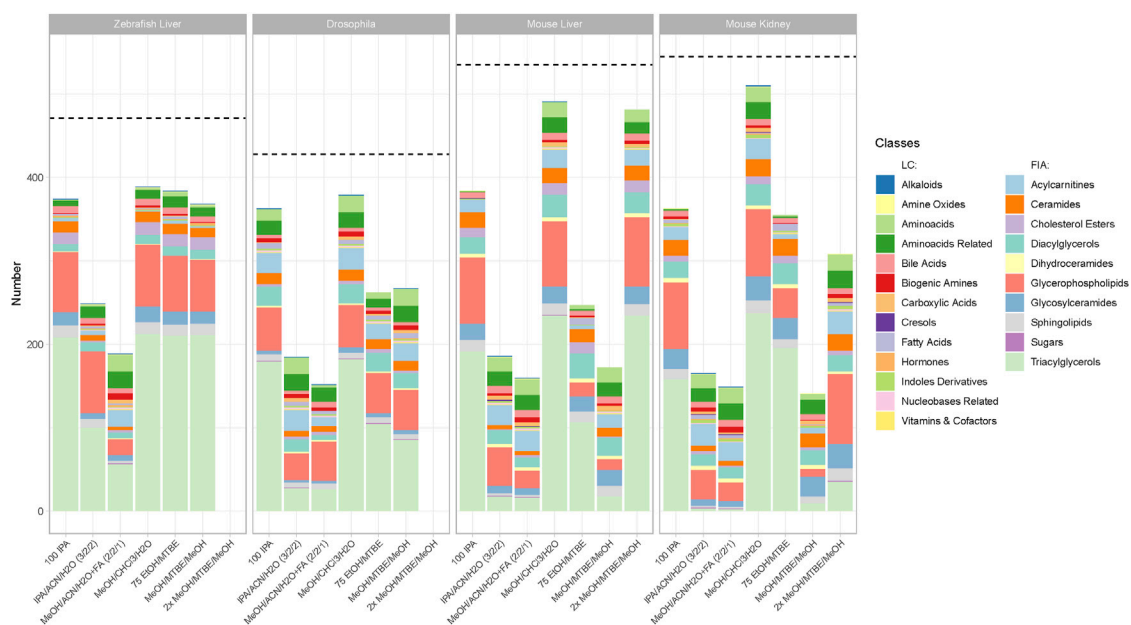


FIGURE 3 | Number of metabolites per class with the highest concentration per extraction protocol across all sample types and model organisms. Metabolites that appear in the bar chart are only counted when they produce the highest or a non-significantly lower concentration ($p > 0.05$, see Material and Methods) than another tested extraction protocol. The dotted line shows the number of detectable metabolites for each sample type. Indicated by color are the different metabolite classes measured. The legend is categorized between the LC-MS/MS and FIA-MS/MS measurements. A list of the metabolites per extraction protocol can be viewed online in "MetaboExtract". Of note, the metabolite classes that were best suited for a single extraction protocol are depicted in **Supplementary Figure S4**.

the minimal positive value of a given metabolite. Subsequently, to perform statistical analyses, the data was log₂-transformed. We then performed an ANOVA per metabolite considering all metabolites that were detectable with at least a single method. Extraction protocols were used as categorical variables and concentration as dependent variables. A Tukey post-hoc test ($\alpha = 0.05$) was used to determine the extraction protocols with the highest median concentration as well as non-significantly (p -adjusted > 0.05) lower concentrations. These extraction protocols were considered optimal, counted, and depicted in **Figure 3**. Conversely, metabolites that were significantly better extracted in a single extraction protocol are depicted in **Supplementary Figure S4**. We implemented and employed the R package “MetAlyzer” (<https://CRAN.R-project.org/package=MetAlyzer>), which provides an R-S4 object with methods to read output files from the MetIDQ software into R for convenient data processing, statistics and downstream analysis. It covers every step of filtering and analysis with the parameters used in this work to ensure the best possible reproducibility.

R Shiny app

Data can be explored and downloaded using the Shiny app “MetaboExtract” which is available at <http://www.metaboextract.shiny.dkfz.de>. The underlying code is also available at <https://github.com/andresenc/MetaboExtract> (Andresen et al., 2021). **Figures 2, 3** as well as **S3** were extracted from the Shiny app.

RESULTS

The aim of this study was the comparison of seven extraction protocols (**Figure 1**) across three model organisms to determine the optimal extraction procedure with regards to metabolite coverage, their absolute concentration and robustness (CV%). In total, we analyzed 630 metabolites, however, after filtering for low concentrated metabolites below the limit of detection (LOD), we continued the analyses using this processed data. **Supplementary Figure S1** shows the ratio of LOD, LOQ and valid measurements per extraction protocol across all sample types and model organisms.

Biphasic Extractions Generate the Highest Coverage and Concentration

The metabolic profiling kit (Biocrates MxP Quant 500) used for this study quantifies polar as well as non-polar metabolites across 14 small molecule and nine different lipid classes. Therefore, an extraction procedure is required that enables solubilization ranging from very polar metabolites (e.g., carbohydrates and amino acids) to very non-polar metabolites such as triacylglycerols (**Figure 2**). While the maximum coverage between the different model organisms is expected to be variable, the general performance of the respective protocol remained similar. **Figure 2** shows the detected metabolites per extraction protocol across all sample types and model organisms.

The ordering of the protocols from left to right also indicates the level of complexity and time required for the protocol (**Figure 1**).

Clear performance trends between the monophasic (100IPA, IPA/ACN/H₂O, MeOH/ACN/H₂O + FA) and biphasic (MeOH/CHCl₃/H₂O, 75EtOH/MTBE, (2x)MeOH/MTBE) extractions were apparent. The protocol using MeOH/CHCl₃/H₂O resulted in the highest metabolite coverage in all sample types and across all organisms (zebrafish liver (422), Drosophila (388), mouse liver (509), mouse kidney (530)). Similarly, 75EtOH/MTBE, as well as both MeOH/MTBE protocols, produced a broad coverage across all metabolite classes. In other words, all biphasic extractions performed well and were comparable regarding their metabolite coverage.

While 100IPA, a rapid and simple single solvent extraction protocol, produced fair coverage, the remaining protocols, both containing acetonitrile, achieved the lowest coverage regardless of the sample type or organism. Comparison of the different metabolite classes reveal that these monophasic extraction protocols failed to extract several lipids, such as di- and triacylglycerols as well as ceramides or cholesterol esters.

Although the coverage of a given extraction is essential, the concentration of a metabolite may vary across the different extraction procedures. Here, we consider an extraction protocol as better when higher concentration of metabolites can be achieved. To scrutinize the extraction protocols regarding this criterion we performed an ANOVA (see material and method part) counting the metabolites that reached the highest or a non-significantly lower concentration in a given extraction protocol per model organism (**Figure 3**). Therefore, high counts of metabolites in **Figure 3** indicate that a given protocol extracted the highest concentration. Vice versa, lower counts in **Figure 3** indicate that other protocols extracted significantly higher concentrations generating an overview and elucidate trends in performance. A list of the metabolites that are extracted with the highest concentration (or a non-significantly lower concentration that another protocol) is available online in “MetaboExtract”.

In **Figure 3** a similar pattern compared to the metabolite coverage (**Figure 2**) emerged. The protocol using MeOH/CHCl₃/H₂O resulted in the highest concentrations of metabolites measured within each metabolite class across all organisms (zebrafish liver (392), Drosophila (379), mouse liver (493), mouse kidney (510)). The remaining biphasic extraction protocols performed comparable, apart from MeOH/MTBE in mouse liver and kidney, showing significantly lower concentrations per metabolite than the other protocols with a strong reduction in triacylglycerols. Within the group of MTBE protocols the combination with EtOH was superior to the MeOH extraction resulting in higher or comparable metabolite concentrations. Comparing both MeOH variations, in mice, 2xMeOH/MTBE resulted in higher concentrations than the MeOH/MTBE extraction. Of note, in mouse liver, 2xMeOH/MTBE generated the highest concentrations within the group of MTBE protocols indicating strong differences between the sample types. In-depth comparison of several metabolites using “MetaboExtract” shows that while not counted in

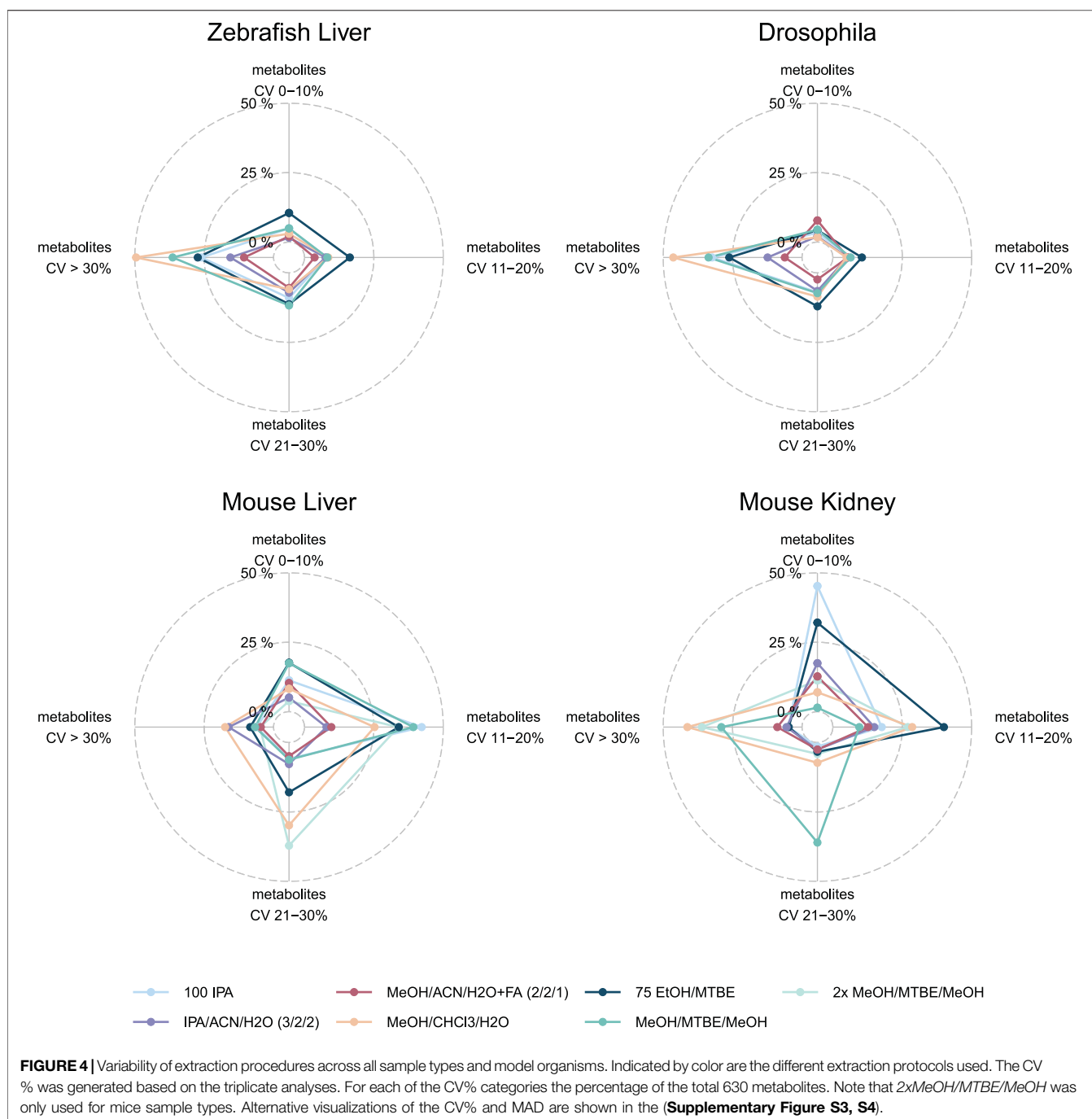
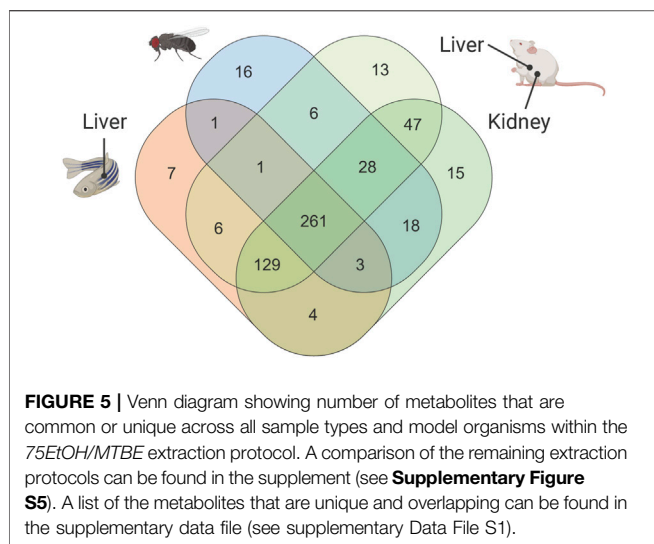


Figure 3, MTBE containing protocols perform comparable across most model organisms and sample types.

Similarly to the coverage of metabolites, both acetonitrile-containing protocols performed worse across all model organisms and sample types overall with the exception of very few metabolite classes. For example, *MeOH/ACN/H₂O* + *FA* extracted amino acids and their related metabolites at higher concentrations across all model organisms. Lastly, the rapid *100IPA* protocol produced comparable or higher concentrations than the MTBE protocols across most metabolite classes.

Extraction Protocol Variability as an Essential Quality Parameter

While coverage and concentrations are important to determine the optimal extraction protocol for the broadest range of metabolite classes, the variability or the coefficient of variance (CV%) of each metabolite between the analysis of biological triplicates informs about the robustness of a protocol. To better understand the variability across the different protocols and compare it alongside the coverage we plotted both as a spider plot in **Figure 4**. There, the variability of the measurements



between the triplicates per metabolite in CV% ranges from 0–10% (= excellent), 11–20% (= good), 21–30% (= acceptable) and >30% (= not acceptable). The percentage ranges were calculated from the total of 630 possible metabolites, elucidating the variability of a method but also the number of detectable metabolites per method. For example, in mouse kidney, 75EtOH/MTBE results in 202 (32.1%) metabolites with an excellent CV, 252 (40%) metabolites with a good CV, 21 (3.3%) metabolites with a CV that is acceptable CV and finally, 30 (4.8%) metabolites with a high CV that is not acceptable. Similarly, 100IPA appears as a well performing choice in this sample type with most measurements in a CV% range from 0–10% (= excellent).

This visualization enables the comparison of several extraction protocols across all sample types regarding their robustness and coverage at once (**Figure 4**). The protocol using MeOH/CHCl₃/H₂O which resulted in the highest coverage and concentration performed the worst across all sample types and model organisms with most of the metabolites with a CV of >30% (zebrafish liver (312), Drosophila (292), mouse liver (110), mouse kidney (260)). Similarly, 2xMeOH/MTBE generates a high variability but also a high coverage as well as concentrations in mouse sample types. Amongst the other model organisms (Drosophila and zebrafish), a single extraction with MeOH/MTBE resulted in a high portion of CV >30% (= not acceptable) compared to 75EtOH/MTBE. Yet, differences could be seen in mouse sample types, where 75EtOH/MTBE performed better in mouse kidney than mouse liver and conversely, for MeOH/MTBE.

75EtOH/MTBE resulted in acceptable levels of variance across all sample types and model organisms (<30%). An alternative visualization of the CV% across the different extraction protocols can be found in **Supplementary Figure S2**. The median and median absolute deviation (MAD) of the coefficient of variation (CV) across the seven extraction protocols is depicted in the **Supplementary Figure S3**. Both visualizations strengthen the conclusion described above. Notably, Drosophila and zebrafish samples show overall higher variability in the measurements.

As a next step, we used the 75EtOH/MTBE extraction protocol as an example to visualize the overlap and the uniquely determined metabolites across the different sample types and model organisms in a Venn diagram (**Figure 5**).

Strong Overlap of Detectable Compounds Between Analyzed Sample Types Using 75EtOH/MTBE

Figure 5 shows the common and uniquely extracted metabolites per model organism within the 75EtOH/MTBE protocol. Overall, the 75EtOH/MTBE protocol resulted in adequate coverage and metabolite concentrations of the evaluated protocols while also showing excellent to acceptable levels of variance between the measurements. Within this protocol 261 common metabolites out of 630 possible compounds could be extracted across all matrices. Additional 129 metabolites were shared between the liver and kidney samples (mouse and zebrafish). Only very few metabolites were unique to each sample type, highlighting the broad coverage of the 75EtOH/MTBE extraction protocol. Venn diagrams for the remaining extraction protocols are provided in **Supplementary Figure S5** together with the list of shared or unique metabolites in supplementary Data File S1. There, MeOH/CHCl₃/H₂O is once more the protocol producing the highest coverage across all sample types and model organism (304 metabolites).

“MetaboExtract” - An Interactive Resource to Explore Metabolite Extractions and Baseline Concentrations of Model Organisms

The presented data provides an attempt to inform about the optimal extraction protocol for a standardized profiling assay. However, it harbors further information such as baseline concentrations for sample types and whole model organisms. To access this information researchers may explore the data set via the easy-to-use interactive R/shiny app “MetaboExtract” (Andresen et al., 2021). There, the already present metabolite data on human tissue and cells was expanded by our data set focused on model organisms. Since all data was generated using the standardized MxP Quant 500 assay it is highly comparable. Organisms, tissues, extraction methods and classes of metabolites may be (de)selected to focus on the data of interest that are then provided in comprehensive and interactive visualizations. The data presented in **Figure 2** and in **Supplementary Figure S4** were generated using MetaboExtract. Its standardized nature provides the potential for further expansion via additional MxP Quant 500 assay measurements.

DISCUSSION

Model organisms enable standardized laboratory-controlled handling, sampling and experiments. This level of standardization in the pre-analytical phase benefits metabolic profiling due to the dynamic nature of the

metabolome, rapid turnover rates of metabolites and the influence of the environment (Edison et al., 2016; Saoi and Britz-mckibbin, 2021).

Here, we focused on the extraction and processing of diverse sample types, one of the most important aspects in the analytical phase requiring strict standardization for reproducibility of data. To this end, we used a targeted metabolic profiling approach (Biocrates MxP Quant 500) quantifying up to 630 metabolites and validated it across three commonly used model organisms (*Drosophila*, mouse and zebrafish) to find a robust, easy-to-use extraction protocol yielding a comprehensive coverage of the target analytes (Figure 1). This metabolic profiling assay quantifies polar as well as non-polar metabolites across 14 hydrophilic and 9 different lipid classes. Hence, it requires the extraction of a chemically diverse range of metabolites from solid samples. Besides broad metabolite coverage and high concentrations with little loss during the extraction, we evaluated the robustness of a given method as well as the practicability and effort of performing the protocols.

Biphasic Extractions are Superior to Monophasic Extractions

In our study, biphasic extractions (*MeOH/CHCl₃/H₂O*, *75EtOH/MTBE*, *(2x)MeOH/MTBE*) resulted in superior coverage and concentrations across all model organisms and sample types. Here, the complementary phases, composed of an organic lipid-rich phase and an aqueous phase containing primary and secondary metabolites, were combined and dried in the final step of each protocol allowing for a greater coverage as compared to monophasic extractions. Chloroform based biphasic extractions by Bligh and Dyer (1959) have been dominantly used over the years due to the focus on the lipid fraction, however, MTBE (methyl tert-butyl ether, i.e., TBME) is more frequently used as a non-toxic and non-carcinogenic alternative to chloroform (Matyash et al., 2008; Furse et al., 2015). Here, both strong hydrophobic solvents in combination with another organic solvent of lower hydrophobicity such as ethanol or methanol resulted in comparable metabolite coverage. Importantly, the chloroform-based extraction resulted in the highest concentrations as well as broadest coverage, however, substituting it with MTBE resulted in similar but less variable measurements (Figures 3, 4).

Monophasic extractions (*100IPA*, *IPA/ACN* and *MeOH/ACN*) require less solvent and are performed more rapidly as compared to biphasic ones, which is a big advantage when processing large numbers of samples. While the robustness of monophasic extractions was comparable to that of the other well performing biphasic extractions, i.e., *75EtOH/MTBE*, they provided lower compound coverage due to the lack of certain lipids that were poorly extracted, with the exception of *100IPA*, which provided adequate coverage and concentrations in most cases. This easy-to-use and rapid protocol achieved adequate lipid coverage and reproducibility in most model organisms and sample types. However, the concentration for amino acids and amino acid

related metabolites were lower as compared to biphasic extraction. Several other lipidomic studies concluded that isopropanol is an adequate alternative to more complex and time-consuming biphasic extractions. There, utilizing isopropanol in a ratio to water, e.g., 90:10 v/v or 75:25 v/v, performed well and was regarded as excellent alternative for lipidomic analyses (Calderón et al., 2019). Although such monophasic extractions are in general well suited for lipidomic approaches, the broad nature of the standardized metabolic profiling assay requires a trade-off between coverage, extracted concentration as well as reproducibility across all metabolite classes. The latter criterion was recently highlighted by Ghorasaini et al. (2021) in an interlaboratory assessment of extraction protocols for lipidomic analyses. The authors showed that the extraction with *MeOH/MTBE* performed better and was more practical than the comparable Bligh and Dyer extraction.

In line with this notion and matching the discussed criteria, we suggest the protocol *75EtOH/MTBE* as a suitable broadly applicable biphasic extraction with MTBE. Importantly, similar conclusions could be drawn for other sample types. Erben et al. (2021) compared several extraction protocols for metabolic profiling of human stool samples via MxP Quant 500 and Andresen et al. (2021) of human cells from different tissues (human liver and bone marrow) or cell lines (adherent: HEK and non-adherent: HL60). Both studies concluded that protocols including methanol or ethanol with MTBE are suitable for these sample types confirming our findings.

No one Size Fits all Approach

The biphasic MTBE extractions achieve a broad coverage, high concentrations and little variability in between extractions. These attributes make it a versatile extraction method suitable for the different model organisms and sample types tested.

However, the extraction protocol of choice depends highly on the target as well as the sample type. There is no universal extraction protocol that is optimal in all instances. While our study aimed to find the most versatile protocol, it also showed that other protocols extracted certain metabolite classes more efficiently than the broader biphasic extractions. For instance, *MeOH/ACN/H₂O* + FA was superior in the extraction of amino acids in zebrafish and of glycerophospholipids in *Drosophila* as compared to the other protocols (Supplementary Figure S4). Due to the fact that the *75EtOH/MTBE* protocol is quite time and labor consuming, the rapid *100IPA* protocol may provide an adequate alternative for large sample cohorts where high-throughput is required. Hence, the most suitable extraction protocol highly depends on the type of analysis (quantitative or qualitative assessment), the coverage needed (a small set of targets within one metabolite class or a broad screening), as well as the size, type, and number of samples to process.

To find the most adequate protocol for a given scenario we included this data in a publicly available shiny app - "MetaboExtract" (Andresen et al., 2021). This open access resource is expandable and makes use of the comparability of standardized assays such as MxP Quant 500. MetaboExtract enables users to review and explore standardized extractions and infer baseline concentrations of

metabolites across a variety of sample types and organisms. There, users can search for a metabolite or metabolite class of interest, review or compare measured concentrations following a variety of mono- or biphasic extraction protocols across human cells, cell lines and tissue and, now, model organisms.

DATA AVAILABILITY STATEMENT

The custom R scripts (R version 4.0.4) that were used for analysis and visualization are accessible at https://github.com/nilsmechtel/MO_extractions and <https://CRAN.R-project.org/package=MetAlyzer>. The underlying code for “MetaboExtract” is available at <https://github.com/andresenc/MetaboExtract> (Andresen et al., 2021).

ETHICS STATEMENT

The animal study was reviewed and approved by Regierungspräsidium Karlsruhe, Germany (T-40/20) Regierungspräsidium Karlsruhe and by Medical Faculty Mannheim (I-19/02).

AUTHOR CONTRIBUTIONS

Conceptualization, HG, EH, NM, RH, and GP.; sample generation, AW, FC, and KB.; sample processing and analysis, EH and NM.; data analysis, NM, HG, and GP.; writing—original draft preparation, HG, NM, RH, and GP.; writing—original draft preparation, HG, NM, RH, and GP.; writing—review and editing, all authors; visualization, NM and HG.; project administration, RH and GP.; funding acquisition, TF, MF, AT, JK, RH and GP. All authors contributed to the article and approved the submitted version.

REFERENCES

- Abbiss, H., Maker, G., and Trengove, R. (2019). Metabolomics Approaches for the Diagnosis and Understanding of Kidney Diseases. *Metabolites* 9 (2), 34. doi:10.3390/metabo9020034
- Adamski, J. (2016). Key Elements of Metabolomics in the Study of Biomarkers of Diabetes. *Diabetologia* 59 (12), 2497–2502. Springer Verlag. doi:10.1007/s00125-016-4044-y
- Andresen, C., Boch, T., Gegner, H. M., Mechtel, N., Narr, A., Birgin, E., et al. (2021). Comparison of Extraction Methods for Intracellular Metabolomics. *BioRxiv*. doi:10.1101/2021.12.15.470649
- Arneth, B., Arneth, R., and Shams, M. (2019). Metabolomics of Type 1 and Type 2 Diabetes. *Int. J. Mol. Sci.* 20 (10), 2467. doi:10.3390/ijms20102467
- Bell, J. A., Santos Ferreira, D. L., Fraser, A., Soares, A. L. G., Howe, L. D., Lawlor, D. A., et al. (2021). Sex Differences in Systemic Metabolites at Four Life Stages: Cohort Study with Repeated Metabolomics. *BMC Med.* 19 (1), 1–13. doi:10.1186/s12916-021-01929-2
- Bligh, E. G., and Dyer, W. J. (1959). Canadian Journal of Biochemistry and Physiology. *Can. J. Biochem. Physiol.* 37 (8), 911–917.
- Brennan, L., and Gibbons, H. (2020). Sex Matters: a Focus on the Impact of Biological Sex on Metabolomic Profiles and Dietary Interventions. *Proc. Nutr. Soc.* 79 (2), 205–209. doi:10.1017/S002966511900106X

FUNDING

HG and parts of the study were funded by the German Federal Ministry of Education and Research within the SMART-CARE consortium under the funding code 161L0212. EH and NM. and parts of the study were funded by grants from Deutsche Forschungsgemeinschaft (CRC 1118 and IRTG 1874/2 DIAMICOM). The Metabolomics Core Technology Platform is supported by the Excellence cluster “CellNetworks” (Heidelberg University) and the Deutsche Forschungsgemeinschaft (Grant ZUK 40/2010-3009262). CA. is supported by an Add-on Fellowship of the Joachim Herz Foundation. The responsibility for the content of this publication lies with the authors.

ACKNOWLEDGMENTS

The authors gratefully acknowledge the data storage service SDS@hd supported by the Ministry of Science, Research and the Arts Baden-Württemberg (MWK) and the German Research Foundation (DFG) through grant INST 35/1314-1 FUGG and INST 35/1503-1 FUGG. We are grateful for support by the Zebrafish Core Unit Mannheim. Additionally, the authors would like to thank the technicians of the MCTP, Nina Kunze-Rohrbach, Eva-Maria Kaeshammer-Lorenz and Michael Schulz for their excellent work in the laboratory. Lastly, we would like to note that **Figure 1** was created using BioRender.com.

SUPPLEMENTARY MATERIAL

The Supplementary Material for this article can be found online at: <https://www.frontiersin.org/articles/10.3389/fchem.2022.869732/full#supplementary-material>

- Calderón, C., Sanwald, C., Schlotterbeck, J., Drotleff, B., and Lämmerhofer, M. (2019). Comparison of Simple Monophasic versus Classical Biphasic Extraction Protocols for Comprehensive UHPLC-MS/MS Lipidomic Analysis of Hela Cells. *Analytica Chim. Acta* 1048, 66–74. doi:10.1016/j.aca.2018.10.035
- Edison, A., Hall, R., Junot, C., Karp, P., Kurland, I., Mistrik, R., et al. (2016). The Time Is Right to Focus on Model Organism Metabolomes. *Metabolites* 6 (1), 8. doi:10.3390/metabo6010008
- Erben, V., Poschet, G., Schrotz-King, P., and Brenner, H. (2021). Evaluation of Different Stool Extraction Methods for Metabolomics Measurements in Human Faecal Samples. *BMJ Nutr. Prev. Health* 4, 374–384. doi:10.1136/bmjnp-2020-000202
- Furse, S., Egmond, M. R., and Killian, J. A. (2015). Isolation of Lipids from Biological Samples. *Mol. Membr. Biol.* 32 (3), 55–64. doi:10.3109/09687688.2015.1050468
- Ghorasaini, M., Mohammed, Y., Adamski, J., Bettcher, L., Bowden, J. A., Cabruja, M., et al. (2021). Cross-Laboratory Standardization of Preclinical Lipidomics Using Differential Mobility Spectrometry and Multiple Reaction Monitoring. *Anal. Chem.* 93, 16369–16378. doi:10.1021/acs.analchem.1c02826
- Ivanisevic, J., Zhu, Z.-J., Plate, L., Tautenhahn, R., Chen, S., O'Brien, P. J., et al. (2013). Toward 'Omic Scale Metabolite Profiling: A Dual Separation-Mass Spectrometry Approach for Coverage of Lipid and Central Carbon Metabolism. *Anal. Chem.* 85 (14), 6876–6884. doi:10.1021/ac401140h
- Johnson, C. H., Patterson, A. D., Idle, J. R., and Gonzalez, F. J. (2012). Xenobiotic Metabolomics: Major Impact on the Metabolome. *Annu. Rev. Pharmacol. Toxicol.* 52, 37–56. doi:10.1146/annurev-pharmtox-010611-134748

- Lin, C. Y., Wu, H., Tjeerdema, R. S., and Viant, M. R. (2007). Evaluation of Metabolite Extraction Strategies from Tissue Samples Using NMR Metabolomics. *Metabolomics* 3 (1), 55–67. doi:10.1007/s11306-006-0043-1
- Lippi, G., Von Meyer, A., Cadamuro, J., and Simundic, A.-M. (2020). PREDICT: A Checklist for Preventing Preanalytical Diagnostic Errors in Clinical Trials. *Clin. Chem. Lab. Med.* 58 (4), 518–526. doi:10.1515/cclm-2019-1089
- Lisec, J., Schauer, N., Kopka, J., Willmitzer, L., and Fernie, A. R. (2006). Gas Chromatography Mass Spectrometry-Based Metabolite Profiling in Plants. *Nat. Protoc.* 1 (1), 387–396. doi:10.1038/nprot.2006.59
- Matyash, V., Liebisch, G., Kurzchalia, T. V., Shevchenko, A., and Schwudke, D. (2008). Lipid Extraction by Methyl-Tert-Butyl Ether for High-Throughput Lipidomics. *J. Lipid Res.* 49 (5), 1137–1146. doi:10.1194/jlr.D700041-JLR200
- Mellert, W., Kapp, M., Strauss, V., Wiemer, J., Kamp, H., Walk, T., et al. (2011). Nutritional Impact on the Plasma Metabolome of Rats. *Toxicol. Lett.* 207 (2), 173–181. doi:10.1016/j.toxlet.2011.08.013
- Nicholson, J. K., Holmes, E., and Elliott, P. (2008). The Metabolome-Wide Association Study: A New Look at Human Disease Risk Factors. *J. Proteome Res.* 7 (9), 3637–3638. doi:10.1021/pr8005099
- Pallister, T., Jackson, M. A., Martin, T. C., Glastonbury, C. A., Jennings, A., Beaumont, M., et al. (2017). Untangling the Relationship between Diet and Visceral Fat Mass through Blood Metabolomics and Gut Microbiome Profiling. *Int. J. Obes.* 41 (7), 1106–1113. doi:10.1038/ijo.2017.70
- Rabinowitz, J. D., and Kimball, E. (2007). Acidic Acetonitrile for Cellular Metabolome Extraction from *Escherichia C.* *Anal. Chem.* 79 (16), 6167–6173. doi:10.1021/ac070470c
- Saoi, M., and Britz-mckibbin, P. (2021). New Advances in Tissue Metabolomics: A Review. *Metabolites* 11 (10), 672. doi:10.3390/metabo11100672
- Shao, Y., and Le, W. (2019). Recent Advances and Perspectives of Metabolomics-Based Investigations in Parkinson's Disease. *Mol. Neurodegeneration* 14 (1), 1–12. doi:10.1186/s13024-018-0304-2
- Sindelar, M., Stancliffe, E., Schwaiger-Haber, M., Anbukumar, D. S., Adkins-Travis, K., Goss, C. W., et al. (2021). Longitudinal Metabolomics of Human Plasma Reveals Prognostic Markers of COVID-19 Disease Severity. *Cel Rep. Med.* 2 (8), 100369. doi:10.1016/j.xcrm.2021.100369
- Siskos, A. P., Jain, P., Römisch-Margl, W., Bennett, M., Achaintre, D., Asad, Y., et al. (2017). Interlaboratory Reproducibility of a Targeted Metabolomics Platform for Analysis of Human Serum and Plasma. *Anal. Chem.* 89 (1), 656–665. doi:10.1021/acs.analchem.6b02930
- Weir, T. L., Manter, D. K., Sheflin, A. M., Barnett, B. A., Heuberger, A. L., and Ryan, E. P. (2013). Stool Microbiome and Metabolome Differences between Colorectal Cancer Patients and Healthy Adults. *PLoS ONE* 8 (8), e70803. doi:10.1371/journal.pone.0070803
- Wilkins, J. M., and Trushina, E. (2018). Application of Metabolomics in Alzheimer's Disease. *Front. Neurol.* 8 (JAN), 1–20. doi:10.3389/fneur.2017.00719
- Yin, P., Lehmann, R., and Xu, G. (2015). Effects of Pre-Analytical Processes on Blood Samples Used in Metabolomics Studies. *Anal. Bioanal. Chem.* 407 (17), 4879–4892. doi:10.1007/s00216-015-8565-x
- Zukunft, S., Prehn, C., Röhring, C., Möller, G., Hrabě de Angelis, M., Adamski, J., et al. (2018). High-Throughput Extraction and Quantification Method for Targeted Metabolomics in Murine Tissues. *Metabolomics* 14 (1), 1–12. doi:10.1007/s11306-017-1312-x

Conflict of Interest: The authors declare that the research was conducted in the absence of any commercial or financial relationships that could be construed as a potential conflict of interest.

Publisher's Note: All claims expressed in this article are solely those of the authors and do not necessarily represent those of their affiliated organizations, or those of the publisher, the editors and the reviewers. Any product that may be evaluated in this article, or claim that may be made by its manufacturer, is not guaranteed or endorsed by the publisher.

Copyright © 2022 Gegner, Mechtel, Heidenreich, Wirth, Cortizo, Bennewitz, Fleming, Andresen, Freichel, Teleman, Kroll, Hell and Poschet. This is an open-access article distributed under the terms of the Creative Commons Attribution License (CC BY). The use, distribution or reproduction in other forums is permitted, provided the original author(s) and the copyright owner(s) are credited and that the original publication in this journal is cited, in accordance with accepted academic practice. No use, distribution or reproduction is permitted which does not comply with these terms.



Gut Bacteria Regulate the Pathogenesis of Huntington's Disease in *Drosophila* Model

Anjalika Chongtham¹, Jung Hyun Yoo¹, Theodore M. Chin¹, Ngozi D. Akingbesote¹, Ainul Huda¹, J. Lawrence Marsh² and Ali Khoshnan^{1*}

¹ Biology and Bioengineering, California Institute of Technology (Caltech), Pasadena, CA, United States, ² Developmental and Cell Biology, University of California, Irvine, Irvine, CA, United States

OPEN ACCESS

Edited by:

Frank Hirth,
King's College London,
United Kingdom

Reviewed by:

Pedro Domingos,
Universidade Nova de Lisboa,
Portugal

Amber L. Southwell,
University of Central Florida,
United States

*Correspondence:

Ali Khoshnan
Khoshnan@caltech.edu

Specialty section:

This article was submitted to
Neurodegeneration,
a section of the journal
Frontiers in Neuroscience

Received: 22 March 2022

Accepted: 12 May 2022

Published: 02 June 2022

Citation:

Chongtham A, Yoo JH, Chin TM, Akingbesote ND, Huda A, Marsh JL and Khoshnan A (2022) Gut Bacteria Regulate the Pathogenesis of Huntington's Disease in *Drosophila* Model. *Front. Neurosci.* 16:902205. doi: 10.3389/fnins.2022.902205

Changes in the composition of gut microbiota are implicated in the pathogenesis of several neurodegenerative disorders. Here, we investigated whether gut bacteria affect the progression of Huntington's disease (HD) in transgenic *Drosophila melanogaster* (fruit fly) models expressing full-length or N-terminal fragments of human mutant huntingtin (HTT) protein. We find that elimination of commensal gut bacteria by antibiotics reduces the aggregation of amyloidogenic N-terminal fragments of HTT and delays the development of motor defects. Conversely, colonization of HD flies with *Escherichia coli* (*E. coli*), a known pathobiont of human gut with links to neurodegeneration and other morbidities, accelerates HTT aggregation, aggravates immobility, and shortens lifespan. Similar to antibiotics, treatment of HD flies with small compounds such as luteolin, a flavone, or crocin a beta-carotenoid, ameliorates disease phenotypes, and promotes survival. Crocin prevents colonization of *E. coli* in the gut and alters the levels of commensal bacteria, which may be linked to its protective effects. The opposing effects of *E. coli* and crocin on HTT aggregation, motor defects, and survival in transgenic *Drosophila* models support the involvement of gut-brain networks in the pathogenesis of HD.

Keywords: Huntington's disease, microbiota, gut-brain, neurodegeneration, crocin (PubChem CID: 5281233)

INTRODUCTION

Huntington's disease (HD) is a progressive genetically inherited neurodegenerative disorder characterized by debilitating motor, psychiatric, and cognitive symptoms (Bates et al., 2015; Ghosh and Tabrizi, 2018). Expansion of a CAG repeat (>35) in exon 1 of the huntingtin (HTT) gene, which translates into an abnormal polyglutamine (polyQ) tract, is the underlying cause of HD (Huntington's Disease Collaborative Research Group, 1993). The expanded polyQ enhances the amyloidogenic properties of HTT exon1 (HTT_{ex1}) peptide, which misfolds and forms insoluble protein assemblies in neurons (DiFiglia et al., 1997). Expansion of the polyQ repeat is a major determinant of disease onset in HD, however, multiple genetic and environmental factors may affect the development and progression of symptoms. One potential modifier is neuroinflammation exemplified by elevated levels of inflammatory microglia and TH17.1 cells in the brains of pre-manifest HD patients. An increase in the activated immune cells coincides with elevated production of inflammatory cytokines, which persists during the symptomatic stages of HD (Björkqvist et al., 2008; Politis et al., 2015; von Essen et al., 2020). Although mutant HTT has been directly implicated in the activation of inflammatory pathways, the environmental inducers of inflammation in HD remain to be investigated (Khoshnan et al., 2004; Trager et al., 2014; Khoshnan et al., 2017).

Commensal and acquired gut microorganisms are prominent sources of inflammogens implicated in neurological disorders. Within the last decade, extensive studies demonstrate that the gastrointestinal (GI) tract and its resident microbes (collectively known as microbiota, and their genomes as microbiome) regulate the nervous system physiology. For example, the gut microbiota influences neurodevelopment, neurodegeneration, neurotrophin and neurotransmitter production, neuropsychiatric and motor behaviors, and neuroinflammation (Sampson et al., 2016; Sharon et al., 2016; Morais et al., 2021). Changes in the homeostasis of gut microbiota (dysbiosis) have been linked to the pathogenesis of several neurological and neurodegenerative disorders, including, autism spectrum disorder (ASD), multiple sclerosis (MS), Alzheimer's disease (AD), Parkinson's disease (PD), and amyotrophic lateral sclerosis (ALS) (Hsiao et al., 2013; Sampson et al., 2016; Marizzoni et al., 2020; Takewaki et al., 2020; Zeng et al., 2020). Neuroinflammation is a prominent feature of gut dysbiosis in neurodegenerative disorders, which includes the activation of microglia and subsequent production of inflammatory cytokines (Sampson et al., 2016; Abdel-Haq et al., 2019). Notably, inflammatory bacteria such as *Enterobacteriaceae* are elevated in the gut of PD patients and their abundance correlates with the worsening of the neurological and pathological symptoms (Keshavarzian et al., 2015; Scheperjans et al., 2015; Li et al., 2017). Moreover, lipopolysaccharides (LPS), major components of gram negative bacteria, which include *Enterobacteriaceae*, have been implicated in the pathogenesis of PD (Perez-Pardo et al., 2019). Gut dysbiosis manifested by reduced alpha diversity in the bacterial communities were recently reported in a cohort of HD patients. Notably, in these studies changes in the abundance of *Eubacterium halii* and potentially other candidates coincide with altered cognition (Wasser et al., 2020). Another gut microbiome analysis of a group of HDs patient's links blooming of the gram-negative bacteria *Bilophila* species to elevated levels of inflammatory cytokines (Du et al., 2021). In transgenic mouse models of HD expressing the neurotoxic mutant HTT^{ex1} fragment, gut dysbiosis has been linked to weight loss, motor deficit, metabolic changes, and disruption in the intestinal epithelium (Kong et al., 2020; Stan et al., 2020; Kong et al., 2021). These promising studies highlight a potential role of gut microbiota in the pathogenesis of HD. However, the mechanisms of how a specific bacterium may affect disease manifestation remain to be investigated.

Drosophila melanogaster (fruit fly) is emerging as a useful model to study the impact of gut-brain interactions in the development and progression of neurological disorders (Wu et al., 2017; Douglas, 2018). Similar to mammals, gut homeostasis in *Drosophila* is regulated by the interaction of bacteria with the enteric neurons and intestinal epithelium including the enteroendocrine cells, which produce antimicrobial peptides (AMPs) involved in immunity against invasive pathogens and maintaining optimal abundance of commensal bacteria (Hanson and Lemaitre, 2020). *Drosophila* has a handful of commensal gut bacteria, which can easily be manipulated for studies on gut-brain communications (Douglas, 2018; Ankrah et al., 2021).

Lactobacillus and *Acetobacter* species are the two most abundant bacterial genera, which regulate nutrient acquisition, growth, metabolism, immune development, and locomotion (Schretter et al., 2018; Storelli et al., 2018; Henriques et al., 2020; Yamauchi et al., 2020; Ankrah et al., 2021). The *Drosophila* models of HD display several hallmarks of disease progression including protein aggregation, motor defects, and aberrant expression of genes including those implicated in systemic inflammation (Barbaro et al., 2015; Al-Ramahi et al., 2018). The simplicity of *Drosophila* gut microbiota offers a useful platform to examine the influence of endogenous and single exogenous bacterial species on HD pathogenesis and to investigate the role of HTT in gut-brain pathways. As a first step, we explored whether elimination of gut bacteria in HD *Drosophila* models or colonization with the human pathobiont *E. coli* influences disease development. Here, we report that gut bacteria promote the aggregation of amyloidogenic N-terminal fragments of HTT, contribute to development of aberrant motor behavior and reduce the life span of female HD flies. We further provide evidence that modifying the gut environment of female HD flies ameliorates HD phenotypes. These studies and models facilitate future dissection of gut-brain interaction in HD at a molecular level and are useful for the discovery of gut-based therapeutics.

MATERIALS AND METHODS

Fly Stocks

The huntingtin expressing transgenic *Drosophila* lines used in this study were M{UAS-HTT^{ex1}.Q25} (B#68414), M{UAS-HTT^{ex1}.Q120} (B#76352), and M{UAS-HTT⁵⁸⁶.Q120} (B#68447), M{UAS-HTT^{FL}.Q25} (B#68397), M{UAS-hHTT^{FL}.Q120} (Barbaro et al., 2015; Chongtham et al., 2020). Human HTT 586, full-length HTT and HTT^{ex1} (90 aa) transgenes were inserted into the same chromosomal location (51D) and in the same orientation in a common inbred host *Drosophila* line using the phiC31 targeted-insertion system (Bischof et al., 2007). The Gal4/UAS system (Brand and Perrimon, 1993) was used to express the HTT transgenes by crossing the transgenes under the control of the UAS promoter to a driver line having the yeast Gal4 transcriptional activator. The GAL4 drivers used were the pan-neuronal *elav*-Gal4 C155 driver (Bloomington Stock Number B#458) and the ubiquitous *da*-Gal4 (B#8641). Fly cultures were maintained on standard cornmeal/sugar/agar media on a 12:12 h light:dark cycle. Appropriate crosses were carried out to obtain desired progeny. Briefly, standard food vials with ten UAS-HTT males and ten *da*-Gal4 or *elav*-Gal4 driver females were allowed to mate for 2 days and then passed into new vials at 20°C. All assays used female progeny, which were collected after the eclosion and maintained at 20°C for 2–3 days until enough flies had been collected.

Treatment of Flies With Antibiotics or Small Molecules

For drug treatment, groups of 15–20 female flies were placed in vials containing standard cornmeal/sugar/agar food alone for

non-treatment control experiments or standard food mixed with 1 mg/ml of water-soluble test compounds crocin (cat# 17304 Sigma), rifaximin (cat# Y0001074, Sigma), luteolin (# L9283 Sigma), or 1% penicillin-streptomycin (cat#15140-122; Gibco). The flies were transferred to 25°C and passaged to fresh vials every 2nd or 3rd day. For treatment with live bacteria, curli producing (MC4100) and curli deficient (Δ csg) *E. coli* strains from -80°C frozen stocks were grown on YESCA (1% Casamino Acids, 0.12% yeast extract, 2% Bacto agar) agar plates at 25°C for 48 h. The *Lactobacillus rhamnosus* strain (JB-1, ATCC) from frozen stock was streaked on MRS agar (cat#OXCM0361B, Fisher) plates and grown at 37°C overnight. The *Acetobacter* stock was prepared by grinding adult flies in PBS followed by culturing of isolated bacteria on mannitol agar plates. Isolated colonies were grown in liquid manitol broth at 37°C in a bacterial shaker. The bacterial cultures were harvested by centrifugation (3000×g, 5 min), washed and suspended in PBS. The bacterial suspension (0.5 OD or 5×10^7 cells) was then mixed with standard food and groups of 15–20 female progeny that had first been treated with 1% penicillin-streptomycin-supplemented food for 3–4 days, were transferred to the bacteria supplemented food. The flies were transferred to new food with the live bacteria every 2nd or 3rd day at 25°C.

To examine the effects of crocin on *E. coli* treated flies, crocin (1mg/mL) and *E. coli* (0.5 OD or 5×10^7 cells) were both mixed with standard food and flies, that had been treated with 1% penicillin-streptomycin for 3–4 days, were transferred to the crocin and *E. coli* mixed food. Flies were transferred to fresh food every 2nd or 3rd day and their bacterial load and motor behavior was monitored.

Western Blotting

At least 10 wandering third instar larvae or adult flies were lysed and homogenized in RIPA buffer (25 mM Tris-HCl pH 7.6, 150 mM NaCl, 1% NP-40, 1 mM EDTA) with protease inhibitors (Complete, Mini Protease Inhibitor Cocktail, and Roche Applied Science). The lysates were then boiled at 95°C for 5 min, and equal amounts of protein were separated by SDS/PAGE on pre-cast 4–20% polyacrylamide gradient gels (Cat# 5671094, Biorad) and transferred to immune-blot PVDF membrane (Merck cat# IPVH00010). Membranes were blocked with blocking solution (5% non-fat milk in 0.05% Tween in PBS) and incubated with primary anti-HTT antibody PHP1 (1:1,000 in blocking solution) overnight at 4°C. The blots were then treated with HRP-conjugated goat anti-mouse secondary antibody (1:10,000) diluted in blocking solution for 1 h and developed with enhanced chemiluminescent (ECL) substrate (Cat#1705060, Biorad).

To separate SDS-resistant amyloid assemblies, semi-denaturing detergent agarose gel electrophoresis (SDD-AGE) was performed (Halfmann and Lindquist, 2008) with some modifications. Fly lysates were prepared as described above and resolved by electrophoresis in SDD-AGE gels (1.5% agarose, 1X TAE, 0.1% SDS). Proteins were transferred to immune-blot PVDF membrane by overnight downward capillary action using 1X TBS. Membranes were then treated as western blots above.

Immunostaining of Larval Brains and Guts of Adult Flies

Wandering third instar larvae were cut into anterior and posterior halves, and the anterior halves were turned inside out and placed in PBS on ice. These halves were then fixed by rocking for 30 min at RT with 4% formaldehyde made in PBST (PBS + 0.2% Triton X-100). After fixation, halves were washed three times with PBST, blocked with 5% BSA in PBT for 1 h at RT, probed overnight with primary antibody (s) at 4°C, washed, blocked again, and incubated with secondary antibody (s) for 2 h and washed again. Larval brains were then dissected out and mounted in Vectashield-DAPI medium. The primary antibodies were rat-Elav-7E8A10 anti-elav (used at 1:200 dilution in PBS; Developmental Studies Hybridoma Bank), PHP1 anti-HTT (used at 1:500 dilution in PBS; Ko et al., 2018). The secondary antibodies were Alexa Fluor 488 goat anti-mouse (green) and Alexa Fluor 568 goat anti-rat (red) (used at 1:250 dilution in blocking solution, Life Technologies).

Whole guts of adult flies were dissected out in PBS, fixed in 4% formaldehyde in PBST for 1 h, washed with PBST and incubated with blocking buffer for 1 h at RT. The guts were then probed with anti-*E. coli* monoclonal antibody (produced in house) overnight at 4°C. After washing with PBST, guts were incubated with Alexa Fluor 488 goat anti-mouse antibody diluted in blocking buffer for 2 h at RT and washed. The guts were mounted in Vectashield-DAPI medium. Images of mounted tissues were captured using a Leica Sp8 laser scanning microscope and analyzed using Leica Application Suite X (LAS X) software.

Seeding Assay

Seeding assay was according to recent protocols published recently (Chongtham et al., 2021). Briefly, 5 µg of fly lysate from control, *E. coli* and *E. coli* (curli+) fed flies was preincubated with 0.01 µg/mL of proteinase K at 37°C for 1 h and heat inactivated at 75°C for 10 min. The proteinase K treated fly lysate was then incubated with 100 µg of total protein from human neural lysates for 4 h at 25°C with continuous agitation. Semi-denaturing detergent agarose gel electrophoresis (SDD-AGE) was performed to analyze the seeded products.

Climbing Assay

For monitoring the locomotor ability, 10 flies were gently tapped to the bottom of a vertical glass vial (diameter, 2.2 cm), as adapted from Liu et al. (2008). The number of flies that climbed to a height of 5 cm within 10 s was recorded. The test was repeated three times each for four vials of 10 flies at 1 min intervals.

Longevity Assay

A longevity assay was performed as described previously with slight modifications (Barbaro et al., 2015). Briefly, eighty eclosed female flies (1–3 days old) were divided into four tubes of 20 each with the indicated treatment in the figure legends and were maintained at 20°C with a 12:12 h light:dark cycle. Longevity assays in the presence of *E. coli* were performed at 25°C to accommodate bacterial growth. Progeny were collected and transferred to fresh vials with standard food ± treatment.

Cultures were monitored every other day and the number of dead flies counted.

Congo Red Staining of Bacterial Colonies and Colony Forming Unit Counting

To determine the *E. coli* (Curli-producing) load in the gut, flies were surface sterilized with 70% ethanol for 1 min and washed three times with sterile 1X PBS. Flies were then homogenized in groups of five in 500 μ L of sterile 1X PBS using a motorized pestle. Microbial counts were determined by serial dilution plating of the homogenates on YESCA agar plates supplemented with 50 μ g/mL of Congo Red (CR) (Sigma). The YESCA CR plates were incubated at 25°C for 2 days to induce curli production and the number of red colonies that showed curli expression were counted.

Quantification of Dead Pupae

Four groups of 10 UAS-HTTex1-120Q males and elav-Gal4 female virgins were allowed to mate for 2 days at 20°C and passaged daily into vials with standard food supplemented with crocin (1 mg/mL) or 1% penicillin-streptomycin for a span of 4 days. Twenty days after crosses were made, all flies were emptied from the vials, and empty pupal cases and cases containing dead flies were counted to calculate the percentage of pupal survival (Hatfield et al., 2015).

PCR Amplification Bacteria

Flies were surface sterilized with 70% ethanol for 1 min and washed three times with sterile 1X PBS. Bacterial DNA was extracted from equal number of HTTex1 (25Qs or 103Qs) using stool DNA kit (Omega Bio-tek, Norcross, Georgia) according to the provided procedures. Bacterial DNA was amplified from 5 ng of total DNA from each batch of fly by q-PCR using the universal primer Eub340F: 5'-TCCTACGGGAGGCAGCAGT-3' and Eub781R: 5'-GGACTACCAGGGTATCTAATCCTGTT-3' (Nadkarni et al., 2002) in a 7300 real-time PCR system. Data were analyzed comparatively by the formula $2^{(-\Delta\Delta CT)}$.

Construction of pLenti6-csgA-6x his Plasmid

E. coli genomic DNA was isolated from ~1 mL of overnight culture using QIAamp DNA Mini Kit (QIAGEN), following the manufacturer's protocol. C-terminally hexahistidine-tagged CsgA without N-terminal SEC secretion signal sequence (Evans et al., 2015) was amplified via standard PCR method using the following primers: csgA F: 5'-TCAAGGGAATTCACCATGGGTGTTGTTCTCAGTACGG-3', csgA R: 5'-TCAACGGGATCCCTAGTGATGATGGTGGTGA TGGTACTGATGAGCGGTCGCGTTG-3'. Thermal cycling program used for the PCR is as follows: 94°C, 5 min \rightarrow 33x [94°C, 30 s \rightarrow 58°C, 30 s \rightarrow 72°C, 30 s] \rightarrow 72°C, 7 min \rightarrow 4°C. The resulting PCR amplicon was gel-purified using QIAquick Gel Extraction kit (QIAGEN) and then assembled into pLenti6/V5-D-TOPO vector (Invitrogen) following the manufacturer's protocol. The cloned plasmid was subsequently transformed into One Shot TOP10 chemically competent *E. coli* (Invitrogen) and spread on LB + Ampicillin (100 μ g/mL) agar plate

for selection. Several plasmid clones were isolated using QIAprep Spin Miniprep kit (QIAGEN) and then screened via agarose gel electrophoresis after digesting them with *Eco*RI and *Bam*HI. The correct clone was sequenced using CMV-F primer (5'-CGCAAATGGGCGGTAGGCGTG-3') and named pLenti6-V5-D-TOPO:csgA-6x His.

Co-transfection of HTTex1 Q103-EGFP and csgA Plasmids in HEK293 Cells

HEK293 cells were seeded in a 6-well plate with approximately 25% density and let grow overnight at 37°C, 5% CO₂. The cells were then transfected using calcium phosphate transfection method. In brief, 0.1 μ g Lenti-HTTex1 Q103-EGFP plasmid and differential amounts of Lenti-csgA-6x His plasmid (0, 0.2, or 0.3 μ g), were added in each snap-cap tube. Beta-galactosidase cDNA cloned in similar vector was used as control. The total amount of DNA in each transfection mixture was normalized using an empty plasmid backbone. 2 M CaCl₂ was subsequently added (0.12 M final concentration), and the volume of mixture was brought up to 100 μ L with ddH₂O. 100 μ L 2x HBS was added next dropwise and part of solution was squirted into the rest by pipetting for aeration. Entire volume of each transfection mixture was added to the cells and incubation was done overnight at 37°C, 5% CO₂. The transfected cells were subjected to widefield fluorescence microscopy for quantifying HTTex1 Q103-EGFP aggregates and then harvested for SDS-PAGE and western blotting analyses for HTTex1 Q103-EGFP (probed with PHP2 antibody, 1:1,000 dilution) and CsgA-6x His (probed with mouse anti-His antibody, from Thermo Fisher, 1:5,000 dilution).

16S Sequencing of Gut Bacteria

Female flies were harvested on the indicated days post-eclosion, gently disinfected in 70% ethanol and three subsequent rinses in PBS to remove any external bacteria and stored immediately at -80°C. Similar samples for different batches of flies were mixed and shipped to the sequencing facility at Zymo Research Irvine, CA, United States. Briefly, bacterial DNA was extracted using ZymoBIOMICS-96 MagBead DNA kit (Zymo Research Irvine, CA, United States). The DNA samples were prepared for targeted sequencing with the Quick-16S NGS library Prep kit and 16S primer set V3-V4 (Zymo Research Irvine, CA, United States). The final library was sequenced on Illumina MiSeq with a V3 reagent Kit (600 cycles). The sequencing was performed with 10% PhiX Spike-in.

Bioinformatics Analysis of Bacteria

Unique amplicon sequences were inferred from raw reads using the Dada2 pipeline (Callahan et al., 2016). Chimeric sequences were also removed with the Dada2 pipeline. Taxonomy assignment was performed using Uclust from Qiime v.1.9.1. Taxonomy was assigned with the Zymo Research Database, a 16S database that is internally designed and curated, as reference. Composition visualization, alpha-diversity, and beta-diversity analyses were performed with Qiime v.1.9.1 (Caporaso et al., 2010). If applicable, taxa that have significant abundance among different groups were identified by LefSe (Segata et al., 2011).

using default settings. Other analyses such as heatmaps, Taxa2SV_decomposer, and PCoA plots were performed with internal scripts.

Absolute Abundance Quantification

Quantitative real-time PCR was set up with a standard curve. The standard curve was made with plasmid DNA containing one copy of the 16S gene and one copy of the fungal ITS2 region prepared in 10-fold serial dilutions. The primers used were the same as those used in Targeted Library Preparation. The equation generated by the plasmid DNA standard curve was used to calculate the number of gene copies in the reaction for each sample. The PCR input volume (2 μ l) was used to calculate the number of gene copies per microliter in each DNA sample. The number of genome copies per microliter DNA sample was calculated by dividing the gene copy number by an assumed number of gene copies per genome. The value used for 16S copies per genome is 4. The value used for ITS copies per genome is 200. The amount of DNA per microliter DNA sample was calculated using an assumed genome size of 4.64×10^6 bp, the genome size of *Escherichia coli*, for 16S samples, or an assumed genome size of 1.20×10^7 bp, the genome size of *Saccharomyces cerevisiae*, for ITS samples. This calculation is shown below: Calculated Total DNA = Calculated Total Genome Copies \times Assumed Genome Size (4.64×10^6 bp) \times Average Molecular Weight of a DNA bp (660 g/mole/bp) \div Avogadro's Number ($6.022 \times 1,023/\text{mole}$).

Statistical Analysis

Error bars show Standard Error of the Mean (SEM = standard deviation/square root of n). Statistical significance was established using analysis of variance (ANOVA) on Prism software (GraphPad). A one-way ANOVA was performed to analyze the effect of bacterial or drug treatment on motor behavior and survival. A two-way ANOVA was performed to analyze the effect of bacterial or drug treatment, and the timeline of treatment on motor behavior and survival. A two-way ANOVA was performed to check the effect of genotype (WT and mutant HTT expression) and age of flies (days post eclosion) on microbial load of flies. A two-way ANOVA was also performed to investigate the impact of bacterial treatment or gender, and genotype (Da > Gal4, WT-HTT, and mutant HTT) on motor behavior. The ANOVA results are summarized in **Supplementary Table 1** (* = $P < 0.05$, ** = $P < 0.01$, and *** = $P < 0.001$).

RESULTS

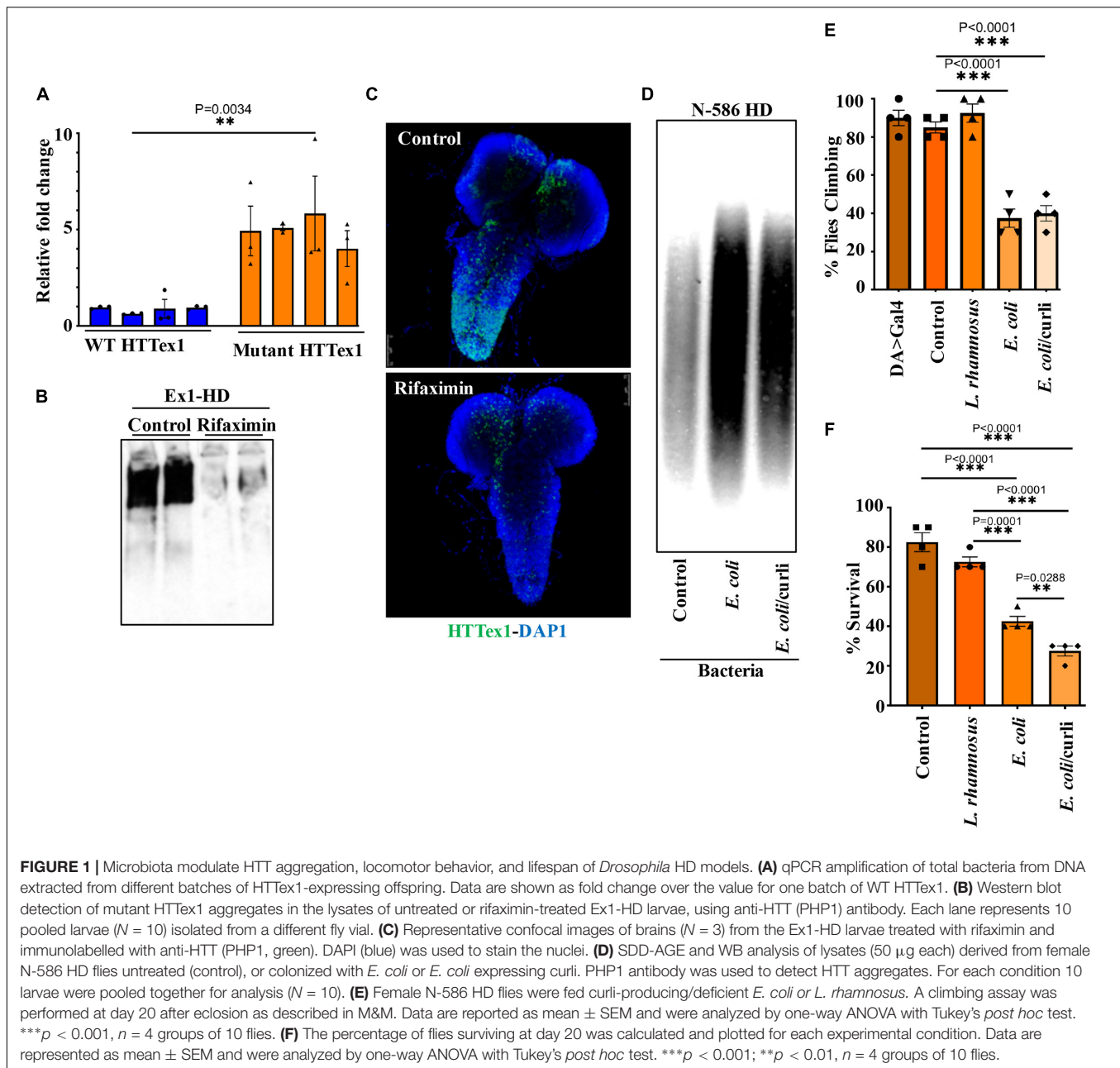
Gut Bacteria Promote the Aggregation of Amyloidogenic HTT Fragments in *Drosophila*

Transgenic *Drosophila* expressing HTTex1 (120Qs) under the control of the pan-neuronal driver *elav*-Gal4 (Ex1-HD) display gut dysbiosis exemplified by elevated levels of total bacteria when compared to a line expressing WT HTTex1 (25Qs) (**Figure 1A** and **Supplementary Figures 1A,B**). To examine

whether gut bacteria influence the aggregation of mutant HTTex1, we generated larvae of the Ex1-HD line in the presence of a gut-specific antibiotic, rifaximin, to eliminate bacteria (**Supplementary Figure 1C**) and examined for the accumulation of aggregates by Western blots (WBs) and immunohistochemistry (IHC). Rifaximin treatment significantly reduces the levels of HTTex1 aggregates in the nervous system of Ex1-HD larvae (**Figures 1B,C**). Given that HTTex1 is selectively expressed in neurons, these findings suggest that gut bacteria may alter neuronal physiology and pathways which regulate the misfolding and aggregation of HTTex1. We then asked whether gut bacteria with links to neurodegeneration in humans may have a similar effect. *Escherichia coli* (*E. coli*), a gut pathobiont, has been implicated in the pathogenesis of PD. In particular, colonization of transgenic mice expressing human α -synuclein, or normal rats with an *E. coli* strain expressing the functional bacterial amyloids curli accelerates the aggregation of α -synuclein in the brain, induces neuroinflammation and worsens motor symptoms (Chen et al., 2016; Sampson et al., 2020). We used a *Drosophila* line ubiquitously expressing the N-terminal 586 amino acids (AA) fragment of mutant HTT (120Qs) (N-586 HD) to explore the impact of *E. coli* on aggregation. Protein aggregates in this line accumulate much slower than in the Ex1-HD line thus, making it ideal for these assays (Barbaro et al., 2015). N-586 HD larvae were generated on food containing an *E. coli* strain expressing curli or an isogenic mutant where the operon for curli has been deleted (Reichhardt et al., 2015). We find that colonization with either strain accelerates the aggregation of N-586 HTT fragment (**Figure 1D**). Although we do not observe any selective effects of curli on HTT proteostasis in the N-586 female HD flies, recombinant curli promotes the aggregation of mutant HTTex1-EGFP when co-expressed in HEK-293 tissue culture cells (**Supplementary Figure 2**). A likely explanation is that direct interaction of curli with mutant HTT may be essential to induce misfolding, whereas other aggregation-promoting components of *E. coli* common to both strains may function by indirect pathways. Collectively, these findings identify gut bacteria as modifiers of HTT aggregation in fruit fly models of HD. We also explored whether *E. coli* induces protein aggregation in transgenic female flies ubiquitously expressing full-length mutant HTT (120Qs) (FL-HD flies). Using various aggregate-specific antibodies (Ko et al., 2018; Chongtham et al., 2021), we did not detect any HTT aggregates in HD flies treated with or without *E. coli* (**Supplementary Figure 3**). However, we cannot rule out the formation of unstable oligomers or novel conformations, which may not bind to antibodies used in these studies.

Gut Bacteria Contribute to Immobility and Death of Female Flies Expressing Mutant HTT

Abnormal motor behavior is a cardinal symptom of HD. Gut bacteria have been implicated in the locomotion of *Drosophila* (Schretter et al., 2018). Given that *E. coli* promotes HTT aggregation, we asked whether it may alter the mobility of HD flies. The N-586 HD flies do not develop mutant HTT-mediated motor defects at a young age (Barbaro et al., 2015),



however, colonization of female flies with *E. coli* significantly impairs their climbing ability, whereas *Lactobacillus rhamnosus* (JB-1 strain) (*L. rhamnosus*), a gram-positive human probiotic has no effects (**Figure 1E**). Moreover, *E. coli* does not alter the mobility of non-transgenic female flies or those expressing WT HTT (**Supplementary Figure 4A**). These findings suggest that *E. coli* may promote the toxicity of the N-586 HTT fragment, which manifests as motor defects in the transgenic flies. *E. coli* also shortens the lifespan of N-586 HD flies; by day 20 ~50% of the flies die and the rest remain immobile and expire within few days (**Figure 1F**). Curli-producing *E. coli* appears more toxic than the isogenic mutant strain indicating that the bacterial amyloids may affect the mortality of N586-HD

flies independent of HTT aggregation and locomotor defects (**Figure 1F**). Seeding of mutant HTT species isolated from the brains of HD *Drosophila* models has been linked to disease progression and toxicity (Ast et al., 2018). We recently reported that seeding-competent HTTex1 species produce neurotoxic assemblies in human neurons and neuronal lysates. The seeding competency of HTT species isolated from mouse models of HD is induced by proteinase-K (PK) treatment (Chongtham et al., 2021). To determine whether *E. coli* colonization enhances the seeding competency of mutant HTT in the N-586 HD flies, we performed seeding assays with or without PK treatment. Using equivalent amount of brains lysates as seeds, we find that the seeding activity of mutant HTT treated with PK is enhanced

in flies colonized with *E. coli* \pm curli (**Figure 2**). The elevated seeding activity is consistent with mobility defects and enhanced mortality of *E. coli*-treated N586-HD flies and suggest that gut bacteria may influence the production and/or the stability of seeding-competent and toxic HTT species.

Ubiquitously expressed full-length mutant HTT produces various abnormalities such as failure to elicit metamorphosis, cryptocephal phenotype, defects in abdominal and thoracic dorsal closure and rotated genitalia in the adult flies. These phenotypes are less severe when progenies are raised at low temperature (20°C) and this condition provides sufficient offspring with minimal or no visible structural defects. The progressive immobility of FL-HD flies is comparable between males and females (**Supplementary Figure 4B**). However, even at low temperature the rotated genitalia and abdominal cleft phenotype are more pronounced in males than in females. To avoid any compounding effects, which may arise from these and/or other undetected phenotypic and genotypic differences between the male and female HD flies, we selected a homogenous population of females with no visible structural pathology for the following studies.

To examine the role of gut bacteria on the mobility of FL-HD, we treated ~3 day old adult female flies with rifaximin or penicillin-streptomycin and evaluated their climbing ability at different intervals. Antibiotic treatment ameliorates the motor defects of FL-HD flies (**Figures 3A, 4A**). Conversely, colonization of FL-HD flies with *E. coli* exacerbates the climbing defects but has no effects on the non-transgenic flies or those expressing full-length WT HTT (**Figure 3B** and **Supplementary Figure 4A**). Colonization of FL-HD or control flies with *L. rhamnosus* does not alter their climbing abilities. (**Figure 3B** and **Supplementary Figure 4A**). Notably, feeding excess *Acetobacter senegalensis* (*A. senegalensis*), a commensal gram-negative bacterium of *Drosophila* also accelerates the motor defects of FL-HD flies (**Figure 3B**). The similar debilitating climbing defects induced by two *E. coli* strains and *A. senegalensis* are consistent with a pathogenic role of gram-negative bacteria in the motor behavior of female HD flies. *E. coli* colonization also significantly reduces the lifespan of FL-HD flies and similar to the N-586 HD model, the curli-producing strain appears more pathogenic (**Figure 3C**). Immunostaining the gut of *E. coli*-fed female HD flies (FL-HD or the N-586 HD) shows colonization of *E. coli* in the midgut (**Figure 3D** and **Supplementary Figure 5**), which contains enterocytes and enteric neurons regulating host-microorganism interactions (Dutta et al., 2015; Capo et al., 2019). The localized accumulation of *E. coli* in the midgut is noteworthy as it confirms spatial colonization and a niche, which may participate in gut-brain communications in flies.

Crocin Ameliorates Huntington's Disease Phenotypes in Female *Drosophila* Models

Gut-based regulation of mutant HTT neurotoxicity is a potential therapeutic target. Given that rifaximin treatment of Ex1-HD flies reduces the buildup of neurotoxic HTTex1 assemblies in neurons (**Figures 1B,C**), we examined whether gut-based natural

compounds might have a similar effect. We focused on anti-inflammatory compounds since inflammation occurs early in pre-manifest HD patients and is recognized as a modifier of HD pathogenesis (Politis et al., 2015). Moreover, inflammation is a prominent outcome of dysbiosis linked to neurodegeneration (Sampson et al., 2016; Goyal et al., 2021). Toward this end, we generated Ex1-HD larvae on foods containing luteolin, a flavone which we have found to inhibit the IKK β -dependent aggregation of HTTex1 in human neurons (Khoshnan et al., 2017), or crocin, a carotenoid abundant in the medicinal plant *Crocus sativus* (saffron), also known for its anti-inflammatory properties and inhibiting the aggregation of amyloidogenic proteins like α -synuclein (Inoue et al., 2018; Shafiee et al., 2018). We find that similar to antibiotics (rifaximin or penicillin-streptomycin), treatment with luteolin or crocin reduces the aggregation of HTTex1 in the nervous system of Ex1-HD larvae (**Figures 1B,C, 5A,B**, and **Supplementary Figure 6**). Crocin or antibiotics also enhance the eclosion efficiency of Ex1-HD flies (**Figure 5C**) further reinforcing gut-mediated regulation of HTTex1 aggregation, toxicity and survival.

Notably, addition of crocin, rifaximin or luteolin to fly food also ameliorates the motor defects of female FL-HD flies with crocin being the most potent compound (**Figure 4A**). Crocin also improves the severe motor defects of the FL-HD flies colonized with *E. coli* (**Figure 4B**). In survival assays, crocin extends the lifespan of female FL-HD flies and those treated with *E. coli* \pm curli (**Figures 4C,D**, respectively). Mechanistically, we find that crocin treatment blocks the colonization and accumulation *E. coli* in the flies' gut (**Figure 4E** and **Supplementary Figure 7**). Crocin does not inhibit the growth of *E. coli* in culture thus, its inhibitory effects on gut colonization may be due to the induction of flies' anti-microbial defense pathways and/or altering the abundance and/or physiology of gut microbiota.

Crocin Modulates the Composition of Gut Bacteria in Female Huntington's Disease Flies

We performed culture assays to examine any potential dysbiosis in the gut of female FL-HD flies. Notably, compared to flies expressing WT HTT, FL-HD flies begin to show dysbiosis by day 5 post eclosion exemplified by lower colony-forming units (CFUs) of *Lactobacilli* but elevated CFUs of *Acetobacter* (**Figure 6**). These findings are similar to results in Ex1-HD flies (**Figure 1A** and **Supplementary Figure 1**) and support an expanded polyQ-mediated disruption in the composition of gut bacteria. To gain better insights into the composition of gut bacteria and the impact of crocin, we performed 16S rRNA sequencing. Our *Drosophila* stocks including those with human HTT transgenes predominantly harbor several *Lactobacilli* strains and *Acetobacter senegalensis* (*A. senegalensis*) species. Notably, *Lactobacilli* and *Acetobacter* show temporal fluctuation in abundance independent of any transgenes, which may be related to flies' physiology and nutritional demand (Schretter et al., 2018; Storelli et al., 2018; Henriques et al., 2020; Yamauchi et al., 2020; Ankrah et al., 2021) (**Figures 7A–C** and

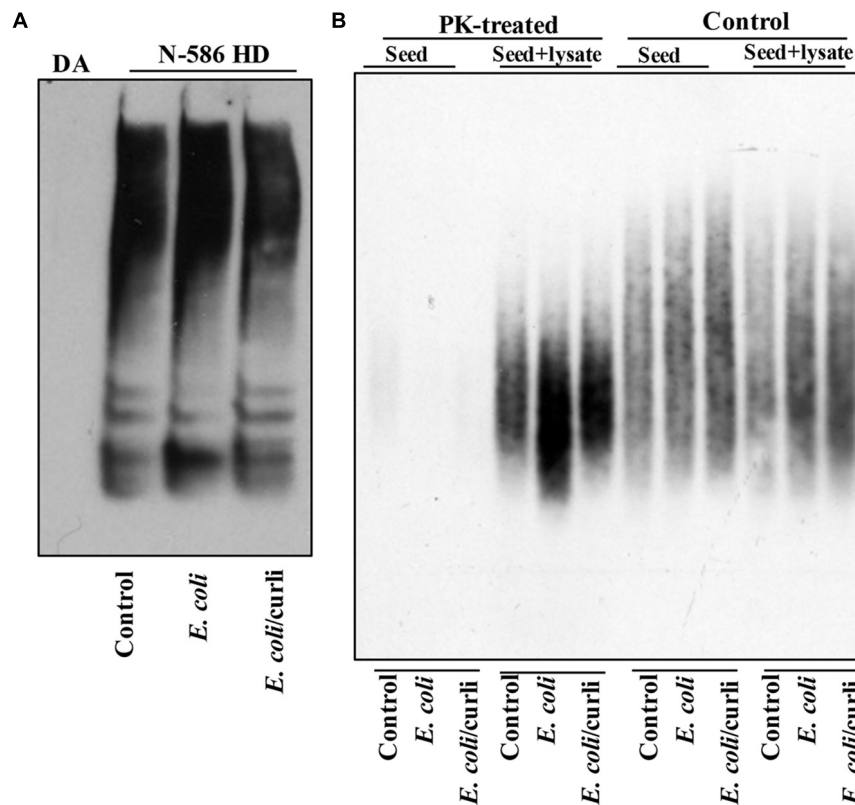


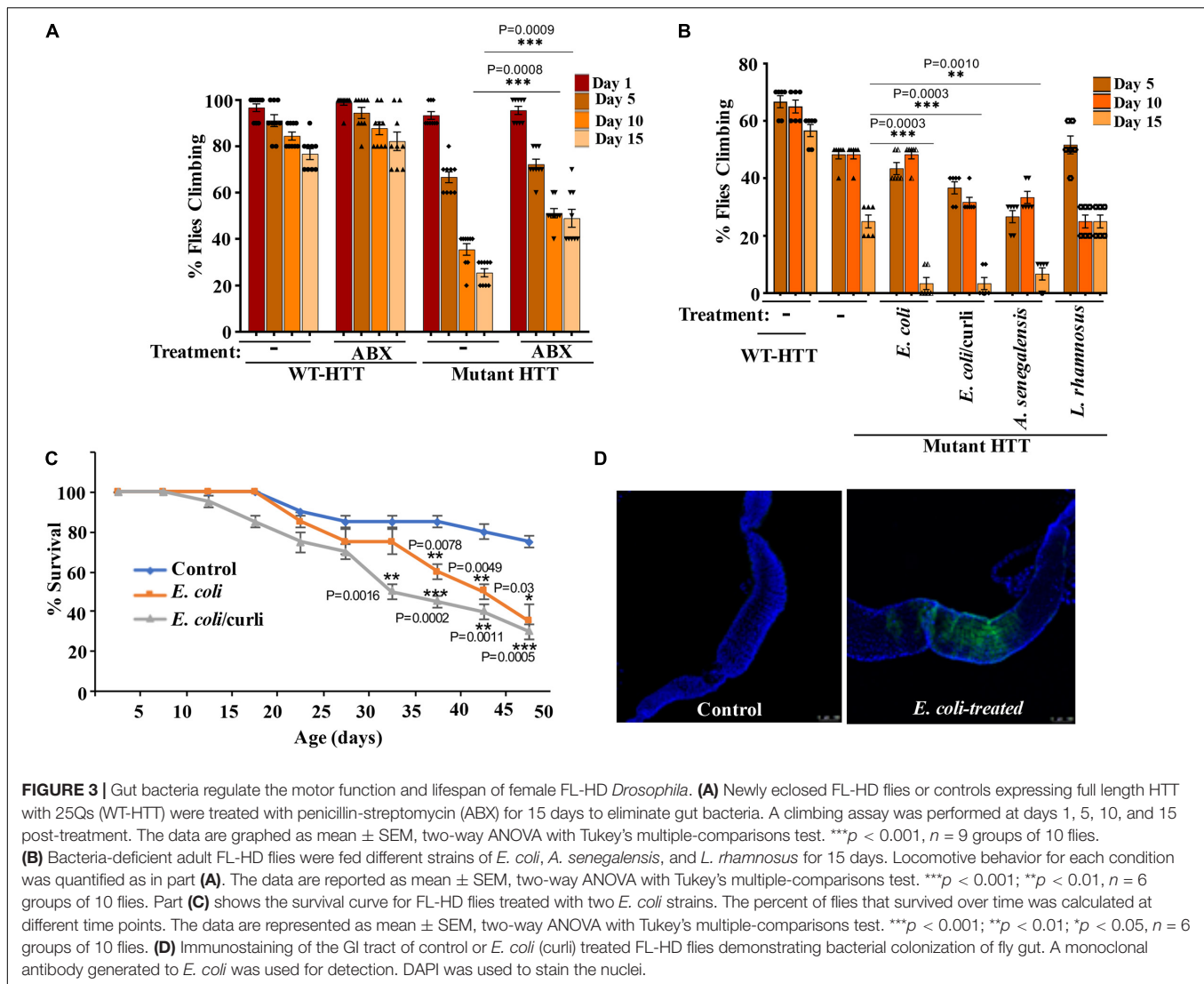
FIGURE 2 | *E. coli* enhances the seeding activity of mutant HTT assemblies in female N-586 HD flies. **(A)** SDS-PAGE analysis of brain lysates followed by WBs of ~15-day old non-transgenic (DA) or N-586 HD flies treated with *E. coli* probed with anti-HTT PHP1. Details are provided in the section “Materials and Methods.” **(B)** SDD-AGE of equal amounts of seeds from lysates in part A added to 50 µg of human neuronal lysates before or after treatment with proteinase-K (PK) (0.5 µg/ml of PK at RT for 30 min and subsequently inactivated by heating at 75°C (Chongtham et al., 2020). Seeds mixed with neuronal lysates were incubated at RT for 4 h and subsequently examined by SDD-AGE. Products were probed with PHP1 antibody.

Supplementary Figure 8A). Flies ubiquitously expressing HTT transgenes (WT or mutant) differ with respect to the relative abundance of *Lactobacilli* and *A. senegalensis* when compared to control flies (Da-Gal4) (Figures 7A–C and Supplementary Figure 8A). Consistent with culture findings, female FL-HD flies harbor elevated levels of *Acetobacter* and changes in the abundance of various *Lactobacilli* species when compared to normal flies or those expressing WT HTT (Figure 7C and Supplementary Figure 8A). Interestingly, elevation of *Acetobacter* has been linked to induced mortality in *Drosophila* (Obata et al., 2018). Indeed, female HD flies fed excess *A. senegalensis* develop severe motor defects, which are similar in magnitude to those induced by *E. coli* (Figure 3B). These data are consistent with the induction of dysbiosis by mutant HTT in *Drosophila* and a potential link to disease progression. Crocin treatment alters the abundance of *Acetobacter* and *Lactobacillus* in all tested fly lines independent of HTT transgene expression (Figures 7D–F and Supplementary Figure 8B). Crocin also reduces the elevated levels of *Acetobacter* but increases the abundance of *Lactobacillus*-NA (not annotated in data bank) in 5-day old female FL-HD flies, however, the effects do not persist (Figure 7F and Supplementary Figure 8B). We predict that crocin may alter the signaling pathways, which regulate the

abundance and/or the physiology of *Lactobacilli* and *Acetobacter* species based on the flies’ nutritional demand (Storelli et al., 2018; Yamauchi et al., 2020). Such systemic and complex metabolic changes may translate into protection observed in the crocin-treated HD flies and remain to be investigated at a molecular level.

DISCUSSION

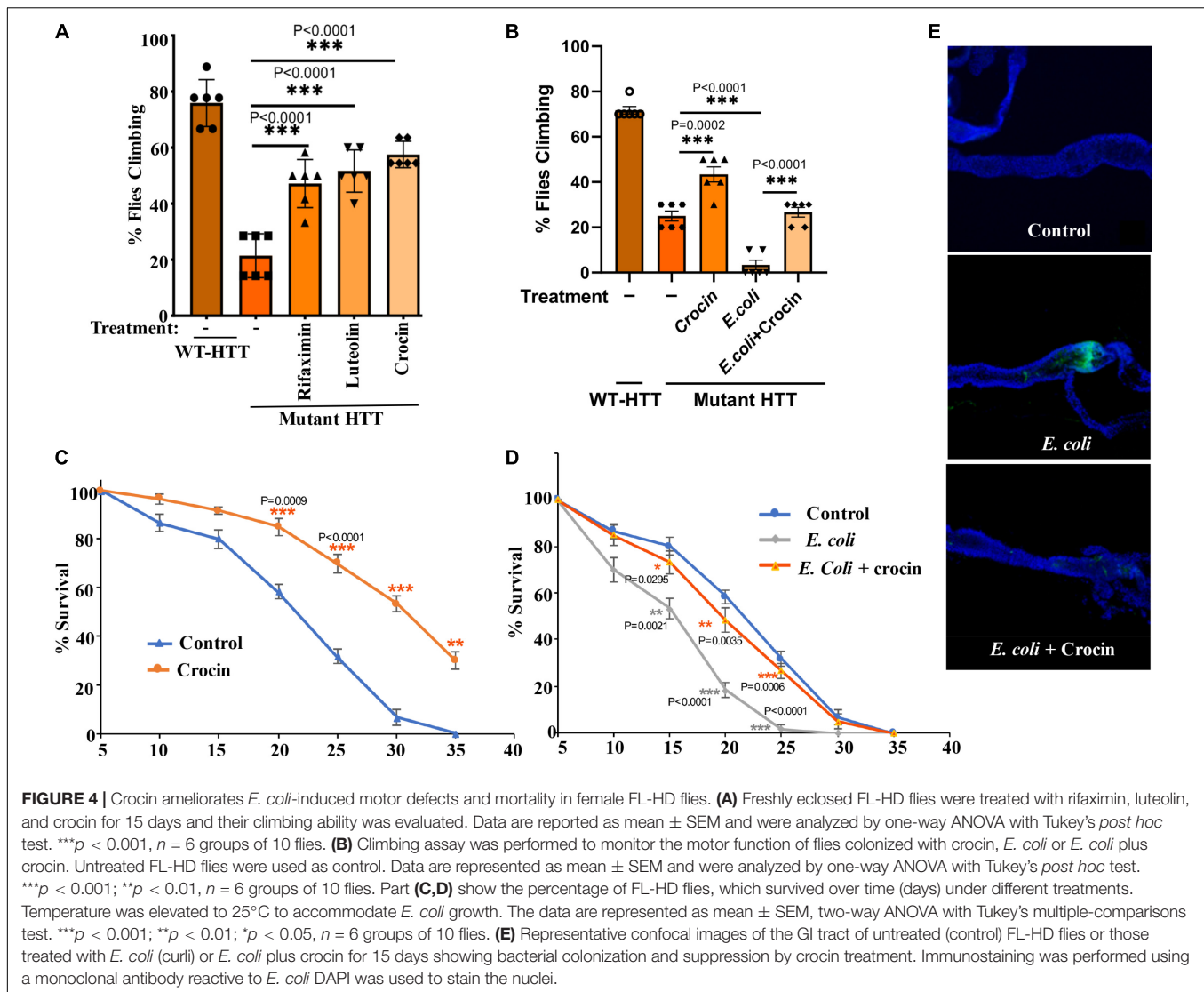
We took advantage of the simplicity of microbiota in *Drosophila* to reveal how bacteria may affect the development of HD. We provide evidence that gut bacteria promote mutant HTT aggregation, impair locomotion and reduce the lifespan of transgenic female HD flies. More specifically, we have identified the gram-negative *Acetobacter*, a commensal fly bacterium, and *E. coli* a human pathobiont, as modifiers of HD pathogenesis. As a proof of concept, we have further demonstrated that modifying the gut environment of HD flies by a gut-specific antibiotic rifaximin, which is approved to treat dysbiosis in Hepatic Encephalopathy patients (Bureau et al., 2021), or small nutraceuticals such as luteolin or crocin delays HD progression. These studies are a prelude to future mechanistic investigations



of microbiota-brain interactions in HD and identification of pathway, which may serve as targets for gut-based therapeutic interventions. A limitation of the current study however, is the use of just female flies in behavioral studies. While both sexes display HD phenotypes including HTT aggregation and immobility, the response of male *Drosophila* expressing mutant HTT to microbial and dietary manipulations of the gut environment may differ from females and remains to be investigated.

Our results indicate that elimination of gut bacteria by antibiotics in the Ex1-HD flies significantly reduces the aggregation of amyloidogenic N-terminal HTTex1. These findings are further reinforced by the induction of mutant HTT aggregation by two strains of *E. coli* in the N-586 HD flies. Interestingly, *E. coli* colonization elevated the seeding activity of mutant HTT (Figure 2), which is linked to severity of symptoms in HD animal models and neurotoxicity in human neurons (Ast et al., 2018; Chongtham et al., 2021). The notion that gut bacteria may alter the toxicity of mutant HTT assemblies

is a novel finding, which requires biophysical investigation to identify any potential neurotoxic conformations (Ko et al., 2018; Chongtham et al., 2021). Recent studies indicate that gram-negative bacteria promote the aggregation of polyQ peptides and impair the motility of *Caenorhabditis elegans* by disrupting proteostasis in neurons, muscle and intestinal cells (Walker et al., 2021). Our studies are consistent with these findings and underscore the regulatory role of gut bacteria in promoting the misfolding and aggregation of amyloidogenic HTT fragments and the production of neurotoxic assemblies. Surprisingly, several bacterial species have been detected in the brain tissues of HD patients. Among them are members of *Enterobacteriaceae* family, which include *E. coli* and other gram-negative bacteria (Alonso et al., 2019). How bacteria gain access to the brains of HD patients and whether they affect the proteostasis of HTT remains unknown. Our results however, indicate that bacteria such as *E. coli* may promote the aggregation of HTT from the gut. Notably, antibiotic treatments of Ex1-HD flies (expressing mutant HTTex1 selectively in neurons) reduce the aggregation of



HTTex1 (Figures 1B,C, 5A,B) thus, supporting an indirect role for gut microbiota regulating the aggregation of amyloidogenic HTT fragments in the nervous system. Ex1-HD flies also show signs of gut dysbiosis (Figure 1A). Given that enteric neurons directly interact with the intestinal epithelium, we speculate that mutant HTTex1 may disrupt neuronal signals essential for gut microbial homeostasis. While details remain to be understood, the findings support the notion that gut dysbiosis in HD flies may also be triggered by neuronal defects. Collectively, we predict that aberrant bidirectional signaling may feed one another and contribute to gut-brain dysfunction in HD.

E. coli expressing the functional amyloids curli in the gut has been implicated in α -synuclein aggregation in the brains of rodents, which coincides with PD pathology (Chen et al., 2016; Sampson et al., 2020). Our data did not show a selective impact of curli-producing *E. coli* on HTT aggregation and impaired locomotion of female HD flies but curli had a negative effect on lifespan and promoted HTTex1 aggregation

when co-expressed in mammalian tissue culture (Figures 1, 3 and Supplementary Figure 2). These findings suggest that curli amyloids may need close contact with HTT to promote its aggregation and that they are potentially unable to enter *Drosophila* cells. Moreover, the negative effects of curli on the survival of female HD flies may be independent of HTT aggregation. Notably, *E. coli* and elevated *Acetobacter* (a fly commensal) produced similar debilitating effects on locomotion, which is consistent with gram-negative bacteria being modifiers of HD symptoms. A recent study demonstrated a correlation between the abundance of the gram-negative *Bilophila* species and elevated inflammatory cytokine response in HD patients (Du et al., 2021). Our findings along with studies on the microbiota of HD patients and mammalian models support the potential involvement of specific clades (or a specific clade) of gut bacteria regulating HD progression and severity (Kong et al., 2020; Stan et al., 2020; Wasser et al., 2020; Du et al., 2021; Kong et al., 2021).

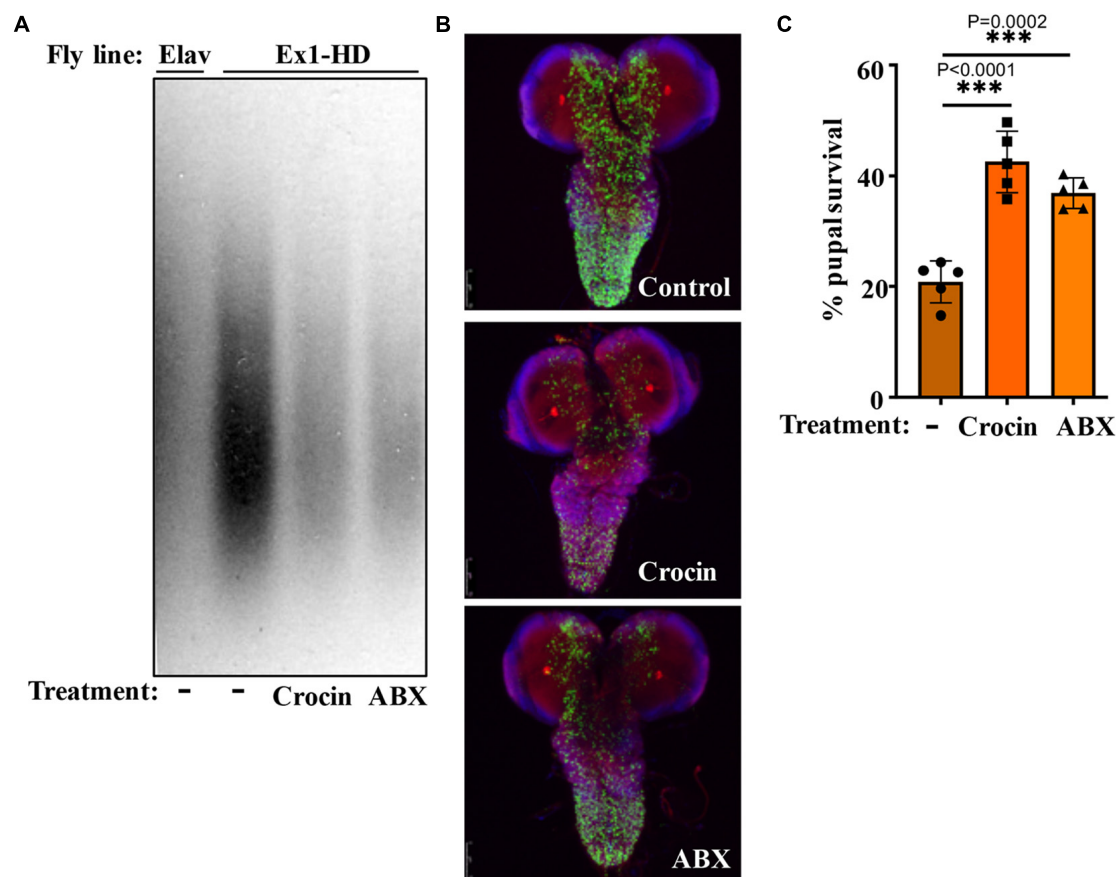


FIGURE 5 | Crocin and antibiotics reduce HTTEx1 aggregation and mortality. **(A)** SDD-AGE and WB analysis of lysates generated from the Ex1-HD larvae treated with crocin or penicillin/streptomycin (ABX). PHP1 antibody was used to detect aggregates. Elav-Gal4 larvae were used as a negative control. For each condition, ten larvae ($n = 10$) were pooled and analyzed. **(B)** Representative confocal images of brains from Ex1-HD larvae untreated (Control) and treated with crocin or ABX, and immunolabelled with PHP1 (green), anti-Elav antibody (red), and DAPI (blue). Part **(C)** shows the percent of pupal survival of Ex1-HD larvae treated with crocin or ABX. The data are represented as mean \pm SEM, one-way ANOVA with Tukey's *post hoc* test. $n = 5$ independent crosses for each condition, *** $p < 0.001$.

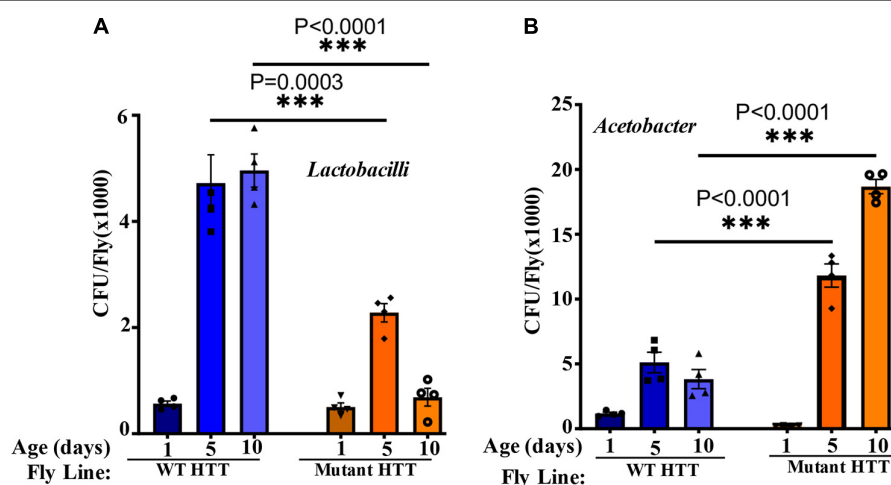


FIGURE 6 | FL-HD female flies have lower abundance of *Lactobacilli* but elevated levels of *Acetobacter*. Microbial counts were determined by serial dilution plating of fly homogenates on MRS or Mannitol agar plates (section "Materials and Methods"). **(A,B)** Time course of the relative abundance of colony forming units (CFU) of *Lactobacilli* and *Acetobacter*, respectively. The data are represented as mean \pm SEM, two-way ANOVA and Sidak's multiple comparison Test. $n = 4$ agar plates for each condition, *** $p < 0.001$.

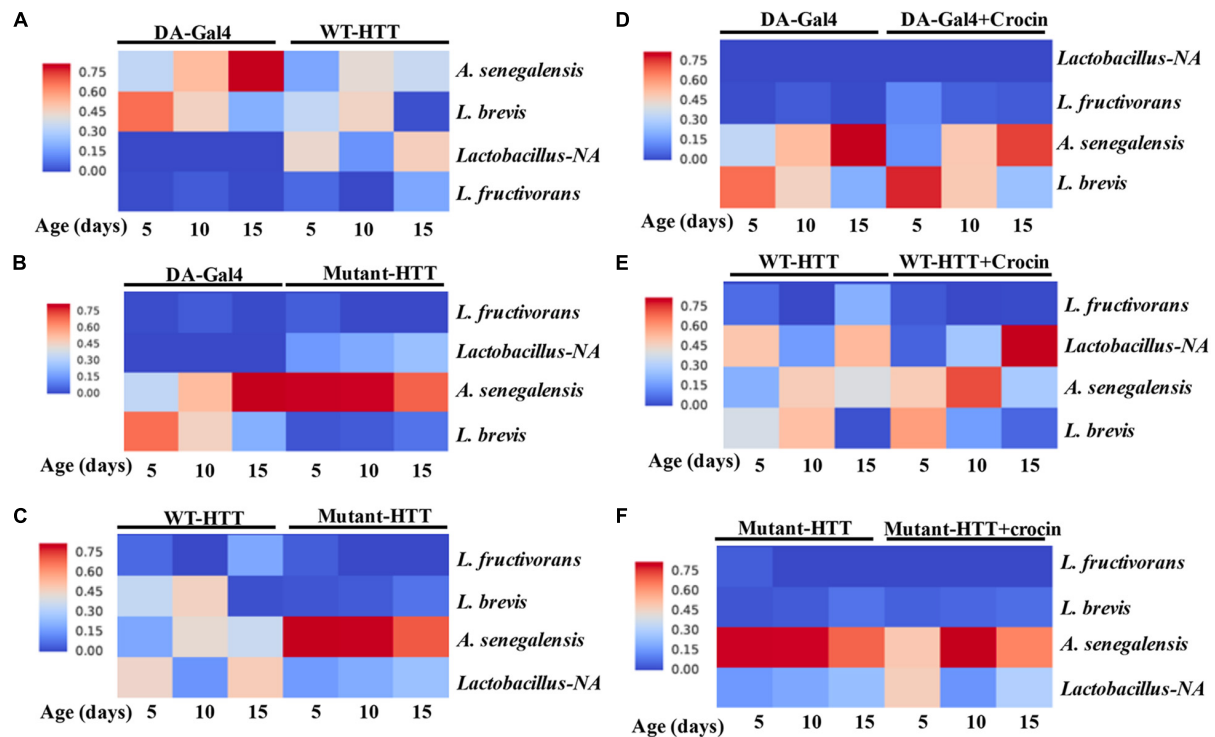


FIGURE 7 | Relative abundance of *Lactobacilli* strains and *A. senegalensis* in the gut of female HD flies by 16S rRNA gene sequence analysis. **(A)** Comparative analysis of Da-Gal4 flies with those expressing WT-HTT, **(B)** Da-Gal4 with FL-HD flies, and **(C)** WT-HTT with FL-HD. Parts **(D–F)** show the effects of crocin on the abundance of bacteria in Da-Gal4, WT-HTT, and FL-HD flies, respectively. All analyses were performed as described in the section “Materials and Methods” by Zymogen’s computational biologists. *Lactobacillus-NA* strain was not detected in the data base.

The ability to modify HD pathology from the gut is therapeutically useful and attractive. Inclusion of crocin in the diet suppressed HTT aggregation, ameliorated locomotive defects, and increased the survival of female HD flies including those colonized with *E. coli*. The effects of crocin on the diversity of gut bacteria in *Drosophila* were difficult to dissect due to few commensal species. However, crocin treatment altered the abundance of *Lactobacillus* and *Acetobacter* in the young female FL-HD flies (Figure 7F) and prevented *E. coli* colonization in the gut (Figure 4E and Supplementary Figure 7). In rodents, crocin modifies gut microbiota, which coincides with the inhibition of neurodegeneration in cerebral ischemia models (Zhang et al., 2019), and mitigates glucocorticoids-induced dysbiosis in mice by increasing the alpha diversity of gut bacteria and subsequent normalization of aberrant lipid metabolism (Xie et al., 2019). Crocin and its major byproduct crocetin do not penetrate the gut epithelium in mammals suggesting that its protective effects are potentially induced by modification of gut physiology and/or its microbiota (Xie et al., 2019; Zhang et al., 2019). Given that alpha diversity of gut bacteria is decreased in HD patients and in HD mice (Kong et al., 2020; Stan et al., 2020; Wasser et al., 2020; Du et al., 2021), the application of crocin as a promoter of bacterial diversity in HD models with complex microbiota may provide useful knowledge on specific species, which regulate HD progression.

In summary, our data support a link between gut bacteria and disease progression in transgenic *Drosophila* models of HD and highlight the involvement of gram-negative bacteria in regulating the abundance and toxicity of mutant HTT. The neurotoxic phenotypes such as protein aggregation, motor defects and mortality induced by *E. coli* are useful biomarkers to investigate the gut-brain circuits at a cellular and molecular level. The *Drosophila* GI tract shares anatomical and functional similarities to the mammalian equivalent (Apidianakis and Rahme, 2011). The midgut where *E. coli* colonizes (Figures 3 and 5) is enriched in numerous cell types including the enteroendocrine (EE) cells, which perform similar tasks as in human GI cells and are nodes for gut-brain networks implicated in neurodegeneration (Chandra et al., 2017). Future knowledge on the transcriptome and proteomics of EE cells in HD *Drosophila* models may identify some of the earliest events, which may trigger the neurotoxicity of mutant HTT in the nervous system. The inclusion of crocin as an inhibitory agent of *E. coli* toxicity may also identify overlapping pathways, potentially functioning in the opposite directions, or compensatory circuits beneficial to HD. Crocin has a long history of medicinal use and has produced favorable outcomes in clinical and preclinical trials in CNS disorders including AD, PD, ischemia, mood disorders, and LPS-induced cognitive decline (Rajaei et al., 2016; Zhang et al., 2018; Haeri et al., 2019; Zhang et al., 2019; Azmand and Rajaei, 2021). The therapeutic benefits

of crocin in subjects with depression have been attributed to the induction of neurotrophin expression including brain-derived neurotrophic factor (BDNF) (Ghasemi et al., 2015; Moghadam et al., 2021). This property of crocin may prove useful for HD considering the role of HTT in BDNF expression and transport, biological activities that are diminished in neurons expressing mutant HTT (Zuccato and Cattaneo, 2014). These features and the gut-modifying properties of crocin make it or its derivatives attractive therapeutic candidates for HD.

DATA AVAILABILITY STATEMENT

The original contributions presented in this study are included in the article/**Supplementary Material**. Further inquiries can be directed to the corresponding author/s.

AUTHOR CONTRIBUTIONS

AK conceived the idea, wrote the manuscript, and acquired the funding. AC contributed to writing and editing the manuscript. AC, JY, TC, NA, and AH performed the experiments. AK, AC,

and JY analyzed the data. JM provided the fly stocks. All authors have read and approved the manuscript.

FUNDING

Funding was provided through awards to AK by the Huntington's Disease Society of America (HDSA) and Hereditary Disease Foundation (HDF).

ACKNOWLEDGMENTS

We are grateful to Segelski at Stanford for providing the *E. coli* strains used in these studies, and Yelim Lee for technical assistance.

SUPPLEMENTARY MATERIAL

The Supplementary Material for this article can be found online at: <https://www.frontiersin.org/articles/10.3389/fnins.2022.902205/full#supplementary-material>

REFERENCES

- Abdel-Haq, R., Schlachetzki, J. C. M., Glass, C. K., and Mazmanian, S. K. (2019). Microbiome-microglia connections via the gut-brain axis. *J. Exp. Med.* 216, 41–59. doi: 10.1084/jem.20180794
- Alonso, R., Pisa, D., and Carrasco, L. (2019). Brain microbiota in huntington's disease patients. *Front. Microbiol.* 10:2622. doi: 10.3389/fmicb.2019.02622
- Al-Ramahi, I., Lu, B., Di Paola, S., Pang, K., de Haro, M., Peluso, I., et al. (2018). High-throughput functional analysis distinguishes pathogenic, nonpathogenic, and compensatory transcriptional changes in neurodegeneration. *Cell Syst.* 7, 28–40. doi: 10.1016/j.cels.2018.05.010
- Ankrah, N. Y. D., Barker, B. E., Song, J., Wu, C., McMullen, J. G. II, and Douglas, A. E. (2021). Predicted metabolic function of the gut microbiota of drosophila melanogaster. 6:e1369. doi: 10.1128/mSystems.01369-20
- Apidianakis, Y., and Rahme, L. G. (2011). Drosophila melanogaster as a model for human intestinal infection and pathology. *Dis. Model Mech.* 4, 21–30. doi: 10.1242/dmm.003970
- Ast, A., Buntru, A., Schindler, F., Hasenkopf, R., Schulz, A., Brusendorf, L., et al. (2018). mHTT seeding activity: a marker of disease progression and neurotoxicity in models of huntington's disease. *Mol. Cell.* 71, 675–688. doi: 10.1016/j.molcel.2018.07.032
- Azmand, M. J., and Rajaei, Z. (2021). Effects of crocin on spatial or aversive learning and memory impairments induced by lipopolysaccharide in rats. *Avicenna J. Phytomed.* 11, 79–90.
- Barbaro, B. A., Lukacsovich, T., Agrawal, N., Burke, J., Bornemann, D. J., Purcell, J. M., et al. (2015). Comparative study of naturally occurring huntingtin fragments in Drosophila points to exon 1 as the most pathogenic species in Huntington's disease. *Hum. Mol. Genet.* 24, 913–925. doi: 10.1093/hmg/ddu504
- Bates, G. P., Dorsey, R., Gusella, J. F., Hayden, M. R., Kay, C., Leavitt, B. R., et al. (2015). Huntington disease. *Nat. Rev. Dis. Prim.* 1:15005.
- Bischof, J., Maeda, R. K., Hediger, M., Karch, F., and Basler, K. (2007). An optimized transgenesis system for Drosophila using germ-line-specific phiC31 integrases. *Proc. Natl Acad. Sci. USA* 104, 3312–3317. doi: 10.1073/pnas.0611511104
- Björkqvist, M., Wild, E. J., Thiele, J., Silvestroni, A., Andre, R., Lahiri, N., et al. (2008). A novel pathogenic pathway of immune activation detectable before clinical onset in Huntington's disease. *J. Exp. Med.* 205, 1869–1877. doi: 10.1084/jem.20080178
- Brand, A. H., and Perrimon, N. (1993). Targeted gene expression as a means of altering cell fates and generating dominant phenotypes. *Development* 118, 401–415. doi: 10.1242/dev.118.2.401
- Bureau, C., Thabut, D., Jezequel, C., Archambeau, I., D'Alteroche, L., Dharancy, S., et al. (2021). The use of rifaximin in the prevention of overt hepatic encephalopathy after transjugular intrahepatic portosystemic shunt : a randomized controlled trial. *Ann. Intern. Med.* 174, 633–640.
- Callahan, B. J., McMurdie, P. J., Rosen, M. J., Han, A. W., Johnson, A. J., and Holmes, S. P. (2016). DADA2: High-resolution sample inference from Illumina amplicon data. *Nat. Methods.* 13, 581–583. doi: 10.1038/nmeth.3869
- Capo, F., Wilson, A., and Di Cara, F. (2019). The intestine of drosophila melanogaster: an emerging versatile model system to study intestinal epithelial homeostasis and host-microbial interactions in humans. *Microorganisms* 2019:7. doi: 10.3390/microorganisms7090336
- Caporaso, J., Kuczynski, J., Stombaugh, J., Bittinger, K., Bushman, F. D., Costello, E. K., et al. (2010). QIIME allows analysis of high-throughput community sequencing data. *Nat. Methods* 7, 335–336. doi: 10.1038/nmeth.f.303
- Chandra, R., Hiniker, A., Kuo, Y. M., Nussbaum, R. L., and Liddle, R. A. (2017). alpha-Synuclein in gut endocrine cells and its implications for Parkinson's disease. *JCI Insight* 2017:2. doi: 10.1172/jci.insight.92295
- Chen, S. G., Stribinski, V., Rane, M. J., Demuth, D. R., Gozal, E., Roberts, A. M., et al. (2016). Exposure to the functional bacterial amyloid protein curli enhances alpha-synuclein aggregation in aged fischer 344 rats and caenorhabditis elegans. *Sci. Rep.* 6:34477. doi: 10.1038/srep34477
- Chongtham, A., Bornemann, D. J., Barbaro, B. A., Lukacsovich, T., Agrawal, N., Syed, A., et al. (2020). Effects of flanking sequences and cellular context on subcellular behavior and pathology of mutant HTT. *Hum. Mol. Genet.* 29, 674–688. doi: 10.1093/hmg/ddaa001
- Chongtham, A., Isas, J. M., Pandey, N. K., Rawat, A., Yoo, J. H., Mastro, T., et al. (2021). Amplification of neurotoxic HTTex1 assemblies in human neurons. *Neurobiol. Dis.* 159:105517. doi: 10.1016/j.nbd.2021.105517
- DiFiglia, M., Sapp, E., Chase, K. O., Davies, S. W., Bates, G. P., Vonsattel, J. P., et al. (1997). Aggregation of huntingtin in neuronal intranuclear inclusions and dystrophic neurites in brain. *Science* 277, 1990–1993. doi: 10.1126/science.277.5334.1990
- Douglas, A. E. (2018). The Drosophila model for microbiome research. *Lab. Anim.* 47, 157–164. doi: 10.1038/s41684-018-0065-0

- Du, G., Dong, W., Yang, Q., Yu, X., Ma, J., Gu, W., et al. (2021). Altered gut microbiota related to inflammatory responses in patients with huntington's disease. *Front. Immunol.* 11:603594. doi: 10.3389/fimmu.2020.603594
- Dutta, D., Dobson, A. J., Houtz, P. L., Glasser, C., Revah, J., Korzeli, J., et al. (2015). Regional cell-specific transcriptome mapping reveals regulatory complexity in the adult drosophila midgut. *Cell Rep.* 12, 346–358. doi: 10.1016/j.celrep.2015.06.009
- Evans, M. L., Chorell, E., Taylor, J. D., Åden, J., Götheson, A., Li, F., et al. (2015). The bacterial curli system possesses a potent and selective inhibitor of amyloid formation. *Mol. Cell* 57, 445–455. doi: 10.1016/j.molcel.2014.12.025
- Ghasemi, T., Abnous, K., Vahdati, F., Mehri, S., Razavi, B. M., and Hosseinzadeh, H. (2015). Antidepressant effect of crocus sativus aqueous extract and its effect on CREB, BDNF, and VGF transcript and protein levels in rat hippocampus. *Drug Res.* 65, 337–343. doi: 10.1055/s-0034-1371876
- Ghosh, R., and Tabrizi, S. J. (2018). Clinical features of huntington's disease. *Adv. Exp. Med. Biol.* 1049, 1–28.
- Goyal, D., Ali, S. A., and Singh, R. K. (2021). Emerging role of gut microbiota in modulation of neuroinflammation and neurodegeneration with emphasis on Alzheimer's disease. *Prog. Neuropsychopharmacol. Biol. Psychiatry* 106:110112. doi: 10.1016/j.pnpbp.2020.110112
- Haeri, P., Mohammadipour, A., Heidari, Z., and Ebrahimzadeh-Bideskan, A. (2019). Neuroprotective effect of crocin on substantia nigra in MPTP-induced Parkinson's disease model of mice. *Anat. Sci. Int.* 94, 119–127. doi: 10.1007/s12565-018-0457-7
- Halfmann, R., and Lindquist, S. (2008). Screening for amyloid aggregation by Semi-denaturing detergent-agarose gel electrophoresis. *J. Vis. Exp.* 17:838. doi: 10.3791/838
- Hanson, M. A., and Lemaitre, B. (2020). New insights on Drosophila antimicrobial peptide function in host defense and beyond. *Curr. Opin. Immunol.* 62, 22–30. doi: 10.1016/j.coi.2019.11.008
- Hatfield, I., Harvey, I., Yates, E. R., Redd, J. R., Reiter, L. T., and Bridges, D. (2015). The role of TORC1 in muscle development in Drosophila. *Sci. Rep.* 5:9676. doi: 10.1038/srep09676
- Henriques, S. F., Dhakan, D. B., Serra, L., Francisco, A. P., Carvalho-Santos, Z., Baltazar, C., et al. (2020). Metabolic cross-feeding in imbalanced diets allows gut microbes to improve reproduction and alter host behaviour. *Nat. Commun.* 11:4236. doi: 10.1038/s41467-020-18049-9
- Hsiao, E. Y., McBride, S. W., Hsien, S., Sharon, G., Hyde, E. R., McCue, T., et al. (2013). Microbiota modulate behavioral and physiological abnormalities associated with neurodevelopmental disorders. *Cell* 155, 1451–1463. doi: 10.1016/j.cell.2013.11.024
- Huntington's Disease Collaborative Research Group. (1993). A novel gene containing a trinucleotide repeat that is expanded and unstable on Huntington's disease chromosomes. *Cell* 72, 971–983. doi: 10.1016/0092-8674(93)90585-e
- Inoue, E., Shimizu, Y., Masui, R., Hayakawa, T., Tsubonoya, T., Hori, S., et al. (2018). Effects of saffron and its constituents, crocin-1, crocin-2, and crocetin on alpha-synuclein fibrils. *J. Nat. Med.* 72, 274–279. doi: 10.1007/s11418-017-1150-1
- Keshavarzian, A., Green, S. J., Engen, P. A., Voigt, R. M., Naqib, A., Forsyth, C. B., et al. (2015). Colonic bacterial composition in Parkinson's disease. *Mov. Disord.* 30, 1351–1360.
- Khosnhan, A., Ko, J., Watkin, E. E., Paige, L. A., Reinhart, P. H., and Patterson, P. H. (2004). Activation of the IkappaB kinase complex and nuclear factor-kappaB contributes to mutant huntingtin neurotoxicity. *J. Neurosci.* 24, 7999–8008. doi: 10.1523/JNEUROSCI.2675-04.2004
- Khosnhan, A., Sabbaugh, A., Calamini, B., Marinero, S. A., Dunn, D. E., Yoo, J. H., et al. (2017). IKKbeta and mutant huntingtin interactions regulate the expression of IL-34: implications for microglial-mediated neurodegeneration in HD. *Hum. Mol. Genet.* 26, 4267–4277. doi: 10.1093/hmg/ddx315
- Ko, J., Isas, J. M., Sabbaugh, A., Yoo, J. H., Pandey, N. K., Chongtham, A., et al. (2018). Identification of distinct conformations associated with monomers and fibril assemblies of mutant huntingtin. *Hum. Mol. Genet.* 27, 2330–2343. doi: 10.1093/hmg/ddy141
- Kong, G., Cao, K. L., Judd, L. M., Li, S., Renoir, T., and Hannan, A. J. (2020). Microbiome profiling reveals gut dysbiosis in a transgenic mouse model of Huntington's disease. *Neurobiol. Dis.* 135:104268. doi: 10.1016/j.nbd.2018.09.001
- Kong, G., Ellul, S., Narayana, V. K., Kanojia, K., Ha, H. T. T., Li, S., et al. (2021). An integrated metagenomics and metabolomics approach implicates the microbiota-gut-brain axis in the pathogenesis of Huntington's disease. *Neurobiol. Dis.* 148:105199. doi: 10.1016/j.nbd.2020.105199
- Li, W., Wu, X., Hu, X., Wang, T., Liang, S., Duan, Y., et al. (2017). Structural changes of gut microbiota in Parkinson's disease and its correlation with clinical features. *Sci. China Life Sci.* 60, 1223–1233. doi: 10.1007/s11427-016-9001-4
- Liu, Z., Wang, X., Yu, Y., Li, X., Wang, T., Jiang, H., et al. (2008). A drosophila model for LRRK2-linked parkinsonism. *Proc. Natl. Acad. Sci. USA* 105, 2693–2698. doi: 10.1073/pnas.0708452105
- Marizzoni, M., Cattaneo, A., Mirabelli, P., Festari, C., Lopizzo, N., Nicolosi, V., et al. (2020). Short-chain fatty acids and lipopolysaccharide as mediators between gut dysbiosis and amyloid pathology in alzheimer's disease. *J. Alzheimers Dis.* 78, 683–697. doi: 10.3233/JAD-200306
- Moghadam, B. H., Bagheri, R., Roozbeh, B., Ashtary-Larky, D., Gaeini, A. A., Duthiel, F., et al. (2021). Impact of saffron (*Crocus Sativus* Linn) supplementation and resistance training on markers implicated in depression and happiness levels in untrained young males. *Physiol. Behav.* 233:113352. doi: 10.1016/j.physbeh.2021.113352
- Morais, L. H., Schreiber, H., and Mazmanian, S. K. (2021). The gut microbiota-brain axis in behaviour and brain disorders. *Nat. Rev. Microbiol.* 19, 241–255. doi: 10.1038/s41579-020-00460-0
- Nadkarni, M. A., Martin, F. E., Jacques, N. A., and Hunter, N. (2002). Determination of bacterial load by real-time PCR using a broad-range (universal) probe and primers set. *Microbiology* 148, 257–266. doi: 10.1099/00221287-148-1-257
- Obata, F., Fons, C. O., and Gould, A. P. (2018). Early-life exposure to low-dose oxidants can increase longevity via microbiome remodelling in Drosophila. *Nat. Commun.* 9:975. doi: 10.1038/s41467-018-03070-w
- Perez-Pardo, P., Dodiya, H. B., Engen, P. A., Forsyth, C. B., Huscens, A. M., Shaikh, M., et al. (2019). Role of TLR4 in the gut-brain axis in Parkinson's disease: a translational study from men to mice. *Gut* 68, 829–843. doi: 10.1136/gutjnl-2018-136844
- Politis, M., Lahiri, N., Niccolini, F., Su, P., Wu, K., Giannetti, P., et al. (2015). Increased central microglial activation associated with peripheral cytokine levels in premanifest Huntington's disease gene carriers. *Neurobiol. Dis.* 83, 115–121.
- Rajaei, Z., Hosseini, M., and Alaei, H. (2016). Effects of crocin on brain oxidative damage and aversive memory in a 6-OHDA model of Parkinson's disease. *Arg. Neuropsychiatr.* 74, 723–729. doi: 10.1590/0004-282X20160131
- Reichhardt, C., Jacobson, A. N., Maher, M. C., Uang, J., McCrate, O. A., Eckart, M., et al. (2015). Congo Red Interactions with Curli-Producing E. coli and native curli amyloid fibers. *PLoS One* 10:e0140388. doi: 10.1371/journal.pone.0140388
- Sampson, T. R., Challis, C., Jain, N., Moiseyenko, A., Ladinsky, M. S., Shastri, G. G., et al. (2020). A gut bacterial amyloid promotes alpha-synuclein aggregation and motor impairment in mice. *Elife* 2020:9. doi: 10.7554/eLife.53111
- Sampson, T. R., Debelius, J. W., Thron, T., Janssen, S., Shastri, G. G., Ilhan, Z. E., et al. (2016). Gut Microbiota regulate motor deficits and neuroinflammation in a model of parkinson's disease. *Cell* 167, 1469–1480. doi: 10.1016/j.cell.2016.11.018
- Scheperjans, F., Aho, V., Pereira, P. A., Koskinen, K., Paulin, L., Pekkonen, E., et al. (2015). Gut microbiota are related to Parkinson's disease and clinical phenotype. *Mov. Disord.* 30, 350–358. doi: 10.1002/mds.26069
- Schretter, C. E., Vielmetter, J., Bartos, I., Marka, Z., Marka, S., Argade, S., et al. (2018). A gut microbial factor modulates locomotor behaviour in Drosophila. *Nature* 563, 402–406. doi: 10.1038/s41586-018-0634-9
- Segata, N., Izard, J., Waldron, L., Gevers, D., Miropolsky, L., Garrett, W. S., et al. (2011). Metagenomic biomarker discovery and explanation. *Genome Biol.* 12:R60. doi: 10.1186/gb-2011-12-6-r60
- Shafee, M., Arekhi, S., Omranzadeh, A., and Sahebkar, A. (2018). Saffron in the treatment of depression, anxiety and other mental disorders: current evidence and potential mechanisms of action. *J. Affect. Disord.* 227, 330–337. doi: 10.1016/j.jad.2017.11.020
- Sharon, G., Sampson, T. R., Geschwind, D. H., and Mazmanian, S. K. (2016). The Central nervous system and the gut microbiome. *Cell* 167, 915–932.
- Stan, T. L., Soylu-Kucharz, R., Burleigh, S., Prykhodko, O., Cao, L., Franke, N., et al. (2020). Increased intestinal permeability and gut dysbiosis in the R6/2

- mouse model of Huntington's disease. *Sci. Rep.* 10:18270. doi: 10.1038/s41598-020-75229-9
- Storelli, G., Strigini, M., Grenier, T., Bozonnet, L., Schwarzer, M., Daniel, C., et al. (2018). *Drosophila* perpetuates nutritional mutualism by promoting the fitness of its intestinal symbiont *Lactobacillus plantarum*. *Cell Metab.* 27, 362–377. doi: 10.1016/j.cmet.2017.11.011
- Takewaki, D., Suda, W., Sato, W., Takayasu, L., Kumar, N., Kimura, K., et al. (2020). Alterations of the gut ecological and functional microenvironment in different stages of multiple sclerosis. *Proc. Natl. Acad. Sci. USA* 117, 22402–22412. doi: 10.1073/pnas.2011703117
- Trager, U., Andre, R., Lahiri, N., Magnusson-Lind, A., Weiss, A., Grueninger, S., et al. (2014). HTT-lowering reverses Huntington's disease immune dysfunction caused by NF- κ B pathway dysregulation. *Brain* 137, 819–833. doi: 10.1093/brain/awt355
- von Essen, M. R., Hellem, M. N. N., Vinther-Jensen, T., Ammitzboll, C., Hansen, R. H., Hjermand, L. E., et al. (2020). Early Intrathecal T Helper 17.1 cell activity in huntington disease. *Ann. Neurol.* 87, 246–255. doi: 10.1002/ana.25647
- Walker, A. C., Bhargava, R., Vaziryan-Sani, A. S., Pourciau, C., Donahue, E. T., Dove, A. S., et al. (2021). Colonization of the *Caenorhabditis elegans* gut with human enteric bacterial pathogens leads to proteostasis disruption that is rescued by butyrate. *PLoS Pathog.* 17:e1009510. doi: 10.1371/journal.ppat.1009510
- Wasser, C. I., Mercieca, E. C., Kong, G., Hannan, A. J., McKeown, S. J., Glikmann-Johnston, Y., et al. (2020). Gut dysbiosis in Huntington's disease: associations among gut microbiota, cognitive performance and clinical outcomes. *Brain Commun.* 2:fcaa110. doi: 10.1093/braincomms/fcaa110
- Wu, S. C., Cao, Z. S., Chang, K. M., and Juang, J. L. (2017). Intestinal microbial dysbiosis aggravates the progression of Alzheimer's disease in *Drosophila*. *Nat. Commun.* 8:24. doi: 10.1038/s41467-017-00040-6
- Xie, X., Xiao, Q., Xiong, Z., Yu, C., Zhou, J., and Fu, Z. (2019). Crocin-I ameliorates the disruption of lipid metabolism and dysbiosis of the gut microbiota induced by chronic corticosterone in mice. *Food Funct.* 10, 6779–6791. doi: 10.1039/c9fo01533g
- Yamauchi, T., Oi, A., Kosakamoto, H., Akuzawa-Tokita, Y., Murakami, T., Mori, H., et al. (2020). Gut bacterial species distinctively impact host purine metabolites during aging in *drosophila*. *iScience* 2020:101477. doi: 10.1016/j.isci.2020.101477
- Zeng, Q., Shen, J., Chen, K., Zhou, J., Liao, Q., Lu, K., et al. (2020). The alteration of gut microbiome and metabolism in amyotrophic lateral sclerosis patients. *Sci. Rep.* 10:12998. doi: 10.1038/s41598-020-69845-8
- Zhang, L., Previn, R., Lu, L., Liao, R. F., Jin, Y., and Wang, R. K. (2018). Crocin, a natural product attenuates lipopolysaccharide-induced anxiety and depressive-like behaviors through suppressing NF- κ B and NLRP3 signaling pathway. *Brain Res. Bull.* 142, 352–359. doi: 10.1016/j.brainresbull.2018.08.021
- Zhang, Y., Geng, J., Hong, Y., Jiao, L., Li, S., Sun, R., et al. (2019). Orally administered crocin protects against cerebral ischemia/reperfusion injury through the metabolic transformation of crocetin by gut microbiota. *Front. Pharmacol.* 10:440. doi: 10.3389/fphar.2019.00440
- Zuccato, C., and Cattaneo, E. (2014). Huntington's disease. *Handb. Exp. Pharmacol.* 220, 357–409.

Conflict of Interest: The authors declare that the research was conducted in the absence of any commercial or financial relationships that could be construed as a potential conflict of interest.

Publisher's Note: All claims expressed in this article are solely those of the authors and do not necessarily represent those of their affiliated organizations, or those of the publisher, the editors and the reviewers. Any product that may be evaluated in this article, or claim that may be made by its manufacturer, is not guaranteed or endorsed by the publisher.

Copyright © 2022 Chongtham, Yoo, Chin, Akingbesote, Huda, Marsh and Khoshnan. This is an open-access article distributed under the terms of the Creative Commons Attribution License (CC BY). The use, distribution or reproduction in other forums is permitted, provided the original author(s) and the copyright owner(s) are credited and that the original publication in this journal is cited, in accordance with accepted academic practice. No use, distribution or reproduction is permitted which does not comply with these terms.



New Enclosure for *in vivo* Medical Imaging of Zebrafish With Vital Signs Monitoring

A. C. M. Magalhães¹, P. M. M. Correia¹, R. G. Oliveira¹, P. M. C. C. Encarnação¹, I. Domingues², J. F. C. A. Veloso¹ and A. L. M. Silva^{1*}

¹Department of Physics, I3N, University of Aveiro, Aveiro, Portugal, ²CESAM, Department of Biology, University of Aveiro, Aveiro, Portugal

OPEN ACCESS

Edited by:

Jose Fernando Lopez-Olmeda,
University of Murcia, Spain

Reviewed by:

Yonghe Ding,
Mayo Clinic, United States
William Holmes,
University of Glasgow,
United Kingdom

*Correspondence:

A. L. M. Silva
analuisa.silva@ua.pt

Specialty section:

This article was submitted to
Aquatic Physiology,
a section of the journal
Frontiers in Physiology

Received: 28 March 2022

Accepted: 16 May 2022

Published: 29 June 2022

Citation:

Magalhães ACM, Correia PMM, Oliveira RG, Encarnação PMCC, Domingues I, Veloso JCA and Silva ALM (2022) New Enclosure for *in vivo* Medical Imaging of Zebrafish With Vital Signs Monitoring. *Front. Physiol.* 13:906110. doi: 10.3389/fphys.2022.906110

Lately, the use of zebrafish has gained increased interest in the scientific community as an animal model in preclinical research. However, there is a lack of *in vivo* imaging tools that ensure animal welfare during acquisition procedures. The use of functional imaging techniques, like Positron Emission Tomography (PET), in zebrafish is limited since it requires the animal to be alive, representing a higher instrumentation complexity when compared to morphological imaging systems. In the present work, a new zebrafish enclosure was developed to acquire *in vivo* images while monitoring the animal's welfare through its heartbeat. The temperature, dissolved oxygen, and pH range in a closed aquatic environment were tested to ensure that the conditions stay suitable for animal welfare during image acquisitions. The developed system, based on an enclosure with a bed and heartbeat sensors, was tested under controlled conditions in anesthetized fishes. Since the anesthetized zebrafish do not affect the water quality over time, there is no need to incorporate water circulation for the expected time of PET exams (about 30 min). The range of values obtained for the zebrafish heart rate was 88–127 bpm. The developed system has shown promising results regarding the zebrafish's heart rate while keeping the fish still during the long imaging exams. The zebrafish enclosure ensures the animal's well-being during the acquisition of *in vivo* images in different modalities (PET, Computer Tomography, Magnetic Resonance Imaging), contributing substantially to the preclinical research.

Keywords: Zebrafish physiology, non-invasive sensors, vital signs monitoring, zebrafish heart rate, small animal imaging

1 INTRODUCTION

Most preclinical experimental studies are conducted in animal models, traditionally mammals, like rodents. This is mainly due to the homology of the mammalian genome, anatomy, cellular biology, and physiology (Merrifield et al., 2017). However, these models have significant disadvantages, such as the high maintenance cost and complex genomes (Volkoff, 2019). On the other hand, non-mammalian vertebrates, mainly fishes, have genetic, endocrine, and physiological features, brain mechanisms, and essential gut functions similar to humans (Volkoff, 2019). These similarities allow using fishes as models of human diseases (Barbazuk et al., 2000; Kari, Rodeck and Dicker, 2007; Lieschke and Currie, 2007; Feitsma and Cuppen, 2008; Sun et al., 2008; Howe et al., 2013; Jones and Norton, 2015; Meshalkina et al., 2017; Sieber et al., 2019).

Zebrafish have short life cycles, and when compared with mammalian models, they have lower maintenance costs and fewer ethical issues involved in conducting experiments, facilitating genetic manipulation (Kari, Rodeck and Dicker, 2007; Volkoff, 2019) and allowing faster and cheaper large-scale studies when compared with other vertebrate models (Bufkin and Leevy, 2015). Zebrafish also has a unique natural ability to regenerate some tissues, and its genome has already been sequenced, which makes it very attractive to different research areas, such as evolutionary biology, and regenerative medicine (Lieschke and Currie, 2007; Howe et al., 2013; Marques, Lupi and Mercader, 2019). Due to its advantages, zebrafish models are becoming increasingly important and used in preclinical research. There is a clear interest in using and studying this animal model using medical imaging (Yao, Lecomte and Crawford, 2012); however, the imaging systems are rarely used (Browning, 2013), mainly due to the lack of technology and tools oriented to the acquisition of *in vivo* zebrafish images (Koba, Jelicks and Fine, 2013). Furthermore, its small size and physiological requirements make it very challenging and require the development of a dedicated housing capable of keeping the fish still and monitoring physiological parameters to ensure the animal's welfare during imaging procedures.

Positron Emission Tomography (PET) is a powerful image research tool for many biological research activities. The non-invasive image provided by PET technology and its ability to detect changes in metabolic, biological, chemical, and molecular processes may provide new scientific discoveries and economic advantages in research with zebrafish (Bufkin and Leevy, 2015; Dorsemans et al., 2017). However, only a few studies using PET in zebrafish are reported in the literature (Bufkin and Leevy, 2015; Dorsemans et al., 2017; Jones et al., 2017; Snay, 2017; Tucker et al., 2021). In all of those, the equipment used has been particularly rudimentary for physiological preservation and animal welfare. In these *in vivo* studies, zebrafish were either upright or wrapped in absorbent tissue (Bufkin and Leevy, 2015; Dorsemans et al., 2017; Jones et al., 2017; Snay, 2017; Tucker et al., 2021). These conditions are not natural for the fish, adding undesirable physiological stress.

More recently, new dedicated chambers have been developed ((Koth et al., 2017; Merrifield et al., 2017; Seeger et al., 2022)) that have water circulation ensuring a continuous supply of fresh water and anesthetics. Despite the monitoring of the environmental conditions, these chambers did not monitor the zebrafish's physiological stability. In addition to being able to monitor the well-being of the fish over time, this information will also be helpful to use as cardiac gating in the various imaging modalities (e.g., Merrifield et al., 2013).

Therefore, to address these challenges, a new dedicated zebrafish enclosure capable of keeping it still and monitoring the animal's vital signs during the imaging exam is presented, demonstrating the capability to predict critical injuries of the animal and prevent them in time during acquisitions procedures.

2 ZEBRAFISH ETHICAL PRINCIPLES

The zebrafish used in this study were protected under the directive 2010/63/EU, following the 3Rs principle (Replace,

Reduce, and Refine). Therefore, the experimental design was meticulously planned to decrease the chance of errors and unsuccessful experiments; additionally, to avoid unnecessary testing, an extensive literature review, covering a broad number of areas involving the problem, was carried out. Furthermore, the fish's well-being, including anesthesia administration and recovery, was assessed during the experiments to minimize suffering. Finally, euthanasia was performed according to the methods approved by the competent entities when needed.

3 ZEBRAFISH PREPARATION

The zebrafish used in this work were kept in tanks with proper conditions at the bioterium of the Biology Department of the University of Aveiro. Adult zebrafish were maintained in carbon-filtered water with salt (*Instant Ocean Synthetic Sea Salt*) under a 12:12 h (light: dark) cycle and at $26 \pm 1^\circ\text{C}$. The water was continuously renewed, and physicochemical parameters were controlled (pH 7.5 ± 0.5 ; conductivity $750 \pm 50 \mu\text{S}$ and dissolved oxygen above 95% saturation).

The experiments with zebrafish required their immobilization using an anesthetic like *tricaine methanesulfonate* (MS222), which is the most used and well-established for this species (Collymore et al., 2014). The anesthetic works as a muscle relaxant, reducing the muscle action potentials and spontaneous contractions (including sensory inputs and reflexes) (Matthews and Varga, 2012). The protocol followed in the present work to anesthetize zebrafish is described in **Figure 1** and was based on the one reported in (Merrifield et al., 2017).

The protocol starts by emerging the zebrafish on a solution of MS222 (125 mg/L) until reaching the surgical level of anesthesia, which can be identified through the loss of equilibrium, no reflex response, and the slowdown of opercular movements. After reaching this level of anesthesia, the zebrafish is transferred to a 100 mg/L of MS222 solution, where it is kept to maintain the anesthesia effect. The anesthetized zebrafish tend to be laid on their back, so we decided to maintain them in this position in the enclosure during our measurements. However, there is no technical limitation in doing the heartbeat measurements with the zebrafish in its natural position when awaked.

4 ZEBRAFISH ENCLOSURE

The developed enclosure consists in a closed cylindrical chamber made with PMMA (Poly (methyl methacrylate)). The chamber material was chosen due to its transparency, enabling the visualization of the fish and ensuring that the animal does not exhibit signals of stress. In addition, the material has a reduced atomic number (water equivalent), which has less interaction with the radiation during the imaging exam minimizing the image deterioration. The chamber includes inside a bed support to accommodate the zebrafish in a position aligned with the heartbeat sensors. Beyond these sensors, the developed enclosure also contains a thermistor to measure the water temperature (**Figure 2**).

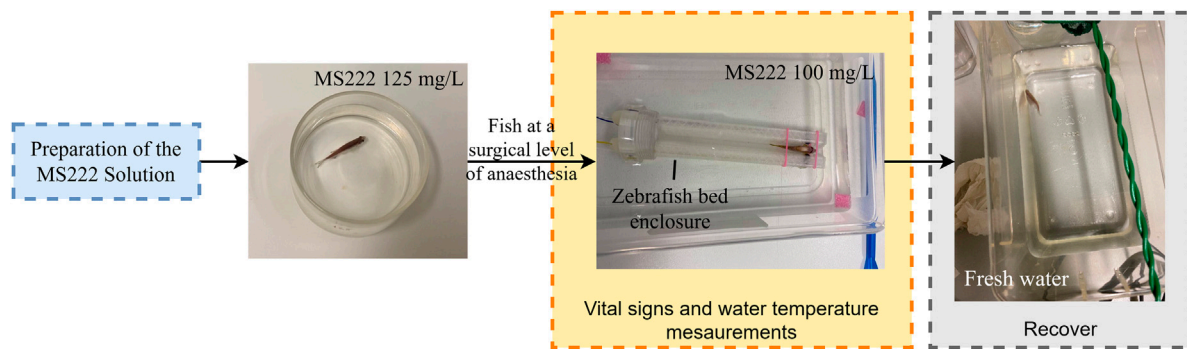


FIGURE 1 | Anesthesia protocol followed in the present work.

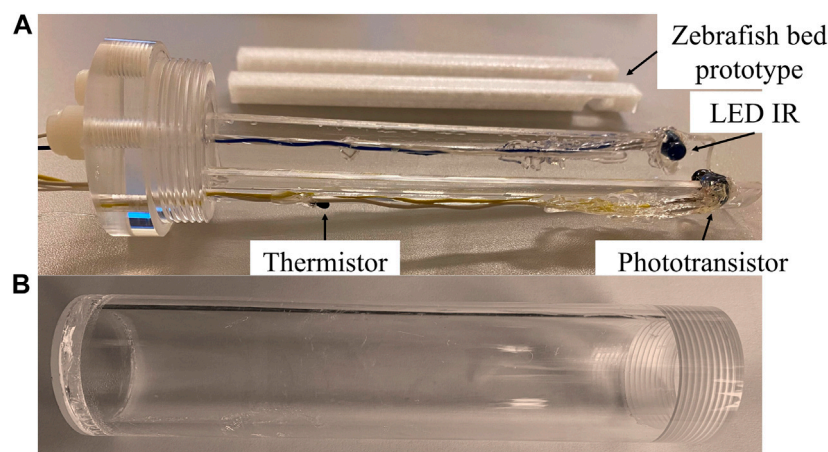


FIGURE 2 | Enclosure prototype developed (A) Bed support block to accommodate zebrafish (B) Block to seal the container.

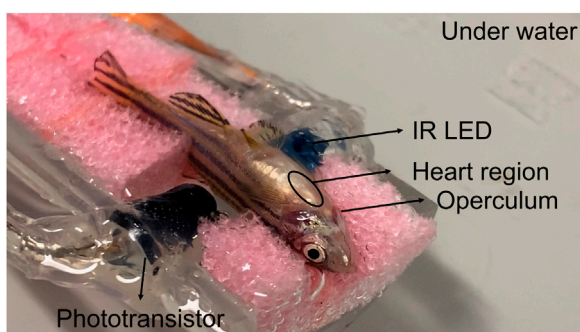


FIGURE 3 | Zebrafish in the bed with a sponge to improve immobilization and positioning of zebrafish.

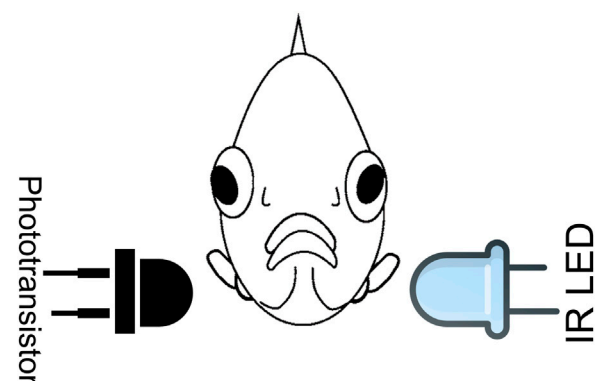
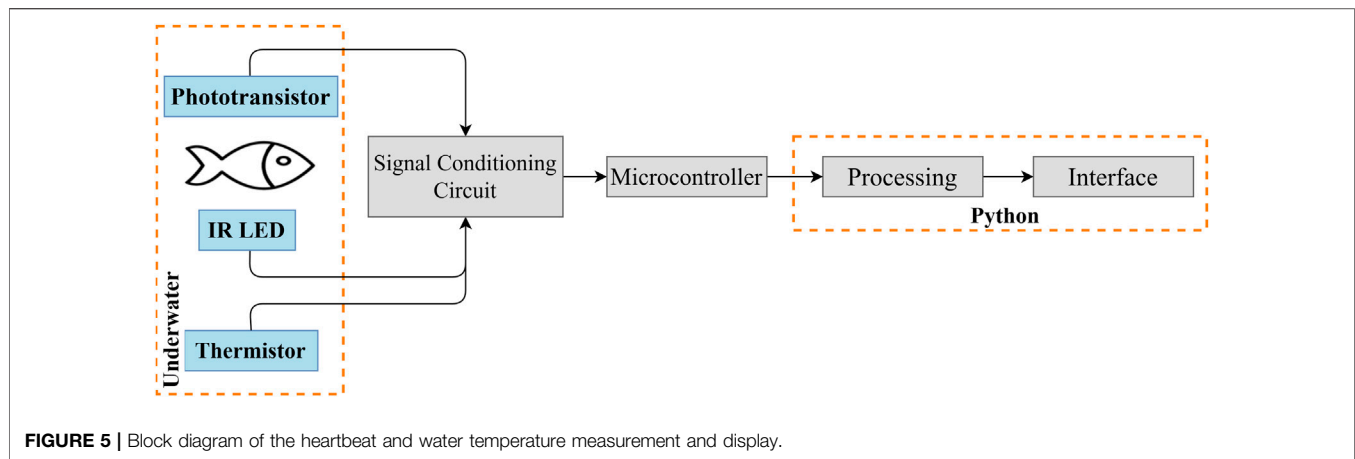


FIGURE 4 | Sensor arrangement relative to the zebrafish (front view). Adapted from (Yoshida, Hirano and Shima, 2009).

The proposed bed configuration intends to improve the zebrafish placement in a horizontal position, preventing the fish from moving as well as allowing an effortless sealing of the container when filled with the anesthetic solution.

Additionally, a sponge was added to the support block of the zebrafish's bed to immobilize it more efficiently (**Figure 3**). Since the opercula need to move freely and without the interference of



the immobilization material, the sponge has a broad aperture in the zebrafish's head region. In order to ensure that the animal stays still during the data acquisition, the tail was positioned in a tighter region of the sponge.

5 MONITORING SYSTEM

The heartbeat monitoring system consists of a transmitter, an infrared light-emitting diode (IR LED), and a receiver based on a phototransistor (optical sensor). These components were placed on opposite sides of the zebrafish body, as illustrated in **Figure 4** (Yoshida, Hirano and Shima, 2009). The IR LED emits infrared photons being partially absorbed by the fish's body. Since the number of photons absorbed varies with the blood volume, there is a correlation between the electrical signal produced and fish heartbeat.

Besides the unit responsible for the heartbeat monitoring, it was also necessary to assemble a unit for the water temperature monitoring. The temperature sensor is based on a Negative Temperature Coefficient (NTC) thermistor from Betatherm^{®1}.

The block diagram from **Figure 5** provides a functional view of the system developed, from the data acquisition stage (sensors and microcontroller) to the data processing and system control, which is executed by dedicated software. As shown in **Figure 5**, the sensors are underwater in the same environment as the zebrafish. First, the signal is filtered and amplified in the conditioning circuit. Then, the microcontroller (Arduino Uno R3) reads and converts the analog signal to digital and sends the data to a Python (v. 3.8) program. Finally, the data is processed and displayed in a Graphical User Interface (GUI), developed using Qt Creator (v. 4.14.1) and PyQt 5.

5.1 Hardware

Regarding the hardware, the heartbeat signal acquired is filtered through a simple low pass filter circuit (cutoff frequency of 2.34 Hz) and has an amplification stage (with a gain of 100). Next, the amplified signal is filtered through a high pass filter with

a cutoff frequency of around 1 Hz to block the DC component and is further amplified by another amplification stage, with a gain of 45. In this way, we set the signal to be within the voltage readout range of the analog converter.

Concerning the electronic circuit that was developed to monitor the water temperature, the thermistor and a resistor (10 kΩ) were positioned in a voltage divider configuration to obtain a suitable signal for the microcontroller.

5.2 Firmware and Software

The microcontroller reads the signals produced by the sensors and conditioning circuits for posterior processing.

The analog value given by the water temperature conditioning circuit (A_{therm}) is converted to voltage (V_o) by applying (1). The resistance of the thermistor (R_{Therm}) correspondent to V_o is then obtained with the voltage divider formula (2). Finally, the Steinhart-Hart Equation (3) converts the thermistor's resistance to a temperature reading (T) (in Kelvin), which is converted to the Celsius degree scale.

$$V_o = 5 \times \frac{A_{therm}}{1023} \quad (1)$$

$$R_{Therm} = R1 \times \frac{V_{in} - V_o}{V_o} = 10 \text{ k}\Omega \times \frac{5 - V_o}{V_o} \quad (2)$$

$$\frac{1}{T} = C1 + C2 \times \ln(R_{Therm}) + C3 \times (\ln(R_{Therm}))^3 \quad (3)$$

where $R1$ is the resistor of the voltage divider circuit, V_{in} is the voltage supply of the circuit, and $C1$, $C2$, and $C3$ are the thermistor's Steinhart-Hart coefficients.

The obtained temperature data and the analog readings from the heart rate conditioning circuit are then sent via serial communication (USB) from the microprocessor to the computer. This data is further processed in a dedicated software and displayed in a graphical interface based on multithreading and multiprocessing programming, enabling the processing and displaying of the data acquired in real-time.

The heartbeat raw data sent to the computer is filtered using a bandpass Butterworth filter, with cutoff frequencies of 0.2 and 7 Hz (**Figure 6**). In this way, both the signal's DC component and higher noisy frequencies are eliminated. The heart rate calculations were

¹BetaCurve Interchangeable Thermistor 10 kΩ with an α_{25} of $-4.39\%/^{\circ}\text{C}$.

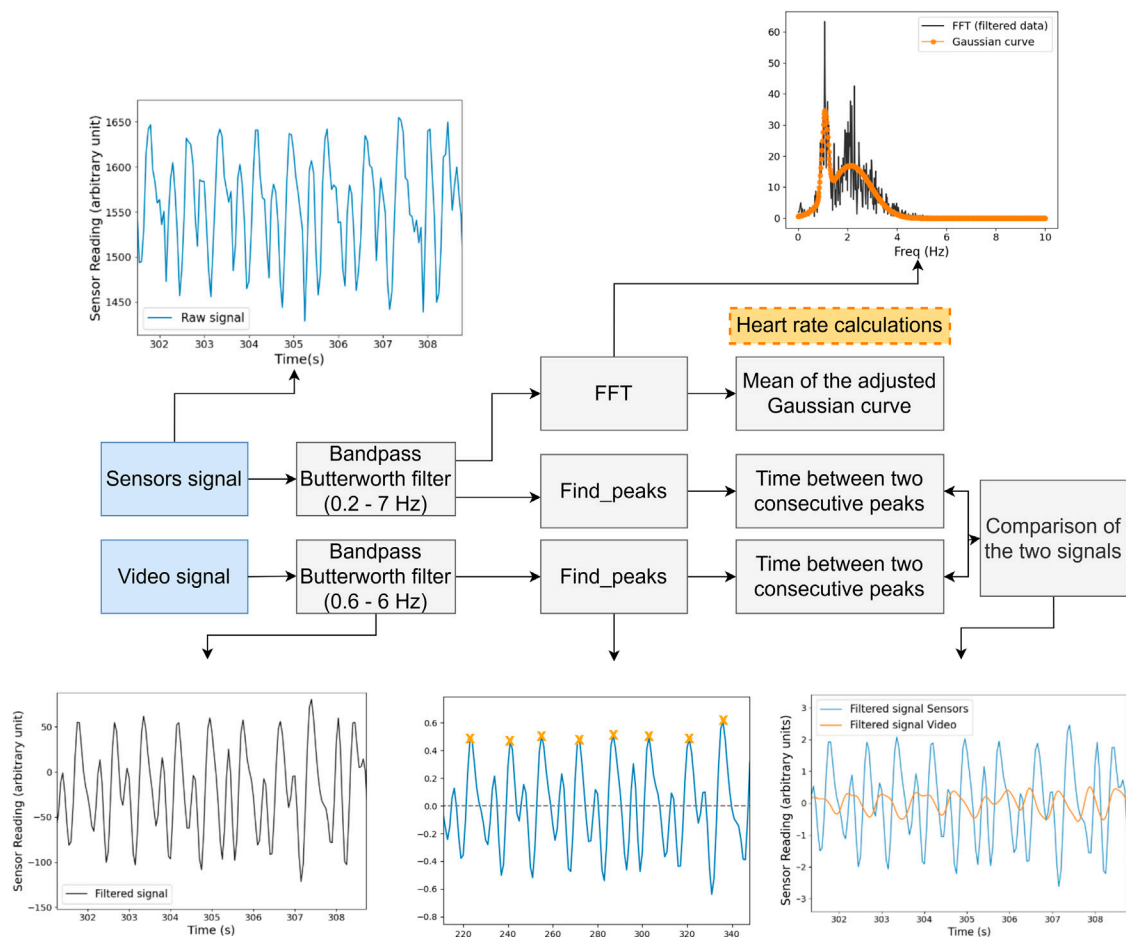


FIGURE 6 | Block diagram of the analysis applied to the acquired signals, both by the sensors and the video.

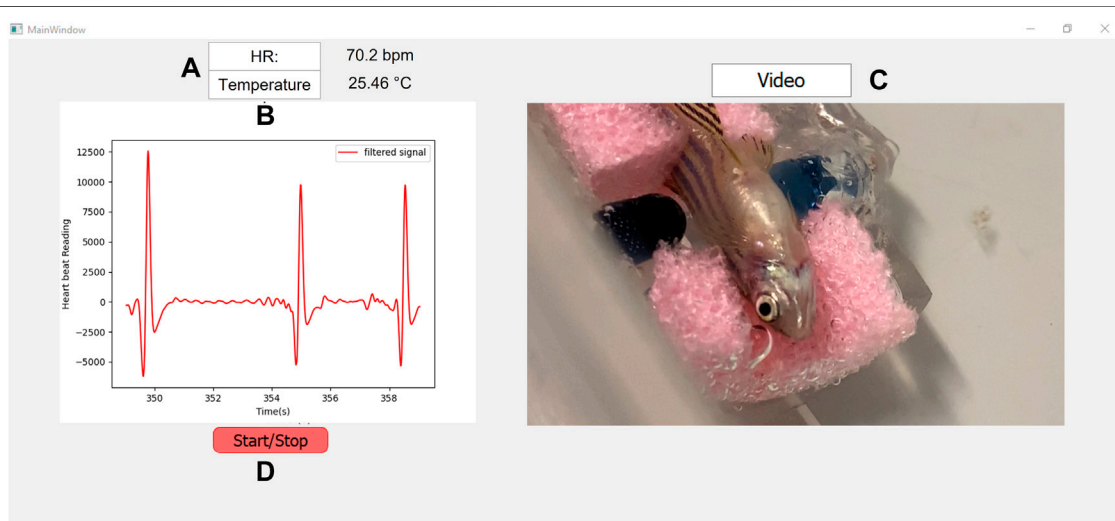


FIGURE 7 | Graphical interface developed, during the signal acquisition.



FIGURE 8 | Interface of the computer vision software and ROI selection.

based on a *find_peaks* Python function (Scipy library) (`scipy.signal.find_peaks`—SciPy v1.7.1 Manual, no date) that finds the local maxima inside a signal by comparing neighboring values. With the position of the peak information, it was possible to extract the time between two consecutive peaks (Δt), and thus, possible to know the number of beats per minute ($bpm = 60/\Delta t$).

Regarding the GUI design and operation, the sensor's data are displayed in the plot area (**Figure 7B**). In addition, the heartbeat frequency and temperature measurements calculations are carried out parallel to the acquisition, almost in real-time, and displayed in **Figure 7A**.

During acquisitions, a live video of the zebrafish enclosure is also displayed for a better examination of the fish welfare (**Figure 7C**). The video is also recorded and synchronized with the heartbeat signal for further processing using Computer Vision algorithms.

The video recordings were used to validate the results obtained by the sensors. The video analysis basic principle is based on the evident variation of pixels intensity value when zebrafish heartbeats. Therefore, the algorithm developed converts the frames from the video recordings to grayscale (pixel's value varies between 0 and 255) and allows the user to choose a Region of Interest (ROI) in the image (**Figure 8**).

The average pixels intensity value inside the ROI is calculated for each individual video frame and represented as a time series, showing the signal corresponding to the heartbeat. After, the signal is processed and analyzed similarly to the method performed for the sensors' signals.

6 RESULTS AND DISCUSSION

6.1 Dissolved Oxygen and pH Measurements

The water parameters - dissolved oxygen and pH - were measured in a recipient with a similar volume to the developed enclosure.

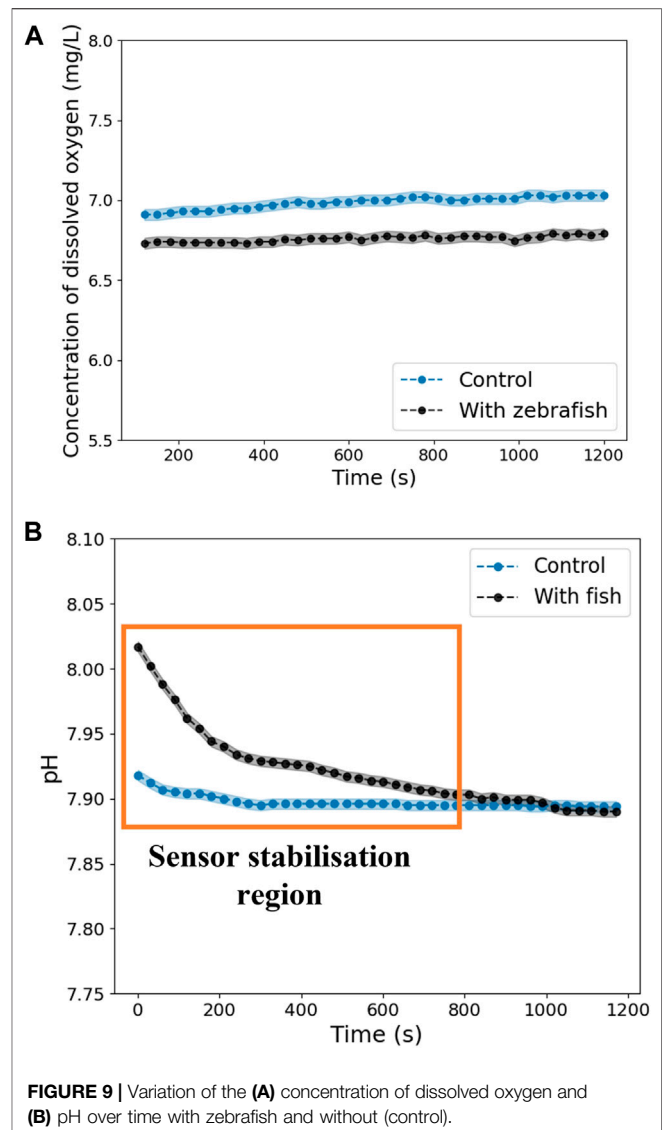


FIGURE 9 | Variation of the (A) concentration of dissolved oxygen and (B) pH over time with zebrafish and without (control).

By monitoring these parameters over time, we checked that the zebrafish remains stable along with its well-being guaranteed for approximately 20 min. pH and dissolved oxygen were monitored over time since these two parameters are regularly checked in zebrafish tanks. A multi-parameter system (*Multi 3410*) was used with digital sensors, one for pH (*SenTix® 940*) and another for dissolved oxygen (*FDO® 925*).

Zebrafishes were anesthetized according to the protocol defined in **Section 3** and transferred to a close recipient, free of air, with a similar volume of the zebrafish enclosure to be used. pH and dissolved oxygen concentration were registered every 30 seconds to evaluate how these values change over time.

Figure 9A shows that the dissolved oxygen concentration remains practically constant even with the zebrafish presence. Relative to the pH graph (**Figure 9B**), it is possible to verify that the measurement takes time to stabilize. However, after that period, it is observed that the pH follows the tendency of the

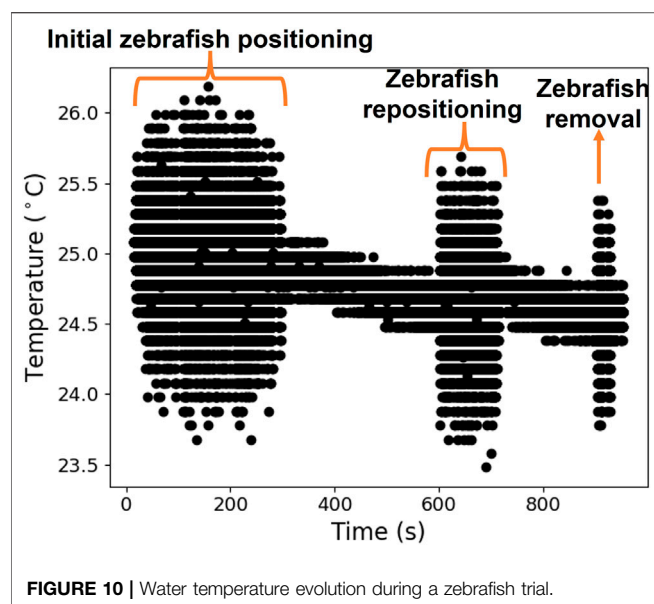


FIGURE 10 | Water temperature evolution during a zebrafish trial.

control study. Both graphs evidence that the zebrafish does not significantly change the environment concentration of dissolved oxygen and pH, maintaining these values within acceptable values throughout the experiments, between 6–8 mg/L (Hammer, 2019) and 6–8 (Avdesh et al., 2012), respectively.

Considering the results obtained, it was concluded that it is possible to perform PET exams on zebrafish in a closed volume without increasing the system's complexity by including a water renewal system.

6.2 Water Temperature Measurements

The water temperature was monitored during the zebrafish's vital signs measurements. The water temperature throughout the experiments varied between 24.5°C and 25.5°C, as shown in **Figure 10**. These values are within the expected and optimal range for zebrafish (24–29°C) reported in the literature (Avdesh et al., 2012; Hammer, 2019). During the vital signs measurements, it was necessary to adjust the fish positioning, which generated some movement in the water, leading to rapid changes in the thermistor response, as evidenced in **Figure 10**.

6.3 Validation of the Vital Signs Monitoring System

Before testing the vital signs monitoring system developed in zebrafish, it was decided to validate it first in human volunteers.

For this purpose, a commercial heart rate meter (Oximeter MD300C29, ChoiceMMed) was used to compare its results with the proposed system. Volunteers were asked to put one finger on the commercial heart rate meter, and another finger from the other hand between the IR LED and the phototransistor. The volunteers remained in this position for about 2 minutes, and the pulse rate was registered from both the heart rate meter and sensors every 10 seconds.

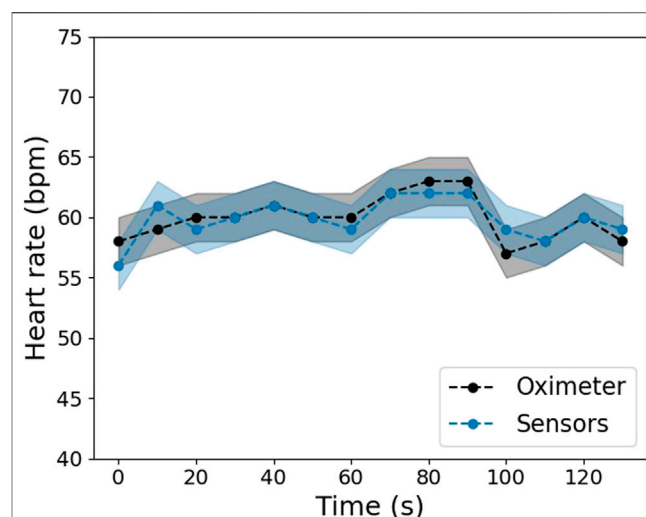


FIGURE 11 | Comparison of the heart rate values obtained by the developed system's sensors and a commercial heart rate meter in one volunteer.

TABLE 1 | Identification of the zebrafish.

Parameters	Zebrafish			
	1	2	3	4
Weight (mg)	774	800	740	380
Gender	Female	Female	Male	-
Recovered anesthesia	Yes	Yes	Yes	No

The monitoring system's response is illustrated in **Figure 11**. The slightly changes of the heart rate values over time observed in the graph can be due to some agitation or stress of the volunteers caused by the measurement *per se*. Besides, the differences between the sensors and the commercial meter may be because it is more challenging to position the finger without moving it in the developed system. This movement can induce changes in the sensor measurements. Nevertheless, despite a 3% of the maximum difference, the heart rate values calculated by the developed system are within the error range of the commercial heart rate meter, which indicates the correct functioning of the developed system.

6.4 Zebrafish Vital Signs Measurements

Zebrafish vital signs measurements were performed in the Biology Department bioterium of the University of Aveiro, using the developed enclosure. Four data samples are presented in **Table 1** for demonstration purposes once the remaining adult zebrafish samples contain similar information.

The raw data acquired for each zebrafish was done during 30 min and were filtered and processed according to the procedure described in **Section 5** (**Figure 6**).

For each fish, the heart rate obtained by the sensors was compared with the value calculated using the developed computer vision algorithm for zebrafish heart rate detection. The raw and filtered signals obtained from two zebrafish are

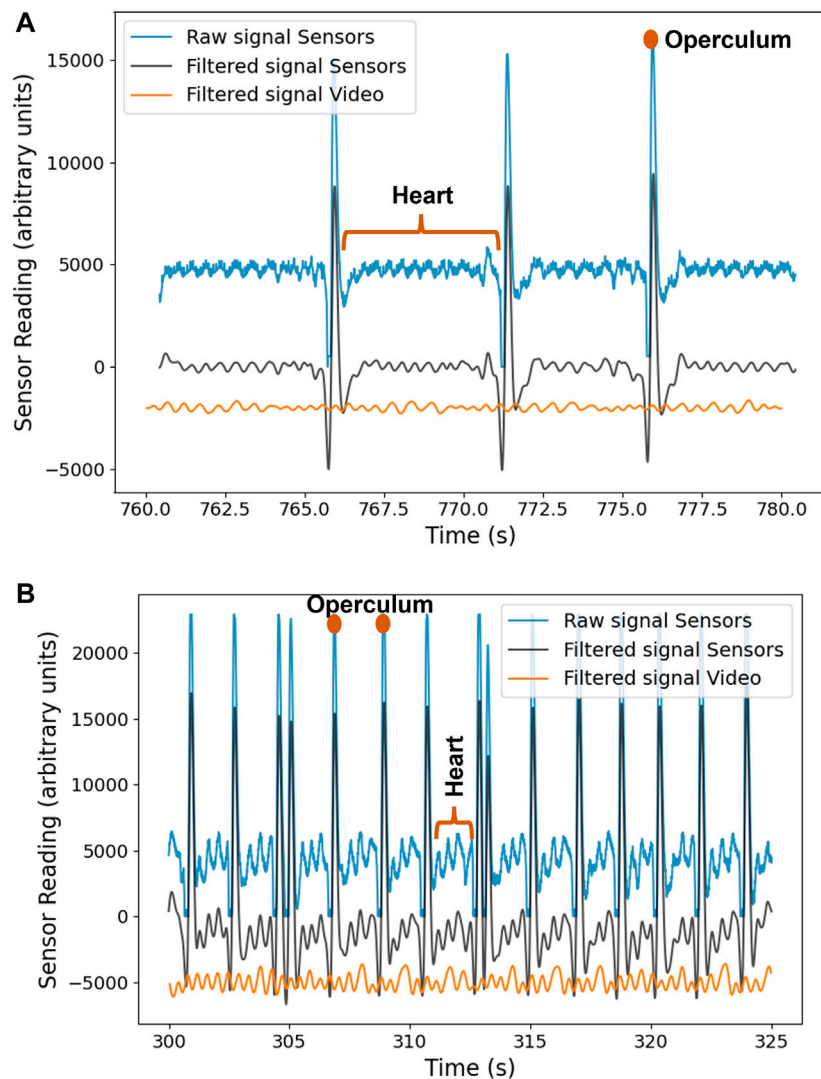


FIGURE 12 | (A) Signal acquired from zebrafish 1 **(B)** Signal acquired from zebrafish 2.

shown in **Figure 12**. Both graphs make it possible to distinguish between the peaks that correspond to the heartbeat (peaks with lower amplitude) and the opercular aperture (peaks with higher amplitude). The only difference between the two signals is that the opercular aperture of the zebrafish 2 (**Figure 12B**) has a bigger frequency, as verified in **Table 2**.

Comparing the signals obtained by the sensors and the video (**Figure 12**), it can be observed that some peaks are not perfectly synchronized, which is likely due to limitations of the video method (incorrect ROI selection, fish movements, or light reflections), as the SNR is lower for that method. Besides, the synchronization method is manually tuned and not done automatically by the software, contributing to a not perfect synchronization. However, despite that, the results between the two methods are in good agreement, as summarized in **Table 2**.

TABLE 2 | Zebrafish heart and operculum rates obtained with the sensors and video analysis method.

Zebrafish	Fig	Signal	Sensors (bpm)	Video (bpm)
1	Figure 12A	Heart	120 ± 10	127 ± 10
		Operculum	12 ± 3	12 ± 2
2	Figure 12B	Heart	88 ± 5	93 ± 2
		Operculum	32 ± 4	33 ± 5
3	—	Heart	118 ± 4	117 ± 2
		Operculum	41 ± 11	49 ± 15
4	—	Heart	115 ± 15	—
		Operculum	Nonexistent	Nonexistent

Analyzing **Table 2**, it is observed that the zebrafish heart rate varies between 88–127 bpm, and the operculum rate varies between 12–49 bpm. Besides, it is noticeable that both operculum and heart

rate values are similar within errors when measured with the sensors' signal or with the video; the more significant difference between the two methods found is only 8 bpm.

Regarding zebrafish 4, it was impossible to perform a video analysis due to undesired camera movements. Zebrafish 4 revealed a particular behavior since the opercular aperture was nonexistent at the end of the acquisition, which implies that the signal only contained the heartbeat pulse. Therefore, despite the zebrafish's visible heartbeat on the acquired signal, the nonexistence of the opercular aperture indicated that the zebrafish entered into the overdose anesthesia level, leading to a non-recovery from the anesthesia even after being placed in freshwater.

Summarily, by the analysis of the graphs and **Table 2**, it is observed that the two methods of heart rate determination are consistent. In addition, it is possible to detect the heart rate and the presence of opercular movement, both indicators of the zebrafish's well-being.

The obtained heart rate values compare favorably to the values found in the literature (Pereira et al., 2015; Wang et al., 2017; Santoso et al., 2020), validating our results. Nevertheless, some other discrepancies in the literature can be pointed out (Pereira et al., 2015; Wang et al., 2017; Santoso et al., 2020). For example, the different protocols and environmental conditions could justify minor discrepancies between the literature studies and the present work.

7 CONCLUSION

A suitable enclosure for *in vivo* imaging of adult zebrafish, incorporating a heart rate, opercular movement, and water temperature monitoring system, was successfully developed and implemented. As a result, the zebrafish were successfully maintained and recovered, without renewing water, for up to 30 min, the typical time for *in vivo* medical image acquisition.

The heartbeat signals obtained in zebrafish trials were in accordance with results from the video analysis, using computer vision methods. The maximum difference noticed between both methods was within the errors of the developed system.

The heart rate values obtained were between 88 and 127 bpm, which agrees with the values reported in the literature (63–125 bpm) (Wang et al., 2017).

Monitoring the opercula aperture could give information about the zebrafish's well-being since the nonexistent opercular movement means that the zebrafish is entering the overdose anesthesia level. The developed system was able to detect the opercula aperture failure and correlate this effect with a posterior non-recovery from anesthesia, demonstrating the capability to predict critical injuries of the animal and prevent them in time.

The developed system has shown promising results presenting a challenging but interesting solution to be applied in different preclinical imaging modalities and to perform different studies combining zebrafish models and *in vivo* medical imaging.

DATA AVAILABILITY STATEMENT

The original contributions presented in the study are included in the article/Supplementary Material, further inquiries can be directed to the corresponding author.

ETHICS STATEMENT

The animal study was reviewed and approved by Committee responsible for animal experimentation and welfare (CREBEA) at the Department of Biology, University of Aveiro. Moreover, the 3Rs policy concerning the use of animals in science is strictly followed according to the EU (Directive 2010/63/EC) and national (DL 113/2013) legislation. Zebrafish facilities and staff people are accredited by the Portuguese competent authority (Direção-Geral de Alimentação e Veterinária, DGAV).

AUTHOR CONTRIBUTIONS

AM, PMC, RO, JV, and AS contributed to the conception and design of the study. AM performed the experiments, developed the software used in the study, analyzed the data, and wrote the manuscript. ID guided the zebrafish experiments. PMC contributed to the electronics and hardware developments. RO contributed to signal and video processing and data analysis. PME contributed to the implementation of real time software solutions for data acquisition and visualization. All authors contributed to the analysis, interpretation, and discussion of the results. All authors contributed to the manuscript revision and have read and approved the final version of the manuscript.

FUNDING

This work was supported by project CENTRO-01-0247-FEDER-039880 (iPET) and project PTDC/EMD-EMD/2140/2020 (easyPET-CT). This work was developed within the scope of the i3N (UIDB/50025/2020 & UIDP/50025/2020) and CESAM (UIDP/50017/2020 and UIDB/50017/2020), financed by national funds through the FCT/MEC COMPETE, FEDER and POCI programs. RO and PME are grateful to FCT (Lisbon) for scholarships SFRH/BI/10638/2020, and SFRH/BD/143964/2019, respectively.

ACKNOWLEDGMENTS

Authors would like to thank the staff of the CESAM bioterium and i3N for their availability and cooperation.

REFERENCES

- Avdesh, A., Chen, M., Martin-Iverson, M. T., Mondal, A., Ong, D., Rainey-Smith, S., et al. (2012). Regular Care and Maintenance of a Zebrafish (*Danio rerio*) Laboratory: An Introduction. *JoVE* 69, 1–8. doi:10.3791/4196
- Barbazuk, W. B., Korf, I., Kadavi, C., Heyen, J., Tate, S., Wun, E., et al. (2000). The Syntenic Relationship of the Zebrafish and Human Genomes. *Genome Res.* 10 (9), 1351–1358. doi:10.1101/gr.144700
- Browning, Z. S. (2013). *Using Advanced Imaging to Study Fish*.
- Bufkin, K., and Leevy, M. (2015). Multimodal Imaging Trials with Zebrafish Specimens. *Winthrop McNair Res. Bull.* 1 (3), 1–5.
- Collymore, C., Tolwani, A., Lieggi, C., and Rasmussen, S. (2014). Efficacy and Safety of 5 Anesthetics in Adult Zebrafish (*Danio rerio*). *J. Am. Assoc. Lab. Anim. Sci.* 53 (2), 198–203.
- Dorsemans, A.-C., Lefebvre d'Helencourt, C., Ait-Arsa, I., Jestin, E., Meilhac, O., and Diotel, N. (2017). Acute and Chronic Models of Hyperglycemia in Zebrafish: A Method to Assess the Impact of Hyperglycemia on Neurogenesis and the Biodistribution of Radiolabeled Molecules. *JoVE* 2017 (124). doi:10.3791/55203
- Feitsma, H., and Cuppen, E. (2008). Zebrafish as a Cancer Model. *Mol. Cancer Res.* 6 (5), 685–694. doi:10.1158/1541-7786.MCR-07-2167
- Hammer, H. S. (2020). Water Quality for Zebrafish Culture. *Zebrafish Biomed. Res. Biol. Husb. Dis. Res. Appl.* 2020, 321–335. doi:10.1016/B978-0-12-812431-4.00029-4
- Howe, K., Clark, M. D., Torroja, C. F., Torrance, J., Berthelot, C., Muffato, M., et al. (2013). The Zebrafish Reference Genome Sequence and its Relationship to the Human Genome. *Nature* 496 (7446), 498–503. doi:10.1038/nature12111
- Jones, E., Henderson, F., Midey, A., Hurlstone, A., Forster, D., Johnston, H., et al. (2017). Comparison of Lipid Imaging in a Zebrafish Melanoma Model by Positron Emission Tomography (PET) and Desorption Electrospray Ionization-Mass Spectrometry (DESI-MS). *Drug Metabolism Pharmacokinet.* 32 (1), S42–S43. doi:10.1016/j.dmpk.2016.10.181
- Jones, L. J., and Norton, W. H. J. (2015). Using Zebrafish to Uncover the Genetic and Neural Basis of Aggression, a Frequent Comorbid Symptom of Psychiatric Disorders. *Behav. Brain Res.* 276, 171–180. doi:10.1016/j.bbr.2014.05.055
- Kari, G., Rodeck, U., and Dicker, A. P. (2007). Zebrafish: An Emerging Model System for Human Disease and Drug Discovery. *Clin. Pharmacol. Ther.* 82 (1), 70–80. doi:10.1038/sj.clpt.6100223
- Koba, W., Jelicks, L. A., and Fine, E. J. (2013). MicroPET/SPECT/CT Imaging of Small Animal Models of Disease. *Am. J. Pathol.* 182 (2), 319–324. doi:10.1016/j.ajpath.2012.09.025
- Koth, J., Maguire, M. L., McClymont, D., Diffley, L., Thornton, V. L., Beech, J., et al. (2017). High-Resolution Magnetic Resonance Imaging of the Regenerating Adult Zebrafish Heart. *Sci. Rep.* 7 (1), 1–12. doi:10.1038/s41598-017-03050-y
- Lieschke, G. J., and Currie, P. D. (2007). Animal Models of Human Disease: Zebrafish Swim into View. *Nat. Rev. Genet.* 8 (5), 353–367. doi:10.1038/nrg2091
- Marques, I. J., Lupi, E., and Mercader, N. (2019). Model Systems for Regeneration: Zebrafish. *Co. Biol. Ltd* 146 (18), 1–12. doi:10.1242/dev.167692
- Matthews, M., and Varga, Z. M. (2012). Anesthesia and Euthanasia in Zebrafish. *ILAR J.* 53 (2), 192–204. doi:10.1093/ilar.53.2.192
- Merrifield, G. D., Mullin, J., Tucker, C. S., Denvir, M. A., and Holmes, W. M. (2013). Development of Cardiac MRI for Studying Zebrafish Models of Cardiovascular Disease. *Proc. Intl Soc. Mag. Reson. Med.* 21, 1387.
- Merrifield, G. D., Mullin, J., Gallagher, L., Tucker, C., Jansen, M. A., Denvir, M., et al. (2017). Rapid and Recoverable *In Vivo* Magnetic Resonance Imaging of the Adult Zebrafish at 7T. *Magn. Reson. Imaging* 37, 9–15. doi:10.1016/j.mri.2016.10.013
- Meshalkina, D. A., Kysil, E. V., Warnick, J. E., Demin, K. A., and Kalueff, A. V. (2017). Adult Zebrafish in CNS Disease Modeling: a Tank That's Half-Full, Not Half-Empty, and Still Filling. *Lab. Anim.* 46 (10), 378–387. doi:10.1038/lab.1345
- Pereira, A., Marins, F., Rodrigues, B., Portela, F., Santos, M. F., Machado, J., et al. (2015). Improving Quality of Medical Service with Mobile Health Software. *Procedia Comput. Sci.* 63 (1ct), 292–299. doi:10.1016/j.procs.2015.08.346
- Santoso, F., Farhan, A., Castillo, A. L., Malhotra, N., Saputra, F., Kurnia, K. A., et al. (2020). An Overview of Methods for Cardiac Rhythm Detection in Zebrafish. *Biomedicines* 8 (9), 329. doi:10.3390/biomedicines8090329
- SciPy *scipy.signal.find_peaks* — SciPy v1.7.1 Manual (No Date). Available at: https://docs.scipy.org/doc/scipy/reference/generated/scipy.signal.find_peaks.html (Accessed: December 7, 2022).
- Seeger, S., Zvolský, M., Melikov, S., Frerkes, M., and Rafecas, M. (2022). Dedicated Chamber for Multimodal *In Vivo* Imaging of Adult Zebrafish. *Zebrafish* 19 (2), 67–70. Available at: <https://home.liebertpub.com/zeb>. doi:10.1089/ZEB.2021.0066
- Sieber, S., Grossen, P., Bussmann, J., Campbell, F., Kros, A., Witzgmann, D., et al. (2019). Zebrafish as a Preclinical *In Vivo* Screening Model for Nanomedicines. *Adv. Drug Deliv. Rev.* 151–152, 152–168. doi:10.1016/j.addr.2019.01.001
- Snay, E., Dang, M., Fahey, F., and Zon, L. (2017). Developing a Practical Approach to Imaging PET/CT of Zebrafish. *J. Nucl. Med.* 58 (Suppl. 1), 1127. Available at: https://jnm.snmjournals.org/content/58/supplement_1/1127 (Accessed: December 6, 2021).
- Sun, L., Lien, C.-L., Xu, X., and Shung, K. K. (2008). *In Vivo* Cardiac Imaging of Adult Zebrafish Using High Frequency Ultrasound (45–75 MHz). *Ultrasound Med. Biol.* 34 (1), 31–39. doi:10.1016/j.ultrasmedbio.2007.07.002
- Tucker, C., Collins, R., Denvir, M. A., and McDougald, W. A. (2021). PET/CT Technology in Adult Zebrafish: A Pilot Study toward Live Longitudinal Imaging. *Front. Med.* 8 (October), 1–7. doi:10.3389/fmed.2021.725548
- Volkoff, H. (2019). Fish as Models for Understanding the Vertebrate Endocrine Regulation of Feeding and Weight. *Mol. Cell. Endocrinol.* 497, 10437. doi:10.1016/j.mce.2019.04.017
- Wang, L. W., Huttner, I. G., Santiago, C. F., Kesteven, S. H., Yu, Z. Y., Feneley, M. P., et al. (2017). Standardized Echocardiographic Assessment of Cardiac Function in Normal Adult Zebrafish and Heart Disease Models. *Dis. Model Mech.* 10, 63–76. doi:10.1242/dmm.026989
- Yao, R., Lecomte, R., and Crawford, E. S. (2012). Small-animal PET: What Is it, and Why Do We Need it? *J. Nucl. Med. Technol.* 40 (3), 157–165. doi:10.2967/jnmt.111.098632
- Yoshida, M., Hirano, R., and Shima, T. (2009). Photocardiography: A Novel Method for Monitoring Cardiac Activity in Fish. *Zoological Sci.* 26 (5), 356–361. doi:10.2108/zsj.26.356

Conflict of Interest: The authors declare that the research was conducted in the absence of any commercial or financial relationships that could be construed as a potential conflict of interest.

Publisher's Note: All claims expressed in this article are solely those of the authors and do not necessarily represent those of their affiliated organizations, or those of the publisher, the editors and the reviewers. Any product that may be evaluated in this article, or claim that may be made by its manufacturer, is not guaranteed or endorsed by the publisher.

Copyright © 2022 Magalhães, Correia, Oliveira, Encarnação, Domingues, Veloso and Silva. This is an open-access article distributed under the terms of the Creative Commons Attribution License (CC BY). The use, distribution or reproduction in other forums is permitted, provided the original author(s) and the copyright owner(s) are credited and that the original publication in this journal is cited, in accordance with accepted academic practice. No use, distribution or reproduction is permitted which does not comply with these terms.



Lung Organoids—The Ultimate Tool to Dissect Pulmonary Diseases?

Veronika Bosáková^{1,2}, Marco De Zuani¹, Lucie Sládková^{3,4}, Zuzana Garlíková¹, Shyam Sushama Jose¹, Teresa Zelante⁵, Marcela Hortová Kohoutková¹ and Jan Frič^{1,3*}

¹International Clinical Research Center, St. Anne's University Hospital Brno, Brno, Czechia, ²Department of Biology, Faculty of Medicine, Masaryk University, Brno, Czechia, ³Institute of Hematology and Blood Transfusion, Prague, Czechia, ⁴Department of Cell Biology, Faculty of Science, Charles University, Prague, Czechia, ⁵Department of Medicine and Surgery, University of Perugia, Perugia, Italy

OPEN ACCESS

Edited by:

Tobias Raabe,
University of Pennsylvania,
United States

Reviewed by:

Sandra Leibel,
University of California, San Diego,
United States
Anas Rabata,
Cedars-Sinai Medical Center,
United States

*Correspondence:

Jan Frič
jan.fric@fnusa.cz

Specialty section:

This article was submitted to
Stem Cell Research,
a section of the journal
Frontiers in Cell and Developmental
Biology

Received: 18 March 2022

Accepted: 24 June 2022

Published: 13 July 2022

Citation:

Bosáková V, De Zuani M, Sládková L,
Garlíková Z, Jose SS, Zelante T,
Hortová Kohoutková M and Frič J
(2022) Lung Organoids—The Ultimate
Tool to Dissect Pulmonary Diseases?
Front. Cell Dev. Biol. 10:899368.
doi: 10.3389/fcell.2022.899368

Organoids are complex multicellular three-dimensional (3D) *in vitro* models that are designed to allow accurate studies of the molecular processes and pathologies of human organs. Organoids can be derived from a variety of cell types, such as human primary progenitor cells, pluripotent stem cells, or tumor-derived cells and can be co-cultured with immune or microbial cells to further mimic the tissue niche. Here, we focus on the development of 3D lung organoids and their use as disease models and drug screening tools. We introduce the various experimental approaches used to model complex human diseases and analyze their advantages and disadvantages. We also discuss validation of the organoids and their physiological relevance to the study of lung diseases. Furthermore, we summarize the current use of lung organoids as models of host-pathogen interactions and human lung diseases such as cystic fibrosis, chronic obstructive pulmonary disease, or SARS-CoV-2 infection. Moreover, we discuss the use of lung organoids derived from tumor cells as lung cancer models and their application in personalized cancer medicine research. Finally, we outline the future of research in the field of human induced pluripotent stem cell-derived organoids.

Keywords: induced pluripotent stem cells, lung organoids, cystic fibrosis - CF, human disease modelling, 3D structure, chronic obstructive pulmonary disease, lung cancer

1 INTRODUCTION

Respiratory disorders such as asthma, chronic obstructive pulmonary disease (COPD), and idiopathic pulmonary fibrosis (IPF) affect millions of people worldwide, accounting for approximately 8% of global mortality (Dwyer-Lindgren et al., 2017). Lung tumors and airborne infections add to the burden of lung disease-associated morbidity and mortality, with the ongoing COVID-19 pandemic demonstrating the potential impact of viral lung disease on the worldwide population (Pollard et al., 2020; Kumar et al., 2021). Despite intensive research efforts spanning decades, our knowledge of lung biology and its interaction with the disease process remains incomplete. For example, key questions remain around the nature of lung stem cells, their roles in tissue regeneration and their therapeutic potential. A better understanding of the lung stem cell progenitor's capacity to generate the various cell types of the adult lung and unraveling the pathways involved in their responses to injury could lead to the discovery of more efficient treatments for numerous pulmonary diseases. Thus, there is a persistent and urgent need to develop more relevant *in vitro* models of the human lung that authentically recapitulate the organ's physiology and can be used to elucidate the mechanisms and biomarkers of pulmonary disease, as well as to test and guide the development of new treatments for conditions affecting the airways.

Studies of lung biology have, until recently, been limited by the unique structural and cellular complexity of the organ. The human lung comprises over 40 different types of cells (Franks et al., 2008; Cunliffe et al., 2021; Varghese et al., 2022), arranged in a complex three-dimensional (3D) architecture that is designed to withstand the continuous dynamic mechanical stress associated with respiratory movements (Nossa et al., 2021) while existing and functioning at the air-tissue-interface, in the presence of a varied and interactive microbiota (Paolicelli et al., 2019; Barcik et al., 2020). Studies of primary tissue *ex vivo* cannot provide dynamic information, while the relative inaccessibility of the lung and its constant movement have precluded the widespread use of intra-vital imaging in pre-clinical models. Together, these challenges have driven researchers to develop and explore the use of lung organoids (LOs). These 3D *in vitro* models of the lung incorporate multiple cell types derived from induced pluripotent stem cells (iPSCs) (Clevers, 2016; Paolicelli et al., 2019; Jose et al., 2020; Wang et al., 2020a) and offer the potential to answer long-standing questions about lung biology in health and disease.

In this review we outline the unique features of the lung that make studying the organ and its pathologies such a challenge, then summarize the pre-organoid era leading to the development of these latest models. We then review the different approaches used to generate LOs, and report the latest findings made in the field, before finally looking at the direction of pulmonary research in the future.

2 THE PRE-ORGANOID ERA: EARLY ATTEMPTS TO MODEL THE HUMAN LUNG

While all organs are, to some degree, complex, the human lung is remarkably so. While the stomach (Busslinger et al., 2021) and liver (Ramachandran et al., 2020), for example, are comprised of four or five main cell types, the lung contains more than 40 (Franks et al., 2008; Cunliffe et al., 2021; Varghese et al., 2022), varying in proportion depending on the region of the lung and exhibiting clear patterns of polarization at the air-liquid interface (Castellani et al., 2018). Thus, the development of reliable *in vitro* lung models is a challenge on a grand scale (Castellani et al., 2018).

Accordingly, for many years, studies of lung tissue either employed a reductionist approach based on 2D culture of human cells, or relied on animal models, in which the 3D structure of the lung is intact. Together with increasing use of tools such as genetic engineering and inducible gene expression, these approaches have enabled us to better understand the molecular basis of some lung diseases (Guilbault et al., 2007; Williams and Roman, 2016; Lambrecht et al., 2019). However, 2D cultures of human cells have clear drawbacks for the study of an organ with a function that is tightly linked to its 3D organization and multiple studies have shown that the overall ability of rodent models in particular to accurately replicate human pulmonary diseases is limited (Shmidt and Nitkin, 2004; Matute-Bello et al., 2008; Wang et al., 2008). Thus, there is mounting evidence for the need to develop human cell-based systems to study pulmonary disease.

2.1 Basic 2D Cultures of Human Lung Cells

Prior to the advent of 3D tissue culture methods, many studies of the lung used human primary cells and/or cell lines derived from healthy pulmonary or tumor tissues, grown in monolayer cultures (Gottschling et al., 2012). The 2D models are ideal for high-throughput drug screening and their generation from cell lines with histological and genetic changes allows modeling of different clinical conditions and drug responses (Huang et al., 2021). Gazdar et al. (2010) reviewed the important discoveries made using 2D models such as, the spectrum of TP53 gene mutations in lung cancer (Takahashi et al., 1989), mechanisms of resistance in EGFR mutant cells (Kwak et al., 2005; Pao et al., 2005; Engelman et al., 2007) and the description of BRAF mutations in various tumors, including lung (Davies et al., 2002; Pratilas et al., 2008).

While these models have the advantage of human origin, they are constrained by the culture's limited amount of extracellular matrix and the absence of different lung cell subtypes—including progenitors—and their inability to replicate the morphology or structural features of the *in vivo* lung architecture. The significance of these factors has become even more apparent in recent years: for example, we now know that lung-infiltrating immune cells are fundamental to the biology of several lung diseases, including COPD (Huang et al., 2019; David et al., 2021), IPF (Tanabe et al., 2020; van Geffen et al., 2021; Zhu et al., 2021), and non-small cell lung cancer (Tamminga et al., 2020). Furthermore, recent studies have illustrated the central role of tissue polarity in lung conditions, which can alter the functions of native cells in terms of spreading, migrating, and sensing soluble factors and other ligands (Duval et al., 2017). This implies limited relevance of findings from 2D cell cultures or isolated primary cells.

2.2 Rodent Models of Human Pulmonary Disorders

Although the etiology of human lung diseases is complicated and multi-factorial, there are three broad underlying forces: genetic mutation/variation/predisposition, environmental exposure/influences, and infection by a pathogen. Animal models have been used widely to investigate the mechanisms of each of these forces. While such studies have generated important insights into human lung disorders, there is a growing body of evidence that indicates their lack of ability to achieve progress in the field. Molecular characterization of human lungs using proteomic, transcriptomic, and *in silico* approaches, such as the Molecular Atlas of Lung Development Program (LungMAP), revealed major molecular differences between mouse and human lung epithelial tissues (Ardini-Poleske et al., 2017; Pan et al., 2019). Recent studies also showed that human lungs significantly differ from those of mouse models in several key metabolic processes as well as molecular pathways regulating the development and function of the lung extracellular matrix (Wang et al., 2015; Aichler et al., 2018). The main differences between human and mouse lungs are summarized in **Figure 1**. Below, we note key examples of the types of animal models commonly in use, acknowledging the advances and also noting their limitations that are driving the design of ever better LOs.

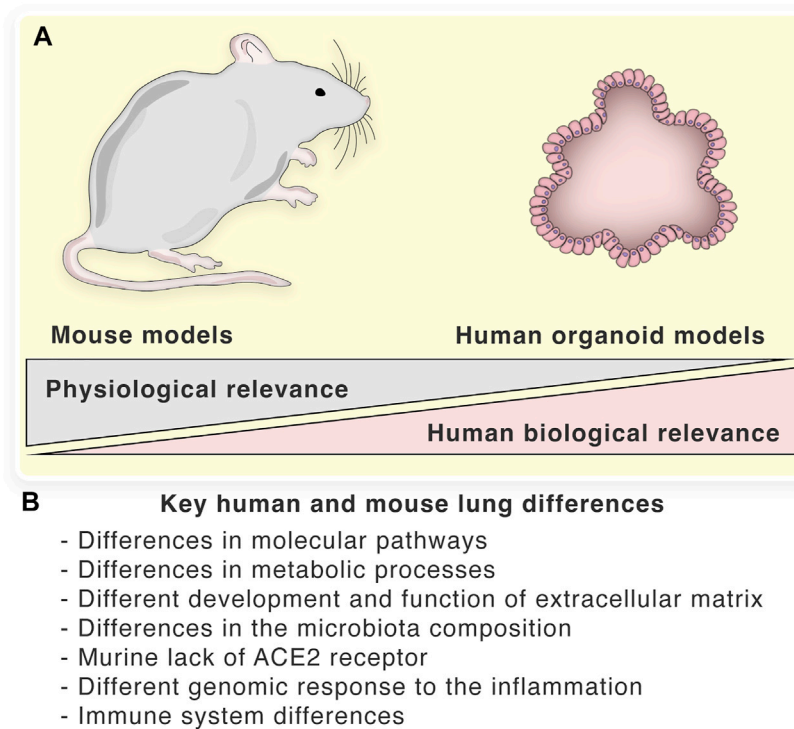


FIGURE 1 | Key human and mouse lung differences: **(A)**—Biological and physiological relevance of mouse and organoid models. **(B)**—The main differences between human and mouse lungs.

2.2.1 Models of Genetic Diseases Affecting the Lungs

CF is among the most common autosomal recessive diseases in humans and is caused by mutation of the cystic fibrosis transmembrane conductance regulator (*CFTR*) gene. Genetically modified rodents bearing one or several of the more than 2,000 *CFTR* mutations that can result in CF in humans (De Boeck, 2020) have been used to model the condition, as reviewed by Semaniakou et al. (2018). However, although these models bear mutations known to be associated with the onset of CF in humans, the disease phenotypes in these mice vary in severity and pathology. These differences have been attributed to the rodent's lack of specific cell types, receptors, and mediators involved in CF (Grubb and Boucher, 1999; Pan et al., 2019). Recent studies indicate that the differences in the microbial composition of the murine and human lung could also be a key factor (Semaniakou et al., 2018). Taken together, the distinct microbiota, alongside the molecular and physiological differences between mouse and human lungs, mean that murine models of CF are limited in their ability to advance our knowledge.

The same pattern emerges for the study of IPF—a chronic progressive disease characterized by scarring of the lung tissue—which has incompletely understood environmental and genetic components to its etiology (Chanda et al., 2019). The main mouse model of IPF involves the induction of pulmonary fibrosis by direct administration of bleomycin into the lungs of rodents (Walters and Kleeberger, 2008), with more recent developments including transgenic overexpression of pro-

fibrotic cytokines such as TGF- β , TNF- α , IL-1 β , and IL-13 in mice (Tashiro et al., 2017). However, despite showing fibrotic features, mouse models of IPF often display heterogeneous disease kinetics, especially in terms of the severity and extent of pulmonary lesions and levels of different cytokines (Moeller et al., 2008). Humanized mice have also been used as recipients of injected IPF patient lung biopsy material or tissue explants, which has allowed researchers to study the biology of the resulting lung remodeling and fibrotic lung phenotype (Habel et al., 2018). As a result of murine studies, two IPF drugs have been developed, pirfenidone (King et al., 2014) and nintedanib (Richeldi et al., 2014), but neither are able to cure the disease and patient survival remains poor, with a median lifespan of 3.8 years post-diagnosis (Raghu et al., 2014).

2.2.2 Models of Pulmonary Infections

Another challenge is the development of relevant preclinical models of human pulmonary infections. Rodents and humans differ in their susceptibility to many pulmonary pathogens. This is particularly clear in mouse models of lung conditions that, in humans, develop through recurrent exacerbations of pulmonary infections including those by *Staphylococcus aureus*, *Haemophilus influenzae*, *Pseudomonas aeruginosa*, and *Burkholderia cepacia* (Semaniakou et al., 2018). Again, the difference in the microbes colonizing laboratory mice and humans is likely a major factor limiting the applicability of these models, and it is not yet clear whether this challenge can

be overcome, although some attempts are being made [reviewed in Chang *et al.* (Chang and Sharma, 2020)]. Human viral lung infections are also difficult to study in murine models. For instance, investigations of human infection with the pathogenic avian influenza virus H5N1 in these models is impeded by the absence of the epithelial receptor for viral entry in mice (Ibricevic *et al.*, 2006). Similarly, mice lack the ACE2 receptor required for severe acute respiratory syndrome coronavirus 2 (SARS-CoV-2) infection, initially dramatically limiting their applicability in this field. Although the development of a mouse model expressing the human ACE2 receptor was recently reported (Cleary *et al.*, 2020), it is still unclear whether the response of mice to the virus mimics that of humans, and whether they express other as yet unidentified co-factors involved in infection/pathology.

Sepsis is a condition characterized by life-threatening organ dysfunction, and is caused by the host response to infection, most commonly by bacteria (Minasyan, 2019; Reyes *et al.*, 2020) but also by some viruses (Singer *et al.*, 2016; Hortova-Kohoutkova *et al.*, 2020; Hortova-Kohoutkova *et al.*, 2021). In the respiratory system, sepsis manifests clinically as acute lung injury (ALI) or, the more severe acute respiratory distress syndrome (ARDS) (Sevransky *et al.*, 2009; Angus and van der Poll, 2013). Sepsis-induced ALI is marked by a “cytokine storm” that triggers inflammation and is followed by uncontrolled infiltration of pulmonary tissue by neutrophils (Aziz *et al.*, 2013), while ARDS also involves pulmonary edema caused by alveolar injury that results in dangerously low oxygen levels in the blood (Sweeney and McAuley, 2016). Respiratory-infection-linked sepsis deaths totaled 1.8 million globally in 2017 (Rudd *et al.*, 2020) driving urgent research into the condition. Sepsis has been experimentally induced in rodents by the administration of microbial components or living pathogens (e.g., *Escherichia coli*, or *S. aureus*) into the bloodstream, peritoneal cavity, or trachea (Karzai *et al.*, 2003; Wang *et al.*, 2004; Charavaryamath *et al.*, 2006; Stahl *et al.*, 2013; Kapicibasi *et al.*, 2020). These models have shown that sepsis induced in mice by injection of peptidoglycan causes organ injury, organ, and systemic inflammation (Wang *et al.*, 2004). Similarly, injection of a high dose of LPS and alpha toxin induces a systemic inflammatory response syndrome in rodents (Stahl *et al.*, 2013). However, despite extensive animal studies, clinical translation has been largely unsuccessful. In this case, one of the reasons for the poor translation of the mouse data to humans is likely due to their markedly different genomic response to inflammation. A study comparing mouse and human endotoxemia showed no correlation between the top 10 most downregulated signaling pathways in the two species. In contrast to mouse models, the response to injury in humans was dominated by upregulation of genes related to innate immune response and downregulation of pathways related to adaptive immunity (Seok *et al.*, 2013). Therefore, one must conclude that the balance of harm to the animal—in this case significant suffering is induced during sepsis modeling—and the low potential for valuable clinical insight, renders the use of such models highly undesirable for future research (Nandi *et al.*, 2020).

2.2.3 Animal Models of Human Lung Cancer

Since the first animal model of leukemia was reported in 1950, many types of animal models of cancer have been developed to understand tumor biology and test drug efficacy. One of the simplest human tumor models is created by injecting tumor cell lines into immunodeficient mice. However, the pressure to develop more standardized model emerged due to unanticipated and unpredictable phenotype alterations compared to the original tumor. The patient-derived xenograft (PDX) model represents a reliable translation research tool that accurately mimics parental tumor tissue. It is generated by implanting a small tissue sample into highly immunodeficient mice. The great advantages of PDX models are in preserving the histologic features, genetic aberrations and gene expression profiles of the original tumor, as well as matching the characteristics of inflammation and the responses to chemotherapeutics and other anti-tumor drugs of the parental tissue. Therefore, PDX models are a valuable tool in tumor biology research, development of novel anti-cancer therapeutics, and pre-clinical drug screening (Lai *et al.*, 2017; Bleijs *et al.*, 2019; Yoshida, 2020). Although PDX models represent highly complex systems that accurately replicate tumor tissue *in vivo*, they also have several drawbacks, for example, the low success rate (30%–40%, lack of efficacy and the high cost of their establishment in terms of time and money, as well as their limited potential for application in high-throughput studies (Kim *et al.*, 2019; Li *et al.*, 2020). These features render PDX models unsuitable for use in the personalized treatment industry and other models suitable for high-throughput research are urgently required.

In lung cancer modeling, PDXs were reported in development of a novel anti-tumor therapeutic approaches, for example, in evaluation of microwave hyperthermia therapy (Motomura *et al.*, 2010). Furthermore, PDX models of lung cancer have been used in pre-clinical drug testing (Hai *et al.*, 2020; Li *et al.*, 2020; Shi *et al.*, 2020; Wang *et al.*, 2020b), which is discussed in the following sections.

3 THE BIRTH OF HUMAN LUNG ORGANIDS: PHYSIOLOGICALLY RELEVANT MODELS OF PULMONARY TISSUES

To overcome the limitations of classical 2D cultures and inter-species models, the use of lung tissue organoids has been pioneered in the field of lung research. Organoids are 3D “organ in a dish” models that aim to recreate key aspects of the *in vivo* structure of tissues using a mixture/variety of cell types from the species of interest to generate a relevant microenvironment in which cells within the organoid exhibit key aspects of the function of that organ (Lancaster and Huch, 2019).

Research into organoids was initially pioneered in the field of cancer studies, with cultured 3D structures based on simple air-medium interface system used to characterize the histological

features of tumors (Kondo and Inoue, 2019). A significant advance in our ability to model non-malignant cells was the innovative demonstration by Sato et al. (2009) that individual Lgr5⁺ stem cells isolated from small intestinal crypts of adult mice could be grown and maintained in 3D cultures in which they regenerated the intestinal niche, comprising villus-like structures and fully differentiated epithelial cells. Since then, the use of tissue organoids in disease modeling research has expanded rapidly, with more than 3,000 scientific articles now published in this field alone (Lancaster and Huch, 2019).

It is now possible to generate LOs from cultures of pluripotent stem cells (PSCs) (including embryonic stem cells), induced PSCs (iPSCs), or adult stem cells (ASCs). Regardless of the source cell type, a key procedure common across all protocols for organoid derivation is the embedding of cells in extracellular matrix, which serves as the basal lamina for tissue culture and supports the development of the 3D architecture (Schutgens and Clevers, 2020). Fully differentiated organoids can then be passaged, further expanded, and used for basic tissue research (Tian et al., 2021), cell interaction studies (Nikolic and Rawlins, 2017), and cancer drug testing (Clevers, 2016; Drost and Clevers, 2018; Kim et al., 2019).

3.1 Different Methods for Generating Lung Organoids

As mentioned above, human LOs can now be derived through several routes and different biological materials, each with its own strengths and limitations. Selecting the most appropriate method for each application is of key importance, but with careful application of the methodologies mentioned below, valuable insights into lung biology and disease pathology can be made.

3.1.1 Generation of Primary Lung Progenitor Cell-Derived Organoids

Early protocols for LO differentiation were based on the use of primary lung progenitor cells (Leeman et al., 2019; Rabata et al., 2020; Schutgens and Clevers, 2020), or transformed lung cancer cells (Neal and Kuo, 2016; Sato et al., 2017). Several methods have been published describing the isolation of these cells from lung tissue that was first subjected to mechanical disruption followed by digestion using enzymes (Katsura et al., 2020; Salahudeen et al., 2020; Lamers et al., 2021; Tindle et al., 2021). Once a single-cell suspension has been generated, the cells are either directly seeded into Matrigel droplets for organoid culture or sorted based on the expression of cell-type-specific markers for organoid cultures that require a more homogeneous population of a particular cell type (Katsura et al., 2020).

Importantly, it is also possible to generate LOs from specific lung regions to model their physiology more accurately. For example, human lung basal cells can be isolated from either the trachea or upper bronchia, after which they are expanded *ex vivo* and stem cells are isolated for embedding into the matrix (Schutgens and Clevers, 2020). Similarly, alveolar-like organoids can be generated by sorting of type II alveolar cells identified as CD45[−]CD31[−]Epcam⁺HTII⁺ cells from dissociated lung tissue dissociation and mixing them with MRC5 fibroblasts before

embedding in Matrigel (Barkauskas et al., 2013). A second method of alveolar organoid generation involves co-culture of epithelial progenitors with stromal fibroblasts (Tan et al., 2017), although this approach is less commonly used. More advanced LOs exhibiting a limited lung-like structure have been generated by mixing epithelial and fibroblastic cells using multi-layered microfluidic devices that enable the formation of differentiated LOs with morphological and secretory cellular phenotypes similar to those in human lungs (Hegab et al., 2015; Gkatzis et al., 2018). Similarly, organoids derived from alveolar or small airway epithelial cells have been co-cultured with mesenchymal stromal cells (MSCs) to promote alveolar organoid formation (Leeman et al., 2019). Leeman et al. (2019) also showed that ASC-derived LOs exhibit increased alveolar differentiation and decreased self-renewal when cultured with MSC-conditioned medium, thus demonstrating that MSC-secreted factors are important for the self-organization of lung epithelial organoids. Despite the achievements in the field of primary lung progenitor cell-derived organoid research, some limitations of these *in vitro* models remain. First, primary cell-derived LOs lack the mesenchymal cells that produce factors to support LO growth and differentiation (Leeman et al., 2019). Therefore, the successful generation of LOs requires either co-cultivation with mesenchymal cells or supplementation of the medium with these factors. Furthermore, cell-derived organoids are formed from only a limited number of cell types, which does not accurately mirror the complex structures of the human lung. Finally, primary cell-derived organoids require lung tissue biopsies, which provide only a limited amount of material for LO differentiation.

3.1.2 Generation of Induced Pluripotent Stem Cells-Derived Lung Organoids

iPSC-based organoids can be generated by reprogramming somatic cells from patients (often easily accessible skin fibroblasts or peripheral blood mononuclear cells), making them a uniquely valuable and versatile tool for clinical research (Figure 2). This approach has revolutionized the study of genetic disorders in particular, superseding the previous ASC-based organoids, that were limited by their lack of MSCs and fibroblastic stromal cells, which are required for tissue-like structures and functions (Schutgens and Clevers, 2020). Thus, the use of PSCs to generate LOs with both epithelial and mesenchymal components has been a breakthrough in the field, and these organoids are now being utilized to study lung development and lung diseases across a broad range of fields (Choi et al., 2016).

The process of LO differentiation follows that of normal embryogenesis, in which fetal lungs arise from the anterior foregut endoderm, forming the bronchial, and alveolar tissues (Schittny, 2017). *In vitro*, this process is driven/directed by sequential activation and inhibition of different signaling pathways using growth factors and small molecules. The iPSC-derived LO differentiation protocol was firstly described by Dye et al. (2015). This protocol involves the initial differentiation of either ESCs or iPSCs into definitive endoderm by treatment with activin A for a period of 4 days

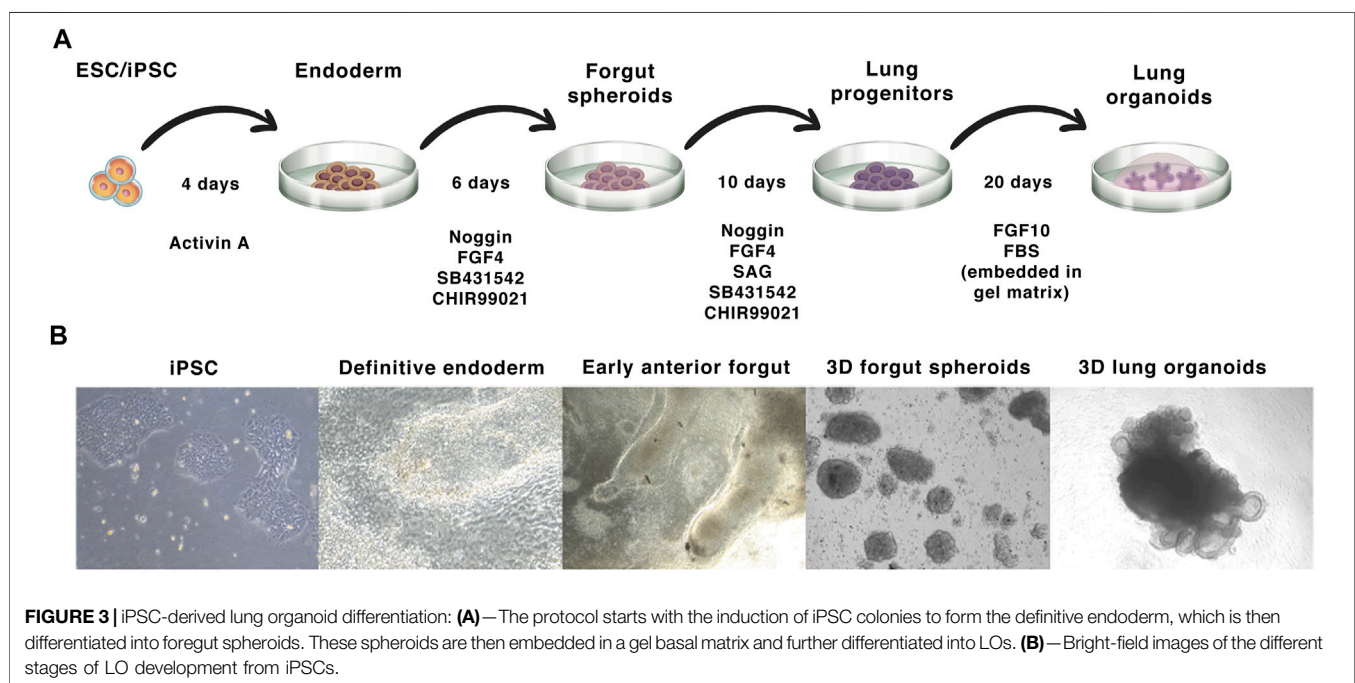
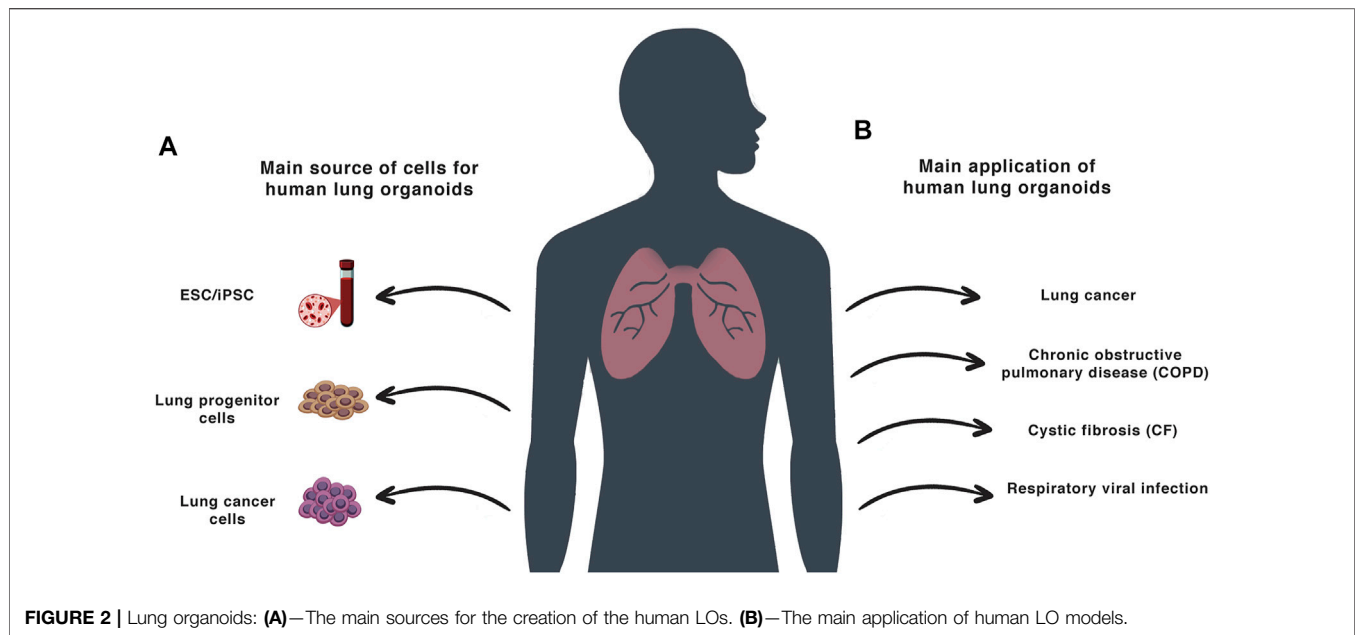
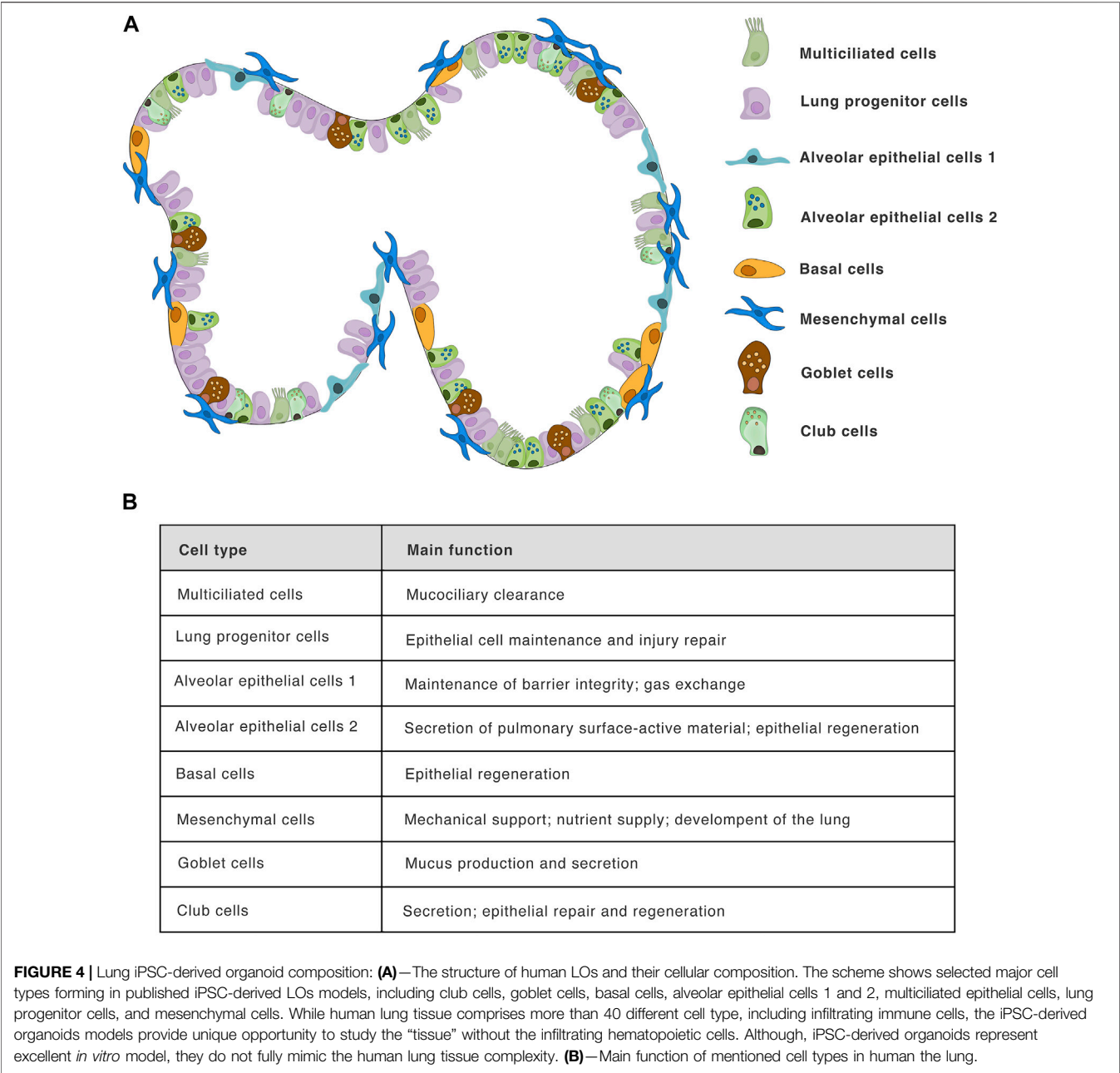


(Figure 3, days 1–4). This endodermal layer is then differentiated to form anterior foregut spheroids by using a combination of noggin, the TGF β /activin/NODAL pathway inhibitor SB431542, FGF4, and the GSK3 inhibitor CHIR99021 (Figure 3, days 4–10). These signals are sufficient to induce both mesenchymal and epithelial cell populations within the anterior foregut spheroids. The activation of the WNT and FGF pathway and the simultaneous inhibition of the BMP/TGF β signalling in PSCs was found to be optimal for the generation of lung tissue

expressing NKX2.1⁺, a key transcription factor that regulates pulmonary development (Minoo et al., 1995; Choi et al., 2016). For the generation of NKX2.1⁺ E-cadherin⁺ foregut spheroids, the sonic hedgehog activator SAG is also added on days 4–10. Finally, NKX2.1⁺ SOX9⁺ spheroids are embedded into a gel matrix and expanded in an FGF10-containing medium, leading to the development of 3D LOs comprising both P63⁺ basal cells and FOXJ1⁺ ciliated epithelial cells (Dye et al., 2015; De Luca et al., 2017). Importantly, these organoids also exhibit tissue polarity,



evidenced by the localization of acetyl-tubulin and E-cadherin markers (Jose et al., 2020). As previously mentioned, human lung tissue comprises more than 40 cell types (Franks et al., 2008; Cuniff et al., 2021; Varghese et al., 2022), including infiltrating immune cells. However, iPSC-derived organoids do not consist of any cells of hematopoietic origin, which can be an experimental advantage allowing controlled cocultures, such as Jose et al. (2020) showed for monocytes. Moreover, distinct protocols differ in the cell types composition within the organoids. The composition of several cell types forming iPSC-derived organoids is shown in Figure 4, the overall complexity of iPSCs model indeed does not reach completely the normal lungs.

A recent advance in LO research is represented by reporter iPSCs, which allows the differentiation of different cell types to be tracked within the organoid. Pioneered by Sharma et al. (2018), this method involves fluorescent tagging of endogenous proteins in a stable human iPSC line using CRISPR/Cas9 genome editing technology (Sharma et al., 2018). Since almost any intracellular protein can be tagged, this system represents a powerful tool with the potential for application in many fields of research. Notably, this technique has recently been used in our own laboratory to study the activation of transcriptional factors such as NF-κB during LO differentiation and stimulation (Jose et al., 2020). Hawkins et al. (2021) published the protocol for directed differentiation of human iPSCs into airway basal cells allowing

TABLE 1 | Lung organoids used for disease investigation: Disease studies where 3D LOs were used as experimental models.

Disease modeled	Source cell type	References
Lung cancer	Human primary tumor tissue/cells Patient-derived xenograft models Human lung cancer cell lines Human ESCs	Jung et al. (2019); Kim et al. (2019) Shi et al. (2020) Ramamoorthy et al. (2019) Chen et al. (2017)
COPD	Primary human lung epithelial cells Human lung epithelial cell lines	Ng-Blichfeldt et al. (2018) Tan et al. (2017)
CF	Patient-derived iPSCs Lung cell pellet from the broncho-alveolar lavage fluid of patients	Mou et al. (2012); Wong et al. (2012); Firth et al. (2015) Sachs et al. (2019)
IPF	Patient-derived iPSCs Human ESCs	Wilkinson et al. (2017); Strikoudis et al. (2019) Chen et al. (2017)
Neonatal respiratory distress syndrome	Patient-derived iPSCs	Jacob et al. (2017)
Interstitial lung disease	Patient-derived iPSCs	Leibel et al. (2019)
Bronchopulmonary dysplasia	Human fetal lung fibroblasts	Sucre et al. (2016)
Pulmonary metaplasia	Normal primary human epithelial cells	Danahay et al. (2015)
Pulmonary edema	Human pulmonary epithelial cells and microvascular endothelial cells used to form 3D-lung organoids on a chip	Huh et al. (2012)
Lung inflammation	Human 3D differentiated airway epithelium cultured on-chip (inflammation induced by IL-13) Mouse lung tissue (inflammation induced by bacterial flagellar hooks stimulation) Mouse type 2 alveolar epithelial cells (inflammation induced by IL-1 β and TNF α)	Benam et al. (2016) Shen et al. (2017) Katsura et al. (2019)
Lung tissue injury and regeneration Respiratory viral infection	Primary mouse lung epithelial cells, endothelial cells, and MSCs <i>IRF7</i> mutant patient-derived iPSCs (influenza virus infection) Mouse epithelial stem/progenitor cells (influenza virus infection) Human ESCs (respiratory syncytial virus infection) Human ESCs (parainfluenza virus infection) Human airway epithelial cell cultures (parechovirus infection) Human alveolar epithelial type II of KRT5+ basal cells (severe acute respiratory syndrome coronavirus 2) Human alveolar type 2 cells/pneumocytes (severe acute respiratory syndrome coronavirus 2) Human epithelial progenitor cells (severe acute respiratory syndrome coronavirus 2) Human alveolar type 2 cells (severe acute respiratory syndrome coronavirus 2) Primary human lung tissue (enterovirus infection)	Leeman et al. (2019); Riemondy et al. (2019) Ciancanelli et al. (2015) Quantius et al. (2016) Chen et al. (2017) Porotto et al. (2019) Karelehto et al. (2018) Salahudeen et al. (2020) Katsura et al. (2020) Xu et al. (2021) Ebisudani et al. (2021) van der Sanden et al. (2018)

Used abbreviations: COPD, chronic obstructive pulmonary disease; CF, cystic fibrosis; IPF, idiopathic pulmonary fibrosis; ESCs, embryonal stem cells; iPSCs, induced pluripotent stem cells; MSCs, mesenchymal stromal cells.

use of the iPSC NKX2-1^{GFP}/TP63^{tdTomato} dual reporter system. This protocol facilitates tracking of the differentiation state of the cells and sorting of the positive population to obtain pure culture of lung progenitor cells (Hawkins et al., 2021). In another study, the fluorescent reporter NKX2-1 and SFTPC iPSCs line were used to generate and purify alveolar epithelial type 2 cells (AEC2s) (Jacob et al., 2017). Importantly, this approach provides opportunities to study AEC dysfunction, which has been implicated in the pathogenesis of many lung disorders (Hawkins et al., 2021).

Advances in iPSC-derived LO generation have led to the generation of organoids with close transcriptional similarities to human fetal lung (Dye et al., 2016); however, their ability to

recapitulate the characteristics of the adult tissue remains to be fully defined.

4 THE APPLICATION OF LUNG ORGANOIDS

The special characteristics of organoids make them an excellent model for a wide range of basic and translational investigations, including drug testing, genetic screening, and disease modeling (Table 1). The major advantage of LO cultures is the interdependent existence of epithelial and mesenchymal cell populations, which—alongside epithelial polarization—is required for proper pulmonary function *in vivo* (Tan et al., 2017).

4.1 Lung Organoids as Models of Genetic Diseases Affecting the Lungs

LOs have been used successfully to investigate the pathogenesis of CF and protocols have been published for generating disease-specific lung progenitor cells from human CF patient-derived iPSCs (Mou et al., 2012; Wong et al., 2012). The value of this approach lies in the use of a human model, as the murine models may not be exact phenocopy of the human lung disease (Clarke et al., 1992; Snouwaert et al., 1992; Guilbault et al., 2007; Mou et al., 2012). Moreover, patient-derived iPSCs can be used to study the clinical variability of CF without the need for prior analysis of the genetic background of patients (Mou et al., 2012). Furthermore, Mou et al. (2012) used modified RNAs as a replacement for viral vectors to establish iPSC lines that are not genetically modified and therefore, provide an advantage for potential clinical use. Wong et al. (2012) validated the applicability of iPSC-derived epithelial cells as an *in vitro* model for the drug screening. In this study, CF patient-specific iPSC-derived lung epithelial cells were used to test a novel small molecule compound called a “corrector”, which is able to restore the trafficking of a mutant CFTR protein to the plasma membrane. “Corrector” treatment of cells with the F508del CF mutation resulted in the enhanced plasma membrane localization of the CFTR protein (Wong et al., 2012). Finally, this approach provides the ability to test drugs for personalized medicine and the possible future development of regenerative medicine for lung disorders. An additional advantage of iPSC-derived LOs in the study of lung fibrosis lies in their capacity for expansion of lung stem cell populations and the induction of differentiated cells from very limited amounts of starting material. In one study, Firth et al. (2015) took advantage of this feature to generate iPSC-derived LOs from CF patient fibroblasts. These organoids exhibited fibrotic characteristics *in vitro*, which were abrogated by CRISPR-mediated CFTR correction, ultimately giving rise to normal LOs (Firth et al., 2015). Alongside these disease-modelling successes, LOs have been instrumental in advances in CF drug testing (Kim et al., 2021). In one study, fibrotic response and collagen accumulation were ameliorated in a LO model of CF by treatment with NP-011, a novel potential anti-fibrotic drug (Kim et al., 2021). In the future, the use of patient-derived organoids may hold the potential for improved diagnostics (Dekkers et al., 2013), with the hope of achieving greater insight into disease processes, and perhaps even personalized therapies for CF (Berkers et al., 2019).

The limitations of mouse models of IPF also make LOs the natural choice for advancing knowledge in the field. This is especially so given the important role of altered extracellular matrix (ECM) composition in IPF pathology, which is readily studied in organoid models of the IPF lung (Kim et al., 2021; Suezawa et al., 2021). These models have yielded important insights, including the identification of new inhibitors of fibrinogenesis, such as NP-011, which was shown to ameliorate fibrosis induced by TGF β (Kim et al., 2021). Moreover, similar results were obtained using in a mouse model of pulmonary fibrosis, suggesting the important potential of LOs for respiratory disease modeling and drug

testing (Kim et al., 2021). Another condition extensively studied using LOs is fibrotic lung injury and the associated repair mechanisms. For instance, Chen et al. (2017) recapitulated fibrotic lung disease *in vitro* in normal iPSC line-derived LOs by the introduction of a mutation in the *HPS1* gene. ECM and MSCs accumulated in affected LOs, in processes similar to those observed in *HPS1* mutant-driven lung fibrosis *in vivo* (Chen et al., 2017).

Cytokine stimulation of organoids has been investigated in the field of pulmonary research. IL-1 β is produced by lung interstitial macrophages in mouse lungs following bleomycin-induced injury (Choi et al., 2020). In the alveolar region, IL-1 β induces differentiation of AT2 cells into damage-associated transition progenitors (DAPTs), which further differentiate into AT1 and AT2 cells to regenerate the alveolar compartment (Choi et al., 2020). This also occurs in IL-1 β -stimulated mouse AT2 organoids (Choi et al., 2020), indicating the suitability of cytokine treatment of organoids for the study of inflammation and regeneration after injury. Choi et al. (2020) also demonstrated that chronic inflammation can be mimicked by IL-1 β treatment of LOs, with sustained stimulation with IL-1 β found to impair the terminal differentiation of AT1 cells and cause accumulation of DAPTs. Such an increase in the number of cells with expression profiles similar to DAPTs also occurs in the lung tissue of patients with IPF (Choi et al., 2020). Interestingly, withdrawing IL-1 β after 14 days of LO stimulation resulted in increased terminal differentiation of AT1 cells (Choi et al., 2020), suggesting the potential benefits of therapies targeting IL-1 β in the treatment of IPF. These examples of organoid models of immune responses in various tissues indicate a promising trajectory for basic and preclinical immunological research.

4.2 Lung Organoids to Model Lung Infections—The Model of SARS-CoV-2 Infection

The inflammatory response plays a crucial role in pathology as well as in the regeneration of lung tissue (Lechner et al., 2017). For example, cytokine storm and cytokine-release syndrome are life-threatening systemic inflammatory events involving elevated levels of circulating cytokines and immune cell hyperactivation (Fajgenbaum and June, 2020). In experimental settings, the induction of cytokine storm-like environments can be achieved by infection of lung tissue with a pathogenic agent or by direct stimulation with relevant cytokines. The cytokine approach has the advantage of mimicking the inflammatory niches in culture, even in relatively simplified *in vitro* tissue models, which lack the complete milieu of naturally occurring cell types.

Airway epithelial cells serve as a first line of defense against pathogen attack or inflammatory stimuli. Accordingly, LOs have been exploited to help understand how epithelial cell function/dysfunction contributes to the pathogenesis of various inflammatory lung diseases and infections (Gkatzis et al., 2018).

Several organoid-based *in vitro* models of lung infection have been established, which have provided valuable insights into the

underlying host-pathogen interactions at the cellular and molecular levels. The recent SARS-CoV-2 pandemic has increased the demand for, and focus on, *in vitro* models of human lung tissue to facilitate disease pathology investigations and drug testing experiments. A seminal work in the field of LO infection models was published by Chen et al. (2017), who presented a protocol to generate PSC-derived lung bud organoids consisting of mesodermal (Vim⁺, CD90⁺) and pulmonary endodermal (FOXA2⁺, NKX2.1⁺, EPCAM⁺, SOX9⁺) cells. These organoids were shown to undergo branch morphogenesis when cultured in 3D Matrigel or transplanted into a mouse, rendering the model highly relevant as branching morphogenesis is a critical step in lung tissue development (Schittny, 2017). The researchers also infected the organoids with respiratory syncytial virus (RSV), which causes small airway obstruction and bronchiolitis in infants. They revealed a process of shedding of swollen, infected cells similar to that seen in infected human lungs (Chen et al., 2017). Therefore, RSV-infected LOs represent a useful model for RSV infection research, especially as most commonly used mouse models are limited by crucial differences between human and murine physiology, especially in metabolism, which may also be due to the fact that model organisms develop faster than humans (Kim et al., 2020).

A system for the culture of organoids derived from a single adult human alveolar epithelial type II cell (AT2) has also been developed. The resulting organoids successfully supported the differentiation of AT2 cells into AT1 cells (Salahudeen et al., 2020), which together form the human lung epithelium, in which AT2 cells produce pulmonary surfactant proteins, and AT1 cells cover most of the surface area of the alveoli and perform the function of gas exchange (Cunniff et al., 2021). These organoids have also been used to model human SARS-CoV-2 infection (Salahudeen et al., 2020). Around 10% of AT2-derived organoids (specifically the SFPTC⁺ cells) and 10% of basal cell-derived organoids (specifically SCGB1A1⁺ club cells) were infected with SARS-CoV-2. These results indicate that AT2 cells are directly infected by SARS-CoV-2 and that club cells are a distal lung target population (Salahudeen et al., 2020).

Xu et al. (2021) used LOs to examine the innate cellular immune response of lung tissue during SARS-CoV-2 infection. They found that expression of receptor interacting serine/threonine-protein kinase 1 (RIPK1), an important mediator of inflammation and cell death (Mifflin et al., 2020), is upregulated in patients with COVID-19 who experience a cytokine storm, and is also activated in SARS-CoV-2-infected primary LOs. Interestingly, treating infected LOs with the RIPK1-inhibitor Nec-1s reduced the transcription of proinflammatory cytokines, as well as ACE2 and the epidermal growth factor receptor (EGFR), which mediate viral entry (Xu et al., 2021).

Clinical trials of the immunomodulatory and clinical effects of another RIPK1 inhibitor, SAR443122, in patients with severe COVID-19 are currently in progress. Interestingly, these studies conducted in LOs, show the applicability of these organoids as suitable models to dissect the pathological mechanisms underlying infectious diseases. Moreover, LOs can be used for rapid screening of the infectivity of emerging human airway

pathogens and to test disease-specific therapeutics. Using LO models to test the safety and efficacy of potential drugs instead of time-consuming and costly clinical trials can greatly contribute to faster and cheaper development of new drugs. Indeed, an LO model has been used to test drugs for SARS-CoV-2 infection (Ebisudani et al., 2021). In this model, infected LOs were treated with physiologically relevant concentrations of lopinavir, nelfinavir, and remdesivir (Ebisudani et al., 2021). Lopinavir and nelfinavir are protein inhibitors commonly used in combination with other drugs for the treatment of HIV-1 infection in adults, adolescents and children (Croxtall and Perry, 2010). Remdesivir is an adenosine nucleotide analogue with broad-spectrum activity against viruses from various families (Lamb, 2020). Although lopinavir and nelfinavir significantly decreased the viral titer, SARS-CoV-2 viral replication was not halted. Interestingly, remdesivir inhibited the replication of the virus in infected organoids (Ebisudani et al., 2021). These results correlate with clinical data of patients infected by SARS-CoV-2 (Beigel et al., 2020; Grein et al., 2020; Ebisudani et al., 2021) and thus, suggest that LOs represent appropriate models for the study of infectious lung diseases.

To conclude, organoids have been already used successfully as models of human disease caused by infections with viruses such SARS-CoV-2 and RSV. These models represent effective and relatively cheap tools for preclinical and clinical trials of potential treatment strategies. Furthermore, LO models of human lung tissue and infectious disease offer possibilities for comparison with, and validation of, serological data from the patients in the clinic.

4.3 Lung Organoids in Cancer Research

Compared to conventional 2D monolayers and suspension cell cultures, LOs used in cancer research provide a valuable opportunity to develop physiologically, genetically, and histologically relevant tumor models. LOs can mimic some of the high cellular organization, tumor microenvironment, and cell interactions of *in vivo* tumor tissue. As such, LOs have been used in various contexts from carcinogenesis, to personalized medicine and drug development (Gunti et al., 2021).

Lung cancer organoids (tumoroids) precisely reflect the histological features of primary lung tumors and maintain their genomic abnormalities during long-term expansion *in vitro*. Recognizing that these models represent a valuable resource, Kim et al. (2019) created a biobank of 80 lung tumoroids from the five most frequent subtypes of lung cancers, and five normal bronchial organoids as controls, which replicate the unique histological features of the primary tissues. Such biobanks serve as a beneficial platform for drug testing and pre-clinical research to advance personalized medicine approaches.

Similar to LOs derived from primary lung progenitors, organoids established from lung cancer cell lines or primary tumor cells contain only a few cell types and so fail to completely replicate the tumor *in vitro* (Fiorini et al., 2020). Nevertheless, these systems have been used successfully in drug sensitivity studies. In one such study, high-throughput screening

of anticancer agents on liver organoids indicated that patient-derived organoids can mimic a patient's response to a particular therapy. Thus, these types of organoids could potentially be used for the development of personalized medicine approaches or as part of clinical trials (Vlachogiannis et al., 2018). Indeed, others have shown that cancer-cell-derived LOs can serve as a tool for pre-treatment drug screening and personalized medicine. Hai et al. (2020) developed genetically modified mouse LOs to mimic human lung squamous cell carcinoma (LSCC) and used this model to demonstrate that treatment with the WEE1 inhibitor (AZD1775) and the adjuvant PD-1 inhibitor enhanced T-cell anti-tumour activity. This demonstrates the importance of drug efficacy screening for identifying more efficient therapeutic drug combinations for evaluation in future clinical trials (Hai et al., 2020). Shi et al. (2020) published a protocol for *in vitro* generation of non-small cell lung cancer (NSCLC) organoids that mimic the histological attributes of the original tumor tissue. Moreover, these NSCLC organoids retained the molecular profile of matching tumor tissue long-term, even after multiple passages (>3 months, >10 passages). Next, they and others showed that NSCLC organoids and PDX models from the same parental tissue exhibit similar drug responses and proposed that organoid cancer models are a valid pre-clinical model to explore novel therapeutic options for NSCLC disease (Hai et al., 2020; Li et al., 2020; Shi et al., 2020; Wang et al., 2020b). Li et al. (2020) established organoid models of lung adenocarcinoma (LADC), the most common subtype of NSCLC. They also showed that the *in vitro* generated organoids preserve the key tumor features and therefore, can be used as a valuable pre-clinical tool. Using LADC organoids derived from 12 cancer lines they performed high-throughput drug response screening and showed that the sensitivity to a particular drug was consistent throughout individual passages and also that the response to the drug varied among different organoid lines (Li et al., 2020). Moreover, they discovered unpredicted drug sensitivity regardless of genetic markers. For example, the ACI-3_O line and SOL-4_O line responded to gefitinib despite the lack of EGFR mutations. Again, their conclusions highlight the benefits of drug response screening on organoids (Li et al., 2020). Kim et al. (2019) used LOs generated from patient-derived cells to dissect the genetic and phenotypic basis of heterogeneous responses to anticancer therapy. They demonstrated that variability in drug responses correlated with particular genomic mutations and persisted during multiple organoid passages. For example, organoids with a *BRCA2* gene mutation showed increased sensitivity to the PARP inhibitor, Olaparib (Kim et al., 2019). Moreover, PDX derived from these organoids also responded to Olaparib treatment. On the other hand, although two organoids derived from different tissues expressed the same EGFR mutation, their responses to erlotinib and crizotinib differed due to secondary mutations. Overall, these studies highlight the critical importance of the LO biobank mentioned above for anti-tumor drug screening to predict individual patient drug responses (Kim et al., 2019).

The results mentioned above demonstrate that organoids are suitable for high-throughput screening while providing the advantages of 3D cancer models which, combined with clinical

evaluation of specific genetic alterations, can serve as a tool for personalized therapy. Indeed, another recent study by Hu et al. (2021) proved that LOs successfully mimic original tumor tissue features and preserve them after *in vitro* cultivation. Moreover, they developed an integrated superhydrophobic microwell array chip (InSMAR-chip) suitable for high-throughput testing. With this set-up, they analyzed drugs administered during patient treatment and obtained results showing 100% accuracy and specificity in 10 of 21 samples. The remaining 11 on-chip samples could not be compared to relative patient responses due to differences in subsequent treatment. Nevertheless, this study showed a strong correlation of the drug response with genetic mutation and clinical outcomes and therefore, confirmed this as a promising approach for predicting the most effective drugs for individual patients (Hu et al., 2021).

As a result of such successes, LOs derived from patients with various lung pathologies have now entered clinical trials to establish their efficacy in predicting individual patients' responses to a specific therapy (Table 2).

These studies of high-throughput screening have highlighted the potential of cancer organoids as a promising tool for personalized treatment. Using such progressive methods, organoids can be generated for each individual patient and used to screen drug responses based on the initial clinical tests of specific genetic mutations and gene expression profiles. This approach holds great potential for achieving better clinical outcomes and prolonged survival of patients. High-throughput testing also offers a great advantage for screening samples currently available in biobanks. Furthermore, as more patient-derived samples are contributed, the collection of unique genetic alterations and their specific combinations will expand. Thus, we expect that this approach will provide a standardized tool for rapid development and testing of new anti-tumor treatments.

5 Lung Organoids: Future Prospects and Remaining Challenges

So far, we have discussed the great progress made using primary lung progenitor cell-derived and iPSC-derived LOs in modeling human diseases such as CF, IPF, lung cancer, and SARS-CoV-2 infection. However, certain challenges still need to be addressed to improve the relevance of these models to *in vivo* conditions. Several approaches have been developed to further enhance the physiological resemblance of *in vitro* 3D models to lung tissue *in vivo*. One is based on the cultivation of lung epithelial cells at an air-liquid interface, where the basolateral side of the epithelial cells is immersed in culture medium while the apical side is exposed to humidified air. This approach was used by Mas et al. (2016) to develop OncoCilAir™ tumor-stroma airway model by co-culture of lung adenocarcinoma cells, human primary bronchial cells, and lung fibroblasts. This model provides an alternative means of testing drug efficacy and toxicity that could replace animal models by overcoming the disadvantages of differences in rodent cancer physiology and genetic features. Specifically, the major drawback of animal lung models is the diversity in progression of lung disease and response to therapy (Mas et al., 2016).

TABLE 2 | Clinical trials in lung organoids: List of the clinical trials using 3D LOs as *in vitro* models.

Disease	Model	Source of the cells	Purpose of the study	ClinicalTrials.gov Identifier
Lung cancer	Spheroids Patient-derived LOs 3D model OncoCilAir™ (OncoTheis)	Lung tumor biopsies	Characterization of the consistency and accuracy of the organoids derived from patient lung biopsies to predict clinical response to the chemotherapy	NCT03979170
Lung cancer	Patient-derived normal and cancer LOs Blood samples	Biopsies from endobronchial tumors or lymph nodes	Biobanking of normal and primary lung cancer organoids. Analysis of microvesicles secreted by lung cancer cells in organoid-derived culture supernatants and patient blood samples. Comparison of the response to the drugs in normal and cancer LOs	NCT05092009
Lung cancer	Patient-derived organoids Xenografts	Tumor tissue biopsies	Comparison of the xenografts with donor tissue. Testing novel anti-cancer treatment. Developing assays to predict tumor response to the drug	NCT04859166
CF	Organoids derived from the tissue of patients with the R334W-CFTR mutation	Rectal biopsies	Study of the response of organoids to CFTR modulators, which will be compared to the patients' response to the same drug in the next study	NCT04254705
Lung cancer	Patient-derived LOs	Lung tumor biopsies	Biobanking of organoids derived from stage I–IV lung cancer patients	NCT03655015
Lung cancer	Patient-derived LOs	Non-small cell lung cancer patient biopsies	Use of organoids for the drug sensitivity testing and comparison with clinical treatment data	NCT03453307
COPD and IPF	Patient-derived LOs	Lung tissue biopsies from patients with emphysema or pulmonary fibrosis	Characterization of the stem cell niche in different tissues (healthy, emphysematous and fibrotic pulmonary tissue). Further use of the organoids for drug screening and personalized medicine	NCT02705144
Lung cancer	Patient-derived LOs	Non-small cell lung cancer patient biopsies	Testing of different drugs <i>in vitro</i> using organoids. Evaluation of the responders to Osimertinib and screening of alternative therapies for non-responders <i>in vitro</i>	NCT05136014
Lung cancer	Patient-derived LOs Microfluidic system	Tumor biopsies Blood samples	Use of organoids and a microfluidic system as an innovative model of the tumor microenvironment and HUVECS or endothelial cells as a model of tumor vascularization, to create a tool for personalized medicine	NCT04826913
Lung cancer	Patient-derived organoids from lung tumors or other solid tumors TILs or/and peripheral T-cells	Lung cancer tissue or solid tumor biopsies	Co-cultivation of organoids with lymphocytes to screen for tumor-responsive T-cells, which will be further expanded and used as immunotherapy for the patient	NCT03778814
CF	Patient-derived organoids	Not specified	Use of an <i>ex vivo</i> organoid model to establish the correlation between the clinical response of CF patients to Vx-770 (Ivacaftor)	NCT03390985

Used abbreviations: COPD, chronic obstructive pulmonary disease; CF, cystic fibrosis; IPF, idiopathic pulmonary fibrosis; LOs, lung organoids; 3D, three-dimensional; CFTR, cystic fibrosis transmembrane conductance regulator.

The newly developed cultures that incorporate an extracellular scaffold represent a further advance that enables standardized long-term cultivation conditions and reproducibility (Zscheppang et al., 2018). Moreover, this approach facilitates exploration of the interaction between the ECM and lung cells in the context of aberrant repair or regeneration. The scaffolds are generated by decellularization of healthy human lung tissue or tissue derived from patients with conditions such as IPF. These models will contribute greatly to our understanding of the pathogenesis of lung disease and evaluation of the role of ECM in the onset and course of these pathologies (Zscheppang et al., 2018).

While 3D models have many advantages compared to conventional 2D models, many still fail to fully represent

even a small fraction of the dynamic features of human lungs, such as the processes of nutrient and gas exchange, the mechanical forces created by breathing movements, and dynamic flow conditions. The tumor-on-a-chip model however, was designed to overcome these limitations (Barros et al., 2021). These microfluidic models of lung tumors are often derived from established lung cancer cell lines, which form a spheroid in the microchannel, adding a further 3D aspect to these studies (Mehta et al., 2022). Microfluidic devices have been used to study drug resistance, the efficiency of photodynamic therapy, the influence of mechanical forces in the lungs on tumor progression and drug resistance, and characterization of cell-cell communication in the tumor microenvironment (Del Piccolo et al., 2021). For example, Xu et al. (2013) developed

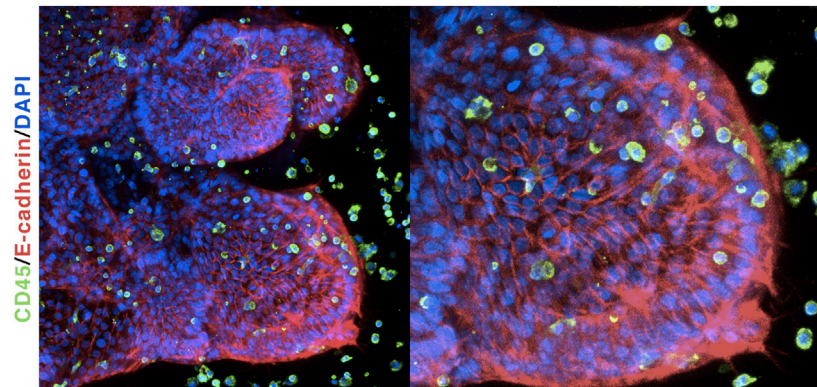


FIGURE 5 | Lung organoids co-cultured with primary monocytes: Immunofluorescent labeling of human LOs shows tissue polarity and recruitment of human monocytes.

a microfluidic device to study drug sensitivity of a co-cultured human non-small cell lung cancer cell line (SPCA-1) and stromal cells. They also established a culture of fresh lung cancer tissues from eight patients in their microchip device, in order to identify personalized medical treatments. This approach accomplished replication of the actual condition of the solid tumor *in vivo*. Microfluidic devices provide an easy way to administer single or combined anti-cancer treatments in high-throughput assays, which is beneficial for the development of personalized medicine. Further advantages are that these devices require only small amounts of samples and reagents, short assay time and high sensitivity. Microfluidic devices can also be used with various tissue set-ups, such as cell line monolayers or co-culture of cancer cell lines and stromal cells, to more accurately recapitulate tumor tissue *in vivo*, or even primary fresh tissue. This approach revealed significant differences in treatment sensitivity, with the poorest detected in fresh tissue (Xu et al., 2013). Thus, further studies are warranted to develop methods for cultivation of patient tumor tissue *in vitro* while closely maintaining the physiological features of the human body that can be used to exploit the potential of organoids in the development of personalized therapy.

Sepsis and septic shock greatly contribute to the mortality of human population (Rudd et al., 2020). Therefore, the development of an *in vitro* model of sepsis represents another prospect for the LO approach for defining the exact pathogenesis of the disease and identifying potential therapeutic strategies and new biomarkers. However, an *in vitro* model of sepsis-induced lung injury based on LO technology may require a complex set-up due to the number of different cell types and their specific effects in septic reactions. For instance, hypoxemia, which is an important factor in the pathophysiology of ALI/ARDS, is caused by neutrophil entrapment in the pulmonary microvasculature (Park et al., 2019). Therefore, to create a relevant *in vitro* model of sepsis might warrant culture under hypoxic conditions. Nevertheless, similar to the situation for infectious diseases, a great advantage of LOs as a model of human sepsis is in the possibility of comparison with, and validation of, serological data from patients in the clinic.

The use of iPSCs to derive LOs has rapidly advanced the field in recent years; however, these models are not yet perfect. LOs developed from iPSCs resemble fetal tissues rather than adult lungs and, therefore, transplantation into a living organism may be required to fully recapitulate the adult lung phenotype (Dye et al., 2015). This engraftment procedure has been successfully achieved using humanized/immunodeficient mouse recipients to develop mature intestinal (Cortez et al., 2018; Poling et al., 2018; Boyle et al., 2021), brain (Dong et al., 2021), and kidney (van den Berg et al., 2018) organoids, but it is not so commonly practiced with LOs. An early study by Dye et al. (2016) demonstrated that human ESC-derived LOs can be maintained for up to 15 weeks after engraftment into the epididymal fat pad of male NOD-scid IL2R γ null mice. After the engraftment, LOs improved their cellular differentiation of secretory lineages and formed airway-like structures that were similar to adult human lungs, including vasculature and smooth muscles. However, a bioartificial microporous poly (lactide-co-glycolide) (PLG) scaffold niche was necessary for proper engraftment (Dye et al., 2016), which requires advanced techniques for its fabrication. Nevertheless, alternative approaches such as decellularized lung scaffolds are also available to provide relevant physical and environments for the generation of organized lung structures (Gilpin et al., 2014).

A notable drawback of iPSC-derived LOs is the lack of a pulmonary immune cell populations. The human lung comprises both tissue-resident immune cells (such as pulmonary macrophages) as well as infiltrating immune cells, such as neutrophils, monocytes, and T-cells, which are not found in LOs. This immune cell-deprived scenario renders such a model unsuitable for studying diseases in which immune cells have a major role—including microbial infections and inflammation. However, recent studies have demonstrated that immune cells can be co-cultured with organoids to generate a more physiologically relevant model. Our own findings show that iPSC-derived LOs, although deprived of immune cell populations, can respond to microbial ligands and are able to recruit human primary monocytes *in vitro* (Jose et al., 2020). Interestingly, co-cultured monocytes interacted closely with the

organoid tissue and significantly changed their phenotype (Figure 5). Similarly, another study showed that RSV-infected airway organoids were able to recruit and interact with human neutrophils (Sachs et al., 2019). Taken together, these results suggest that co-culturing LOs with primary immune cells will allow a better dissection of the interactions of immune cells with human tissues and thus, contribute to a better understanding of complex pathologies.

As already mentioned, the local microbiota plays a crucial role in the pathology and homeostasis of the lung tissue (Paolicelli et al., 2019; Barcik et al., 2020). Although many studies have focused on the role of the microbiota in the gastrointestinal tract using human intestinal organoids (Min et al., 2020), few studies using LOs have been reported. Therefore, future research should focus on dissection of the cell-cell interaction of the microbiota with lung tissue and the molecular mechanisms by which the microbiota influences the development, pathology, and homeostasis of human lung.

6 DISCUSSION

Using 3D organoids as a tool to understand lung development and function holds great potential for generating important insights not only into genetic lung disorders, but also into diseases such as COPD, CF, and lung infections. The generation of LOs from human PSCs is crucial for overcoming the obstacles to *in vitro* studies of human cells, which for many years have relied on the scant availability of post-mortem tissues. LOs can bridge the knowledge gap between lung disease pathways identified in rodent models and therapeutic possibilities in their human counterparts. The end of our long-term dependence on rodent models for genetic manipulation studies may also be heralded by the emergence of novel genome editing techniques such as CRISPR, which could be used to generate genetic models of pulmonary disease using organoids. This approach would facilitate mechanistic studies in a physiological setting that closely resembles the human respiratory system without the need for presumably costly and time-consuming animal research. The recent advances in the use of iPSC-derived LO in clinical trials are also promising in terms of drug screening for personalized treatment or transplantation of healthy tissues, especially allogenic tissues, in patients, and hints at a future that includes “organoid-based treatment” of pulmonary diseases.

In summary, we believe that organoids represent the future of lung disease modeling as they allow long-term cultivation of

human lung tissue, maintaining many of its phenotypical, and functional characteristics. LOs represent one of the best tools for translational research, due to the comparatively inexpensive and increasingly biologically-relevant methodology. The past 10 years have seen an increasing number of studies leveraging organoids to shed light on previously unexplained pathologies of diseases such as IPF (Chen et al., 2017; Kim et al., 2021; Suezawa et al., 2021), CF (Dekkers et al., 2013; Firth et al., 2015; Kim et al., 2021), and lung cancer (Hai et al., 2020; Li et al., 2020; Shi et al., 2020; Wang et al., 2020b; Gunti et al., 2021; Hu et al., 2021). Harnessing the potential that LOs have to offer will promote the design of new treatments and diagnostic methodologies and thus, finally improve the quality of life of people affected by various pulmonary diseases.

AUTHOR CONTRIBUTIONS

VB prepared the figures and table and wrote the manuscript. MZ wrote and critically reviewed the manuscript. LS and ZG wrote the manuscript. SJ prepared the table and wrote the manuscript. MH and TZ critically reviewed the manuscript. JF conceptualized, wrote, and critically reviewed the manuscript. All authors contributed to the article and approved the submitted version.

FUNDING

The authors were supported by the European Social Fund and European Regional Development Fund—Project MAGNET (No. CZ.02.1.01/0.0/0.0/15_003/0000492) and ENOCH (CZ.02.1.01/0.0/0.0/16_019/0000868), and by the Ministry of Health of the Czech Republic—DRO (Institute of Hematology and Blood Transfusion—IHBT, 00023736) and grant nr. NU22-A-121. All rights reserved. MZ was supported by the European Regional Development Fund—Project Support of MSCA IF fellowships at FNUA-ICRC (No. CZ.02.2.69/0.0/0.0/19_074/0016274).

ACKNOWLEDGMENTS

Authors would like to thank Lucy Robinson and Jessica Tamanini of Insight Editing London for critically reviewing the manuscript before submission.

REFERENCES

- Aichler, M., Kunzke, T., Buck, A., Sun, N., Ackermann, M., Jonigk, D., et al. (2018). Molecular Similarities and Differences from Human Pulmonary Fibrosis and Corresponding Mouse Model: MALDI Imaging Mass Spectrometry in Comparative Medicine. *Lab. Invest.* 98, 141–149. doi:10.1038/labinvest.2017.110
- Angus, D. C., and van der Poll, T. (2013). Severe Sepsis and Septic Shock. *N. Engl. J. Med.* 369, 840–851. doi:10.1056/nejmra1208623
- Ardini-Poleske, M. E., Clark, R. F., Ansong, C., Carson, J. P., Corley, R. A., Deutsch, G. H., et al. (2017). LungMAP: The Molecular Atlas of Lung Development Program. *Am. J. Physiology-Lung Cell. Mol. Physiology* 313, L733–L740. doi:10.1152/ajplung.00139.2017
- Aziz, M., Jacob, A., Yang, W. L., Matsuda, A., and Wang, P. (2013). Current Trends in Inflammatory and Immunomodulatory Mediators in Sepsis. *J. Leukoc. Biol.* 93, 329–342. doi:10.1189/jlb.0912437
- Barcik, W., Boutin, R. C. T., Sokolowska, M., and Finlay, B. B. (2020). The Role of Lung and Gut Microbiota in the Pathology of Asthma. *Immunity* 52, 241–255. doi:10.1016/j.immuni.2020.01.007

- Barkauskas, C. E., Cronce, M. J., Rackley, C. R., Bowie, E. J., Keene, D. R., Stripp, B. R., et al. (2013). Type 2 Alveolar Cells Are Stem Cells in Adult Lung. *J. Clin. Invest.* 123, 3025–3036. doi:10.1172/jci68782
- Barros, A. S., Costa, A., and Sarmento, B. (2021). Building Three-Dimensional Lung Models for Studying Pharmacokinetics of Inhaled Drugs. *Adv. drug Deliv. Rev.* 170, 386–395. doi:10.1016/j.addr.2020.09.008
- Beigel, J. H., Tomashek, K. M., Dodd, L. E., Mehta, A. K., Zingman, B. S., Kalil, A. C., et al. (2020). Remdesivir for the Treatment of Covid-19 - Final Report. *N. Engl. J. Med.* 383, 1813–1826. doi:10.1056/nejmoa2007764
- Benam, K. H., Villenave, R., Lucchesi, C., Varone, A., Hubeau, C., Lee, H. H., et al. (2016). Small Airway-On-A-Chip Enables Analysis of Human Lung Inflammation and Drug Responses *In Vitro*. *Nat. Methods* 13, 151–157. doi:10.1038/nmeth.3697
- Berkers, G., van Mourik, P., Vonk, A. M., Kruisselbrink, E., Dekkers, J. F., de Winter-de Groot, K. M., et al. (2019). Rectal Organoids Enable Personalized Treatment of Cystic Fibrosis. *Cell Rep.* 26, 1701–1708. e3. doi:10.1016/j.celrep.2019.01.068
- Bleijis, M., van de Wetering, M., Clevers, H., and Drost, J. (2019). Xenograft and Organoid Model Systems in Cancer Research. *EMBO J.* 38, e101654. doi:10.15252/embj.2019101654
- Boyle, M. A., Sequeira, D. J., McNeill, E. P., Criss, Z. K., 2nd, Shroyer, N. F., and Speer, A. L. (2021). Vivo Transplantation of Human Intestinal Organoids Enhances Select Tight Junction Gene Expression. *J. Surg. Res.* 259, 500–508. doi:10.1016/j.jss.2020.10.002
- Busslinger, G. A., Weusten, B. L. A., Bogte, A., Begthel, H., Brosens, L. A. A., and Clevers, H. (2021). Human Gastrointestinal Epithelia of the Esophagus, Stomach, and Duodenum Resolved at Single-Cell Resolution. *Cell Rep.* 34, 108819. doi:10.1016/j.celrep.2021.108819
- Castellani, S., Di Gioia, S., di Toma, L., and Conese, M. (2018). Human Cellular Models for the Investigation of Lung Inflammation and Mucus Production in Cystic Fibrosis. *Anal. Cell Pathol. (Amst)* 2018, 3839803. doi:10.1155/2018/3839803
- Chanda, D., Otoupalova, E., Smith, S. R., Volckaert, T., De Langhe, S. P., and Thannickal, V. J. (2019). Developmental Pathways in the Pathogenesis of Lung Fibrosis. *Mol. Aspects Med.* 65, 56–69. doi:10.1016/j.mam.2018.08.004
- Chang, D., and Sharma, L. (2020). Harnessing Murine Microbiome Models to Study Human Lung Microbiome. *Chest* 157, 776–778. doi:10.1016/j.chest.2019.12.011
- Charavaryamath, C., Janardhan, K. S., Caldwell, S., and Singh, B. (2006). Pulmonary Intravascular Monocytes/macrophages in a Rat Model of Sepsis. *Anat. Rec. A Discov. Mol. Cell Evol. Biol.* 288, 1259–1271. doi:10.1002/ar.a.20401
- Chen, Y. W., Huang, S. X., de Carvalho, A., Ho, S. H., Islam, M. N., Volpi, S., et al. (2017). A Three-Dimensional Model of Human Lung Development and Disease from Pluripotent Stem Cells. *Nat. Cell Biol.* 19, 542–549. doi:10.1038/ncb3510
- Choi, J., Iich, E., and Lee, J. H. (2016). Organogenesis of Adult Lung in a Dish: Differentiation, Disease and Therapy. *Dev. Biol.* 420, 278–286. doi:10.1016/j.ydbio.2016.10.002
- Choi, J., Park, J. E., Tsakogeorga, G., Yanagita, M., Koo, B. K., Han, N., et al. (2020). Inflammatory Signals Induce AT2 Cell-Derived Damage-Associated Transient Progenitors that Mediate Alveolar Regeneration. *Cell Stem Cell* 27, 366–382 e7. doi:10.1016/j.stem.2020.06.020
- Ciancanelli, M. J., Huang, S. X., Luthra, P., Garner, H., Itan, Y., Volpi, S., et al. (2015). Infectious Disease. Life-Threatening Influenza and Impaired Interferon Amplification in Human IRF7 Deficiency. *Science* 348, 448–453. doi:10.1126/science.aaa1578
- Clarke, L. L., Grubb, B. R., Gabriel, S. E., Smithies, O., Koller, B. H., and Boucher, R. C. (1992). Defective Epithelial Chloride Transport in a Gene-Targeted Mouse Model of Cystic Fibrosis. *Science* 257, 1125–1128. doi:10.1126/science.257.5073.1125
- Cleary, S. J., Pitchford, S. C., Amison, R. T., Carrington, R., Robaina Cabrera, C. L., Magnen, M., et al. (2020). Animal Models of Mechanisms of SARS-CoV-2 Infection and COVID-19 Pathology. *Br. J. Pharmacol.* 177, 4851–4865. doi:10.1111/bph.15143
- Clevers, H. (2016). Modeling Development and Disease with Organoids. *Cell* 165, 1586–1597. doi:10.1016/j.cell.2016.05.082
- Cortez, A. R., Poling, H. M., Brown, N. E., Singh, A., Mahe, M. M., and Helmrath, M. A. (2018). Transplantation of Human Intestinal Organoids into the Mouse Mesentery: A More Physiologic and Anatomic Engraftment Site. *Surgery* 164, 643–650. doi:10.1016/j.surg.2018.04.048
- Croxtall, J. D., and Perry, C. M. (2010). Lopinavir/Ritonavir: a Review of its Use in the Management of HIV-1 Infection. *Drugs* 70, 1885–1915. doi:10.2165/11204950-000000000-00000
- Cunniff, B., Druso, J. E., and van der Velden, J. L. (2021). Lung Organoids: Advances in Generation and 3D-Visualization. *Histochem Cell Biol.* 155, 301–308. doi:10.1007/s00418-020-01955-w
- Danahay, H., Pessotti, A. D., Coote, J., Montgomery, B. E., Xia, D., Wilson, A., et al. (2015). Notch2 Is Required for Inflammatory Cytokine-Driven Goblet Cell Metaplasia in the Lung. *Cell Rep.* 10, 239–252. doi:10.1016/j.celrep.2014.12.017
- David, B., Bafadhel, M., Koenderman, L., and De Soyza, A. (2021). Eosinophilic Inflammation in COPD: from an Inflammatory Marker to a Treatable Trait. *Thorax* 76, 188–195. doi:10.1136/thoraxjnl-2020-215167
- Davies, H., Bignell, G. R., Cox, C., Stephens, P., Edkins, S., Clegg, S., et al. (2002). Mutations of the BRAF Gene in Human Cancer. *Nature* 417, 949–954. doi:10.1038/nature00766
- De Boeck, K. (2020). Cystic Fibrosis in the Year 2020: A Disease with a New Face. *Acta Paediatr.* 109, 893–899. doi:10.1111/apa.15155
- De Luca, A., Pariano, M., Cellini, B., Costantini, C., Vilella, V. R., Jose, S. S., et al. (2017). The IL-17F/IL-17RC Axis Promotes Respiratory Allergy in the Proximal Airways. *Cell Rep.* 20, 1667–1680. doi:10.1016/j.celrep.2017.07.063
- Dekkers, J. F., Wiegierinck, C. L., de Jonge, H. R., Bronsveld, L., Janssens, H. M., de Winter-de Groot, K. M., et al. (2013). A Functional CFTR Assay Using Primary Cystic Fibrosis Intestinal Organoids. *Nat. Med.* 19, 939–945. doi:10.1038/nm.3201
- Del Piccolo, N., Shirure, V. S., Bi, Y., Goedegebuure, S. P., Gholami, S., Hughes, C. W., et al. (2021). Tumor-on-chip Modeling of Organ-specific Cancer and Metastasis. *Adv. drug Deliv. Rev.* 175, 113798. doi:10.1016/j.addr.2021.05.008
- Dong, X., Xu, S. B., Chen, X., Tao, M., Tang, X. Y., Fang, K. H., et al. (2021). Human Cerebral Organoids Establish Subcortical Projections in the Mouse Brain after Transplantation. *Mol. psychiatry* 26, 2964–2976. doi:10.1038/s41380-020-00910-4
- Drost, J., and Clevers, H. (2018). Organoids in Cancer Research. *Nat. Rev. Cancer* 18, 407–418. doi:10.1038/s41568-018-0007-6
- Duval, K., Grover, H., Han, L.-H., Mou, Y., Pegoraro, A. F., Fredberg, J., et al. (2017). Modeling Physiological Events in 2D vs. 3D Cell Culture. *Physiology* 32, 266–277. doi:10.1152/physiol.00036.2016
- Dwyer-Lindgren, L., Bertozzi-Villa, A., Stubbs, R. W., Morozoff, C., Shirude, S., Naghavi, M., et al. (2017). Trends and Patterns of Differences in Chronic Respiratory Disease Mortality Among US Counties, 1980–2014. *Jama* 318, 1136–1149. doi:10.1001/jama.2017.11747
- Dye, B. R., Dedhia, P. H., Miller, A. J., Nagy, M. S., White, E. S., Shea, L. D., et al. (2016). A Bioengineered Niche Promotes *In Vivo* Engraftment and Maturation of Pluripotent Stem Cell Derived Human Lung Organoids. *Elife* 5. doi:10.7554/eLife.19732
- Dye, B. R., Hill, D. R., Ferguson, M. A., Tsai, Y. H., Nagy, M. S., Dyal, R., et al. (2015). *In Vitro* generation of Human Pluripotent Stem Cell Derived Lung Organoids. *Elife* 4. doi:10.7554/eLife.05098
- Ebisudani, T., Sugimoto, S., Haga, K., Mitsuishi, A., Takai-Todaka, R., Fujii, M., et al. (2021). Direct Derivation of Human Alveolospheres for SARS-CoV-2 Infection Modeling and Drug Screening. *Cell Rep.* 35, 109218. doi:10.1016/j.celrep.2021.109218
- Engelman, J. A., Zejnullahu, K., Mitsudomi, T., Song, Y., Hyland, C., Park, J. O., et al. (2007). MET Amplification Leads to Gefitinib Resistance in Lung Cancer by Activating ERBB3 Signaling. *Science* 316, 1039–1043. doi:10.1126/science.1141478
- Fajgenbaum, D. C., and June, C. H. (2020). Cytokine Storm. *N. Engl. J. Med.* 383, 2255–2273. doi:10.1056/nejmra2026131
- Fiorini, E., Veghini, L., and Corbo, V. (2020). Modeling Cell Communication in Cancer with Organoids: Making the Complex Simple. *Front. Cell Dev. Biol.* 8, 166. doi:10.3389/fcell.2020.00166
- Firth, A. L., Menon, T., Parker, G. S., Qualls, S. J., Lewis, B. M., Ke, E., et al. (2015). Functional Gene Correction for Cystic Fibrosis in Lung Epithelial Cells Generated from Patient iPSCs. *Cell Rep.* 12, 1385–1390. doi:10.1016/j.celrep.2015.07.062

- Franks, T. J., Colby, T. V., Travis, W. D., Tuder, R. M., Reynolds, H. Y., Brody, A. R., et al. (2008). Resident Cellular Components of the Human Lung: Current Knowledge and Goals for Research on Cell Phenotyping and Function. *Proc. Am. Thorac. Soc.* 5, 763–766. doi:10.1513/pats.200803-025hr
- Gazdar, A. F., Girard, L., Lockwood, W. W., Lam, W. L., and Minna, J. D. (2010). Lung Cancer Cell Lines as Tools for Biomedical Discovery and Research. *J. Natl. Cancer Inst.* 102, 1310–1321. doi:10.1093/jnci/djq279
- Gilpin, S. E., Ren, X., Okamoto, T., Guyette, J. P., Mou, H., Rajagopal, J., et al. (2014). Enhanced Lung Epithelial Specification of Human Induced Pluripotent Stem Cells on Decellularized Lung Matrix. *Ann. Thorac. Surg.* 98, 1721–1729. doi:10.1016/j.athoracsur.2014.05.080
- Gkatzis, K., Taghizadeh, S., Huh, D., Stainier, D. Y. R., and Bellusci, S. (2018). Use of Three-Dimensional Organoids and Lung-On-A-Chip Methods to Study Lung Development, Regeneration and Disease. *Eur. Respir. J.* 52. doi:10.1183/13993003.00876-2018
- Gottschling, S., Jauch, A., Kuner, R., Herpel, E., Mueller-Decker, K., Schnabel, P. A., et al. (2012). Establishment and Comparative Characterization of Novel Squamous Cell Non-small Cell Lung Cancer Cell Lines and Their Corresponding Tumor Tissue. *Lung cancer* 75, 45–57. doi:10.1016/j.lungcan.2011.05.020
- Grein, J., Ohmagari, N., Shin, D., Diaz, G., Asperges, E., Castagna, A., et al. (2020). Compassionate Use of Remdesivir for Patients with Severe Covid-19. *N. Engl. J. Med.* 382, 2327–2336. doi:10.1056/nejmoa2007016
- Grubb, B. R., and Boucher, R. C. (1999). Pathophysiology of Gene-Targeted Mouse Models for Cystic Fibrosis. *Physiol. Rev.* 79, S193–S214. doi:10.1152/physrev.1999.79.1.s193
- Guilbault, C., Saeed, Z., Downey, G. P., and Radzioch, D. (2007). Cystic Fibrosis Mouse Models. *Am. J. Respir. Cell Mol. Biol.* 36, 1–7. doi:10.1165/rcmb.2006-0184tr
- Gunti, S., Hoke, A. T. K., Vu, K. P., and London, N. R., Jr. (2021). Organoid and Spheroid Tumor Models: Techniques and Applications. *Cancers* 13. doi:10.3390/cancers13040874
- Habel, D. M., Espindola, M. S., Coelho, A. L., and Hogaboam, C. M. (2018). Modeling Idiopathic Pulmonary Fibrosis in Humanized Severe Combined Immunodeficient Mice. *Am. J. Pathology* 188, 891–903. doi:10.1016/j.ajpath.2017.12.020
- Hai, J., Zhang, H., Zhou, J., Wu, Z., Chen, T., Papadopoulos, E., et al. (2020). Generation of Genetically Engineered Mouse Lung Organoid Models for Squamous Cell Lung Cancers Allows for the Study of Combinatorial Immunotherapy. *Clin. Cancer Res.* 26, 3431–3442. doi:10.1158/1078-0432.ccr-19-1627
- Hawkins, F. J., Suzuki, S., Beermann, M. L., Barilla, C., Wang, R., Villacorta-Martin, C., et al. (2021). Derivation of Airway Basal Stem Cells from Human Pluripotent Stem Cells. *Cell stem Cell* 28, 79–95 e8. doi:10.1016/j.stem.2020.09.017
- Hegab, A. E., Arai, D., Gao, J., Kuroda, A., Yasuda, H., Ishii, M., et al. (2015). Mimicking the Niche of Lung Epithelial Stem Cells and Characterization of Several Effectors of Their *In Vitro* Behavior. *Stem Cell Res.* 15, 109–121. doi:10.1016/j.scr.2015.05.005
- Hortova-Kohoutkova, M., De Zuani, M., Laznickova, P., Bendickova, K., Mrkva, O., Andrejcinova, I., et al. (2021). Polymorphonuclear Cells Show Features of Dysfunctional Activation during Fatal Sepsis. *Front. Immunol.* 12, 741484. doi:10.3389/fimmu.2021.741484
- Hortova-Kohoutkova, M., Tidu, F., De Zuani, M., Sramek, V., Helan, M., and Fric, J. (2020). Phagocytosis-Inflammation Crosstalk in Sepsis: New Avenues for Therapeutic Intervention. *Shock* 54, 606–614. doi:10.1097/shk.0000000000001541
- Hu, Y., Sui, X., Song, F., Li, Y., Li, K., Chen, Z., et al. (2021). Lung Cancer Organoids Analyzed on Microwell Arrays Predict Drug Responses of Patients within a Week. *Nat. Commun.* 12, 2581. doi:10.1038/s41467-021-22676-1
- Huang, H., Feng, H., and Zhuge, D. (2019). M1 Macrophage Activated by Notch Signal Pathway Contributed to Ventilator-Induced Lung Injury in Chronic Obstructive Pulmonary Disease Model. *J. Surg. Res.* 244, 358–367. doi:10.1016/j.jss.2019.06.060
- Huang, Y., Huang, Z., Tang, Z., Chen, Y., Huang, M., Liu, H., et al. (2021). Research Progress, Challenges, and Breakthroughs of Organoids as Disease Models. *Front. Cell Dev. Biol.* 9, 740574. doi:10.3389/fcell.2021.740574
- Huh, D., Leslie, D. C., Matthews, B. D., Fraser, J. P., Jurek, S., Hamilton, G. A., et al. (2012). A Human Disease Model of Drug Toxicity-Induced Pulmonary Edema in a Lung-On-A-Chip Microdevice. *Sci. Transl. Med.* 4, 159ra147. doi:10.1126/scitranslmed.3004249
- Ibricevic, A., Pekosz, A., Walter, M. J., Newby, C., Battaile, J. T., Brown, E. G., et al. (2006). Influenza Virus Receptor Specificity and Cell Tropism in Mouse and Human Airway Epithelial Cells. *J. virology* 80, 7469–7480. doi:10.1128/jvi.02677-05
- Jacob, A., Morley, M., Hawkins, F., McCauley, K. B., Jean, J. C., Heins, H., et al. (2017). Differentiation of Human Pluripotent Stem Cells into Functional Lung Alveolar Epithelial Cells. *Cell stem Cell* 21, 472–488 e10. doi:10.1016/j.stem.2017.08.014
- Jose, S. S., De Zuani, M., Tidu, F., Hortová Kohoutková, M., Pazzagli, L., Forte, G., et al. (2020). Comparison of Two Human Organoid Models of Lung and Intestinal Inflammation Reveals Toll-like Receptor Signalling Activation and Monocyte Recruitment. *Clin. Transl. Immunol.* 9, e1131. doi:10.1002/cti2.1131
- Jung, D. J., Shin, T. H., Kim, M., Sung, C. O., Jang, S. J., and Jeong, G. S. (2019). A One-Stop Microfluidic-Based Lung Cancer Organoid Culture Platform for Testing Drug Sensitivity. *Lab a chip* 19, 2854–2865. doi:10.1039/c9lc00496c
- Kapicibasi, H. O., Kiraz, H. A., Demir, E. T., Adali, Y., and Elmas, S. (2020). Pulmonary Effects of Ozone Therapy at Different Doses Combined with Antibioticotherapy in Experimental Sepsis Model. *Acta Cir. Bras.* 35, e202000604. doi:10.1590/s0102-865020200060000004
- Karelehto, E., Cristella, C., Yu, X., Sridhar, A., Hulsdouw, R., de Haan, K., et al. (2018). Polarized Entry of Human Parechoviruses in the Airway Epithelium. *Front. Cell. Infect. Microbiol.* 8, 294. doi:10.3389/fcimb.2018.00294
- Karzai, W., Cui, X., Mehlhorn, B., Straube, E., Hartung, T., Gerstenberger, E., et al. (2003). Protection with Antibody to Tumor Necrosis Factor Differs with Similarly Lethal *Escherichia coli* versus *Staphylococcus aureus* Pneumonia in Rats. *Anesthesiology* 99, 81–89. doi:10.1097/0000542-200307000-00016
- Katsura, H., Kobayashi, Y., Tata, P. R., and Hogan, B. L. M. (2019). IL-1 and TNFalpha Contribute to the Inflammatory Niche to Enhance Alveolar Regeneration. *Stem Cell Rep.* 12, 657–666. doi:10.1016/j.stemcr.2019.02.013
- Katsura, H., Sontake, V., Tata, A., Kobayashi, Y., Edwards, C. E., Heaton, B. E., et al. (2020). Human Lung Stem Cell-Based Alveolospheres Provide Insights into SARS-CoV-2-Mediated Interferon Responses and Pneumocyte Dysfunction. *Cell Stem Cell* 27, 890–904. e8. doi:10.1016/j.stem.2020.10.005
- Kim, J. H., An, G. H., Kim, J. Y., Rasaei, R., Kim, W. J., Jin, X., et al. (2021). Human Pluripotent Stem-Cell-Derived Alveolar Organoids for Modeling Pulmonary Fibrosis and Drug Testing. *Cell Death Discov.* 7, 48. doi:10.1038/s41420-021-00439-7
- Kim, J., Koo, B. K., and Knoblich, J. A. (2020). Human Organoids: Model Systems for Human Biology and Medicine. *Nat. Rev. Mol. Cell Biol.* 21, 571–584. doi:10.1038/s41580-020-0259-3
- Kim, M., Mun, H., Sung, C. O., Cho, E. J., Jeon, H. J., Chun, S. M., et al. (2019). Patient-derived Lung Cancer Organoids as *In Vitro* Cancer Models for Therapeutic Screening. *Nat. Commun.* 10, 3991. doi:10.1038/s41467-019-11867-6
- King, T. E., Jr., Bradford, W. Z., Castro-Bernardini, S., Fagan, E. A., Glaspole, I., Glassberg, M. K., et al. (2014). A Phase 3 Trial of Pirfenidone in Patients with Idiopathic Pulmonary Fibrosis. *N. Engl. J. Med.* 370, 2083–2092. doi:10.1056/nejmoa1402582
- Kondo, J., and Inoue, M. (2019). Application of Cancer Organoid Model for Drug Screening and Personalized Therapy. *Cells* 8. doi:10.3390/cells8050470
- Kumar, A., Singh, R., Kaur, J., Pandey, S., Sharma, V., Thakur, L., et al. (2021). Wuhan to World: The COVID-19 Pandemic. *Front. Cell. Infect. Microbiol.* 11, 596201. doi:10.3389/fcimb.2021.596201
- Kwak, E. L., Sordella, R., Bell, D. W., Godin-Heymann, N., Okimoto, R. A., Brannigan, B. W., et al. (2005). Irreversible Inhibitors of the EGF Receptor May Circumvent Acquired Resistance to Gefitinib. *Proc. Natl. Acad. Sci. U.S.A.* 102, 7665–7670. doi:10.1073/pnas.0502860102
- Lai, Y., Wei, X., Lin, S., Qin, L., Cheng, L., and Li, P. (2017). Current Status and Perspectives of Patient-Derived Xenograft Models in Cancer Research. *J. Hematol. Oncol.* 10, 106. doi:10.1186/s13045-017-0470-7
- Lamb, Y. N. (2020). Remdesivir: First Approval. *Drugs* 80, 1355–1363. doi:10.1007/s40265-020-01378-w
- Lambrecht, B. N., Hammad, H., and Fahy, J. V. (2019). The Cytokines of Asthma. *Immunity* 50, 975–991. doi:10.1016/j.immuni.2019.03.018

- Lamers, M. M., van der Vaart, J., Knoop, K., Rieseboom, S., Breugem, T. I., Mykityn, A. Z., et al. (2021). An Organoid-Derived Bronchioalveolar Model for SARS-CoV-2 Infection of Human Alveolar Type II-like Cells. *EMBO J.* 40, e105912. doi:10.15252/embj.2020105912
- Lancaster, M. A., and Huch, M. (2019). Disease Modelling in Human Organoids. *Dis. Model Mech.* 12. doi:10.1242/dmm.039347
- Lechner, A. J., Driver, I. H., Lee, J., Conroy, C. M., Nagle, A., Locksley, R. M., et al. (2017). Recruited Monocytes and Type 2 Immunity Promote Lung Regeneration Following Pneumectomy. *Cell Stem Cell* 21, 120–134. e7. doi:10.1016/j.stem.2017.03.024
- Leeman, K. T., Pessina, P., Lee, J. H., and Kim, C. F. (2019). Mesenchymal Stem Cells Increase Alveolar Differentiation in Lung Progenitor Organoid Cultures. *Sci. Rep.* 9, 6479. doi:10.1038/s41598-019-42819-1
- Leibel, S. L., Winquist, A., Tseu, L., Wang, J., Luo, D., Shojiaie, S., et al. (2019). Reversal of Surfactant Protein B Deficiency in Patient Specific Human Induced Pluripotent Stem Cell Derived Lung Organoids by Gene Therapy. *Sci. Rep.* 9, 13450. doi:10.1038/s41598-019-49696-8
- Li, Z., Qian, Y., Li, W., Liu, L., Yu, L., Liu, X., et al. (2020). Human Lung Adenocarcinoma-Derived Organoid Models for Drug Screening. *iScience* 23, 101411. doi:10.1016/j.isci.2020.101411
- Mas, C., Boda, B., Caul Futy, M., Huang, S., Wisniewski, L., and Constant, S. (2016). Establishment of a Tumour-Stroma Airway Model (OncoCilAir) to Accelerate the Development of Human Therapies against Lung Cancer. *Altern. Lab. Anim.* 44, 479–485. doi:10.1177/026119291604400509
- Matute-Bello, G., Frevert, C. W., and Martin, T. R. (2008). Animal Models of Acute Lung Injury. *Am. J. Physiology-Lung Cell. Mol. Physiology* 295, L379–L399. doi:10.1152/ajplung.00010.2008
- Mehta, P., Rahman, Z., Ten Dijke, P., and Boukany, P. E. (2022). Microfluidics Meets 3D Cancer Cell Migration. *Trends Cancer* S2405-8033 (22), 00072–00073. doi:10.1016/j.trecan.2022.03.006
- Mifflin, L., Ofengeim, D., and Yuan, J. (2020). Receptor-interacting Protein Kinase 1 (RIPK1) as a Therapeutic Target. *Nat. Rev. Drug Discov.* 19, 553–571. doi:10.1038/s41573-020-0071-y
- Min, S., Kim, S., and Cho, S. W. (2020). Gastrointestinal Tract Modeling Using Organoids Engineered with Cellular and Microbiota Niches. *Exp. Mol. Med.* 52, 227–237. doi:10.1038/s12276-020-0386-0
- Minasyan, H. (2019). Sepsis: Mechanisms of Bacterial Injury to the Patient. *Scand. J. Trauma Resusc. Emerg. Med.* 27, 19. doi:10.1186/s13049-019-0596-4
- Minoo, P., Hamdan, H., Bu, D., Warburton, D., Stepanik, P., and deLemos, R. (1995). TTF-1 Regulates Lung Epithelial Morphogenesis. *Dev. Biol.* 172, 694–698. doi:10.1006/dbio.1995.8080
- Moeller, A., Ask, K., Warburton, D., Gauldie, J., and Kolb, M. (2008). The Bleomycin Animal Model: a Useful Tool to Investigate Treatment Options for Idiopathic Pulmonary Fibrosis? *Int. J. Biochem. Cell Biol.* 40, 362–382. doi:10.1016/j.biocel.2007.08.011
- Motomura, T., Ueda, K., Ohtani, S., Hansen, E., Ji, L., Ito, K., et al. (2010). Evaluation of Systemic External Microwave Hyperthermia for Treatment of Pleural Metastasis in Orthotopic Lung Cancer Model. *Oncol. Rep.* 24, 591–598. doi:10.3892/or.00000896
- Mou, H., Zhao, R., Sherwood, R., Ahfeldt, T., Lapey, A., Wain, J., et al. (2012). Generation of Multipotent Lung and Airway Progenitors from Mouse ESCs and Patient-specific Cystic Fibrosis iPSCs. *Cell Stem Cell* 10, 385–397. doi:10.1016/j.stem.2012.01.018
- Nandi, M., Jackson, S. K., Macrae, D., Shankar-Hari, M., Tremoleda, J. L., and Lilley, E. (2020). Rethinking Animal Models of Sepsis - Working towards Improved Clinical Translation whilst Integrating the 3Rs. *Clin. Sci.* 134, 1715–1734. doi:10.1042/cs20200679
- Neal, J. T., and Kuo, C. J. (2016). Organoids as Models for Neoplastic Transformation. *Annu. Rev. Pathol.* 11, 199–220. doi:10.1146/annurev-pathol-012615-044249
- Ng-Blichfeldt, J. P., Schrik, A., Kortekaas, R. K., Noordhoek, J. A., Heijink, I. H., Hiemstra, P. S., et al. (2018). Retinoic Acid Signaling Balances Adult Distal Lung Epithelial Progenitor Cell Growth and Differentiation. *EBioMedicine* 36, 461–474. doi:10.1016/j.ebiom.2018.09.002
- Nikolic, M. Z., and Rawlins, E. L. (2017). Lung Organoids and Their Use to Study Cell-Cell Interaction. *Curr. Pathobiol. Rep.* 5, 223–231.
- Nossa, R., Costa, J., Cacopardo, L., and Ahluwalia, A. (2021). Breathing *In Vitro*: Designs and Applications of Engineered Lung Models. *J. Tissue Eng.* 12, 20417314211008696. doi:10.1177/20417314211008696
- Pan, H., Deutsch, G. H., Deutsch, G. H., Wert, S. E., and Consortium, N. M. A. o. L. D. P. (2019). Comprehensive Anatomic Ontologies for Lung Development: A Comparison of Alveolar Formation and Maturation within Mouse and Human Lung. *J. Biomed. Semant.* 10, 18. doi:10.1186/s13326-019-0209-1
- Pao, W., Miller, V. A., Politi, K. A., Riely, G. J., Somwar, R., Zakowski, M. F., et al. (2005). Acquired Resistance of Lung Adenocarcinomas to Gefitinib or Erlotinib Is Associated with a Second Mutation in the EGFR Kinase Domain. *PLoS Med.* 2, e73. doi:10.1371/journal.pmed.0020073
- Paolicelli, G., Luca, A. D., Jose, S. S., Antonini, M., Teloni, I., Fric, J., et al. (2019). Using Lung Organoids to Investigate Epithelial Barrier Complexity and IL-17 Signaling during Respiratory Infection. *Front. Immunol.* 10, 323. doi:10.3389/fimmu.2019.00323
- Park, I., Kim, M., Choe, K., Song, E., Seo, H., Hwang, Y., et al. (2019). Neutrophils Disturb Pulmonary Microcirculation in Sepsis-Induced Acute Lung Injury. *Eur. Respir. J.* 53. doi:10.1183/13993003.00786-2018
- Poling, H. M., Wu, D., Brown, N., Baker, M., Hausfeld, T. A., Huynh, N., et al. (2018). Mechanically Induced Development and Maturation of Human Intestinal Organoids *In Vivo*. *Nat. Biomed. Eng.* 2, 429–442. doi:10.1038/s41551-018-0243-9
- Pollard, C. A., Morran, M. P., and Nestor-Kalinoski, A. L. (2020). The COVID-19 Pandemic: a Global Health Crisis. *Physiol. genomics* 52, 549–557. doi:10.1152/physiolgenomics.00089.2020
- Porotto, M., Ferren, M., Chen, Y. W., Siu, Y., Makhosou, N., Rima, B., et al. (2019). Authentic Modeling of Human Respiratory Virus Infection in Human Pluripotent Stem Cell-Derived Lung Organoids. *mBio* 10. doi:10.1128/mBio.00723-19
- Pratilas, C. A., Hanrahan, A. J., Halilovic, E., Persaud, Y., Soh, J., Chitale, D., et al. (2008). Genetic Predictors of MEK Dependence in Non-small Cell Lung Cancer. *Cancer Res.* 68, 9375–9383. doi:10.1158/0008-5472.can-08-2223
- Quantius, J., Schmoldt, C., Vazquez-Armendariz, A. I., Becker, C., El Agha, E., Wilhelm, J., et al. (2016). Influenza Virus Infects Epithelial Stem/Progenitor Cells of the Distal Lung: Impact on Fgfr2b-Driven Epithelial Repair. *PLoS Pathog.* 12, e1005544. doi:10.1371/journal.ppat.1005544
- Rabata, A., Fedr, R., Soucek, K., Hampl, A., and Koledova, Z. (2020). 3D Cell Culture Models Demonstrate a Role for FGF and WNT Signaling in Regulation of Lung Epithelial Cell Fate and Morphogenesis. *Front. Cell Dev. Biol.* 8, 574. doi:10.3389/fcell.2020.00574
- Raghu, G., Chen, S.-Y., Yeh, W.-S., Maroni, B., Li, Q., Lee, Y.-C., et al. (2014). Idiopathic Pulmonary Fibrosis in US Medicare Beneficiaries Aged 65 Years and Older: Incidence, Prevalence, and Survival, 2001–11. *Lancet Respir. Med.* 2, 566–572. doi:10.1016/s2213-2600(14)70101-8
- Ramachandran, P., Matchett, K. P., Dobie, R., Wilson-Kanamori, J. R., and Henderson, N. C. (2020). Single-cell Technologies in Hepatology: New Insights into Liver Biology and Disease Pathogenesis. *Nat. Rev. Gastroenterol. Hepatol.* 17, 457–472. doi:10.1038/s41575-020-0304-x
- Ramamoorthy, P., Thomas, S. M., Kaushik, G., Subramaniam, D., Chastain, K. M., Dhar, A., et al. (2019). Metastatic Tumor-In-A-Dish, a Novel Multicellular Organoid to Study Lung Colonization and Predict Therapeutic Response. *Cancer Res.* 79, 1681–1695. doi:10.1158/0008-5472.can-18-2602
- Reyes, M., Filbin, M. R., Bhattacharyya, R. P., Billman, K., Eisenhaure, T., Hung, D. T., et al. (2020). An Immune-Cell Signature of Bacterial Sepsis. *Nat. Med.* 26, 333–340. doi:10.1038/s41591-020-0752-4
- Richeldi, L., du Bois, R. M., Raghu, G., Azuma, A., Brown, K. K., Costabel, U., et al. (2014). Efficacy and Safety of Nintedanib in Idiopathic Pulmonary Fibrosis. *N. Engl. J. Med.* 370, 2071–2082. doi:10.1056/nejmoa1402584
- Riemyndy, K. A., Jansing, N. L., Jiang, P., Redente, E. F., Gillen, A. E., Fu, R., et al. (2019). Single Cell RNA Sequencing Identifies TGFbeta as a Key Regenerative Cue Following LPS-Induced Lung Injury. *JCI Insight* 5. doi:10.1172/jci.insight.123637
- Rudd, K. E., Johnson, S. C., Agesa, K. M., Shackelford, K. A., Tsoi, D., Kievlan, D. R., et al. (2020). Global, Regional, and National Sepsis Incidence and Mortality, 1990–2017: Analysis for the Global Burden of Disease Study. *Lancet* 395, 200–211. doi:10.1016/s0140-6736(19)32989-7

- Sachs, N., Papaspyropoulos, A., Zomer-van Ommen, D. D., Heo, I., Bottinger, L., Klay, D., et al. (2019). Long-term Expanding Human Airway Organoids for Disease Modeling. *EMBO J.* 38. doi:10.15252/embj.2018100300
- Salahudeen, A. A., Choi, S. S., Rustagi, A., Zhu, J., van Unen, V., de la, O. S., et al. (2020). Progenitor Identification and SARS-CoV-2 Infection in Human Distal Lung Organoids. *Nature* 588, 670–675. doi:10.1038/s41586-020-3014-1
- Sato, T., Morita, M., Tanaka, R., Inoue, Y., Nomura, M., Sakamoto, Y., et al. (2017). *Ex Vivo* model of Non-small Cell Lung Cancer Using Mouse Lung Epithelial Cells. *Oncol. Lett.* 14, 6863–6868. doi:10.3892/ol.2017.7098
- Sato, T., Vries, R. G., Snippert, H. J., van de Wetering, M., Barker, N., Stange, D. E., et al. (2009). Single Lgr5 Stem Cells Build Crypt-Villus Structures *In Vitro* without a Mesenchymal Niche. *Nature* 459, 262–265. doi:10.1038/nature07935
- Schittny, J. C. (2017). Development of the Lung. *Cell Tissue Res.* 367, 427–444. doi:10.1007/s00441-016-2545-0
- Schutgens, F., and Clevers, H. (2020). Human Organoids: Tools for Understanding Biology and Treating Diseases. *Annu. Rev. Pathol.* 15, 211–234. doi:10.1146/annurev-pathmechdis-012419-032611
- Semaniakou, A., Croll, R. P., and Chappe, V. (2018). Animal Models in the Pathophysiology of Cystic Fibrosis. *Front. Pharmacol.* 9, 1475. doi:10.3389/fphar.2018.01475
- Seok, J., Warren, H. S., Cuenca, A. G., Mindrinos, M. N., Baker, H. V., Xu, W., et al. (2013). Host Response to Injury, Genomic Responses in Mouse Models Poorly Mimic Human Inflammatory Diseases. *Proc. Natl. Acad. Sci. U. S. A.* 110, 3507–3512. doi:10.1073/pnas.1222878110
- Sevransky, J. E., Martin, G. S., Shanholtz, C., Mendez-Tellez, P. A., Pronovost, P., Brower, R., et al. (2009). Mortality in Sepsis versus Non-sepsis Induced Acute Lung Injury. *Crit. Care* 13, R150. doi:10.1186/cc8048
- Sharma, A., Toepfer, C. N., Ward, T., Wasson, L., Agarwal, R., Conner, D. A., et al. (2018). CRISPR/Cas9-Mediated Fluorescent Tagging of Endogenous Proteins in Human Pluripotent Stem Cells. *Curr. Protoc. Hum. Genet.* 96, 21.11.1–21.11.20. doi:10.1002/cphg.52
- Shen, Y., Chen, L., Wang, M., Lin, D., Liang, Z., Song, P., et al. (2017). Flagellar Hooks and Hook Protein FlgE Participate in Host Microbe Interactions at Immunological Level. *Sci. Rep.* 7, 1433. doi:10.1038/s41598-017-01619-1
- Shi, R., Radulovich, N., Ng, C., Liu, N., Notsuda, H., Cabanero, M., et al. (2020). Organoid Cultures as Preclinical Models of Non-small Cell Lung Cancer. *Clin. Cancer Res.* 26, 1162–1174. doi:10.1158/1078-0432.ccr-19-1376
- Shmidt, E. N., and Nitkin, A. Y. (2004). Pathology of Mouse Models of Human Lung Cancer. *Comp. Med.* 54, 23–26.
- Singer, M., Deutschman, C. S., Seymour, C. W., Shankar-Hari, M., Annane, D., Bauer, M., et al. (2016). The Third International Consensus Definitions for Sepsis and Septic Shock (Sepsis-3). *JAMA* 315, 801–810. doi:10.1001/jama.2016.0287
- Snouwaert, J. N., Brigman, K. K., Latour, A. M., Malouf, N. N., Boucher, R. C., Smithies, O., et al. (1992). An Animal Model for Cystic Fibrosis Made by Gene Targeting. *Science* 257, 1083–1088. doi:10.1126/science.257.5073.1083
- Stahl, O., Löffler, B., Haier, J., Mardin, W. A., and Mees, S. T. (2013). Mimicry of Human Sepsis in a Rat Model—Prospects and Limitations. *J. Surg. Res.* 179, e167–75. doi:10.1016/j.jss.2012.01.042
- Strikoudis, A., Cieslak, A., Loffredo, L., Chen, Y. W., Patel, N., Saqi, A., et al. (2019). Modeling of Fibrotic Lung Disease Using 3D Organoids Derived from Human Pluripotent Stem Cells. *Cell Rep.* 27, 3709–3723. e5. doi:10.1016/j.celrep.2019.05.077
- Sucre, J. M., Wilkinson, D., Vijayaraj, P., Paul, M., Dunn, B., Alva-Ornelas, J. A., et al. (2016). A Three-Dimensional Human Model of the Fibroblast Activation that Accompanies Bronchopulmonary Dysplasia Identifies Notch-Mediated Pathophysiology. *Am. J. physiology. Lung Cell. Mol. physiology* 310, L889–L898. doi:10.1152/ajplung.00446.2015
- Suezawa, T., Kanagaki, S., Moriguchi, K., Masui, A., Nakao, K., Toyomoto, M., et al. (2021). Disease Modeling of Pulmonary Fibrosis Using Human Pluripotent Stem Cell-Derived Alveolar Organoids. *Stem Cell Rep.* 16, 2973–2987. doi:10.1016/j.stemcr.2021.10.015
- Sweeney, R. M., and McAuley, D. F. (2016). Acute Respiratory Distress Syndrome. *Lancet* 388, 2416–2430. doi:10.1016/s0140-6736(16)00578-x
- Takahashi, T., Nau, M. M., Chiba, I., Birrer, M. J., Rosenberg, R. K., Vinocour, M., et al. (1989). p53: a Frequent Target for Genetic Abnormalities in Lung Cancer. *Science* 246, 491–494. doi:10.1126/science.2554494
- Tamminga, M., Hiltermann, T. J. N., Schuurin, E., Timens, W., Fehrmann, R. S., and Groen, H. J. (2020). Immune Microenvironment Composition in Non-small Cell Lung Cancer and its Association with Survival. *Clin. Transl. Immunol.* 9, e1142. doi:10.1002/cti2.1142
- Tan, Q., Choi, K. M., Sicard, D., and Tschumperlin, D. J. (2017). Human Airway Organoid Engineering as a Step toward Lung Regeneration and Disease Modeling. *Biomaterials* 113, 118–132. doi:10.1016/j.biomaterials.2016.10.046
- Tanabe, N., McDonough, J. E., Vasilescu, D. M., Ikezoe, K., Verleden, S. E., Xu, F., et al. (2020). Pathology of Idiopathic Pulmonary Fibrosis Assessed by a Combination of Microcomputed Tomography, Histology, and Immunohistochemistry. *Am. J. pathology* 190, 2427–2435. doi:10.1016/j.ajpath.2020.09.001
- Tashiro, J., Rubio, G. A., Limper, A. H., Williams, K., Elliot, S. J., Ninou, I., et al. (2017). Exploring Animal Models that Resemble Idiopathic Pulmonary Fibrosis. *Front. Med.* 4, 118. doi:10.3389/fmed.2017.00118
- Tian, L., Gao, J., Garcia, I. M., Chen, H. J., Castaldi, A., and Chen, Y. W. (2021). Human Pluripotent Stem Cell-Derived Lung Organoids: Potential Applications in Development and Disease Modeling. *Wiley Interdiscip. Rev. Dev. Biol.* 10, e399. doi:10.1002/wdev.399
- Tindle, C., Fuller, M., Fonseca, A., Taheri, S., Ibeawuchi, S. R., Beutler, N., et al. (2021). Adult Stem Cell-Derived Complete Lung Organoid Models Emulate Lung Disease in COVID-19. *Elife* 10. doi:10.7554/eLife.66417
- van den Berg, C. W., Ritsma, L., Avramut, M. C., Wiersma, L. E., van den Berg, B. M., Leuning, D. G., et al. (2018). Renal Subcapsular Transplantation of PSC-Derived Kidney Organoids Induces Neo-Vasculogenesis and Significant Glomerular and Tubular Maturation *In Vivo*. *Stem Cell Rep.* 10, 751–765. doi:10.1016/j.stemcr.2018.01.041
- van der Sanden, S. M. G., Sachs, N., Koekkoek, S. M., Koen, G., Pajkrt, D., Clevers, H., et al. (2018). Enterovirus 71 Infection of Human Airway Organoids Reveals VP1-145 as a Viral Infectivity Determinant. *Emerg. microbes Infect.* 7, 84. doi:10.1038/s41426-018-0077-2
- van Geffen, C., Deissler, A., Quante, M., Renz, H., Hartl, D., and Kolahian, S. (2021). Regulatory Immune Cells in Idiopathic Pulmonary Fibrosis: Friends or Foes? *Front. Immunol.* 12, 663203. doi:10.3389/fimmu.2021.663203
- Varghese, B., Ling, Z., and Ren, X. (2022). Reconstructing the Pulmonary Niche with Stem Cells: a Lung Story. *Stem Cell Res. Ther.* 13, 161. doi:10.1186/s13287-022-02830-2
- Vlachogiannis, G., Hedayat, S., Vatsiou, A., Jamin, Y., Fernandez-Mateos, J., Khan, K., et al. (2018). Patient-derived Organoids Model Treatment Response of Metastatic Gastrointestinal Cancers. *Science* 359, 920–926. doi:10.1126/science.aao2774
- Walters, D. M., and Kleeberger, S. R. (2008). Mouse Models of Bleomycin-Induced Pulmonary Fibrosis. *Curr. Protoc. Pharmacol.* Chapter 5, Unit 5.46. doi:10.1002/0471141755.ph0546s40
- Wang, H. M., Bodenstein, M., and Markstaller, K. (2008). Overview of the Pathology of Three Widely Used Animal Models of Acute Lung Injury. *Eur. Surg. Res.* 40, 305–316. doi:10.1159/000121471
- Wang, J. E., Dahle, M. K., Yndestad, A., Bauer, I., McDonald, M. C., Aukrust, P., et al. (2004). Peptidoglycan of *Staphylococcus aureus* Causes Inflammation and Organ Injury in the Rat. *Crit. Care Med.* 32, 546–552. doi:10.1097/01.ccm.0000109775.22138.8f
- Wang, J., Li, X., and Chen, H. (2020). Organoid Models in Lung Regeneration and Cancer. *Cancer Lett.* 475, 129–135. doi:10.1016/j.canlet.2020.01.030
- Wang, L., Liu, H., Jiao, Y., Wang, E., Clark, S., Postlethwaite, A., et al. (2015). Differences between Mice and Humans in Regulation and the Molecular Network of Collagen, Type III, Alpha-1 at the Gene Expression Level: Obstacles that Translational Research Must Overcome. *Int. J. Mol. Sci.* 16, 15031–15056. doi:10.3390/ijms160715031
- Wang, R., McCauley, K. B., Kotton, D. N., and Hawkins, F. (2020). Differentiation of Human Airway-Organoids from Induced Pluripotent Stem Cells (iPSCs). *Methods Cell Biol.* 159, 95–114. doi:10.1016/bs.mcb.2020.03.008
- Wilkinson, D. C., Alva-Ornelas, J. A., Sucre, J. M., Vijayaraj, P., Durra, A., Richardson, W., et al. (2017). Development of a Three-Dimensional Bioengineering Technology to Generate Lung Tissue for Personalized Disease Modeling. *Stem cells Transl. Med.* 6, 622–633. doi:10.5966/sctm.2016-0192

- Williams, K., and Roman, J. (2016). Studying Human Respiratory Disease in Animals - Role of Induced and Naturally Occurring Models. *J. Pathol.* 238, 220–232. doi:10.1002/path.4658
- Wong, A. P., Bear, C. E., Chin, S., Pasceri, P., Thompson, T. O., Huan, L. J., et al. (2012). Directed Differentiation of Human Pluripotent Stem Cells into Mature Airway Epithelia Expressing Functional CFTR Protein. *Nat. Biotechnol.* 30, 876–882. doi:10.1038/nbt.2328
- Xu, G., Li, Y., Zhang, S., Peng, H., Wang, Y., Li, D., et al. (2021). SARS-CoV-2 Promotes RIPK1 Activation to Facilitate Viral Propagation. *Cell Res.* 31, 1230–1243. doi:10.1038/s41422-021-00578-7
- Xu, Z., Gao, Y., Hao, Y., Li, E., Wang, Y., Zhang, J., et al. (2013). Application of a Microfluidic Chip-Based 3D Co-culture to Test Drug Sensitivity for Individualized Treatment of Lung Cancer. *Biomaterials* 34, 4109–4117. doi:10.1016/j.biomaterials.2013.02.045
- Yoshida, G. J. (2020). Applications of Patient-Derived Tumor Xenograft Models and Tumor Organoids. *J. Hematol. Oncol.* 13, 4. doi:10.1186/s13045-019-0829-z
- Zhu, F., Zuo, L., Hu, R., Wang, J., Yang, Z., Qi, X., et al. (2021). Effect of Immune Cell Infiltration on Occurrence of Pulmonary Hypertension in Pulmonary Fibrosis Patients Based on Gene Expression Profiles. *Front. Med.* 8, 671617. doi:10.3389/fmed.2021.671617
- Zscheppang, K., Berg, J., Hedtrich, S., Verheyen, L., Wagner, D. E., Suttorp, N., et al. (2018). Human Pulmonary 3D Models for Translational Research. *Biotechnol. J.* 13. doi:10.1002/biot.201700341

Conflict of Interest: The authors declare that the research was conducted in the absence of any commercial or financial relationships that could be construed as a potential conflict of interest.

Publisher's Note: All claims expressed in this article are solely those of the authors and do not necessarily represent those of their affiliated organizations, or those of the publisher, the editors and the reviewers. Any product that may be evaluated in this article, or claim that may be made by its manufacturer, is not guaranteed or endorsed by the publisher.

Copyright © 2022 Bosáková, De Zuani, Sládková, Garlíková, Jose, Zelante, Hortová Kohoutková and Frič. This is an open-access article distributed under the terms of the Creative Commons Attribution License (CC BY). The use, distribution or reproduction in other forums is permitted, provided the original author(s) and the copyright owner(s) are credited and that the original publication in this journal is cited, in accordance with accepted academic practice. No use, distribution or reproduction is permitted which does not comply with these terms.



OPEN ACCESS

EDITED BY

Kusum K. Kharbanda,
University of Nebraska Medical Center,
United States

REVIEWED BY

Johnson V. John,
Terasaki Institute for Biomedical
Innovation, United States
Jingwei Xie,
University of Nebraska Medical Center,
United States

*CORRESPONDENCE

Chunjie Wu,
wucjcdutcm@163.com
Linjiang Song,
songlinjiang@cdutcm.edu.cn

SPECIALTY SECTION

This article was submitted to
Gastrointestinal Sciences,
a section of the journal
Frontiers in Physiology

RECEIVED 31 May 2022

ACCEPTED 30 June 2022

PUBLISHED 18 July 2022

CITATION

Liu Q, Zeng A, Liu Z, Wu C and Song L
(2022), Liver organoids: From
fabrication to application in
liver diseases.
Front. Physiol. 13:956244.
doi: 10.3389/fphys.2022.956244

COPYRIGHT

© 2022 Liu, Zeng, Liu, Wu and Song. This
is an open-access article distributed
under the terms of the [Creative
Commons Attribution License \(CC BY\)](#).
The use, distribution or reproduction in
other forums is permitted, provided the
original author(s) and the copyright
owner(s) are credited and that the
original publication in this journal is
cited, in accordance with accepted
academic practice. No use, distribution
or reproduction is permitted which does
not comply with these terms.

Liver organoids: From fabrication to application in liver diseases

Qianglin Liu¹, Anqi Zeng², Zibo Liu³, Chunjie Wu^{3*} and
Linjiang Song^{1*}

¹School of Medical and Life Sciences, Chengdu University of Traditional Chinese Medicine, Chengdu, China, ²Institute of Translational Pharmacology and Clinical Application, Sichuan Academy of Chinese Medical Science, Chengdu, China, ³School of Pharmacy, Chengdu University of Traditional Chinese Medicine, Chengdu, China

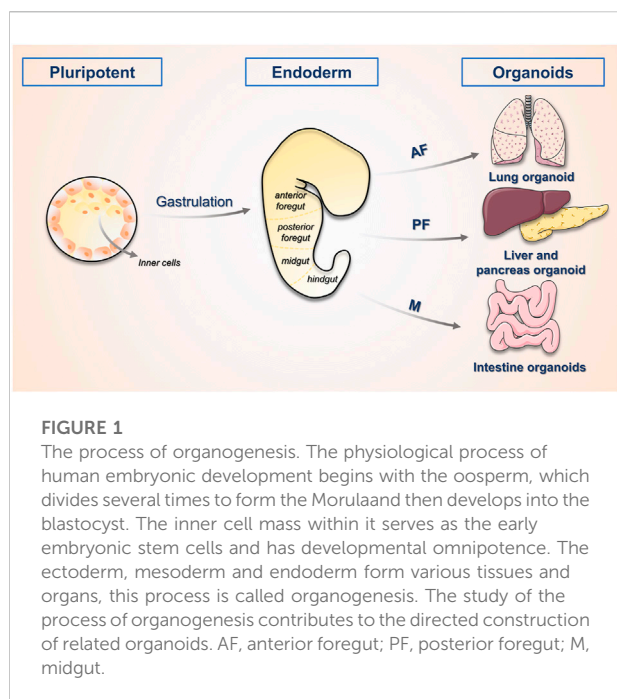
As the largest internal organ, the liver is the key hub for many physiological processes. Previous research on the liver has been mainly conducted on animal models and cell lines, in which not only there are deficiencies in species variability and retention of heritable material, but it is also difficult for primary hepatocytes to maintain their metabolic functions after *in vitro* expansion. Because of the increased burden of liver disease worldwide, there is a growing demand for 3D *in vitro* liver models—Liver Organoids. Based on the type of initiation cells, the liver organoid can be classified as PSC-derived or ASC-derived. Liver organoids originated from ASC or primary sclerosing cholangitis, which are co-cultured in matrix gel with components such as stromal cells or immune cells, and eventually form three-dimensional structures in the presence of cytokines. Liver organoids have already made progress in drug screening, individual medicine and disease modeling with hereditary liver diseases, alcoholic or non-alcoholic liver diseases and primary liver cancer. In this review, we summarize the generation process of liver organoids and the current clinical applications, including disease modeling, drug screening and individual medical treatment, which provide new perspectives for liver physiology and disease research.

KEYWORDS

liver organoid, 3D culture, co-culture, disease modelling, drug screen

1 Introduction

As the largest internal organ, the liver is the key hub for many physiological processes. It not only participates in the metabolism of major nutrients, but also has diverse roles in the regulation of the immune system and the decomposition of heterogeneous biological compounds (Trefts et al., 2017), including many drugs, and other functions. Therefore, liver disease has an enormous impact on human health. Liver disease causes approximately two million deaths worldwide each year (Asrani et al., 2019), and epidemiological studies have shown that the burden of liver disease varies among people of different ethnicities, genders, geographic regions, financial positions and social ladders. In addition, certain liver diseases also show genetic correlations. With the aging of the global population, the prevalence of obesity, diabetes and other diseases is gradually increasing, which also increases the incidence rates of non-alcoholic steatohepatitis and chronic liver disease (Estes et al., 2018).



The development of the liver is first initiated by the inner cell mass, which progressively develops into an embryo. As illustrated in [Figure 1](#), the posterior foregut of the endoderm develops into the liver as the triple germ layer forms. The liver is formed by the growth of the ventral foregut epithelium, which is first to develop into the hepatic bud structure. The hepatic buds generate hepatocytes and the cholestatic epithelium, while the adjacent mesenchymal stroma of mesodermal origin constitutes hepatic fibroblasts and stellate cells ([Lancaster and Knoblich, 2014](#)). The growth of the liver also involves the establishment of innervation, extensive vascularization and interactions between various types of cells, and it eventually develops into an organ with complex architecture and function. In an *in vitro* model, bile duct cells and hepatocytes complete cyclic renewal every 60 and 150 days, respectively ([Magami et al., 2002](#)). Although this is slower than the turnover rate of other organs of endothelial origin, the liver demonstrates a remarkable ability to regenerate after suffering injury.

To define the pathological changes of these diseases and discover the potential treatment approaches, researchers require an array of approaches to understand the development of liver structure and function, the pathogenesis of liver diseases, and the responses to related treatments. During the past few decades, most *in vitro* studies of chronic liver diseases have used two-dimensional (2D) cultured cell lines. Cell lines from benign or malignant tumours of the liver and primary human hepatocytes (PHHs) are the main sources for these *in vitro* studies because cancer-derived hepatocyte lines lack their normal liver cell counterparts, despite their ability to proliferate indefinitely. Most importantly, they lack most of the cell types that differentiate into primary tissues ([Schutgens and Clevers, 2020](#)). Although PHHs retain many of the characteristics of normal

hepatocytes, their viability in culture is limited to a few days, so there is a constant need for fresh donor tissues, which are often difficult to obtain. In addition, their initial establishment involves not only extensive genetic but also phenotypic adaptation to culture conditions ([Nuciforo and Heim, 2021](#)). Two-dimensional cultured cell models, such as PHHs and induced pluripotent stem cells (iPSCs) also lose the polarity that hepatocytes exhibit *in vivo* because they are forced to adopt a flat morphology *in vitro* ([Shulman and Nahmias, 2013](#)).

By contrast, the *in vivo* models for studying the pathogenesis of liver-related diseases are mainly animal models ([Aqeilan, 2020](#)), which facilitates a greater and more sophisticated dimension of understanding. While animal models used to study liver disease mechanisms and targeted therapeutics share key biological and histological features with the liver in humans ([Prior et al., 2019](#)), the intrinsic differences between animal models and humans cannot be easily resolved, especially in replicating the key aspects of the complex structure and metabolic functions of the liver in humans, which has severely affected several potentially effective therapeutic agents in clinical trials. In addition, most of the animal models used in preclinical studies are based on inbred lines with genetic homogeneity that lack the heterogeneous genetic diversity of humans.

Organoids are established over long periods of time and maintain genetic sustainability, thereby achieving more complex structures similar to those of the mammalian body, and they have been applied to rodents ([Kuijk et al., 2016](#)), canines ([Nantasanti et al., 2015](#); [Gabriel et al., 2022](#)), cats ([Kruitwagen et al., 2017](#)) and humans. In addition, while both *in vitro* models and organoids are capable of providing causal evidence of pharmacological and genetic targeting, the assay throughput of organoids is well beyond the maximum capacity of mouse models ([Takebe et al., 2017](#)). For the past few years, researchers have introduced transcriptomics, proteomics and metabolomics into studies of organoid cultures, promoting new discoveries and complementary investigations in 2D cultures and animal models. We summarize the advantages and disadvantages of different *in vitro* models in [Table 1](#). In recent years, much progress has been made in establishing several different organoid culture protocols to simulate the human liver and model liver-related diseases. In addition, organoids have potential for drug testing and even organ replacement. Here, we describe the principal derivation procedures, as well as the classification of liver organoids, and discuss their present and emerging applications in disease modeling, drug screening, and regenerative medicine. Finally, we highlight some of the challenges that remain in the field.

2 Overview of the liver and organoids

2.1 Origin of liver organoids

In 1981, Evans and others established pluripotent stem cells from mouse embryos ([Lancaster and Knoblich, 2014](#)) and in

TABLE 1 Comparison of different hepatic *in vitro* model systems.

Classifications	Sources	Advantages	Disadvantages	Reference
Animals	rodents, canines, cats, etc.	Experimental materials are relatively easy to obtain	Differences in structure and physiological state exist; lack the heterogeneous genetic diversity of humans	Broutier, et al. (2016) Kruitwagen, et al. (2017) Kuijk, et al. (2016) Magami, et al. (2002) Nantasanti, et al. (2015)
PHH	Liver tissue	Less experimental investment; Retaining genetic background; proliferate indefinitely	Lack of complexity of morphology; lose the polarity that hepatocytes exhibit <i>in vivo</i>	Huch, et al. (2013) Kang, et al. (2016) Nuciforo and Heim (2021)
iPSCs	Fibroblasts and others	Retaining genetic background High throughput screening	Lack of complexity of morphology More experimental expenses	Asai, et al. (2017) Coll, et al. (2018) Ohnuki and Takahashi (2015) Sampaziotis, et al. (2015) Schutgens and Clevers, (2020) Takebe, et al. (2013) Takebe, et al. (2017) Wang, et al. (2016)
Organoids	Adult liver, foetal liver, and pluripotent stem cells	Possesses a complex three-dimensional structure Preservation of gene stability and ability to perform genetic manipulation	Difficulty of the experiment process More time and materials spent on the experiment	Bao, et al. (2021) Broutier, et al. (2017) Clevers, (2016) Drost and Clevers (2018) Lancaster and Knoblich, (2014) Leite, et al. (2016) Mccauley and Wells, (2017)

PHH, Primary human hepatocytes; iPSCs, induced pluripotent stem cells.

1988, the first human embryonic stem cell line was isolated and cultured from human blastocysts by Thomson et al. (1998). In 1987, Bissell and colleagues reported that extracellular matrix (ECM) extracts play an important role in epithelial organization into 3D ducts and conduits in a mammary model (Li et al., 1987). However, it was not until 2009 that Clevers and colleagues generated intestinal organoids from adult intestinal stem cells by 3D culture of stromal gels (Sato et al., 2009), which is believed to be the first organoid ever established *in vitro*.

The definition of an organoid is the collection of organ-specific cell types that develop from stem cells or organ progenitors and self-organize through cell sorting and spatially-restricted lineage commitment in a manner similar to that *in vivo* (Lancaster and Knoblich, 2014). Self-organisation, the basis for organoid establishment, is achieved through direct cell-cell interactions (Asai et al., 2017). The general ability of cells to separate and reorganise through the process known as “cell sorting” forms generations with histogenic characteristics that

are identical to those *in vivo*. Self-organisation depends not only on the classification of cells, but also on the correct execution of genealogical decisions for progenitor cells, which includes the appropriate direction of stem cell division, the correlation of synchronous and non-synchronous divisions, and the migration of differentiated daughter cells to particular locations within a specific tissue (Lancaster and Knoblich, 2014).

2.2 Derivation methods for liver organoids

Organoids are based on the ability of cells to self-organise, which is influenced by the physical characteristics of the culture environment, the requirement for endogenous and/or exogenous signals and the starting cell type and system conditions (Rossi et al., 2018). Different parameter selections of these characteristics can ultimately affect the features and the extent of applicability of the organoid as a biological prototype system.

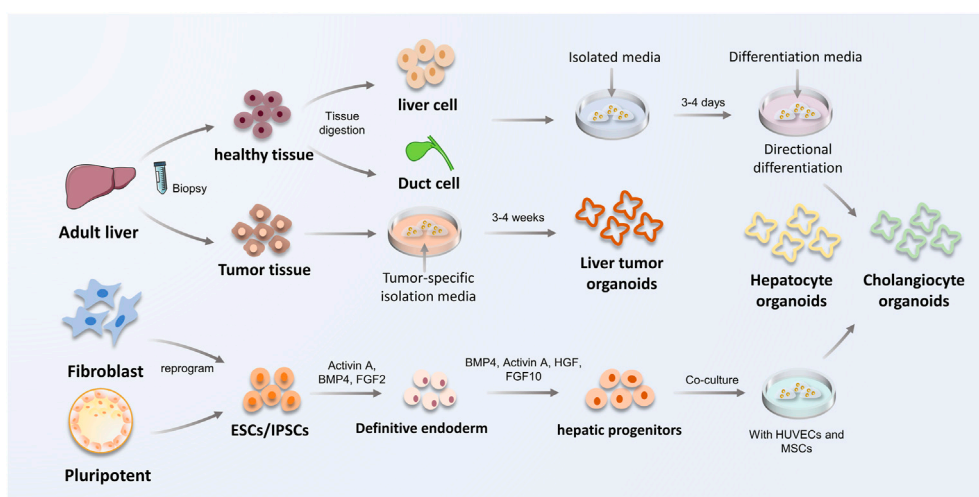


FIGURE 2

The construction procedure of ASC and PSC-derived liver organoids. The process of constructing liver organoids is divided into ASC and PSC origin. ASC are mainly derived from biopsy of adult tissues to obtain healthy or tumor tissues. Hepatocytes or bile duct tissues obtained from biopsies were inoculated in isolation medium, and subsequently hepatocyte organoids and cholangiocyte organoids were constructed using defined differentiation media. PSCs can be obtained by reprogramming fibroblasts *in vivo*, in addition to inner cell mass, which are capable to form hepatic progenitor cells by co-culture and special signal-mediated differentiation towards endoderm, and eventually obtain hepatocyte organoids and cholangiocyte organoids. HUVECs, vein endothelial cells; MSCs, mesenchymal stem cells.

Until now, several approaches for the generation of liver organoids have been published. The current mainstream approaches for the generation of liver organoids involve a PSC-derived approach, including transdifferentiation (Sun et al., 2019), and an ASC-derived approach. The different approaches for the generation of liver organoids and their characteristics are described in further detail below.

3 Classification of liver organoids

Depending on the type of starting cell, organoids can be classified as PSC-derived or ASC-derived. Because each cell type originates at a different developmental stage, the maturity level of the organoid that can be derived from each type of starting cell is variable. The process of PSC- and ASC-derived organoid establishment is presented in Figure 2.

3.1 Pluripotent stem cells-derived organoids

Pluripotent stem cells (PSCs) are a type of cell that can self-renew and differentiate into specialized cell types that comprise one of the three germ layers *in vivo* (Liu et al., 2020). Thus, PSCs, which contain embryonic stem cells (ESCs) and induced pluripotent stem cells (IPSCs), are primarily used to study organogenesis and progression events that result in tissue

generation (Schutgens and Clevers, 2020). PSCs are induced into hepatic endodermal cells by the action of activin A and then complete differentiation in response to developmental signaling pathways from FGF and BMP (Clevers, 2016).

IPSC generated by reprogramming of skin fibroblasts (Sun et al., 2019) can differentiate into all cell types in the body and precisely differentiate into different cell and tissue types under the control of induction signals (Asai et al., 2017; McCauley and Wells, 2017). In addition, co-cultured with stromal cells, human umbilical vein endothelial cells (HUVECs) and human mesenchymal stem cells (MSCs), all of which have stem cell potential, can help liver endodermal cells from human IPSCs (IPSC-HEs) recapitulate early organogenesis (Takebe et al., 2013; Rossi et al., 2018).

To address the lack of homologous substrate components, Ouchi et al. (2019) generated a foregut model by recapitulating early organogenic differentiation. The authors embedded foregut globules in a stromal gel, followed by co-culture with retinoic acid (RA) to directionally differentiate PSCs into foregut-derived organoids, thereby generating more complete organoids containing both epithelial components and mesenchymal cells which can differentiate into supporting lineages. Recently, in response to the disadvantage that PSC-derived organoids exhibit only immature fetal characteristics, Mun et al. (2021) used microbial short-chain fatty acids (SCFAs) to simulate changes in the microenvironment of the liver during postnatal development. This approach could increase albumin secretion and P450 activity, as well as the expression of hepatocyte genes

(Aloia et al., 2019), which improved the metabolic ripening of iPSC-derived liver organoids.

3.2 Adult stem cells-derived organoids

Adult stem cells (ASCs) are undifferentiated lineage-committed cells. Terminally differentiated cholangiocytes or hepatocytes can also become activated by appropriate liver injury, which causes them to restart the cell cycle and induce liver regenerative repair by forming ASCs (Liu et al., 2020). However, other ASCs, such as hematopoietic stem cells, do not have this characteristic. Compared to PSC-derived organoids, ASCs can only differentiate into components associated with the organ or tissue from which they are derived. However, ASC-derived organoids are more stable at chromosomal and structural levels, while having a lower incidence of single base changes (Huch et al., 2015). This is due to the presence of inherited and epigenetic abnormalities in iPSC-derived organoids during iPSC reprogramming and organ differentiation, which occur infrequently in ASC-derived organoids (Ohnuki and Takahashi, 2015).

ASCs are located in a very specific microenvironment, namely, the stem cell niche, which ensures that the cells are able to renew themselves. Stem cell niches are functional domains within stem cell populations capable of controlling the dynamics of tissue homeostasis under different conditions (Vining and Mooney, 2017), and they communicate with stem cells through mechanical signals that regulate cell fate and steer their developmental processes with a high degree of plasticity (Voog and Jones, 2010). ASCs are usually obtained from isolated cells or dissected tissue fragments of normal or tumour tissues (Schutgens and Clevers, 2020). The cells of tissue origin used to establish liver organoids, including hepatocytes and duct cells, usually have a slow turnover rate but can exhibit a remarkable capacity for tissue self-renewal and damage restoration after liver injury (Aloia et al., 2019). ASC-derived liver organoids of hepatocyte origin are perhaps slightly superior to those of bile duct origin in terms of maturity and physiological relevance. However, there is still no alternative to cholangiocyte-based liver organoids, for example, to study the function and pathology of the bile duct. Meanwhile, bile duct-derived liver organoids are inoculated more efficiently than hepatocyte-derived liver organoids, with EpCAM + hepatic duct cell-derived organoids having a higher efficiency than hepatocyte-derived organoids, even in the presence of TNF- α (Peng et al., 2018). ASCs obtained from biopsy specimens, such as tumour tissues, allow the generation of patient-derived organoids (PDOs). Liver organoids derived from healthy tissues initially form a monolayer of epithelial structures, which transdifferentiate into pseudo-lamellar epithelial cells (Broutier et al., 2017), while tumouroids can directly recapitulate the features of the various tumour subtypes.

Furthermore, they retain histologic, genetic and transcriptomic features to mirror the original tumour tissue (Li et al., 2019).

Following chronic liver injury, oval cells, a population of bipotent progenitor cells derived from biliary epithelial cells (BECs) in the Hering duct that emanates from the biliary tree, trigger regeneration by restoring both hepatocytes and cholangiocytes, suggesting that they are an alternative source for new cell therapies. Following acute liver injury, such as partial hepatectomy (PHx), total liver chemical-induced damage or infection (Broutier et al., 2016), mature hepatocytes respond by proliferating. Interestingly, no significant dedifferentiation to a progenitor state was observed during this process (Nuciforo and Heim, 2021). Based on the reparative mechanism of acute liver injury, mature hepatocyte-derived liver organoids can be generated directly, cultured and expanded *in vitro* for long periods of time (Hu et al., 2018).

The Wnt signaling pathway is comprised of extracellular development-related proteins, and this pathway is responsible for initiating sustained tissue renewal by promoting stem cell activity; otherwise, tissue renewal is impaired (Clevers et al., 2014). Lgr5, which is one of the target genes of Wnt, is a commonly used stem cell marker (Clevers, 2016). When CCl₄ was used to induce liver injury, the damaged tissue showed increased expression of Axin2-LacZ16 compared to healthy tissue. Furthermore, Lgr5⁺ cells not only express multiple Wnt target genes but also have features of bi-potent liver progenitors, which allows them to achieve *in vitro* expansion (Huch et al., 2013).

4 Characteristics of the culture environment

Organoid differentiation of PSCs consists of several stages. First, the differentiation of iPSCs to the definitive endoderm is followed by the directed derivation to foregut progenitors, which is a crucial step, and finally in the presence of BMP and RPMI, among other factors, to hepatoblasts (Sampaziotis et al., 2015). Subsequently, hepatic progenitors with bidirectional differentiation potential can differentiate into hepatocytes or bile duct cells in different settings, a process that usually requires co-culture with mesoderm-derived stromal components embedded in ECM, which promotes three-dimensional (3D) growth and organoid formation.

4.1 Co-culture

As most liver organoids are typical of cystic organoids, containing only epithelial cell types, co-culture is needed to generate organoids. As displayed in Figure 3, co-culture methods are essential to study the interaction of organ tissues with immune cells, stromal cells, and fibroblasts, as well as to

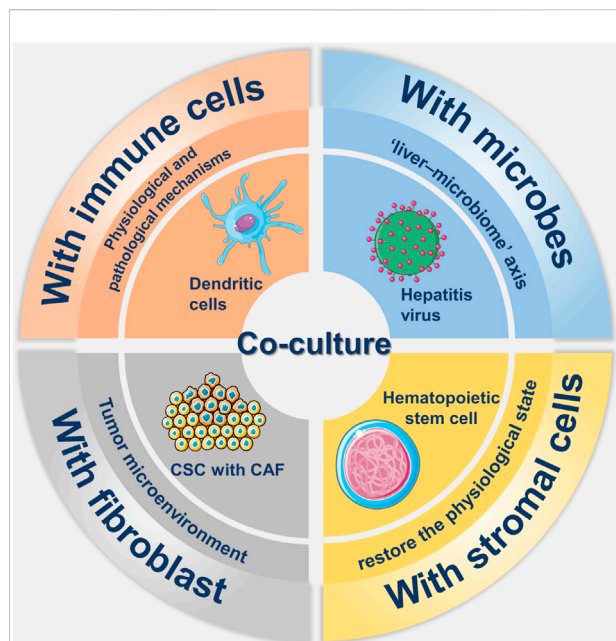


FIGURE 3

Overview about co-culture of liver organoids. There have been many researches in the field in co-culture of liver organoid, which mainly includes co-culture with immune cells, stromal cells, fibroblasts and microorganisms. The involvement of immune cells such as dendritic cells and stromal cells such as hematopoietic stem cells in co-culture helps to simulate the real environment *in vivo*. Co-culture with hepatitis virus not only reflects the role of the liver-microbe axis, but also allows for participation in disease modeling. Co-culture with cancer-associated fibroblast (CAF) in tumor modeling not only mimics the tumor microenvironment but also promotes the growth of cancer stem cells (CSCs).

achieve the optimal reproduction of the actual environment *in vivo*.

4.2.1 Organoids and immune cells

The co-culture of liver organoids with immune cells facilitates the exploration of the physiological state of the liver and the mechanisms of disease, in addition to promoting the investigation of the dynamic interactions between expanding tumours and immune systems (Bresnahan et al., 2020).

There are three types of systems in which organoids are co-cultured with immune cells (Bar-Ephraim et al., 2019). In the first system, immune-related cytokines are added to organoid media. In the second system, organoids are dissociated into single-cell suspensions and co-cultured with immune cells for a defined period of time before establishing organoids. In the third system, activated immune cells are co-cultured with organoids. However, of these three approaches, the first simply adds cytokines and lacks the relevant immune cell component, while the second is a co-culture of immune cells with organoids that have been digested into single cells, which does not prove that a co-

culture system was established after digestion. By contrast, the third approach constitutes a putative co-culture system of immune cells. In addition, Yuki et al. (2020) described a method for establishing tumour-derived organoids, while preserving immune, stromal and mesenchymal cells from the same tumour specimen. The authors named this system “a native model,” which provides a holistic approach to the study of the tumour microenvironment and allows better simulation of tumour metastasis.

4.2.2 Organoids and microbes

Many liver diseases, such as primary sclerosing cholangitis (PSC) and hepatic encephalopathy (HE) due to cirrhosis, have been reported to associate with microbial characteristics. For example, microbes play an essential role in liver inflammation, with the liver impacting and communicating with microbes through mediators such as bile acids or inflammatory signals. This connection is known as the liver-microbiome axis (Adolph et al., 2018). Therefore, the co-culture of organoids and microbial organisms can be used to study infectious or non-infectious liver inflammation.

The co-culture of organoids with viruses, which can mimic virus infection, has potential for infectious disease models. For example, Nie et al. (2018) generated an *in vitro* infection model with hepatitis B virus (HBV) after co-culture of PSCs with stromal cells on 3D microtiter plates, which developed into vascularised and functional tissue after transplantation. The significant release of viruses from infected iPSC-derived organoids in this assay and the high expression of the infection-promoting factors GPC5, PPARA and CEBPA in iPSC-derived liver organoids demonstrated the stability of this differentiated infection model.

During the COVID-19 epidemic, organoids were similarly applied to related research areas. Researchers reported that liver organoids were highly sensitive to SARS-CoV-2 infection and showed high expression of chemokines following infection, which is consistent with findings in lung specimens from human COVID-19 autopsies (Yang et al., 2020). In addition, co-culture of patient-derived organoids with microbes provides new insights on the roles played by microbes in the disease process (McCarron et al., 2021). Liver organoids, as an emerging *in vitro* model, provide an effective way to investigate the human tissue response to SARS-CoV-2 infection.

4.2.3 Organoids and fibroblasts

The co-culture of organoids and fibroblasts has been widely used in tumour patient-derived organoids. Cancer associated fibroblasts (CAF), which are derived from tissue-residual fibroblasts, endothelial cells and vascular smooth muscle cells, play an essential role in the establishment of the tumour microenvironment (Yamamura et al., 2015). CAFs can mold stem cell niches to maintain and facilitate the growth of cancer stem cells (CSCs) through direct contact with tumour cells or a

paracrine pathway (Liu et al., 2021). The co-culture of CAFs with liver tumour-derived organoids promoted the growth of organoids, and the results showed that the effect of CAFs was achieved by expanding the volume of organoids instead of the number, although the effectiveness on organoid initiation was not confirmed.

In addition to the growth promoting effects on CSCs and liver tumour-derived organoids, CAFs can induce tumour drug resistance (Xiong et al., 2018). CAFs cause tumour drug resistance by affecting the tumour-specific microenvironment, including increasing tumour mesenchymal pressure and inducing vascular collapse. CAFs can also alter the immune response through ECM remodeling, thereby preventing the regulation of tumour tissue by immune cells (Liu et al., 2021). In addition to co-culture with organoids, co-transplantation of CAFs with organoids can result in more efficient tumour formation.

4.2.4 Organoids and stromal cells

Hepatocytes and bile duct cells in the liver differentiate from the epithelium of the ventral foregut in the endoderm and the mesenchyme transforms from the mesoderm, so that hepatic progression represents a complex interplay between tissues of endodermal and mesodermal origins. To achieve this physiological state as much as possible, Takebe et al. (2013) generated functional vascularized liver buds by co-culture of iPSCs with stromal cell populations such as human umbilical vein endothelial cells (HUVECs) and human mesenchymal stem cells (MSCs). In addition to direct hepatocyte-stromal cell interactions, the stromal cell population also activates FGF and BMP through a paracrine pathway, which is necessary for the generation of 3D liver buds *in vitro*. However, due to the heterogeneity of iPSCs, common culture protocols do not guarantee that the cells used for organoid generation have the same characteristics, even if they come from the same cohort. To demonstrate the difference between the TGF β 1-induced artificial liver fibrosis model and the liver fibrosis caused by the natural development of NAFLD, Ali et al. established HepaRG-based bioengineered multicellular liver microtissues (BE-MLMs). HepaRG (cell line), HUVECs (human primary), KCs (human primary), and HSCs (human primary) were co-cultured in spheroid-laden hydrogels at different ratios while simulating liver tissue native configuration, such as nutrients/O₂ gradients and direct cell-cell contacts between different cell types inside spheroids (Bao et al., 2021). Organoid of the HepaRG-based BE-MLMs is more complex and further describes the structural and metabolic environment of the liver. A new method for the co-culture of vascular endothelial cells and organoids was recently described by Pettinato and others. The authors reported that suppression of the Sonic hedgehog and Notch signalling pathways at an initial phase of differentiation significantly increased the expression of key proteins and the activity of enzymes (Pettinato et al., 2021).

Overall, co-cultures play an irreplaceable role in the construction of organoids, bridging the cellular and structural deficiencies of single germ layer-derived organoids in immune, neural and vascular aspects. In terms of disease modeling, co-cultured organoids can personalize the simulation of the patient's *in vivo* environment and construct more effective disease models. However, there are differences between HUVEC and mature hepatic sinusoidal endothelial cells, which may lead to differences in subsequent applications for disease modeling. In addition, the current co-culture of TME components other than immune cells and fibroblasts with organoids still needs to be improved to further enhance the effectiveness of organoids.

4.2 Culture environment of liver organoids

4.2.1 Matrigel method

The two-dimensional (2D) culture of hepatocytes primarily consists of monolayers on collagen gels and cultures covered with matrix or collagen gels, which are defined as “sandwich cultures” (Peng et al., 2021), but hepatocytes cultured in this way rapidly exhibit defects in their morphology. In organoid cultures, hepatocytes are mainly co-cultured with mesenchymal cells and supported by the matrix gel, which induces the aggregation into 3D spheroids. Table 2 compares and summarizes the characteristics of biomaterials from matrigel sources and non-matrigel sources.

Matrigel is an extract from Engelbreth-Holm Swarm mouse sarcoma with components similar to those of a true basement membrane that can form a hydrogel at temperatures of 30°C and above (Benton et al., 2014; Aisenbrey and Murphy, 2020), and the effectiveness of matrix gel-based cultures for organoid generation has been widely demonstrated (Guan et al., 2017; Giobbe et al., 2019). However, the generation of Matrigel-based liver organoids suffers from a lack of cell function and maturation. Furthermore, the complex and uncertain composition of Matrigel makes it difficult to precisely demonstrate its role in organoid generation.

4.2.2 Matrigel-free methods

The matrix gels prepared by decellularization, as described above, are of animal origin, and their residual animal protein content may induce an immune response in the host (Giobbe et al., 2019; Kozłowski et al., 2021). Therefore, the advent of chemically-synthesized matrices has remedied this shortcoming. A purely chemically-synthesized matrix that integrates key ECM proteins found in the liver, such as type IV collagen and fibronectin, was prepared using poly ethylene glycol (PEG) hydrogels as the skeleton and successfully used to culture liver organoids. In addition to the benefits of complete chemical synthesis and avoidance of immunological factors, the stable cross-linking of the PEG gel matrix allowed for the stable culture of liver organoids for more than 14 days (Sorrentino et al., 2020). In addition to purely chemically-synthesized substrates, the

TABLE 2 Comparing the differences between different organoid construction biomaterials.

	Sources	Biomaterial	Existing research
MATRIGEL	Natural	EHS tumor tissue	widely used for studies on cell differentiation, angiogenesis, and tumor growth
	Natural	Alginate Collagen gels	supported differentiation and maturation of the organoids inducing fibroblast differentiation during matrix remodeling
MATRIGEL-FREE		Hyaluronic Acid (HA)	Improved cell-cell and cell-ECM interactions
		Silk	High stromal cell infiltration in the silk scaffolds
	Synthetic	PEG (Poly ethylene Glycol)	Improved growth and expansion of the organoids
		PLGA (Poly Lactic Glycolic Acid)	Improved wound healing
		PCL (Poly Caprolactone)	Improved tumoroid formation with porous PCL substrate
		Hybrid hydrogels	Low immunogenicity

EHS, Engelbreth-Holm-Swarm; ECM, extracellular matrix.

bioplotting poly-L-lactic acid scaffold (Wang et al., 2016), which permitted cells to develop in three dimensions and form cell-cell connections, was applied by Wang and colleagues. The cells grown within the ECM scaffold had markedly higher P450 activity and metabolizing enzymatic activity compared to iPSC-derived hepatocytes grown in a 2D matrix gel.

4.2.3 Liver on-chip

With the development of organoid chips in recent years, liver chips have received much attention and investigation. The types of cells and culture approaches used for liver microarrays are constantly improving, and the overall model can be classified as simple microwell microarrays (Wiedenmann et al., 2021), complex microfluidic microarrays (Ya et al., 2021) and body on chip (Tao et al., 2021), a collection of multiple organoids. Microfluidic organoids not only enable more precise control of culture conditions, but also reduce the influence of human factors by imposing physical and mechanical controls (Telles-Silva et al., 2022). Based on the standardized nature of organoids, this model implies more consistent drug responses and more reliable results.

The liver organoids generated of the rat, dog and human involved using micro-engineered organoids containing primary hepatocytes and stromal cells. Primary hepatocytes of the three sources were located in the porous membrane with two parallel microchannels within the ECM sandwich, while stromal cells were located on the other side of the sandwich. Ya et al. (2021) used engineered liver lobule canines (LLC) to generate liver organoids. The addition of an oxygen concentration regulation chip (ORC) on top of this could more accurately reflect the blood supply and blood oxygen content of the hepatic arterial and venous systems in the actual liver. The advantages of this organoid over those cultured in a matrix gel are that it solves the issue of vascularization and the establishment of a naturally perusable hepatic sinusoidal system, which prolongs the application of the liver organoid.

4.2.4 Other biomaterials methods

In vitro cells self-organizing into organoids are limited by the lack of circulatory system as well as oxygen and nutrients, which leads to the appearance of central organoid necrosis. To address this problem, vascularization methods have been applied to the construction of organoids, and interspersing fibers of endothelial cells between fibers containing parenchymal cells can facilitate vascularization and anastomosis with the host tissue *in vivo*. In addition to this, 3D printing techniques have been applied to construct vascularized frameworks for tissue development and differentiation of organoids in response to endothelial-parenchymal interactions (Leong et al., 2013).

Biomaterial scaffolds are mainly used for compartmentalization or restriction during organoid construction and are important for determining the final organoid structure and function. For example, the initial arrangement of epithelial and mesenchymal cells that initiate the development of ectodermal appendages in co-culture can be constructed by 3D modeling, which later consists of multiple parallel adjacent fibrous compartments filled with epithelial and mesenchymal cells as a whole (Pan et al., 2013).

5 Validation of liver organoids

After the liver organoid is generated, its performance can usually be assessed *in vitro* by morphological tests (Broutier et al., 2016; Aloia et al., 2019; Ogoke et al., 2022), functional tests (Akbari et al., 2019), such as P450 activity assays, and single-cell sequencing (Elbadawy et al., 2020). Compared to morphological and functional tests, single-cell sequencing is more reflective of the similarity between the organoid and the primary liver. The Human Cell Atlas Project is a worldwide study that characterizes cellular and tissue components through a single cell genomics approach, and it meticulously identifies different cells and tissues and defines all cell types in the human body based on their unique molecular profiles (Lindeboom et al., 2021). Single-cell

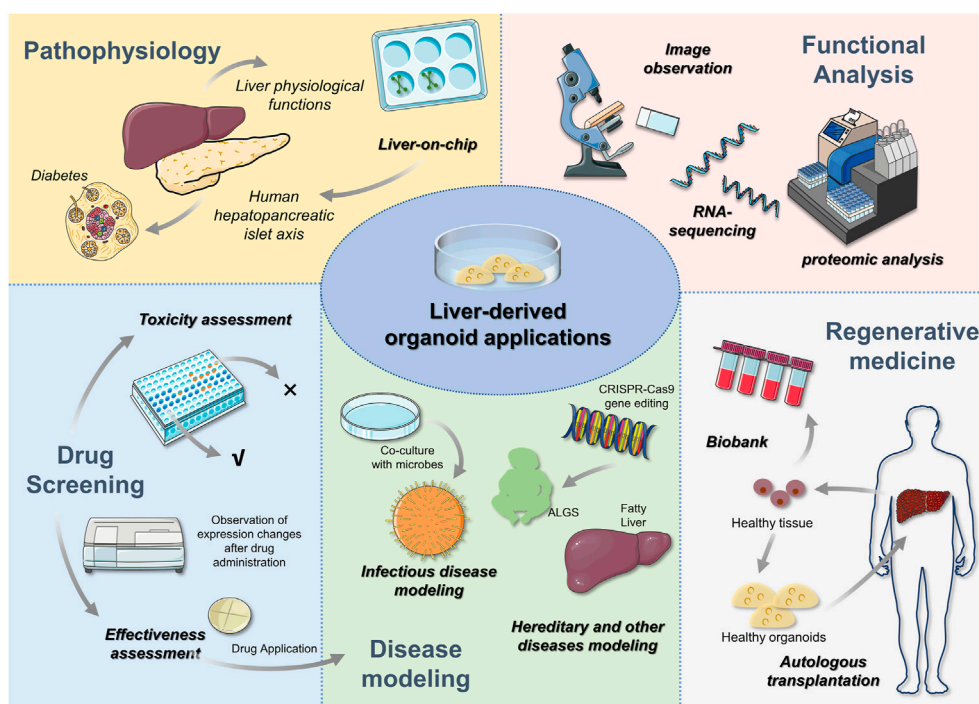


FIGURE 4

Liver-derived organoid applications After the liver organoid has been constructed, relevant expressions can be examined by morphology, RNA sequencing and proteomic analysis to determine the validity of the organoid. Subsequently, liver organoids can be used for liver pathophysiology research, disease modeling, drug screening and regenerative medicine. In addition to further understanding of liver physiology, *in vitro* 3D organoids can be used to construct multi-organ systems to study the role of different organs through liver-on-chip. For example, the role of hepatopancreatic islet axis in diabetes. Drug analysis includes efficacy and toxicity analysis, which contributes to the clinical application of drugs. Disease modeling is a popular area for liver organoids applications. Congenital and genetic diseases have been constructed through gene editing techniques. The availability of liver organoids also offers the hope to autologous organ transplantation. Healthy liver tissues in patients are able to be expanded and then transplanted, which can avoid the emergence of anti-host reactions. In addition to this, biopsied liver tissue is able to expand the biobank.

transcriptomics also plays an important role in the validation of organoids. A single-cell genomic approach can quantify the similarity of cells within liver organoids to the primary liver tissue, and this approach offers superior resolution and accuracy compared to bulk RNA-sequencing (Brazovskaja et al., 2019; Shinozawa et al., 2021). Camp et al. (2017) reported the regeneration of PSCs to a hepatocyte lineage by applying single-cell RNA sequencing at a 2D level, and a 3D liver bud was generated by co-culture of hepatocytes and stromal cells. Furthermore, the similarity to fetal hepatocytes was demonstrated based on the results of single-cell RNA sequencing, thereby proving the validity of the liver organoid.

6 Application of liver organoids

Existing disease models, such as cancer models, only reproduce a patient's tumour, and the lack of a functional holistic component in these models leads to limitations in their application. Commonly used animal models, while

contributing to the fundamental field of disease research, can require long culture and experimental periods and often do not adequately reflect the histological complexity and genetic specificity of the human body (Drost and Clevers, 2018; Nuciforo and Heim, 2021). By contrast, organoids can serve as preclinical models because they are physiologically and functionally similar to their primary organs. As such, the study of disease is not only limited to basic theory; instead, it also contributes to the development of clinical therapeutics, which is superior to other established 2D models. The current use of liver organoids is summarized in Figure 4.

6.1 Disease modelling

The sources of the disease models used to generate organoids can be classified as patient-derived organoids and CRISPR + organoids. Patient-derived normal or abnormal specimens preserve the genetic background of the respective individual, and thus, are important in disease modelling of monogenic

diseases and cancers, as patient-derived tissues include specific genetic mutations. In addition, they can be used to develop individualized drug tests or treatment plans for patients (Nuciforo and Heim, 2021).

CRISPR-Cas9-mediated genome engineering is one of the most popular gene editing technologies, and it mainly includes gene knock-in and knock-out techniques. After CRISPR-Cas9-induced double-strand breaks occur, the induced breaks can be repaired by non-homologous end joining or homology-directed repair (Zhan et al., 2019; Hendriks et al., 2020). Compared to patient-derived organoids, CRISPR + organoids can overcome the limitation of the sample source. In addition, after oncogene knock-out (Artegiani et al., 2019), it is possible to continuously observe the changes in the organoid and to further intervene in various stages of the disease. In addition to disease modelling, genome-scale CRISPR screening can identify new genes for cancer research (Zhan et al., 2019; Ringel et al., 2020).

6.1.1 Genetic diseases

Alagille syndrome (ALGS) is an autosomal dominant disorder that results in multiple organ abnormalities due to mutations in *JAG1*, which blocks the Notch signalling pathway. The main hepatic lesion is chronic cholestasis due to the lack of intrahepatic bile ducts (Turnpenny and Ellard, 2012). In a study by Huch et al. (2015), structural defects in the biliary tract were generated using biopsies derived from patients to model ALGS disease. The inhibition of nicotinamide, R-spondin, etc., was found to lead to a reduction in biliary marker expression and biliary cell apoptosis in ALGS patient-derived organoids. Guan et al. (2017) prepared iPSCs using fibroblasts from patients and generated iPSC-derived liver organoids expressing *ALGS1*. The pathogenic *ALGS1* mutation C829X was introduced and restored in iPSC-derived liver organoids and controls by CRISPR-Cas9 genome editing, and it was found that bile duct formation in liver organoids was increased following reversal of the *ALGS1* mutation. The efficiency of organoid formation and biliary transit function were also closely associated with the *JAG1* mutation.

Citrullinemia type 1 (CTLN1) is a relatively rare inherited metabolic disorder that causes severe and fatal neonatal hyperammonemia. It is mainly due to a mutation in arginosuccinate synthetase (ASS1) that affects the detoxification function of the liver, thereby blocking the urea cycle and causing a significant accumulation of ammonia in the body that cannot be converted to urea, ultimately leading to hyperammonemia (Nuciforo and Heim, 2021). Research into this disease is hampered by the high clinical variability of the disease and the lack of models that can predict the severity of the phenotype early in the course of the disease. Akbari et al. (2019) performed disease modelling of CTLN1 by generating liver organoids using biopsies from patients. The expression of *ASS1* was not detected in patient-derived organoids, but it could be detected in healthy donors, indicating the

importance of *ASS1* defects in CTLN1. The ability to reverse disease-associated ammonia accumulation by genetic manipulation techniques to achieve the expression of *ASS1* suggests that the model is suitable for genetic manipulation. This study also provides early evidence for the role of organoids in genetically-corrected treatments for genetic disorders.

Mitochondrial DNA deficiency syndrome (MDS) is a serious genetic disorder caused by iron overload in the body, which is mainly due to mutations in *DGUOK*. The liver, as the main storage site for iron in the body, is more sensitive to the oxidative stress caused by iron overload, which ultimately leads to severe liver damage. However, the process from iron overload to liver failure is not known. Recently, Guo et al. (2021) used iPSCs from patients carrying a *DGUOK* mutation to generate liver organoids *in vitro*, a model that not only has the characteristics of hepatocytes, but also includes the patient's genetic context. In addition, corrections by CRISPR/Cas9 gene editing enable more accurate controls. The ability of n-acetylcysteine (NAC) to reduce the sensitivity of NCOA4-dependent ferritin degradation-mediated iron pendant disease in lysosomes to iron overload has led to the further study of MDS.

6.1.2 Alcohol-related and non-alcoholic fatty liver diseases

Alcoholic liver disease (ALD) is a liver disease that is closely related to alcohol use. Chronic alcohol abuse (>60 g/day) plays an important role in the development of the disease, and genetic factors, such as patatin-like phospholipase domain containing 3 (PNPLA3) and transmembrane six superfamily member 2 (TM6SF2) expression, viral infections, obesity or malnutrition, are also associated with ALD (Lackner and Tiniakos, 2019). ESC-derived liver organoids co-cultured with human fetal liver mesenchymal cells can mimic the pathophysiological and developmental stages of the disease, including oxidative stress and inflammatory-mediated fibrosis. This disease model can also be used for the study of steatohepatitis that follows ALD. As this model shows significant long-term expansion potential over 20 generations, it can be applied as an industrial-scale model for studying the potential mechanisms of the disease, screening of drugs and conducting research related to ALD prevention and treatment (Wang et al., 2019).

Unlike ALD, the causative factors for non-alcoholic fatty liver diseases (NAFLD) may include high-energy diet, sedentary lifestyle, obesity, diabetes and hyperlipidemia (Younossi et al., 2019). When liver organoids were exposed to free fatty acid, hepatocytes showed steatosis and ballooning, with increased levels of pro-inflammatory cytokines and collagen, demonstrating the role of inflammation and fibrosis in the disease, and thus, recapitulating key features of non-alcoholic steatohepatitis (NASH) (Soret et al., 2020). Patient-derived organoids are capable of modeling specific diseases, while patient-derived NASH organoids show strikingly diverse transcriptomes and functions, including increased growth

kinetics, lipid accumulation and sensitivity to apoptotic stimuli. The co-culture of NASH organoids with hepatic stellate cells, T cells and Kupffer cells can effectively validate NASH-related inflammation, fibrosis and tumour development. As such, this approach more accurately reflects the hepatic microenvironment of NASH patients than the NASH model constructed from healthy liver organoids (Mccarron et al., 2021). The upregulation of some novel genes in NASH organoids (Elbadawy et al., 2020) may provide a possible pathway for the use of liver organoids in the diagnosis and treatment of NASH in the future.

6.1.3 Infectious diseases

Viral hepatitis, mainly caused by hepatophilic viruses, causes acute hepatocyte necrosis, degeneration and inflammation. Hepatitis B virus (HBV), which causes chronic infection in more than 200 million individuals worldwide, is the predominant infectious agent of the liver (Wose Kinge et al., 2020). HBV exhibits significant heterogeneity, including clinical manifestations ranging from self-limiting infection to cirrhosis or hepatocellular carcinoma development, and different outcomes in response to the same drug therapy. This has led to the difficulty in providing a complete overview of the HBV replication cycle and the deficiency in representing individualized genetic backgrounds in the study of related diseases. By co-culturing iPSCs with mesenchymal and endothelial cells, iPSC-derived organoids are a good model for HBV research, which encompasses patient-specific genetic backgrounds and susceptibility to HBV infection compared to iPSC-derived hepatic-like cells (Nie et al., 2018). In addition to healthy liver organoids, the use of HBV-infected chronic cirrhotic liver tissues to generate HBV-infected patient-derived liver organoids enables the study of HBV development. Despite the lack of phenotypic evidence for abnormal growth, HBV-infected non-tumorigenic patient-derived liver organoids exhibit early cancer gene profiles (De Crignis et al., 2021), which may provide an approach for the early personalized treatment of HBV-associated hepatocellular carcinoma (HCC).

Due to the ACE2+/TMPRSS2+ expressing cell population in human bile ducts, human liver ductal organoids can be used for SARS-CoV-2 disease modelling. By co-culturing with SARS-CoV-2, human liver ductal organoids exhibited susceptibility and supported robust viral replication (Zhao et al., 2020; Lui et al., 2022). In addition to healthy human liver ductal organoids, patient-derived organoids can respond to the relationship between different diseases. For example, NASH-derived organoids demonstrate the permissibility to SARS-CoV-2 pseudovirus, providing a possible explanation for the severe outcome of COVID-19 in NASH patients (Mccarron et al., 2021).

6.1.4 Liver fibrosis

Hepatic fibrosis is a dynamic pathological process that essentially results from the excessive accumulation of

heterologous hepatic myofibroblastic components, leading to abnormal production of connective tissue in the liver (Parola and Pinzani, 2019). Initially, chronic inflammation in the liver occurs in response to various pathogenic factors such as hepatitis virus infection, fatty liver disease, immune disorders and drug or chemical exposure. Inflammation primarily activates hepatic stellate cells within the liver interstitium, which is the central event in liver fibrosis. Furthermore, hematopoietic stem cells are activated and differentiate into myofibroblasts, whose increase leads to the massive accumulation of ECM (Bao et al., 2021). The chronic inflammatory process also produces several immune cells that are driven by inflammatory factors, which damages hepatocytes and causes them to lose their robust regenerative capacity, ultimately leading to the development of irreversible cirrhosis.

Three-dimensional liver organoids were constructed by co-culture with HepaRG and hepatic stellate cells. After exposure to allyl alcohol and methotrexate, the organoids showed enhanced activity of hepatic stellate cells and secretion and deposition of collagen, providing evidence for the establishment of a fibrosis model based on HepaRG-derived liver organoids. In addition, acetaminophen use results in hepatocyte injury-dependent activation and collagen production in hepatic stellate cells, while histone deacetylase suppression prevents activation in these cells (Leite et al., 2016). One of the clinical manifestations of autosomal recessive polycystic kidney disease (ARPKD) is congenital hepatic fibrosis. The generation of liver organoids with a common pathogenic mutation in ARPKD demonstrated that the increased TGF β expression generated by this mutation in bile duct cells could stimulate myofibroblasts to form collagen fibers (Guan et al., 2021), which ultimately resulted in the development of liver fibrosis.

6.1.5 Cancer

ACS-derived liver organoids and patient-derived xenografts (PDXs) are common sources of 3D *in vitro* liver tumour models. However, PDXs associate with a low implantation rate, and thus, they have limited application in disease modelling (Cavalloni et al., 2016). Patient-derived tumour organoids have been shown to retain the histology, gene expression and oncogenic potential of the original tumour based on long-term *in vitro* expansion, and these features can also be seen in patients after transplantation (Broutier et al., 2017).

Li et al. (2019) generated PDOs from tissues of different regional biopsy sources and investigated the effects of 129 FDA-approved drugs, demonstrating the roles of intra- and inter-patient factors in drug response heterogeneity, which may explain why promising drugs succeed in preclinical models but fail in clinical settings. Liver tissues from tumour patients obtained by needle biopsy, including tissues from various clinical stages of HCC of different etiologies (Nuciforo et al., 2018), have been used to construct HCC organoids. While retaining the biomarkers of the original tumour, HCC organoids are

significantly different morphologically from those of non-tumour derived organoids. HCC organoids, which more closely resemble the tumour-specific microenvironment of the original tumour, may be used to further investigate individualized therapies. However, tumour-derived organoids, such as HCC organoids, are affected by the overgrowth of healthy contaminant-derived organoids, which may be due to differences in genetic stability. To avoid the growth of healthy contaminant-derived organoids, the time of tissue digestion should be increased (Broutier et al., 2017). Furthermore, the outcome of organoid generation correlates with the degree of differentiation of the original tumour, with only one quarter of HCC biopsies progressing to organoids and those are usually derived from undifferentiated specimens (Nuciforo et al., 2018).

Current sources of organoid models for Cholangiocarcinoma (CCA) include biopsy tissue from CCA patients and genetically engineered human cholangiocyte, and have been useful in disease metabolism studies, drug screening and individualized medicine (Massa et al., 2020). BRCA1-associated protein 1 (BAP1), a tumour suppressor, was introduced into human cholangiocyte organoids by CRISPR-Cas9 using a loss-of-function technique, and the organoids were injected into mice subcutaneously, as well as into the liver, after editing to demonstrate tumorigenic ability. After adding doxorubicin to induce BAP1 expression, the morphology of the organoid gradually reverted to a monolayer (Artegiani et al., 2019), demonstrating that BAP1 plays an important role in the development of cholangiocarcinoma. By manipulating classical genes, such as *P53*, *RB*, *MYC2* and other oncogenes, Sun et al. (2019) demonstrated that oncogenesis in hepatocytes could be prevented by inhibiting both Notch and JAK-STAT signalling pathways. By RNA sequencing of co-cultured and monocultured cells, the results showed upregulation of gene expression associated with TNF signaling. Hepatocellular carcinoma cell-endothelial vascular secretory signaling in the co-culture model differentiated macrophages toward a pro-inflammatory and pro-angiogenic phenotype, suggesting that endothelial cells induce an inflammatory microenvironment in hepatocellular carcinoma cells by recruiting immune cells (Lim et al., 2022).

6.2 Drug screening

6.2.1 Effectiveness assessment

Polycystic liver disease is a type of cystic lesion caused by the presence of fetal cholestatic cells in the liver (Raynaud et al., 2011), which leads to a dominant effect in the bile ducts, thereby increasing fluid secretion into the lumen, enhancing bile duct cell proliferation and leading to impaired liver function. Bile duct organoids were used to examine the effects of drugs on shrinking cysts in the treatment of polycystic liver disease. Octreotide, a synthetic analogue of a growth inhibitor, has been used in clinical settings to reduce the size of cysts in polycystic liver disease by

eliminating the effects of secretin on cystic lesions (Sampaziotis et al., 2015).

Hepatic lipid deposition is a unique and common condition in cats in which fats are broken down into free fatty acids and then transported through the bloodstream to the liver, where they accumulate as triacylglycerols in hepatocytes. Using a feline liver organoid system to examine the effects of drugs on treating hepatic lipid deposition in cats, Haaker et al. (2020) validated the effects of AICAR, T863 and PF 06424439 on hepatic lipid deposition by quantitative TAG assays, lipid droplet staining analyses and quantitative polymerase chain reactions to further provide evidence for *in vitro* studies of hepatic lipid deposition.

In addition, traditional Chinese medicines play important roles in the treatment of liver diseases. After applying cholesterol + MIX (mainly cholesterol and other small molecules), Wu et al. (2019) showed increased expression of mature hepatocyte and bile duct cell markers in hepatobiliary analogs, which also showed improved drug metabolism, glycogen storage capacity and Alb secretion capacity compared to analogs in the absence of the medicine, demonstrating the positive benefits of herbal medicines in liver health.

6.2.2 Toxicity assessment

As the toxicity of certain drugs, such as the proprietary compound JNJ-2, can associate with significant species variability, liver organoids provide a considerably more accurate tool for drug toxicity testing than animal models (Jang et al., 2019). For drug-induced liver injury, the applicability of more than 200 marketed drugs and their resulting cholestatic effect and/or mitochondrial toxicity has been assessed by high-throughput liver organoid models (Shinozawa et al., 2021).

Liver organoids are also used to assess drug toxicity in cells of different origins. For example, Kang et al. (2016) established ESC-, PSC- and primary hepatocyte-derived organoids. The hepatotoxicity of acetaminophen (AAP) and aflatoxin B1 (AFB1) was evaluated, and it was found that AAP decreased cell viability and increased lactate dehydrogenase activity in a dose-dependent manner in all cell types. Furthermore, AFB1 showed different dose-dependent responses depending on the cell type and rapidly decreased cell survival in primary hepatocyte-derived organoids.

6.2.3 *In vitro* studies of liver physiology and regenerative medicine

The properties of organoids derived from normal tissues have a unique role in the study of liver physiology. The normal state of the hepatopancreatic islet axis is closely related to the normal functions of the liver and other organs of the mammalian body. Tao et al. (2021) simulated the human hepatopancreatic islet axis under normal conditions by generating a microfluidic multi-organ system that contained two separated regions connected by a network of microchannels. Due to the circulating perfusion conditions of this

system, iPSC-derived liver and pancreatic organoids were able to persist in long-term culture.

Regenerative medicine is a field of medical research based on the natural healing ability of tissues that each organism possesses within itself. The liver, due to its powerful regenerative capacity, has opened up a wide range of prospects for the clinical application of hepatocyte transplantation and artificial liver generation using hepatocytes. Monogenic inherited liver diseases are caused by genetic defects in hepatocyte function in the absence of stem cell damage, and thus, liver transplantation can play an important role in the treatment of monogenic inherited diseases (Peng et al., 2021).

7 Conclusion and perspective

In summary, PSC- or ASC-derived liver organoids are gradually replacing cell lines and animal models as promising *in vitro* models for clinical studies of the liver due to their ability to better mimic the *in vivo* environment. Organoids have demonstrated their potential in modeling infectious, genetic, and alcoholic liver diseases, as well as in drug screening and personalized medicine.

iPSC-derived organoids have the advantage of not relying on primary tissue resection because patient-derived iPSC lines can generate multiple cell types indefinitely and repeatedly (Takebe et al., 2014). Unfortunately, there are genetic and epigenetic abnormalities associated with this process that are difficult to control. Thus, in disease modeling, patient biopsy-derived organoids may be superior to iPSC-derived organoids because they retain the patient's true epigenetic characteristics, which are often greatly influenced by non-genetic environmental factors. Multiple tissue biopsies combined with PDO drug screening platforms can support drug efficacy studies, leading to individualized treatment (Li et al., 2019). Although the clinical availability of patient-derived biopsy tissues is a major shortcoming, the positive contributions to drug screening and toxicity evaluation following the application of organoid disease models may increase patient acceptance of biopsies in the future. In addition, organoids can be a valuable method for early-

decision making in the development of expensive anti-tumour drugs (Bertolini et al., 2015). Regardless, the emergence of organoids has addressed ethical issues to some extent (Rossi et al., 2018), and thus, the potential of organoids in clinical settings in the future is enormous. We are excited to see more comprehensive development of organoids in the future, including the application of new biomaterials that can be constructed not only in basic research, but increasingly used in actual clinical treatments.

Author contributions

Conceptualization: LS and CW; Writing—original draft preparation: QL; Writing—review and editing: QL, AZ, ZL, and LS; Visualization: AZ and LS. All authors have read and agreed to the published version of the manuscript.

Funding

Xinglin project of Chengdu University of Traditional Chinese Medicine (ZKYY 2019, MPRC2021012).

Conflict of interest

The authors declare that the research was conducted in the absence of any commercial or financial relationships that could be construed as a potential conflict of interest.

Publisher's note

All claims expressed in this article are solely those of the authors and do not necessarily represent those of their affiliated organizations, or those of the publisher, the editors and the reviewers. Any product that may be evaluated in this article, or claim that may be made by its manufacturer, is not guaranteed or endorsed by the publisher.

References

- Adolph, T. E., Grander, C., Moschen, A. R., and Tilg, H. (2018). Liver-microbiome Axis in health and disease. *Trends Immunol.* 39, 712–723. doi:10.1016/j.it.2018.05.002
- Aisenbrey, E. A., and Murphy, W. L. (2020). Synthetic alternatives to matrigel. *Nat. Rev. Mat.* 5, 539–551. doi:10.1038/s41578-020-0199-8
- Akbari, S., Sevinc, G. G., Ersoy, N., Basak, O., Kaplan, K., Sevinc, K., et al. (2019). Robust, long-term culture of endoderm-derived hepatic organoids for disease modeling. *Stem Cell Rep.* 13, 627–641. doi:10.1016/j.stemcr.2019.08.007
- Aloia, L., Mckie, M. A., Vernaz, G., Cordero-Espinoza, L., Aleksieva, N., Van Den Amele, J., et al. (2019). Epigenetic remodelling licences adult cholangiocytes for organoid formation and liver regeneration. *Nat. Cell Biol.* 21, 1321–1333. doi:10.1038/s41556-019-0402-6
- Aqeilan, R. I. (2020). Engineering organoids: A promising platform to understand biology and treat diseases. *Cell Death Differ.* 28, 1–4. doi:10.1038/s41418-020-00680-0
- Artegiani, B., Van Voorthuisen, L., Lindeboom, R. G. H., Seinstr, D., Heo, I., Tapia, P., et al. (2019). Probing the tumor suppressor function of BAP1 in CRISPR-engineered human liver organoids. *Cell Stem Cell* 24, 927–943. doi:10.1016/j.stem.2019.04.017
- Asai, A., Aihara, E., Watson, C., Mourya, R., Mizuochi, T., Shivakumar, P., et al. (2017). Paracrine signals regulate human liver organoid maturation from iPSC. *Development* 144 (6), 1056–1064. doi:10.1242/dev.142794
- Asrani, S. K., Devarbhavi, H., Eaton, J., and Kamath, P. S. (2019). Burden of liver diseases in the world. *J. Hepatol.* 70, 151–171. doi:10.1016/j.jhep.2018.09.014

- Bao, Y. L., Wang, L., Pan, H. T., Zhang, T. R., Chen, Y. H., Xu, S. J., et al. (2021). Animal and organoid models of liver fibrosis. *Front. Physiol.* 12, 666138. doi:10.3389/fphys.2021.666138
- Bar-Ephraim, Y. E., Kretschmar, K., and Clevers, H. (2019). Organoids in immunological research. *Nat. Rev. Immunol.* 20, 279–293. doi:10.1038/s41577-019-0248-y
- Benton, G., Arnaoutova, I., George, J., Kleinman, H. K., and Koblinski, J. (2014). Matrigel: From discovery and ECM mimicry to assays and models for cancer research. *Adv. Drug Deliv. Rev.* 79–80, 3–18. doi:10.1016/j.addr.2014.06.005
- Bertolini, F., Sukhatme, V. P., and Bouche, G. (2015). Drug repurposing in oncology—patient and health systems opportunities. *Nat. Rev. Clin. Oncol.* 12, 732–742. doi:10.1038/nrclinonc.2015.169
- Brazovskaja, A., Treutlein, B., and Camp, J. G. (2019). High-throughput single-cell transcriptomics on organoids. *Curr. Opin. Biotechnol.* 55, 167–171. doi:10.1016/j.copbio.2018.11.002
- Bresnahan, E., Ramadori, P., Heikenwalder, M., Zender, L., and Lujambio, A. (2020). Novel patient-derived preclinical models of liver cancer. *J. Hepatol.* 72, 239–249. doi:10.1016/j.jhep.2019.09.028
- BROUTIER, L., Andersson-Rolf, A., Hindley, C. J., Boj, S. F., Clevers, H., Koo, B. K., et al. (2016). Culture and establishment of self-renewing human and mouse adult liver and pancreas 3D organoids and their genetic manipulation. *Nat. Protoc.* 11, 1724–1743. doi:10.1038/nprot.2016.097
- BROUTIER, L., Mastrogianni, G., Verstegen, M. M., Francies, H. E., Gavarro, L. M., Bradshaw, C. R., et al. (2017). Human primary liver cancer-derived organoid cultures for disease modeling and drug screening. *Nat. Med.* 23, 1424–1435. doi:10.1038/nm.4438
- Camp, J. G., Sekine, K., Gerber, T., Loeffler-Wirth, H., Binder, H., Gac, M., et al. (2017). Multilineage communication regulates human liver bud development from pluripotency. *Nature* 546, 533–538. doi:10.1038/nature22796
- Cavalloni, G., Peraldo-Neia, C., Sassi, F., Chiorino, G., Sarotto, I., Aglietta, M., et al. (2016). Establishment of a patient-derived intrahepatic cholangiocarcinoma xenograft model with KRAS mutation. *Bmc Cancer* 16, 90. doi:10.1186/s12885-016-2136-1
- Clevers, H., Loh, K. M., and Nusse, R. (2014). Stem cell signaling. An integral program for tissue renewal and regeneration: Wnt signaling and stem cell control. *Science* 346, 1248012. doi:10.1126/science.1248012
- Clevers, H. (2016). Modeling development and disease with organoids. *Cell* 165, 1586–1597. doi:10.1016/j.cell.2016.05.082
- Coll, M., Perea, L., Boon, R., Leite, S. B., Vallverdú, J., Mannaerts, I., et al. (2018). Generation of hepatic stellate cells from human pluripotent stem cells enables *in vitro* modeling of liver fibrosis. *Cell Stem Cell* 23 (1), 101–113.e7.
- De Crignis, E., Hossain, T., Romal, S., Carofiglio, F., Moulos, P., Khalid, M. M., et al. (2021). Application of human liver organoids as a patient-derived primary model for HBV infection and related hepatocellular carcinoma. *Elife* 10, e60747. doi:10.7554/eLife.60747
- Drost, J., and Clevers, H. (2018). Organoids in cancer research. *Nat. Rev. Cancer* 18, 407–418. doi:10.1038/s41568-018-0007-6
- Elbadawy, M., Yamanaka, M., Goto, Y., Hayashi, K., Tsunedomi, R., Hazama, S., et al. (2020). Efficacy of primary liver organoid culture from different stages of non-alcoholic steatohepatitis (NASH) mouse model. *Biomaterials* 237, 119823. doi:10.1016/j.biomaterials.2020.119823
- Estes, C., Anstee, Q. M., Arias-Loste, M. T., Bantel, H., Bellentani, S., Caballeria, J., et al. (2018). Modeling NAFLD disease burden in China, France, Germany, Italy, Japan, Spain, United Kingdom, and United States for the period 2016–2030. *J. Hepatology* 69 (4), 896–904. doi:10.1016/j.jhep.2018.05.036
- Gabriel, V., Zdyski, C., Sahoo, D. K., Dao, K., Bourgois-Mochel, A., Kopper, J., et al. (2022). Standardization and maintenance of 3D canine hepatic and intestinal organoid cultures for use in biomedical research. *J. Vis. Exp.* 1, 1. doi:10.3791/63515
- Giobbe, G. G., Crowley, C., Luni, C., Campinoti, S., Khedr, M., Kretschmar, K., et al. (2019). Extracellular matrix hydrogel derived from decellularized tissues enables endodermal organoid culture. *Nat. Commun.* 10, 5658. doi:10.1038/s41467-019-13605-4
- Guan, Y., Enejder, A., Wang, M., Fang, Z., Cui, L., Chen, S. Y., et al. (2021). A human multi-lineage hepatic organoid model for liver fibrosis. *Nat. Commun.* 12, 6138. doi:10.1038/s41467-021-26410-9
- Guan, Y., Xu, D., Garfin, P. M., Ehmer, U., Hurwitz, M., Enns, G., et al. (2017). Human hepatic organoids for the analysis of human genetic diseases. *JCI Insight* 2, 94954. doi:10.1172/jci.insight.94954
- Guo, J., Duan, L., He, X., Li, S., Wu, Y., Xiang, G., et al. (2021). A combined model of human iPSC-derived liver organoids and hepatocytes reveals ferroptosis in DGUOK mutant mtDNA depletion syndrome. *Adv. Sci.* 8, 2004680. doi:10.1002/advsc.202004680
- Haaker, M. W., Kruitwagen, H. S., Vaandrager, A. B., Houweling, M., Penning, L. C., Molenaar, M. R., et al. (2020). Identification of potential drugs for treatment of hepatic lipidosis in cats using an *in vitro* feline liver organoid system. *J. Vet. Intern. Med.* 34, 132–138. doi:10.1111/jvim.15670
- Hendriks, D., Artegiani, B., Hu, H., Chuva De Sousa Lopes, S., and Clevers, H. (2020). Establishment of human fetal hepatocyte organoids and CRISPR–Cas9-based gene knockin and knockout in organoid cultures from human liver. *Nat. Protoc.* 16, 182–217. doi:10.1038/s41596-020-00411-2
- Hu, H., Gehart, H., Artegiani, B., C. L. O.-I., Dekkers, F., Basak, O., et al. (2018). Long-term expansion of functional mouse and human hepatocytes as 3D organoids. *Cell* 175, 1591–1606. doi:10.1016/j.cell.2018.11.013
- Huch, M., Dorrell, C., Boj, S. F., Van Es, J. H., Li, V. S., Van De Wetering, M., et al. (2013). *In vitro* expansion of single Lgr5+ liver stem cells induced by Wnt-driven regeneration. *Nature* 494, 247–250. doi:10.1038/nature11826
- Huch, M., Gehart, H., Van boxtel, R., Hamer, K., Blokzijl, F., Verstegen, Monique m. A., et al. (2015). Long-term culture of genome-stable bipotent stem cells from adult human liver. *Cell* 160, 299–312. doi:10.1016/j.cell.2014.11.050
- Jang, K. J., Otieno, M. A., Ronxhi, J., Lim, H. K., Ewart, L., Kodella, K. R., et al. (2019). Reproducing human and cross-species drug toxicities using a Liver-Chip. *Sci. Transl. Med.* 11, eaax5516. doi:10.1126/scitranslmed.aax5516
- Kang, S. J., Lee, H. M., Park, Y. I., Yi, H., Lee, H., So, B., et al. (2016). Chemically induced hepatotoxicity in human stem cell-induced hepatocytes compared with primary hepatocytes and HepG2. *Cell Biol. Toxicol.* 32, 403–417. doi:10.1007/s10565-016-9342-0
- Kozłowski, M. T., Crook, C. J., and Ku, H. T. (2021). Towards organoid culture without Matrigel. *Commun. Biol.* 4, 1387. doi:10.1038/s42003-021-02910-8
- Kruitwagen, H. S., Oosterhoff, L. A., Vernooij, I. G. W. H., Schraal, I. M., Van Wolferen, M. E., Bannink, F., et al. (2017). Long-term adult feline liver organoid cultures for disease modeling of hepatic steatosis. *Stem Cell Rep.* 8, 822–830. doi:10.1016/j.stemcr.2017.02.015
- Kuijk, E. W., Rasmussen, S., Blokzijl, F., Huch, M., Gehart, H., Toonen, P., et al. (2016). Generation and characterization of rat liver stem cell lines and their engraftment in a rat model of liver failure. *Sci. Rep.* 6, 22154. doi:10.1038/srep22154
- Lackner, C., and Tiniakos, D. (2019). Fibrosis and alcohol-related liver disease. *J. Hepatol.* 70, 294–304. doi:10.1016/j.jhep.2018.12.003
- Lancaster, M. A., and Knoblich, J. A. (2014). Organogenesis in a dish: Modeling development and disease using organoid technologies. *Science* 345, 1247125. doi:10.1126/science.1247125
- Leite, S. B., Roosens, T., El Taghdouini, A., Mannaerts, I., Smout, A. J., Najimi, M., et al. (2016). Novel human hepatic organoid model enables testing of drug-induced liver fibrosis *in vitro*. *Biomaterials* 78, 1–10. doi:10.1016/j.biomaterials.2015.11.026
- Leong, M. F., Toh, J. K., Du, C., Narayanan, K., Lu, H. F., Lim, T. C., et al. (2013). Patterned prevascularised tissue constructs by assembly of polyelectrolyte hydrogel fibres. *Nat. Commun.* 4, 2353. doi:10.1038/ncomms3353
- Li, L., Knutsdottir, H., Hui, K., Weiss, M. J., He, J., Philosophie, B., et al. (2019). Human primary liver cancer organoids reveal intratumor and interpatient drug response heterogeneity. *JCI Insight* 4, 121490. doi:10.1172/jci.insight.121490
- Li, M. L., Aggeler, J., Farson, D. A., Hatier, C., Hassell, J., Bissell, M. J., et al. (1987). Influence of a reconstituted basement membrane and its components on casein gene expression and secretion in mouse mammary epithelial cells. *Proc. Natl. Acad. Sci. U. S. A.* 84, 136–140. doi:10.1073/pnas.84.1.136
- Lim, J. T. C., Kwang, L. G., Ho, N. C. W., Toh, C. C. M., Too, N. S. H., Hooi, L., et al. (2022). Hepatocellular carcinoma organoid co-cultures mimic angiocrine crosstalk to generate inflammatory tumor microenvironment. *Biomaterials* 284, 121527. doi:10.1016/j.biomaterials.2022.121527
- Lindeboom, R. G. H., Regev, A., and Teichmann, S. A. (2021). Towards a human cell Atlas: Taking notes from the past. *Trends Genet.* 37, 625–630. doi:10.1016/j.tig.2021.03.007
- Liu, G., David, B. T., Trawczynski, M., and Fessler, R. G. (2020). Advances in pluripotent stem cells: History, mechanisms, technologies, and applications. *Stem Cell Rev. Rep.* 16, 3–32. doi:10.1007/s12015-019-09935-x
- Liu, J., Li, P., Wang, L., Li, M., Ge, Z., Noordam, L., et al. (2021). Cancer-associated fibroblasts provide a stromal niche for liver cancer organoids that confers trophic effects and therapy resistance. *Cell. Mol. Gastroenterol. Hepatol.* 11, 407–431. doi:10.1016/j.jcmgh.2020.09.003
- Lui, V. C., Hui, K. P., Babu, R. O., Yue, H., Chung, P. H., Tam, P. K., et al. (2022). Human liver organoid derived intra-hepatic bile duct cells support SARS-CoV-2 infection and replication. *Sci. Rep.* 12, 5375. doi:10.1038/s41598-022-09306-6
- Magami, Y., Azuma, T., Inokuchi, H., Kokuno, S., Moriyasu, F., Kawai, K., et al. (2002). Cell proliferation and renewal of normal hepatocytes and bile duct cells in adult mouse liver. *Liver* 22, 419–425. doi:10.1034/j.1600-0676.2002.01702.x

- Massa, A., Varamo, C., Vita, F., Tavolari, S., Peraldo-Neia, C., Brandi, G., et al. (2020). Evolution of the experimental models of cholangiocarcinoma. *Cancers (Basel)* 12, E2308. doi:10.3390/cancers12082308
- Mccarron, S., Bathon, B., Conlon, D. M., Abbey, D., Rader, D. J., Gawronski, K., et al. (2021). Functional characterization of organoids derived from irreversibly damaged liver of patients with NASH. *Hepatology* 74, 1825–1844. doi:10.1002/hep.31857
- McCauley, H. A., and Wells, J. M. (2017). Pluripotent stem cell-derived organoids: Using principles of developmental biology to grow human tissues in a dish. *Development* 144, 958–962. doi:10.1242/dev.140731
- Mun, S. J., Lee, J., Chung, K. S., Son, M. Y., and Son, M. J. (2021). Effect of microbial short-chain fatty acids on CYP3A4-mediated metabolic activation of human pluripotent stem cell-derived liver organoids. *Cells* 10, 126. doi:10.3390/cells10010126
- Nantasanti, S., Spee, B., Kruitwagen, H. S., Chen, C., Geijsen, N., Oosterhoff, L. A., et al. (2015). Disease modeling and gene therapy of copper storage disease in canine hepatic organoids. *Stem Cell Rep.* 5, 895–907. doi:10.1016/j.stemcr.2015.09.002
- Nie, Y.-Z., Zheng, Y.-W., Miyakawa, K., Murata, S., Zhang, R.-R., Sekine, K., et al. (2018). Recapitulation of Hepatitis B virus–host interactions in liver organoids from human induced pluripotent stem cells. *EBioMedicine* 35, 114–123. doi:10.1016/j.ebiom.2018.08.014
- Nuciforo, S., Fofana, I., Matter, M. S., Blumer, T., Calabrese, D., Boldanova, T., et al. (2018). Organoid models of human liver cancers derived from tumor needle biopsies. *Cell Rep.* 24, 1363–1376. doi:10.1016/j.celrep.2018.07.001
- Nuciforo, S., and Heim, M. H. (2021). Organoids to model liver disease. *JHEP Rep.* 3, 100198. doi:10.1016/j.jhepr.2020.100198
- Ogoke, O., Guiggey, D., Mon, T., Shamul, C., Ross, S., Rao, S., et al. (2022). Spatiotemporal imaging and analysis of mouse and human liver bud morphogenesis. *Dev. Dyn.* 251, 662–686. doi:10.1002/dvdy.429
- Ohnuki, M., and Takahashi, K. (2015). Present and future challenges of induced pluripotent stem cells. *Philosophical Trans. R. Soc. B-Biological Sci.* 370, 20140367. doi:10.1098/rstb.2014.0367
- Ouchi, R., Togo, S., Kimura, M., Shinozawa, T., Koido, M., Koike, H., et al. (2019). Modeling steatohepatitis in humans with pluripotent stem cell-derived organoids. *Cell Metab.* 30, 374–384. doi:10.1016/j.cmet.2019.05.007
- Pan, J., Yung Chan, S., Common, J. E., Amini, S., Miserez, A., Birgitte Lane, E., et al. (2013). Fabrication of a 3D hair follicle-like hydrogel by soft lithography. *J. Biomed. Mat. Res. A* 101, 3159–3169. doi:10.1002/jbm.a.34628
- Parola, M., and Pinzani, M. (2019). Liver fibrosis: Pathophysiology, pathogenetic targets and clinical issues. *Mol. Asp. Med.* 65, 37–55. doi:10.1016/j.mam.2018.09.002
- Peng, W. C., Kraaier, L. J., and Kluiver, T. A. (2021). Hepatocyte organoids and cell transplantation: What the future holds. *Exp. Mol. Med.* 53, 1512–1528. doi:10.1038/s12276-021-00579-x
- Peng, W. C., Logan, C. Y., Fish, M., Anbarchian, T., Aguisanda, F., Álvarez-Varela, A., et al. (2018). Inflammatory cytokine TNF α promotes the long-term expansion of primary hepatocytes in 3D culture. *Cell* 175, 1607–1619. e1615. doi:10.1016/j.cell.2018.11.012
- Pettinato, G., Coughlan, M. F., Zhang, X., Chen, L., Khan, U., Glyavina, M., et al. (2021). Spectroscopic label-free microscopy of changes in live cell chromatin and biochemical composition in transplantable organoids. *Sci. Adv.* 7, eabj2800. doi:10.1126/sciadv.abj2800
- Prior, N., Inacio, P., and Huch, M. (2019). Liver organoids: From basic research to therapeutic applications. *Gut* 68, 2228–2237. doi:10.1136/gutjnl-2019-319256
- Raynaud, P., Tate, J., Callens, C., Cordi, S., Vandersmissen, P., Carpentier, R., et al. (2011). A classification of ductal plate malformations based on distinct pathogenic mechanisms of biliary dysmorphogenesis. *Hepatology* 53, 1959–1966. doi:10.1002/hep.24292
- Ringel, T., Frey, N., Ringnald, F., Janjuha, S., Cherkaoui, S., Butz, S., et al. (2020). Genome-scale CRISPR screening in human intestinal organoids identifies drivers of TGF- β resistance. *Cell Stem Cell* 26, 431–440. doi:10.1016/j.stem.2020.02.007
- Rossi, G., Manfrin, A., and Lutolf, M. P. (2018). Progress and potential in organoid research. *Nat. Rev. Genet.* 19, 671–687. doi:10.1038/s41576-018-0051-9
- Sampaziotis, F., De Brito, M. C., Madrigal, P., Bertero, A., Saeb-Parsy, K., Soares, F. A. C., et al. (2015). Cholangiocytes derived from human induced pluripotent stem cells for disease modeling and drug validation. *Nat. Biotechnol.* 33, 845–852. doi:10.1038/nbt.3275
- Sato, T., Vries, R. G., Snippert, H. J., Van De Wetering, M., Barker, N., Stange, D. E., et al. (2009). Single Lgr5 stem cells build crypt-villus structures *in vitro* without a mesenchymal niche. *Nature* 459, 262–265. doi:10.1038/nature07935
- Schutgens, F., and Clevers, H. (2020). Human organoids: Tools for understanding biology and treating diseases. *Annu. Rev. Pathol.* 15, 211–234. doi:10.1146/annurev-pathmechdis-012419-032611
- Shinozawa, T., Kimura, M., Cai, Y. Q., Saiki, N., Yoneyama, Y., Ouchi, R., et al. (2021). High-fidelity drug-induced liver injury screen using human pluripotent stem cell-derived organoids. *Gastroenterology* 160, 831–846. e10. doi:10.1053/j.gastro.2020.10.002
- Shulman, M., and Nahmias, Y. (2013). Long-term culture and coculture of primary rat and human hepatocytes. *Methods Mol. Biol.* 945, 287–302. doi:10.1007/978-1-62703-125-7_17
- Soret, P. A., Magusto, J., Housset, C., and Gautheron, J. (2020). *In vitro* and *in vivo* models of non-alcoholic fatty liver disease: A critical appraisal. *J. Clin. Med.* 10, E36. doi:10.3390/jcm10010036
- Sorrentino, G., Rezakhani, S., Yildiz, E., Nuciforo, S., Heim, M. H., Lutolf, M. P., et al. (2020). Mechano-modulatory synthetic niches for liver organoid derivation. *Nat. Commun.* 11, 3416. doi:10.1038/s41467-020-17161-0
- Sun, L. L., Wang, Y. Q., Cen, J., Ma, X. L., Cui, L., Qiu, Z. X., et al. (2019). Modelling liver cancer initiation with organoids derived from directly reprogrammed human hepatocytes. *Nat. Cell Biol.* 21, 1015–1026. doi:10.1038/s41556-019-0359-5
- Takebe, T., Sekine, K., Enomura, M., Koike, H., Kimura, M., Ogaeri, T., et al. (2013). Vascularized and functional human liver from an iPSC-derived organ bud transplant. *Nature* 499, 481–484. doi:10.1038/nature12271
- Takebe, T., Sekine, K., Kimura, M., Yoshizawa, E., Ayano, S., Koido, M., et al. (2017). Massive and reproducible production of liver buds entirely from human pluripotent stem cells. *Cell Rep.* 21, 2661–2670. doi:10.1016/j.celrep.2017.11.005
- Takebe, T., Zhang, R. R., Koike, H., Kimura, M., Yoshizawa, E., Enomura, M., et al. (2014). Generation of a vascularized and functional human liver from an iPSC-derived organ bud transplant. *Nat. Protoc.* 9, 396–409. doi:10.1038/nprot.2014.020
- Tao, T., Deng, P., Wang, Y., Zhang, X., Guo, Y., Chen, W., et al. (2021). Microengineered multi-organoid system from hiPSCs to recapitulate human liver-islet Axis in normal and type 2 diabetes. *Adv. Sci.* 9, e2103495. doi:10.1002/adv.202103495
- Telles-Silva, K. A., Pacheco, L., Komatsu, S., Chianca, F., Caires-Junior, L. C., Araujo, B. H. S., et al. (2022). Applied hepatic bioengineering: Modeling the human liver using organoid and liver-on-a-chip technologies. *Front. Bioeng. Biotechnol.* 10, 845360. doi:10.3389/fbioe.2022.845360
- Thomson, J. A., Itskovitz-Eldor, J., Shapiro, S. S., Waknitz, M. A., Swiergiel, J. J., Marshall, V. S., et al. (1998). Embryonic stem cell lines derived from human blastocysts. *Science* 282, 1145–1147. doi:10.1126/science.282.5391.1145
- Trefts, E., Gannon, M., and Wasserman, D. H. (2017). The liver. *Curr. Biol.* 27, R1147–R1151. doi:10.1016/j.cub.2017.09.019
- Turnpenny, P. D., and Ellard, S. (2012). Alagille syndrome: Pathogenesis, diagnosis and management. *Eur. J. Hum. Genet.* 20, 251–257. doi:10.1038/ejhg.2011.181
- Vining, K. H., and Mooney, D. J. (2017). Mechanical forces direct stem cell behaviour in development and regeneration. *Nat. Rev. Mol. Cell Biol.* 18, 728–742. doi:10.1038/nrm.2017.108
- Voog, J., and Jones, D. L. (2010). Stem cells and the niche: A dynamic duo. *Cell Stem Cell* 6, 103–115. doi:10.1016/j.stem.2010.01.011
- Wang, B., Jakus, A. E., Baptista, P. M., Soker, S., Soto-Gutierrez, A., Abecassis, M. M., et al. (2016). Functional maturation of induced pluripotent stem cell hepatocytes in extracellular matrix-A comparative analysis of bioartificial liver microenvironments. *Stem Cells Transl. Med.* 5, 1257–1267. doi:10.5966/sctm.2015-0235
- Wang, S., Wang, X., Tan, Z., Su, Y., Liu, J., Chang, M., et al. (2019). Human ESC-derived expandable hepatic organoids enable therapeutic liver repopulation and pathophysiological modeling of alcoholic liver injury. *Cell Res.* 29, 1009–1026. doi:10.1038/s41422-019-0242-8
- Wiedenmann, S., Breunig, M., Merkle, J., Von Toerne, C., Georgiev, T., Moussus, M., et al. (2021). Single-cell-resolved differentiation of human induced pluripotent stem cells into pancreatic duct-like organoids on a microwell chip. *Nat. Biomed. Eng.* 5, 897–913. doi:10.1038/s41551-021-00757-2
- Wose Kinge, C. N., Bhoola, N. H., and Kramvis, A. (2020). *In vitro* systems for studying different genotypes/sub-genotypes of hepatitis B virus: Strengths and limitations. *Viruses* 12, 353. doi:10.3390/v12030353
- Wu, F., Wu, D., Ren, Y., Huang, Y., Feng, B., Zhao, N., et al. (2019). Generation of hepatobiliary organoids from human induced pluripotent stem cells. *J. Hepatol.* 70, 1145–1158. doi:10.1016/j.jhep.2018.12.028
- Xiong, S., Wang, R. H., Chen, Q., Luo, J., Wang, J. L., Zhao, Z. X., et al. (2018). Cancer-associated fibroblasts promote stem cell-like properties of hepatocellular carcinoma cells through IL-6/STAT3/Notch signaling. *Am. J. Cancer Res.* 8, 302–316.
- Ya, S., Ding, W., Li, S., Du, K., Zhang, Y., Li, C., et al. (2021). On-chip construction of liver lobules with self-assembled perfusable hepatic sinusoid

networks. *ACS Appl. Mat. Interfaces* 13, 32640–32652. doi:10.1021/acsami.1c00794

Yamamura, Y., Asai, N., Enomoto, A., Kato, T., Mii, S., Kondo, Y., et al. (2015). Akt-Girdin signaling in cancer-associated fibroblasts contributes to tumor progression. *Cancer Res.* 75, 813–823. doi:10.1158/0008-5472.CAN-14-1317

Yang, L., Han, Y., Nilsson-Payant, B. E., Gupta, V., Wang, P., Duan, X., et al. (2020). A human pluripotent stem cell-based platform to study SARS-CoV-2 tropism and model virus infection in human cells and organoids. *Cell Stem Cell* 27, 125–136. e127. doi:10.1016/j.stem.2020.06.015

Younossi, Z., Tacke, F., Arrese, M., Chander Sharma, B., Mostafa, I., Bugianesi, E., et al. (2019). Global perspectives on nonalcoholic fatty liver

disease and nonalcoholic steatohepatitis. *Hepatology* 69, 2672–2682. doi:10.1002/hep.30251

Yuki, K., Cheng, N., Nakano, M., and Kuo, C. J. (2020). Organoid models of tumor immunology. *Trends Immunol.* 41, 652–664. doi:10.1016/j.it.2020.06.010

Zhan, T. Z., Rindtorff, N., Betge, J., Ebert, M. P., and Boutros, M. (2019). CRISPR/Cas9 for cancer research and therapy. *Semin. Cancer Biol.* 55, 106–119. doi:10.1016/j.semcancer.2018.04.001

Zhao, B., Ni, C., Gao, R., Wang, Y., Yang, L., Wei, J., et al. (2020). Recapitulation of SARS-CoV-2 infection and cholangiocyte damage with human liver ductal organoids. *Protein Cell* 11, 771–775. doi:10.1007/s13238-020-00718-6



Patient-Derived Organoid Facilitating Personalized Medicine in Gastrointestinal Stromal Tumor With Liver Metastasis: A Case Report

Ying Cao¹, Xi Zhang², Qianyun Chen², Xi Rao², Enming Qiu², Gang Wu³, Yu Lin⁴, Ziqi Zeng⁴, Bin Zheng⁵, Zhou Li², Zhai Cai², Huaiming Wang⁶ and Shuai Han^{2*}

¹ The Second School of Clinical Medicine, Southern Medical University, Guangzhou, China, ² Department of Gastrointestinal Surgery, General Surgery Center, Zhujiang Hospital, The Second Affiliated Hospital of Southern Medical University, Guangzhou, China, ³ Department of Oncology, Zhujiang Hospital, The Second Affiliated Hospital of Southern Medical University, Guangzhou, China, ⁴ Department of Pathology, Zhujiang Hospital, The Second Affiliated Hospital of Southern Medical University, Guangzhou, China, ⁵ Guangdong Research Center of Organoid Engineering and Technology, Accurate International Biotechnology Company, Guangzhou, China, ⁶ Department of Colorectal Surgery, The Sixth Affiliated Hospital of Sun Yat-sen University, Guangzhou, China

OPEN ACCESS

Edited by:

Xiangsong Wu,
Shanghai Jiao Tong University School
of Medicine, China

Reviewed by:

Jinhui Zhu,
Zhejiang University, China
Zizhen Zhang,
Shanghai Jiao Tong University, China
Yijian Zhang,
Shanghai Jiao Tong University, China

*Correspondence:

Shuai Han
gzhanbo0624@smu.edu.cn

Specialty section:

This article was submitted to
Cancer Molecular Targets
and Therapeutics,
a section of the journal
Frontiers in Oncology

Received: 15 April 2022

Accepted: 04 May 2022

Published: 02 August 2022

Citation:

Cao Y, Zhang X, Chen Q, Rao X, Qiu E,
Wu G, Lin Y, Zeng Z, Zheng B, Li Z,
Cai Z, Wang H and Han S (2022)
Patient-Derived Organoid Facilitating
Personalized Medicine in
Gastrointestinal Stromal Tumor With
Liver Metastasis: A Case Report.
Front. Oncol. 12:920762.
doi: 10.3389/fonc.2022.920762

The gastrointestinal stromal tumors (GIST) are a rare gastrointestinal tract malignancy. The two primary mutation sites are found in KIT and platelet-derived growth factor receptor- α (PDGFR- α) genes. The current study reports on a point mutation within the exon 11 of KIT, named KIT p.V560E. Patient-derived organoids (PDOs) are potential 3D *in vitro* models of tissues that can be used to identify sensitivity toward specific targets in patients with tumors and allow for personalized medicine when drugs specific for newly identified genetic locus mutations are not yet available. This study describes a 68-year-old patient who complained of diffused abdominal pain and intermittent melena lasting more than 10 days. He has no other gastrointestinal abnormalities, prior abdominal surgery, or related family history. Surgery was conducted first to remove the lesions and ascertain the disease through histology and immunohistochemical stains of the mass. Immunohistochemistry revealed that the tumor was positive for CD117 and Dog-1. Based on the above findings, he was diagnosed with GISTs. Gene detection analysis and organoid culture were then performed to verify clinical decisions. KIT p.V560E and the reduced number of RB1 copies were identified as two obvious mutations, so the patient was administrated first-line treatment of imatinib 400 mg/d. However, progressive disease prompted us to switch to sunitinib, and his condition gradually improved. Meanwhile, organoid culture showed sensitivity to sunitinib and tolerance to imatinib with half-maximal inhibitory concentration (IC50) values of 0.89 and >20, respectively. In summary, to the best of our knowledge, this is the first time that the established organoid culture indicated that the GISTs organoid could identify the sensitivity to target therapies and facilitate individual-based treatment.

Keywords: gastrointestinal stromal tumor, patient-derived organoid, KIT exon 11 mutations, p.V560E, personalized medicine

INTRODUCTION

As the most common mesenchymal gastrointestinal tumors, gastrointestinal stromal tumors (GISTs) account for 0.1%–3% of all gastrointestinal tract malignancy (1). GISTs are considered to originate from the interstitial cells of Cajal (ICC), the pacemaker for the peristaltic movement of the gastrointestinal tract (2, 3). These tumors are primarily the result of KIT mutations and/or platelet-derived growth factor receptor- α (PDGFR- α) mutations which activate downstream signaling and cytogenetic changes that promote tumor occurrence and progression (4). CD117 and CD34 are expressed in approximately 95% and 80% of GISTs, respectively (5) and later discovered on gastrointestinal stromal tumor 1 (Dog-1), also suggested to be a positive diagnostic marker in pathological immunohistochemistry (6). Both immunohistochemical panel (CD117/Dog-1) and molecular analysis (KIT/PDGFR- α), the gold standard, make it possible to accurately diagnose GISTs (7). The stomach (51%), the small intestine (36%), and the colon (7%) are the most common pathological entities of GISTs (8); additionally, they usually metastasize inside the abdominal cavity like the liver (50%–60%) and peritoneum (20%–43%) (9). Patients with GISTs exhibit symptoms like gastrointestinal bleeding (hematemesis, anemia, and azotemia), tiredness, abdominal pain, or intestinal obstruction (2). Current ESMO-EURACAN-GENTURIS Clinical Practice Guidelines have reached a consensus on the management of GISTs: surgical/endoscopic resection is the standard approach to tumors ≥ 2 cm in size, and active surveillance is suggested when the evidence for diagnosis is inadequate. Imatinib is the standard treatment for patients whose stromal tumors have progressed locally, metastasized, or are inoperative. It is also recommended for patients who well tolerated imatinib and with all the lesions removed postoperation (10). While patients with the PDGFR- α exon 18 D842V-mutation are not as sensitive to imatinib, they are significantly more responsive to this drug than to avapritinib (11). When patients are intolerant to imatinib or having advanced disease, sunitinib as the standard second-line therapy (50 mg/d 4 weeks on/2 weeks off) was approved by the Food and Drug Administration (FDA) (12). Additionally, patients with c-KIT exon 9 mutations may gain more benefits from sunitinib than imatinib treatment (13).

The novel *in vitro* 3D culture technologies, patient-derived organoids (PDOs), offer us more opportunities to study human cancer models physiologically. Even with the increased development of targeted regimens and immunotherapies for cancer, relief and recovery from tumors remain a significant challenge. Current animal models cannot perfectly mirror human tumors, simulate progression, or identify genetic

heterogeneity, making it difficult to translate findings into clinical practice (14). Therefore, patient-derived cancer organoids are being prioritized for use in guiding personalized medicine. Thus far, no precedents have reported the utilization of PDOs to test the sensitivity toward KIT-targeted inhibitors in patients with GISTs. The current case report describes a GIST patient with liver metastasis and identifies a role for PDO in optimizing treatment and informing clinical decision-making.

CASE PRESENTATION

A 68-year-old man with a diagnosis of primary hypertension presented to the general surgery department on August 24, 2021 for diffused abdominal pain and intermittent melena lasting more than ten days. The man denied other gastrointestinal abnormalities, prior abdominal surgery, or related family history. Abdominal tenderness, especially in the epigastric, tenderness without rebound tenderness or Murphy's sign was observed in the physical examination on admission. His blood test results revealed that he was anemic, with red blood cell (RBC), hemoglobin (Hb), hematocrit value (Hct), and mean corpuscular hemoglobin concentration (MCHC) of $3.3 \times 10^{12}/L$ [normal range $(4.3\text{--}5.8) \times 10^{12}/L$], 94 g/L (normal range, 130–175 g/L), 0.3 L/L (normal range, 0.4–0.5 L/L), and 312 g/L (normal range, 316–354 g/L), respectively. Liver and kidney function and electrolyte levels showed results within the normal range. In addition, no abnormality was observed in his serum levels of carbohydrate antigen (CA) 199 was 9 KU/L (normal range, <34 KU/L) and carcinoembryonic antigen (CEA) was 1.1 ng/ml (normal range, ≤ 5 ng/ml). A computed tomography (CT) scan indicated small liver lesions with multiple hypodense nodules about 30–33 Hu value, and in contrast-enhanced CT observed ring-shaped enhanced nodules with a maximum diameter of 17 mm (**Figure 1A**). The CT report considered liver cirrhosis and possible liver metastases that required confirmation based on clinical symptoms and other examination results. The capsule endoscopy found an ulcerated bulge covered with yellow-white digesta and bloodstains (**Supplementary Figures 1A–C**). Narrowing of the intestinal lumen required a slow descending of capsule endoscopy, delaying and terminating intestinal inspection. Additionally, abundant fresh blood was visible beside the bulge. Abdominal plain film examination revealed no expansion of the enteric cavity, gas-fluid, or subphrenic air.

Surgery of resecting intestinal and liver metastases was conducted on September 1, 2021 to conduct a hemostasia operation and ascertain the disease through pathological and immunohistochemical stains of the small intestine and liver masses: GIST (small intestine, liver), high risk, and mitotic $>10/50$ HPF. Immunohistochemistry results were CD117 (+), Dog-1 (+), smooth muscle actin (+), Vim (+), CK (–), CD34 (–), and SOX-10 (–) (**Figures 2A–D**). Meanwhile, gene detection and organoid culture were performed to verify the clinical diagnosis. Targeted genetic tests using next-generation sequencing of the resected tumors from the small intestine and liver were performed to clarify somatic gene mutation: we observed two significant gene

Abbreviations: GIST, gastrointestinal stromal tumor; PDGFR- α , platelet-derived growth factor receptor- α ; PDOs, patient-derived organoids; ICC, interstitial cells of Cajal; Dog-1, discovered on gastrointestinal stromal tumor 1; RBC, red blood cell; Hb, hemoglobin; Hct, hematocrit value; MCHC, mean corpuscular hemoglobin concentration; CA, carbohydrate antigen; CEA, carcinoembryonic antigen; TMB, tumor mutational burden; Muts/Mb, mutational loads per million bases; IC, inhibitory concentration; MSS, microsatellite stable; mTOR, mammalian target of rapamycin.

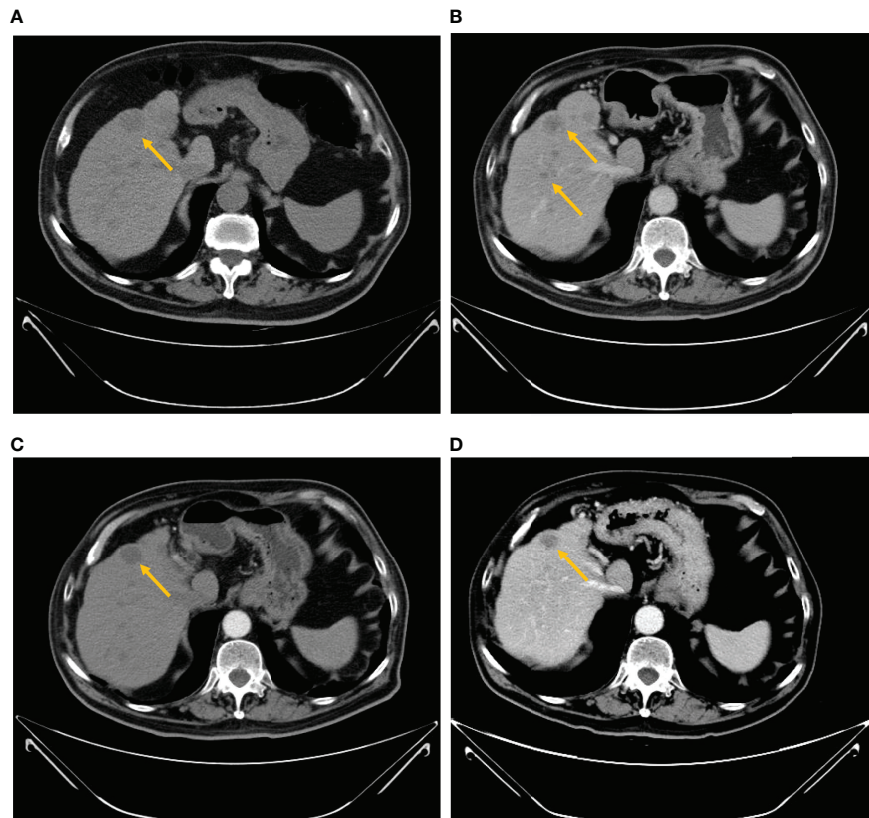


FIGURE 1 | Abdominal computed tomography scan. **(A)** The baseline CT scan performed on August 26, 2021 showed multiple large hypodense lesions in the liver. Contrast-enhanced CT showed ring-shaped enhanced nodules with the maximum diameter of 17 mm. **(B)** After 2 months of treatment with imatinib, a CT scan was performed on October 25, 2021, a relapse of disease (growth of the longest lesion's diameter from 17 to 25 mm) of the hepatic lesion and multiple hepatic metastases with slight reinforcement was observed. **(C)** The venous phase of the CT scan performed on November 25, 2021 demonstrated decreased hypodense lesions (growth of the longest lesion's diameter from 25 to 23 mm) with peripheral rim enhancement. **(D)** After two cycles of sunitinib, a CT scan was performed on January 19, 2022 and revealed a smaller, irregular hypodense intrahepatic metastatic mass.

mutations, KIT p.V560E and the reduced number of RB1 copies. KIT p.V560E indicated that the valine in the 560 codon of the KIT gene was mutated to glutamate, and it was within the exon 11 of KIT, and KIT mutation accounts for 60% of GISTs (**Supplementary Figures 2A, B**) (15). We also analyzed the sensitivity and applicability to immunotherapy: microsatellite stable; microsatellite instability where the tumor mutational burden (TMB) was rated medium of 2.23 Muts/Mb (mutational load per million bases), lower than 57% of patients with GISTs (small intestine); and no mismatch-repair gene deficiency detected (**Supplementary Figures 2C, D**).

Subsequently, we also established the organoid model with small intestinal during surgical resection (**Supplementary Figures 3A–C**) to assess the drug response to currently widely used KIT-targeted drugs (16). The liver organoid was also cocultured but the cell viability was inferior to the small intestinal organoid. The genetic testing results obtained from the small intestine and liver had the same gene mutation sites, so the small intestine organoid could predict treatment response that corresponded with the patient. Briefly, the patient tumor tissue

was minced and digested into small cell clusters (**Supplementary Figure 3A**) and passed through a 70- μ m filter. The cell suspension was then mixed with the Matrigel matrix (Corning Inc, Corning, NY), transferred to a culture plate, and incubated at 37°C and 5% CO₂ cell culture incubator for 30 min. On complete gelation, the culture medium was added and cultured until enough PDOs were formed (**Supplementary Figures 3B, C**). Both the hematoxylin-eosin and immunochemical staining demonstrated that cultured PDOs retained key phenotypic characteristics of the parent GISTs like nuclear pleomorphism, mitotic rate, and immunoreactive profiles (**Supplementary Figures 3D, E**). The maximal tumor inhibition was 98.89% for sunitinib and 99.28% inhibition for regorafenib. The drug sensitivity of GIST-PDO against widely used target drugs including imatinib, sunitinib, and regorafenib was examined. To compare the drug sensitivities of the tested drugs, the relative half-maximal inhibitory concentration (IC₅₀) of each drug was determined using the “Accurate drug sensitivity cut-off database.” The IC₅₀ of each drug can be divided into sensitive (0–0.5), undefined (0.5–1), and resistant (>1) groups. The concentration–response curves manifested that PDOs were

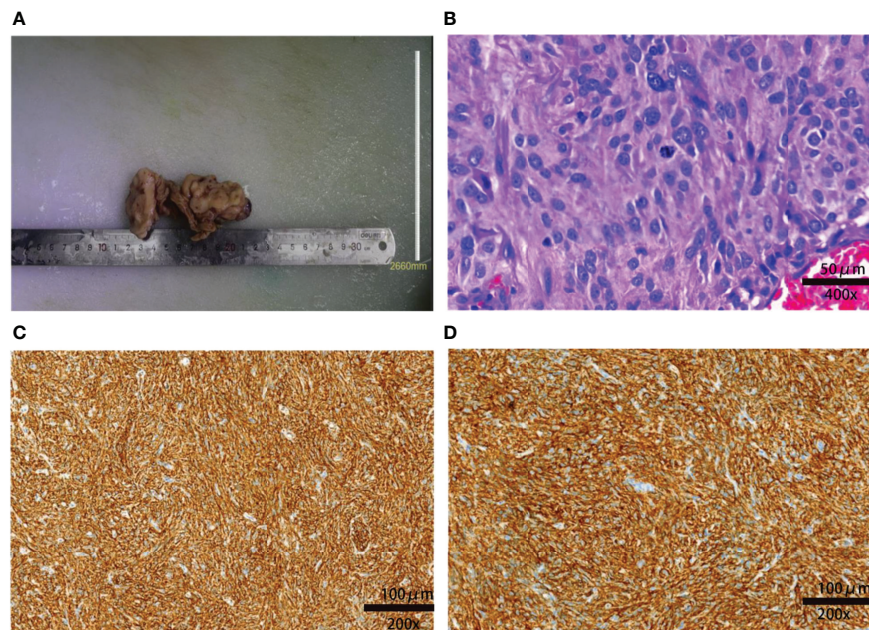


FIGURE 2 | Macroscopic and microscopic findings of the resected tumor. **(A)** The resected specimen of the small intestine measured $10 \times 5 \times 2$ cm. **(B)** Postoperative pathology indicated that the tumor was a high-risk GIST: the lesion had significant nuclear pleomorphism with mitotic $>10/50$ HPF (hematoxylin and eosin staining). The spindle or ovoid cells are deeply stained with coarse chromatin and obvious atypia ($\times 400$). **(C)** Immunochemical staining showing that the tissue was CD117+ ($\times 200$). **(D)** Immunochemical staining showing that the tissue Dog-1+ ($\times 200$).

resistant to both imatinib (IC_{50} : $>20\times$) and regorafenib (IC_{50} : $1.57\times$), and sensitive to sunitinib (IC_{50} : $0.89\times$) (**Figure 3**). Although regorafenib has a cytotoxic effect on neoplastic cells, it was not recommended to the patient, as its IC_{50} surpassed $1\times$, and sunitinib was ranked the optimal regimen according to the PDOs results. Notwithstanding, we administrated imatinib 400 mg daily to the patient a week postoperation, the standard first-line

treatment FDA-approved treatment. Approximately 2 months later, the patient complained of epigastric pain and CT indicated more enlarged nodules with a maximum diameter of 25 mm, increased parietal thickness, and increasing nodules (**Figure 1B**). Thus, the therapy was switched to sunitinib (continuous 50 mg/d for 4 weeks with a 2-week interval) on November 1, 2021. CT demonstrated a well-defined, shrunk homogeneous soft-tissue

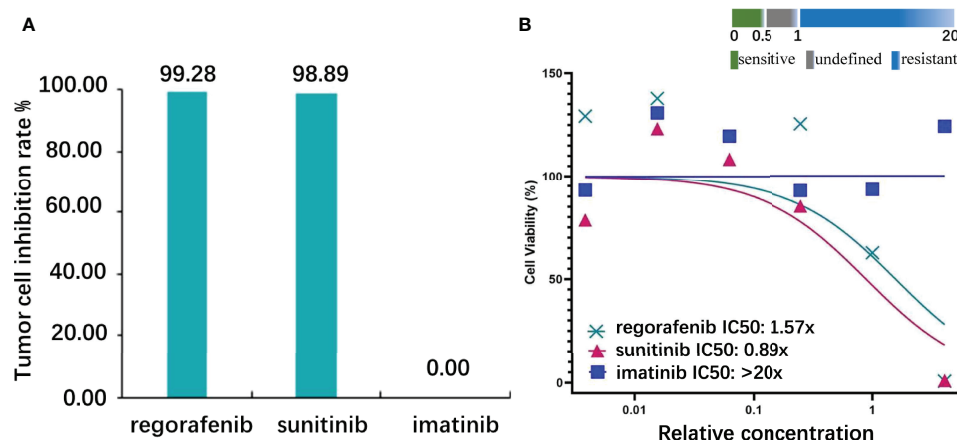


FIGURE 3 | Target drug susceptibilities. **(A)** The inhibition rate of the highest concentration: regorafenib, sunitinib, and imatinib were 99.28, 98.89, and 0.00, respectively (the control cells received no treatment, and the cell viability was 100%). **(B)** Half-maximal inhibitory concentration (IC_{50}): regorafenib, sunitinib, and imatinib were 1.57, 0.89, and >20 , respectively (definition: sensitive, $IC_{50}<0.5$; undefined, $0.5<IC_{50}<1$; resistant, $IC_{50}>1$).

mass on November 25, 2021 (**Figure 1C**). By Jan 19, 2022, CT scans showed partial lesion absorption (**Figure 1D**). The patient expressed abdominal pain relief demonstrating that he had experienced a partial response (PR). During the whole diagnosis and treatment periods, his CA199 and CEA remained normal. The diagnosis and treatment strategy timeline schematic is presented in **Figure 4**.

DISCUSSION

The first application of organoid culture in 2009 (17) opened a new era for cancer research by allowing researchers and clinicians to observe the tumors' biological features, discover novel biomarkers, and improve personalized treatments. Organoids derived from surgical procedures or tumor biopsies can inform clinical decision-making by providing a mechanism for reliably testing drug sensitivity and IC50 value (18). Meanwhile, large cohorts and randomized controlled trials can then be used to validate the results of organoids or, paralleled with genetic testing, to implement individualized cancer therapy.

Here, we report a case of a patient of GIST with liver metastasis whose response to treatment matched the intestine organoid culture results. Surgical resection (reaching the greatest extent possible) and segmental liver resection with laparoscopic surgery were recommended as the first therapeutic option in order to eliminate the possible life-threatening symptom of melena, determine the accuracy of the diagnosis using histological and immunohistochemical stains of the tumor, activate cancer cells' sensitivity to adjuvant therapy as a result of the decreased tumor load, and preserve tumor tissue for organoid development to assist clinical decision-making (19). Regular postoperation monitoring and supplementary target therapy are essential for a better prognosis. A retrospective study reported that resection of liver metastases in GIST patients combined with imatinib may lead to improved prognosis with 1- and 3-year progression-free survival of 93% and 67% respectively (20). The case reported here was not appropriate for immunotherapy: because he was microsatellite stable (MSS), had a medium TMB, and was no mismatch-repair gene deficient. A high TMB may be associated with a positive response to immunotherapy, but the cutoff point is dependent on where cancer originated (21, 22). The TMB of our patient was lower than 57% of small intestinal GIST patients. Molecular genotyping results demonstrated that mismatch-repair deficient or

microsatellite instability-high colorectal cancer have adequate immune activation required to respond with immunotherapeutic agents (23, 24). Therefore, imatinib 400 mg/d was administrated to the patient as the standard first-line therapy, however, GIST progression was observed a month later. Research indicates that patients with KIT exon 11 mutation appeared to benefit less than those with the KIT exon 9 mutation when imatinib is increased to 800 mg/d to halt disease progression (25). As a result, the case reported here was switched to sunitinib 50 mg/d for 4 weeks followed by a 2-week rest (26). The patient's right epigastrium pain was relieved after being administrated with sunitinib, and CT scans revealed the presence of homogeneous shrunk lesions.

In this case report, we sought to explore the reasons for liver metastases' recurrence and disease progression. On the one hand, several studies have confirmed that KIT-associated tumors progression when combined with additional sporadic mutations (27, 28), such as the decreased RB1 copies seen in this case. This could potentially incur GISTs' metastasis in the liver. On the other hand, it was expected that imatinib treatment would improve recurrence-free and overall survival of this high-risk patient (29). Instead, the KIT p.V560E appeared to incur resistance to imatinib, a finding not reported previously. Generally, it is acknowledged that KIT exon 9 mutations or GIST without PDGFR- α or KIT mutations are more likely to acquire resistance than KIT exon 11 mutations, accounting to 10% of advanced GISTs patients (30, 31). Our patient's gene detection reported KIT p.V560E, whose valine in the 560 codon of the KIT exon 11 gene was mutated to glutamate. A previous study found that motesanib could inhibit autophosphorylation of KIT mutants V560D more potently than imatinib in transfected Ba/F3 cells, with IC50 values of 3 and 7 nM, respectively (32). In our case, we consider that sunitinib could exhibit superior efficacy than imatinib, with IC50 values of 0.89 and >20, respectively. The possible mechanical explanation could be that mutated glutamate changed the juxtamembraneous domain of KIT, small sunitinib may bind to the ATP-binding pocket of the KIT protein, and this gatekeeper mutation hindered the incorporation of large imatinib (33).

Of note, the postoperative efficacy of the chosen drugs was consistent with the results obtained from suggesting that tumor organoids could inform treatment decisions because they could retain the original cancer gene mutation. Other examples of successful organoid use are evident in the literature. A recent case of oligometastatic colorectal cancer, for example, underwent surgical resection and followed systemic FOLFOX treatment

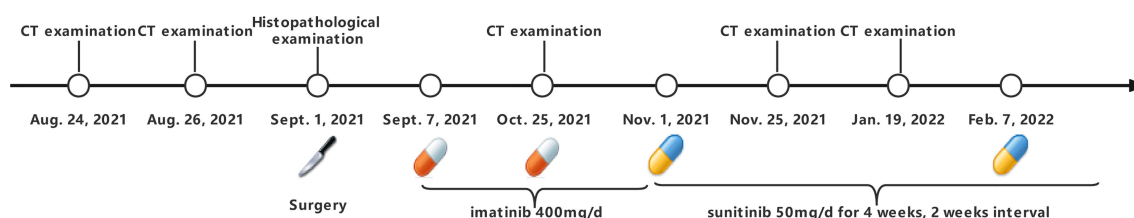


FIGURE 4 | Timeline of the diagnostic and therapeutic process.

regimen. However, the prognosis was not as expected; the patient relapsed and a clinical decision was made to switch to 5-fluorouracil and SN-38 treatment based on pharmacologic organoid screening. The case exhibited promising tumor shrinkage and experienced a partial recovery, and this case could inform us of the organoids' role in drug sensitivity testing, supporting personalized clinical choice (18). Vlachogiannis et al. used a living biobank of patient-derived organoids collected from pretreated metastatic colorectal and gastroesophageal cancer tissues to identify PDOs' credibility to predict clinical efficacy (34). The results were courageous because PDOs could recapitulate original tumor mutations and match drug monitoring susceptibility of the patient.

Current treatments focus on precise and individualized medicine for different genome and transcriptome landscapes, lifestyles, and progressive disease courses. The novel prominent choice, gene-targeting therapy, emerged to be powerful; however, not all patients could gain the expected effect of the recommended target drugs (35), as our patient reported above. Exact explanations from theoretical mechanisms remain challenging. In general, patient-derived organoids could potentially compensate for this gap through their ability to retain the original mutation of the patient tumor and recapitulate drug responses. Organoid culture results could be a promising supplement or alternative to gene detection; moreover, it can be used to elucidate possible genetic alterations linked to drug resistance. For example, if a patient acquires secondary resistance to sunitinib and the combination of sunitinib, its downstream signaling, mammalian target of rapamycin (mTOR) may be a promising strategy (36). Notwithstanding credible efficacy data, we could utilize the organoid culture technology to provide preliminary validation.

While PDOs encountered dramatic progression in clinical therapy over the past decade, their intrinsic property limited their advance. Because the tissues or tumors are acquired from the individual patient, heterogeneity can attribute to diverse treatment options that make consensus a challenge. Besides, not all tumors could adapt to the external environment or retain their original mutations *in vitro* (37). Growth rates varied among different tumor tissues and some tumors, such as breast cancer, may take 6 months to become organoids (38), so fastened culture processes despite neoplasms' histological type are urgently needed. Additionally, it is critical to maintain the primary genetics of the tumor. Maintaining primary genetics is foremost. In the future, standardization of organoid culture and identification process, improvement of culture success rate, accurate drug sensitivity detection methods, and optimization of drug sensitivity related parameters still need to be ascertained; especially, large cohort clinical trials are essential to validate the patient-tailored treatment. We believe that following additional clinical observational and interventional studies, the organoid models will inevitably be regularly used to improve the cancer therapy and patients' quality of life.

In conclusion, this study describes the first reported use of GISTs' organoids to identify sensitivity to target drugs and facilitate individual-based treatment. The results indicated that GISTs with KIT p.V560E may be more sensitive to sunitinib than imatinib, suggesting that sunitinib may be a preferred treatment in

the treatment of GISTs with KIT p.V560E. Furthermore, our study demonstrated that GIST-PDO could represent a faithful tumor model and validate drug responses *in vivo*; it may be promising to combine current guidelines with PDO results before initiating treatment to elucidate possibly the most appropriate regimens and advance precision cancer medicine.

DATA AVAILABILITY STATEMENT

The original contributions presented in the study are included in the article/**Supplementary Material**. Further inquiries can be directed to the corresponding author.

ETHICS STATEMENT

Written informed consent was obtained from the individual(s) for the publication of any potentially identifiable images or data included in this article.

AUTHOR CONTRIBUTIONS

Material preparation and data analysis were performed by XZ, EQ, and GW. The first draft of the manuscript was written by YC, QC, XR, and HW. ZL, ZC, GW, and SH treated the patient. BZ and his affiliated company conducted the organoids culture. SH is the guarantor of this work and, as such, had full access to all of the data in the study and takes responsibility for the integrity of the data and the accuracy of the data analysis. All authors contributed to the article and approved the submitted version.

ACKNOWLEDGMENTS

We would like to thank the patient who voluntarily took part in the study, as well as the Accurate International Biotechnology (Guangzhou) Company for the technical support in organoid culture. We thankfully acknowledge Yaoyu Chen and Mengli Huang from 3D Medicine Genetic Testing Center for their technical support.

SUPPLEMENTARY MATERIAL

The Supplementary Material for this article can be found online at: <https://www.frontiersin.org/articles/10.3389/fonc.2022.920762/full#supplementary-material>

Supplementary Figure 1 | Capsule endoscopy. (A) A swelling mass found in the upper small intestine. **(B)** Local ulceration, including abundant fresh blood, yellow-white digesta and food scraps were observed. **(C)** Narrow intestinal lumen delayed observation of the capsule endoscopy. The capsule remained in the middle part of the small intestine so the examination was not completed.

Supplementary Figure 2 | Results of genetic testing. **(A)** KIT 560point mutation identified in next-generation sequence read from tumor tissue: the novel point mutation (V to E) was identified within the KIT gene. (V=Val=Valine; E=Glu=Glutamic acid) **(B)** Gene copy number changes in this patient's sample: no mutations of clinical significance were observed. (The horizontal axis represents the location of the chromosomes. The vertical axis represents next-generation sequencing (NGS)-based copy number variant (CNV) detection for the analyzed tumor sample). **(C)** MSS: the patient's MSI score was much lower than the cutoff. **(D)** TMB was 2.23Muts/Mb, lower than 57% small intestinal GIST patients. (TMB is defined as

mutational load per million bases (Mb) in tumor within targeting coding regions. high: 0-25% medium; 26-75% low; 76%-100%).

Supplementary Figure 3 | Images of organoid culture cells. **(A)** The patient tumor tissue was minced and digested into small cell clusters. **(B, C)** Microscopic image of culture cells showing an intermediate proliferation rate and activity. There were 2000 tumor organoids with the average diameter of 41.11µm. **(D)** Hematoxylin and eosin staining of culture cells. (× 400). **(E)** Immunochemical staining showing that Dog-1 was positive. (× 400).

REFERENCES

- Navarrete A, Momblan D, Almenara R, Lacy A. Giant Gastric Gastrointestinal Stromal Tumor (GIST). *J Gastrointest Surg* (2017) 21:202–4. doi: 10.1007/s11605-016-3196-x
- Akahoshi K, Oya M, Koga T, Shiratsuchi Y. Current Clinical Management of Gastrointestinal Stromal Tumor. *World J Gastroenterol* (2018) 24:2806–17. doi: 10.3748/wjg.v24.i26.2806
- Yi JH, Sim J, Park BB, Lee YY, Jung WS, Jang HJ, et al. The Primary Extra-Gastrointestinal Stromal Tumor of Pleura: A Case Report and a Literature Review. *Jpn J Clin Oncol* (2013) 43:1269–72. doi: 10.1093/jjco/hyt158
- Heinrich MC, Corless CL, Duensing A, McGreevey L, Chen CJ, Joseph N, et al. PDGFRA Activating Mutations in Gastrointestinal Stromal Tumors. *Science* (2003) 299:708–10. doi: 10.1126/science.1079666
- He JP, Feng JX. CD117 is Not Always Positive in Infantile Gastrointestinal Stromal Tumor. *World J Pediatr* (2018) 14:100–3. doi: 10.1007/s12519-018-0123-0
- Miettinen M, Wang ZF, Lasota J. DOG1 Antibody in the Differential Diagnosis of Gastrointestinal Stromal Tumors: A Study of 1840 Cases. *Am J Surg Pathol* (2009) 33:1401–8. doi: 10.1097/PAS.0b013e3181a90e1a
- Wu CE, Tzen CY, Wang SY, Yeh CN. Clinical Diagnosis of Gastrointestinal Stromal Tumor (GIST): From the Molecular Genetic Point of View. *Cancers (Basel)* (2019) 11(5):679. doi: 10.3390/cancers11050679
- Tran T, Davila JA, El-Serag HB. The Epidemiology of Malignant Gastrointestinal Stromal Tumors: An Analysis of 1,458 Cases From 1992 to 2000. *Am J Gastroenterol* (2005) 100:162–8. doi: 10.1111/j.1572-0241.2005.40709.x
- Ozan E, Oztekin O, Alacacioglu A, Aykas A, Postaci H, Adibelli Z. Esophageal Gastrointestinal Stromal Tumor With Pulmonary and Bone Metastases. *Diagn Interv Radiol* (2010) 16:217–20. doi: 10.4261/1305-3825.DIR.1861-08.2
- Casali PG, Blay JY, Abecassis N, Bajpai J, Bauer S, Biagini R, et al. Gastrointestinal Stromal Tumours: ESMO-EURACAN-GENTURIS Clinical Practice Guidelines for Diagnosis, Treatment and Follow-Up. *Ann Oncol* (2022) 33:20–33. doi: 10.1016/j.annonc.2021.09.005
- Dhillon S. Avapritinib: First Approval. *Drugs* (2020) 80:433–9. doi: 10.1007/s40265-020-01275-2
- Adams VR, Leggas M. Sunitinib Malate for the Treatment of Metastatic Renal Cell Carcinoma and Gastrointestinal Stromal Tumors. *Clin Ther* (2007) 29:1338–53. doi: 10.1016/j.clinthera.2007.07.022
- Parab TM, DeRogatis MJ, Boaz AM, Grasso SA, Issack PS, Duarte DA, et al. Gastrointestinal Stromal Tumors: A Comprehensive Review. *J Gastrointest Oncol* (2019) 10:144–54. doi: 10.21037/jgo.2018.08.20
- Olson B, Li Y, Lin Y, Liu ET, Patnaik A. Mouse Models for Cancer Immunotherapy Research. *Cancer Discov* (2018) 8:1358–65. doi: 10.1158/2159-8290.CD-18-0044
- Bachet JB, Hostein I, Le Cesne A, Brahimi S, Beauchet A, Tabone-Eglinger S, et al. Prognosis and Predictive Value of KIT Exon 11 Deletion in GISTs. *Br J Cancer* (2009) 101:7–11. doi: 10.1038/sj.bjc.6605117
- Wang T, Pan W, Zheng H, Zheng H, Wang Z, Li JJ, et al. Accuracy of Using a Patient-Derived Tumor Organoid Culture Model to Predict the Response to Chemotherapy Regimens in Stage IV Colorectal Cancer: A Blinded Study. *Dis Colon Rectum* (2021) 64:833–50. doi: 10.1097/DCR.0000000000001971
- Sato T, Vries RG, Snippert HJ, van de Wetering M, Barker N, Stange DE, et al. Single Lgr5 Stem Cells Build Crypt-Villus Structures *In Vitro* Without a Mesenchymal Niche. *Nature* (2009) 459:262–5. doi: 10.1038/nature07935
- Mauri G, Durinikova E, Amatu A, Tosi F, Cassingena A, Rizzetto F, et al. Empowering Clinical Decision Making in Oligometastatic Colorectal Cancer: The Potential Role of Drug Screening of Patient-Derived Organoids. *JCO Precis Oncol* (2021) 5:PO.21.00143. doi: 10.1200/PO.21.00143
- Li Q, Xu X, Su D, Zhou T, Wang G, Li Z. Long-Term Survival of an Elderly Patient With Advanced Gastric Cancer After Combination Therapy: A Case Report and Literature Review. *BMC Cancer* (2019) 19:459. doi: 10.1186/s12885-019-5683-4
- Seesing MF, Tielen R, van Hillegersberg R, van Coevorden F, de Jong KP, Nagtegaal ID, et al. Resection of Liver Metastases in Patients With Gastrointestinal Stromal Tumors in the Imatinib Era: A Nationwide Retrospective Study. *Eur J Surg Oncol* (2016) 42:1407–13. doi: 10.1016/j.ejso.2016.02.257
- Hu CT, Zhou YC, Zu LD, Fu GH, Li Q. High Tumor Mutation Burden in a Patient With Metastatic Gastric Cancer Sensitive To Trastuzumab: A Case Report. *Ann Palliat Med* (2021) 10:5846–52. doi: 10.21037/apm-20-132
- Samstein RM, Lee CH, Shoushtari AN, Hellmann MD, Shen R, Janjigian YY, et al. Tumor Mutational Load Predicts Survival After Immunotherapy Across Multiple Cancer Types. *Nat Genet* (2019) 51:202–6. doi: 10.1038/s41588-018-0312-8
- Kreidieh M, Mukherji D, Temraz S, Shamseddine A. Expanding the Scope of Immunotherapy in Colorectal Cancer: Current Clinical Approaches and Future Directions. *BioMed Res Int* (2020) 2020:9037217. doi: 10.1155/2020/9037217
- Puccini A, Battaglin F, Iaia ML, Lenz HJ, Salem ME. Overcoming Resistance to Anti-PD1 and Anti-PD-L1 Treatment in Gastrointestinal Malignancies. *J Immunother Cancer* (2020) 8(1):e000404. doi: 10.1136/jitc-2019-000404
- Blanke CD, Rankin C, Demetri GD, Ryan CW, von Mehren M, Benjamin RS, et al. Phase III Randomized, Intergroup Trial Assessing Imatinib Mesylate at Two Dose Levels in Patients With Unresectable or Metastatic Gastrointestinal Stromal Tumors Expressing the Kit Receptor Tyrosine Kinase: S0033. *J Clin Oncol* (2008) 26:626–32. doi: 10.1200/JCO.2007.13.4452
- Poveda A, Garcia DMX, Lopez-Guerrero JA, Cubedo R, Martinez V, Romero I, et al. GEIS Guidelines for Gastrointestinal Sarcomas (GIST). *Cancer Treat Rev* (2017) 55:107–19. doi: 10.1016/j.ctrv.2016.11.011
- Meir M, Maurus K, Kuper J, Hankir M, Wardelmann E, Rosenwald A, et al. The Novel KIT Exon 11 Germline Mutation K558N is Associated With Gastrointestinal Stromal Tumor, Mastocytosis, and Seminoma Development. *Genes Chromosomes Cancer* (2021) 12:827–32. doi: 10.1002/gcc.22988
- Kikuchi H, Miyazaki S, Setoguchi T, Hiramatsu Y, Ohta M, Kamiya K, et al. Rapid Relapse After Resection of a Sunitinib-Resistant Gastrointestinal Stromal Tumor Harboring a Secondary Mutation in Exon 13 of the C-KIT Gene. *Anticancer Res* (2012) 32:4105–9.
- DeMatteo RP, Ballman KV, Antonescu CR, Corless C, Kolesnikova V, von Mehren M, et al. Long-Term Results of Adjuvant Imatinib Mesylate in Localized, High-Risk, Primary Gastrointestinal Stromal Tumor: ACOSOG Z9000 (Alliance) Intergroup Phase 2 Trial. *Ann Surg* (2013) 258:422–9. doi: 10.1097/SLA.0b013e3182a15eb7
- Casali PG, Abecassis N, Aro HT, Bauer S, Biagini R, Bielack S, et al. Gastrointestinal Stromal Tumours: ESMO-EURACAN Clinical Practice Guidelines for Diagnosis, Treatment and Follow-Up. *Ann Oncol* (2018) 29:v68–78. doi: 10.1093/annonc/mdy095
- Blay JY, Kang YK, Nishida T, von Mehren M. Gastrointestinal Stromal Tumours. *Nat Rev Dis Primers* (2021) 7:22. doi: 10.1038/s41572-021-00254-5

32. Caenepeel S, Renshaw-Gegg L, Baher A, Bush TL, Baron W, Juan T, et al. Motesanib Inhibits Kit Mutations Associated With Gastrointestinal Stromal Tumors. *J Exp Clin Cancer Res* (2010) 29:96. doi: 10.1186/1756-9966-29-96
33. Gajiwala KS, Wu JC, Christensen J, Deshmukh GD, Diehl W, DiNitto JP, et al. KIT Kinase Mutants Show Unique Mechanisms of Drug Resistance to Imatinib and Sunitinib in Gastrointestinal Stromal Tumor Patients. *Proc Natl Acad Sci USA* (2009) 106:1542–7. doi: 10.1073/pnas.0812413106
34. Vlachogiannis G, Hedayat S, Vatsiou A, Jamin Y, Fernandez-Mateos J, Khan K, et al. Patient-Derived Organoids Model Treatment Response of Metastatic Gastrointestinal Cancers. *Science* (2018) 359:920–6. doi: 10.1126/science.aao2774
35. Xia X, Li F, He J, Aji R, Gao D. Organoid Technology in Cancer Precision Medicine. *Cancer Lett* (2019) 457:20–7. doi: 10.1016/j.canlet.2019.04.039
36. Kelly CM, Gutierrez SL, Chi P. The Management of Metastatic GIST: Current Standard and Investigational Therapeutics. *J Hematol Oncol* (2021) 14:2. doi: 10.1186/s13045-020-01026-6
37. Bleijs M, van de Wetering M, Clevers H, Drost J. Xenograft and Organoid Model Systems in Cancer Research. *EMBO J* (2019) 38:e101654. doi: 10.15252/embj.2019101654
38. Chakradhar S. Put to the Test: Organoid-Based Testing Becomes a Clinical Tool. *Nat Med* (2017) 23:796–9. doi: 10.1038/nm0717-796

Conflict of Interest: BZ was employed by Accurate International Biotechnology Company.

The remaining authors declare that the research was conducted in the absence of any commercial or financial relationships that could be construed as a potential conflict of interest.

Publisher's Note: All claims expressed in this article are solely those of the authors and do not necessarily represent those of their affiliated organizations, or those of the publisher, the editors and the reviewers. Any product that may be evaluated in this article, or claim that may be made by its manufacturer, is not guaranteed or endorsed by the publisher.

Copyright © 2022 Cao, Zhang, Chen, Rao, Qiu, Wu, Lin, Zeng, Zheng, Li, Cai, Wang and Han. This is an open-access article distributed under the terms of the Creative Commons Attribution License (CC BY). The use, distribution or reproduction in other forums is permitted, provided the original author(s) and the copyright owner(s) are credited and that the original publication in this journal is cited, in accordance with accepted academic practice. No use, distribution or reproduction is permitted which does not comply with these terms.



OPEN ACCESS

EDITED BY

Christopher R. Cederroth,
Swiss 3R Competence
Centre, Switzerland

REVIEWED BY

Laura Calvillo,
Italian Auxological Institute
(IRCCS), Italy
Dimitri De Bundel,
Vrije University Brussel, Belgium
Nikola Cesarovic,
ETH Zürich, Switzerland

*CORRESPONDENCE

Kai Diederich
kai.diederich@bfr.bund.de

[†]These authors have contributed
equally to this work

SPECIALTY SECTION

This article was submitted to
Animal Behavior and Welfare,
a section of the journal
Frontiers in Veterinary Science

RECEIVED 18 March 2022

ACCEPTED 19 July 2022

PUBLISHED 18 August 2022

CITATION

Mieske P, Hobbiesiefken U,
Fischer-Tenhagen C, Heintz C,
Hohlbaum K, Kahnau P, Meier J,
Wilzopolski J, Butzke D, Rudeck J,
Lewejohann L and Diederich K (2022)
Bored at home?—A systematic review
on the effect of environmental
enrichment on the welfare of
laboratory rats and mice.
Front. Vet. Sci. 9:899219.
doi: 10.3389/fvets.2022.899219

COPYRIGHT

© 2022 Mieske, Hobbiesiefken,
Fischer-Tenhagen, Heintz, Hohlbaum,
Kahnau, Meier, Wilzopolski, Butzke,
Rudeck, Lewejohann and Diederich.
This is an open-access article
distributed under the terms of the
Creative Commons Attribution License
(CC BY). The use, distribution or
reproduction in other forums is
permitted, provided the original
author(s) and the copyright owner(s)
are credited and that the original
publication in this journal is cited, in
accordance with accepted academic
practice. No use, distribution or
reproduction is permitted which does
not comply with these terms.

Bored at home?—A systematic review on the effect of environmental enrichment on the welfare of laboratory rats and mice

Paul Mieske^{1†}, Ute Hobbiesiefken^{1†}, Carola Fischer-Tenhagen¹,
Céline Heintz¹, Katharina Hohlbaum¹, Pia Kahnau¹,
Jennifer Meier¹, Jenny Wilzopolski¹, Daniel Butzke¹,
Juliane Rudeck¹, Lars Lewejohann^{1,2} and Kai Diederich^{1*}

¹German Center for the Protection of Laboratory Animals (Bf3R), German Federal Institute for Risk Assessment (BfR), Berlin, Germany, ²Institute of Animal Welfare, Animal Behavior and Laboratory Animal Science, Freie Universität Berlin, Berlin, Germany

Boredom is an emotional state that occurs when an individual has nothing to do, is not interested in the surrounding, and feels dreary and in a monotony. While this condition is usually defined for humans, it may very well describe the lives of many laboratory animals housed in small, barren cages. To make the cages less monotonous, environmental enrichment is often proposed. Although housing in a stimulating environment is still used predominantly as a luxury good and for treatment in preclinical research, enrichment is increasingly recognized to improve animal welfare. To gain insight into how stimulating environments influence the welfare of laboratory rodents, we conducted a systematic review of studies that analyzed the effect of enriched environment on behavioral parameters of animal well-being. Remarkably, a considerable number of these parameters can be associated with symptoms of boredom. Our findings show that a stimulating living environment is essential for the development of natural behavior and animal welfare of laboratory rats and mice alike, regardless of age and sex. Conversely, confinement and understimulation has potentially detrimental effects on the mental and physical health of laboratory rodents. We show that boredom in experimental animals is measurable and does not have to be accepted as inevitable.

KEYWORDS

animal behavior, animal welfare, enriched environment, boredom, abnormal behavior, impoverished environment, laboratory animals (mouse and rat)

Introduction

Recommendations for the husbandry of laboratory animals have been developed primarily with a view to standardizing experimental conditions and providing basic needs like water and food (1, 2). While satisfying basic needs helps avoid obvious pain and suffering in laboratory animals, in modern animal husbandry, saving resources

and personnel costs is certainly also an important factor. For the planning of animal experiments, compromises are made between the various interests of researchers, animal caretakers, animal house managers, and animal welfare advocates. The guidelines of the EU-directive for example contains basic recommendations including that social animals should be kept in groups and that all laboratory animals should be given the opportunity to develop a wide range of normal behavior by providing a housing condition with sufficient complexity (Directive 2010/63/EU). Moreover, species-specific recommendations for rats and mice call for the provision of environmental enrichment to make laboratory animal housing more diverse (e.g., <https://www.nc3rs.org.uk/3rs-resources/housing-and-husbandry-mouse>). However, the type of housing referred to as “enriched environment” has changed significantly in the last decades (3, 4). For example, some of what was described as enriched animal husbandry 25 years ago nowadays just meets the basic recommendations [i.e., a cardboard tube (5, 6)]. Moreover, not only has the concept of enrichment changed over time, but so has the related conventional housing, which usually reflects the actual state of housing and legal requirements at the time of publication. Still, the current housing of most laboratory animals reflects an impoverished environment compared to truly species-specific housing. More specifically, one must assume that the lack of stimuli has far-reaching consequences for the well-being and health status of laboratory animals. In fact, Cait et al. (7) showed in a meta-analysis of 214 studies that conventional housing increases morbidity and mortality in research rodents. This is backed up by the here reviewed research on comparing laboratory conventional housing to a more varied enriched housing using more space, social contact, and/or physical items, which conclusively describe positive effects on well-being and behavior of mice provided with enrichment.

Environmental enrichment was initially introduced to laboratory animals for studies investigating the effect of environment on neurobiological parameters and learning behavior (8). For this very purpose it is still being used, for example, enrichment has been proven to be an effective therapeutic intervention in animal models of various diseases including stroke (9) and neurodegenerative diseases like Alzheimer's disease (10). Moreover, a stimulating environment improves learning and memory formation and is a potent trigger for neuroplastic events in the adult brain—a process originally thought to occur only in the young developing brain (11). In addition to disease models and neurobiological studies, increasing focus has been placed on the effect of stimulating environments on animal welfare. Stress-responses were mitigated under enriched housing conditions and the activity of natural-killer cells was enhanced (12). Expression of abnormal repetitive behaviors (i.e., stereotypies) were reduced in mice living in an enrichment environment (13–16) as were behavioral measures related to anxiety (13, 17). In summary,

most publications indicate that enriched and varied housing conditions improve the well-being of laboratory animals. However, due to the low stimuli of conventional housing systems compared to a species-appropriate environment, this conclusion might be validly expressed in the opposite sense, that confined housing of laboratory animals compromises animal welfare and health.

Conventional husbandry of laboratory animals in research laboratories is characterized by confinement, monotony, and lack of challenge. In humans, such conditions are usually accompanied by a condition known as boredom. Boredom is an emotional state that usually relates to individuals having nothing to do, are not interested in their surroundings, and feel that life is dull and tedious (18, 19). This state could also very aptly describe the life of many laboratory animals housed in small barren cages. Few studies have directly addressed the issue of animal boredom so far. However, based on the findings from human studies (20), some behavioral abnormalities observed in captive animals can be readily linked to boredom (21).

For example, barbering behavior in animals has recently been related to Trichotillomania (“hair-pulling disorder”), a human disorder reportedly triggered by boredom (22, 23). Common abnormalities in captive animals are stereotypies, which are often related to a lack of stimulation in laboratory animals. Stereotypic behavior in mice like wire gnawing/bar-mouthing (6), circling at the cage lid, back-flipping, route tracing, and twirling (13, 14) was shown to be decreased under more stimulating enriched housing conditions. Another symptom of human boredom is an altered perception of time, in which time does not seem to pass in monotonous situations (24). In animals, this phenomenon can be measured objectively by training them to expect a specific event or reward after a predictable period and measuring their anticipatory behavior after being exposed to monotonous tasks or environments (21). This method was successfully trained in starlings using pecking a key as an anticipatory behavior (25). It is reasonable to assume that laboratory rodents also experience such a perceptual shift, but as far as we know this has not been investigated until now. Overall, it is not unfounded to speculate that the great overlap between human symptoms of boredom and similar phenomena in rodents indeed indicates that boredom in animals is both real and underestimated in laboratory animals.

Since a sufficient form of stimulation is lacking in boring situations, sensation-seeking or stimulus-seeking behavior also occurs in animals (21). This is seen as a form of escape from the unpleasant, boring situation. Indeed, it has been described that it is sometimes of little importance whether the stimulus has a positive or negative valence if interaction is possible at all (26). Burn et al. (27) showed stimulus seeking in ferrets as increased contact to negative and ambiguous stimuli compared to a control group which were provided a 1 h daily play time. Furthermore, ferrets without playtime spent more time lying awake with their eyes open, screeched

more but sat and stood less, than after playtime (27). This form of awake inactivity as a form of suboptimal arousal can be seen as an indicator of bored animals as well and was also more apparent under non-stimulating housing conditions in mink (26, 28) and mice (29). Moreover, Meagher et al. (28) found increased interest in different external stimuli in mink in non-enriched environments as a form of sensation seeking of potentially bored animals. These two almost opposite extremes of boredom symptomatology—sensation seeking vs. awake inactivity—illustrate the multifaceted nature of the expression of boredom and thus the difficult search for a fixed definition for this distressing and damaging emotional condition. In psychology and medicine, boredom is gaining increasing recognition as a potentially harmful emotional state and as a field of research for translational studies (19, 30). Regarding animal welfare, boredom becomes a serious concern with an urgent need for research. In this systematic review, we therefore examined the literature on enriched environment with specific regard to the effects of housing conditions on well-being in laboratory mice and rats. Moreover, we examine the existing body of literature specifically related to boredom symptoms. By identifying measures of boredom as well as clues to potential cures for boredom in laboratory rodents, we aim to lay the groundwork for addressing this pressing issue in the context of modern animal research.

Materials and methods

Search strategy

In accordance with PRISMA guidelines, we searched the database Web of Science on July 5th, 2019, and again on February 24th, 2021, before data analysis commenced. We performed a supplementary search on Web of Science, Embase, and PubMed on March 29th, 2022. In terms of population, we focused on mice and rats, the most widely used laboratory animals in experimental research. Enriched housing conditions were included as intervention and a corresponding non-enriched/conventional housing as a comparator. At least one behavioral observation or test should have been performed as an outcome parameter for animal welfare. For further specialization of the resulting search string boredom and its synonyms were as well-included as their respective counterpart. To achieve a high outcome of relevant research papers in the final search, truncations with wildcards and synonyms were used in the search string establishment.

Searchstring:

TS = (*boredom OR tedium OR ennui OR tediousness OR stuffiness OR dullness OR boringness OR monotony OR bor* OR monoton* OR motivat* OR stimulat* OR excit* OR activ* OR "affective state"*)

AND TS = (*hous* OR husbandry OR "animal keeping" OR environment**)

AND TS = (*mice OR mouse OR rat OR rats*)

AND TS = (*behavior* OR behavior**)

AND TS = (*standard OR conventional OR barren OR restricted OR impoverished*)

AND TS = (*enrich* OR seminatural OR semi-naturalistic*)

Selection of studies and information extraction

Abstract screening was done by nine reviewers (PM, UH, CF-T, CH, KH, PK, JM, JW, and KD) using the systematic reviewing online tool SyRF (<http://www.syrf.org.uk/>). Exclusion criteria included the use of other animals than rats and mice, no behavioral observation or experiment, use of only one housing condition, use of psychoactive drugs, use of a disease or transgenic models. We excluded editorials, conference abstracts, and review papers.

Ten reviewers (PM, UH, CF-T, CH, KH, PK, JM, JW, LL, and KD) independently screened full text and extracted information from eligible studies into a standardized form. Extracted parameters included species, strain, sex, age at the start of the housing period and the beginning of the behavioral experiment, the presence of a focus on animal welfare, the disease/lesion model, genetic modification, psychoactive substances/stimulations, enrichment category (social, object, space of home cage) and description, number of groups including control group and their housing, the mean behavioral outcome parameter and the used behavioral test. Compliance with scientific quality criteria in the included studies was assessed by ascertaining whether the allocation of animals to experimental groups was randomized and the assessment of outcomes was blinded. Any discrepancies were resolved by consensus. Randomization was done with the sample() function in the statistical computing software R (<https://www.r-project.org/>).

Categorization and classification of age and durations of housing

Outcome parameters were categorized as follows: social behavior, aggressive behavior, abnormal behavior, affective well-being, activity, cognition, nociception, motor function, circadian rhythm, and exploratory behavior. An overview of the behavioral tests used in the studies and the assignment to the categories is shown in [Supplementary Table 1](#). In addition, we extracted information about glucocorticoid hormones to evaluate effects of housing on stress. However, determination of stress hormones regarding sample source, number, and

sampling-time was very heterogeneous. We therefore included glucocorticoids only in the main overview.

For a detailed examination of the effects of enrichment on animal welfare, the results of each study were considered in terms of sex of experimental animals, age of experimental animals, and duration of housing in the respective housing environments. For age classification, animals were designated as postnatal from 0 to 21 days of age, adolescent from 21 to 60 days of age, adult from 60 to 750 days of age, and post reproductive from more than 750 days of age (31). Duration of husbandry was classified in short, mid, and long-term housing duration with short defined as 0 to 30 days, mid with 30–90 days and long-term with more than 90 days.

For an in-depth investigation of boredom, all selected publications were screened again for boredom-specific parameters. Because few studies have explicitly examined boredom in animals, especially laboratory animals, the classification of boredom parameters was based on the symptomatology of human boredom and relevant translatable phenomena in mice and rats. The sources for these parameters were literature on human boredom (20, 32) and Charlotte Burn's pioneering review article on animal boredom (21). All studies selected in this systematic review were examined regarding these parameters. For the examination of the parameter “drug seeking behavior”, the studies related to the use of psychoactive substances that were excluded for the main analysis were re-integrated into this single analysis. Results of this part of the analysis are summarized in Table 1.

Analysis

Analysis and illustrations were done using the software environment R (version 3.6.3, <https://www.r-project.org/>, R Foundation for Statistical Computing, Vienna, Austria) and the development software and graphical user interface RStudio (version 1.2.1.335, RStudio, Inc., Boston, MA, United States).

To assess the impact of enrichment on the defined categories, it was determined whether the selected studies reported an increase or a decrease in the respective categories; if no change was found, the result was classified as neutral. In the figures, the bars represent the studies that reported an increase, a decrease, or no change in the respective parameter in the corresponding category. The thickness of the bars reflects the amount of identified and investigated studies for this category. The numbers indicate the observed effect of the enrichment as a decimal number. If this value reaches 1, all studies in this category have observed an increase; correspondingly, a decrease if the value reaches -1 . A bar located further to the right of the scale thus indicates an increasing effect of the applied enrichment on the category under consideration. The numbers correspond to the principle of a Likert scale.

Results

Study inclusion and study characteristics

Search strategy and study selection results are presented in Figure 1. After removal of duplicates, 884 titles/abstracts were screened, of which 438 were excluded. Full texts of the remaining 446 records were then screened, and 228 did not meet the eligibility criteria. This left 186 articles for qualitative synthesis.

71.6% of studies reported randomization of animals to treatment groups and only 24.3% of studies indicated blinding of outcome assessors.

Figure 2 shows the parameters that were examined in the context of environmental enrichment. The figure also shows the parameters that were defined as indicators of boredom and explicitly searched for in the publications. There is a large overlap between the factors examined in the studies and the boredom-related parameters.

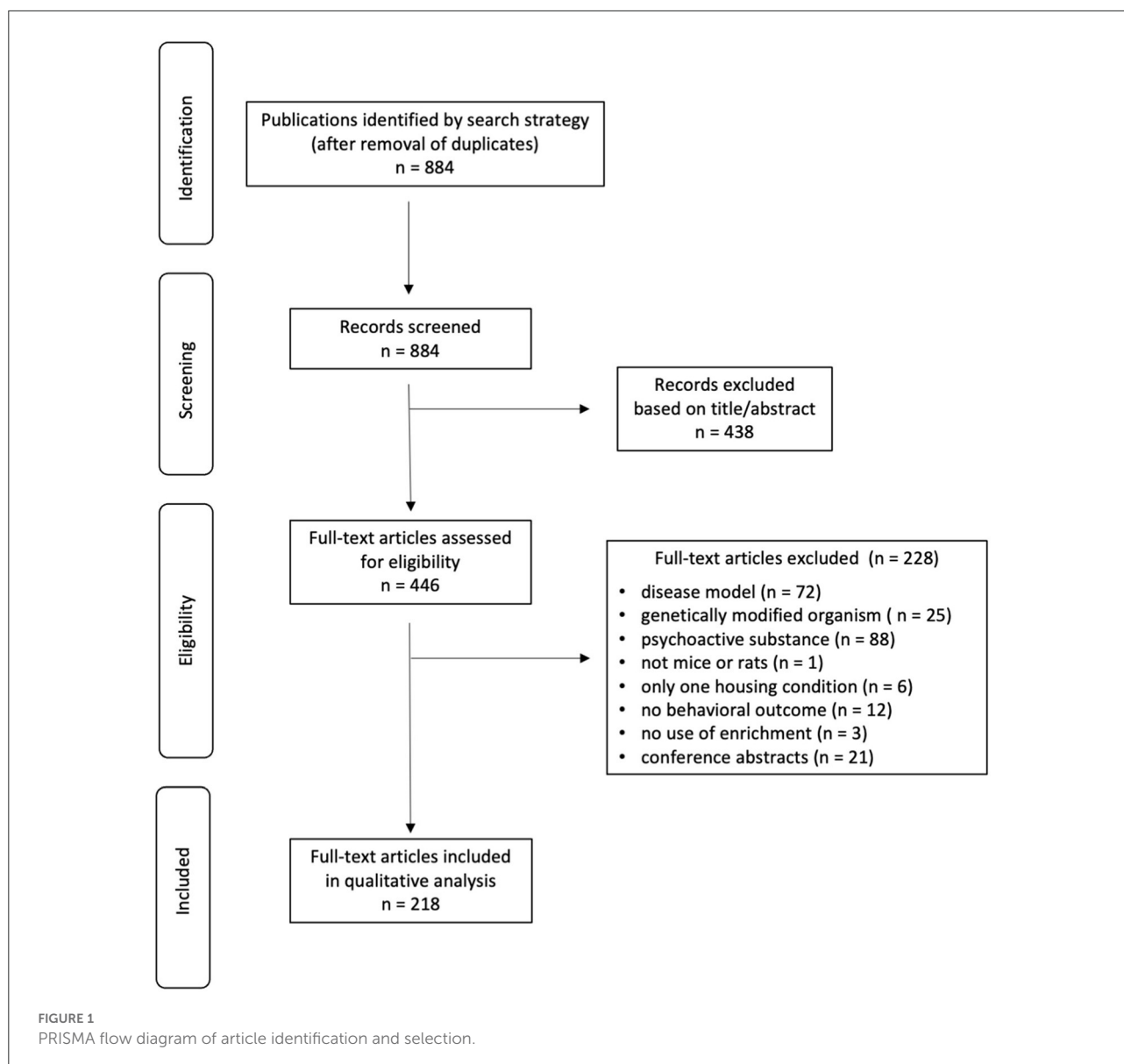
Increasing number of publications about home cage enrichment

The number of studies examining the effects of enriched housing on mouse and rat behavior has steadily increased, particularly over the past decade, with peaks in 2013, 2015, and 2018 (Figure 3). In 2022, three papers were included in the parameter extraction with one of them focusing on animal welfare. All studies that explicitly aimed to improve the housing conditions of laboratory animals and thus were dedicated to refining animal experiments were categorized as “Focus on animal welfare”. Although the absolute number of publications with a focus on animal welfare was slightly increasing over time, its overall proportion is still low.

Results on reviewed methods and experimental designs

Rats have been used more frequently than mice to study the effects of housing conditions on behavior and for both species, mainly males were examined (Figure 4). The most frequently used rat strain was Sprague-Dawley (48 studies) followed by Wistar (44 studies). Twenty-two studies housed Long-Evans rats as experimental animals. Eighteen different strains of mice were studied in the context of environmental enrichment. The most used strains were C57BL/6 (39 studies), BALB/C (13 references) and CD-1 mice (11 references).

The enrichment applied in the examined studies was divided into three categories. “Social enrichment” was defined as being housed in a group or provided with a cage partner. When additional space by increasing the home cage size was used to provide enrichment, the category

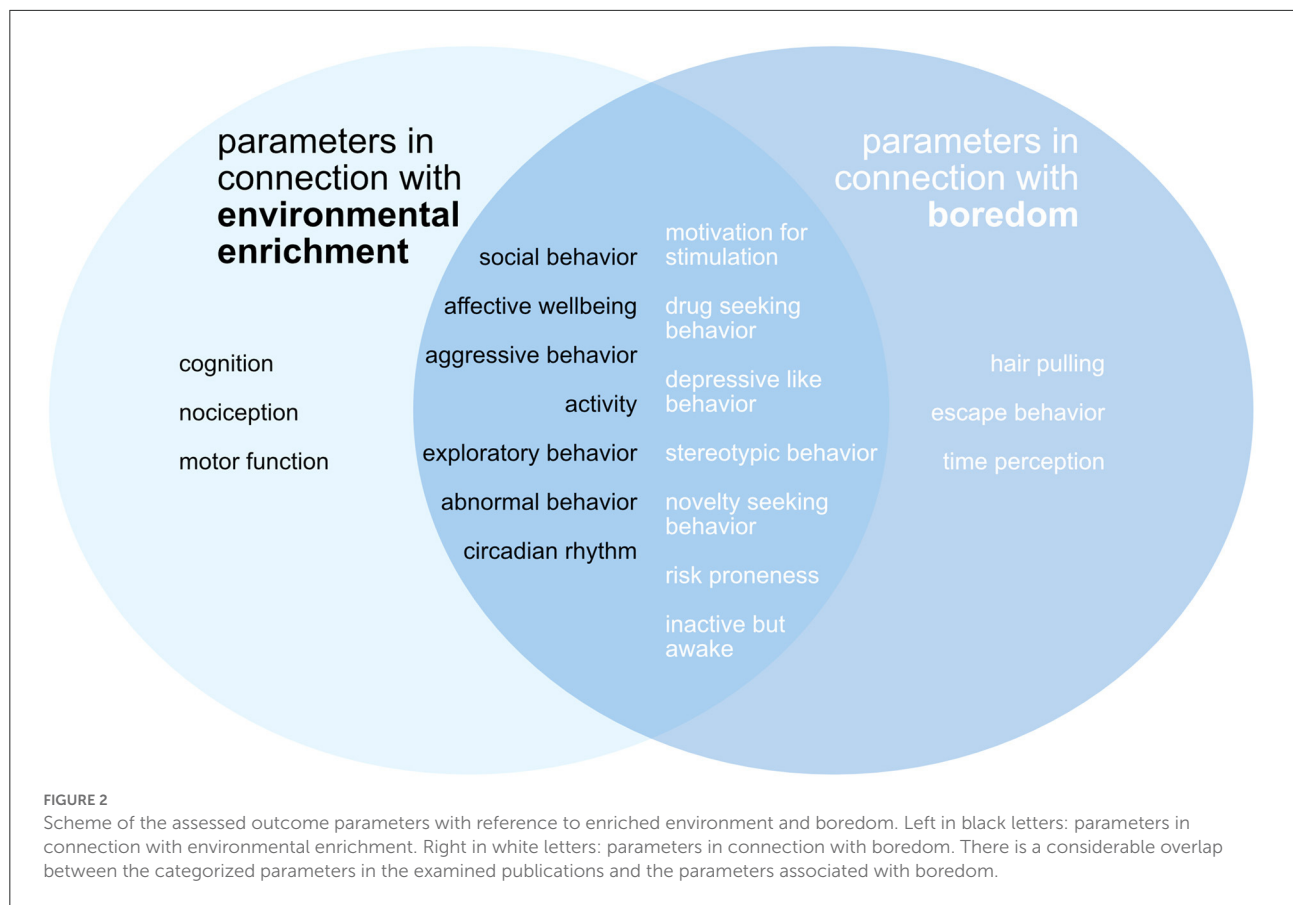


‘size enrichment’ was indicated. The “object enrichment” category was assigned when the environment was changed by the introduction of objects of any kind (toys, climbing opportunities, structural elements).

Most studies used a combination of all three types of enrichment in their experiments (104 studies). This was followed by a combination of object enrichment and size enrichment of the home cage (55 studies). Social enrichment alone (6 studies), enrichment of home cage space alone (3 studies) and the combination of social and spatial enrichment (3 studies) were the least used types of enrichment. Three studies used environmental enrichment in their experiments but did not mention the type.

A stimulating environment is essential for the development of natural behavior and animal welfare

Providing animals with an enriched environment substantially improves cognitive skills. Motor function, social behaviors and affective state were positively affected, and abnormal behaviors were considerably decreased compared to conventional or barren housed animals, also indicating a positive protective effect. The effects of enrichment on the categories aggressive behavior and activity though remain inconclusive. There is no clear tendency for stress hormones to increase or decrease in relation to housing conditions (Figure 5).



Enriched housing promotes well-being in mice and rats, and regardless of sex and age

The reported effects of environmental enrichment on animal welfare are largely independent of the animal species compared in this study. Mice and rats benefit similarly from enrichment of their living environment (Figure 6A).

Most of the studies examined were performed on males (123 studies, Figure 6B). Fifty-eight studies examined both sexes whereas only 31 studies did experiments on female animals. Enrichment increases cognition, social behavior and motor function and decreases abnormal behavior in females and males, with these effects being more pronounced in females. Regardless of sex, a similar number of studies reported an impairment, a reduction, or no effect on activity. Exploration and aggressive behavior in females increased with the provision of enrichment. Eight studies examined the effect of enrichment on aggressive behavior in male animals. In four of these studies, an increase in aggressive behavior was observed.

Most of the studies reviewed were conducted with adolescent animals (117 studies, Figure 6C). Seventy studies used adult animals and 29 studies used postnatal animals.

Two studies used post-reproductive animals. Apart from this discrepancy in the use of animals of different ages, the effects of enrichment on cognition, affective well-being, social behavior, and the development of abnormal behavior proved generally positive for all age groups. Motor function was positively affected by enrichment but data in postnatal and adult animals are lacking here as well as in post-reproductive animals. Ambiguous results of the effect of enrichment on aggressive behavior, exploratory behavior, and activity with an increase, decrease as well as a neutral or no effect could be detected.

The longer the period of housing in an enriched environment, the higher the benefit to welfare

Most of the included studies applied a medium housing period (30–90 days, 124 studies). The most beneficial effect of enrichment was obtained with a long housing duration (more than 90 days, 33 studies) but all durations could improve motor function, cognition and affective well-being and exert a protective effect against the development of abnormal behavior (Figure 7). The effect of enrichment duration on aggressive

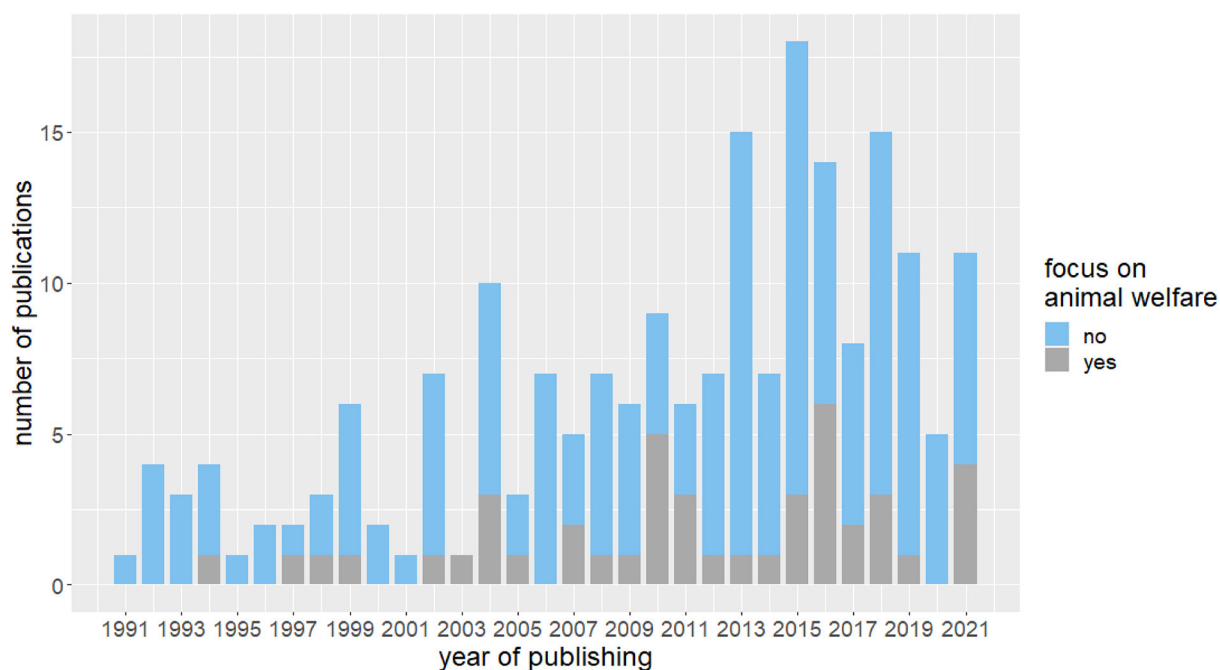


FIGURE 3

Absolute number of included publications in the years 1991 to 2022. Indicated is the number of publications with and without explicit focus on animal welfare in the publications.

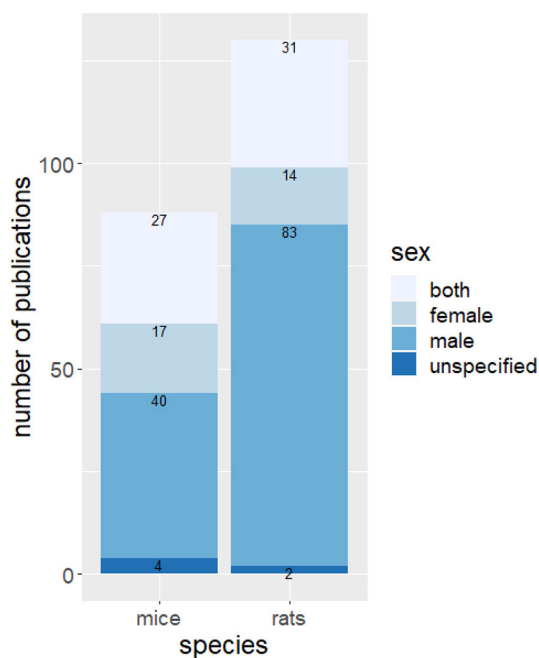


FIGURE 4

Number of publications using rats and mice and sex bias. Indicated is the absolute number of publications with the specified species and sexes.

behavior and activity remained inconclusive with a tendency to an increase in aggressive behavior and activity in a long-term provision of enrichment.

Discussion

Environmental enrichment has been a popular research topic for some time, not excessively but continually researched. Neuroscience research has provided some fundamental results in this field, elucidating the close relationship of animal housing conditions on the structure and function of the central nervous system. Most published studies use enrichment as an intervention in animal models of various diseases, including stroke (127, 128), traumatic brain injury (129), and Alzheimer's disease (10). Although this is a highly exciting field of research, these studies were deliberately not included in this systematic review. This systematic review instead focuses on enriched environment as a means of preventing boredom-like symptoms and improving the welfare of laboratory animals.

While research activity on enriched environments has increased steadily over the years, only a small fraction of the investigated studies dealt specifically with animal welfare. This is perhaps not surprising, since there are various definitions of animal welfare (130), and no consensus on how to improve it.

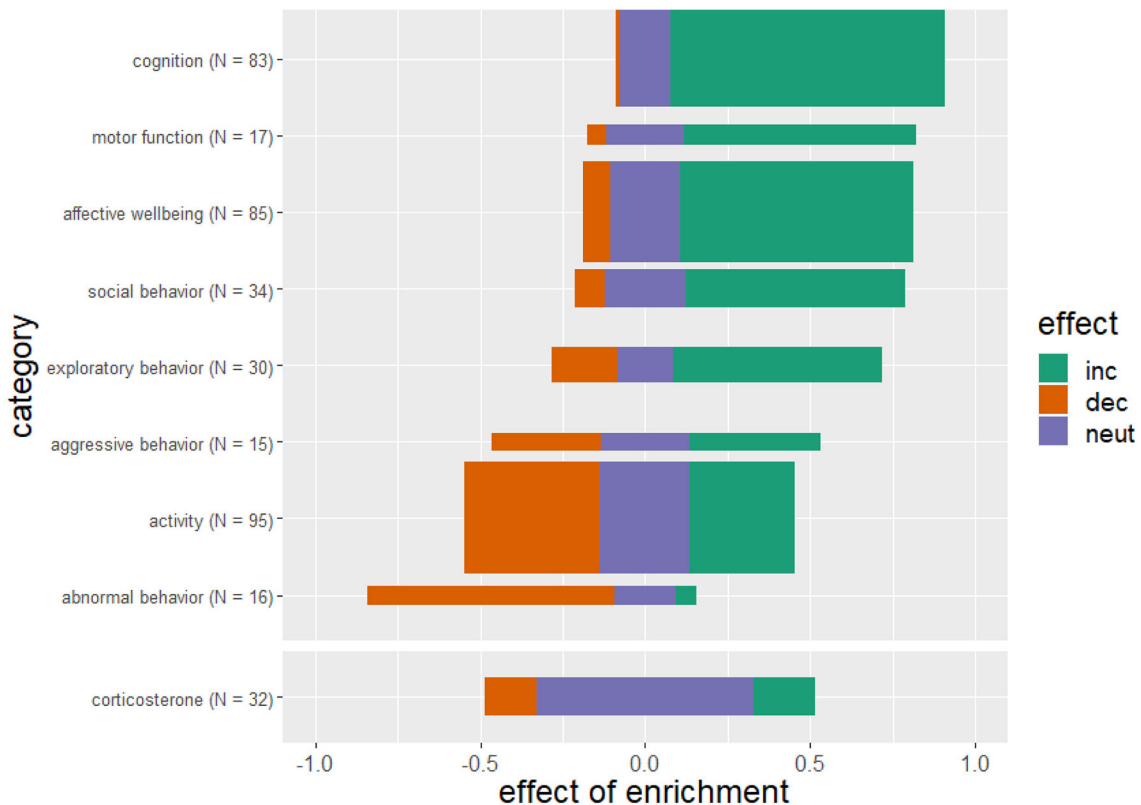


FIGURE 5

Effects of enriched housing on behavioral outcome and corticosterone level. Bars represent the studies that reported an increase (inc), a decrease (dec) or no change (neut) in the parameters of the corresponding category. Values indicate the observed effect of the enrichment as a decimal number. The thickness of the bars reflects the number of investigated studies for this category. The sum of references per category is greater than $N = 218$ studies because some studies examined more than one outcome parameter.

However, our data show that the proportion of studies with a specific focus on improving the living conditions of laboratory animals in enrichment research is slightly rising. As animal welfare research gains increasing recognition as an established research discipline, the number of research papers in the field will likely continue to grow. For example, recent research shows that tunnel handling can improve physiological well-being and often the handling tunnel is used as an additional enrichment item (131).

Our analysis shows that rats are used more frequently than mice in enrichment research and that different strains of both species are used. Nevertheless, rats and mice benefit similarly from an enriched living environment and there is no evidence that housing conditions affect the welfare of strains differently. Females are underrepresented in studies with mice and even more so in studies with rats. Among the studies using mice, 31% reported the use of both sexes, 46% the use of male, and 19% the use of female mice. In the rat studies, 24% used both sexes, 64% used male, and only 11% used female rats. A similar bias toward the use of male subjects has been found in preclinical animal research (132). The underrepresentation

of female subjects in animal research is based on the belief that females are more variable than males due to their estrous cycle. However, for most applications including behavioral measures, female rodents display no more variation than males do; and female estrus cycles therefore need not necessarily be given special consideration (133). The underrepresentation of females in animal research is still pervasive, and the scientific understanding of female biology is compromised by these persistent disparities. To address the inadequate inclusion of female animals, the US National Institutes of Health has implemented policies in 2014 that require applicants to indicate their plans for a balance of males and females in preclinical studies in all future applications, unless sex inclusion is not warranted due to strictly defined exceptions (134). The bias toward male subjects in animal research is receiving additional attention due to a plausible implication in the much-discussed translational crisis. Less consideration has so far been devoted to the obvious ethical implications of this sex imbalance. Since no fewer females than males are born in breeding facilities for laboratory animals, the question inevitably arises as to what happens to the “surplus” females (130).

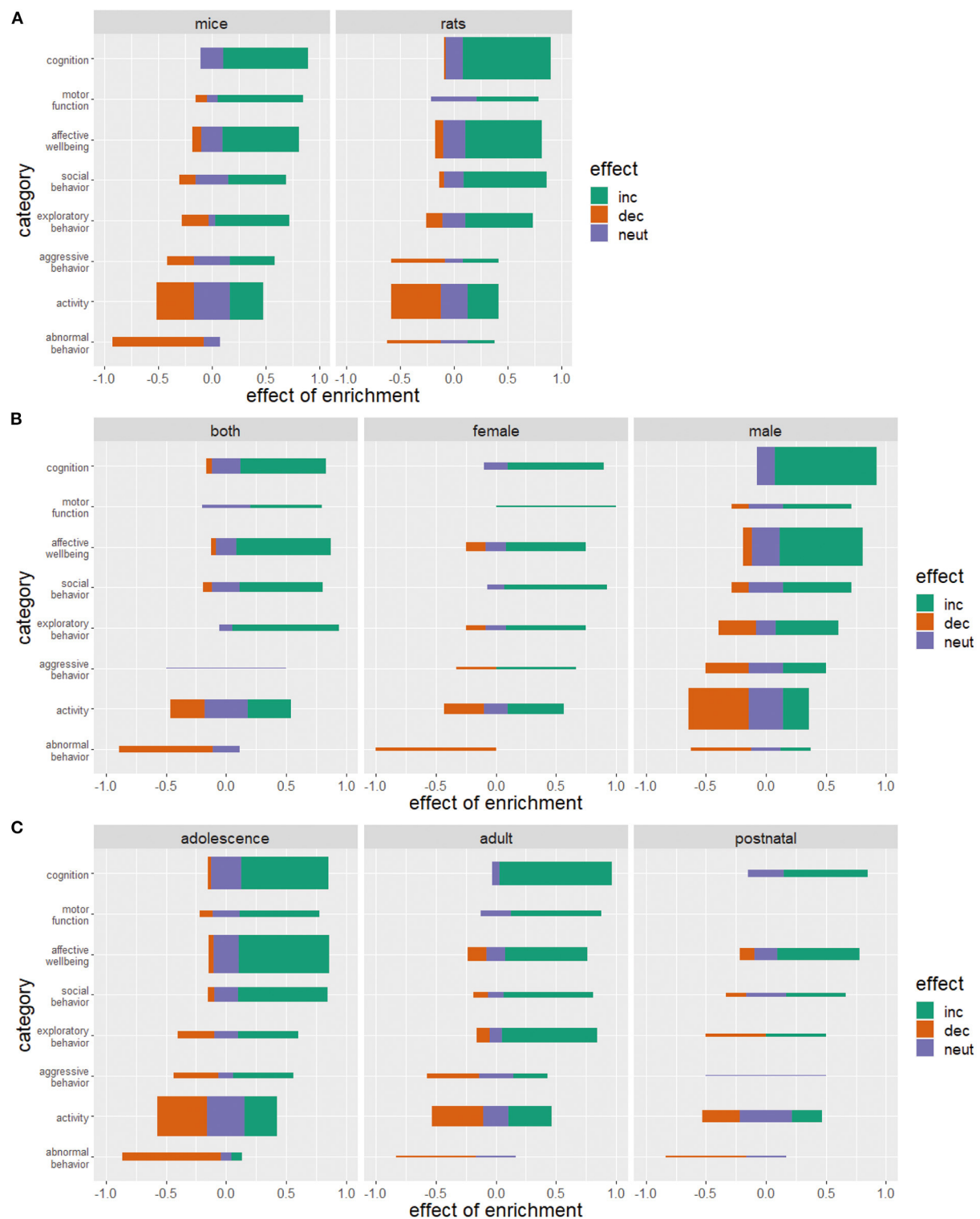
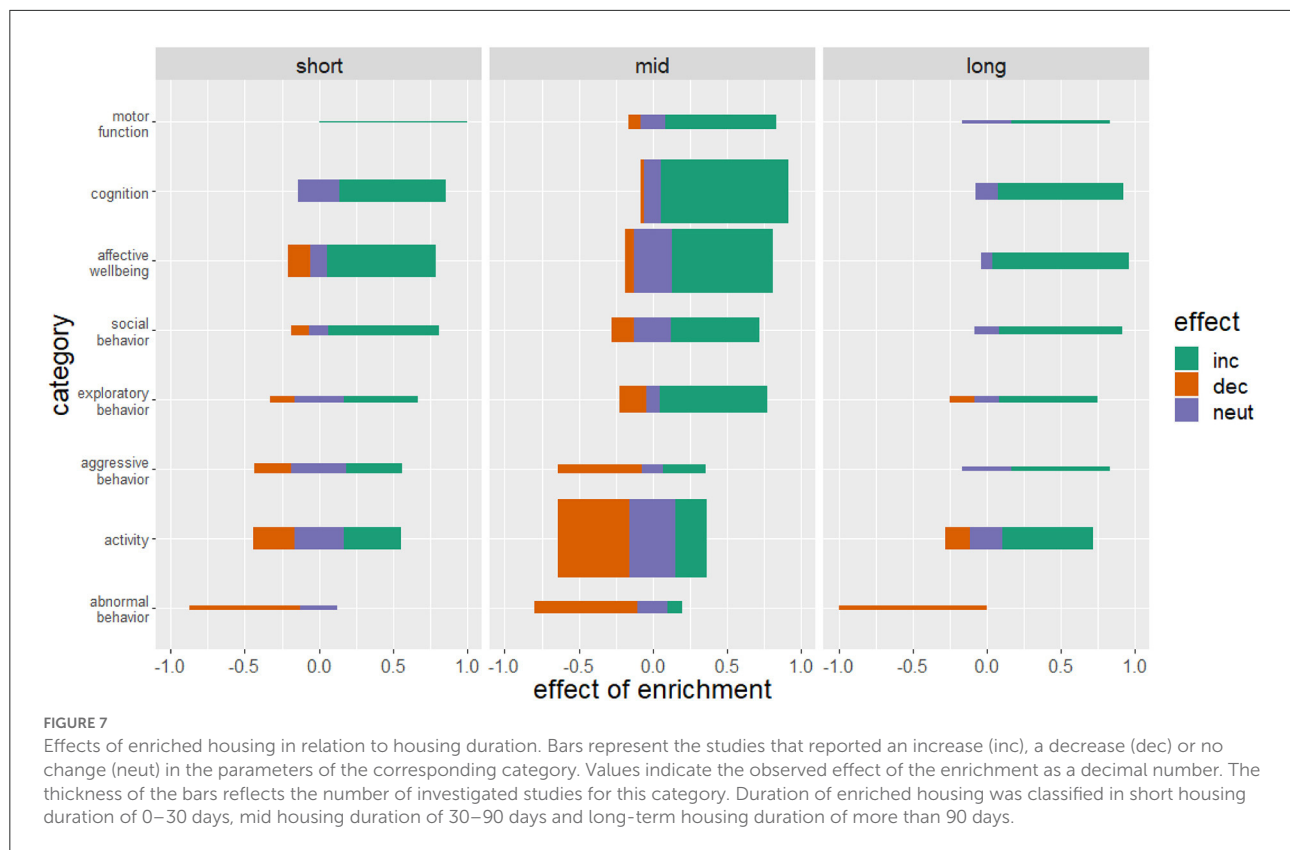


FIGURE 6

Effects of enriched housing on mice and rats (A), in relation to sex (B), and age (C). Bars represent the studies that reported an increase (inc), a decrease (dec) or no change (neut) in the parameters of the corresponding category. Values indicate the observed effect of the enrichment as a decimal number. The thickness of the bars reflects the number of investigated studies for this category. (C) Animals were considered postnatal at the age of 0–21 days, adolescent at the age of 21–60 days, adult at the age of 60–750 days and post reproductive at the age of more than 750 days.



Age is another important experimental factor in animal research that is often inadequately considered in experimental design and poorly reported in publications. Animals used in the examined enrichment studies tend to be young. In most of the studies, the housing phase in the enriched cages started at 0–4 weeks of age. In the behavioral tests, many of the animals were then tested at 6–14 weeks of age. This corresponds to the average age of 8–12 weeks at which laboratory animals are usually used in animal research (135). At this age, many developmental processes are not yet complete. It is therefore important to note that age-related physiological changes can have a major influence on experimental outcomes.

The positive effects of a diversified housing on physical, cognitive, and affective health of laboratory animals have been demonstrated by numerous publications analyzed in this review. Motor function, cognition, affective well-being, and social behavior benefited most from enriched housing. A reduction in abnormal behavior was also frequently reported with enriched housing. The effect of enrichment on activity remains inconclusive. One possible reason for the ambiguous results on the activity parameter is the broad definition of the parameter, which might limit the interpretability. Another reason could be the observed decrease in abnormal behaviors (stereotypies) due to housing in an enriched environment, which are usually accompanied by a significant level of activity.

Since an enriched environment is often associated with more space and/or the provision of a running wheel, animals in these housing conditions clearly have more opportunity for physical activity than animals in confined housing. Mice housed in enriched cage systems outperformed conventionally housed animals on the rotarod, indicating that enrichment stimulates motor coordination and presumably fitness, even when no running wheel or disc is provided (136). Numerous studies on animals and humans have evidenced the beneficial influence of physical activity on the musculoskeletal system (137, 138). It is therefore a reasonable assumption that keeping laboratory animals in confined cages can harm the bone structure and musculature of laboratory animals.

Interestingly, we did not detect a clear increase or decrease in glucocorticoid stress hormones associated with housing conditions. In a recent review, however, it was suggested that conventional laboratory housing was found to be associated with chronic stress (7). Instead of a chronic increase in stress hormones, we suggest that conventional housing may rather reduce the capacity of the stress axis to cope with environmental challenges and that the health impairments result from constant under-stimulation. This would be in line with the proposed non-linear relation of stress and welfare as proposed by Korte et al. (139). However, it should be noted that the determination of stress hormones in the included publications was very

TABLE 1 Overview of publications addressing boredom related parameters, the respective outcome, and the behavioral test used.

Boredom related parameter	Publications	Outcome	Behavioral test
novelty seeking behavior	(33)	increase	open field, behavioral observation
	(34)	increase	Y-maze
	(35)	increase	open field, light-dark test
	(36)	increase	open field, behavioral observation
	(37)	increase	open field, object recognition test
	(38)	decrease	elevated plus maze, open field
	(39)	decrease	open field
	(40)	decrease	activity cage
	(41)	decrease	open field, behavioral observation
	(42)	decrease	two-lever operant conditioning chamber
	(43)	increase	object recognition test, open field
	(44)	increase	behavioral observation
	(45)	increase	radial-arm maze
	(46)	increase	open field, Y-maze
	(47)	increase	open field, Y-maze, light-dark test
	(48)	increase	Y-maze, object recognition test
	(49)	increase	barrier test, group test, intruder test
	(50)	decrease	open field, light-dark test
	(51)	increase	elevated plus maze, light-dark test, concentric square field test
	(52)	increase	Y-maze, light-dark test
	(53)	increase	object recognition test
	(54)	increase	corridor field task
	(55)	decrease	behavioral observation, elevated plus maze
	(56)	increase	open field
	(57)	increase	open field elevated plus maze, light-dark test
	(58)	increase	hole board test
	(59)	increase	light-dark test, concentric square field test
	(60)	decrease	open field, elevated plus maze
	(61)	increase	open field, light-dark test, hole board test
	(62)	decrease	novelty place preference
	(63)	increase	object recognition, passive avoidance test
	(64)	decrease	elevated plus maze, open field
	(65)	decrease	lever-responding task
depressive like behavior	(66)	decrease	forced swim test
	(67)	increase	forced swim test
	(68)	neutral	forced swim test
	(69)	decrease	forced swim test
	(70)	decrease	forced swim test
	(71)	decrease	forced swim test
	(72)	neutral	tail suspension test
	(73)	decrease	forced swim test
	(74)	neutral	forced swim test
	(75)	increase	tail suspension test
	(76)	increase	forced swim test, sucrose preference
	(77)	increase	forced swim test
	(78)	neutral	forced swim test

(Continued)

TABLE 1 Continued

Boredom related parameter	Publications	Outcome	Behavioral test
drug-seeking behavior	(79)	decrease	forced swim test
	(50)	decrease	forced swim test, sucrose preference
	(80)	decrease	tail suspension test
	(81)	decrease	forced swim test
	(82)	decrease	forced swim test
	(83)	decrease	forced swim test
	(29)	decrease	forced swim test
	(84)	decrease	forced swim test
	(85)	decrease	sucrose preference
	(86)	decrease	forced swim test
	(87)	decrease	conditioned place preference
	(88)	decrease	conditioned place preference
	(89)	decrease	conditioned place preference
	(90)	decrease	conditioned place preference
	(91)	decrease	cocaine context renewal test
	(92)	decrease	operant conditioning chamber
	(93)	decrease	conditioned place preference
	(94)	decrease	conditioned place preference
	(95)	decrease	operant conditioning chamber
	(96)	decrease	conditioned place preference
	(97)	decrease	drinking in the dark test
	(98)	decrease	operant conditioning chamber
	(84)	decrease	two-bottle choice test
	(99)	decrease	operant conditioning chamber
	(100)	decrease	conditioned place preference
	(101)	decrease	operant conditioning chamber
	(102)	neutral	operant conditioning chamber
	(103)	decrease	context induced relapse test
	(104)	decrease	conditioned place preference
	(105)	decrease	operant conditioning chamber
	(106)	decrease	liquid consumption
	(107)	neutral	sign tracking
	(108)	decrease	conditioned place preference
stereotypic behavior	(65)	decrease	alcohol self-administration
	(6)	decrease	behavioral observation
	(109)	decrease	behavioral observation
	(110)	decrease	behavioral observation
	(44)	neutral	behavioral observation
	(111)	decrease	behavioral observation
	(112)	decrease	behavioral observation
	(113)	neutral	behavioral observation
	(114)	decrease	behavioral observation
	(76)	decrease	activitymeter, behavioral observation
	(115)	neutral	behavioral observation
	(116)	decrease	behavioral observation

(Continued)

TABLE 1 Continued

Boredom related parameter	Publications	Outcome	Behavioral test
motivation for stimulation	(29)	decrease	behavioral observation
	(117)	decrease	activity testing chamber
	(118)	neutral	behavioral observation
	(13)	decrease	behavioral observation
	(16)	decrease	behavioral observation
	(119)	increase	running wheel, open field
	(120)	increase	operant training
	(121)	decrease	operant conditioning test
	(50)	increase	open field, hole board
Inactive but awake	(122)	decrease	behavioral observation
	(110)	decrease	behavioral observation
	(123)	decrease	open field, behavioral observation
	(29)	decrease	behavioral observation
risk proneness	(124)	decrease	behavioral observation, open field
	(125)	increase	open field, radial water maze
	(51)	increase	elevated plus maze, light-dark test
	(126)	neutral	open field, elevated plus maze, inhibitory avoidance

The table is sorted showing the boredom related behaviors with the largest number of publications first. The publications investigating the specific behaviors are sorted by year ascending in order to show actual trends in this field of research. The boredom related parameters escape behavior, hair pulling and time perception were not investigated in the reviewed publications.

heterogeneous in terms of sample source, number, and timing and that these parameters were not assessed. This evaluation was not a central topic of this work, and measurement of glucocorticoid stress hormones was not a part of the search strategy. However, our preliminary data suggest that a more thorough analysis of this parameter may be warranted.

The effects of a stimulus-rich environment on cognition and affective well-being are well-documented and there is accumulating evidence for potential underlying brain structures and neurophysiological mechanisms. These extend from brain region volume and morphology to neuron complexity and excitability, adult neurogenesis, synaptic plasticity, and a plethora of molecular responses including gene-environment interactions, inflammation, and trophic factors (140–143). Many of these effects are likely linked to the increased physical activity associated with an enriched housing. However, there are processes that are directly attributable to the stimulative elements of enrichment. These include the successful differentiation and long-term survival of newly formed neurons during neurogenesis, processes that can be clearly distinguished from the proliferation of neural cells, which in turn is facilitated in particular by physical activity (144).

In the studies reviewed, a variety of housing, bedding, and nesting materials, as well as various items or any combination thereof, were used as enrichment. It is worth noting that pre-build shelters can have different effects than providing material for building their own nests (145). Historically,

all additions to housing cages were considered enrichment. In this way, “enrichment” became an umbrella term for a variety of shelters, bedding and nesting materials, and miscellaneous items, or any combination thereof, and lacked a general theoretical framework for what should be considered enrichment (4). This is also reflected in the studies reviewed. In most publications, a combination of social, object and spatial enrichment was used (Supplementary Table 2). Because of the widespread simultaneous use of all types of enrichment, there is no clear consensus on which form is most effective in preventing housing-specific behavioral disorders.

Enriched environment alleviates boredom-like symptoms in laboratory animals

Some of the outcomes extracted in this review may be directly related to boredom in laboratory animals. These included abnormal behaviors like stereotypic, hyperactivity, and inactive-but-awake behavior, as well as novelty-seeking, drug-seeking, and depressive like behavior. Thirty-three publications dealt with novelty-seeking behavior in the broadest sense (Table 1). This parameter is often investigated with the open field test or elevated plus maze, but also by observing the behavior or activity in newly presented home cages. While novelty seeking is assumed to be an indicator of boredom, the measurement

of novelty seeking is often linked to activity and exploration in a range of different tests. This makes it difficult to clearly attribute the results of tests classified as novelty seeking in terms of boredom. Therefore, there is no unequivocal effect of environmental enrichment on novelty seeking behavior.

Twenty-three of the included publications investigated depressive like behavior in connection with environmental enrichment. This was mostly done with the forced swim test and tail suspension test. Fifteen studies (65%) describe a decrease and four (17, 4%) an increase in symptomatology in animals housed in an enriched environment. The 10 most recent studies published since 2014 uniformly show a decrease in depressive-like behavior in animals housed in enriched environments.

Twenty-four publications were identified as studies on drug-seeking behavior. Here, a consistently positive effect of environmental enrichment was reported.

Sixteen studies examined stereotypic behavior in mice and rats were. There was an overall decrease of stereotypic behavior under enriched housing conditions. Although the occurrence of stereotypic behavior appears to be a multifactorial event in animals (6, 15), it can be observed more frequently under barren restrictive housing conditions and has been shown to be reduced by the use of enrichment in zoo animals (146). Burn (21) argued that stereotypic behaviors increase under monotonous situations and identified abnormal repetitive behaviors as a potential measurable boredom parameter in captive animals.

Very poorly represented are the boredom parameters motivation for stimulation, inactive but awake and risk proneness with 12 publications in total. These characteristics, which closely relate to human boredom, are also influenced by environmental enrichment. Motivation for stimulation is a parameter that has been reported to be both increased and decreased by an enriched environment. This parameter is usually derived from the activity behavior of the animals and determined by a variety of tests that lead to inconclusive results. Awake inactivity was reduced by enriched environment in every included publication. Two studies found increased, and one found unchanged risk proneness, in animals living in an enriched environment. However, with only three publications related to risk proneness in our body of literature, this statement should be viewed with caution.

Escape behavior, hair pulling, or a possible shift of time perception were not examined by any publication. Overall, it must be noted that in only a few cases boredom was specifically mentioned at all.

Methodological considerations

Although boredom is resonant in many enrichment studies, it is almost never directly examined and rarely mentioned at all. Due to limited data availability, conducting a meta-analysis on

this particular topic is not feasible. Nevertheless, to approach the topic, we developed a systematic review in which we investigate the effect of animal husbandry on the welfare of laboratory animals and assign some of the extracted welfare parameters to typical symptoms of boredom. Since boredom and animal welfare are multifaceted conditions, this work is not based on the investigation of a single outcome, as considered in the classical PICO scheme but examines a set of parameters related to welfare and potentially boredom of laboratory animals.

The evaluation of the compliance with the established scientific quality criteria in the examined studies revealed a common lack of reported blinding. The percentage of about 25% of studies reporting blinding seems to be relatively low especially compared to preclinical biomedical studies (147) and also compared with a recent meta-analysis of the effects of housing on mortality in animal models of disease (7). One possible reason for this could be that behavioral studies are increasingly automated and/or conducted in the home cage without any required intervention with a (blinded) experimenter. In the case of behavioral observations in the (enriched) home cage, blinding of the observer is difficult to implement; in the case of automated behavioral analyses, it may not be necessary. This was not explored in this work; however, a systematic review of the use of automated and home cage-based systems for behavior analysis would be intriguing.

Although the study protocol was determined a priori, the protocol of this systematic review was not pre-registered. While this was not done in this work, it should be emphasized here that prospective registration of systematic reviews and meta-analyses reduces the potential for bias and fosters transparency (148).

Conclusion

Our findings show that a stimulating environment can be considered essential for the development of natural behavior and animal welfare of research rodents. Although boredom is almost never studied directly and rarely mentioned, this theme clearly resonates in many studies of the effects of improved housing conditions. Chronic boredom as a consequence of living in a barren and confined environment can pose a health risk to laboratory animals, limiting their validity as model organisms for biomedical research. A stimulating living environment sustains the well-being of laboratory rats and mice alike, regardless of age and sex. Although a longer period of housing might be more beneficial, even a short period in a stimulating environment improves essential parameters of animal welfare. Providing animals with adequate space, social contact, and a stimulating environment should not be considered a luxury or a treatment, but a necessity to ensure mental and physical health and a foundation for the expression of natural behaviors.

Data availability statement

The original contributions presented in the study are included in the article/Supplementary material, further inquiries can be directed to the corresponding author.

Author contributions

PM, UH, DB, LL, and KD: developed the study concept and design. PM, UH, CF-T, CH, KH, PK, JM, JR, JW, LL, and KD: were involved in data acquisition and analysis. PM, UH, LL, and KD: drafted the manuscript and figures. All authors contributed to the article and approved the submitted version.

Funding

This work was funded by the German Federal Institute for Risk Assessment.

References

- Olsson IAS, Dahlborn K. Improving housing conditions for laboratory mice: a review of "environmental enrichment" *Lab Anim.* (2002) 36:243–70. doi: 10.1258/002367702320162379
- van Zutphen LFM, Baumans V, Beynen AC. *Principles of Laboratory Animal Science: A Contribution to the Humane Use and Care of Animals and to the Quality of Experimental Results*. 1st ed. Amsterdam, NY: Elsevier (2001). p. 389.
- Ratuski AS, Weary DM. Environmental enrichment for rats and mice housed in laboratories: a metareview. *Animals*. (2022) 12:414. doi: 10.3390/ani12040414
- Newberry RC. Environmental enrichment: increasing the biological relevance of captive environments. *Appl Anim Behav Sci.* (1995) 44:229–43. doi: 10.1016/0168-1591(95)00616-Z
- Würbel H. Ideal homes? Housing effects on rodent brain and behaviour. *Trends Neurosci.* (2001) 24:207–11. doi: 10.1016/S0166-2236(00)01718-5
- Würbel H, Chapman R, Rutland C. Effect of feed and environmental enrichment on development of stereotypic wire-gnawing in laboratory mice. *Appl. Anim. Behav. Sci.* (1998) 60:69–81. doi: 10.1016/S0168-1591(98)00150-6
- Scott RW, Winder CB, Mason GJ. Conventional laboratory housing increases morbidity and mortality in research rodents: results of a meta-analysis. *BMC Biol.* (2022) 20:1–22. doi: 10.1186/s12915-021-01184-0
- Hebb DO. *The Organization of Behavior; A Neuropsychological Theory*. Oxford, England: Wiley (1949). p. 335.
- Johansson BB. Functional outcome in rats transferred to an enriched environment 15 days after focal brain ischemia. *Stroke.* (1996) 27:324–6. doi: 10.1161/01.STR.27.2.324
- Herring A, Lewejohann L, Panzer AL, Donath A, Kröll O, Sachser N, et al. Preventive and therapeutic types of environmental enrichment counteract beta amyloid pathology by different molecular mechanisms. *Neurobiol Dis.* (2011) 42:530–8. doi: 10.1016/j.nbd.2011.03.007
- van Praag H, Kempermann G, Gage FH. Neural consequences of environmental enrichment. *Nat Rev Neurosci.* (2000) 1:191–8. doi: 10.1038/35044558
- Benaroya-Milshtein N, Hollander N, Apter A, Kukulansky T, Raz N, Wilf A, et al. Environmental enrichment in mice decreases anxiety, attenuates stress responses and enhances natural killer cell activity. *Eur J Neurosci.* (2004) 20:1341–7. doi: 10.1111/j.1460-9568.2004.03587.x
- Bailoo JD, Murphy E, Boada-Sana M, Varholick JA, Hintze S, Baussiere C, et al. Effects of cage enrichment on behavior, welfare and outcome variability in female mice. *Front Behav Neurosci.* (2018) 12:232. doi: 10.3389/fnbeh.2018.00232
- Garner JP. Stereotypies and other abnormal repetitive behaviors: Potential impact on validity, reliability, and replicability of scientific outcomes. *ILAR J.* (2005) 46:106–17. doi: 10.1093/ilar.46.2.106
- Würbel H, Freire R, Nicol CJ. Prevention of stereotypic wire-gnawing in laboratory mice: Effects on behaviour and implications for stereotypy as a coping response. *Behav Processes.* (1998). doi: 10.1016/S0376-6357(97)00062-4
- Hobbiesiefken U, Mieske P, Lewejohann L, Diederich K. Evaluation of different types of enrichment - their usage and effect on home cage behavior in female mice. *PLoS ONE.* (2021) 16:e0261876. doi: 10.1371/journal.pone.0261876
- Hüttenrauch M, Salinas G, Wirths O. Effects of long-term environmental enrichment on anxiety, memory, hippocampal plasticity and overall brain gene expression in C57BL6 mice. *Front Mol Neurosci.* (2016) 9:1–11. doi: 10.3389/fnmol.2016.00062
- Smith JL, Wagaman J, Handley IM. Keeping it dull or making it fun: Task variation as a function of promotion versus prevention focus. *Motiv Emot.* (2009) 33:150–60. doi: 10.1007/s11031-008-9118-9
- Goldberg YK, Eastwood JD, Laguardia J, Danckert J. Boredom: an emotional experience distinct from apathy, anhedonia, or depression. *J Soc Clin Psychol.* (2011) 30:647–66. doi: 10.1521/jscp.2011.30.6.647
- Vodanovich SJ, Verner KM. Boredom proneness: its relationship to positive and negative affect. *Psychol Rep.* (1991) 69:1139–46. doi: 10.2466/pr0.1991.69.3f.1139
- Burn CC. Bestial boredom: a biological perspective on animal boredom and suggestions for its scientific investigation. *Anim Behav.* (2017) 130:141–51. doi: 10.1016/j.anbehav.2017.06.006
- Kurien BT, Gross T, Scofield RH. Barbering in mice: a model for trichotillomania. *Br. Med. J.* (2005) 331:1503–1505. doi: 10.1136/bmj.331.7531.1503
- Mansueto CS, Townsley Stemberger RM, McCombs Thomas A, Goldfinger Golomb R. Trichotillomania: a comprehensive behavioral model. *Clin Psychol Rev.* (1997) 17:567–57. doi: 10.1016/S0272-7358(97)00028-7[[i]]

Conflict of interest

The authors declare that the research was conducted in the absence of any commercial or financial relationships that could be construed as a potential conflict of interest.

Publisher's note

All claims expressed in this article are solely those of the authors and do not necessarily represent those of their affiliated organizations, or those of the publisher, the editors and the reviewers. Any product that may be evaluated in this article, or claim that may be made by its manufacturer, is not guaranteed or endorsed by the publisher.

Supplementary material

The Supplementary Material for this article can be found online at: <https://www.frontiersin.org/articles/10.3389/fvets.2022.899219/full#supplementary-material>

24. Hawkins MF, Tedford WH. Effects of interest and relatedness on estimated duration of verbal material. *Bull Psychon Soc.* (1976) 8:301–2. doi: 10.3758/BF03335146
25. Bateson M, Kacelnik A. Preferences for fixed and variable food sources: variability in amount and delay. *J Exp Anal Behav.* (1995) 63:313–29. doi: 10.1901/jeab.1995.63-313
26. Meagher RK, Mason GJ. Environmental enrichment reduces signs of boredom in caged mink. *PLoS ONE.* (2012) 7:e49180 doi: 10.1371/journal.pone.0049180
27. Burn CC, Raffle J, Bizley JK. Does “playtime” reduce stimulus-seeking and other boredom-like behaviour in laboratory ferrets? *Anim Welf.* (2020) 29:19–26. doi: 10.7120/09627286.29.1.019
28. Meagher RK, Campbell DLM, Mason GJ. Boredom-like states in mink and their behavioural correlates: a replicate study. *Appl Anim Behav Sci.* (2017) 197:112–9. doi: 10.1016/j.applanim.2017.08.001
29. Fureix C, Walker M, Harper L, Reynolds K, Saldivia-Woo A, Mason G. Stereotypic behaviour in standard non-enriched cages is an alternative to depression-like responses in C57BL/6 mice. *Behav. Brain Res.* (2016) 305:186–90. doi: 10.1016/j.bbr.2016.02.005
30. Fahlman SA, Mercer-Lynn KB, Flora DB, Eastwood JD. Development and validation of the multidimensional state boredom scale. *Assessment.* (2013) 20:68–85. doi: 10.1177/1073191111421303
31. Brust V, Schindler PM, Lewejohann L. Lifetime development of behavioural phenotype in the house mouse (*Mus musculus*). *Front. Zool.* (2015) 12:17. doi: 10.1186/1742-9994-12-S1-S17
32. Wilson TD, Reinhard DA, Westgate EC, Gilbert DT, Ellerbeck N, Hahn C, et al. Just think: the challenges of the disengaged mind. *Science.* (2014) 345:75–7. doi: 10.1126/science.1250830
33. Manosevitz M, Joel U. Behavioral effects of environmental enrichment in randomly bred mice. *J Comp Physiol Psychol.* (1973) 85:373–82. doi: 10.1037/h0035041
34. Inglis IR. Enriched sensory experience in adulthood increases subsequent exploratory behaviour in the rat. *Ani Behav.* (1975) 23:932–40. doi: 10.1016/0003-3472(75)90117-7
35. Swanson HH, McConnell P, Uylings HB, Van Oyen HG, Van de Poll NE. Interaction between pre-weaning undernutrition and post-weaning environmental enrichment on somatic development and behaviour in male and female rats. *Behav Processes.* (1983) 8:1–20. doi: 10.1016/0376-6357(83)90039-6
36. Van De Weerd HA, Van Loo PLP, Van Zutphen LFM, Koolhaas JM, Baumans V. Nesting material as environmental enrichment has no adverse effects on behavior and physiology of laboratory mice. *Physiol Behav.* (1997) 62:1019–28. doi: 10.1016/S0031-9384(97)00232-1
37. Tees RC. The influences of sex, rearing environment, and neonatal choline dietary supplementation on spatial and non-spatial learning and memory in adult rats. *Dev Psychobiol.* (1999) 35:328–42. doi: 10.1002/(SICI)1098-2302(199912)35:4<328::AID-DEV7>3.0.CO;2-4
38. Roy V, Belzung C, Delarue C, Chapillon P. Environmental enrichment in BALB/c mice - effects in classical tests of anxiety and exposure to a predatory odor. *Physiol Behav.* (2001) 74:313–20. doi: 10.1016/S0031-9384(01)00561-3
39. Van de Weerd HA, Aarsen EL, Mulder A, Kruitwagen CLJJ, Hendriksen CFM, Baumans V. Effects of environmental enrichment for mice: variation in experimental results. *J Appl Anim Welf Sci.* (2002) 5:87–109. doi: 10.1207/S15327604JAWS0502_01
40. Bezard E, Dovero S, Belin D, Duconger S, Jackson-Lewis V, Przedborski S, et al. Enriched environment confers resistance to 1-methyl-4-phenyl-1,2,3,6-tetrahydropyridine and cocaine: involvement of dopamine transporter and trophic factors. *J Neurosci.* (2003) 23:10999–1007. doi: 10.1523/JNEUROSCI.23-35-10999.2003
41. Pietropaolo S, Branchi I, Cirulli F, Chiarotti F, Aloe L, Alleva E. Long-term effects of the periadolescent environment on exploratory activity and aggressive behaviour in mice: social versus physical enrichment. *Physiol Behav.* (2004) 81:443–53. doi: 10.1016/j.physbeh.2004.02.022
42. Cain ME, Green TA, Bardo MT. Environmental enrichment decreases responding for visual novelty. *Behav Processes.* (2006) 73:360–6. doi: 10.1016/j.beproc.2006.08.007
43. Gresack JE, Kerr KM, Frick KM. Short-term environmental enrichment decreases the mnemonic response to estrogen in young, but not aged, female mice. *Brain Res.* (2007) 1160:91–101. doi: 10.1016/j.brainres.2007.05.033
44. Abou-Ismaïl UA, Burman OHP, Nicol CJ, Mendl M. The effects of enhancing cage complexity on the behaviour and welfare of laboratory rats. *Behav Processes.* (2010) 85:172–80. doi: 10.1016/j.beproc.2010.07.002
45. Franks B, Champagne FA, Higgins ET. How Enrichment Affects Exploration Trade-Offs in Rats: Implications for Welfare and Well-Being. *PLoS ONE.* (2013) 8:e83578. doi: 10.1371/journal.pone.0083578
46. Hughes RN. Modification by environmental enrichment of acute caffeine's behavioral effects on male and female rats. *J Caffeine Res.* (2013) 3:156–62. doi: 10.1089/jcr.2013.0018
47. Hughes RN, Otto MT. Anxiolytic effects of environmental enrichment attenuate sex-related anxiogenic effects of scopolamine in rats. *Prog Neuropsychopharmacol Biol Psychiatry.* (2013) 40:252–9. doi: 10.1016/j.pnpbp.2012.10.009
48. Doulames V, Lee S, Shea TB. Environmental enrichment and social interaction improve cognitive function and decrease reactive oxidative species in normal adult mice. *Int J Neurosci.* (2014) 124:369–76. doi: 10.3109/00207454.2013.848441
49. Lima FB, Spinelli de Oliveira E. What is the impact of low testosterone levels on the anatomical and behavioral repertoire of long-term enriched housing of male mice? *Behav Processes.* (2014) 108:57–64. doi: 10.1016/j.beproc.2014.09.025
50. Badowska DM, Brzózka MM, Chowdhury A, Malzahn D, Rossner MJ. Data calibration and reduction allows to visualize behavioural profiles of psychosocial influences in mice towards clinical domains. *Eur Arch Psychiatry Clin Neurosci.* (2015) 265:483–96. doi: 10.1007/s00406-014-0532-6
51. Berardo LR, Fabio MC, Pautassi RM. Post-weaning environmental enrichment, but not chronic maternal isolation, enhanced ethanol intake during periadolescence and early adulthood. *Front Behav Neurosci.* (2016) 10:195. doi: 10.3389/fnbeh.2016.00195
52. Garcia EJ, Haddon TN, Saucier DA, Cain ME. Differential housing and novelty response: Protection and risk from locomotor sensitization. *Pharmacol Biochem Behav.* (2017) 154:20–30. doi: 10.1016/j.pbb.2017.01.004
53. Melani R, Chelini G, Cenni MC, Berardi N. Enriched environment effects on remote object recognition memory. *Neuroscience.* (2017) 352:296–305. doi: 10.1016/j.neuroscience.2017.04.006
54. Faraji J, Karimi M, Soltanpour N, Rouhzadeh Z, Roudaki S, Hosseini SA, et al. Intergenerational sex-specific transmission of maternal social experience. *Sci Rep.* (2018) 8:10529. doi: 10.1038/s41598-018-28729-8
55. Sparling JE, Baker SL, Bielajew C. Effects of combined pre- and post-natal enrichment on anxiety-like, social, and cognitive behaviours in juvenile and adult rat offspring. *Behav Brain Res.* (2018) 353:40–50. doi: 10.1016/j.bbr.2018.06.033
56. Mendes F, da Paixao L, Diniz CWP, Sosthenes MCK. Environmental impoverishment, aging, and reduction in mastication affect mouse innate repertoire to explore novel environments and to assess risk. *Front Neurosci.* (2019) 13:107. doi: 10.3389/fnins.2019.00107
57. Dixon EI, Hughes RN. Treatment with 1-benzylpiperazine (BZP) during adolescence of male and female hooded rats exposed to environmental enrichment: Subsequent behavioral outcomes. *Int J Dev Neurosci.* (2019) 73:32–40. doi: 10.1016/j.ijdevneu.2018.12.005
58. Rabadan R, Ramos-Campos M, Redolat R, Mesa-Gresa P. Physical activity and environmental enrichment: behavioural effects of exposure to different housing conditions in mice. *Acta Neurobiol Exp.* (2019) 79:374–85. doi: 10.21307/ane-2019-035
59. Suárez A, Fabio MC, Bellia F, Fernández MS, Pautassi RM. Environmental enrichment during adolescence heightens ethanol intake in female, but not male, adolescent rats that are selectively bred for high and low ethanol intake during adolescence. *Am J Drug Alcohol Abuse.* (2020) 46:553–64. doi: 10.1080/00952990.2020.1770778
60. Soeda F, Toda A, Masuzaki K, Miki R, Koga T, Fujii Y, Takahama K. Effects of enriched environment on micturition activity in freely moving C57BL/6J mice. *Low Urin tract Symptoms.* (2021) 13:400–9. doi: 10.1111/luts.12376
61. van der Geest JN, Spoor M, Frens MA. Environmental Enrichment Improves Vestibular Oculomotor Learning in Mice. *Front Behav Neurosci.* (2021) 15:676416. doi: 10.3389/fnbeh.2021.676416
62. Vazquez-Sanroman DB, Wilson GA, Bardo MT. Effects of social isolation on perineuronal nets in the amygdala following a reward omission task in female rats. *Mol Neurobiol.* (2021) 58:348–61. doi: 10.1007/s12035-020-02125-8
63. Yazdanfar N, Mard SA, Mahmoudi J, Bakhtiari N, Sarkaki A, Farnam A. Maternal morphine exposure and post-weaning social isolation impair memory and ventral striatum dopamine system in male offspring: is an enriched environment beneficial? *Neuroscience.* (2021) 461:80–90. doi: 10.1016/j.neuroscience.2021.02.024
64. Dos Anjos-Garcia T, Kanashiro A, De Campos AC, Coimbra NC. Environmental enrichment facilitates anxiety in conflict-based tests but inhibits predator threat-induced defensive behaviour in male mice. *Neuropsychobiology.* (2022) 81:225–36. doi: 10.1159/000521184

65. Maccioni P, Bratzu J, Lobina C, Acciaro C, Corrias G, Capra A, et al. Exposure to an enriched environment reduces alcohol self-administration in Sardinian alcohol-preferring rats. *Physiol Behav.* (2022) 249:113771. doi: 10.1016/j.physbeh.2022.113771
66. Paré WP, Kluczynski J. Developmental factors modify stress ulcer incidence in a stress-susceptible rat strain. *J Physiol Paris.* (1997) 105–111. doi: 10.1016/S0928-4257(97)89473-9
67. Branchi I, Alleva E. Communal nesting, an early social enrichment, increases the adult anxiety-like response and shapes the role of social context in modulating the emotional behavior. *Behav Brain Res.* (2006) 172:299–306. doi: 10.1016/j.bbr.2006.05.019
68. Abramov U, Puusaar T, Raud S, Kurrikoff K, Vasar E. Behavioural differences between C57BL/6 and 129SvEv strains are reinforced by environmental enrichment. *Neurosci Lett.* (2008) 443:223–7. doi: 10.1016/j.neulet.2008.07.075
69. Brenes JC, Rodríguez O, Fornaguera J. Differential effect of environment enrichment and social isolation on depressive-like behavior, spontaneous activity and serotonin and norepinephrine concentration in prefrontal cortex and ventral striatum. *Pharmacol Biochem Behav.* (2008) 89:85–93. doi: 10.1016/j.pbb.2007.11.004
70. Brenes JC, Padilla M, Fornaguera J, A. detailed analysis of open-field habituation and behavioral and neurochemical antidepressant-like effects in postweaning enriched rats. *Behav Brain Res.* (2009) 197:125–37. doi: 10.1016/j.bbr.2008.08.014
71. Nowakowska E, Czubak A, Kus K, Metelska J, Burda K, Nowakowska A. Effect of lamotrigine and environmental enrichment on spatial memory and behavioral functions in rats. *Arzneimittelforschung.* (2010) 60:307–14. doi: 10.1055/s-0031-1296292
72. Silva CF, Duarte FS, Lima TCM De, De Oliveira CL. Effects of social isolation and enriched environment on behavior of adult Swiss mice do not require hippocampal neurogenesis. *Behav Brain Res.* (2011) 225:85–90. doi: 10.1016/j.bbr.2011.07.007
73. Workman JL, Fonken LK, Gusfa J, Kassouf KM, Nelson RJ. Post-weaning environmental enrichment alters affective responses and interacts with behavioral testing to alter nNOS immunoreactivity. *Pharmacol Biochem Behav.* (2011) 100:25–32. doi: 10.1016/j.pbb.2011.07.008
74. Simpson J, Kelly JP. The effects of isolated and enriched housing conditions on baseline and drug-induced behavioural responses in the male rat. *Behav Brain Res.* (2012) 234:175–83. doi: 10.1016/j.bbr.2012.06.015
75. Ros-Simó C, Valverde O. Early-life social experiences in mice affect emotional behaviour and hypothalamic-pituitary-adrenal axis function. *Pharmacol Biochem Behav.* (2012) 102:434–41. doi: 10.1016/j.pbb.2012.06.001
76. Yildirim E, Erol K, Ulupinar E. Effects of sertraline on behavioral alterations caused by environmental enrichment and social isolation. *Pharmacol Biochem Behav.* (2012) 101:278–87. doi: 10.1016/j.pbb.2011.12.017
77. Kallioikoski O, Jacobsen KR, Darusman HS, Henriksen T, Weimann A, Poulsen HE, et al. Mice do not habituate to metabolism cage housing—a three week study of male BALB/c mice. *PLoS ONE.* (2013) 8:e58460. doi: 10.1371/journal.pone.0058460
78. Nishijima T, Llorens-Martin M, Tejeda GS, Inoue K, Yamamura Y, Soya H, et al. Cessation of voluntary wheel running increases anxiety-like behavior and impairs adult hippocampal neurogenesis in mice. *Behav Brain Res.* (2013) 245:34–41. doi: 10.1016/j.bbr.2013.02.009
79. Cao WY, Duan J, Wang XQ, Zhong XL, Hu ZL, Huang FL, et al. Early enriched environment induces an increased conversion of proBDNF to BDNF in the adult rat's hippocampus. *Behav Brain Res.* (2014) 265:76–83. doi: 10.1016/j.bbr.2014.02.022
80. Martinez AR, Brunelli SA, Zimmerberg B. Communal nesting exerts epigenetic influences on affective and social behaviors in rats selectively bred for an infantile trait. *Physiol Behav.* (2015) 139:97–103. doi: 10.1016/j.physbeh.2014.11.007
81. Mosafari B, Babri S, Ebrahimi H, Mohaddes G. Enduring effects of post-weaning rearing condition on depressive- and anxiety-like behaviors and motor activity in male rats. *Physiol Behav.* (2015) 142:131–6. doi: 10.1016/j.physbeh.2015.02.015
82. Arndt DL, Peterson CJ, Cain ME. Differential rearing alters forced swim test behavior, fluoxetine efficacy, and post-test weight gain in male rats. *PLoS ONE.* (2015) 10:e0131709. doi: 10.1371/journal.pone.0131709
83. Zanca RM, Braren SH, Maloney B, Schrott LM, Luine VN, Serrano PA. Environmental enrichment increases glucocorticoid receptors and decreases GluA2 and protein kinase M Zeta (PKMζ) trafficking during chronic stress: a protective mechanism? *Front Behav Neurosci.* (2015) 9:303. doi: 10.3389/fnbeh.2015.00303
84. Pooriamehr A, Sabahi P, Miladi-Gorji H. Effects of environmental enrichment during abstinence in morphine dependent parents on anxiety, depressive-like behaviors and voluntary morphine consumption in rat offspring. *Neurosci Lett.* (2017) 656:37–42. doi: 10.1016/j.neulet.2017.07.024
85. Nip E, Adcock A, Nazal B, MacLellan A, Niel L, Choleris E, et al. Why are enriched mice nice? Investigating how environmental enrichment reduces agonism in female C57BL/6, DBA/2, and BALB/c mice. *Appl Anim Behav Sci.* (2019) 217:73–82. doi: 10.1016/j.applanim.2019.05.002
86. Nwachukwu K, Rhoads E, Meek S, Bardi M. Back to nature: herbal treatment, environmental enrichment, and social play can protect against unpredictable chronic stress in Long-Evans rats (*Rattus norvegicus*). *Psychopharmacology.* (2021) 238:2999–3012. doi: 10.1007/s00213-021-05917-5
87. Xu ZW, Hou B, Gao Y, He FC, Zhang CG. Effects of enriched environment on morphine-induced reward in mice. *Exp Neurol.* (2007) 204:714–9. doi: 10.1016/j.expneurol.2006.12.027
88. El Rawas R, Thiriet N, Lardeux V, Jaber M, Solinas M. Environmental enrichment decreases the rewarding but not the activating effects of heroin. *Psychopharmacology.* (2009) 203:561–70. doi: 10.1007/s00213-008-1402-6
89. De Carvalho CR, Pandolfo P, Pamplona FA, Takahashi RN. Environmental enrichment reduces the impact of novelty and motivational properties of ethanol in spontaneously hypertensive rats. *Behav Brain Res.* (2010) 208:231–6. doi: 10.1016/j.bbr.2009.11.043
90. Chauvet C, Lardeux V, Jaber M, Solinas M. Brain regions associated with the reversal of cocaine conditioned place preference by environmental enrichment. *Neuroscience.* (2011) 184:88–96. doi: 10.1016/j.neuroscience.2011.03.068
91. Ranaldi R, Kest K, Zellner M, Hachimine-Semprebom P. Environmental enrichment, administered after establishment of cocaine self-administration, reduces lever pressing in extinction and during a cocaine context renewal test. *Behav Pharmacol.* (2011) 22:347–53. doi: 10.1097/FBP.0b013e3283487365
92. Smith MA, Pitts EG. Access to a running wheel inhibits the acquisition of cocaine self-administration. *Pharmacol Biochem Behav.* (2011) 100:237–43. doi: 10.1016/j.pbb.2011.08.025
93. Chauvet C, Goldberg SR, Jaber M, Solinas M. Effects of environmental enrichment on the incubation of cocaine craving. *Neuropharmacology.* (2012) 63:635–41. doi: 10.1016/j.neuropharm.2012.05.014
94. Turner PV, Sunohara-Neilson J, Ovari J, Healy A, Leri F. Effects of single compared with pair housing on hypothalamic-pituitary-adrenal axis activity and low-dose heroin place conditioning in adult male Sprague-Dawley rats. *J Am Assoc Lab Anim Sci.* (2014) 53:161–7. Available online at: <https://www.ncbi.nlm.nih.gov/pmc/articles/PMC3966272/>
95. Peck JA, Galaj E, Eshak S, Newman KL, Ranaldi R. Environmental enrichment induces early heroin abstinence in an animal conflict model. *Pharmacol Biochem Behav.* (2015) 138:20–5. doi: 10.1016/j.pbb.2015.09.009
96. Bahi A. Environmental enrichment reduces chronic psychosocial stress-induced anxiety and ethanol-related behaviors in mice. *Prog Neuropsychopharmacol Biol Psychiatry.* (2017) 77:65–74. doi: 10.1016/j.pnpbp.2017.04.001
97. Holgate JY, Garcia H, Chatterjee S, Bartlett SE. Social and environmental enrichment has different effects on ethanol and sucrose consumption in mice. *Brain Behav.* (2017) 7:e00767. doi: 10.1002/brb3.767
98. Li C, Frantz KJ. Abstinence environment contributes to age differences in reinstatement of cocaine seeking between adolescent and adult male rats. *Pharmacol Biochem Behav.* (2017) 158:49–56. doi: 10.1016/j.pbb.2017.06.003
99. Ewing S, Ranaldi R. Environmental enrichment facilitates cocaine abstinence in an animal conflict model. *Pharmacol Biochem Behav.* (2018) 166:35–41. doi: 10.1016/j.pbb.2018.01.006
100. Khalaji S, Bigdeli I, Ghorbani R, Miladi-Gorji H. Environmental enrichment attenuates morphine-induced conditioned place preference and locomotor sensitization in maternally separated rat pups. *Basic Clin Neurosci.* (2018) 9:181–90. doi: 10.32598/bcn.9.4.241
101. Wang R, Hausknecht KA, Shen YL, Haj-Dahmane S, Vezina P, Shen RY. Environmental enrichment reverses increased addiction risk caused by prenatal ethanol exposure. *Drug Alcohol Depend.* (2018) 191:343–7. doi: 10.1016/j.drugalcdep.2018.07.013
102. Arndt DL, Wukitch TJ, Garcia EJ, Cain M. Histone deacetylase inhibition differentially attenuates cue-induced reinstatement: an interaction of environment and acH3K9 expression in the dorsal striatum. *Behav Neurosci.* (2019) 133:478–88. doi: 10.1037/bne000333
103. Campbell EJ, Jin S, Lawrence AJ. Environmental enrichment reduces the propensity to relapse following punishment-imposed abstinence of alcohol seeking. *Physiol Behav.* (2019) 210:112638. doi: 10.1016/j.physbeh.2019.11.2638

104. Haider S, Nawaz A, Batool Z, Tabassum S, Perveen T. Alleviation of diazepam-induced conditioned place preference and its withdrawal-associated neurobehavioral deficits following pre-exposure to enriched environment in rats. *Physiol Behav.* (2019) 208:112564. doi: 10.1016/j.physbeh.2019.112564
105. Garcia EJ, Cain ME. Environmental enrichment and a selective metabotropic glutamate receptor(2/3) [mGluR(2/3)] agonist suppress amphetamine self-administration: Characterizing baseline differences. *Pharmacol Biochem Behav.* (2020) 192:172907. doi: 10.1016/j.pbb.2020.172907
106. Salinas-Velarde ID, Bernal-Morales B, Pacheco-Cabrera P, Sánchez-Aparicio P, Pascual-Mathey LI, Venebra-Muñoz A. Lower Δ FosB expression in the dopaminergic system after stevia consumption in rats housed under environmental enrichment conditions. *Brain Res Bull.* (2021) 177:172–80. doi: 10.1016/j.brainresbull.2021.10.001
107. Vigorito M, Lopez MJ, Pra Sisto AJ. Sign tracking in an enriched environment: a potential ecologically relevant animal model of adaptive behavior change. *Cogn Affect Behav Neurosci.* (2021) 192:172907. doi: 10.3758/s13415-021-00897-7
108. Yazdanfar N, Farnam A, Sadigh-Eteghad S, Mahmoudi J, Sarkaki A. Enriched environment and social isolation differentially modulate addiction-related behaviors in male offspring of morphine-addicted dams: The possible role of μ -opioid receptors and Δ FosB in the brain reward pathway. *Brain Res Bull.* (2021) 170:98–105. doi: 10.1016/j.brainresbull.2021.02.005
109. Callard MD, Bursten SN, Price EO. Repetitive backflipping behaviour in captive roof rats (*Rattus rattus*) and the effects of cage enrichment. *Anim Welf.* (2000) 9:139–52. Available online at: <https://www.ingentaconnect.com/contentone/ufaw/aw/2000/00000009/00000002/art00003>
110. Olsson IAS, Sherwin CM. Behaviour of laboratory mice in different housing conditions when allowed to self-administer an anxiolytic. *Lab Anim.* (2006) 40:392–9. doi: 10.1258/002367706778476389
111. Tilly S-LC, Dallaire J, Mason GJ. Middle-aged mice with enrichment-resistant stereotypic behaviour show reduced motivation for enrichment. *Anim Behav.* (2010) 80:363–73. doi: 10.1016/j.anbehav.2010.06.008
112. Latham N, Mason G. Frustration and perseveration in stereotypic captive animals: Is a taste of enrichment worse than none at all? *Behav Brain Res.* (2010) 211:96–104. doi: 10.1016/j.bbr.2010.03.018
113. Pawlowicz A, Demner A, Lewis MH. Effects of access to voluntary wheel running on the development of stereotypy. *Behav Processes.* (2010) 83:242–6. doi: 10.1016/j.beproc.2009.11.008
114. Jones MA, Mason G, Pillay N. Early environmental enrichment protects captive-born striped mice against the later development of stereotypic behaviour. *Appl Anim Behav Sci.* (2011) 135:138–45. doi: 10.1016/j.applanim.2011.08.015
115. Hajheidari S, Miladi-gorji H, Bigdeli I. Effects of environmental enrichment during induction of methamphetamine dependence on the behavioral withdrawal symptoms in rats. *Neurosci Lett.* (2015) 605:39–43. doi: 10.1016/j.neulet.2015.08.010
116. Joshi S, Pillay N. Personality predicts the responses to environmental enrichment at the group but not within-groups in stereotypic African striped mice, *Rhabdomys dilectus*. *Appl Anim Behav Sci.* (2016) 182:44–52. doi: 10.1016/j.applanim.2016.06.006
117. Bechard AR, Bliznyuk N, Lewis MH. The development of repetitive motor behaviors in deer mice: Effects of environmental enrichment, repeated testing, and differential mediation by indirect basal ganglia pathway activation. *Develop Psychobiol.* (2017) 59:390–9. doi: 10.1002/dev.21503
118. Joshi S, Pillay N. Is wheel running a re-directed stereotypic behaviour in striped mice *Rhabdomys dilectus*? *Appl Anim Behav Sci.* (2018) 204:113–21. doi: 10.1016/j.applanim.2018.04.011
119. Joseph R, Gallagher RE. Gender and early environmental influences on activity, overresponsiveness, and exploration. *Develop Psychobiol.* (1980) 13:527–44. doi: 10.1002/dev.420130512
120. Rose FD, Love S, Dell PA. Differential reinforcement effects in rats reared in enriched and impoverished environments. *Physiol Behav.* (1986) 36:1139–45. doi: 10.1016/0031-9384(86)90491-9
121. Holm L, Ladewig J. The effect of housing rats in a stimulus rich versus stimulus poor environment on preference measured by sigmoid double demand curves. *Appl Anim Behav Sci.* (2007) 107:342–54. doi: 10.1016/j.applanim.2006.09.019
122. Makowska IJ, Weary DM. Differences in anticipatory behaviour between rats (*rattus norvegicus*) housed in standard versus semi-naturalistic laboratory environments. *PLoS ONE.* (2016) 11:e0147595. doi: 10.1371/journal.pone.0147595
123. Vakhnin VA, Bryukhin GV. Effects of environmental conditions on behavior in an open field test in rats born to females with chronic alcoholization. *Neurosci Behav Physiol.* (2015) 45:1003–9. doi: 10.1007/s11055-015-0179-4
124. Núñez-Murrieta MA, Noguez P, Coria-Avila GA, García-García F, Santiago-García J, Bolado-García VE, et al. Maternal behavior, novelty confrontation, and subcortical c-Fos expression during lactation period are shaped by gestational environment. *Behav Brain Res.* (2021) 412. doi: 10.1016/j.bbr.2021.113432
125. Garrido P, De Blas M, Ronzoni G, Cordero I, Antón M, Giné E, et al. Differential effects of environmental enrichment and isolation housing on the hormonal and neurochemical responses to stress in the prefrontal cortex of the adult rat: relationship to working and emotional memories. *J Neural Transm.* (2013) 120:829–43. doi: 10.1007/s00702-012-0935-3
126. Molina SJ, Lietti AE, Carreira Caro CS, Buján GE, Guelman LR. Effects of early noise exposure on hippocampal-dependent behaviors during adolescence in male rats: influence of different housing conditions. *Anim Cogn.* (2022) 25:103–20. doi: 10.1007/s10071-021-01540-1
127. Biernaskie J, Corbett D. Enriched rehabilitative training promotes improved forelimb motor function and enhanced dendritic growth after focal ischemic injury. *J Neurosci.* (2001) 21:5272–80. doi: 10.1523/JNEUROSCI.21-14-05272.2001
128. Murphy TH, Corbett D. Plasticity during stroke recovery: from synapse to behaviour. *Nat Rev Neurosci.* (2009) 10:861–72. doi: 10.1038/nrn2735
129. Radabaugh HL, LaPorte MJ, Greene AM, Bondi CO, Lajud N, Radabaugh HL, et al. Refining environmental enrichment to advance rehabilitation based research after experimental traumatic brain injury. *Clin Exp Neurol.* (2017) 294:12–8. doi: 10.1016/j.expneurol.2017.04.013[[i]]
130. Lewejohann L, Schwabe K, Häger K, Jirkof P. Impulse for animal welfare outside the experiment. *Lab Anim.* (2020) 54:150–8. doi: 10.1177/0023677219891754
131. Gouveia K, Hurst JL. Improving the practicality of using non-aversive handling methods to reduce background stress and anxiety in laboratory mice. *Sci Rep.* (2019) 9:20305. doi: 10.1038/s41598-019-56860-7
132. Flórez-Vargas O, Brass A, Karystianis G, Bramhall M, Stevens R, Cruickshank S, et al. Bias in the reporting of sex and age in biomedical research on mouse models. *Elife.* (2016) 5:1–14. doi: 10.7554/eLife.13615
133. Becker JB, Prendergast BJ, Liang JW. Female rats are not more variable than male rats: A meta-analysis of neuroscience studies. *Biol Sex Differ.* (2016) 7:1–7. doi: 10.1186/s13293-016-0087-5
134. Clayton JA, Collins FS, NIH. To balance sex in cell and animal studies. *Nature.* (2014) 509:282–3. doi: 10.1038/509282a
135. Jackson SJ, Andrews N, Ball D, Bellantuono I, Gray J, Hachoumi L, et al. Does age matter? The impact of rodent age on study outcomes. *Lab Anim.* (2017) 51:160–9. doi: 10.1177/0023677216653984
136. Korholz JC, Zocher S, Grzyb AN, Morisse B, Poetzsch A, Ehret F, et al. Selective increases in inter-individual variability in response to environmental enrichment in female mice. *Elife.* (2018) 7:e35690. doi: 10.7554/eLife.35690
137. Kell RT, Bell G, Quinney A. Musculoskeletal fitness, health outcomes and quality of life. *Sports Med.* (2001) 31:863–73. doi: 10.2165/00007256-200131120-00003
138. Schmitt A, Herzog P, Röchner F, Brändle AL, Fragasso A, Munz B. Skeletal muscle effects of two different 10-week exercise regimens, voluntary wheel running, and forced treadmill running, in mice: a pilot study. *Physiol Rep.* (2020) 8:1–15. doi: 10.14814/phy2.14609
139. Korte SM, Olivier B, Koolhaas JM. A new animal welfare concept based on allostasis. *Physiol Behav.* (2007) 92:422–8. doi: 10.1016/j.physbeh.2006.10.018
140. Kempermann G. Environmental enrichment, new neurons and the neurobiology of individuality. *Nat Rev Neurosci.* (2019) 20:235–45. doi: 10.1038/s41583-019-0120-x
141. Zocher S, Overall RW, Lesche M, Dahl A, Kempermann G. Environmental enrichment preserves a young DNA methylation landscape in the aged mouse hippocampus. *Nat Commun.* (2021) 12:3892. doi: 10.1038/s41467-021-23993-1
142. Xiao R, Ali S, Caligiuri MA, Cao L. Enhancing effects of environmental enrichment on the functions of natural killer cells in mice. *Front Immunol.* (2021) 12:1–10. doi: 10.3389/fimmu.2021.695859
143. Landeck L, Kaiser ME, Heffer D, Draguhn A, Both M. Enriched environment modulates sharp wave-ripple (SPW-R) activity in hippocampal slices. *Front Neural Circuits.* (2021) 15:1–12. doi: 10.3389/fncir.2021.758939
144. Fabel K, Wolf SA, Ehninger D, Babu H, Leal-García P, Kempermann G. Additive effects of physical exercise and environmental enrichment on adult hippocampal neurogenesis in mice. *Front Neurosci.* (2009) 3:1–7. doi: 10.3389/neuro.22.002.2009

145. Hess SE, Rohr S, Dufour BD, Gaskill BN, Pajor EA, Garner JP. Home improvement: C57BL/6J mice given more naturalistic nesting materials build better nests. *J Am Assoc Lab Anim Sci.* (2008) 47:25–31. Available online at: <https://www.ncbi.nlm.nih.gov/pmc/articles/PMC2687128/>
146. Shyne A. Meta-analytic review of the effects of enrichment on stereotypic behavior in zoo mammals. *Zoo Biol.* (2006) 25:317–37. doi: 10.1002/zoo.20091
147. Babor Z, Liao J, Macleod MR, Bannach-Brown A, McCann SK, Wever KE, et al. Risk of bias reporting in the recent animal focal cerebral ischaemia literature. *Clin Sci (Lond).* (2017) 131:2525–32. doi: 10.1042/CS20160722
148. Stewart L, Moher D, Shekelle P. Why prospective registration of systematic reviews makes sense. *Syst Rev.* (2012) 1:7. doi: 10.1186/2046-4053-1-7



OPEN ACCESS

EDITED BY

Adelino Sanchez Ramos da Silva,
University of São Paulo, Brazil

REVIEWED BY

Yifan Zhai,
Shandong Academy of Agricultural
Sciences, China
Subhash Rajpurohit,
Ahmedabad University, India

*CORRESPONDENCE

Lan Zheng,
Lanzheng@hunnu.edu.cn

SPECIALTY SECTION

This article was submitted to
Developmental Epigenetics,
a section of the journal
Frontiers in Cell and Developmental
Biology

RECEIVED 11 June 2022

ACCEPTED 22 August 2022

PUBLISHED 09 September 2022

CITATION

Ding M, Li H and Zheng L (2022),
Drosophila exercise, an emerging
model bridging the fields of exercise and
aging in human.
Front. Cell Dev. Biol. 10:966531.
doi: 10.3389/fcell.2022.966531

COPYRIGHT

© 2022 Ding, Li and Zheng. This is an
open-access article distributed under
the terms of the [Creative Commons
Attribution License \(CC BY\)](#). The use,
distribution or reproduction in other
forums is permitted, provided the
original author(s) and the copyright
owner(s) are credited and that the
original publication in this journal is
cited, in accordance with accepted
academic practice. No use, distribution
or reproduction is permitted which does
not comply with these terms.

Drosophila exercise, an emerging model bridging the fields of exercise and aging in human

Meng Ding, Hongyu Li and Lan Zheng*

Key Laboratory of Physical Fitness and Exercise Rehabilitation of Hunan Province, Hunan Normal University, Changsha, China

Exercise is one of the most effective treatments for the diseases of aging. In recent years, a growing number of researchers have used *Drosophila melanogaster* to study the broad benefits of regular exercise in aging individuals. With the widespread use of *Drosophila* exercise models and the upgrading of the *Drosophila* exercise apparatus, we should carefully examine the differential contribution of regular exercise in the aging process to facilitate more detailed quantitative measurements and assessment of the exercise phenotype. In this paper, we review some of the resources available for *Drosophila* exercise models. The focus is on the impact of regular exercise or exercise adaptation in the aging process in *Drosophila* and highlights the great potential and current challenges faced by this model in the field of anti-aging research.

KEYWORDS

Drosophila, exercise, aging, obesity, cardiac aging, lipid metabolism

1 Introduction

Exercise is a serious challenge to systemic homeostasis and it causes a wide range of effects in a variety of cells, tissues and organs (Hawley et al., 2014). Indeed, a single exercise session is sufficient to produce acute changes at the transcriptional level (Williams et al., 1996), (Pilegaard et al., 2003). Multiple repetitions of exercise can produce exercise adaptation and more lasting effects on protein function (McGee and Hargreaves, 2020). Planned regular exercise can delay the development of chronic metabolic diseases, including cardiovascular diseases (CVDs), type 2 diabetes (T2D), insulin resistance and obesity (Hawley and Krook, 2016), (Fiuza-Luces et al., 2018), (Umpierre et al., 2011), (Goodyear and Kahn, 1998), (Castaño et al., 2020), (Houghton et al., 2017).

Aging is a major risk factor for CVDs, T2D and neurodegenerative diseases (Paneni et al., 2017), (Laiteerapong et al., 2019), (Hou et al., 2019). Epidemiological studies have shown that the increase in human lifespan has led to a high incidence of aging-related diseases, which places a huge burden on the world health care system (Partridge et al., 2018). Therefore, healthy aging will become one of the most important goals to be addressed today. Aging is determined by complex interactions between biology, environment, and society, which are beyond the control of the individual (Myint and Welch, 2012). But, lifestyle interventions can help to maintain health, such as increasing

exercise as well as controlling diet (Partridge et al., 2018). It is well known that lifespan has heritable properties and therefore has a genetic basis. This was shown in studies in *Drosophila*, where differences in lifespan can be almost twofold across genetic backgrounds and these differences are heritable, supporting the model of genetic determination of lifespan (Campisi et al., 2019). *Drosophila* has powerful genetic tools and short lifespan characteristics, which make it an ideal model organism for studying lifespan and aging (Helfand and Rogina, 2003), (Makarova et al., 2015). In addition, *Drosophila* models have many notable achievements in age-related diseases, such as CVDs, sarcopenia and neurodegenerative diseases (Diop and Bodmer, 2015), (Hunt et al., 2021), (Feany and Bender, 2000), (Lu and Vogel, 2009).

Although exercise is an economical and effective treatment for age-related diseases (Li et al., 2020a), (Fiuza-Luces et al., 2018), (Batsis and Villareal, 2018), there are still many limitations in human and animal studies due to life cycle limitations (Blice-Baum et al., 2019). In recent years, *Drosophila* exercise models with short lifespan and mature genetic tools have become the optimal choice for researchers (Li et al., 2020b), (Kim et al., 2020), (Wen et al., 2016).

2 Development of a *Drosophila* exercise model for cardiovascular aging research

CVDs are the leading cause of death worldwide, with an estimated 17.9 million deaths from CVDs in 2019, accounting for 32% of global deaths (WHO (World Health Organization), 2017). Aging is a major risk factor for CVDs, including atherosclerosis, hypertension, myocardial infarction, and stroke (Paneni et al., 2017), (North and Sinclair, 2012). Exercise therapy is an economical and effective therapy to reduce mortality and risk of heart disease (Goenka and Lee, 2017). These studies are equally applicable in flies. In aged *Drosophila*, exercise enhances cardiac function and improves cardiomyocyte ultrastructure and heart failure (Piazza et al., 2009), (Li et al., 2020b). Nicotinamide adenine dinucleotide (NAD⁺) is a central metabolite associated with atherosclerosis, ischemic, diabetic, arrhythmogenic, hypertrophic or dilated cardiomyopathy, and different forms of heart failure (Abdellatif et al., 2021). Recently, several studies using *Drosophila* models have shown that NAD⁺ supplementation improves mitochondrial mass, delays accelerated aging and extends lifespan through DCT-1 and ULK-1 (Fang et al., 2019). Consistently, mice prolong lifespan by supplementation with the NAD⁺ precursor nicotinamide riboside (NR) (Zhang et al., 2016). In addition, high expression of NAD⁺ synthase protein positively affected cardiac function in aging flies, including increased cardiac output and reduced heart failure (Wen et al., 2016). Similarly, NAD⁺ precursor treatment also improved cardiac function in aged MDX mice with

cardiomyopathy and improved mitochondrial and cardiac function in a mouse model of iron deficiency heart failure (Ryu et al., 2016), (Xu et al., 2015). During physical exercise, cellular energy requirements change all the time, including NAD⁺ and NADH concentrations (White and Schenk, 2012). In mice, swimming increased NAD⁺ levels in muscle (Cantó et al., 2010). In rats, endurance exercise resulted in a sustained increase in NAD⁺ levels in the gastrocnemius muscle of young and aging rats (Koltai et al., 2010). A recent study showed that exercise increased cardiac NAD⁺ levels and PGC-1 α activity to improve lipotoxic cardiomyopathy in aged flies, which was associated with NAD⁺/dSir2/PGC-1 α pathway activation (Wen et al., 2019a). *Drosophila* dSir2, a homolog of mammalian Sir2, encodes deacetylase activity that prolongs flies lifespan (Rosenberg and Parkhurst, 2002), (Griswold et al., 2008). In addition, exercise activates the cardiac dSir2/Foxo/SOD and dSir2/Foxo/bmm pathways and reduces the occurrence of diastolic dysfunction as well as enhances cardiac contractility (Wen et al., 2019b). Exercise not only improves CVDs in aging *Drosophila*, but also resists the stress on the heart caused by a high-fat, high-sugar and high-salt diet. For example, lipid levels in the heart are significantly increased in dFatphet mutants, and exercise rescues myocardial lipid content and cardiac function (Sujkowski et al., 2012). Long-term exercise resists high salt-induced premature cardiac failure by blocking CG2196 (salt)/TOR/oxidative stress and activating dFOXO/PGC-1 α (Wen et al., 2021a). Electrical pacing produced a significantly increased rate of heart failure when flies were exposed to a high sucrose diet (Bazzell et al., 2013). Aging is an important cause of arrhythmias (Chadda et al., 2018). In aged flies, early physical exercise improves arrhythmias, mainly by reducing the incidence of fibrillation and increasing the occurrence of bradycardia (Zheng et al., 2017). These facts show a great similarity, and humans compared to rats. For humans, exercise training is important for the prevention and treatment of CVDs (Lavie et al., 2015). For example, persistent regular exercise provides benefits in a variety of diseases, including atherosclerosis, atrial fibrillation, heart failure, and cardiac lipotoxic injury (Rognmo et al., 2012), (Risom et al., 2017), (Cattadori et al., 2018), (Schrauwen-Hinderling et al., 2010). In mice, the same beneficial effects of exercise on the heart have been reported (Fiuza-Luces et al., 2018), (Harris et al., 2020), (Vujic et al., 2018), (Börzsei et al., 2021), (Cheedipudi et al., 2020). In conclusion, this illustrates the significance of the *Drosophila* exercise model for the study of cardiac function.

3 Development of *Drosophila* exercise models in circadian rhythm studies

Aging leads to a weakening of circadian rhythms, such as the sleep/wake cycle. These rhythms are generated by biological

clocks, which are based on cell-autonomous negative feedback loops involving clock genes that display molecular oscillations in approximately 24-h cycles. Clock genes are conserved from *Drosophila* to humans, and their oscillatory activity coordinates rhythms at the molecular, physiological and behavioral levels (Rakshit et al., 2013). *Drosophila* exhibits a sleep-like state that is regulated by both circadian rhythms and homeostasis (Shaw et al., 2000). It has been reported that knockdown of dATF-2 in pacemaker neurons decreases sleep duration, while ectopic expression of dATF-2 increases sleep duration (Shimizu et al., 2008). However, the degree of dATF-2 phosphorylation can be enhanced by forced exercise of the dp38 pathway (Shimizu et al., 2008). This suggests that dATF-2 is the regulator that links sleep to exercise. Furthermore, both chronic hypoxia and exercise improved sleep quality and climbing ability and extended maximum lifespan in aged flies, but exercise was insensitive to improvements in circadian rest/activity rhythms (Li et al., 2020b), (Zheng et al., 2017). Neuropeptide F (NPF) positive clock neurons have been reported to be critical for the control of nocturnal activity in *Drosophila* (Hermann et al., 2012). Interestingly, *Drosophila* exercise is similar to humans in maintaining and improving circadian rhythms (Rakshit et al., 2013), (Gabriel and Zierath, 2019). However, in *Drosophila*, the link between regular exercise and NPF remains poorly understood. Another study showed that exercise increased the duration of nighttime sleep by decreasing nocturnal activity, while also increasing the number of second deep sleeps and the intensity of daytime activity (Li et al., 2020b). Therefore, it will be interesting to study the effect of exercise and NPF on circadian rhythms. In contrast, one study reported that regular exercise did not improve circadian rhythms or lifespan in wild-type flies, but the clock mutant *per 01* significantly reduced climbing ability with or without exercise, suggesting a role for some specific clock genes in maintaining health as part of healthy aging (Rakshit et al., 2013). The paradoxes that lead to the results may be due to differences in model building, including exercise devices, protocols and detection means. As an excellent model of circadian biology and aging, *Drosophila* is well suited to be combined with exercise to explore the molecular pathways between exercise and circadian rhythms. However, we must carefully consider the experimental errors caused by different exercise devices and protocols, otherwise revealing the intrinsic connection between exercise and circadian rhythms will become difficult.

4 Development of *Drosophila* exercise models in obesity-related diseases

Obesity is a global epidemic that is associated with aging and diet (Santos and Sinha, 2021). Obesity increases the risk of many health problems, including T2D, metabolic syndrome, CVDs,

and cancer, and therefore leads to higher mortality (Aune et al., 2016), (Global BMI Mortality Collaboration Di Angelantonio et al., 2016). Physical exercise prevents obesity, reduces visceral fat and maintains body weight (Oppert et al., 2021), (Swift et al., 2018), (Villareal et al., 2017). *Drosophila* has become an excellent model for metabolic and diet-related diseases due to its powerful genetic tools and stable reproducible phenotype (Birse et al., 2010), (Musselman and Kühnlein, 2018). Although exercise is believed to mitigate the damage caused by obesity, it remains controversial (Waters et al., 2013). Therefore, the *Drosophila* exercise model serves as a bridge to reveal the intrinsic relation between exercise and obesity. *Drosophila* need only be fed a diet containing 30% coconut oil for 5 days to exhibit a phenotype similar to that of the mammalian metabolic syndrome, including increased glucose levels and decreased insulin-like peptide 2 (Dilp2) levels (Birse et al., 2010). The TOR pathway is associated with nutrient-sensing signaling in flies (Luong et al., 2006). Reducing the function of the TOR pathway may accelerate lipolytic metabolism and may also reduce lipid anabolism or storage (Birse et al., 2010). These results are similar to those in humans and rodents in that elevated TG levels induced by high-fat diets are associated with disruptions in lipid and glucose homeostasis, and mitochondrial function, which may lead to lipid accumulation and lipotoxic damage (Ouwens et al., 2005), (Unger, 2003), (Schaffer, 2003). Recent studies have found that regular exercise reduces aging-induced increases in cardiac triglycerides, which may be associated with activation of the cardiac dSir2 pathway (Wen et al., 2019b). Regular exercise is also able to increase antioxidant defense and control the production of RS required for cellular metabolic regulation, improving adiposity and glycemia (Dahleh et al., 2021). In addition, exercise may also reduce high-fat diet-induced whole-body hypertriglyceride levels by decreasing the expression of apoLpp (Ding et al., 2021). It is well known that high-fat diet-induced obesity induces cardiac lipid accumulation and leads to the development of lipotoxic cardiomyopathy. A study showed that lipotoxic cardiomyopathy can be reversed by exercise activation of the Nmnat/NAD⁺/SIR2 pathway (Wen et al., 2021b). These results have similarities with some studies in humans and mammals, such as exercise improving dyslipidemia and insulin resistance by reducing apolipoprotein B in patients with T2D (Alam et al., 2004), and in aged rats, exercise training promoting SIRT1 activity and improving antioxidant defenses in heart and adipose tissue (Ferrara et al., 2008). Another recent study showed that exercise and cold stimulation were able to alter the expression levels of the brown fat and beige fat markers *ucp1*, *serca2b*, β 3-adrenergic receptor, *prdm16*, *ampk*, and *camk*, and reduce lipid accumulation (Huang et al., 2022). Although the above studies are not sufficient to prove whether exercise has an effect on lipid browning in flies, they provide indirect evidence, which suggests that exercise holds great potential in the regulation of lipid metabolism in flies.

5 *Drosophila* exercise model in skeletal muscle aging

In humans, the mortality and pathogenesis of many age-related diseases are related to the functional status, metabolic demands and mass of skeletal muscle, suggesting that skeletal muscle is a key regulator of whole-body aging (Anker et al., 1997) (Metter et al., 2002) (Nair, 2005) (Ruiz et al., 2008). In *Drosophila melanogaster*, the organization and metabolism of skeletal muscle fibers is similar to that of mammals (Piccirillo et al., 2014). But, muscles undergo more drastic age-related degeneration, which may be due to the lack of satellite stem cells and the limited muscle repair capacity of this organism (Grotewiel et al., 2005). A major difference between *Drosophila* and mammalian muscles is the lack of muscle stem cells. This feature makes *Drosophila* muscle, excellent models for identifying the mechanisms by which assembled sarcomeres are maintained and repaired without the confounding influence of regeneration as found in mammalian muscle (Christian and Benian, 2020). In addition, *Drosophila* muscle function can be analyzed by measuring their ability to fly and climb (Gargano et al., 2005). Due to these properties, flies are emerging as a useful model organism to study muscle aging together with mammalian models.

Skeletal muscle aging is a risk factor for the development of several age-related diseases, such as sarcopenia, metabolic syndrome, cancer, Alzheimer's disease, and Parkinson's disease (Christian and Benian, 2020), (Ruiz et al., 2011), (Demontis et al., 2013a). Exercise and muscle function are important predictors of age-related mortality in humans (Anker et al., 1997), (Metter et al., 2002), (Demontis et al., 2013b). For example, exercise protects transgenic mice with Alzheimer's disease and Parkinson's disease from neurodegeneration (Zigmond et al., 2009). Endurance exercise rescues mitochondrial defects and premature aging in mice defective in proofreading-exonuclease activity of mitochondrial DNA polymerase γ (Safdar et al., 2011). Another study showed that Sestrins are necessary and sufficient for beneficial adaptations to muscle function and metabolism in *Drosophila* and mice (Kim et al., 2020). Knockdown of Sestrins reduced endurance and flight in exercise-adapted flies (Sujkowski and Wessells, 2021). Similarly, knockdown of Sestrins in exercise mice impeded endurance and metabolic benefits (Sujkowski and Wessells, 2021). *Drosophila* muscle-specific dSesn expression replicates similar improvements in aging mobility by exercise and mediates changes in lysosomal activity in a variety of tissues, and both adaptations are dependent on TORC2-Akt activity and PGC1 α (Sujkowski and Wessells, 2021). In addition, *Drosophila* muscle can play an important role in delaying aging (Rai et al., 2021). The first finding was that adult muscle-specific overexpression of dFOXO prolongs lifespan in *Drosophila* (Demontis and Perrimon, 2010). Although these findings

underscore the fundamental role of muscle in regulating systemic aging, the molecular mechanisms involved in this inter-tissue communication are largely unknown.

Exercise not only produces beneficial effects in one's own muscles but also has the potential to trigger beneficial effects in other tissues. Examples include increased energy expenditure and clearance of ectopic lipid stores (Hawley et al., 2014), improved insulin sensitivity and lower circulating insulin levels (Hawley et al., 2014), and increased secretion of exercise-regulated myokines, including irisin (Whitham et al., 2018) and extracellular vesicles (Arnold et al., 2011). Myokines can act on distant tissues such as adipose tissue, liver, pancreatic β -cells and endothelium (Pedersen and Febbraio, 2012). Insulin-like growth factor-1 (IGF-1) is an actin produced by muscles in response to exercise (Pedersen and Febbraio, 2012), (Hede et al., 2012). In *Drosophila*, Impl2 is a member of the immunoglobulin superfamily, similar to mammalian IGFBP7, which binds to Dilps and inhibits insulin signaling and promotes mitochondrial autophagy (Owusu-Ansah et al., 2013). Mild muscle mitochondrial damage preserves mitochondrial function, inhibits age-dependent degeneration of muscle function and structure, and prolongs lifespan (Copeland et al., 2009), (Kirchman et al., 1999), (Dillin et al., 2002), (Liu et al., 2005). Although muscle-derived insulin-like growth factor binding protein is not detected in the circulation, it induces muscle hypertrophy after exercise in an autocrine/paracrine manner (Vinciguerra et al., 2010), (Silverman et al., 1995). It is well known that physical exercise counteracts the deleterious effects of secondary aging by preventing the decline in mitochondrial respiration, attenuating the loss of muscle mass associated with aging, and enhancing insulin sensitivity (Cartee et al., 2016). Although the *Drosophila* exercise model is not well studied in the field of skeletal muscle aging, its evolutionarily conserved myokines and short lifespan characteristics make it an excellent model for studying the role in intertissue communication.

6 Different genetic backgrounds of *Drosophila* exercise models

A growing number of studies have used *Drosophila* exercise to mimic phenotypes similar to those of humans, including increased endurance, improved age-related decreases in mobility and cardiac function, improved lipid metabolism, and increased lifespan (Wen et al., 2016), (Ding et al., 2021), (Lowman et al., 2018), (Piazza et al., 2009). *Drosophila* exercise is a complex multifactorial response and it has different exercise performance in different genetic backgrounds, including climbing speed and endurance (Damschroder et al., 2020). In addition, age, diet and gender are also factors that influence exercise performance. For example, climbing speed, endurance and flight performance decrease with age (Damschroder et al., 2020), (Sujkowski et al., 2019). The effect of

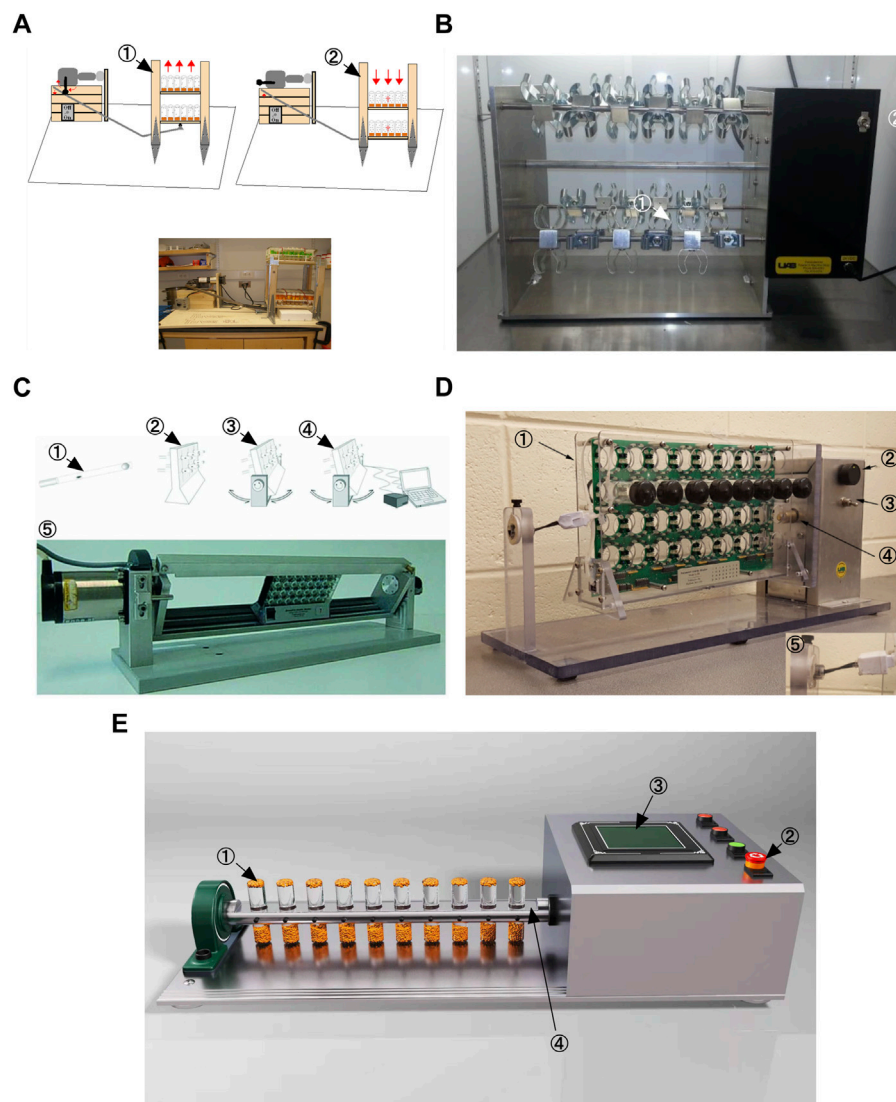


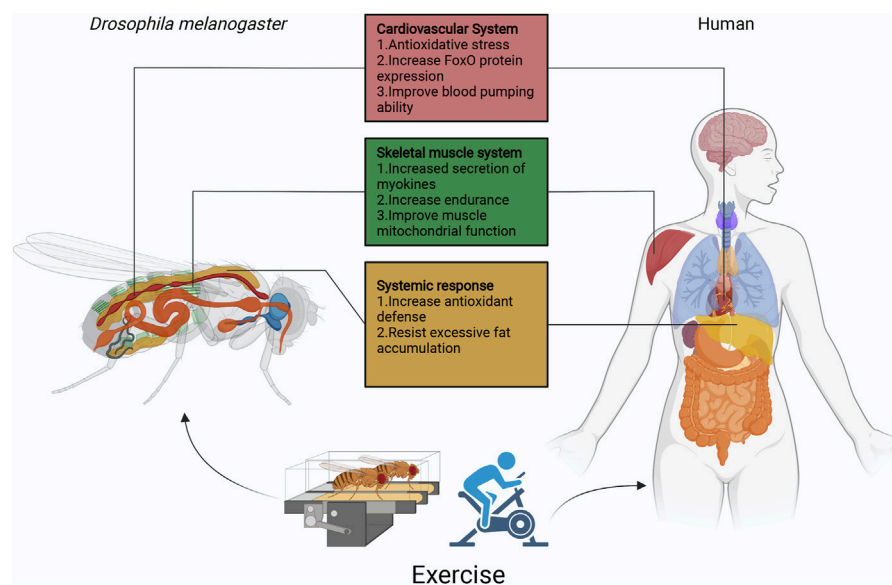
FIGURE 1

Different *Drosophila* exercise devices. (A) Power Tower. This is adapted from [Piazza et al., 2009](#). (B) TreadWheel. This is adapted from [Mendez et al., 2016](#). (C) Swing Boat. This is adapted from [Berlandi et al., 2017](#). (D) REQS. This is adapted from [Watanabe and Riddle, 2018](#). (E) Flip Bottle.

diet on endurance is dramatic and affects acute endurance and adaptation to chronic exercise training, with diet composition having a greater effect than calorie content ([Bazzell et al., 2013](#)). In addition, the effect of gender on exercise is equally important; when looking at the distribution of activity levels during the same 2-h exercise session, there is a strong correlation between gender and exercise, with females experiencing an early burst of activity and males maintaining activity levels throughout the exercise session ([Sujkowski et al., 2020](#)). The mechanisms that lead to genotypic variation in exercise capacity are important to uncover the genetic pathways of exercise, and we should take advantage of cross-species genetics to better explore the interactions between exercise and aging-related diseases.

7 *Drosophila* exercise device

More than 40 years ago, scientists discovered that *Drosophila* exhibit an inherent behavior of crawling against gravity when at the bottom of a vial, a behavior commonly referred to as negative geotaxis ([Miquel et al., 1976](#)). Negative geotaxis in *Drosophila* requires Johnston's organ, a mechanosensory structure located in the tentacles that also detects near-field sounds ([Kamikouchi et al., 2009](#)), ([Sun et al., 2009](#)). To date, five *Drosophila* exercise devices have been described. A decade ago, a first generation locomotion device, the Power Tower, was developed based on the negative tropism of *Drosophila* ([Piazza et al., 2009](#)). The Power Tower device lifts up flies fixed to a platform by a motor and then

**FIGURE 2**

Overview of the function of *Drosophila* exercise in different organs. Currently, *Drosophila* exercise models have made some achievements in cardiovascular, skeletal muscle, and fat body. Exercise activates the cardiomyocyte dSir2/FoxO/SOD and dSir2/FoxO/bmm pathways to delay cardiac aging. In Sestrins, *Sesn1* is mainly expressed in muscle, where it is involved in the metabolic response to exercise and is associated with TORC2-Akt activity and PGC1 α . In addition, skeletal muscle secretes myokines (ImpL2) that inhibit insulin signaling and promote mitochondrial autophagy. Exercise through apoLpp to regulate abnormal lipid metabolism, it also activates Nmnat/NAD⁺/dSir2 to resist lipotoxicity. In exception to the heart, fat body and skeletal muscles, *Drosophila* has other systems similar to those of humans, such as the central nervous system represented by the *Drosophila* and human brain, the digestive system represented by the *Drosophila* and human intestine, the respiratory system represented by the *Drosophila* thorax and human lungs, and the reproductive system represented by the *Drosophila* and human ovaries/testes. The effects of exercise on aging individuals are complex, but the use of simple *Drosophila* exercise models will be exciting for exploring the role of exercise in different biological processes, while facing various difficulties and challenges.

lets the platform fall freely with gravity, causing the flies to fall to the bottom of the bottle (Figure 1A). Due to their negative geostasis response, the flies crawl upward until the motor makes them fall to the bottom of the bottle once again. The TreadWheel device stimulates flies to crawl upward in a fully rotating manner and avoids some physical shocks during locomotion (Mendez et al., 2016), (Katzenberger et al., 2013) (Figure 1B). The Swing Boat device allows the tube to be rotated alternately 30° to each side and also allows the collection of data during locomotion in combination with the *Drosophila* Monitoring System (DAMSystem) (Berlandi et al., 2017) (Figure 1C). REQS is an upgraded version of the TreadWheel, similar to the Swing Boat, allowing the combination of a DAMSystem to quantify the level of movement of flies (Watanabe and Riddle, 2018) (Figure 1D). In addition, the Key Laboratory of Physical and Exercise Rehabilitation of Hunan Province also developed a *Drosophila* exercise device in an experiment in which a motor was controlled to drive the flip of the vial on the platform (Figure 1E). The difference is that each rotation of the device is 180 and this stimulates the flies to actively walk upwards inside the vial (Zheng et al., 2015). This device is called “Flip Bottle” because it keeps turning the bottle

during its operation. All in all, the other four devices are mainly rotational in design compared to the Power Tower device. The “rotational” approach allows for greater avoidance of physical damage during the exercise of flies. Although the upgrade of the exercise device reduces the possibility of physical damage, there are still some questions about the efficiency of flies’ exercise in the vial and how to accurately determine the intensity of exercise. Various research protocols currently use motor rotation speed and time as key factors in determining exercise intensity (Katzenberger et al., 2013), (Berlandi et al., 2017), (Watanabe and Riddle, 2018). In short, Power Tower triggers *Drosophila* exercise through mechanical vibration, while the other four trigger exercise through rotation, including full rotation for TreadWheel and REQS, alternating 30 per side for Swing Boat, and alternating 180° per side for Flip Bottle. In addition, Swing Boat and REQS incorporate the DAMSystem, which makes them more objective in monitoring the intensity of exercise. However, in previous studies it was found that flies exhibited a passive tendency to climb after exercising for a period of time (usually after 20–30 min) (Watanabe and Riddle, 2017). This means that flies stay in a certain location in the vial and their range of movement decreases dramatically, which makes it more

TABLE 1 Exercise-related genes in *Drosophila* aging.

Gene	Participation path	Main findings	Reference
<i>spargel</i>		The PGC-1 α <i>Drosophila</i> homolog <i>spargel</i> is required for adequate motor capacity in <i>Drosophila</i>	Tinkerhess et al. (2012)
<i>Sestrins</i>	TORC-1/TORC-2; AKT	Sestrins are necessary and sufficient for beneficial adaptations of muscle function and metabolism in <i>Drosophila</i> and mice	Kim et al., (2020), Sujkowski and Wessells, (2021)
<i>Pink1</i>		<i>Pink1</i> -expression of the mitochondrial proteome in <i>Drosophila</i> generally decreases in response to exercise	Ebanks et al. (2021)
<i>γ-oryzanol</i>		Combined use of γ -oryzanol and exercise enhances exercise capacity and viability in <i>Drosophila</i> without increasing cellular oxidative state	Kang et al. (2013)
<i>Nmnat</i>	NAD ⁺ /dSir2/FOXO	Cardiac <i>Nmnat</i> /NAD ⁺ /SIR2 pathway activation is an important underlying molecular mechanism by which endurance exercise and cardiac <i>Nmnat</i> overexpression protect <i>Drosophila</i> from lipotoxic cardiomyopathy	Grotewiel et al. (2005)
<i>salt</i>	salt/TOR/oxidative stress; dFOXO/PGC-1 α	Endurance exercise improved the climbing capacity and survival in salt-overexpression <i>Drosophila</i>	Harris et al., (2020), Wen et al., (2020)
<i>ATXN2 Q117</i>		Endurance exercise has a significant positive effect on SCA2 (type of spinocerebellar ataxia) in <i>Drosophila</i>	Sujkowski et al. (2022)
<i>dSir2</i>	dSir2/Foxo/SOD; dSir2/Foxo/bmm	The activation of cardiac dSir2/Foxo/SOD and dSir2/Foxo/bmm pathways may be two important molecular mechanisms through which exercise works against heart aging in <i>Drosophila</i>	Cattadori et al. (2018)
<i>CG9940</i>	NAD (+)	Both normal expression and overexpression of <i>CG9940</i> positively affected cardiac function, activity, and lifespan adaptation to exercise in aging <i>Drosophila</i>	Wen et al., (2016), Lavie et al., (2015)
<i>dFatp</i>		Endurance exercise can reverse increased lipid storage in the myocardium and deleterious cardiac function conferred by <i>dFatp</i> mutations	Schrauwen-Hinderling et al. (2010)

difficult to determine the intensity of exercise. It is well known that regular exercise can bring great benefits for healthy aging, and the emergence of *Drosophila* exercise models will further reveal the relationship between exercise and aging. Therefore, precise quantification of exercise intensity and the development of more advanced *Drosophila* exercise devices will become highly relevant in the future.

8 Summary

Drosophila and other animal models are widely used to study the relationship between exercise and aging, such as mice and zebrafish (Murphy et al., 2021), (van Praag et al., 2005). But because of the complexity of these systems, we need simpler model organisms to overcome these challenges. *Drosophila* has the obvious advantage of being a first-line model for testing hundreds of potential longevity enhancers in multicellular organisms and can be easily adapted to mammalian models. *Drosophila* exercise produces physiological characteristics similar to those of humans (Figure 2). As described in this review, the *Drosophila* exercise model provides some new insights into cardiac aging, abnormal lipid metabolism, circadian rhythm disorders, and skeletal muscle aging. In addition to this, exercise regulates a variety of neurological disorders, including neuroendocrine, neurotransmitter, neuroinsulin signaling, antioxidant and anti-inflammatory responses, and cell survival and death pathways

(Virus, 1992), (Meeusen and De Meirleir, 1995), (Lovatell et al., 2013), (Monteiro-Junior et al., 2015), (Kurgan et al., 2019), (Serra et al., 2019), (Kang et al., 2013). Surprisingly, however, *Drosophila* exercise models have only been reported in studies of octopamine and its receptors, a powerful neuromodulator that affects sensory and cognitive functions in insects (Zheng et al., 2015), (Sujkowski et al., 2017), (Farooqui, 2007). Many neuronal genes and neuronal transcriptional regulators were reported in a recent study to be affected by the exercise of the genus *Drosophila* (Watanabe and Riddle, 2021). Therefore, in the future, more studies will apply *Drosophila* exercise models to explore neurological disorders.

Drosophila exercise models have made remarkable achievements in this decade or so, but there are still some limitations awaiting the development of future methods and tools. Specifically, *Drosophila* exercise models are currently used primarily to study endurance exercise, but human exercise types also include exercises to improve strength, flexibility, and balance. In addition to increasing endurance, human exercise needs often include improving muscle strength or muscle tone, altering body composition, or increasing flexibility. Therefore, new methods and tools are needed to match *Drosophila* exercise to human exercise models. Although the *Drosophila* model has a limited redundancy of conserved pathways, it is still of great value for such studies. Therefore, it is important to further investigate the molecular mechanisms behind the physiological changes in exercise and aging. Furthermore, elucidating the role of

exercise-related genes in *Drosophila* aging would provide evidence for a potential role of their human counterparts in aging (eg Table 1). *Drosophila* exercise models could provide therapeutic targets for exercise treatment of aging-related diseases. Of course these exercise-related genes need to be validated by extensive experiments before they hold promise as new therapeutic approaches.

Author contributions

MD and HL: Conceptualization, writing—original draft; LZ: Funding acquisition, Supervision, writing—review & editing.

Funding

This research was funded by The Key scientific research project of Hunan Education Department was funded, grant number 19A328, and the National Natural Science Foundation of China, grant number 32071175.

References

- Abdellatif, M., Sedej, S., and Kroemer, G. (2021). NAD⁺ metabolism in cardiac health, aging, and disease. *Circulation* 144 (22), 1795–1817. doi:10.1161/CIRCULATIONAHA.121.056589
- Alam, S., Stolin, M., Pentecost, C., Boroujerdi, M. A., Jones, R. H., Sonksen, P. H., et al. (2004). The effect of a six-month exercise program on very low-density lipoprotein apolipoprotein B secretion in type 2 diabetes. *J. Clin. Endocrinol. Metab.* 89 (2), 688–694. doi:10.1210/jc.2003-031036
- Anker, S. D., Ponikowski, P., Varney, S., Chua, T. P., Clark, A. L., Webb-Peploe, K. M., et al. (1997). Wasting as independent risk factor for mortality in chronic heart failure. *Lancet* 349 (9058), 1050–1053. doi:10.1016/S0140-6736(96)07015-8
- Arnold, A. S., Egger, A., and Handschin, C. (2011). PGC-1 α and myokines in the aging muscle - a mini-review. *Gerontology* 57 (1), 37–43. doi:10.1159/000281883
- Aune, D., Sen, A., Prasad, M., Norat, T., Janszky, I., Tonstad, S., et al. (2016). BMI and all cause mortality: Systematic review and non-linear dose-response meta-analysis of 230 cohort studies with 3.74 million deaths among 30.3 million participants. *BMJ* 353, i2156. PMID: 27146380; PMCID: PMC4856854. doi:10.1136/bmj.i2156
- Batsis, J. A., and Villareal, D. T. (2018). Sarcopenic obesity in older adults: Aetiology, epidemiology and treatment strategies. *Nat. Rev. Endocrinol.* 14 (9), 513–537. PMID: 30065268; PMCID: PMC6241236. doi:10.1038/s41574-018-0062-9
- Bazzell, B., Ginzberg, S., Healy, L., and Wessells, R. J. (2013). Dietary composition regulates *Drosophila* mobility and cardiac physiology. *J. Exp. Biol.* 216 (5), 859–868. Epub 2012 Nov 15. PMID: 23155082; PMCID: PMC3571989. doi:10.1242/jeb.078758
- Berlandi, J., Lin, F. J., Ambrée, O., Rieger, D., Paulus, W., and Jeibmann, A. (2017). Swing Boat: Inducing and recording locomotor activity in a *Drosophila* melanogaster model of Alzheimer's disease. *Front. Behav. Neurosci.* 11, 159. PMID: 28912696; PMCID: PMC5582087. doi:10.3389/fnbeh.2017.00159
- Birse, R. T., Choi, J., Reardon, K., Rodriguez, J., Graham, S., Diop, S., et al. (2010). High-fat-diet-induced obesity and heart dysfunction are regulated by the TOR pathway in *Drosophila*. *Cell Metab.* 12 (5), 533–544. PMID: 21035763; PMCID: PMC3026640. doi:10.1016/j.cmet.2010.09.014
- Blice-Baum, A. C., Guida, M. C., Hartley, P. S., Adams, P. D., Bodmer, R., and Cammarato, A. (2019). As time flies by: Investigating cardiac aging in the short-lived *Drosophila* model. *Biochim. Biophys. Acta Mol. Basis Dis.* 1865 (7), 1831–1844. Epub 2018 Nov 27. PMID: 30496794; PMCID: PMC6527462. doi:10.1016/j.bbdis.2018.11.010
- Börzsei, D., Priks, D., Szabó, R., Bombicz, M., Karácsonyi, Z., Puskás, L. G., et al. (2021). Exercise-mitigated sex-based differences in aging: From genetic alterations

Acknowledgments

We thank Ying Guo, Qiufang Li and Shiyi He for discussions on this manuscript.

Conflict of interest

The authors declare that the research was conducted in the absence of any commercial or financial relationships that could be construed as a potential conflict of interest.

Publisher's note

All claims expressed in this article are solely those of the authors and do not necessarily represent those of their affiliated organizations, or those of the publisher, the editors and the reviewers. Any product that may be evaluated in this article, or claim that may be made by its manufacturer, is not guaranteed or endorsed by the publisher.

to heart performance. *Am. J. Physiol. Heart Circ. Physiol.* 320 (2), H854–H866. Epub 2020 Dec 18. PMID: 33337964. doi:10.1152/ajpheart.00643.2020

Campisi, J., Kapahi, P., Lithgow, G. J., Melov, S., Newman, J. C., and Verdin, E. (2019). From discoveries in ageing research to therapeutics for healthy ageing. *Nature* 571 (7764), 183–192. Epub 2019 Jul 10. PMID: 31292558; PMCID: PMC7205183. doi:10.1038/s41586-019-1365-2

Cantó, C., Jiang, L. Q., Deshmukh, A. S., Matak, C., Coste, A., Lagouge, M., et al. (2010). Interdependence of AMPK and SIRT1 for metabolic adaptation to fasting and exercise in skeletal muscle. *Cell Metab.* 11 (3), 213–219. PMID: 20197054; PMCID: PMC3616265. doi:10.1016/j.cmet.2010.02.006

Cartee, G. D., Hepple, R. T., Bamman, M. M., and Zierath, J. R. (2016). Exercise promotes healthy aging of skeletal muscle. *Cell Metab.* 23 (6), 1034–1047. PMID: 27304505; PMCID: PMC5045036. doi:10.1016/j.cmet.2016.05.007

Castano, C., Mirasierra, M., Vallejo, M., Novials, A., and Parrizas, M. (2020). Delivery of muscle-derived exosomal miRNAs induced by HIIT improves insulin sensitivity through down-regulation of hepatic FoxO1 in mice. *Proc. Natl. Acad. Sci. U. S. A.* 117 (48), 30335–30343. Epub 2020 Nov 16. PMID: 33199621; PMCID: PMC7720135. doi:10.1073/pnas.2016112117

Cattadori, G., Segurini, C., Picozzi, A., Padeletti, L., and Anzà, C. (2018). Exercise and heart failure: An update. *Esc. Heart Fail.* 5 (2), 222–232. Epub 2017 Dec 13. PMID: 29235244; PMCID: PMC5880674. doi:10.1002/ehf2.12225

Chadda, K. R., Ajijola, O. A., Vaseghi, M., Shivkumar, K., Huang, C. L., and Jeevaratnam, K. (2018). Ageing, the autonomic nervous system and arrhythmia: From brain to heart. *Ageing Res. Rev.* 48, 40–50. Epub 2018 Oct 6. PMID: 30300712. doi:10.1016/j.arr.2018.09.005

Cheedipudi, S. M., Hu, J., Fan, S., Yuan, P., Karmouch, J., Czernuszewicz, G., et al. (2020). Exercise restores dysregulated gene expression in a mouse model of arrhythmogenic cardiomyopathy. *Cardiovasc Res.* 116 (6), 1199–1213. PMID: 31350552; PMCID: PMC7177479. doi:10.1093/cvr/cvz199

Christian, C. J., and Benian, G. M. (2020). Animal models of sarcopenia. *Aging Cell* 19 (10), e13223. Epub 2020 Aug 28. PMID: 32857472; PMCID: PMC7576270. doi:10.1111/acer.13223

Copeland, J. M., Cho, J., Lo, T., Jr, Hur, J. H., Bahadorani, S., Arabyan, T., et al. (2009). Extension of *Drosophila* life span by RNAi of the mitochondrial respiratory chain. *Curr. Biol.* 19 (19), 1591–1598. Epub 2009 Sep 10. PMID: 19747824. doi:10.1016/j.cub.2009.08.016

Dahleh, M. M. M., Araujo, S. M., Bortolotto, V. C., Pinheiro, F. C., Poetini, M. R., Musachio, E. A. S., et al. (2021). Exercise associated with γ -oryzanol

supplementation suppresses oxidative stress and prevents changes in locomotion in *Drosophila melanogaster*. *Free Radic. Res.* 55 (2), 198–209. Epub 2021 May 18. PMID: 33655816. doi:10.1080/10715762.2021.1895992

Damschroder, D., Richardson, K., Cobb, T., and Wessells, R. (2020). The effects of genetic background on exercise performance in *Drosophila*. *Fly. (Austin)* 14 (1–4), 80–92. PMID: 33100141; PMCID: PMC7714460. doi:10.1080/19336934.2020.1835329

Demontis, F., and Perrimon, N. (2010). FOXO/4E-BP signaling in *Drosophila* muscles regulates organism-wide proteostasis during aging. *Cell* 143 (5), 813–825. PMID: 21111239; PMCID: PMC3066043. doi:10.1016/j.cell.2010.10.007

Demontis, F., Piccirillo, R., Goldberg, A. L., and Perrimon, N. (2013). Mechanisms of skeletal muscle aging: Insights from *Drosophila* and mammalian models. *Dis. Model. Mech.* 6 (6), 1339–1352. Epub 2013 Oct 2. PMID: 24092876; PMCID: PMC3820258. doi:10.1242/dmm.012559

Demontis, F., Piccirillo, R., Goldberg, A. L., and Perrimon, N. (2013). The influence of skeletal muscle on systemic aging and lifespan. *Aging Cell* 12 (6), 943–949. Epub 2013 Jul 17. PMID: 23802635; PMCID: PMC3838468. doi:10.1111/acel.12126

Dillin, A., Hsu, A. L., Arantes-Oliveira, N., Lehrer-Graiwer, J., Hsin, H., Fraser, A. G., et al. (2002). Rates of behavior and aging specified by mitochondrial function during development. *Science* 298 (5602), 2398–2401. Epub 2002 Dec 5. PMID: 12471266. doi:10.1126/science.1077780

Ding, M., Zheng, L., Li, Q. F., Wang, W. L., Peng, W. D., and Zhou, M. (2021). Exercise-training regulates apolipoprotein B in *Drosophila* to improve HFD-mediated cardiac function damage and low exercise capacity. *Front. Physiol.* 12, 650959. PMID: 34305631; PMCID: PMC8294119. doi:10.3389/fphys.2021.650959

Diop, S. B., and Bodmer, R. (2015). Gaining insights into diabetic cardiomyopathy from *Drosophila*. *Trends Endocrinol. Metab.* 26 (11), 618–627. Epub 2015 Oct 16. PMID: 26482877; PMCID: PMC4638170. doi:10.1016/j.tem.2015.09.009

Ebanks, B., Ingram, T. L., Katyal, G., Ingram, J. R., Moiso, N., and Chakrabarti, L. (2021). The dysregulated Pink1-*Drosophila* mitochondrial proteome is partially corrected with exercise. *Aging (Albany NY)* 13 (11), 14709–14728. Epub 2021 Jun 1. PMID: 34074800; PMCID: PMC8221352. doi:10.18632/aging.203128

Fang, E. F., Hou, Y., Lautrup, S., Jensen, M. B., Yang, B., SenGupta, T., et al. (2019). NAD⁺ augmentation restores mitophagy and limits accelerated aging in Werner syndrome. *Nat. Commun.* 10 (1), 5284. PMID: 31754102; PMCID: PMC6872719. doi:10.1038/s41467-019-13172-8

Farooqui, T. (2007). Octopamine-mediated neuromodulation of insect senses. *Neurochem. Res.* 32 (9), 1511–1529. Epub 2007 May 5. PMID: 17484052. doi:10.1007/s11064-007-9344-7

Feany, M. B., and Bender, W. W. (2000). A *Drosophila* model of Parkinson's disease. *Nature* 404 (6776), 394–398. doi:10.1038/35006074

Ferrara, N., Rinaldi, B., Corbi, G., Conti, V., Stiuso, P., Boccuti, S., et al. (2008). Exercise training promotes SIRT1 activity in aged rats. *Rejuvenation Res.* 11 (1), 139–150. doi:10.1089/rej.2007.0576

Fiuzza-Luces, C., Santos-Lozano, A., Joyner, M., Carrera-Bastos, P., Picazo, O., Zugaza, J. L., et al. (2018). Exercise benefits in cardiovascular disease: Beyond attenuation of traditional risk factors. *Nat. Rev. Cardiol.* 15 (12), 731–743. doi:10.1038/s41569-018-0065-1

Gabriel, B. M., and Zierath, J. R. (2019). Circadian rhythms and exercise - re-setting the clock in metabolic disease. *Nat. Rev. Endocrinol.* 15 (4), 197–206. PMID: 30655625. doi:10.1038/s41574-018-0150-x

Gargano, J. W., Martin, I., Bhandari, P., and Grotewiel, M. S. (2005). Rapid iterative negative geotaxis (RING): A new method for assessing age-related locomotor decline in *Drosophila*. *Exp. Gerontol.* 40 (5), 386–395. Epub 2005 Mar 19. PMID: 15919590. doi:10.1016/j.exger.2005.02.005

Global BMI Mortality Collaboration Di Angelantonio, E., Bhupathiraju, S., Wormser, D., Gao, P., Kaptoge, S., Berrington de Gonzalez, A., et al. (2016). Body-mass index and all-cause mortality: Individual-participant-data meta-analysis of 239 prospective studies in four continents. *Lancet* 388 (10046), 776–786. Epub 2016 Jul 13. PMID: 27423262; PMCID: PMC4995441. doi:10.1016/S0140-6736(16)30175-1

Goenka, S., and Lee, I. M. (2017). Physical activity lowers mortality and heart disease risks. *Lancet* 390 (10113), 2609–2610. Epub 2017 Sep 21. PMID: 28943265. doi:10.1016/S0140-6736(17)32104-9

Goodyear, L. J., and Kahn, B. B. (1998). Exercise, glucose transport, and insulin sensitivity. *Annu. Rev. Med.* 49, 235–261. PMID: 9509261. doi:10.1146/annurev.med.49.1.235

Griswold, A. J., Chang, K. T., Runko, A. P., Knight, M. A., and Min, K. T. (2008). Sir2 mediates apoptosis through JNK-dependent pathways in *Drosophila*. *Proc. Natl. Acad. Sci. U. S. A.* 105 (25), 8673–8678. Epub 2008 Jun 17. PMID: 18562277; PMCID: PMC2438412. doi:10.1073/pnas.0803837105

Grotewiel, M. S., Martin, I., Bhandari, P., and Cook-Wiens, E. (2005). Functional senescence in *Drosophila melanogaster*. *Ageing Res. Rev.* 4 (3), 372–397. PMID: 16024299. doi:10.1016/j.arr.2005.04.001

Harris, J. E., Pinckard, K. M., Wright, K. R., Baer, L. A., Arts, P. J., Abay, E., et al. (2020). Exercise-induced 3'-sialyllactose in breast milk is a critical mediator to improve metabolic health and cardiac function in mouse offspring. *Nat. Metab.* 2 (8), 678–687. Epub 2020 Jun 29. PMID: 32694823; PMCID: PMC7438265. doi:10.1038/s42255-020-0223-8

Hawley, J. A., Hargreaves, M., Joyner, M. J., and Zierath, J. R. (2014). Integrative biology of exercise. *Cell* 159 (4), 738–749. doi:10.1016/j.cell.2014.10.029

Hawley, J. A., and Krook, A. (2016). Metabolism: One step forward for exercise. *Nat. Rev. Endocrinol.* 12 (1), 7–8. Epub 2015 Nov 27. PMID: 26610411. doi:10.1038/nrendo.2015.201

Hede, M. S., Salimova, E., Piszczek, A., Perlas, E., Winn, N., Nastasi, T., et al. (2012). E-peptides control bioavailability of IGF-1. *PLoS One* 7 (12), e51152. Epub 2012 Dec 10. PMID: 23251442; PMCID: PMC3519493. doi:10.1371/journal.pone.0051152

Helfand, S. L., and Rogina, B. (2003). Genetics of aging in the fruit fly, *Drosophila melanogaster*. *Annu. Rev. Genet.* 37, 329–348. PMID: 14616064. doi:10.1146/annurev.genet.37.040103.095211

Hermann, C., Yoshii, T., Dusik, V., and Helfrich-Förster, C. (2012). Neuropeptide F immunoreactive clock neurons modify evening locomotor activity and free-running period in *Drosophila melanogaster*. *J. Comp. Neurol.* 520 (5), 970–987. PMID: 21826659. doi:10.1002/cne.22742

Hou, Y., Dan, X., Babbar, M., Wei, Y., Hasselbalch, S. G., Croteau, D. L., et al. (2019). Ageing as a risk factor for neurodegenerative disease. *Nat. Rev. Neurol.* 15 (10), 565–581. Epub 2019 Sep 9. PMID: 31501588. doi:10.1038/s41582-019-0244-7

Houghton, D., Thoma, C., Hallsworth, K., Cassidy, S., Hardy, T., Burt, A. D., et al. (2017). Exercise reduces liver lipids and visceral adiposity in patients with nonalcoholic steatohepatitis in a randomized controlled trial. *Clin. Gastroenterol. Hepatol.* 15 (1), 96–102. e3. Epub 2016 Aug 10. PMID: 27521509; PMCID: PMC5196006. doi:10.1016/j.cgh.2016.07.031

Huang, T., Jian, X., Liu, J., Zheng, L., Li, F. Q., Meng, D., et al. (2022). Exercise and/or cold exposure alters the gene expression profile in the fat body and changes the heart function in *Drosophila*. *Front. Endocrinol. (Lausanne)* 13, 790414. PMID: 35418948; PMCID: PMC8995477. doi:10.3389/fendo.2022.790414

Hunt, L. C., Schadeberg, B., Stover, J., Haugen, B., Pagala, V., Wang, Y. D., et al. (2021). Antagonistic control of myofiber size and muscle protein quality control by the ubiquitin ligase UBR4 during aging. *Nat. Commun.* 12 (1), 1418. PMID: 33658508; PMCID: PMC7930053. doi:10.1038/s41467-021-21738-8

Kamikouchi, A., Inagaki, H. K., Effertz, T., Hendrich, O., Fiala, A., Göpfert, M. C., et al. (2009). The neural basis of *Drosophila* gravity-sensing and hearing. *Nature* 458 (7235), 165–171. doi:10.1038/nature07810

Kang, E. B., Kwon, I. S., Koo, J. H., Kim, E. J., Kim, C. H., Lee, J., et al. (2013). Treadmill exercise represses neuronal cell death and inflammation during Aβ-induced ER stress by regulating unfolded protein response in aged presenilin 2 mutant mice. *Apoptosis* 18 (11), 1332–1347. doi:10.1007/s10495-013-0884-9

Katzenberger, R. J., Loewen, C. A., Wassarman, D. R., Petersen, A. J., Ganetzky, B., and Wassarman, D. A. (2013). A *Drosophila* model of closed head traumatic brain injury. *Proc. Natl. Acad. Sci. U. S. A.* 110 (44), E4152–E4159. Epub 2013 Oct 14. PMID: 24127584; PMCID: PMC3816429. doi:10.1073/pnas.1316895110

Kim, M., Sujkowski, A., Namkoong, S., Gu, B., Cobb, T., Kim, B., et al. (2020). Sestrins are evolutionarily conserved mediators of exercise benefits. *Nat. Commun.* 11 (1), 190. PMID: 31929512; PMCID: PMC6955242. doi:10.1038/s41467-019-13442-5

Kirchman, P. A., Kim, S., Lai, C. Y., and Jazwinski, S. M. (1999). Interorganelle signaling is a determinant of longevity in *Saccharomyces cerevisiae*. *Genetics* 152 (1), 179–190. PMID: 10224252; PMCID: PMC1460582. doi:10.1093/genetics/152.1.179

Koltai, E., Szabo, Z., Atalay, M., Boldogh, I., Naito, H., Goto, S., et al. (2010). Exercise alters SIRT1, SIRT6, NAD and NAMPT levels in skeletal muscle of aged rats. *Mech. Ageing Dev.* 131 (1), 21–28. Epub 2009 Nov 12. PMID: 19913571; PMCID: PMC2872991. doi:10.1016/j.mad.2009.11.002

Kurgan, N., Noaman, N., Pergande, M. R., Cologna, S. M., Coorsen, J. R., and Klenstrup, P. (2019). Changes to the human serum proteome in response to high intensity interval exercise: A sequential top-down proteomic analysis. *Front. Physiol.* 10, 362. PMID: 31001142; PMCID: PMC6454028. doi:10.3389/fphys.2019.00362

Laiteerapong, N., Ham, S. A., Gao, Y., Moffet, H. H., Liu, J. Y., Huang, E. S., et al. (2019). The legacy effect in type 2 diabetes: Impact of early glycemic control on future complications (the diabetes & aging study). *Diabetes Care* 42 (3), 416–426. Epub 2018 Aug 13. PMID: 30104301; PMCID: PMC6385699. doi:10.2337/dci17-1144

Lavie, C. J., Arena, R., Swift, D. L., Johannsen, N. M., Sui, X., Lee, D. C., et al. (2015). Exercise and the cardiovascular system: Clinical science and cardiovascular outcomes. *Circ. Res.* 117 (2), 207–219. PMID: 26139859; PMCID: PMC4493772. doi:10.1161/CIRCRESAHA.117.305205

- Li, H., Hastings, M. H., Rhee, J., Trager, L. E., Roh, J. D., and Rosenzweig, A. (2020). Targeting age-related pathways in heart failure. *Circ. Res.* 126 (4), 533–551. Epub 2020 Feb 13. PMID: 32078451; PMCID: PMC7041880. doi:10.1161/CIRCRESAHA.119.315889
- Li, Q. F., Wang, H., Zheng, L., Yang, F., Li, H. Z., Li, J. X., et al. (2020). Effects of modest hypoxia and exercise on cardiac function, sleep-activity, negative geotaxis behavior of aged female *Drosophila*. *Front. Physiol.* 10, 1610. PMID: 32038290; PMCID: PMC6985434. doi:10.3389/fphys.2019.01610
- Liu, X., Jiang, N., Hughes, B., Bigras, E., Shoubridge, E., and Hekimi, S. (2005). Evolutionary conservation of the clk-1-dependent mechanism of longevity: Loss of mclk1 increases cellular fitness and lifespan in mice. *Genes Dev.* 19 (20), 2424–2434. Epub 2005 Sep 29. PMID: 16195414; PMCID: PMC1257397. doi:10.1101/gad.1352905
- Lovatel, G. A., Elsner, V. R., Bertoldi, K., Vanzella, C., Moysés Fdos, S., Vizuete, A., et al. (2013). Treadmill exercise induces age-related changes in aversive memory, neuroinflammatory and epigenetic processes in the rat hippocampus. *Neurobiol. Learn. Mem.* 101, 94–102. Epub 2013 Jan 26. PMID: 23357282. doi:10.1016/j.nlm.2013.01.007
- Lowman, K. E., Wyatt, B. J., Cunneely, O. P., and Reed, L. K. (2018). The TreadWheel: Interval training protocol for gently induced exercise in *Drosophila melanogaster*. *J. Vis. Exp.* 27 (135), 57788. PMID: 29939171; PMCID: PMC6101642. doi:10.3791/57788
- Lu, B., and Vogel, H. (2009). *Drosophila* models of neurodegenerative diseases. *Annu. Rev. Pathol.* 4, 315–342. PMID: 18842101; PMCID: PMC3045805. doi:10.1146/annurev.pathol.3.121806.151529
- Luong, N., Davies, C. R., Wessells, R. J., Graham, S. M., King, M. T., Veech, R., et al. (2006). Activated FOXO-mediated insulin resistance is blocked by reduction of TOR activity. *Cell Metab.* 4 (2), 133–142. PMID: 16890541. doi:10.1016/j.cmet.2006.05.013
- Makarova, K. S., Wolf, Y. I., Alkhnbashi, O. S., Costa, F., Shah, S. A., Saunders, S. J., et al. (2015). An updated evolutionary classification of CRISPR-Cas systems. *Nat. Rev. Microbiol.* 13 (11), 722–736. Epub 2015 Sep. PMID: 26411297; PMCID: PMC5426118. doi:10.1038/nrmicro3569
- McGee, S. L., and Hargreaves, M. (2020). Exercise adaptations: Molecular mechanisms and potential targets for therapeutic benefit. *Nat. Rev. Endocrinol.* 16 (9), 495–505. Epub 2020 Jul 6. PMID: 32632275. doi:10.1038/s41574-020-0377-1
- Meeusen, R., and De Meirleir, K. (1995). Exercise and brain neurotransmission. *Sports Med.* 20 (3), 160–188. PMID: 8571000. doi:10.2165/00007256-199520030-00004
- Mendez, S., Watanabe, L., Hill, R., Owens, M., Moraczewski, J., Rowe, G. C., et al. (2016). The TreadWheel: A novel apparatus to measure genetic variation in response to gently induced exercise for *Drosophila*. *PLoS One* 11 (10), e0164706. PMID: 27736996; PMCID: PMC5063428. doi:10.1371/journal.pone.0164706
- Metter, E. J., Talbot, L. A., Schragger, M., and Conwit, R. (2002). Skeletal muscle strength as a predictor of all-cause mortality in healthy men. *J. Gerontol. A Biol. Sci. Med. Sci.* 57 (10), B359–B365. PMID: 12242311. doi:10.1093/gerona/57.10.b359
- Miquel, J., Lundgren, P. R., Bensch, K. G., and Atlan, H. (1976). Effects of temperature on the life span, vitality and fine structure of *Drosophila melanogaster*. *Mech. Ageing Dev.* 5 (5), 347–370. PMID: 823384. doi:10.1016/0047-6374(76)90034-8
- Monteiro-Junior, R. S., Cevada, T., Oliveira, B. R., Lattari, E., Portugal, E. M., Carvalho, A., et al. (2015). We need to move more: Neurobiological hypotheses of physical exercise as a treatment for Parkinson's disease. *Med. Hypotheses* 85 (5), 537–541. Epub 2015 Jul 17. PMID: 26209418. doi:10.1016/j.mehy.2015.07.011
- Murphy, L. B., Santos-Ledo, A., Dhanaseelan, T., Eley, L., Burns, D., Henderson, D. J., et al. (2021). Exercise, programmed cell death and exhaustion of cardiomyocyte proliferation in aging zebrafish. *Dis. Model Mech.* 14 (7), dmm049013. Epub 2021 Jul 22. PMID: 34296752; PMCID: PMC8319546. doi:10.1242/dmm.049013
- Musselman, L. P., and Kühnlein, R. P. (2018). *Drosophila* as a model to study obesity and metabolic disease. *J. Exp. Biol.* 221 (1), jeb163881. doi:10.1242/jeb.163881
- Myint, P. K., and Welch, A. A. (2012). Healthier ageing. *BMJ* 344, e1214. PMID: 22411918. doi:10.1136/bmj.e1214
- Nair, K. S. (2005). Aging muscle. *Am. J. Clin. Nutr.* 81 (5), 953–963. doi:10.1093/ajcn/81.5.953
- North, B. J., and Sinclair, D. A. (2012). The intersection between aging and cardiovascular disease. *Circ. Res.* 110 (8), 1097–1108. PMID: 22499900; PMCID: PMC3366686. doi:10.1161/CIRCRESAHA.111.246876
- Oppert, J. M., Bellicha, A., and Ciangura, C. (2021). Physical activity in management of persons with obesity. *Eur. J. Intern. Med.* 93, 8–12. Epub 2021 May 21. PMID: 34024703. doi:10.1016/j.ejim.2021.04.028
- Ouwens, D. M., Boer, C., Fodor, M., de Galan, P., Heine, R. J., Maassen, J. A., et al. (2005). Cardiac dysfunction induced by high-fat diet is associated with altered myocardial insulin signalling in rats. *Diabetologia* 48 (6), 1229–1237. Epub 2005 Apr 30. PMID: 15864533. doi:10.1007/s00125-005-1755-x
- Owusu-Ansah, E., Song, W., and Perrimon, N. (2013). Muscle mitohormesis promotes longevity via systemic repression of insulin signaling. *Cell* 155 (3), 699–712. Epub 2013 Oct 24. PMID: 24243023; PMCID: PMC3856681. doi:10.1016/j.cell.2013.09.021
- Paneni, F., Diaz Cañestro, C., Libby, P., Lüscher, T. F., and Camici, G. G. (2017). The aging cardiovascular system: Understanding it at the cellular and clinical levels. *J. Am. Coll. Cardiol.* 69 (15), 1952–1967. PMID: 28408026. doi:10.1016/j.jacc.2017.01.064
- Partridge, L., Deelen, J., and Slagboom, P. E. (2018). Facing up to the global challenges of ageing. *Nature* 561 (7721), 45–56. Epub 2018 Sep 5. PMID: 30185958. doi:10.1038/s41586-018-0457-8
- Pedersen, B. K., and Febbraio, M. A. (2012). Muscles, exercise and obesity: Skeletal muscle as a secretory organ. *Nat. Rev. Endocrinol.* 8 (8), 457–465. doi:10.1038/nrendo.2012.49
- Piazza, N., Gosangi, B., Devilla, S., Arking, R., and Wessells, R. (2009). Exercise-training in young *Drosophila melanogaster* reduces age-related decline in mobility and cardiac performance. *PLoS One* 4 (6), e5886. PMID: 19517023; PMCID: PMC2691613. doi:10.1371/journal.pone.0005886
- Piccirillo, R., Demontis, F., Perrimon, N., and Goldberg, A. L. (2014). Mechanisms of muscle growth and atrophy in mammals and *Drosophila*. *Dev. Dyn.* 243 (2), 201–215. Epub 2013 Oct 24. PMID: 24038488; PMCID: PMC3980484. doi:10.1002/dvdy.24036
- Pilegaard, H., Saltin, B., and Neufer, P. D. (2003). Exercise induces transient transcriptional activation of the PGC-1 α gene in human skeletal muscle. *J. Physiol.* 546 (3), 851–858. PMID: 12563009; PMCID: PMC2342594. doi:10.1113/jphysiol.2002.034850
- Rai, M., Coleman, Z., Curley, M., Nityanandam, A., Platt, A., Robles-Murguía, M., et al. (2021). Proteasome stress in skeletal muscle mounts a long-range protective response that delays retinal and brain aging. *Cell Metab.* 33 (6), 1137–1154. e9. Epub 2021 Mar 26. PMID: 33773104; PMCID: PMC8172468. doi:10.1016/j.cmet.2021.03.005
- Rakshit, K., Wambua, R., Giebltowicz, T. M., and Giebltowicz, J. M. (2013). Effects of exercise on circadian rhythms and mobility in aging *Drosophila melanogaster*. *Exp. Gerontol.* 48 (11), 1260–1265. Epub 2013 Aug 2. PMID: 23916842; PMCID: PMC3798010. doi:10.1016/j.exger.2013.07.013
- Risom, S. S., Zwisler, A. D., Johansen, P. P., Sibillit, K. L., Lindschou, J., Gluud, C., et al. (2017). Exercise-based cardiac rehabilitation for adults with atrial fibrillation. *Cochrane Database Syst. Rev.* 2 (2), CD011197. pub2. PMID: 28181684; PMCID: PMC6464537. doi:10.1002/14651858.CD011197
- Rognmo, Ø., Moholdt, T., Bakken, H., Hole, T., Mølsted, P., Myhr, N. E., et al. (2012). Cardiovascular risk of high- versus moderate-intensity aerobic exercise in coronary heart disease patients. *Circulation* 126 (12), 1436–1440. Epub 2012 Aug 9. PMID: 22879367. doi:10.1161/CIRCULATIONAHA.112.123117
- Rosenberg, M. I., and Parkhurst, S. M. (2002). *Drosophila* Sir2 is required for heterochromatic silencing and by euchromatic Hair/E(Spl) bHLH repressors in segmentation and sex determination. *Cell* 109 (4), 447–458. PMID: 12086602. doi:10.1016/s0092-8674(02)00732-8
- Ruiz, J. R., Morán, M., Arenas, J., and Lucia, A. (2011). Strenuous endurance exercise improves life expectancy: it's in our genes. *Br. J. Sports Med.* 45 (3), 159–161. Epub 2010 Sep 27. PMID: 20876590. doi:10.1136/bjsm.2010.075085
- Ruiz, J. R., Sui, X., Lobelo, F., Morrow, J. R., Jr, Jackson, A. W., Sjöström, M., et al. (2008). Association between muscular strength and mortality in men: Prospective cohort study. *BMJ* 337 (7661), a439. PMID: 18595904; PMCID: PMC2453303. doi:10.1136/bmj.a439
- Ryu, D., Zhang, H., Ropelle, E. R., Sorrentino, V., Mázala, D. A., Mouchiroud, L., et al. (2016). NAD⁺ repletion improves muscle function in muscular dystrophy and counters global PARYlation. *Sci. Transl. Med.* 8 (361), 361ra139. PMID: 27798264; PMCID: PMC5535761. doi:10.1126/scitranslmed.aaf5504
- Safdar, A., Bourgeois, J. M., Ogborn, D. I., Little, J. P., Hettinga, B. P., Akhtar, M., et al. (2011). Endurance exercise rescues progeroid aging and induces systemic mitochondrial rejuvenation in mtDNA mutator mice. *Proc. Natl. Acad. Sci. U. S. A.* 108 (10), 4135–4140. Epub 2011 Feb 22. PMID: 21368114; PMCID: PMC3053975. doi:10.1073/pnas.1019581108
- Santos, A. L., and Sinha, S. (2021). Obesity and aging: Molecular mechanisms and therapeutic approaches. *Ageing Res. Rev.* 67, 101268. Epub 2021 Feb 5. PMID: 33556548. doi:10.1016/j.arr.2021.101268
- Schaffer, J. E. (2003). Lipotoxicity: When tissues overeat. *Curr. Opin. Lipidol.* 14 (3), 281–287. PMID: 12840659. doi:10.1097/00041433-200306000-00008
- Schrauwen-Hinderling, V. B., Hesselink, M. K., Meex, R., van der Made, S., Schär, M., Lamb, H., et al. (2010). Improved ejection fraction after exercise training in obesity is accompanied by reduced cardiac lipid content. *J. Clin. Endocrinol. Metab.* 95 (4), 1932–1938. Epub 2010 Feb 19. PMID: 20173015. doi:10.1210/jc.2009-2076

- Serra, F. T., Carvalho, A. D., Araujo, B. H. S., Torres, L. B., Cardoso, F. D. S., Henrique, J. S., et al. (2019). Early exercise induces long-lasting morphological changes in cortical and hippocampal neurons throughout of a sedentary period of rats. *Sci. Rep.* 9 (1), 13684. PMID: 31548605; PMCID: PMC6757043. doi:10.1038/s41598-019-50218-9
- Shaw, P. J., Cirelli, C., Greenspan, R. J., and Tononi, G. (2000). Correlates of sleep and waking in *Drosophila melanogaster*. *Science* 287 (5459), 1834–1837. PMID: 10710313. doi:10.1126/science.287.5459.1834
- Shimizu, H., Shimoda, M., Yamaguchi, T., Seong, K. H., Okamura, T., and Ishii, S. (2008). *Drosophila* ATF-2 regulates sleep and locomotor activity in pacemaker neurons. *Mol. Cell. Biol.* 28 (20), 6278–6289. Epub 2008 Aug 11. PMID: 18694958; PMCID: PMC2577423. doi:10.1128/MCB.02242-07
- Silverman, L. A., Cheng, Z. Q., Hsiao, D., and Rosenthal, S. M. (1995). Skeletal muscle cell-derived insulin-like growth factor (IGF) binding proteins inhibit IGF-I-induced myogenesis in rat L6E9 cells. *Endocrinology* 136 (2), 720–726. doi:10.1210/endo.136.2.7530651
- Sujkowski, A., Gretzinger, A., Soave, N., Todi, S. V., and Wessells, R. (2020). Alpha- and beta-adrenergic octopamine receptors in muscle and heart are required for *Drosophila* exercise adaptations. *PLoS Genet.* 16 (6), e1008778. PMID: 32579604; PMCID: PMC7351206. doi:10.1371/journal.pgen.1008778
- Sujkowski, A., Ramesh, D., Brockmann, A., and Wessells, R. (2017). Octopamine drives endurance exercise adaptations in *Drosophila*. *Cell Rep.* 21 (7), 1809–1823. PMID: 29141215; PMCID: PMC5693351. doi:10.1016/j.celrep.2017.10.065
- Sujkowski, A., Richardson, K., Prifti, M. V., Wessells, R. J., and Todi, S. V. (2022). Endurance exercise ameliorates phenotypes in *Drosophila* models of spinocerebellar ataxias. *Elife* 11, e75389. PMID: 35170431; PMCID: PMC8871352. doi:10.7554/eLife.75389
- Sujkowski, A., Saunders, S., Tinkerhess, M., Piazza, N., Jennens, J., Healy, L., et al. (2012). dFATP regulates nutrient distribution and long-term physiology in *Drosophila*. *Aging Cell* 11 (6), 921–932. Epub 2012 Aug 27. PMID: 22809097; PMCID: PMC3533766. doi:10.1111/j.1474-9726.2012.00864.x
- Sujkowski, A., Spierer, A. N., Rajagopalan, T., Bazzell, B., Safdar, M., Imsirovic, D., et al. (2019). Mito-nuclear interactions modify *Drosophila* exercise performance. *Mitochondrion* 47, 188–205. Epub 2018 Nov 6. PMID: 30408593; PMCID: PMC7035791. doi:10.1016/j.mito.2018.11.005
- Sujkowski, A., and Wessells, R. (2021). Exercise and sestrin mediate speed and lysosomal activity in *Drosophila* by partially overlapping mechanisms. *Cells* 10 (9), 2479. PMID: 34572128; PMCID: PMC8466685. doi:10.3390/cells10092479
- Sun, Y., Liu, L., Ben-Shahar, Y., Jacobs, J. S., Eberl, D. F., and Welsh, M. J. (2009). TRPA channels distinguish gravity sensing from hearing in Johnston's organ. *Proc. Natl. Acad. Sci. U. S. A.* 106 (32), 13606–13611. Epub 2009 Jul 28. PMID: 19666538; PMCID: PMC2717111. doi:10.1073/pnas.0906377106
- Swift, D. L., McGee, J. E., Earnest, C. P., Carlisle, E., Nygard, M., and Johannsen, N. M. (2018). The effects of exercise and physical activity on weight loss and maintenance. *Prog. Cardiovasc. Dis.* 61 (2), 206–213. Epub 2018 Jul 9. PMID: 30003901. doi:10.1016/j.pcad.2018.07.014
- Tinkerhess, M. J., Healy, L., Morgan, M., Sujkowski, A., Matthys, E., Zheng, L., et al. (2012). The *Drosophila* PGC-1 α homolog spargel modulates the physiological effects of endurance exercise. *PLoS One* 7 (2), e31633. Epub 2012 Feb 13. PMID: 22348115; PMCID: PMC3278454. doi:10.1371/journal.pone.0031633
- Umpierre, D., Ribeiro, P. A., Kramer, C. K., Leitão, C. B., Zucatti, A. T., Azevedo, M. J., et al. (2011). Physical activity advice only or structured exercise training and association with HbA1c levels in type 2 diabetes: A systematic review and meta-analysis. *JAMA* 305 (17), 1790–1799. doi:10.1001/jama.2011.576
- Unger, R. H. (2003). Minireview: Weapons of lean body mass destruction: The role of ectopic lipids in the metabolic syndrome. *Endocrinology* 144 (12), 5159–5165. Epub 2003 Sep 4. PMID: 12960011. doi:10.1210/en.2003-0870
- van Praag, H., Shubert, T., Zhao, C., and Gage, F. H. (2005). Exercise enhances learning and hippocampal neurogenesis in aged mice. *J. Neurosci.* 25 (38), 8680–8685. PMID: 16177036; PMCID: PMC1360197. doi:10.1523/JNEUROSCI.1731-05.2005
- Villareal, D. T., Aguirre, L., Gurney, A. B., Waters, D. L., Sinacore, D. R., Colombo, E., et al. (2017). Aerobic or resistance exercise, or both, in dieting obese older adults. *N. Engl. J. Med.* 376 (20), 1943–1955. PMID: 28514618; PMCID: PMC5552187. doi:10.1056/NEJMoa1616338
- Vinciguerra, M., Musaro, A., and Rosenthal, N. (2010). Regulation of muscle atrophy in aging and disease. *Adv. Exp. Med. Biol.* 694, 211–233. PMID: 20886766. doi:10.1007/978-1-4419-7002-2_15
- Viru, A. (1992). Plasma hormones and physical exercise. *Int. J. Sports Med.* 13 (3), 201–209. doi:10.1055/s-2007-1021254
- Vujic, A., Lerchenmüller, C., Wu, T. D., Guillemer, C., Rabolli, C. P., Gonzalez, E., et al. (2018). Exercise induces new cardiomyocyte generation in the adult mammalian heart. *Nat. Commun.* 9 (1), 1659. PMID: 29695718; PMCID: PMC5916892. doi:10.1038/s41467-018-04083-1
- Watanabe, L. P., and Riddle, N. C. (2017). Characterization of the rotating exercise quantification system (REQS), a novel *Drosophila* exercise quantification apparatus. *PLoS One* 12 (10), e0185090. PMID: 29016615; PMCID: PMC5634558. doi:10.1371/journal.pone.0185090
- Watanabe, L. P., and Riddle, N. C. (2021). GWAS reveal a role for the central nervous system in regulating weight and weight change in response to exercise. *Sci. Rep.* 11 (1), 5144. PMID: 33664357; PMCID: PMC7933348. doi:10.1038/s41598-021-84534-w
- Watanabe, L. P., and Riddle, N. C. (2018). Measuring exercise levels in *Drosophila melanogaster* using the rotating exercise quantification system (REQS). *J. Vis. Exp.* 8 (136), 57788. PMID: 29889199; PMCID: PMC6101427. doi:10.3791/57751
- Waters, D. L., Ward, A. L., and Villareal, D. T. (2013). Weight loss in obese adults 65 years and older: A review of the controversy. *Exp. Gerontol.* 48 (10), 1054–1061. Epub 2013 Feb 10. PMID: 23403042; PMCID: PMC3714333. doi:10.1016/j.exger.2013.02.005
- Wen, D. T., Wang, W. Q., Hou, W. Q., Cai, S. X., and Zhai, S. S. (2020). Endurance exercise protects aging *Drosophila* from high-salt diet (HSD)-induced climbing capacity decline and lifespan decrease by enhancing antioxidant capacity. *Biol. Open* 9 (5), bio045260. PMID: 32414766; PMCID: PMC7272356. doi:10.1242/bio.045260
- Wen, D. T., Zheng, L., Li, J. X., Cheng, D., Liu, Y., Lu, K., et al. (2019). Endurance exercise resistance to lipotoxic cardiomyopathy is associated with cardiac NAD⁺/dSIR2/PGC-1 α pathway activation in old *Drosophila*. *Biol. Open* 8 (10), bio044719. PMID: 31624074; PMCID: PMC6826281. doi:10.1242/bio.044719
- Wen, D. T., Zheng, L., Li, J. X., Lu, K., and Hou, W. Q. (2019). The activation of cardiac dSIR2-related pathways mediates physical exercise resistance to heart aging in old *Drosophila*. *Aging (Albany NY)* 11 (17), 7274–7293. Epub 2019 Sep 10. PMID: 31503544; PMCID: PMC6756900. doi:10.18632/aging.102261
- Wen, D. T., Zheng, L., Lu, K., and Hou, W. Q. (2021). Activation of cardiac Nmnat/NAD⁺/SIR2 pathways mediates endurance exercise resistance to lipotoxic cardiomyopathy in aging *Drosophila*. *J. Exp. Biol.* 224 (18), jeb242425. Epub 2021 Sep 15. PMID: 34495320. doi:10.1242/jeb.242425
- Wen, D. T., Zheng, L., Lu, K., and Hou, W. Q. (2021). Physical exercise prevents age-related heart dysfunction induced by high-salt intake and heart salt-specific overexpression in *Drosophila*. *Aging (Albany NY)* 13 (15), 19542–19560. Epub 2021 Aug 12. PMID: 34383711; PMCID: PMC8386524. doi:10.18632/aging.203364
- Wen, D. T., Zheng, L., Ni, L., Wang, H., Feng, Y., and Zhang, M. (2016). The expression of CG9940 affects the adaptation of cardiac function, mobility, and lifespan to exercise in aging *Drosophila*. *Exp. Gerontol.* 83, 6–14. Epub 2016 Jul 19. PMID: 27448710. doi:10.1016/j.exger.2016.07.006
- White, A. T., and Schenk, S. (2012). NAD⁺/NADH and skeletal muscle mitochondrial adaptations to exercise. *Am. J. Physiol. Endocrinol. Metab.* 303 (3), E308–E321. Epub 2012 Mar 20. PMID: 22436696; PMCID: PMC3423123. doi:10.1152/ajpendo.00054.2012
- Whitham, M., Parker, B. L., Friedrichsen, M., Hingst, J. R., Hjorth, M., Hughes, W. E., et al. (2018). Extracellular vesicles provide a means for tissue crosstalk during exercise. *Cell Metab.* 27 (1), 237–251. e4. PMID: 29320704. doi:10.1016/j.cmet.2017.12.001
- WHO (World Health Organization) (2017). *Cardiovascular diseases (CVDs)*. WHO. Available at: [https://www.who.int/news-room/fact-sheets/detail/cardiovascular-diseases-\(cvds\)](https://www.who.int/news-room/fact-sheets/detail/cardiovascular-diseases-(cvds)).
- Williams, R. S., and Neuffer, P. D. (1996). "Regulation of gene expression in skeletal muscle by contractile activity," in *The handbook of physiology. Exercise: Regulation and integration of multiple systems*. Editors L. B. Rowell and J. T. Shepherd (New York, USA: Oxford University Press), 1124–1150.
- Xu, W., Barrientos, T., Mao, L., Rockman, H. A., Sauve, A. A., and Andrews, N. C. (2015). Lethal cardiomyopathy in mice lacking transferrin receptor in the heart. *Cell Rep.* 13 (3), 533–545. Epub 2015 Oct 8. PMID: 26456827; PMCID: PMC4618069. doi:10.1016/j.celrep.2015.09.023
- Zhang, H., Ryu, D., Wu, Y., Gariani, K., Wang, X., Luan, P., et al. (2016). NAD⁺ repletion improves mitochondrial and stem cell function and enhances life span in mice. *Science* 352 (6292), 1436–1443. Epub 2016 Apr 28. PMID: 27127236. doi:10.1126/science.1269363
- Zheng, L., Feng, Y., Wen, D. T., Wang, H., and Wu, X. S. (2015). Fatiguing exercise initiated later in life reduces incidence of fibrillation and improves sleep quality in *Drosophila*. *Age (Dordr.)* 37 (4), 9816. Epub 2015 Jul 24. PMID: 26206392; PMCID: PMC4512962. doi:10.1007/s11357-015-9816-7
- Zheng, L., Li, Q. F., Ni, L., Wang, H., Ruan, X. C., and Wu, X. S. (2017). Lifetime regular exercise affects the incident of different arrhythmias and improves organismal health in aging female *Drosophila melanogaster*. *Biogerontology* 18 (1), 97–108. Epub 2016 Oct 27. PMID: 27787741. doi:10.1007/s10522-016-9665-5
- Zigmond, M. J., Cameron, J. L., Leak, R. K., Mirnics, K., Russell, V. A., Smeyne, R. J., et al. (2009). Triggering endogenous neuroprotective processes through exercise in models of dopamine deficiency. *Park. Relat. Disord.* 15 (3), S42–S45. PMID: 20083005. doi:10.1016/S1353-8020(09)70778-3



REPLACING ANIMAL TESTING: HOW AND WHEN?

Thomas Hartung^{1,2*}

¹Center for Alternatives to Animal Testing (CAAT), Johns Hopkins University, Baltimore, MD, United States

²CAAT-Europe, University of Konstanz, Konstanz, Germany

YOUNG REVIEWERS

Internat
School
Lausann

INTERNA-
TIONAL
SCHOOL
OF
LAUSANNE

AGES: 11–12

An important discussion in today's society is whether we should make animals suffer for the sake of science and product development. In this article, I present four examples of animal tests that were introduced in the past to protect patients and consumers, and I discuss attempts to replace those animal tests with other methods. When we started using small animals such as mice and rats for testing more than 100 years ago, there were not many alternatives. Today, we have more knowledge and a greater number of options. Scientists can now create tiny functioning organs in the laboratory, and even combine multiple mini-organs, to help us understand how the human body works when it is healthy or sick. This increased understanding will allow scientists to move beyond the use of animals in many cases, which will improve both the accuracy of the scientific tests and the welfare of animals.

Thanks to the endeavors of the **Swiss 3RCC**, these articles have been translated into the three main Swiss languages of **German**, **French**, and **Italian**.

3RS PRINCIPLE

An attempt to replace animals with other forms of testing, reduce the number of animals used in tests, and refine animal tests so that they are more humane.

BIOENGINEERING

The field of engineering that applies the life sciences, physical sciences, mathematics, and engineering to solve problems in biology and medicine.

PYROGENS

A group of microbial substances that lead to fever and inflammation.

ANIMAL TESTING IS CONTROVERSIAL

There is much debate over whether we should allow laboratory animals to suffer for the sake of science or the development of products such as cosmetics, drugs, and pesticides: about 50% of Americans and 60% of Europeans oppose animal testing, but individuals hold varied positions in terms of what should be allowed and what should not. In 1959, two scientists named Bill Russel and Rex Burch developed the **3Rs principle** (reduce, replace, refine), which is a sort of compromise. Instead of completely banning animal research or allowing it in all cases, they called on scientists to do as much as possible to replace animal testing. Where replacement is *not* possible, scientists are encouraged to reduce the numbers of animals used and refine their experiments to minimize animal suffering. Russel and Burch said, "Refinement is never enough, and we should always seek further for reduction and, if possible, replacement."

Back when Russel and Burch came up with the 3Rs principle, there were not many alternatives to animal experiments—but knowledge of the life sciences doubles every 7 years, so we now know over 1,000 times more than we did then! Scientists know much more about growing cells in the laboratory and, using human stem cell technologies and **bioengineering**, we can now recreate the structure and function of some organs in the lab and even combine multiple lab-generated organs to create a "human" system in the laboratory. A detailed understanding of how the body works in health and disease will help researchers create tests that are more accurate than animal testing and that save the lives of laboratory animals.

HISTORY: ANIMAL TESTS TO SOLVE RESEARCH PROBLEMS

Now I will describe four different medical-safety problems of the past that were solved through animal testing. These historic cases have shaped how we ensure the safety of drugs and consumer products, and the examples can help us understand the progress made using new technologies.

Pyrogens

The term **pyrogen** comes from a Greek word meaning something that generates fire. Today we use the word pyrogen to mean something that generates fever. In the early 1900s, scientists started to synthesize disease-curing drugs, including some that had to be injected into the body. Physicians often observed fever in their patients following drug injections, and sometimes even life-threatening reactions. They named the unknown fever-causing substances pyrogens. In 1912, the rabbit pyrogen test was invented: a dose of the drug ten times greater than what would be used in humans was injected into rabbits. If the rabbits did not develop fever, the drug was deemed safe for

human use. Today we know that these pyrogens come from bacterial contamination during drug production, and even killing the microbes by sterilization does not eliminate them. When the patient's immune system recognizes the bacterial pyrogens, fever results.

Eye Irritation

The eyes are especially sensitive to chemicals. In the US in the early 1930s, a cosmetic used to dye the eyelashes (called Lash Lure) led to more than 3,000 cases of eye irritation, five cases of blindness, and one death. Subsequently, the rabbit eye test was developed to prevent this from happening again. A drop of the chemical is applied directly into the eye of a rabbit and the animal is observed for several days.

REPEAT-DOSE TESTING

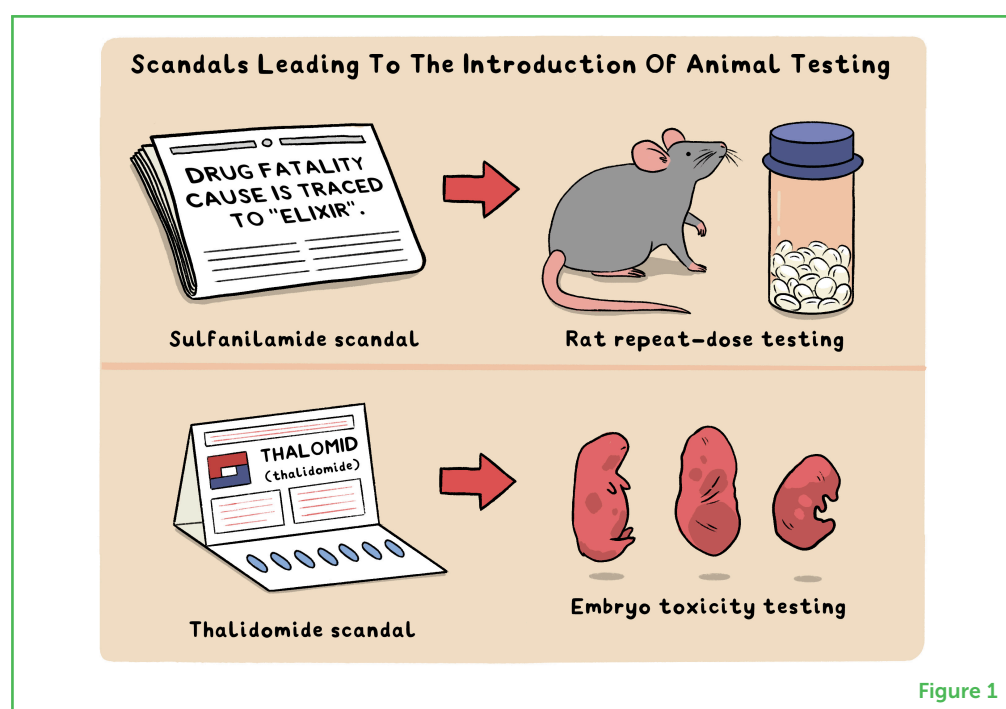
Giving a drug to animals multiple times over 28–90 days, to look for unexpected toxic effects on their organs.

Unexpected Toxicities

In 1936, more than 100 children died in the US from a cough syrup (Figure 1). The antibiotic contained in the syrup had been used for years without problems, but a substance called glycol, used to dissolve the antibiotic, was toxic. This started what is called **repeat-dose testing**, usually performed in rats and dogs, in which the drug is given for 28 or even 90 days orally, by inhalation, or on the skin (depending on the use of the drug). Afterward, the animals are killed and their organs are checked for possible effects.

Figure 1

Scandals leading to the introduction of animal testing. Scandals prompted a lot of the animal tests we use today. Two examples are the repeat-dose testing for unexpected toxicities and embryotoxicity in response to health problems caused by Sulfanilamide and Thalidomide.



Embryotoxicity Testing

In the late 1950s, a German pharmaceutical company introduced a drug called thalidomide that became very popular for "morning sickness"—the frequent nausea experienced by pregnant women. About 2,000 unborn babies died from the drug and more than 10,000 children were born with malformations of their limbs (Figure

EMBRYOTOXICITY TESTING

Animal testing of drugs on pregnant animals, to see if the drugs are safe or will have dangerous effects on (human) embryos.

HORSESHOE CRAB PYROGEN TEST

A test using the blood of horseshoe crabs, which coagulates (clots) in response to an important group of pyrogens.

Figure 2

History of pyrogen testing. In the early 1900s, scientists and doctors noticed high fevers and some deaths in their patients after the injection of certain drugs. In 1912, the rabbit pyrogen test was developed to screen injected drugs for these dangerous effects. Since then, various techniques have been developed to decrease or completely end the use of rabbits in these tests. These attempts are ongoing and, by 2030, rabbit testing should be eliminated in the EU.

1). In response, broad testing of toxicity against embryos, called **embryotoxicity testing**, was introduced—using 3,200 rats and 2,100 rabbits per drug (Figure 1).

In all these cases, the scientific solution was to use animals to make sure drugs and other chemicals were safe for use in humans. But the use of animals to mirror what might happen in people is far from perfect—mice and rats predict each other's response to drugs often not better than 60%, and sometimes specific strains of mice react completely differently from each other in these tests. Sometimes animals react like humans in response to drugs or other chemicals, but sometimes they do not.

REPLACING ANIMAL TESTING: A PYROGEN EXAMPLE

A timeline of pyrogen testing is shown in Figure 2. Scientists first discovered certain bacterial contaminations of drugs that were causing fever reactions back in the 1950s. In the 1960s, it was discovered that the same bacterial substances made the blood of horseshoe crabs clot. This spurred the development of a new test relying on sampling horseshoe crabs' blood, the **Horseshoe crab pyrogen test**, which replaced 90% of rabbit testing starting in the 1980s. Then, in 1995, another laboratory test was developed based on the advancing knowledge of the human immune system—particularly,

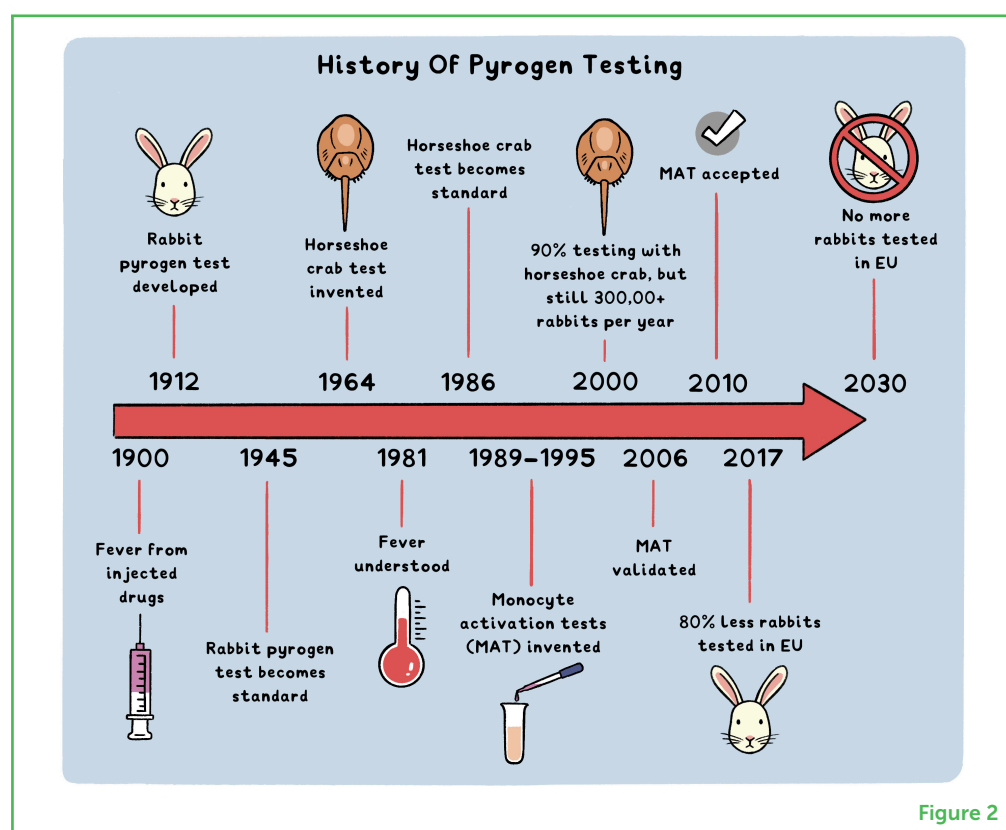


Figure 2

MONOCYTE ACTIVATION TEST

A laboratory test that measures whether substances are contaminated with pyrogens based on the reaction of monocytes (cells of the human immune system).

white blood cells called monocytes, which emit the chemical signals that cause fever. These tests are now called **monocyte activation tests**, and they measure whether substances are contaminated with pyrogens based on the reaction of monocytes. I developed one of these tests and led an international study with other scientists who had developed similar tests, demonstrating that such tests could replace the animal test for pyrogens [1, 2]. Following a thorough review by experts, the monocyte activation test was validated in 2006 and accepted by a number of agencies across the world in the years that followed. However, the actual replacement of the animal test is still ongoing: by 2017, 80% of rabbit pyrogen testing had been replaced in Europe, and by 2030 all rabbit testing in Europe should end. Other parts of the world lag behind. So, it took about 30 years for the horseshoe crab test to replace about 90% of rabbit testing, and another 30 years for monocyte activation tests to replace the remainder. Too slow, but we learn from these forerunners! Once scientists understand what happens in the human body, it will be easier to use non-animal test systems.

PROGRESS IN OTHER AREAS

Eye irritation testing has seen enormous progress (Figure 3A). Several new tests use simple cell cultures of skin cells, others the eyes of chickens or cows that are killed for our food. Bioengineered human eye structures have also been developed and validated. Unfortunately, no single test can fully replace the rabbit test yet. Some can only identify strongly toxic substances; others can only identify substances that have no effect. Some tests work only with certain types of chemicals. But various combinations of new tests *can* replace animals for most uses.

Embryotoxicity testing is the most demanding animal test, with respect to the numbers of animals needed. Some tests require more than 5,000 rats as well as rabbits and their embryos. Progress to replace animals for embryotoxicity testing is slow, primarily because embryo development is extremely complex and varies between species. Only three out of five chemicals tested in one species give the same results in a different species. Major progress in recent years has included the development of stem cells, which allow scientists to learn more about early human embryo development (Figure 3B). The stem cell tests that have been developed are bringing scientists closer to replacing the animal test.

Unexpected toxicities are still a key problem. How can we prepare for the unexpected? There are hundreds of tissues in the human body, and each could be the target! However, as it becomes more obvious that animals often react differently to toxic substances than humans do, we have no choice but to develop new, human-relevant tests (Figure 3C). Enormous progress has been made with modern

Figure 3

Progress in replacing animal testing. **(A)** Eye irritation testing. **(B)** Embryotoxicity testing. **(C)** Unexpected toxicity testing. Various technological advances allow the replacement of animal tests, including cell culture, slaughterhouse materials, bioengineered organs, stem cell technology, test combinations, and computational methods.

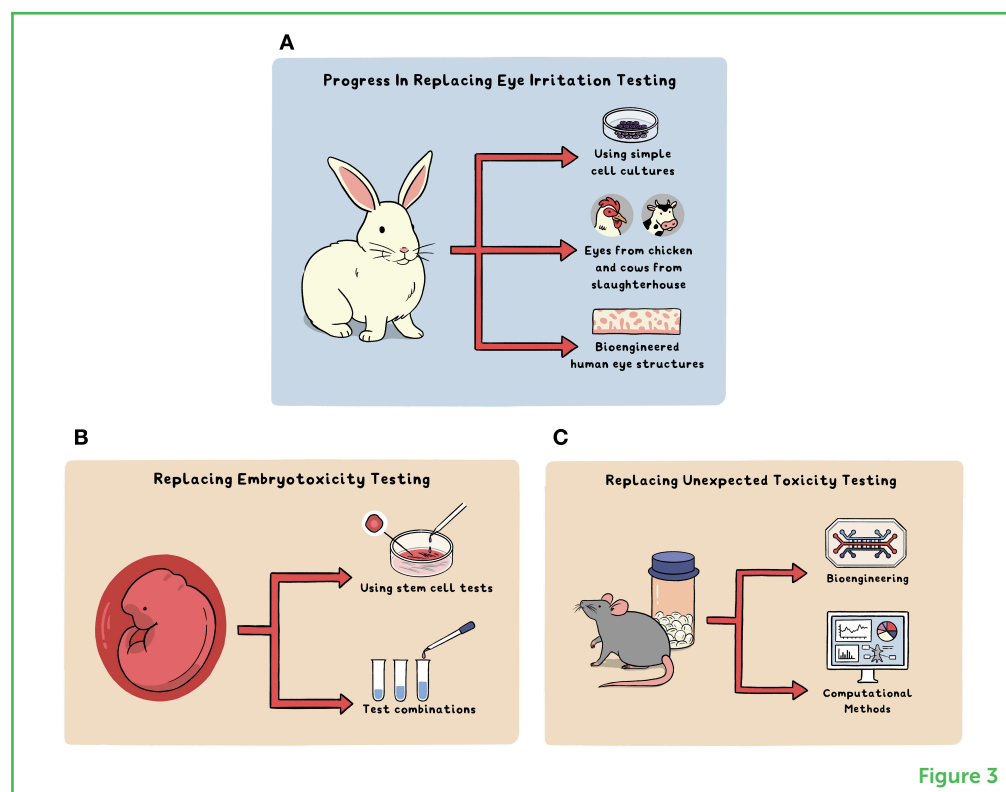


Figure 3

ORGANOIDS

Cell cultures that replicate organ architecture and function. They can be 2D or 3D, on "chips," and multiple organoids can be joined together to create human-on-chip models.

cell culture: bioengineering allows us to recreate the structure and function of bodily organs in the lab. These **organoids** can be combined on chips and connected by tiny fluid-filled channels that act like blood vessels. These human-on-chip models are exciting because they enable scientists to study reactions in human-like systems. At the same time, artificial intelligence (AI), which involves the increasing ability of computers to learn and analyze data, is helping us combine the accumulated knowledge of recent decades. Millions of scientific papers and tons of data from experiments can be combined by AI systems to predict unexpected effects of substances on the human body and thus avoid animal tests. So, gains in computer power are helping scientists to model what is happening in the body and to make sense of large datasets, to predict toxic effects.

THE CHALLENGE AHEAD

These examples illustrate that science is continuously advancing. While this article has focused on the safety of drugs, similar stories could be told for other areas of research. New laboratory and computer-based methods can be used on their own and are even more powerful if combined. These new approaches are often as good or better than traditional animal experiments. The challenge now is figuring out how to change the habit of relying on animal testing for safety assessments of drugs and new consumer products. Recent

advances have made testing processes more relevant to the human body and, most importantly, more humane.

FURTHER READING

Goldberg, A., and Hartung, T. 2006. Protecting more than animals. *Sci. Am.* 294:84–91. doi: 10.1038/scientificamerican0106-84

Hartung, T. 2018. "Alternatives to animal testing," in *Toxicology and Risk Assessment: A Comprehensive Introduction, 2nd edn*, eds H. Greim, and R. Snyder (Hoboken, NJ: Wiley). p. 461–47.

REFERENCES

1. Hartung, T. 2015. The human whole blood pyrogen test – lessons learned in twenty years. *ALTEX*. 32:79–100. doi: 10.14573/altex.1503241
2. Hartung, T. 2021. Pyrogen testing revisited on occasion of the 25th anniversary of the whole blood test. *ALTEX*. 38:3–19. doi: 10.14573/altex.2101051

SUBMITTED: 01 June 2022; **ACCEPTED:** 05 September 2022;

PUBLISHED ONLINE: 11 October 2022.

EDITOR: Robert T. Knight, University of California, Berkeley, United States

SCIENCE MENTOR: Christopher R. Cederroth

CITATION: Hartung T (2022) Replacing Animal Testing: How and When? *Front. Young Minds* 10:959496. doi: 10.3389/frym.2022.959496

CONFLICT OF INTEREST: The author consults a number of companies on alternative methods.

COPYRIGHT © 2022 Hartung. This is an open-access article distributed under the terms of the Creative Commons Attribution License (CC BY). The use, distribution or reproduction in other forums is permitted, provided the original author(s) and the copyright owner(s) are credited and that the original publication in this journal is cited, in accordance with accepted academic practice. No use, distribution or reproduction is permitted which does not comply with these terms.

YOUNG REVIEWERS

INTERNATIONAL SCHOOL OF LAUSANNE, AGES: 11–12

ISL is a non-profit, independent, International Baccalaureate (IB) World School. Since 1962, we have grown to almost 1,000 students, aged 3–18 years, who come from more than 60 nations. We believe in strong values, the courage to think independently, and cooperation across cultural boundaries—ideas that form the heart of a progressive approach to learning.





AUTHOR

THOMAS HARTUNG

Thomas Hartung has spent more than three decades of his career promoting technologies to replace animal testing. From 2002 to 2008 he led the European Center for the Validation of Alternative Methods (to animal experiments) of the European Commission in Italy and since 2009 Centers for Alternatives to Animal Testing in the US and Europe. He is active in many different fields of science: starting with studies of biochemistry, human medicine and mathematics/informatics, he became first doctor (MD Ph.D.) and then professor for both pharmacology and toxicology. He expanded his work to immunology, microbiology and engineering. Today he holds five professorships at Johns Hopkins University and Georgetown University in the US as well as at the University of Konstanz in Germany. He is chief editor of *Frontiers in Artificial Intelligence*. *THartung@jhu.edu



REDUCING THE NUMBER OF RESEARCH ANIMALS: HOW IMAGING TECHNOLOGIES CAN HELP

Jordi L. Tremoleda^{1,2*}

¹Neuroscience, Surgery and Trauma, Blizard Institute, Queen Mary University, London, United Kingdom

²Biological Services, Queen Mary University London, London, United Kingdom

YOUNG REVIEWERS



INTER-
NATIONAL
SCHOOL
OF
LAUSANNE

AGES: 11–12

Even when no other alternatives are available for scientific experiments, the use of research animals is still a difficult decision. To promote more ethical animal research, scientists must follow the 3Rs principle. Reduction is one of the 3Rs—it involves keeping the number of animals used to a minimum, by obtaining information from fewer animals or obtaining more information from the same number of animals. Imaging technologies allow scientists to see inside of the bodies of live animals without harming them, so that the animals do not need to be killed for scientists to study their organs. Using imaging techniques, scientists can study illness and responses to treatments. Animals can be imaged multiple times in long-term studies, so imaging techniques protect animal welfare by reducing the number of animals used in research.

Thanks to the endeavors of the **Swiss 3RCC**, these articles have been translated into the three main Swiss languages of **German**, **French**, and **Italian**.

RESEARCH IS NECESSARY

Our world continues to be challenged by devastating diseases, as illustrated only too well by the health emergencies brought on by the Covid-19 pandemic. Understanding how the bodies of humans and animals work is very important, because it helps scientists discover new treatments for animal and human diseases. The use of animals in research has been vital in supporting major medical breakthroughs, such as the discovery of vaccines and antibiotics that can prevent and treat dangerous infections. Research animals have also advanced our understanding of genetics and our knowledge of how the body's cells regenerate [1]¹.

¹ <https://www.animalresearch.info/en/medical-advances/medical-discovery-timeline/>

3RS

Scientific principles that replace, reduce, and refine the use of animal in scientific experiments, to ensure humane and caring animal research.

However, animals are living, feeling beings that can suffer pain and distress, so using them for research is a difficult decision and must always be completely necessary and ethically justifiable. Most national and international laws protect the care and welfare of research animals, both for the wellbeing of the animals and as a way to support the highest-quality science. More than 60 years ago, two English biologists, Russel and Burch, set up the **3Rs principle** for performing humane animal research [2]. The 3Rs principle includes replacement of animals by alternative methods when possible, reduction of the number of animals used in research studies, and refinement of experimental methods and housing conditions to minimize the suffering of laboratory animals.

WHY DO WE STILL USE ANIMALS IN RESEARCH?

Despite great progress in the use of non-animal alternatives (for example using human samples or computer models), there are circumstances when animal studies are unavoidable—such as when studying a disease or testing a new medicine. Testing new drugs on humans is not ethically possible and, so far, there are no alternatives to animals that can replicate the complex, interacting parts of a living body (for example the effects of the heart beating and blood circulating under the control of the brain). Researchers have a legal and ethical responsibility to ensure that the treatments they are studying are safe to be used in humans or in the animals those treatments are designed for. There is still an urgent need for better medicines and vaccines to treat life-threatening conditions like cancer, brain disorders, or pandemics like Covid-19.

Mice are the most-used animals in research. Although much smaller than humans, mice have very similar body functions and share 95% of their genes with humans. This means that the way a mouse body functions and responds to medicines is often very similar to what is seen in humans, so using mice in research can be a very informative way for scientists to understand a disease and how it might respond to treatment. More recently, scientists are increasingly using fish, flies,

or worms to study body functions and new drug treatments, but the anatomy and the body-function differences between these animals and humans can be much greater, so there are limits to what these experiments can tell us.

LET US TALK ABOUT THE 3RS: WHY REDUCTION IS NEEDED

The 3Rs guide all research that uses animals, promoting the best animal care to support the highest-quality science. As scientists become better at understanding human diseases by looking at patients and working with alternative tests, these approaches will help to replace the use of animals in research. But in other cases, possibly during the final stages of testing the safety of new medicines in complex diseases like cancer or brain disorders, scientists may still need to use animals. When doing studies that require the use of animals, scientists must follow the reduction and refinement principles, to reduce the number of animals used and to ensure that they avoid or at least minimize any harm to the animals.

REDUCTION

One of the 3Rs principles that promotes the use of the smallest number of animals possible, while still obtaining valuable research information.

Reduction aims to use the smallest number of animals possible, by obtaining information from fewer animals or by obtaining a greater amount of information from the same number of animals. When planning a research study to test a new medicine, scientists should plan how many animals will be needed. This number includes those animals that will be used to test the new medicine and a group of animals that will experience the same living conditions but do not receive the medicine, called the control group. Scientists must also think about how many times the animals must be tested or investigated. For example, animals may receive a medicine that changes their heart function, so a scientist might need to check the animals' heart rates every so many hours, days, or weeks, to study the medicine's effects. But the scientist might also need to examine the heart directly, which can only be done after the animal is humanely killed. This means that, if the scientist wants to study animals at multiple time points, many animals would need to be killed. To avoid killing the animals, it would be ideal to be able to visualize internal tissues and organs in a living animal, without causing it harm. Visualizing the internal structures of a living animal would allow scientists to study how the animal's tissues are affected during a disease and whether any tissue damage improves with new medicines. **Imaging technologies** is a technique that allows scientists to do precisely this—to look inside an animal's body while it is alive, without causing it any harm, to study the animal's organs and functions (Figure 1).

IMAGING TECHNOLOGIES

Creating pictures of the inside of a living body for analysis. These include techniques such as X-rays and ultrasound.

Figure 1

During imaging, the animal is anesthetized so that it does not move and does not feel distress. Imaging technologies help us to look directly inside an animal's body—at its skeleton or internal organs like the heart—without causing any harm. Once the animal has been imaged, it is monitored closely while it recovers from the anesthesia, and then it is transferred back to its housing with the other animals. Most imaging sessions take 15–30 min and animals recover well after a short anesthesia.

ANESTHESIA

The use of medicines to ensure that an animal is unconscious and free of pain during a medical procedure like imaging.

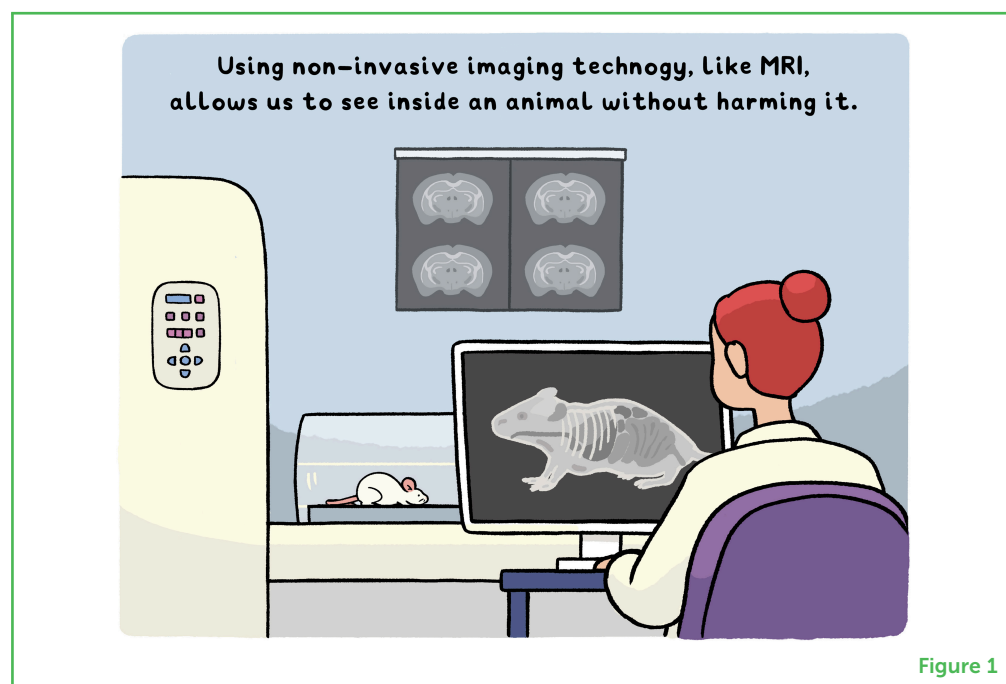


Figure 1

IMAGING TO REDUCE USE OF LABORATORY ANIMALS

Non-harmful imaging technologies, such x-rays or ultrasound, allow scientists to visualize the skeletons of live animals, to see their hearts beating, or to observe their brain function. Thus, imaging technologies help scientists to study how animals' bodies are affected by illnesses and how they respond to treatments in real time, without the need to harm or kill them [3].

Imaging is used extensively in animal research, using equipment similar to that used for humans but adapted to the smaller size of mice, rats, or fish. Unlike humans, animals will generally be put to sleep using **anesthesia**, so that they do not move around or panic when they are placed in an unfamiliar environment to be imaged. Imaging technologies allow scientists to look at the size and shape of an animal's organs, to detect tumor growth or a bone fracture, for example. Imaging also allows scientists to study how organs function, for example to study an animal's heart beating or blood moving through the blood vessels to carry oxygen around the body. Importantly, scientists can also see how an animal's cells and tissues respond to inflammation or injury by measuring how much oxygen or energy these cells or tissue use.

The ability to take a picture of the structure and function of internal organs helps scientists get more detailed information from a single animal, which improves the quality of their research studies. Imaging also helps scientists understand animal bodies, which helps them detect any signs of discomfort so they can act quickly to provide

animals with better-quality care. This helps to improve animal welfare (Figure 2).

Figure 2

Imaging helps scientists see how internal organs change as an animal grows or when it is treated with a drug. For example, if animals have a high body temperature that causes inflammation in the brain, scientists can use imaging to see whether brain inflammation could be treated by various medicines. Imaging a living animal can provide a lot of information, which helps reduce the number of animals needed for research studies.

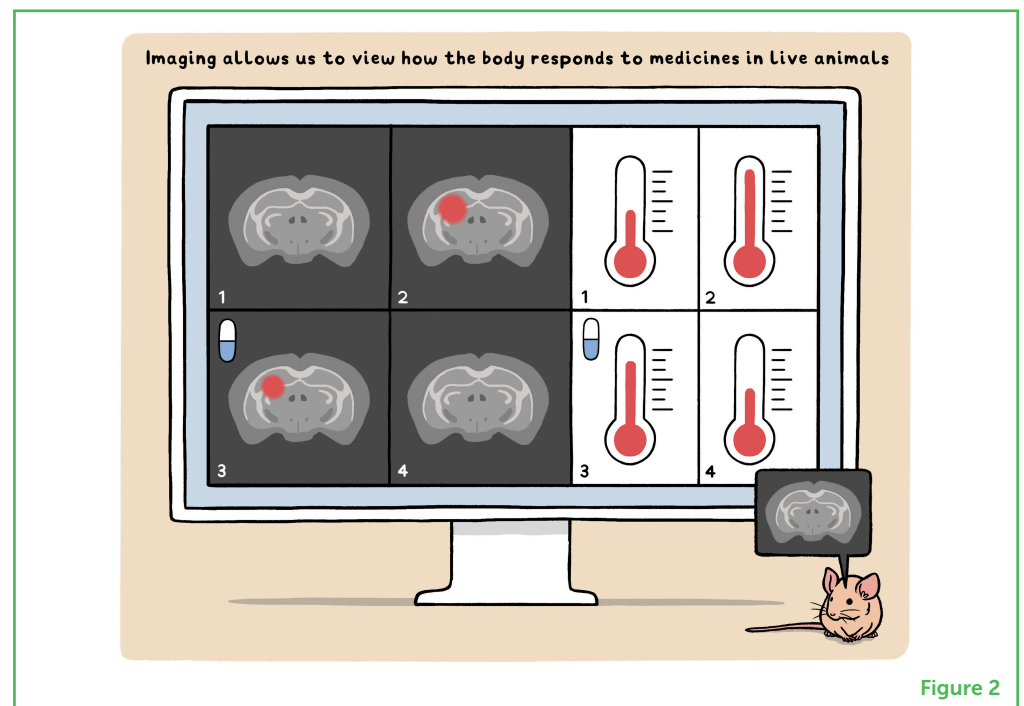


Figure 2

HOW IMAGING WORKS

There are several imaging techniques commonly used for laboratory animals (Figure 3) [3, 4].

One of the most-used methods is called computed tomography (CT) scans. CT produces 3D, x-ray-based images of solid tissues like bones, allowing scientists to study the structure of bone tissue. This method is very useful for studying bone fractures or changes in the skeleton.

Magnetic resonance imaging (MRI) maps water molecules in the tissues to create pictures of soft internal organs such as the heart, brain, liver, or digestive system. This technique is most often used to analyse the nervous system, especially the brain and spinal cord.

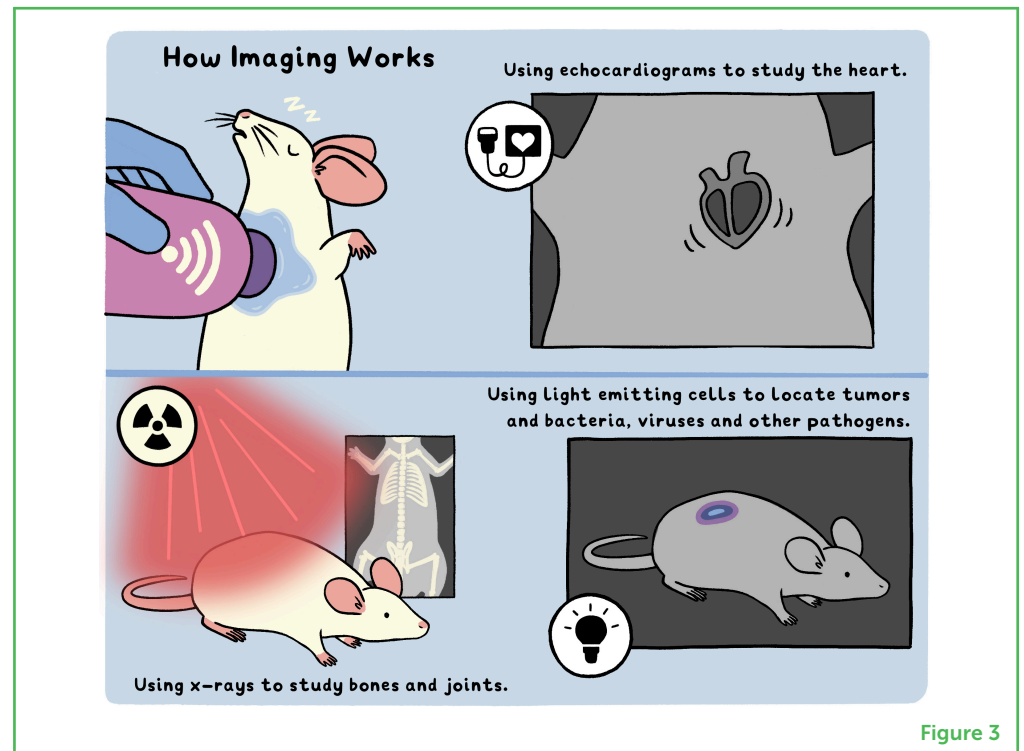
Nuclear imaging detects radiation emitted by small radioactive tracer molecules injected into the body, to analyse the functions of internal organs. Typically, tracers are molecules chemically similar to glucose, the body's main energy source. We can image whether these tracers are rapidly taken up by cancer cells and/or inflamed cells inside the animal's body. This allows scientists to map where these diseased cells are located.

Figure 3

Animals are imaged with technologies similar to those used to image humans. Non-harmful physical and chemical techniques such X-rays, the detection of light-emitting cells, or ultrasound (echocardiograms) are used to look at the skeleton, examine cell growth, or assess blood flow through the heart, for example. Viewing cell/tissue structure and function in real time is very important for studying diseases and for finding effective treatments, without harming or killing animals.

ECHOCARDIOGRAM

Imaging the heart function using ultrasound.



Optical imaging is used to detect cells inside animals' bodies that can emit light. This technique is based on the ability of organisms like fireflies to make light in their abdomens by a controlled chemical reaction. Using the same chemical reaction, animal cells can be modified to emit visible light, which helps scientists to identify their locations inside the animal's body. Detecting these glowing cells is useful for studying cell growth and energy use in cancer cells, for example.

Ultrasound uses high-frequency sound waves produced by the movement of organs, like the sound waves produced by the heart beating. These sound waves travel across the animal's body, are collected, and turned into a moving image. This imaging technique is commonly used for studying heart function.

Before an imaging study, researchers must confirm the total number of number of times that an animal will be imaged and anesthetised. Only a limited number of imaging sessions is allowed per animal (generally one to three sessions), and researchers must monitor the health and wellbeing of the animals during the entire study.

CONCLUSION

Imaging has dramatically improved animal studies, enabling scientists to monitor disease progression in real time and to study the responses of animals to medicines without causing them harm [4]. Imaging

allows scientists to get detailed information on the anatomy and functions of animals' bodies without the need to kill them to access their internal organs. This is an important step for reducing the number of animals used in research. Importantly, imaging helps scientists to better understand an animal's body functions and how they may be affected by experimental procedures. This allows scientists to detect early signs of illness or suffering that could cause further distress in the animals. Identifying such effects early helps scientists to take immediate actions to improve animal care and welfare and to prevent or minimize suffering (for example by giving painkillers or more nutritious food). Overall, imaging directly benefits animal welfare and improves scientific research through reducing the number of research animals used—a key component of the 3Rs principle.

REFERENCES

1. National Research Council (US) and Institute of Medicine (US) Committee on the Use of Laboratory Animals in Biomedical and Behavioral Research. 1988. *Use of Laboratory Animals in Biomedical and Behavioral Research. Benefits Derived from the Use of Animals*. (Washington, DC: National Academies Press). p. 3. Available online at: <https://www.ncbi.nlm.nih.gov/books/NBK218274/> (accessed September 12, 2022).
2. Russell, W., and Burch R. 1959. *The Principles of Humane Experimental Technique*. Wheathampstead: Universities Federation for Animal Welfare.
3. Tremoleda, J. L., and Sosabowski, J. 2015. Imaging technologies and basic considerations for welfare of laboratory rodents. *Lab. Anim.* 44:97–105. doi: 10.1038/labanim.665
4. Lauber, D. T., Fülöp, A., Kovács, T., Szigeti, K., Máthé, D., Sziártó, A. 2017. State of the art *in vivo* imaging techniques for laboratory animals. *Lab Anim.* 51:465–478. doi: 10.1177/0023677217695852

SUBMITTED: 26 May 2022; **ACCEPTED:** 05 September 2022;

PUBLISHED ONLINE: 11 October 2022.

EDITOR: Robert T. Knight, University of California, Berkeley, United States

SCIENCE MENTOR: Christopher R. Cederroth

CITATION: Tremoleda JL (2022) Reducing the Number of Research Animals: How Imaging Technologies Can Help. *Front. Young Minds* 10:953662. doi: 10.3389/frym.2022.953662

CONFLICT OF INTEREST: The author declares that the research was conducted in the absence of any commercial or financial relationships that could be construed as a potential conflict of interest.

COPYRIGHT © 2022 Tremoleda. This is an open-access article distributed under the terms of the Creative Commons Attribution License (CC BY). The use, distribution or reproduction in other forums is permitted, provided the original author(s) and

the copyright owner(s) are credited and that the original publication in this journal is cited, in accordance with accepted academic practice. No use, distribution or reproduction is permitted which does not comply with these terms.

YOUNG REVIEWERS

INTERNATIONAL SCHOOL OF LAUSANNE, AGES: 11–12

ISL is a non-profit, independent, International Baccalaureate (IB) World School. Since 1962, we have grown to almost 1,000 students, aged 3–18 years, who come from more than 60 nations. We believe in strong values, the courage to think independently, and cooperation across cultural boundaries-ideas that form the heart of a progressive approach to learning.



AUTHOR

JORDI L. TREMOLEDA

Jordi L. Tremoleda is a veterinarian working with laboratory animals used in research. He is responsible for the health, care, and welfare of the animals and, importantly, ensures that experiments follow all the ethical and legal requirements. Jordi is an Associate Professor at Queen Mary University in London, UK, where he teaches animal welfare and ethics. He gained experience in animal imaging at the Imperial College London; has a doctorate from Utrecht University, a Masters in Bioethics and Law from the University of Barcelona and a degree in Veterinary Medicine from the Universitat Autònoma de Barcelona. *j.lopez-tremoleda@qmul.ac.uk





REFINING RESEARCH TO IMPROVE THE LIVES OF LABORATORY MICE

Paulin Jirkof*

Office for Animal Welfare and 3Rs, University of Zurich, Zurich, Switzerland

YOUNG REVIEWERS



INTER-
NATIONAL
SCHOOL
OF
LAUSANNE

AGES: 11–12

Some scientific research includes experiments performed using animals. Many of the animals used in research are sentient, which means they have emotions or feelings that are probably similar to the positive and negative emotions that humans experience. Some experiments can cause animals to experience negative emotions like pain or fear. While animals can sometimes be replaced with other methods or used sparingly, in other situations there is no easy way to perform experiments without using animals. In these cases, scientists can protect animals by using refinement, which describes all efforts to improve the housing conditions, care, and scientific procedures that the animals experience. Refinement aims to avoid or lessen negative experiences or pain and to improve the animals' wellbeing. For example, scientists work hard to develop methods to give drugs to mice without using force, or to pick mice up more gently so the animals do not feel stress.

Thanks to the endeavors of the **Swiss 3RCC**, these articles have been translated into the three main Swiss languages of **German**, **French**, and **Italian**.

ANIMAL EXPERIMENTS AND THE 3RS PRINCIPLE

ORGANISM

A living thing made up of one or more cells, for example a human, a fish, or a mouse.

UNETHICAL

Actions or behaviors that do not follow the accepted rules of our society.

3RS PRINCIPLE

A principle formulated by two scientists in 1959, to make animal research less harmful for the animals. The 3Rs are replacement, reduction, and refinement.

¹ <https://caat.jhsph.edu/principles/the-principle-s-of-humane-experimental-technique>

REPLACEMENT

Attempting to avoid the use of animals in research by replacing them with other methods.

REDUCTION

Applying methods to minimize the number of animals used for research.

REFINEMENT

Applying methods to minimize suffering and to improve welfare in animals used for research.

Animals are used in research for many different reasons. For example, they are used to develop new medicines or to test potential medicines for safety and effectiveness before these drugs are tested on people. Animals are also used to check the safety of chemicals that we use in our daily lives, like cleaning products. Scientists also use animals to learn about diseases that affect both humans and animals. Many of the diseases scientists work on involve processes that can only be studied in living **organisms**—not in cells that scientists grow in the laboratory. For example, if scientists want to understand diseases of the brain, often only animal studies can help them do so. Several animal species are biologically similar to humans and suffer from some of the same diseases we do. It is often easier to perform experiments on animals than on humans, for two main reasons. First, scientists can control the environments that research animals live in, for example what the animals eat or how they are housed. This cannot be done with humans. Second, research on humans could expose those humans to health risks, which would be **unethical**.

Many people worry about the use of animals in research and would like to see animal research replaced with alternative methods. To protect animals as much as possible, scientists apply the **3Rs principle** to avoid or reduce animal use in research whenever possible. The 3Rs principle was formulated by two scientists, William Russel and Rex Burch, in 1959¹. Their aim was to make animal research less harmful for the animals. The first R is **replacement**, which describes all efforts to completely avoid using animals in research, for example by using computers to simulate what happens in a human or animal brain. The principle of **reduction** deals with methods to reduce the number of animals used in research. Modern research methods that maximize the knowledge that scientists can get from each animal help to reduce the total number of animals needed. The third R is **refinement**, which describes changes in how scientists house and treat laboratory animals to reduce their suffering and increase their wellbeing.

Although the first and most important R is replacement, for some experiments it is impossible to use alternative methods like computer simulations or cells grown in the lab. Despite efforts to replace animal experimentation, around 12 million animals are still used every year in Europe for scientific experiments [1]. Because of this, refinement, the third R, is important. In most countries, the wellbeing of animals is protected by animal welfare laws that forbid cruel treatment of animals, which can include any treatments that let animals suffer unnecessarily. The laws also describe how animals should be housed and cared for. For example, these laws describe how much space a lab animal should have in its stable or cage. However, the refinement principle goes beyond the conditions that are set out by animal welfare laws—it strives to reduce negative impacts on research animals as

much as possible, and to make their lives better by continuously improving their living conditions.

SENTIENT ANIMALS CAN EXPERIENCE NEGATIVE EMOTIONS

Why do we care that lab animals are treated well and that their living conditions are good? Some animals, including many of those used in science, are sentient. Being sentient means these animals have emotions that are probably similar to the positive and negative emotions that humans experience. Some experiments can cause sentient animals to experience negative emotions, like pain or fear. When sentient animals, including humans, experience very strong negative emotions, or even mild negative emotions for a long time, they may suffer.

Which animals are sentient and can therefore experience suffering? This is not an easy question to answer, and there are many differing opinions on the issue. In the future, research on animal **sentience** may change our minds, but currently all vertebrates (animals with backbones) are believed to be sentient, including mammals, birds, fish, reptiles, and amphibians. Invertebrates (animals without backbones) like insects and worms are not currently thought to experience positive and negative emotions the same way humans and vertebrates do [2]. Therefore, at this point in time, most invertebrates are not considered sentient by most scientists (Figure 1). However, there are certain invertebrates—like the lobster and the octopus—that *do* react similarly to vertebrates when they experience painful situations. So, some scientists include these animals in the group of sentient animals and ask for their strict protection. Switzerland, for example, includes octopi in its animal welfare laws.

SENTIENCE

Being sentient means to have (positive and negative) emotions.

Figure 1

Sentient animals are believed to experience positive and negative emotions similar to those experienced by humans. At this time, non-sentient animals are not currently thought to experience positive and negative emotions the same way humans and vertebrates do.

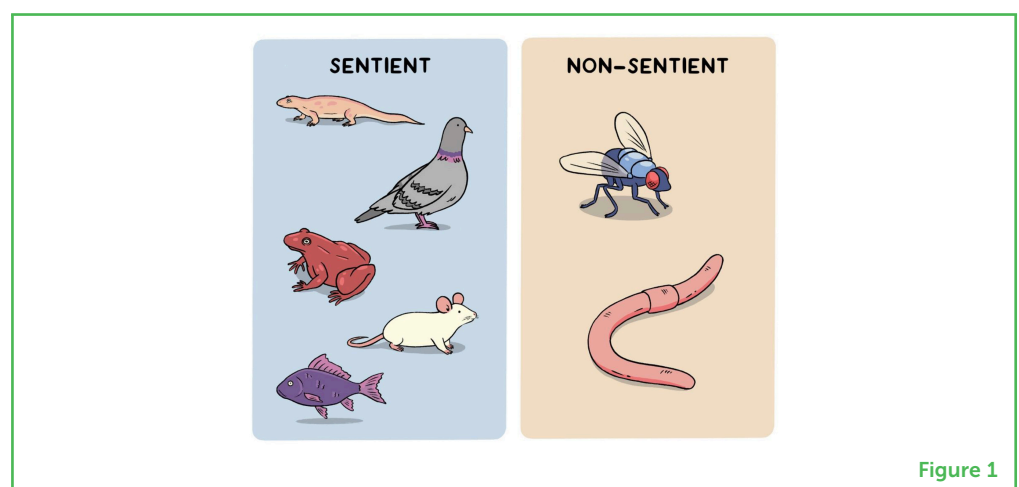


Figure 1

GENETIC MODIFICATION

Changing the characteristics of an organism by changing its DNA. DNA is the material that carries all the information about how an organism looks and functions.

FREQUENCIES

Here, audio frequency. Frequency is how many sound waves are produced by the animal per second.

IMPROVING THE LIVES OF LABORATORY MICE

To describe how refinement efforts can improve animal welfare, we will concentrate on mice because mice are the most widely used research animals around the globe. Depending on the country, mice make up 50–75% of all animals used in research, mainly because mice reproduce or breed quickly and can be easily housed in the laboratory. Mice are tiny mammals that have many things in common with humans, including much of their genetic information and many bodily processes. The genetic information of the mouse is also easy for scientists to change, which makes mice good for many experiments. Research using **genetically modified** mice allows scientists to imitate and study human diseases in mice, as well as to find new medicines to treat these diseases.

The welfare of mice is important because they are sentient animals that interact with each other socially. For example, did you know that male mice sing love songs for female mice, in **frequencies** that are beyond the level of human hearing [3]? Or that mice can tell if another mouse is feeling unwell and change their behavior accordingly—for example, by reacting more strongly to negative experiences like pain [4]? In humans we call this empathy—the ability to understand or feel what others are feeling.

Mice need certain conditions to live healthy, happy lives. Good conditions for mice include having material to build cozy nests to keep themselves warm, living in groups with other mice, and being cared for by humans who understand their needs. There are also many ways that experiments can be improved to reduce the negative emotions mice experience, like pain or fear. Examples include helping mice to get used to being around humans before the experiments start or giving mice pain killers when painful experiments are performed.

A SPOONFUL OF SUGAR HELPS THE MEDICINE GO DOWN

When mice are used in experiments in which they must take medicines—to prove that a new drug helps to treat a disease, for example—these medicines must sometimes be swallowed by the mice. Mice do not swallow all medicines willingly, especially if the drugs taste bitter. To get around this, scientists sometimes give the medicines through a tube inserted into the mouse's mouth directly into its stomach. This is unpleasant for the mouse, so even though the procedure is allowed by law when it is scientifically necessary, scientists try to use the refinement principle to make giving drugs more pleasant for mice. For example, scientists from the University of Zurich, Switzerland [5], use this easy solution: mice like fatty, sweet food, so they mix the drug with a tasty substance like sweetened condensed

milk. Mice will happily lick up all the medicated condensed milk from a measuring device called a pipette (Figure 2).

Figure 2

Feeding a drug mixed with sweetened condensed milk to a mouse. Mice like to eat sweet and fatty substances, so they will easily lick up drugs that are mixed with foods like Nutella, peanut butter, or raspberry jam.

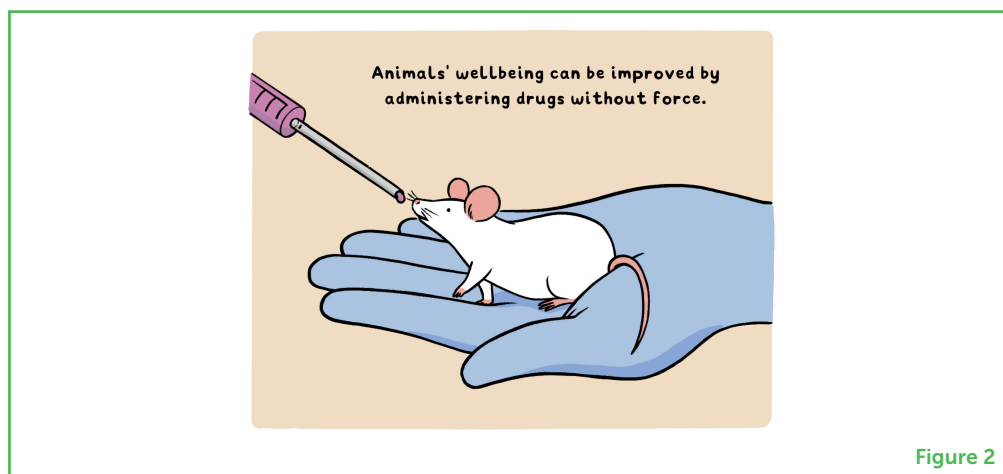


Figure 2

Other good ways of getting mice to swallow drugs without using any kind of force include mixing the medicine with Nutella, peanut butter, or raspberry jam. These methods avoid unpleasant experiences for the mice and also make scientists' lives easier because the mice will willingly eat these substances—so the scientists know that their mice have swallowed the full dose of the drug they are investigating.

A PLEASANT RIDE: USING PLASTIC TUNNELS TO GENTLY PICK UP MICE

For many years, scientists picked up lab mice by their tails to move them from place to place (Figure 3A). It was easy for scientists to catch the mice this way without being bitten, but some scientists thought it might be unpleasant for mice and did research on better ways to pick them up. In the wild, mice live in burrows with tunnels. A researcher in Liverpool, England named Jane Hurst therefore checked whether mice prefer to be transported in a tunnel—and they do! Mice transported in tunnels are tamer and more relaxed than those picked up by their tails [6]. This is good for the wellbeing of the mice, and it makes the mice easier for scientists to work with. More and more scientists are training their mice to enter little plastic tunnels², which the scientists use to transport the mice (Figure 3B).

² <https://www.nc3rs.org.uk/3rs-resources/mouse-handling>

OUTLOOK

In most countries, these and many other refinement techniques are not yet required by law, meaning scientists do not *have to* use them—but even though they are not required, these techniques are still being increasingly used these days. Use of refinement techniques is important because it helps to reduce animal suffering and improves animal welfare whenever we cannot fully replace animals in research.

Figure 3

(A) In the past, most scientists caught mice by the tail to transport them. (B) Using plastic tunnels to transport mice keeps the mice more relaxed, which is both good for the mice and helpful for the scientists who work with them.

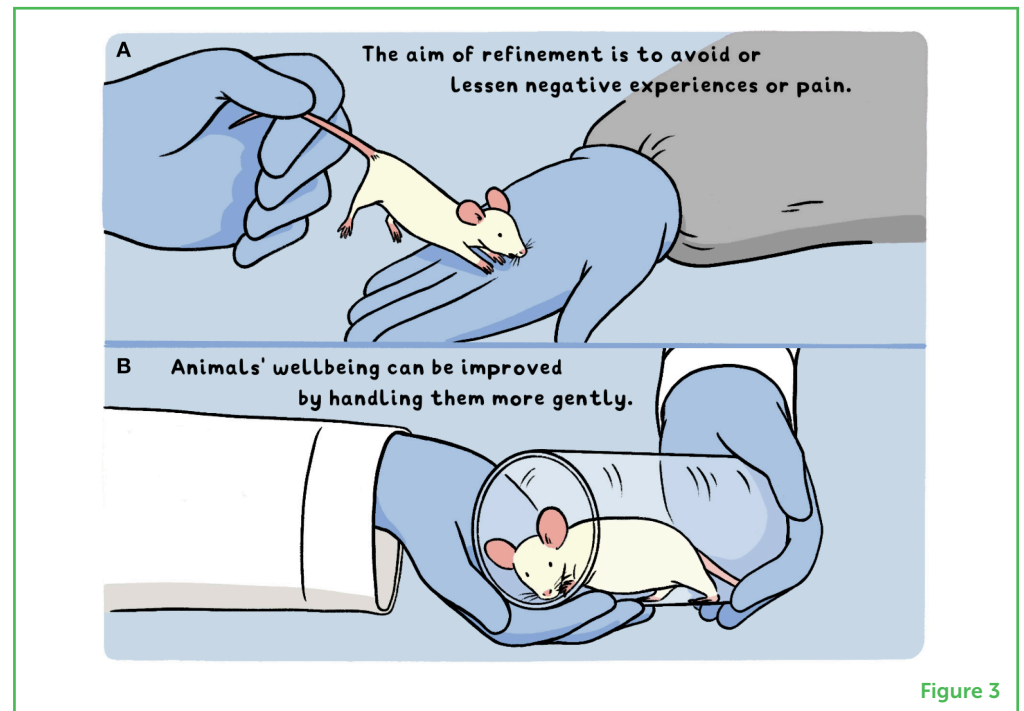


Figure 3

All around the globe, scientists are trying to convince their colleagues to implement more refinement into their animal experiments. How do you think we could increase the happiness and reduce the suffering of lab animals, and how could we best convince others to follow these practices?

REFERENCES

1. European Commission. 2021. *Summary Report on the statistics on the use of animals for scientific purposes in the Member States of the European Union and Norway in 2018*.
2. Sneddon, L. U., Elwood, R. W., Adamo, S. A., and Leach, M. C. 2014. Defining and assessing animal pain. *Anim. Behav.* 97:201–12. doi: 10.1016/j.anbehav.2014.09.007
3. Hammerschmidt, K., Radyushkin, K., Ehrenreich, H., and Fischer, J. 2009. Female mice respond to male ultrasonic 'songs' with approach behaviour. *Biology letters*, 5:589–92. doi: 10.1098/rsbl.2009.0317
4. Langford, D. J., Crago, S. E., Shehzad, Z., Smith, S. B., Sotocinal, S. G., Levenstadt, J. S., et al. 2006. Social modulation of pain as evidence for empathy in mice. *Science* 312:1967–70. doi: 10.1126/science.1128322
5. Scarborough, J., Mueller, F., Arban, R., Dorner-Ciossek, C., Weber-Stadlbauer, U., Rosenbrock, H., et al. 2020. Preclinical validation of the micropipette-guided drug administration (MDA) method in the maternal immune activation model of neurodevelopmental disorders. *Brain Behav. Immunity* 88:461–70. doi: 10.1016/j.bbi.2020.04.015
6. Hurst, J. L., and West, R. S. 2010. Taming anxiety in laboratory mice. *Nat. Methods* 7:825–6. doi: 10.1038/nmeth.1500

SUBMITTED: 27 May 2022; **ACCEPTED:** 05 September 2022;
PUBLISHED ONLINE: 11 October 2022.

EDITOR: Robert T. Knight, University of California, Berkeley, United States

SCIENCE MENTOR: Christopher R. Cederroth

CITATION: Jirkof P (2022) Refining Research to Improve the Lives of Laboratory Mice. *Front. Young Minds* 10:954413. doi: 10.3389/frym.2022.954413

CONFLICT OF INTEREST: The author declares that the research was conducted in the absence of any commercial or financial relationships that could be construed as a potential conflict of interest.

COPYRIGHT © 2022 Jirkof. This is an open-access article distributed under the terms of the Creative Commons Attribution License (CC BY). The use, distribution or reproduction in other forums is permitted, provided the original author(s) and the copyright owner(s) are credited and that the original publication in this journal is cited, in accordance with accepted academic practice. No use, distribution or reproduction is permitted which does not comply with these terms.

YOUNG REVIEWERS

INTERNATIONAL SCHOOL OF LAUSANNE, AGES: 11–12

ISL is a non-profit, independent, International Baccalaureate (IB) World School. Since 1962, we have grown to almost 1,000 students, aged 3–18 years, who come from more than 60 nations. We believe in strong values, the courage to think independently, and cooperation across cultural boundaries—ideas that form the heart of a progressive approach to learning.

AUTHOR

PAULIN JIRKOF

Paulin Jirkof is a biologist, trained in neuroscience and behavior. She works as a 3Rs coordinator at the University of Zurich, Switzerland. In this position she helps scientists, teachers and animal care staff to use the 3Rs principle in their daily work (replacement, reduction and refinement of animal experimentation). She is fascinated by animal behavior and especially interested in the behavior of small laboratory species like mice and rats. With her research she tries to reduce suffering in animal experiments and to improve the lives of laboratory animals.
*paulin.jirkof@uzh.ch





OPEN ACCESS

EDITED BY

Jun-ichi Hikima,
University of Miyazaki, Japan

REVIEWED BY

Diana Boraschi,
Shenzhen Institute of Advanced
Technology (SIAT) (CAS), China
Sylvia Dominika Tyrkalska,
University of Murcia, Spain

*CORRESPONDENCE

Michael R. Taylor
michael.taylor@wisc.edu

SPECIALTY SECTION

This article was submitted to
Comparative Immunology,
a section of the journal
Frontiers in Immunology

RECEIVED 07 September 2022

ACCEPTED 14 October 2022

PUBLISHED 26 October 2022

CITATION

Sebo DJ, Fetsko AR, Phipps KK and
Taylor MR (2022) Functional
identification of the zebrafish
Interleukin-1 receptor in an embryonic
model of IL-1 β -induced
systemic inflammation.
Front. Immunol. 13:1039161.
doi: 10.3389/fimmu.2022.1039161

COPYRIGHT

© 2022 Sebo, Fetsko, Phipps and Taylor.
This is an open-access article
distributed under the terms of the
Creative Commons Attribution License
(CC BY). The use, distribution or
reproduction in other forums is
permitted, provided the original
author(s) and the copyright owner(s)
are credited and that the original
publication in this journal is cited, in
accordance with accepted academic
practice. No use, distribution or
reproduction is permitted which does
not comply with these terms.

Functional identification of the zebrafish Interleukin-1 receptor in an embryonic model of IL-1 β -induced systemic inflammation

Dylan J. Sebo¹, Audrey R. Fetsko¹, Kallie K. Phipps^{1,2}
and Michael R. Taylor^{1,2*}

¹Division of Pharmaceutical Sciences, School of Pharmacy, University of Wisconsin–Madison, Madison, WI, United States, ²Pharmacology and Toxicology Program, School of Pharmacy, University of Wisconsin–Madison, Madison, WI, United States

Interleukin-1 β (IL-1 β) is a potent proinflammatory cytokine that plays a vital role in the innate immune system. To observe the innate immune response *in vivo*, several transgenic zebrafish lines have been developed to model IL-1 β -induced inflammation and to visualize immune cell migration and proliferation in real time. However, our understanding of the IL-1 β response in zebrafish is limited due to an incomplete genome annotation and a lack of functional data for the cytokine receptors involved in the inflammatory process. Here, we use a combination of database mining, genetic analyses, and functional assays to identify zebrafish Interleukin-1 receptor, type 1 (IL1r1). We identified putative zebrafish *il1r1* candidate genes that encode proteins with predicted structures similar to human IL1R1. To examine functionality of these candidates, we designed highly effective morpholinos to disrupt gene expression in a zebrafish model of embryonic IL-1 β -induced systemic inflammation. In this double transgenic model, *ubb:Gal4-EcR*, *uas:il1 β ^{mat}*, the zebrafish ubiquitin *b* (*ubb*) promoter drives expression of the modified Gal4 transcription factor fused to the ecdysone receptor (EcR), which in turn drives the tightly-regulated expression and secretion of mature IL-1 β only in the presence of the ecdysone analog tebufenozide (Teb). Application of Teb to *ubb:Gal4-EcR*, *uas:il1 β ^{mat}* embryos causes premature death, fin degradation, substantial neutrophil expansion, and generation of reactive oxygen species (ROS). To rescue these deleterious phenotypes, we injected *ubb:Gal4-EcR*, *uas:il1 β ^{mat}* embryos with putative *il1r1* morpholinos and found that knockdown of only one candidate gene prevented the adverse effects caused by IL-1 β . Mosaic knockout of *il1r1* using the CRISPR/Cas9 system phenocopied these results. Taken together, our study identifies the functional zebrafish IL1r1 utilizing a genetic model of IL-1 β -induced inflammation and provides valuable new insights to study inflammatory conditions specifically driven by IL-1 β or related to IL1r1 function in zebrafish.

KEYWORDS

zebrafish, interleukin - 1 β , interleukin 1 receptor type 1, inflammation, neutrophils, ROS - reactive oxygen species, UAS/Gal4

Introduction

Zebrafish (*Danio rerio*) have emerged as a valuable vertebrate model to study inflammation due to several important features including rapid development of the innate immune system, optical transparency for *in vivo* imaging, and the accessibility of genetic tools and experimental methods (1–3). The relative ease of transgenesis in zebrafish (4) has given rise to several genetic models of inflammation driven by the expression of the potent proinflammatory cytokine Interleukin-1 β (IL-1 β). These models include heat-shock-inducible IL-1 β (5), cell-specific expression of IL-1 β (6), and a doxycycline-inducible model (7). A variety of non-genetic zebrafish inflammation models have also been characterized, including infection models using bacteria (8–10), viruses (11), fungi (12, 13), and lipopolysaccharide (LPS) (14) as well as several wound-induced models (15–20). Similar to the genetic models, wound-induced models stimulate IL-1 β expression and promote IL-1 β dependent migration of neutrophils to the site of injury (5, 21). Additionally, morpholino knockdown of zebrafish IL-1 β decreases the recruitment of neutrophils demonstrating that IL-1 β plays a specific role in regulating neutrophil migration during injury-induced inflammation (5). More recently, we generated a genetically inducible model of systemic inflammation using the Gal4-EcR/UAS system (22). In this model, the mature form of IL-1 β is secreted in response to the ecdysone analog tebufenozide resulting in dose-dependent neutrophil expansion, reactive oxygen species (ROS) generation, morbidity, and mortality (23).

During an innate immune response to foreign antigens, IL-1 β is produced as an inactive precursor that is processed by caspase-1 and the inflammasome to produce mature IL-1 β for secretion (24). Once secreted, IL-1 β (as well as IL-1 α) binds specifically to the Interleukin-1 receptor, type 1 (IL1R1) causing a conformational change that allows for binding of the co-receptor Interleukin-1 receptor accessory protein (IL1RAP; also known as IL1R3) that forms a trimeric complex that promotes a strong proinflammatory signal (25). To demonstrate functionality, previous studies showed that targeted disruption of the murine genes encoding either IL1R1 (26, 27) or IL1RAP (28) block IL-1 signaling, indicating that IL1R1 and IL1RAP are both required to elicit an immune response. While IL1R1 and IL1RAP share some structural similarities, both receptors possess unique primary sequences and distinct genomic locations in both human and mouse. As IL1R1 binds specifically to IL-1 β and serves as a primary therapeutic target for treating inflammation in a broad spectrum of diseases, our current study focuses on the identification of the zebrafish Interleukin-1 receptor, type 1 (Il1r1).

Given the prominent role of IL-1 β in the inflammatory response, it is particularly surprising that the zebrafish Il1r1

has not been identified. Indeed, the discovery and validation of functional orthologs in zebrafish can be challenging for a variety of reasons. While comparison of the human and zebrafish reference genomes reveals that approximately 70% of human genes have at least one obvious zebrafish ortholog, the sequence divergence of many genes is so great that they cannot be recognized or confirmed as orthologs without experimental validation (29). Furthermore, members of the Teleostei infraclass, including zebrafish, underwent a teleost-specific whole-genome duplication event (30). This further complicates the identification of human - zebrafish orthologs due to the possibility of 1) functionally redundant paralogs, 2) mutually exclusive, overlapping, or redundant expression patterns of the paralogs, or 3) the presence of pseudogenes.

In this study, we perform an *in silico* analysis and identify putative zebrafish Il1r1 orthologs with low sequence identities but with predicted protein structures highly similar to human IL1R1. To determine if these proteins function as the receptor for IL-1 β , we utilize our validated *in vivo* zebrafish model of IL-1 β -induced systemic inflammation (23). Here, we knockdown the expression of putative receptors and examine the phenotypic rescue of inflammation by performing multiple functional assays. Using this experimental approach, we identify the functional ortholog for zebrafish Il1r1 and demonstrate that it is absolutely required for the IL-1 β -driven inflammatory response and the associated disease phenotypes. Given the increasing interest in zebrafish models of inflammation, our findings provide valuable new tools to dissect signaling pathways, cellular responses, and disease models that are specifically driven by or related to Il1r1 function.

Materials and methods

Zebrafish husbandry

Zebrafish lines were maintained using guidelines established in The Zebrafish Book (31). The AB wild-type (WT) strain was acquired from the Zebrafish International Resource Center. Transgenic lines *Tg(ubb:IVS2GVEcR, cmcl2:EGFP)*, herein abbreviated as *ubb:Gal4-EcR*, and *Tg(uas:GSP-Il1 β^{mat} , cmcl2:mCherry)*, herein abbreviated as *uas:Il1 β^{mat}* were previously generated in our lab (23). The *Tg(mpx:mCherry)^{uwm7}* transgenic line, herein abbreviated as *mpx:mCherry*, was a gift from Dr. Anna Huttenlocher (UW-Madison). Embryos were maintained at 28.5°C in egg water (0.03% Instant Ocean reconstituted in reverse osmosis water). For imaging, 0.003% phenylthiourea (PTU) was used to inhibit melanin production. All experiments were performed in accordance with the University of Wisconsin-Madison Institutional Animal Care and Use Committee.

Database mining for putative zebrafish interleukin-1 receptors

To identify putative zebrafish Interleukin-1 receptor(s), type 1 (IL1R1), we performed database searches for zebrafish homologs. The human IL1R1 protein sequence (accession number P14778) was used to search the zebrafish genome at Ensembl (assembly GRCz11) using the TBLASTN search tool. Sequence identities and phylogenetic analysis of protein sequences was performed using the Clustal V Method in MegAlign (DNASTAR). Predicted protein structures for human IL1R1 (<https://alphafold.ebi.ac.uk/entry/P14778>), zebrafish CABZ01054965 (<https://alphafold.ebi.ac.uk/entry/E7FGC6>), and zebrafish ZMP:0000000936 (<https://alphafold.ebi.ac.uk/entry/E7F5V6>) were identified using AlphaFold (32, 33).

Morpholino antisense oligonucleotide design and microinjection

Morpholino antisense oligonucleotides (MO) were designed against zebrafish *cabz01054965* and *zmp:0000000936* using the manufacturers recommendations (GeneTools). The *cabz01054965* splice donor morpholino sequence 5'-TGTGCATCAGGGTTTACCTTTCGC-3' was designed against the splice donor site (underlined) located between exon 4 and intron 5. The *zmp:0000000936* splice donor morpholino sequence 5'-GTGATATGAAAGGCTCACCTGCAC-3' was designed against the splice donor site (underlined) located between exon 5 and intron 6. The *zmp:0000000936* start site morpholino sequence 5'-ACCAATCGACCCATATCTACAGCCG-3' was designed to span across the translation start site (underlined). For control morpholino injections, the standard GeneTools control oligo was used 5'-CCTCTTACCTCAGTTACAATTTATA-3'. Uninjected embryos were used as controls for some experiments as indicated.

Morpholinos were resuspended in dH₂O at a stock concentration of 2 mM. For microinjection, morpholinos were diluted to 0.1–0.5 mM in dH₂O containing phenol red (0.05%) as an injection tracer. Microinjection needles were fabricated from 1.2 mm thin wall glass capillaries (WPI; TW120F-4) using a Sutter Instrument Flaming/Brown Micropipette Puller (Model P-97). Approximately 2 nl were microinjected into the yolk of single-celled embryos from pairwise crosses of the relevant genotypes. Damaged embryos identified with gross morphological defects as a result of microinjection were removed from the study prior to analyses. All morpholinos were found to be effective at a concentration of 0.25 mM (~2 ng) without any obvious off-target effects.

Generation of IL-1 β -induced embryonic systemic inflammation

The transgenic lines *ubb:Gal4-EcR* and *uas:Il1 β ^{mat}* were used to generate IL-1 β -induced embryonic systemic inflammation in the presence of the ecdysone analog, tebufenozide (Teb), as previously described (23). Teb was prepared as a 1 mM stock solution in 100% DMSO. Adults carrying the transgenes were bred, embryos were injected with morpholino at the one-cell stage or left uninjected, and then treated at 1 or 2 days postfertilization (dpf) with 1 μ M Teb or 0.1% DMSO (untreated controls). Embryos were selected for both transgenesis markers *cmlc2:EGFP* (green heart) and *cmlc2:mCherry* (red heart) using a Nikon SMZ18 epifluorescence stereomicroscope prior to further analyses. For neutrophil experiments, the *ubb:Gal4-EcR* and *uas:Il1 β ^{mat}* lines were bred to *mpx:mCherry*. All experimental embryos were heterozygous for all transgenes.

Mosaic rescue of IL-1 β -induced embryonic systemic inflammation with CRISPR/Cas9

To phenocopy the *zmp* splice-donor and start-site morpholino rescue of IL-1 β -induced embryonic systemic inflammation, we used a CRISPR/Cas9 strategy utilizing the crRNA:tracrRNA duplex format with recombinant *S. Pyogenes* Cas9 nuclease (Cas9) from Integrated DNA Technologies (IDT). Using the Alt-R Custom Cas9 crRNA Design Tool (IDT), we designed two CRISPR RNAs (crRNAs): cr1.*zmp:0000000936.ex8* 5'-/AltR1/ucgacugcuggacaccagacguuuuagagcuaugcu/AltR2/-3' and cr2.*zmp:0000000936.ex9* 5'-/AltR1/uuaagguggagcuggucuuaguuuuagagcuaugcu/AltR2/-3' against exon 8 and exon 9, respectively. For CRISPR-Cas9 ribonucleoprotein (RNP) preparation and microinjection, we followed the IDT demonstrated protocol "Zebrafish embryo microinjection" modified from Dr. Jeffrey Essner (Iowa State University). The crRNAs and transactivating crRNA (tracrRNA) were resuspended to 100 μ M in nuclease-free TE buffer, pH 8.0, the individual crRNAs were combined with tracrRNA at 1:1 molar ratio in nuclease-free Duplex Buffer (IDT) to create 3 μ M gRNA complexes (cr1 and cr2). The solutions were heated to 95°C for 5 min, then cooled to room temperature. Recombinant Cas9, glycerol-free (IDT) was diluted to 0.5 μ g/ μ l in PBS, pH 7.4. The RNP complex was assembled by combining 3 μ l of gRNA complexes with 3 μ l of diluted Cas9, incubated at 37°C for 10 min, then cooled to room temperature. Approximately 2 nl of the RNP complexes with either cr1, cr2, or combined cr1/cr2 (1:1) was microinjected into *ubb:Gal4-EcR*, *uas:Il1 β ^{mat}* single-cell embryos and monitored for morbidity and mortality. PCR was performed on individual embryos using *zmp:0000000936*-

specific primers: forward primer 5'-tatgtgtcctcttcagCG-3' and reverse primer 5'-tggtatcacgacacCTGTGG-3' located in intron 7 and intron 9, respectively. Percentages of survival (alive), morbidity (sick), and mortality (dead) were plotted for each group using Excel (Microsoft). To test for differences between groups, a chi-square test of independence was performed, followed by a *post hoc* test using adjusted residuals and a *p*-value Bonferroni adjustment.

RNA extraction, cDNA synthesis, and RT-PCR

Embryos from 0–3 dpf (20–30 per group in duplicate) were anesthetized in 0.02% Tricaine, transferred into RNase/DNase-free 1.5 ml microcentrifuge tubes with fitted pestle (Kontes), homogenized in TRIzol, and total RNA was extracted according to the manufacturer's protocol (Invitrogen). cDNA was synthesized by reverse transcription using the SuperScript IV First-Strand Synthesis System using Oligo(dT) primers according to the manufacturer's protocol (Invitrogen). Reverse transcription polymerase chain reaction (RT-PCR) amplified a 578 bp fragment of *cabz01054965* using forward primer 5'-ACGCACCTGACACATCGTAA-3' and reverse primer 5'-GTTTGACTTGGCTTCGGGTA-3', a 577 bp fragment of *zmp:0000000936* using forward primer 5'-GCGAGATGACC TCAGAAACC-3' and reverse primer 5'-TCCTCCGACACA TGAGACAC-3', and a 932 bp fragment of *actin, beta 1 (actb1)* as an RT-PCR control using forward primer 5'-CCCTCCATTGTTGGACGAC-3' and reverse primer 5'-CCG ATCCAGACGGAGTATTTG -3'. All primers were designed using Primer3 (34).

Whole-mount *in situ* hybridization

WISH was performed using protocols adapted from Vauti et al. and Thisse and Thisse (35, 36). This new protocol afforded greater probe penetration into the central nervous system (CNS) and trunk of 1–3 dpf animals used for this study. Briefly, WT embryos from 1–3 dpf were fixed in 4% paraformaldehyde/PBS at 4°C overnight, dehydrated in 100% methanol, then stored at –20°C. For probe synthesis, *cabz01054965* (forward primer 5'-AATTAACCCTCACTAAAGGGGCGAGATGACCTC AGAAACC-3'; reverse primer 5'-TAATACGACTCACTAT AGGGACCTCCTCCTCTTCCAG-3') and *zmp:0000000936* (forward primer 5'-AATTAACCCTCACTAAAGGGGCG AGATGACCTCAGAAACC-3'; reverse primer 5'-TAAT ACGACTCACTATAGGGACCTCCTCCTCTTCCAG-3') were PCR amplified from WT zebrafish cDNA to produce products of 1,227 and 1,293 bp, respectively. Both forward primers contained a 5'-T3 RNA polymerase binding site (*italics*) and both reverse primers contained a 5'-T7 RNA polymerase

binding site (*italics*). PCR products were then purified using the QIAquick PCR purification kit (Qiagen). Approximately 1 µg of purified PCR product was used to synthesize sense and antisense digoxigenin (DIG)-labeled RNA probes with T3 and T7 RNA polymerase, respectively, using a DIG RNA Labeling Kit (Roche). Prepared embryos (n=8 per group) were transitioned to ethanol, treated with ethanol/xylol (1:1 vol/vol), rehydrated in H₂O with 0.1% Tween, permeabilized in 80% Acetone, and bleached in H₂O₂, according to Vauti et al., 2020 (36). Embryos were prehybridized at 70°C for 2 hr, then hybridized with DIG-labeled RNA probes at 70°C overnight. After washing and blocking, the embryos were incubated with anti-DIG-AP Fab fragment (Roche) at 4°C overnight then stained with BM Purple, AP precipitating substrate (Roche), containing NBT and BCIP, until the desired signal intensity appeared (35). Images were captured using a Nikon SMZ18 stereomicroscope equipped with a Nikon DS-Fi2 color camera and Nikon NIS-Elements software.

Survival analysis

To examine IL-1β-induced mortality, double transgenic *ubb:Gal4-EcR, uas:Il1β^{mat}* embryos were induced with 1 µM Teb at 1 dpf and survival was monitored until 6 dpf. All survival assays were performed in 100x15 mm petri dishes (Falcon). In our previous survival studies, Teb (concentration range: 10 nM–10 µM) was added at 2 dpf, which caused mortality beginning at 5 dpf (23). Therefore, in the current study, we added Teb at 1 dpf to expedite mortality as morpholino effectiveness may be reduced past 3 dpf (37). Survival was tallied daily as dead embryos were identified and removed from the petri dishes. Teb was replaced daily with freshly prepared solution. Kaplan-Meier curves were made using Excel (Microsoft) and log rank tests were used to evaluate statistical significance.

Gross morphology

Transgenic *ubb:Gal4-EcR* and *uas:Il1β^{mat}* embryos (10–20 per group) were induced with 1 µM Teb at 2 dpf and maintained in fresh Teb until 4 dpf. Three embryos per group (except for *cabz* +Teb; n=2), were randomly selected and imaged. Lateral images were acquired by confocal microscopy using the TD channel at 4 dpf. Regions of interest were quantified using FIJI ROI selection and measurement tools. Mean cross sectional area + standard deviation was plotted using Excel (Microsoft).

Neutrophil quantification

The neutrophil reporter line *mpx:mCherry* was bred to *ubb:Gal4-EcR, uas:Il1β^{mat}* double transgenics to produce triple heterozygous transgenic embryos. Systemic inflammation was

induced at 2 dpf with 1 μ M Teb (10–20 per group). Three embryos per group (except for *cabz* +Teb; *n*=2), were randomly selected and neutrophils were imaged by confocal microscopy at 4 dpf. Neutrophils were quantified by manually counting the number of mCherry-positive cells throughout the entire volume rendered image using FIJI Cell Counter Plugin (38). Mean + standard deviation was plotted using Excel (Microsoft).

Reactive oxygen species analysis

Transgenic *ubb:Gal4-EcR, uas:Il1 β ^{mat}* embryos (10–20 per group) were induced with 1 μ M Teb at 2 dpf and maintained in Teb until 3 dpf. CM-H₂DCFDA (Invitrogen), a fluorescent cell-permeant indicator for ROS, was freshly prepared as a 10 mM stock in DMSO. Embryos were incubated with 2.5 μ M CM-H₂DCFDA (Invitrogen) for 30 min in the dark, then washed in egg water (3 x 10 minutes each wash) prior to imaging. Three embryos per group (except for *cabz* +Teb; *n*=2), were randomly selected and imaged by confocal microscopy at 3 dpf. Quantification of fluorescent signal was completed on 2D projections of 3D confocal z-stacks, created using the Nikon NIS-Elements Maximum Intensity Projection algorithm. Regions of interest were identified using FIJI ROI selection tools, then the fluorescence was quantified using the FIJI ‘mean grey value’ measurement tool. Values were normalized to uninjected no Teb controls and normalized mean + standard deviation was plotted using Excel (Microsoft).

Confocal laser scanning microscopy

Zebrafish from 1 to 4 dpf were anesthetized in 0.02% Tricaine and immobilized in 1.2% low melting point agarose (Invitrogen) in glass bottom culture dishes (MatTek). Confocal microscopy was performed using a Nikon Eclipse Ti microscope equipped with a Nikon A1R. For images of whole embryos and larvae, large images (4 x 1 mm) were captured and stitched together with a 15% overlap. All images are 2D projections of 3D confocal z-stacks using the Nikon NIS-Elements Maximum Intensity Projection algorithm or are single frame lateral TD images. All image manipulation for brightness or contrast (*via* Nikon NIS-Elements software) was applied to all pixels, equally, and does not affect interpretation of data.

Statistical analysis

Statistical differences of mean values among multiple groups were determined using one-way analysis of variance (ANOVA) followed by Tukey’s HSD *post-hoc* test. The criterion for statistical significance was set at *P* < 0.05. Values

represent means \pm standard deviation. Error bars show +1 standard deviation.

Results

Identification of the putative zebrafish interleukin-1 receptor, type 1

Using the human IL1R1 protein sequence (accession number: P14778), we performed a TBLASTN against the zebrafish genome at Ensembl. We identified three genes, *cabz01054965*, (accession number: ENSDARG00000090844), *zmp:0000000936* (accession number: ENSDARG00000088672), and *cu855885*, (accession number: ENSDARG00000101527) on zebrafish chromosome (chr.) 9 with sequence similarities to human IL1R1. In addition, these three genes showed partial synteny to the IL-1 Receptor Cluster on human chr. 2q (39) and mouse chr. 1 (Figure 1A). The *cu855885* gene has previously been identified as the zebrafish ortholog for human Interleukin-1 receptor-like 1 (*IL1RL1*) (40), herein referred to as zebrafish *il1rl1*. Protein sequence alignment using the Clustal V Method in MegAlign (DNASTAR) indicated percent identities to the human IL1R1 protein sequence of 19.6%, 21.4%, and 19.1% for the proteins encoded by the zebrafish genes *cabz01054965*, *zmp:0000000936*, and *il1rl1*, respectively.

Phylogenetic analysis of human IL1R1 (P14778), human IL1RL1 (Q01638), human IL1RL2 (Q9HB29), zebrafish CABZ01054965, zebrafish ZMP:0000000936, and zebrafish *Il1rl1* was also performed using the Clustal V Method in MegAlign (Figure 1B). As predicted, zebrafish *Il1rl1* was found to be most similar to human IL1RL1, confirming the previously established annotation (40). However, our analysis was unable to definitively distinguish whether CABZ01054965 or ZMP:0000000936 were functional zebrafish orthologs or paralogs for either human IL1R1 or IL1RL2.

We next examined the structural similarities between human IL1R1, zebrafish CABZ01054965 (abbreviated herein as CABZ), and ZMP:0000000936 (abbreviated herein as ZMP) using the AlphaFold Protein Structure Database (32, 33). As shown in Figure 1C, human IL1R1 consists of an N-terminal signal peptide (SP), 3 extracellular immunoglobulin-like (Ig-I) domains, a single transmembrane domain (TM), and an intracellular Toll/Interleukin-1 receptor (TIR) domain (41–43). Despite the low sequence similarities between the human and zebrafish proteins, AlphaFold predicted conserved protein structures and domains for human IL1R1, zebrafish CABZ, and zebrafish ZMP (Figure 1C). However, these structures did not distinguish functionality between the two zebrafish proteins.

We also examined the zebrafish genome for *IL1RAP* and the three additional *IL1R* genes found within the human and mouse IL-1 receptor clusters (i.e. *IL1R2*, *IL18R1*, and *IL18RAP*). As IL-1 signaling requires the association of IL1RAP with the IL-1 β /

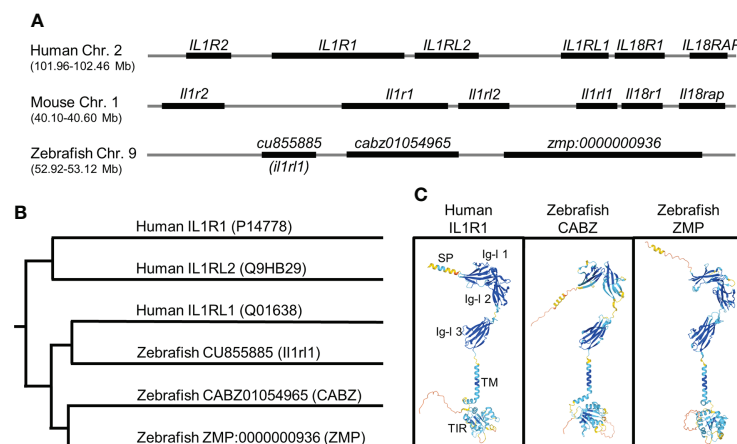


FIGURE 1

In silico identification of the putative zebrafish interleukin-1 receptor, type 1 (*IL1R1*). **(A)** Alignment of human, mouse, and zebrafish genomic regions showing conserved synteny. Shown here are the human and mouse *IL-1* receptor clusters and the putative zebrafish *IL-1* receptor cluster (not to scale). **(B)** Phylogenetic alignment of human *IL1R* protein sequences with putative zebrafish *IL1r* protein sequences. **(C)** Predicted protein structures of human *IL1R1*, zebrafish CABZ (CABZ01054965), and zebrafish ZMP (ZMP:0000000936) showing conserved domains: N-terminal signal peptide (SP), 3 extracellular immunoglobulin-like (Ig-I) domains (Ig-I 1, Ig-I 2, and Ig-I 3), a single transmembrane domain (TM), and an intracellular Toll/Interleukin-1 receptor (TIR).

IL1R1 complex, we mined the zebrafish genome for the gene encoding the zebrafish ortholog for *IL1rap*. BLAST analysis using human *IL1RAP* localized the putative zebrafish *il1rap* gene (*cabz01068246*) to chr. 15 near the zebrafish *fgf12b* gene (data not shown). This genomic region in zebrafish shares conserved synteny with both the human and mouse genomes, which show colocalization of the *IL1RAP* and *FGF12* genes. In addition, BLAST analysis using human *IL1R2* localized the putative zebrafish *il1r2* (*cabz01078737*) near the proximal telomere of chr. 9 adjacent to zebrafish *map4k4* (data not shown). This genomic region shows conserved synteny between *il1r2* and *map4k4* in human, mouse, and zebrafish, albeit at a distant genomic region in the zebrafish genome, with respect to the zebrafish *IL-1* receptor cluster. No obvious zebrafish orthologs for human or mouse *IL18R1* or *IL18RAP* were identified using BLAST analysis. However, the previously annotated zebrafish gene products *IL1rap1a*, *IL1rap1b*, and *IL1rap12* (44) share partial sequence alignment to human and mouse *IL18R1* and *IL18RAP*, indicating the potential for conserved function.

Developmental expression of putative zebrafish interleukin-1 receptors

To examine the developmental expression of the zebrafish *cabz* and *zmp* transcripts, we performed reverse-transcription polymerase chain reaction (RT-PCR) and whole-mount *in situ* hybridization (WISH). No antibodies against the zebrafish proteins are currently available for protein expression analysis, and no expression data for either zebrafish transcript is currently

available. For RT-PCR, we extracted total RNA from embryos at 0, 1, 2, and 3 days postfertilization (dpf), synthesized cDNA, and PCR amplified using sequence-specific DNA primers (see Materials and Methods). As shown in Figure 2A, the *cabz* transcript was not detected maternally, whereas the *zmp* transcript demonstrated maternally derived expression at 0 dpf. Both the *cabz* and *zmp* transcripts showed robust expression from 1-3 dpf, indicating that both transcripts are developmentally expressed (Figure 2A).

To examine the spatiotemporal expression of the zebrafish *cabz* and *zmp* transcripts, we performed WISH. Using wild-type (WT) embryos at 1, 2, and 3 dpf, we analyzed transcript expression using antisense and sense digoxigenin (DIG)-labeled RNA probes. As expected, sense probes did not detect any expression (data not shown). We found that the *cabz* and *zmp* antisense probes exhibited unrestricted expression of both transcripts at all three developmental stages examined (Figure 2B). The unrestricted expression of these zebrafish *il1r* genes is consistent with low tissue specificity of the human *IL1R1* transcript as demonstrated by RNAseq, microarray, and SAGE analysis (see <https://www.proteinatlas.org/ENSG00000115594-IL1R1/tissue> and <https://www.genecards.org/cgi-bin/carddisp.pl?gene=IL1R1#expression>).

Morpholino knockdown of the putative zebrafish interleukin-1 receptors

Based upon sequence homology and transcript expression results, we were unable to conclusively identify the functional

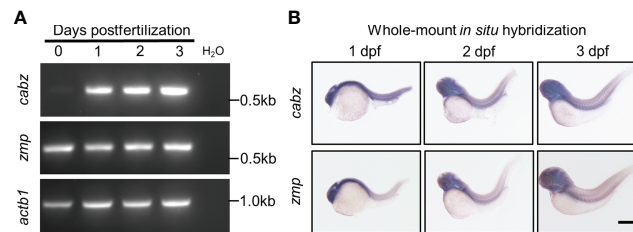


FIGURE 2

Developmental expression of putative zebrafish *Il1r1*. (A) RT-PCR from WT embryos at 0–3 dpf showed expression of *cabz* beginning at 1 dpf, maternal expression of *zmp* at 0 dpf, and *actin beta 1* (*actb1*) transcript as an experimental control. Molecular weight markers are shown on the right. (B) Whole-mount *in situ* hybridization using antisense DIG-labeled riboprobes against *cabz* or *zmp* transcripts showed unrestricted expression of both transcripts at 1, 2, and 3 dpf. Scale bar in (B) is 200 μm.

homolog(s) for zebrafish *Il1r1*. Therefore, we designed morpholino oligonucleotides (MO) against splice donor sites to functionally knockdown the expression of both CABZ and ZMP by disrupting pre-mRNA splicing (45). Morpholinos were injected into WT embryos at the single-cell stage. The resulting morphants were raised to 2 dpf, total RNA was extracted, then morphant transcripts were analyzed by RT-PCR using DNA primers designed to span the splice donor sites of *cabz* and *zmp*, or the *actin beta 1* (*actb1*) transcript as a control. We found that injection of the *cabz* splice donor morpholino resulted in the loss of the WT transcript (578 bp) and the formation of a single alternatively spliced transcript of approximately 400 bp (Figure 3A; top panel). In addition, we found that injection of the *zmp* splice donor morpholino resulted in the loss of the WT transcript (577 bp) and the formation of three aberrantly spliced transcripts of approximately 2,100, 570, and 400 bp (Figure 3A; middle panel). As expected, the standard control morpholino (Con.) supplied by GeneTools showed no effect on the *zmp*, *cabz*, or *actb1* transcripts. To further examine the splicing effects of both morpholinos, we gel purified and sequenced the aberrantly spliced transcripts. For the *cabz* morphants, we found that the ~400 bp band was due to exclusion of exon 4 (-ex4), which was predicted to result in a non-functional product (Figures 3A, B). For the *zmp* morphants, we found that the ~2,100 bp band was due to the inclusion of intron 5 (+in5), the ~570 bp band was due to a cryptic splicing site (css) in exon 5 twelve bases upstream of the authentic splice-donor site, and the ~400 bp band was due to exclusion of exon 5 (-ex5) (Figures 3A, C). All three alternatively spliced *zmp* morphant transcripts were predicted to result in non-functional products. Importantly, the ~570 bp band from the *zmp* splice-site morphants is slightly smaller than the WT band and no WT transcript was detected in the *zmp* splice-site morphants using DNA sequence analysis. In fact, no WT transcripts were detected in either of the *cabz* or *zmp* morphants at the developmental stages examined. Thus, both the *cabz* and *zmp* morpholinos provide valuable genetic tools that disrupt the expression of these transcripts.

To test the functional consequences of the *cabz* and *zmp* morpholinos, we utilized our transgenic zebrafish model of *Il-1β*-induced systemic inflammation (23). We previously generated two transgenic zebrafish lines *Tg(ubb:IVS2GVEcR, cmcl2:EGFP)*, herein abbreviated as *ubb:Gal4-EcR*, and *Tg(uas:GSP-Il1β^{mat}, cmcl2:mCherry)*, herein abbreviated as *uas:Il1β^{mat}*. This model uses the Gal4-EcR/UAS system (22), where mature *Il-1β* (*Il1β^{mat}*) is ubiquitously secreted only in the presence of the ecdysone analog, Tebufenozide (Teb). In order to identify the functional *Il1r1* in zebrafish, we used our model to examine 1) survival, 2) morphology, 3) neutrophils (*mpx:mCherry*), and 4) reactive oxygen species (ROS) in the putative *Il1r1* morphants (Figure 3D).

Survival analysis of *Il-1β*-induced mortality

Our previous studies established *Il-1β*-induced mortality in double transgenic *ubb:Gal4-EcR, uas:Il1β^{mat}* larvae in the presence of Teb in a dose-dependent manner (23). To accelerate mortality in our current study, we modified the original experimental paradigm by generating inflammation at 1 dpf, which coincides with the onset of innate immunity in zebrafish (10, 46, 47). Here, double transgenic *ubb:Gal4-EcR, uas:Il1β^{mat}* embryos were 1) injected with control, *cabz*, or *zmp* morpholinos at the single-cell stage or left uninjected, 2) treated with 1 μM Teb or no Teb (0.1% DMSO) at 1 dpf, and then 3) observed daily for survival up to 6 dpf. As shown in Figure 4A, all untreated *ubb:Gal4-EcR, uas:Il1β^{mat}* controls (*ubb/uas* Uninj No Teb) and all wild type controls (WT Uninj No Teb and WT Uninj + 1 μM Teb) survived to 6 dpf and beyond. Moreover, none of the morpholino injections or Teb treatments significantly reduced survival in WT embryos at the concentrations used (Supplemental Figure 1). In contrast, when *ubb:Gal4-EcR, uas:Il1β^{mat}* embryos were treated with 1 μM Teb, the majority of uninjected controls (*ubb/uas* Uninj + 1 μM Teb; *n*=32) and control morphants (*ubb/uas* Con MO + 1 μM Teb; *n*=36) died by 3 dpf (Figure 4A). As control MO showed no effect on morbidity and mortality, the remainder of controlled experiments were conducted with uninjected embryos only.

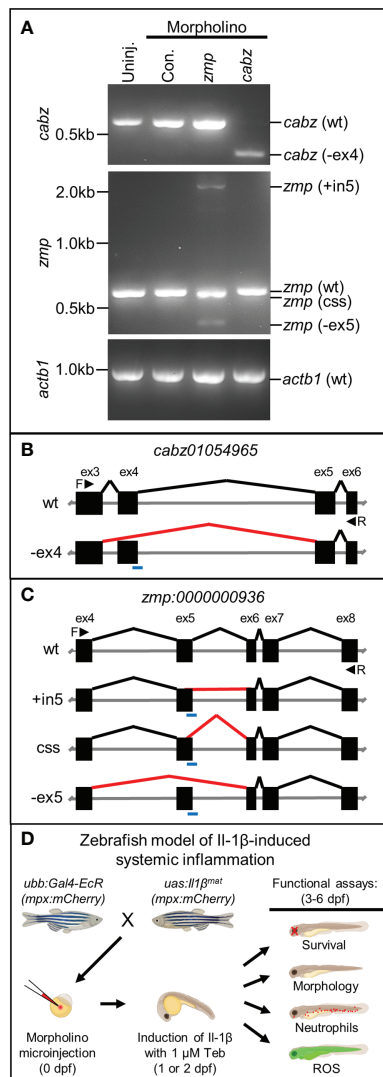


FIGURE 3

Morpholino knockdown of putative zebrafish *Il1r1*. (A) RT-PCR of *cabz*, *zmp*, and *actb1* transcripts from uninjected embryos, control morpholino injected embryos, and *cabz* and *zmp* morphants. (B) Schematic of the *cabz01054965* (*cabz*) gene showing exons 3-6, forward (F) and reverse (R) primers used for analysis (black arrowheads), the location of the splice donor site morpholino (blue line), normal splicing of wt (black lines), and aberrant splicing with the *cabz* morpholino (red line) that excludes exon 4 (-ex4). (C) Schematic of the *zmp:0000000936* (*zmp*) gene showing exons 4-8, forward (F) and reverse (R) primers used for analysis (black arrowheads), the location of the splice donor site morpholino (blue line), normal splicing of wt (black lines), and aberrant splicing with the *zmp* morpholino (red lines) that includes intron 5 (+in5), introduce a cryptic splice sites (css), or excludes exon 5 (-ex5). (D) Diagram of the experimental paradigm used to functionally identify zebrafish *Il1r1*. A zebrafish model of Il-1 β -induced systemic inflammation was generated by breeding transgenic lines *ubb:Gal4-EcR* and *uas:Il1 β^{mat}* with or without the neutrophil reporter line *mpx:mCherry*. Single-celled embryos were injected with morpholino, inflammation was induced with 1 μ M Teb, and functional analyses were performed from 3-6 dpf to assess morpholino rescue of Il-1 β -induced inflammation.

These results demonstrate that Teb-treated *ubb:Gal4-EcR*, *uas:Il1 β^{mat}* embryos are extremely susceptible to mortality and that this experimental paradigm provides a high level of reproducibility.

Concurrently, we monitored survival of the putative *il1r1* morphants. We reasoned that if Il-1 β -induced mortality is mediated by the activation of zebrafish *Il1r1*, then morpholino knockdown of the appropriate receptor(s) would reduce death

and increase survival. As shown in Figure 4B, we found that the *cabz* splice-site morphants treated with 1 μ M Teb (*ubb/uas cabz* Spl + 1 μ M Teb; $n=34$) died at a rate comparable to the uninjected and control MO injected Teb treated embryos, indicating that Il-1 β -induced death is not mediated through zebrafish CABZ. In contrast, the *zmp* splice-site morphants treated with 1 μ M Teb (*ubb/uas zmp* Spl + 1 μ M Teb; $n=37$) survived equally to No Teb embryos (Figures 4A, B). To confirm the effects of the *zmp* splice-

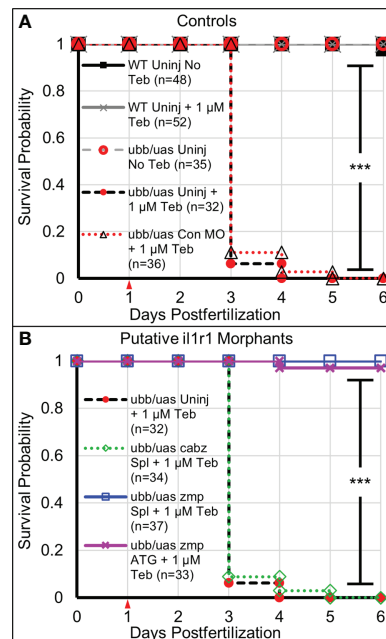


FIGURE 4

Survival analysis of Il-1 β -induced mortality. **(A)** Kaplan-Meier representations of the survival of WT larvae left untreated (WT Uninj No Teb), or Teb treated (WT Uninj + 1 μ M Teb), *ubb:Gal4-EcR, uas:Il1 β^{mat}* larvae with no Teb treatment (*ubb/uas Uninj No Teb*), with Teb (*ubb/uas Uninj + 1 μ M Teb*), or injected with control morpholino with Teb (*ubb/uas Con MO + 1 μ M Teb*). **(B)** Kaplan-Meier representations of the survival of *ubb:Gal4-EcR, uas:Il1 β^{mat}* larvae left uninjected with Teb treatment (*ubb/uas Uninj + 1 μ M Teb*) injected with the *cabz* splice donor morpholino with Teb (*ubb/uas cabz Spl + 1 μ M Teb*), *zmp* splice donor morpholino with Teb (*ubb/uas zmp Spl + 1 μ M Teb*), or *zmp* start site morpholino with Teb (*ubb/uas zmp ATG + 1 μ M Teb*). Teb was added to the embryos at 1 dpf (red arrowhead). Note that only the *zmp* morpholinos rescued Il-1 β -induced death. *** $p < 0.001$.

site morpholino, we designed and injected a *zmp* start-site morpholino (*zmp ATG*) to block translation of the *zmp* transcript (48). As with the *zmp* splice morphants, the *zmp* start morphants (*ubb/uas zmp ATG + 1 μ M Teb*; $n=33$) survived at a frequency comparable to No Teb embryos (Figures 4A, B).

To further verify and phenocopy the *zmp* morpholino rescue of Il-1 β -induced morbidity and mortality, we microinjected CRISPR-Cas9 ribonucleoprotein (RNP) complexes targeting the *zmp* gene into *ubb:Gal4-EcR, uas:Il1 β^{mat}* embryos to generate mosaic knockouts. Two RNPs, cr1 and cr2, targeting exon 8 and exon 9, respectively, were injected independently or in combination at 1:1 molar ratio (Supplemental Figure 2A) then treated with 1 μ M Teb (+ Teb) or untreated (No Teb). As shown in Supplemental Figure 2B, uninjected control embryos (Con.) treated with Teb at 1 dpf showed ~80% dead, ~15% sick (fin degradation and general morbidity), and ~5% alive by 4 dpf. In contrast, the RNP-injected embryos showed a dramatic increase in survival with ~85% of cr1/cr2, ~94% of cr1, and ~50% of cr2 alive at 4 dpf. Injection of RNPs had no effect on survival in the absence of Teb treatment. As cr1/cr2 injection could result in a deletion mutation, we analyzed crispants by PCR. We found that the controls, cr1, and cr2 produced a predicted 508 bp band, whereas the cr1/cr2 combination resulted in the 508 bp band as

well as a smaller ~160 bp band in three of the four samples shown (Supplemental Figure 2C). As the protospacer adjacent motif (PAM) site of cr1 and cr2 are ~350 bp apart, this smaller band likely represents a genomic deletion between cr1 and cr2. We also conclude that the cr1 and cr2 crispants must cause in a small inactivating insertion or deletion (indel) in *il1r1* as both rescued Il-1 β -induced mortality.

Our data demonstrate that knockdown of zebrafish ZMP function by disrupting pre-mRNA splicing, blocking translation, or mosaic CRISPR/Cas9 knockout rescues Il-1 β -dependent mortality. Since both *zmp* splice-site and *zmp* start-site morpholinos equally rescued death and worked as effectively as mosaic knockout with CRISPR/Cas9, we used the splice-site morpholinos for the remainder of experiments described below.

Rescue of Il-1 β -induced gross morphological defects

Double transgenic *ubb:Gal4-EcR, uas:Il1 β^{mat}* embryos were 1) uninjected, injected with *cabz* morpholino (*cabz*), or injected with *zmp* morpholino (*zmp*), 2) untreated (No Teb) or treated with 1 μ M Teb at 2 dpf, and then 3) imaged for gross

morphology at 4 dpf. We previously demonstrated that $Il-1\beta$ -induced systemic inflammation results in fin degradation and general morbidity prior to death (23). As shown in Figure 5A, untreated larvae (No Teb) maintained normal morphology, whereas Teb-treated larvae (+Teb) showed extensive fin degradation and an overall unhealthy phenotype (Figure 5A; top panels). Untreated *cabz* morphants also displayed normal fin morphology, whereas Teb-treated embryos showed extensive fin degradation similar to the uninjected controls (Figure 5A; middle panels). In contrast, *zmp* morphants displayed normal fin morphology with and without Teb treatment, indicating rescue of the inflammation phenotype (Figure 5A; bottom panels). Furthermore, quantification of fin degradation revealed that the *zmp* morpholino, but not the *cabz* morpholino, prevented $Il-1\beta$ -dependent morbidity in our model. We found that the total fin area was significantly decreased with Teb treatment in the uninjected and the *cabz* morphants, whereas the *zmp* morphants maintained normal fin area similar to untreated larvae (Figure 5B). We also measured the effects on total body area between the different groups. We found that Teb-induced larvae had a smaller cross-sectional area compared to untreated controls (Figure 5C). However, all cross-sectional area differences were a consequence of fin degradation only (Figure 5D). No other gross morphological differences were observed between the groups. In addition, Teb-treatment (even up to 10 μ M Teb) showed no effect on morphology in WT embryos without the *ubb:Gal4-EcR*, *uas:Il1 β^{mat}* transgenes (Supplemental Figure 3).

Inhibition of $Il-1\beta$ -induced neutrophil expansion

Neutrophils are innate immune cells responsive to proinflammatory cytokines such as $Il-1\beta$. In zebrafish, neutrophils become functional during early development (10, 46), after which they can expand and migrate in response to inflammatory events such as tissue damage or microbial infection (18, 49). Here, we investigated whether our putative *il1r1* morpholinos were able to block $Il-1\beta$ -dependent neutrophil activity. Triple transgenic *ubb:Gal4-EcR*, *uas:Il1 β^{mat}* , *mpx:mCherry* embryos were 1) uninjected, injected with *cabz* morpholino (*cabz*), or injected with *zmp* morpholino (*zmp*), 2) untreated (No Teb) or treated with 1 μ M Teb at 2 dpf, and then 3) imaged and quantified at 4 dpf. As shown in Figure 6A, untreated larvae (No Teb), showed a stereotypical distribution of neutrophils primarily located in the caudal hematopoietic tissue (CHT) with few cells dispersed throughout the larvae (left panels). When treated with Teb (+Teb), uninjected larvae and *cabz* morphants showed an extensive expansion of neutrophils within the CHT and throughout the larvae, whereas *zmp* morphants were phenotypically similar to untreated (No Teb) larvae. Teb showed no effects on neutrophil numbers or distribution in *mpx:mCherry* embryos (Supplemental Figure 4). To quantify these results, we counted total neutrophils in the whole larvae (Figure 6B). In uninjected larvae and *cabz* morphants, Teb treatment caused a significant increase in the total number of

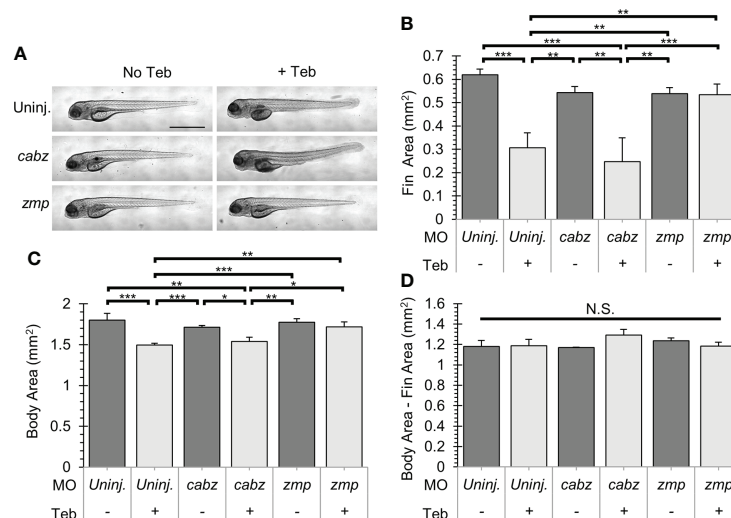


FIGURE 5

Gross morphological analysis of $Il-1\beta$ -induced morbidity. (A) Representative images of *ubb:Gal4-EcR*, *uas:Il1 β^{mat}* larvae showing gross morphology. Shown here are uninjected larvae, *cabz* morphants, and *zmp* morphants without Teb (No Teb) and with Teb treatment (+Teb). Note that *zmp* morphants +Teb showed normal morphology with no gross defects. (B–D) Mean Cross-Sectional Fin Area (B), Body Area (C), and the product of Body Area – Fin Area (D) was plotted in mm² for each group. Error Bars are +1 standard deviation. Asterisks indicate significant differences * p < 0.05 ** p < 0.01 *** p < 0.001; N.S., not significant; by one-way ANOVA followed by Tukey's HSD Test. Scale bar in (A) is 1 mm.

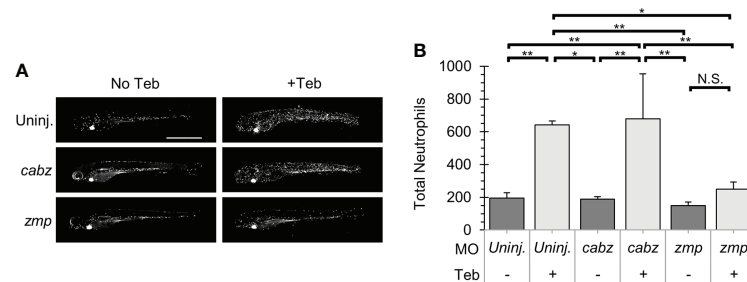


FIGURE 6

IL-1 β -induced neutrophil recruitment. (A) Representative confocal images of *ubb:Gal4-EcR, uas:Il1 β ^{mat}, mpx:mCherry* larvae. Shown here are uninjected larvae, *cabz* morphants, and *zmp* morphants without Teb (No Teb) and with Teb treatment (+Teb). (B) Neutrophils were counted using FIJI Cell Counter and Total Neutrophil counts were plotted for each group. Error Bars are +1 standard deviation. Asterisks indicate significant differences * $p < 0.05$ ** $p < 0.01$; N.S., not significant; by one-way ANOVA followed by Tukey's HSD Test. Scale bar in (A) is 1 mm.

neutrophils. In contrast, the Teb-treated *zmp* morphants showed no significant neutrophil expansion, indicating complete phenotypic rescue by the *zmp* morpholino.

Prevention of IL-1 β -induced reactive oxygen species

ROS are central to the progression of many inflammatory diseases and are produced by cells, such as neutrophils, that are involved in the host-defense response to various cytokines (50). For this study, we examined whether our putative *il1r1* morpholinos were capable of blocking IL-1 β -dependent ROS production. Double transgenic *ubb:Gal4-EcR, uas:Il1 β ^{mat}* embryos were 1) uninjected, injected with *cabz* morpholino (*cabz*), or injected with *zmp* morpholino (*zmp*), 2) untreated (No Teb) or treated with 1 μ M Teb at 2 dpf, 3) exposed to CM-H₂DCFDA, a fluorescent cell-permeant indicator for ROS, at 4 dpf, and 4) imaged and quantified for relative fluorescence. Here,

we show an overlay of brightfield and fluorescent images (Figure 7A; left panels) and the area of fluorescence quantified (Figure 7A; right panels, white boundaries). As untreated larvae showed fluorescence in the yolk, gut, and heart from autofluorescence, CM-H₂DCFDA cleavage, and *cmlc2:EGFP*, respectively, we excluded these regions from quantification. To quantify the signal, we measured the fluorescence within the white boundaries using FIJI Mean Gray Value Measurement as described in Methods. As shown in Figure 7B, addition of Teb caused a significant increase in the fluorescent signal in the uninjected controls, demonstrating IL-1 β -dependent ROS production. Similarly, the *cabz* morphants showed a dramatic increase in ROS, indicating that the *cabz* morpholino did not block this process. In contrast, the *zmp* morphants showed almost no fluorescent signal, equivalent to the uninjected larvae without Teb. These data indicate that the *zmp* morpholino blocks IL-1 β -dependent ROS production.

Given that 1) the *zmp* gene shares conserved synteny between the human, mouse, and zebrafish genomes, 2) *zmp*

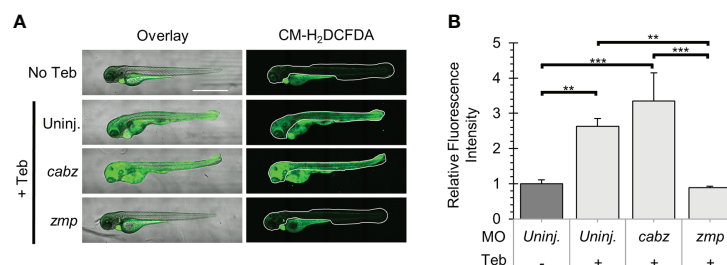


FIGURE 7

Analysis of Reactive Oxygen Species in IL-1 β -induced inflammation. (A) Representative confocal images of *ubb:Gal4-EcR, uas:Il1 β ^{mat}* larvae treated with CM-H₂DCFDA. Shown here are the overlay of brightfield and CM-H₂DCFDA fluorescence (left panels) and CM-H₂DCFDA fluorescence only (right panels). Fluorescence signal was quantified from the region of interest outlined with a white border in the CM-H₂DCFDA images. (B) Relative Fluorescence Intensity (RFI) was quantified using FIJI 'mean grey value' measurement. All mean RFIs were normalized to uninjected No Teb mean values. Error Bars are +1 standard deviation. Asterisks indicate significant differences ** $p < 0.01$ *** $p < 0.001$ by one-way ANOVA followed by Tukey's HSD Test. Scale bar in (A) is 1 mm.

morpholinos rescued mortality, gross morphology, neutrophil counts, and prevented ROS in our model of IL-1 β -induced embryonic systemic inflammation, and 3) mosaic CRISPR/Cas9 knockout phenocopies the morpholino rescue, we have genetically and functionally demonstrated that the *zmp:0000000936* gene encodes zebrafish IL1r1.

Discussion

In this study, we use a combination of database mining, genetic analyses, and functional assays to identify zebrafish IL1r1. Although our *in silico* analysis revealed several putative genes that encode for proteins with partial alignment to human IL1R1, we discovered two putative candidate genes with conserved synteny to the human and mouse genomes. The proteins encoded by these genes show relatively low sequence identities to human IL1R1 but have highly similar predicted protein structures. To examine functionality of these candidates, we designed highly effective morpholinos that disrupted normal splicing or transcription with no obvious off-target effects. We found that knockdown of only one candidate rescued neutrophil expansion, ROS generation, morbidity, and mortality in our zebrafish model of embryonic IL-1 β -induced systemic inflammation. We also designed effective gRNAs for mosaic knockout using the CRISPR/Cas9 system that phenocopied the knockdown effects of the morpholinos. We therefore conclude that the zebrafish genome contains only one functional ortholog of IL1r1. Our study highlights the importance of functional data to accurately identify and annotate zebrafish orthologs of inflammation genes and provides essential insights to the inflammatory response driven by IL-1 β .

As a potential caveat of our results, IL1rap is also required for IL-1 signaling and our study has not conclusively eliminated the possibility that *zmp:0000000936* could encode IL1rap. For example, knockdown of either zebrafish IL1r1 or IL1rap could both result in the rescue of IL-1 β -induced inflammation as previously demonstrated by knockouts of either mouse IL1r1 or IL1rap (26–28). However, based upon conserved synteny and protein alignments, we predict that zebrafish IL1rap is most likely encoded by the *cabz01068246* gene (see Results), although we do not present functional data for this observation. In addition, by process of elimination, we predict that the *cabz01054965* gene, which is adjacent to *zmp:0000000936*, likely encodes the zebrafish IL1r2 ortholog as shown by conserved synteny. Based upon our collective data, we are confident that we have identified zebrafish IL1r1, but have not conclusively demonstrated receptor functionality without a formal biochemical analysis of receptor/ligand binding.

Prior to our study, zebrafish IL1r1 was not accurately annotated in the zebrafish genome. Previous studies used the zebrafish genomic sequence to identify putative genes encoding Toll-like receptors (TLR) and interleukin receptors that contain a Toll/IL-1 receptor (TIR) domain. For example, Meijer et al.

identified several predicted TLR proteins, one putative IL1r, and one putative IL18r (51). This study confirmed the expression of the predicted transcripts by RT-PCR and investigated their expression in *Mycobacterium*-infected zebrafish. Ultimately, the authors concluded that other *il1r* and *il18r* homologues may exist as the expression levels of the putative *il1r* and *il18r* transcripts were unaffected by *Mycobacterium* infection. On review of this work, we determined that the transcript-specific primers used to amplify *il1r* and *il18r* by RT-PCR are actually against *cu855885* (annotated as *il1rl1*) located on chr. 9 and *il18r* (annotated as *il1rap12*) located on chr. 14, respectively. More recently, Frame et al. described the identification of the zebrafish gene encoding Interleukin-1 receptor-like 1 (IL1rl1), a predicted homolog of zebrafish IL1r1. This study found upregulation of zebrafish *il1rl1* in Flk1⁺ cMyb⁺ hematopoietic stem and progenitor cells (HSPCs) in response to IL-1 β stimulation by macrophages. The authors also found reduced *runx1/cmyb* expression and reduced numbers of CD41⁺ HSPCs following morpholino knockdown of *il1rl1* and suggest that IL-1 β promotes IL1rl1⁺ HSPC production *via* inflammasome activity (40). Based upon the results we present in our study; it would be interesting to examine the expression and knockdown of zebrafish *il1rl1* in this model of HSPC production.

To identify the functional zebrafish IL1r1, we implemented our validated transgenic model of embryonic IL-1 β -induced systemic inflammation and used morpholino oligonucleotides to knockdown the expression of putative IL1r1 orthologs. In our model, the mature form of IL-1 β is secreted only in the presence of the ecdysone analog tebufenozide (Teb), resulting in adverse inflammation-related phenotypes. Other inducible transgenic models, such as Tet-On/Tet-Off and Cre-ER recombinase often have unintended consequences due to antibiotic- and estrogen receptor-mediated effects that may complicate data interpretation (52). In contrast, we used the Teb-inducible UAS/Gal4-EcR system as there is no endogenous ecdysone receptor in vertebrates, no known off-target effects, and markedly low toxicity (22). Further, our inflammation model is driven by a single proinflammatory cytokine, IL-1 β . Unlike wound-induced or infection-based models that cause inflammation *via* a myriad of damage-associated molecular patterns (DAMPs) and pathogen-associated molecular patterns (PAMPs), the use of a single molecular effector allowed for our targeted, morpholino-based approach. To demonstrate morpholino effectiveness in our model, we showed 1) disrupted pre-mRNA splicing as demonstrated by RT-PCR and DNA sequencing, 2) phenocopy of the splice-site morpholino using an independent *il1r1* start-site morpholino, 3) no obvious off-target phenotypes, and 4) complete rescue of the deleterious phenotypes caused by induced expression of IL-1 β . Thus, our experimental paradigm, with appropriate caveats considered, follows the basic guidelines for morpholino use in zebrafish as described by Stainier et al. (53).

While newer technologies enable targeted gene disruption in zebrafish, including the CRISPR/Cas9 system, transcription

activator-like effector nucleases (TALENs), and zinc finger nucleases (ZFNs) (54), these strategies require significant time and resources compared to validated, highly effective morpholinos. For example, the successful design and generation of CRISPR/Cas9 knockouts in combination with breeding schemes to produce double or triple transgenic zebrafish in a mutant background could take years to successfully accomplish. Furthermore, these analyses generally target one gene at a time, so if two paralogs were to have overlapping function, both genes would need to be targeted and bred into the appropriate background to observe the desired phenotypes. These analyses could be further complicated by compensatory networks that buffer against deleterious mutations (55). Given these limitations, we were surprised to find that mosaic CRISPR/Cas9 knockout of zebrafish *Il1r1* effectively phenocopied the knockdown effects of the morpholinos. Thus, our study highlights the effective use of morpholinos and mosaic CRISPR/Cas9 to identify gene function in a relevant embryonic disease model simply by rescuing the deleterious phenotypes.

In conclusion, our study provides important new tools and insights for investigating the role of *Il-1 β* and *Il1r1* in a broad spectrum of diseases, such as autoinflammatory diseases, metabolic syndromes, acute and chronic inflammation, and malignancies (25, 56). As an example, neonatal-onset multisystem inflammatory disease (NOMID), a rare congenital inflammatory disorder, is caused by autosomal dominant mutations in the *NLRP3* gene, also known as Cryopyrin or *CIAS1* (57). Clinical manifestations in NOMID, similar to our zebrafish inflammation model, are caused by increased release of *Il-1 β* . Current therapies for NOMID and related disorders primarily involve biologics against *IL1R1* signaling such as Anakinra (a recombinant *IL1R* antagonist), Canakinumab (an antibody targeting *Il-1 β*), and Rilonacept (a soluble decoy receptor). Given that many inflammatory conditions are driven by *Il-1 β* and that there are no known small molecule inhibitors of *IL1R1* (25, 56), identification of *Il1r1* in our zebrafish model provides a novel platform to identify new drugs for the treatment of *Il-1 β* -related diseases.

Data availability statement

The original contributions presented in the study are included in the article/Supplementary Material. Further inquiries can be directed to the corresponding author.

Ethics statement

The animal study was reviewed and approved by University of Wisconsin-Madison, Institutional Animal Care and Use Committee.

Author contributions

DS conducted the experiments, collected, assembled, analyzed the data, and wrote the manuscript. AF provided experimental support, helped in data analysis, and edited the manuscript. KP provided experimental support and helped in data analysis. MT conceived the study, designed experiments, interpreted data, and wrote the manuscript. All authors contributed to the article and approved the submitted version.

Funding

Funding was provided by NIH RO1NS116043. AF was supported by the UW-Madison Biotechnology Training Program, NIH T32GM008349 and T32GM135066.

Acknowledgments

We thank Dr. Anna Huttenlocher (University of Wisconsin-Madison) for providing the *Tg(mpx:mCherry)^{uwm7}* transgenic line. We also wish to thank Randall Kopielski and Jessica Fairbanks for assistance with zebrafish husbandry and animal facility care and maintenance.

Conflict of interest

The authors declare that the research was conducted in the absence of any commercial or financial relationships that could be construed as a potential conflict of interest.

Publisher's note

All claims expressed in this article are solely those of the authors and do not necessarily represent those of their affiliated organizations, or those of the publisher, the editors and the reviewers. Any product that may be evaluated in this article, or claim that may be made by its manufacturer, is not guaranteed or endorsed by the publisher.

Supplementary material

The Supplementary Material for this article can be found online at: <https://www.frontiersin.org/articles/10.3389/fimmu.2022.1039161/full#supplementary-material>

References

- Campos-Sanchez JC, Esteban MA. Review of inflammation in fish and value of the zebrafish model. *J Fish Dis* (2021) 44(2):123–39. doi: 10.1111/jfd.13310
- Xie Y, Meijer AH, Schaaf MJM. Modeling inflammation in zebrafish for the development of anti-inflammatory drugs. *Front Cell Dev Biol* (2020) 8:620984. doi: 10.3389/fcell.2020.620984
- Zanandrea R, Bonan CD, Campos MM. Zebrafish as a model for inflammation and drug discovery. *Drug Discovery Today* (2020) 25(12):2201–11. doi: 10.1016/j.drudis.2020.09.036
- Kwan KM, Fujimoto E, Grabher C, Mangum BD, Hardy ME, Campbell DS, et al. The Tol2kit: a multisite gateway-based construction kit for Tol2 transposon transgenesis constructs. *Dev Dyn* (2007) 236(11):3088–99. doi: 10.1002/dvdy.21343
- Yan B, Han P, Pan L, Lu W, Xiong J, Zhang M, et al. IL-1 β and reactive oxygen species differentially regulate neutrophil directional migration and basal random motility in a zebrafish injury-induced inflammation model. *J Immunol* (2014) 192(12):5998–6008. doi: 10.4049/jimmunol.1301645
- Delgadillo-Silva LF, Tsakmaki A, Akhtar N, Franklin ZJ, Konantz J, Bewick GA, et al. Modelling pancreatic beta-cell inflammation in zebrafish identifies the natural product wedelolactone for human islet protection. *Dis Model Mech* (2019) 12(1):1–12. doi: 10.1242/dmm.036004
- Ibrahim S, Harris-Kawano A, Haider I, Mirmira RG, Sims EK, Anderson RM. A novel cre-enabled tetracycline-inducible transgenic system for tissue-specific cytokine expression in the zebrafish: CETI-PIC3. *Dis Model Mech* (2020) 13(6):1–12. doi: 10.1242/dmm.042556
- Deng Q, Harvie EA, Huttenlocher A. Distinct signalling mechanisms mediate neutrophil attraction to bacterial infection and tissue injury. *Cell Microbiol* (2012) 14(4):517–28. doi: 10.1111/j.1462-5822.2011.01738.x
- Hall CJ, Flores MV, Oehlers SH, Sanderson LE, Lam EY, Crosier KE, et al. Infection-responsive expansion of the hematopoietic stem and progenitor cell compartment in zebrafish is dependent upon inducible nitric oxide. *Cell Stem Cell* (2012) 10(2):198–209. doi: 10.1016/j.stem.2012.01.007
- Le Guyader D, Redd MJ, Colucci-Guyon E, Murayama E, Kissa K, Briolat V, et al. Origins and unconventional behavior of neutrophils in developing zebrafish. *Blood* (2008) 111(1):132–41. doi: 10.1182/blood-2007-06-095398
- Goody M, Jurczyk D, Kim C, Henry C. Influenza a virus infection damages zebrafish skeletal muscle and exacerbates disease in zebrafish modeling duchenne muscular dystrophy. *PLoS Curr* (2017) 9. doi: 10.1371/currents.mdm.8a7e35c50fa2b48156799d3c39788175
- Davis JM, Huang M, Botts MR, Hull CM, Huttenlocher A. A zebrafish model of cryptococcal infection reveals roles for macrophages, endothelial cells, and neutrophils in the establishment and control of sustained fungemia. *Infect Immun* (2016) 84(10):3047–62. doi: 10.1128/IAI.00506-16
- Voelz K, Gratacap RL, Wheeler RT. A zebrafish larval model reveals early tissue-specific innate immune responses to mucor circinelloides. *Dis Model Mech* (2015) 8(11):1375–88. doi: 10.1242/dmm.019992
- Philip AM, Wang Y, Mauro A, El-Rass S, Marshall JC, Lee WL, et al. Development of a zebrafish sepsis model for high-throughput drug discovery. *Mol Med* (2017) 23:134–48. doi: 10.2119/molmed.2016.00188
- Cvejic A, Hall C, Bak-Maier M, Flores MV, Crosier P, Redd MJ, et al. Analysis of WASp function during the wound inflammatory response—live-imaging studies in zebrafish larvae. *J Cell Sci* (2008) 121(Pt 19):3196–206. doi: 10.1242/jcs.032235
- Hasegawa T, Hall CJ, Crosier PS, Abe G, Kawakami K, Kudo A, et al. Transient inflammatory response mediated by interleukin-1 β is required for proper regeneration in zebrafish fin fold. *Elife* (2017) 6:1–22. doi: 10.7554/eLife.22716
- Mathias JR, Perrin BJ, Liu TX, Kanki J, Look AT, Huttenlocher A. Resolution of inflammation by retrograde chemotaxis of neutrophils in transgenic zebrafish. *J Leukoc Biol* (2006) 80(6):1281–8. doi: 10.1189/jlb.0506346
- Renshaw SA, Loynes CA, Trushell DM, Elworthy S, Ingham PW, Whyte MK. A transgenic zebrafish model of neutrophilic inflammation. *Blood* (2006) 108(13):3976–8. doi: 10.1182/blood-2006-05-024075
- Sipka T, Perocesi R, Hassan-Abdi R, Gross M, Ellett F, Begon-Pescia C, et al. Damage-induced calcium signaling and reactive oxygen species mediate macrophage activation in zebrafish. *Front Immunol* (2021) 12:636585. doi: 10.3389/fimmu.2021.636585
- Yoo SK, Huttenlocher A. Spatiotemporal photolabeling of neutrophil trafficking during inflammation in live zebrafish. *J Leukoc Biol* (2011) 89(5):661–7. doi: 10.1189/jlb.1010567
- Ogryzko NV, Hoggett EE, Solaymani-Kohal S, Tazzyman S, Chico TJ, Renshaw SA, et al. Zebrafish tissue injury causes upregulation of interleukin-1 and caspase-dependent amplification of the inflammatory response. *Dis Model Mech* (2014) 7(2):259–64. doi: 10.1242/dmm.013029
- Esengil H, Chang V, Mich JK, Chen JK. Small-molecule regulation of zebrafish gene expression. *Nat Chem Biol* (2007) 3(3):154–5. doi: 10.1038/nchembio858
- Lanham KA, Nedden ML, Wise VE, Taylor MR. Genetically inducible and reversible zebrafish model of systemic inflammation. *Biol Open* (2022) 11(3):1–12. doi: 10.1242/bio.058559
- Lopez-Castejon G, Brough D. Understanding the mechanism of IL-1 β secretion. *Cytokine Growth Factor Rev* (2011) 22(4):189–95. doi: 10.1016/j.cytogfr.2011.10.001
- Kaneko N, Kurata M, Yamamoto T, Morikawa S, Masumoto J. The role of interleukin-1 in general pathology. *Inflamm Regen* (2019) 39:12. doi: 10.1186/s41232-019-0101-5
- Glaccum MB, Stocking KL, Charrier K, Smith JL, Willis CR, Maliszewski C, et al. Phenotypic and functional characterization of mice that lack the type I receptor for IL-1. *J Immunol* (1997) 159(7):3364–71.
- Labow M, Shuster D, Zetterstrom M, Nunes P, Terry R, Cullinan EB, et al. Absence of IL-1 signaling and reduced inflammatory response in IL-1 type I receptor-deficient mice. *J Immunol* (1997) 159(5):2452–61.
- Cullinan EB, Kwee L, Nunes P, Shuster DJ, Ju G, McIntyre KW, et al. IL-1 receptor accessory protein is an essential component of the IL-1 receptor. *J Immunol* (1998) 161(10):5614–20.
- Howe K, Clark MD, Torroja CF, Torrance J, Berthelot C, Muffato M, et al. The zebrafish reference genome sequence and its relationship to the human genome. *Nature* (2013) 496(7446):498–503. doi: 10.1038/nature12111
- Meyer A, Scharl M. Gene and genome duplications in vertebrates: the one-to-four (-to-eight in fish) rule and the evolution of novel gene functions. *Curr Opin Cell Biol* (1999) 11(6):699–704. doi: 10.1016/S0955-0674(99)00039-3
- Westerfield M. *The zebrafish book: University of Oregon press*. (Eugene, Oregon: University of Oregon Press) (1995).
- Jumper J, Evans R, Pritzel A, Green T, Figurnov M, Ronneberger O, et al. Highly accurate protein structure prediction with AlphaFold. *Nature* (2021) 596(7873):583–9. doi: 10.1038/s41586-021-03819-2
- Varadi M, Anyango S, Deshpande M, Nair S, Natassia C, Yordanova G, et al. AlphaFold protein structure database: massively expanding the structural coverage of protein-sequence space with high-accuracy models. *Nucleic Acids Res* (2022) 50(D1):D439–D44. doi: 10.1093/nar/gkab1061
- Untergasser A, Cutcutache I, Koressaar T, Ye J, Faircloth BC, Remm M, et al. Primer3—new capabilities and interfaces. *Nucleic Acids Res* (2012) 40(15):e115. doi: 10.1093/nar/gks596
- Thisse C, Thisse B. High-resolution *in situ* hybridization to whole-mount zebrafish embryos. *Nat Protoc* (2008) 3(1):59–69. doi: 10.1038/nprot.2007.514
- Vauti F, Stegemann LA, Vogele V, Koster RW. All-age whole mount *in situ* hybridization to reveal larval and juvenile expression patterns in zebrafish. *PLoS One* (2020) 15(8):e0237167. doi: 10.1371/journal.pone.0237167
- Bill BR, Petzold AM, Clark KJ, Schimmenti LA, Ekker SC. A primer for morpholino use in zebrafish. *Zebrafish* (2009) 6(1):69–77. doi: 10.1089/zeb.2008.0555
- Schindelin J, Arganda-Carreras I, Frise E, Kaynig V, Longair M, Pietzsch T, et al. Fiji: an open-source platform for biological-image analysis. *Nat Methods* (2012) 9(7):676–82. doi: 10.1038/nmeth.2019
- Dale M, Nicklin MJ. Interleukin-1 receptor cluster: gene organization of IL1R2, IL1R1, IL1RL2 (IL-1R β), IL1RL1 (T1/ST2), and IL18R1 (IL-1R α) on human chromosome 2q. *Genomics* (1999) 57(1):177–9. doi: 10.1006/geno.1999.5767
- Frame JM, Kubaczka C, Long TL, Esain V, Soto RA, Hachimi M, et al. Metabolic regulation of inflammasome activity controls embryonic hematopoietic stem and progenitor cell production. *Dev Cell* (2020) 55(2):133–49 e6. doi: 10.1016/j.devcel.2020.07.015
- Fields JK, Gunther S, Sundberg EJ. Structural basis of IL-1 family cytokine signaling. *Front Immunol* (2019) 10:1412. doi: 10.3389/fimmu.2019.01412
- O'Neill LA, Bowie AG. The family of five: TIR-domain-containing adaptors in toll-like receptor signalling. *Nat Rev Immunol* (2007) 7(5):353–64. doi: 10.1038/nri2079
- Riva F, Bonavita E, Barbati E, Muzio M, Mantovani A, Garlanda C. TIR8/SIGIRR is an interleukin-1 Receptor/Toll like receptor family member with regulatory functions in inflammation and immunity. *Front Immunol* (2012) 3:322. doi: 10.3389/fimmu.2012.00322
- Yoshida T, Mishina M. Zebrafish orthologue of mental retardation protein IL1RAPL1 regulates presynaptic differentiation. *Mol Cell Neurosci* (2008) 39(2):218–28. doi: 10.1016/j.mcn.2008.06.013

45. Draper BW, Morcos PA, Kimmel CB. Inhibition of zebrafish *fgf8* pre-mRNA splicing with morpholino oligos: a quantifiable method for gene knockdown. *Genesis* (2001) 30(3):154–6. doi: 10.1002/gene.1053
46. Bader A, Gao J, Riviere T, Schmid B, Walzog B, Maier-Begandt D. Molecular insights into neutrophil biology from the zebrafish perspective: Lessons from CD18 deficiency. *Front Immunol* (2021) 12:677994. doi: 10.3389/fimmu.2021.677994
47. Herbomel P, Thisse B, Thisse C. Ontogeny and behaviour of early macrophages in the zebrafish embryo. *Development* (1999) 126(17):3735–45. doi: 10.1242/dev.126.17.3735
48. Nasevicius A, Ekker SC. Effective targeted gene 'knockdown' in zebrafish. *Nat Genet* (2000) 26(2):216–20. doi: 10.1038/79951
49. Harvie EA, Huttenlocher A. Neutrophils in host defense: new insights from zebrafish. *J Leukoc Biol* (2015) 98(4):523–37. doi: 10.1189/jlb.4MR1114-524R
50. Mittal M, Siddiqui MR, Tran K, Reddy SP, Malik AB. Reactive oxygen species in inflammation and tissue injury. *Antioxid Redox Signal* (2014) 20(7):1126–67. doi: 10.1089/ars.2012.5149
51. Meijer AH, Gabby Krens SF, Medina Rodriguez IA, He S, Bitter W, Ewa Snaar-Jagalska B, et al. Expression analysis of the toll-like receptor and TIR domain adaptor families of zebrafish. *Mol Immunol* (2004) 40(11):773–83. doi: 10.1016/j.molimm.2003.10.003
52. Wust RCI, Houtkooper RH, Auwerx J. Confounding factors from inducible systems for spatiotemporal gene expression regulation. *J Cell Biol* (2020) 219(7):1–4. doi: 10.1083/jcb.202003031
53. Stainier DYR, Raz E, Lawson ND, Ekker SC, Burdine RD, Eisen JS, et al. Guidelines for morpholino use in zebrafish. *PLoS Genet* (2017) 13(10):e1007000. doi: 10.1371/journal.pgen.1007000
54. Lawson ND. Reverse genetics in zebrafish: Mutants, morphants, and moving forward. *Trends Cell Biol* (2016) 26(2):77–9. doi: 10.1016/j.tcb.2015.11.005
55. Rossi A, Kontarakis Z, Gerri C, Nolte H, Holper S, Kruger M, et al. Genetic compensation induced by deleterious mutations but not gene knockdowns. *Nature* (2015) 524(7564):230–3. doi: 10.1038/nature14580
56. Dinarello CA, Simon A, van der Meer JW. Treating inflammation by blocking interleukin-1 in a broad spectrum of diseases. *Nat Rev Drug Discov* (2012) 11(8):633–52. doi: 10.1038/nrd3800
57. Goldbach-Mansky R, Dailey NJ, Canna SW, Gelabert A, Jones J, Rubin BI, et al. Neonatal-onset multisystem inflammatory disease responsive to interleukin-1beta inhibition. *N Engl J Med* (2006) 355(6):581–92. doi: 10.1056/NEJMoa055137



OPEN ACCESS

EDITED BY

Santiago Grijalvo,
Biomaterials and Nanomedicine
(CIBER-BBN), Spain

REVIEWED BY

Elena Dellacasa,
University of Genoa, Italy
John F. Trant,
University of Windsor, Canada
Yücel Başpınar,
Ege University, Turkey

*CORRESPONDENCE

María de la Fuente,
maria.de.la.fuente.freire@sergas.es

SPECIALTY SECTION

This article was submitted to
Translational Pharmacology,
a section of the journal
Frontiers in Pharmacology

RECEIVED 29 July 2022

ACCEPTED 14 October 2022

PUBLISHED 31 October 2022

CITATION

Cascallar M, Hurtado P, Lores S,
Pensado-López A, Quelle-Regaldie A,
Sánchez L, Piñeiro R and de la Fuente M
(2022), Zebrafish as a platform to
evaluate the potential of lipidic
nanoemulsions for gene therapy
in cancer.
Front. Pharmacol. 13:1007018.
doi: 10.3389/fphar.2022.1007018

COPYRIGHT

© 2022 Cascallar, Hurtado, Lores,
Pensado-López, Quelle-Regaldie,
Sánchez, Piñeiro and de la Fuente. This
is an open-access article distributed
under the terms of the [Creative
Commons Attribution License \(CC BY\)](#).
The use, distribution or reproduction in
other forums is permitted, provided the
original author(s) and the copyright
owner(s) are credited and that the
original publication in this journal is
cited, in accordance with accepted
academic practice. No use, distribution
or reproduction is permitted which does
not comply with these terms.

Zebrafish as a platform to evaluate the potential of lipidic nanoemulsions for gene therapy in cancer

María Cascallar^{1,2,3}, Pablo Hurtado^{2,4}, Saínza Lores^{1,3},
Alba Pensado-López^{5,6}, Ana Quelle-Regaldie⁵,
Laura Sánchez^{5,7}, Roberto Piñeiro^{2,4} and
María de la Fuente^{1,2,3,8*}

¹Nano-Oncology and Translational Therapeutics Group, Health Research Institute of Santiago de Compostela (IDIS), SERGAS, Santiago de Compostela, Spain, ²Centro de Investigación Biomédica en Red Cáncer (CIBERONC), Madrid, Spain, ³Universidade de Santiago de Compostela (USC), Santiago de Compostela, Spain, ⁴Roche-Chus Joint Unit, Translational Medical Oncology Group, Oncomet, Health Research Institute of Santiago de Compostela, Santiago de Compostela, Spain, ⁵Department of Zoology, Genetics and Physical Anthropology, Universidade de Santiago de Compostela, Campus de Lugo, Lugo, Spain, ⁶Center for Research in Molecular Medicine and Chronic Diseases (CIMUS), Campus Vida, Universidade de Santiago de Compostela, Santiago de Compostela, Spain, ⁷Preclinical Animal Models Group, Health Research Institute of Santiago de Compostela (IDIS), Santiago de Compostela, Spain, ⁸DIVERSA Technologies S.L., Santiago de Compostela, Spain

Gene therapy is a promising therapeutic approach that has experienced significant growth in recent decades, with gene nanomedicines reaching the clinics. However, it is still necessary to continue developing novel vectors able to carry, protect, and release the nucleic acids into the target cells, to respond to the widespread demand for new gene therapies to address current unmet clinical needs. We propose here the use of zebrafish embryos as an *in vivo* platform to evaluate the potential of newly developed nanosystems for gene therapy applications in cancer treatment. Zebrafish embryos have several advantages such as low maintenance costs, transparency, robustness, and a high homology with the human genome. In this work, a new type of putrescine-sphingomyelin nanosystems (PSN), specifically designed for cancer gene therapy applications, was successfully characterized and demonstrated its potential for delivery of plasmid DNA (pDNA) and miRNA (miR). On one hand, we were able to validate a regulatory effect of the PSN/miR on gene expression after injection in embryos of 0 hpf. Additionally, experiments proved the potential of the model to study the transport of the associated nucleic acids (pDNA and miR) upon incubation in zebrafish water. The biodistribution of PSN/pDNA and PSN/miR *in vivo* was also assessed after microinjection into the zebrafish vasculature, demonstrating that the nucleic acids remained associated with the PSN in an *in vivo* environment, and could successfully reach disseminated cancer cells in zebrafish xenografts. Altogether, these results demonstrate the potential of zebrafish as an *in vivo* model to evaluate nanotechnology-based gene therapies for cancer treatment, as well as the capacity of the developed versatile PSN formulation for gene therapy applications.

KEYWORDS

zebrafish, nanomedicine, gene therapy, miRNA, plasmid, cancer

1 Introduction

Over the past decades, gene therapy has flourished. The basis of this therapy is focused on the use of exogenous therapeutic nucleic acids (NAs) that have the capacity to modify the expression of disease-related genes. NAs involved in gene therapy are micro RNAs (miRs), small interfering RNAs (siRNAs), short hairpin RNAs (shRNAs), antisense oligonucleotides (ASOs) and DNA plasmids (pDNAs) (Sayed et al., 2022).

One of the main limitations in the development of novel gene therapies is the need for efficient carriers capable of protecting and transporting them to their site of action. Viral vectors are the carriers that have moved most quickly to clinical trials, due to the ability of the virus to carry and protect the genetic material to specific cells (Santiago-Ortiz and Schaffer, 2016; Mohammadinejad et al., 2020). Despite this, viral vectors accumulate several disadvantages, such as limitation in the length of the cargo (e.g., 10 kb in lentiviral vectors), insertional mutagenesis, and immunogenicity due to the antibodies against these common viruses produced throughout life (Walther and Drugs, 2000; Amer, 2014; Mohammadinejad et al., 2020; Zu and Gao, 2021). In this sense, non-viral vectors have been proven to successfully resolve the limitations of viral vectors (Mohammadinejad et al., 2020). A clear example is nanomedicine, which arises from the application of nanotechnology in the field of biomedicine, providing several advantages for the intracellular delivery of macromolecules, such as NAs. As proof of this, in recent years several breakthroughs have taken place. In 2018, Onpattro® became the first FDA-approved lipid nanoparticle for gene therapy (Hoy, 2018; Akinc et al., 2019). Additionally, in 2021, mRNA-based vaccines against Covid-19 reached the market (Corbett et al., 2020; Polack et al., 2020), opening a new era for the engineering and application of gene therapy.

Despite the successful advances of the past few years, translating more gene nanomedicines from bench to bedside is still a challenge. In this sense, the use of robust preclinical models that can better predict the future behavior of nanosystems is essential for their development and validation, improving the translation process (Wick et al., 2015; Sahlgren et al., 2017; Sieber et al., 2019b; Bouzo et al., 2020; Boix-Montesinos et al., 2021). *In vivo* models are needed to evaluate biodistribution, toxicity and efficacy, among other parameters. Rodents, the most common animal model, have multiple advantages, such as anatomical and genomic similarities to humans. Nevertheless, they entail certain disadvantages, including the high cost of maintenance and small progeny that prevents the possibility of carrying out large studies (Lieschke and Currie, 2007a; Sieber et al., 2019). A valuable alternative as an *in vivo* platform to evaluate the potential of

nanomedicine is the zebrafish (Gutiérrez-Lovera et al., 2017; Pearce et al., 2018; Sieber et al., 2019; Cascallar et al., 2022).

The use of the zebrafish (*Danio rerio*) in developmental biology and genetics studies dates back to the 1970s (Streisinger et al., 1981). Since then, applications have expanded to study multiple human pathologies, such as cancer, as well as biodistribution, toxicity and pharmacological screening of new drugs (Jia et al., 2019). The success of zebrafish in research is based on their biological characteristics (Zon, 1999). Specifically, their small size enables easy handling, and large number of individuals can be maintained in optimal experimental conditions. Due to their short life cycle, the main organs develop practically within 48 h, sexual maturity is reached at approximately 3 months of life, and large offspring allow large-scale studies to be carried out (Kimmel et al., 1995). Additionally, the zebrafish reference genome has revealed that approximately 80% of the genes have a human orthologue related to diseases (Howe et al., 2013).

Based on these features, in the field of nanomedicine this model is being proposed to assess the biocompatibility and toxicity of several nanomaterials, but also to validate their therapeutic efficacy (Gutiérrez-Lovera et al., 2017; Sieber, Grossen, Bussmann, et al., 2019; Wang et al., 2019; Pensado-López et al., 2021; Cascallar et al., 2022). The presence in zebrafish of organs and metabolic pathways analogous to those of humans allows toxicological and biocompatibility evaluations, and the large number of offspring enables high-throughput and multi- and transgenerational screens (Horzmann and Freeman, 2018). In addition, the response of zebrafish to several substances has been reported to be concordant with that observed in mammalian models (Sipes et al., 2011). In the context of cancer, the transparency of embryos and the availability of fluorescently labelled transgenic zebrafish lines offer the possibility to track cancer cells in xenograft assays or genetic models and thus understand their behavior, dissemination, metastasis, extravasation, or interaction with the tumor microenvironment or immune cells (Lawson & Weinstein, 2002; Renshaw et al., 2006; Ellett et al., 2011). On the other hand, the transparency of zebrafish allows the determination of the toxicity of nanosystems in different anatomical sites of the fish and their tracking to establish biodistribution and interaction profiles with tumor cells without the need for invasive techniques (Lee et al., 2017). In this sense, transgenic zebrafish models allow for real-time tracking of tumor cells without the need to immunostain cells, thus avoiding non-specific labeling and imaging issues derived. As a consequence of the abovementioned, several nanomedicines have been developed and tested in zebrafish, including gene therapies (Wang et al., 2019; Al-Thani et al., 2021; Saraiva et al., 2021).

TABLE 1 compilation of sequences of the miR used in this work.

	Sequence
miR control	5'CAGUACUUUUGUGUAGUACAA3'
miR control-Cy5	5'Cy5-CAGUACUUUUGUGUAGUACAA3'
miR 145	5'GUCCAGUUUCCAGGAAUCCCU3'

In our group, we have previously developed different types of nanosystems for miR-based gene therapy for cancer treatment. These nanocarriers, protamine nanocapsules and sphingomyelin-based nanosystems, demonstrated their *in vitro* potential to interfere in the cancer process (Reimondez-Troitiño et al., 2019; Nagachinta et al., 2020). On subsequent studies by our group, Lores et al. (2022) developed putrescine-sphingomyelin nanosystems (PSN) for cancer gene therapy applications establishing for the first time the use of the natural polyamine putrescine for the development of non-viral vectors, taking advantage of the cationic nature of this compound and the greater affinity of cancer cells for this type of molecules (Thomas et al., 2016; Tracy et al., 2016). In this work, a therapeutic plasmid DNA (pDNA) encoding for the Fas Ligand protein, which promotes the activation of apoptotic pathways, was associated with PSN, and the potential of the developed formulation confirmed *in vitro*, in a triple negative breast cancer cell line (MDA-MB-231), and *in vivo*, in both a zebrafish embryo xenograft model and in an orthotopic mouse model, evidencing a high correlation in terms of efficacy. Based on this data, the present work aimed to further demonstrate the potential of zebrafish embryos as an intermediate model between *in vitro* and *in vivo* mammalian models for the evaluation of novel gene therapies, using for this purpose PSN associated with two different types of nucleic acids, miR and pDNA (Lores et al., 2022).

2 Materials and methods

2.1 Materials

All the miRs used in this work (Table 1) were purchased from Eurofins Genomics (Ebersberg, Germany). Penicillin-Streptomycin, Hoechst 33342, DiI (1,1'-Diiododecyl-3,3,3',3'-Tetramethylindocarbocyanine Perchlorate), agarose and SYBR Gold were provided by Thermo Fisher (Massachusetts, United States). C11 TopFluor Sphingomyelin (N-[11-(dipyrrometheneboron difluoride)undecanoyl]-D-erythro-sphingosylphosphorylcholine was purchased from Avanti Polar Lipids (Alabama, United States). Brilliant III Ultra-Fast SYBR Green QPCR Master Mix Kit was acquired from Agilent Technologies (California, United States). Nuclease-free water was provided by Corning (New York, United States). NYZol reagent was purchased from NYZotech (Lisboa, Portugal). Dulbecco's Modified Eagle's Medium (DMEM), Phosphate Buffered Saline (PBS),

Tricaine methanesulfonate, Vitamin E (DL- α -Tocopherol), N-Phenylthiourea (PTU), Polyvinylpyrrolidone (PVP), Trypsin-EDTA Solution and MOWIOL® 4-88 Reagent were kindly provided by Merck (Darmstadt, Germany). Ethanol of analytical grade was purchased from VWR (Barcelona, Spain). Paraformaldehyde was provided by IESMAT (Madrid, España). Sphingomyelin (Lipoid E SM) was acquired from Lipoid GmbH (Ludwigshafen, Germany). Oleamide-modified putrescine ((9Z)-N-(4-Aminobutyl)-9-octadecenamide, CAS RN: 1005454-33-0) was provided by GalChimia (A Coruña, Spain). The plasmid pcDNA4TO-mito-mCherry-10xGCN4_v4 was purchased in AddGene (Plasmid #60914; <http://n2t.net/addgene:60914>; RRID: Addgene_60914) (Massachusetts, United States).

2.2 Formulation of the nanosystems and nucleic acid association

As previously described (Lores et al., 2022), putrescine nanosystems were formulated by ethanol injection method. Briefly, 5 mg of vitamin E (VitE), 0.5 mg of sphingomyelin (SM) and 0.25 mg of putrescine modified with oleamide (Pt) were dissolved in 100 μ l of ethanol and injected under magnetic stirring at 700 RPM in 1 ml of Molecular Grade Water. The suspension was kept under stirring at room temperature for 5 min. Then, 5 μ g of miR were dissolved in 100 μ l of H₂O nuclease-free and added over 100 μ l of preformed nanocarriers, for 20 min under magnetic stirring at 500 RPM to achieve the association.

Moreover, previously to the pDNA-Cy5 association with the PSN, it was labelled with Cy5 with the Label IT® Tracker™ Intracellular Nucleic Acid Localization Kit (Mirus Bio, Madison, United States).

2.3 Physicochemical characterization

Physicochemical characterization of the nanosystems were performed using a Zetasizer® Nano ZS (Malvern Instruments, England), which provides mean size, polydispersity index (PdI) and zeta potential (ZP). Dynamic light scattering (DLS) allows to perform size and PdI measurements of samples previously diluted 1:10 in MilliQ water. Samples were analysed in disposable microcuvettes (ZEN0040, Malvern Instruments) with a detection angle of 173° at room temperature. Laser Doppler anemometry (LDA) allows to evaluate ZP using folded capillary cells cuvettes (DTS 1070, Malvern Instruments) and a 1:40 diluted sample in MilliQ water.

2.4 Association efficiency

An 3% agarose gel electrophoresis was performed to evaluate the association efficiency of the miR. A known amount of miR

(2 µg) was mixed with Loading buffer, Tris-Borate-EDTA (TBE) buffer and SYBR Gold. The agarose gel was prepared in TAE buffer, composed by Tris, acetic acid and EDTA 0.5 M. Prepared samples were loaded, and the gel was run at 80 V for 40 min, making use of a Mini-Sub Cell GT Cell (BioRad, California, United States). The result was evaluated with the ChemiDoc™ MP Imaging System (Bio-Rad, California, United States), in which not-associated miR appears as a band in the gel. In the case of pDNA, 0.2 µg was loaded in a 1% agarose gel, following the same protocol.

2.5 miR-145 effects in sox9b and gata6 expression-zebrafish as a feasible model for gene therapy

2.5.1 Zebrafish husbandry and microinjection

Zebrafish embryos were obtained by mating wild type adults, which were maintained in 30-L tanks with a 14 h/10 h light/dark cycle and a temperature of 28.5°C. Embryos of 0 h post fertilization (hpf) were collected, placed in 90 mm × 15 mm Petri dishes, and subsequently microinjected with 1–3 nl of free miR Control, free miR145, PSN alone, PSN/miR Control or PSN/miR 145 (0.25 µg/µl). Microinjected embryos as well as controls were kept at 28.5°C until 72 hpf. All the procedures described for zebrafish were performed in agreement with the Animal Care and Use Committee of the University of Santiago de Compostela and the standard protocols (Directive 2012–63-UE).

2.5.2 Real-time quantitative polymerase chain reaction

Real-time quantitative polymerase chain reaction (RT-qPCR) was performed with three biological replicates (10 embryos/pool) and three technical replicates for each. Total RNA was isolated from the embryos with the NYzol reagent and the purification was based on a phenol-chloroform protocol. Reverse transcription was performed with the AffinityScript Multiple Temperature cDNA Synthesis Kit (Agilent) following the manufacturer's protocol. RT-qPCR was performed using the Brilliant III Ultra-Fast SYBR Green QPCR Master Mix Kit and the Stratagene Mx3005P Thermal Cycler (Agilent Technologies). To analyze the expression levels, the $\Delta\Delta CT$ method was applied, using the *actb2* gene as housekeeping and statistical analyses were performed in SPSS Statistics (IBM) through a T Student test. Statistical significance was considered if $p < 0.05$. The *actb2* primers (Forward: ACTTCA CGCCGACTCAAAC; Reverse: ATCCTGAGTCAAGCG CCAAA) were designed using Primer BLAST (Altschul et al., 1990), while those for *sox9b* (Forward: AGCTCAGCAAAA CACTCGGC; Reverse: CCGTCTGGGCTGGTATTTGT) (Steeman et al., 2021) and *gata6* (Forward: AAACCTCAG AAGCGCATGTC; Reverse: AGACCACAGGCGTTGCAC) (Zeng et al., 2009) were obtained in the literature.

2.6 Cell culture

MDA-MB-231 (CRM-HTB-26™) triple negative breast cancer cell line and MCF7 (HTB-22™) breast cancer cell line were obtained from the American Type Cell Culture (ATCC). Cells were cultured in Dulbecco's Modified Eagle's Medium (DMEM) - high glucose, supplemented with 10% Fetal bovine serum and 1% penicillin/streptomycin. Cells were maintained in a humid atmosphere (95%), 5% of CO₂ and 37°C.

2.7 Cellular uptake

Internalization assays were performed on MDA-MB-231 cells to evaluate nanoemulsions labelled with sphingomyelin TopFluor® (4.5 µg/nanoemulsion). Cells were seeded on an 8-well chambered slide at 40,000 cell/well. After 24 h of incubation at 37°C, cells were washed with PBS and 200 µl of non-supplemented DMEM were added per well. Nanocarriers with and without associated miR-Cy5 were mixed in each well at a concentration of 0.2 mg/ml. Cells were incubated with the nanocarriers for 4 h at 37°C. After this time, cells were washed twice with PBS and fixed with 4% (w/v) paraformaldehyde for 15 min. Cells were again washed twice with PBS and cellular nuclei were stained with Hoechst (0.01 mg/ml in PBS) for 5 min in darkness at room temperature. After that, cells were washed 3 times for 5 min with PBS, which was aspirated after the last wash. Then, walls were removed and Mowiol® 4-88 was added for placing a coverslip; after that, samples were kept drying in darkness overnight. Uptake results were evaluated by confocal microscopy (SP8 Laser Microscope, Leica).

2.8 Zebrafish maintenance

Wildtype zebrafish embryos were maintained in E3 medium with 1-phenyl 2-thiourea (PTU) at 28.5°C. E3 is a saline medium composed by NaCl, KCl, CaCl₂ · 2H₂O and MgSO₄ (Murphey and Zon, 2006), traditionally used for maintaining the embryos, whereas PTU is a compound that inhibits the melanogenesis (Karlsson et al., 2001), maintaining the transparency of embryos for a longer time and avoiding the pigmentation, which could interfere later in confocal microscopy. PTU was only used in the assays evaluated by confocal imaging to improve the transparency of the embryos.

2.9 In vivo uptake

Nanoemulsions labelled with TopFluor were incubated with the embryos in a 96-well plate with a final volume of 100 µl per well, for 72 h at 34°C. The lipidic concentration used in these assays was 0.5 mg/ml and the concentration of TopFluor was 20 µg/ml.

Internalization was tested in three different conditions with at least 16 replicates per condition: Control (MilliQ water), PSN, PSN/miR, and PSN/pDNA (with Cy5-labelled miR and pDNA). Permeability was evaluated by confocal microscope after embryos suppression with tricaine overdose, fixation with paraformaldehyde 4% for 30 min, and wash with PBS twice.

Moreover, in the case of PSN and PSN/pDNA, mortality assessment was performed to evaluate the toxicity of the nanosystems. Embryos were evaluated each 24 h and mortality was observed.

2.10 Nanoemulsions biodistribution *in vivo*

To evaluate the biodistribution of nanoemulsions *in vivo*, 48 hpf zebrafish embryos were microinjected in the duct of Cuvier with TopFluor-labelled PSN (with and without Cy5-labelled miR/pDNA) previously concentrated 10 times by the SpeedVac Concentrator (Savant SPD111V-120, Cambridge Scientific, Massachusetts, United States). The microinjection was carried out with a binocular loupe (SMZ745, Nikon), the IM 300 Microinjector (Narishige, Tokyo, Japan), and needles made with the PC-10 Puller (Narishige, Tokyo, Japan) from glass capillaries (Harvard Apparatus, Massachusetts, United States). After 48 h from the microinjection, embryos were processed as explained in Section 2.9 and nanoemulsions biodistribution was evaluated by confocal microscopy.

2.11 Nanoemulsions behavior in xenografted zebrafish

In order to evaluate the behavior of the nanoemulsions in a metastatic-like *in vivo* environment, 48 hpf zebrafish embryos were xenografted with MDA-MB-231 cells, previously labelled with DiI. Cells were resuspended in PVP 2% and 200–300 cells were injected into the perivitelline space, as explained in Section 2.9. After 24 h, TopFluor-labelled PSN (with and without Cy5-labelled miR/pDNA), previously concentrated 10 times by the SpeedVac Concentrator, were microinjected into the Duct of Cuvier. *In vivo* behaviour and interaction between developed nanocarriers and cancer cells were evaluated by confocal microscopy subsequent to following the same protocol as explained in Section 2.9.

3 Results

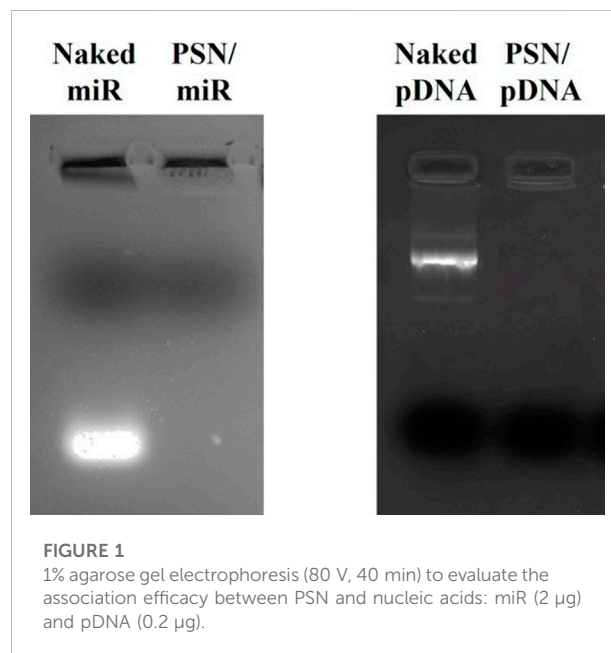
3.1 Nanoemulsions (PSN) characterization

In this work, we wanted to evaluate the potential of zebrafish to test novel gene nanotherapies, and for that purpose, we associated two different types of NAs to versatile PSN, namely miR and pDNA. To formulate the PSN, we followed the ethanol

TABLE 2 Physicochemical characterization of PSN with and without different miR associated by DLS and LDA.

Formulation	Length (bp)	Size (nm)	PdI	ZP (mV)
PSN	—	91 ± 6	0,23	+58 ± 6
PSN/miR control	21	123 ± 2	0,17	+45 ± 1
PSN/miR 145	23	108 ± 3	0,20	+40 ± 2
PSN/pDNA	6,717	164 ± 4	0,09	+44 ± 5

Abbreviations: PdI, polydispersity index; ZP, zeta potential.



injection method, as previously described (Bouzo et al., 2020; Lores et al., 2022). PSN have a mean size below 100 nm, a positive zeta potential (ZP) (around +60 mV) and a polydispersity index (PdI) of about 0.2 (Table 2), as determined by Dynamic Light Scattering (DLS) and Laser Doppler Anemometry (LDA).

The conditions for an efficient NA association preserving the colloidal properties of the nanocarriers were conveniently adjusted. As can be observed in Table 2, in all tested conditions, an increase in the hydrodynamic size and a decrease in the ZP were observed after the association of the NA, due to the interaction between their phosphate groups and the primary amines from the putrescine. Particularly, the association of the miR showed an increase in the size of around 30 nm. After the incubation with the pDNA, a higher increase in size was observed, which could be due to the higher molecular weight of the NA (near 7,000 bp compared to the 21–23 bp of the miRs). In both cases, the resulting changes in the physicochemical parameters suggest a successful association, as was shown in other works (Liu et al., 2016; Nagachinta et al., 2020). Moreover, the PdI remained below 0.2 after NAs

association, demonstrating that the PSN population is homogeneous. Even though these results indicate an efficient association of the NAs, an agarose gel electrophoresis was performed to provide additional evidence. (Figure 1). As observed, miR and pDNA were successfully retained in the well, as consequence of their interaction with PSN. Only naked NA molecules, loaded for control, freely moved in the gel.

Morover, in our previous work by Lores et al., PSN stability experiments were carried out. PSN stability under storage conditions, at 4°C, was evaluated, and the results demonstrate that they are stable for up to 21 days, according to the lack of variation in size, PDI, and ZP. Furthermore, the association between the pDNA and the PSN was studied and confirmed to remain stable by agarose gel electrophoresis. The conditions evaluated were the stability upon incubation with complete cellular medium, after incubation with DNases and after 3 months of storage at 4°C, demonstrating the high stability of the association as well as the protective role of PSN against DNases (Lores et al., 2022).

3.2 Transfection efficacy in the zebrafish embryo: *In vivo* effects of PSN/miR 145 in *sox9b* and *gata6* expression

The characterization of PNS demonstrates the correct association of different NAs, however, for the PNS to exert the desired therapeutic effect, a key factor is the release of the cargo inside the cells. In this sense, zebrafish embryos allow us to evaluate *in vivo* the transfection capacity of the NAs. As mentioned before, zebrafish compile characteristics that make them highly appropriate to evaluate gene therapies. In this specific case, embryo robustness, their external fecundation, and the ease with which they are genetically manipulated make zebrafish the ideal model for this kind of assessment.

With the aim of studying the correct release of the associated NAs inside the cells, miR 145 was chosen due to its effect on gene expression in the zebrafish embryo. This miR is known to downregulate *sox9b* and *gata6* genes when overexpressed in zebrafish (Zeng et al., 2009; Steeman et al., 2021). Embryos of 0 hpf, one-cell stage, were microinjected with PSN associated and non-associated with miR (Control and 145), and with free miR (Control and 145). The chosen stage to start the treatment was 0 hpf to potentially modulate the genes during the first cell division and avoid possible interference in successive stages. Furthermore, microinjection was the selected method to ensure the introduction of the PSN/miR 145 into zebrafish embryos.

In order to determine if the microinjected PSN miR145 or the free miR145 were able to modify *sox9b* and/or *gata6* expression, a RT-qPCR was performed 3 days later (72 hpf). In accordance with previous observations (Zeng et al., 2009; Steeman et al., 2021), miR145 increase led to a significant decrease in *sox9b* (*p*

value 0,0347) and *gata6* (*p* value 0,0364) expression but only when associated in PSN (Figure 2), and not when microinjected alone, in 72 hpf zebrafish embryos. Similarly, neither free miR control nor PSN alone nor PSN/miR control were able to modify their expression.

3.3 PSN/miR-pDNA *in vivo* uptake

Zebrafish is also characterized by being transparent in their first embryonic stages, and this fact allows us to evaluate fluorescent-labelled compounds as well as cells and nanoparticles (Gutiérrez-Lovera et al., 2017; Sieber, Grossen, Bussmann, et al., 2019). It is relevant that nanosystem internalization experiments based on incubation are easily performed in zebrafish embryos, however, this cannot be done in rodents, demonstrating the advantages of zebrafish as a model. Taking advance of this, an *in vivo* internalization assay was performed in 48 hpf embryos to study PSN behavior.

Cy5-labelled miR and pDNA were respectively associated with fluorescent PSN (labelled with TopFluor®-sphingomyelin). The use of zebrafish embryos for this type of assay allows us to easily incubate NA-loaded PSN in their media, in this case, 72 h. The results, which were obtained by confocal microscopy, demonstrated a high internalization by cells of the fluorescent PSN, and most importantly, allowed also to determine the presence of the associated NAs, miR and pDNA (Figure 3). Furthermore, experiments confirmed the co-localization (in cyan) of PSN (in green) and NAs (in blue) in an *in vivo* model with a superior level of complexity (Figure 3). This colocalization proves that PSN and NAs remain associated during the uptake process, allowing the efficient transport of NAs into the cells, which is a key step for successful gene therapy.

Furthermore, these uptake studies demonstrated the low toxicity of the nanocarriers (Supplementary Figure S1), producing less than 20% of mortality in the embryos.

3.4 PSN/miR-pDNA *in vivo* biodistribution

Following the same strategy of leveraging zebrafish embryo transparency, a PSN biodistribution assay was subsequently performed. Zebrafish transparency, which lasts until 24 hpf and can be extended with the use of PTU (Karlsson et al., 2001), allowed us to demonstrate the potential of PSN to be a carrier for gene therapy since we can monitor their stability and biodistribution in the circulatory system of the fish (Sieber, Grossen, Bussmann, et al., 2019).

For this purpose, 48 hpf embryos were microinjected in the Duct of Cuvier with the PNS, associated and non-associated with NAs (miR and pDNA), as well as free NAs. After 48 h of incubation, embryos were fixed and analyzed by confocal microscopy. The obtained results show the biodistribution

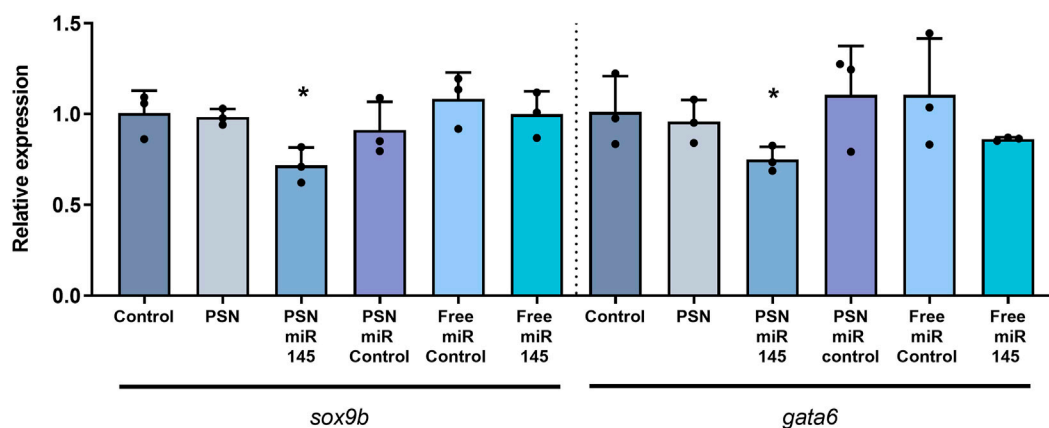


FIGURE 2

RT-qPCR results of the effect of miR 145 associated and non-associated with PSN in the relative expression of *sox9b* and *gata6* genes in zebrafish embryos.

of PSN along the zebrafish embryo body through the vasculature and their accumulation in the tail (Figure 4). In the case of PSN associated with NAs (PSN/miR and PSN/pDNA), it is observed that the association between NAs and nanocarriers after the microinjection in circulation is maintained *in vivo*. This maintenance is reflected by the cyan signal observed, which is a result of the co-localization of the green fluorescence of the nanosystems (with SM-TopFluor) and the blue fluorescence from the NAs (labelled with Cy5). Both PSN and PSN associated with NAs display an accumulation pattern that does not appear in the case of the naked miR and pDNA, which are spreading along the zebrafish body.

3.5 PSN/miR-pDNA *in vivo* interaction with cancer cells

Another zebrafish embryo property that makes it suitable as an *in vivo* model for gene therapy nanomedicine is the late activation of the immune system, which is not complete until 4–6 wpf (Lam et al., 2004). This allows us to perform xenotransplantation of cancer cells without the necessity of using genetically engineered immunodeficient *in vivo* models. Furthermore, the use of fluorescent-labelled cells, as well as fluorescent PSN and NAs, allows to evaluate how they behave in an *in vivo* tumor-like environment and how they interact with cancer cells.

Zebrafish embryos of 48 hpf were microinjected in the Duct of Cuvier with MDA-MB-231 cells, previously labelled with DiI. The result of this injection was a metastasis-like environment with cancer cells spread in the tail of the embryos, a key milieu to evaluate PSN interactions with cancer cells. Twenty-four hours

after the xenograft, PSN with SM-TopFluor, associated and non-associated Cy5-NAs, were microinjected in the Duct of Cuvier. Forty-eight hours post-PSN injection, embryos were scanned by confocal microscopy. The results show that the fluorescent signal of the NAs (in blue) co-localize with the PSN (in green), corroborating the results obtained in the biodistribution assay (Figure 5). Further to this, it is observed some co-localization of the fluorescence signal of the PSN (with and without associated NAs) with the fluorescence of cancer cells; whereas free nucleic acids do not show any signal overlapping with the cancer cells. It is also important to highlight that the association between the carrier and the NA is stable 48 h after the microinjection, along the zebrafish circulatory, verifying the stability of the NA-loaded PSN.

4 Discussion

Even though zebrafish is widely used as a model to evaluate therapies for cancer treatment (Cascallar et al., 2022; Kwiatkowska et al., 2022), its use to develop and validate innovative gene therapy nanomedicines has not yet been fully investigated. With this aim, this work was carried out to demonstrate the potential of zebrafish as a key model in the study of new gene therapies based on nanotechnology.

Zebrafish is an interesting *in vivo* platform that allows us to perform assays that cannot easily be performed with other *in vivo* model systems, such as rodents. Probably, the most characteristic feature of zebrafish is the transparency present in the embryonic stages (Lieschke & Currie, 2007a; Sieber, Grossen, Bussmann, et al., 2019). As mentioned before, transparency allows the simple visualization of fluorescently labelled molecules, cells, and nanoparticles (Gutiérrez-Lovera

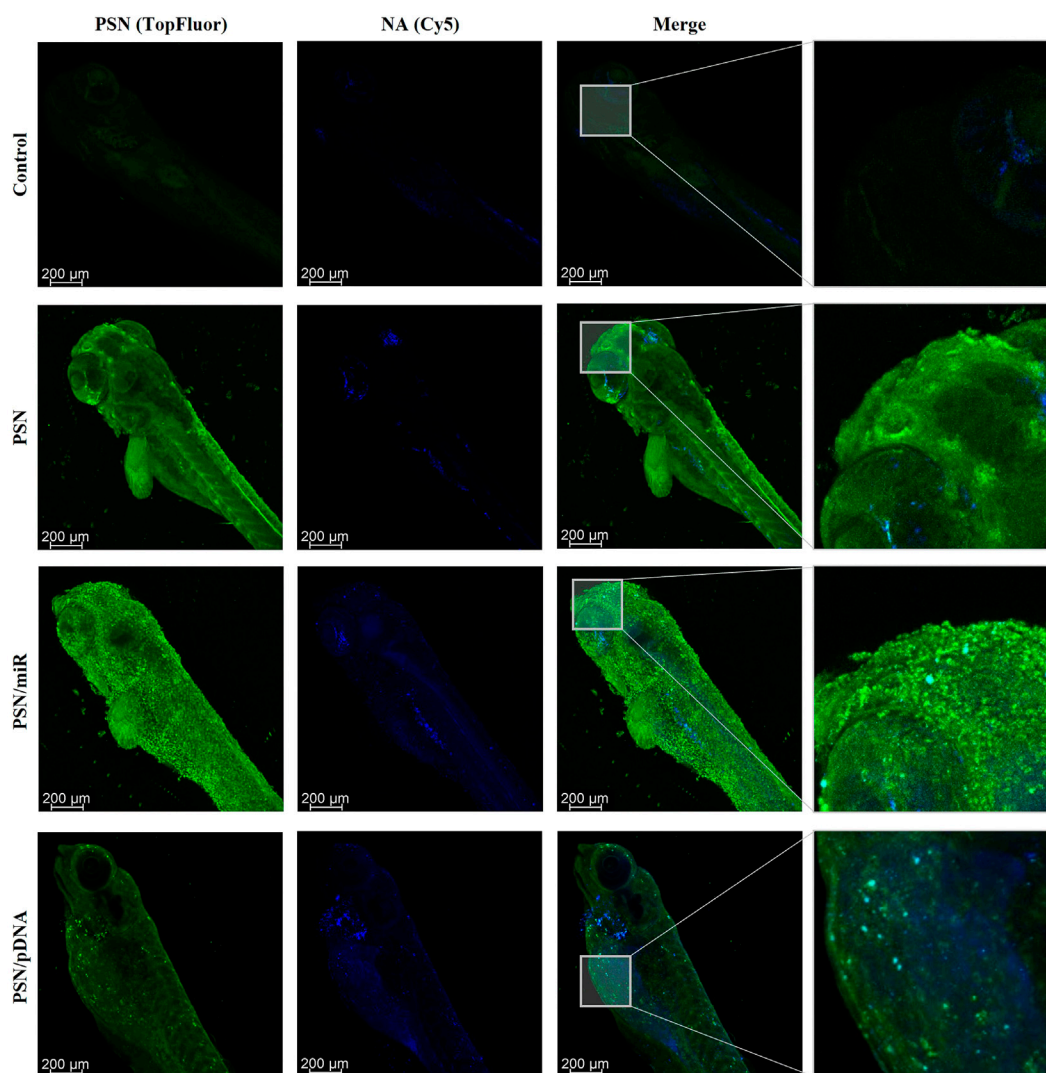


FIGURE 3

Confocal images of zebrafish embryos after a 72 h incubation with TopFluor-PSN (in green) associated and non-associated with Cy5-labelled miR and pDNA (in blue).

et al., 2017; Sieber, Grossen, Bussmann, et al., 2019). This advantage, in synergy with fluorescence/confocal microscopy, permits *in vivo* monitoring of specific structures, such as nanoparticles. As a result, we were able not only to observe how PNS behave *in vivo*, and how they interact with cancer cells, but also to confirm their stability and the maintenance of the association with NAs in an environment similar to that of patients. Our results are in line with several publications that use zebrafish as a model to evaluate nanomedicines (not for gene therapy purposes) and demonstrate how zebrafish can be used to evaluate novel cationic lipidic nanoemulsions *in vivo* with associated NAs (Sieber, Grossen, Bussmann, et al., 2019; Saez Talens et al., 2020; Rességuier et al., 2021; Cascallar et al., 2022).

Although zebrafish transparency plays a key role in carrying out these types of assays, this is not the only interesting advantage of this model system. Both embryos and adults have a small size and can be easily stored and maintained. This characteristic allows cost-effective, large scale assays with a large number of specimens, with enough replicates to validate the experiments (Lieschke & Currie, 2007b; Delvecchio et al., 2011; Veinotte et al., 2014). These types of assays are inconceivable in mice, considering the high maintenance cost and the small number of progeny (Veinotte et al., 2014). In addition, zebrafish genome has a great homology with the human genome, and the body with several vertebrate structures (Lieschke & Currie, 2007b; Delvecchio et al., 2011).

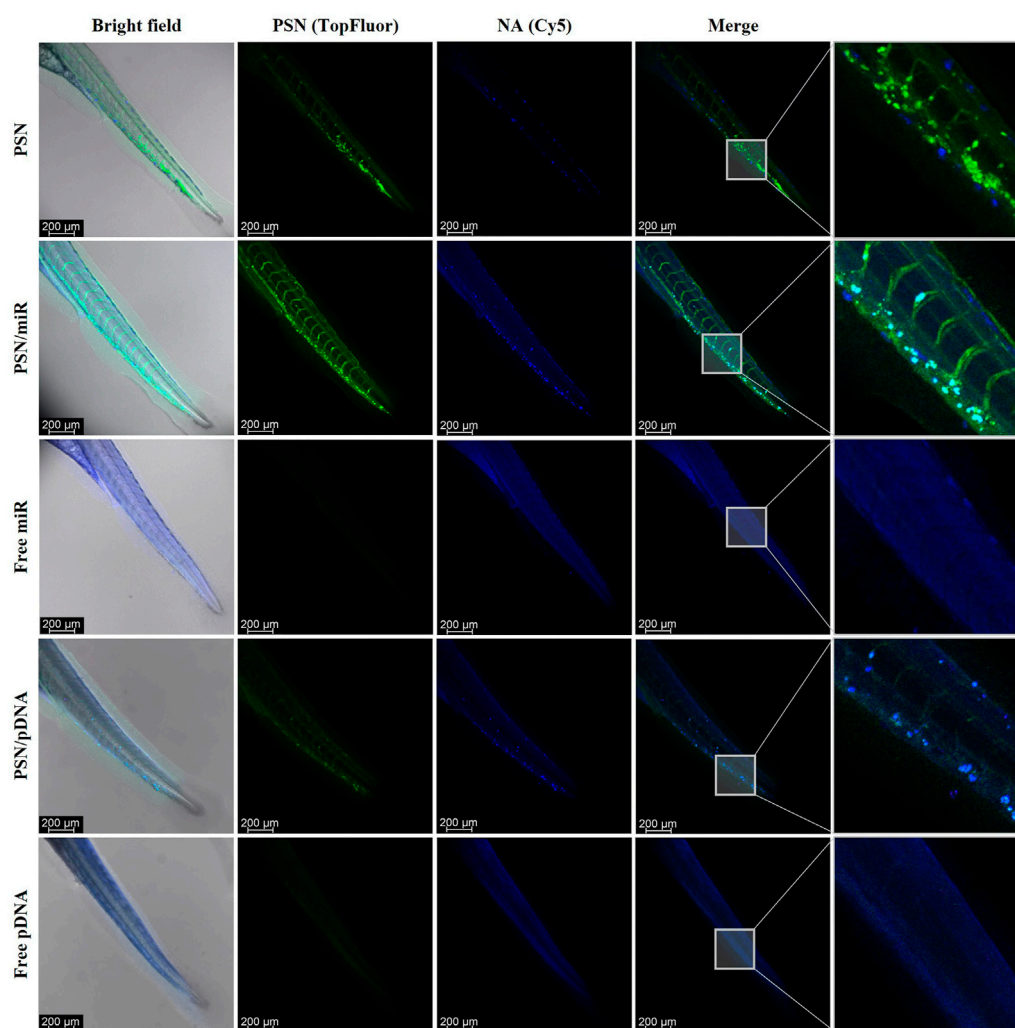


FIGURE 4

Confocal images of *in vivo* biodistribution of TopFluor-labelled nanoemulsions (green) with and without miR-Cy5 and pDNA (blue), after 48 h incubation in microinjected 48 hpf zebrafish embryos.

Certainly, zebrafish embryo has several advantages that make it suitable as a model platform to evaluate cancer nanotechnology-based therapies, resulting in a plethora of diverse experiments that can be done to optimize and select the best treatments. However, it also has limitations in terms of similarity with humans. For instance, the lack of the physiological complexity of a non-mammalian organism implies the need to combine the zebrafish with other models, such as mice and rats, in certain types of experiments. However, in the context of animal welfare, combining the use of zebrafish embryo with more complex models may help to implement the 3R's rule: replace, reduce, and refine (MacArthur Clark, 2018; Lewis, 2019). Because the zebrafish is an intermediate model between cell cultures and rodents, all experiments that can be performed in zebrafish

models would inversely affect the number of mice that will be needed in subsequent experiments.

Our group has previously developed a new type of cationic nanosystems composed by Vitamin E, Sphingomyelin and a Putrescine derivative, PSN (Lores et al., 2022). This formulation is an optimization of previous sphingomyelin nanosystems (Bouzo et al., 2020; Nagachinta et al., 2020; Bidan et al., 2022), for cancer gene therapy applications, taking advantage of the intrinsic properties of putrescine. Among others, putrescine provides a cationic charge that can establish electrostatic interactions with negative-charged molecules such as NAs (Rowe et al., 2009; Chakraborty and Jiang, 2013; Agostinelli et al., 2015). In addition, cancer cells show a higher affinity for putrescine compared to normal cells, in order to maintain their metabolic activities, in which natural

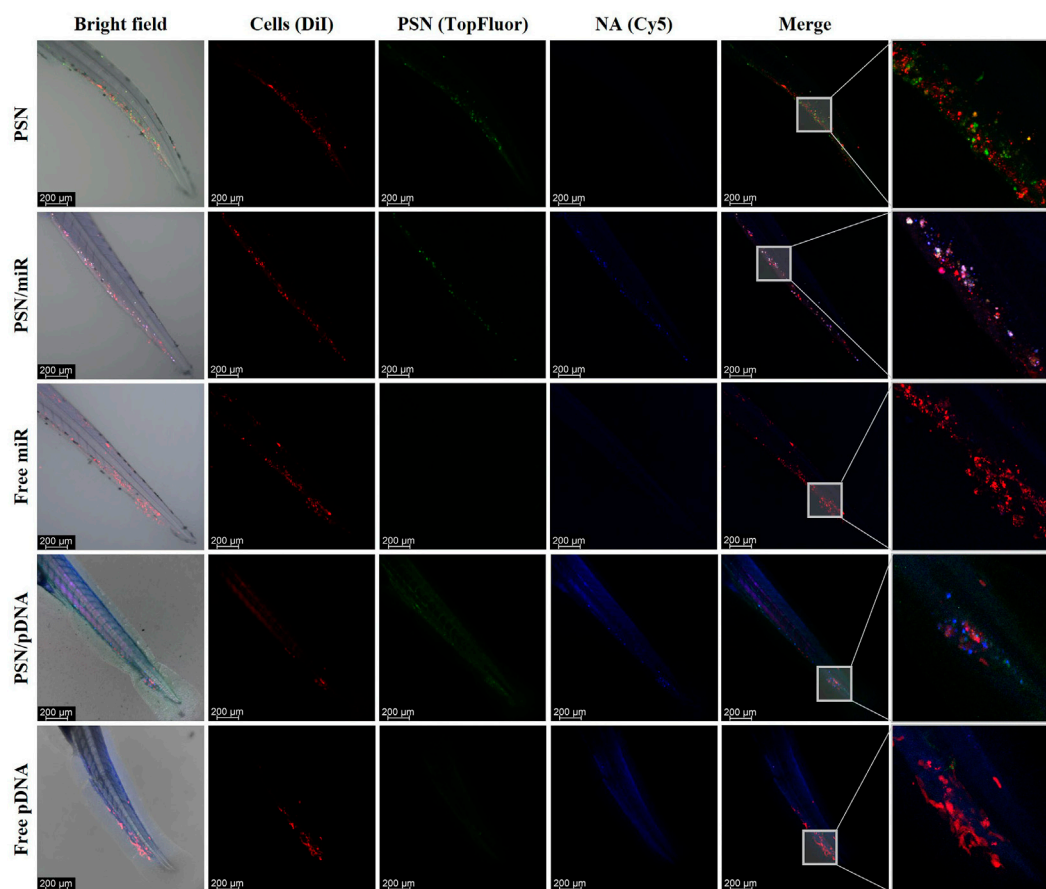


FIGURE 5

Images of the *in vivo* interaction between nanoemulsions, labelled with TopFluor (green), and associated and non-associated miR and pDNA Cy5-labelled (blue) with DiI-MDA-MB-231 cancer cells (red), by confocal microscopy.

polyamines are involved (Tracy et al., 2016; Casero et al., 2018). Our previous results show the potential of PSN to efficiently carry anti-cancer therapeutic pDNA, achieving a therapeutic effect in cell culture. Most importantly, the results show a tumor reduction in murine models of cancer, which correlates with the reduction previously observed in xenografted zebrafish embryos (Lores et al., 2022).

Furthermore, the experiments performed in the present work allowed us to validate the adaptability of our PSN cationic nanoemulsions (Lores et al., 2022). PSN demonstrated to be an innovative carrier for gene therapy showing a high versatility due to their ability to carry different types of NAs, not only with a huge difference in length but also with different nature, desoxyribonucleic (pDNA) and ribonucleic acids (miR). Moreover, results obtained in 0 hpf embryos confirmed that miR145 is able to develop its regulatory role in zebrafish genes when associated with nanoemulsions; and therefore, the PSN are capable of releasing their cargo inside the cell. This fact

highlights the potential of zebrafish to study the transfection efficiency of gene delivery nanosystems. It is important to emphasize that this type of experiment, with 0 hpf embryos, cannot be performed in the common models used in experimentation, such as mice and rats. These models, with higher complexity, have internal fertilization, thus this assay becomes complicated by the need to perform *in vitro* fecundation.

The accumulation of PSN observed in tumor cells could be related to the incorporation of putrescine and the fact that polyamine uptake is increased in cancer cells through Polyamine Transport Systems (Novita Sari et al., 2021). Importantly, we observed that PSN were stable in an *in vivo* environment, maintaining an efficient association of the NAs, which were then successfully released inside the cells. This proved the ability of putrescine to protect the NAs against *in vivo* barriers due to its capacity to condense nucleic acids achieving an improvement in the transport inside the cells

(Thomas et al., 2016). In this sense, zebrafish allow us to observe/visualize the interaction of PSN with cancer cells in a more complex system than the one represented by a cell culture since different cell types from the tumor environment are present in the fish. Interaction studies verified that PSN/miR-pDNA are able to travel along the embryos and reach the cancer cells. These results corroborate the ones observed in uptakes performed in cancer cell lines, demonstrating that the PSN interaction with cancer cells happens both *in vitro* and *in vivo* (Supplementary Figures S2,S3). In other words, these results confirm that we have developed an efficient and stable nanocarrier able to transport its cargo to the cancer cells. Furthermore, the working times between cell cultures and zebrafish embryos are quite similar, obtaining more complex and reliable results.

In conclusion, our results demonstrate the huge potential that zebrafish embryos have as an *in vivo* platform to evaluate nanomedicines for gene therapy in a fast, cost-effective and reliable way in contrast with other animal models. In the same vein, the experiments presented here validated the capacity of PSN to successfully associate and transport different types of NAs into a living organism.

Data availability statement

The original contributions presented in the study are included in the article/Supplementary Material, further inquiries can be directed to the corresponding author.

Author contributions

Conceptualization, MC, PH, LS, RP, and MF; writing—original draft preparation, MC, SL, and AP-L; writing—review and writing, MC, PH, SL, AP-L, LS, RP, and MF; experiments conduction, MC, PH, SL, AP-L, and AQ-R; supervision, RP and MF; funding acquisition, RP and MF.

Funding

This research was funded by the Instituto de Salud Carlos IIIISCIII and the European Regional Development Fund (FEDER) (AC18/00107, AC18/00045, PI18/00176); by the ERA-NET EURONANOMED III project METASTARG

References

Agostinelli, E., Vianello, F., Magliulo, G., Thomas, T., and Thomas, T. J. (2015). Nanoparticle strategies for cancer therapeutics: Nucleic acids, polyamines, bovine serum amine oxidase and iron oxide nanoparticles (Review). *Int. J. Oncol.* 46 (1), 5–16. doi:10.3892/ijo.2014.2706

(Grant Number JTC 2018-045) and the ERA-NET EURONANOMED III project PANIPAC (Grant Number JTC 2018/041); and by Axencia Galega de Innovación (GAIN), Consellería de Economía, Emprego e Industria (IN607B2021/14). RP was supported by Roche-Chus Joint Unit (IN853B 2018/03) funded by Axencia Galega de Innovación (GAIN), Consellería de Economía, Emprego e Industria. SL, PH, and AP-L. were funded by a Predoctoral fellowship (IN606A-2019/003, IN606A-2018/019 and ED481A-2018/095) from Axencia Galega de Innovación (GAIN, Xunta de Galicia).

Acknowledgments

We gratefully thank Miguel Ramallo for his help in the *in vitro* experiments; and Marta Picado and Monserrat García for their support in confocal microscopy.

Conflict of interest

Author MD is the co-founder of the company DIVERSA Technologies S.L.

The remaining authors declare that the research was conducted in the absence of any commercial or financial relationships that could be construed as a potential conflict of interest.

Publisher's note

All claims expressed in this article are solely those of the authors and do not necessarily represent those of their affiliated organizations, or those of the publisher, the editors and the reviewers. Any product that may be evaluated in this article, or claim that may be made by its manufacturer, is not guaranteed or endorsed by the publisher.

Supplementary material

The Supplementary Material for this article can be found online at: <https://www.frontiersin.org/articles/10.3389/fphar.2022.1007018/full#supplementary-material>

Akinc, A., Maier, M. A., Manoharan, M., Fitzgerald, K., Jayaraman, M., Barros, S., et al. (2019). The Onpatro story and the clinical translation of nanomedicines containing nucleic acid-based drugs. *Nat. Nanotechnol.* 14 (12), 1084–1087. doi:10.1038/s41565-019-0591-y

- Al-Thani, H. F., Shurbaji, S., and Yalcin, H. C. (2021). Zebrafish as a model for anticancer nanomedicine studies. *Pharmaceutics* 14 (7), 625. doi:10.3390/PH14070625
- Altschul, S. F., Gish, W., Miller, W., Myers, E. W., and Lipman, D. J. (1990). Basic local alignment search tool. *J. Mol. Biol.* 215 (3), 403–410. doi:10.1016/S0022-2836(05)80360-2
- Amer, M. H. (2014). Gene therapy for cancer: Present status and future perspective. *Mol. Cell. Ther.* 2 (1), 27. doi:10.1186/2052-8426-2-27
- Bidan, N., Lores, S., Vanhecke, A., Nicolas, V., Domenichini, S., López, R., et al. (2022). Before *in vivo* studies: *In vitro* screening of sphingomyelin nanosystems using a relevant 3D multicellular pancreatic tumor spheroid model. *Int. J. Pharm.*, 617. doi:10.1016/j.ijpharm.2022.121577
- Boix-Montesinos, P., Soriano-Teruel, P. M., Armiñán, A., Orzáez, M., and Vicent, M. J. (2021). The past, present, and future of breast cancer models for nanomedicine development. *Adv. Drug Deliv. Rev.* 173, 306–330. doi:10.1016/J.ADDR.2021.03.018
- Bouzo, B. L., Calvelo, M., Martín-Pastor, M., García-Fandiño, R., and de La Fuente, M. (2020). *In vitro*-in silico modeling approach to rationally designed simple and versatile drug delivery systems. *J. Phys. Chem. B* 124 (28), 5788–5800. doi:10.1021/acs.jpcc.0c02731
- Cascallar, M., Alijas, S., Pensado-López, A., Vázquez-Ríos, A. J., Sánchez, L., Piñero, R., et al. (2022). What zebrafish and nanotechnology can offer for cancer treatments in the age of personalized medicine. *Cancers* 14 (9), 2238. doi:10.3390/CANCERS14092238
- Casero, R. A., Murray Stewart, T., and Pegg, A. E. (2018). Polyamine metabolism and cancer: Treatments, challenges and opportunities. *Nat. Rev. Cancer* 18 (11), 681. doi:10.1038/S41568-018-0050-3
- Corbett, K. S., Edwards, D. K., Leist, S. R., Abiona, O. M., Boyoglu-Barnum, S., Gillespie, R. A., et al. (2020). SARS-CoV-2 mRNA vaccine design enabled by prototype pathogen preparedness. *Nature* 586 (7830), 567–571. doi:10.1038/s41586-020-2622-0
- Delvecchio, C., Tiefenbach, J., and Krause, H. M. (2011). The zebrafish: A powerful platform for *in vivo*, hts drug discovery. *Assay. Drug Dev. Technol.* 9 (4), 354–361. doi:10.1089/adt.2010.0346
- Ellett, F., Pase, L., Hayman, J. W., Andrianopoulos, A., and Lieschke, G. J. (2011). mpeg1 promoter transgenes direct macrophage-lineage expression in zebrafish. *Blood* 117 (4), e49–e56. doi:10.1182/BLOOD-2010-10-314120
- Gutiérrez-Lovera, C., Vázquez-Ríos, A. J., Guerra-Varela, J., Sánchez, L., and de la Fuente, M. (2017). The potential of zebrafish as a model organism for improving the translation of genetic anticancer nanomedicines. *Genes* 8, 349. doi:10.3390/genes8120349
- Horzmann, K. A., and Freeman, J. L. (2018). Making waves: New developments in toxicology with the zebrafish. *Toxicol. Sci.* 163 (1), 5–12. doi:10.1093/TOXSCI/KFY044
- Howe, K., Clark, M. D., Torroja, C. F., Torrance, J., Berthelot, C., Muffato, M., et al. (2013). The zebrafish reference genome sequence and its relationship to the human genome. *Nature* 496 (7446), 498–503. doi:10.1038/nature12111
- Hoy, S. M. (2018). Patisiran: First global approval. *Drugs* 78 (15), 1625–1631. doi:10.1007/S40265-018-0983-6
- Jia, H. R., Zhu, Y. X., Duan, Q. Y., Chen, Z., and Wu, F. G. (2019). Nanomaterials meet zebrafish: Toxicity evaluation and drug delivery applications. *J. Control. Release* 311–312, 301–318. Elsevier. doi:10.1016/j.jconrel.2019.08.022
- Karlsson, J., von Hofsten, J., and Olsson, P. E. (2001). Generating transparent zebrafish: A refined method to improve detection of gene expression during embryonic development. *Mar. Biotechnol.* 3 (6), 522–527. doi:10.1007/s1012601-0053-4
- Kimmel, C. B., Ballard, W. W., Kimmel, S. R., Ullmann, B., and Schilling, T. F. (1995). Stages of embryonic development of the zebrafish. *Dev. Dyn.* 203 (3), 253–310. doi:10.1002/AJA.1002030302
- Kwiatkowska, I., Hermanowicz, J. M., Iwinska, Z., Kowalczyk, K., Iwanowska, J., and Pawlak, D. (2022). Zebrafish—an optimal model in experimental oncology. *Molecules* 27 (13), 4223. doi:10.3390/MOLECULES27134223
- Lam, S. H., Chua, H. L., Gong, Z., Lam, T. J., and Sin, Y. M. (2004). Development and maturation of the immune system in zebrafish, *Danio rerio*: A gene expression profiling, *in situ* hybridization and immunological study. *Dev. Comp. Immunol.* 28 (1), 9–28. doi:10.1016/S0145-305X(03)00103-4
- Lawson, N. D., and Weinstein, B. M. (2002). *In vivo* imaging of embryonic vascular development using transgenic zebrafish. *Dev. Biol.* 248 (2), 307–318. doi:10.1006/DBIO.2002.0711
- Lee, K. Y., Jang, G. H., Byun, C. H., Jeun, M., Searson, P. C., and Lee, K. H. (2017). Zebrafish models for functional and toxicological screening of nanoscale drug delivery systems: Promoting preclinical applications. *Biosci. Rep.* 37 (3), BSR20170199–13. doi:10.1042/BSR20170199
- Lewis, D. I. (2019). Animal experimentation: Implementation and application of the 3Rs. *Emerg. Top. Life Sci.* 3 (6), 675–679. doi:10.1042/ETLS20190061
- Lieschke, G. J., and Currie, P. D. (2007a). Animal models of human disease: Zebrafish swim into view. *Nat. Rev. Genet.* 8 (5), 353–367. doi:10.1038/nrg2091
- Lieschke, G. J., and Currie, P. D. (2007b). Animal models of human disease: Zebrafish swim into view. *Nat. Rev. Genet.* 8 (5), 353–367. Nature Publishing Group. doi:10.1038/nrg2091
- Liu, J., Meng, T., Yuan, M., Wen, L. J., Cheng, B. L., Liu, N., et al. (2016). MicroRNA-200c delivered by solid lipid nanoparticles enhances the effect of paclitaxel on breast cancer stem cell. *Int. J. Nanomedicine* 11, 6713–6725. doi:10.2147/IJN.S111647
- Lores, S., Gámez-Chiachio, M., Cascallar, M., Ramos-Nebot, C., Hurtado, P., Alijas, S., et al. (2022). Effectiveness of a novel gene nanotherapy based on putrescine for cancer treatment. Submitted: Biomaterials Science.
- MacArthur Clark, J. (2018). The 3Rs in research: A contemporary approach to replacement, reduction and refinement. *Br. J. Nutr.* 120 (1), S1–S7. doi:10.1017/S0007114517002227
- Mohammadinejad, R., Dehshahri, A., Sagar Madamsetty, V., Zahmatkeshan, M., Tavakol, S., Makvandi, P., et al. (2020). *In vivo* gene delivery mediated by non-viral vectors for cancer therapy. *J. Control. Release* 325, 249–275. doi:10.1016/j.jconrel.2020.06.038
- Murphy, R. D., and Zon, L. I. (2006). Small molecule screening in the zebrafish. *Methods* 39 (3), 255–261. doi:10.1016/J.YMETH.2005.09.019
- Nagachinta, S., Bouzo, B. L., Vazquez-Rios, A. J., Lopez, R., and de la Fuente, M. (2020). Sphingomyelin-based nanosystems (SNs) for the development of anticancer miRNA therapeutics. *Pharmaceutics* 12 (2), E189. doi:10.3390/pharmaceutics12020189
- Novita Sari, I., Setiawan, T., Seock Kim, K., Toni Wijaya, Y., Won Cho, K., and Young Kwon, H. (2021). Metabolism and function of polyamines in cancer progression. *Cancer Lett.* 519, 91–104. doi:10.1016/J.CANLET.2021.06.020
- Pearce, M. C., Gamble, J. T., Kopparapu, P. R., O'Donnell, E. F., Mueller, M. J., Jang, H. S., et al. (2018). Induction of apoptosis and suppression of tumor growth by Nur77-derived Bcl-2 converting peptide in chemoresistant lung cancer cells. *Oncotarget* 9 (40), 26072–26085. doi:10.18632/oncotarget.25437
- Pensado-López, A., Fernández-Rey, J., Reimunde, P., Crecente-Campo, J., Sánchez, L., and Torres Andón, F. (2021). Zebrafish models for the safety and therapeutic testing of nanoparticles with a focus on macrophages. *Nanomaterials* 11 (7), 1784. doi:10.3390/NANO11071784
- Polack, F. P., Thomas, S. J., Kitchin, N., Absalon, J., Gurtman, A., Lockhart, S., et al. (2020). Safety and efficacy of the BNT162b2 mRNA covid-19 vaccine. *N. Engl. J. Med.* 383 (27), 2603–2615. doi:10.1056/nejmoa2034577
- Reimondez-Troitiño, S., González-Aramundiz, J. v., Ruiz-Bañobre, J., López-López, R., Alonso, M. J., Csaba, N., et al. (2019). Versatile protamine nanocapsules to restore miR-145 levels and interfere tumor growth in colorectal cancer cells. *Eur. J. Pharm. Biopharm.* 142, 449–459. doi:10.1016/j.ejpb.2019.07.016
- Renshaw, S. A., Loynes, C. A., Trushell, D. M. I., Elworthy, S., Ingham, P. W., and Whyte, M. K. B. (2006). A transgenic zebrafish model of neutrophilic inflammation. *Blood* 108 (13), 3976–3978. doi:10.1182/BLOOD-2006-05-024075
- Rességuier, J., Levraud, J. P., Dal, N. K., Fenaroli, F., Primard, C., Wohlmann, J., et al. (2021). Biodistribution of surfactant-free poly(lactic-acid) nanoparticles and uptake by endothelial cells and phagocytes in zebrafish: Evidence for endothelium to macrophage transfer. *J. Control. Release* 331, 228–245. doi:10.1016/J.JCONREL.2021.01.006
- Rowe, R., Sheskey, P., and Quinn, M. (2009). *Handbook of pharmaceutical excipients*. <http://repositorio.ub.edu.ar/handle/123456789/5143>.
- Saez Talens, V., Arias-Alpizar, G., Makurat, D. M. M., Davis, J., Bussmann, J., Kros, A., et al. (2020). Stab2-Mediated clearance of supramolecular polymer nanoparticles in zebrafish embryos. *Biomacromolecules* 21 (3), 1060–1068. doi:10.1021/acs.biomac.9b01318
- Sahlgren, C., Meinander, A., Zhang, H., Cheng, F., Preis, M., Xu, C., et al. (2017). Tailored approaches in drug development and diagnostics: From molecular design to biological model systems. *Adv. Healthc. Mat.* 6 (21), 1700258. doi:10.1002/adhm.201700258
- Santiago-Ortiz, J. L., and Schaffer, D. V. (2016). Adeno-associated virus (AAV) vectors in cancer gene therapy. *J. Control. Release* 240, 287–301. doi:10.1016/j.jconrel.2016.01.001
- Saraiva, S. M., Gutiérrez-Lovera, C., Martínez-Val, J., Lores, S., Bouzo, B. L., Díez-Villares, S., et al. (2021). Edelfosine nanoemulsions inhibit tumor growth of triple

negative breast cancer in zebrafish xenograft model. *Sci. Rep.* 11 (1), 9873. doi:10.1038/S41598-021-87968-4

Sayed, N., Allawadhi, P., Khurana, A., Singh, V., Navik, U., Pasumarthi, S. K., et al. (2022). Gene therapy: Comprehensive overview and therapeutic applications. *Life Sci.* 294. Elsevier Inc. doi:10.1016/j.lfs.2022.120375

Sieber, S., Grossen, P., Busmann, J., Campbell, F., Kros, A., Witzigmann, D., et al. (2019). Zebrafish as a preclinical *in vivo* screening model for nanomedicines. *Adv. Drug Deliv. Rev.* 151, 152–168. Elsevier. doi:10.1016/j.addr.2019.01.001

Sieber, S., Grossen, P., Uhl, P., Detampel, P., Mier, W., Witzigmann, D., et al. (2019). Zebrafish as a predictive screening model to assess macrophage clearance of liposomes *in vivo*. *Nanomedicine* 17, 82–93. doi:10.1016/j.nano.2018.11.017

Sipes, N. S., Padilla, S., and Knudsen, T. B. (2011). Zebrafish—as an integrative model for twenty-first century toxicity testing. *Birth Defects Res. C Embryo Today* 93 (3), 256–267. doi:10.1002/BDRC.20214

Steeman, T. J., Rubiolo, J. A., Sánchez, L. E., Calcaterra, N. B., and Weiner, A. M. J. (2021). Conservation of zebrafish miRNA-145 and its role during neural crest cell development. *Genes* 12 (7), 1023. doi:10.3390/genes12071023

Streisinger, G., Walker, C., Dower, N., Knauber, D., and Singer, F. (1981). Production of clones of homozygous diploid zebra fish (*Brachydanio rerio*). *Nature* 291 (5813), 293–296. doi:10.1038/291293a0

Thomas, T. J., Tajmir-Riahi, H. A., and Thomas, T. (2016). Polyamine–DNA interactions and development of gene delivery vehicles. *Amino Acids* 48 (10), 2423–2431. doi:10.1007/s00726-016-2246-8

Tracy, R. M. S., Woster, P. M., and Casero, R. A. (2016). Targeting polyamine metabolism for cancer therapy and prevention. *Biochem. J.* 473 (19), 2937–2953. doi:10.1042/BCJ20160383

Veinotte, C. J., Delaire, G., and Berman, J. N. (2014). Hooking the big one: The potential of zebrafish xenotransplantation to reform cancer drug screening in the genomic era. *Dis. Model. Mech.* 7 (7), 745–754. doi:10.1242/dmm.015784

Walther, W., Drugs, U. S., and Stein, U. (2000). Viral vectors for gene transfer: A review of their use in the treatment of human diseases. *Drugs* 60 (2), 249–271. doi:10.2165/00003495-200060020-00002

Wang, F., Wang, X., Gao, L., Meng, L. Y., Xie, J. M., Xiong, J. W., et al. (2019). Nanoparticle-mediated delivery of siRNA into zebrafish heart: A cell-level investigation on the biodistribution and gene silencing effects. *Nanoscale* 11 (39), 18052–18064. doi:10.1039/C9NR05758G

Wick, P., Chortarea, S., Guenat, O. T., Roeslein, M., Stucki, J. D., Hirn, S., et al. (2015). *In vitro-ex vivo* model systems for nanosafety assessment. *Eur. J. Nanomedicine* 7 (3), 169–179. doi:10.1515/ejnm-2014-0049

Zeng, L., Carter, A. D., and Childs, S. J. (2009). miR-145 directs intestinal maturation in zebrafish. *Proc. Natl. Acad. Sci. U. S. A.* 106 (42), 17793–17798. doi:10.1073/PNAS.0903693106/SUPPL_FILE/0903693106SI

Zon, L. I. (1999). Zebrafish: A new model for human disease: Figure 1. *Genome Res.* 9 (2), 99–100. doi:10.1101/GR.9.2.99

Zu, H., and Gao, D. (2021). Non-viral vectors in gene therapy: Recent development, challenges, and prospects. *Nat. Publ. Group* 23, 78. doi:10.1208/s12248-021-00608-7



OPEN ACCESS

EDITED BY

Serban Morosan,
INSERM US28 Phénotypage du Petit
Animal, France

REVIEWED BY

Gabrielle Christine Musk,
University of Western
Australia, Australia
Laura Calza,
University of Bologna, Italy

*CORRESPONDENCE

André Bleich
bleich.andre@mh-hannover.de

[†]These authors share first authorship

[‡]These authors share senior authorship

SPECIALTY SECTION

This article was submitted to
Animal Behavior and Welfare,
a section of the journal
Frontiers in Veterinary Science

RECEIVED 06 May 2022

ACCEPTED 24 October 2022

PUBLISHED 11 November 2022

CITATION

Talbot SR, Struve B, Wassermann L,
Heider M, Weegh N, Knape T,
Hofmann MCJ, von Knethen A,
Jirkof P, Häger C and Bleich A (2022)
RELSA—A multidimensional procedure
for the comparative assessment of
well-being and the quantitative
determination of severity in
experimental procedures.
Front. Vet. Sci. 9:937711.
doi: 10.3389/fvets.2022.937711

COPYRIGHT

© 2022 Talbot, Struve, Wassermann,
Heider, Weegh, Knape, Hofmann, von
Knethen, Jirkof, Häger and Bleich. This
is an open-access article distributed
under the terms of the [Creative
Commons Attribution License \(CC BY\)](#).
The use, distribution or reproduction
in other forums is permitted, provided
the original author(s) and the copyright
owner(s) are credited and that the
original publication in this journal is
cited, in accordance with accepted
academic practice. No use, distribution
or reproduction is permitted which
does not comply with these terms.

RELSA—A multidimensional procedure for the comparative assessment of well-being and the quantitative determination of severity in experimental procedures

Steven R. Talbot^{1†}, Birgitta Struve^{1†}, Laura Wassermann^{1†},
Miriam Heider¹, Nora Weegh¹, Tilo Knape²,
Martine C. J. Hofmann², Andreas von Knethen^{2,3}, Paulin Jirkof⁴,
Christine Häger^{1†} and André Bleich^{1*†}

¹Institute for Laboratory Animal Science and Central Animal Facility, Hannover Medical School, Hanover, Germany, ²Fraunhofer Institute for Translational Medicine and Pharmacology (ITMP), Frankfurt, Germany, ³Department of Anaesthesiology, Intensive Care Medicine and Pain & Therapy, University Hospital Frankfurt, Frankfurt, Germany, ⁴Office for Animal Welfare and 3Rs, University of Zurich, Zurich, Switzerland

Good science in translational research requires good animal welfare according to the principles of 3Rs. In many countries, determining animal welfare is a mandatory legal requirement, implying a categorization of animal suffering, traditionally dominated by subjective scorings. However, how such methods can be objectified and refined to compare impairments between animals, subgroups, and animal models remained unclear. Therefore, we developed the RELative Severity Assessment (RELSA) procedure to establish an evidence-based method based on quantitative outcome measures such as body weight, burrowing behavior, heart rate, heart rate variability, temperature, and activity to obtain a relative metric for severity comparisons. The RELSA procedure provided the necessary framework to get severity gradings in TM-implanted mice, yielding four distinct RELSA thresholds L1<0.27, L2<0.59, L3<0.79, and L4<3.45. We show further that severity patterns in the contributing variables are time and model-specific and use this information to obtain contextualized *between* animal-model and subgroup comparisons with the severity of sepsis > surgery > restraint stress > colitis. The bootstrapped 95% confidence intervals reliably show that RELSA estimates are conditionally invariant against missing information but precise in ranking the quantitative severity information to the moderate context of the transmitter-implantation model. In conclusion, we propose the RELSA as a validated tool for an objective, computational

approach to comparative and quantitative severity assessment and grading. The RELSA procedure will fundamentally improve animal welfare, data quality, and reproducibility. It is also the first step toward translational risk assessment in biomedical research.

KEYWORDS

severity assessment, laboratory animal, animal welfare, data science, animal experiments, sepsis model, colitis model, surgical models

Introduction

Good science and high-quality data from animal experiments in basic and translational research require good animal welfare. Consequently, researchers are obligated to ensure the best possible welfare of their research animals, in line with the refinement principle in the 3Rs (1, 2). Therefore, the determination of laboratory animal welfare is embedded in many international animal protection guidelines and acts, e.g., the Guide for the Care and Use of Laboratory Animals (3) and the European Directive on the protection of animals used for scientific purposes (4).

Animal welfare describes the status of life quality, which relies on the consideration and promotion of things to achieve good animal welfare (5, 6). Its assessment requires monitoring animal affective states with positive and negative valence (7). The term severity assessment emphasizes categorizing negative affective states in animals, explicitly under experimental conditions. It aims to recognize signs of suffering and is essential for possible interventions to relieve the burden during experiments and promotes the refinement of procedures. Nevertheless, to comply with scientific and regulatory requirements, an accurate, evidence-based severity assessment and the classification of severity conditions are needed (8).

These aims raise the need for a more precise and data-centered evaluation of impaired animals, resulting in a more holistic analysis less influenced by human decision bias. Further, integrating multimodal and multivariate methods requires increased methodological awareness and integration into severity assessment, in general, to ensure, for example, inter-animal-model comparability.

Currently, outcome measures from physiology, biochemistry, clinical sciences, and the behavioral sciences are considered to best capture the welfare state of the animals under experimentation (7). This notion often leads to an assortment of results whose interpretation and categorization remain with the scientist. However, few veterinary studies combine multiple collected variables to provide a more comprehensive method for evaluating animal wellbeing. For example, Principal Component Analysis (PCA) was performed in a study assessing the severity of procedures conducted in

three epilepsy models. In this study, multiple behavioral and biochemical parameters were analyzed. The PCA revealed the most informative orthogonal parameters and combined them in a Composite Measures Scheme (CMS) used in comparative severity assessment (9). However, the PCA method can be misleading when data are highly collinear.

In another study investigating the severity of neuroscientific surgeries in rats, a supervised Machine Learning method with a radial Support Vector Machine kernel was used to classify distinct invasive procedures (10), e.g., with the heart rate and activity information as input dimensions. These studies support the concept that incorporating mathematical methods to explain higher-dimensional relationships in the data beyond the traditional scope of simple inferential statistics successfully helps determine states of wellbeing and the severity of experimental procedures (11–13).

Consequently, our study aimed to develop an algorithm-based composite system that provides an objective animal welfare assessment with an arbitrary number of input variables and further introduces the concept of adding relational context to the quantitative severity assessment. With this methodology, and, e.g., using the same measured variables in three independent animal models, we will show that relative severity can be used to compare states of wellbeing between individual animals, treatment groups, and animal models.

Furthermore, this level of comparability is achieved with a collection of physiological, clinical, and behavioral outcome measures from a surgical mouse model, resulting in the development and application of the Relative Severity Assessment (RELSA) procedure. We hypothesize that the individual outcome measures can signal changes in severity in laboratory animals, but they do so at different reporting characteristics over time. Thus, using a weighted composite like the RELSA score helps minimize information loss when variables are missing and allows severity comparisons at different levels, such as the individual or model scale.

The current study is divided into two parts: first, objective parameters were utilized for an actual severity assessment to show the general applicability of RELSA in a well-established method (TM implantation). This surgical model has the advantage of providing a collection of objective variables

such as heart rate, heart rate variability, and activity and is officially classified as moderate severity according to the EU directive. In the second part, we aim at the severity grading of different animal models involving inflammation, stress, and sepsis based on identical variables using RELSA. This analysis resulted in an evidence-based severity comparison of experimental procedures, providing scientists and regulators with more precise estimates of severity gradings for experiments and tangible approaches for refinement. Furthermore, these results show that the reference data derived from the surgical model already provide a basis for routine use of this method, e.g., in daily severity monitoring, without the need to gain this data on additional animals. Furthermore, with the RELSA method, researchers are free to define their reference data when needed, as recently shown in a study comparing the severity of genetic, stress-based, and pharmacological depression models (14). The RELSA procedure is, therefore, not bound to an invasive procedure and can be applied as an objective severity measure in a wide range of research models.

Methods

Ethical statement

Experiments involving surgery, DSS colitis, and stress were approved by the Local Institutional Animal Care and Research Advisory Committee and permitted by the Lower Saxony State Office for Consumer Protection and Food Safety (LAVES, Oldenburg, Lower Saxony, Germany; license 15/1905). The application for the animal experiments involving sepsis (authorization no. V54–19 c 20/15 - F152/1016) was approved by the local Ethics Committee for Animal Research (Darmstadt, Hessen, Germany). All procedures followed the German animal protection law and the European Directive 2010/63/EU.

Animals, housing conditions, and husbandry

Female C57BL/6J mice undergoing surgery only (transmitter implantation and Sham groups), DSS colitis, or stress induction were obtained from the Central Animal Facility, Hannover Medical School, Hannover, Germany. For the sepsis study, male C57BL/6N mice were obtained from Charles River Laboratories, Sulzfeld, Germany (for an overview of the studies, mice, and animal numbers, see [Supplementary Table 1](#)). The mice were free of the viral, bacterial, and parasitic pathogens listed in the Federation of European Laboratory Animal Science Association (15). A sentinel program monitored their health status throughout the experiments. The mice were housed at the Central Animal Facilities of the MHH (surgery, colitis, stress groups) in macrolon type-II cages (360 cm²; Tecniplast, Italy),

which were changed once per week. Cages were bedded with autoclaved softwood shavings (poplar wood; AB 368P, AsBe-wood GmbH, Buxtehude, Germany), paper nesting material (AsBe-wood GmbH, Buxtehude, Germany), and two cotton nesting pads (AsBe-wood GmbH, Buxtehude, Germany). Room conditions were standardized (22 ± 1°C; humidity: 50–60%; 14:10 h light/dark cycle). Mice were fed standard rodent food (Altromin 1324, Altromin, Lage, Germany) *ad libitum*, and autoclaved (135°C/60 min) distilled water was provided *ad libitum*. Two female persons handled the mice. For the sepsis experiments, the mice were housed at the animal facility of Fraunhofer IME-TMP, Frankfurt, Germany, in IVC cages (501 cm²; GM500, Tecniplast, Italy), which were changed once per week (but never during sepsis). These cages were bedded with softwood shavings (H0234-200, ssniff Spezialdiäten GmbH, Germany), paper nesting material (Sizzlenest, H4201-11, ssniff Spezialdiäten GmbH, Germany) and a mouse igloo (#13100 Plexx BV, Netherlands). Room conditions were standardized (22 ± 2°C; humidity: 45–65%; 12:12 h light/dark cycle including a 30 min twilight phase at the beginning and end of the light/dark phases). The mice were fed standard rodent food (V1534-000, ssniff Spezialdiäten GmbH, Germany) *ad libitum*, and tap water was provided *ad libitum*. Animals were allocated randomly to the testing groups and habituated to the experimental environment before the surgical procedure.

Transmitter implantation

The mice for the surgery, colitis, and stress studies were 9–10 weeks old. Transmitters (ETA-F10 or HD-X11; DSI, St Paul, MN, USA) were aseptically implanted into the intraperitoneal cavity with electrodes placed subcutaneously for a bipolar lead II configuration under general isoflurane anesthesia. Sham-operated mice underwent aseptic surgery without implantation of the transmitters. General anesthesia was induced in an induction chamber (15 × 10 × 10 cm) with 5 vol% isoflurane (Isofluran CP®, CP Pharma, Burgdorf, Germany) and an oxygen flow (100% oxygen) of 6 l/min. After confirming the absence of the righting reflex and removal from the chamber, anesthesia was maintained via an inhalation mask with 1.5–2.5 vol% isoflurane and an oxygen flow of 1 l/min. The corneal reflex was used in combination with the eyelid-closing reflex and the toe pinch reflex to determine the depth of anesthesia. Personnel involved have been trained and were experienced in performing these assays carefully and very softly to omit any damage. The eyes were moistened with eye ointment to protect them from drying out (Bepanthen®, Bayer AG, Leverkusen, Germany). After reaching total anesthesia, the surgical area was shaved, and the mice were placed in the surgical field in dorsal recumbency with the head toward the surgeon. During the entire duration of the anesthesia, the mice were placed on a heating pad at 37.0 ± 1.0°C to prevent hypothermia. EMLA®

cream (25 mg/g Lidocain + 25 mg/g Prilocain; Aspen Germany GmbH, Munich, Germany) was used for local anesthesia at the incision sites. The mice that underwent only surgery received either preoperative 200 mg/kg metamizole (Novaminsulfon 500 mg Lichtenstein, Zentiva Pharma GmbH, Frankfurt am Main, Germany) subcutaneously (s.c.) and postoperative 200 mg/kg metamizole orally via the drinking water until day 3 or preoperative 5 mg/kg carprofen (Rimadyl, Zoetis Deutschland GmbH, Berlin, Germany) s.c. and postoperative 2.5 mg/kg s.c. every 12 h until day 3. The mice that underwent additional colitis or stress induction were treated using the metamizole analgesia regimen.

In the CLP study, mice aged 12–14 weeks were anesthetized via s.c. injection of 120 mg/kg in 10 ml/kg ketamine (Ketaset®, Zoetis Deutschland GmbH, Berlin, Germany) and 8 mg/kg in 10 ml/kg xylazine (Rompun®, Bayer Vital GmbH, Leverkusen, Germany). Perioperative management was the same as described above. The blood pressure catheter was placed in the left carotid artery and positioned so that the gel-filled sensing region of the catheter was ~2 mm in the aortic arch. The telemetry transmitter was placed along the lateral flank between the forelimb and hindlimb, close to the back midline. Biopotential ECG leads were tunneled subcutaneously to achieve positioning analogous to lead II in human ECG. For postsurgical analgesia, 200 mg/kg metamizole s.c. (Novaminsulfon 1,000 mg Lichtenstein, Zentiva Pharma GmbH, Frankfurt/Main, Germany) was administered at the first signs of waking up. For postsurgical analgesia, 5 mg/kg carprofen (Rimadyl, Zoetis Deutschland GmbH, Berlin, Germany) was administered s.c. on the evening of the day of the surgery and the morning and evening of day 1 and day 2 after surgery. After fully recovering from the anesthesia, mice were put back into their home cage, and the continuous data acquisition of all physiological parameters began immediately. Mice were randomly allocated to the testing groups and habituated to the experimental environment before the surgical CLP or CLP Sham procedure.

Sham surgery

Sham-operated mice were used as controls for assessing the severity of transmitter implantation and underwent an aseptic laparotomy without transmitter implantation (Sham mice or animals) under the same conditions as described above (surgery studies), including anesthetic and analgesic regimens.

Burrowing behavior

One week before intraperitoneal transmitter implantation or the corresponding Sham surgery, the mice were housed pairwise in type II macrolon cages filled with aspen bedding material

(AsBewood GmbH, Buxtehude, Germany) and two compressed cotton nesting pads (AsBewood GmbH, Buxtehude, Germany). On days five and four before surgery, the burrowing apparatus was provided to the animals to train them in the burrowing behavior (16). Baseline measurements were taken on days two and one before surgery. A 250 mL plastic bottle with a length of 15 cm, a diameter of 5.5 cm, and a port diameter of 4 cm was used as a burrowing apparatus. It was filled with 140 ± 1.5 g of the standard diet pellets of the mice (Altromin1324, Lage, Germany). For burrowing testing after surgeries (1st, 2nd, 3rd, 5th, and 7th night after surgery), mice were singly housed in a type-II macrolon cage with autoclaved hardwood shavings. The burrowing bottles were placed in the left corner. Half of the used nesting material from the home cage was provided as a shelter in the right corner. The tests started 3 h before the dark phase. The bottles containing the remaining pellets were placed back into the cages and weighed the following day (burON, “overnight burrowing performance”) again.

Cecal ligation and puncture surgery

At the earliest 6 days or after reestablishing a regular circadian rhythm after the surgical implantation of the telemetry transmitter device, male C57BL/6JN mice were used for the CLP experiments. The CLP surgery and the subsequent start of the experiments were conducted in the morning to control circadian variations. The mice were weighed, and 30 min before surgery, 0.05 mg/kg buprenorphine was injected s.c. (Bupresol® 0.3 mg/ml, CP-Pharma HmbH, Burgdorf, Germany). The mice were anesthetized using isoflurane (2–3% Forene®, AbbVie Deutschland GmbH & Co. KG, Wiesbaden, Germany) and placed on their back on a heating pad while continuously connected to the isoflurane anesthesia. The eyes were moistened with eye ointment. Xylocaine (Xylocain® Pumpspray Dental, AstraZeneca GmbH, Wedel, Germany) was used for local anesthesia using two puffs of a ready-to-use pump spray containing 10 mg lidocaine per puff at the incision site. The corneal reflex was used in combination with the eyelid-closing reflex and the toe pinch reflex to determine the depth of anesthesia. Personnel involved have been trained and were experienced in performing these assays carefully and very softly to omit any damage. During the entire period of anesthesia, the mice were on a heating pad at $37.0 \pm 1.0^\circ\text{C}$. The abdominal cavity was aseptically opened via a midline laparotomy incision of approximately 3 cm, and the cecum was exposed. Subsequently, the cecum was 2/3 ligated (Nylon Monofilament Suture 6/0, Fine Science Tools GmbH, Heidelberg, Germany) distal to the ileocecal valve, while care was taken that the intestinal continuity was maintained. The exposed cecum was punctured twice, “through-and-through,” with a 21-gauge needle. Next, sufficient pressure was applied to the cecum to extrude fecal material from each puncture site

(~ 1 mm). The cecum was returned to the abdominal cavity and placed in the upper central abdomen. Following this procedure, the peritoneum was closed with three-knot fissures with non-resorbable sterile suture material (Nylon Monofilament Suture 7/0, Fine Science Tools GmbH, Heidelberg, Germany), and the upper skin layer was stapled with sterile clips (Michel Suture Clips 7.5 × 1.75 mm, Fine Science Tools GmbH, Heidelberg, Germany). For the mice undergoing a Sham laparotomy, the same procedure was performed without CLP. After fully recovering from the anesthesia, the mice were put back into their home cage, after which the continuous data acquisition of all physiological parameters began immediately. The mice received 0.1 mg/kg buprenorphine s.c. 3 h after surgery and subsequently every 8 h for the rest of the experiment. At the end of the experiments, mice were anesthetized deeply with isoflurane and killed by cervical dislocation.

Colitis induction and restraint stress

After intraperitoneal transmitter implantation and 28 days of postoperative recovery, the female C57BL6/J mice were exposed to 0% (control; receiving water only) or 1% DSS (colitis; mol wt 36,000–50,000; MP Biomedicals, Eschwege, Germany) in drinking water for 5 consecutive days to induce intestinal inflammation. The mice were weighed daily, and the telemetry-derived parameters were recorded: hr, hrv, activity, and temperature. The third group of mice was subjected to restraint stress (colitis + stress) and DSS treatment. The mice were inserted into restraint tubes on 10 consecutive days (d1–d10) for 60 min (from 09:00 to 10:00 a.m.). The restraint tubes (23-mm internal diameter, 93-mm length) consisted of transparent acrylic glass with ventilation holes (8 mm diameter) and a whole distance spanning 7-mm-wide opening along the upper side of the tube. The ends of the tubes were sealed on one side by a piece of acrylic glass with a slot for the animals' tail and the other side by a fixed solid plastic ring. The mice could rotate around their axis but could not move horizontally.

Data characterization and RELSA pre-processing

Data were brought into the tabular format required for RELSA analysis (Supplementary material 2). Up to six outcome measures were used in the calculations (body weight change [bwc], burrowing overnight [burON], heart rate [hr], heart rate variability [hrv], body temperature [temp], and activity [act]). Five parameters were used in the animal model comparisons because burON was not determined in all included studies. The RELSA pre-processing was initiated with the normalization process. The quantitative data were normalized to the range [0;100]% with 100% as starting values [e.g., based

on physiological or baseline conditions, e.g., on pre-surgery day (–1), Supplementary material 2 for an example].

The RELSA methodology required a reference set

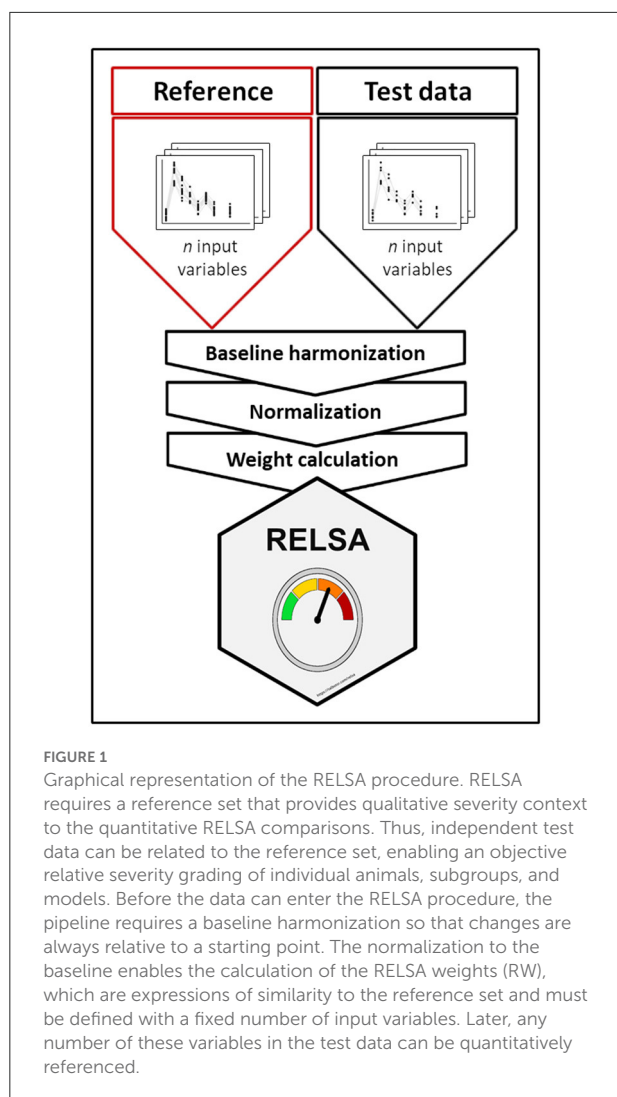
Therefore, the surgery model was defined as the RELSA reference set. According to Annex XIII of the EU directive, surgical interventions under general anesthesia, such as TM implantations or Sham surgeries, are categorized as “moderate” in terms of severity. Since the subsequent RELSA analyses were referenced to the values in the reference set (self-reference is possible), they also obtained a relative qualitative severity level. More information on the RELSA procedure is available in Supplementary material 3. A graphical representation of the RELSA procedure is shown in Figure 1. Further, in Supplementary material 4, a simple explanation of the RELSA is demonstrated with examples.

At each observed point in time (t), differences to the normalized baseline in each contributing outcome measure (i) were calculated. Then, to establish the quantitative severity context, the differences were divided by the normalized maximum-reached differences in the respective variables in the reference set. This operation yielded the RELSA weights (RW, see formula 1). Again, care was taken to include the direction of unfolding severity in each outcome measure (e.g., impairments decreased bwc but heightened hr in the included models). The RW were expressions of similarity concerning the maximum-reached value observed in the reference set at any observed point in time. This step also regularized differences in variable contributions at any given severity level, especially in highly collinear contributors.

Larger differences were given more weight, and the final RELSA score was calculated by the root mean square (RMS) of the available RW divided by the number of variables (N) (see formula 2). Missing variables did not contribute to the RELSA, whereas values equal to or above baseline level contributed zero. Furthermore, levels of severity in the reference data were calculated using the *k*-means algorithm (11). The number of clusters was determined heuristically with a Scree plot (Supplementary Figure 5A). A RELSA value of 1 meant that all contributing variables in a test animal reached the same values as the largest observed deviations in the reference set at the defined severity level (here, “moderate”).

$$R_{wi}(t) = \frac{(|100 - i|)}{\left(100 - \max_{i,ref}\right)} \quad (1)$$

$$RELSA(t) = \sqrt{\frac{\sum_1^i R_{wi}^2}{N}} \quad (2)$$



Statistics

Data were tested against the hypothesis of normality using the Shapiro-Wilk test. In the case of a rejected Null hypothesis, non-parametric methods were used for group comparisons (e.g., the Kruskal-Wallis and Mann-Whitney U-test). When the assumptions of normal distribution were met, parametric analyses were performed, e.g., with an analysis of variance (ANOVA) and reported with a type III error structure due to the presence of interactions. Singular group comparisons were analyzed with the *t*-test (plus Welch's correction in cases of unequal variances). Multiple comparisons were adjusted with the Tukey-Kramer *post-hoc* test. Comparisons to the baseline were calculated with an ANOVA using a control group, followed by Dunnett's *post-hoc* test. The RELSA_{max} and cluster centroids were bootstrapped 10,000-fold to yield estimates as well as 95% bias-corrected and

accelerated (BCa) confidence intervals. With either method, the resulting *p*-values were considered to be significant at the following levels: 0.05 (*), 0.01 (**), 0.001 (***), and 0.0001 (****).

Software, R-packages, and raw data availability

RELSA was developed in R (version 4.0.3). The following packages were used for analysis and visualization: ggplot2, factoextra, effsize, plyr, emmeans, car, and boot. In addition, radar charts were realized using the fsmb package. The RELSA algorithm and the raw data are available as an R package with complete documentation on GitHub: <https://github.com/mytalbot/relsa>. The RELSA procedure can also be tested with a limited set of variables in a stand-alone web application: <https://calliope.shinyapps.io/RELSAapp/>. Finally, raw data are available as text files in the following location: https://github.com/mytalbot/RELSA/tree/master/raw_data.

Results

Severity assessment after surgery using single outcome measures

We utilized the surgical model of TM implantation to generate well-defined variables that first can be used as single outcome measures to characterize the model itself (this section) and later for developing and validating the RELSA algorithm (following sections), also providing a reference for assessment of further mouse models. After transmitter (TM) implantation or the corresponding Sham surgeries, we monitored the animals' relative body weight change (bwc) as one of the most frequently used clinical parameters (Figure 2A). TM animals showed an average loss of 10.89% (SD = 2.29%) in body weight on the day of surgery (day 0), which was significantly ($p < 0.0001$) higher than Sham animals which showed only an average loss of 3.78% (SD = 2.93%) which was also significant ($p = 0.002$). No animal lost more than 15.45% in body weight. The bwc values in TM mice returned to baseline levels on day ten after surgery and in Sham animals as early as day six after surgery. Both treatment groups showed weight gain in the progress of the experiment. Further, we observed the overnight burrowing performance (burON). The burrowing also dropped compared to initial values, down to an average of 25.64% (SD = 21.13%). However, in the Sham animals, the loss in burrowing performance was less prominent at an average of 83% (SD = 14.34%) (Figure 2B). The burrowing parameter showed regular burrowing activity on day 2 – two days after surgery. The difference between Sham and TM animals on surgery day was significant ($p < 0.0001$). From the implanted transmitters, additional variables

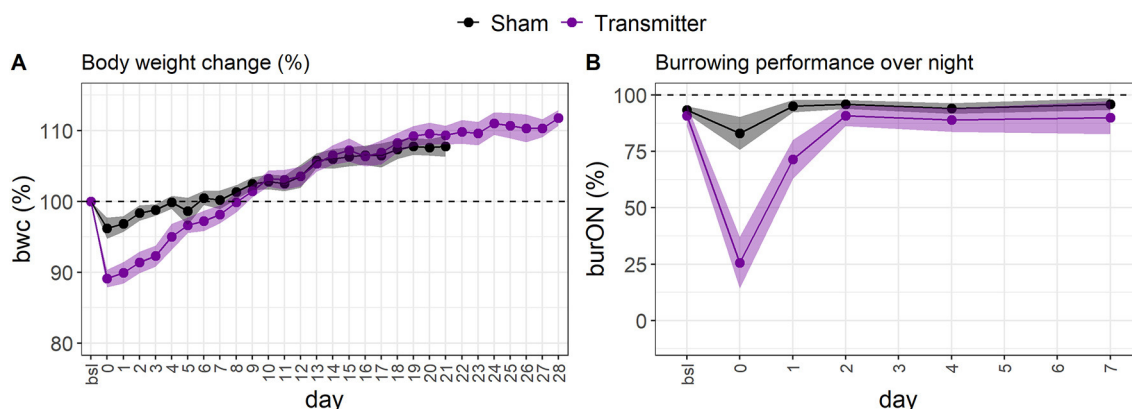


FIGURE 2

(A) The standardized, average body weight change indicates impairments to animal welfare in female C57BL6/J mice. The loss in bwc is most extensive after surgery (day 0) in the TM-implanted group (mauve, $n = 13$). The loss in body weight is less severe in the Sham group (black dots, $n = 15$). On average, the animals recovered back to baseline levels at around day eight. After day eight, the animals gained weight. The errors are depicted as 95% confidence bands. (B) The standardized, average overnight burrowing performance (burON) in female C57BL6/J mice also showed a sharp drop after surgery (day 0). However, the performance loss is higher in the TM group ($n = 13$) than in the Sham group ($n = 15$). The burrowing behavior returns faster back to baseline levels than the bwc variable. The animals regained normal burrowing behavior on day 2.

were obtained. The heart rate (hr) spiked after surgery (day 0) at an average of 642.25 ($SD = 36.12$) bpm and returned to baseline levels on day 7 (Figure 3A). The heart rate variability (hrv) showed decreased values after surgery. Its average was lowered to 3.45 ($SD = 1.52$) ms (Figure 3B), corresponding to a 76.1% drop in values. The animals recovered back to baseline on day 14. The body core temperature was measured in a small range ($[34.10; 37.52]^{\circ}\text{C}$) and showed ambiguous results. After surgery on day 0, there was a slight drop of 0.73% in temp (-0.26°C), followed by an increase on day 1 to 37.35 ($SD = 0.14^{\circ}\text{C}$), again followed by a recovery back to baseline levels on day 7 [36.51 ($SD = 0.17^{\circ}\text{C}$), Figure 3C]. The general activity was reduced after surgery, dropping from an average of 1011.98 ($SD = 443.14$) counts/min to 137.04 ($SD = 68.87$) counts/min. The activity parameter showed recovery to baseline levels on day 14 (Figure 3D). The Supplementary material 6 shows additional inferential statistics on the day-to-baseline and between treatment contrasts of the single variables used to indicate changes in severity. Further, the animals were evaluated daily using a clinical score ranging from 0 (no impairment) to 6 (severe impairment) comprising the body weight, the visual evaluation of activity, general health condition, and behavior. An increase to score 2.15 ($CI_{95\%}[1.93; 2.38]$) was observed on day 0 (post-op) and returned back to pre-op level on day 9 post-op (Supplementary material 7.1).

This surgery model served as the reference model for the subsequent RELSA development and its validation. The raw data of this and the other animal models with their individual set of variables are available under the following link: https://github.com/mytalbot/RELSA/tree/master/raw_data.

Severity assessment after surgery using multiple outcome measures in the composite RELSA score

While single variables showed differences, e.g., in recovery times (hrv [day 14] vs. burrowing [day 2]) and escalation magnitudes (e.g., a maximum loss in burON of 0%, and a maximum increase of hr at 688.18 bpm), it remained unclear what this contradicting information meant in the context of severity assessment. Therefore, we analyzed how the severity information developed when different variables were combined in the RELSA. As such, the full model (bwc, burON, hr, hrv, temp, and act) was plotted against the TM variables (hr, hrv, temp, and act), the body weight change (bwc), and the burrowing performance overnight (burON), and the body weight change plus the burrowing parameter (bwc+burON) in the TM animals (Figure 4A). Here, the point of maximum severity in the animals was identified as the peak in all models at day 0 (after surgery). The full model showed a mean RELSA score of $RELSA_{full,0} = 0.75$ ($SD = 0.05$), the TM model $RELSA_{TM,0} = 0.76$ ($SD = 0.06$), the bwc $RELSA_{bwc,0} = 0.71$ ($SD = 0.15$), the burON $RELSA_{burON,0} = 0.71$ ($SD = 0.24$), and bwc+burON $RELSA_{bwc+burON,0} = 0.73$ ($SD = 0.15$) (see inset plot in Figure 4A). On day 0, neither the TM group [$F_{(4,60)} = 0.36$, $p = 0.84$], nor the Sham group [$F_{(2,42)} = 2.69$, $p = 0.08$] showed differences in RELSA performances. The exemplary variable permutations reached a mean of $RELSA_{mean,0} = 0.73$ at a high level of precision with the 95% confidence interval in the range $CI_{95\%}[0.71; 0.76]$. Therefore, the maximum RELSA score was relatively

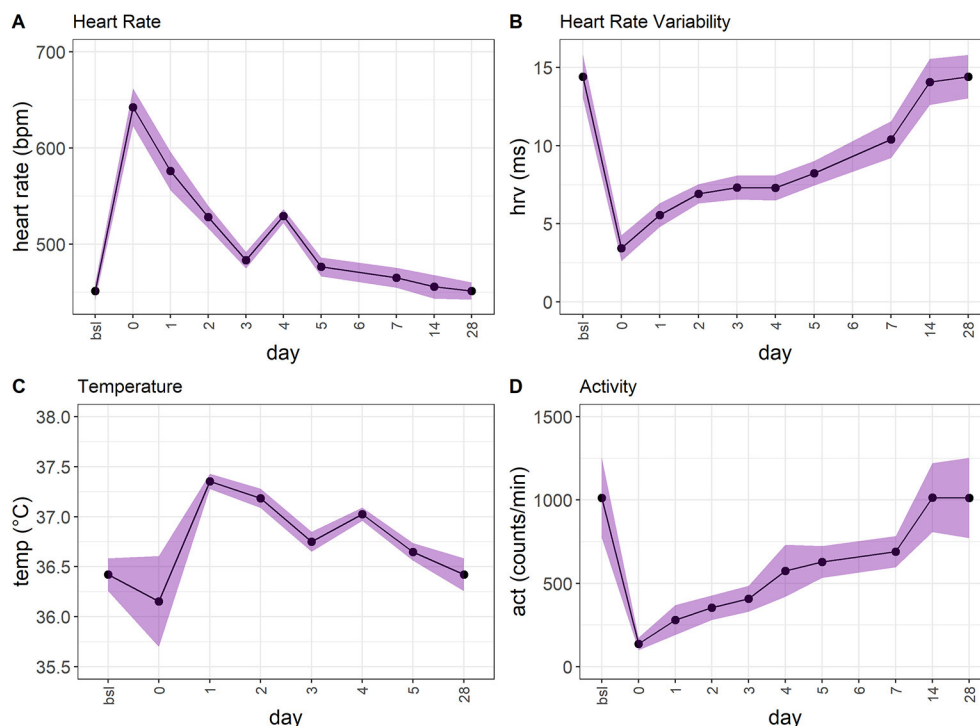


FIGURE 3

(A) The heart rate (hr) in TM-implanted female C57BL6/J mice ($n = 13$) shows an increase on surgery day and returns back to baseline levels. However, the recovery is much slower than, e.g., in burON and bwc. (B) The heart rate variability (hrv) shows a similar development to hr. The maximum drop occurs after surgery (day 0). After that, the animals recover over 28 days. (C) The temperature shows an ambiguous development. There is a slight drop after surgery, followed by an increase that slowly returns to baseline levels. However, the range of the temperature variable is small ($[34.10; 37.52]^{\circ}\text{C}$). (D) The activity (act) variable shows a drop after surgery (day 0) and returns back to baseline levels over the next 14 days.

invariant against small changes in singular variables. This result was corroborated by analyzing the Sham animals, where bwc, burON, and their combination were analyzed using the RELSA. The animals not only showed lower severities than the TM animals with $\text{RELSA}_{\text{bwc}+\text{burON},0} = 0.22$ ($\text{SD} = 0.15$), $\text{RELSA}_{\text{bwc},0} = 0.25$ ($\text{SD} = 0.19$), and $\text{RELSA}_{\text{burON},0} = 0.12$ ($\text{SD} = 0.13$) but also that the RELSA incorporated the short-term spiking of the burON variable on day 0 (Figure 4B) by lowering the average on day zero in the combined model as a consequence of the weighting in the RELSA formula. The difference between the averages of $\text{RELSA}_{\text{bwc}+\text{burON},0}$ and $\text{RELSA}_{\text{bwc},0} = 0.25$ was $\Delta_{\text{RELSA}} = 0.03$. Consequently, the average RELSA in the Sham group showed lower precision $\text{RELSA}_{\text{Sham},0} = 0.12$ ($\text{CI}_{95\%}[0.03; 0.36]$) than the models above with more contributing variables.

These results show that RELSA enables detection of severity after TM implantation, discriminates different treatments (here: TM implantation vs. Sham operation) and is robust toward the selection of variables. To validate the RELSA performance, we used the clinical score data. The clinical score correlated highly with the RELSA ($r = 0.98$, $\text{CI}_{95\%}[0.95; 0.99]$, $t = 22.81$, $df =$

27, $p < 0.0001$), thereby validating the algorithm. Details on the validation are shown in [Supplementary material 7](#).

The comparison of severity in individual animals and experimental subgroups can be achieved with the RELSA score and the $\text{RELSA}_{\text{max}}$ Value

The RELSA procedure was calculated with six variables in the TM group (bwc, burON, hr, hrv, temp, and act) and two in the Sham group (bwc, burON). On day 0, there were no *between-model* differences in the RELSA score due to the high collinearity of the contributing variables (see Figures 4A,B). Subsequently, the individual RELSA scores in the TM animals reached higher values than the Sham animals (Figure 5A). However, at least three animals in the Sham group showed severity anomalies (e.g., $\text{RELSA} > 0.4$). These animals were identified as animals 18, 21, and 22 (Figure 5A). Therefore, the RELSA outcome was used to identify the source of these higher severities. The analysis

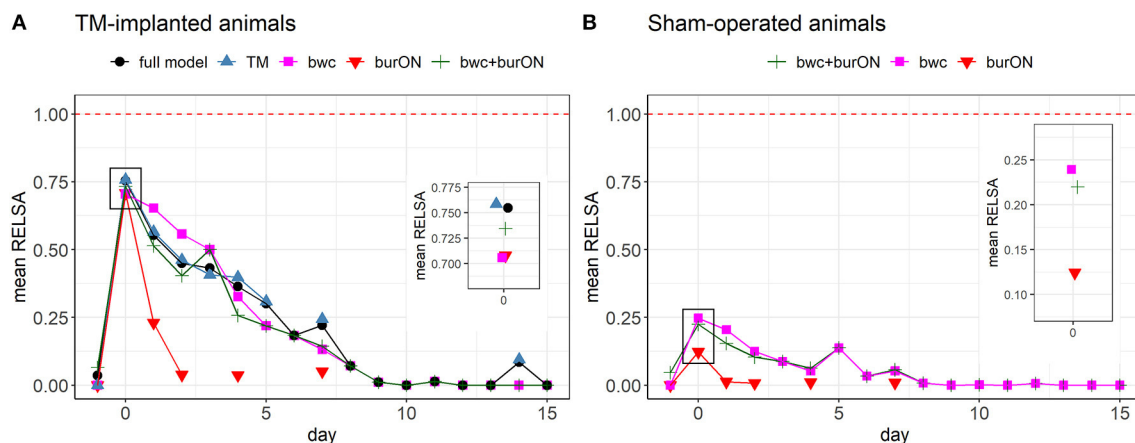


FIGURE 4

(A) Comparison of RELSA performances using different input variables in the TM-implanted animals ($n = 13$). The red dashed line (RELSA = 1) represents the maximum in the reference model. The full model comprised the outcome measures bwc, burON, hr, hrv, act, and temp. The inset plot focuses on the RELSA values on day 0 (after surgery). Here, the average RELSA values are highest and close together $RELSA_{mean,0} = 0.73$ ($SD = 0.02$, range = [0.71; 0.76]) at a low error rate. The highest-performing models are the TM outcomes (hr, hrv, act, and temp, mean = 0.76), followed by the full model (mean = 0.75). During recovery, the performances vary due to changing contributions to the RELSA score. However, the models appear interchangeable as the RELSA weighs and regularizes missing information, especially in highly collinear data. (B) Comparison of RELSA performances using different input variables in the Sham-operated animals ($n = 15$). The maximum RELSA is indicated by bwc (mean = 0.24). Note that burON alone has a lower RELSA value than bwc on day 0 (mean = 0.12). However, the combination of bwc and burON can capture most of the severity information on day 0 as indicated by bwc (see inset plot). Consequently, the combination of bwc and burON (mean = 0.22) performs slightly lower than bwc alone. The burrowing behavior was not measured on all days, so the main RELSA information is dependent on bwc in these cases. The RELSA is relative invariant against missing input variables when multiple measures are included.

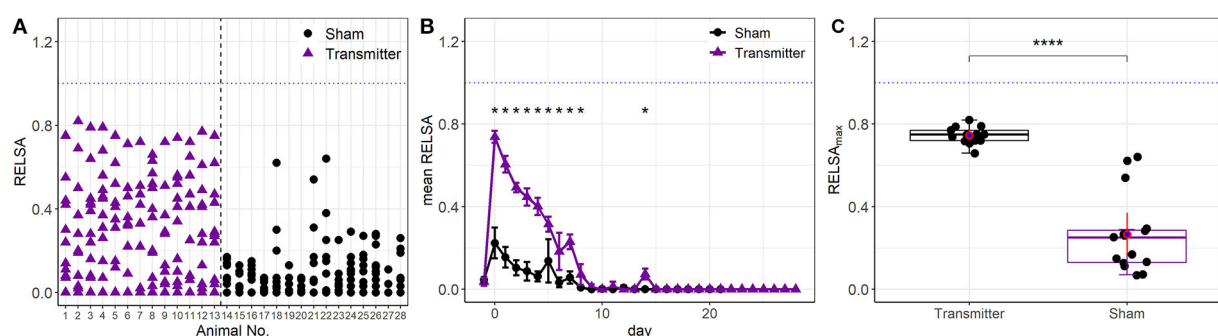


FIGURE 5

(A) Single animal analysis with the full RELSA model (bwc, burON, hr, hrv, act, and temp). The average RELSA score was higher in the TM group than in the Sham group (average $RELSA_{max, TM} = 0.75$ vs. average $RELSA_{max, Sham} = 0.26$). In addition, at least three animals in the Sham group have high severity ($RELSA > 0.4$). These animals showed higher losses in bwc and burON than the other animals in the Sham group and were correctly identified. (B) Animals in the time-resolved RELSA curves of the Sham and TM groups show a significant treatment:day interaction [$F_{(1, 29)} = 59.78$, $p > 0.0001$]. The subsequent *post-hoc* tests indicate significant differences between treatments ($*p < 0.05$). On day 14, small spikes in hrv and act unrelated to the surgery occurred and were detected with the RELSA. (C) There is a general between-groups difference in severity ($RELSA_{max}$) concerning the TM-implanted ($n = 13$) and Sham animals [$n = 15$, $t_{(26)} = 8.9$, $p < 0.0001$ ****].

showed that animal 18 had lower values in both outcomes, bwc (89.36%) and burON (46.51%), on day zero, while animals 21 and 22 showed only lowered bwc on day 5 (91.70% and 90.1%) compared to the other Sham animals, e.g., displaying a mean bwc value of 93.02% on day 0. Furthermore, the average RELSA score indicated the higher general severity of the TM-animals at $RELSA_{TM,0} = 0.73$ ($SD = 0.05$) compared to the Sham animals with $RELSA_{Sham,0} = 0.22$ ($SD = 0.15$). In addition,

the treatment:day interaction was significant in an ANOVA [$F_{(1,29)} = 59.78$, $p > 0.0001$], and the subsequent *post-hoc* tests showed significant differences between Sham and TM animals on the days 0–8 ($p < 0.0001$) and 14 ($p < 0.0018$) (Figure 5B). The maximum RELSA values from the individual animals were combined into the $RELSA_{max}$ value and used in a subsequent *between-subgroups* comparison. The analysis showed that the highest achieved severity from an integrated set of six variables

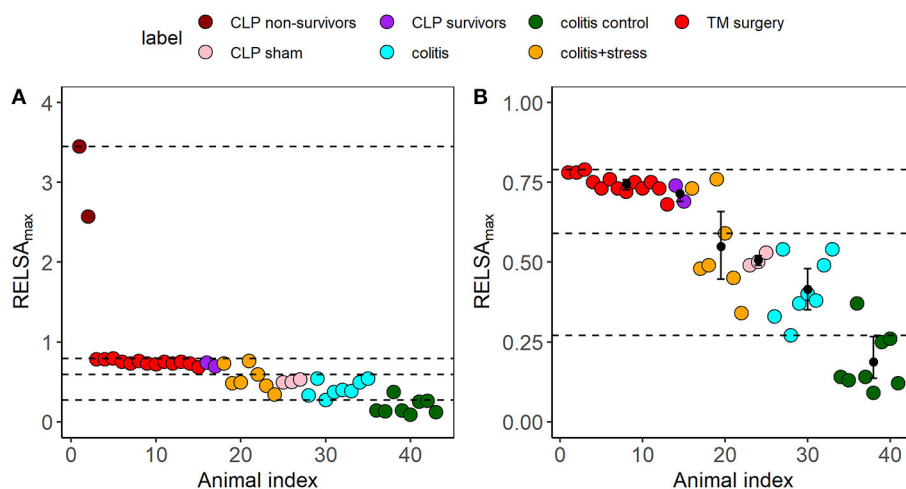


FIGURE 6

(A) Cluster analysis and severity categorization of six distinct subgroups from the three independent animal studies cecal ligation puncture (CLP, sepsis), surgery (TM implantation), and colitis/restraint stress using the RELSA_{max} as the maximum experienced severity information. Each dot represents an animal. In all subgroups, the outcome measures bwc, hr, hrv, temp, and act were used to calculate the RELSA_{max}. The dashed lines represent the four severity thresholds from a k-means clustering (L1 < 0.27, L2 < 0.59, L3 < 0.79, and L4 < 3.45) to enable a comparative grading and categorization of the models and animals. The highest severity was reached by the two CLP non-survivors (RELSA_{max} > 2.5). (B) The bootstrapped cluster centers with 95% confidence intervals show that except for the colitis + stress model data, the 95% CIs remain within the identified cluster levels, indicating highly stable severity estimates. Individual animals in the colitis control group showed increased severity due to a drop in activity. Note that the RELSA scale focuses on the range RELSA[0;1]; therefore, the two CLP non-survivors are not visible.

was significantly different in TM and Sham animals [$t_{(26)} = 8.9$, $p < 0.0001$, Figure 5C].

The clustering of RELSA_{max} values revealed objective severity levels

In addition to the data for building the RELSA reference set from TM-implanted mice and showing the possible comparisons *between* individual animals and experimental subgroups, we further explored the RELSA as a tool for severity comparisons *between* different animal models. We included three additional animal studies (colitis, stress, and sepsis), with data available on five outcome values (bwc, hr, hrv, temp, and act). Each study was analyzed using the RELSA methodology and was, therefore, referenced against the data from the TM-implanted mice. This quantitative referencing provided the necessary framework for grading the severity information. In addition, we used the individual RELSA_{max} values, as previously described, to map the maximum achieved severity of each animal in each study against the RELSA reference set. This allowed classification of severity levels based on the standardized values from each study. With these data, *k*-means clustering was used to segment the ordered univariate RELSA_{max} outputs into distinct clusters.

First, we estimated the number of clusters to $k = 4$ using Scree analysis. The heuristics of this selection process are shown in the Supplementary Figures 5A,B. The

resulting limits of the clustering are shown as dashed lines in Supplementary Figures 5B, 8. The four RELSA_{max} cluster thresholds were L1 < 0.27, L2 < 0.59, L3 < 0.79, and L4 < 3.45.

Second, we analyzed and compared the additional studies in terms of severity, using the cluster levels to attribute severity gradings. The other data included mice suffering from colitis induced by dextran sulfate sodium (DSS) and colitis plus additional stress (colitis+stress). In the latter group, the animals received DSS and were subjected to immobilization stress for 1 h on ten consecutive days. The corresponding colitis control animals were treated with water only. Furthermore, we refined data from a study on cecal ligation puncture (CLP) surgery for sepsis induction and the corresponding Sham-operated animals (CLP Sham). Here, the data were divided into CLP survivors and non-survivors. The cluster analysis revealed the highest severity level in CLP non-survivors, followed by a cluster of TM-implanted animals (which comprised the RELSA reference set), followed by CLP survivors. Data from the colitis+stress and colitis study formed the lower severity clusters and CLP Sham-operated animals. Colitis control animals were allocated to the lowest severity cluster (Figure 6).

Furthermore, we investigated how stable the RELSA_{max} distributions were in their group estimates and cluster positions. Some studies or subgroups involved small sample sizes (Supplementary material 1). Therefore, we applied 10,000-fold bootstrapping to assess the 95% confidence intervals of the RELSA_{max} centroids. Except for the colitis + stress study, the confidence intervals remained within their relative *k*-means

cluster levels. The confidence interval of the colitis control group did not overlap with any other higher-level confidence interval and did not cross the L1 cluster threshold.

RELSA generalized model-specific changes in outcome patterns into global severity information

The surgery data in this study showed that outcome measures varied in magnitude and showed differences concerning recovery times. In addition, the natural variance of biological systems is also part of any quantitative severity assessment [e.g., three individual animals in the Sham-group significantly deviated from the global RELSA mean (see [Figure 4A](#))]. Therefore, to assess the contributions of individual outcome variables to the RELSA analysis, we monitored the average RELSA weight contributions of the surgery intervention [TM-implanted animals ([Figure 7](#))] with radar charts.

The analysis of exemplary time points showed that the development in the variables changed over time. First, before the intervention (Baseline), the variables showed no contribution to the RELSA ($AUC = 0$). After surgery (post-op), all five variables showed substantial contributions ($AUC = 0.66$), e.g., the most notable contributor was the act variable with a weight contribution of $RW_{act,Bsl} = 0.89$. At the same time, temp contributed the least with $RM_{temp,Bsl} = 0.10$ ([Figure 7](#) Baseline). Finally, the contribution patterns changed over time, e.g., when the animals recovered. While all variables returned to their baseline positions, hrv and act remained more elevated than others.

The contribution patterns over time were animal-model specific. We also analyzed the additional studies for which RELSA analyses were performed. The RELSA performances of these studies are visualized in the [Supplementary materials 8A–F](#). The corresponding radar charts/contribution patterns can also be found in the [Supplementary material 9](#). Here, we saw, e.g., that the RELSA in the CLP model was dominated by the large differences in the temperature variable. However, the other outcome measures, except for bwc, also contributed but were not as strong as the temperature. Note that the time was reported in hours in the CLP study, not days ([Supplementary materials 9.1–9.3](#)). The sampling time or lag in bwc could not keep track of the fast changes in the severity status.

Interestingly, activity was the most contributing variable in CLP Sham animals ([Supplementary material 9.3](#)), but temperature and heart rate also contributed to the RELSA. Over the first days, the activity was the dominating variable in animals suffering from colitis with stress ([Supplementary material 9.5](#)) and colitis without stress ([Supplementary material 9.4](#)). Still, on day 7, body weight became more relevant.

As expected, RELSA weights from colitis control mice showed only minor changes within any observed variables ([Supplementary material 9.6](#)).

Discussion

More objective, comparable, evidence-based severity assessment methods are highly demanded. They offer a plethora of quality improvements regarding, e.g., (a) science, with higher standards in hypothesis testing, (b) the ability to monitor the best-possible individual animal welfare, (c) the ethical prerequisite for experimental refinement procedures, e.g., such as reducing the burdens in animals, and, (d) higher data quality, e.g., to counter the adverse effects of the reproducibility crisis. Finally, from a legal point of view, ensuring animal welfare and severity assessment is mandatory in many countries, e.g., in all EU member states (4). However, the large number and diversity of animal models and the lack of validated methods hinder clear definitions of severity categories (17). Consequently, this raises legal uncertainties for scientists and authorities, resulting in potential bias, e.g., in the actual and prospective severity ratings.

With the RELSA procedure, we addressed these critical points in laboratory animal science and developed a tool enabling an evidence-based severity assessment. RELSA uses an arbitrary number of outcome measures to compute a composite metric for welfare assessment and severity grading (18–20). To our knowledge, this is the first attempt in preclinical science to combine phenotypical data with the necessary experimental severity context to allow a qualitative grading between individual animals, subgroups, and models. This approach contrasts with current standards using human judgment to generate numerical scores for assessing welfare.

Addressing our initial hypothesis, we demonstrated that variables differed in performance and showed changing patterns in relative contributions over time, e.g., during the recovery phase. This empowers time-resolved refinement procedures, in which specific markers, e.g., for pain and temperature models, can be identified. Furthermore, the fact that these contribution patterns were highly animal-model-specific strengthens the concept of a multimodal severity assessment. Finally, RELSA paves the way for the field of comparative quantitative severity assessment, allowing the direct comparison of distinct animal models concerning severity levels. Ultimately, we speculate that the RELSA procedure will also apply to the human clinical context.

RELSA in the current practice of composite scoring

The principle of composite scoring is based on systems utilized for clinical monitoring and risk assessment in human

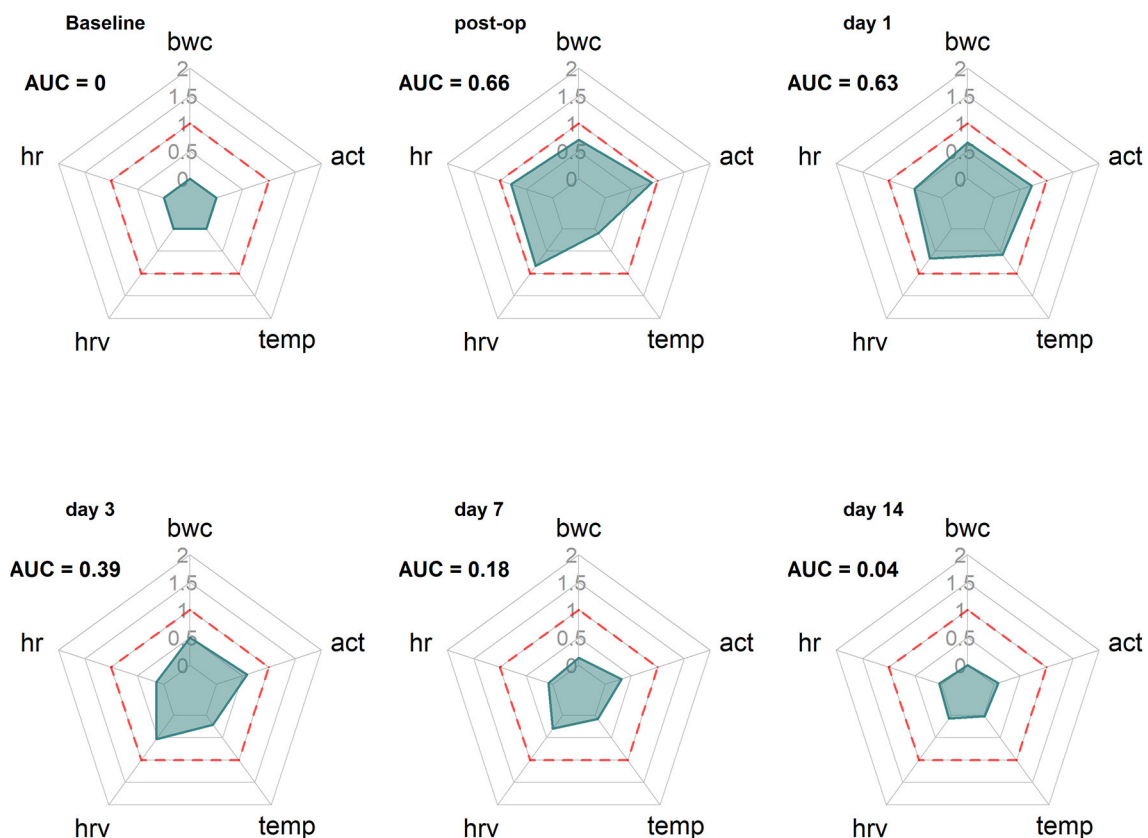


FIGURE 7

Radar charts reveal the time-dependent changing contribution of the outcome measures bwc, act, temp, hrv, and hr to the RELSA. The RELSA weights (RW) from the TM-implantation subgroup ($n = 13$) are averaged on six days (baseline, post-op day 0, day 1, day 3, day 7, and day 14) of the experiment. The dashed red line indicates the RELSA reference level of 1. Note, e.g., how the hrv stays elevated longer than the other outcome measures, showing the different and animal-model dependent qualities that single variables can assume in severity assessment.

medicine. One example in humans is the Acute Physiology And Chronic Health Evaluation (APACHE II) score, first reported in 1985. The APACHE II score comprises 12 physiological and laboratory parameters with an additional weighting for age and preadmission health status to predict the risk of death (21, 22). In contrast, the Sequential Organ Failure Assessment (SOFA) score, established in 1996, consists of 6 different scores assessing distinct organ dysfunction and failure (23, 24). The score describes the status of morbidity and critical illness but does not predict the outcome. Currently, the SOFA score is used in the severity assessment of COVID-19 patients to characterize mortality among intensive care unit (ICU) patients (25). In veterinary medicine and laboratory animal science, there are various composite scores available, e.g., the clinical severity index for acute pancreatitis in canines (26), composite behavior scores for pain assessment in rodents (27, 28), or composite measure schemes for rat epilepsy models (9). These are elaborated systems tailored to model-specific characteristics which provide valuable insights into animal welfare.

To create a more generalized severity assessment approach that also addresses the specific needs of scientists and authorities working in laboratory animal science, we developed a procedure with the potential of combining any outcome measurement from clinical and behavioral examinations, thus widening the applicability across scientific fields. According to the EU directive, a severity classification is mandatory in the authorization process of animal experiments. However, the current classification poses several ambiguities as it is not comprehensive, not based on objective parameters, and does not consider refinement measures. Therefore, a comprehensive overview of classified models using evidence-based parameters will resolve this situation. RELSA provides a means to achieve this goal. From a scientific point of view, comparing the severity of different animal models on a multidimensional scale offers deep insight into the quantitative nature of animal wellbeing. This kind of severity mapping is a crucial feature that many in the 3R community request.

In addition, this approach considers the multidimensional nature of severity, reflecting pain and distress and affective,

emotional states. We showed that not every variable reports the same severity information and that the content changes over time. Thus, the chosen parameters for severity assessment should be multimodal (12, 29). Furthermore, such a holistic approach enables refinement procedures. Multiple outcome variables indicate different sources of disturbed animal wellbeing over time, which is challenging or impossible to observe using single parameters. In addition, the RELSA procedure enables the comparison of models that differentially impact the welfare of animals on a relative scale. Of course, knowing these differences also allowed severity assessment in a well-understood and characterized model, using just the most prominent contributing variables. Therefore, when developing RELSA, we aimed at a quantitative grading of severity, while current methods in the veterinary sciences are characterized mainly by qualitative scorings.

Outcome measures

In the present study, we used a comprehensive panel of methods to monitor the welfare of animals after various experimental procedures, e.g., with TM implantation as a use case. To exclude selection bias, we calculated the models' severity levels with a set of available outcome measures: body weight change, burrowing behavior, and telemetry-derived parameters, including hr, hrv, temperature, and activity. These outcome measures were selected based on increasing evidence of their suitability in various model systems as well as several round-table discussions within our German Research Foundation (DFG)-funded research consortium 2591, which focuses on severity assessment in animal-based research (www.severity-assessment.de) (7, 8, 29).

We observed that although some variables showed high sensitivity toward the implantation procedure, the change was short-lived. The most prominent example here is the burON variable. Burrowing is a highly motivated behavior of mice and is impaired under painful conditions or in mouse models of anxiety and schizophrenia (30, 31). In this study, burrowing was highly sensitive in detecting changes in welfare but only immediately after TM implantation. Likewise, bwc sensitively indicated the impact of TM surgery but quickly recovered within 4–6 days after the operation. Body weight is considered one of the most critical parameters in classic clinical scoring of rodents (32). However, monitoring body weight as a severity assessment parameter was model-specific and should be combined with other parameters (32).

In contrast, the telemetry-derived parameters hr, hrv, and act showed strong changes on the post-op day and indicated a longer-lasting impact on the animals, suggesting an extended recovery period (up to day 14). Telemetry is a frequently used method in biomedical research. For example, it has been shown that hr and hrv are suited for indicating distress and pain

(33, 34), and hr and body temp serve as critical parameters in sepsis studies (35).

Our findings make us assume that the various parameters reflected different facets of severity (e.g., pain) better than others or that the animals lose some aspects over time. However, this exciting hypothesis remains elusive. The present results underpin the need for a combination of parameters to fully assess the (severity) situation, including physiological outcome measures. Therefore, the “usefulness” of outcome measures is dependent on the analytical purpose (e.g., acute pain vs. long-term impairment). We plan on expanding the RELSA applicability to this field.

Using RELSA in comparisons

Usually, animals in a study are monitored over time, and the intervention effect is present somewhere on that timeline. However, in the TM-implantation model, the RELSA outcomes were skewed toward the time point with the most dominant deviations in the contributing outcome (post-op day). Since the exact maximum depends on the animal model under observation, a better choice for comparisons is the individual RELSA_{max} values representing each animal's time-independent maximally achieved RELSA values. The most extreme values reveal the maximally achieved severity better than the average. If the animal model is stable (e.g., showing consistent variance), the resulting RELSA_{max} values can be used, e.g., in animal model comparisons (Figure 6). Comparing the RELSA_{max} values revealed that TM implantation exhibited higher severity than Sham operations. However, the Sham operation also showed minimal severity due to natural variance.

Validating the RELSA procedure

The RELSA procedure was validated using data from models with different forms and grades of impairments. In addition, data from an acute DSS-colitis model, an acute DSS colitis combined with repeated restraint stress, and a CLP sepsis model were assessed. Figure 6 shows that the RELSA_{max} values remained within the moderate frame of the four *k*-means cluster levels except for the CLP non-survivors and did not exceed the RELSA reference level of 1. In addition, the colitis RELSA_{max} values are reliably clustered in level L2, indicating a lower severity for the DSS-colitis model than in the TM-implantation study. However, 3 animals had to be euthanized in the colitis + stress study because the humane endpoint (max. of 20% weight loss) was reached. According to the project authorization, this was set to ensure that animals experience only a maximum of moderate severity levels. However, this also resulted in the loss of quantitative severity information. And although the RELSA values indicated increased suffering

(Supplementary material 8D), they also implied that the animals might have been euthanized too soon, challenging the 20% loss in body weight threshold as an objective endpoint to ensure moderate severity levels. Even though the predefined endpoint in a single variable was reached, the remaining variables did not support a general increase in overall suffering concerning the reference set. Data from the CLP study revealed very high RELSA values in the animals that did not survive the procedure ($RELSA_{max} \geq 2.60$) and lower values for the prevailing and Sham animals ($RELSA_{max} < 1$). The main factor responsible for the high values was the decrease in temperature, but hrv and act also indicated increases in severity. Here, more than one variable points toward increased suffering and an increased impairment in wellbeing. In addition to the between-model validation of the procedure, we validated RELSA internally for the reference data. Since we were not seeking to challenge established “gold-standard” procedures, we ensured that RELSA was at least comparable to or even better than clinical scoring (Supplementary material 7.1). Furthermore, the interval validation showed that RELSA is more precise with the current parameters and reveals information that subjective scoring could not catch (Supplementary material 7.2). Together with the model comparison capability of the RELSA, these features substantially improve the current standard of any severity assessment.

RELSA principle and critical issues

RELSA enables scientists to quantify severity. The procedure can classify animals, subgroups, and animal models in a qualitative framework, e.g., mild, moderate, and severe. The necessary context must be provided as a reference set for such a qualitative grading. Ideally, this should be an animal model from which the qualitative severity context can be extrapolated while offering multiple outcome measures that consistently substantiate the quantitative scale. The caveat that makes up for the word “relative” in RELSA is that researchers must provide some qualitative estimate about the reference set’s severity—ultimately, a step that still involves human judgment. However, once defined, a new experiment can be put into a quantitative severity context, always regarding the development in the reference set. This unique concept allows an evidence-based comparison of models within actual statutory provisions and guidelines. The Supplementary material explains the RELSA procedure so researchers can apply this method easily (Supplementary material 4).

In addition to providing context, the reference set has another purpose: it regularizes the possible ranges of the input variables. This can prove essential in severity assessment, as variables in negatively affected animals behave differently. For example, a loss of 17% in body weight is generally recognized as a threat to animal health (32). At the same time, the burrowing

behavior may drop to zero. In this case, a difference of 17% in one variable is equivalent to a 100% difference in the other variable. For an optimal representation of this bias, we calculated individual RELSA weights (RW) as effect sizes for each variable and day, contributing to the final calculation. These weights can be considered a particular form of effect size somewhat related to Glass’ Δ (36). However, for the RW values, the differences are that they are not standardized to the standard deviation in the control group but instead to the difference of the respective variable to its maximum deviation in the reference set. This approach estimates *within*-animal effect sizes and measurements of a particular variable’s importance. We concluded that variables with larger deviations should have more impact on the generalization of the weights. In comparison, smaller deviations primarily represent noise and effects that are less prominent within a cohort. In statistics, this is followed by the root mean square (RMS) concept, e.g., in error and regression analysis. In contrast to a pure sum score, the RMS has the advantage that it directly translates to the scale of the individual weights and is considered more accurate in showing the best fit.

Another critical issue is the study-dependent sampling and measurement frequency of the outcome measure. For example, body weight is measured once per day (in the morning) and the burrowing behavior after a particular time (e.g., overnight). The sampling rates in these cases are (a) not equal and (b) not frequent enough to catch minute-by-minute changes. Transient changes in such variables thus appear as “all-or-nothing” parameters. Here, the biological changes happen faster than the sampling rates, so the exact development over time cannot be seen. Although the sampling rate cannot be corrected with RELSA, the skewness in distribution can be adjusted to a certain degree by including extreme values of a reference model with known severity in the calculation. This way, a model is backward compatible on the time scale, as we have shown with the CLP data, sampled on an hourly basis compared to the daily data in the reference model. To be comparable, we suggest that measurements in the reference set be from roughly the same reporting frame (e.g., day). This will also pave the way to a possible RELSA focusing on short-term bursts in severity changes (e.g., pain models) that were not covered in this study.

Outlook and conclusion

RELSA was designed to assess the multidimensional severity facets that an animal experiences under impaired welfare conditions. Therefore, combining objective outcome measures into a composite metric has the advantage of an unbiased severity assessment without the need for interpretation or analysis. Furthermore, we have shown that such a hybrid model can be built, tested, and validated. In the future, comparing more animal models will lead to a severity map that can be

used to better understand the multivariate nature of severity in laboratory animals. Finally, we have provided a framework that can be easily implemented into any severity-related research project's daily routine via the RELSA R package or web application. Eventually, assessing the severity and enabling the ranking of animal models in terms of their welfare impairment will become much more precise. This aspect may also reveal more generalized or specific variables for monitoring severity. With the development of home cage monitoring systems, RELSA will enable an automatic and continuous assessment of the animals and, thereby, an early warning system helping to identify animals at risk.

Data availability statement

The datasets presented in this study can be found in online repositories. The names of the repository/repositories and accession number(s) can be found in the article/[Supplementary material](#).

Ethics statement

Experiments involving surgery, DSS colitis, and stress were reviewed and approved by the Local Institutional Animal Care and Research Advisory Committee and permitted by the Lower Saxony State Office for Consumer Protection and Food Safety (LAVES, Oldenburg, Lower Saxony, Germany; license 15/1905). The application for the animal experiments involving sepsis (authorization no. V54 – 19c 20/15 – F152/1016) was approved by the local Ethics Committee for Animal Research (Darmstadt, Hessen, Germany). All procedures were carried out following the German law for animal protection and the European Directive 2010/63/EU.

Author contributions

ST, CH, and AB conceptualized the study and drafted the manuscript. CH and AB designed the TM implantation and

colitis study. CH, BS, LW, NW, MHe, LK, PJ, TK, MHo, and AK conducted the experiments, collected and annotated the data, and performed the descriptive analysis. ST redesigned the data annotations, developed, and coded the RELSA procedure, developed the R package and its applications, and conducted the corresponding (statistical) analyses. All authors discussed the results and commented on the manuscript.

Acknowledgments

This research was supported by the DFG research group FOR 2591 (HA6483/1-2, BL953/10-1 and 10-2, BL953/11-1 and 11-2) and by the research funding program Landes-Offensive zur Entwicklung wissenschaftlich-ökonomischer Exzellenz (LOEWE) of the State of Hesse, Germany.

Conflict of interest

The authors declare that the research was conducted in the absence of any commercial or financial relationships that could be construed as a potential conflict of interest.

Publisher's note

All claims expressed in this article are solely those of the authors and do not necessarily represent those of their affiliated organizations, or those of the publisher, the editors and the reviewers. Any product that may be evaluated in this article, or claim that may be made by its manufacturer, is not guaranteed or endorsed by the publisher.

Supplementary material

The Supplementary Material for this article can be found online at: <https://www.frontiersin.org/articles/10.3389/fvets.2022.937711/full#supplementary-material>

References

1. Poole T. happy animals make good science. *Lab Anim.* (1997) 31:116–24. doi: 10.1258/002367797780600198
2. Russell WMS, Burch RL. *The Principles of Humane Experimental Technique*. Wheathampstead: Universities Federation for Animal Welfare (1959).
3. Council NR. *Guide for the Care and Use of Laboratory Animals: Eighth Edition*. Washington, DC: The National Academies Press (2011). p. 246.
4. Directive 2010/63/Eu of the European parliament and of the council of 22 september 2010 on the protection of animals used for scientific purposes. *Official J Eur Union.* (2010) L276:33–79.
5. Mellor DJ. Operational details of the five domains model and its key applications to the assessment and management of animal welfare. *Animals.* (2017) 7:60. doi: 10.3390/ani7080060
6. Lewejohann L, Schwabe K, Häger C, Jirkof P. Impulse for animal welfare outside the experiment. *Lab Anim.* (2020) 54:150–8. doi: 10.1177/0023677219891754
7. Jirkof P, Rudeck J, Lewejohann L. Assessing affective state in laboratory rodents to promote animal welfare-what is the progress in applied refinement research? *Animals.* (2019) 9:1026. doi: 10.3390/ani9121026

8. Bleich A, Tolba RH. How can we assess their suffering? German research consortium aims at defining a severity assessment framework for laboratory animals. *Lab Anim.* (2017) 51:667. doi: 10.1177/0023677217733010
9. van Dijk RM, Koska I, Bleich A, Tolba R, Seiffert I, Möller C, et al. Design of composite measure schemes for comparative severity assessment in animal-based neuroscience research: a case study focussed on rat epilepsy models. *PLoS ONE.* (2020) 15:e0230141. doi: 10.1371/journal.pone.0230141
10. Wassermann L, Helgers SOA, Riedesel AK, Talbot SR, Bleich A, Schwabe K, et al. Monitoring of heart rate and activity using telemetry allows grading of experimental procedures used in neuroscientific rat models. *Front Neurosci.* (2020) 14:587760. doi: 10.3389/fnins.2020.587760
11. Häger C, Keubler LM, Talbot SR, Biernot S, Weegh N, Buchheister S, et al. Running in the wheel: defining individual severity levels in mice. *PLoS Biol.* (2018) 16:e2006159. doi: 10.1371/journal.pbio.2006159
12. Abdelrahman A, Kumstel S, Zhang X, Liebig M, Wendt EHU, Eichberg J, et al. A novel multi-parametric analysis of non-invasive methods to assess animal distress during chronic pancreatitis. *Sci Rep.* (2019) 9:14084. doi: 10.1038/s41598-019-50682-3
13. Kumstel S, Tang G, Zhang X, Kerndl H, Vollmar B, Zechner D. Grading distress of different animal models for gastrointestinal diseases based on plasma corticosterone kinetics. *Animals.* (2019) 9:145. doi: 10.3390/ani9040145
14. Mallien AS, Pfeiffer N, Brandwein C, Inta D, Sprengel R, Palme R, et al. Comparative severity assessment of genetic, stress-based, and pharmacological mouse models of depression. *Front Behav Neurosci.* (2022) 16:908366. doi: 10.3389/fnbeh.2022.908366
15. Mähler M, Berard M, Feinstein R, Gallagher A, Illgen-Wilcke B, Pritchett-Corning K, et al. Felasa recommendations for the health monitoring of mouse, rat, hamster, guinea pig and rabbit colonies in breeding and experimental units. *Lab Anim.* (2014) 48:178–92. doi: 10.1177/0023677213516312
16. Deacon RM. Burrowing in rodents: a sensitive method for detecting behavioral dysfunction. *Nat Protoc.* (2006) 1:118–21. doi: 10.1038/nprot.2006.19
17. Hemsworth PH, Mellor DJ, Cronin GM, Tilbrook AJ. Scientific assessment of animal welfare. *N Z Vet J.* (2015) 63:24–30. doi: 10.1080/00480169.2014.966167
18. Baumgaertner H, Mullan S, Main DC. Assessment of unnecessary suffering in animals by veterinary experts. *Vet Rec.* (2016) 179:307. doi: 10.1136/vr.103633
19. Zintzsch A, Noe E, Reissmann M, Ullmann K, Krämer S, Jerchow B, et al. Guidelines on severity assessment and classification of genetically altered mouse and rat lines. *Lab Anim.* (2017) 51:573–82. doi: 10.1177/0023677217718863
20. Smith D, Anderson D, Degryse AD, Bol C, Criado A, Ferrara A, et al. Classification and reporting of severity experienced by animals used in scientific procedures: Felasa/Eclan/Eslav working group report. *Lab Anim.* (2018) 52:5–57. doi: 10.1177/0023677217744587
21. Knaus WA, Zimmerman JE, Wagner DP, Draper EA, Lawrence DE. Apache-acute physiology and chronic health evaluation: a physiologically based classification system. *Crit Care Med.* (1981) 9:591–7. doi: 10.1097/00003246-198108000-00008
22. Knaus WA, Draper EA, Wagner DP, Zimmerman JE. Apache II: a severity of disease classification system. *Crit Care Med.* (1985) 13:818–29. doi: 10.1097/00003246-198510000-00009
23. Vincent JL, Moreno R, Takala J, Willatts S, De Mendonca A, Bruining H, et al. The sofa (sepsis-related organ failure assessment) score to describe organ dysfunction/failure. On behalf of the working group on sepsis-related problems of the European society of intensive care medicine. *Intensive Care Med.* (1996) 22:707–10. doi: 10.1007/BF01709751
24. Vincent JL, de Mendonca A, Cantraine F, Moreno R, Takala J, Suter PM, et al. Use of the sofa score to assess the incidence of organ dysfunction/failure in intensive care units: results of a multicenter, prospective study. Working group on “sepsis-related problems” of the European society of intensive care medicine. *Crit Care Med.* (1998) 26:1793–800. doi: 10.1097/00003246-199811000-00016
25. Zhou F, Yu T, Du R, Fan G, Liu Y, Liu Z, et al. Clinical course and risk factors for mortality of adult inpatients with COVID-19 in Wuhan, China: a retrospective cohort study. *Lancet.* (2020) 395:1054–62. doi: 10.1016/S0140-6736(20)30566-3
26. Mansfield CS, James FE, Robertson ID. Development of a clinical severity index for dogs with acute pancreatitis. *J Am Vet Med Assoc.* (2008) 233:936–44. doi: 10.2460/javma.233.6.936
27. Roughan JV, Wright-Williams SL, Flecknell PA. Automated analysis of postoperative behaviour: assessment of homecagescan as a novel method to rapidly identify pain and analgesic effects in mice. *Lab Anim.* (2009) 43:17–26. doi: 10.1258/la.2008.007156
28. Wright-Williams S, Flecknell PA, Roughan JV. Comparative effects of vasectomy surgery and buprenorphine treatment on faecal corticosterone concentrations and behaviour assessed by manual and automated analysis methods in C57 and C3h mice. *PLoS ONE.* (2013) 8:e75948. doi: 10.1371/journal.pone.0075948
29. Keubler LM, Hoppe N, Potschka H, Talbot SR, Vollmar B, Zechner D, et al. Where are we heading? Challenges in evidence-based severity assessment. *Lab Anim.* (2020) 54:50–62. doi: 10.1177/0023677219877216
30. Jirkof P. Burrowing and nest building behavior as indicators of wellbeing in mice. *J Neurosci Methods.* (2014) 234:139–46. doi: 10.1016/j.jneumeth.2014.02.001
31. Barkus C, Feyder M, Graybeal C, Wright T, Wiedholz L, Izquierdo A, et al. Do glua1 knockout mice exhibit behavioral abnormalities relevant to the negative or cognitive symptoms of schizophrenia and schizoaffective disorder? *Neuropharmacology.* (2012) 62:1263–72. doi: 10.1016/j.neuropharm.2011.06.005
32. Talbot SR, Biernot S, Bleich A, van Dijk RM, Ernst L, Häger C, et al. Defining body-weight reduction as a humane endpoint: a critical appraisal. *Lab Anim.* (2020) 54:99–110. doi: 10.1177/0023677219883319
33. Arras M, Rettich A, Cinelli P, Kasermann HP, Burki K. Assessment of post-laparotomy pain in laboratory mice by telemetric recording of heart rate and heart rate variability. *BMC Vet Res.* (2007) 3:16. doi: 10.1186/1746-6148-3-16
34. Cesarovic N, Jirkof P, Rettich A, Arras M. Implantation of radiotelemetry transmitters yielding data on ecg, heart rate, core body temperature and activity in free-moving laboratory Mice. *J Vis Exp.* (2011) 57:3260. doi: 10.3791/3260
35. Lewis AJ, Yuan D, Zhang X, Angus DC, Rosengart MR, Seymour CW. Use of biotelemetry to define physiology-based deterioration thresholds in a murine cecal ligation and puncture model of sepsis. *Crit Care Med.* (2016) 44:e420–31. doi: 10.1097/CCM.0000000000001615
36. Kavale KA, Glass GV. Meta-analysis and the integration of research in special education. *J Learn Disabil.* (1981) 14:531–8. doi: 10.1177/002221948101400909



OPEN ACCESS

EDITED BY

Annamarie Lang,
University of Pennsylvania,
United States

REVIEWED BY

Shari Cohen,
The University of Melbourne, Australia
Abbie Viscardi,
Kansas State University, United States

*CORRESPONDENCE

Carola Fischer-Tenhagen
carola.fischer-tenhagen@bfr.bund.de

SPECIALTY SECTION

This article was submitted to
Animal Behavior and Welfare,
a section of the journal
Frontiers in Veterinary Science

RECEIVED 25 July 2022

ACCEPTED 09 November 2022

PUBLISHED 06 December 2022

CITATION

Fischer-Tenhagen C, Meier J and
Pohl A (2022) "Do not look at me like
that": Is the facial expression score
reliable and accurate to evaluate pain
in large domestic animals? A
systematic review.
Front. Vet. Sci. 9:1002681.
doi: 10.3389/fvets.2022.1002681

COPYRIGHT

© 2022 Fischer-Tenhagen, Meier and
Pohl. This is an open-access article
distributed under the terms of the
[Creative Commons Attribution License](#)
(CC BY). The use, distribution or
reproduction in other forums is
permitted, provided the original
author(s) and the copyright owner(s)
are credited and that the original
publication in this journal is cited, in
accordance with accepted academic
practice. No use, distribution or
reproduction is permitted which does
not comply with these terms.

"Do not look at me like that": Is the facial expression score reliable and accurate to evaluate pain in large domestic animals? A systematic review

Carola Fischer-Tenhagen^{1*}, Jennifer Meier¹ and Alina Pohl²

¹German Centre for the Protection of Laboratory Animals (Bf3R), German Federal Institute for Risk Assessment (BfR), Berlin, Germany, ²Clinic of Animal Reproduction, Freie Universität Berlin, Berlin, Germany

Introduction: Facial expression scoring has proven to be useful for pain evaluation in humans. In the last decade, equivalent scales have been developed for various animal species, including large domestic animals. The research question of this systematic review was as follows: is facial expression scoring (intervention) a valid method to evaluate pain (the outcome) in large domestic animals (population)?

Method: We searched two databases for relevant articles using the search string: "grimace scale" OR "facial expression" AND animal OR "farm animal" NOT "mouse" NOT "rat" NOT "laboratory animal." The risk of bias was estimated by adapting the Quality Assessment of Diagnostic Accuracy Studies (QUADAS) checklist.

Results: The search strategy extracted 30 articles, with the major share on equids and a considerable number on cows, pigs, and sheep. Most studies evaluated facial action units (FAUs), including the eye region, the orbital region, the cheek or the chewing muscles, the lips, the mouth, and the position of the ears. Interobserver reliability was tested in 21 studies. Overall FAU reliability was substantial, but there were differences for individual FAUs. The position of the ear had almost perfect interobserver reliability (interclass coefficient (ICC): 0.73–0.97). Validity was tested in five studies with the reported accuracy values ranging from 68.2 to 80.0%.

Discussion: This systematic review revealed that facial expression scores provide an easy method for learning and reliable test results to identify whether an animal is in pain or distress. Many studies lack a reference standard and a true control group. Further research is warranted to evaluate the test accuracy of facial expression scoring as a live pen side test.

KEYWORDS

grimace scales, assessment, pain, facial action, large animal

Introduction

Reliable and accurate pain assessment is necessary for pain management and, specifically, the impact of interventions on animals in experiments. Only if pain is correctly recognized and classified, it can be successfully managed. Pain is defined as "an unpleasant sensory and emotional experience associated with, or resembling that

associated with, actual or potential tissue damage” (1, 2). Pain not only is a question of the severity of trauma or tissue damage but also has a time dimension. Acute pain occurs in injuries or specific diseases and is associated with the activation of the sympathetic nervous system. Chronic pain persists for more than 3 months and is considered a disease state (3). In addition, pain also has an emotional and individual component. Therefore, pain is a subjective experience with multiple dimensions, all of which can have an influence on individual pain perception and expression. To estimate the pain sensation of the human individual patient, a numerical or visual rating scale from 1 to 10 was introduced to improve adequate pain management (4). Animals cannot verbally communicate their pain experience. Therefore, the gold standard for measuring pain in humans is not available in animals.

Current methods for assessing pain in animals focus on changes in behavior and physiology. Animals in pain feed less, play less, and have a change in activity and lying behavior (5, 6). The release of glucocorticoids (7), the change in heart rate variability (8), or the variation in the composition of immune cells (9) are useful physiological parameters for assessing aversive situations. However, on-farm or pen side pain identification techniques should rely on immediate rather than retrospective indicators of pain. This ensures that humane intervention can be applied promptly without leaving animals in distress for an extended period of time (10).

In non-verbal humans, like infants, facial expressions provide a reliable indicator of pain (11, 12). Facial expression is the measure of changes in the face or in groups of muscles, known as “action units” in relation to a stimulus. Ekman (13) developed the Facial Action Coding System (FACS). This system enabled trained persons to code over 40 distinct muscle movements in the face (14). The benefits of externalizing pain through facial expressions are thought to be evolutionary and effective in increasing the chances of survival by inducing empathy in other individuals (15, 16).

Facial expressions have been shown to be consistent during the induction of pain by various modalities of nociceptive stimulation in humans. The human pain face comprises five action units: brow lowering, lid tightening, wrinkled nose, raised upper lip, and eye closure (17). Darwin (18) also observed that animals express emotions through facial expressions similar to humans. Across the different species, there are similar facial movements and action units expressed in the presence of pain (19). Thus, facial expressions are considered honest signals of the affective state and pain intensity (20).

In 2010, Langford et al. (21) introduced a facial expression score to assess pain in mice by comparing the facial expressions of painless and painful animals. Since then, similar comparable “grimace scales” or “facial expression scores” were developed and reported for various species, such as rats (22), rabbits (23), ferrets (24), sheep (25), horses (26), pigs (27), cattle (28), and

cats (29). In most of these studies, scientists produced frames out of videos pre and post painful experiences in animals. Scientists could demonstrate that observers blinded to treatment could identify specific pain faces and scored frames of animals with pain higher than animals without pain.

Cows and sheep are often described as especially stoic and showing no pain (30). Modern cows, extensively managed ruminants, and their wild ancestors are still considered prey species. It is thought that showing evidence of injury could attract potential predators. As they do not inherently portray pain, it makes it even more difficult for humans to determine their welfare needs. Therefore, pain assessment in farm animals is especially critical. Several studies report evidence that facial expressions are valid and reliable for evaluating pain in farm or large domestic animals (25, 26).

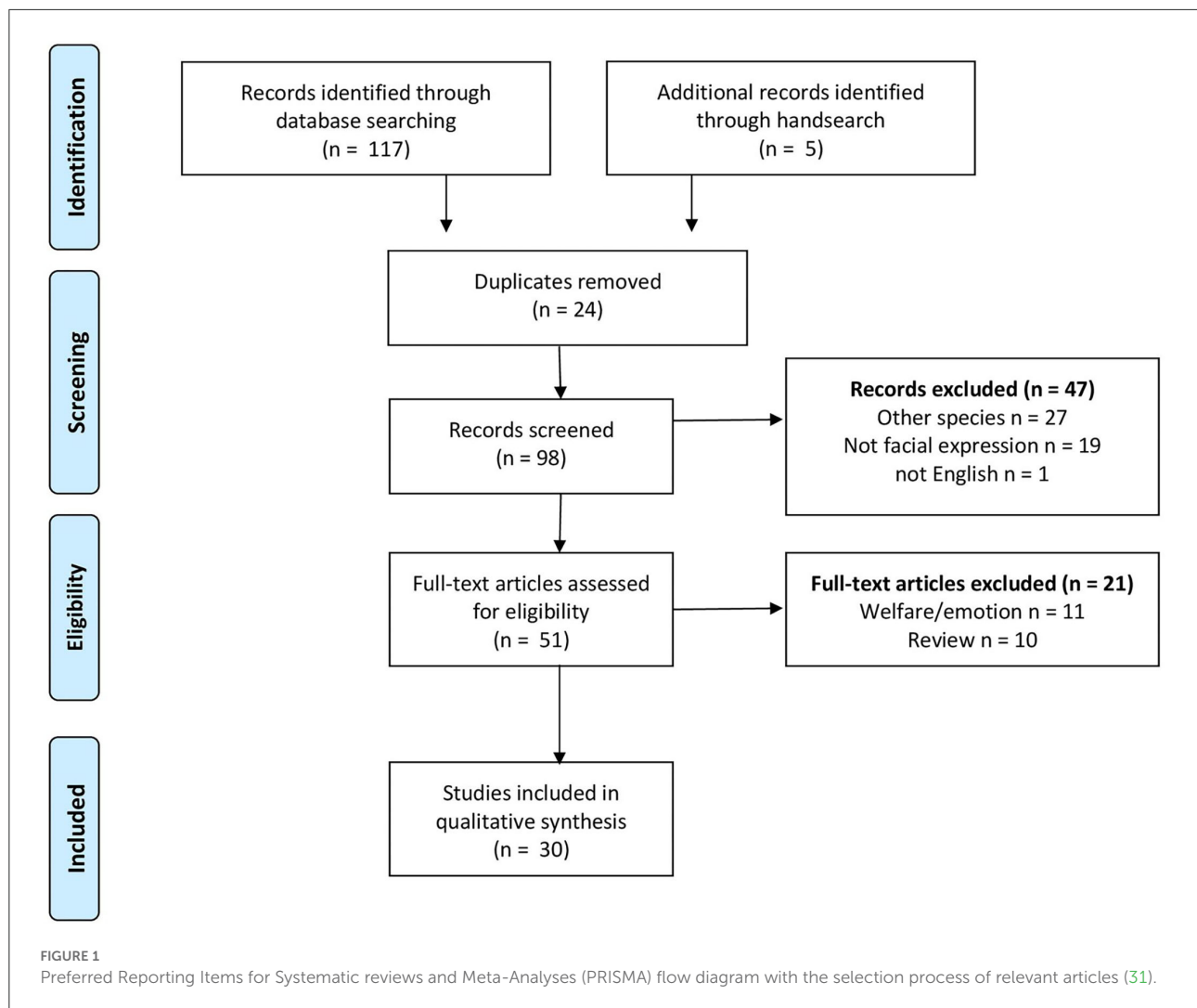
The objectives of this systematic review were to summarize and categorize the results of recent papers on the facial expression score in large domestic animals. Our specific research question was: Is the facial expression score (intervention) a valid method to evaluate pain (the outcome) in large domestic animals (population)? We wanted to evaluate the risk of bias in these studies and compare the results in terms of reliability and accuracy. As a result, we wanted to identify the best practice for the use of facial expression scoring in large domestic animals, point out the flaws and challenges with this technique, and identify the need for further research in this field.

Materials and methods

To identify the literature relevant to the question, we developed a search strategy in the PubMed (<https://pubmed.ncbi.nlm.nih.gov>) and Web of Science (<https://apps.webofknowledge.com>) databases including the following keywords: “grimace scale” OR “facial expression” AND “pain” AND “animal” OR “farm animal” NOT “mouse” NOT “rat” NOT “laboratory animal.” We searched the database on 20 January 2022. Relevant articles found in the reference list of retained articles were included as “hand search.” The selection strategy is illustrated in Figure 1.

The data collection process was performed by the first author (CFT) and crosschecked by JM and AP to ensure the integrity of the contents. Articles were screened by title and abstract, and we included articles with the full text published in peer-reviewed journals, written in English, and evaluating pain assessment with facial expressions in large domestic animals. We excluded studies evaluating emotions or welfare *via* facial expressions. Conference abstracts and articles with only an abstract in English were also excluded.

To categorize and evaluate the articles, we assessed them according to the following criteria: the type of study (clinical study, case report, and data-based study), species involved in the study, sample size, qualification and number of observers,



reference (gold) standard, the method of observation (real time, video, and pictures), interobserver reliability test, additional pain assessment methods (composition pain score, behavioral assessment), the number of facial action unit (FAU) scored, and scale range. The reference standard in this review is defined as the best available method to establish the presence or absence of the target condition; a gold standard would be an error-free reference standard (32). Data were extracted into Microsoft Excel (version 2013; Microsoft Corp., Redmond, WA, USA). Descriptive and explorative statistics were performed using SPSS for Windows (version 22.0; SPSS, Inc.). For other methods of addressing study quality, such as sensitivity analysis, subgroup analysis, or meta-regression analysis, the included studies were too low in number and too diverse in design for meaningful investigations.

We assessed the risk of bias in the individual study by adapting the Quality Assessment of Diagnostic Accuracy Studies (QUADAS) checklist (33). The final checklist consists of 12

questions that evaluate items with a potential risk of bias (Figure 3). The percentage of studies with a low, high, or unclear risk of bias for the respective item was summarized in a bar chart. Initially, the assessment was independently done by CFT and AP. In case of disagreement (5% of the answers on the checklist), both authors found a consensus after reviewing the manuscripts again.

Results

Our search strategy resulted in 117 articles from the databases. Five additional articles were retrieved by scanning the reference list of relevant articles. We excluded duplicates ($n = 24$), non-English articles ($n = 1$), reviews ($n = 10$), articles evaluating welfare or emotions ($n = 11$), articles not focusing on large domestic animals ($n = 27$), or articles where the grimace scale or facial expressions were not the objectives

TABLE 1 General characteristics of articles ($n = 30$) included in this review.

First Author	Year	Species	number of animals	Type of study	Pain type	Score Type	Number of score criteria	number of observer	observation
Coneglien	2020	Horse	33	Clinical study	Dental treatment	HGS	6	8	Real time
Dai	2020	Horse	N.A.	Proof of concept	N.A	HGS	6	206	Photo
Dalla Costa	2014	Horse	46	Clinical study	Castration	HGS	6	6	Frame from video
Dalla Costa	2016	Horse	10	Clinical study	Acute laminitis	HGS	6	6	Video and photo
Dalla Costa	2021	Horse	11	Clinical study	Castration	HGS	6	4	Frame from video
Diego	2016	Horse	21	Clinical study	Follicular puncture	HGS	3	N.A.	Real time
Dierendonck	2020	Donkey	254	Clinical study	Painful diseases	FAP	12	6	Real time
Dyson	2017	Horse	101	Observation	Lameness	FEPP	14	1	Photograph
Giminiani	2016	Pig	23	Clinical study	Tail docking, castration	PGS	10	30	Frame from video
Gleerup	2015	Bovine	139	Clinical study	Clinical disease	FEE	6	4	Real time
Gleerup	2015	Horse	6	Clinical study	Capiscain, tournique	Painface	6	1	Photo
Guesgen	2016	Sheep	18	Clinical study	Tail docking	Ear	4	5	Frame from video
Häger	2017	Sheep	14	Clinical study	Tibiatomy	SGS	3	6	Frame from video
Lencioni	2021	Horse	7	Observation	Castration	HGS		1	Photo
McLennan	2016	Sheep	113	Clinical study	Disease	SGS	6	6	Photo
Mullard	2017	Horse	30	Observation	Lameness	FEE	14	13	Photo
Muller	2019	Bovine	35	Clinical study	Hot iron branding	FEE	15	1	Frame from video
Navarro	2020	Pig	21	Clinical study	Farrowing	PGS	5	8	Frame from video
Orth	2020	Donkey	9	Clinical study	Castration	DGS	9	12	Photo
Rashid	2020	Horse	27	Observation	Disease	FACS	27	1	Video
VanLoon	2021	Horse	53	Clinical study	None	FAP	9	2	Real time
VanLoon	2021	Donkey	77	Clinical study	None	FAP	12	2	Real time
VanLoon	2019	Horse	77	Clinical study	Trauma, surgery	FAP	9	2	Real time
VanLoon	2015	Horse	50	Clinical study	Colic	FAP	9	4	Real time
Viscardi	2017	Pig	19	Clinical study	Tail docking, castration	GS	3	2	Frame from video
Viscardi	2021	Sheep	30	Clinical study	Laparatomy	GS	6	3	Photo
Viscardi	2019	Pig	120	Clinical study	Castration	GS	3	8	Photo
Viscardi	2018	Pig	60	Clinical study	Castration	GS	3	4	Photo
Vullo	2020	Pig	10	Clinical study	Castration	GS	3	3	Frame from video
Yamada	2021	Bovine	45	Clinical study	Dental treatment	FAU	4	nk	Photo

NA, not applicable; HGS, horse grimace scale; PGS, pig grimace scale; DGS, donkey grimace scale; SGS, sheep grimace scale; GS, grimace scale; FAP, facial assessment of pain; FEE, facial expression ethogram; FACS, facial action coding system.

of the study ($n = 19$) (Figure 1). We included 30 articles for further evaluation. The general characteristics of the studies are summarized in Table 1.

Twenty-eight studies included animals for data collection. The number of animals included ranged from 6 to 254, with a median of 30 and an interquartile range (IQR) of 43. Two-thirds of studies included animals undergoing general veterinary treatment; all other studies used animals explicitly for their experiment (experimental animals). Two utilized pictures/videos from previous studies for analysis. Species involved were horses ($n = 14$), pigs (sows $n = 1$ and piglets $n = 5$), sheep (adult $n = 2$ and lambs $n = 2$), cattle ($n = 3$), and donkeys ($n = 3$).

Most studies were designed as a clinical study ($n = 27$). Two studies performed specific data analysis, and one manuscript described a training program for learning facial expressions. Clinical studies were categorized as observational studies ($n = 7$), randomized clinical controlled studies ($n = 5$), case-control studies ($n = 12$), and cohort studies ($n = 3$).

The number of observers included in this study was reported in 28 studies, ranging from 1 to 206 with a median of 4.0 and an IQR of 6. Observers in these studies were veterinarians or students of veterinary medicine ($n = 13$), animal scientists or animal professionals ($n = 8$), lay people ($n = 1$), or non-specified ($n = 8$).

The observation modes were real-time ($n = 8$), videos ($n = 1$), and photographs ($n = 2$). Two studies evaluated videos and photos, and 10 studies picked frames out of videos to score FAUs. The number of FAU scored ranged from 3 to 27 with a median of 6. The scale ranged from 2 (yes/no) to 4, including the options “don’t know” or “cannot see.”

Seventeen studies used or evaluated a grimace scale, whereas the rest of the studies evaluated pain by developing a facial expression ethogram with 1 to 27 FAUs. Twenty-one studies assessed and reported interobserver reliability for the scale including all FAUs. Interclass correlation (ICC, $n = 19$) and Kappa coefficient, Kendall, Cronbach’s alpha (one each) were used as statistical methods (Table 2). The reported reliability coefficient ranged from 0.45 to 0.92. Eleven groups evaluated reliability for individual FAU ranging from 0.2 to 1.0 (Figure 2). Twenty-one studies evaluated differences in the grimace scale between animals in the pain and painless control groups, and 17 of these studies reported a significantly higher score for animals in pain. Three studies reported the accuracy of this method to identify pain ranging from 68.2 to 80%, and two groups reported the sensitivity and specificity of this method with 57/87.5% and 90.5/88%, respectively.

Four studies reported the values of facial expression scores pre- and post-intervention. Intervention is meant as the measure taken to provoke pain in the experiment. The horse grimace scale (maximum score 12) had a 3.5- and 2.3-point higher score after castration. Pigs (maximum score of 5) had a 1.14-point higher score after castration, and the sheep grimace scale

(maximum score of 7) rose by 1.3 points after an orthopedic intervention. Different score systems, species, and the type of intervention did not allow any analysis of the effect of the intervention on the pain score.

To assess the risk of bias in these studies, we adapted the checklist for QUADAS (33). CFT and AP independently evaluated the articles with respect to 12 questions (Figure 3). In the following analysis of our evaluation, we found a 95% agreement.

We identified a high risk of selection bias, as, in the majority (28/30) of studies, the study population was a convenience sample. Study animals were either recruited on specific farms (commercial or research) or in animal hospitals or sanctuaries. If the selection of the study population involves evaluating a diagnostic test, the generalizability of the results may be limited. Sample size calculation was not reported in any study. Control groups were found to be not appropriate in 12 studies. Animals in the control group should be handled in the same way as the treatment group to exclude as many confounding variables as possible. Twenty-two studies used the same animal as control (pretreatment and posttreatment), where the effect of time, habituation, and other variables could influence the facial score (35). We agreed that, in most studies, the intervention produced or relieved pain as the target condition.

The number of observers in the studies were appropriate, as two observers are needed for testing interobserver reliability (36). More than two observers assessed FAUs in the majority of studies. The selection of observers included both genders and different levels of experience and expertise with the species of interest; we rated a low risk of selection bias in this respect. Most authors reported that the observers were blinded to the treatment, but in 16 out of 20 studies using videos or frames, the selection of these was not blinded. Pain assessment with other methods as the reference was performed in 24 studies. If the observer is aware of the result of this additional assessment, this can influence their judging in facial expression scoring (33). This issue was not addressed in these studies.

In most studies, all FAUs scored were included in the analysis. However, some FAUs were not present or very rare in experiments. The authors excluded those from the analysis. Unfortunately, there was no consensus among the studies on the number of FAUs in a composite score or the scale range. As such, a one-to-one comparison of the study results is not possible. The validity, a core criterion for the quality of a diagnostic test, was evaluated in only five studies. Without data on test accuracy, an evaluation of the test quality is not possible.

Discussion

Animals cannot communicate verbally regarding their perception of pain or distress. To ensure the good welfare of animals under human care, it is essential to be able to recognize

TABLE 2 Effect of treatment on facial expressions and statistical methods used for analysis.

First Author	Year	Treatment	Effect	Statistics
Coneglien	2020	Dental treatment	Lower pain score	Wilcoxon test
Dai	2020	N.A.	N.A.	N.A.
Dalla Costa	2014	Castration	Effect on pain scores	GLENMIX; ANOVA
Dalla Costa	2016	Acute laminitis	Lower pain score	Wilcoxon signed rank test
Dalla Costa	2021	Castration	Higher pain score	Friedmantest; <i>post hoc</i> Bonferoni
Diego	2016	Follicular puncture	No effect	Mann–Whitney U
Dierendonck	2020	Painful diseases	Higher pain score	Mann–Whitney U
Dyson	2017	Lameness	Higher pain score	Mann–Whitney U
Giminiani	2016	Tail docking, castration	Difference only orbital tightening	Wilcoxon matched pair test
Gleerup	2015	Clinical disease	Higher pain scores	One-tailed <i>t</i> -test with Welch correction
Gleerup	2015	Capiscain, tourniquet	More pain face features	Wilcoxon signed rank test
Guesgen	2016	Tail docking,	Higher pain score	GLENMIX
Häger	2017	Tibiatomy	Higher pain score	ANOVA
Lencioni	2021	Castration	N.A.	N.A.
McLennan	2016	Disease	Higher pain score	Spearman's rank correlations
Mullard	2017	Lameness	N.A.	N.A.
Muller	2019	Hot iron branding	4 FAU with association to pain	McNemar test
Navarro	2020	Farrowing	N.A.	N.A.
Orth	2020	Castration	N.A.	N.A.
Rashid	2020	Disease	Chewing indicative for pain	paired <i>t</i> -test
VanLoon	2021	Chronic pain	Higher pain score only 1 day	Mann–Whitney U
VanLoon	2021	Chronic pain	Higher pain score	Mann–Whitney U
VanLoon	2019	Trauma, surgery	Higher pain score	Mann–Whitney U
VanLoon	2015	Colic	Higher pain score	Mann–Whitney U
Viscardi	2017	Tail docking, castration	Higher pain score	ANOVA
Viscardi	2021	Laparotomy	No effect on pain score	GLENMIX
Viscardi	2019	Castration	Effect on pain score	GLENMIX
Viscardi	2018	Castration	No effect on pain score	GLENMIX
Vullo,	2020	Castration	Higher pain score 6h post treatment	Paired Sample <i>t</i> -test
Yamada	2021	Dental treatment	Positive correlation for eye and above eye	Logistic regression, <i>post hoc</i> Tukey's test

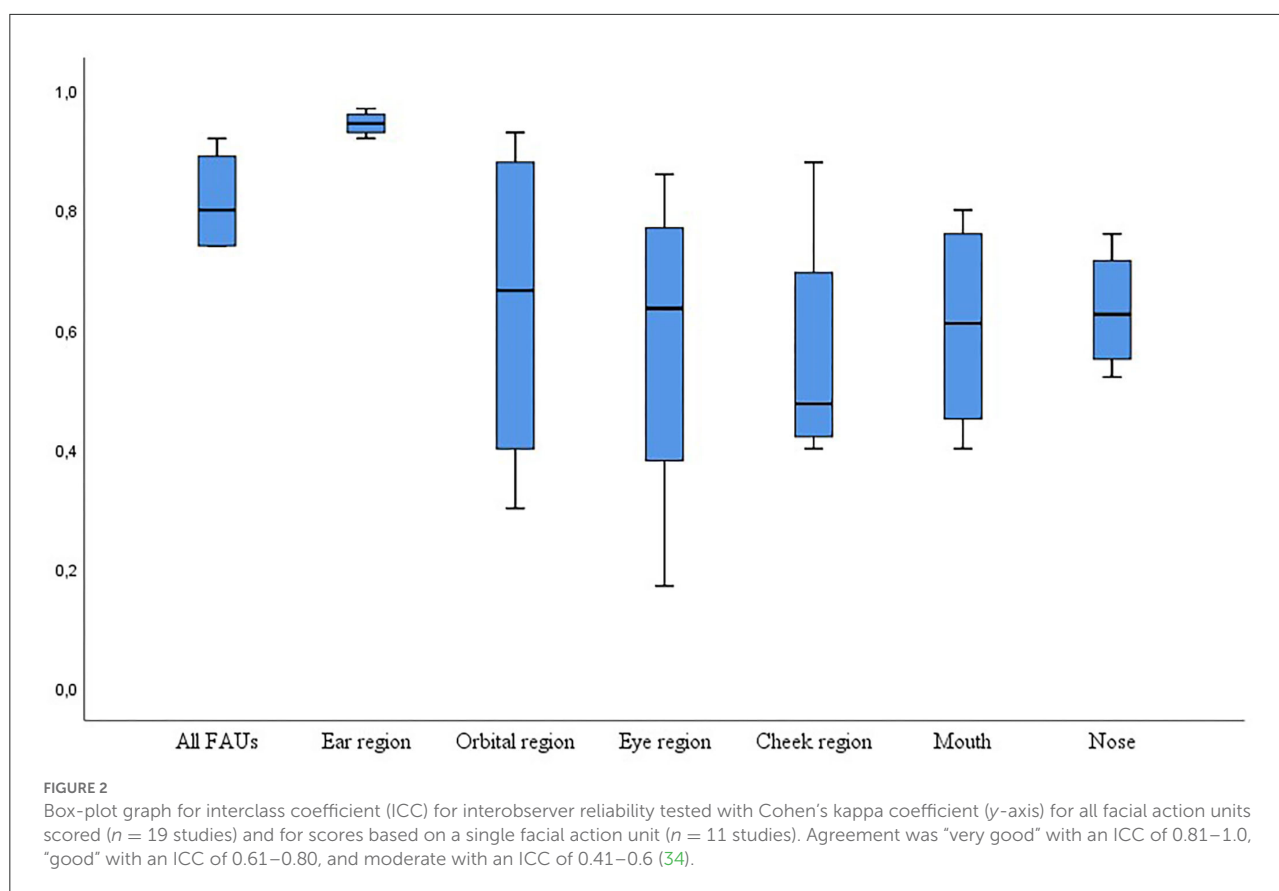
NA, not applicable; ANOVA, analysis of variance; GLENMIX, general linear mixed model; FAU, facial action unit.

and assess pain or distress. This is true for animal husbandry and veterinary issues, especially in animal experiments. For animal experiments, the EU Directive 2010/63/EU requires the assessment of the severity of all procedures in an experiment. In this context, severity describes all adverse effects that animals may experience in an experiment, including discomfort, pain, distress, fear, nutritional deprivation, and behavioral deprivation (37).

As Langford et al. (21) introduced a grimace scale for pain assessment in laboratory mice, a variety of studies aimed at the development and validation of facial expression scores or grimace scales in a variety of species (10) [for a review, see Mota-Rojas (38)]. Although facial expression scores seem to offer an easy-to-learn and cheap pain assessment method, they are not yet widely integrated into the daily routine of animal research (38). These authors concluded that, in their

review on grimace scales in laboratory animals, currently, the retrospective character and time-consuming implementation can hinder the establishment of grimace scales in research practice. In our systematic review, we focused on large domestic animals. The housing and handling of large domestic animals are substantially different from those of laboratory animals. This can have an influence on the usefulness and effectivity of a pain scoring system. We wanted to assess the validity and repeatability of this method for large domestic animals and identify the best practice for veterinary practice and farm animals in research.

Following our search criteria, we included 30 articles, the majority of which were published by European working groups. A systematic literature search is always a snapshot of the date of the search (20 January 2022). Therefore, more recent papers are not included in this review.

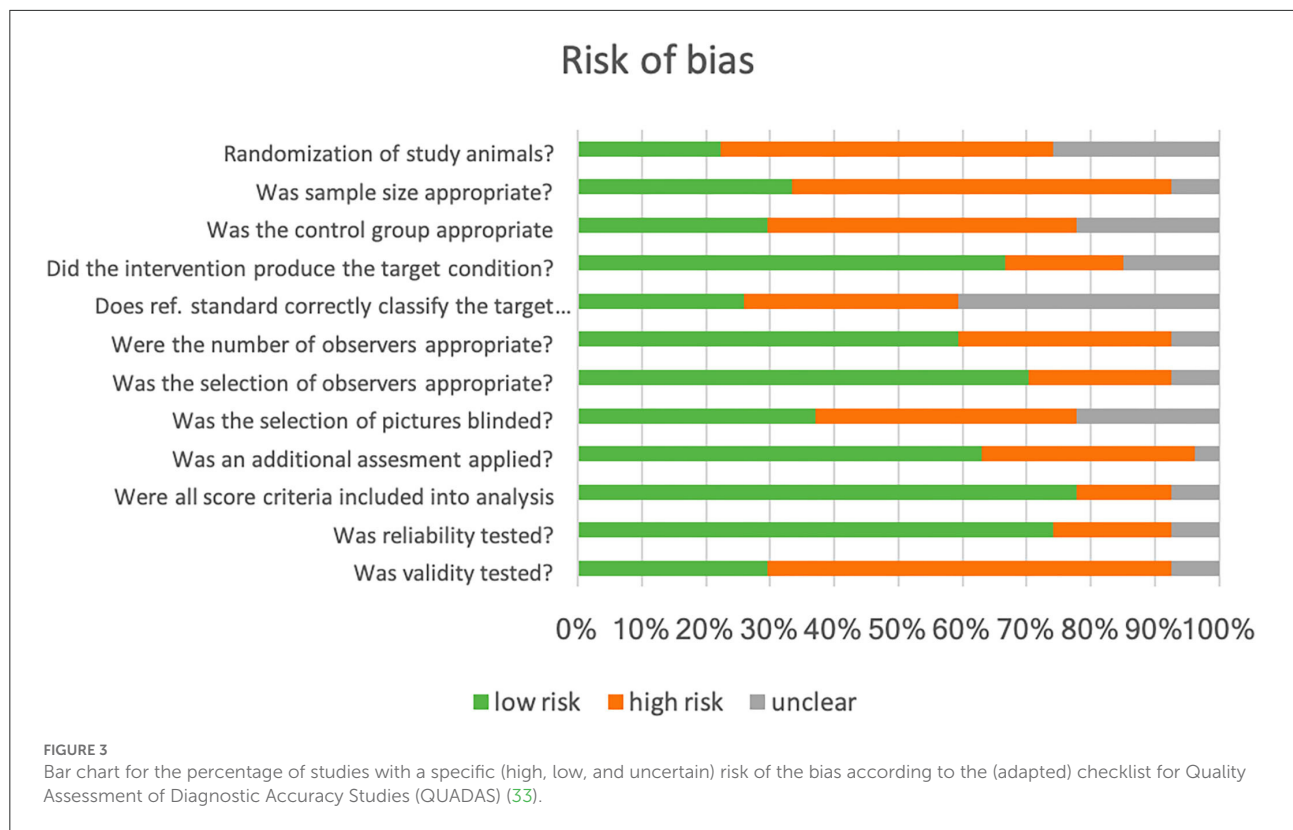


The EU Directive EU/2010/63 demands valid methods for assessing pain in animals used in experiments. Although farm animals are regularly included in animal experiments, we found only a few articles focusing on large domestic animals as experimental animals. Equids (horses and donkeys) are the major species in the included articles. In the human–animal relationship, speciesism is described. Different motivations to keep an animal have been suggested: instrumental, empathy, or identification; and values or beliefs (39). The attitude of how humans treat an animal depends on the culture of the person, the type of animal, and the function of the animal (40). Companion animals, such as horses, fall into the empathy group, whereas farm animals usually count for the instrumental group. This could lead to a greater interest in a reliable pain assessment tool for horses.

The objective of most studies was to develop a scoring system based on facial expressions. Furthermore, some groups aimed at the validation of these scores as pain assessment methods. For the quality assessment of the studies included in this review, we adapted the Diagnostic Accuracy Studies (QUADAS) checklist (33) to analyze the potential risk of bias. Reliability and validity describe the quality of a test. Interobserver reliability is the consistency of results between different observers, whereas intra-observer reliability refers to

the consistency within one observer when evaluating repeatedly. To test the interobserver reliability, at least two observers are needed (36). The number of observers included in the study was stated in 28 studies, and in five studies, only one observer was assessed and no interobserver reliability was tested. Observer variability assessment is calculated by ICC. An ICC ≥ 0.7 is accepted as sufficient (41); this was reported in 5 out of 18 studies investigating interobserver reliability for all FAUs.

Facial expression scoring is promoted as an easy-to-learn test method (42). Previous work experience or qualification of the observer should have no influence on the reliability of the test. Observers with a wide range of experiences are needed for reliability testing to avoid selection bias. In this context, a selection bias would arise if the experience or qualification of the observers would influence their ability to score FAU. The authors found that, in 70% of the studies, the selection of observers was appropriate. Their qualification ranged from no experience to animal professionals, animal scientists, and veterinarians (27). Navarro et al. (43) found no effect on interobserver reliability related to the level of pig experience of the observer. This is in agreement with Mullard et al. (44). They found no influence of professional background in scoring ridden horses. Dai et al. (42) showed that only 30 min of training significantly improved the agreement between the observers; training observers had a great



variability in scoring horse FAUs. Additionally, Navarro et al. (43) reported an effect of the gender of the six observers on the score, with the four female observers having higher reliability than male observers. For any best practice guideline, before using facial expression scoring, observers should receive specific training for scoring systems to ensure reliable results (42).

Facial expressions of pain in humans are characterized by lowering of the eyebrows, squeezing of the eyes, wrinkling of the nose, raising of the upper lip, and opening of the mouth (45). Equivalent FAUs were implemented for assessing pain in large domestic animals [as in laboratory animals (21)]. The assessment included FAUs in the eye area, the orbital region, the cheek or the chewing muscles, the lips, the mouth, and, in addition to the human pain face, the position of ears.

The ability and reliability to score a respective FAU varied considerably (Figure 2). In horses, the evaluation of “ear position” seemed easy, but 21% of observers noted “not able to score” for tension above the eye, strained mouth, and pronounced chin (26, 46). The frequency of appearance of the FAUs also had an influence. When only moderately presented, Czycholl et al. (47) could not detect any reliability for “orbital tightening” or “tension above the eye area” in a study on welfare assessment in horses. In pigs, “orbital tightening” was easy to recognize for the observer, whereas 72% had difficulties with “nostril dilatation” (27). In sheep suffering painful clinical diseases, all five FAUs investigated seemed to be easy to score,

with a maximum of 12% “not able to score” for orbital tightening (25). However, the agreement was low in lambs undergoing tail docking, when scoring “mouth changes” and “cheek flattening” in contrast to the strong agreement for “ear posture” (48). This can imply that age and the type of painful condition can influence the visibility of specific FAU. The agreement for FAU “ear position” was a “very good” agreement [ICC 0.81–1, (34)], whereas the agreement for all other FAUs varied between moderate (0.41–0.6) and good (0.61–0.8, Figure 2).

It seems that the ear position is easy to score, whereas tension above the eye, orbital tightening, and FAU around the mouth are sometimes difficult to score, which can affect the reliability of these specific FAUs. Giving the scores with higher reliability, more power in a composite score might improve the overall reliability.

Twenty-one studies in this review scored pictures captured from videos of the study animals. This procedure has limitations. First, there is a substantial risk of bias as only 20% of the authors reported that the selection of the frames was blinded or done by a person not familiar with FAU scoring. There is a risk that frames are selected with respect to the prominence of specific FAUs. Next, these pictures represent the face of an animal only for a fraction of a second. This bears the danger of missing important FAU activities. Gleerup et al. (49) remarked that facial expressions were altered during pain induction and that not all features identified were present simultaneously at

all times. As such, a frame would express a different pain face rather than a live image over time. Dalla Costa et al. (50) found no significant differences in the horse grimace scale between still images and 15-s video sequences, but they had a higher variation of scores between the observers when scoring videos. In laboratory animals, live grimace scores were found to be significantly lower than retrospective scores of still images or videos (51, 52). This is in agreement with the findings of Conegelian et al. (53) evaluating dental pain in horses. In their study, pain scores evaluated in motion were always lower than scores from photographic evaluators. Thus, it seems that facial expression scoring in pictures has different challenges from scoring in real time or videos, and each method potentially has to be assessed separately. To establish facial expression scoring as a pen-side pain assessment, validation has to be done under field conditions as well. Further research is required here. A pain assessment method is only valuable for clinical decision-making, when the result is promptly available while examining the animal rather than retrospectively. In laboratory mice, some research has been done to automate frame selection (54) to enhance the effectivity of pain scoring, research on the use of the algorithm for facial expression scoring in farm animals is only limited (55, 56).

Another limitation of pictures or videos for scoring is the selection process. Although the observers were blinded to the treatment, the selection of pictures or videos was sometimes not blinded. These studies are at risk of overestimating the presence of FAU characteristics for pain. This can also happen if persons with expertise select photographs or videos for evaluation in facial expression scoring.

A test method not only has to be reliable but also valid. Validity is a measure of how accurately a test system describes the real situation (57). Testing “true” or criterion-related validity needs a gold standard as the reference. Pain is a subjective experience, and animals cannot express themselves verbally. Approximately 75% of the studies in this review had difficulties in defining a reference gold standard method, so there is a substantial risk of verification bias. In the absence of an error-free reference standard, a gold standard construct or content validity is a possible measure to describe the quality of a pain test for animals. These methods compare the results of the test to be evaluated with other indirect test methods (i.e., cortisol measurements or behavior assessment) or with specific plausible procedures (i.e., castration or tail docking), respectively. All studies in this review that tested validity compared the results of scoring FAU to painful diseases or surgical intervention as the reference of pain.

There are challenges to pain scoring systems as pain has multiple dimensions. Two of these dimensions are intensity and length. Van Loon et al. evaluated a chronic pain score for horses and donkeys (58, 59). While the chronic pain scale identified pain in chronically diseased donkeys, it was not so reliable for horses with chronic pain. Also, in humans,

facial expressions of chronic pain are challenging. The lack of a pain-free baseline for comparison and the overload of emotional components make it difficult to describe a chronic pain face (15).

Methods of assessing pain intensity are needed for adequate pain management. Human subjects were asked to describe their pain experience on a scale from 1 to 10 (4). Based on the studies in this review, animals were classified as either in pain or pain-free. The framework of Directive 2010/63/EU demands a classification of the animal's burden in the experiment into low, middle, or severe. Further research is warranted if pain intensity can be evaluated with facial expression scoring.

Conclusion

Facial expression scores or grimace scales have been developed for a wide range of species, including large domestic animals. This review revealed that the reliability of these scores is satisfactory. In the majority of the studies, it was demonstrated that facial expressions changed during painful events. To ensure substantial reliability, observers should receive training on the scoring system. Composite scores should consider that some FAUs are easier to score and occur more frequently than others. The assessment of the validity of grimace scales continues to be challenging. Before implementing facial expression scoring as a real-time assessment method, further validation of live scoring is still needed. Overall, the facial expression score seems to be suitable for identifying animals in acute pain even though the validity of measuring the intensity of pain has not been validated yet.

Data availability statement

The raw data supporting the conclusions of this article will be made available by the authors, without undue reservation.

Author contributions

Conceptualization and writing—original draft preparation: CF-T. Validation and writing—review and editing: CF-T, JM, and AP. Formal analysis: CF-T and AP. Data curation: AP. All authors contributed to the article and approved the submitted version.

Conflict of interest

The authors declare that the research was conducted in the absence of any commercial or financial relationships that could be construed as a potential conflict of interest.

Publisher's note

All claims expressed in this article are solely those of the authors and do not necessarily represent those of their affiliated

organizations, or those of the publisher, the editors and the reviewers. Any product that may be evaluated in this article, or claim that may be made by its manufacturer, is not guaranteed or endorsed by the publisher.

References

- Hagemeister K, Ernst L, Kadaba Srinivasan P, Tanaka H, Fukushima K, Tolba R. Severity assessment in pigs after partial liver resection: evaluation of a score sheet. *Lab Anim.* (2020) 54:251–60. doi: 10.1177/0023677219871585
- Raja SN, Carr DB, Cohen M, Finnerup NB, Flor H, Gibson S et al. The revised International Association for the Study of Pain definition of pain: concepts, challenges, and compromises. *Pain.* (2020) 161:1976–82. doi: 10.1097/j.pain.0000000000001939
- Swieboda P, Filip R, Prystupa A, Drozd M. Assessment of pain: types, mechanism and treatment. *Pain.* (2013) 2, 2–7.
- Affairs DV. *Pain as the 5th Vital Sign Toolkit*. Washington, DC: Department of Veterans Affairs (2000).
- Weary D, Fraser D. *Identifying Pain in Farm Animals. Scientific Assessment and Management of Animal Pain.* (2008). p. 157–71.
- Hudson C, Whay H, Huxley J. Recognition and management of pain in cattle. *In Pract.* (2008) 30:126–34. doi: 10.1136/inpract.30.3.126
- Palme R. Monitoring stress hormone metabolites as a useful, non-invasive tool for welfare assessment in farm animals. *Animal Welfare UFAW J.* (2012) 21:331. doi: 10.7120/09627286.21.3.331
- Nagel C, Aurich J, Trenk L, Ille N, Drillich M, Pohl W et al. Stress response and cardiac activity of term and preterm calves in the perinatal period. *Theriogenology.* (2016) 86:1498–505. doi: 10.1016/j.theriogenology.2016.05.008
- Caroprese M, Albenzio M, Marzano A, Schena L, Annicchiarico G, Sevi A. Relationship between cortisol response to stress and behavior, immune profile, and production performance of dairy ewes. *J Dairy Sci.* (2010) 93:2395–403. doi: 10.3168/jds.2009-2604
- Cohen S, Beths T. Grimace scores: tools to support the identification of pain in mammals used in research. *Animals.* (2020) 10:1726. doi: 10.3390/ani10101726
- Grunau RV, Craig KD. Pain expression in neonates: facial action and cry. *Pain.* (1987) 28:395–410. doi: 10.1016/0304-3959(87)90073-X
- Hadjistavropoulos T, Baeyer CV, Craig KD. Pain assessment in persons with limited ability to communicate. In: Turk DC and Melzack R editors. *Handbook of pain assessment*. New York, NY: The Guilford Press. (2001) 134–149.
- Ekman P. *The Argument and Evidence about Universals in Facial Expressions. Handbook of Social Psychophysiology.* Hoboken, NJ: John Wiley & Sons (1989). p. 143–64.
- Ekman P, Friesen W, Hager J. *Facial Action Coding System (FACS): Manual.* Salt Lake City: A Human Face (2002).
- Williams AD. Facial expression of pain: an evolutionary account. *Behav Brain Sci.* (2002) 25:439–55. doi: 10.1017/S0140525X02000080
- Prkachin KM, Currie NA, Craig KD. Judging non-verbal expressions of pain. *Canad J Behav Sci.* (1983) 15:409. doi: 10.1037/h0080757
- Prkachin KM. The consistency of facial expressions of pain: a comparison across modalities. *Pain.* (1992) 51:297–306. doi: 10.1016/0304-3959(92)90213-U
- Darwin C. "The expression of the emotions in man and animals," In: *The Origin of Species*. ed Murray. Vol. 6th edn. Chicago, IL: University of Chicago Press (1873).
- Chambers CT, Mogil JS. Ontogeny and phylogeny of facial expression of pain. *Pain.* (2015) 156:798–9. doi: 10.1097/j.pain.000000000000133
- McLennan KM. Why pain is still a welfare issue for farm animals, and how facial expression could be the answer. *Agriculture-Basel.* (2018) 8:127. doi: 10.3390/agriculture8080127
- Langford DJ, Bailey AL, Chanda ML, Clarke SE, Drummond TE, Echols S, et al. Coding of facial expressions of pain in the laboratory mouse. *Nat Methods.* (2010) 7:447–U52. doi: 10.1038/nmeth.1455
- Sotocina SG, Sorge RE, Zaloum A, Tuttle AH, Martin LJ, Wieskopf JS, et al. The rat grimace scale: a partially automated method for quantifying pain in the laboratory rat via facial expressions. *Molecular Pain.* (2011) 7:1744–8069. doi: 10.1186/1744-8069-7-55
- Keating SC, Thomas AA, Flecknell PA, Leach MC. Evaluation of EMLA cream for preventing pain during tattooing of rabbits: changes in physiological, behavioural and facial expression responses. *PLoS ONE.* (2012) 7:e44437. doi: 10.1371/journal.pone.0044437
- Reijgwart ML, Schoemaker NJ, Pascuzzo R, Leach MC, Stodel M, de Nies L, et al. The composition and initial evaluation of a grimace scale in ferrets after surgical implantation of a telemetry probe. *PLoS ONE.* (2017) 12:e0187986. doi: 10.1371/journal.pone.0187986
- McLennan KM, Rebelo CJ, Corke MJ, Holmes MA, Leach MC, Constantino-Casas F. Development of a facial expression scale using footrot and mastitis as models of pain in sheep. *Appl Anim Behav Sci.* (2016) 176:19–26. doi: 10.1016/j.applanim.2016.01.007
- Dalla Costa E, Minero M, Lebelt D, Stucke D, Canali E, Leach MC. Development of the Horse Grimace Scale (HGS) as a pain assessment tool in horses undergoing routine castration. *PLoS ONE.* (2014) 9:e92281. doi: 10.1371/journal.pone.0092281
- Di Giminiani P, Brierley VL, Scollo A, Gottardo F, Malcolm EM, Edwards SA et al. The assessment of facial expressions in piglets undergoing tail docking and castration: toward the development of the piglet grimace scale. *Front Vet Sci.* (2016) 3:100. doi: 10.3389/fvets.2016.00100
- Gleerup KB, Andersen PH, Munksgaard L, Forkman B. Pain evaluation in dairy cattle. *Appl Anim Behav Sci.* (2015) 171:25–32. doi: 10.1016/j.applanim.2015.08.023
- Evangelista MC, Watanabe R, Leung VS, Monteiro BP, O'Toole E, Pang DS et al. Facial expressions of pain in cats: the development and validation of a Feline Grimace Scale. *Sci. Rep.* (2019) 9:1–11. doi: 10.1038/s41598-019-55693-8
- Blackie N, Bleach EC, Amory JR, Scaife JR. Associations between locomotion score and kinematic measures in dairy cows with varying hoof lesion types. *J Dairy Sci.* (2013) 96:3564–72. doi: 10.3168/jds.2012-5597
- Moher D, Altman DG, Liberati A, Tetzlaff J. PRISMA statement. *Epidemiology.* (2011) 22:128. doi: 10.1097/EDE.0b013e3181fe7825
- Bossuyt PM, Reitsma JB, Bruns DE, Gatsonis CA, Glasziou PP, Irwig L et al. STARD 2015: an updated list of essential items for reporting diagnostic accuracy studies. *Clin Chem.* (2015) 61:1446–52. doi: 10.1373/clinchem.2015.246280
- Whiting P, Rutjes AW, Reitsma JB, Bossuyt PM, Kleijnen J. The development of QUADAS: a tool for the quality assessment of studies of diagnostic accuracy included in systematic reviews. *BMC Med Res Methodol.* (2003) 3:1–13. doi: 10.1186/1471-2288-3-25
- Landis JR, Koch GG. The measurement of observer agreement for categorical data. *Biometrics.* (1977) 33:159–174. doi: 10.2307/2529310
- Flannelly KJ, Flannelly LT, Jankowski KR. Threats to the internal validity of experimental and quasi-experimental research in healthcare. *J Health Care Chaplain.* (2018) 24:107–30. doi: 10.1080/08854726.2017.1421019
- Popović ZB, Thomas JD. Assessing observer variability: a user's guide. *Cardiovasc Diagn Ther.* (2017) 7:317. doi: 10.21037/cdt.2017.03.12
- Fenwick N, Ormandy E, Gauthier C, Griffin G. Classifying the severity of scientific animal use: a review of international systems. *Animal Welfare.* (2011) 20:281–301.
- Mota-Rojas D, Olmos-Hernández A, Verduzco-Mendoza A, Hernández E, Martínez-Burnes J, Whittaker AL. The utility of grimace scales for practical pain assessment in laboratory animals. *Animals.* (2020) 10:1838. doi: 10.3390/ani10101838
- Hills AM. The motivational bases of attitudes toward animals. *Soc Anim.* (1993) 1:111–28. doi: 10.1163/156853093X00028
- Spencer S, Decuyper E, Aerts S, De Tavernier J. History and ethics of keeping pets: comparison with farm animals. *J Agric Environ Ethics.* (2006) 19:17–25. doi: 10.1007/s10806-005-4379-8

41. Terwee CB, Mokkink LB, Knol DL, Ostelo RW, Bouter LM, de Vet HC. Rating the methodological quality in systematic reviews of studies on measurement properties: a scoring system for the COSMIN checklist. *Quality Life Res.* (2012) 21:651–7. doi: 10.1007/s11136-011-9960-1
42. Dai F, Leach M, MacRae AM, Minero M, Dalla Costa E. Does thirty-minute standardised training improve the inter-observer reliability of the horse grimace scale (HGS)? A case study. *Animals.* (2020) 10:781. doi: 10.3390/ani10050781
43. Navarro E, Mainau E, Manteca X. Development of a facial expression scale using farrowing as a model of pain in sows. *Animals.* (2020) 10:2113. doi: 10.3390/ani10112113
44. Mullard J, Berger JM, Ellis AD, Dyson S. Development of an ethogram to describe facial expressions in ridden horses (FEReq). *J Vet Behav Clin Appl Res.* (2017) 18:7–12. doi: 10.1016/j.jveb.2016.11.005
45. Craig KD, Prkachin KM, Grunau RE. The facial expression of pain. In: Turk DC, Melzack R editors. *Handbook of pain assessment.* New York, NY: The Guilford Press (2011) 117–33. doi: 10.2217/pmt.11.22
46. Schanz L, Krueger K, Hintze S. Sex and age don't matter, but breed type does-factors influencing eye wrinkle expression in horses. *Front Vet Sci.* (2019) 6:154. doi: 10.3389/fvets.2019.00154
47. Czychołł I, Klingbeil P, Krieter J. Interobserver reliability of the animal welfare indicators welfare assessment protocol for horses. *J Equine Vet Sci.* (2019) 75:112–21. doi: 10.1016/j.jevs.2019.02.005
48. Guesgen MJ, Beausoleil NJ, Leach M, Minot EO, Stewart M, Stafford KJ. Coding and quantification of a facial expression for pain in lambs. *Behav Processes.* (2016) 132:49–56. doi: 10.1016/j.beproc.2016.09.010
49. Gleerup KB, Forkman B, Lindegaard C, Andersen PH. An equine pain face. *Vet Anaesth Analg.* (2015) 42:103–14. doi: 10.1111/vaa.12212
50. Dalla Costa E, Stucke D, Dai F, Minero M, Leach MC, Lebelt D. Using the horse grimace scale (HGS) to assess pain associated with acute laminitis in horses (*Equus caballus*). *Animals.* (2016) 6:47. doi: 10.3390/ani6080047
51. Miller AL, Leach MC. The effect of handling method on the mouse grimace scale in two strains of laboratory mice. *Lab Anim.* (2016) 50:305–7. doi: 10.1177/0023677215622144
52. Chartier LC, Hebart ML, Howarth GS, Whittaker AL. Affective state determination in a mouse model of colitis-associated colorectal cancer. *PLoS ONE.* (2020) 15:e0228413. doi: 10.1371/journal.pone.0228413
53. Coneglian MM, Borges TD, Weber SH, Bertagnon HG, Michelotto PV. Use of the horse grimace scale to identify and quantify pain due to dental disorders in horses. *Appl. Anim Behav. Sci.* (2020) 225:104970. doi: 10.1016/j.applanim.2020.104970
54. Kopaczka M, Ernst L, Heckelmann J, Schorn C, Tolba R, Merhof D. “Automatic key frame extraction from videos for efficient mouse pain scoring,” In: *2018 5th International Conference on Signal Processing and Integrated Networks.* Noida (2018). p. 248–52. doi: 10.1109/SPIN.2018.8474046
55. Lu Y, Mahmoud M, Robinson P. “Estimating sheep pain level using facial action unit detection,” In: *2017 12th IEEE International Conference on Automatic Face & Gesture Recognition (FG 2017)* Washington, DC: IEEE (2017). doi: 10.1109/FG.2017.56
56. Lencioni GC, de Sousa RV, de Souza Sardinha EJ, Corrêa RR, Zanella AJ. Pain assessment in horses using automatic facial expression recognition through deep learning-based modeling. *PLoS ONE.* (2021) 16:e0258672. doi: 10.1371/journal.pone.0258672
57. LoBiondo-Wood G, Haber J. “Reliability and validity,” In: *Nursing Research. Methods and Critical Appraisal for Evidence Based Practice.* (2014). p. 289–309. doi: 10.1016/S2155-8256(15)30102-2
58. van Loon JP, Macri L. Objective assessment of chronic pain in horses using the horse chronic pain scale (HCPS): a scale-construction study. *Animals.* (2021) 11:1826. doi: 10.3390/ani11061826
59. van Loon JP, de Grauw JC, Burden F, Vos KJ, Bardelmeijer LH, Rickards K. Objective assessment of chronic pain in donkeys using the donkey chronic pain scale (DCPS): a scale-construction study. *Vet J.* (2021) 267:105580. doi: 10.1016/j.tvjl.2020.105580



OPEN ACCESS

EDITED BY

Edward Narayan,
The University of Queensland, Australia

REVIEWED BY

Benjamin Lecorps,
University of Bristol, United Kingdom
Sonja Sara Schmucker,
University of Hohenheim, Germany
Ruedi Nager,
University of Glasgow, United Kingdom

*CORRESPONDENCE

Inga Tiemann
✉ inga.tiemann@uni-bonn.de

SPECIALTY SECTION

This article was submitted to
Animal Behavior and Welfare,
a section of the journal
Frontiers in Veterinary Science

RECEIVED 27 May 2022

ACCEPTED 12 December 2022

PUBLISHED 06 January 2023

CITATION

Tiemann I, Fijn LB, Bagaria M,
Langen EMA, van der Staay FJ,
Arndt SS, Leenaars C and Goerlich VC
(2023) Glucocorticoids in relation to
behavior, morphology, and physiology
as proxy indicators for the assessment
of animal welfare. A systematic
mapping review.
Front. Vet. Sci. 9:954607.
doi: 10.3389/fvets.2022.954607

COPYRIGHT

© 2023 Tiemann, Fijn, Bagaria,
Langen, van der Staay, Arndt, Leenaars
and Goerlich. This is an open-access
article distributed under the terms of
the [Creative Commons Attribution
License \(CC BY\)](#). The use, distribution
or reproduction in other forums is
permitted, provided the original
author(s) and the copyright owner(s)
are credited and that the original
publication in this journal is cited, in
accordance with accepted academic
practice. No use, distribution or
reproduction is permitted which does
not comply with these terms.

Glucocorticoids in relation to behavior, morphology, and physiology as proxy indicators for the assessment of animal welfare. A systematic mapping review

Inga Tiemann^{1*}, Lisa B. Fijn², Marc Bagaria²,
Esther M. A. Langen², F. Josef van der Staay³, Saskia S. Arndt²,
Cathalijn Leenaars⁴ and Vivian C. Goerlich²

¹Faculty of Agriculture, Institute of Agricultural Engineering, University of Bonn, Bonn, Germany,

²Division of Animals in Science and Society, Department of Population Health Sciences, Faculty of Veterinary Medicine, Utrecht University, Utrecht, Netherlands, ³Division of Farm Animal Health, Behaviour and Welfare Group, Department of Population Health Sciences, Faculty of Veterinary Medicine, Utrecht University, Utrecht, Netherlands, ⁴Institute for Laboratory Animal Science, Hannover Medical School, Hanover, Germany

Translating theoretical concepts of animal welfare into quantitative assessment protocols is an ongoing challenge. Glucocorticoids (GCs) are frequently used as physiological measure in welfare assessment. The interpretation of levels of GCs and especially their relation to welfare, however, is not as straightforward, questioning the informative power of GCs. The aim of this systematic mapping review was therefore to provide an overview of the relevant literature to identify global patterns in studies using GCs as proxy for the assessment of welfare of vertebrate species. Following a systematic protocol and a-priori inclusion criteria, 509 studies with 517 experiments were selected for data extraction. The outcome of the experiments was categorized based on whether the intervention significantly affected levels of GCs, and whether these effects were accompanied by changes in behavior, morphology and physiology. Additional information, such as animal species, type of intervention, experimental set up and sample type used for GC determination was extracted, as well. Given the broad scope and large variation in included experiments, meta-analyses were not performed, but outcomes are presented to encourage further, in-depth analyses of the data set. The interventions did not consistently lead to changes in GCs with respect to the original authors hypothesis. Changes in GCs were not consistently paralleled by changes in additional assessment parameter on behavior, morphology and physiology. The minority of experiment quantified GCs in less invasive sample matrices compared to blood. Interventions showed a large variability, and species such as fish were underrepresented, especially in the assessment of behavior. The inconclusive effects on GCs and additional assessment parameter urges for further validation of techniques and welfare proxies. Several conceptual and

technical challenges need to be met to create standardized and robust welfare assessment protocols and to determine the role of GCs herein.

KEYWORDS

welfare proxy, readout parameters, endocrine biomarkers, hormone metabolites, stress, animal husbandry, systematic review, welfare indicator

1. Introduction

Safeguarding and improving the welfare of animals under human care, irrespective of species and context, is a goal recognized by science and society. Many theoretical frameworks have been put forward to conceptualize what “good” welfare is and how animal welfare could be quantified. These concepts lay the basis for practical recommendation for assessing animal welfare and measures for improving animal welfare [e.g., (1)]. The concept of the “Five Freedoms,” proposed by the Brambell committee in 1965 (2), is the earliest and most influential approach to defining the basic aspects of husbandry necessary to safeguard welfare especially of farmed animals. Meanwhile, next to the mere absence of negative states, the importance of the inclusion of positive states in welfare has been emphasized (3). Current concepts incorporate several domains, such as behavior, naturalness, health, and physiology [e.g., the “Five Domains” concept; (4, 5)]. In this review, we use the following conceptual approach to animal welfare: animal welfare is a dynamic process, not a momentary snapshot, to which both positive and negative states contribute (3, 6). The ability to cope and adapt to environmental stimuli and stressors, delimited by the animal’s adaptive capacity, is the basis for the animal to “[...] reach a state that it perceives as positive [...]” (6). The mental and emotional state of an animal, which is accompanied by correlated physiological patterns, therefore forms a crucial part of welfare (7–9). Establishing the potential relation between these aspects, however, needs further research.

While many different concepts contribute valuable insight into animal welfare, the assessment of welfare is an ongoing challenge. The identification of measurements concerning health, behavior, and/or physiology to derive readout parameters indicative of a positive, or negative, welfare state is a much-debated goal in animal welfare research (10). Ultimately, if one or a few well-validated parameters would correlate highly with other parameters that are considered valid proxies/biomarkers of animal welfare, these could serve as index of welfare [iceberg indicators, e.g., (11)]. In this case, one could dispense with a multitude of measurements in animal welfare research and focus on few key indicators.

Despite critical evaluations of the usefulness of GC values as a proxy indicator for stress (12) and welfare states (13–17), the assumption of animals exhibiting high levels of GCs, and therefore experiencing a diminished welfare, remains

widespread (18). Given that welfare is a multidimensional concept, it should therefore be assessed using a combination of behavioral, morphological, and physiological indicators (14). A broad range of additional parameters has been investigated as potential proxy indicators of animal welfare. Some may be measurable directly and quantitatively, e.g., the presence of wounds or infections, others can only be inferred, such as subjective mental states and cognitive bias (19).

In search for key indicators of animal welfare, the measurement of a physiological parameter may imply objectiveness and straightforward interpretation. Glucocorticoids (GCs), in particular the steroid hormones cortisol and corticosterone, have gained much popularity in research on welfare of vertebrate species. External and internal stimuli and stressors may affect an individual’s welfare, and an individual’s welfare state may affect its ability to cope with these. GCs mediate the endocrine stress response, which is orchestrated by the hypothalamus–pituitary–adrenal (HPA) axis in mammals, birds and reptiles, and the hypothalamic–pituitary–interrenal (HPI) axis in fish and amphibians (20). Notably, next to being a key player in the endocrine response to stressors, GCs induce a manifold of behavioral and physiological processes to promote restoring homeostasis and survival (21). Given the pleiotropic actions of GCs, the interpretation of GC levels and release patterns proves complex (12, 21–23). GCs may rise not only in response to a stressor with potentially negative consequences, but also in response to stimuli such as environmental enrichment or sexual encounters (13, 24–26). Notably, the interpretation of the valence of the stimulus, whether it is perceived as positive or as negative and potentially threatening, may depend on the individual’s personality and cognitive traits (18, 27, 28). Adding onto the biological complexity of interpreting GC levels, are the variations in techniques to sample and determine GC levels in various tissues. To make robust assumptions on the relation between welfare and GCs, methodological limitations need to be identified and overcome.

Welfare is dynamic and describes the individual’s coping with stimuli and stressors (14). In combination, GC levels may add information on the activation of the HPA axis and arousal, aiding the interpretation of an animal’s response to an intervention aimed at affecting welfare. The usefulness of GCs in assessing an animal’s welfare may very well depend on the time frame within which GC levels are monitored. GCs

are time-sensitive in their excretion after a triggering event, but also with regard to biological rhythms (29). GCs excretion follows ultradian, circadian and seasonal rhythms, leading to measurable variation in levels under undisturbed circumstances (14, 30, 31). Given the circadian rhythm, an animal should ideally be monitored for at least 24 h to infer information on deviation in GC release (32). Moreover, the genomic actions of GCs need several hours to come into action (21). Finally, considering the central role of the animal's ability to cope and adapt in welfare concepts, monitoring should ideally last longer than 24 h.

Given the popularity, and criticism, of GC measurements in welfare assessment, we performed a mapping review of the research field to identify general trends and provide a basis for future, in-depth analyses. A mapping review “is a high-level review with a broad research question and presents the global results” (33). It follows a systematic search of literature and data extraction, but does not provide detailed information on a meta-analysis level. Rather, the results aid the identification of trends and gaps in knowledge and suggests avenues for future studies.

Based on strict a-priori criteria, we examined experimental studies which tested an intervention aimed at affecting the welfare of a target population. We were interested in the consistency of patterns of GCs, and welfare read out parameters in the domains behavior, morphology, and physiology, in welfare assessment studies. Following our conceptual approach to welfare being a multidimensional construct, we selected studies which measured GCs and concurrently parameters related to behavior, morphology, and physiology to evaluate the effects of interventions (15). Moreover, as we see welfare as being dynamic and comprising more than the peak GC response to a stressor [which typically lasts <24 h (30, 34), but may exert longer impact on the animal (32)], we restricted our search to studies following animals longer than 24 h after an acute intervention or studies that investigated long-term interventions.

From the included studies, we extracted data on the effects of the intervention on GCs and behavior, morphology, and physiology. We then categorized the impact of the welfare intervention on the outcomes within the four domains into “no effect,” “homogenous effect,” and “heterogenous effect” (Table 1) to provide an overview of the outcome of interest in relation the study characteristics. These within-domain categorizations are presented next to each other to reflect patterns across readout parameters.

We expected GC levels to change in response to welfare interventions in congruence with changes in readout parameters related to behavior, morphology, and physiology (e.g., in both domains “behavior and “GCs” a homogenous effect). Moreover, we expected GC outcomes to follow the author hypothesis. To provide an overview of the experiments, we report general aspects of the experimental studies, such as animal species,

TABLE 1 Conceptual approach to animal welfare underlying the selection of studies included in this mapping review and categorization of parameter outcomes within the four domains GCs, behavior, morphology or physiology (B, M, P).

Concept	Working definition
Animal welfare	A dynamic process delimited by the animal's capacity to cope with the environment to reach a state that it perceives as positive (6).
Intervention effect (on GC and/or other parameters measured)	Yes: The original authors observed a statistically significant effect of the intervention on the readout parameters within the four domains (GCs, B, M, P) compared to baseline or the control group according to the original analyses. No: The original authors did not observe a significant effect of the intervention on the readout parameters.
Homogeneous effects	Significant and consistent effect of the welfare intervention on the readout parameters within the four domains (GCs, B, M, P); consistent effect refers to a distinct change in readout parameters compared to baseline/control irrespective of direction (increase or decrease). This term covers the specificity of GCs to show an acute response, i.e., an increase in time proximity to the intervention/event and a decrease afterwards.
Heterogeneous effects	Inconclusive or inconsistent effect of the welfare intervention on the readout parameters within the four domains (GCs, B, M, P); inconclusive effect refers to significant but ambiguous pattern in changes of the readout parameters compared to baseline/control; inconsistent effect refers to the occurrence of significant as well as non-significant changes of the readout parameters compared to baseline/control.

experimental design, and sample matrix for GC determination, as well.

With more than 500 records included, we present one of the largest mapping reviews focusing on GC measurements in the field of animal welfare assessment. Our results provide an overview of the field of research on animal welfare, describing the available evidence on the relation between GCs, additional readout parameters and welfare of vertebrate species.

2. Material and methods

2.1. Literature search strategy

The research question leading to this mapping review was: Do GCs change consistently in response to a welfare intervention? For the comprehensive search strategy, the question was rephrased according to the PICO-format (35) to:

do GCs (Outcome) consistently change due to interventions potentially affecting welfare (Intervention) compared to within- or between-subject control conditions (Condition) in non-human vertebrate animals (Population)?

Therefore, this mapping review is based on a comprehensive search strategy, using multiple databases: PubMed, Embase and Web of Science. The searches for each database consisted of three search components [SCs, (36)]: SC1 welfare; SC2 glucocorticoids; SC3 all non-human vertebrates. The detailed search strings covered synonyms, alternative spellings and related terms, such as wellbeing for welfare.

For PubMed and Embase searches, both thesaurus-terms (MeSH for PubMed and Emtree for Embase) and title/abstract/keywords terms were included (Web of Science does not use an internal thesaurus). SC1 (animal welfare) covered the terms animal welfare and animal wellbeing, SC2 (GCs) was adapted from Leenaars et al. (33), SC3 (animals) from the Syrcle animal filter (37), with invertebrates removed, and some terms added (title-abstract terms for additional avian species, e.g., “turkey”). The complete search strings can be found in the [Supplementary material 1](#). All searches were performed in June 2020.

2.2. Study selection

Search results were imported into the reference manager Zotero, where duplicate and triplicate records were removed. All remaining records were imported into Rayyan QCRI (<https://www.rayyan.ai/>) for screening (38, 39).

In the following sections we refer to “records” as the reference to a study or book, etc., “report” and “study” as the published research paper, and “experiment” to the independent interventions investigated within a study.

The reviewer team (five people) were first trained to apply the inclusion and exclusion criteria consistently, using a set of 10 randomly chosen studies from the retrieved records. The retrieved reports were then screened for relevance in two steps: first title and abstract, then full text. Reports were sorted on title and allocated randomly to the reviewers. Screening of each report took place by at least two independent reviewers. Discrepancies were solved by discussion among the team based on the conceptual approach detailed in [Table 1](#).

2.3. Inclusion and exclusion criteria

We included original research publications reporting the assessment of GCs and welfare in non-human vertebrates. We used the following exclusion criteria in title-abstract screening: (1) invertebrate or human study population, (2) no glucocorticoids measured in the study, (3) wrong publication

type (no primary data, reviews, theses, conference abstracts), (4) animal welfare not primary focus. During full text screening we used the same exclusion criteria, in addition: (5) lack of an appropriate control for the intervention, and (6) non-English publication. We did not apply any publication date restriction.

The exclusion criterion (4) “animal welfare not primary focus” was operationalized as follows: studies needed to examine parameters of at least one additional domain (behavior, morphology, physiology) next to GCs, as welfare is more than purely the peak GC response to a stressor. As welfare is dynamic and should be monitored over a longer timeframe, we included only studies that followed the animals at least 24 h post intervention. These studies either investigated the long-term response to a short-term intervention, or the effects of a long-term intervention (chronic and/or repeated). Of these studies, all data covering GC, behavioral, morphological, and physiological measurements, thus also those collected within the first 24 h, were taken into consideration. Studies investigating welfare-related parameters over a period of <24 h after the intervention were excluded.

The “appropriate control” could either be a pre-intervention baseline in within-subject experimental designs, or a separate group of animals not exposed to the intervention. Studies comparing groups without a clear control group (e.g., studies comparing different housing densities or diets where none was explicitly designated as control by the authors) were excluded.

2.4. Data extraction and analyses

From the final set of 509 included studies, we extracted the domains intervention, animals, sampling, and outcome. In total, 17 different categories of information were extracted per experiment included, such as numeric data (number of animals) and descriptive data [species, category, strain/breed (free text), and sex] for the domain “animals.” Other information categories covered descriptive data on the authors hypothesis, the type of welfare intervention, experimental design, sampling regime, and sample type used for determination of GCs (see [Supplementary material 2](#)). A priori, we agreed on a list of potential interventions, based on our experience with the field of research. If, during extraction, an intervention did not fit into one of these categories, it was labeled as “other.” If an intervention comprised several categories, it was labeled as “combination” and further specified in a free text column. The authors original hypothesis on the effect of the experimental intervention was classified as welfare *enhancing*, *diminishing*, or *no hypothesis*, based on agreement of at least three of the five reviewers.

Similarly, the impact of the intervention was scored for each readout parameter within the domains GCs, behavior, morphology, physiology (GCs, B, M, P). Based on agreement of

at least three of the five reviewers, the outcome was scored as no effect or significant effect compared to baseline/control. Effects were scored as significant based on analytical statistics reported per experiment. The outcome within each domain was scored as homogenous if there was a consistent change in readout parameters compared to baseline/control, i.e., a distinct effect of the intervention on all readout parameters included in the statistical analyses. The outcome within each domain was scored as heterogenous if readout parameters showed inconclusive or inconsistent effects compared to baseline/control (see Table 1). We did not differentiate between an increase or decrease of single parameters, as we were interested in detecting changes in readout parameters caused by the intervention rather than judging on whether an increase or decrease of a readout parameter indicates an increase or decrease in welfare.

To avoid vote counting (40), statistical comparison of outcome categories within parameter domains (GCs, B, M, P) were not performed, but descriptive statistics are reported. The quantitative, but from a statistical point of view not analytical, description of the extracted information of the set of included studies was first organized in Excel (Microsoft Corporation, Redmond, WA, USA). Next, the percentage distribution was calculated for each result category and presented graphically (using SigmaPlot 14, Systat Software, San Jose, CA) or in tabular form. In general, *n* represents the number of studies and *k* the number of experiments included in the analyses.

We used VOSviewer for the exploratory visualization of the terms in the title and the abstracts (version 1.6.16; <https://www.vosviewer.com/>). The result are maps based on the co-occurrence of terms used in the titles and abstracts of the studies included. To simplify the set of terms, VOSviewer calculates clusters, indicated by distinct groups in the same color (41). The size of the circles and of the labels reflects the frequency of occurrence. Labels with low frequencies might not be shown to avoid overlapping. The relatedness is reflected as distance between two items and based on the VOS mapping technique using a similarity matrix. The total link strength indicates the sum of link strengths as a weight attribute, where the link strength is defined as number of links of an item with another item.

3. Results

3.1. Reference flow

Our literature searches provided 717 results from PubMed, 1,092 from Embase, and 1,948 from Web of Science. After duplicate removal, 2,428 records remained for title-abstract screening. After applying the exclusion criteria during title-abstract and subsequent full text screening, *n* = 509 studies were included in this mapping review [Figure 1, (42); see

Supplementary material 3]. Four of these 509 studies, reported two independent experimental interventions, and one reported five independent experimental interventions, resulting in a total of *k* = 517 experiments for data extraction.

3.2. Network visualization

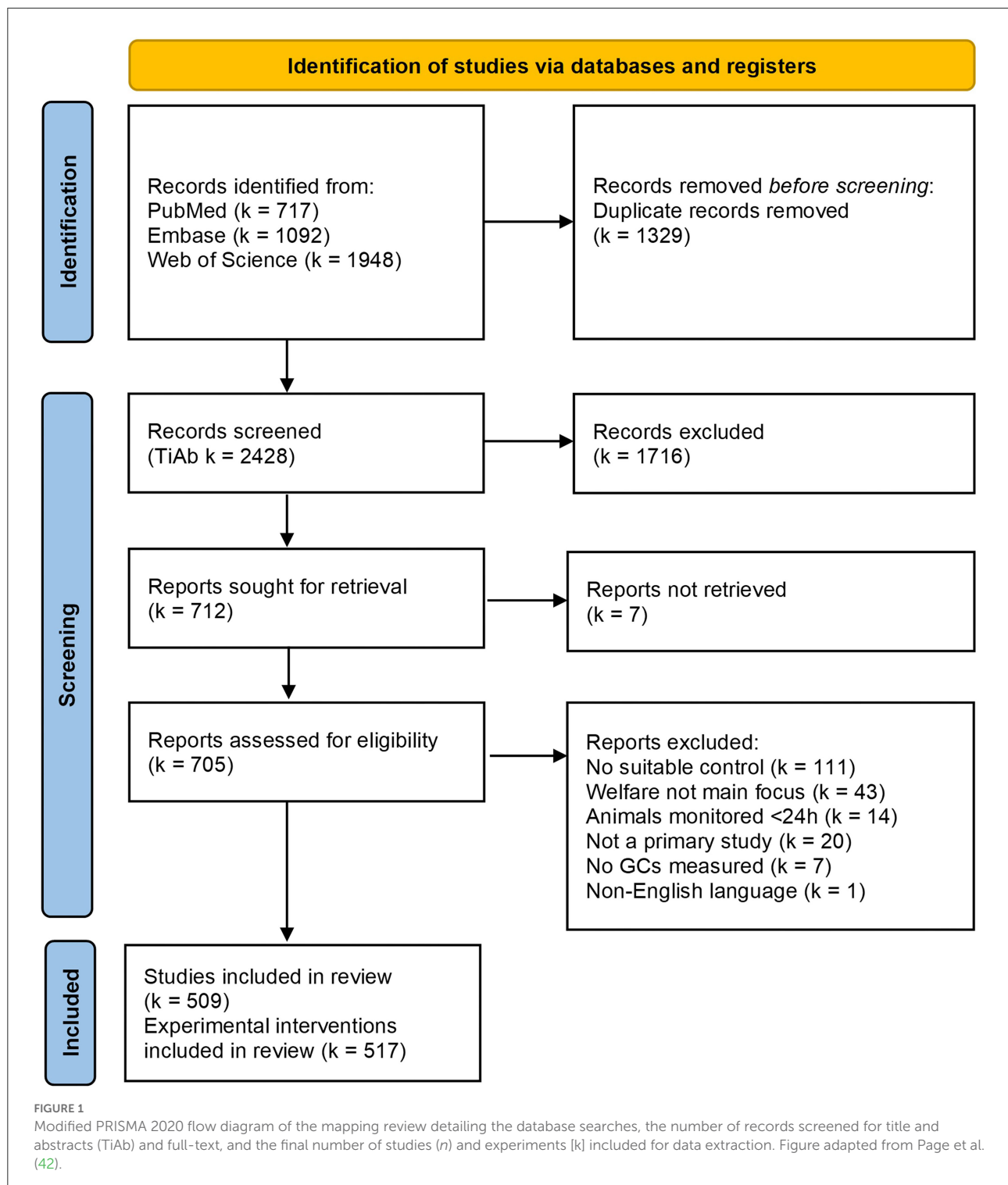
A link cloud was calculated based on the terms used in the abstracts of all included records (setting applied: min. occurrence of words: 7; resulting in items: 488; cluster: 9; links: 14,714; total link strength: 109,316; Figure 2). The main clusters revealed the different animal species investigated in the studies: pigs, cows, small rodents, and birds. The clusters also provide a first insight into the research topics predominantly investigated in these species. For pigs, the housing system as well as management including reproduction were frequently occurring themes. Comparable topics were relevant for cows, especially calves, although in this genus, the major focus was on castration. For mice and rats, research focused on the impact of housing and cage design on welfare. For birds, mainly chickens, the stocking density and husbandry system and their impact on welfare was commonly investigated. Research focused on zoo animals and their interaction with visitors is indicated by “penguin” and “exhibit.”

3.3. Effects on glucocorticoids

We scored whether the experimental intervention led to a statistically significant effect on GCs which could either be an increase or decrease of GC levels compared to control or pre-intervention baseline (homogenous effect) or a heterogenous effect (the intervention not leading to a clear and distinct change in GC levels, Table 1). Of the analyzed experiments, 39.26% (*k* = 203) found no significant effect of the intervention on GC levels, 38.10% (*k* = 197) found a homogenous effect and 22.63% (*k* = 117) of the experiments reported a heterogenous effect. Note that outcomes in which the GC response showed the typical course of an initial increase and following decrease were scored as homogenous.

3.4. Additional assessment parameters

In line with our conceptual approach to welfare, additional parameters from all three domains behavior, morphology, and physiology were assessed most frequently amongst the experiments (32.30%, *k* = 167). The combination of behavior and physiology (22.82%, *k* = 118) was most common in experiments assessing two additional parameters, while behavior was the most occurring single domain (13.93%, *k* = 72).

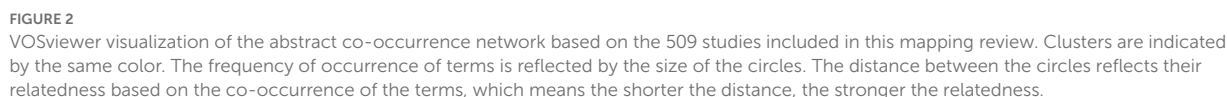


3.5. Outcomes related to study hypothesis

We were interested in the distribution of interventions and whether the experimental outcome aligned with the *a-priori* research hypotheses stated by the respective study authors

(Table 2). The hypotheses were classified based on the expected direction of impact of the experimental intervention on animal welfare as stated by the authors of the studies (increasing or diminishing welfare compared to control/baseline).

Most of the experiments investigated a putative welfare improving intervention, followed by a putative welfare



If the intervention was expected to improve welfare, most of the experiments found no effect on GC levels, followed by homogenous changes in GC levels. If the intervention was expected to diminish welfare, most of the experiments found a homogenous effect on GC levels, followed by no effect. If authors did not formulate a directional hypothesis, most of the experiments found no effect on GC levels, followed by heterogenous effects. Outcomes in the domain behavior were most often heterogenous (mean 47.18%), irrespective of the hypotheses. Morphological parameters were most frequently not measured (mean 41.87%), or were found not affected by the intervention (mean 24.12%). Effects on physiology were most often heterogenous (mean 37.41%), again, irrespective of the original research hypotheses.

The proportion of homogenous, heterogeneous or no effects on GCs, depending on the number of sampling timepoints is depicted in [Figure 3](#). GCs were measured four and more times (43.13%, $k = 223$), followed by experiments measuring GC two (16.83%, $k = 87$), and three times (16.25%, $k = 84$). GCs were measured only once in roughly one quarter of the experiments (23.79%, $k = 123$).

With an increasing number of sampling timepoints throughout the experimental period, the proportion of experiments finding no effect on GC levels declined, similarly to experiments finding a homogenous effect. However, the percentage of experiments finding heterogenous effects on GC levels rose with number of GC measurements.

TABLE 2 Categorization of the proportion and total numbers of experiments (517 experiments in 509 studies) of the research hypothesis (A, B, C) stated by the respective authors of the reviewed studies reporting an effect on GC levels and/or the three additional assessment parameter, behavior, morphology and physiology.

Hypothesis	GC	Behavior	Morphology	Physiology
A. Enhancing welfare (51.06%, k = 264)				
Homogenous effect	38.64%	23.48%	19.70%	15.15%
	k = 102	k = 62	k = 52	k = 40
Heterogenous effect	20.08%	48.48%	18.18%	33.71%
	k = 53	k = 128	k = 48	k = 89
No effect	41.29%	11.74%	20.83%	22.35%
	k = 109	k = 31	k = 55	k = 59
Not measured	N/A	16.29%	41.29%	28.79%
		k = 63	k = 109	k = 76
B. Diminishing welfare (28.63%, k = 148)				
Homogenous effect	45.95%	20.95%	15.54%	19.59%
	k = 68	k = 31	k = 23	k = 29
Heterogenous effect	19.59%	42.57%	16.22%	38.51%
	k = 29	k = 63	k = 48	k = 57
No effect	34.46%	12.16%	22.97%	22.30%
	k = 51	k = 18	k = 55	k = 33
Not measured	N/A	24.32%	45.27%	19.59%
		k = 36	k = 109	k = 29
C. Neutral/no directional hypothesis (20.31%, k = 105)				
Homogenous effect	25.71%	17.14%	7.62%	8.57%
	k = 27%	k = 18	k = 8	k = 9
Heterogenous effect	33.33%	50.48%	24.76%	40.00%
	k = 35	k = 53	k = 26	k = 42
No effect	40.95%	16.19%	28.57%	19.05%
	k = 43	k = 17	k = 30	k = 20
Not measured	N/A	16.19%	39.05%	32.38%
		k = 17	k = 41	k = 34

Effects are categorized according to the definitions of homogenous (consistent change in readout parameters compared to baseline/control), heterogenous (inconsistent change in readout parameters compared to baseline/control), or no effect (see Table 1). Results are presented in proportions [%] and total number of experiments [k]. The outcomes of the assessment parameters add up to 100% per hypothesis.

Samples for GC determination were most frequently collected under undisturbed circumstances (aiming at determining baseline concentrations, 78.92%, k = 408). In only 14.70% of the experiments (k = 76), GCs were measured after applying a stressor or challenge (e.g., ACTH), or a combination of both (6.38%, k = 33). If a stressor was applied, 32.89% (k = 25) of the studies found a homogenous effect on GCs, whereas 46.05% (k = 35) did not find an effect. In case there was no stressor applied, 40.44% of the experiments (k = 165) found a homogenous effect on GC, whereas 38.48% (k = 157) did not find an effect.

Regarding the sample matrix and prominent GC metabolite, GC levels were predominantly determined from blood samples, in which mainly cortisol was quantified (Table 3). Less-invasive sampling techniques, such as sampling feces or saliva, ranked second and third, respectively. Table 3 also shows the outcome categories in relation to the sample matrices. Of the experiments that sampled blood and saliva, 40.20% (k = 123) and 45.28% (k = 24), respectively, found homogenous effects, while of the experiments that quantified GCs in feces or urine, 58.33% (k = 49) and 42.86% (k = 9) found no effect.

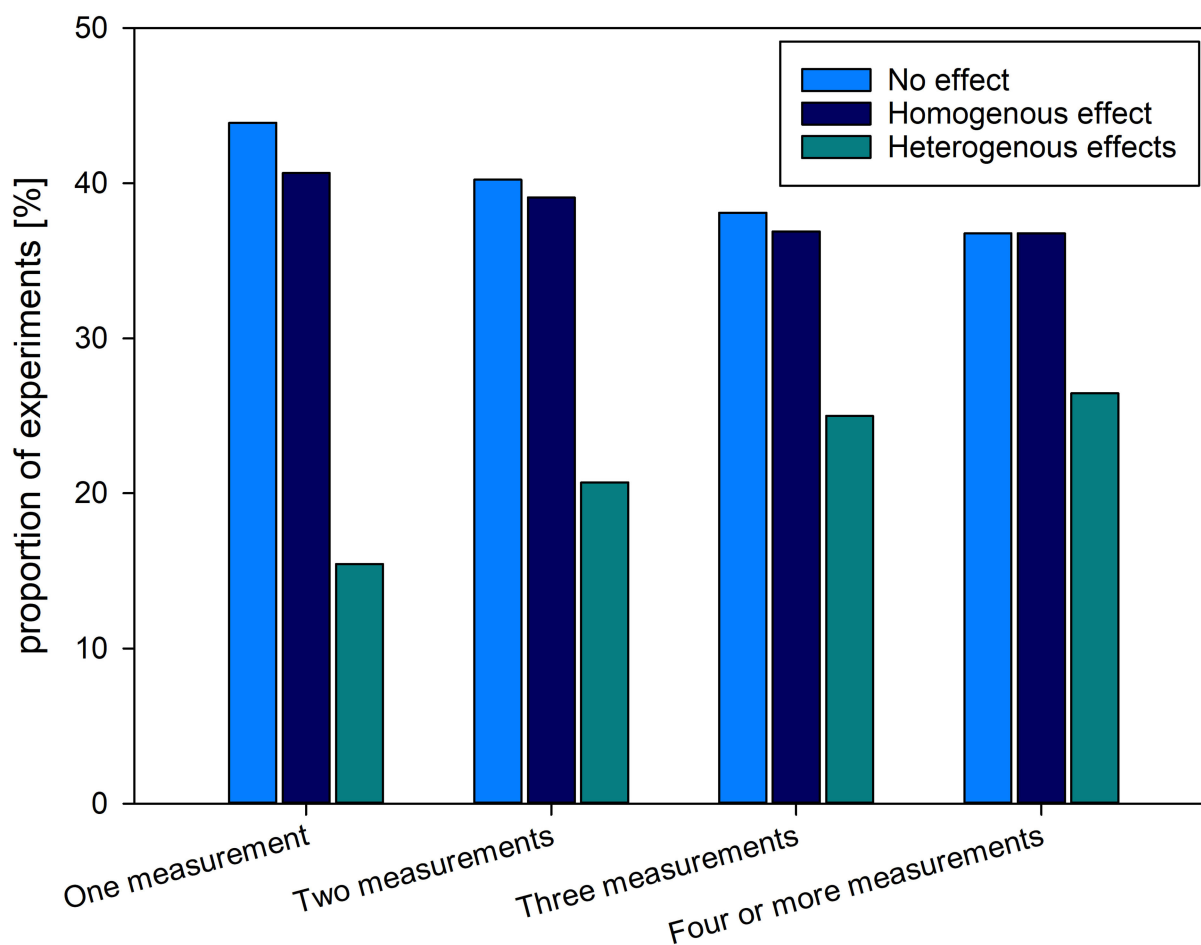


FIGURE 3

Proportion and total numbers of experiments (517 experiments in 509 studies) finding a homogenous (consistent change in readout parameter compared to baseline/control), heterogenous (inconsistent change in readout parameter compared to baseline/control) or no effect of the intervention on GC levels among the different experimental designs with regard to the number of timepoints at which GC was measured during the experiment. Results are presented in proportions [%], left vertical axis] and total number of experiments [(k), right vertical axis].

3.7. Experimental design

Most experiments, compared treatment to control groups (56.87%, $k = 294$). Of these experiments, 37.07% ($k = 109$) found a homogenous effect on GC levels, whereas 40.48% ($k = 119$) found no effect. A within-subject design was used by 16.44% ($k = 85$) of the experiments, and 49.25% ($k = 33$) found a homogenous effect, whereas 32.84% ($k = 22$) did not find an effect. The combination of between and within subject design was used by 26.69% ($k = 138$) experiments, of which 3.48% ($k = 18$) used a cross-over design.

Duration of the intervention was categorized as days to weeks for almost two thirds of the experiments (58.61%, $k = 303$), followed by months to years (16.83%, $k = 87$). A proportion of 11.61% ($k = 60$) of the experiments investigated acute treatments (lasting minutes to hours), 5.03% ($k = 26$) investigated permanent treatments (from birth till

sampling/euthanasia), followed by experimental treatments that were repeatedly continuing (days to weeks; 4.06%, $k = 21$), repeatedly acute (minutes to hours; 3.29%, $k = 17$) or repeatedly long-term (months to years; 0.58%, $k = 3$). Within the category of acute interventions, 46.47% ($k = 28$) of experiments found homogenous effects on GC responses, in 26.67% ($k = 16$) no effect was reported. Of the experiments investigating interventions that lasted from days to week, 37.95% ($k = 115$) found homogenous effects on GC, and 37.62% ($k = 114$) reported no effects on GC levels. Homogenous effects on GC levels were found in 39.08% ($k = 34$) of the experiments that investigated long-term interventions, whereas 41.38% ($k = 36$) found no effect.

Sample size of the experimental animals used in the reviewed experiments ranged from 1 (orangutan) to 650 (tilapia). In all three GC outcome categories, the median sample size ranged from 32 to 40 individual animals (no effect, homogenous,

TABLE 3 Ranking of the proportion and total numbers of experiments (517 experiments in 509 studies) of biological sample types used for determination of GC levels, the corresponding most commonly determined GC metabolite and the outcome of the GC assessment.

Sample	Proportion of total studies	GC metabolite (most frequently measured in the corresponding sample)	GC outcome (based on all samples)		
			Homogenous effect	Heterogenous effect	No effect
Blood	59.19% (k = 306)	Cortisol (70.26%, k = 215)	40.20% (k = 123)	23.20% (k = 71)	36.60% (k = 112)
Feces	16.25% (k = 84)	Corticosterone (51.19%, k = 43)	29.76% (k = 25)	11.90% (k = 10)	58.33% (k = 49)
Saliva	10.25% (k = 53)	Cortisol (100.00%, k = 53)	45.28% (k = 24)	22.64% (k = 12)	32.08% (k = 17)
Multiple sample types	6.19% (k = 32)	Cortisol (56.25%, k = 18)	31.25% (k = 10)	40.63% (k = 13)	28.13% (k = 9)
Urine	4.06% (k = 21)	CORT: Creatinine ratio (66.67%, k = 14) [71.43% cortisol (k = 10), 28.57% corticosterone (k = 4)]	38.10% (k = 8)	19.05% (k = 4)	42.86% (k = 9)
Other	2.32% (k = 12)	Cortisol [66.67%, k = 8; whole (fish) body 87.5% (k = 7), milk 12.5% (k = 1)]; Corticosterone [33.33%, k = 4; eggs (avian) 50.00% (k = 2), water (fish) 50.00% (k = 2)]	33.33% (k = 4)	41.67% (k = 5)	25.00% (k = 3)
Hair	1.16% (k = 6)	Cortisol (100.00%, k = 6)	50.00% (k = 3)	50.00% (k = 3)	–
Feathers	0.58% (k = 3)	Corticosterone (100.00%, k = 3)	–	66.67% (k = 2)	33.33% (k = 1)

Note that the most frequently reported GC metabolite is probably confounded by the species most commonly sampled (e.g., cortisol in blood from mammals). Results are given in proportions [%] and total numbers [k] in brackets.

TABLE 4 Categorization of the proportion and total numbers of experiments (517 experiments in 509 studies) of animal class, occurrence, primary GC sample type, primary additional assessment parameters (B, Behavior; M, Morphology; P, Physiology), primary investigated sex, and average sample size tested for GC levels (N).

Class	Proportion of total studies	GC sample type	Primary additional parameter(s)	Primary investigated sex	Average sample size
Mammalian	76.02% (k = 393)	Blood (53.94%, k = 212)	M & B & P (31.81%, k = 125)	Female (35.88%, k = 141)	49 [1; 329]
Avian	14.70% (k = 76)	Blood (76.32%, k = 58)	M & B & P (46.05%, k = 35)	Female (56.58%, k = 43)	74 [6; 576]
Fish	7.93% (k = 41)	Blood (82.93%, k = 34)	M & P (46.34%, k = 19)	Not reported (60.98%, k = 25); both (26.83%, k = 11)	84 [12; 650]
Reptile	0.77% (k = 4)	Blood and Feces (50% each, k = 2)	M & B & P (50.00%, k = 2)	Both (75.00%, k = 3)	16 [3; 49]
Amphibian	0.58% (k = 3)	Water extraction (66.67%, k = 2)	Physiology (66.67%, k = 2)	Both (66.67%, k = 2)	47 [15; 90]

Results are given in proportions [%] and total numbers [k] in brackets. Average sample size is given in mean numbers of animals [min; max].

heterogenous, [Figure 4](#)). We further summarized the sample size per class of animals in [Table 4](#).

3.8. Study population

The reviewed experiments comprised a wide variety of animal species, ranging from zebrafish to elephants. Most of the experiments investigated the welfare of pigs, cows, chicken and sheep (i.e., farm animals, 51.06%, k = 264), or mice and rats (i.e., laboratory animals, 14.70%, k = 76, [Figure 5](#)).

We combined the information given for the animal class, the prevalence among experiments, the welfare parameters assessed as well as sex of the animals investigated and sample size of the

experiments. To identify over- or under representation of animal classes in welfare research, we combined species to classes to assess their proportion in the reviewed experiments. As welfare assessment may differ between species and classes, we also related the additional assessment parameters to the respective class ([Table 4](#)). Three quarters of the selected studies investigated mammals. Blood as GC sampling matrix was most commonly used across animal classes, as also was the combinatory assessment of behavioral, morphological, and physiological parameters. Females were the most often investigated sex in mammals and avian species, whereas in fish studies, sexes were most often not reported. The mean sample size ranged from 16 individuals in reptiles to 84 in fish, with a minimum of 1 in mammals and 650 in avian species.

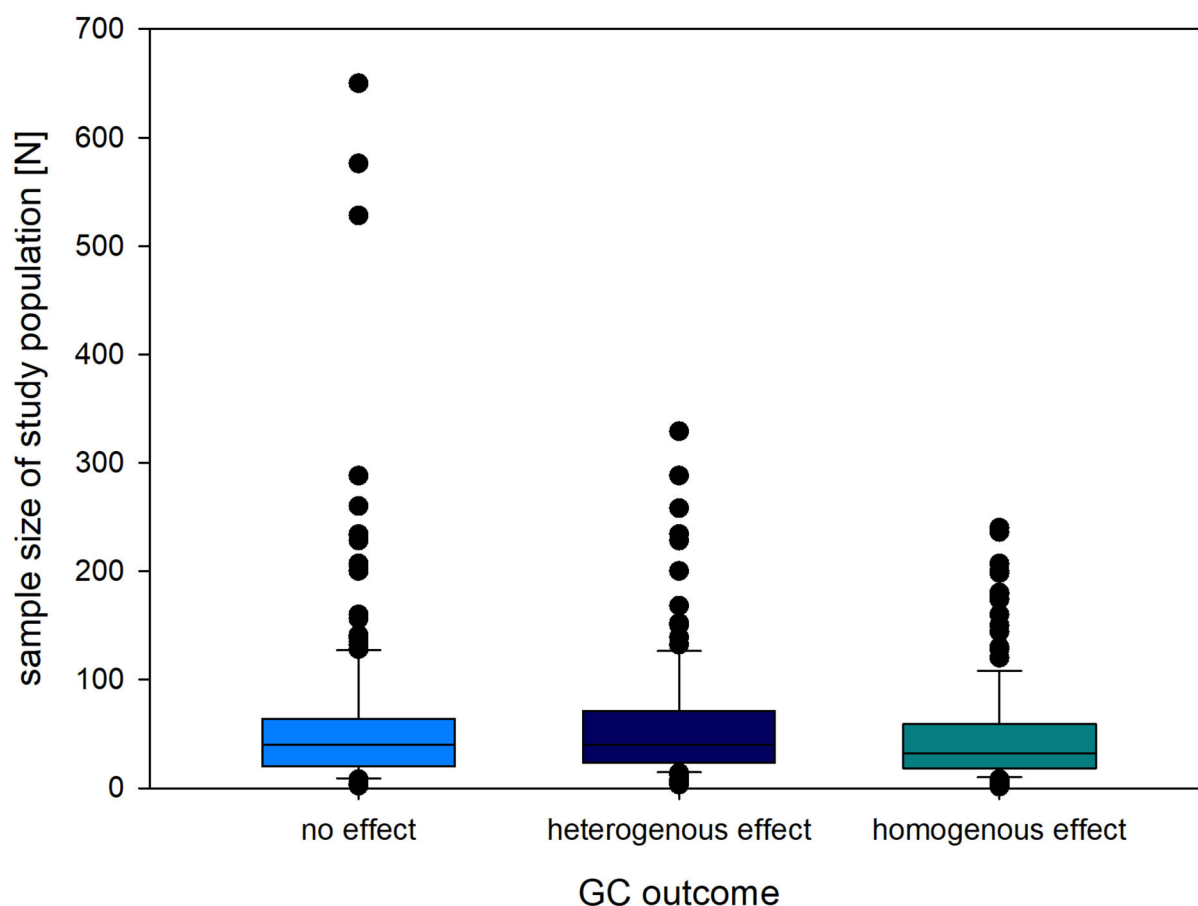


FIGURE 4

Sample size (N) of animals sampled for GCs in studies finding a homogenous (consistent change in readout parameter compared to baseline/control), heterogenous (inconsistent change in readout parameter compared to baseline/control) or no effect of the intervention on GC levels. The box plots represent the median (and 10th, 25th, 75th and 90th percentile) as well as outliers (outside percentiles).

3.9. Interventions

Among the interventions aimed at affecting welfare, most of the experiments used a combination of interventions, followed by structural enrichments, other treatments (e.g., milking procedures in dairy cows being the most commonly applied single treatment), combinations of enrichments, and nutrition/nutritional supplementation (Figure 6).

4. Discussion

The question leading to this mapping review was whether GCs change consistently in response to a welfare intervention, and whether changes were also reflected in measures of behavior, morphology and physiology. With help of a systematic mapping review of the relevant literature, we examined 509 studies including 517 independent experiments. The included experiments used measurements of GCs in combination with

measurements of behavior, morphology, and physiology, to assess the welfare of non-human vertebrates in response to an intervention expected to affect animal welfare. We were specifically interested in the added value of GCs as a proxy indicator in animal welfare studies. While this mapping review started with a comprehensive search and screening, the search and screening were restricted to studies with a focus on welfare. Relevant information from publications with another focus was thus not included, as we were specifically interested in the added value of GCs as a proxy indicator in animal welfare studies.

For a mapping review, the goal is not to perform in-depth (meta) analyses, but rather to describe the available literature, in this case on the use of GCs in the assessment of animal welfare. We present an overview on aspects of experimental set-ups and sampling regimes, the sample types analyzed for quantification of GCs, and the species and sex of the target animals. To identify global patterns in the outcome of GC monitoring as proxy for animal welfare, the interventions and original authors' hypotheses were categorized according

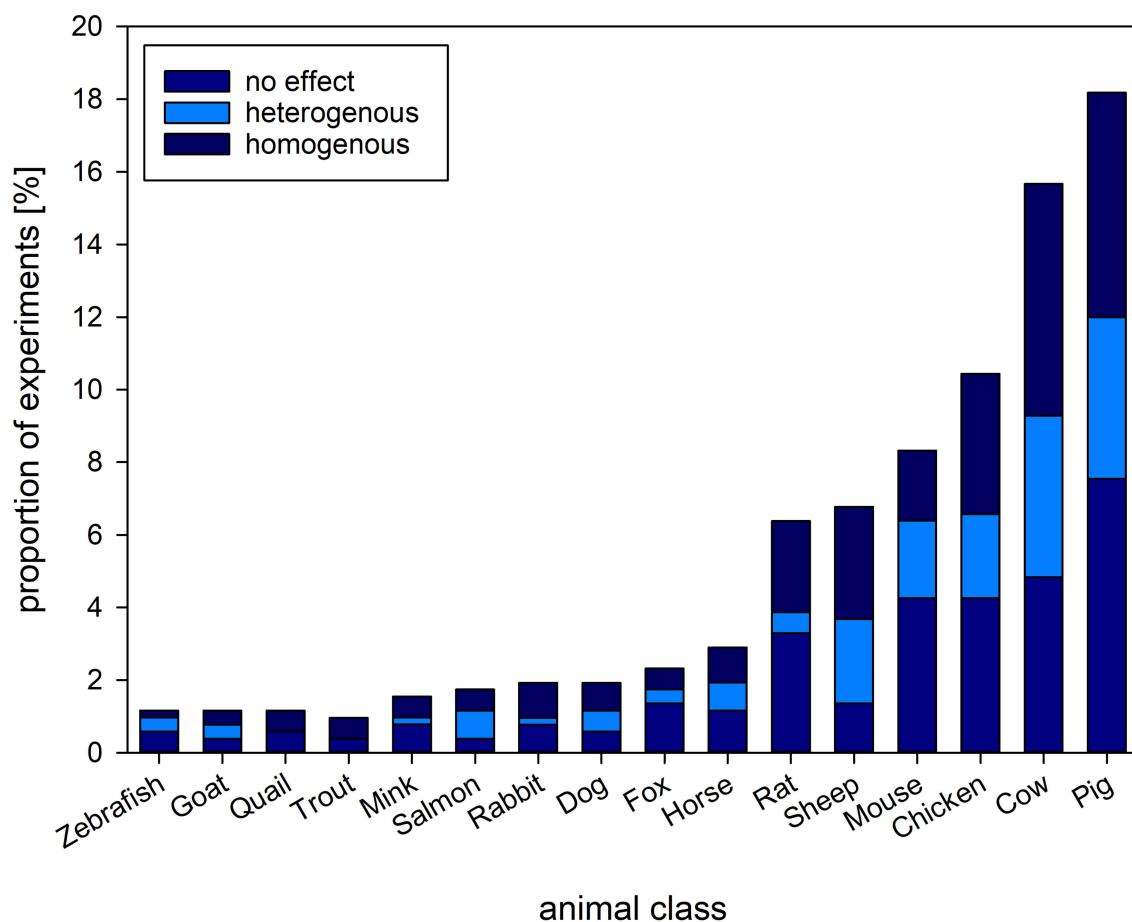


FIGURE 5

Proportion [%] of experiments and the types of animals investigated. Stacked bars refer to the proportion of experiments reporting on homogenous (consistent change in readout parameter compared to baseline/control), heterogenous (inconsistent change in readout parameter compared to baseline/control) or no effect of an intervention on GC levels found among the species investigated. The figure shows the types of animals with a proportion above 1% of the complete set of experiments.

to the effects of the interventions on GC levels. Finally, we were interested in whether a significant change in GCs was accompanied by changes in behavioral, morphologic, and physiological parameters.

4.1. Network visualization

The network visualization reveals the diversity of welfare-related topics in which GCs are assessed. The clusters formed in the network analyses match current societal and scientific welfare concerns across animals in different contexts such as farm, laboratory and zoological exhibitions (43, 44). Examples are husbandry (light and density), procedures of commercial livestock management (castration), health issues of farm animals (lameness), and the aim to assess emotional states (fear). The selection

criteria thus resulted in a representative coverage of the relevant literature.

4.2. Effects on glucocorticoids

The results suggest that the prevalence of effects on GC driven by welfare-related interventions is ambiguous. To make informed conclusions, and avoid vote counting, however, the experimental outcomes need to be analyzed on a more detailed level, ideally using meta-analysis approach. Almost two thirds of the reviewed experiments found an effect of the experimental intervention on GC levels, even if heterogenous effects, thus not all measurements showing significant effects, or inconsistent effects. The probability for an intervention to result in heterogenous effects within a domain may rise with the number of readout parameters. For GCs, however, the

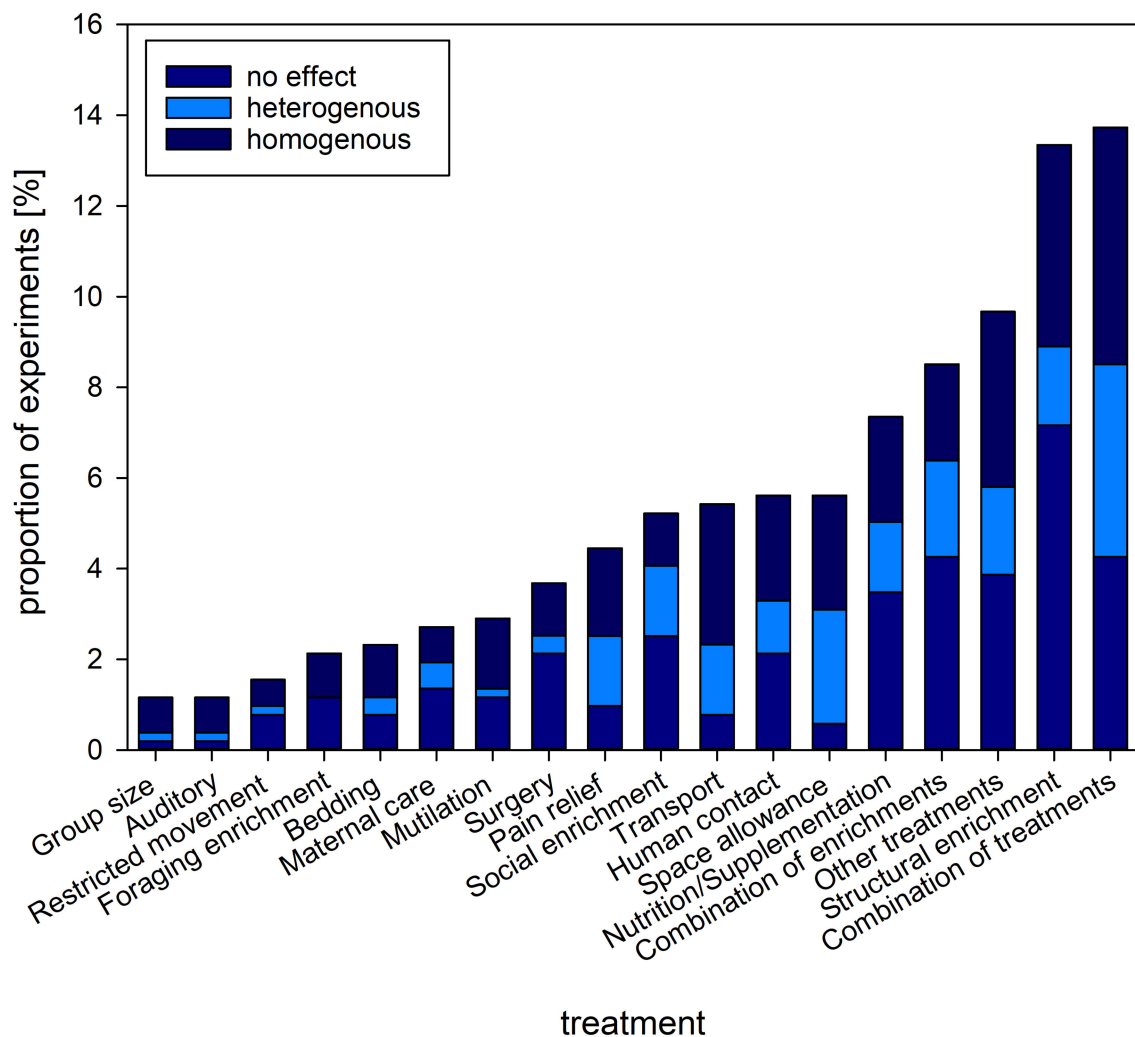


FIGURE 6

Proportion [%] of experiments and the type of interventions investigated. Stacked bars refer to the proportion of experiments reporting on homogenous (consistent change in readout parameter compared to baseline/control), heterogenous (inconsistent change in readout parameter compared to baseline/control) or no effect of the intervention on GC levels. The figure shows the types of interventions with a proportion above 1% of the complete set of experiments.

spread across the outcome categories was similar across number of sampling moments. Note that to statistically confirm these patterns, further detailed analyses are necessary.

The large number of records and variation in experimental set-ups and analyses prevented a clear distinction of outcomes into increase or decrease of GCs with respect to control/baseline. Notably, rather than the direction of change of GC levels, change itself, may be an indicator of an animal being in a state of arousal (45).

Even if GC levels do not change in response to an intervention, this does not mean that modulation of HPA axis and stress responsivity has not taken place. Under some circumstances, changes in patterns of GC release may only be visible when accounting for circadian rhythms [e.g., (46, 47)].

We included only studies which followed the animals longer than 24 h. Short-term GC responses may point to the animal experiencing acute stress, however, to identify and impact on welfare and the individual's capacity to cope and adapt, an animal needs to be followed over a longer period of time (6, 48).

Animals may also develop a hypo- or hyperresponsiveness to stressors, after being exposed to prolonged periods of chronic or repeated stressors (49–51). This modulation of GC baseline and peak levels in response to chronic exposure to stressors may hamper the interpretation of GC responses to interventions, as individuals in the stressor group may have lower baseline GC levels compared to controls (52). The animal may have adapted to the challenge in order to cope by a new physiological setpoint [allostatic state, (48, 53)]. The crucial point is whether

adjusted setpoints have negative consequences on the physical and emotional wellbeing of the individual, or on the animal's capacity to reach a state that it perceives as positive.

Also, persisting changes in GC levels can be, but are not necessarily accompanied by structural changes in organs, e.g., changes in the morphology of the adrenal glands (54). Even more variation is added by the sample type reflecting free or bound fractions of GCs or even GC metabolites (30). These may differ between species (29, 55) and need to be identified prior to measuring and interpreting concentrations with respect to the effects of an intervention (56). We show variation in GC metabolites per sample matrix. This pattern may be influenced by the sample matrices that are typically used withing a particular animal class. However, whether the probability to find an effect of a welfare intervention depends on the sample matrix, remains to be investigated. The lack of validation of GC (metabolite) quantification in alternative sample types such as feces, for example, may lead to erroneous results (30).

Other influential factors in the interpretation of GC levels are corticosteroid binding globulins (CBGs), which regulate bioavailability of GCs. The measurement and correction for CBG levels is not yet widely being applied in research on stress and animal welfare, though recognized by critical reviews on the usefulness of GCs for welfare assessment (13–15). Thus, basing conclusions concerning the effect of a welfare related intervention solely on an effect found on the animal's GC levels appears unsubstantiated by the literature. Regarding the determination of GCs, conceptual, and technical challenges need to be met to create standardized and robust data on GC levels, and to aid the interpretation of changes in GC patterns.

4.3. Additional assessment parameters

GC levels alone are of limited informational value without additional information about the animal, at least about its current behavior, morphology, and physiology, ideally accompanied by information on ontogeny and previous experiences. The value of GCs may be adding information to other welfare proxies while the correlation between different welfare readout parameters needs further study.

Although the measurement of GCs is often considered to represent valid "welfare measurements," GCs alone do not seem to be valid indicators of welfare, and additional (or even more suitable) readout parameters need to be identified and used. As we limited our review to studies about welfare assessment, we only included studies in our mapping review that measured additional morphological, behavioral, and/or physiological parameters.

The combination of sampling of GC and collection of parameters from the three domains, behavior, morphology, and physiology, was applied most frequently. This reflects the general consensus that welfare comprises several domains (8). Behavior

was the most often assessed additional parameter. This might be due to the unanimous opinion that behavior is the main non-invasive readout parameter to assess the welfare state of an animal, across species and between breeds (57–59). How an individual valences its own emotional state cannot be assessed by other non-invasive procedures than behavioral observations (60). Promising indicators for assessing pain and distress in animals, for example, have been obtained through the analyses of vocalizations (61, 62) and by analyzing the animal's facial expressions, using grimace scales. The latter have successfully been developed for several species (63).

When behavior was assessed as additional parameter to GC values, studies reported heterogenous results. This finding indicates that, if there was an effect of the intervention, measurements of different behavioral traits did not show consistent changes. We did not extract information on type and details of behavioral observations, but the high variability in outcomes urges for adaptation, standardization and validation of tests, a common definition of test aims (i.e., which domain is tested in the animal, e.g., exploration, fear, habituation), and detailed description of test setups.

While we acknowledge behavior as the most important indicator of an individual's emotional state, the use of parameters related to health, morphology, and physiology may be indispensable for a comprehensive approach to welfare. The measurement of physiological parameters is subjected to the same issues as GC measurements, thus variability due to sampling regimen or due to individual phenotypes. Moreover, there is a great variety of parameters to choose from, and therefore it was not surprising that studies reported no or heterogenous effects. The large variation in parameters (and outcomes) calls for detailed reviews identifying overarching patterns in effects on specific readout parameters. While there are many promising physiological parameters to monitor and assess welfare, these also need a thorough validation and should be evaluated in a more in-depth review [e.g., (64, 65)].

Morphological parameters are thought to be closely linked to animal welfare, since physical health is often considered a prerequisite for welfare. In our data set, however, the majority of experiments did not monitor parameters related to morphology. Notably, an animal in good health is not automatically in a state of positive welfare, and vice versa. As long as the individual has not reached the limits of its adaptive capacity, and the health status does not prevent it from reaching a state that it perceives as positive, compromised health may not lead to seriously compromised welfare (66). Monitoring clinical signs and body mass is common practice to assess welfare, as these traits are relatively easy to assess. Monitoring weight loss has been shown to be indicative of severe suffering in laboratory animals, but assessing (milder forms of) distress requires the measurement of additional parameters (67). Therefore, also the use of body mass as primary welfare indicator for at least laboratory animals should be questioned [e.g., (68)]. Regarding animals selected for

high productivity, the relation between body mass and welfare may be distorted, e.g., in broiler chicken or pigs, where fear of humans, indicative of a negative welfare state, and productivity are inversely correlated (69, 70).

4.4. Outcomes related to study hypothesis

A considerable number of experiments yielded results that were inconsistent with the hypotheses (i.e., no effect while enhancing/diminishing welfare was hypothesized). While this finding can be explained by the ambiguous effects that welfare related interventions may have on assessment parameters, it also highlights the importance of formulating *a-priori*, testable, and clear research hypotheses. Hypothesis-driven studies are especially needed in the field of stress and welfare research, which is complex and faced with subjective attitudes and interpretations (71). Also, the underlying conceptual approach to welfare, and a hypothesis about why GC levels should increase/decrease in response to a certain intervention, should be explicitly stated. Interventions aimed at affecting welfare and not resulting in changes in GCs may support the critical literature on the validity of GCs for the assessment of welfare (13–16). Alternatively, the interventions may have been unsuccessful in affecting welfare. Teasing apart these two aspects requires a critical evaluation of the design of interventions, and its appropriateness for the study population.

It is a common misperception that GC levels equal the levels of stress an animal experiences (12), and that stress equals diminished welfare (72). We argue that an animal resides in a positive welfare state as long as it can cope and adapt to the demands of its (prevailing) environmental circumstances, enabling it to reach a state that it perceives as positive, e.g., that evokes positive emotions (3, 6). Thus, when investigating the effects of stressors, these aspects should be considered when formulating the research hypothesis.

Since we extracted the hypotheses as they were presented in the final publications, our results may have been affected by authors adapting their hypotheses in the writing phase to improve storytelling. Recent work shows that this phenomenon, generally referred to as “HARKing” (Hypothesizing After Results are Known) also exists in animal welfare research (19). The high incidence of inconsistency between the hypotheses and results reported in the set of reviewed studies suggests that HARKing in the welfare field is less common. Alternatively, the proportion of inconclusive results may even be larger than can be deduced from the published records, i.e., the proportion of inconsistent results may be an underrepresentation of the real number of studies that did not support the (original) hypothesis. This idea may become testable as soon as a *a priori* protocol

registration becomes common practice and original hypotheses can reliably be retrieved.

4.4.1. Glucocorticoid sampling

To elucidate potential improvements regarding the informative value of GCs as welfare proxy, we extracted information on sampling methods. Most often, experiments sampled GCs more than once, in line with our conceptual approach to welfare, which is dynamic (3, 6). The proportion of experiments finding homogenous effects or no effects were comparable across the number of GC measurements, but the proportion of experiments reporting heterogenous effects increased. Note that long-term experiments, in which the GC levels initially changed due to the intervention and then returned to control or baseline levels, were not scored as heterogenous but included in the homogenous category because this change was considered as temporary.

To identify patterns of GC release in response to an acute stressor, multiple measurements on the dynamics of the GC response may prove to be more informative about the animal's coping style and resilience (73). Further long-term and in-depth analyses are needed to understand the time course of HPA axis regulation, the role of allostasis and resilience, and the consequences for welfare (74).

Blood sampling for cortisol was the most common procedure. Animal species differ in the glucocorticoid that is predominantly produced by the adrenals, e.g., corticosterone in birds and rodents, and cortisol in most other mammals. However, research has shown that local GC and GC metabolite synthesis may lead to local differences in which glucocorticoid is present at a higher level, challenging the idea that species are corticosterone or cortisol dominant [e.g., (75)]. In addition, cortisol and corticosterone concentrations might not correlate (76). Especially studies investigating the immune system as index of welfare should consider measuring several GC metabolites when trying to elucidate mechanisms [e.g., (77)].

Nearly half of the experiments collected sample matrices such as feces, urine, hair, or other substances (e.g., milk or eggs) to quantify GC levels. These matrices allow for less invasive sampling than blood collection. Additionally, the procedures necessary to collect blood samples may affect levels of GCs themselves (78). Therefore, alternative sample matrices are promising for repeatedly sampling to avoid accumulation of discomfort. Notably, handling to collect alternative samples, e.g., placing the animal in a separate cage [e.g., (79)], may affect GC levels in subsequent samples. Moreover, the relation between GC levels in blood and in alternative matrices needs more investigation. Sample matrices reflect different time periods of GC accumulation (56), thus relative levels might not relate between sample types (23). Interestingly, minimally invasively measured levels of GCs, e.g., in feces or in feathers, have been shown to reflect biologically meaningful patterns (80, 81).

Further validation of measurements, e.g., by challenging animals with ACTH and subsequently collecting samples over a period of time to determine peak GC concentrations, is highly recommended (29, 30).

Next to handling of the animals, several technical challenges may account, at least partly, for the variation in the relation between GCs and additional proxies of welfare. Sampling regimens should account for variation on the individual instead of group/cage level (82–84). A circadian and circannual rhythm [e.g., (85)] may lead to additional variation, which needs to be controlled experimentally and statistically. The subsequent processing of samples in the laboratory—i.e., whether and how the sample is extracted and purified, the choice of antibody and assay type—may further impact measured concentrations (86), though a recent meta-analysis did not find an effect of assay method (87).

4.5. Experimental design

A between-subject design was applied in most of the reviewed experiments, comparing the effects of a treatment with a control group. Regarding to the importance of the individual in welfare concepts, data on pre-intervention values would add valuable information about individual profiles (88). Vice versa, studies investigating within-individual changes may miss the comparison to a control group over time. One third of the reviewed studies did indeed use a combined experimental set-up, thus included within- and between individual, or group, measurements. Long-term effects of an intervention may then become visible, which is important in view of the concept that welfare is dynamic and dependent on the individuals' adaptive capacity.

All three GC outcome domains were prevalent across a range of sample sizes, but detailed analyses are needed to infer the likelihood of finding effects on GC levels are driven by the number of animals sampled. Information on sample size for GC measurements proved rather difficult to retrieve. We therefore urge the reporting of precise sample sizes along with the statistics or graphical representations of GC levels. A sufficiently large sample size and appropriate statistical power is an issue across research topics. Guidelines for animal welfare research have been published to ensure the appropriate samples size in animal welfare studies, especially when investigating adverse interventions (89).

4.5.1. Study population

Most of the experiments focused on farm animals such as pigs, cows, and chicken, and on laboratory animals such as mice and rats, followed by other domesticated species. These results may indicate the great effort of researchers investigating welfare and welfare-related interventions in the two most frequently

used animal clusters (44). The proportion of studies aiming to study the welfare of a given species might also be linked to the perceived ethical conflict regarding the intrinsic value of animals, urging to safeguard the animal's integrity on the one side, and the use of animals for human purposes, on the other (90). The perceived need for improvement of husbandry circumstances seems to be highest in pigs as well as other species used for meat production.

Despite the increasing production of fish in commercial aquaculture, studies investigating a welfare related intervention in fish were scarce in our data set. The small number of studies represented in our review may be due to our selection criteria, as research on fish welfare often assesses measurements directly relating to the stress response and does not include additional parameter such as behavior. Given the large numbers of fish used in intensive aquaculture, and the large variety of fish species used, more research on their biological needs and potential welfare, using appropriate readout parameter is clearly needed (91, 92). We therefore advocate investigating the biological needs and to identify readout parameters suitable for assessing welfare in species underrepresented in our data set, such as amphibians, reptiles, and fish (93–96).

4.6. Interventions

Prior to data extraction, the team of reviewers defined a set of categories of interventions, based on our knowledge of the field. We were able to assign the major part of the experiments to these categories, however, ten percent were defined as “other intervention.” The outcome confirms the broad scope of welfare related research, and the complexity of factors to which the animals are exposed to. The clusters found are similar to the clusters of the network analysis from Freire and Nicol (44).

The variation of interventions, even within categories, may partly explain the variation in outcome of welfare proxies such as GCs, and behavior, morphology, and physiology. It remains to be statistically evaluated whether certain interventions lead to specific patterns in GC responses. Moreover, the type and array of welfare assessment parameters should be adjusted to the type of intervention.

Structural enrichment was the main category of single interventions, followed by a combination of enrichments. Enrichment aims to trigger different motivational systems and stimulates the animal to express its full behavioral repertoire (97). Similarly, space allowance and restricted movement were often investigated. Both determine which behaviors an animal can express, as some systems severely restrict movement (e.g., gestation stalls in sows). Expressing natural and/or normal behavior is recognized as a biological need and crucial for the animal to reach a positive welfare state (98, 99). Assessment of welfare based on GCs and other physiological

parameters may not be appropriate in these systems, as physical exercise may affect the outcomes, leading to e.g., higher GC levels (100).

4.7. Limitations

This mapping review provides an overview of experiments systematically in- or excluded according to a list of a priori criteria. While some of the exclusion criteria were based on a clear go/no go decision, others may be debatable. The first exclusion criterium, invertebrate, or human study population, served to limit the review to animal species in which GCs are components of the stress response. Based on the recent insights into emotional capacities in invertebrate species, we urge to extend welfare concepts and assessment protocols to these taxa (101).

Given the variety of opinions on welfare, the decision whether an experiment was assessing welfare or purely focused on the physiological response to stressors was challenging. Based on the conceptual approach that welfare is dynamic and comprises several domains (4), we established the criterium that, next to GCs, additional parameters needed to be measured (out of the domains, behavior, morphology and physiology) and that the experiment needed to follow the animals longer than 24 h. The 24 h cut-off was chosen to distinguish the acute GC stress response from long-term consequences affecting the coping capacity of animals (32). Nevertheless, we claim that 24 h are certainly not long enough to truly reflect coping capacity and welfare. Welfare assessment of an individual should take its lifetime experiences into account, positive as well as negative, as reflected by concepts such as “a Life Worth Living” (102, 103). Important for the welfare of an individual is that also acute interventions may have long-term effects, especially if applied during sensitive phases such as early life or adolescence, or even prenatally (104–106). If we, however, would have selected only studies across a lifetime of an animal, we would have significantly limited our sample size, as permanent interventions represented only a very small proportion of our set of publications. Nevertheless, our dataset offers the future possibility to investigate the included studies in more detail.

We did not extract detailed quantitative information about GC levels or the other outcome parameter. Instead, we chose to provide an overview of studies measuring GCs as part of assessing animal welfare. We did not analyze relations between experimental characteristics and outcome parameter to prevent “vote counting” (40). Vote counting, thus adding up the number of studies finding an effect, while omitting the statistical analysis of these studies, may lead to a false interpretation and over- or underestimation of effect sizes. While summations may suggest an effect of an intervention (or the absence thereof), reliable interpretation is only possible

by performing a weighted meta-analysis on the summarized data, taking means and variation into account (40). Keeping this in mind, we describe GC, behavioral, morphological, and physiological outcomes to provide an overview of the field, not inferring statistical implications. The here-presented results therefore do not allow for causal inferences, rather serves as inspiration. Further exploration of the data set, focusing on a carefully selected and defined subset of limited criteria and parameters, offers the opportunity to perform a meta-analysis and support further results by applying appropriate statistical analyses.

5. Conclusions and recommendations

The variation in outcomes of GCs, behavioral, morphological, and physiological parameter indicates that we have not yet developed the toolbox to decide with sufficient certainty whether an intervention improves or compromises welfare. Further research relating these parameters to the emotional experience of an individual, e.g., in terms of positive welfare indicators, is crucial (107). The complexity and multidimensional nature of welfare assessment needs, and benefits from, more than one assessment dimension (108).

This mapping review provides one of the largest explorative analyses of experimental studies using GCs as one of the parameters to assess the effects of interventions on animal welfare. The results are meant to encourage further extraction and quantitative meta-analysis of the relationships between parameter, for example testing effects on GCs in relation to intervention or sample matrix. Further research aiding our understanding of the interplay of GCs and behavioral, morphological and physiological processes, is clearly needed.

Data availability statement

The data that support the findings of this study are available from the corresponding author, IT upon reasonable request: inga.tiemann@uni-bonn.de.

Author contributions

VG and IT conceived the presented idea. IT, LE, MB, CL, and VG defined the literature search. IT, LE, MB, EL, and VG carried out the literature search. IT and VG wrote the paper with input from all the co-authors. All authors contributed to the article and approved the submitted version.

Funding

The publication was supported by the Open Access Publication Fund of the University of Bonn.

Acknowledgments

We thank Malika Weima, Eveline Giersberg, Thea Kranz, Laura Kröger, and Josefine Stuff for their help with the data extraction.

Conflict of interest

The authors declare that the research was conducted in the absence of any commercial or financial relationships

that could be construed as a potential conflict of interest.

Publisher's note

All claims expressed in this article are solely those of the authors and do not necessarily represent those of their affiliated organizations, or those of the publisher, the editors and the reviewers. Any product that may be evaluated in this article, or claim that may be made by its manufacturer, is not guaranteed or endorsed by the publisher.

Supplementary material

The Supplementary Material for this article can be found online at: <https://www.frontiersin.org/articles/10.3389/fvets.2022.954607/full#supplementary-material>

References

1. Welfare Quality®. *Welfare Quality® Assessment Protocol for Cattle*. Lelystad: Welfare Quality® (2009).
2. Brambell FW, Barbour DS, Lady Barnett, Ewer TK, Hobson A, Pitchforth H, et al. *Report of the Technical Committee to Enquire Into the Welfare of Animals Kept Under Intensive Livestock Husbandry Systems*. London (1965).
3. Ohl F, van der Staay FJ. Animal welfare: at the interface between science and society. *Vet J*. (2012) 192:13–9. doi: 10.1016/j.tvjl.2011.05.019
4. Mellor DJ, Beausoleil NJ, Littlewood KE, McLean AN, McGreevy PD, Jones B, et al. The 2020 five domains model: including human–animal interactions in assessments of animal welfare. *Animals*. (2020) 10:1870. doi: 10.3390/ani10101870
5. Mellor DJ, Reid C. Concepts of animal well-being and predicting the impact of procedures on experimental animals. In: *Improving the Well-Being of Animals in the Research Environment*. Glen Osmond, SA: WellBeing International (1994). p. 3–18. Available online at: <https://www.wellbeingintlstudiesrepository.org/exprawel/7/>
6. Arndt SS, Goerlich VC, van der Staay FJ. A dynamic concept of animal welfare: the role of appetitive and adverse internal and external factors and the animal's ability to adapt to them. *Front Anim Sci*. (2022) 3:908513. doi: 10.3389/fanim.2022.908513
7. Boissy A, Manteuffel G, Bak Jensen M, Oppermann Moe R, Spruijt B, Keeling LJ, et al. Assessment of positive emotions in animals to improve their welfare. *Physiol Behav*. (2007) 92:375–97. doi: 10.1016/j.physbeh.2007.02.003
8. Mellor DJ. Operational details of the five domains model and its key applications to the assessment and management of animal welfare. *Animals*. (2017) 7:60. doi: 10.3390/ani7080060
9. Rushen J. Using aversion learning techniques to assess the mental state, suffering, and welfare of farm animals. *J Anim Sci*. (1996) 74:1990–5. doi: 10.2527/1996.7481990x
10. Mason G, Mendl M. Why is there no simple way of measuring animal welfare? *Anim. Welf*. (1993) 2:301–19.
11. Farm Animal Welfare Council. *Farm Animal Welfare in Great Britain: Past, Present and Future*. London (2009).
12. MacDougall-Shackleton SA, Bonier F, Romero LM, Moore IT. Glucocorticoids and “stress” are not synonymous. *Integrat Organ Biol*. (2019) 1:obz017. doi: 10.1093/iob/obz017
13. Otovic P, Hutchinson E. Limits to using HPA axis activity as an indication of animal welfare. *ALTEX Alter Anim Exp*. (2015) 32:41–50. doi: 10.14573/altex.1406161
14. Mormède P, Andanson S, Aupérin B, Beerda B, Guémené D, Malmkvist J, et al. Exploration of the hypothalamic–pituitary–adrenal function as a tool to evaluate animal welfare. *Physiol Behav*. (2007) 92:317–39. doi: 10.1016/j.physbeh.2006.12.003
15. Ralph CR, Tilbrook AJ. The usefulness of measuring glucocorticoids for assessing animal welfare. *J Anim Sci*. (2016) 94:457–70. doi: 10.2527/jas.2015-9645
16. Rushen J. Problems associated with the interpretation of physiological data in the assessment of animal welfare. *Appl Anim Behav Sci*. (1991) 28:381–6. doi: 10.1016/0168-1591(91)90170-3
17. Wiepkema PR, Koolhaas JM. Stress and animal welfare. *Anim Welf*. (1993) 2:195–218.
18. Veissier I, Boissy A. Stress and welfare: two complementary concepts that are intrinsically related to the animal's point of view. *Physiol Behav*. (2007) 92:429–33. doi: 10.1016/j.physbeh.2006.11.008
19. van der Schot AA, Phillips C. Publication bias in animal welfare scientific literature. *J Agric Environ Ethics*. (2013) 26:945–58. doi: 10.1007/s10806-012-9433-8
20. Harris BN, Carr JA. The role of the hypothalamus–pituitary–adrenal/interrenal axis in mediating predator-avoidance trade-offs. *Gen Comp Endocrinol*. (2016) 230:110–42. doi: 10.1016/j.ygcen.2016.04.006
21. Sapolsky RM, Romero LM, Munck AU. How do glucocorticoids influence stress responses? Integrating permissive, suppressive, stimulatory, and preparative actions. *Endocrine Rev*. (2000) 21:55–89. doi: 10.1210/edrv.21.1.0389
22. Jimeno B, Hau M, Verhulst S. Corticosterone levels reflect variation in metabolic rate, independent of ‘stress’. *Sci Rep*. (2018) 8:13020. doi: 10.1038/s41598-018-31258-z
23. Cook NJ. Review: minimally invasive sampling media and the measurement of corticosteroids as biomarkers of stress in animals. *Can J Anim Sci*. (2012) 92:227–59. doi: 10.4141/cjas2012-045
24. Borg KE, Esbensen KL, Johnson BH. Cortisol, growth hormone, and testosterone concentrations during mating behavior in the bull and boar. *J Anim Sci*. (1991) 69:3230–40. doi: 10.2527/1991.6983230x
25. Buwalda B, Scholte J, Boer SF de, Coppens CM, Koolhaas JM. The acute glucocorticoid stress response does not differentiate between rewarding and aversive social stimuli in rats. *Horm Behav*. (2012) 61:218–26. doi: 10.1016/j.yhbeh.2011.12.012
26. Fairhurst GD, Frey MD, Reichert JF, Szelest I, Kelly DM, Bortolotti GR. Does environmental enrichment reduce stress? An integrated measure of corticosterone from feathers provides a novel perspective. *PLoS ONE*. (2011) 6:e17663. doi: 10.1371/journal.pone.0017663

27. Bienertova-Vasku J, Lenart P, Scherlinger M. Eustress and distress: neither good nor bad, but rather the same? *BioEssays*. (2020) 42:1900238. doi: 10.1002/bies.201900238
28. Meehan CL, Mench JA. The challenge of challenge: can problem solving opportunities enhance animal welfare? *Appl Anim Behav Sci*. (2007) 102:246–61. doi: 10.1016/j.applanim.2006.05.031
29. Touma C, Palme R. Measuring fecal glucocorticoid metabolites in mammals and birds: the importance of validation. *Ann N Y Acad Sci*. (2005) 1046:54–74. doi: 10.1196/annals.1343.006
30. Palme R. Non-invasive measurement of glucocorticoids: advances and problems. *Physiol Behav*. (2019) 199:229–43. doi: 10.1016/j.physbeh.2018.11.021
31. Spencer RL, Deak T. A users guide to HPA axis research. *Physiol Behav*. (2017) 178:43–65. doi: 10.1016/j.physbeh.2016.11.014
32. García A, Martí O, Vallés A, Dal-Zotto S, Armario A. Recovery of the hypothalamic-pituitary-adrenal response to stress. *NEN*. (2000) 72:114–25. doi: 10.1159/000054578
33. Leenaars CH, van der Mierden S, Durst M, Goerlich-Jansson VC, Ripoli FL, Keubler LM, et al. Measurement of corticosterone in mice: a protocol for a mapping review. *Lab Anim*. (2020) 54:26–32. doi: 10.1177/0023677219868499
34. Cockrem JF. Individual variation in glucocorticoid stress responses in animals. *Gen Comp Endocrinol*. (2013) 181:45–58. doi: 10.1016/j.ygcen.2012.11.025
35. Eriksen MB, Frandsen TF. The impact of patient, intervention, comparison, outcome (PICO) as a search strategy tool on literature search quality: a systematic review. *JMLA*. (2018) 106:420–31. doi: 10.5195/jmla.2018.345
36. Leenaars M, Hooijmans CR, van Veggel N, Riet G ter, Leeflang M, Hooft L, et al. A step-by-step guide to systematically identify all relevant animal studies. *Lab Anim*. (2012) 46:24–31. doi: 10.1258/la.2011.011087
37. de Vries R, Hooijmans CR, Tillema A, Leenaars M, Ritskes-Hoitinga M. Updated version of the Embase search filter for animal studies. *Lab Anim*. (2014) 48:88. doi: 10.1177/0023677213494374
38. Ouzzani M, Hammady H, Fedorowicz Z, Elmagarmid A. Rayyan—a web and mobile app for systematic reviews. *Syst Rev*. (2016) 5:210. doi: 10.1186/s13643-016-0384-4
39. van der Mierden S, Tsaionn K, Bleich A, Leenaars CH. Software tools for literature screening in systematic reviews in biomedical research. *ALTEX Alter Anim Exp*. (2019) 36:508–17. doi: 10.14573/altex.1902131
40. Borenstein M, Hedges LV, Higgins JP, Rothstein HR. *Introduction to Meta-Analysis*. Oxford: John Wiley and Sons (2021).
41. Waltman L, van Eck NJ, Noyons EC. A unified approach to mapping and clustering of bibliometric networks. *J Informetr*. (2010) 4:629–35. doi: 10.1016/j.joi.2010.07.002
42. Page MJ, McKenzie JE, Bossuyt PM, Boutron I, Hoffmann TC, Mulrow CD, et al. The PRISMA 2020 statement: an updated guideline for reporting systematic reviews. *BMJ*. (2021) 372:n71. doi: 10.1136/bmj.n71
43. Walker M, Diez-Leon M, Mason G. Animal welfare science: recent publication trends and future research priorities. *Int J Consum Stud*. (2014) 27:80–100. doi: 10.46867/ijcp.2014.27.013
44. Freire R, Nicol CJ. A bibliometric analysis of past and emergent trends in animal welfare science. *Anim Welf*. (2019) 28:465–85. doi: 10.7120/09627286.28.4.465
45. Dickens MJ, Romero LM. A consensus endocrine profile for chronically stressed wild animals does not exist. *Gen Comp Endocrinol*. (2013) 191:177–89. doi: 10.1016/j.ygcen.2013.06.014
46. de Jong IC, Prelle I, Vandeburgwal J, Lambooi E, Korte S, Blokhuis H, et al. Effects of environmental enrichment on behavioral responses to novelty, learning, and memory, and the circadian rhythm in cortisol in growing pigs. *Physiol Behav*. (2000) 68:571–8. doi: 10.1016/S0031-9384(99)00212-7
47. Naderi F, Hernández-Pérez J, Chivite M, Soengas JL, Míguez JM, López-Patiño MA. Involvement of cortisol and sirtuin1 during the response to stress of hypothalamic circadian system and food intake-related peptides in rainbow trout, *oncorhynchus mykiss*. *Chronobiol Int*. (2018) 35:1122–41. doi: 10.1080/07420528.2018.1461110
48. Korte SM, Olivier B, Koolhaas JM. A new animal welfare concept based on allostasis. *Physiol Behav*. (2007) 92:422–8. doi: 10.1016/j.physbeh.2006.10.018
49. Cyr NE, Michael Romero L. Chronic stress in free-living European starlings reduces corticosterone concentrations and reproductive success. *Gen Comp Endocrinol*. (2007) 151:82–9. doi: 10.1016/j.ygcen.2006.12.003
50. Rich EL, Romero LM. Exposure to chronic stress downregulates corticosterone responses to acute stressors. *Am J Physiol Regul Integrat Comp Physiol*. (2005) 288:R1628–36. doi: 10.1152/ajpregu.00484.2004
51. Wulsin AC, Wick-Carlson D, Packard BA, Morano R, Herman JP. Adolescent chronic stress causes hypothalamo-pituitary-adrenocortical hypo-responsiveness and depression-like behavior in adult female rats. *Psychoneuroendocrinology*. (2016) 65:109–17. doi: 10.1016/j.psyneuen.2015.12.004
52. Romero LM, Beattie UK. Common myths of glucocorticoid function in ecology and conservation. *J Exp Zool Part A Ecol Integrat Physiol*. (2022) 337:7–14. doi: 10.1002/jez.2459
53. McEwen BS. Stress, adaptation, and disease: allostasis and allostatic load. *Ann N Y Acad Sci*. (1998) 840:33–44. doi: 10.1111/j.1749-6632.1998.tb09546.x
54. Kasanen IH, Inhilä KJ, Vainio OM, Kiviniemi VV, Hau J, Scheinin M, et al. The diet board: welfare impacts of a novel method of dietary restriction in laboratory rats. *Lab Anim*. (2009) 43:215–23. doi: 10.1258/la.2008.008066
55. Gayrard V, Alvinerie M, Toutain PL. Interspecies variations of corticosteroid-binding globulin parameters. *Domest Anim Endocrinol*. (1996) 13:35–45. doi: 10.1016/0739-7240(95)00042-9
56. Gormally BM, Romero LM, Angelier F. What are you actually measuring? A review of techniques that integrate the stress response on distinct time-scales. *Funct Ecol*. (2020) 34:2030–44. doi: 10.1111/1365-2435.13648
57. Dawkins MS. Using behaviour to assess animal welfare. *Anim Welf*. (2004) 13:3–7.
58. Mason GJ, Mench J. Using behaviour to assess animal welfare. In: *Animal Welfare*. Wallingford: CAB International (2021). p. 127–41.
59. Meuser V, Weinhold L, Hillemacher S, Tiemann I. Welfare-related behaviors in chickens: characterization of fear and exploration in local and commercial chicken strains. *Animals*. (2021) 11:679. doi: 10.3390/ani11030679
60. Mendl M, Burman OH, Paul ES. An integrative and functional framework for the study of animal emotion and mood. *Proc R Soc B Biol Sci*. (2010) 277:2895–904. doi: 10.1098/rspb.2010.0303
61. Manteuffel G, Puppe B, Schön PC. Vocalization of farm animals as a measure of welfare. *Appl Anim Behav Sci*. (2004) 88:163–82. doi: 10.1016/j.applanim.2004.02.012
62. McLoughlin MP, Stewart R, McElligott AG. Automated bioacoustics: methods in ecology and conservation and their potential for animal welfare monitoring. *J R Soc Interf*. (2019) 16:20190225. doi: 10.1098/rsif.2019.0225
63. Mogil JS, Pang DS, Silva Dutra GG, Chambers CT. The development and use of facial grimace scales for pain measurement in animals. *Neurosci Biobehav Rev*. (2020) 116:480–93. doi: 10.1016/j.neubiorev.2020.07.013
64. von Borell E, Langbein J, Després G, Hansen S, Leterrier C, Marchant-Forde J, et al. Heart rate variability as a measure of autonomic regulation of cardiac activity for assessing stress and welfare in farm animals — a review. *Physiol Behav*. (2007) 92:293–316. doi: 10.1016/j.physbeh.2007.01.007
65. Jerez-Cepa I, Ruiz-Jarabo I. Physiology: an important tool to assess the welfare of aquatic animals. *Biology*. (2021) 10:61. doi: 10.3390/biology10010061
66. Duncan IJ, Petherick JC. The implications of cognitive processes for animal welfare. *J Anim Sci*. (1991) 69:5017–22. doi: 10.2527/1991.69125017x
67. Talbot SR, Biernot S, Bleich A, van Dijk RM, Ernst L, Häger C, et al. Defining body-weight reduction as a humane endpoint: a critical appraisal. *Lab Anim*. (2020) 54:99–110. doi: 10.1177/0023677219883319
68. Kalliokoski O, Jacobsen KR, Darusman HS, Henriksen T, Weimann A, Poulsen HE, et al. Mice do not habituate to metabolism cage housing—a three week study of male BALB/c mice. *PLoS ONE*. (2013) 8:e58460. doi: 10.1371/journal.pone.0058460
69. Hemsworth PH, Barnett JL, Hansen C. The influence of handling by humans on the behavior, growth, and corticosteroids in the juvenile female pig. *Horm Behav*. (1981) 15:396–403. doi: 10.1016/0018-506X(81)90004-0
70. Hemsworth PH, Coleman GJ, Barnett JL, Jones RB. Behavioural responses to humans and the productivity of commercial broiler chickens. *Appl Anim Behav Sci*. (1994) 41:101–14. doi: 10.1016/0168-1591(94)90055-8
71. Harris BN. Stress hypothesis overload: 131 hypotheses exploring the role of stress in tradeoffs, transitions, and health. *Gen Comp Endocrinol*. (2020) 288:113355. doi: 10.1016/j.ygcen.2019.113355
72. Tilbrook AJ, Ralph CR. Hormones, stress and the welfare of animals. *Anim Product Sci*. (2018) 58:408. doi: 10.1071/AN16808
73. Ericsson M, Fallahsharoudi A, Bergquist J, Kushnir MM, Jensen P. Domestication effects on behavioural and hormonal responses to acute stress in chickens. *Physiol Behav*. (2014) 133:161–9. doi: 10.1016/j.physbeh.2014.05.024
74. Nazar FN, Estevez I. The immune-neuroendocrine system, a key aspect of poultry welfare and resilience. *Poult Sci*. (2022) 101:101919. doi: 10.1016/j.psj.2022.101919

75. Schmidt KL, Soma KK. Cortisol and corticosterone in the songbird immune and nervous systems: local vs. systemic levels during development. *Am J Physiol Regulat Integrat Comp Physiol.* (2008) 295:R103–R110. doi: 10.1152/ajpregu.00002.2008
76. Koren L, Whiteside D, Fahlman Å, Ruckstuhl K, Kutz S, Checkley S, et al. Cortisol and corticosterone independence in cortisol-dominant wildlife. *Gen Comp Endocrinol.* (2012) 177:113–9. doi: 10.1016/j.ygcen.2012.02.020
77. Tetel V, Tonissen S, Fraley GS. Sex difference in changes in heterophil to lymphocyte ratios in response to acute exposure of both corticosterone and cortisol in the Pekin duck. *Poult Sci.* (2022) 101:101914. doi: 10.1016/j.psj.2022.101914
78. Newman AE, Hess H, Woodworth BK, Norris DR. Time as tyrant: the minute, hour and day make a difference for corticosterone concentrations in wild nestlings. *Gen Comp Endocrinol.* (2017) 250:80–4. doi: 10.1016/j.ygcen.2017.05.022
79. Nicholson A, Malcolm RD, Russ PL, Cough K, Touma C, Palme R, et al. The response of C57BL/6J and BALB/cJ mice to increased housing density. *J Am Assoc Lab Anim Sci.* (2009) 48:14.
80. Lind M-A, Hörak P, Sepp T, Meitern R. Corticosterone levels correlate in wild-grown and lab-grown feathers in greenfinches (*Carduelis chloris*) and predict behaviour and survival in captivity. *Horm Behav.* (2020) 118:104642. doi: 10.1016/j.yhbeh.2019.104642
81. Sheriff MJ, Krebs CJ, Boonstra R. Assessing stress in animal populations: do fecal and plasma glucocorticoids tell the same story? *Gen Comp Endocrinol.* (2010) 166:614–9. doi: 10.1016/j.ygcen.2009.12.017
82. Alm M, Wall H, Holm L, Wichman A, Palme R, Tauson R. Welfare and performance in layers following temporary exclusion from the litter area on introduction to the layer facility. *Poult Sci.* (2015) 94:565–73. doi: 10.3382/ps/pev021
83. Gjendal K, Sørensen DB, Kiersgaard MK, Ottesen JL. Hang on: an evaluation of the hemp rope as environmental enrichment in C57BL/6 mice. *Anim Welf.* (2017) 26:437–47. doi: 10.7120/09627286.26.4.437
84. Ronca AE, Moyer EL, Talyansky Y, Lowe M, Padmanabhan S, Choi S, et al. Behavior of mice aboard the international space station. *Sci Rep.* (2019) 9:4717. doi: 10.1038/s41598-019-40789-y
85. Rao R, Androulakis IP. The physiological significance of the circadian dynamics of the HPA axis: interplay between circadian rhythms, allostasis and stress resilience. *Horm Behav.* (2019) 110:77–89. doi: 10.1016/j.yhbeh.2019.02.018
86. Beyl HE, Jimeno B, Lynn SE, Breuner CW. Assay temperature affects corticosteroid-binding globulin and free corticosterone estimates across species. *Gen Comp Endocrinol.* (2021) 310:113810. doi: 10.1016/j.ygcen.2021.113810
87. van der Mierden S, Leenaars CH, Boyle EC, Ripoli FL, Gass P, Durst M, et al. Measuring endogenous corticosterone in laboratory mice - a mapping review, meta-analysis, and open source database. *ALTEX Alter Anim Exp.* (2021) 38:111–22. doi: 10.14573/altex.2004221
88. van der Goot MH, Boleij H, van den Broek J, Salomons AR, Arndt SS, van Lith HA. An individual based, multidimensional approach to identify emotional reactivity profiles in inbred mice. *J Neurosci Methods.* (2020) 343:108810. doi: 10.1016/j.jneumeth.2020.108810
89. Hampton JO, MacKenzie DI, Forsyth DM. How many to sample? Statistical guidelines for monitoring animal welfare outcomes. *PLoS ONE.* (2019) 14:e0211417. doi: 10.1371/journal.pone.0211417
90. Röcklinsberg H, Gamborg C, Gjerris M. A case for integrity: gains from including more than animal welfare in animal ethics committee deliberations. *Lab Anim.* (2014) 48:61–71. doi: 10.1177/0023677213514220
91. Franks B, Ewell C, Jacquet J. Animal welfare risks of global aquaculture. *Sci Adv.* (2021) 7:eabg0677. doi: 10.1126/sciadv.abg0677
92. Toni M, Manciocco A, Angiulli E, Alleva E, Cioni C, Malavasi S. Review: assessing fish welfare in research and aquaculture, with a focus on European directives. *Animal.* (2019) 13:161–70. doi: 10.1017/S1751731118000940
93. Colson V, Mure A, Valotaire C, Le Calvez JM, Goardon L, Labbé L, et al. A novel emotional and cognitive approach to welfare phenotyping in rainbow trout exposed to poor water quality. *Appl Anim Behav Sci.* (2019) 210:103–12. doi: 10.1016/j.applanim.2018.10.010
94. Michaels CJ, Downie JR, Campbell-Palmer R. The importance of enrichment for advancing amphibian welfare and conservation goals: a review of a neglected topic. *Biodiversity.* (2014) 8:17.
95. Pasmans F, Bogaerts S, Braeckman J, Cunningham AA, Hellebuyck T, Griffiths RA, et al. Future of keeping pet reptiles and amphibians: towards integrating animal welfare, human health and environmental sustainability. *Vet Rec.* (2017) 181:450. doi: 10.1136/vr.104296
96. Silla AJ, Calatayud NE, Trudeau VL. Amphibian reproductive technologies: approaches and welfare considerations. *Conserv Physiol.* (2021) 9:coab011. doi: 10.1093/conphys/coab011
97. Newberry RC. Environmental enrichment: increasing the biological relevance of captive environments. *Appl Anim Behav Sci.* (1995) 44:229–43. doi: 10.1016/0168-1591(95)00616-Z
98. Bracke MB, Hopster H. Assessing the importance of natural behavior for animal welfare. *J Agric Environ Ethics.* (2006) 19:77–89. doi: 10.1007/s10806-005-4493-7
99. Špinka M. How important is natural behaviour in animal farming systems? *Appl Anim Behav Sci.* (2006) 100:117–28. doi: 10.1016/j.applanim.2006.04.006
100. Veissier I, Andanson S, Dubroeuq H, Pomiès D. The motivation of cows to walk as thwarted by tethering. *J Anim Sci.* (2008) 86:2723–9. doi: 10.2527/jas.2008-1020
101. Horvath K, Angeletti D, Nascetti G, Carere C. Invertebrate welfare: an overlooked issue. *Ann Ist Super Sanita.* (2013) 49:9–17. doi: 10.4415/ANN_13_01_04
102. Mellor DJ. Updating animal welfare thinking: moving beyond the “five freedoms” towards “a life worth living”. *Animals.* (2016) 6:21. doi: 10.3390/ani6030021
103. Yeates JW. Is ‘a life worth living’ a concept worth having? *Anim Welf.* (2011) 20:397–406.
104. Begni V, Sanson A, Pfeiffer N, Brandwein C, Inta D, Talbot SR, et al. Social isolation in rats: effects on animal welfare and molecular markers for neuroplasticity. *PLoS ONE.* (2020) 15:e0240439. doi: 10.1371/journal.pone.0240439
105. Costa JH, Cantor MC, Adderley NA, Neave HW. Key animal welfare issues in commercially raised dairy calves: social environment, nutrition, and painful procedures. *Can J Anim Sci.* (2019) 99:649–60. doi: 10.1139/cjas-2019-0031
106. Rutherford K, Donald R, Arnott G, Rooke J, Dixon L, Mehers JJ, et al. Farm animal welfare: assessing risks attributable to the prenatal environment. *Anim Welf.* (2012) 21:419–29. doi: 10.7120/09627286.21.3.419
107. Kremer L, Klein Holkenborg SEJ, Reimert I, Bolhuis JE, Webb LE. The nuts and bolts of animal emotion. *Neurosci Biobehav Rev.* (2020) 113:273–86. doi: 10.1016/j.neubiorev.2020.01.028
108. Botreau R, Veissier I, Butterworth A, Bracke MB, Keeling LJ. Definition of criteria for overall assessment of animal welfare. *Anim Welf.* (2007) 16:225–8.



OPEN ACCESS

EDITED BY

E. Tobias Krause,
Friedrich-Loeffler-Institute, Germany

REVIEWED BY

Antje Schubert,
Friedrich-Loeffler-Institute, Germany
Hayley Randle,
Charles Sturt University, Australia

*CORRESPONDENCE

Leigh P. Gaffney
✉ lgaffney@uvic.ca

[†]These authors have contributed
equally to this work and share
first authorship

SPECIALTY SECTION

This article was submitted to
Animal Welfare and Policy,
a section of the journal
Frontiers in Animal Science

RECEIVED 05 October 2022

ACCEPTED 29 December 2022

PUBLISHED 16 January 2023

CITATION

Gaffney LP, Lavery JM, Schiestl M,
Trevvarthen A, Schukraft J, Miller R,
Schnell AK and Fischer B (2023) A
theoretical approach to improving
interspecies welfare comparisons.
Front. Anim. Sci. 3:1062458.
doi: 10.3389/fanim.2022.1062458

COPYRIGHT

© 2023 Gaffney, Lavery, Schiestl, Trevvarthen,
Schukraft, Miller, Schnell and Fischer. This is
an open-access article distributed under the
terms of the [Creative Commons Attribution
License \(CC BY\)](#). The use, distribution or
reproduction in other forums is permitted,
provided the original author(s) and the
copyright owner(s) are credited and that
the original publication in this journal is
cited, in accordance with accepted
academic practice. No use, distribution or
reproduction is permitted which does not
comply with these terms.

A theoretical approach to improving interspecies welfare comparisons

Leigh P. Gaffney^{1*†}, J. Michelle Lavery^{2†}, Martina Schiestl^{3†},
Anna Trevvarthen^{4†}, Jason Schukraft⁵, Rachael Miller^{6,7}, Alexandra
K. Schnell⁶ and Bob Fischer^{8,9}

¹Fisheries Ecology and Marine Conservation Lab, Department of Biology, University of Victoria, Victoria, BC, Canada, ²Campbell Centre for the Study of Animal Welfare, Department of Integrative Biology, University of Guelph, Guelph, ON, Canada, ³Faculty for Veterinary Medicine, University of Veterinary Science, Brno, Czechia, ⁴Independent Researcher, Gloucestershire, United Kingdom, ⁵Open Philanthropy, San Francisco, CA, United States, ⁶Department of Psychology, University of Cambridge, Cambridge, United Kingdom, ⁷School of Life Sciences, Anglia Ruskin University, Cambridge, United Kingdom, ⁸Rethink Priorities, San Francisco, CA, United States, ⁹Department of Philosophy, Texas State University, San Marcos, TX, United States

The number of animals bred, raised, and slaughtered each year is on the rise, resulting in increasing impacts to welfare. Farmed animals are also becoming more diverse, ranging from pigs to bees. The diversity and number of species farmed invite questions about how best to allocate currently limited resources towards safeguarding and improving welfare. This is of the utmost concern to animal welfare funders and effective altruism advocates, who are responsible for targeting the areas most likely to cause harm. For example, is tail docking worse for pigs than beak trimming is for chickens in terms of their pain, suffering, and general experience? Or are the welfare impacts equal? Answering these questions requires making an interspecies welfare comparison; a judgment about how good or bad different species fare relative to one another. Here, we outline and discuss an empirical methodology that aims to improve our ability to make interspecies welfare comparisons by investigating welfare range, which refers to how good or bad animals can fare. Beginning with a theory of welfare, we operationalize that theory by identifying metrics that are defensible proxies for measuring welfare, including cognitive, affective, behavioral, and neuro-biological measures. Differential weights are assigned to those proxies that reflect their evidential value for the determinants of welfare, such as the Delphi structured deliberation method with a panel of experts. The evidence should then be reviewed and its quality scored to ascertain whether particular taxa may possess the proxies in question to construct a taxon-level welfare range profile. Finally, using a Monte Carlo simulation, an overall estimate of comparative welfare range relative to a hypothetical index species can be generated. Interspecies welfare comparisons will help facilitate empirically informed decision-making to streamline the allocation of resources and ultimately better prioritize and improve animal welfare.

KEYWORDS

interspecies comparisons, comparative cognition, animal welfare range, empirical methodology, effective altruism

1 Introduction

1.1 A case for the need to make interspecies welfare comparisons

The number of animals bred, raised, and slaughtered each year for food and other purposes is on the rise (Béné et al., 2015). On an annual basis, over 70 billion terrestrial animals and nearly a trillion aquatic animals, across a wide variety of species, are raised or captured for food (FAO, 2021; Franks et al., 2021). This trend has led to an increase in intensive production practices that significantly impact the welfare (see Table 1 for key definitions) of the various species involved and may lead to increased pain, suffering, and other negative experiences (e.g., Lundmark et al., 2014; Broom, 2019; Keeling et al., 2019; Xu et al., 2019). One major challenge for animal welfare science is the difficulty of making meaningful comparisons between the welfare impacts of certain practices on different species (Bracke, 2006; Cohen, 2009; Wong, 2016; Budolfson & Spears, 2019; Browning, 2020). That is, it is difficult to assess whether some species are made worse off by such practices than others.

There are many examples of how intensive production can impact welfare. Globally, for instance, most intensive pork production systems dock piglets' tails in their first week of life (Sutherland et al., 2008). This involves using clippers that are heated so that they both cut the tail and cauterize the wound at the same time. The procedure is done without anesthesia and can cause acute pain that disrupts normal behavior in the short run (2011; Sutherland et al., 2008). In the long run, tail docking can result in the growth of neuromas (i.e., nerve tumors) that are permanently sensitive (Sutherland et al., 2008). Production system managers argue that tail docking is necessary to reduce injury from other piglets, who often bite at tails if they are left long (Sutherland et al., 2008). In most

intensive egg production facilities worldwide, beak trimming (i.e., the partial removal of the upper portion of a hen's beak) is a standard procedure performed on young hens (Bessei, 2018). It involves removing roughly a third of the upper beak, or sometimes both the upper and lower beak (Lonsdale et al., 1957), with a hot blade that both cuts and cauterizes (Henderson et al., 2009). Like tail docking, beak trimming can cause acute pain that disrupts normal behavior (Duncan et al., 1989) and also result in the growth of neuromas that are permanently sensitive (Kuenzel, 2007). Production system managers argue that beak trimming is necessary to reduce feed waste and avoid pecking-related injuries that can lead to cannibalism and increase chicken mortality (Allen and Perry, 1975).

Mass marking of salmon by fin clipping (i.e., the partial or full removal of a fish's fins) is a procedure commonly used in intensive aquaculture and hatcheries to distinguish farmed or hatchery-reared salmon from wild salmon (Uglen et al., 2020). Similarly, to tail docking and beak trimming, fin clipping may cause pain and injury in fish and alter swimming efficiency (Roques et al., 2010; Buckland-Nicks et al., 2021; Schroeder & Sneddon, 2017; Thomson et al., 2020; Uglen et al., 2020). Production system managers argue that fin clipping is the easiest method to identify fish because it is inexpensive, quick, and requires minimal equipment and training (Hammer and Lee Blankenship, 2001).

These practices raise questions that need to be addressed to inform future directions in welfare in intensive production. For example, are the welfare impacts of tail-docking pigs worse than beak trimming chickens? Are the welfare impacts of beak trimming chickens worse than fin clipping salmon? Or are the welfare impacts equal? What empirical evidence exists that could be used to make this assessment? Considering whether one practice has greater welfare impacts than the other is a primary concern for animal advocates (see Table 1 for key definitions) who have to make choices about how to allocate limited resources. Many of these advocates, including

TABLE 1 Key definitions.

Term	Definition
Affective states	Affective states refer to the experience of feeling the underlying emotional state (Hogg et al., 2010).
Cardinal utility	Cardinal measurement of utility refers to the measurement (or expression) of utility in terms of units like 2, 4, 6 and 8. Cardinality means that utility can be measured in numbers (Baumol, 1958).
Effective altruism	Effective altruism is a research field and conceptual approach emerging from a social community, using data-driven reasoning, aiming to find the best ways to help others, and put them into practice (Broad, 2018).
Empirical methodology	Empirical research is a type of research methodology that makes use of verifiable evidence in order to arrive at research outcomes, meaning it relies solely on evidence obtained through scientific data collection.
Hedonism	The word 'hedonism' comes from the ancient Greek word for 'pleasure'. If hedonism is true, then what matters is how an animal feels - its subjective experiences (Weijers, 2011).
Proxy/Indicator	Proxies or indicators, are defined as measures relevant to cognition, behavior, welfare, and physiology (e.g., measures of brain power, working memory capacity, self-awareness) (Fischer, 2022).
Stakeholder	A person with an interest or concern in something, especially a business.
Valenced	Valence, or hedonic tone, is the affective quality referring to the intrinsic attractiveness - goodness (positive valence) or averseness - badness (negative valence) of an event, object, or situation. The term also characterizes and categorizes specific emotions (Lindquist et al., 2016; Bruckner, 2020)
Welfare	The term "welfare" refers to the state of an individual in relation to its environment, and this can be measured (Broom, 1991; Broom, 1996; Bruckner, 2020).
Welfare range	An animal's welfare range is the difference between how well and poorly that animal can fare at a time (Fischer, 2022).

effective altruists (see Table 1 for key definitions), want to allocate funding in a way that maximizes returns on welfare investments (i.e., produces the largest welfare improvement per dollar spent). Likewise, many members of the general public wish to make informed decisions around their food and purchasing choices. Individuals may, for instance, choose to become pescatarians, vegetarians, or vegans, or simply avoid one kind of animal product while eating others (e.g., those who abstain from eating veal or foie gras). These decisions are largely based around their perceptions and understanding of the impacts of farming on different animals. However, without relevant empirical data, such decisions, for stakeholders (see Table 1 for key definitions) of all types, are invariably *ad-hoc* or subjective, and thus unlikely to achieve their intended aims. Interspecies welfare comparisons can provide a pathway to make informed decisions about which areas and which taxa to prioritize for various purposes.

Making interspecies welfare comparisons can have other implications, particularly in relation to identifying bias in discussions of animal welfare. Animal welfare concerns have primarily been directed at terrestrial vertebrates used in agriculture, laboratory research, and as companion animals (e.g., Russell & Burch, 1959; Lundmark et al., 2014; Cardoso et al., 2017; Franks et al., 2021; Gaffney and Lavery, 2022). However, many species used in intensive production systems, such as fish, shrimp, and silkworms, have received little attention and consequently, their welfare is often regarded with less concern (e.g., Elder & Fischer, 2017). Furthermore, the production numbers of these latter species tend to amount to considerably more overall in comparison to the more ‘traditional’ ones (Franks et al., 2021). Such attitudes may be based on arbitrary distinctions, with humans tending to care more about species that are evolutionarily closer and often more familiar, like mammals, than those that are more distant and different, like insects. Or, there may be legitimate reasons to be less concerned about the welfare of some species compared to others. Nevertheless, without tools to compare welfare across species, it is difficult to answer these questions.

Interspecies welfare comparisons can also improve welfare guidelines for scientific research. Such comparisons become particularly important when implementing the imperative to “reduce, refine, and replace” (the 3Rs; Fenwick et al., 2009). For example, when possible, researchers are required to replace animal models with non-animal models (Burden et al., 2015). However, in situations where replacement is not possible (given research objectives), some scientists defer to using animals, which are thought to be “cognitively less-sophisticated” animals. For example, zebrafish are often used as a substitute for ostensibly “cognitively more-sophisticated” animals, like mice (Hamilton et al., 2016; 2018). These decisions are based on the assumption that members of one species would be harmed less by the research than members of another (Schaeck et al., 2013; Message & Greenhough, 2019; Sloman et al., 2019; Almstedt et al., 2022). Inevitably, without interspecies welfare comparisons, such subjective judgements could introduce unjustified bias towards certain species over others.

Our goal is to outline a theoretical approach to improving interspecies welfare comparisons using an empirical methodology (see Table 1 for definition and details). We propose investigating welfare ranges (see Table 1 for key definitions), which refer to the differences between how well or poorly various animals can fare at a

time. This theoretical construct allows us to compare the severity of harms and benefits across species.

1.2 Conceptual issues associated with interspecies welfare comparisons

We need to consider several conceptual issues before turning to our method for making interspecies welfare comparisons.

First, we should acknowledge that there are many theories of welfare. For example, here are four that have had some influence in agriculture, conservation biology, animal welfare science, and philosophy:

1. Welfare as bodily health: animals have positive welfare insofar as their bodies are functioning properly (Dawkins, 2021).
2. Welfare as engaging in or expressing natural behavior: animals have positive welfare insofar as they exhibit (or can exhibit) natural behavior (Bruckner, 2020).
3. Welfare as subjective experiences: animals have positive welfare insofar as they are experiencing sufficiently many positive affective states (see Table 1 for definition and details) relative to negative affective states (Robbins et al., 2018).
4. Welfare as hedonism/desire satisfaction: animals have positive welfare insofar as they “get what they want” (Dawkins, 2021).

Theories of welfare differ over the determinants of welfare. Nevertheless, these theories are sometimes combined: the classic triadic theory discussed by Fraser (2008), for instance, proposes that welfare is jointly determined by bodily health, natural behavior, and subjective experiences. Similarly, the Five Freedoms (Webster, 1994) has had considerable influence as a framework for animal welfare assessment in policy-making spaces and incorporates elements of subjective experience, bodily health, and natural behavior into its conceptualization of welfare. Balancing the overall valence of lifetime subjective experiences and incorporating aspects of hedonism, the concept of a “life worth living” (FAWC, 2009; Yeates, 2011) has been used to determine minimum standards for the treatment of farm animals in some policies and guidelines. Many of these theories have received criticism (e.g., Korte et al., 2007; McCulloch, 2013; Duncan, 2016), but are generally unified by some degree of concern about an animal’s subjective experiences.

Second, aside from aligning with a theory of welfare, we must also consider the different types of interspecies welfare comparisons. List (2003) distinguishes between two types of comparisons. The first type is the more basic: it concerns the valences of experiences (see Table 1 for key definitions)—i.e., whether they are positive, negative, or neutral. Imagine, for instance, a sow who is physically restricted (e.g., in a farrowing crate) and cannot reach her piglets and a healthy chicken who is pecking at some corn in a safe environment. It seems likely that the sow’s experience is negatively valenced whereas the chicken’s is positively valenced. So, we can plausibly conclude that, at least with respect to their experiential states, the chicken is faring better than the sow.

The second type of interspecies welfare comparisons are level comparisons, that is, differences within a given valence, which

introduces additional complexity. Imagine a recently tail-docked pig and a hen which has not eaten for eight hours. Both animals are likely to be having negatively valenced experiences (acute pain and some degree of hunger, respectively). However, while it may seem plausible that the docked pig is worse off than the hungry chicken, it is difficult to provide a detailed justification for this judgment. We may inherently think about how we, as humans, may feel in a comparable situation, reflecting on our own experiences. However, without knowing the extent to which other animals experience pain or hunger comparably to us (or to one another), we cannot accurately make such a distinction. At present, there is no agreed-upon method for making such interspecies welfare level comparisons.

Finally, it is important to recognize that our assessment of a given animal's welfare is based on objective measures of the animal's subjective state (Sandøe & Jensen, 2011). However, subjective states are not directly measurable, and we cannot ask animals directly how they feel. Thus, we are left measuring "indicators" or "proxies" of welfare (see Table 1 for key definitions), rather than the momentary state itself. Validation of such proxies of welfare is therefore of particular importance and is especially pressing in cases where we have a limited understanding of animals' physiology and behavior (e.g., the pain debate in fishes and insects; see Vettese et al., 2020 and Gibbons et al., 2022). Further, it is unclear how to theoretically aggregate proxies into a measure of overall welfare, even within a species (e.g., see Botreau et al., 2007 for a review).

Our proposed solution avoids these problems for now, by investigating animals' welfare ranges with the aim of creating a tool that could inform interspecies welfare comparisons. An animal's welfare refers to how well or poorly an individual is faring (Broom, 1986); so, an animal's welfare range refers to the difference between how well or poorly an animal can fare at a time. The contrast here is between the actual state of an animal (welfare) and possible states of that animal (welfare range). Animals with relatively large welfare ranges can be harmed to greater degrees than animals with relatively small welfare ranges. Notice that welfare range profiles can be created for animals at the individual-level, but our methods have been designed to create welfare range profiles at the species-level.

As the definition of welfare ranges suggests, talk of "larger" and "smaller" welfare range is a simplification, overlooking potential dissociations between the various dimensions and multiple theories of animal welfare (see review by Bruckner, 2020). According to a pluralistic theory of welfare, there are multiple determinants of welfare. Dawkins (2021) has such a theory, which states that animal welfare is determined by two factors: namely, animals being healthy and getting what they want. By contrast, a monistic theory of welfare suggests there is a single determinant of welfare, such as hedonism (see Table 1 for key definitions). This theory states that animal welfare is determined by the quality of their subjective experiences (Robbins et al., 2018), where all and only positive experiences are good for animals, whilst all and only negative experiences are bad for them.

While it is possible to investigate differences in welfare ranges assuming any theory of welfare, it is impossible to do that in a single paper. So, for simplicity, we assume hedonism. This theory of welfare is compatible with the view that it matters whether animals are healthy and whether they can express species-typical behaviors (Robbins et al., 2018). Following hedonism, we will assume that

welfare at a time is determined by the qualities of experiential states, i.e., the strength of how good or bad an animal's overall experience is. So, if there could be variation among species in terms of the potential intensity of their experience, then there could be differences in their welfare ranges.

Animals differ with respect to their evolutionary history, neurophysiology, and neurobiology. This seems to have led to variation in their cognitive, affective, and sensory capabilities. It seems plausible, then, that there would be considerable differences in their experiential lives. Indeed, Birch et al. (2020) argue that there are five dimensions of variation: Perceptual Richness, Evaluative Richness, Integration at a Time, Integration across Time and Self-Consciousness. They argue that traditional one-dimensional scales of consciousness neglect these important dimensions of variation across taxa. Using a multi-dimensional approach by investigating taxa against each proposed dimension would create "consciousness profiles" that capture variation and highlight where a taxon is likely to fit in the space of possible forms of experience.

If different species encounter differences in their experiential lives, then it is plausible that there are characteristic differences in the determinants of the qualities of experiential states. Differences in intensity are perhaps the most familiar to us, such as pain perception, which is variable in humans (Hu & Iannetti, 2019). However, there is a difference between variations in the strength of the stimulus to produce a given response and variation in maximum response capacity. Given apparent differences among humans, who broadly share social, affective, intellectual, behavioral, and neurobiological characteristics, it is not hard to imagine more profound differences among nonhuman animals, a possibility that is explicitly raised in the literature (e.g., Yeates, 2012).

1.3 Why could differences in welfare ranges be relevant to interspecies welfare comparisons?

In brief, we can use standard welfare assessments, interpreted with welfare ranges, can be used to estimate the relative badness of harms or the goodness of benefits. This is because, from a philosophical perspective, when we assess animals' welfare, we assess it relative to a species-typical neutral point. Given that neutral point, we assess both valence and strength of valence is assessed. For example, we can say that a particular state is positive or negative and that it is more positive or negative than some other state (e.g., Mendl et al., 2010). So, while we use measures with cardinal utility are used (see Table 1 for key definitions) to assess welfare, such as the duration of protective behavior, cortisol levels, time to return to normal feeding behavior, and changes in time spent resting vs. active, we aggregate them to produce an ordinal ranking of welfare states (Botreau et al., 2007). When it comes to intraspecies welfare comparisons, what matters is not, for instance, the duration of protective behavior per se, but one of two comparisons:

1. The duration of protective behavior that one individual displays in response to a given stimulus compared to the duration of protective behavior that the individual displays in

response to a different stimulus, i.e., an individual-level focus, for example, using individual-based measures of welfare (see [Blokhuis et al., 2010](#)), or

2. The duration of protective behavior that one individual displays compared to the typical duration of protective behavior that individuals of that species display in response to a range of stimuli and / or stimuli of that kind, i.e. a species-level focus, for example, using group-level measures of welfare (see [Main et al., 2003](#)).

We typically, validate measures of welfare are validated by making either individual-level or species-level comparisons; we assess the impacts of particular stimuli in terms of how they affect animals by comparing their response relative to another individual or species. These relative rankings are essential, as we cannot ask animals directly how they are faring. This implies, however, that when we make interspecies welfare comparisons are made, we are starting out with species-relative data. As such, it is safe to assume that apparently equivalent harms reduce the welfare of members of each species by an approximately equivalent percentage of their respective welfare ranges. To see this, consider [Figure 1](#).

[Figure 1](#)'s conceptualization of "welfare units" and welfare ranges provides a tentative way to quantify the relative welfare impacts of

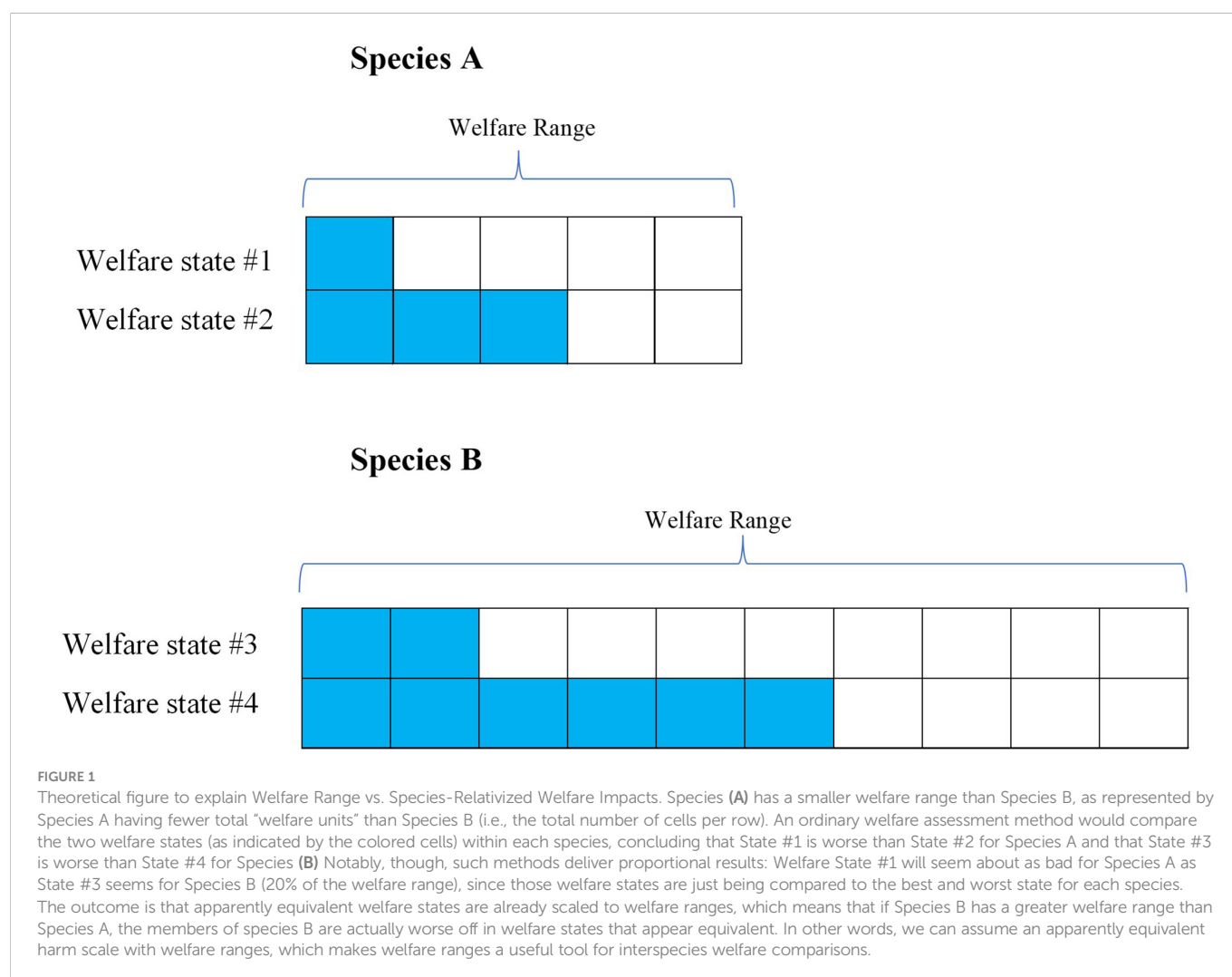
different harms and benefits. While obviously imprecise, it may still be the case that they are useful for many practical purposes. That being said, the usefulness of welfare ranges depends entirely on our ability to empirically assess and quantify it. If there is no way to do that, then we cannot use welfare ranges to tackle the problem of interspecies welfare comparisons.

2 Proposed methodology

Our aim in this section is to propose a basic methodology for assessing welfare ranges. This is summarized in [Figure 2](#).

The *first* task is to specify features that are intrinsic, rather than extrinsic, determinants of welfare, and so of welfare ranges. This part requires selecting a theory of welfare; (see section 1.2).

Importantly, we do not suggest that the theories of welfare outlined in section 1.2 are equally plausible or that the options we mentioned represent the only possibilities available. Our goal here is to set out the methodology, not to defend particular choices within it. If, for instance, we conclude that welfare is determined by bodily health, we would then turn to the task of operationalizing bodily health in ways that lend it to empirical investigation.



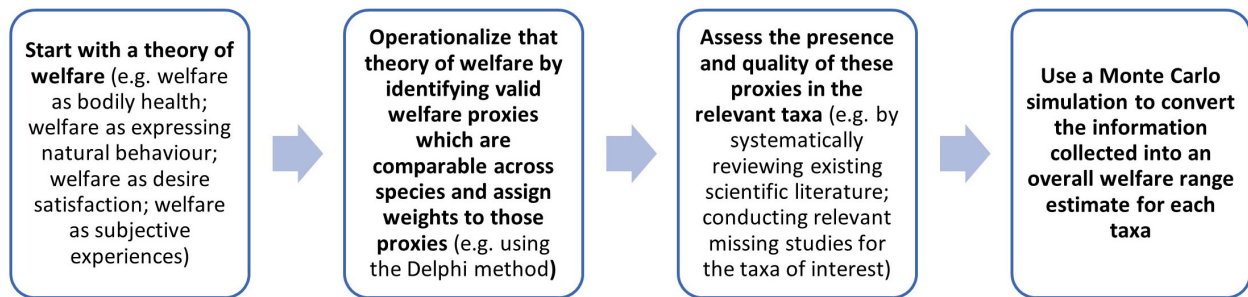


FIGURE 2

A summary of the proposed methodology for determining a welfare range estimate for taxa of interest to enable interspecies welfare comparisons.

The *second* task involves turning the determinants of welfare enumerated during the first stage into measurable proxies. Notice that, at the outset, there is a tremendous amount of empirical uncertainty about the extent to which different animals display different welfare-relevant proxies. But that does not negate the value of describing a theoretical methodology built on such proxies, as it can assist in prioritizing research efforts such that our empirical certainty increases, and the estimates produced by the methodology are refined. These proxies should ideally be valid and amenable to operationalization, comparable across taxa, and chosen with an understanding of their ecological relevance to the taxa being compared. Further, there are considerable theoretical and practical challenges involved in comparing morally relevant features across phylogenetically distant animals. For example, the presence of nociceptors provides some evidence of the capacity for negative subjective experiences, but it is not definitive, since there can be nociception without any subjective experience at all in humans (Dubin and Patapoutian, 2010). Moreover, these proxies may relate to cognition, affect, behavior and neuro-biology. We therefore suggest that the best way forward is to weigh the chosen proxies in terms of the quality of the evidence they provide for the factors that are taken to be determinants of welfare. One way to select and provide these precise proxy weights is to use the Delphi method (Linstone and Turoff, 1975). In brief, the Delphi method is a form of structured deliberation. It begins with the selection of a panel of experts. Then the experts answer questionnaires in at least two revisions. After each revision, the experts send their answers to a facilitator who returns an anonymized summary of the experts' assessments to each member of the panel.

The *third* task involves assessing the evidence for these proxies in the relevant taxa. To begin, this task involves systematically reviewing the existing scientific literature. For more in depth knowledge about how this can be done, please refer to our pre-printed review about the relationship between cognition and welfare in 10 farmed animal taxa (Miller et al., 2022b pre-print). Notice that to apply our empirical methodology in full, we would likely need to conduct various relevant new studies that have not been completed for the taxa of interest. In primates, for instance, perspective-taking is associated with self-awareness, theory of mind, and empathy (Bulloch et al., 2008; de Waal, 2008; Towner, 2010). Specifically, perspective-taking involves reasoning about the mental states of others (e.g., their intentions, desires, and knowledge) and has been linked to possessing strong emotional capacities (Healey and Grossmann, 2018). Consequently,

perspective-taking may be considered a suitable proxy for some cognitive capacities that are either determinants of welfare or are themselves associated with determinants of welfare. There is ample evidence of perspective-taking in pigs: they can learn to follow other pigs who they recognize to have information about the location of food (Held et al., 2000), they can adjust their own behavior to prevent other pigs from exploiting their knowledge in this way (Held et al., 2002a), they can detect whether humans are paying attention to them *via* head cues (Nawroth et al., 2013a), and they can follow human hand signals to find food (Nawroth et al., 2013b). However, there is very little evidence as to whether chickens engage in perspective-taking (Smith et al., 2011), suggesting that additional research would be valuable.

Before we can draw any conclusions about the value of additional research, it is critical to identify the quantity and quality of the evidence that has already been published. For each publication found in the review, it would be important to record the estimate of the credibility of that paper and either its conclusion regarding the presence, absence or magnitude of the proxy, depending on whether the proxy is discrete or continuous. The strength of evidence could be rated along a scale. For example, a recent review of sentience in invertebrates used a scaled rating method ranging from 'lean no' to 'yes' (Rethink Priorities, 2020; Table 2). Another review on the evidence of sentience in cephalopod molluscs and decapod crustaceans used a scaled rating method that graded evidence in terms of how many of criteria for sentience were satisfied (8 criteria in total) (Birch et al., 2021). Specifically, evidence was graded as 'extremely strong' if 7–8 criteria were satisfied, 'strong' if 5–6 criteria were satisfied, 'substantial' if 3–4 criteria were satisfied, 'some' if only 2 criteria were satisfied, and 'unknown or unlikely' if 0–1 criteria were satisfied. Using scaled rating methods can generate welfare range profiles per taxa that simultaneously highlights the quality and quantity of evidence *and* identifies gaps in the current literature. We note that all estimates of scalar proxies should be normalized to a hypothetical index species that possesses the maximum observed value for any proxy that might matter for that particular welfare comparison. Since it is essential to compare all the values in the table to some reference value possessed by the index species, the absence of a proxy in the index species entails that the welfare range of other species goes to infinity, or some other arbitrarily large number.

The *fourth* task involves turning the data into overall welfare range estimates using a Monte Carlo simulation. Although other

TABLE 2 Examples of potential literature review output and rating scale for some example proxies and species, using the rating approach from **Rethink Priorities (2020)**.

Proxy	Species A (e.g., pig)	Species B (e.g., chicken)	Species C (e.g., salmon)	Species D (e.g., crayfish)	Species E (e.g., bee)
Judgment bias	Likely yes (Düppan et al., 2013)	Likely yes (Crump et al., 2018)	Unknown	Lean yes (Bacqué-Cazenave et al., 2017)	Likely yes (Bateson et al., 2011)
Social learning	Likely yes (Oostindjer et al., 2011)	Likely yes (Nicol & Pope, 1994)	Likely yes (Bajer et al., 2010)	Lean yes (Jiménez-Morales et al., 2018)	Likely yes (Alem et al., 2016)
Boredom-like behavior	Likely yes (Wemelsfelder, 1985)	Likely yes (Newberry, 1999)	Unknown	Unknown	Unknown

methods may also be possible, Monte Carlo methods are the preferred choice for modeling phenomena with significant uncertainty in inputs (Kroese et al., 2014). They reduce the need for using human judgment, which is often unreliable when dealing with complex questions. They also allow a complex probability density function to be presented as an output, rather than just a point estimate or a simple range, which is especially important for this project because it makes it easier to appreciate the degree of uncertainty in particular welfare range estimates. One way to proceed is to survey experts, using a formal, pre-registered, structured way of aggregating the survey results into a useful bottom-line estimate that preserves all information about the range of judgments that the experts make. This process reduces the need to make decisions about how to aggregate information that could influence or bias the results.

Each sample used as input for the Monte Carlo method is the judgment of one expert in the field, combined with the results of one paper that studies each proxy that the expert considers to be important. The result of this sample is plotted on a histogram and the process is repeated thousands of times. The resulting histogram represents the scale of possibilities for the welfare range typical for a given species, given different judgments and lines of evidence. This histogram can be used to produce averages, confidence intervals, and other ways of summarizing or reporting the data.

Given a specific theory of welfare and a set of welfare determinants, each repetition of the simulation will:

1. Randomly choose one expert in the Delphi panel. Then, assign a weight to each proxy based on that expert's estimates for the proxy weights.
2. Randomly choose one paper for each proxy, based on the credibility assigned to that paper. Pull a sample of the numerical value of that proxy from its adjusted distribution.
3. Calculate a weighted average of the capacity, using the values from Step 2 and the weights in Step 1.

The simulation should be run at least 10,000 times, producing a histogram of results. Again, this histogram will be the probability distribution of the species' welfare range as a fraction of the hypothetical index species.

There are bound to be gaps in the available proxy-relevant research for some species and we have a choice about how to manage this. One option is not to intervene, simply ignoring

unknown values. As a result, the weight of the other proxies (for which there is known information) would be increased proportionally when performing weighted average calculations. So, if a species has (average) values of 0.2, 0.3, 0.4, and unknown across four proxies, with equal weight on them all, the average would be 0.3. However, this has the effect of amplifying the significance of the other sources of variance.

A second option is to replace all unknown values with the corresponding values from the target comparison species. The hypothetical index species has the maximum observed value for each proxy across all actual species. So, entering values from the hypothetical index species would produce empirically implausible results, e.g., attributing cognitive capacities that we know a species lacks simply because its specific capacities have not been studied. For example, if pigs are compared to chickens, and there are lots of unknowns for chickens then we replace unknown values for chickens with the known values for pigs. This would have the effect of reducing the significance of the other sources of variance and would amount to a "curve" in favor of no variance. This would reflect the judgment that we should err on the side of welfare ranges being distributed more equally across the target taxa. Moreover, it may mean that we are unable to identify any differences in welfare ranges between some taxa, which will result in there being a narrower range of cases where we can draw on welfare range differences to make interspecies welfare comparisons. However, a narrower range of cases might still be a practically significant range of cases. Then finally, with our estimate in place, it is possible to make certain interspecies welfare comparisons.

3 Discussion

Our aim has been to propose a method for making interspecies welfare comparisons *via* estimates of comparative welfare ranges. We do not assume that this methodology will reveal differences (or similarities) in welfare ranges. Instead, we believe that *if* there are differences across taxa, ours is a promising method for discovering them. Furthermore, as our description suggests, this is a substantial research program that could only be completed over a significant period of time with extensive interdisciplinary collaboration. There are still some aspects of the method that deserve special attention, which we discuss below.

Depending on the theory of welfare used, the method could become more complex. If applying a pluralistic theory of welfare (such as Fraser, 2008's triadic theory) or using multiple theories of welfare at once, a separate Delphi method for each theory or component of the theory (e.g., bodily health, natural behavior, and subjective experiences; Fraser, 2008) would need to be conducted. The method can become more complicated because it might be necessary to use a different panel of experts appropriate to that theory or component. Empirical research would then need to be focused on the proxies, if any, that are shared across components or theories and are found by consensus to be important for each theory.

Depending on the proxies that are chosen and the taxa that are compared, a lack of relevant literature reporting evidence of those proxies may represent a significant limitation. Gaps in the literature may also make choosing proxies difficult. For instance, neuron counts (Herculano-Houzel et al., 2015; Raji & Potter, 2021) are relatively easy to compare across species and there are already data for many taxa of interest. However, it is not clear how neuron counts are linked to the welfare of an animal. To properly compare neurons, we need to know where they are located and how they are connected to each other. So, insofar as neuron counts are worth investigating and comparing, they must be handled carefully as proxies for other characteristics of interest (Von Bartheld et al., 2016). It may be, for example, that neuron count is associated with affective sophistication, intensity of valenced experiences, or general intelligence, though extensive research would be required before such conclusions could be drawn (Dicke & Roth, 2016). Our approach helps to identify where these gaps in the literature exist and highlights which proxies should be prioritized for future research.

Beyond a lack of literature, comparing phylogenetically distant taxa may pose additional challenges. For instance, if it turns out that sentience (assuming it is a feature relevant to the theory of welfare in use) is the product of convergent evolution, with multiple independent origins (Brown, 2020), then we might never find proxies that work across those taxonomic gaps. Even if it turns out that sentience is not the product of convergent evolution, we will end up relying heavily on the field of comparative cognition. Fortunately, there has been a recent surge of interest in comparing species across metrics that may bear on questions about welfare ranges (MacLean et al., 2014; Cauchoix et al., 2018; Miller et al., 2022a). There has been a concomitant surge in theoretical discussions about how to compare features across species, as seen in Weiss et al. (2019), which outlines a quantitative measure of social complexity that works across species. Similarly, Anderson and Andolphins (2014) developed a framework for studying emotions across species. Such research provides reason for optimism about the potential of comparative cognition research.

However, it should be noted that comparative cognition is a heterogeneous field with respect to the reliability and reproducibility of research findings. Some areas of comparative cognition research have been criticized for their low rates of reproducibility, largely owing to small sample sizes, inappropriate or noisy measurements, and implausible hypotheses (Forstmeier et al., 2017; Farrar et al.,

2020). By contrast, other areas of comparative cognition research appear to be less affected by low reproducibility rates due to the use of robust designs that can easily be replicated; for instance, the use of within-subject designs where subjects experience many trials multiple times (Smith and Little, 2018). The field of comparative cognition also bears hallmarks of the publication bias towards positive results. Specifically, the field is biased towards confirming more exceptional cognitive abilities in animals, since academic journals appear to favor papers with surprising results over papers which merely confirm the expected (Mlinarić et al., 2017).

Nevertheless, the unexpected is not always favored equally across species since there are differences in how abilities are perceived among different taxa. For example, a study recently demonstrated that a tiny fish, the cleaner wrasse (*Labroides dimidiatus*) passed the mirror mark test (Kohda et al., 2019), joining an 'elite' handful of other species including chimpanzees (Gallup, 1970), dolphins (Reiss & Marino, 2001), Asian elephants (Plotnik et al., 2006) and Eurasian magpies (Prior et al., 2008). Other animals such as pigs and parrots might be suitable candidates for passing the mirror mark test, as they are able to use a mirror as visual information to find hidden items (Pepperberg et al., 1995; Broom et al., 2009). The mirror mark test involves placing a mark on an animal in a location that can only be seen in a mirror reflection. Passing the mirror mark test involves performing self-directed behaviors in the mirror (i.e., exploring areas of the body that cannot be observed without the mirror), showing interest in the mark on the body and ultimately attempting to remove the mark. The test is considered a benchmark for investigating mirror self-recognition and self-awareness. The study on cleaner wrasse was strongly criticized and triggered debate about whether researchers included robust and appropriate controls to rule-out alternative explanations for the observed behaviors (Frans de Waal, 2019; Gallup & Anderson, 2020; but see Kohda et al., 2022). Moreover, skeptics were not convinced that self-scraping behavior in fish could be considered equivalent to mark-directed self-exploration with hands or trunks in humans, apes, and elephants. Notice that the interpretation of results from mirror mark tests in other animals are also subject to wide debate, particularly about the certainty with which behavioral responses during the test can be used as evidence of self-awareness (1995; Heyes, 1994; Anderson and Gallup, 2015). While it is important that all scientific findings are met with healthy skepticism, the response to the cleaner wrasse study hints that sophisticated cognitive capacities ascribed to intuitively perceived "lower-order" species can be met with stronger skepticism.

Our method could also be prone to bias if proxies are chosen without an understanding of their ecological relevance to the taxa of interest. Suppose we conclude, for instance, that the capacity for emotional contagion is a good proxy for the presence of certain subjective experiences that we take to be relevant to welfare (Düppjan et al., 2020). This proxy might be suitable for species that live in social groups or form affiliative relationships with conspecifics because sharing social experiences is thought to facilitate emotional contagion (Herrando & Constantinides, 2021). By contrast,

emotional contagion (Adriaense et al., 2019) might be practically useless for making interspecies welfare comparisons across relatively solitary species that do not form strong social bonds with other individuals (e.g., octopuses: Schnell and Clayton, 2019; silkworms: Zhu et al., 2021). As a result, including it would heavily bias against less social species, not because we have some positive reason to think that the relevant sorts of subjective experiences are absent, but because our method of assessment is skewed toward some species relative to others. However, this could be partially circumvented by building welfare range profiles at the class- or family-level rather than species-level. This becomes relevant when there is social variation within a taxonomic group of animals. For example, there are both solitary and eusocial species across the four main bee families. There are also both solitary (i.e., octopuses) and group living species (i.e., schooling squid) within the class Cephalopoda.

Other biases when choosing relevant proxies might arise because our human perspective may render the method prone to false negatives (e.g., Ioannidis, 2005). If this method does not uncover differences in welfare ranges between certain taxa, we caution against assuming that no differences exist. Regardless of the theory of welfare used, ultimately proxies will likely be chosen with some attention to what we perceive to be relevant determinants of welfare for humans. This anthropocentrism is present throughout animal welfare science. For example, many welfare indicators are validated using humans as a form of gold standard (e.g., Mendl et al., 2022). However, such decisions about which proxies to examine may introduce unconscious biases towards or against certain options and may indeed miss entire categories of proxies relevant for detecting differences in welfare ranges between taxa. A complete view of a given taxa's welfare range is, at present, difficult, given the literature constraints and other challenges discussed in this section. As such, our method provides an approximation that should be interpreted with care.

In any theory in which valenced experiences are determinants of welfare, it is plausible that differences in the possible intensity of those experiences will matter. Unfortunately, assessing potential differences in the intensity range of valenced experiences is a difficult task. Specifically, it is notoriously difficult to establish a scale and measure the intensity of an internal state, and harder still to do so across species. For example, it might be true that, in general, members of a species show shorter latencies to move toward more desirable rewards (Davies et al., 2015). However, there may be variation within species in terms of willingness to work for a reward that does not track the intensity of internal states. Across species, any number of factors may make it difficult to use differences in latency as a proxy, including ecological role (i.e., predator or prey) and physical anatomy (i.e., appendages that facilitate swimming, walking, crawling, or flying). This is true even for some closely-related species, but it becomes more pronounced as phylogenetic distance increases (e.g., Dobromylskyy et al., 2000; Mogil, 2019; Browning, 2020; and Stasiak et al., 2003). In

these cases, the use of careful controls in experimental design is critical, for instance, comparing a baseline latency with a test latency to construct a difference score per individual (Miller et al., 2022a). While there is little question about intensity of valenced experiences being a determinant of welfare, and intensity range being a factor that influences welfare range, it will be extremely difficult to make any progress on the problem of differences in intensity range. However, this is not necessarily a problem for the methodology. Experts can simply assign very low scores to any proxy for intensity, which means that while it will be included, its impact will be significantly attenuated. That is, even if there are large differences in the empirical assessments of that proxy across species, they will have only minor impacts on the overall welfare range estimate, with small or uncertain differences being almost irrelevant.

Finally, we foresee potential challenges in reaching consensus around which proxies are most relevant and how to weigh them. Using subjective, expert judgments in the Delphi method is an accepted, robust option as described in the previous section. However, in practice, such expert judgments may cause new tensions in already often politically-fraught conversations about animal welfare (e.g., the fish pain debate, Mason and Lavery, 2022; conversations about “wicked problems”, Bolton and Von Keyserlingk, 2021). To be clear, this is not a reason not to use this method; instead, it is a call to employ the results of the method with care for context, and with attention to how they may be received by diverse stakeholders.

4 Conclusion

From a theoretical perspective, the method we propose for assessing comparative welfare ranges is an attempt to answer fundamental questions about differences in the experiential lives of nonhuman animals. From a practical perspective, the method we propose is an attempt to improve daily judgments about how to allocate and prioritize resources to relieve animal suffering. We also acknowledge that there are risks and limitations to undertaking such a project. However, interspecies welfare comparisons are important and common: they are already being made on one basis or another, primarily without empirical evidence. Our methodological framework can facilitate comparisons which are based on a transparent and empirically informed process. Ultimately, interspecies welfare comparisons can help us direct our attention to issues that will be most important for improving estimates of comparative welfare ranges and allow us to conduct sensitivity analyses to determine where additional information has the highest value relative to that end. We hope that this methodology provides a starting point for developing empirical interspecies welfare comparisons, while highlighting priorities for future research and promoting interdisciplinary collaborations to achieve this.

Data availability statement

The original contributions presented in the study are included in the article/supplementary material. Further inquiries can be directed to the corresponding author.

Author contributions

BF and JS contributed to the conception of the methodology. BF wrote the first draft of the manuscript. LG, JML, MS, and AT wrote sections of the manuscript and prepared it for submission. All authors contributed to the article and approved the submitted version.

Acknowledgments

We would like to thank Richard Bruns, Marcus Davis, Adam Shriver, and Michael St. Jules for their discussion of the ideas presented in this paper and our reviewers for their constructive

feedback. We would also like to extend our gratitude to Open Philanthropy and Rethink Priorities for facilitating and funding this work. A preprint of this article (Gaffney et al., 2022) can be found on preprints.org.

Conflict of interest

The authors declare that the research was conducted in the absence of any commercial or financial relationships that could be construed as a potential conflict of interest.

Publisher's note

All claims expressed in this article are solely those of the authors and do not necessarily represent those of their affiliated organizations, or those of the publisher, the editors and the reviewers. Any product that may be evaluated in this article, or claim that may be made by its manufacturer, is not guaranteed or endorsed by the publisher.

References

- Adriaense, J. E. C., Martin, J. S., Schiestl, M., Lamm, C., and Bugnyar, T. (2019). Negative emotional contagion and cognitive bias in common ravens (*Corvus corax*). *PNAS* 116, 11547–11552. doi: 10.1073/pnas.1817066116
- Alem, S., Perry, C. J., Zhu, X., Loukola, O. J., Ingraham, T., Søvik, E., et al. (2016). Correction: Associative mechanisms allow for social learning and cultural transmission of string pulling in an insect. *PLoS Biol.* 14 (12), e1002589. doi: 10.1371/journal.pbio.1002589
- Allen, J., and Perry, G. C. (1975). Feather pecking and cannibalism in a caged layer flock. *Br. Poultry Sci.* 16, 441–451. doi: 10.1080/00071667508416212
- Almstedt, E., Rosén, E., Gloger, M., Stockgard, R., Hekmati, N., Koltowska, K., et al. (2022). Real-time evaluation of glioblastoma growth in patient-specific zebrafish xenografts. *Neuro-oncology* 24, 726–738. doi: 10.1093/neuonc/noab264
- Anderson, D. J., and Adolphs, R. (2014). A framework for studying emotions across species. *Cell* 157, 187–200. doi: 10.1016/j.cell.2014.03.003
- Anderson, J. R., and Gallup, G. G. (2015). Mirror self-recognition: a review and critique of attempts to promote and engineer self-recognition in primates. *Primates* 56, 317–326. doi: 10.1007/s10329-015-0488-9
- Bacqué-Cazenave, J., Cattaert, D., Delbecq, J. P., and Fossat, P. (2017). Social harassment induces anxiety-like behaviour in crayfish. *Sci. Rep.* 7, 1–7. doi: 10.1038/srep39935
- Bajer, P. G., Lim, H., Travaline, M. J., Miller, B. D., and Sorensen, P. W. (2010). Cognitive aspects of food searching behavior in free-ranging wild common carp. *Environ. Biol. Fish.* 88, 295–300. doi: 10.1007/s10641-010-9643-8
- Bateson, M., Desire, S., Gartside, S. E., and Wright, G. A. (2011). Agitated honeybees exhibit pessimistic cognitive biases. *Curr. Biol.* 21, 1070–1073. doi: 10.1016/j.cub.2011.05.017
- Baumol, W. J. (1958). The cardinal utility which is ordinal. *Econ. J.* 68, 665–672. doi: 10.2307/2227278
- Béné, C., Barange, M., Subasinghe, R., Pinstrup-Andersen, P., Merino, G., Hemre, G. I., et al. (2015). Feeding 9 billion by 2050—putting fish back on the menu. *Food Secur.* 7, 261–274. doi: 10.1007/s12571-015-0427-z
- Bessei, W. (2018). Impact of animal welfare on worldwide poultry production. *World's Poultry Sci. J.* 74, 211–224. doi: 10.1017/S0043933918000028
- Birch, J., Burn, C., Schnell, A. K., Browning, H., and Crump, A. (2021). Review of the evidence of sentience in cephalopod molluscs and decapod crustaceans. LSE consulting. LSE enterprise Ltd. *London School Econ. Politic. Sci.* Available at: <https://www.lse.ac.uk/News/News-Assets/PDFs/2021/Sentience-in-Cephalopod-Molluscs-and-Decapod-Crustaceans-Final-Report-November-2021.pdf>. (Accessed August 10, 2022).
- Birch, J., Schnell, A. K., and Clayton, N. S. (2020). Dimensions of animal consciousness. *Trends Cogn. Sci.* 24, 789–801. doi: 10.1016/j.tics.2020.07.007
- Blokhuys, H. J., Veissier, I., Miele, M., and Jones, B. (2010). The welfare quality project and beyond: safeguarding farm animal well-being. *Acta Agric. Scand. Sect. A.* 60, 129–140. doi: 10.1080/09064702.2010.523480
- Bolton, S. E., and Von Keyserlingk, M. A. (2021). The dispensable surplus dairy calf: Is this issue a “wicked problem” and where do we go from here? *Front. Vet. Sci.* 8. doi: 10.3389/fvets.2021.660934
- Botreau, R., Bonde, M., Butterworth, A., Perny, P., Bracke, M., Capdeville, J., et al. (2007). Aggregation of measures to produce an overall assessment of animal welfare. part 1: A review of existing methods. *Animal* 1, 1179–1187. doi: 10.1017/S1751731107000535
- Bracke, M. B. M. (2006). Providing cross-species comparisons of animal welfare with a scientific basis. *NJAS-Wageningen J. Life Sci.* 54, 61–75. doi: 10.1016/S1573-5214(06)80004-7
- Broad, G. M. (2018). Effective animal advocacy: effective altruism, the social economy, and the animal protection movement. *Agric. Hum. Values* 35, 777–789. doi: 10.1007/s10460-018-9873-5
- Broom, D. M. (1986). Indicators of poor welfare. *Br. Vet. J.* 142, 524–526. doi: 10.1016/0007-1935(86)90109-0
- Broom, D. M. (1991). Animal welfare: concepts and measurement. *J. Anim. Sci.* 69, 4167–4175. doi: 10.2527/1991.69104167x
- Broom, D. M. (1996). Attempts to cope with the environment. *Acta Agric. Scand. Sec. A. Anim. Sci. Suppl.* 27, 22–28.
- Broom, D. M. (2019). Animal welfare complementing or conflicting with other sustainability issues. *Appl. Anim. Behav. Sci.* 219, 104829. doi: 10.1016/j.applanim.2019.06.010
- Broom, D. M., Sena, H., and Moynihan, K. L. (2009). Pigs learn what a mirror image represents and use it to obtain information. *Anim. Behav.* 78, 1037–1041. doi: 10.1016/j.anbehav.2009.07.027
- Brown, C. (2020). Convergent evolution of sentience? *Anim. Sentience* 5, 25. doi: 10.51291/2377-7478.1617
- Browning, H. (2020). If I could talk to the animals: Measuring subjective animal welfare [Doctoral dissertation, the Australian national university]. *ProQuest Dissert. Pub.* 1–212. doi: 10.25911/5f1572fb1b5be
- Bruckner, D. W. (2020). Animal welfare science, varieties of value and philosophical methodology. *Anim. Welf.* 29, 387–397. doi: 10.7120/09627286.29.4.387
- Buckland-Nicks, J. A., Gillis, M., and Reimchen, T. E. (2021). Neural network detected in a presumed vestigial trait: ultrastructure of the salmonid adipose fin. *Proc. R. Soc. B: Biol. Sci.* 279, 553–563. doi: 10.1098/rspb.2011.1009
- Budolfson, M., and Spears, D. (2019). “Quantifying animal well-being and overcoming the challenge of interspecies comparisons,” in *The routledge handbook of animal ethics*, vol. 92-101. Ed. B. Fischer (New York, United States: Routledge).
- Bullock, M. J., Boysen, S. T., and Furlong, E. E. (2008). Visual attention and its relation to knowledge states in chimpanzees, pan troglodytes. *Anim. Behaviour* 76, 1147–1155. doi: 10.1016/j.anbehav.2008.01.033
- Burden, N., Chapman, K., Sewell, F., and Robinson, V. (2015). Pioneering better science through the 3Rs: an introduction to the national centre for the replacement,

refinement, and reduction of animals in research (NC3Rs). *J. Am. Assoc. Lab. Anim. Sci.* 54, 198–208.

Cardoso, S. D., Faraco, C. B., de Sousa, L., and Pereira, G. D. G. (2017). History and evolution of the European legislation on welfare and protection of companion animals. *J. Vet. Behav.* 19, 64–68. doi: 10.1016/j.jvbeh.2017.01.006

Cauchois, M., Chow, P. K. Y., Van Horik, J. O., Atance, C. M., Barbeau, E. J., Barragan-Jason, G., et al. (2018). The repeatability of cognitive performance: a meta-analysis. *Philos. Trans. R. Soc. B: Biol. Sci.* 373, 20170281. doi: 10.1098/rstb.2017.0281

Cohen, A. I. (2009). Contractarianism and interspecies welfare conflicts. *Soc. Philos. Policy* 26, 227–257. doi: 10.1017/S0265052509090104

Crump, A., Arnott, G., and Bethell, E. J. (2018). Affect-driven attention biases as animal welfare indicators: review and methods. *Animals* 8, 136. doi: 10.3390/ani8080136

Davies, A. C., Nicol, C. J., and Radford, A. N. (2015). Effect of reward downshift on the behaviour and physiology of chickens. *Anim. Behaviour* 105, 21–28. doi: 10.1016/j.anbehav.2015.04.005

Dawkins, M. S. (2021). *The science of animal welfare: Understanding what animals want* (Oxford, United Kingdom: Oxford University Press).

de Waal, F. B. M. (2008). Putting the altruism back into altruism: the evolution of empathy. *Annu. Rev. Psychol.* 59, 279–300. doi: 10.1146/annurev.psych.59.103006.093625

de Waal, F. B. M. (2019). Fish, mirrors, and a gradualist perspective on self-awareness. *PLoS Biol.* 17, e3000112. doi: 10.1371/journal.pbio.3000112

Dicke, U., and Roth, G. (2016). Neuronal factors determining high intelligence. *Philos. Trans. R. Soc. B: Biol. Sci.* 371, 20150180. doi: 10.1098/rstb.2015.0180

Dobromylyskij, P., Flecknell, P. A., Lascelles, B. D., Livingston, A., Taylor, P., and Waterman-Pearson, A. (2000). “Chapter 4 – pain assessment,” in *Pain management in animals* (Philadelphia, Pennsylvania, United States: W.B. Saunders), 53–79. doi: 10.1016/B978-0-7020-1767-4.50007-2

Dubin, A. E., and Patapoutian, A. (2010). Nociceptors: the sensors of the pain pathway. *J. Clin. Invest.* 120, 3760–3772. doi: 10.1172/JCI42843

Duncan, I. J. (2016). Is sentience only a nonessential component of animal welfare? *Anim. Sentience* 1, 6. doi: 10.51291/2377-7478.1023

Duncan, I. J. H., Slee, G. S., Seawright, E., and Breward, J. (1989). Behavioural consequences of partial beak amputation (beak trimming) in poultry. *Br. Poultry Sci.* 30, 479–488. doi: 10.1080/00071668908417172

Düppan, S., Krause, A., Moscovice, L. R., and Nawroth, C. (2020). Emotional contagion and its implications for animal welfare. *CABI Rev.* 15, 1–6. doi: 10.1079/PAVSNNR202015046

Düppan, S., Ramp, C., Kanitz, E., Tuchscherer, A., and Puppe, B. (2013). A design for studies on cognitive bias in the domestic pig. *J. Vet. Behavior* 8, 485–489. doi: 10.1016/j.jvbeh.2013.05.007

Elder, M., and Fischer, B. (2017). Focus on fish: a call to effective altruists. *Essays Philos.* 18, 107–129. doi: 10.7710/1526-0569.1567

FAO (2021) *Crops and livestock products* (Food and Agriculture Organization of the United Nations). Available at: www.fao.org/faostat/en/#data/QCL (Accessed August 10, 2022).

Farrar, B. G., Boeckle, M., and Clayton, N. S. (2020). Replications in comparative cognition: What should we expect and how can we improve? *Anim. Behav. Cogn.* 7, 1. doi: 10.26451/abc.07.01.02.020

FAWC (2009). Farm animal welfare in Great Britain: Past, present and future. *Farm Anim. Welf. Council*. Available at: https://www.gov.uk/government/uploads/system/uploads/attachment_data/file/319292/Farm_Animal_Welfare_in_Great_Britain_-_Past_Present_and_Future.pdf (Accessed August 15, 2022).

Fenwick, N., Griffin, G., and Gauthier, C. (2009). The welfare of animals used in science: How the “Three Rs” ethic guides improvements. *Can. Vet. J.* 50, 523.

Fischer, B. (2022) *The welfare range table: effective altruism forum*. Available at: <https://forum.effectivealtruism.org/posts/tNsg6o7cHFLc395/the-welfare-range-table> (Accessed November 16th, 2022).

Forstmeier, W., Wagenmakers, E.-J., and Parker, T. H. (2017). Detecting and avoiding likely false-positive findings—a practical guide. *Biol. Rev. Cambridge Philos. Soc.* 92, 1941–1968. doi: 10.1111/brv.12315

Franks, B., Ewell, C., and Jacquet, J. (2021). Animal welfare risks of global aquaculture. *Sci. Adv.* 7, eabg0677. doi: 10.1126/sciadv.abg0677

Fraser, D. (2008). Understanding animal welfare. *Acta Vet. Scandinavica* 50, 1–7. doi: 10.1186/1751-0147-50-S1-S1

Gaffney, L. P., and Lavery, J. M. (2022). Research before policy: identifying gaps in salmonid welfare research that require further study to inform evidence-based aquaculture guidelines in Canada. *Front. Vet. Sci.*, 1533. doi: 10.3389/fvets.2021.7685

Gaffney, L. P., Lavery, J. M., Schiestl, M., Trevathen, A., Schukraft, J., Miller, R., et al. (2022). A method for improving interspecies welfare comparisons. *Preprints* 8, 2022100012. doi: 10.20944/preprints202210.0012.v1

Gallup, G. G. Jr. (1970). Chimpanzees: Self-recognition. *Science* 167 (3914), 86–87. doi: 10.1126/science.167.3914.86

Gallup, Jr. G. G., and Anderson, J. R. (2020). Self-recognition in animals: Where do we stand 50 years later? lessons from cleaner wrasse and other species. *Psychol. Consciousness: Theory Res. Pract.* 7, 46. doi: 10.1037/cns0000206

Gibbons, M., Sarlak, S., and Chittka, L. (2022). Descending control of nociception in insects? *Proc. R. Soc. B* 289, 20220599. doi: 10.1098/rspb.2022.0599

Gordon, G. G. (1970). Chimpanzees: self-recognition. *Science* 167, 86–87. doi: 10.1126/science.167.3914.86

Hamilton, T. J., Myggland, A., Duperreault, E., May, Z., Gallup, J., Powell, R. A., et al. (2016). Episodic-like memory in zebrafish. *Anim. Cogn.* 19, 1071–1079. doi: 10.1007/s10071-016-1014-1

Hamilton, N., Sabroe, I., and Renshaw, S. A. (2018). A method for transplantation of human HSCs into zebrafish, to replace humanised murine transplantation models. *F1000Research* 7, 1–19. doi: 10.12688/f1000research.14507.2

Hammer, S. A., and Lee Blankenship, H. (2001). Cost comparison of marks, tags, and mark-with-tag combinations used in salmonid research. *North Am. J. Aquacult.* 63, 171–178. doi: 10.1577/1548-8454(2001)063<0171:CCOMTA>2.0.CO;2

Healey, M. L., and Grossman, M. (2018). Cognitive and affective perspective-taking: evidence for shared and dissociable anatomical substrates. *Front. Neurol.* 9, 491. doi: 10.3389/fneur.2018.00491

Held, S., Mendl, M., Devereux, C., and Byrne, R. W. (2000). Social tactics of pigs in a competitive foraging task: the ‘informed forager’ paradigm. *Anim. Behaviour* 59, 579–576. doi: 10.1006/anbe.1999.1322

Held, S., Mendl, M., Devereux, C., and Byrne, R. W. (2002a). Foraging pigs alter their behaviour in response to exploitation. *Anim. Behaviour* 64, 157–165. doi: 10.1006/anbe.2002.3044

Henderson, S. N., Barton, J. T., Wolfenden, A. D., Higgins, S. E., Higgins, J. P., Kuenzel, W. J., et al. (2009). Comparison of beak-trimming methods on early broiler breeder performance. *Poultry Sci.* 88, 57–60. doi: 10.3382/ps.2008-00104

Herculano-Houzel, S., Catania, K., Manger, P. R., and Kaas, J. H. (2015). Mammalian brains are made of these: a dataset of the numbers and densities of neuronal and nonneuronal cells in the brain of glires, primates, scandentia, eulipotyphlans, afrotherians and artiodactyls, and their relationship with body mass. *Brain Behav. Evol.* 86, 145–163. doi: 10.1159/000437413

Herrando, C., and Constantinides, E. (2021). Emotional contagion: A brief overview and future directions. *Front. Psychol.* 12. doi: 10.3389/fpsyg.2021.712606

Heyes, C. M. (1994). Reflections on self-recognition in primates. *Anim. Behav.* 47, 909–919. doi: 10.1006/anbe.1994.1123

Heyes, C. M. (1995). Self-recognition in primates: further reflections create a hall of mirrors. *Anim. Behav.* 50, 1533–1542. doi: 10.1016/0003-3472(95)80009-3

Hogg, M. A., Abrams, D., and Martin, G. N. (2010). “Social cognition and attitudes,” in *Psychology*. Eds. G. N. Martin, N. R. Carlson and W. Buskist (Harlow: Pearson Education Limited), 646–677.

Hu, L., and Iannetti, G. D. (2019). Neural indicators of perceptual variability of pain across species. *Proc. Natl. Acad. Sci.* 116, 1782–1791. doi: 10.1073/pnas.1812499116

Ioannidis, J. P. (2005). Why most published research findings are false. *PLoS Med.* 2, e124. doi: 10.1371/journal.pmed.0020124

Jiménez-Morales, N., Mendoza-Ángeles, K., Porras-Villalobos, M., Ibarra-Coronado, E., Roldán-Roldán, G., and Hernández-Falcón, J. (2018). Who is the boss? individual recognition memory and social hierarchy formation in crayfish. *Neurobiol. Learn. Memory* 147, 79–89. doi: 10.1016/j.nlm.2017.11.017

Keeling, L., Tunón, H., Olmos Antillón, G., Berg, C., Jones, M., Stuardo, L., et al. (2019). Animal welfare and the United Nations sustainable development goals. *Front. Vet. Sci.* 6. doi: 10.3389/fvets.2019.0033

Kohda, M., Hotta, T., Takeyama, T., Awata, S., Tanaka, H., Asai, J. Y., et al. (2019). If a fish can pass the mark test, what are the implications for consciousness and self-awareness testing in animals? *PLoS Biol.* 17, e3000021. doi: 10.1371/journal.pbio.3000021

Kohda, M., Sogawa, S., Jordan, A. L., Kubo, N., Awata, S., Satoh, S., et al. (2022). Further evidence for the capacity of mirror self-recognition in cleaner fish and the significance of ecologically relevant marks. *PLoS Biol.* 20, e3001529. doi: 10.1371/journal.pbio.3001529

Korte, S. M., Olivier, B., and Koolhaas, J. M. (2007). A new animal welfare concept based on allostasis. *Physiol. Behav.* 92, 422–428. doi: 10.1016/j.physbeh.2006.10.018

Kroese, D. P., Brereton, T., Taimre, T., and Botev, Z. I. (2014). Why the Monte Carlo method is so important today. *Wiley Interdiscip. Reviews: Comput. Stat.* 6, 386–392. doi: 10.1002/wics.1314

Kuenzel, W. J. (2007). Neurobiological basis of sensory perception: welfare implications of beak trimming. *Poultry Sci.* 86, 1273–1282. doi: 10.1093/ps/86.6.1273

Lindquist, K. A., Satpute, A. B., Wager, T. D., Weber, J., and Barrett, L. F. (2016). The brain basis of positive and negative affect: evidence from a meta-analysis of the human neuroimaging literature. *Cereb. Cortex* 26, 1910–1922. doi: 10.1093/cercor/bhv001

Linstone, H. A., and Turoff, M. (1975). “The delphi method,” in *Reading* (MA: Addison-Wesley), 3–12.

List, C. (2003). Are interpersonal comparisons of utility indeterminate? *Erkenntnis* 58, 229–260. doi: 10.1023/A:1022094826922

Lonsdale, M. B., Vondell, R. M., and Ringrose, R. C. (1957). Debeaking at one day of age and the feeding of pellets to broiler chickens. *Poultry Sci.* 36, 565–571. doi: 10.3382/ps.0360565

Lundmark, F., Berg, C., Schmid, O., Behdadi, D., and Röcklinsberg, H. (2014). Intentions and values in animal welfare legislation and standards. *J. Agric. Environ. Ethics* 27, 991–1017. doi: 10.1007/s10806-014-9512-0

MacLean, E. L., Hare, B., Nunn, C. L., Addessi, E., Amici, F., Anderson, R. C., et al. (2014). The evolution of self-control. *Proc. Natl. Acad. Sci.* 111, E2140–E2148. doi: 10.1073/pnas.1323533111

- Main, D. C. J., Kent, J. P., Wemelsfelder, F., Ofner, E., and Tuytens, F. A. M. (2003). Applications for methods of on-farm welfare assessment. *Anim. Welf.* 12, 523–528.
- Mason, G. J., and Lavery, J. M. (2022). What is it like to be a bass? red herrings, fish pain and the study of animal sentience. *Front. Vet. Sci.* 9. doi: 10.3389/fvets.2022.788289
- McCulloch, S. P. A. (2013). Critique of FAWC's five freedoms as a framework for the analysis of animal welfare. *J. Agri. Environ. Ethics* 26, 959–975. doi: 10.1007/s10806-012-9434-7
- Mendl, M., Burman, O. H. P., and Paul, E. S. (2010). An integrative and functional framework for the study of animal emotion and mood. *Proc. R. Soc. B.* 277, 2895–2904. doi: 10.1098/rspb.2010.0303
- Mendl, M., Neville, V., and Paul, E. S. (2022). Bridging the gap: Human emotions and animal emotions. *Affect. Sci.* 3 (4), 703–712. doi: 10.1007/s42761-022-00125-6
- Message, R., and Greenhough, B. (2019). “But it's just a fish”: understanding the challenges of applying the 3Rs in laboratory aquariums in the UK. *Animals* 9, 1075. doi: 10.3390/ani9121075
- Miller, R., Lambert, M., Frohnwieser, A., Brecht, K., Bugnyar, T., Crampton, I., et al. (2022a). Socio-ecological correlates of neophobia in corvids. *Curr. Biol.* 32 (1), 74–85. doi: 10.1016/j.cub.2021.10.045
- Miller, R., Schiestl, M., Trevarthen, A., Gaffney, L., Lavery, J. M., Fischer, B., et al. (2022b). From pigs to silkworms: Cognition and welfare across 10 farmed taxa. *bioRxiv* 11, 516141. doi: 10.1101/2022.11.11.516141
- Mlinarić, A., Horvat, M., and Šupak Smolčić, V. (2017). Dealing with the positive publication bias: Why you should really publish your negative results. *Biochem. med.* 27, 447–452. doi: 10.11613/BM.2017.030201
- Mogil, J. S. (2019). The translatability of pain across species. *Philos. Trans. R. Soc. B.* 374, 20190286. doi: 10.1098/rstb.2019.0286
- Nawroth, C., Ebersbach, M., and von Borell, E. (2013a). Are juvenile domestic pigs (*Sus scrofa domestica*) sensitive to the attentive states of humans? – the impact of impulsivity on choice behavior. *Behav. Processes* 96, 53–58. doi: 10.1016/j.beproc.2013.03.002
- Nawroth, C., Ebersbach, M., and von Borell, E. (2013b). Juvenile domestic pigs (*Sus scrofa domestica*) use human-given cues in an object choice task. *Anim. Cogn.* 17, 701–713. doi: 10.1007/s10071-013-0702-3
- Newberry, R. C. (1999). Exploratory behaviour of young domestic fowl. *Appl. Anim. Behav. sci.* 63, 311–321. doi: 10.1016/S0168-1591(99)00016-7
- Nicol, C. J., and Pope, S. J. (1994). Social learning in small flocks of laying hens. *Anim. Behaviour* 47, 1289–1296. doi: 10.1006/anbe.1994.1177
- Oostindjer, M., Bolhuis, J. E., Mendl, M., Held, S., van den Brand, H., and Kemp, B. (2011). Learning how to eat like a pig: effectiveness of mechanisms for vertical social learning in piglets. *Anim. Behav.* 82, 503–511. doi: 10.1016/j.anbehav.2011.05.031
- Pepperberg, I. M., Garcia, S. E., Jackson, E. C., and Marconi, S. (1995). Mirror use by African grey parrots (*Psittacus erithacus*). *J. Comp. Psychol.* 109, 182. doi: 10.1037/0735-7036.109.2.182
- Plotnik, J. M., De Waal, F. B., and Reiss, D. (2006). Self-recognition in an Asian elephant. *Proc. Natl. Acad. Sci.* 103, 17053–17057. doi: 10.1073/pnas.0608062103
- Prior, H., Schwarz, A., and Güntürkün, O. (2008). Mirror-induced behavior in the magpie (*Pica pica*): evidence of self-recognition. *PloS Biol.* 6, e202. doi: 10.1371/journal.pbio.0060202
- Raji, J. I., and Potter, C. J. (2021). The number of neurons in drosophila and mosquito brains. *PloS One* 16, e0250381. doi: 10.1371/journal.pone.0250381
- Reiss, D., and Marino, L. (2001). Mirror self-recognition in the bottlenose dolphin: A case of cognitive convergence. *Proc. Natl. Acad. Sci.* 98, 5937–5942. doi: 10.1073/pnas.101086398
- Rethink Priorities (2020) *Invertebrate sentience table*. Available at: <https://rethinkpriorities.org/invertebrate-sentience-table> (Accessed September 7, 2022).
- Robbins, J., Franks, B., and von Keyserlingk, M. A. (2018). ‘More than a feeling’: An empirical investigation of hedonistic accounts of animal welfare. *PloS One* 13, e0193864. doi: 10.1371/journal.pone.0193864
- Roques, J. A., Abbink, W., Geurds, F., van de Vis, H., and Flik, G. (2010). Tailfin clipping, a painful procedure: studies on Nile tilapia and common carp. *Physiol. Behav.* 101, 533–540. doi: 10.1016/j.physbeh.2010.08.001
- Russell, W. M. S., and Burch, R. L. (1959). The principles of humane experimental technique. *Methuen*.
- Sandoe, P., and Jensen, K. K. (2011). “The idea of animal welfare—developments and tensions,” in *Veterinary & animal ethics: Proceedings of the first international conference on veterinary and animal ethics* (Oxford, UK: Blackwell Publishing Ltd), 19–31.
- Schaeck, M., Van den Broeck, W., Hermans, K., and Decostere, A. (2013). Fish as research tools: alternatives to in vivo experiments. *Altern. to Lab. Anim.* 41, 219–229. doi: 10.1177/026119291304100305
- Schnell, A. K., and Clayton, N. S. (2019). Cephalopod cognition. *Curr. Biol.* 29, R726–R732. doi: 10.1016/j.cub.2019.06.049
- Schroeder, P. G., and Sneddon, L. U. (2017). Exploring the efficacy of immersion analgesics in zebrafish using an integrative approach. *Appl. Anim. Behav. Sci.* 187, 93–102. doi: 10.1016/j.applanim.2016.12.003
- Slooman, K. A., Bouyoucos, I. A., Brooks, E. J., and Sneddon, L. U. (2019). Ethical considerations in fish research. *J. Fish Biol.* 94, 556–577. doi: 10.1111/jfb.13946
- Smith, P. L., and Little, D. R. (2018). Small is beautiful: In defense of the small-n design. *Psychon. Bull. Rev.* 6, 2083–2101. doi: 10.3758/s13423-018-1451-8
- Smith, C. L., Taylor, A., and Evans, C. S. (2011). Tactical multimodal signaling in birds: facultative variation in signal modality reveals sensitivity to social costs. *Anim. Behav.* 82, 521–527. doi: 10.1016/j.anbehav.2011.06.002
- Stasiak, K. L., Maul, D., French, E., Hellyer, P. W., and Vandewoude, S. (2003). Species-specific assessment of pain in laboratory animals. *J. Am. Assoc. Lab. Anim. Sci.* 42, 13–20.
- Sutherland, M. A., Bryer, P. J., Krebs, N., and McGlone, J. J. (2008). Tail docking in pigs: acute physiological and behavioural responses. *Animal* 2, 292–297. doi: 10.1017/S1751731107001450
- Sutherland, M. A., Davis, B. L., and McGlone, J. J. (2011). The effect of local or general anesthesia on the physiology and behavior of tail docked pigs. *Animal* 5, 1237–1246. doi: 10.1017/S175173111100019X
- Thomson, J. S., Deakin, A. G., Cossins, A. R., Spencer, J. W., Young, I. S., and Sneddon, L. U. (2020). Acute and chronic stress prevents responses to pain in zebrafish: evidence for stress-induced analgesia. *J. Exp. Biol.* 223, jeb224527. doi: 10.1242/jeb.224527
- Towner, S. (2010). Concept of mind in non-human primates. *Biosci. Horizons* 3, 96–104. doi: 10.1093/biohorizons/hzq011
- Uglen, I., Kristiansen, T. S., Mejdell, C. M., Basic, D., and Mortensen, S. (2020). Evaluation of large-scale marking methods in farmed salmonids for tracing purposes: Impact on fish welfare. *Rev. Aquacult.* 12, 600–625. doi: 10.1111/raq.12342
- Vettese, T., Franks, B., and Jacquet, J. (2020). The great fish pain debate. *Issues Sci. Technol.* 36, 49–53.
- Von Bartheld, C. S., Bahney, J., and Herculano-Houzel, S. (2016). The search for true numbers of neurons and glial cells in the human brain: A review of 150 years of cell counting. *J. Comp. Neurol.* 524, 3865–3895. doi: 10.1002/cne.24040
- Webster, J. (1994). “Assessment of animal welfare: The five freedoms,” in *Animal welfare: A cool eye towards Eden* (Oxford, UK: Blackwell Science), 10–14.
- Weijers, D. (2011). *Hedonism. Internet encyclopedia of philosophy* (London, Ontario, Canada: The PhilPapers Foundation).
- Weiss, M. N., Franks, D. W., Croft, D. P., and Whitehead, H. (2019). Measuring the complexity of social associations using mixture models. *Behav. Ecol. Sociobiol.* 73, 8. doi: 10.1007/s00265-018-2603-6
- Wemelsfelder, F. (1985). “Animal boredom: is a scientific study of the subjective experiences of animals possible?,” in *Advances in animal welfare science* (Dordrecht: Springer), 115–154.
- Wong, K. (2016). Counting animals: On effective altruism and the prospect of interspecies commensurability [Doctoral dissertation, BA thesis, Princeton university, Princeton, NJ]. *Academia*. 1–67. Available at: <http://arks.princeton.edu/ark:/88435/dsp0144558g929> (Accessed August 20, 2022).
- Xu, L., Yang, X., Wu, L., Chen, X., Chen, L., and Tsai, F. S. (2019). Consumers' willingness to pay for food with information on animal welfare, lean meat essence detection, and traceability. *Int. J. Environ. Res. Public Health* 16, 3616. doi: 10.3390/ijerph16193616
- Yeates, J. W. (2011). Is ‘a life worth living’ a concept worth having? *Anim. Welf.* 20, 397–406. doi: 10.1017/S0962728600002955
- Yeates, J. W. (2012). “Brain-pain: Do animals with higher cognitive capacities feel more pain? insights for species selection in scientific experiments,” in *Large Animals as biomedical models: Ethical, societal, legal and biological aspects*. Eds. K. Hagen, A. Schnieke and F. Thiele (Europäische Akademie), 24–46.
- Zhu, Z., Tan, Y., Xiao, S., Guan, Z., Zhao, W., Dai, Z., et al. (2021). Solitary living brings a decreased weight and an increased ability to the domestic silkworm, *bombyx mori*. *Insects* 12, 809. doi: 10.3390/insects12090809



OPEN ACCESS

EDITED BY

Michael Paul Kim,
University of Texas MD Anderson Cancer
Center, United States

REVIEWED BY

Maria Concetta Scuto,
University of Catania, Italy
Colin Rae,
University of Glasgow, United Kingdom

*CORRESPONDENCE

Chen Yuanneng
✉ cyn60668@aliyun.com
Zhang Tao
✉ zhangtao41@aliyun.com

SPECIALTY SECTION

This article was submitted to
Molecular and Cellular Oncology,
a section of the journal
Frontiers in Oncology

RECEIVED 08 November 2022

ACCEPTED 04 January 2023

PUBLISHED 26 January 2023

CITATION

Shuoxin Y, Shuping W, Xinyue Z, Tao Z and
Yuanneng C (2023) Progress of research
on tumor organoids: A bibliometric analysis
of relevant publications from 2011 to 2021.
Front. Oncol. 13:1092870.
doi: 10.3389/fonc.2023.1092870

COPYRIGHT

© 2023 Shuoxin, Shuping, Xinyue, Tao and
Yuanneng. This is an open-access article
distributed under the terms of the [Creative
Commons Attribution License \(CC BY\)](#). The
use, distribution or reproduction in other
forums is permitted, provided the original
author(s) and the copyright owner(s) are
credited and that the original publication in
this journal is cited, in accordance with
accepted academic practice. No use,
distribution or reproduction is permitted
which does not comply with these terms.

Progress of research on tumor organoids: A bibliometric analysis of relevant publications from 2011 to 2021

Yin Shuoxin¹, Wang Shuping¹, Zhang Xinyue², Zhang Tao^{2*}
and Chen Yuanneng^{2*}

¹Graduate School of Guangxi University of Chinese Medicine, Nanning, Guangxi, China, ²Department of Gastroenterology, Ruikang Hospital Affiliated to Guangxi University of Chinese Medicine, Nanning, Guangxi, China

Background: Research on tumor organoids has developed rapidly over the past 20 years, but a systematic analysis of current research trends is lacking. Researchers in the field need relevant references and knowledge of current research hot spots. Bibliometric analysis and visualization is a systematic method of acquiring an in-depth understanding of the status of research on tumor organoids.

Methods: CiteSpace, VOSviewer and the Bibliometric Online Analysis Platform from the Web of Science Core Collection were used to analyze and predict publishing trends and research hot spots worldwide in the field of tumor organoids.

Results: A total of 3,666 publications on tumor organoids were retrieved, and 2,939 eligible articles were included in the final analysis. The number of publications has grown significantly, with the United States of America as the leading country for research on tumor organoids. Among journals, *Cancers* published the largest number of articles. Harvard Medical School published the highest number of articles among all institutions. The Chinese Academy of Sciences was ranked highest among all contributing institutions on the importance of their publications. A trend in multi-disciplinary collaboration was observed in studies on tumor organoids. Keywords indicated that the current research largely concentrated on optimizing the construction of organoid models to use for medication development and screening in the clinical setting, and to provide patients with individualized treatment for gastric cancer and colorectal cancer, which are newly emerging research hotspots. Gastric and colorectal cancers were the top two tumors that have received increasing attention and have become the focal points of recent studies.

Conclusion: This study analyzed 2,939 publications covering the topic of tumor organoids. Although optimizing the construction of organoid models has always been a hot topic in this field, the application of tumor organoids to the development of medications and screenings will foster individualized treatment for patients, which is another emerging hot spot in this field of research.

KEYWORDS

tumor organoids, bibliometric analysis, drug screening, precise medicine, antioxidant polyphenols, CiteSpace, VOSviewer

Introduction

The International Agency for Research on Cancer reported 19.3 million new cases of cancer and approximately 10 million deaths due to cancer worldwide in 2020. Approximately 28.4 million new cases of cancer are expected worldwide in 2040, which is an increase of 47%. Cancer has become a key problem endangering global public health (1). In recent years, the treatment of patients with cancer has evolved from interventions based on tumor types to those based on the tumor's molecular characteristics or microenvironment. This approach, known as precision medicine or individualized treatment, has saved many patients with advanced cancer. At present, commonly used tumor models, such as the 2D cell culture (2), genetically engineered mouse models (3) and the human-derived tumor xenograft models (4), although essential for tumor research, are difficult to simulate perfectly the actual state of tumors *in vivo*, resulting in the failures of many clinical trials. Organoids are derived from the stem cells of 3D cultures, which can reproduce the structural and functional characteristics of a native organ and simulate the development of diseases of human organs in culture dishes (5). Tumor organoids are *in vitro* models established by surgical resection or tissue biopsy to obtain tumor tissue in patients, followed by mincing and enzymatic hydrolysis of tumor tissue and the 3D culture of the tumor cells in it (6). Compared with traditional tumor models, tumor organoids not only reflect the genetic characteristics and tissue structure heterogeneity of a patient's tumor tissues, but they also maintain gene stability during self-renewal and throughout long-term expansion. Given these reasons, they can be used to study cancers caused by infection or gene mutation, and have unique advantages for clinical drug development and guiding individualized treatment (7).

Although the research on tumor organoids has developed rapidly in recent years, a scientific and systematic analysis of their status and trends is lacking. Therefore, we used the Web of Science Core Collection (WoSCC) as our data source to perform a quantitative analysis of the literature in the field of tumor organoid research, in order to understand and determine the research hot spots and frontiers, and to provide a relevant reference for scientific researchers in the field.

Materials and methods

Data sources and search strategies

All of the data in this study were derived from the WoSCC. The search terms were: Tumor or Neoplasm (TS) = ("Cancer" or "Tumor" or "Neoplasm" or "Neoplasia" or "Malignant Neoplasm" or "Malignancy" or "Malignant Neoplasms" or "Benign Neoplasms" or "carcinoma") AND ("Organoid" or "Organoids") AND Language = English. The search period was from January 1, 2011 to December 31, 2021 and the required language was English. A total of 3,666 articles were retrieved and 727 were excluded from the analysis because either they were not research reports or they were review articles. Thus, 2,939 articles were included in the final sample for the subsequent metrological analysis, as shown in Figure 1. All data in the text were

extracted on September 14, 2022 (the same day) to avoid deviations due to daily updates of the database.

Study procedures

The full records and cited references of the eligible publications were downloaded from the WoSCC database and saved in TXT format; then they were imported into the CiteSpace software V5.8.R3 SE, 64 bits. CiteSpace is visual analysis software based on the JAVA environment developed by Chen Chaomei. The software is designed to analyze information in the scientific literature. The user can detect the development of rules and the distribution of scientific knowledge in a field through visualization, and identify key points in the development of a field of study based on the existing data, especially turning points and key points in the field of knowledge (8). VOSviewer is visualization software developed by the Science and Technology Research Center in Leiden, the Netherlands. The user can also build a visual network map based on information in the scientific literature and acquire a comprehensive understanding of trends in the scientific structure and dynamic development of a field (9). The full records and cited references of these publications were downloaded from the WoSCC database, saved as a tab-delimited file and imported into the Bibliometrics Online Analysis Platform¹. We chose the "total literature analysis" option to examine trends in publications of different countries and the "partnership analysis" option to explore collaborations between countries and regions.

Study metrics

In this bibliometric analysis, the quantity and quality of the research results were evaluated using indicators, such as the number of articles published, the frequency of citations of the article and the impact factor, which reflect the level of research and academic status of a region, institution or author in a certain field. The number of papers published is an important indicator for evaluating the capacity for scientific research output. Frequency of citations in bibliometric analysis, refers to the number of times a published paper is cited in other articles, which reflect the value of the paper to a field and the degree of attention it has received. The H-index refers to rankings of articles published using relevant statistical measures, based on an articles' frequency of citations (from high to low). Articles with the lowest H-index have the least amount of citations, which we used as a measure to assess the number of scientific research outputs and the quality of the research in this bibliometric analysis. The journal's impact factor and other metrics were retrieved from the 2021 edition of Journal Citation Reports. These are important indicators of the academic level and quality of the journals and the articles.

Results

Changing trend in the quantity of articles published

To clarify the rate of the development of research on tumor organoids, global trends in the volume of published research articles

Abbreviations: Web of Science Core Collection, WoSCC; United States of America, USA.

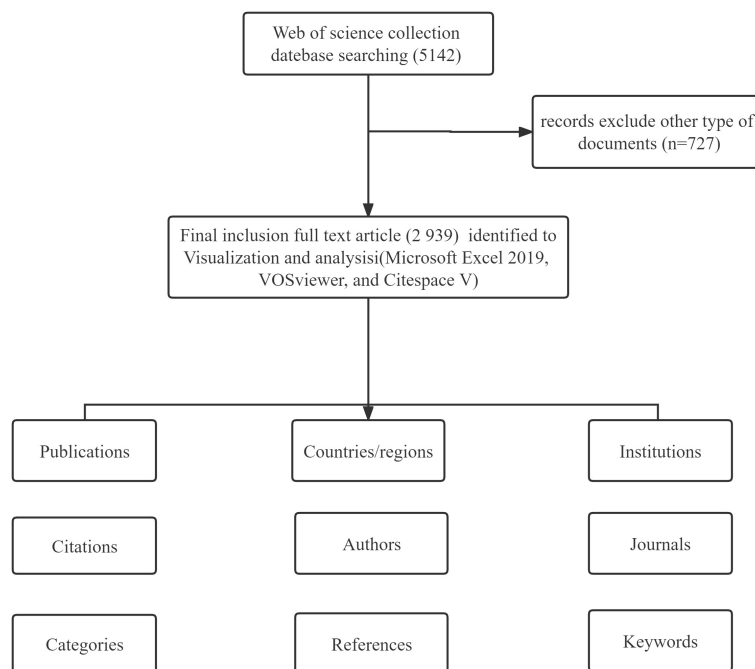


FIGURE 1
Flowchart of the research literature selection.

from 2011 to 2021 were plotted, as shown in Figure 2. Only 129 articles were published worldwide from 2011 to 2014. With the global shift to a rapid growth of research on tumor organoids before and after 2017, as of 2021, 912 studies have been published worldwide, accounting for 31.03% of the total number of articles published from 2011 to 2021, indicating that research on tumor organoids has become a focus of global enquiry. Given the upward trend line in Figure 2, the global number of publications in 2022 is expected to be significantly higher than the number of articles published last year.

Cooperation between research publishing countries and institutions

Between 2011 and 2021, there were 72 countries worldwide that published research on tumor organoids, as shown in Figure 3. Indicators of the top ten countries with the highest number of articles are shown in Table 1. The highest and most significant number of articles were published in the United States of America (USA) (1,320, 44.91%) and China (447, 15.21%), followed by

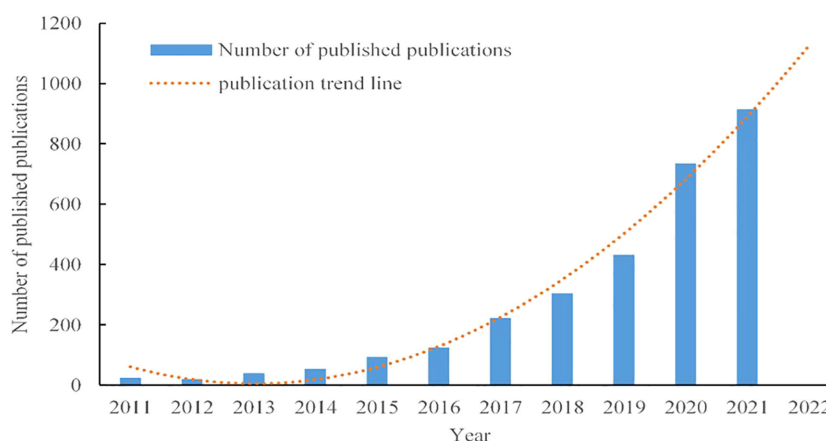
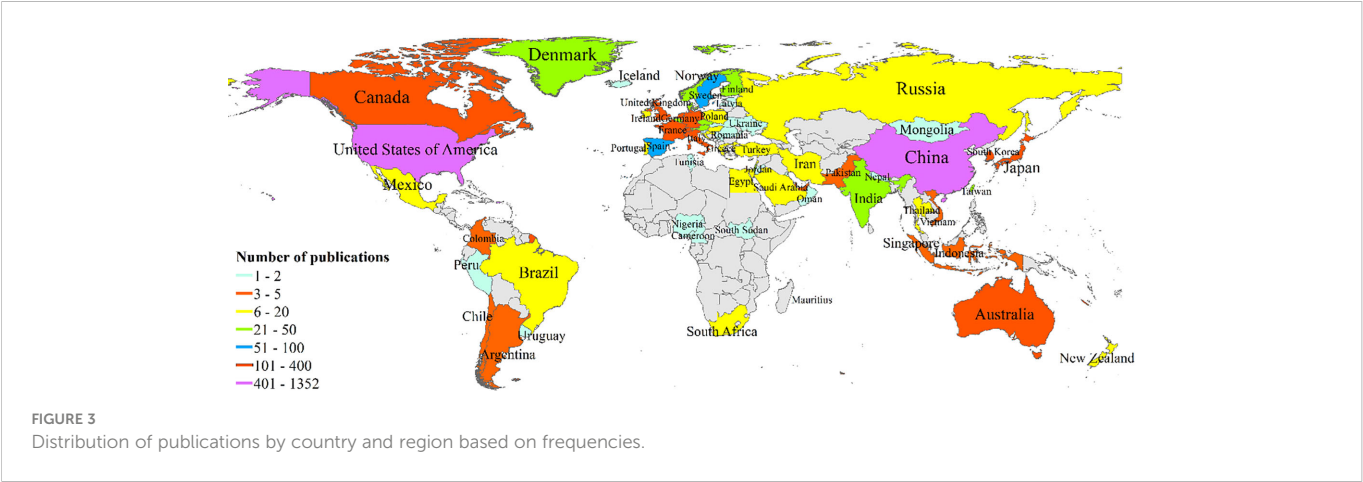


FIGURE 2
Upward trends in the volume of published research on tumor organoids from 2011 to 2021.



Germany (329, 11.19%), Japan (297, 10.10%) and the Netherlands (289, 9.83%). The H-indices of the USA, the Netherlands and Germany were 93, 67 and 48, respectively, ranking them among the top three countries with the highest H-indices. Articles from the USA, the Netherlands and England with 44,814, 25,368 and 10,089 citations, respectively, were ranked among the top three countries with the highest total number of citations, and articles from the Netherlands, England and Switzerland, with an average of 87.78, 42.93 and 36.17 citations per paper respectively, were ranked among the top three countries for the highest average number of citations per article.

All relevant information was exported from the WoSCC database and saved as a tab-delimited file. International cooperation between the countries publishing relevant research was analyzed using the Bibliometric Online Analysis Platform¹, as shown in Figure 4A, with the USA having the highest frequency of international cooperation, followed by Germany and the Netherlands. China had close cooperative relationships with the USA, the Netherlands and Singapore. The mediation centrality of the publishing countries was analyzed using CiteSpace software, as shown in Figure 4B. Mediation centrality refers to the ratio of the shortest path passing through a certain point and connecting these two points in the network to the

total number of shortest path lines between these two points, which is an indicator used to characterize the importance of the node. The numerical value indicates that the node is in a key position in the network and has influence. The information in Figure 4B was exported to report the rankings of centrality of the top five nations' publications in Table 2. The USA (0.38), Germany (0.21), the England (0.21), France (0.19) and Italy (0.19) exhibited high degrees of centrality, which is represented by purple in Figure 4B. The above results indicate that these countries play an important role in tumor organoid research, and the academic influence of their research results influence countries worldwide. The reliability, quality and innovation of the relevant research from these countries are far ahead of other countries.

Academic cooperation between institutions is crucial for strengthening exchanges between scholars and for disseminating advanced experiences. CiteSpace software was used in this study to conduct network co-occurrence analysis of the publishing institution, as shown in Figure 5. The information in Figure 5 was exported to report the rankings of centrality and the number of publications among the top five institutions in Table 3. Harvard Medical School (111), the University Medical Center of Utrecht (102), Memorial Sloan Kettering Cancer Center (88), Johns Hopkins University (61)

TABLE 1 Publication metrics of articles on tumor organoids of the top ten countries by number of publications.

Rank	Country	Number of publications	Total frequency of citations	Average number of citations per paper	H-index
1	USA	1 320	44 814	33.95	94
2	China	477	7 525	15.78	43
3	Germany	329	8 314	25.27	48
4	Japan	297	9794	32.98	43
5	Netherlands	289	25 368	87.78	67
6	England	235	10 089	42.93	45
7	Italy	164	4 619	28.16	28
8	Canada	141	4 071	28.87	31
9	France	121	2 243	18.54	22
10	Switzerland	115	4 160	36.17	25

USA, United States of America.

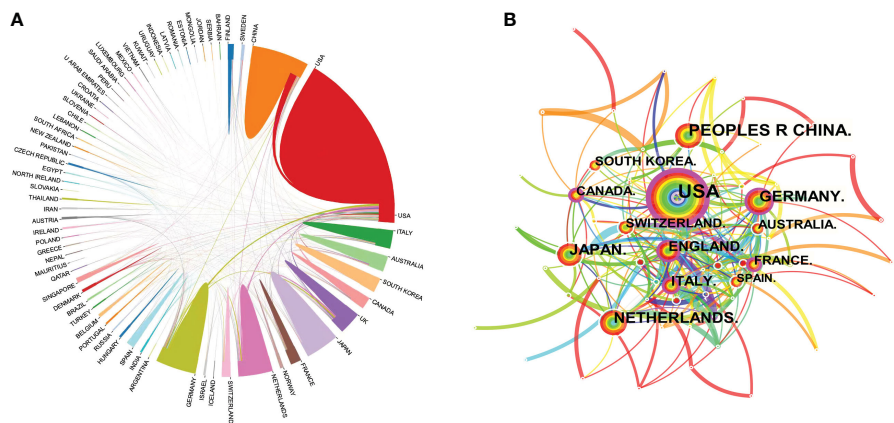


FIGURE 4 Map of the co-occurrence of tumor organoid research by nation. Figure 4 (A) illustrates the international cooperation among countries. These countries are represented by different colors; the links represent international cooperation and links between countries represent connections between countries. Figure 4 (B) shows the centrality of the articles. Each node represents a country, and the node size represents the number of articles published by the country. The larger the node, the more articles that were published. The purple color in the outermost ring represents a central node or the central location of the cooperation between the institution and other institutions.

and Vanderbilt University (54) were the top five research institutions in terms of their numbers of published articles. The Chinese Academy of Sciences (0.32), Dana Farber Cancer Institute (0.30), the University of Nebraska Medical Center (0.24), Columbia University (0.23) and Memorial Sloan Kettering Cancer Center (0.22) were the top five research institutions in terms of intermediary centrality. These institutions occupy core positions in the field of tumor organoid research and engage in cooperative academic research with most institutions.

Authors of publications and their cooperative relationships

A total of 20,139 scholars published articles in the field of tumor organoid research worldwide. The indicators of the top ten scholars as shown in Table 4. Four articles were published by the top ten scholars; five scholars were from the USA and three were from the Netherlands, Japan and England. Clevers H (103) at the University Medical Center of Utrecht, Sato T (34) at the Keio University School of Medicine and Chen Y (32) at Memorial Sloan Kettering Cancer Center were identified as the top three authors with the highest number of published articles. Clevers H also ranked first in the total number of citations received, the average frequency of citations per paper and

the H-index. These authors have influenced tumor organoid research worldwide.

Based on the cooperative network analysis of the authors with high numbers of published articles using the VOSviewer, we further defined “core authors” as those who had at least 5 publications, which included 316 authors in the analysis. We found some collaborative research teams had a high publication volume, as shown in Figure 6. Clevers H, Sato T, Drost J, Chen Y, Sansom OJ, Braker N and Van Der collaborated closely, but most of the inter-author collaborations were limited to intra-team collaborations, with little international collaboration, such as several small cooperative networks in the periphery (e.g., Hippo Y, Onuma K and Inoue M., and Jun P, Meyer TF and Bartfeld S). If cooperative research between authors can be strengthened, especially between authors from different countries or institutions, exchanges and innovations will likely improve significantly.

Journal publications of tumor organoid research

Journals play a crucial role in promoting international cooperation and progress in the level of scientific research. Between 2011 and 2021, 752 journals worldwide published academic papers on

TABLE 2 Centrality rankings of the top five nations’ publications in the field of tumor organoids.

Country	Year	Centrality	Number of publications
USA	2011	0.33	1 320
Germany	2013	0.15	329
England	2011	0.13	235
France	2011	0.12	121
Italy	2012	0.11	164

USA, United States of America.

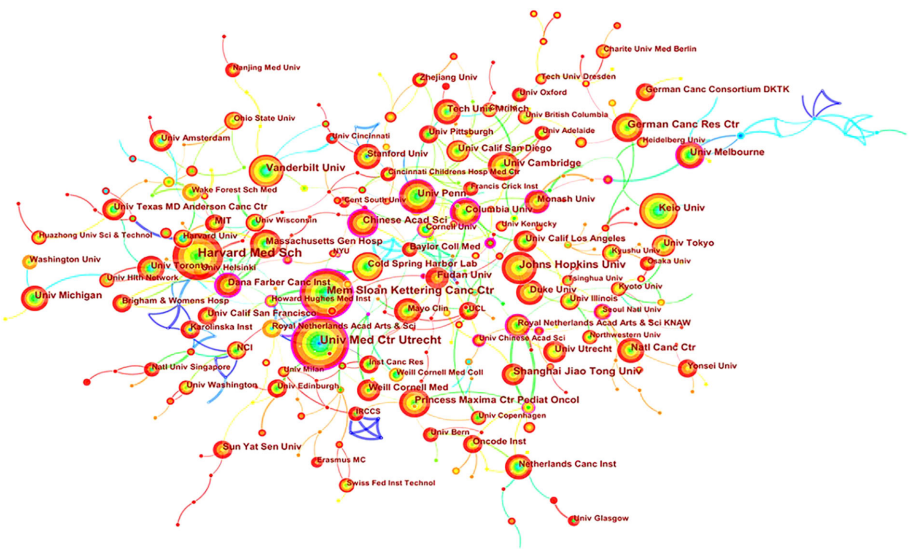


FIGURE 5
Map of cooperation in tumor organoid research. The nodes in Figure 5 represent different institutions, and the size of the nodes represents the number of articles published. The purple ring in the outermost circle indicates a central node, which has a central position in the cooperation between this institution and other institutions. The wired lines indicate cooperation among institutions.

tumor organoid research, of which the top ten journals published 5 papers on the topic as shown in Table 5. *Cancers* published the most research results, with 130 articles, accounting for 4.42% of the total publication volume, followed by *Scientific Reports* and *Nature Communications*, which published 85 and 74 articles, respectively, accounting for 2.89% and 2.51% of the total volume of publications. *Gastroenterology* ranked first in both citation frequency and the H-index. Among the top ten journals, eight journals belonged to partition Q1, 2 belonged to partition Q2 and 1 to partition Q3, with an impact factor ranging from 1.696 to 23.937, and *Gastroenterology* having the highest impact factor. The analysis shows that these international journals were the academic authorities on the findings of tumor organoid research, which were most likely to be of concern to scholars in various countries.

Research directions

The 2,939 articles in this study were classified into 95 research directions. It should be noted that the sum of the percentages of all the studies' directions exceeded 100% because the same article could be classified into multiple research directions. Changing trends in research directions in recent years is shown in Figure 7. The most

articles published were in the direction of Oncology with a total of 802, accounting for 27.25% of the total number of articles published. These were followed by Cell Biology and Multidisciplinary Sciences, with 599 and 362 articles, respectively, followed by Biochemistry Molecular Biology and Gastroenterology Hepatology. Experimental Medicine Research, Genetics Heredity, Pathology, Cell Tissue Engineering and Pharmacology Pharmacy, with more than 100 articles. Thus, this study of tumor organoids showed the developing characteristics of multidisciplinary intersection. Given the changes in the number of articles published in each research direction over time, the top five research directions of the articles indicated an increasing trend in fluctuations before 2016. All research directions reached a state of rapid growth after 2016, with Oncology developing most rapidly.

Frequently cited papers

The total frequencies of citations of the top ten articles were derived from the citation reports of the WoSCC. These articles were cited more than 600 times, of which 9 were from the team led by Clevers H (Table 6). In 2011, the Clevers H team successfully constructed a small intestinal crypt-villus structure *in vitro* without

TABLE 3 Centrality rankings and number of publications of the top five institutions in the field of tumor organoid research.

Rank	Institution	Number of publications	Rank	Institution	Centrality
1	Harvard Medical School	111	1	Chinese Academy of Sciences	0.32
2	University Medical Center Utrecht	102	2	Dana Farber Cancer Institute	0.3
3	Memorial Sloan Kettering Cancer Center	88	3	University of Nebraska Medical Center	0.24
4	Johns Hopkins University	61	4	Columbia University	0.23
5	Vanderbilt University	54	5	Memorial Sloan Kettering Cancer Center	0.22

TABLE 4 Productivity, citations and H-indices of the top ten authors of tumor organoid research.

Author	Country	Number of publications	Total citations	Average number of citations per paper	H-index
Clevers H	Netherlands	103	20 939	201.34	59
Sato T	Japan	34	6 615	194.56	18
Chen Y	USA	32	2 806	87.69	19
Cuppen E	Netherlands	22	4 425	201.14	17
Van Boxtel R	Netherlands	20	4 009	200.45	15
Ewald AJ	USA	19	752	39.58	10
Tuveson DA	USA	19	3 276	172.42	17
Skardal A	USA	18	899	49.94	14
Sansom OJ	England	18	1 008	56.00	9
Sawyers CL	USA	14	2 000	117.65	14

USA, United States of America.

mesenchymal conditions from a single LGR5 stem cell (10). The team then added different growth factors or inhibitors to different organoids, based on previous studies, so that the replication potential of the adult stem cells was not limited *in vitro*. This improvement promoted the use of organoid models as a tool for investigating diseases with increasing complexity (11–13). The team also constructed a variety of tumor organoid models, such as models of colorectal, prostate and pancreatic cancers (14–19). These constructed models had a better fit with real tumor growth and development, and the organoid tumor models that were constructed using the patient’s own tumor cells facilitated a more individualized approach to the treatment of tumors. These studies have opened up a

new path for acquiring a more in-depth understanding of the mechanism of tumorigenesis and development, and clinical drug development and screening.

Analysis of keywords

Table 7 shows the top twenty most frequently occurring keywords analyzed by CiteSpace. Nodes were set as keywords with a time interval of 2011–2021 and yearly time slices. We found that “stem cells,” “cancer,” “*in vitro*,” “colorectal cancer,” “model,” “culture,” “differentiation” and “growth” were the most frequently occurring

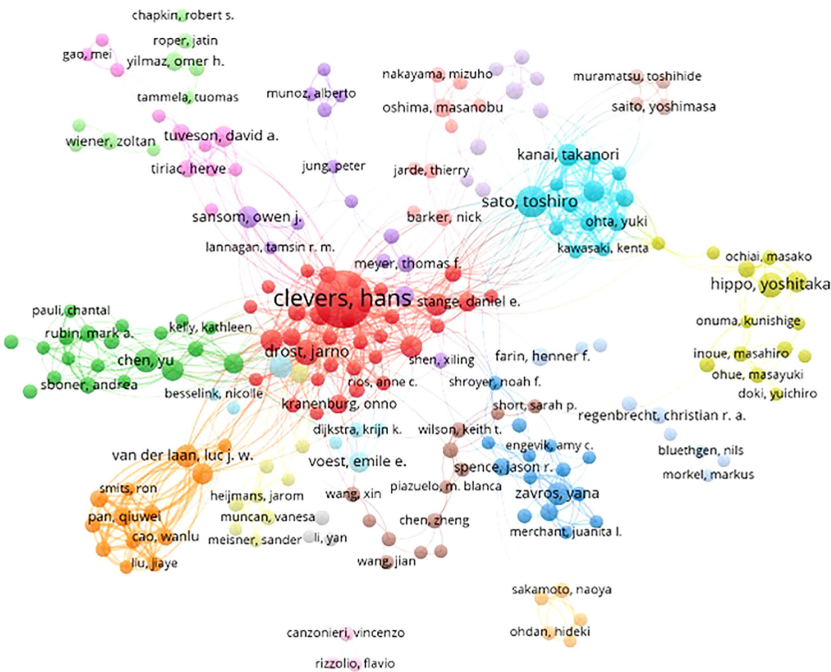


FIGURE 6 Collaborative networks among authors with a high publication volume of tumor organoid research.

TABLE 5 The top ten journals that published papers on tumor organoid research.

Rank	Journal	Count	Average number of citations per paper	H-index	Impact factors	Zone
1	<i>Cancers</i>	130	6.55	16	6.999	Q1
2	<i>Scientific Reports</i>	85	17.21	19	5.134	Q1
3	<i>Nature Communications</i>	74	30.57	26	15.805	Q1
4	<i>Gastroenterology</i>	54	81.30	27	23.937	Q1
5	<i>Cancer Research</i>	50	28.14	19	12.843	Q1
6	<i>Oncogene</i>	48	17.71	18	8.858	Q1
7	<i>Cell Reports</i>	44	35.70	24	10.394	Q1
8	<i>Frontiers in Cell and Developmental Biology</i>	44	4.89	9	7.219	Q1
9	<i>Cells</i>	43	14.00	14	6.663	Q2
10	<i>Jove Journal of Visualized Experiments</i>	40	7.83	8	1.696	Q3

keywords, and “3D culture,” “tumor model,” “beta catenin,” “inflammatory bowel disease,” “small intestine,” “P53” and “cancer metabolism” were the most central keywords.

A K-means cluster analysis of the keywords was performed using CiteSpace, and 19 clusters were obtained (Table 8; Supplementary Figure 1). The keyword co-occurrence network in the field of research on tumor organoids is shown in Supplementary Figure 1. The main research directions were divided into the following categories: #0 (cell), #1 (stem cell), #2 (generation), #3 (expression), #4 (cerebral organoid), #5 (extracellular matrix), #8 (*in vitro*), #9 (landscape), #13 (*in vitro*) and #14 (culture) the culture and characteristics of the tumor organoid models. Categories: #6 (gastric cancer), #7 (rectal cancer), #10 (inflammatory bowel disease), #12 (colorectal cancer) and #17 (cancer) were classified as diseases currently used in tumor organoids, and categories #11 (precision medicine), #15 (personalized medicine), #16 (progression) and #18 (photo thermal medicine) were classified as current research and trends in tumor organoids. These 19 clusters summarize the process of development of tumor organoid research, and highlight research hot spots.

Discussion

Applications and advantages of tumor organoids

Although the 3D culture was proposed more than 100 years ago, it was not until 2009 that the first organoid model of a single stem cell source was established, and Clevers' laboratory demonstrated that a single LGR5 stem cell could successfully construct small intestinal crypt-villous structures *in vitro* in the absence of interstitial space (20, 21). In recent years, the application of 3D culture models in cancer research has developed rapidly, and studies of almost every tumor have solved a wide variety of research problems. In contrast to the widely used 2D cell culture and animal models, organoids are an important preclinical model for cancer research with distinct advantages. The 2D cell culture is simpler, cheaper and allows more direct genetic manipulation than the 3D culture models permits; however many cell lines cannot mimic the real situation of tumors accurately due to the lack of spatial organization and the tumor's micro-environment. Increasing the dimension of the

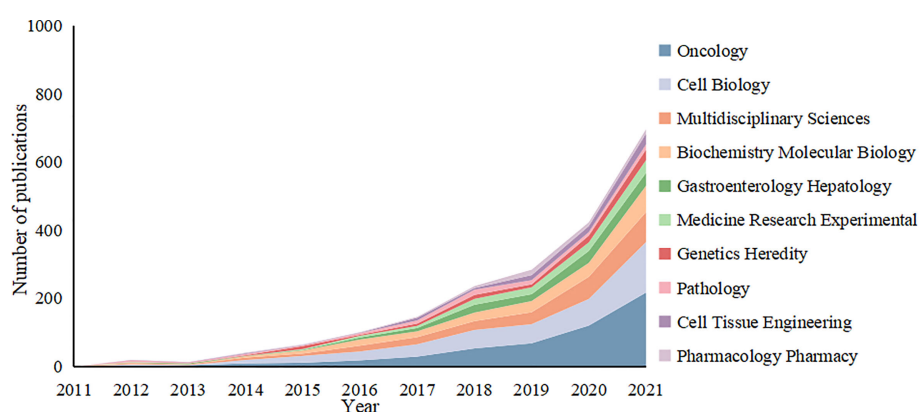


FIGURE 7
Variation curve of the number of published papers by main research direction of the tumor organoid research.

TABLE 6 The total number of citations of the top ten journal articles related to tumor organoids.

No.	Journal articles	Citation	Year
1	Long-term Expansion of Epithelial Organoids From Human Colon, Adenoma, Adenocarcinoma, and Barrett's Epithelium	1740	2011
2	Paneth cells constitute the niche for Lgr5 stem cells in intestinal crypts	1520	2011
3	Modeling Development and Disease with Organoids	1116	2016
4	Prospective Derivation of a Living Organoid Biobank of Colorectal Cancer Patients	1093	2015
5	Organoid Models of Human and Mouse Ductal Pancreatic Cancer	971	2015
6	Distinct populations of inflammatory fibroblasts and myofibroblasts in pancreatic cancer	793	2017
7	Organoid Cultures Derived from Patients with Advanced Prostate Cancer	768	2014
8	Growing Self-Organizing Mini-Guts from a Single Intestinal Stem Cell: Mechanism and Applications	670	2013
9	Patient-derived organoids model treatment response of metastatic gastrointestinal cancers	630	2018
10	Single-cell messenger RNA sequencing reveals rare intestinal cell types	625	2015

extracellular matrix from 2D to 3D significantly improved cell proliferation, differentiation and survival, and the success rate of patient-derived tumor organoid cultures (22, 23). The patient-derived xenograft model is similar to the original tumor in terms of its histological expression and biological behavior, such as protein expression, tumor biomarker status and genetic status, which cannot be achieved by tumor organoid models (24). However, patient-derived xenograft model transplantation is difficult to perform (25) and time consuming (26), and its cost is relatively high. In addition, genetically engineered mouse models can be used to assess *in vivo* phenotypes and incorporate the complexity of the syngeneic tumor microenvironment. However, the complexities of time, cost and genetic manipulation are significant drawbacks of these models, compared to those of the organoid models (24). The advantages and disadvantages of the organoid model compared with other models are summarized in [Supplementary Figure 2](#).

Drug development and screening

Non-clinical testing was used to determine the potential risk of drugs and their efficacy in humans. However, the most commonly

used 2D *in vitro* cell culture system lacked heterogeneity and could not accurately describe or mimic the rich environment *in vivo* and the complex process of disease formation. Significant flaws were also found in animal studies, with species differences causing most drugs to exhibit different drug sensitivities in different *in vitro* models (27). The 3D cell culture models have been developed to reflect drug sensitivity in humans more accurately. Compared to the 2D cell culture systems, the 3D cell culture models can replicate the complex micro-ecological environment of human organs can be used for drug safety assessments and combination studies and they can provide key pharmacokinetic and biomarker data (28–30). The intestinal epithelium is an important site for drug absorption and metabolism and plays an important role in the oral bioavailability of drugs. In particular, intestinal epithelial cells serve as gatekeepers for drug and nutrient absorption (31). The data from cell and animal models related to intestinal nutrient absorption, metabolism and oral bioavailability of drugs have poor accuracy due to tumor heterogeneity and species differences. In contrast, intestinal organoids are used to examine different aspects of bioavailability, including drug distribution, individual differences, and high-throughput screening (32). Furthermore, the establishment of

TABLE 7 The top twenty most frequently occurring keywords and their centrality in research related to tumor organoids.

No.	Keywords	Count	Centrality	No.	Keywords	Centrality	Count
1	stem cell	604	0.00	1	3d culture	0.17	69
2	Cancer	570	0.03	2	tumor model	0.17	10
3	Expression	507	0.01	3	beta catenin	0.16	72
4	<i>in vitro</i>	469	0.11	4	inflammatory bowel disease	0.12	44
5	colorectal cancer	333	0.01	5	adult stem cell	0.12	9
6	Model	292	0.03	6	<i>in vitro</i>	0.11	469
7	Cell	284	0.07	7	<i>in vivo</i>	0.11	59
8	differentiation	249	0.01	8	small intestine	0.11	44
9	Growth	196	0.05	9	p53	0.11	37
10	Culture	191	0.05	10	cancer metabolism	0.11	3

P53, Tumor suppressor protein.

TABLE 8 Keyword clusters from the analysis of tumor organoids.

Cluster ID	Count	Silhouette	Year	Cluster name
#0	42	0.973	2015	Cell
#1	40	0.884	2015	Stem cell
#2	39	0.882	2016	Generation
#3	39	0.882	2014	Expression
#4	36	0.848	2019	Cerebral organoid
#5	35	0.886	2017	Extracellular matrix
#6	34	0.901	2017	Gastric cancer
#7	33	0.869	2018	Rectal cancer
#8	32	0.946	2015	<i>In vitro</i> expansion
#9	31	0.938	2019	Landscape
#10	30	0.82	2017	Inflammatory bowel disease
#11	29	0.834	2018	Precision medicine
#12	27	0.908	2018	Colorectal cancer
#13	27	0.955	2016	<i>In vitro</i>
#14	25	0.924	2015	Culture
#15	22	0.879	2015	Personalized medicine
#16	21	0.873	2013	Progression
#17	21	0.942	2015	Cancer
#18	7	0.961	2018	Photothermal therapy

organoid models for the liver, kidney and blood-brain barrier meet the basic requirements for evaluating the different pharmacological aspects of drugs (33). In addition to efficacy, drug metabolism and toxicological mechanisms are also important to assess. Simplified culture models of primary human hepatocytes or liver cell lines that are currently used differ considerably from *in vivo* physiology in terms of drug toxicity, often resulting in failed drug conversion (34). Therefore, the determination of toxicological properties relies mainly on animals. However, due to species differences between humans and animals, the results might not be consistent with the real situation (35). At present, a reproducible human liver organoid model can detect bile acid uptake and excretion in modified human liver organoids in real time by knocking out bile acid transporter genes. The assay platform can be used for large-scale compound screening and has been shown to be genotype-specific sensitive to bosentan-induced cholestasis. This powerful assay will facilitate diagnoses, functional studies, drug development and individualized therapies (36).

Individualized treatment

Traditional cancer treatments (chemotherapy and radiation therapy) are ineffective or have a positive effect in only a subset of patients due to the heterogeneity of malignancies. To ensure the effectiveness of the treatment, it is necessary to consider the patient's personal characteristics (37). Precision medicine has been propelled forward by current large-scale tumor sequencing efforts and

numerous therapeutic targets that have been identified as a result. Despite the reports of many successful cases based on DNA sequencing, the need for effective treatment remains significant for the majority of patients with cancer (38). However, genetic changes in a small percentage of coding regions do not adequately describe the complexities of cancer progression. Although DNA sequencing provides information about cancer drivers that are relatively well-preserved during cancer progression, it does not include the effects of other regulatory factors, such as epigenetic changes or non-coding regions, which are more dynamic and their relevance is more difficult to understand (39, 40). Therefore, a dynamic and versatile model system is needed to analyze tumor biology from multiple dimensions accurately and to reflect the behavior of the original tumor in the patient. The ability of tumor organoids to retain the original tumor characteristics makes them unique in studies at the individual level of patients with cancer, and they have been proposed as a model for precision medicine. For example, a study established a bank of living tumor samples from patients with advanced rectal cancer who received adjuvant chemo-radiotherapy. The combined clinical trial data confirmed that the chemo-radiotherapy response of the patients was a very close match with the organoid response of the rectal cancer, with an accuracy of 84.43%, a sensitivity of 78.01% and a specificity of 91.97% (41). Organoids have also successfully predicted the sensitivity of colorectal cancer (42), gastric cancer (43), ovarian cancer (44) and prostate cancer (45) to drugs. It appears at the present time that extracting samples from patient tumor tissues, creating and culturing organoids, exposing patient-derived tumor organoids to various drugs to find the best drug or drug combination to treat

patients, revealing potential weaknesses of individual treatments based on gene mutation profiles and treatment responses of organoids and determining the next treatment route when first-line treatment is ineffective will become the ultimate mode of treatment for cancer (46, 47)¹.

According to the latest literature and further analysis of keywords, the chemopreventive and therapeutic effects of antioxidant polyphenols on tumors were found to have received increasing attention from the scientific community in recent years. In an examination of antioxidant polyphenols, the complex technology of organoids as a new anti-cancer strategy has displayed unique advantages. Polyphenols that largely exist in plants serve as reactive oxygen species scavengers with prominent antioxidant activity, which exert the inhibitory effects on inflammation by manipulating the inflammation-related signaling pathways and suppressing the release of inflammatory mediators (48, 49). Not only contributing to treating non-neoplastic diseases, such as natural inducers from saffron targeting Nrf2/vitagen pathway to suppress oxidative stress and neuroinflammation and consequently inhibiting cognitive dysfunction (50), polyphenols could also play their roles in preventing and treating tumors by regulating cell apoptosis, autophagy, cell-cycle progression, inflammation, invasion, and metastasis through the activation of tumor suppressor genes and the inhibition of oncogenes (51, 52). Professor Scuto M's team demonstrated that, polyphenols with low concentrations could suppress oxidative stress and inflammation, and induced the apoptotic of brain cancer cells by activating Nrf2/vitagen pathway (53), in addition, the supplementation of dietary polyphenols and vitamin D can also manipulate oxidative stress, inflammation and autophagy dysfunction in tumor cells through Nrf2/vitagen pathway, the low concentrated polyphenols and vitamin D could serve as cytotoxic agents of pro-oxidants, in the form of molecular activation through reactive oxygen species production and several survival pathways (e. g., glutathione) to induce apoptosis and cell-cycle arrest in tumor cells, for the chemoprevention and treatment of tumors in the presence of metal ions. Furthermore, the study has fully investigated a range of potential interventions in tumor organoid models depending on plant polyphenols and vitamin D, which is required to be introduced into clinical practice combined to powerful and novel technique through future interventions incorporating redox mesums of oxidative stress (54). The establishment of tumor model aims to approach 100% simulate the practical condition of the true tumor in the patient, so as to contribute to preclinical research and clinical application. Patient-derived organoids as a stable biology could facilitate gene operation, which is suitable for high-throughput sequencing analysis, and can reproduce the development from native tissue to the whole process of tumor occurrence (55). Currently some studies have taken tumor organoids as a model to explore the effect of polyphenols in tumor treatment, the results indicated that the low-dose polyphenols combined with chemotherapeutic drugs could not only optimize the efficacy, but also alleviate cytotoxicity and prevent the drug resistance (56). Another study with patient-derived organoids model revealed that the oligomeric proanthocyanidins combined to the curcumin

attenuated the expression of cyclin D1, PCNA, and HSPA 5, which could serve as a method that preferentially targets cancer cells without affecting normal cells (57). The latest development of organoid models provides an excellent preclinical platform for the research of tumors, as well as makes the personalization of tumor therapy, evaluation of drug efficacy easier, contributing to the more in-depth exploration the mechanisms of cancer.

In summary, organoids mimic the structural and functional properties of native tumors, and compared to traditional tumor models, tumor organoids maintain gene stability while self-renewing and expanding over the long-term, and reflecting the genetic characteristics and tissue structure heterogeneity of the patients' tumor tissues. In recent years, the study of tumor organoids has steadily increased, and effective organoid cultures have made it possible to screen individualized drugs within the time line of clinical treatment and apply them to translational medicine and individualized treatment. The use of organoids as precise and high-throughput preclinical tools for precision medicine is an unavoidable future trend. CiteSpace and VOSview software were used in this paper to analyze the bibliometrics and visualize the data derived from tumor organoid research.

Data availability statement

The original contributions presented in the study are included in the article/supplementary material. Further inquiries can be directed to the corresponding authors.

Author contributions

YS is responsible for conception design, article writing and proofreading. WS and ZX are responsible for literature collection, analysis and summary. CY and ZT are responsible for project guidance. All authors contributed to the article and approved the submitted version.

Funding

This work was supported by the National Natural Science Foundation of China (grant number 81360531), the Natural Science Foundation of Guangxi Zhuang Autonomous Region, China (grant number 2020GXNSFAA238030), the Innovation Project of Guangxi Graduate Education of Guangxi University of Chinese Medicine, China (grant number YCSZ2022018), and the Top Talents Program of Guangxi University of Chinese Medicine, China (grant number: 2022C001).

Acknowledgments

All claims expressed in this article are solely those of the authors and do not necessarily represent those of their affiliated organizations, or those of the publisher, the editors and the reviewers. Any product that may be evaluated in this article, or claim that made by its manufacturer, is not guaranteed or endorsed by the publisher.

¹ <https://bibliometric.com>

Conflict of interest

The authors declare that the research was conducted in the absence of any commercial or financial relationships that could be construed as a potential conflict of interest.

Publisher's note

All claims expressed in this article are solely those of the authors and do not necessarily represent those of their affiliated

organizations, or those of the publisher, the editors and the reviewers. Any product that may be evaluated in this article, or claim that may be made by its manufacturer, is not guaranteed or endorsed by the publisher.

Supplementary material

The Supplementary Material for this article can be found online at: <https://www.frontiersin.org/articles/10.3389/fonc.2023.1092870/full#supplementary-material>

References

- Sung H, Ferlay J, Siegel RL, Laversanne M, Soerjomataram I, Jemal A, et al. Global cancer statistics 2020: GLOBOCAN estimates of incidence and mortality worldwide for 36 cancers in 185 countries. *CA Cancer J Clin* (2021) 71(3):209–49. doi: 10.3322/caac.21660
- Kuenzi BM, Park J, Fong SH, Sanchez KS, Lee J, Kreisberg JF, et al. Predicting drug response and synergy using a deep learning model of human cancer cells. *Cancer Cell* (2020) 38(5):672–84. doi: 10.1016/j.ccell.2020.09.014
- Weber J, Rad R. Engineering CRISPR mouse models of cancer. *Curr Opin Genet Dev* (2019) 54:88–96. doi: 10.1016/j.gde.2019.04.001
- Hansel-Hertsch R, Simeone A, Shea A, Hui WWL, Zyner KG, Marsico G, et al. Landscape of G-quadruplex DNA structural regions in breast cancer. *Nat Genet* (2020) 52(9):878–83. doi: 10.1038/s41588-020-0672-8
- Yi SA, Zhang Y, Rathnam C, Pongkulap T, Lee KB. Bioengineering approaches for the advanced organoid research. *Adv Mater* (2021) 33(45):e2007949. doi: 10.1002/adma.202007949
- LeSavage BL, Suhar RA, Broguiere N, Lutolf MP, Heilshorn SC. Next-generation cancer organoids. *Nat Mater* (2022) 21(2):143–59. doi: 10.1038/s41563-021-01057-5
- Bock C, Boutros M, Camp JG, Clarke L, Clevers H, Knoblich JA, et al. The organoid cell atlas. *Nat Biotechnol* (2021) 39(1):13–7. doi: 10.1038/s41587-020-00762-x
- Synnestvedt MB, Chen C, Holmes JH. CiteSpace II: visualization and knowledge discovery in bibliographic databases. *AMIA Annu Symp Proc* (2005), 724–8.
- van Eck NJ, Waltman L. Software survey: VOSviewer, a computer program for bibliometric mapping. *Scientometrics* (2010) 84(2):523–38. doi: 10.1007/s11192-009-0146-3
- Sato T, van Es JH, Snippert HJ, Stange DE, Vries RG, van den Born M, et al. Paneth cells constitute the niche for Lgr5 stem cells in intestinal crypts. *Nature* (2011) 469(7330):415–8. doi: 10.1038/nature09637
- Boj SF, Hwang CI, Baker LA, Chio II, Engle DD, Corbo V, et al. Organoid models of human and mouse ductal pancreatic cancer. *Cell* (2015) 160(1–2):324–38. doi: 10.1016/j.cell.2014.12.021
- Grün D, Lyubimova A, Kester L, Wiebrands K, Basak O, Sasaki N, et al. Single-cell messenger RNA sequencing reveals rare intestinal cell types. *Nature* (2015) 525(7568):251–5. doi: 10.1038/nature14966
- Sato T, Stange DE, Ferrante M, Vries RG, Van Es JH, Van den Brink S, et al. Long-term expansion of epithelial organoids from human colon, adenoma, adenocarcinoma, and barrett's epithelium. *Gastroenterology* (2011) 141(5):1762–72. doi: 10.1053/j.gastro.2011.07.050
- Sato T, Clevers H. Growing self-organizing mini-guts from a single intestinal stem cell: mechanism and applications. *Science* (2013) 340(6137):1190–4. doi: 10.1126/science.1234852
- Gao D, Vela I, Sboner A, Iaquinata PJ, Karthaus WR, Gopalan A, et al. Organoid cultures derived from patients with advanced prostate cancer. *Cell* (2014) 159(1):176–87. doi: 10.1016/j.cell.2014.08.016
- van de Wetering M, Francies HE, Francis JM, Bounova G, Iorio F, Pronk A, et al. Prospective derivation of a living organoid biobank of colorectal cancer patients. *Cell* (2015) 161(4):933–45. doi: 10.1016/j.cell.2015.03.053
- Clevers H. Modeling development and disease with organoids. *Cell* (2016) 165(7):1586–97. doi: 10.1016/j.cell.2016.05.082
- Öhlund D, Handly-Santana A, Biffi G, Elyada E, Almeida AS, Ponz-Sarvis M, et al. Distinct populations of inflammatory fibroblasts and myofibroblasts in pancreatic cancer. *J Exp Med* (2017) 214(3):579–96. doi: 10.1084/jem.20162024
- Vlachogiannis G, Hedayat S, Vatsiou A, Jamin Y, Fernández-Mateos J, Khan K, et al. Patient-derived organoids model treatment response of metastatic gastrointestinal cancers. *Science* (2018) 359(6378):920–6. doi: 10.1126/science.aao2774
- Wilson HV. A new method by which sponges may be artificially reared. *Science* (1907) 25(649):912–5. doi: 10.1126/science.25.649.912
- Sato T, Vries RG, Snippert HJ, van de Wetering M, Barker N, Stange DE, et al. Single Lgr5 stem cells build crypt-villus structures *in vitro* without a mesenchymal niche. *Nature* (2009) 459(7244):262–5. doi: 10.1038/nature07935
- Duval K D, Grover H, Han LH, Mou Y, Pegoraro AF, Fredberg J, et al. Modeling physiological events in 2D vs. 3D cell culture. *Physiol (Bethesda)* (2017) 32(4):266–77. doi: 10.1152/physiol.00036.2016
- Sarin V, Yu K, Ferguson ID, Gugliemini O, Nix MA, Hann B, et al. Evaluating the efficacy of multiple myeloma cell lines as models for patient tumors *via* transcriptomic correlation analysis. *Leukemia* (2020) 34(10):2754–65. doi: 10.1038/s41375-020-0785-1
- Wood LD, Ewald AJ. Organoids in cancer research: a review for pathologist-scientists. *J Pathol* (2021) 254(4):395–404. doi: 10.1002/path.5684
- Zhang X, Claerhout S, Prat A, Dobrolecki LE, Petrovic I, Lai Q, et al. A renewable tissue resource of phenotypically stable, biologically and ethnically diverse, patient-derived human breast cancer xenograft models. *Cancer Res* (2013) 73(15):4885–97. doi: 10.1158/0008-5472.CAN-12-4081
- Hidalgo M, Amant F, Biankin AV, Budinská E, Byrne AT, Caldas C, et al. Patient-derived xenograft models: an emerging platform for translational cancer research. *Cancer Discovery* (2014) 4(9):998–1013. doi: 10.1158/2159-8290.CD-14-0001
- Fontoura JC, Viezzer C, Dos Santos FG, Ligabue RA, Weinlich R, Puga RD, et al. Comparison of 2D and 3D cell culture models for cell growth, gene expression and drug resistance. *Mater Sci Eng C Mater Biol Appl* (2020) 107:110264. doi: 10.1016/j.msec.2019.110264
- Dame K, Ribeiro AJ. Microengineered systems with iPSC-derived cardiac and hepatic cells to evaluate drug adverse effects. *Exp Biol Med (Maywood)* (2021) 246(3):317–31. doi: 10.1177/1535370220959598
- Breslin S, O'Driscoll L. Three-dimensional cell culture: the missing link in drug discovery. *Drug Discovery Today* (2013) 18(5–6):240–9. doi: 10.1016/j.drudis.2012.10.003
- Mittal R, Woo FW, Castro CS, Cohen MA, Karanxha J, Mittal J, et al. Organ-on-chip models: Implications in drug discovery and clinical applications. *J Cell Physiol* (2019) 234(6):8352–80. doi: 10.1002/jcp.27729
- Macedo MH, Araújo F, Martínez E, Barrias C, Sarmento B. iPSC-derived enterocyte-like cells for drug absorption and metabolism studies. *Trends Mol Med* (2018) 24(8):696–708. doi: 10.1016/j.molmed.2018.06.001
- Zietek T, Boomgaarden W, Rath E. Drug screening, oral bioavailability and regulatory aspects: A need for human organoids. *Pharmaceutics* (2021) 13(8):1280. doi: 10.3390/pharmaceutics13081280
- Wang H, Brown PC, Chow EY, Ewart L, Ferguson SS, Fitzpatrick S, et al. 3D cell culture models: Drug pharmacokinetics, safety assessment, and regulatory consideration. *Clin Transl Sci* (2021) 14(5):1659–80. doi: 10.1111/cts.13066
- Gupta R, Schroeders Y, Hauser D, van Herwijnen M, Albrecht W, Ter Braak B, et al. Comparing *in vitro* human liver models to *in vivo* human liver using RNA-seq. *Arch Toxicol* (2021) 95(2):573–89. doi: 10.1007/s00204-020-02937-6
- Hedrich WD, Panzica-Kelly JM, Chen SJ, Strassle B, Hasson C, Lecureux L, et al. Development and characterization of rat duodenal organoids for ADME and toxicology applications. *Toxicology* (2020) 446:152614. doi: 10.1016/j.tox.2020.152614
- Shinozawa T, Kimura M, Cai Y, Saiki N, Yoneyama Y, Ouchi R, et al. High-fidelity drug-induced liver injury screen using human pluripotent stem cell-derived organoids. *Gastroenterology* (2021) 160(3):831–46. doi: 10.1053/j.gastro.2020.10.002
- Supplitt S, Karpinski P, Sasiadek M, Laczmanska I. Current achievements and applications of transcriptomics in personalized cancer medicine. *Int J Mol Sci* (2021) 22(3):1422. doi: 10.3390/ijms22031422
- Cobain EF, Wu YM, Vats P, Chugh R, Worden F, Smith DC, et al. Assessment of clinical benefit of integrative genomic profiling in advanced solid tumors. *JAMA Oncol* (2021) 7(4):525–33. doi: 10.1001/jamaoncol.2020.7987

39. Perri F, Longo F, Giuliano M, Sabbatino F, Favia G, Ionna F, et al. Epigenetic control of gene expression: Potential implications for cancer treatment. *Crit Rev Oncol Hematol* (2017) 111:166–72. doi: 10.1016/j.critrevonc.2017.01.020
40. van Galen P. Decoding the noncoding cancer genome. *Cancer Discovery* (2020) 10(5):646–7. doi: 10.1158/2159-8290.CD-20-0285
41. Yao Y, Xu X, Yang L, Zhu J, Wan J, Shen L, et al. Patient-derived organoids predict chemoradiation responses of locally advanced rectal cancer. *Cell Stem Cell* (2020) 26(1):17–26. doi: 10.1016/j.stem.2019.10.010
42. Amodio V, Yaeger R, Arcella P, Cancelliere C, Lamba S, Lorenzato A, et al. EGFR blockade reverts resistance to KRAS(G12C) inhibition in colorectal cancer. *Cancer Discovery* (2020) 10(8):1129–39. doi: 10.1158/2159-8290.CD-20-0187
43. Seidlitz T, Koo BK, Stange DE. Gastric organoids-an *in vitro* model system for the study of gastric development and road to personalized medicine. *Cell Death Differ* (2021) 28(1):68–83. doi: 10.1038/s41418-020-00662-2
44. Tao M, Wu X. The role of patient-derived ovarian cancer organoids in the study of PARP inhibitors sensitivity and resistance: from genomic analysis to functional testing. *J Exp Clin Cancer Res* (2021) 40(1):338. doi: 10.1186/s13046-021-02139-7
45. Pamarthy S, Sabaawy HE. Patient derived organoids in prostate cancer: improving therapeutic efficacy in precision medicine. *Mol Cancer* (2021) 20(1):125. doi: 10.1186/s12943-021-01426-3
46. Veninga V, Voest EE. Tumor organoids: Opportunities and challenges to guide precision medicine. *Cancer Cell* (2021) 39(9):1190–201. doi: 10.1016/j.ccell.2021.07.020
47. Yao J, Yang M, Atteh L, Liu P, Mao Y, Meng W, et al. A pancreas tumor derived organoid study: from drug screen to precision medicine. *Cancer Cell Int* (2021) 21(1):398. doi: 10.1186/s12935-021-02044-1
48. Kopustinskiene DM, Jakstas V, Savickas A, Bernatoniene J. Flavonoids as anticancer agents. *Nutrients* (2020) 12(2):457. doi: 10.3390/nu12020457
49. Kim HH, Ha SE, Vetrivel P, Bhosale PB, Kim SM, Kim GS, et al. Potential antioxidant and anti-inflammatory function of gynura procumbens polyphenols ligand. *Int J Mol Sci* (2021) 22(16):8716. doi: 10.3390/ijms22168716
50. Scuto M, Modafferi S, Rampulla F, Zimbone V, Tomasello M, Spano S, et al. Redox modulation of stress resilience by crocus sativus l. for potential neuroprotective and anti-neuroinflammatory applications in brain disorders: From molecular basis to therapy. *Mech Ageing Dev* (2022) 205:111686. doi: 10.1016/j.mad.2022.111686
51. Patra S, Pradhan B, Nayak R, Behera C, Das S, Patra SK, et al. Dietary polyphenols in chemoprevention and synergistic effect in cancer: Clinical evidences and molecular mechanisms of action. *Phytomedicine* (2021) 90:153554. doi: 10.1016/j.phymed.2021.153554
52. Arrigoni R, Ballini A, Santacroce L, Cantore S, Inchingolo A, Inchingolo F, et al. Another look at dietary polyphenols: Challenges in cancer prevention and treatment. *Curr Med Chem* (2022) 29(6):1061–82. doi: 10.2174/0929867328666210810154732
53. Scuto M, Ontario ML, Salinaro AT, Caligiuri I, Rampulla F, Zimbone V, et al. Redox modulation by plant polyphenols targeting vitagenes for chemoprevention and therapy: Relevance to novel anti-cancer interventions and mini-brain organoid technology. *Free Radic Biol Med* (2022) 179:59–75. doi: 10.1016/j.freeradbiomed.2021.12.267
54. Scuto M, Trovato SA, Caligiuri I, Ontario ML, Greco V, Sciuto N, et al. Redox modulation of vitagenes via plant polyphenols and vitamin d: Novel insights for chemoprevention and therapeutic interventions based on organoid technology. *Mech Ageing Dev* (2021) 199:111551. doi: 10.1016/j.mad.2021.111551
55. Weeber F, van de Wetering M, Hoogstraat M, Dijkstra KK, Krijgsman O, Kuilman T, et al. Preserved genetic diversity in organoids cultured from biopsies of human colorectal cancer metastases. *Proc Natl Acad Sci U.S.A.* (2015) 112(43):13308–11. doi: 10.1073/pnas.1516689112
56. Ye HS, Gao HF, Li H, Nie JH, Li TT, Lu MD, et al. Higher efficacy of resveratrol against advanced breast cancer organoids: A comparison with that of clinically relevant drugs. *Phytother Res* (2022) 36(8):3313–24. doi: 10.1002/ptr.7515
57. Ravindranathan P, Pasham D, Balaji U, Cardenas J, Gu J, Toden S, et al. A combination of curcumin and oligomeric proanthocyanidins offer superior anti-tumorigenic properties in colorectal cancer. *Sci Rep* (2018) 8(1):13869. doi: 10.1038/s41598-018-32267-8



OPEN ACCESS

EDITED BY

Christopher R. Cederroth,
Swiss 3R Competence Centre, Switzerland

REVIEWED BY

Hanno Wuerbel,
University of Bern, Switzerland

*CORRESPONDENCE

Adrian J. Smith
✉ adrian.smith@norecopa.no

SPECIALTY SECTION

This article was submitted to
Animal Behavior and Welfare,
a section of the journal
Frontiers in Veterinary Science

RECEIVED 12 December 2022

ACCEPTED 18 January 2023

PUBLISHED 02 February 2023

CITATION

Smith AJ (2023) Norecopa: A global knowledge
base of resources for improving animal
research and testing.
Front. Vet. Sci. 10:1119923.
doi: 10.3389/fvets.2023.1119923

COPYRIGHT

© 2023 Smith. This is an open-access article
distributed under the terms of the [Creative
Commons Attribution License \(CC BY\)](#). The use,
distribution or reproduction in other forums is
permitted, provided the original author(s) and
the copyright owner(s) are credited and that
the original publication in this journal is cited, in
accordance with accepted academic practice.
No use, distribution or reproduction is
permitted which does not comply with these
terms.

Norecopa: A global knowledge base of resources for improving animal research and testing

Adrian J. Smith*

Norecopa, c/o Norwegian Veterinary Institute, Ås, Norway

There are good ethical, legal and scientific reasons for ensuring that our use of animals in research and testing is limited to the lowest number of animals, and that those which are used are treated as humanely as possible, while at the same time providing reliable, reproducible and translatable data which is adequately reported. Unfortunately, there is widespread evidence that there is room for improvement in all these areas. This paper describes the Norecopa website, which offers links to global resources which can be used to resolve these issues. Much of the website content is linked to the PREPARE guidelines for planning any research or testing which appears to need animals. Attention to detail on all steps of the pathway from early planning to manuscript submission should lead to better science, improved animal welfare, and fewer health and safety accidents. This will also minimize the chances of manuscript rejection due to inadequate planning, avoiding a waste of human resources and animal lives.

KEYWORDS

animal research, testing, guidelines, replacement, reduction and refinement, PREPARE, quality

1. Introduction

The implication that animal research can be improved may appear provocative to senior scientists. If their research has been funded, and the animal studies approved by an ethics committee and the relevant authorities, what more is to be gained?

Unfortunately, there is widespread evidence that animal research has suffered from poor reproducibility and translatability for many years [e.g., (1, 2)], and that the standard of reporting could be significantly improved [e.g., (3, 4)]. Better reporting depends upon better planning, for which there are now over 400 guidelines available worldwide,¹ in addition to the wealth of advice available at individual institutions.

The devil is often in the details in animal research and testing (5, 6). Norecopa has worked for the last 15 years to collect links to resources about the practical issues which decide the quality of this work. Many of these issues may appear obvious, but they regularly affect experiments which on paper look to be well-designed. Norecopa and coworkers have published the PREPARE guidelines (7) to offer scientists and animal care staff an overview of issues which should be considered when planning studies which appear to need animals, as aid to the advancement of the three Rs (Replacement, Reduction, Refinement) of Russell and Burch (8). PREPARE is based on experience gained from accrediting animal facilities, and from dialogue with scientists, animal technicians, regulators and veterinarians.

1 3R Guide. <https://norecopa.no/3Rguide> (accessed 8 January, 2022).

The PREPARE guidelines cover three main areas:

1. Formulation of the study
2. Dialogue between scientists and the animal facility
3. Quality control of the components in the study

PREPARE consists of a checklist (see [Figure 1](#), currently available in 34 languages) with 15 main topics covering these areas, and a website with links to more information, guidelines and scientific papers on each subject. The checklist is available in three different formats. The website is continuously updated, as new guidelines and relevant scientific papers are published. Many of these are announced first in Norecopa's newsletters.²

Some of the overarching aims behind the PREPARE guidelines are to promote:

1. The production of valid data (reflecting a true treatment effect, not artifacts caused, for example, by stress) from reproducible experiments. If the animal studies are designed to cast light on conditions in other species or humans, the results must be translatable to these.
2. Best possible animal welfare.
3. Attention to the health and safety of all those who are in any way affected by the animal studies, including other animals in the facility and visitors.
4. A good culture of care in the animal facility and research group.
5. Communication of best practice to other researchers and to the other stakeholders, including the general public.

A few brief examples from these areas are given below. Many more are cited on the PREPARE website.³

2. Valid, reproducible, and translatable data

There is ample evidence of both poor experimental design and reporting in the literature. Briefly, the major concerns (9) are:

- Lack of randomization and blinding.
- Low statistical power.
- Over-reliance on *p*-values, and *p*-value hacking.
- HARKing (hypothesizing after the results are known).
- Publication bias (under-reporting of negative or null results).

An overview of the concerns about the use of statistics has been published by Rowe (10).

What may be less clear to researchers is the need to modify their protocols to take into account the characteristics of the animals which they plan to use. The correct choice of species should be based upon knowledge of the hypothesis to be tested and the characteristics which a research animal must possess to be able to test the hypothesis, not solely upon which species have previously been used in the area. Among other things, physically smaller animals will in general have higher metabolic rates (11), which will affect the optimal dose rates.

Housing and husbandry conditions, and methods of handling and immobilization^{4,5} may all cause artifacts or stress which, in the worst case, can cause larger effects on the parameters to be measured than the experimental treatment itself [see also examples in (12)]. For example, laboratory animal diets have a far greater impact on experimental results than many realize (13). Åhlgren and Voikar (14) demonstrated how C57BL/6 mice purchased from two different suppliers showed behavioral differences which would affect the results of behavioral tests. Measurements of cardiac function are another example: Labitt et al. (15) identified changes in cardiac rhythm in mice for up to 6 mins following simple scruffing, an effect which could be eliminated by choosing a different method of grasping the skin on the neck.

3. Welfare

Adequate consideration of the welfare aspects of animal research must cover both animal and human welfare. Animal research has been dubbed “reversed veterinary medicine,” because it involves the procurement of healthy animals which are then treated in such a way that they become ill. This is the very opposite of the ideals imprinted in the education of animal care staff, and time must be set aside to inform all those who are skeptical about a new study of the benefits that will hopefully come from it, despite the very real likelihood of harm to the research animals themselves.

A good culture of care at an animal facility will help this process (see below), and will ensure that anyone who has reservations about a planned study has the confidence to speak their mind without fear of ridicule or reprisals.

Injections and blood samples which are relatively harmless in larger animals may cause significant distress in smaller ones. The stress of injections or oral gavaging can often be prevented by training animals for voluntary ingestion.⁶ The route and amount of blood sampling, which scientists may not be so focused upon, can dramatically affect the quality of the parameters to be measured in the samples and the welfare of the animals (16). Bleeding techniques may be evaluated against a number of subjective criteria based upon common sense:

- Is the blood vessel visible?
- Can the bleeding (including any internal blood loss) be easily stopped?
- Might the method damage surrounding tissue?
- Can the blood be collected quickly, to avoid artifacts in the samples due to variations in storage time before processing, or to mechanical damage caused by having to “milk” the vein to extract blood?

Considerable time may have to be spent designing studies which are minimally invasive and which cause the least effect on the animals' physiology. If humans are really the final target of a research

2 <https://norecopa.no/news/newsletters> (accessed 8 January, 2022).


3 <https://norecopa.no/PREPARE> (accessed 8 January, 2022).

4 <https://www.na3rsc.org/refined-mouse-handling> (accessed 8 January, 2022).

5 <https://norecopa.no/prepare/12-housing-and-husbandry/12a/general-principles> (accessed 8 January, 2022).

6 <https://www.ri.se/en/what-we-do/expertises/3r-focus-on-animal-welfare> (accessed 8 January, 2022).

PREPARE



The PREPARE Guidelines Checklist
Planning Research and Experimental Procedures on Animals: Recommendations for Excellence
 Adrian J. Smith¹, R. Eddie Clutton², Elliot Lilley³, Kristine E. Aa. Hansen⁴ & Trond Brattøyd⁵

¹Norecopa, c/o Norwegian Veterinary Institute, P.O. Box 750 Sentrum, 0108 Oslo, Norway; ²Royal (Dick) School of Veterinary Studies, Easter Bush, Midlothian, EH25 9RG, U.K.; ³Research Animals Department, Science Group, RSPCA, Wilberforce Way, Southmead, Horsham, West Sussex, RH13 9RS, U.K.; ⁴Section of Experimental Biomedicine, Department of Production Animal Clinical Sciences, Faculty of Veterinary Medicine, Norwegian University of Life Sciences, P.O. Box 8140 Dep., 0033 Oslo, Norway; ⁵Division for Research Management and External Funding, Western Norway University of Applied Sciences, 5020 Bergen, Norway.

PREPARE[®] consists of planning guidelines which are complementary to reporting guidelines such as ARRIVE[®]. PREPARE covers the three broad areas which determine the quality of the preparation for animal studies:

1. Formulation of the study
2. Dialogue between scientists and the animal facility
3. Quality control of the components in the study

The topics will not always be addressed in the order in which they are presented here, and some topics overlap. The PREPARE checklist can be adapted to meet special needs, such as field studies. PREPARE includes guidance on the management of animal facilities, since in-house experiments are dependent upon their quality. The full version of the guidelines is available on the Norecopa website, with links to global resources, at <https://norecopa.no/PREPARE>. The PREPARE guidelines are a dynamic set which will evolve as more species- and situation-specific guidelines are produced, and as best practice within Laboratory Animal Science progresses.

Topic	Recommendation
(A) Formulation of the study	
1. Literature searches	<input type="checkbox"/> Form a clear hypothesis, with primary and secondary outcomes. <input type="checkbox"/> Consider the use of systematic reviews. <input type="checkbox"/> Decide upon databases and information specialists to be consulted, and construct search terms. <input type="checkbox"/> Assess the relevance of the species to be used, its biology and suitability to answer the experimental questions with the least suffering, and its welfare needs. <input type="checkbox"/> Assess the reproducibility and translatability of the project.
2. Legal issues	<input type="checkbox"/> Consider how the research is affected by relevant legislation for animal research and other areas, e.g. animal transport, occupational health and safety. <input type="checkbox"/> Locate relevant guidance documents (e.g. EU guidance on project evaluation).
3. Ethical issues, harm-benefit assessment and humane endpoints	<input type="checkbox"/> Construct a lay summary. <input type="checkbox"/> In dialogue with ethics committees, consider whether statements about this type of research have already been produced. <input type="checkbox"/> Address the 3Rs (replacement, reduction, refinement) and the 3Ss (good science, good sense, good sensibilities). <input type="checkbox"/> Consider pre-registration and the publication of negative results. <input type="checkbox"/> Perform a harm-benefit assessment and justify any likely animal harm. <input type="checkbox"/> Discuss the learning objectives, if the animal use is for educational or training purposes. <input type="checkbox"/> Allocate a severity classification to the project. <input type="checkbox"/> Define objective, easily measurable and unequivocal humane endpoints. <input type="checkbox"/> Discuss the justification, if any, for death as an end-point.
4. Experimental design and statistical analysis	<input type="checkbox"/> Consider pilot studies, statistical power and significance levels. <input type="checkbox"/> Define the experimental unit and decide upon animal numbers. <input type="checkbox"/> Choose methods of randomisation, prevent observer bias, and decide upon inclusion and exclusion criteria.
(B) Dialogue between scientists and the animal facility	
5. Objectives and timescale, funding and division of labour	<input type="checkbox"/> Arrange meetings with all relevant staff when early plans for the project exist. <input type="checkbox"/> Construct an approximate timescale for the project, indicating the need for assistance with preparation, animal care, procedures and waste disposal/decontamination. <input type="checkbox"/> Discuss and disclose all expected and potential costs. <input type="checkbox"/> Construct a detailed plan for division of labour and expenses at all stages of the study.
6. Facility evaluation	<input type="checkbox"/> Conduct a physical inspection of the facilities, to evaluate building and equipment standards and needs. <input type="checkbox"/> Discuss staffing levels at times of extra risk.
7. Education and training	<input type="checkbox"/> Assess the current competence of staff members and the need for further education or training prior to the study.
8. Health risks, waste disposal and decontamination	<input type="checkbox"/> Perform a risk assessment, in collaboration with the animal facility, for all persons and animals affected directly or indirectly by the study. <input type="checkbox"/> Assess, and if necessary produce, specific guidance for all stages of the project. <input type="checkbox"/> Discuss means for containment, decontamination, and disposal of all items in the study.
(C) Quality control of the components in the study	
9. Test substances and procedures	<input type="checkbox"/> Provide as much information as possible about test substances. <input type="checkbox"/> Consider the feasibility and validity of test procedures and the skills needed to perform them.
10. Experimental animals	<input type="checkbox"/> Decide upon the characteristics of the animals that are essential for the study and for reporting. <input type="checkbox"/> Avoid generation of surplus animals.
11. Quarantine and health monitoring	<input type="checkbox"/> Discuss the animals' likely health status, any needs for transport, quarantine and isolation, health monitoring and consequences for the personnel.
12. Housing and husbandry	<input type="checkbox"/> Attend to the animals' specific instincts and needs, in collaboration with expert staff. <input type="checkbox"/> Discuss acclimatization, optimal housing conditions and procedures, environmental factors and any experimental limitations on these (e.g. food deprivation, solitary housing).
13. Experimental procedures	<input type="checkbox"/> Develop refined procedures for capture, immobilisation, marking, and release or rehoming. <input type="checkbox"/> Develop refined procedures for substance administration, sampling, sedation and anaesthesia, surgery and other techniques.
14. Humane killing, release, reuse or rehoming	<input type="checkbox"/> Consult relevant legislation and guidelines well in advance of the study. <input type="checkbox"/> Define primary and emergency methods for humane killing. <input type="checkbox"/> Assess the competence of those who may have to perform these tasks.
15. Necropsy	<input type="checkbox"/> Construct a systematic plan for all stages of necropsy, including location, and identification of all animals and samples.

References
 1. Smith AJ, Clutton RE, Lilley E, Hansen KEA & Brattøyd T (2018) PREPARE Guidelines for Planning Animal Research and Testing. *Laboratory Animals*, 52(2):135–141. <https://doi.org/10.1177/002387717724823>
 2. Pearce du Sert N, Hurst V, Ahluwalia A, Alam S, Avey M, Baker M et al. (2020) The ARRIVE guidelines 2.0: Updated guidelines for reporting animal research. *PLoS Biol* 18(7): e3000410. <https://doi.org/10.1371/journal.pbio.3000410>

Further information
<https://norecopa.no/PREPARE> | post@norecopa.no | [@norecopa](https://twitter.com/norecopa)

FIGURE 1
 The PREPARE checklist (<https://norecopa.no/PREPARE/prepare-checklist>, accessed 8 January, 2022).

programme, efforts should be made to see if animal studies can in fact be replaced by methods which use human materials.

Scientists and facility staff must both contribute to this process, not least because they are specialists in two different areas, both of which must be addressed when animal studies are planned. Scientists will naturally be mostly focused on the scientific hypotheses to be tested, and the more “mathematical” aspects of experimental design such as group size, experimental units and statistical analyses. Animal care staff will be more focused on practical issues related to space, equipment, staffing needs, competency and costs. They will also be more aware than the scientists of the potential sources of variability in the study that can be caused by intrinsic factors (e.g., genetic and microbial variation within the animals) and extrinsic factors such as the stress of transportation, social re-grouping, capture and handling, and environmental parameters (e.g., room temperature, humidity, and noise levels). Many of these are subtle and are still poorly understood or appreciated. While the potential causes of direct suffering in an experiment may be obvious, it may be more difficult to identify causes of what Russell and Burch called contingent suffering, i.e., pain and distress caused by other factors than the experiment itself, such as fighting when new social groups are established, or boredom in barren environments. A comprehensive slide deck describing the 3Rs has recently been published.⁷

4. Health and safety

Many research protocols, which appear scientifically sound on paper, present practical problems when preparations are made to implement them in an animal facility—or in the field. It is essential that maximum effort is made to avoid harm to anyone entering the area, or who may be exposed indirectly to harm from the experiment. This includes not only people but also other research animals. Many potentially harmful substances, such as radioactive isotopes, micro-organisms and carcinogenic drugs, are invisible and steps must be taken to ensure that they are properly contained. In addition to making sure that there are detailed protocols for their use, and emergency procedures in case someone is exposed to them, the facility must have adequate signage so that those entering the building are immediately made aware of the potential hazards and how to avoid them. Without adequate signs describing the presence of potential hazards, visitors to the facility, particularly if these are out of normal working hours, may accidentally be exposed.

Researchers who have worked with potential hazardous agents for many years will have developed their own routines for safe handling. They may not be aware of the need to inform animal care staff of these routines and, if necessary, to adjust them to the particular conditions in the animal facility, which may be very different from their laboratories. Likewise, their preferred methods of administration may not be realistic in the animals in question, necessitating a discussion. In many cases, the use of hazardous agents will lead to extra expense, for example to purchase additional

⁷ <https://norecopa.no/3Rs> (accessed 8 January, 2022).

protective clothing and to decontaminate the rooms afterwards. Discussions must include clarification of whom is to bear these costs.

Most significant accidents are caused by the presence of a number of smaller events which in themselves are relatively harmless, but which when they occur together trigger a significant event—the so-called Swiss Cheese effect (17).⁸ Threat and error management⁹ is an important part of running an animal facility, building in redundancy at critical steps, and including the establishment of contingency plans based upon a risk assessment (both of the facility and the research study).

Early dialogue between the research group and those who will be taking care of the animals is the clue to better science, better welfare and sufficient attention to health and safety. It is essential to clarify the responsibilities and costs at all stages of the study. These are, broadly speaking:

- Who is to perform which tasks?
- Who will be paying for equipment, procedures, training and staffing, over and above the standard functions of the facility?

They apply from the earliest preparations for a study all the way until the facility has been thoroughly decontaminated after the study and all material correctly disposed of.

These clarifications should be documented with an agreement signed by both parties. Such a document will greatly reduce the chances of research data being lost because one party had assumed that the other was going to collect them. A Master Plan should also be constructed, both for the study and for the animal facility itself, displaying the critical steps to be carried out and documentation of who has performed these. Standard Operating Procedures (SOPs) should be readily available for all of these steps, to aid harmonization. Discussions of all these stages of an experiment can greatly improve the quality of the study, as they tend to unearth potential challenges that might otherwise have been forgotten.

More advice on contingency plans and master plans is available on the Norecopa website.¹⁰ Loss of data can in the worst case result in inability to publish animal experiments, with a waste both of human resources and animal lives.

5. Culture of care

A Culture of Care is a commitment throughout a research facility to ensure mutual respect, so that everyone has the security and confidence to discuss potential concerns with an experiment or with the way in which the facility is managed. This commitment will automatically lead to an improvement in the scientific quality of the research, and the welfare of the animals in its care. The

8 https://en.wikipedia.org/wiki/Swiss_cheese_model (accessed January 8, 2022).

9 <https://www.montereynavyflyclub.org/Safety%20Presentations/Intro%20to%20TEM%20Training%20v7a%20with%20VMax.pdf> (Accessed January 8, 2022).

10 <https://norecopa.no/more-resources/master-plan-and-sops> (accessed January 8, 2022).

culture of care should also extend to transparency about the research, not least to the general public who in many cases are indirectly financing the research. A facility that has embraced this culture to its maximal extent will be a pleasant workplace producing high quality science from animals living in harmony with their surroundings.

Norecopa hosts the website of the International Culture of Care Network,¹¹ which provides a forum to discuss ways in which this culture can be achieved and practical examples of resources and events that have been shown to work.

Since a caring environment empowers all employees to be able to raise their concerns, it will also embrace a Culture of Challenge (18), whereby staff look for acceptable methods of work, rather than being satisfied with what has been accepted.

The PREPARE guidelines emphasize the need for involvement of animal carers and technicians from the earliest stage of planning. There are a number of good reasons for this:

- they have a right to know about the aims of animal studies, and will be more motivated if they understand these,
- they, better than anyone else, know the possibilities (and limitations) inherent in the animal facility,
- they often possess a large range of practical skills and are good at lateral thinking from one species or project to another,
- they know the animals best,
- the animals know them best,
- lack of involvement creates anxiety, depression and opposition to animal research, as well as limiting creativity which might improve the experiments.

6. Communication of best practice

Improvements to protocols and facility management should be communicated quickly and widely so that others may benefit. In some cases this may entail writing a separate methodology paper to highlight the improvement. For example, the technique of blood sampling rodents from the saphenous vein was first described in one sentence in a research paper on a totally different subject (19), and it first became widely known and adopted after publication of a paper devoted entirely to it (20). These papers do not have to be published in journals with high impact factor, since the most important issue is to make them accessible as rapidly as possible to search engines.

Recently, a Refinement Wiki¹² was created to allow even faster dissemination of such improvements, including more anecdotal accounts, with room for discussion.

Communication also entails honesty about failures or accidents. If others are to avoid the same mistakes, scientists must be prepared to report them. A service called CIRS-LAS (*Critical Incident Reporting System-Laboratory Animal Science*)¹³ has been designed for this purpose. Reports are submitted anonymously and published with a commentary

11 <https://norecopa.no/coc> (accessed January 8, 2022).

12 <https://wiki.norecopa.no/> (accessed January 8, 2022).

13 <https://www.cirs-las.de/> (accessed January 8, 2022).

on the CIRS-LAS website. The database can be searched for specific incidents.

7. The value of guidelines and checklists (standard operating procedures)

Although the 3R Guide database (see footnote 1) includes descriptions of over 400 guidelines, many more are still needed. In particular, species-specific guidelines need to be developed for housing and procedures. No better example of this is the need for more guidelines for fish, which are often treated as one group rather than separate species with very different needs.

Guidelines should be used as the basis for constructing checklists (or standard operating procedures as they are referred to in the realm of Good Laboratory Practice¹⁴) for ensuring the quality of each critical step of a study. In a busy research lab, there may be a tendency to look upon them as unnecessarily bureaucratic and time consuming, increasing the already substantial paperwork involved in animal research. On the contrary, just like a kitchen recipe (once it is written down), they save time, avoid errors, and ensure that the result is repeatable.

Checklists have many advantages. They are used extensively in the aviation industry to maintain their excellent safety record:

- They reduce risk of forgetting to carry out vital actions.
- They ensure that procedures are carried out in the correct sequence.
- They encourage cooperation and cross-checking between all players.
- They make sure that everyone is “on the same page.”

Norecopa has spent considerable resources on creating a website with links to global resources within animal research (both in the laboratory and in the field) and testing, animal welfare and related topics which can be helpful when planning, conducting and writing up animal studies. The website currently consists of roughly 9,000 pages, organized as one large searchable database. It includes a number of smaller databases such as NORINA (an inventory of ~2,800 alternatives or supplements to animal use in education and training),¹⁵ 3R Guide (a global collection of ~400 guidelines for animal research)¹⁶ and TextBase (~1,500 textbooks and other literature of relevance to this field).¹⁷ The website also contains information about, and links to, over 70 external databases which scientists may have use for.¹⁸

Access to these global resources has been facilitated by the overarching PREPARE Guidelines (7).

8. Concluding remarks

The pathway to better science consists of many steps, including some which are not the subject of this paper. Planning guidelines such as PREPARE (7) are, for example, complementary to reporting guidelines such as ARRIVE (4).

All too often, researchers are confronted at the submission stage with questions from reviewers which they are unable to answer, largely because these have not been addressed during the planning stage of the study. Conscientious use of planning guidelines, which act as an overarching checklist, will help researchers to identify and address these issues while it is still possible to act on them—for example to ensure that data which reviewers may later consider critical to the study is in fact recorded. Thorough planning will make it easier to perform adequate reporting, which in turn will greatly increase the likelihood of a manuscript being accepted for publication so that researchers will find that: “We ARRIVED because we were PREPARED.”

Data availability statement

The original contributions presented in the study are included in the article/supplementary material, further inquiries can be directed to the corresponding author.

Author contributions

The author confirms being the sole contributor of this work and has approved it for publication.

Funding

AS is a full-time employee of the Norwegian Veterinary Institute, which handles the administration of Norecopa's secretariat. Norecopa receives core funding from two Norwegian Ministries via the Veterinary Institute, and fees from its members. In addition, Norecopa receives occasional grants from animal welfare organizations and others, for specific projects. A list of those who have sponsored Norecopa is available.¹⁹

Acknowledgments

The author acknowledges sponsors and members of Norecopa, who have made it possible to fund development of the resources mentioned in this paper, and to many colleagues who have contributed scientific material to Norecopa.

Conflict of interest

AS is lead author of the PREPARE guidelines and manager of the Norecopa website, including the Refinement Wiki.

14 <https://www.oecd.org/chemicalsafety/testing/good-laboratory-practiceglp.htm> (accessed January 8, 2022).

15 <https://norecopa.no/NORINA> (accessed January 8, 2022).

16 <https://norecopa.no/3RGuide> (accessed January 8, 2022).

17 <https://norecopa.no/TextBase> (accessed January 8, 2022).

18 https://norecopa.no/search?fq=type:%22Databases%22&sort=name_s%20asc&q=*%26facet.limit=125 (accessed January 8, 2022).

19 <https://norecopa.no/Sponsors> (accessed January 8, 2022).

Publisher's note

All claims expressed in this article are solely those of the authors and do not necessarily represent those of their affiliated

organizations, or those of the publisher, the editors and the reviewers. Any product that may be evaluated in this article, or claim that may be made by its manufacturer, is not guaranteed or endorsed by the publisher.

References

1. Baker M. 1,500 scientists lift the lid on reproducibility. *Nature*. (2016) 533:452–4. doi: 10.1038/533452a
2. Macleod M, Mohan S. Reproducibility and rigor in animal-based research. *ILAR J*. (2019) 60:17–23. doi: 10.1093/ilar/ilz015
3. Kilkenny C, Parsons N, Kadyszewski E, Festing MW, Cuthill IC, Fry D, et al. Survey of the quality of experimental design, statistical analysis and reporting of research using animals. *PLoS ONE*. (2009) 4:e7824–e7824. doi: 10.1371/journal.pone.0007824
4. Percie du Sert N, Hurst V, Ahluwalia A, Alam S, Avey MT, Baker M, et al. The ARRIVE guidelines 2.0: updated guidelines for reporting animal research. *PLoS Biol*. (2020) 18:e3000410. doi: 10.1186/s12917-020-02451-y
5. Avey MT, Moher D, Sullivan KJ, Fergusson D, Griffin G, Grimshaw JM, et al. The devil is in the details: incomplete reporting in preclinical animal research. *PLoS ONE*. (2016) 11:e0166733. doi: 10.1371/journal.pone.0166733
6. Hay AM, Howie HL, Gorham JD, D'Alessandro A, Spitalnik SL, Hudson KE, et al. Mouse background genetics in biomedical research: the devil's in the details. *Transfusion*. (2021) 61:3017–25. doi: 10.1111/trf.16628
7. Smith AJ, Clutton RE, Lilley E, Hansen KEA, Brattelid T. PREPARE: guidelines for planning animal research and testing. *Lab Anim*. (2018) 52:135–41. doi: 10.1177/0023677217724823
8. Russell WMS, Burch RL. *The Principles of Humane Experimental Technique*. London: Methuen and Co. (1959).
9. Munafò MR, Nosek BA, Bishop DV, Button KS, Chambers CD, Percie du Sert N, et al. A manifesto for reproducible science. *Nat Hum Behav*. (2017) 1:1–9. doi: 10.1038/s41562-016-0021
10. Rowe A. Recommendations to improve use and reporting of statistics in animal experiments. *Lab Anim*. (2022) 2022:00236772221140669. doi: 10.1177/00236772221140669
11. Hawk TC, Leary S, Morris TH. *Formulary for Laboratory Animals*. 216 pp. Blackwell Publishing (2005). Available online at: <https://www.usf.edu/research-innovation/comparative-medicine/documents/formulary-lab-animals.pdf> (accessed December 6, 2022).
12. Percie du Sert N, Alfieri A, Allan SM, Carswell HV, Deuchar GA, Farr TD, et al. The IMPROVE guidelines (ischaemic models: procedural refinements of in vivo experiments). *J Cerebr Blood Flow Metab*. (2017) 37:3488–517. doi: 10.1177/0271678X1709185
13. Pellizzon MA, Ricci MR. Choice of laboratory rodent diet may confound data interpretation and reproducibility. *Curr Dev Nutr*. (2020) 4:nzaa031. doi: 10.1093/cdn/nzaa031
14. Åhlgren J, Voikar V. Experiments done in Black-6 mice: what does it mean? *Lab Anim*. (2019) 48:171–80. doi: 10.1038/s41684-019-0288-8
15. Labitt RN, Oxford EM, Davis AK, Butler SD, Daugherty EK. A validated smartphone-based electrocardiogram reveals severe bradyarrhythmias during immobilizing restraint in mice of both sexes and four strains. *J Am Assoc Lab Anim Sci*. (2021) 60:201–12. doi: 10.30802/AALAS-JAALAS-20-000069
16. Diehl K-H, Hull R, Morton D, Pfister R, Rabemampianina Y, Smith D, et al. A good practice guide to the administration of substances and removal of blood, including routes and volumes. *J Appl Toxicol*. (2001) 21:15–23. doi: 10.1002/jat.727
17. Reason J. Human error: models and management. *BMJ*. (2000) 320:768–70. doi: 10.1136/bmj.320.7237.768
18. Louhimies S. Refinement facilitated by the culture of care. In: *Proceedings of the EUSAAT 2015-Linz 2005 Congress, Linz, Austria, 20–23 September 2015*; Volume 4, p. 154 (2015). Available online at: http://eusaat-congress.eu/images/2015/Abstractbook_EUSAAT_2015_Linz_2015.pdf (accessed on December 6, 2022).
19. Aaberge IS, Michaelsen TE, Rolstad AK, Groeng EC, Solberg P, Løvik M. SCID-Hu mice immunized with a pneumococcal vaccine produce specific human antibodies and show increased resistance to infection. *Infect Immun*. (1992) 60:4146–53. doi: 10.1128/iai.60.10.4146-4153.1992
20. Hem A, Smith AJ, Solberg P. Saphenous vein puncture for blood sampling of the mouse, rat, hamster, guinea pig, ferret and mink. *Lab Anim*. (1998) 32:364–8. doi: 10.1258/002367798780599866



OPEN ACCESS

EDITED BY

Christopher R. Cederroth,
Swiss 3R Competence Centre, Switzerland

REVIEWED BY

Stefano Gaburro,
Tecniplast, Italy
Brian Hansen,
Aarhus University, Denmark

*CORRESPONDENCE

Elin Törnqvist
✉ elin.tornqvist@sva.se

SPECIALTY SECTION

This article was submitted to
Emotion Regulation and Processing,
a section of the journal
Frontiers in Behavioral Neuroscience

RECEIVED 28 November 2022

ACCEPTED 16 January 2023

PUBLISHED 02 February 2023

CITATION

Swan J, Boyer S, Westlund K, Bengtsson C,
Nordahl G and Törnqvist E (2023) Decreased
levels of discomfort in repeatedly handled
mice during experimental procedures,
assessed by facial expressions.
Front. Behav. Neurosci. 17:1109886.
doi: 10.3389/fnbeh.2023.1109886

COPYRIGHT

© 2023 Swan, Boyer, Westlund, Bengtsson,
Nordahl and Törnqvist. This is an open-access
article distributed under the terms of the
[Creative Commons Attribution License \(CC BY\)](https://creativecommons.org/licenses/by/4.0/).
The use, distribution or reproduction in other
forums is permitted, provided the original
author(s) and the copyright owner(s) are
credited and that the original publication in this
journal is cited, in accordance with accepted
academic practice. No use, distribution or
reproduction is permitted which does not
comply with these terms.

Decreased levels of discomfort in repeatedly handled mice during experimental procedures, assessed by facial expressions

Julia Swan^{1,2}, Scott Boyer^{3,4}, Karolina Westlund⁵,
Camilla Bengtsson^{4,6}, Gunnar Nordahl⁷ and Elin Törnqvist^{4,8,9*}

¹Research Unit of Biomedicine, Department of Pharmacology and Toxicology, University of Oulu, Oulu, Finland, ²Biocenter Oulu, University of Oulu, Oulu, Finland, ³Chemotargets SL, Barcelona, Spain, ⁴Global Safety Assessment, AstraZeneca R&D, Södertälje, Sweden, ⁵ILLIS Animal Behaviour Courses, Stockholm, Sweden, ⁶Independent Consultant, Strömsund, Sweden, ⁷Sweden Operations, AstraZeneca, Södertälje, Sweden, ⁸Department of Animal Health and Antimicrobial Strategies, Swedish National Veterinary Institute (SVA), Uppsala, Sweden, ⁹Institute of Environmental Medicine, Karolinska Institutet, Solna, Sweden

Mice are the most commonly used laboratory animal, yet there are limited studies which investigate the effects of repeated handling on their welfare and scientific outcomes. Furthermore, simple methods to evaluate distress in mice are lacking, and specialized behavioral or biochemical tests are often required. Here, two groups of CD1 mice were exposed to either traditional laboratory handling methods or a training protocol with cup lifting for 3 and 5 weeks. The training protocol was designed to habituate the mice to the procedures involved in subcutaneous injection, e.g., removal from the cage, skin pinch. This protocol was followed by two common research procedures: subcutaneous injection and tail vein blood sampling. Two training sessions and the procedures (subcutaneous injection and blood sampling) were video recorded. The mouse facial expressions were then scored, focusing on the ear and eye categories of the mouse grimace scale. Using this assessment method, trained mice expressed less distress than the control mice during subcutaneous injection. Mice trained for subcutaneous injection also had reduced facial scores during blood sampling. We found a clear sex difference as female mice responded to training faster than the male mice, they also had lower facial scores than the male mice when trained. The ear score appeared to be a more sensitive measure of distress than the eye score, which may be more indicative of pain. In conclusion, training is an important refinement method to reduce distress in mice during common laboratory procedures and this can best be assessed using the ear score of the mouse grimace scale.

KEYWORDS

3R, mouse grimace scale, refinement, repeated handling, habituation, sex differences

1. Introduction

Laboratory animal welfare is influenced by handling procedures. This includes housing and routines which range from arriving at the research facility until the animals are sacrificed at the end of the study. Stress and suffering may compromise the animals' health and welfare, as well as introduce problematic, confounding factors that may interfere with the interpretation of biomedical results (Ghosal et al., 2015; Ono et al., 2016). The development of methods and activities for refinement is therefore important to reduce stress before, during and after the

animal experiment. Refinement activities are often associated with improved housing conditions and environmental enrichment (Baumans and Van Loo, 2013). This can include the usage of non-aversive animal handling methods (Hurst and West, 2010) and animal training (Westlund, 2015).

Stress has the potential to impact physiological responses in two ways: increasing variability (Koolhaas et al., 2010; Fridgeirsdottir et al., 2014; Nakamura and Suzuki, 2018) or acting as a confounding factor (Rowan, 1990; Strekalova et al., 2005; Ghosal et al., 2015; Ono et al., 2016). Consequently, proper acclimation (adaptation to environmental conditions), including handling and sampling procedures, is crucial to safeguard the quality of the data from acute stress reactions.

In addition to improved housing and enrichment, gentle handling, and training should be employed as a refinement protocol before any experimental procedure is performed. Animal training or structured human-animal interactions reduces laboratory animal stress and has been effective for numerous lab animal species. For example, in primates, training has been shown to reduce fear and associated stress responses (Westlund, 2015) and, in rats, tickling reduces the stress of repeated intraperitoneal injections (Cloutier et al., 2014).

However, there have been limited studies on the refinement effects of mouse training, although they are the most used laboratory animal (with 5.5 million being used in EU, constituting approximately 52.5% of laboratory animals) (European Commission, 2022). Hurst and West (2010) compared the anxiety levels induced by differing mouse handling methods. Mice lifted by their tails exhibited high anxiety and handler aversion compared to those lifted in their shelters/tubes, or in an open hand (cup) (Hurst and West, 2010). Gouveia and Hurst (2019) later investigated the duration and handling frequency needed to familiarize mice with these different lifting methods (tail, tube, and cup lifting). More handling sessions were needed to habituate mice to be cupped on an open hand, compared with tube lifting (Gouveia and Hurst, 2019). Moreover, a strong handler aversion was observed after only a short duration and frequency of tail lifting. The positive effects of frequent handling with non-aversive techniques (tube lifting for instance) were not affected by scuffing or subcutaneous injections (Gouveia and Hurst, 2019). This suggests that these handling techniques have practical application in laboratory settings where mice are frequently required to be restrained for routine procedures.

The refinement aspect of the 3Rs concept is defined as a method which alleviates or minimizes potential pain, suffering, and distress, and which enhances animal well-being (MacArthur Clark, 2018). This study focuses on the refinement component of 3Rs. Understanding mouse behavior and signs of welfare vs. distress is pertinent to evaluate efforts aiming at refinement (Brown et al., 2006). General welfare assessment protocols for scoring animal suffering have been used to measure the effects of refinement strategies for research animals (Hawkins et al., 2011), and for specific experimental animal models, e.g., experimental autoimmune encephalomyelitis (Wolfensohn et al., 2013). In 2010, Langford et al. (2010) published the Mouse Grimace Scale (MGS) for assessment of facial expressions of pain in the laboratory mouse. This highly cited method, not only allows identification of the degree of pain in mice, but also shows that mice express feelings of pain using facial expressions, just like humans (Leach et al., 2012). Could mice also reflect feelings of distress in their facial expressions?

In this study we investigate effects of mouse training during acclimation by scoring the ear and eye appearance according to the MGS (Langford et al., 2010) during subsequent injection and blood sampling. We hypothesize that trained mice are less stressed than mice handled using traditional handling methods. In addition, we assess the usefulness of the MGS during non-painful as well as painful handling procedures. Here, we adapted this scoring method to assess stress and discomfort in mice, by focusing on the ear and eye categories of the scoring system.

2. Materials and methods

2.1. Animals and housing

Twenty male and 20 female, 4-week-old, CD1 mice were purchased from Charles River where they were tail lifted. The mice were randomized into groups of two or three per cage. Randomization was done by placing the first mouse lifted from their travel cage in group 1, the second in group 2, the third in group 1, etc. This was done within each gender group so that there were 20 animals per group (10 males and 10 females). The mice were housed in Macrolon 3H cages with bedding (Aspen bedding), nesting material (happy mats and sizzle nest) and a cardboard house and tunnel. They were provided standard chow and tap water ad libitum. Their cages were changed once weekly and they were maintained with a 12 h light/dark cycle, temperature between 19 and 21°C, and humidity of 40–70%. The study was approved by the Swedish Research Animal Ethics Committee (Stockholms södra djurförsöksetiska nämnd).

2.2. Study design

In an experiment setting, the facial expressions of trained, cup lifted (test group) and non-trained, tail lifted (control group) mice were compared during common research procedures; namely subcutaneous (s.c.) injection and tail vein blood sampling (Figure 1A). The mice were handled by the same female technician for all procedures and all staff interacting with the mice were also female. The group allocation was known by the animal handlers during conduction of the experiment, i.e., in training sessions as well as s.c. injection and blood sampling.

The control group was handled using traditional handling techniques. This means that the mice were acclimated for 1 week and had daily observations through the cage, followed by a thorough examination once weekly. This was accompanied by regular cage changes. These mice were always lifted by their tails, including during cage changes.

The test group was acclimated for 1 week, thereafter, they were trained according to a schedule. In the schedule, mice were trained five times a week for 3 weeks (before s.c. injection) and then trained for a further 2 weeks (a total of 5 weeks of training) before blood sampling. The training procedure was designed to prepare the mice for dosing and sampling procedures commonly used in toxicological studies: the mice were cupped in the technician's hand and put on a soft piece of fabric/soft pad placed on the procedure table. The skin was lifted/pinched, simulating skin lifting at subcutaneous injection, at four possible injection sites and the mouse was cupped in the hand again and transferred back to the cage (Supplementary Video 1).

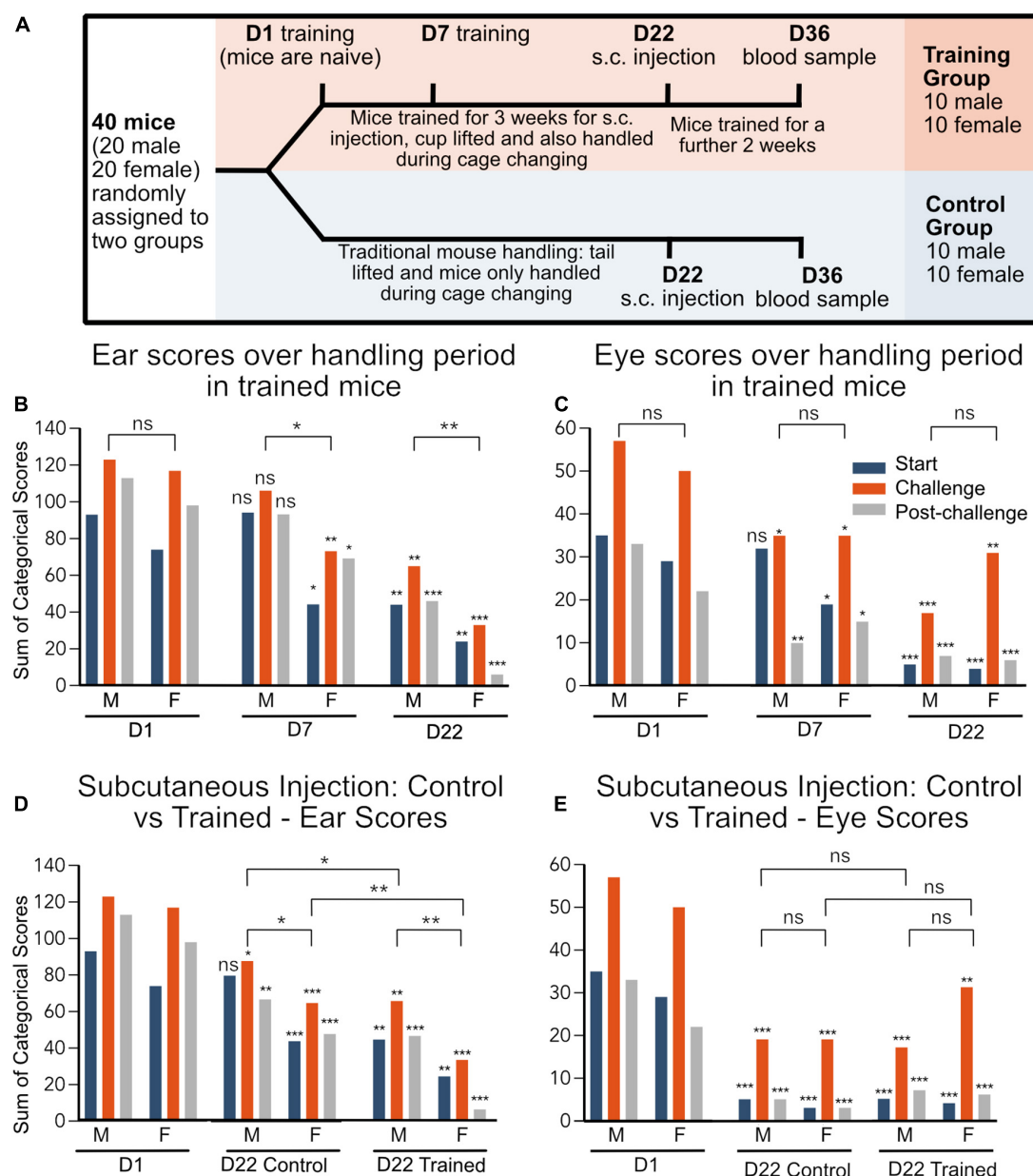


FIGURE 1

(A) Experimental timeline. D1 of training is used as a baseline as this is the first handling session. (B–E) Data are represented as the sum of categorical scores: the sum of facial scores from all evaluators (7 evaluators for ear and 6 evaluators for eye) for all mice in each treatment group ($n = 10$). Maximum possible score for ear: 140, maximum possible score for eye: 120. * $p < 0.05$, ** $p < 0.01$, *** $p < 0.001$. Significance indicated directly above each bar indicates comparison to Day 1 category of the same sex group and handling observation, e.g., start, challenge, and post-challenge. Comparisons between groups for sex during training effect (combined start, challenge, and post-challenge scores) are indicated by lines above the bars. D1, day 1; D22, day 22 and corresponds to s.c. injection.

Each session lasted approximately 8–10 seconds. The mice were always lifted by cupping, including during cage changes.

After 3 weeks of training, both groups were injected subcutaneously, but no substance was administered. The test group was then trained for a further 2 weeks (a total of 5 weeks of training) and on day 36, mice from both groups had blood sampled *via* the tail vein (Figure 1A). The subcutaneous injections and blood sampling *via* the tail vein were performed using a non-restrained method in all groups. Here, the mouse was placed on a soft piece of fabric on the lab bench where all training and experimental procedures were performed. The injections and sampling were done in groups of 10 according to the treatment groups.

Each animal in the test group was filmed at the first and seventh day of training, and each mouse from both groups (test and control) were filmed at day 22 and day 36, when injected subcutaneously and blood was sampled intravenously, respectively.

2.3. Scoring protocol

Ear scoring and eye scoring were performed using a three grade scale from the MGS (Langford et al., 2010): 0 = normal ear position and eye appearance (Supplementary Videos 1, 2), 1 = slightly changed ear position and slightly altered eye appearance

([Supplementary Videos 3, 4](#)) and 2 = totally changed ear position and altered eye appearance ([Supplementary Videos 5, 6](#)). Example videos of blood sampling can be seen in [Supplementary Video 7](#) (control) and [Supplementary Video 8](#) (trained).

Each animal was scored at three time points in each film: before, during and after the challenge (pinch/injection/needle puncture). The scoring was done by seven evaluators, all of them experienced animal technicians working with mice in toxicity studies (see [Supplementary Table 1](#) for an example of the scoring sheet).

The films were randomized, all identifiers removed and shown to all evaluators at the same occasion. All films were displayed twice, and evaluators registered their score on separate sheets without conferring with each other. Ear and eye scores were recorded in the same viewing session. The evaluators scored in total 120 films (80 films from the trained group and 40 from the non-trained group). In addition, as an internal validation of the scoring procedure, 16 of these films were randomly selected and displayed twice, once in the beginning of the session and a second time at the end to evaluate the scoring stability over the day. The evaluators' individual scoring was also compared.

2.4. Statistics

Each mouse was considered a single experimental unit and no unit or data point was excluded during the analysis, thus the sample size was 10, unless stated otherwise.

The results of both ear and eye scores were analyzed separately and grouped by sex, treatment (and day) and by handling event (pre-challenge, challenge, and post-challenge). Comparisons between groups used individual scores from the evaluators and were treated as three-level ordinal variables (Score 0, 1, 2). Group comparisons were performed using Ordinal Logistic Regression (OLR) ([Venables and Ripley, 2002](#)) using the MASS function¹ in RStudio (2022.07.1 Build 554). Significance values, expressed as *p*-values, were derived from an ANOVA with a *post hoc* Chi-squared test comparing the null-hypothesis. All regression coefficients from the OLR are set to zero to the OLR derived from the group comparisons. The observed *p*-values are reported as not significant (ns) ($p \geq 0.05$) or significant at $p < 0.05$, $p < 0.01$, and $p < 0.001$.

For the evaluation of training effect on specific responses, pre-challenge, challenge, and post-challenge responses were compared to their day 1, within-sex response. For the evaluation of sex effects and overall training effects all within-sex scores (pre-challenge, challenge, and post-challenge) were grouped for each training/evaluation occasion (day). Overall training effects and sex differences were evaluated using these grouped scores.

Evaluation of the uniformity of observer scores ($n = 7$ for ear and $n = 6$ for eye) was performed using OLR in RStudio (2022.07.1 Build 554) with a chi-squared statistic with the group of scores for each observer across all test conditions grouped and compared to all other observers.

To control for observer scoring consistency, 16 films were displayed twice, to evaluate the scoring stability over the day ($n = 16$). Normality was evaluated using the Shapiro–Wilk test. The scores recorded at the start of the session were compared to those scored at the end of the session using a repeated measures

t-test (normal distribution) or a repeated measures Mann Whitney test (non-normal distribution). This was conducted in GraphPad Prism Version 9.

3. Results

3.1. Trained mice display less discomfort than non-trained mice

At day 22, the mice had a s.c. injection, the facial scores were recorded and, later, scored. Both male and female trained mice had lower ear and eye scores, when compared to the first day of training for this procedure ([Figures 1B, C](#)). Furthermore, when the facial expressions of the control vs. trained group were compared at D22, trained mice had lower ear scores than the control mice, showing reduced discomfort ([Figure 1D](#)). However, there were no differences in eye score between trained and control mice ([Figure 1E](#)).

The facial expressions of the control group were also compared with that of the training group's facial scores on day 1. Facial scores on day 1 provide a baseline for all the mice as this was the first time that the trained mice were handled, thus at this point, they are considered naïve ([Figure 1A](#)). Interestingly, at day 22, the untrained mice had lower ear and eye scores when compared to day 1 of the training group ([Figures 1D, E](#)). This suggests that, despite not being trained for handling, the mice became habituated to their environment over the 22-day period, which also impacted the facial scores and level of discomfort during s.c. injection.

On day 36, the mice had blood sampled from their tail vein—a procedure for which neither group was specifically trained. The changes in facial expression seen here in the trained group is a result of habituation to general handling. Here, trained mice had lower ear scores than control mice ([Figure 2A](#)) and trained male mice had lower eye scores compared to untrained male mice ([Figure 2B](#)). However, unexpectedly, the female eye score from the trained mice was higher than that of the untrained mice ([Figure 2B](#)).

3.2. Ear scoring was more sensitive than eye scoring, in this study

Data are represented in the graphs as the sum of categorical scores: the sum of facial scores from all evaluators (7 evaluators for ear and 6 evaluators for eye) for all mice in each treatment group ($n = 10$) (mean score and SD for individual groups in [Supplementary Table 2](#)). The maximum possible score is 140 and 120 for the ear and eye, respectively. The maximum recorded ear score was 123 and the maximum recorded eye score was 57. There was also a difference in distribution of the data with a minimum of 6 for the ear and 1 for the eye score. Furthermore, the mean ear score was 73.5 for the ear and 19 for the eye. The larger range of distribution ([Figure 2C](#)) in the ear score, compared to the eye score, suggests that the ear score may be a more sensitive measure of discomfort than the eye scores overall. However, in response to challenge, the eye scores appear to be a more sensitive measure of pain/perceived pain ([Figures 1C, E, 2B](#)).

¹ <https://www.stats.ox.ac.uk/pub/MASS4/>

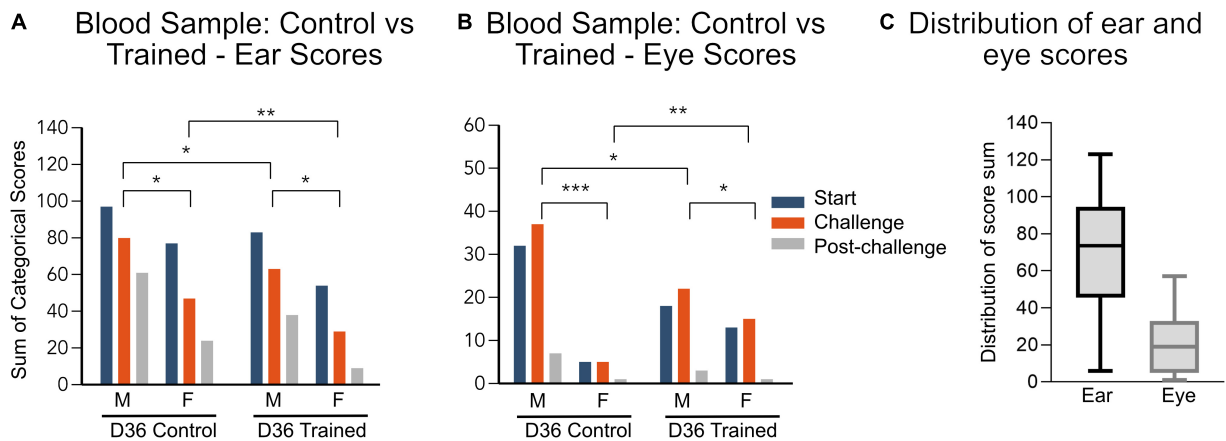


FIGURE 2

(A,B) Data are represented as the sum of categorical scores: the sum of facial scores from all evaluators (7 evaluators for ear and 6 evaluators for eye) for all mice in each treatment group ($n = 10$). Maximum possible score for ear: 140, maximum possible score for eye: 120. Comparisons between groups were performed using grouped data for each sex and training/control group. Significant differences between groups are indicated by lines above the bars, * $p < 0.05$, ** $p < 0.01$, *** $p < 0.001$. D1, day 1; D36, day 36 and corresponds to tail vein blood sample. (C) Distribution of all the ear and eye scores, combining treatment group and sex.

3.3. Females had lower ear scores after training, compared to males

There was no difference in baseline ear and eye scores in male and female mice at day 1. However, after 7 days of training, mimicking subcutaneous injection, there was a reduction in ear score in females but not in males (Figure 1B). Compared to day 1, both male and female mice had reduced challenge and post-challenge eye scores with only the females having reduced start eye scores (Figure 1C).

Only at the subcutaneous injection, after 22 days of training, was the ear score reduced in the male mice (Figure 1B), suggesting that males may require more training sessions than females to reach the same level of habituation to handling. On the other hand, after 22 of training, the eye scores were reduced in both males and females at all time points (start, challenge and post-challenge) (Figure 1C).

In both the trained and untrained group, the females had overall lower scores in both the ear and eye score categories compared to the males. However, this was only statistically significant when evaluated using the ear scores.

3.4. There was no significant difference between scores performed by different test persons

Evaluation of the distribution of scores between observers across all films in this study demonstrated that there does not appear to be any significant difference in the distribution of scores from any one observer and the remaining group of observers or between individual observers.

In addition, there was no significant change in the scores for the 16 films evaluated at the beginning of the day, when compared to the end of the day (an indication of score stability) for the ear score. However, the eye scores recorded at the end of the session were lower (mean 8.3, max 17, min 1) compared to the beginning of the session (mean 10.4, max 24, min 1) (Supplementary Figure 1).

4. Discussion

4.1. Habituated animals are less stressed

In the present study, trained mice were handled five times per week for 3–5 weeks, and during the 8–10 second handling sessions, the handler mimicked procedures associated with a subcutaneous injection: partial restraint by the base of the tail, and four skin lifts on both shoulders and flanks. The control group was handled according to traditional handling procedures, e.g., tail lifted and only handled during cage changing. Trained mice expressed less distress than the control mice during experimental procedures, when evaluated using the orbital tightening and ear position categories of the MGS. However, the ear score was the most sensitive measurement of distress.

Animals may be expected to either sensitize (show an increased stress response over time) or habituate (show a decreased stress response) to a stimulus (McSweeney and Murphy, 2009). Whether one or the other occurs depends on how the introduction to the potentially aversive stimulus is carried out, as well as how aversive it is. In the current study, the aversiveness of the procedure was reduced by lifting the mice in cupped hands, as well as minimizing restraint: the animal was placed on a soft piece of fabric—a possible explanation as to why the animals habituated rather than sensitized in the present study.

Acclimation to certain experimental procedures or situations has previously been shown (Westlund, 2015; Kärrberg et al., 2016; Lindhardt et al., 2022). For example, stress-associated weight change in mice was avoided by acclimating mice to the oral gavage procedure, either by sham gavage or by restraint (Kärrberg et al., 2016). However, the training can be stressful. Body weight loss was observed during the acclimation compared to the untrained mice, which indicates that the training, including restraint, was stressful. Restraint for injections and blood sampling triggers stress in mice (Meijer et al., 2006). Consequently, habituation to general handling should be the

goal of the training sessions, not necessarily training for the specific procedure.

Acclimation to this particular short training procedure is expected to generalize to a variety of different experimental procedures, especially procedures which allow for the mice to be in contact with the fabric/soft pad. During the training sessions, the mice became accustomed to a sequence of events. Firstly, they were enclosed by a gloved hand and removed from the cage—an important step expected to occur with any type of procedure. Within a few seconds, they were placed on a soft fabric pad on the procedure table. In this situation, the tactile, visual, and olfactory sensations of the environment may dominate and, to some extent, even overshadow the subsequent handling/skin lifting/pinching. Finally, after a few seconds, the animals were returned to their cage. As a result, we expect that the mice would have learned that the whole experience (being enclosed within gloved hands, sitting on a soft pad for a few moments and experiencing a plethora of sensations, returning to their home cage) was highly predictable and therefore less stressful over time. Consequently, if we were to keep most of the sequence intact, then we would expect the calming effect of the training to generalize to several types of experimental procedures in the trained mice. This generalized effect of the handling was demonstrated by the reduced stress during blood sampling on habituated animals compared to controls. Such carry-over effects of handling for procedures other than those the animals were specifically trained for has already been previously demonstrated (Gouveia and Hurst, 2019; Marcotte et al., 2021).

Mice have also been successfully trained using intricate positive reinforcement protocols (Leidinger et al., 2017). These require time and trainer skill; in a clicker training study by Leidinger et al. (2017), each training session was 5 min, and the training followed a 38-step training manual. This illustrates that training using operant procedures requires some skill from the handler. Most animal technicians, although skilled in technical laboratory animal procedures such as blood sampling, might not have the training to successfully shape operant responses using positive reinforcement and successive approximations of desired responses (shaping).

However, the acclimation procedure used in the current study was simply exposing the animal to the future experimental procedure multiple times before the experiment started, albeit replacing the final injection with four skin lifts. Furthermore, each training session was only 8–10 seconds long. Two unique additions in the current study that may not be in use in all facilities was to (a) lift the mouse in a cupped hand, and (b) put the mouse on a soft pad rather than use restraint during the experimental procedure. Both techniques require little training to master for the handler, and effectively reduce stress for the animal.

This technique could be further refined by combining systematic desensitization (gradually introducing the handling/stimulus over several training sessions) with counter conditioning (immediately following each training session with access to a desired resource, such as food treats) to prevent and diminish fear and stress. This approach may diminish the stress scores observed in the current study during the initial days of acclimation. Further investigation to reduce the training time is also required for training to be practical and economically viable. Recently, a 3-day training technique was developed to habituate mice to handling (Marcotte et al., 2021). This method involves increased interaction with an individual mouse over a period of 3 days, with different milestones to reach before

moving to the next step. This method could be tested, using facial expressions to determine the optimal number of training sessions needed per strain and sex.

4.2. The mouse grimace scale measures not only pain, but also distress/fear/discomfort

In this study, the positive effects of training laboratory mice were successfully assessed by the ear position of the MGS. The ear score was a more sensitive measure of discomfort, compared to the eye score. Furthermore, the ear score was more stable over the duration of the scoring session, when evaluated using the internal validation test. However, the eye score may be a more sensitive marker of pain or perceived pain. This is evident by the clear peak in eye scores, but not ear scores, during s.c. injections and pinching (Figures 1C, E).

Interestingly, there was also a difference in peak score patterns between the s.c. injection and tail vein blood sampling. During the training sessions and s.c. injection, the ear and eye scores peaked during the challenge. However, during the blood sampling on day 36, the ear score peaked before the challenge, and the eye score peaked at the challenge. This could be attributed to slight differences in handling the mice in the different procedures. During training and s.c. injection, the mouse is briefly held at the tail base, quickly followed by an injection and or pinch. In contrast, during the blood sampling, the mouse is restrained by the tail base for a longer period, during which the tail vein is identified before puncture. This longer duration of restraint may cause additional distress which exceeds that of skin puncture. If the ear is a more sensitive measurement of discomfort, and not pain, this would explain why the peak score was before the challenge and the eye score still peaked during the challenge.

Changes in facial expression is an interspecies indicator of pain and emotional status (Zych and Gogolla, 2021) and facial scoring systems in numerous animal species have been developed to improve animal welfare (Boissy et al., 2011; Bellegarde et al., 2017; Marcet Rius et al., 2018; Lambert and Carder, 2019). The MGS system was initially developed to assess pain in mice (Langford et al., 2010) but, here, the orbital tightening and ear position categories of the MGS were used to assess fear and distress.

The ear is the most mobile part of the face in many animal species and easily assessed. Particular attention to ear position has been given to evaluate emotional states of farm animals. For example, Boissy et al. (2011) found that negative emotional states in sheep were associated with the ears being pulled back and, in positive states, the ears were pulled forward. Similar associations between emotional state and ear position have been found in goats (Bellegarde et al., 2017), cows (Lambert and Carder, 2019), and pigs (Marcet Rius et al., 2018). However, there has been limited investigation into the association between facial expression and emotional states of laboratory animals. Finlayson et al. (2016) used the rat grimace score in combination with other measurements to assess the effect of positive interaction such as tickling on the facial expression of rats. They found that the positive treatment was associated with a pinker ear color and wider ear angle (Finlayson et al., 2016).

In mice, Defensor et al. (2012) used the MGS to evaluate their emotional state in different contexts of stress; such as predator stress,

intruder stress and from the discomfort due to whisker stimulation with a brush, etc. Some components of the MGS, such as the ear position and orbital tightening were strongly associated with direct contact or potential for contact, e.g., when the mouse whiskers were directly touched with a brush, two unfamiliar mice were placed opposite each other across a barrier, or an intruder mouse was placed in the home cage. In contrast, the nose bulge and cheek swell scores were increased more with potential exposure to a predator, i.e., when exposed to the scent of a cat or exposure to a rat across a barrier. This supports our use of the orbital tightening and ear position score to assess mild to moderate stress during handling.

Dolensek et al. (2020) further investigated this link between facial expression and emotional state of mice using image analysis and machine-learning as an alternative to the MGS. They showed that facial expressions are reliable indicators of emotional states and confirmed this thorough optogenetic stimulation of subregions and projections of the insular cortex. They also used optogenetic stimulation to manipulate γ -aminobutyric acid-releasing neurons in the ventral pallidum, which process reward to pleasant stimuli. Although image analysis of facial expressions can provide an objective assessment of the mouse's emotional state, it requires special equipment, expertise which can only be assessed post-handling.

Most methods used to evaluate the success of habituation/gentle-handling techniques on the mouse's stress levels and welfare often require specialized behavioral or biochemical tests. For example, the elevated plus maze test, handler interaction tests, fecal or blood corticosteroid levels, etc. Here, by handlers focusing on the ear position categories of the MGS, they will be able to assess the response of the mouse to their handling/training during each interaction. This is thus a simple, cost-effective tool which can be used daily to evaluate the level of stress in mice to improve welfare.

4.3. Sex difference in response to training

Despite having the same baseline facial expression scores, trained, female mice had, overall, lower scores compared to the males in both the ear and eye score categories. They also had a significant reduction in facial scores after the first week of training, which was not seen in the male mice until day 22.

To improve rigor and translatability of preclinical research, many grant funding organizations now require applicants to include both male and female animals in the experimental design (Shansky and Murphy, 2021). This means that more female mice are expected to be used in preclinical research than in the past. As a result of these funding changes, there is also increasing evidence that male and female, animals and humans alike, respond differently to stress (Bangasser and Wicks, 2017). This evidence supports our findings that male mice respond differently to training compared to female mice.

However, the effects of sex on the number of training sessions required for habituation have not been reported. For example, in the 3-day training technique by Marcotte et al. (2021), habituated male C57BL/6 mice had increased voluntary interaction and decreased anxiety-like behaviors (measured by novelty-suppressed feeding and elevated plus maze), compared to the tail lifted groups. In females, training did not affect these measurements, but did result in decreased serum cortisol levels after 3 days of handling. However, the male and female groups used in that study were different ages,

confounding these sex differences (Marcotte et al., 2021). In another study, testing a 14-day habituation protocol of C57BL/6 mice to magnetic resonance imaging (MRI), male mice had a significant decrease in heart rate after 10 days of training, and females, after 11 days. Females had higher fecal corticosterone metabolite levels, compared to the males, suggesting that they were more stressed throughout the training protocol. However, there were no other indications that the females habituated to the MRI simulation at a different rate than the males (Lindhardt et al., 2022).

4.4. Future areas of research

Here, we show that the ear score, a component of the MGS, is a sensitive method to measure distress in mice. However, further studies are needed to refine this scoring system to focus on signs of distress, rather than pain. In addition, strain differences should also be investigated. Here, only female handlers worked with the mice and handler gender has been shown to influence the level of stress in mice (Sorge et al., 2014), consequently the effect of handler gender on the facial scores should also be studied.

A handful of studies have shown that the methods used to lift mice can affect endpoints used in biomedical (Ghosal et al., 2015; Ono et al., 2016) and behavioral (Novak et al., 2015; Gouveia and Hurst, 2017; Ueno et al., 2020) research. Consequently, a follow up study should assess the effects of training on biochemical parameters of interest in a biomedical study, e.g., severity of a disease model, measurement of metabolic parameters, etc.

4.5. Limitations

The required 3–5-week training duration may be prohibitively long and time consuming within certain fields. In future studies, the training duration could be considerably reduced as an improvement in facial scores, in females, was already seen on day seven. Perhaps, the facial scoring used in this study could be more widely adopted, when combined with the 3-day training protocol (Marcotte et al., 2021). Furthermore, there may have been some group effect as, for logistical reasons, mice were injected and sampled in their treatment groups. Further studies should aim to inject/sample the mice in mixed groups.

The mice were trained in the mornings, during their light cycle/rest period which may have effects on their sleep. This may be a factor which needs to be addressed in all future training protocols used for crepuscular, nocturnal animals. Training should be done at the beginning/end of the dark cycle or during the dark cycle, possibly using a reversed-light cycle or time-shift approach (Hawkins and Golledge, 2018). Although tested to evaluate sleep deprivation in mice, Longordo et al. (2011) did investigate the effects of 3 min disturbance of sleep in mice during the light phase, over 6-days. This is similar to what mice would experience during a training protocol. On all six handling days, there was approximately 25% reduction in resting time and serum cortisone levels were raised. Consequently, routine handling of mice during the light cycle could also introduce confounding effects in behavioral and biomedical studies and needs to be considered when establishing a training protocol (Hawkins and Golledge, 2018).

Lastly, this study investigated training in cup lifted mice and compared it to untrained tail lifted mice. Consequently, some of the changes seen in facial expressions between the two groups may not purely be due to training, but also be influenced by the handling method used.

5. Conclusion/Summary

Habituating mice, through training, to common laboratory procedures for 8–10 seconds during the acclimation period significantly reduces stress. This study was conducted using CD1 mice as they are a general-purpose mouse, commonly used for genetic, toxicology and pharmacology research. However, training is expected to be successful in other strains, such as the C57/BL6 which have previously been shown to be receptive to habituation protocols (Marcotte et al., 2021; Lindhardt et al., 2022). We suggest that general training and gentling protocols, during acclimatization, would reduce stress during experimental situations and therefore improve animal wellbeing. The gentle handling enables whole experiments to be performed with minimum stress placed upon animals and animal handlers, with unrestrained animals. This refinement is also followed by reduction, as better handling during experimental procedures such as dosing, and blood sampling reduces the risk of mistakes at dosing as well as lost samples. Consequently, the number of animals per group could be reduced to a minimum. Furthermore, lowered stress could potentially lead to reduced sample variability, thus requiring less animals while still maintaining statistical power.

Ear scoring is a sensitive, easily observable, and useful tool for assessing lower levels of distress. This method could therefore be an important tool when assessing improvements of animal welfare in 3R projects and method developments.

Data availability statement

The raw data supporting the conclusions of this article will be made available by the authors, without undue reservation.

Ethics statement

The animal study was reviewed and approved by Swedish Research Animal Ethics Committee (Stockholms södra djurförsöksetiska nämnd).

Author contributions

ET designed and conducted the study as well as collected the data. JS, KW, and ET wrote the initial draft of the manuscript. SB performed the final statistical analyses. CB conducted the study. GN designed the scoring system and performed the initial statistical

analysis. All authors contributed to the article and approved the submitted version.

Funding

This research was performed as an internal research project at Global Safety Assessment, AstraZeneca R&D, Södertälje, Sweden, which was closed in 2013.

Conflict of interest

When the study was conducted, ET, SB, and CB were employed by AstraZeneca. GN is still currently employed by AstraZeneca. SB is employed by Chemotargets SL. The authors declare that this study was funded by AstraZeneca. The study was designed and conducted by employees of AstraZeneca. Analysis, decision to publish and preparation of the manuscript was conducted independently of AstraZeneca.

The remaining authors declare that the research was conducted in the absence of any commercial or financial relationships that could be construed as a potential conflict of interest.

Publisher's note

All claims expressed in this article are solely those of the authors and do not necessarily represent those of their affiliated organizations, or those of the publisher, the editors and the reviewers. Any product that may be evaluated in this article, or claim that may be made by its manufacturer, is not guaranteed or endorsed by the publisher.

Supplementary material

The Supplementary Material for this article can be found online at: <https://www.frontiersin.org/articles/10.3389/fnbeh.2023.1109886/full#supplementary-material>

SUPPLEMENTARY FIGURE 1

Sixteen films were displayed twice, once at the start of the session and a second time at the end to evaluate the scoring stability over the day. Data are represented as the sum of categorical scores: the sum of facial scores from all evaluators (7 evaluators for ear and 6 evaluators for eye) for all mice in each treatment group ($n = 10$) and for all time points in each film (start + challenge + post-challenge). (A,C) Total scores for each mouse and day are shown at the start and end of the session. (B,D) Violin plots show changes in distribution of scores between the start and end of the scoring session. $*p < 0.05$.

SUPPLEMENTARY TABLE 1

Example of facial scoring sheet used in the scoring session.

SUPPLEMENTARY TABLE 2

Score per mouse (sum of scores from evaluators) separated by treatment group, day, and time point in the film (start, challenge, and post-challenge). Values are presented as mean \pm standard deviation.

References

- Bangasser, D. A., and Wicks, B. (2017). Sex-specific mechanisms for responding to stress. *J. Neurosci. Res.* 95, 75–82.
- Baumans, V., and Van Loo, P. L. (2013). How to improve housing conditions of laboratory animals: the possibilities of environmental refinement. *Vet. J.* 195, 24–32. doi: 10.1016/j.tvjl.2012.09.023
- Bellegarde, L. G. A., Haskell, M. J., Duvaux-Ponter, C., Weiss, A., Boissy, A., and Erhard, H. W. (2017). Face-based perception of emotions in dairy goats. *Appl. Anim. Behav. Sci.* 193, 51–59. doi: 10.1016/j.applanim.2017.03.014
- Boissy, A., Aubert, A., Désiré, L., Greiveldinger, L., Delval, E., and Veissier, I. (2011). Cognitive sciences to relate ear postures to emotions in sheep. *Anim. Welf.* 20:47.
- Brown, M., Carbone, L., Conlee, K. M., Dawkins, M. S., Duncan, I. J., Fraser, D., et al. (2006). Report of the working group on animal distress in the laboratory. *Lab Anim.* 35, 26–30. doi: 10.1038/labani0906-26
- Cloutier, S., Wahl, K., Baker, C., and Newberry, R. C. (2014). The social buffering effect of playful handling on responses to repeated intraperitoneal injections in laboratory rats. *J. Am. Assoc. Lab. Anim. Sci.* 53, 168–173.
- Defensor, E. B., Corley, M. J., Blanchard, R. J., and Blanchard, D. C. (2012). Facial expressions of mice in aggressive and fearful contexts. *Physiol. Behav.* 107, 680–685. doi: 10.1016/j.physbeh.2012.03.024
- Dolensek, N., Gehrlach, D. A., Klein, A. S., and Gogolla, N. (2020). Facial expressions of emotion states and their neuronal correlates in mice. *Science* 368, 89–94. doi: 10.1126/science.aaz9468
- European Commission. (2022). *Summary Report on the statistics on the use of animals for scientific purposes in the Member States of the European Union and Norway in 2019*. Belgium: European Commission Brussels.
- Finlayson, K., Lampe, J. F., Hintze, S., Würbel, H., and Melotti, L. (2016). Facial indicators of positive emotions in rats. *PLoS One* 11:e0166446. doi: 10.1371/journal.pone.0166446
- Fridgeirsdottir, G. A., Hillered, L., and Clausen, F. (2014). Escalated handling of young C57BL/6 mice results in altered Morris water maze performance. *UPS J. Med. Sci.* 119, 1–9. doi: 10.1090/03009734.2013.847511
- Ghosal, S., Nunley, A., Mahbod, P., Lewis, A. G., Smith, E. P., Tong, J., et al. (2015). Mouse handling limits the impact of stress on metabolic endpoints. *Physiol. Behav.* 150, 31–37. doi: 10.1016/j.physbeh.2015.06.021
- Gouveia, K., and Hurst, J. L. (2017). Optimising reliability of mouse performance in behavioural testing: the major role of non-aversive handling. *Sci. Rep.* 7:44999. doi: 10.1038/srep44999
- Gouveia, K., and Hurst, J. L. (2019). Improving the practicality of using non-aversive handling methods to reduce background stress and anxiety in laboratory mice. *Sci. Rep.* 20305. doi: 10.1038/s41598-019-56860-7
- Hawkins, P., and Golledge, H. D. (2018). The 9 to 5 Rodent- Time for Change? Scientific and animal welfare implications of circadian and light effects on laboratory mice and rats. *J. Neurosci. Methods* 300, 20–25. doi: 10.1016/j.jneumeth.2017.05.014
- Hawkins, P., Morton, D., Burman, O., Dennison, N., Honess, P., Jennings, M., et al. (2011). A guide to defining and implementing protocols for the welfare assessment of laboratory animals: eleventh report of the BVAAWF/FRAME/RSPCA/UEAW Joint Working Group on Refinement. *Lab. Anim.* 45, 1–13. doi: 10.1258/la.2010.010031
- Hurst, J. L., and West, R. S. (2010). Taming anxiety in laboratory mice. *Nat. Methods* 7, 825–826.
- Kärberg, L., Andersson, L., Kastenmayer, R., and Ploj, K. (2016). Refinement of habituation procedures in diet-induced obese mice. *Lab. Anim.* 50, 397–399. doi: 10.1177/0023677216631459
- Koolhaas, J. M., de Boer, S. F., Coppens, C. M., and Buwalda, B. (2010). Neuroendocrinology of coping styles: towards understanding the biology of individual variation. *Front. Neuroendocrinol.* 31:307–321. doi: 10.1016/j.yfrne.2010.04.001
- Lambert, H., and Carder, G. (2019). Positive and negative emotions in dairy cows: Can ear postures be used as a measure? *Behav. Proces.* 158, 172–180. doi: 10.1016/j.beproc.2018.12.007
- Langford, D. J., Bailey, A. L., Chanda, M. L., Clarke, S. E., Drummond, T. E., Echols, S., et al. (2010). Coding of facial expressions of pain in the laboratory mouse. *Nat. Methods* 7, 447–449.
- Leach, M. C., Klaus, K., Miller, A. L., Scotto, di Perrotolo, M., Sotocinal, S. G., et al. (2012). The assessment of post-vasectomy pain in mice using behaviour and the mouse grimace scale. *PLoS One* 7:e35656. doi: 10.1371/journal.pone.0035656
- Leidinger, C., Herrmann, F., Thöne-Reineke, C., Baumgart, N., and Baumgart, J. (2017). Introducing clicker training as a cognitive enrichment for laboratory mice. *JOVE* 12:e55415. doi: 10.3791/55415
- Lindhardt, T. B., Gutiérrez-Jiménez, E., Liang, Z., and Hansen, B. (2022). Male and female c57bl/6 mice respond differently to awake magnetic resonance imaging habituation. *Front. Neurosci.* 16:853527. doi: 10.3389/fnins.2022.853527
- Longordo, F., Fan, J., Steimer, T., Kopp, C., and Lüthi, A. (2011). Do mice habituate to “gentle handling”? A comparison of resting behavior, corticosterone levels and synaptic function in handled and undisturbed C57BL/6 mice. *Sleep* 34, 679–681. doi: 10.1093/sleep/34.5.679
- MacArthur Clark, J. (2018). The 3Rs in research: a contemporary approach to replacement, reduction and refinement. *Br. J. Nutr.* 120, S1–S7. doi: 10.1017/S0007114517002227
- Marcel Rius, M., Pageat, P., Bienboire-Frosini, C., Teruel, E., Monneret, P., Leclercq, J., et al. (2018). Tail and ear movements as possible indicators of emotions in pigs. *Appl. Anim. Behav. Sci.* 205, 14–18. doi: 10.1016/j.applanim.2018.05.012
- Marcotte, M., Bernardo, A., Linga, N., Pérez-Romero, C. A., Guillo, J. L., Sibille, E., et al. (2021). Handling techniques to reduce stress in mice. *J. Vis. Exp.* e62593. doi: 10.3791/62593
- McSweeney, F. K., and Murphy, E. S. (2009). Sensitization and habituation regulate reinforcer effectiveness. *Neurobiol. Learn. Mem.* 92, 189–198.
- Meijer, M., Spruijt, B., Van Zutphen, L., and Baumans, V. (2006). Effect of restraint and injection methods on heart rate and body temperature in mice. *Lab. Anim.* 40, 382–391. doi: 10.1258/002367706778476370
- Nakamura, Y., and Suzuki, K. (2018). Tunnel use facilitates handling of ICR mice and decreases experimental variation. *J. Vet. Med. Sci.* 80, 886–892. doi: 10.1292/jvms.18-0044
- Novak, J., Baloo, J. D., Melotti, L., Rommen, J., and Würbel, H. (2015). An exploration based cognitive bias test for mice: effects of handling method and stereotypic behaviour. *PLoS One* 10:e0130718. doi: 10.1371/journal.pone.0130718
- Ono, M., Sasaki, H., Nagasaki, K., Torigoe, D., Ichii, O., Sasaki, N., et al. (2016). Does the routine handling affect the phenotype of disease model mice? *Jap. J. Vet. Res.* 64, 265–271.
- Rowan, A. N. (1990). Refinement of animal research technique and validity of research data. *Fundam. Appl. Toxicol.* 15, 25–32. doi: 10.1016/0272-0590(90)90159-H
- Shansky, R. M., and Murphy, A. Z. (2021). Considering sex as a biological variable will require a global shift in science culture. *Nat. Neurosci.* 24, 457–464. doi: 10.1038/s41593-021-00806-8
- Sorge, R. E., Martin, L. J., Isbester, K. A., Sotocinal, S. G., Rosen, S., Tuttle, A. H., et al. (2014). Olfactory exposure to males, including men, causes stress and related analgesia in rodents. *Nat. Methods* 11, 629–632. doi: 10.1038/nmeth.2935
- Strelakova, T., Spanagel, R., Dolgov, O., and Bartsch, D. (2005). Stress-induced hyperlocomotion as a confounding factor in anxiety and depression models in mice. *Behav. Pharmacol.* 16, 171–180. doi: 10.1097/00008877-200505000-00006
- Ueno, H., Takahashi, Y., Suemitsu, S., Murakami, S., Kitamura, N., Wani, K., et al. (2020). Effects of repetitive gentle handling of male C57BL/6NCr mice on comparative behavioural test results. *Sci. Rep.* 10, 1–13. doi: 10.1038/s41598-020-60530-4
- Venables, W. N., and Ripley, B. D. (2002). *Modern applied statistics with S*. New York, NY: Springer.
- Westlund, K. (2015). Training laboratory primates – benefits and techniques. *Primate Biol.* 2, 119–132. doi: 10.5194/pb-2-119-2015
- Wolfensohn, S., Hawkins, P., Lilley, E., Anthony, D., Chambers, C., Lane, S., et al. (2013). Reducing suffering in experimental autoimmune encephalomyelitis (EAE). *J. Pharmacol. Toxicol. Methods* 67, 169–176.
- Zych, A. D., and Gogolla, N. (2021). Expressions of emotions across species. *Curr. Opin. Neurobiol.* 68, 57–66. doi: 10.1016/j.conb.2021.01.003



OPEN ACCESS

EDITED BY

Annemarie Lang,
University of Pennsylvania, United States

REVIEWED BY

Valerie J. Bolivar,
Wadsworth Center, United States
Rafal Rygula,
Maj Institute of Pharmacology (PAS), Poland

*CORRESPONDENCE

Sophia Marie Quante
✉ sophia.quante@uni-muenster.de

[†]These authors have contributed equally to this work

SPECIALTY SECTION

This article was submitted to
Emotion Regulation and Processing,
a section of the journal
Frontiers in Behavioral Neuroscience

RECEIVED 30 November 2022

ACCEPTED 21 February 2023

PUBLISHED 16 March 2023

CITATION

Quante SM, Siewert V, Palme R, Kaiser S,
Sachser N and Richter SH (2023) The power of
a touch: Regular touchscreen training but not
its termination affects hormones and behavior
in mice. *Front. Behav. Neurosci.* 17:1112780.
doi: 10.3389/fnbeh.2023.1112780

COPYRIGHT

© 2023 Quante, Siewert, Palme, Kaiser, Sachser
and Richter. This is an open-access article
distributed under the terms of the [Creative
Commons Attribution License \(CC BY\)](#). The use,
distribution or reproduction in other forums is
permitted, provided the original author(s) and
the copyright owner(s) are credited and that
the original publication in this journal is cited, in
accordance with accepted academic practice.
No use, distribution or reproduction is
permitted which does not comply with these
terms.

The power of a touch: Regular touchscreen training but not its termination affects hormones and behavior in mice

Sophia Marie Quante^{1*†}, Viktoria Siewert^{1†}, Rupert Palme²,
Sylvia Kaiser¹, Norbert Sachser¹ and S. Helene Richter¹

¹Department of Behavioural Biology, University of Münster, Münster, Germany, ²Department of Biomedical Sciences, University of Veterinary Medicine, Vienna, Austria

Touchscreen-based procedures are increasingly used in experimental animal research. They not only represent a promising approach for translational research, but have also been highlighted as a powerful tool to reduce potential experimenter effects in animal studies. However, to prepare the animals for a touchscreen-based test, an often time-consuming training phase is required that has itself been shown to cause increased adrenocortical activity and anxiety-like behavior in mice. While these findings point at a potentially negative effect of touchscreen training at first glance, results have also been discussed in light of an enriching effect of touchscreen training. The aim of the present study was therefore to shed more light on recently reported touchscreen training effects, with a particular focus on the termination of the training routine. Specifically, we investigated whether the termination of regular touchscreen training could constitute a loss of enrichment for mice. Thus, we assessed fecal corticosterone metabolites (FCMs), exploratory-, anxiety-like and home cage behavior in touchscreen-trained mice in comparison to food restricted and *ad libitum* fed mice, as a restricted diet is an integral part of the training process. Furthermore, we compared these parameters between mice that were continuously trained and mice whose training was terminated 2 weeks earlier. Our results confirm previous findings showing that a mild food restriction increases the animals' exploratory behavior and shifts their activity rhythm. Moreover, touchscreen training was found to increase FCM levels and anxiety-like behavior of the mice. However, no effect of the termination of touchscreen training could be detected, a finding which contradicts the enrichment loss hypothesis. Therefore, we discuss two alternative explanations for the findings. Yet, the current state of knowledge is not sufficient to draw final conclusions at this stage. In compliance with the refinement endeavors for laboratory animals, further research should assess the severity of touchscreen procedures to ensure a responsible and well-founded use of animals for experimental purposes.

KEYWORDS

cognitive enrichment, anxiety-like behavior, glucocorticoids, anticipation, enrichment loss, stress inoculation, negative contrast, touchscreen technology

1. Introduction

Touchscreen-based procedures are increasingly used in animal research (Bussey et al., 2008). Due to the similarities to human testing techniques [e.g., CANTAB (Fray et al., 1996)], they hold a high translation potential, with some tasks being already successfully translated to rodents (Armbruster et al., 2012; Richter et al., 2014). Besides this, touchscreen

procedures have been highlighted as a powerful tool to reduce potential experimenter effects in animal studies, thereby representing an important refinement strategy (Richter et al., 2014). However, in order to prepare the animals for a touchscreen-based test, an often time-consuming and intense training phase is required that consists of several weeks of daily training (Richter et al., 2014). As it has already been shown that such routinely applied and predictable procedures can have extensive effects on the animals (Bassett and Buchanan-Smith, 2007), it cannot be excluded that the touchscreen training itself can also affect the experimental outcome. Indeed, there are two studies that already report an influence of regular touchscreen training on hormones and behavior in mice. Both show effects on hypothalamus-pituitary-adrenal (HPA) axis activity of touchscreen trained mice across the day, which was highest during the anticipation of a training session (Mallien et al., 2016; Krakenberg et al., 2021). Moreover, we reported increased anxiety-like behavior in touchscreen trained mice in a previous study (Krakenberg et al., 2021). At first glance, these findings might point at a detrimental effect of touchscreen training, indicating impaired welfare in these animals (Paul et al., 2005). However, in light of the so-called “stress inoculation” hypothesis, the findings regarding HPA axis activity could also indicate the opposite effect, namely an enriching effect of touchscreen training. More precisely, according to this hypothesis, mild daily stress is assumed to lead to a higher coping ability with environmental stressors, thus contributing to improved welfare (Crofton et al., 2015; Mallien et al., 2016). In line with these thoughts, we previously developed an alternative explanation, suggesting that an “enrichment loss effect” could account for the increased anxiety-like behavior in the touchscreen trained mice. More specifically, the tests to assess anxiety-like behavior were conducted with a temporal distance of 2 weeks to the termination of the touchscreen training. If the mice indeed perceived touchscreen training as enriching, a termination of training would pose a loss of enrichment, which might be reflected in increased anxiety-like behavior (Krakenberg et al., 2021). This explanation seems to be especially reasonable, as touchscreen training represents a cognitive challenge and cognitively active animals are assumed to be of greater risk to suffer from enrichment removal (Nicol, 1996).

Following up our previous study (Krakenberg et al., 2021), we here aimed to investigate the effects of touchscreen training termination. Hence, we not only included touchscreen trained and control mice in our experiment, but also compared continuously touchscreen trained mice with mice whose training was terminated 2 weeks earlier. As in the mentioned study, we conducted a battery of standardized tests concerning anxiety-like and exploratory behavior and determined fecal corticosterone metabolites (FCMs), which reflect adrenocortical activity (Palme, 2019). However, besides analyzing home cage activity we extended our focus to include stereotypies, which can be used as an indicator for impaired welfare (Latham and Mason, 2010). In line with the stated literature, we hypothesized touchscreen trained mice to display differences in behavioral, as well as endocrinological measurements compared to control mice. Furthermore, we hypothesized continuously touchscreen trained mice to differ from mice whose training was previously terminated concerning the mentioned parameters.

2. Animals, materials and methods

2.1. Animals and housing conditions

The study included 72 male C57BL/6J mice, ordered from Charles River Laboratories (Research Models Services, Germany GmbH, Sulzfeld, Germany) at postnatal day (PND) 28. Mice were delivered in 3 batches, i.e., at three different time points, with always 24 mice per batch. From then on, all individuals were housed singly. Although male mouse housing is a topic of controversial discussion in research (Kappel et al., 2017; Melotti et al., 2019), single housing was chosen in this study, as the applied mild food restriction holds the potential to increase aggressive interactions. The 3 animals that initially shared the same cage were treated as matched triplets for the following experimental phase. The cages (Makrolon Typ III cages: $38 \times 22 \times 15 \text{ cm}^3$) contained wood shavings as bedding material (Tierwohl Super, J. Rettenmaier and Söhne GmbH & Co KG, Rosenberg, Germany), a paper tissue, a wooden stick, and a semi-transparent red plastic house (Mouse HouseTM, Tecniplast Deutschland GmbH, Hohenstein, Germany). In addition, a transparent red plastic tunnel (Mouse Tunnel Red, Plexx B.V., Elst, Netherlands) was added to the cages 1 week before the experimental phase started. Water and food (Altromin 1324, Altromin Spezialfutter GmbH & Co. KG, Lage, Germany) were offered *ad libitum*, except during specific phases of the experiment that required a restricted feeding regime (for details see below). The housing room was maintained at a reversed dark/light cycle with lights off at 9 a.m., a temperature of $\sim 22^\circ\text{C}$, and a relative humidity of about 50%.

2.2. Experimental design

Following the experimental design of Krakenberg et al. (2021), all mice were habituated to tunnel handling 1 week before the start of the different feeding routines and the touchscreen training. This was done by gently guiding the mouse into the tunnel that was already located in the home cage for enrichment purposes. Tunnel handling was found to be less stressful compared to the commonly used tail handling technique (c.f. Hurst and West, 2010). For the subsequent exposure phase (start: PND 69), mice were assigned to one of 3 groups: a touchscreen trained group (TS, $n = 24$), a food restricted control group (FR, $n = 24$), or an *ad libitum* fed control group (AL, $n = 24$) (Figure 1). TS mice were mildly food restricted to 90–95% of their *ad libitum* body weights and trained in 5 sessions per week, each with a duration of 15 min. A restricted diet is usually applied during touchscreen training to increase the animals' motivation to gain food rewards (Horner et al., 2013). Although any touchscreen paradigm could have been used to investigate the effects of the regular training, the present study exemplarily used a Cognitive Judgement Bias task, which is originally used to assess decision making under ambiguity (Krakenberg et al., 2019a). For a detailed description of the touchscreen task please see Supplementary material. The two control groups (FR and AL) were included to differentiate between effects from the touchscreen training and the mild food restriction. Both never received touchscreen training sessions. As TS mice, FR

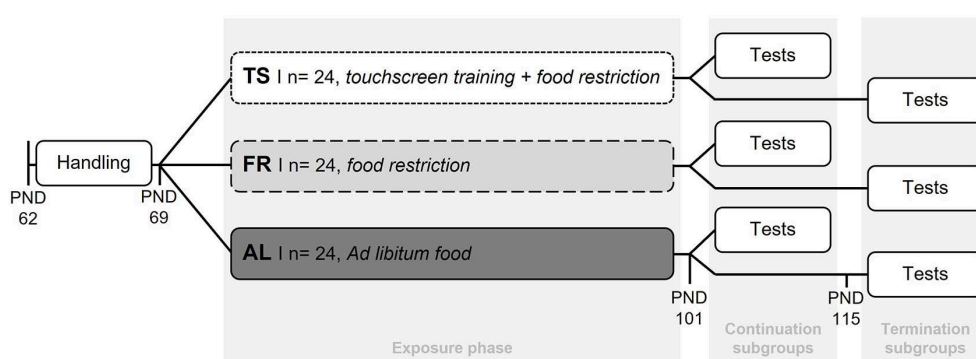


FIGURE 1

Experimental design. After the mice were habituated to tunnel handling (PND 62–69) they were assigned to one of three groups. TS, touchscreen trained and mildly food restricted (90–95% of *ad libitum* feeding weights) group; FR, food restricted group (90–95% of *ad libitum* feeding weights) without touchscreen training; AL, *ad libitum* fed group without touchscreen training. After the 5-week long exposure phase, half of the mice from each group were tested in behavior tests, while their feeding routines and touchscreen training remained unaffected. These subgroups were termed “continuation subgroups”. For the remaining mice from the TS group the touchscreen training was terminated at this point (PND 101). These mice, as well as the remaining mice from the AL and FR group, were tested in behavior tests 2 weeks later (start: PND 115) and termed “termination subgroups”.

mice were restricted to 90–95% of their *ad libitum* body weights (for details see [Supplementary material](#)), while AL mice were fed an *ad libitum* diet. After the exposure phase (PND 101), half of the mice from each group were tested in a battery of standardized behavior tests concerning anxiety-like and exploratory behavior, while their feeding routines and touchscreen training continued as before. These subgroups were termed “continuation subgroups”. The remaining half of mice from each group were labeled “termination subgroups”. Here, the touchscreen training was terminated for mice from the TS subgroup (PND 101) and only the mild food restriction continued. The feeding routines of FR and AL mice from the termination subgroups remained unaffected. To investigate the effects of touchscreen training termination, the termination subgroups were tested for their anxiety-like and exploratory behavior with a temporal distance of 2 weeks to the point of touchscreen training termination (PND 115).

2.2.1. Fecal corticosterone metabolites (FCMs)

To study the effects of touchscreen training on adrenocortical activity, the animals' FCMs were monitored non-invasively over the course of the experiment. Similar to [Krakenberg et al. \(2021\)](#), “baseline” and “reaction” FCMs were measured. The expected effects of touchscreen training and the feeding regime, respectively, can be assumed to subside within only 90 min ([Mallien et al., 2016](#)). Therefore, the here obtained “baseline” FCMs reflect corticosterone levels ~2 h after training and/or the respective feeding routine had been conducted. “Reaction” FCMs represent corticosterone levels directly before (anticipation value), during, and after the respective experimental procedures. As during the dark phase, a peak of FCM concentrations in response to an event can be found 4–6 h later ([Touma et al., 2003](#)), feces collection was adjusted accordingly. Before the start of the exposure phase, FCM “baseline” values were determined for all animals (PND 62). In order to investigate the effect of touchscreen training on adrenocortical activity, FCM “baseline”

and “reaction” values were measured in the middle of the exposure phase (baseline: PND 84; reaction: PND 87). These two measurements were repeated after the exposure phase (baseline: PND 104; reaction: PND 106), before behavioral testing started for the continuation subgroups.

2.2.1.1. Fecal sampling

To collect the feces, regular Makrolon Typ III cages, filled with a small amount of bedding, were prepared. A new mouse house, wooden stick and paper tissue were placed inside each cage. After the mouse was transferred to the cage with the help of the tunnel from the home cage, this tunnel was also left in the sampling cage as enrichment. Before the mouse was handled, it was checked that no old droppings were attached to the tunnel. For food restricted mice, food leftovers were transferred to the sampling cage and back to the home cage later, if still present. Water was offered *ad libitum*. The sampling cages were closed with the lid from the home cage, stacked inside the home cage and placed back to the mouse's rack position. After exactly 3 h, the mice were transferred back to their home cages, together with the enrichment from the sampling cage. Subsequently, the fecal boli were collected with gloves, whereby all feces from one sampling cage were stored in a distinct, labeled 1.5 ml Eppendorf tube (Eppendorf AG, Hamburg, Germany) at -20°C .

2.2.1.2. Extraction and analysis of fecal corticosterone metabolites

For the analysis of the FCMs, the wet weight of the fecal samples was determined (scale: 510–23, Kern, Ballingen, Germany; weighing capacity: 300 g, resolution: 0.001 g). Subsequently, the samples were dried for 2 h at 80°C in an oven (Modell 500, D-06061, Memmert, Schwabach, Germany). The dried feces were weighed again and stored in 2.0 ml safe-lock Eppendorf tubes. In the following, the feces were pulverized with a bead mill (TissueLyser LT, Qiagen, Hilden, Germany) by using a stainless steel ball (diameter: 7 mm, Qiagen, Hilden, Germany). 50 mg of the feces powder was then filled into a new 1.5 ml Eppendorf tube and

TABLE 1 Ethogram for home cage behavior.

Activity	
Active	The mouse shows any kind of locomotor activity (e.g., climbing, gnawing, grooming, digging, etc.). In addition, if a mouse is covered, movements of the nesting material, food pellets or rising bubbles in the water bottle are also considered as active behavior.
Inactive	The mouse does not show any kind of locomotor activity. Tiny whisker, ear or tail movements are excluded.
Stereotypies	
Circling	The mouse shows circular locomotion and completes more than one full circle three times in a row. The mouse can perform this behavior while climbing on the cage lid or while showing locomotion on the floor.
Route tracing	The mouse moves along the same path that it did before at least three times.
Jumping	The mouse pushes itself upwards with its hind legs, followed by a phase when the whole body of the mouse does not touch the ground (the tail can still touch the ground) at least three times in a row.
Back flipping	The mouse throws its head and body backwards and completes a full round in the air before landing on its paws and repeats this sequence at least three times.

Given are the behaviors and their definitions that were used for the home cage analysis.

mixed with 1 ml methanol (80%). If there was <50 mg of powdered feces available in a sample, the amount of methanol was adjusted. The mixture was vortexed for 30 min (Multi-vortex, V-32, Kisker, Steinfurt, Germany) and centrifuged for 10 min with a speed of 5,200 rpm (Centrifuge 5415 R, Eppendorf, Hamburg, Germany). Subsequently, 500 µl of the supernatant that contained FCMs were transferred to a 2.0 ml safe-lock Eppendorf tube and stored at −20°C. In the following, FCM concentrations were analyzed by using a 5α-pregnane-3β,11β,21-triol-20-one enzyme immunoassay (see Touma et al., 2003, 2004).

2.2.2. Home cage behavior

To examine the animals' activity rhythm and the occurrence of stereotypies in relation to touchscreen training and its termination, home cage behavior recordings were taken before, during and after the exposure phase (PND 64–66, 99–101 and 114–115). Please note that the last recording time only included the mice from the termination subgroups, as mice from the continuation subgroups were already tested in the behavior tests. The home cages of the mice were filmed for 24 h and the videos were analyzed concerning activity and stereotypies by using *instantaneous scan sampling* with intervals of 30 min (Bateson and Martin, 2021). Data from the time between 9 and 11 a.m. was not assessed, due to the feeding routines and the touchscreen training being performed. During the analysis of the home cage behavior the experimenter was blinded regarding mice from the FR and TS group. As the experimenter could see continuously filled feeding racks in the cages of AL mice on the videos, AL mice were identifiable on the recordings. On the videos, a mouse was considered *active*, when it showed any kind of motion, excluding tiny whisker, ear or tail movements (Feige-Diller et al., 2020). A stereotypy was counted when a mouse showed *circling*, *route tracing*, *jumping* or *back flipping* (Table 1).

2.2.3. Behavioral tests

In the behavioral test phase, the mice's anxiety-like and exploratory behavior was tested in the Elevated plus maze test (EPM; continuation subgroups: PND 108, termination subgroups: PND 122), Open field test (OF; continuation subgroups: PND 111,

termination subgroups: PND 125), and Free exploration test (FET; continuation subgroups: PND 112/113, termination subgroups: PND 126/127). All behavior tests were performed between 2 p.m. and 4 p.m. in a separate test room. The order in which the mice were tested was always randomized. For the transport to the test room, a Makrolon Typ II cage (floor space: 23 × 17 × 14 cm), covered with a black blanket to protect the mice from the light in the hallway, was used. Before the start of each test, the mouse spent 1 min inside the transportation cage for acclimatization, to make sure that all animals were in the same state of arousal when being tested (Izidio et al., 2005). Inside the test room, the behavior of the mice was recorded and tracked by a camera (DMK 22AUC03, The Imaging Source, Bremen, Germany) and a tracking software (ANY-maze Video Tracking Software, version 6.32, Stoelting Co., Wood Dale, United States), so that the experimenter could leave the room. Before the first mouse, as well as between all mice, the apparatus was cleaned with 70% ethanol and paper tissues.

2.2.3.1. Elevated plus maze test (EPM)

The apparatus of the EPM (Pellow et al., 1985; Lister, 1987) was plus-shaped and made out of gray plastic, with two opposing closed arms (35 × 6 cm), two opposing open arms (35 × 6 cm) and a square center zone (6 × 6 cm). The closed arms were surrounded by 15 cm high walls and the open arms by a 0.2 cm high border, to secure the mice when leaning over the edge. The whole apparatus was elevated 60 cm above the ground and placed in a fixed orientation inside a white plated wooden arena (80 × 80 × 40 cm), to ensure that fallen mice could not escape. The test apparatus was illuminated from above with a light intensity of ~28 Lux. The mouse was put in the center zone of the test apparatus, facing the closed arm pointing away from the experimenter. The test duration was 5 min. The relative time spent on the open arms, the relative number of entries into the open arms and the distance traveled on the open arms were taken as measures of the animals' anxiety-like behavior. The sum of entries made into the open and closed arms of the apparatus and the total distance traveled was taken as a measure of their exploratory locomotion (Rodgers and Johnson, 1995). Parameters regarding the center of the EPM were excluded from the analysis, due to their ambiguous possibilities of interpretation (Shepherd et al., 1994).

2.2.3.2. Open field test (OF)

The apparatus of the OF (Archer, 1973; Treit and Fundytus, 1988) was square-shaped, with a floor space of 80×80 cm, a wall height of 40 cm and made out of gray plastic. The space 20 cm from the walls was defined as the peripheral zone and the space in the middle of the arena (40×40 cm) was defined as the center zone. The test arena was illuminated from above with a light intensity of ~ 30 Lux. The mouse was placed inside the front left corner of the arena, facing the wall. The test duration was 5 min. The time spent in and the numbers of entries made to the center of the apparatus were taken as measures of the animals' anxiety-like behavior. The total distance traveled was taken as a measure of their exploratory locomotion (Krakenberg et al., 2019b).

2.2.3.3. Free exploration test (FET)

Similar to the OF, the apparatus of the FET (Griebel et al., 1993) was square-shaped, with a floor space of 60×60 cm and a wall height of 34 cm. The arena was made of white plated wood and had a hole on the right rear corner, where a square-shaped transparent plastic tunnel ($10 \times 15 \times 9$ cm) was connected. To this tunnel, the home cages of the tested mice could be connected. Therefore, the mice were put into special cages with a slider during the last cage change before the test. Inside the arena, the space 15 cm from the walls was defined as the peripheral zone and the space in the middle of the arena (30×30 cm) was defined as the center zone. The test arena was illuminated from above with a light intensity of ~ 35 Lux. While the mouse spent 1 min inside the transportation cage, the home cage was connected to the test apparatus. Then the mouse was put back into its home cage and the tracking was started. The test had a duration of 15 min. The time spent in and the latency to enter the arena were taken as measures of the animals' anxiety-like behavior. The total distance traveled and the numbers of entries made to the arena were taken as measures of their exploratory locomotion (Krakenberg et al., 2019b).

2.3. Statistics

For the statistical analysis, heteroscedasticity and normal distribution of residuals were examined descriptively and with the Shapiro-Wilk normality test. If the assumptions for parametric analyses were not met, data was transformed. One parameter could not be transformed (FET: arena entries) but simulation studies showed mixed-effect models to be relatively robust against violations of distributional assumptions (Knief and Forstmeier, 2018; Schielzeth et al., 2020). Therefore, the analysis of behavior tests and hormone data was conducted using linear mixed-effect models (LMM). Data concerning the home cage behavior of the animals was analyzed descriptively.

FCM sample points during the handling and exposure phase were analyzed with "group" (3 levels: AL, FR, TS) as fixed factor and "batch" as random factor. Batch refers to the number of animals that were supplied by the animal breeder on the same date (3 levels: 1st, 2nd, 3rd delivery). Afterwards the Tukey's test was performed for *post hoc* comparisons.

$$FCMs \sim group + (1|batch)$$

For the two FCM sample points after the exposure phase, where the animals were split into subgroups, as well as for the behavior test data, the analysis was conducted with "group" and "subgroups" (2 levels: continuation, termination) as fixed factors and "batch" as random factor, followed by Tukey's test for *post hoc* comparisons.

$$FCMs \sim group * subgroups + (1|batch)$$

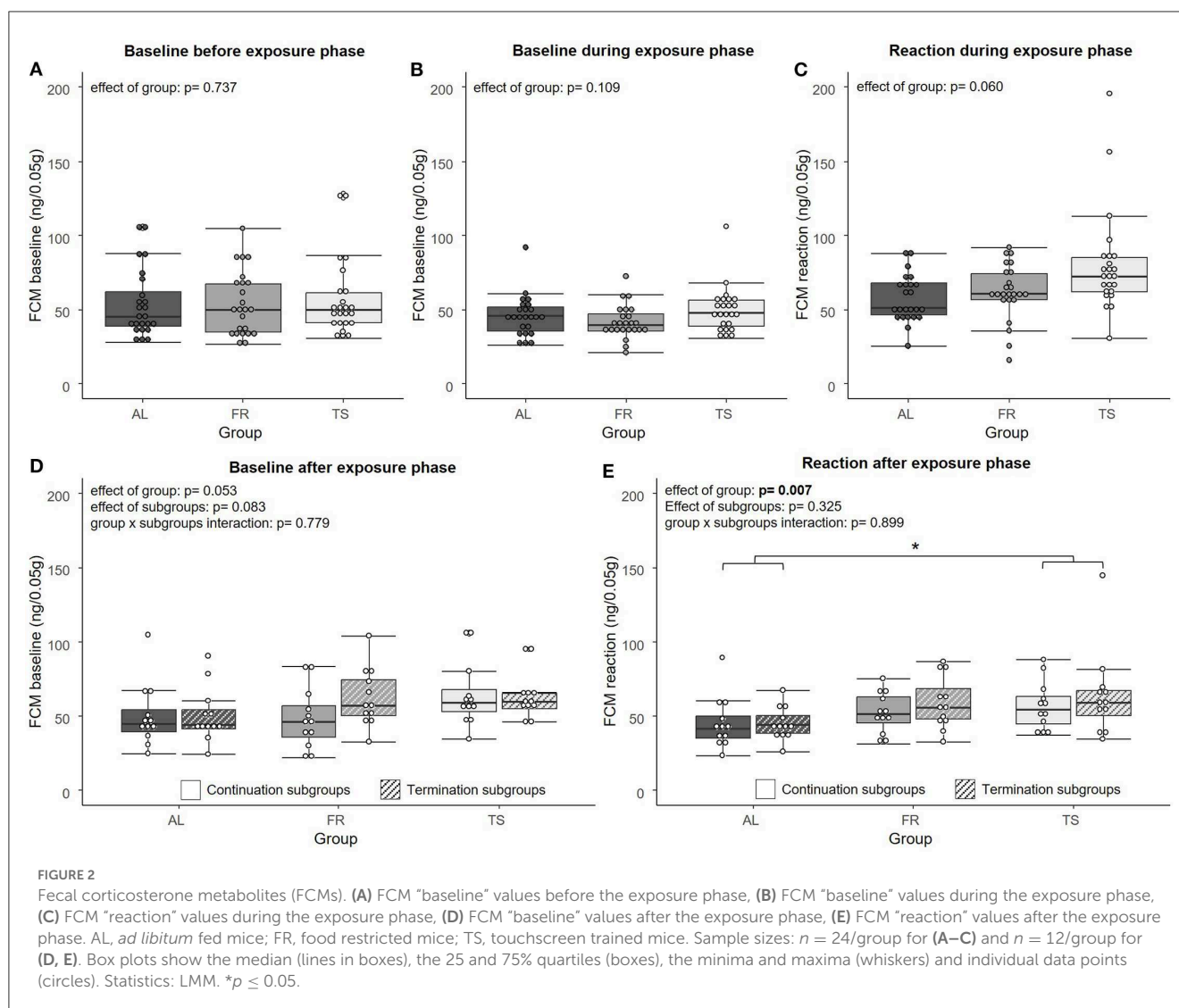
$$Behaviour \sim group * subgroups + (1|batch)$$

Degrees of freedom were always rounded to the nearest integer and differences were considered significant for $p \leq 0.05$. Significance levels of $0.05 < p \leq 0.1$ were considered a trend. To provide a standardized measure for the reported effects, partial eta squared (η^2_p) was calculated (Lakens, 2013). Analyses were carried out using the statistical software R [version 3.5.0 (R Core Team)] and R studio [version 2021.09.0 + 351 (R Core Team)]. The used sample size was determined by performing a power analysis (G*Power Version 3.1.9.6; Faul et al., 2009). We aimed to detect large effects ($f = 0.4$) with a power of 80% regarding the interaction (group*subgroups), which requires a sample size of 11 individuals per group. The presented study included 12 mice per group, to account for possible exclusions during the touchscreen training.

3. Results

3.1. Touchscreen training influenced FCMs

Regarding the FCM analysis, no significant effect of group was found on FCM "baseline" concentrations [LMM, $F_{(2,67)} = 0.307$, $\eta^2_p = 0.009$, $p = 0.737$] before (Figure 2A) and during the exposure phase [LMM, $F_{(2,69)} = 2.294$, $\eta^2_p = 0.062$, $p = 0.109$] (Figure 2B). For the FCM "reaction" values from the exposure phase, a trend for an effect of group was detected [LMM, $F_{(2,66)} = 2.936$, $\eta^2_p = 0.082$, $p = 0.060$] (Figure 2C). On a descriptive level, FR mice showed slightly increased levels compared to AL mice and TS mice showed the highest levels of all three groups. After the exposure phase, FCM "baseline" values revealed a trend for an effect of group [LMM, $F_{(2,63)} = 3.078$, $\eta^2_p = 0.089$, $p = 0.053$] and subgroups [LMM, $F_{(1,63)} = 3.099$, $\eta^2_p = 0.047$, $p = 0.083$], but no effect of group \times subgroups interaction [LMM, $F_{(2,63)} = 0.251$, $\eta^2_p = 0.008$, $p = 0.779$] (Figure 2D). In general, TS mice tended to have higher values than mice from the other two groups and mice from the termination subgroups tended to have higher values than mice from the continuation subgroups. The FCM "reaction" values from the sample point after the exposure phase showed a significant effect of group [LMM, $F_{(2,66)} = 5.334$, $\eta^2_p = 0.139$, $p = 0.007$], with TS mice having significantly higher values compared to AL mice ($p = 0.007$) and FR mice showing a trend for higher values than AL mice ($p = 0.053$) (Figure 2E). No effect was detected for subgroups [LMM, $F_{(1,66)} = 0.982$, $\eta^2_p = 0.015$, $p = 0.325$] and group \times subgroups interaction [LMM, $F_{(2,66)} = 0.107$, $\eta^2_p = 0.003$, $p = 0.899$].



3.2. Only touchscreen training and the feeding regime were found to affect anxiety-like behavior

In the tests for anxiety-like and exploratory behavior, a significant effect of group was found for the relative number of open arm entries [LMM, $F_{(2, 63)} = 3.658$, $\eta^2_p = 0.104$, $p = 0.031$], distance traveled [LMM, $F_{(2, 63)} = 8.101$, $\eta^2_p = 0.205$, $p < 0.001$] and sum of entries in the EPM [LMM, $F_{(2, 63)} = 4.951$, $\eta^2_p = 0.136$, $p = 0.010$]. Also, the time spent in the arena [LMM, $F_{(2, 64)} = 12.094$, $\eta^2_p = 0.274$, $p < 0.001$], the distance traveled there [LMM, $F_{(2, 64)} = 7.574$, $\eta^2_p = 0.191$, $p = 0.001$] and the number of entries made to the arena of the FET [LMM, $F_{(2, 66)} = 5.684$, $\eta^2_p = 0.147$, $p = 0.005$] were influenced by group. *Post hoc* testing revealed that TS mice made significantly less relative open arm entries compared to AL mice ($p = 0.025$), which suggests increased anxiety-like behavior (Figure 3A). Moreover, TS mice traveled a greater distance than AL ($p < 0.001$) and FR mice ($p = 0.012$) (Figure 3B) and showed more EPM arm entries in total compared

to both of the control groups (AL: $p = 0.046$; FR: $p = 0.013$) (Figure 3C), both parameters that indicate increased locomotor behavior. In the FET, TS and FR mice were found to spend more time (TS and FR: $p < 0.001$) (Figure 3E) and travel a greater distance in the FET arena in contrast to AL mice (TS: $p = 0.002$; FR: $p = 0.012$) (Figure 3F). Moreover, TS mice entered the arena more often than AL mice ($p = 0.004$), indicating increased exploratory behavior (Figure 3G). Additionally, there was a trend for an effect of group on the latency to enter the FET arena [LMM, $F_{(2, 64)} = 2.498$, $\eta^2_p = 0.072$, $p = 0.090$]. On a descriptive level, FR and TS mice were faster to enter the arena. No effect of group was detected on relative time spent on the open arms of the EPM and the distance traveled there, as well as on distance traveled in the OF and entries made to and time spent in the center of the OF (LMM, $p > 0.05$ for all comparisons, for details see Supplementary material).

An effect of subgroups was detected for the distance traveled in the EPM [LMM, $F_{(1, 63)} = 4.332$, $\eta^2_p = 0.064$, $p = 0.041$] (Figure 3B) and FET [LMM, $F_{(1, 64)} = 4.203$, $\eta^2_p = 0.062$, $p =$

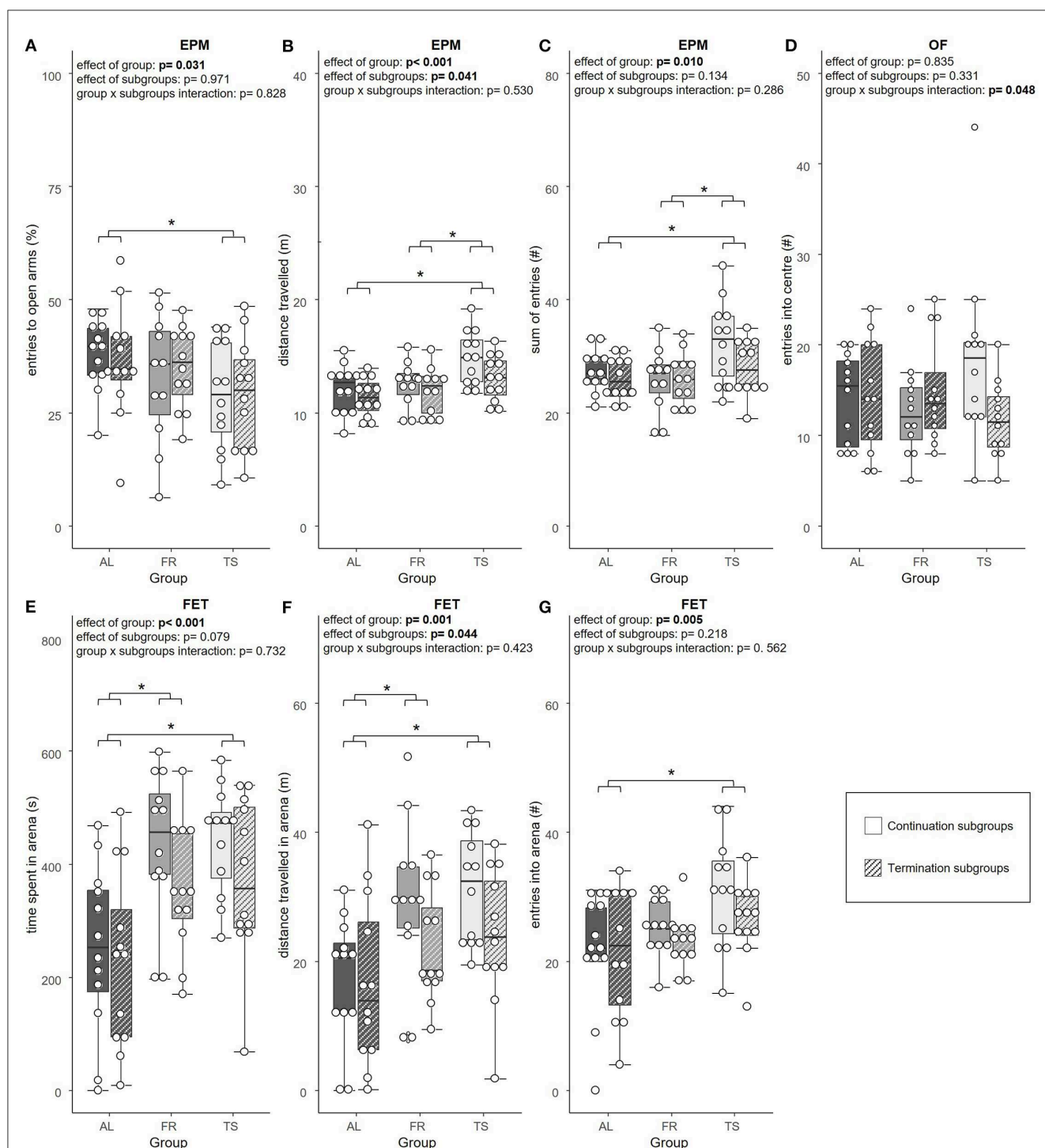
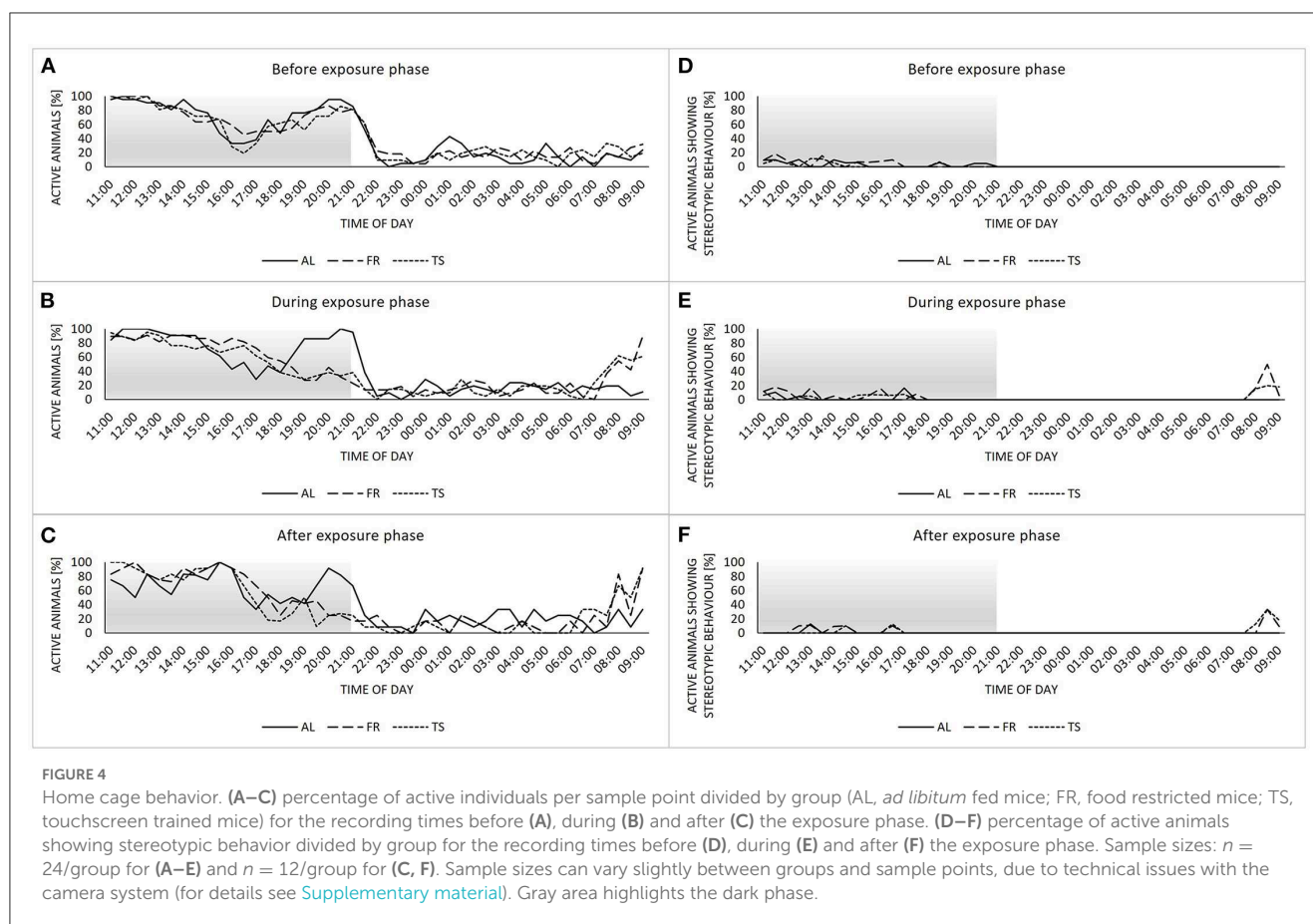


FIGURE 3

Anxiety-like and exploratory behavior. (A) relative number of entries into the open arms of the Elevated plus maze test (EPM), (B) total distance traveled in the EPM, (C) sum of arm entries in the EPM, (D) number of entries into the center of the Open field test (OF), (E) time spent in the arena of the Free exploration test (FET), (F) total distance traveled in the arena of the FET, (G) number of entries into the arena of the FET. AL, *ad libitum* fed mice; FR, food restricted mice; TS, touchscreen trained mice. Sample sizes: $n = 12$ /group. Exception: FR mice from continuation subgroups in A, where $n = 11$. Box plots show the median (lines in boxes), the 25 and 75% quartiles (boxes), the minima and maxima (whiskers) and individual data points (circles). Statistics: LMM. $*p \leq 0.05$.

0.044] (Figure 3F). The continuation subgroups of TS and FR mice traveled a greater distance than the according termination subgroups, indicating increased locomotor behavior. Distance traveled in the OF showed a trend for an effect of subgroups

[LMM, $F_{(1, 64)} = 3.971$, $\eta_p^2 = 0.058$, $p = 0.051$], with mice from the continuation subgroups traveling slightly more than mice from the termination subgroups. Furthermore, there was a trend for an effect of subgroups on arena time in the FET



[LMM, $F_{(1, 64)} = 3.196$, $\eta^2_p = 0.048$, $p = 0.079$], that indicated a tendency for a longer arena time in mice from the continuation subgroups compared to mice from the termination subgroups, which reflect increased exploratory behavior. Subgroups were not found to affect the relative entries made to, the relative time spent on, and the distance traveled on the open arms of the EPM, as well as the sum of arm entries. Also, entries made to the center of the OF, time spent there and latency to enter the arena in the FET and time spent there did not reveal an effect of subgroups (LMM, $p > 0.05$ for all comparisons, for details see [Supplementary material](#)).

Only the number of entries made to the center of the OF revealed a significant group \times subgroups interaction [LMM, $F_{(2, 64)} = 3.177$, $\eta^2_p = 0.090$, $p = 0.048$]. However, *post hoc* testing did not detect any significant differences (Figure 3D). None of the other parameters from the EPM, OF and FET showed a group \times subgroups interaction effect (LMM, $p > 0.05$ for all comparisons, for details see [Supplementary material](#)).

3.3. The feeding regime altered home cage behavior

Concerning the home cage behavior, mice showed a biphasic activity rhythm before the exposure phase, with two activity peaks

divided by a rest, and no noticeable differences between the three groups (Figure 4A). During the exposure phase, the activity rhythms of TS and FR mice changed into a more monophasic profile, with a steady decrease in activity from morning to night (Figure 4B). Also, the onset of activity began earlier compared to AL mice. These differences were maintained after the termination of touchscreen training for TS mice from the termination subgroups (Figure 4C). The display of stereotypic behavior was very low in general and mainly restricted to the dark and therefore active phase of the animals (Figures 4D–F). However, during the exposure phase and beyond, TS and FR mice showed a peak in stereotypic behavior between 8 a.m. and 9 a.m. that could not be observed in AL mice.

4. Discussion

The aim of the present study was to shed more light on recently reported touchscreen training effects, with a particular focus on the termination of the training routine. Two main patterns emerged: First, we confirmed previous findings showing that a restricted feeding regime as an integral part of touchscreen training affects the animals' behavior and activity. Secondly, touchscreen training increased FCMs and anxiety-like behavior of the mice. With regard to our main hypothesis, however, no effect of the termination of touchscreen training could be detected.

4.1. The feeding regime affects exploratory behavior and home cage activity

In the behavior tests as well as in the animals' home cage behavior, effects of the mild food restriction were detected. Regarding the behavior tests, both TS and FR mice showed increased levels of exploratory behavior compared to *ad libitum*-fed animals. This is in line with previous findings showing that a restrictive diet can increase exploration (e.g., Day et al., 1995) and likely reflects a higher motivation of the animals to forage for food. Moreover, TS and FR mice displayed differences in home cage behavior compared to the *ad libitum* fed group. Stereotypic behavior, an indicator of impaired welfare, was slightly increased around the time of exposure to the respective experimental procedures. Yet, the absolute values were too low to allow final conclusions. A comparable increase in stereotypic behavior due to a restricted diet was already reported before when investigating the effects of different food restriction routines (Feige-Diller et al., 2020). Overlapping with the small peak in stereotypies was a peak in activity, also shown by both TS and FR mice. Such an activity-related adaptation to a certain feeding routine, also known as food entrainment, is assumed to reflect anticipatory arousal (Krieger, 1974; Stephan, 2002; Gooley et al., 2006; Refinetti, 2015; Feige-Diller et al., 2020). Activity levels of TS and FR mice not only differed from AL mice shortly before the daily feeding event, but were also shifted during the course of the day. While AL mice displayed a biphasic activity rhythm, which was also reported before in C57BL/6J mice (Bodden et al., 2019), TS and FR mice changed their activity with the onset of the new diet into a more monophasic rhythm. Yet, a welfare-related evaluation of this shift in activity compared to AL mice would be inconclusive, as an *ad libitum* diet has been severely criticized as an appropriate feeding regime for laboratory rodents (for a review see Keenan et al., 1996). Taken together, the observed changes in behavior and activity caused by restricted feeding, which is an integral part of touchscreen training, have important implications for future experiments, as different activity states can affect the performance in other behavior tests as well as the reproducibility of results (Bodden et al., 2019).

4.2. Touchscreen training affected FCMs and anxiety-like behavior

The second main result was that touchscreen training affects HPA axis activity and anxiety-like behavior. Regarding the FCM analysis, touchscreen trained mice showed elevated FCM reaction values. This is consistent with our previous study (Krakenberg et al., 2021), as well as with the results of Mallien et al. (2016), who detected an increase of serum corticosterone in direct anticipation of a training session. Notably, the time directly before training is also reflected in the reaction values we measured. Thus, our results confirm a state of increased arousal in anticipation of and during touchscreen training. As in our previous study, FCM reaction values were still increased after the termination of training, indicating that the anticipation of training persists even beyond the

training phase itself (Krakenberg et al., 2021). In contrast to the reaction values, baseline FCMs were not found to differ between the groups. This is also in line with the literature, where a decrease of FCMs back to baseline ~2 h after the training sessions has been reported (Mallien et al., 2016; Krakenberg et al., 2021). Thus, the animals' state of increased arousal can be assumed to be rather transient, peaking around the time of exposure and decreasing again shortly afterwards.

At first glance, these results might point toward a putatively negative impact of touchscreen training on the welfare of mice, as, traditionally, elevated corticosterone levels are associated with aversive situations [e.g., predator confrontation (Amaral et al., 2010)]. Yet, increased adrenocortical activity can also be observed in reaction to beneficial stimuli [e.g. environmental enrichment (Marashi et al., 2003), see also Koolhaas et al., 2011 for a review]. Particularly the decrease of FCMs back to baseline levels indicates successful coping and the absence of chronic stress caused by the regular training sessions. Thus, the observed hormonal effects could also be interpreted in terms of a potentially enriching effect of touchscreen training by reducing under-stimulation many laboratory animals face (Wemelsfelder, 1985; van Rooijen, 1991; Burn, 2017; Meagher, 2019).

However, in addition to these effects on HPA axis activity, TS mice showed increased levels of anxiety-like behavior, an overall effect that was not dependent on whether TS mice were still trained at the point of testing or not. Specifically, this was reflected in the relative number of open arm entries in the EPM. In our previous study, also other parameters reflecting anxiety-like behavior (e.g., relative open arm time in the EPM) differed significantly between touchscreen-trained and control mice but we can only speculate about the reasons for this. However, descriptively, the present data point into the same direction. This is further underlined by another study conducted at our lab, although with a different research focus: Bračić et al. (2022) also detected increased anxiety-like behavior in touchscreen-trained mice. Again, the respective parameters reflecting anxiety-like behavior differed partly from the two above mentioned studies (e.g., time in the center of the OF). Taken together, there is mounting evidence for touchscreen training to increase anxiety-like behavior in mice, even though the specific parameters reflecting this effect may vary. Moreover, since Bračić et al. investigated female mice, including animals of both the C57BL/6J and B6D2F1 strain, the effect might even be robust across sexes and strains, however, caution is still advisable when generalizing these results.

At the same time, the findings of this study demonstrate that the termination of training is not the critical factor triggering the observed increase in anxiety-like behavior in touchscreen-trained animals. Therefore, the "enrichment loss hypothesis" could not be confirmed in the present study.

Traditionally, increased anxiety-like behavior, similarly to increased FCMs, would be interpreted as an indicator of a negative affective state (Paul et al., 2005; Hurst and West, 2010), suggesting a putatively negative impact of training on our touchscreen groups. As previously argued, however, one alternative explanation for the increased anxiety-like behavior might exist: a potential "negative contrast effect" (Krakenberg et al., 2021). Briefly, a negative contrast emerges if an individual anticipates a rewarding event, but a

comparably less rewarding event actually occurs (e.g., Flaherty, 1982). If touchscreen training was indeed perceived as enriching by the mice, their training anticipation might have been disappointed by being placed on the tests for anxiety-like behavior and not into the touchscreen chamber. This might have caused a negative affective state, reflected in their anxiety-like behavior (Krakenberg et al., 2021).

Taken together, the current state of knowledge is not sufficient to draw final conclusions at this stage, which is why further studies on the effects of touchscreen training are necessary. Yet, the present study successfully reproduced previous findings, showing that (I) a mild food restriction increases exploratory behavior and is capable of shifting the activity rhythm of mice, and (II) that regular touchscreen training transiently increases HPA axis activity and leads to higher levels of anxiety-like behavior. Furthermore, this study provides first evidence that these effects are not caused by the termination of regular touchscreen training. In compliance with the refinement endeavors for laboratory animals, further research should aim for a thorough assessment of the procedure's severity to ensure a responsible and well-founded use of animals for experimental purposes.

Data availability statement

The raw data supporting the conclusions of this article will be made available by the authors upon request.

Ethics statement

All procedures complied with the regulations covering animal experimentation within Germany (Animal Welfare Act) and the EU (European Communities Council DIRECTIVE 2010/63/EU) and were approved by the local (Gesundheits- und Veterinärämter Münster, Nordrhein-Westfalen) and federal authorities (Landesamt für Natur, Umwelt und Verbraucherschutz Nordrhein-Westfalen "LANUV NRW", reference number: 81-02.04.2020.A120).

Author contributions

SHR and VS conceived the study and supervised the project. SK, SHR, NS, and VS designed the experiments. VS trained SQ in conducting the experiments. SQ carried out the experiments. RP

determined and analyzed the hormonal data. SQ and VS conducted the statistical analysis of the data and wrote the initial draft of the manuscript. All authors critically revised the manuscript and gave final approval for publication.

Funding

The authors would like to thank the Ministry of Innovation, Science and Research of the state of North Rhine-Westphalia (MIWF) for supporting the implementation of a professorship for behavioral biology and animal welfare to SHR (Project: Refinement of Animal Experiments). This research was partly funded by the German Research Foundation (DFG) as part of the CRC TRR 212 (NC³)—Project number 396776123.

Acknowledgments

The authors thank Edith Ossendorf and Edith Klobetz-Rassam for excellent technical assistance.

Conflict of interest

The authors declare that the research was conducted in the absence of any commercial or financial relationships that could be construed as a potential conflict of interest.

Publisher's note

All claims expressed in this article are solely those of the authors and do not necessarily represent those of their affiliated organizations, or those of the publisher, the editors and the reviewers. Any product that may be evaluated in this article, or claim that may be made by its manufacturer, is not guaranteed or endorsed by the publisher.

Supplementary material

The Supplementary Material for this article can be found online at: <https://www.frontiersin.org/articles/10.3389/fnbeh.2023.1112780/full#supplementary-material>

References

- Amaral, V. C. S., Santos Gomes, K., and Nunes-de-Souza, R. L. (2010). Increased corticosterone levels in mice subjected to the rat exposure test. *Hormones Behav.* 57, 128–133. doi: 10.1016/j.yhbeh.2009.09.018
- Archer, J. (1973). Tests for emotionality in rats and mice: a review. *Anim. Behav.* 21, 205–235.
- Armbruster, D. J. N., Ueltzhöffer, K., Basten, U., and Fiebach, C. J. (2012). Prefrontal cortical mechanisms underlying individual differences in cognitive flexibility and stability. *J. Cognit. Neurosci.* 24, 2385–2399. doi: 10.1162/jocn_a_00286
- Bassett, L., and Buchanan-Smith, H. M. (2007). Effects of predictability on the welfare of captive animals. *Appl. Anim. Behav. Sci.* 102, 223–245. doi: 10.1016/j.applanim.2006.05.029
- Bateson, M., and Martin, P. (2021). *Measuring Behaviour: An Introductory Guide*. Cambridge: Cambridge University Press. doi: 10.1017/9781108776462
- Bodden, C., von Kortzfleisch, V. T., Karwinkel, F., Kaiser, S., Sachser, N., and Richter, S. H. (2019). Heterogenising study samples across testing time improves reproducibility of behavioural data. *Sci. Rep.* 9, 1–9. doi: 10.1038/s41598-019-44705-2

- Bračić, M., Bohn, L., Siewert, V., von Kortzfleisch, V. T., Schielzeth, H., Kaiser, S., et al. (2022). Once an optimist, always an optimist? Studying cognitive judgment bias in mice. *Behav. Ecol.* 33, 775–788. doi: 10.1093/beheco/ara040
- Burn, C. C. (2017). Bestial boredom: a biological perspective on animal boredom and suggestions for its scientific investigation. *Anim. Behav.* 130, 141–151. doi: 10.1016/j.anbehav.2017.06.006
- Bussey, T. J., Padain, T. L., Skillings, E. A., Winters, B. D., Morton, A. J., and Saksida, L. M. (2008). The touchscreen cognitive testing method for rodents: how to get the best out of your rat. *Learn. Memory* 15, 516–523. doi: 10.1101/lm.987808
- Crofton, E. J., Zhang, Y., and Green, T. A. (2015). Inoculation stress hypothesis of environmental enrichment. *Neurosci. Biobehav. Rev.* 49, 19–31. doi: 10.1016/j.neubiorev.2014.11.017
- Day, J. E. L., Kyriazakis, I., and Lawrence, A. B. (1995). The effect of food deprivation on the expression of foraging and exploratory behaviour in the growing pig. *Appl. Anim. Behav. Sci.* 42, 193–206.
- Faul, F., Erdfelder, E., Buchner, A., and Lang, A.-G. (2009). Statistical power analyses using G*Power 3.1: tests for correlation and regression analyses. *Behav. Res. Methods* 41, 1149–1160. doi: 10.3758/BRM.41.4.1149
- Feige-Diller, J., Krakenberg, V., Bierbaum, L., Seifert, L., Palme, R., Kaiser, S., et al. (2020). The effects of different feeding routines on welfare in laboratory mice. *Front. Vet. Sci.* 6, 1–15. doi: 10.3389/fvets.2019.00479
- Flaherty, C. F. (1982). Incentive contrast: a review of behavioral changes following shifts in reward. *Anim. Learn. Behav.* 10, 409–440.
- Fray, P. J., Robbins, T. W., and Sahakian, B. J. (1996). Neuropsychiatric applications of CANTAB. *Int. J. Geriatr. Psychiatry* 11, 329–336.
- Gooley, J. J., Schomer, A., and Saper, C. B. (2006). The dorsomedial hypothalamic nucleus is critical for the expression of food-entrainable circadian rhythms. *Nat. Neurosci.* 9, 398–407. doi: 10.1038/nn1651
- Griebel, G., Belzung, C., Misslin, R., and Vogel, E. (1993). The free-exploratory paradigm: an effective method for measuring neophobic behaviour in mice and testing potential neophobia-reducing drugs. *Behav. Pharmacol.* 4, 637–644.
- Horner, A. E., Heath, C. J., Hvorslev-Eide, M., Kent, B. A., Kim, C. H., Nilsson, S. R. O., et al. (2013). The touchscreen operant platform for testing learning and memory in rats and mice. *Nat. Protoc.* 8, 1961–1984. doi: 10.1038/nprot.2013.122
- Hurst, J. L., and West, R. S. (2010). Taming anxiety in laboratory mice. *Nat. Methods* 7, 825–826. doi: 10.1038/nmeth.1500
- Izidio, G. S., Lopes, D. M., Spricigo, L., and Ramos, A. (2005). Common variations in the pretest environment influence genotypic comparisons in models of anxiety. *Genes Brain Behav.* 4, 412–419. doi: 10.1111/j.1601-183X.2005.00121.x
- Kappel, S., Hawkins, P., and Mendl, M. T. (2017). To group or not to group? Good practice for housing male laboratory mice. *Animals* 7, 1–25. doi: 10.3390/ani7120088
- Keenan, K. P., Laroque, P., Soper, K. A., Morrissey, R. E., and Dixit, R. (1996). The effects of overfeeding and moderate dietary restriction on Sprague-Dawley rat survival, pathology, carcinogenicity, and the toxicity of pharmaceutical agents. *Exp. Toxicol. Pathol.* 48, 139–144.
- Knief, U., and Forstmeier, W. (2018). Violating the normality assumption may be the lesser of two evils. *BioRxiv* 23, 498931. doi: 10.1101/498931
- Koolhaas, J. M., Bartolomucci, A., Buwalda, B., de Boer, S. F., Flüge, G., Korte, S. M., et al. (2011). Stress revisited: A critical evaluation of the stress concept. *Neurosci. Biobehav. Rev.* 35, 1291–1301. doi: 10.1016/j.neubiorev.2011.02.003
- Krakenberg, V., von Kortzfleisch, V. T., Kaiser, S., Sachser, N., and Richter, S. H. (2019b). Differential effects of serotonin transporter genotype on anxiety-like behavior and cognitive judgment bias in mice. *Front. Behav. Neurosci.* 13, 263. doi: 10.3389/fnbeh.2019.00263
- Krakenberg, V., Wewer, M., Palme, R., Kaiser, S., Sachser, N., and Richter, S. H. (2021). Regular touchscreen training affects faecal corticosterone metabolites and anxiety-like behaviour in mice. *Behav. Brain Res.* 401, 113080. doi: 10.1016/j.bbr.2020.113080
- Krakenberg, V., Woigk, I., Garcia Rodriguez, L., Kästner, N., Kaiser, S., Sachser, N., et al. (2019a). Technology or ecology? New tools to assess cognitive judgement bias in mice. *Behav. Brain Res.* 362, 279–287. doi: 10.1016/j.bbr.2019.01.021
- Krieger, D. T. (1974). Food and water restriction shifts corticosterone, temperature, activity and brain amine periodicity. *Endocrinology* 95, 1195–1201.
- Lakens, D. (2013). Calculating and reporting effect sizes to facilitate cumulative science: a practical primer for *t*-tests and ANOVAs. *Front. Psychol.* 4, 863. doi: 10.3389/fpsyg.2013.00863
- Latham, N., and Mason, G. (2010). Frustration and perseveration in stereotypic captive animals: Is a taste of enrichment worse than none at all? *Behav. Brain Res.* 211, 96–104. doi: 10.1016/j.bbr.2010.03.018
- Lister, R. G. (1987). The use of a plus-maze to measure anxiety in the mouse. *Psychopharmacology* 92, 180–185.
- Mallien, A. S., Palme, R., Richetto, J., Muzzillo, C., Richter, S. H., Vogt, M. A., et al. (2016). Daily exposure to a touchscreen-paradigm and associated food restriction evokes an increase in adrenocortical and neural activity in mice. *Hormones Behav.* 81, 97–105. doi: 10.1016/j.yhbeh.2016.03.009
- Marashi, V., Barnekow, A., Ossendorf, E., and Sachser, N. (2003). Effects of different forms of environmental enrichment on behavioral, endocrinological, and immunological parameters in male mice. *Hormones Behav.* 43, 281–292. doi: 10.1016/S0018-506X(03)00002-3
- Meagher, R. K. (2019). Is boredom an animal welfare concern? *Anim. Welf.* 28, 21–32. doi: 10.7120/09627286.28.1.021
- Melotti, L., Kästner, N., Eick, A. K., Schnelle, A. L., Palme, R., Sachser, N., et al. (2019). Can live with 'em, can live without 'em: Pair housed male C57BL/6J mice show low aggression and increasing sociopositive interactions with age, but can adapt to single housing if separated. *Appl. Anim. Behav. Sci.* 214, 79–88. doi: 10.1016/j.applanim.2019.03.010
- Nicol, C. J. (1996). Farm animal cognition. *Anim. Sci.* 62, 375–391.
- Palme, R. (2019). Non-invasive measurement of glucocorticoids: advances and problems. *Physiol. Behav.* 199, 229–243. doi: 10.1016/j.physbeh.2018.11.021
- Paul, E. S., Harding, E. J., and Mendl, M. (2005). Measuring emotional processes in animals: the utility of a cognitive approach. *Neurosci. Biobehav. Rev.* 29, 469–491. doi: 10.1016/j.neubiorev.2005.01.002
- Pellow, S., Chopin, P., File, S. E., and Briley, M. (1985). Validation of open: closed arm entries in an elevated plus-maze as a measure of anxiety in the rat. *J. Neurosci. Methods* 14, 149–167.
- Refinetti, R. (2015). Comparison of light, food, and temperature as environmental synchronizers of the circadian rhythm of activity in mice. *J. Physiol. Sci.* 65, 359–366. doi: 10.1007/s12576-015-0374-7
- Richter, S. H., Vogel, A. S., Ueltzhöffer, K., Muzzillo, C., Vogt, M. A., Lankisch, K., et al. (2014). Touchscreen-paradigm for mice reveals cross-species evidence for an antagonistic relationship of cognitive flexibility and stability. *Front. Behav. Neurosci.* 8, 1–13. doi: 10.3389/fnbeh.2014.00154
- Rodgers, R. J., and Johnson, N. J. T. (1995). Factor analysis of spatiotemporal and ethological measures in the murine plus-maze test of anxiety. *Pharmacol. Biochem. Behav.* 52, 297–303.
- Schielzeth, H., Dingemanse, N. J., Nakagawa, S., Westneat, D. F., Allee, H., Teplitsky, C., et al. (2020). Robustness of linear mixed-effects models to violations of distributional assumptions. *Methods Ecol. Evol.* 11, 1141–1152. doi: 10.1111/2041-210X.13434
- Shepherd, J. K., Grewal, S. S., Fletcher, A., Bill, D. J., and Dourish, C. T. (1994). Behavioural and pharmacological characterisation of the elevated "zero-maze" as an animal model of anxiety. *Psychopharmacology* 116, 56–64.
- Stephan, F. K. (2002). The "other" circadian system: food as a zeitgeber. *J. Biol. Rhyth.* 17, 284–292. doi: 10.1177/0748730002129002591
- Touma, C., Palme, R., and Sachser, N. (2004). Analyzing corticosterone metabolites in fecal samples of mice: a noninvasive technique to monitor stress hormones. *Hormones Behav.* 45, 10–22. doi: 10.1016/j.yhbeh.2003.07.002
- Touma, C., Sachser, N., Möstl, E., and Palme, R. (2003). Effects of sex and time of day on metabolism and excretion of corticosterone in urine and feces of mice. *Gen. Compar. Endocrinol.* 130, 267–278. doi: 10.1016/S0016-6480(02)00620-2
- Treit, D., and Fundytus, M. (1988). Thigmotaxis as a test for anxiolytic activity in rats. *Pharmacol. Biochem. Behav.* 31, 959–962.
- van Rooijen, J. (1991). Commentary on predictability and boredom. *Appl. Anim. Behav. Sci.* 31, 283–287.
- Wemelsfelder, F. (1985). Animal boredom: is a scientific study of the subjective experiences of animals possible? *Adv. Anim. Welf. Sci.* 85, 115–154.



OPEN ACCESS

EDITED BY

Christopher R. Cederroth,
Swiss 3R Competence Centre, Switzerland

REVIEWED BY

Farhan Chowdhury,
Southern Illinois University Carbondale,
United States
Francesca Della Sala,
Institute of Polymers, National Research
Council (CNR), Italy

*CORRESPONDENCE

Xinjun Lu

✉ luxj33@mail.sysu.edu.cn

Yi Ma

✉ anhuimayi2002@163.com

SPECIALTY SECTION

This article was submitted to
Molecular and Cellular Oncology,
a section of the journal
Frontiers in Oncology

RECEIVED 17 January 2023

ACCEPTED 22 March 2023

PUBLISHED 03 April 2023

CITATION

Zhang L, Liao W, Chen S, Chen Y,
Cheng P, Lu X and Ma Y (2023) Towards
a New 3Rs Era in the construction of
3D cell culture models simulating
tumor microenvironment.
Front. Oncol. 13:1146477.
doi: 10.3389/fonc.2023.1146477

COPYRIGHT

© 2023 Zhang, Liao, Chen, Chen, Cheng, Lu
and Ma. This is an open-access article
distributed under the terms of the [Creative
Commons Attribution License \(CC BY\)](#). The
use, distribution or reproduction in other
forums is permitted, provided the original
author(s) and the copyright owner(s) are
credited and that the original publication in
this journal is cited, in accordance with
accepted academic practice. No use,
distribution or reproduction is permitted
which does not comply with these terms.

Towards a New 3Rs Era in the construction of 3D cell culture models simulating tumor microenvironment

Long Zhang^{1,2}, Weiqi Liao², Shimin Chen², Yukun Chen²,
Pengrui Cheng^{1,3,4}, Xinjun Lu^{5*} and Yi Ma^{1,3,4*}

¹Organ Transplant Center, The First Affiliated Hospital, Sun Yat-sen University, Guangzhou, China, ²Zhongshan School of Medicine, Sun Yat-sen University, Guangzhou, China, ³Guangdong Provincial Key Laboratory of Organ Donation and Transplant Immunology, The First Affiliated Hospital, Sun Yat-sen University, Guangzhou, China, ⁴Guangdong Provincial International Cooperation Base of Science and Technology (Organ Transplantation), The First Affiliated Hospital, Sun Yat-sen University, Guangzhou, China, ⁵Department of Biliary-Pancreatic Surgery, Sun Yat-sen Memorial Hospital, Sun Yat-sen University, Guangzhou, China

Three-dimensional cell culture technology (3DCC) sits between two-dimensional cell culture (2DCC) and animal models and is widely used in oncology research. Compared to 2DCC, 3DCC allows cells to grow in a three-dimensional space, better simulating the *in vivo* growth environment of tumors, including hypoxia, nutrient concentration gradients, micro angiogenesis mimicry, and the interaction between tumor cells and the tumor microenvironment matrix. 3DCC has unparalleled advantages when compared to animal models, being more controllable, operable, and convenient. This review summarizes the comparison between 2DCC and 3DCC, as well as recent advances in different methods to obtain 3D models and their respective advantages and disadvantages.

KEYWORDS

tumor microenvironment, tumor cells, the three dimensional, cell culture, the two dimensional

1 Introduction

Despite significant advances in human research on tumor staging, diagnosis and treatment, tumors remain one of the leading causes of death (1). Cancer cells can grow and metastasize rapidly, which is largely attributed to the ability of cancer cells to create a tumor microenvironment (TME) for themselves and progressively modulate it from an anti-tumor response to a tumor-friendly one (2).

Therefore, establishing an experimental model system that accurately mimics the complexity of the TME is essential. Traditional *in vitro* two-dimensional cell culture systems (2DCC) (on planar scaffold) and animal models have been widely used for cancer research. However, 2DCC systems do not mimic natural TME due to a lack of cell-cell

communication and interactions of cell-cell and cell-matrix (3), while *in vivo* animal models are expensive, ethically problematic, and challenging to set up as they show difficulties in tracking tumor growth and drug screening (4). To address these limitations, the three-dimensional cell culture system (3DCC) is increasingly developed in research and is now crucial for oncology studies due to its ability to accurately maintain TME without any additional manipulation. In this review, we summarize the comparison between 2DCC and 3DCC, as well as recent advances in different methods to obtain 3D models and their advantages and disadvantages.

2 Introduction of the tumor microenvironment

TME refers to the cellular environment in which tumor or cancer stem cells reside which has its own unique characteristics compared to the microenvironment of the normal one. These characteristics are important for the tumor immune escape, growth, survival, and metastasis which include hypoxia, acidic environment, inflammatory microenvironment, specific vascularization (Figure 1). TME consists of the extracellular matrix (ECM) and various tumor-associated cells such as cancer-associated fibroblasts (CAFs), endothelial cells, adipocytes, and immune cells (5, 6). These cells are located around tumor cells and are energized by the vascular network (7). CAFs can be simply defined as fibroblasts (non-epithelial, non-cancerous, non-endothelial, and non-immune cells) located within or adjacent to a tumor and are the major producer of ECM and various other cytokines in the TME. CAFs have functions of immunosuppression, promoting angiogenesis, producing enzymes that degrade ECM

(such as matrix metalloproteinases), and promoting tumor growth and metastasis. However, some CAFs have been shown to inhibit tumor activity (8). Immune cells (T cells, neutrophils, macrophages, etc) play an important role in tumor growth, migration, and immune escape. The pro-tumor inflammation feature within the TME promotes tumor growth by blocking anti-tumor immunity and influent the composition of immune cells within it. Result to the activation of transcription factors in tumor cells, leading to increased inflammation and the production of inflammatory microenvironments adapted to tumor cell growth. Tumor-associated macrophages (TAM) usually divided into M1 type, which mediates antibody-dependent cytotoxic effects (ADCC) to kill tumor cells, and M2 type, which promotes tumor growth, invasion, metastasis and drug resistance. These two cell types can be interconverted (9). Angiogenesis is essential for tumors. Neovascularization provides oxygen and nutrients to the tumor and promotes tumor metastasis. Tumor vascular endothelial cells (TEC) are involved in the metastasis of cancer cells to the neovascular lumen, help generate CAFs, and mediate tumor invasion and metastasis (10). Tumor cells and cancer stem cells (CSCs) secrete molecules that induce a tumor-promoting phenotype, polarizing macrophages to M2 subtype, fibroblasts to CAF, and ECs to TEC (11). ECM is generally defined as the non-cellular component of a tissue that provides metabolic and structural support to its cellular components. Its main components are collagen, proteoglycan, laminin and fibronectin. In the process of tumor progression, a large number of enzymes such as MMP are produced, leading to active remodeling of the extracellular matrix, and changes in collagen degradation or deposition result in loss of ECM homeostasis, which ultimately interferes with cell-cell adhesion, cell polarity and increases growth factor signaling to promote tumor metastasis (12, 13).

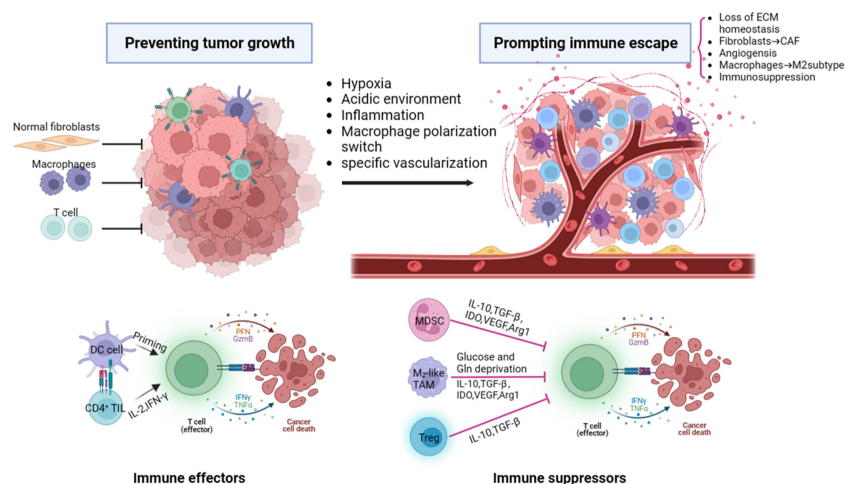


FIGURE 1

The major components and characteristics related to tumor progression within the tumor microenvironment. ECM, extracellular matrix; CAF, cancer-associated fibroblast; DC, dendritic cells; PFN, perforin; GzmB, granzyme B; IFN γ , interferon γ ; TNF α , tumor necrosis factor α ; TGF- β , transforming growth factor- β ; MDSC, myeloid-derived suppressor cell; IDO, indoleamine 2,3-dioxygenase; VEGF, vascular endothelial growth factor; Arg1, arginase 1; Gln, glutamine; Treg, regulatory T cell.

3 2D vs 3D: Introduction of 3DCC model and its advantages

Whether the *in vitro* culture model can effectively mimic TME has become an important basis to investigate its practical value. As a traditional *in vitro* cell culture system, 2DCC has long been used in cancer research. However, 2DCC does not mimic the complexity of 3D tissues *in vivo*, nor does it mimic the interaction between tumor cells and TME. Gradients of nutrient and oxygen concentrations are common in TME (14), but cannot be reproduced in 2DCC (15, 16). To address these limitations, 3D cell culture (3DCC) was developed. The 3D tumor sphere model can narrow the gap between 2DCC and *in vivo* tumor model, making the model closer to the real tumor tissue (17) (Figure 2 and Table 1). At present, 3D sphere models can be divided into four types: multicellular tumor sphere (MCTS), neoplastic sphere, tissue-derived tumor sphere (TDTS), and organotypic multicellular sphere (OMS) (20). The cultural methods and biological characteristics of the different types of models are different. MCTS were produced in single-cell

suspension cultures in conventional FBS supplemented media without the supply of exogenous ECM. But not all cell lines are capable of producing compact MCTS (20). Tumor spheres were established as amplification models of CSCs in a serum-free medium supplemented with growth factors. It was used to enrich CSCs and cells with stem cell-related characteristics (21). TDTS and OMS were obtained from the tumor tissue department. TDTS were observed in an *in vitro* study of colon cancer cell lines (22). The histological features of OMS are very similar to those of tumors *in vivo*, and capillaries can be maintained for up to 6 weeks (23). MCTS is one of the most commonly used models because it is relatively easy to assemble, possesses reproducibility and ability to mimic tumor cell heterogeneity (24). For the study of tumor initiation, smaller, well-oxygenated spheres (optimal diameter of about 200μm) can be used. In contrast, for studies related to tumor expansion, larger spheres are preferred to mimic the hypoxic and necrotic regions observed in hypovascularized tumors (14). The following is a detailed description of how 3DCC is constructed.

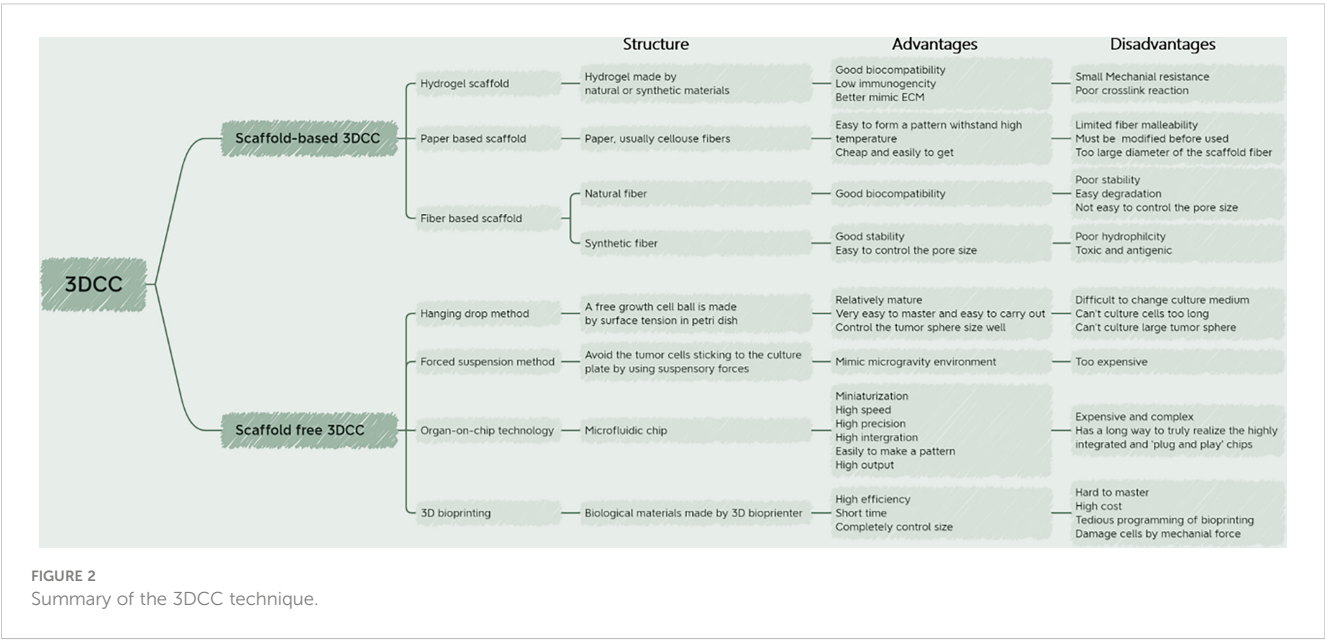


TABLE 1 Comparison of 2DCC and 3DCC (3, 6, 16–19).

	2DCC	3DCC
Morphology	Loss of shape changes and polarization	Actual shape form
Gene expression	To be altered or modified by planar culture or genes	Better representation of tumor gene expression <i>in vivo</i>
TME	None	Mimics TME in tumor tissue
Oxygen, nutrients, signaling molecular gradients in TME	None	Controlled by sphere size and molecular osmotic migration rate
Heterogeneity of tumor	Base	Better approximated by various molecular gradients in the TME
Angiogenesis	Only observational	Functional angiogenesis
Cost	Low	High
Multicellular explore	Suitable for immune response studies	Suitable for cell co-culture

4 3DCC and tumor initiating cells

Tumor initiating cells play a huge role in tumor malignancy and chemotherapy resistance. The niche of cancer stem cells *in vitro* differs significantly from that *in vivo*. One important aspect of the niche is to maintain stem cells in a quiescent state while simultaneously driving a sufficient number of stem cells into proliferation and differentiation pathways to maintain organs' function (25). Many signaling pathways that mediate the interaction of normal stem cells with their niche are also involved in the interaction between cancer stem cells and their niches and can promote tumorigenesis and cancer proliferation. Cancer stem cells tend to be quiescent in the body's milieu interieur, but they exhibit greater proliferative activity *in vitro* than non-cancer stem cells (26).

Currently, the most reliable model for studying cancer stem cells is a 3D assay using an ECM-rich Matrigel, which maintains the growth of heterogeneous layered cancer stem cell cultures. The addition of ECM group stratified adhesins to serum-free medium increases tumor cell growth, self-renewal, and tumorigenic characteristics of glioma cancer stem cells (27). Therefore, the use of 3DCC to study its biological behavior and role in tumors is also a hot topic today. Now some new models are built using 3DCC to study the self-renewing cancer population in depth. For instance, Hubert et al. (28) established CSC cultures derived from the hyperoxia, vegetatively high regions and mixed regions of chronic hypoxia and necrosis regions derived from human glioblastoma. Li et al. (27) constructed a three-dimensional spheroid model of non-small cell lung cancer and used A549 and SK-MES-1 to assess cell growth, migration, drug resistance and other phenomena. In the three-dimensional spheroid model, the commonly used drug tadalafil showed a more pronounced inhibitory effect. Fibrin deposition in the matrix of CRCs proved to be the cause of tumor development. Zhang M et al. (29) used salmon fibrin gel to provide 3D ECM for colon cancer cells and found that 90 Pascal (Pa) fibrin gel was the most effective in isolating and enriching tumor colonies compared to rigid 420 Pa and 1,050 Pa gels. The size and number of colony formations are inversely correlated with gel hardness.

5 3D model construction methods for cancer research and its recent progress

In general, 3DCC construction methods can be divided into scaffold-based and scaffold-free models, each with its own set of advantages and disadvantages (30). The following sections will discuss these two methods individually, and provide an overview of the latest advancements in each.

5.1 Scaffold-based 3DCC model

3D scaffolds can influence tumor cell-cell and cell-TME interactions by affecting mechanical and biochemical signaling

and mimicking the conditions of hypoxia and nutrient deprivation in TME (17). Various forms of materials have been used to construct scaffolds for 3DCC. Depending on the materials, scaffold-based 3DCC can be further classified into hydrogel scaffolds, paper-based scaffolds, and fiber-based scaffolds (15). The support method is simple to operate and easy to disassemble and assemble. However, the disadvantage is that some of the scaffold materials are expensive.

5.1.1 Hydrogel scaffold

Hydrogels consist of one or more different hydrophilic polymers, their unique polymerization mode allows for the free movement of cells and molecules through their pores (31). In the human body, most mammalian cells rely on the extracellular matrix (ECM) for support to carry out life activities. Hydrogels are special because they allow cytokines and growth factors to cross tissue-like gels. Although they contain 95% water, they do provide the solid-liquid level required for cell culture (32). Hydrogels can better replicate the ECM *in vivo*, as they are usually composed of hydrated proteins. They exhibit good biocompatibility and low immunogenicity, but have poor mechanical resistance and crosslinking reactions (17). Hydrogels can be created using natural materials such as collagen, fibrin, hyaluronic acid, and alginate, or synthetic materials like polyethylene glycol (33). The properties of hydrogels, including hydration, porosity, and stiffness, can be fine-tuned by adjusting the components of the material. However, some collagen hydrogels are expensive and have poor renewability (16). Alginate-based hydrogels, like alginate gel beads (ALG beads), are popular 3D substrates for medical applications due to their mild gelation process, biocompatibility, and structural similarity to native tissues (34). Alginate can be cross-linked in the presence of calcium ions and can also be used to degrade scaffolds with sodium citrate to recover cells (35). However, alginate itself does not possess cell adhesion properties due to the lack of interaction with integrins. It also lacks matrix receptors similar to those found in native times, which are important for cell adhesion (34). The pores formed by alginate in the presence of calcium ions are dense and difficult to control accurately, weakening the migration of cells and other biomolecules. Therefore, many improvements have been made to alginate saline gels. Synthetic peptide hydrogels are also a hot research topic. The physicochemical properties of gels can be easily modified by adding or subtracting amino acids or modifying the side chains of amino acid residues (36). There are also many new developments in hydrogel scaffolds of other materials. Table 2 provides an overview of the latest progress of hydrogel scaffolds.

5.1.2 Paper base scaffold

Paper is produced by pressing wet cellulose fibers together. Paper-based scaffolds are rigid and can withstand high temperatures, yet they possess some deformability and can be folded into complex geometries, providing pores for cell growth (15, 53). These scaffolds are also hydrophilic with capillary adsorption capacity (54), making them a convenient and cost-effective option for mass production and utilization (53). A convenient 3D culture environment can be created by combining

TABLE 2 New progress of hydrogel scaffolds.

Research purpose	Innovation	Results	Ref.
Model with fibrous matrix and blood vessels	The embedded gel was prepared by combining type I collagen and fibrin	The model can be used to study tumor-matrix interactions in HCC	(37)
Multicellular heterogeneous spheres	Hanging drop method, co-culture of HCC matrix and fibroblasts, encapsulation of collagen gel,	The model is much closer to ECM	(38)
Novel hydrogel scaffolds	HA3P50 scaffold based on hyaluronic acid and poly (methylethylene ether-Alt-maleic acid)	HepG2 cells were protected from the damaging response on 2D medium	(39)
New tumor microsphere model	Biosynthesis of PEG-fibrinogen gels	Similar in size and shape to tumors <i>in vivo</i>	(40)
New 3D culture platform	Gelatin and alginate complement each other, PEGDA incorporation controls cross-linking density	A 3D alginate culture platform whose pore size can be changed artificially was made	(35)
Alginate gel microarray	Alginate gel micropores were prepared by electrodeposition of alginate gel on ITO electrodes.	HepG2 spheres were successfully prepared	(41)
Porous alginate beads	Dual aqueous emulsion, controllable pore size, good biocompatibility, can directly encapsulate cells	The activity, proliferation of investigated cells were increased	(42)
Peptide hydrogel	Max8β was used as hydrogel to form nanofibrils through hydrophobic collapse and hydrogen bonding	Custom hydrogels for porosity, permeability and mechanical stability	(43)
Soluble gelatin based cell carrier	Temperature sensitive gelatin microspheres were mixed with alginate saline gel as cell carriers.	A new platform was developed for drug testing and oncology	(44)
New gel sphere	Halo-linked 3D microgels of HA-MA and GelMA in air were prepared on superhydrophobic surfaces.	The shape, size and cell number of the microtumor can be easily controlled.	(45)
New gel matrix	The basement membrane extract was gelatinized with Matrigel to form a new matrix	Better mimic a single tumor in the body	(46)
New alginate hybrid gel beads	Acellular liver matrix and alginate constitute new hybrid gel beads	HCCLM3 cells showed higher cell viability and metastatic potential	(34)
Hydrogel microarray	Application of optical crosslinking technology in micro machining and micro forming.	Produce custom size tumor microspheres	(47)
New Liquid Marble Culture Platform	It forms integrates hydrogel components, replaces liquid with hydrogel and removes hydrophobic shell	The liver specific function and DNA content of HM globules increased after long-term culture	(48)
New hydrogel	Magnetic hydrogels were prepared by combining the assembly of magnetic nanoparticles	Enhances cell-cell interactions and promotes spontaneous formation of multicellular spheres	(49)
New hydrogel	The copolymer reversibly gelatinized in aqueous and redissolved without degrading the synthetic scaffolds	A temperature responsive hydrogel was developed	(50)
3D culture and drug resistance system	The resistance of HepG2 cells to Bio-Pa NPs was detected in 2D and 3D cultures, respectively	HepG2 cells in 3D hydrogels were more resistant to Bio-Pa NPs treatment	(51)
New hydrogel	Low temperature CMCH hydrogel solution gelatinizes rapidly at 37°C	Hydrogels promote cell survival and proliferation, and have good biocompatibility	(52)

paper-based scaffolds with hydrogel-simulated ECM (55). The gradient of hypoxia and biomolecules in TME can be imitated by stacking paper-based scaffolds. Disassembling the paper-based scaffold facilitates cell harvesting and analysis of the structure and function of cells in the paper-based scaffold without histological sections. The paper platform is used to culture primary cells, tumor cells, patient biopsies, stem cells, fibroblasts, osteoblasts, immune cells, bacteria, fungi, and plant cells. These platforms are compatible with standard analytical assays commonly used to monitor cell behavior. Due to its thickness and porosity, there is no mass transfer limitation to and from cells in the paper scaffold (56). However, paper-based scaffolds have some limitations, such as limited fiber malleability and the need for physical and chemical modification before use in cell culture (54). Furthermore, the diameter of the

scaffold fiber is much larger than that of body fibrils (about 500nm), with a minimum diameter of 1mm (15).

5.1.3 Fiber base scaffold

Man-made fiber structures date back thousands of years, and they are used as clothing and decoration in the form of textiles (57). Fiber products are also widely used in filtration, cell culture, composite materials and other processes. Fiber-based scaffolds can be constructed using either natural fibers such as collagen, chitosan, and hyaluronic acid, or synthetic fibers such as polylactic acid, polyglycolic acid, and other degradable polyester polymers. Under the premise of ensuring the porosity of hydrogel and the normal growth of cultured cells, the use of fiber materials to build a platform can act as a scaffold to compensate for the lack of

structural rigidity of hydrogels. Adding carbon nanotubes to a hydrogel is a good try (58). Natural fiber scaffolds are known for their good biocompatibility and ability to interact with cell-ECM receptors, which facilitates cell growth. However, these scaffolds have poor stability, are easily degradable, and have a limited ability to control the size of the fiber pore (31). Some fiber production processes, such as electrospinning, use solvents that denature natural fibers (59). In contrast, synthetic fiber scaffolds are stable over a wide range of temperatures and in solution (31). Synthetic fibers are easier to control the pore size and can also be used to mimic the porous structure of ECM (60). However, these fibers may be less hydrophilic, and some may be toxic and antigenic, which can damage cells. Due to these limitations, efforts are being made to enhance their properties while preserving their respective benefits.

In terms of natural materials, Mahmoudzadeh et al. (61) developed collagen-chitosan nanoscaffolds and utilized them to culture 4T1 tumor cells, allowing for the construction of a 3D microenvironment as the tumor cells infiltrated the scaffolds. Koh et al. (62) presented a comprehensive protocol for studying live cell microscopy and immunohistochemistry to quantitatively assess physiological cell-cell contact dynamics. Decellularized natural tissues have also emerged as a source of fibrous scaffolds for cancer research (63), such as decellularized lung scaffolds, which retain the ECM arrangement of the original tissue and allow for better simulation of cell-ECM interactions (64). Tissue engineering can also be employed to construct tumors *in vitro*, as demonstrated by Lu et al. (65), who utilized Tris-trypsin-Triton to treat tumor tissues in multiple steps, creating 3D scaffolds with the ideal spatial arrangement, biomechanical properties, and biocompatibility - a promising approach for modeling the TME.

In terms of synthetic materials, Girard (66) et al. developed the “3P” scaffold, which is produced by electrospinning the block copolymers of poly (lactate-coglycolic acid) (PLGA), polylactic acid (PLA) and mono-methoxy polyethylene glycol (mPEG). Fischbach (67) et al. used polylactide to fabricate fiber scaffolds. Both types of scaffolds are non-toxic to tumor cells and can be produced on a large scale. Additionally, tumor cells grown on these scaffolds exhibit invasion and metastasis characteristics that better replicate the *in vivo* tumor microenvironment. Mazzini (68) et al. and Murakami (69) et al. have both developed 3D tissue culture systems using silicon as a raw material. Mazzini’s team utilized silicon microprocessing technology to produce 3D microarrays for the study of tumor cell invasion. Meanwhile, Murakami’s “Cellbed” culture system is composed of a fibrous polymer made of ultra-fine silica fibers, mimicking the loose connective tissue structure of living organisms. Cancer cells can easily migrate and form 3D structures in this system.

All of the above-mentioned scaffolds are based on natural or artificial materials and are further developed to have more applications as fiber scaffolds.

5.2 Scaffold-free 3DCC model

3DCC without scaffolds mainly uses various methods to prevent cell adherent growth and aggregate tumor pellets in culture medium

(24). These methods include magnetic force, agitation and rotation, hanging drops, low-adhesion culture plates, and advanced technologies such as microfluidic chips and 3D printing. While scaffold-free 3DCC is suitable for only a limited number of cell types and is initially expensive, it allows spontaneously aggregated cells to form their own ECM (24). Scaffold-free 3DCC does not involve vasculogenesis and can restore the heterogeneity of tumors *in vivo*, thus more closely resembling solid tumors *in vivo*. It is not affected by the shear force of scaffold assembly, nor is it limited by the pore size of scaffold fibers, and can produce controllable size tumor microspheres (70). Below, we introduce the main methods and recent advances in scaffold-free 3DCC formation.

5.2.1 Hanging drop method

The hanging drop method is a relatively simple technique. Initially, cells are cultured in two dimensions and allowed to adhere to the wall before being digested into monolayer cells. The resulting digested cell culture liquid is then dropped onto the lid of a Petri dish, which is subsequently inverted. The liquid was drooped to form hanging drops through the action of surface tension, and the desired tumor pellets could be formed in the hanging drops. It usually forms in spheres or sheets within 24 hours but may take longer. The length of time required depends on the type of cells (71). This method is well-established, requiring no specialized equipment and is easy to master. The resulting tumor spheres are easy to control in terms of size, with only one sphere formed per drop. Mesenchymal stem cells cultured by the hanging drop system can secrete a large number of potent anti-inflammatory and antitumor factors (72). However, it is difficult to change the culture medium of the traditional hanging drop method, and the culture time of the cells should not be too long. Large tumor spheres cannot be cultivated due to nutrient supply effects (73). Ratnayaka (74) et al. invented a PDMS platform combining the hanging drop method and polydimethylsiloxane (PDMS) scaffold. By using this method, HepG2 cells could be grown to the level of millimeter, which was much higher than the volume of tumor microspheres obtained by the ordinary hanging drop method. Although the pendant method does not mimic tumor angiogenesis and makes it difficult to grow tumors to the size of advanced tumors *in vivo*, it is still possible to obtain larger tumor microspheres with this method, which provides convenience for tumor research.

5.2.2 Forced suspension method

The forced suspension method is to prevent tumor cells from sticking to the culture plate and forming tumor microspheres by forced suspension. The commonly used method is the liquid covering method, which precoats the surface of the culture plate with low adhesion material in advance to form an ultra-low adhesion culture plate. Tumor cells cannot adhere to the culture plate, so they spontaneously suspend to form tumor microspheres (70). The most commonly used ultra-low adhesion culture plate is a 96-well polystyrene culture plate (70). This method is simple and convenient, and most tumor cells can form tumor microspheres by this method. However, this method cannot control the size and homogeneity of the tumor microspheres formed. Napolitano et al.

(75) used microformed non-viscous hydrogels to conduct forced suspension cell culture, and cells spontaneously self-assembled and reached a structural balance controlled by cell-cell interactions. Shao (76) et al. constructed a novel tumor microsphere model by co-culturing melanoma cells and cancer-associated fibroblasts (CSF). In this model, tumor ECM is completely controlled by CSF, which facilitates the study of the interaction between tumor cells and TME. Beheshti (77) et al. used a combination of the hanging drop method and the liquid covering method to form 3D multicellular spheres to test the anticancer effect of *Ipomoea purpurea*. In addition to these new materials and methods, physical means such as magnetic force and rotation can also be used to achieve the purpose of forced suspension. Magnetic cell suspension is an emerging spheroid-forming technique. To generate spheroids, cells are preloaded with magnetic nanoparticles and then float towards the air/liquid interface within the low-adhesion plate using an externally applied magnetic field to promote cell-cell aggregation and spheroid formation. Glauco R Souza et al. reported a magnetic levitation cell culture model. By controlling the magnetic field, the geometry of the cell can be changed (78). Okochi (79) et al. used magnetite nanoparticles to make cells suspended and gathered in the center of the culture pore through the effect of magnetic force, thus realizing the suspension culture of cells. The rotating cell culture system simulates the microgravity environment by producing laminar flow (80), minimizing the mechanical stress of cell aggregation, making cells grow in suspension and preventing them from sticking to the wall and forming cell spheres. Human mesenchymal stem cells cultured in simulated microgravity have osteogenesis and enhanced adipogenesis (81). This method has been recommended by NASA as an effective tool for modeling microgravity (82). Numerous studies have illustrated the impact of short- and long-term exposure to real and simulated μg on various processes, including differentiation, growth behavior, migration, proliferation, survival, apoptosis, and adhesion, all of which are pertinent to cancer research (83). Thus, the μg -environment facilitates the creation of *in vitro* 3D tumor models, such as multicellular spheroids and organoids, that offer significant potential for preclinical drug targeting, cancer drug development, and the study of cancer progression and metastasis

on a molecular level. In conclusion, as depicted in Figure 3, the forced suspension method is a widely utilized and well-established technique.

5.2.3 Organ on chip technologies

FDA has recently agreed to assess organ on a chip technology, which has the potential to replace animal models altogether. Cancer on-chip technology typically offers the following solutions (84): (1) 2D chips. Single or multi-chamber chips with controlled substance concentration gradients to study the impact of concentration gradients on cancer metastasis; (2) Lumen chips. Lumen consisting of a patterned 3D matrix, suitable for vascular studies of tumors; (3) Partition chip. Chips are divided into several cells with a separator, capable of culturing different types of cells, making them versatile; (4) Y-type chip. Similar to partition chips but with parallel-matrix compartments operating in co-flow mode; (5) Membrane chip. Capable of creating numerous microchannels with porous membranes, facilitating solute gradients at channel interfaces, cell culture, and transfer observation. Summary of the major organ on chip technologies is now illustrated in Table 3. The use of microfluidic chips is an essential component of this technology (Figure 4). Being selected as one of the World Economic Forum's Top 10 Emerging Technologies, Microfluidics integrates sample preparation, reaction, separation, detection, and basic operational units such as cell culture, sorting, and cell lysis (97).

Microfluidics is the science of precisely manipulating fluids and particles in sizes ranging from microns to submicrons (98, 99). The use of Polydimethylsiloxane (PDMS) as a basic material for microfluidic chips is popular due to its low cost, good biocompatibility, high oxygen permeability, light transmittance, and convenience (99, 100). Glass and silicon, which are comparatively expensive and difficult to work with, have been gradually replaced by PDMS. Moreover, hydrogels and paper can also be employed to produce microfluidic chips (101). By integrating cell culture, cell separation, cell detection, and other procedures into a small chip, microfluidic technology offers the benefits of miniaturization, high precision, and high integration. Compared with traditional laboratory techniques in the past, the

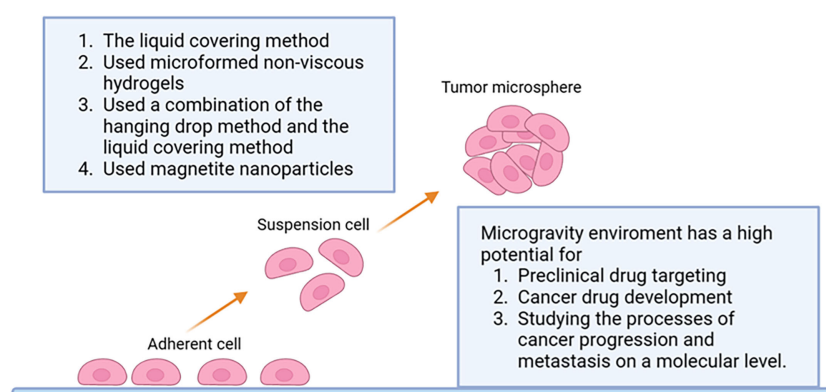


FIGURE 3

Schematic representation of the forced suspension method.

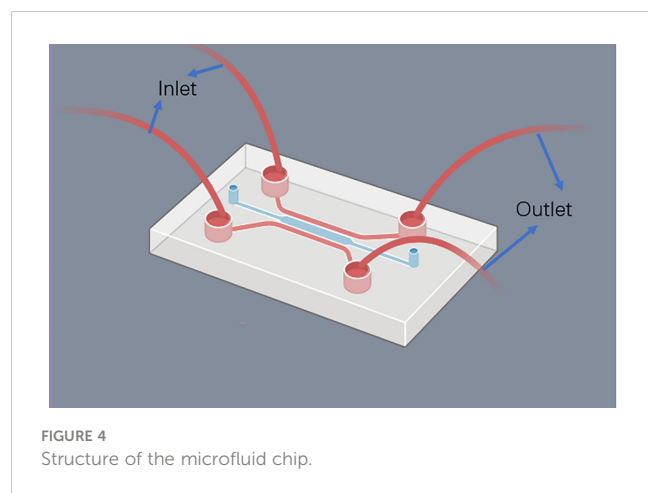
TABLE 3 Summary of the major organ on chip technologies.

Organs	Research type	Results and featured advantages	Ref.
Heart on a chip	Bioprinting 3D microfibrinous scaffolds for engineering endothelialized myocardium	1. Combines 3D printing technology and chip technology 2. Precise control of macroisotropic structure of microfibers 3. Improved alignment capable of spontaneous and synchronous contraction.	(85)
	Heart on chip for high throughput drug studies	1. High throughput, reproducible; submillimeter-sized soft elastomer film cantilever arms. 2. Better recapitulation of engineering tissues of <i>in vivo</i> physiology and quantification of multiple relevant bioanalyses.	(86)
	Heart on a chip for the neuro-cardiac junction	1. A microfluidic device consisting of two separate cell culture chambers was used to co-culture human neurons and human cardiomyocytes. 3. Summarizes the structural and functional properties of the neuro-cardiac connection. 2. Confirmed the presence of a special structure between the two cell types allowing neuromodulation.	(87)
Lung on a chip	A bovine lung-on-chip	1. Successfully generate a co-culture model of the proximal airway of bovines. 2. May replace <i>in vivo</i> experiments. 3. Simulate the blood flow required for systemic administration.	(88)
	A murine lung-on-chip infection model	1. Higher spatiotemporal resolution than animal models by time-lapse imaging technology. 2. The kinetics of host-Mycobacterium tuberculosis interactions at the gas-liquid interface are revealed. 3. The direct role of pulmonary surfactant in early infection is explored.	(89)
	3D Lung-on-Chip Model Based on Biomimetically Microcurved Culture Membranes	1. Reconstruct the main spherical geometry of the cell's native microenvironment. 2. An innovative combination of three-dimensional microfilm molding and ion tracking technology; 3. May lay the groundwork for other microanatomically-inspired membrane-based OoCs in the future.	(90)
Kidney on a chip	Culture and analysis of kidney tubuloids and perfused tubuloid cells-on-a-chip	1. Establish tubule-like cultures, simulate multi-organ interactions and reduce variability. 2. Control The microtubule microenvironment, increase model complexity. 3. Induces flow-induced shear stress.	(91)
	A kidney organoid-vasculature interaction model using a novel organ-on-chip system	1. Supports culture of renal organoids, which exhibit nephron structure. 2. Organoids cultured on a chip show increased maturity in endothelial populations. 3. Establish the first vascularized renal organoids using microfluidic organ-on-chip under HUVEC co-culture conditions.	(92)
	A kidney on a chip model for drug studies	1. Significant upregulation of organic cationic and organic anion transporters improved drug uptake. 2. Perfused 3D proximal tubule model. 3. OPTEC tubules exhibit higher normalized lactate dehydrogenase release when exposed to known nephrotoxins, which are attenuated with the addition of OCT2 and OAT1/3 transport inhibitors.	(93)
Multi organs on a chip (MOC)	A heart/liver/lung-on-a- chip	1. A highly functioning, perfusion-driven, microfluidic multi-tissue organ-on-a-chip system consisting of liver, heart, and lung organoids. 2. Three bioengineered tissue organoids are able to respond independently or synergistically to various external stimuli. 3. When organoids are combined into a single platform, more complex synthetic responses are observed.	(94)
	A lung/liver-on-a-chip	1. Ligate normal human bronchial epithelial cells cultured at the gas-liquid interface and HepaRG™ liver spheres in a single circuit. 2. MOC allows crosstalk between different organs to be studied to assess the safety and efficacy of compounds better than single cultures. 3. Provide new opportunities to study the toxicity of inhaled aerosols or to demonstrate the safety and efficacy of new drug candidates targeting human lungs.	(95)
	A multi-organ chip with matured tissue niches linked by vascular flow	1. Mature niches of heart, liver, bone and skin tissue are connected by a circulating vascular stream. 2. Summarizes the pharmacokinetic and pharmacodynamic profile of human doxorubicin. 3. Allowing the identification of early miRNA biomarkers of cardiotoxicity.	(96)

microfluidic platform has the advantages of requiring fewer samples, high sensitivity, rapid control and so on (102).

The microfluidic chip is the main platform of microfluidic technology. It takes a micropipe network as its main structural feature and microfluidics technology to control the flow of liquid

in the micropipe as its working principle. Microtubules are filled with living cells, and in this way organs or tissues *in vitro* are constructed to study their physiology and pathophysiology mechanisms (103). Due to the structure of the micron scale, the fluid exhibits and produces special properties in it that are



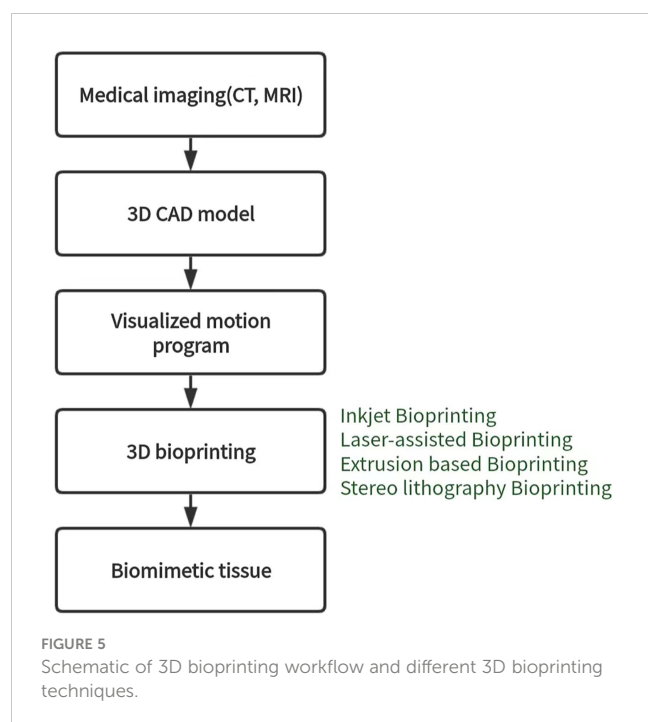
different from those of the macroscopic scale. Hence the development of unique analysis of the resulting performance. Using a microfluidic chip to culture tumor cells can rapidly produce tumor microspheres of controllable size and can also be used for high-throughput analysis of tumor cells at any time. It can be used to simulate the tumor microenvironment, study the invasion and metastasis of cancer cells, simulate tumor angiogenesis, and conduct high-throughput tumor detection (99, 100). Microfluidic chips have the potential to surpass tumor xenograft modeling, which can lead to a significant reduction in animal experimentation and make tumor modeling and research more efficient (104). Despite this, the design and production of microfluidic chips are rather intricate, and there is still a long road ahead before achieving fully integrated and “plug and play” microfluidic chips without costly external auxiliary equipment (105). Table 4 provides an overview of some of the latest microfluidic chips developed.

5.2.4 3D bioprinting

3D bioprinting is a manufacturing technology that accurately distributes biological materials containing cells to construct three-dimensional living tissues and human organs using a 3D printer. Currently, there are four types of 3D bioprinting technology, including inkjet, laser-assisted, extrusion, and stereo lithography, each with its advantages and disadvantages (114) (Figure 5). To construct 3D tumor models *in vitro*, tumors or tumor cells can be combined with TME as printing materials, and bioinks are essential for building effective 3D tumor models. Bioinks are typically biocompatible hydrogels and living cells of interest and play an important role in providing printability of samples (115, 116). Alginate and gelatin are the most commonly used substrates for bioprinting due to their good biocompatibility and mechanical properties. Bioprinting is a new research field. Compared with other cell culture technologies, the biggest advantage of the bioprinting method is that it can form tumor microsphere model with controllable size and shape in a short time, which can be used for various tumor research. However, this method is difficult to master because of its complicated technology, high cost and tedious programming of bioprinting. Inkjet 3D printing is limited due to clogged nozzles, which limits the steady flow of ink, as well as reduced cell viability (72). The mechanical pressure of extrusion printers can also damage cultured cells. Jiang (117) et al. combined alginate and gelatin to form a composite hydrogel similar to a natural tumor matrix. Chen (118) et al. cocultured primary HepG2 human hepatocytes and hepatic stellate cells (HSC) to form spherules. Then the spheres were bioprinted into liver tissue constructs using a Regenova bioprinter to construct a new liver cancer model. Bhattacharjee (119) et al. used packaged granular microgels to make liquid-like solid materials. The material is locally and temporarily fluidized under concentrated applied stress and spontaneously solidifies after the applied stress is removed, facilitating the transport of biomolecules and 3D printing of multicellular structures. In summary, 3D bioprinted cancer models can be valuable as invasion models and serve as an excellent tool to study

TABLE 4 New progress of microfluidic chips.

Research purpose	Innovation	Results	Ref.
Cancer cell migration model	3D collagen barrier is formed through polyelectrolyte composite solidification process	Form 3D aggregates of cells similar to cancer tumors, mimicking the migration of cancer cells <i>in vivo</i>	(106)
Microarray cell culture system	1156 square microcontainers, large capacity, to ensure nutrient supply external bioreactor	Preserve the function of rat primary hepatocytes for more than 2 weeks	(107)
New microfluidic platform	The microfluidic platform can realize the microfluidic control with many repetitions and long duration	High-throughput production of tumors of uniform size; Various 3D tumor microspheres produced in the device	(108)
New cell culture methods	Gelatin-based 384-well ready-to-use microscaffold array	It is suitable for a variety of tumor cells and can be used for drug resistance detection and tumor cell culture	(109)
New manufacturing of cell sphere	Construct a multicellular culture platform using acoustic fluid	This produces more than 6000 tumor spheres per operation and shortens the tumor sphere formation time to one day.	(110)
New microfluidic chip	Polydimethylsiloxane is made of a double casting technique with a thermal aging step	The tumor microsphere culture time of up to 4 weeks can observe the reaction of tumor microsphere for a long time	(111)
Novel TME model	Cancer cells in the microcapsule were encapsulated with a hydrogel shell to form a 3D vascularized tumor	The angiogenesis in the 3D microenvironment of human tumor was simulated	(112)
New 3D co-culture model	Panc-1 tumor spheres were co-cultured with pancreatic stellate cells using microarray chips and	The role of pancreatic stellate cells in tumor development and metastasis was studied	(113)



cancer progression and visualize EMT and metastasis in real-time. Nonetheless, there are still several challenges and limitations that need to be addressed. These include the development of a perfusable, vascularized 3D bioprinted construct, achieving large organ reconstruction *in vitro*, long-term *in vitro* culture, and other related issues.

6 Conclusion

3DCC is increasingly important in oncology research as it better mimics solid tumor conditions *in vivo* with minimal use of animal models. Although 3DCC has obvious advantages over 2DCC, 3DCC cannot completely replace 2DCC (120) at present because the monolayer culture equipment is easy to manufacture, the production cost is low and the technology is easy. As summarized in Figure 2, 3DCC models have unparalleled advantages in simulating the tumor microenvironment. Although tumor-like 3D cultures allow the expansion of the tumor epithelium, they often lack non-epithelial stromal cells from tumors of origin, limiting their usefulness in addressing therapeutic strategies targeting this compartment (121). With the maturation and development of 3DCC technology, its application in the study of tumor metastasis mechanism, tumor microenvironment, tumor cell-ECM interaction

and anti-cancer drug screening will be more extensive and in-depth, making it a promising technology for the future.

Author contributions

LZ, XL and YM contributed to the manuscript's composition, literature review, and drafting and finalization of the manuscript. SC, WL and YC contributed to the literature review and search. PC contributed to the manuscript's drafting and critical review. XL and YM contributed to the approval of the final version of the manuscript.

Funding

This study was supported by grants from the Natural Science Foundation of Guangdong Province (2023A1515011805 and 2022A1515011052), the National Natural Science Foundation of China (81873591), the Science and Technology Planning Project of Guangdong Province (2018A050506030), the Science and Technology Program of Guangzhou (201704020073), the Guangdong Provincial Key Laboratory Construction Projection on Organ Donation and Transplant Immunology (2013A061401007, 2017B030314018, and 2020B1212060026), and the Guangdong Provincial International Cooperation Base of Science and Technology (Organ Transplantation) (2015B050501002 and 2020A0505020003).

Conflict of interest

The authors declare that the research was conducted in the absence of any commercial or financial relationships that could be construed as a potential conflict of interest.

Publisher's note

All claims expressed in this article are solely those of the authors and do not necessarily represent those of their affiliated organizations, or those of the publisher, the editors and the reviewers. Any product that may be evaluated in this article, or claim that may be made by its manufacturer, is not guaranteed or endorsed by the publisher.

References

- Hulvat MC. Cancer incidence and trends. *Surg Clin North Am* (2020) 100:469. doi: 10.1016/j.suc.2020.01.002
- Witz IP. The cross talk between cancer cells and their microenvironments. *Biochem Biophys Res Commun* (2022) 633:59. doi: 10.1016/j.bbrc.2022.09.066
- Atat OE, Farzaneh Z, Pourhamzeh M, Taki F, Abi-Habib R, Vosough M, et al. 3D modeling in cancer studies. *Hum Cell* (2022) 35:23. doi: 10.1007/s13577-021-00642-9
- Robinson NB, Krieger K, Khan FM, Huffman W, Chang M, Naik A. The current state of animal models in research: A review. *Int J Surg* (2019) 72:9. doi: 10.1016/j.ijsu.2019.10.015

5. Côté MF, Turcotte A, Doillon C, Gobeil S. Three-dimensional culture assay to explore cancer cell invasiveness and satellite tumor formation. *J Vis Exp* (2016) (114):54322. doi: 10.3791/54322
6. Gencoglu MF, Barney LE, Hall CL, Brooks EA, Schwartz AD, Corbett DC, et al. Comparative study of multicellular tumor spheroid formation methods and implications for drug screening. *ACS Biomater Sci Eng* (2018) 4:410. doi: 10.1021/acsbomaterials.7b00069
7. Wu T, Dai Y. Tumor microenvironment and therapeutic response. *Cancer Lett* (2017) 387:61. doi: 10.1016/j.canlet.2016.01.043
8. Chen Y, McAndrews KM, Kalluri R. Clinical and therapeutic relevance of cancer-associated fibroblasts. *Nat Rev Clin Oncol* (2021) 18:792. doi: 10.1038/s41571-021-00546-5
9. Pan Y, Yu Y, Wang X, Zhang T. Tumor-associated macrophages in tumor immunity. *Front Immunol* (2020) 11:583084. doi: 10.3389/fimmu.2020.583084
10. Sobierajska K, Ciszewski WM, Sacewicz-Hofman I, Niewiarowska J. Endothelial cells in the tumor microenvironment. *Adv Exp Med Biol* (2020) 1234:71. doi: 10.1007/978-3-030-37184-5_6
11. Colombo E, Cattaneo MG. Multicellular 3D models to study tumour-stroma interactions. *Int J Mol Sci* (2021) 22(4):1633. doi: 10.3390/ijms22041633
12. Walker C, Mojares E, Del Rio Hernández A. Role of extracellular matrix in development and cancer progression. *Int J Mol Sci* (2018) 19(10):3028. doi: 10.3390/ijms19103028
13. Shannon AE, Boos CE, Hummon AB. Co-Culturing multicellular tumor models: Modeling the tumor microenvironment and analysis techniques. *Proteomics* (2021) 21: e2000103. doi: 10.1002/pmic.202000103
14. Thoma CR, Zimmermann M, Agarkova I, Kelm JM, Krek W. 3D cell culture systems modeling tumor growth determinants in cancer target discovery. *Adv Drug Delivery Rev* (2014) 29:69–70. doi: 10.1016/j.addr.2014.03.001
15. Barbosa M, Xavier C, Pereira RF, Petrikaitė V, Vasconcelos MH. 3D cell culture models as recapitulators of the tumor microenvironment for the screening of anti-cancer drugs. *Cancers (Basel)* 14 (2021) 14(1):190. doi: 10.3390/cancers14010190
16. Habanjar O, Diab-Assaf M, Caldefie-Chezet F, Delort L. 3D cell culture systems: Tumor application, advantages, and disadvantages. *Int J Mol Sci* (2021) 22(22):12200. doi: 10.3390/ijms222212200
17. Unnikrishnan K, Thomas IV, Ram KR. Advancement of scaffold-based 3D cellular models in cancer tissue engineering: An update. *Front Oncol* (2021) 11:733652. doi: 10.3389/fonc.2021.733652
18. Hoarau-Véchet J, Rafii A, Touboul C, Pasquier J. Halfway between 2D and animal models: Are 3D cultures the ideal tool to study cancer-microenvironment interactions? *Int J Mol Sci* (2018) 19(1):181. doi: 10.3390/ijms19010181
19. Wang C, Tang Z, Zhao Y, Yao R, Li L, Sun W, et al. Three-dimensional *in vitro* cancer models: a short review. *Biofabrication* (2014) 6:22001. doi: 10.1088/1758-5082/6/2/022001
20. Weiswald LB, Bellet D, Dangles-Marie V. Spherical cancer models in tumor biology. *Neoplasia* (2015) 17:1. doi: 10.1016/j.neo.2014.12.004
21. Ishiguro T, Ohata H, Sato A, Yamawaki K, Enomoto T, Okamoto K, et al. Tumor-derived spheroids: Relevance to cancer stem cells and clinical applications. *Cancer Sci* (2017) 108:283. doi: 10.1111/cas.13155
22. Weiswald LB, Richon S, Validire P, Briffod M, Lai-Kuen R, Cordelières FP, et al. Newly characterised ex vivo colospheres as a three-dimensional colon cancer cell model of tumour aggressiveness. *Br J Cancer* (2009) 101:473. doi: 10.1038/sj.bjc.6605173
23. Kaaijk P, Troost D, Das PK, Leenstra S, Bosch DA. Long-term culture of organotypic multicellular glioma spheroids: a good culture model for studying gliomas. *Neuropathol Appl Neurobiol* (1995) 21:386. doi: 10.1111/j.1365-2990.1995.tb01075.x
24. Ferreira LP, Gaspar VM, Mano JF. Design of spherically structured 3D *in vitro* tumor models -advances and prospects. *Acta Biomater* (2018) 75:11. doi: 10.1016/j.actbio.2018.05.034
25. Iwasaki H, Suda T. Cancer stem cells and their niche. *Cancer Sci* (2009) 100:1166. doi: 10.1111/j.1349-7006.2009.01177.x
26. Bielecka ZF, Maliszewska-Olejniczak K, Safir IJ, Szczylik C, Czarnecka AM. Three-dimensional cell culture model utilization in cancer stem cell research. *Biol Rev Camb Philos Soc* (2017) 92:1505. doi: 10.1111/brev.12293
27. Pollard SM, Yoshikawa K, Clarke ID, Danovi D, Stricker S, Russell R, et al. Glioma stem cell lines expanded in adherent culture have tumor-specific phenotypes and are suitable for chemical and genetic screens. *Cell Stem Cell* (2009) 4:568. doi: 10.1016/j.stem.2009.03.014
28. Hubert CG, Rivera M, Spangler Wu LC Q, Mack SC, Prager BC, et al. A three-dimensional organoid culture system derived from human glioblastomas recapitulates the hypoxic gradients and cancer stem cell heterogeneity of tumors found *In vivo*. *Cancer Res* (2016) 76:2465. doi: 10.1158/0008-5472.CAN-15-2402
29. Zhang M, Xu C, Wang HZ, Peng YN, Li HO, Zhou YJ, et al. Soft fibrin matrix downregulates DAB2IP to promote nanog-dependent growth of colon tumor-repopulating cells. *Cell Death Dis* (2019) 10:151. doi: 10.1038/s41419-019-1309-7
30. Saglam-Metiner P, Gulce-Iz S, Biray-Avci C. Bioengineering-inspired three-dimensional culture systems: Organoids to create tumor microenvironment. *Gene* (2019) 686:203. doi: 10.1016/j.gene.2018.11.058
31. Castiaux AD, Spence DM, Martin RS. Review of 3D cell culture with analysis in microfluidic systems. *Anal Methods* (2019) 11:4220. doi: 10.1039/C9AY01328H
32. Langhans SA. Three-dimensional *in vitro* cell culture models in drug discovery and drug repositioning. *Front Pharmacol* (2018) 9:6. doi: 10.3389/fphar.2018.00006
33. Tibbitt MW, Anseth KS. Hydrogels as extracellular matrix mimics for 3D cell culture. *Biotechnol Bioeng* (2009) 103:655. doi: 10.1002/bit.22361
34. Sun D, Liu Y, Wang H, Deng F, Zhang Y, Zhao S, et al. Novel decellularized liver matrix-alginate hybrid gel beads for the 3D culture of hepatocellular carcinoma cells. *Int J Biol Macromol* (2018) 109:1154. doi: 10.1016/j.ijbiomac.2017.11.103
35. De S, Joshi A, Tripathi DM, Kaur S, Singh N. Alginate based 3D micro-scaffolds mimicking tumor architecture as *in vitro* cell culture platform. *Mater Sci Eng C Mater Biol Appl* (2021) 128:112344. doi: 10.1016/j.msec.2021.112344
36. Worthington P, Pochan DJ, Langhans SA. Peptide hydrogels - versatile matrices for 3D cell culture in cancer medicine. *Front Oncol* (2015) 5:92. doi: 10.3389/fonc.2015.00092
37. Calitz C, Pavlović N, Rosenquist J, Zagami C, Samanta A, Heindryckx F, et al. A biomimetic model for liver cancer to study tumor-stroma interactions in a 3D environment with tunable bio-physical properties. *J Vis Exp* (2020) (162):10.3791/61606. doi: 10.3791/61606
38. Yip D, Cho CH. A multicellular 3D heterospheroid model of liver tumor and stromal cells in collagen gel for anti-cancer drug testing. *Biochem Biophys Res Commun* (2013) 433:327. doi: 10.1016/j.bbrc.2013.03.008
39. Turtoi M, Anghelache M, Bucatariu SM, Deleanu M, Voicu G, Safciuc F, et al. A novel platform for drug testing: Biomimetic three-dimensional hyaluronic acid-based scaffold seeded with human hepatocarcinoma cells. *Int J Biol Macromol* (2021) 185:604. doi: 10.1016/j.ijbiomac.2021.06.174
40. Pradhan S, Clary JM, Seliktar D, Lipke EA. A three-dimensional spheroidal cancer model based on PEG-fibrinogen hydrogel microspheres. *Biomaterials* (2017) 115:141. doi: 10.1016/j.biomaterials.2016.10.052
41. Ozawa F, Ino K, Arai T, Ramón-Azcón J, Takahashi Y, Shiku H, et al. Alginate gel microwell arrays using electrodeposition for three-dimensional cell culture. *Lab chip* (2013) 13:3128. doi: 10.1039/c3lc50455g
42. Liu T, Yi S, Liu G, Hao X, Du T, Chen J, et al. Aqueous two-phase emulsions-templated tailorable porous alginate beads for 3D cell culture. *Carbohydr Polym* (2021) 258:117702. doi: 10.1016/j.carbpol.2021.117702
43. Worthington P, Drake KM, Li Z, Napper AD, Pochan DJ, Langhans SA, et al. Beta-hairpin hydrogels as scaffolds for high-throughput drug discovery in three-dimensional cell culture. *Anal Biochem* (2017) 535:25. doi: 10.1016/j.ab.2017.07.024
44. Leong W, Kremer A, Wang DA. Development of size-customized hepatocarcinoma spheroids as a potential drug testing platform using a sacrificial gelatin microsphere system. *Mater Sci Eng C Mater Biol Appl* (2016) 63:644. doi: 10.1016/j.msec.2016.03.046
45. Antunes J, Gaspar VM, Ferreira L, Monteiro M, Henrique R, Jerónimo C, et al. In-air production of 3D co-culture tumor spheroid hydrogels for expedited drug screening. *Acta Biomater* (2019) 94:392. doi: 10.1016/j.actbio.2019.06.012
46. Benton G, Arnaoutova I, George J, Kleinman HK, Koblinksi J. Matrigel: from discovery and ECM mimicry to assays and models for cancer research. *Adv Drug Delivery Rev* (2014) 3:79–80. doi: 10.1016/j.addr.2014.06.005
47. Singh M, Close DA, Mukundan S, Johnston PA, Sant S. Production of uniform 3D microtumors in hydrogel microwell arrays for measurement of viability, morphology, and signaling pathway activation. *Assay Drug Dev Technol* (2015) 13:570. doi: 10.1089/adt.2015.662
48. Ramadhan W, Ohama Y, Minamihata K, Moriyama K, Wakabayashi R, Goto M, et al. Redox-responsive functionalized hydrogel marble for the generation of cellular spheroids. *J Biosci BIOENG* (2020) 130:416. doi: 10.1016/j.jbiosc.2020.05.010
49. Hu K, Zhou N, Li Y, Ma S, Guo Z, Cao M, et al. Sliced magnetic polyacrylamide hydrogel with cell-adhesive microarray interface: A novel multicellular spheroid culturing platform. *ACS Appl Mater Interfaces* (2016) 8:15113. doi: 10.1021/acsami.6b04112
50. Heffernan JM, Overstreet DJ, Srinivasan S, Le LD, Vernon BL, Sirianni RW, et al. Temperature responsive hydrogels enable transient three-dimensional tumor cultures via rapid cell recovery. *J BioMed Mater Res A* (2016) 104:17. doi: 10.1002/jbm.a.35534
51. Chen H, Wei X, Chen H, Wei H, Wang Y, Nan W, et al. The study of establishment of an *in vivo* tumor model by three-dimensional cells culture systems methods and evaluation of antitumor effect of biotin-conjugated pullulan acetate nanoparticles. *Artif Cells Nanomed Biotechnol* (2019) 47:123. doi: 10.1080/21691401.2018.1544142
52. Liu H, Liu J, Qi C, Fang Y, Zhang L, Zhuo R, et al. Thermosensitive injectable *in-situ* forming carboxymethyl chitin hydrogel for three-dimensional cell culture. *Acta Biomater* (2016) 35:228. doi: 10.1016/j.actbio.2016.02.028
53. Mahadeva SK, Walus K, Stoeber B. Paper as a platform for sensing applications and other devices: a review. *ACS Appl Mater Interfaces* (2015) 7:8345. doi: 10.1021/acsami.5b00373
54. Ng K, Gao B, Yong K, Li Y, Shi M, Zhao X, et al. Paper-based cell culture platform and its emerging biomedical applications. *Mater Today* (2017) 20:32. doi: 10.1016/j.mattod.2016.07.001

55. Derda R, Laromaine A, Mammoto A, Tang SK, Mammoto T, Ingber DE, et al. Paper-supported 3D cell culture for tissue-based bioassays. *Proc Natl Acad Sci U.S.A.* (2009) 106:18457. doi: 10.1073/pnas.0910666106
56. Lantigua D, Kelly YN, Unal B, Camci-Unal G. Engineered paper-based cell culture platforms. *Adv Healthc Mater* (2017) 6(22):10.1002/adhm.201700619. doi: 10.1002/adhm.201700619
57. Tamayol A, Akbari M, Annabi N, Paul A, Khademhosseini A, Juncker D, et al. Fiber-based tissue engineering: Progress, challenges, and opportunities. *Biotechnol Adv* (2013) 31:669. doi: 10.1016/j.biotechadv.2012.11.007
58. Shin SR, Bae H, Cha JM, Mun JY, Chen YC, Tekin H, et al. Carbon nanotube reinforced hybrid microgels as scaffold materials for cell encapsulation. *ACS Nano* (2012) 6:362. doi: 10.1021/nn203711s
59. Liu T, Teng WK, Chan BP, Chew SY. Photochemical crosslinked electrospun collagen nanofibers: synthesis, characterization and neural stem cell interactions. *J BioMed Mater Res A* (2010) 95:276. doi: 10.1002/jbma.a.32831
60. Xue J, Xie J, Liu W, Xia Y. Electrospun nanofibers: New concepts, materials, and applications. *Acc Chem Res* (2017) 50:1976. doi: 10.1021/acs.accounts.7b00218
61. Mahmoudzadeh A, Mohammadpour H. Tumor cell culture on collagen-chitosan scaffolds as three-dimensional tumor model: A suitable model for tumor studies. *J Food Drug Anal* (2016) 24:620. doi: 10.1016/j.jfda.2016.02.008
62. Koh WH, Zayats R, Lopez P, Murooka TT. Visualizing cellular dynamics and protein localization in 3D collagen. *Star Protoc* (2020) 1:100203. doi: 10.1016/j.xpro.2020.100203
63. Li W, Hu X, Yang S, Wang S, Zhang C, Wang H, et al. A novel tissue-engineered 3D tumor model for anti-cancer drug discovery. *Biofabrication* (2018) 11:15004. doi: 10.1088/1758-5090/aae270
64. Stabler CT, Lecht S, Mondrinos JJ, Goulart E, Lazarovici P, Lelkes PI, et al. Revascularization of decellularized lung scaffolds: principles and progress. *Am J Physiol Lung Cell Mol Physiol* (2015) 309:L1273. doi: 10.1152/ajplung.00237.2015
65. Lü WD, Zhang L, Wu CL, Liu ZG, Lei GY, Liu J, et al. Development of an acellular tumor extracellular matrix as a three-dimensional scaffold for tumor engineering. *PLoS One* (2014) 9:e103672. doi: 10.1371/journal.pone.0103672
66. Girard YK, Wang C, Ravi S, Howell MC, Mallela J, Alibrahim M, et al. A 3D fibrous scaffold inducing tumoroids: a platform for anticancer drug development. *PLoS One* (2013) 8:e75345. doi: 10.1371/journal.pone.0075345
67. Fischbach C, Chen R, Matsumoto T, Schmelzle T, Brugge JS, Polverini PJ, et al. Engineering tumors with 3D scaffolds. *Nat Methods* (2007) 4:855. doi: 10.1038/nmeth1085
68. Mazzini G, Carpinano F, Surdo S, Aredia F, Panini N, Torchio M, et al. 3D silicon microstructures: A new tool for evaluating biological aggressiveness of tumor cells. *IEEE Trans Nanobioscience* (2015) 14:797. doi: 10.1109/TNB.2015.2476351
69. Murakami S, Tanaka H, Nakayama T, Taniura N, Miyake T, Tani M, et al. Similarities and differences in metabolites of tongue cancer cells among two- and three-dimensional cultures and xenografts. *Cancer Sci* (2021) 112:918. doi: 10.1111/cas.14749
70. Amaral R, Miranda M, Marcato PD, Swiech K. Comparative analysis of 3D bladder tumor spheroids obtained by forced floating and hanging drop methods for drug screening. *Front Physiol* (2017) 8:605. doi: 10.3389/fphys.2017.00605
71. Foty R. A simple hanging drop cell culture protocol for generation of 3D spheroids. *J Vis Exp* (2011) 51:2720. doi: 10.3791/2720-v
72. Khunmanee S, Park H. Three-dimensional culture for *In vitro* folliculogenesis in the aspect of methods and materials. *Tissue Eng Part B Rev* (2022) 28:1242. doi: 10.1089/ten.teb.2021.0229
73. Huang SW, Tzeng SC, Chen JK, Sun JS, Lin F-H. A dynamic hanging-drop system for mesenchymal stem cell culture. *Int J Mol Sci* (2020) 21(12):4298. doi: 10.3390/ijms21124298
74. Ratnayaka SH, Hillburn TE, Forouzan O, Shevkoplyas SS, Khismatullin DB. PDMS well platform for culturing millimeter-size tumor spheroids. *Biotechnol Prog* (2013) 29:1265. doi: 10.1002/btpr.1764
75. Napolitano AP, Dean DM, Man AJ, Youssef J, Ho DN, Rago AP, et al. Scaffold-free three-dimensional cell culture utilizing micromolded nonadhesive hydrogels. *Biotechniques* (2007) 43:494. doi: 10.2144/000112591
76. Shao H, Moller M, Wang D, Ting A, Boulina M, Liu ZJ, et al. A novel stromal fibroblast-modulated 3D tumor spheroid model for studying tumor-stroma interaction and drug discovery. *J Vis Exp* (2020) 156:10.3791/60660. doi: 10.3791/60660
77. Beheshti F, Shabani AA, AkbariEidgahi MR, Kookhaei P, Vazirian M, Safavi M, et al. Anticancer activity of ipomoea purpurea leaves extracts in monolayer and three-dimensional cell culture. *Evid-Based Compl Alt* (2021) 2021:6666567. doi: 10.1155/2021/6666567
78. Souza GR, Molina JR, Raphael RM, Ozawa MG, Stark DJ, Levin CS, et al. Three-dimensional tissue culture based on magnetic cell levitation. *Nat Nanotechnol* (2010) 5:291. doi: 10.1038/nano.2010.23
79. Okochi M, Takano S, Isaji Y, Senga T, Hamaguchi M, Honda H, et al. Three-dimensional cell culture array using magnetic force-based cell patterning for analysis of invasive capacity of BALB/3T3v-src. *Lab Chip* (2009) 9:3378. doi: 10.1039/b909304d
80. Ryu NE, Lee SH, Park H. Spheroid culture system methods and applications for mesenchymal stem cells. *Cells-Basel* (2019) 8(12):1620. doi: 10.3390/cells8121620
81. Meyers VE, Zayzafoon M, Douglas JT, McDonald JM. RhoA and cytoskeletal disruption mediate reduced osteoblastogenesis and enhanced adipogenesis of human mesenchymal stem cells in modeled microgravity. *J Bone Miner Res* (2005) 20:1858. doi: 10.1359/JBMR.050611
82. Yu B, Yu D, Cao L, Zhao X, Long T, Liu G, et al. Simulated microgravity using a rotary cell culture system promotes chondrogenesis of human adipose-derived mesenchymal stem cells via the p38 MAPK pathway. *Biochem Biophys Res Commun* (2011) 414:412. doi: 10.1016/j.bbrc.2011.09.103
83. Grimm D, Schulz H, Krüger M, Cortés-Sánchez JL, Egli M, Kraus A, et al. The fight against cancer by microgravity: The multicellular spheroid as a metastasis model. *Int J Mol Sci* (2022) 23(6):3073. doi: 10.3390/ijms23063073
84. Sleebom J, Eslami AH, Nair P, Sahlgren CM, den Toonder J. Metastasis in context: modeling the tumor microenvironment with cancer-on-a-chip approaches. *Dis Model Mech* (2018) 11(3):dmm033100. doi: 10.1242/dmm.033100
85. Zhang YS, Arneri A, Bersini S, Shin SR, Zhu K, Goli-Malekbad Z, et al. Bioprinting 3D microfibrous scaffolds for engineering endothelialized myocardium and heart-on-a-chip. *BIOMATERIALS* (2016) 110:45. doi: 10.1016/j.biomaterials.2016.09.003
86. Park J, Wu Z, Steiner PR, Zhu B, Zhang J. Heart-on-Chip for combined cellular dynamics measurements and computational modeling towards clinical applications. *Ann BioMed Eng* (2022) 50:111. doi: 10.1007/s10439-022-02902-7
87. Bernardin AA, Shabani AA, AkbariEidgahi MR, Kookhaei P, Vazirian M, Safavi M, et al. Impact of neurons on patient-derived cardiomyocytes using organ-On-A-Chip and iPSC biotechnologies. *Cells-Basel* (2022) 11(23):3764. doi: 10.3390/cells11233764
88. Ferrari E, Rasponi M. Liver-heart on chip models for drug safety. *APL Bioeng* (2021) 5:31505. doi: 10.1063/5.0048986
89. Thacker VV, Dhar N, Sharma K, Barrile R, Karalis K, McKinney JD, et al. A lung-on-chip model of early mycobacterium tuberculosis infection reveals an essential role for alveolar epithelial cells in controlling bacterial growth. *Elife* (2020) 9:e59961. doi: 10.7554/eLife.59961
90. Baptista D, Moreira Teixeira L, Barata D, Tahmasebi Birgani Z, King J, van Riet S, et al. 3D lung-on-chip model based on biomimetically microcurved culture membranes. *ACS Biomater Sci Eng* (2022) 8:2684. doi: 10.1021/acsbmaterials.1c01463
91. Gijzen L, Yousef YFA, Schutgens F, Vormann MK, Ammerlaan CME, Nicolas A, et al. Culture and analysis of kidney tubuloids and perfused tubuloid cells-on-a-chip. *Nat Protoc* (2021) 16:2023. doi: 10.1038/s41596-020-00479-w
92. Bas-Cristóbal MA, Du Z, vandenBosch TPP, Othman A, Gaio N, Silvestri C. Creating a kidney organoid-vasculature interaction model using a novel organ-on-chip system. *Sci Rep* (2022) 12:20699. doi: 10.1038/s41598-022-24945-5
93. Aceves JO, Heja S, Kobayashi K, Robinson SS, Miyoshi T, Matsumoto T, et al. 3D proximal tubule-on-chip model derived from kidney organoids with improved drug uptake. *Sci Rep* (2022) 12:14997. doi: 10.1038/s41598-022-19293-3
94. Skardal A, Murphy SV, Devarasetty M, Mead I, Kang HW, Seol YJ, et al. Multi-tissue interactions in an integrated three-tissue organ-on-a-chip platform. *Sci Rep* (2017) 7:8837. doi: 10.1038/s41598-017-08879-x
95. Bovard D, Sandoz A, Luettich K, Frentzel S, Iskandar A, Marescotti D, et al. A lung/liver-on-a-chip platform for acute and chronic toxicity studies. *Lab Chip* (2018) 18:3814. doi: 10.1039/C8LC01029C
96. Ronaldson-Bouchard K, Teles D, Yeager K, Tavakoli DN, Zhao Y, Chramiec A, et al. A multi-organ chip with matured tissue niches linked by vascular flow. *Nat BioMed Eng* (2022) 6:351. doi: 10.1038/s41551-022-00882-6
97. Wu Q, Liu J, Wang X, Feng L, Wu J, Zhu X, et al. Organ-on-a-chip: recent breakthroughs and future prospects. *BioMed Eng Online* (2020) 19:9. doi: 10.1186/s12938-020-0752-0
98. Ying L, Wang Q. Microfluidic chip-based technologies: emerging platforms for cancer diagnosis. *BMC Biotechnol* (2013) 13:76. doi: 10.1186/1472-6750-13-76
99. Lin Z, Luo G, Du W, Kong T, Liu C, Liu Z, et al. Recent advances in microfluidic platforms applied in cancer metastasis: Circulating tumor cells (CTCs) isolation and tumor-On-A-Chip. *Small* (2020) 16:e1903899. doi: 10.1002/smll.201903899
100. Fetah KL, DiPardo BJ, Kongadzem EM, Tomlinson JS, Elzagheid A, Elmusrati M, et al. Cancer modeling-on-a-Chip with future artificial intelligence integration. *Small* (2019) 15:e1901985. doi: 10.1002/smll.201901985
101. Regmi S, Poudel C, Adhikari R, Luo KQ. Applications of microfluidics and organ-on-a-Chip in cancer research. *Biosensors (Basel)* (2022) 12(7):459. doi: 10.3390/bios12070459
102. Cho HY, Choi JH, Lim J, Lee SN, Choi JW. Microfluidic chip-based cancer diagnosis and prediction of relapse by detecting circulating tumor cells and circulating cancer stem cells. *Cancers (Basel)* (2021) 13(6):1385. doi: 10.3390/cancers13061385
103. Sontheimer-Phelps A, Hassell BA, Ingber DE. Modelling cancer in microfluidic human organs-on-chips. *Nat Rev Cancer* (2019) 19:65. doi: 10.1038/s41568-018-0104-6
104. Komen J, van Neerven SM, van den Berg A, Vermeulen L, van der Meer AD. Mimicking and surpassing the xenograft model with cancer-on-chip technology. *Ebiomedicine* (2021) 66:103303. doi: 10.1016/j.ebiom.2021.103303
105. Yeo LY, Chang HC, Chan PP, Friend JR. Microfluidic devices for bioapplications. *SMALL* (2011) 7:12. doi: 10.1002/smll.201000946

106. Toh YC, Raja A, Yu H, van Noort D. A 3D microfluidic model to recapitulate cancer cell migration and invasion. *Bioengineering (Basel)* (2018) 5(2):29. doi: 10.3390/bioengineering5020029
107. Gottwald E, Lahni B, Thiele D, Giselbrecht S, Welle A, Weibezahn KF, et al. Chip-based three-dimensional cell culture in perfused micro-bioreactors. *J Vis Exp* (2008) (15):564. doi: 10.3791/564-v
108. Liu W, Tian C, Yan M, Zhao L, Ma C, Li T, et al. Heterotypic 3D tumor culture in a reusable platform using pneumatic microfluidics. *Lab Chip* (2016) 16:4106. doi: 10.1039/C6LC00996D
109. Yan X, Zhou L, Wu Z, Wang X, Chen X, Yang F, et al. High throughput scaffold-based 3D micro-tumor array for efficient drug screening and chemosensitivity testing. *Biomaterials* (2019) 198:167. doi: 10.1016/j.biomaterials.2018.05.020
110. Chen B, Wu Y, Ao Z, Cai H, Nunez A, Liu Y, et al. High-throughput acoustofluidic fabrication of tumor spheroids. *Lab Chip* (2019) 19:1755. doi: 10.1039/C9LC00135B
111. Ziolkowska K, Stelmachowska A, Kwapiszewski R, Chudy M, Dybko A, Brzózka Z, et al. Long-term three-dimensional cell culture and anticancer drug activity evaluation in a microfluidic chip. *Biosens Bioelectron* (2013) 40:68. doi: 10.1016/j.bios.2012.06.017
112. Agarwal P, Wang H, Sun M, Xu J, Zhao S, Liu Z, et al. Microfluidics enabled bottom-up engineering of 3D vascularized tumor for drug discovery. *ACS Nano* (2017) 11:6691. doi: 10.1021/acsnano.7b00824
113. Hwang HJ, Oh MS, Lee DW, Kuh HJ. Multiplex quantitative analysis of stroma-mediated cancer cell invasion, matrix remodeling, and drug response in a 3D co-culture model of pancreatic tumor spheroids and stellate cells. *J Exp Clin Cancer Res* (2019) 38:258. doi: 10.1186/s13046-019-1225-9
114. Mandrycky C, Wang Z, Kim K, Kim DH. 3D bioprinting for engineering complex tissues. *Biotechnol Adv* (2016) 34:422. doi: 10.1016/j.biotechadv.2015.12.011
115. Tiwari AP, Thorat ND, Pridl S, Patil RM, Rohiwal S, Townley H, et al. Bioink: a 3D-bioprinting tool for anticancer drug discovery and cancer management. *Drug Discovery Today* (2021) 26:1574. doi: 10.1016/j.drudis.2021.03.010
116. Xing JL, Wang YX, Du SD. Application and research progress of *in vitro* liver cancer cell culture models. *World Chin J Digestol* (2021) 29:563. doi: 10.11569/wcjd.v29.i11.563
117. Jiang T, Munguia-Lopez J, Flores-Torres S, Grant J, Vijayakumar S, DeLeon-Rodriguez A, et al. Bioprintable Alginate/Gelatin hydrogel 3D *In vitro* model systems induce cell spheroid formation. *J Vis Exp* (2018) (137):57826. doi: 10.3791/57826-v
118. Chen AM, Zhang W, Smith LJ, Walsh J, Sterner J, Gramelspacher E, et al. Hepatocellular carcinoma 3D bioprinted model with 7 days of sorafenib perfusion: Modeling the cancer microenvironment's chemotherapy response. *Transplantation* (2021) 105:14. doi: 10.1097/01.tp.0000789500.50801.c7
119. Bhattacharjee T, Gil CJ, Marshall SL, Urueña JM. Liquid-like solids support cells in 3D. *ACS Biomater Sci Eng* (2016) 2:1787. doi: 10.1021/acsbomaterials.6b00218
120. Altmann B, Welle A, Giselbrecht S, Truckenmüller R, Gottwald E. The famous versus the inconvenient - or the dawn and the rise of 3D-culture systems. *World J Stem Cells* (2009) 1:43. doi: 10.4252/wjsc.v1.i1.43
121. Ciansiosi D, Ansary J, Forbes-Hernandez TY, Regolo L, Quinzi D, Gracia Villar S, et al. The molecular basis of different approaches for the study of cancer stem cells and the advantages and disadvantages of a three-dimensional culture. *MOLECULES* (2021) 26(9):2615. doi: 10.3390/molecules26092615



OPEN ACCESS

EDITED BY

Weiguo Li,
Northwestern University, United States

REVIEWED BY

Vito Antonio Baldassarro,
University of Bologna, Italy
Kejia Cai,
University of Illinois at Chicago, United States

*CORRESPONDENCE

Benjamin Victor Ineichen
✉ benjaminvictor.ineichen@uzh.ch

†These authors have contributed equally to this work and share first authorship

RECEIVED 31 December 2022

ACCEPTED 10 April 2023

PUBLISHED 02 May 2023

CITATION

Cannon AE, Zürcher WE, Zejlou C, Kulcsar Z, Lewandowski S, Piehl F, Granberg T and Ineichen BV (2023) Neuroimaging findings in preclinical amyotrophic lateral sclerosis models—How well do they mimic the clinical phenotype? A systematic review. *Front. Vet. Sci.* 10:1135282. doi: 10.3389/fvets.2023.1135282

COPYRIGHT

© 2023 Cannon, Zürcher, Zejlou, Kulcsar, Lewandowski, Piehl, Granberg and Ineichen. This is an open-access article distributed under the terms of the [Creative Commons Attribution License \(CC BY\)](#). The use, distribution or reproduction in other forums is permitted, provided the original author(s) and the copyright owner(s) are credited and that the original publication in this journal is cited, in accordance with accepted academic practice. No use, distribution or reproduction is permitted which does not comply with these terms.

Neuroimaging findings in preclinical amyotrophic lateral sclerosis models—How well do they mimic the clinical phenotype? A systematic review

Amelia Elaine Cannon^{1†}, Wolfgang Emanuel Zürcher^{1†}, Charlotte Zejlou², Zsolt Kulcsar³, Sebastian Lewandowski⁴, Fredrik Piehl^{4,5}, Tobias Granberg^{2,4} and Benjamin Victor Ineichen ^{1,3,4*}

¹Center for Reproducible Science, University of Zurich, Zurich, Switzerland, ²Department of Neuroradiology, Karolinska University Hospital, Stockholm, Sweden, ³Department of Neuroradiology, Clinical Neuroscience Center, University Hospital Zurich, University of Zurich, Zurich, Switzerland, ⁴Department of Clinical Neuroscience, Karolinska Institutet, Stockholm, Sweden, ⁵Center of Neurology, Academic Specialist Center, Stockholm Health Services, Stockholm, Sweden

Background and objectives: Animal models for motor neuron diseases (MND) such as amyotrophic lateral sclerosis (ALS) are commonly used in preclinical research. However, it is insufficiently understood how much findings from these model systems can be translated to humans. Thus, we aimed at systematically assessing the translational value of MND animal models to probe their external validity with regards to magnetic resonance imaging (MRI) features.

Methods: In a comprehensive literature search in PubMed and Embase, we retrieved 201 unique publications of which 34 were deemed eligible for qualitative synthesis including risk of bias assessment.

Results: ALS animal models can indeed present with human ALS neuroimaging features: Similar to the human paradigm, (regional) brain and spinal cord atrophy as well as signal changes in motor systems are commonly observed in ALS animal models. Blood-brain barrier breakdown seems to be more specific to ALS models, at least in the imaging domain. It is noteworthy that the G93A-SOD1 model, mimicking a rare clinical genotype, was the most frequently used ALS proxy.

Conclusions: Our systematic review provides high-grade evidence that preclinical ALS models indeed show imaging features highly reminiscent of human ALS assigning them a high external validity in this domain. This opposes the high attrition of drugs during bench-to-bedside translation and thus raises concerns that phenotypic reproducibility does not necessarily render an animal model appropriate for drug development. These findings emphasize a careful application of these model systems for ALS therapy development thereby benefiting refinement of animal experiments.

Systematic review registration: <https://www.crd.york.ac.uk/PROSPERO/>, identifier: CRD42022373146.

KEYWORDS

motor neuron disease (MND), magnetic resonance imaging (MRI), systematic review, amyotrophic lateral sclerosis, neuroimaging, external validity, 3R, neuroscience

1. Introduction

Preclinical neuroscience has advanced our understanding of the pathophysiology of neurological diseases, and research in animal models of these diseases has identified many putative treatment targets for human diseases. However, this progress stands in stark contrast to the high attrition rates in drug development, being among the highest in neuroscience (1–4). This gap in bench-to-bedside translation can be attributed to multiple factors (5, 6), some of them inherent to the challenge of developing innovative therapies (7). However, the inappropriate design and conduct of preclinical studies have been flagged as major concerns (8–10). To this end, some attention has focused on external validity (11), i.e., the extent to which an experimental finding can be extrapolated to other settings, e.g., translation from animals to humans (12, 13).

A neuroscience subfield with particularly low bench-to-bedside translation and only exiguous therapeutic options are motor neuron diseases (MND), including entities such as amyotrophic lateral sclerosis (ALS) (4, 14, 15). In these mostly fatal diseases, magnetic resonance imaging (MRI) has become among the most important paraclinical tools for diagnostic workup (16–19). Although unspecific to MND; MRI can present with certain patterns of brain and spinal cord atrophy as well as signal changes in the corticospinal tract and motor cortex (Figure 1).

A variety of MND animal models are used for pathomechanistic investigations of these disorders, most prominently transgenic rodents with mutations in the SOD1 gene, thus mimicking familial ALS (24). However, it is insufficiently understood how well these animal models mimic human MND imaging phenotypes, i.e., what is external validity of these animal models in the neuroimaging domain? Improved understanding of the external validity of these animal models would not only benefit researchers using these models to assess putative drug candidates for MND, but it would also help to implement refinement strategies from the 3R—reduce, replace, refine—within the field (13, 25).

Thus, based on this shortcoming, we here aim at assessing the external validity of motor neuron disease animal models by systematically summarizing MRI features of MND animal models, and to compare these features with human MRI phenotypes. We focus our analysis on structural MRI as used in the clinical routine for MND diagnostic work-up. This study complements a recently published systematic review on structural neuroimaging findings in human MND (20).

2. Methods

2.1. Protocol registration

We registered a prospective study protocol in the International Prospective Register of Systematic Reviews (PROSPERO, CRD42022373146, <https://www.crd.york.ac.uk/PROSPERO/>) and

used the Preferred Reporting Items for Systematic Reviews and Meta-Analysis (PRISMA) guidelines for reporting (26).

2.2. Search strategy

We searched PubMed and Ovid EMBASE for relevant publications from inception up to December 19, 2022. See [Supplementary Table 1](#) for the search strings in each of these databases.

2.3. Inclusion and exclusion criteria

We included original publications that reported on any structural brain or spinal cord MRI outcome in MND animal models. Conference abstracts, non-English articles, and publications which reiterated previously reported quantitative data were excluded. Reviews were excluded but retained as potential sources for additional records. Reference lists of these reviews were screened for additional eligible publications.

2.4. Study selection and data extraction

Titles and abstracts of studies were screened for their relevance in the web-based application Rayyan (27) by two independent reviewers followed by full-text screening. From eligible full texts, the following data was extracted by two independent reviewers: title, authors, publication year, journal, MND model, number of animals in the treatment and control groups, MRI static magnetic field strength, and main findings related to structural neuroimaging.

2.5. Quality assessment

Risk of bias was assessed against a 3-item checklist according to the consensus statement for good laboratory practice in the modeling of stroke (sample size calculations provided, reporting of animal welfare, statement of a potential conflict of interest) (28), as well as four items on reporting any measure of randomization or blinding (29).

3. Results

3.1. General study characteristics

3.1.1. Eligible publications

In total, 364 publications were retrieved from our database search, and an additional 2 publications from reference lists of reviews on related topics. After abstract and title screening, 46 publications were eligible for full-text search. After screening the full text of these records, 34 publications (17% of deduplicated references) were included for the qualitative synthesis (Figure 2).

Abbreviations: ALS, amyotrophic lateral sclerosis; BBB, blood-brain barrier; CNS, central nervous system; CST, corticospinal tract; FTD, frontotemporal dementia; MND, motor neuron disease; MRI, magnetic resonance imaging; SWI, susceptibility-weighted imaging.

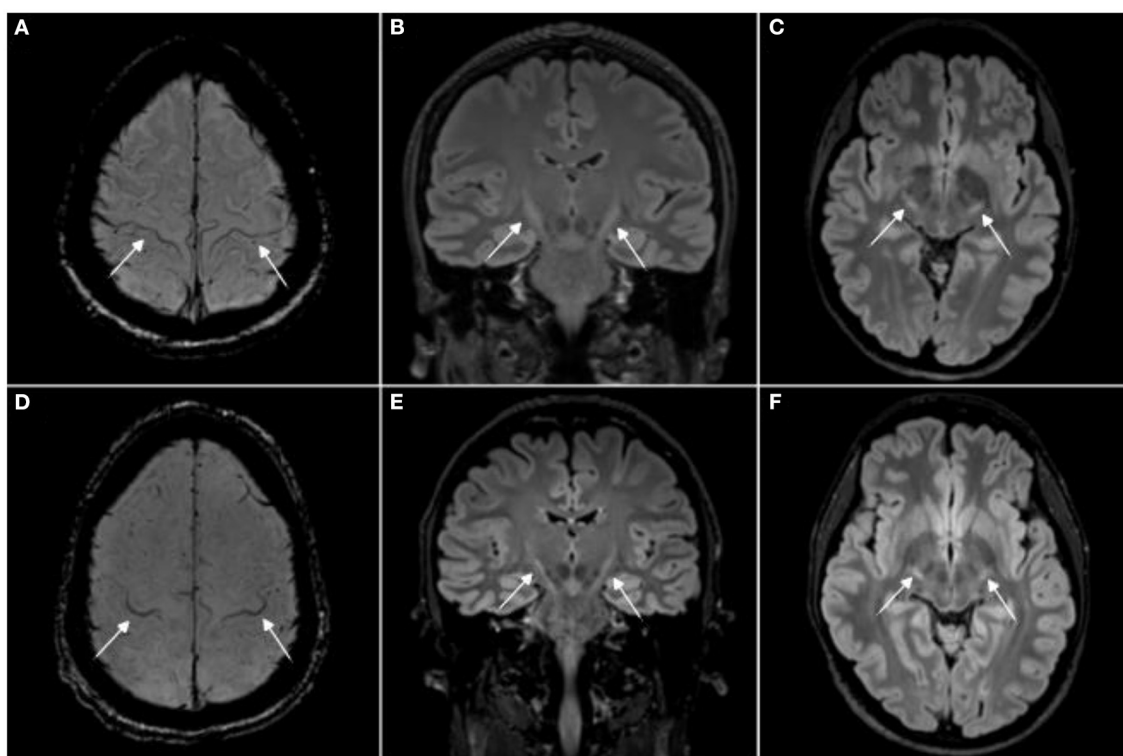


FIGURE 1

Magnetic resonance imaging signs in human amyotrophic lateral sclerosis (ALS). Magnetic resonance imaging (MRI) from two amyotrophic lateral sclerosis (ALS) patients with the “motor band sign,” i.e., motor cortex hypointensities, on susceptibility weighted imaging [SWI, (A, D)] and T2 hyperintensities along the corticospinal tract on 3T 3D T2w-FLAIR (B, C, E, F). Image adjusted from (20). For comparison, T2 signal changes in rodent brain stem motor nuclei are shown in (21–23).

3.1.2. Experimental parameters of eligible publications

The most frequently used MND animal model was the *SOD1*^{G93A} transgenic model, mimicking familial ALS (26 publications, 76%, we will refer to these models as ALS animal models in the remainder of the manuscript). The B6SJL-Tg(*SOD1*^{G93A})1Gur/J was the most commonly used mutant (15 publications, 58%), the B6.Cg-Tg(*SOD1*^{G93A})1Gur/J was only used in one publication, the remaining publications did not further specify the mutant.

Only mice and rats were used in the eligible publications (30 [88%] and 4, [12%], respectively). The employed static magnetic field strengths ranged from 1.5T to 17.6T, with most publications employing 7T (16, 47%). The median sample size of animals was 10 and 5.5 animals for the experimental and control groups, respectively (interquartile range, IQR [7–21.75] and [0.75–7.75], respectively). Four publications did not report the number of used animals.

Seven publications (21%) tested a therapeutic intervention for MND, among them mostly stem cell-based approaches (4 publications, 12%) (21, 30–32). One study each investigated liposomal encapsulated glucocorticoid (33), davunetide (an intranasal neuropeptide therapy) (34), and deferiprone (an iron chelator) (35).

More detailed data on experimental parameters can be found in [Supplementary Table 2](#).

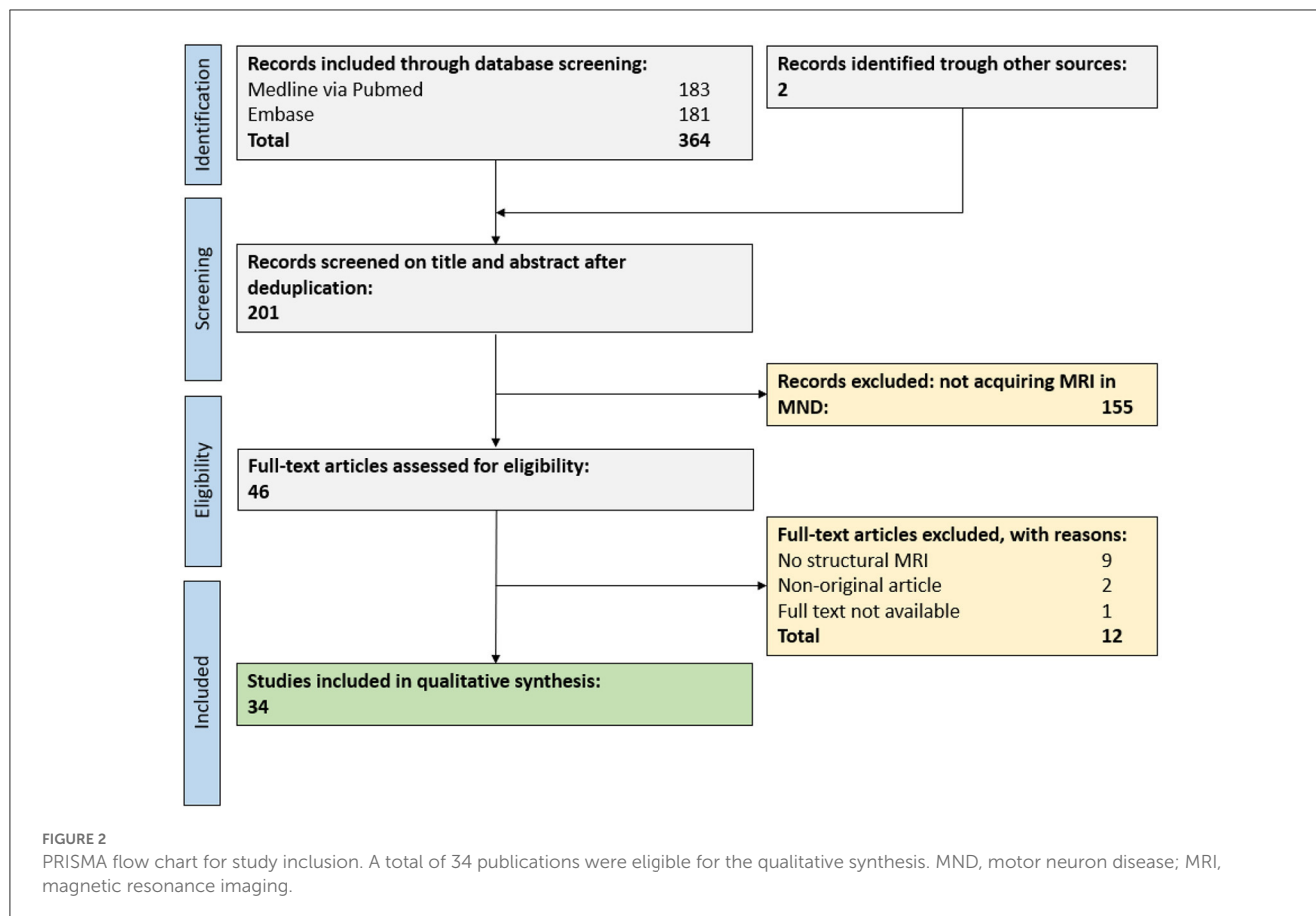
3.1.3. Risk of bias assessment

Most publications showed a low risk of bias in the animal welfare (reported by 29/34 publications, 85%) and conflict of interest domain (19/34, 56%). Yet only few publications reported randomization (7/34, 21%), blinding (6/34, 18%) or sample size calculations for their study (3/34, 9%) ([Supplementary Table 3](#)).

3.2. Neuroimaging findings in motor neuron disease animal models

3.2.1. Atrophy of brain and spinal cord

Neuroimaging has consistently shown local central nervous system (CNS) tissue volume loss in MND animal models. Yet the affected anatomical CNS regions show a high degree of variability between reports. 1-year old mice overexpressing both *APP* and *SOD1* mutations exhibited gray matter atrophy, most pronounced in the hippocampi as well as in entorhinal and cingulate cortices (36). In contrast, mice only overexpressing *SOD1* exhibited atrophy specifically in cortical regions (cingulate, retrosplenial, and temporoparietal cortex) but not in the hippocampi (36). A loss in motor cortex volume has also been observed in the murine *SOD1*^{G93A} model at postnatal day 100 (37). However, such motor cortex atrophy has not been consistent in other study using mice of similar age (38). Along these lines, a report using the *TARDBP*^{Q331K} transgenic mouse strain, i.e., a model for ALS-FTD, found a



more prominent atrophy in the entorhinal cortex compared to the motor cortex (39). Mice fed with cycad toxins (resulting in motor neuron loss) show lower volumes in the substantia nigra, striatum, basal nucleus/internal capsule, and olfactory bulb (40). A more recent study using a conditional TDP-43 mouse model found progressive volume loss of the gray matter in the olfactory bulb, frontal association cortices, lateral and dorsolateral orbital cortices, agranular insular cortices, globus pallidus, hippocampi, dorsal subiculum, secondary visual cortices, as well as in the cerebellum (41). Finally, several studies described atrophy of brain stem nuclei (42), particularly of motor nuclei, e.g., trigeminal, facial, and hypoglossal nuclei (34, 38).

Spinal cord volume loss has been observed in the murine *SOD1^{G93A}* model (37, 43), but also in the cycad toxin animal model (40).

3.2.2. Signal changes of brain and spinal cord

T2w hyperintensities have been described in rodent ALS models in the brain stem (21–23, 44, 45). These hyperintensities seem to parallel or even precede first behavioral ALS symptoms (46, 47). Histopathological correlations found associated vacuolar degeneration (23, 45–49) as well as micro- and astroglial activation (42). Interestingly, magnetic resonance microscopy was able to also detect hyperintensities in the ventral motor tracts within the murine spinal cord (50). Higher T2 values, mainly in the

ventral portions of the spinal cord, have also been observed using conventional sequences at 7T (51).

One study found iron accumulation in the cervical spinal cord (based on T2* contrast), that, however, disappeared with progressing disease (37). Iron changes have also been observed in the medulla oblongata and motor cortex (35).

3.2.3. Contrast enhancement patterns

Overt breakdown of the blood-brain barrier adjacent to lateral ventricles and in the hippocampal region was described in a rat ALS model (22). Such breakdown of the BBB was consistent in another study which also employed Ultrasmall superparamagnetic iron oxide (USPIO) enhanced MRI (52). Here, BBB breakdown was congruent with T cell infiltration. Finally, a study using dynamic contrast-enhanced MRI upon intracisternal injection of gadolinium found altered contrast medium clearance in ALS model mice compared to controls (41).

4. Discussion

4.1. Main findings

The main objective of this study was to systematically summarize the available evidence on structural CNS MRI features in ALS animal models. Frequent MRI features include brain and spinal cord atrophy, signal changes in brain stem motor nuclei

TABLE 1 Synopsis of brain and spinal cord magnetic resonance imaging findings in amyotrophic lateral sclerosis (ALS) animal models.

MRI phenotype in ALS rodent models	MRI phenotype in human ALS
Atrophy of brain and spinal cord	
Cortical gray matter	
Entorhinal (39), cingulate, retrosplenial, temporoparietal (36), motor (37), frontal association, lateral/dorsolateral orbital, agranular insular, and secondary visual cortices (41). No motor cortex atrophy (38)	Motor cortex (53–56); pre- and postcentral gyrus (57). No cortical thinning (58–62)
Subcortical gray matter	
Hippocampi (39), substantia nigra, striatum, and basal nucleus (40, 41) as well as brain stem motor nuclei (34, 38, 42)	Hippocampi (57, 58, 63, 64), thalamus (65–67), caudate nucleus, putamen, amygdala (68), and basal ganglia (69). No subcortical volume loss (58–61)
White matter structures	
Internal capsule (41)	Overall white matter (70); corpus callosum (69, 71)
Other brain structures	
Olfactory bulb (40, 41); cerebellum (41)	Total brain volume (62, 72); cerebellum (73, 74). No cerebellar atrophy (75)
Spinal cord	
Spinal cord atrophy (37, 40, 43)	Spinal cord atrophy (63, 76)
Signal changes of brain and spinal cord	
T2 hyperintensities	
T2 hyperintensities in the brain stem (21–23, 44, 45) and ventral motor tracts of the spinal cord (50, 51)	CST hyperintensity in T2w-FLAIR, but also T2w, PDw, T2*w (77, 78)
Iron accumulation/motor cortex hypointensity	
Iron accumulation in the cervical spinal cord (37), medulla oblongata, and motor cortex (35)	Motor cortex hypointensity (motor band sign) on T2w, T2*w, T2w-FLAIR, or SWI (79–82). Iron deposition in deep subcortical gray matter structures (83)
Contrast enhancement patterns	
Blood-brain barrier breakdown adjacent to lateral ventricles and in the hippocampal region (37, 47). Altered CSF gadolinium clearance (33)	No imaging data

Comparing magnetic resonance imaging (MRI) findings between amyotrophic lateral sclerosis (ALS) animal models and human ALS. Most commonly reported MRI findings in ALS animal models are brain and spinal cord volume loss, T2 and T2* signal changes as well as contrast-enhancement indicating breakdown of the blood-brain barrier.

ALS, amyotrophic lateral sclerosis; CSF, cerebrospinal fluid; CST, corticospinal tract; FLAIR, fluid-attenuated inversion recovery; FTD, frontotemporal dementia; MND, motor neuron disease; MRI, magnetic resonance imaging; PDw, proton density-weighted; SWI, susceptibility weighted imaging.

and the motor cortex as well as breakdown of the blood-brain barrier (Table 1). In the following paragraphs, we will compare this phenotype with MRI features of human ALS.

4.2. Findings in the context of existing evidence

Based on the findings of our systematic review, ALS animal models seem to feature several imaging signs reminiscent of human ALS (Table 1). Among these features is the volume loss of CNS structures with progressive disease. Atrophy in both the motor cortex (37) and the spinal cord (37, 40, 43) has been reported in ALS animal models, similar to the human imaging phenotype (20, 53, 54), which could correspond to the underlying decline of the upper and lower motor neurons (14). These similarities between the human and animal imaging phenotype are particularly interesting since most eligible animal studies used the G93A-SOD1 model thus mimicking familial ALS, a rare clinical phenotype constituting around 10% of ALS patients. It is also noteworthy that, similar to the human population (20), a wide and not always consistent array of CNS structures have been reported to be affected by volume

loss in animal models. For example, motor cortex atrophy has not been consistently shown in ALS animal models (38). It is likely that different methodological approaches for the quantification of atrophy patterns between animal studies is in part responsible for these inconsistencies: This has been emphasized by a human study in ALS-FTD patients which found variable atrophy patterns when comparing different software to assess cortical volumes (FSL, FreeSurfer, and SPM) (84). Further confounders could be technical parameters such as intra-/inter-scanner variability and physiological factors such as hydration state of animals during imaging [reviewed in (85)].

ALS rodent models can present with T2 signal changes in the CNS, potentially corresponding to axonal degeneration (23). In rodents, these signal alterations seem to commonly affect brain stem motor nuclei (21, 22). In ALS patients, T2 signal changes are also commonly observed (20, 77), albeit at different locations, i.e., mostly along the corticospinal tract (Figure 1).

Abnormal iron deposition in the motor cortex and spinal cord has been reported by some rodent ALS studies, measured by T2*-based MRI approaches (35, 37). Although respective publications did not include pictorial examples of iron deposition within the motor cortex, this feature could correspond to the “motor band

sign” (linear motor cortex hypointensity) which is commonly observed in the motor cortex of ALS patients on T2*-based sequences (Figure 1). In ALS, these signal drops seem to correspond to astro- and microglia iron deposition within deep layers of the motor cortex (86).

One imaging feature which seems more specific to rodent ALS models is breakdown of the blood-brain barrier, as visualized by gadolinium enhancement in periventricular and hippocampal regions (22). However, although gadolinium enhancement is not observed in the clinical setting in ALS, several lines of evidence demonstrate damage to the blood-brain and blood-spinal cord barrier in ALS [reviewed in (87)]. Such vascular changes seem to include alterations of tight junction proteins (88) and can be observed already early in the disease process (89). Structural MRI features of preclinical ALS models are summarized in Table 1, alongside with MRI features of human ALS.

4.3. Limitations

To assess the external validity of ALS animal models, we focused our analysis on structural brain and spinal cord MRI features. However, other disease aspects such as patterns of physical disability or also more advanced MRI methods like diffusion-tensor imaging, which are able to more specifically reflect pathogenic disease processes, might enable a more comprehensive comparison between experimental and human phenotypes.

A genuine limitation of this systematic review is that only a limited number of studies employing MRI in ALS animal models was eligible. As a result, it is difficult to map imaging phenotypes of less commonly used ALS models such as cycad toxins or wobbler mice or even for different SOD1^{G93A} mutants. It is possible that certain ALS rodent models might mimic specific human imaging phenotypes better than others (36), similarly to the situation in experimental autoimmune encephalomyelitis (EAE)—a commonly used animal model for multiple sclerosis (90).

Finally, although seven of the eligible publications tested a putative therapeutic intervention for ALS, no corresponding human MRI studies could be identified. Correlating the impact of therapeutic interventions on neuroimaging phenotypes between rodent models and humans would further enhance understanding of the translational value of experimental ALS models.

5. Conclusions

Our systematic review provides high-grade evidence that preclinical ALS models do show imaging features highly reminiscent of human ALS, including certain brain and spinal cord atrophy patterns and signal changes in motor systems (Table 1). Certain imaging features such as breakdown of the BBB are only partly reflected by these experimental models. Thus, ALS rodent models show a high external validity in the neuroimaging domain. This contrasts the high attrition of drugs in clinical ALS trials which have shown promising results in ALS animal models; and this raises concerns that a mere phenotypic comparability between experimental models and corresponding human diseases does not necessarily render an animal model appropriate for drug

development. These findings emphasize a careful application of these model systems for ALS drug development thereby benefiting refinement of animal experiments.

Data availability statement

The original contributions presented in the study are included in the article/Supplementary material, further inquiries can be directed to the corresponding author.

Author contributions

CZ, TG, and BVI conceived the study. AC, WZ, CZ, and BVI performed the literature review and data extraction. BVI wrote the manuscript. All authors provided critical input on the manuscript. All authors contributed to the article and approved the submitted version.

Funding

This study was supported by the *Swiss National Science Foundation* (Grant Nr. P400PM_183884, to BVI) as well as *Region Stockholm* and *CIMED* (to TG). None of the funders had any role in study design, data collection and analysis, decision to publish, or preparation of the manuscript.

Acknowledgments

We cordially thank Emma-Lotta Säätelä and Carl Gornitzki for competent help with the comprehensive medical library database search. We thank Thijs van Leer (Focus) and Claude Debussy for help with data analysis.

Conflict of interest

The authors declare that the research was conducted in the absence of any commercial or financial relationships that could be construed as a potential conflict of interest.

Publisher's note

All claims expressed in this article are solely those of the authors and do not necessarily represent those of their affiliated organizations, or those of the publisher, the editors and the reviewers. Any product that may be evaluated in this article, or claim that may be made by its manufacturer, is not guaranteed or endorsed by the publisher.

Supplementary material

The Supplementary Material for this article can be found online at: <https://www.frontiersin.org/articles/10.3389/fvets.2023.1135282/full#supplementary-material>

References

- Wong CH, Siah KW, Lo AW. Estimation of clinical trial success rates and related parameters. *Biostatistics*. (2019) 20:273–86. doi: 10.1093/biostatistics/kxx069
- I Kola I, Landis J. Can the pharmaceutical industry reduce attrition rates? *Nat Rev Drug Disc.* (2004) 3:711. doi: 10.1038/nrd1470
- Bespalov A, Steckler T, Altevogt B, Koustova E, Skolnick P, Deaver D et al. Failed trials for central nervous system disorders do not necessarily invalidate preclinical models and drug targets. *Nat Rev Drug Disc.* (2016) 15:516–516. doi: 10.1038/nrd.2016.88
- Scott S, Kranz JE, Cole J, Lincecum JM, Thompson K, Kelly N et al. Design, power, and interpretation of studies in the standard murine model of ALS. *Amyotrophic Lateral Sclerosis*. (2008) 9:4–15. doi: 10.1080/17482960701856300
- Waring MJ, Arrowsmith J, Leach AR, Leeson PD, Mandrell S, Owen RM, et al. An analysis of the attrition of drug candidates from four major pharmaceutical companies. *Nat Rev Drug Disc.* (2015) 14:475–86. doi: 10.1038/nrd4609
- Honkala A, Malhotra SV, Kummar S, Junttila MR. Harnessing the predictive power of preclinical models for oncology drug development. *Nat Rev Drug Disc.* (2021) 3:1–16. doi: 10.1038/s41573-021-00301-6
- Bespalov A, Bernard R, Gilis A, Gerlach B, Guillen J, Castagne V, et al. Introduction to the EQIPD quality system. *Elife*. (2021) 10:12. doi: 10.7554/eLife.63294.s2
- Ritskes-Hoitinga M, van Luijk J. How can systematic reviews teach us more about the implementation of the 3Rs and animal welfare? *Animals*. (2019) 9:1163. doi: 10.3390/ani9121163
- Ioannidis JP, Greenland S, Hlatky MA, Khoury MJ, Macleod MR, Moher D, et al. Increasing value and reducing waste in research design, conduct, and analysis. *Lancet*. (2014) 383:166–75. doi: 10.1016/S0140-6736(13)62227-8
- Vollert J, Schenker E, Macleod M, Bespalov A, Wuerbel H, Michel M, et al. Systematic review of guidelines for internal validity in the design, conduct and analysis of preclinical biomedical experiments involving laboratory animals. *BMJ open science*. (2020) 4:e100046. doi: 10.1136/bmjos-2019-100046
- Van der Worp HB, Howells DW, Sena ES, Porritt MJ, Rewell S, O'Collins V, et al. Macleod. Can animal models of disease reliably inform human studies? *PLoS Med.* (2010) 7:e1000245. doi: 10.1371/journal.pmed.1000245
- Ferreira G, Veening-Griffioen DH, Boon WP, Moors EH, Gispén-de Wied CC, Schellekens H, et al. A standardised framework to identify optimal animal models for efficacy assessment in drug development. *PLoS ONE*. (2019) 14:e0218014. doi: 10.1371/journal.pone.0218014
- Ferreira GS, Veening-Griffioen DH, Boon WP, Moors EH, van Meer PJ. Levelling the translational gap for animal to human efficacy data. *Animals*. (2020) 10:1199. doi: 10.3390/ani10071199
- Kiernan MC, Vucic S, Cheah BC, Turner MR, Eisen A, Hardiman O, et al. Amyotrophic lateral sclerosis. *Nat Rev Dis Prim.* (2017) 3:17071. doi: 10.1038/nrdp.2017.72
- Rosenfeld J, Strong MJ. Challenges in the understanding and treatment of amyotrophic lateral sclerosis/motor neuron disease. *Neurotherapeutics*. (2015) 12:317–25. doi: 10.1007/s13311-014-0332-8
- Goodin DS, Rowley HA, Olney RK. Magnetic resonance imaging in amyotrophic lateral sclerosis. *Neurol Res Int.* (2012) 2012:165.
- Kassubek J, Pagani M. Imaging in amyotrophic lateral sclerosis: MRI and PET. *Curr Opin Neurol.* (2019) 32:740–6. doi: 10.1097/WCO.0000000000000728
- Kassubek J, Müller HP. Computer-based magnetic resonance imaging as a tool in clinical diagnosis in neurodegenerative diseases. *Expert Rev Neurother.* (2016) 16:295–306. doi: 10.1586/14737175.2016.1146590
- Bede P, Hardiman O. Lessons of ALS imaging: pitfalls and future directions—a critical review. *NeuroImage: Clinical*. (2014) 4:436–43. doi: 10.1016/j.nicl.2014.02.011
- Zeijl C, Nakhostin D, Winkhofer S, Pangalu A, Kulcsar Z, Lewandowski S, et al. Structural magnetic resonance imaging findings and histopathological correlations in motor neuron diseases—A systematic review and meta-analysis. *Front Neurol.* (2022) 13:947347. doi: 10.3389/fneur.2022.947347
- Bontempi P, Busato A, Bonafede R, Schiaffino L, Scambi I, Sbarbati A, et al. MRI reveals therapeutic efficacy of stem cells: an experimental study on the SOD1(G93A) animal model. *Mag Res Med.* (2018) 79:459–69. doi: 10.1002/mrm.26685
- Andjus PR, Batavelić D, Vanhoutte G, Mitrecic D, Pizzolante F, Djogo N, et al. In vivo morphological changes in animal models of amyotrophic lateral sclerosis and Alzheimer's-like disease: MRI approach. *Anat Record.* (2009) 292:1882–92. doi: 10.1002/ar.20995
- Zang DW, Yang Q, Wang HX, Egan G, Lopes EC, Cheema SS. Magnetic resonance imaging reveals neuronal degeneration in the brainstem of the superoxide dismutase 1 transgenic mouse model of amyotrophic lateral sclerosis. *Eur J Neurosci.* (2004) 20:1745–51. doi: 10.1111/j.1460-9568.2004.03648.x
- Philips T, Rothstein JD. Rodent Models of Amyotrophic Lateral Sclerosis. *Curr. Prof. Pharmacol.* (2015) 69:5.67.1–5.67.21. doi: 10.1002/0471141755.ph0567s69
- Macleod M, Mohan S. Reproducibility and rigor in animal-based research. *ILAR J.* (2019) 60:17–23. doi: 10.1093/ilar/ilz015
- Moher D, Shamseer L, Clarke M, Ghersi D, Liberati A, Petticrew M, et al. Preferred reporting items for systematic review and meta-analysis protocols. (PRISMA-P) 2015 statement. *Syst Rev.* (2015) 4:1. doi: 10.1186/2046-4053-4-1
- Ouzzani M, Hammady H, Fedorowicz Z, Elmagarmid A. Rayyan—a web and mobile app for systematic reviews. *Syst Rev.* (2016) 5:210. doi: 10.1186/s13643-016-0384-4
- Macleod MR, Fisher M, O'collins V, Sena ES, Dirnagl U, Bath PM. Good laboratory practice: preventing introduction of bias at the bench. *J Int Soc Cereb Blood Flow Metabol.* (2009) 29:221–3. doi: 10.1038/jcbfm.2008.101
- Hooijmans CR, Hlavica M, Schuler FA, Good N, Good A, Baumgartner L, et al. Remyelination promoting therapies in multiple sclerosis animal models: a systematic review and meta-analysis. *Sci Rep.* (2019) 9:822. doi: 10.1038/s41598-018-35734-4
- Bigini P, Diana V, Barbera S, Fumagalli E, Micotti E, Sitia L, et al. Longitudinal tracking of human fetal cells labeled with super paramagnetic iron oxide nanoparticles in the brain of mice with motor neuron disease. *PLoS ONE.* (2012) 7:e32326. doi: 10.1371/journal.pone.0032326
- Bonafede R, Turano E, Scambi I, Busato A, Bontempi P, Viri F, et al. ASC-Exosomes ameliorate the disease progression in SOD1(G93A) murine model underlining their potential therapeutic use in human ALS. *Int J Mol Sci.* (2020) 21:15. doi: 10.3390/ijms21103651
- Canzi L, Castellana V, Navone S, Nava S, Dossena M, Zucca I, et al. Human skeletal muscle stem cell antiinflammatory activity ameliorates clinical outcome in amyotrophic lateral sclerosis models. *Mol Med.* (2012) 18:401–11. doi: 10.2119/molmed.2011.00123
- Evans MC, Gaillard PJ, de Boer M, Appeldoorn C, Dorland R, Sibson NR, et al. CNS-targeted glucocorticoid reduces pathology in mouse model of amyotrophic lateral sclerosis. *Acta Neuropathol Commun.* (2014) 2:66. doi: 10.1186/2051-5960-2-66
- Jouroukhin Y, Ostritsky R, Assaf Y, Pelled G, Giladi E, Gozes INAP. (davunetide) modifies disease progression in a mouse model of severe neurodegeneration: protection against impairments in axonal transport. *Neurobiol Dis.* (2013) 56:79–94. doi: 10.1016/j.nbd.2013.04.012
- Moreau C, Danel V, Devedjian JC, Grolez G, Timmerman K, Laloux C, et al. Could Conservative iron chelation lead to neuroprotection in amyotrophic lateral sclerosis? *Antioxid Redox Signal.* (2018) 29:742–8. doi: 10.1089/ars.2017.7493
- Borg J, Chereul E. Differential MRI patterns of brain atrophy in double or single transgenic mice for APP and/or SOD. *J Neurosci Res.* (2008) 86:3275–84. doi: 10.1002/jnr.21778
- Grolez G, Kyheng M, Lopes R, Moreau C, Timmerman K, Auger F, et al. MRI of the cervical spinal cord predicts respiratory dysfunction in ALS. *Sci Rep.* (2018) 8:1828. doi: 10.1038/s41598-018-19938-2
- Marcuzzo S, Zucca I, Mastropietro A, de Rosbo NK, Cavalcante P, Tartari S, et al. Hind limb muscle atrophy precedes cerebral neuronal degeneration in G93A-SOD1 mouse model of amyotrophic lateral sclerosis: a longitudinal MRI study. *Exp Neurol.* (2011) 231:30–7. doi: 10.1016/j.expneurol.2011.05.007
- White MA, Lin Z, Kim E, Henstridge CM, Pena Altamira E, Hunt CK, et al. Sarm1 deletion suppresses TDP–43-linked motor neuron degeneration and cortical spine loss. *Acta Neuropathol Commun.* (2019) 7:166. doi: 10.1186/s40478-019-0800-9
- Wilson JM, Petrik MS, Grant SC, Blackband SJ, Lai J, Shaw CA. Quantitative measurement of neurodegeneration in an ALS-PDC model using MR microscopy. *Neuroimage.* (2004) 23:336–43. doi: 10.1016/j.neuroimage.2004.05.026
- Zamani A, Walker AK, Rollo B, Ayers KL, Farah R, O'Brien TJ, et al. Impaired glymphatic function in the early stages of disease in a TDP–43 mouse model of amyotrophic lateral sclerosis. *Transl Neurodegener.* (2022) 11:17. doi: 10.1186/s40035-022-00291-4
- Evans MC, Serres S, Khrapitchev AA, Stolp HB, Anthony DC, Talbot K, et al. T₂-weighted MRI detects presymptomatic pathology in the SOD1 mouse model of ALS. *J Cereb Blood Flow Metab.* (2014) 34:785–93. doi: 10.1038/jcbfm.2014.19
- Marcuzzo S, Bonanno S, Figini M, Scotti A, Zucca I, Minati L, et al. A longitudinal DTI and histological study of the spinal cord reveals early pathological alterations in G93A-SOD1 mouse model of amyotrophic lateral sclerosis. *Exp Neurol.* (2017) 293:43–52. doi: 10.1016/j.expneurol.2017.03.018
- Grant RA, Sharp PS, Kennerley AJ, Berwick J, Grierson A, Ramesh T, et al. Abnormalities in whisking behaviour are associated with lesions in brain stem nuclei in a mouse model of amyotrophic lateral sclerosis. *Behav Brain Res.* (2014) 259:274–83. doi: 10.1016/j.bbr.2013.11.002
- Batavelić D, Djogo N, Zupunski L, Bajić A, Nicaise C, Pochet R, et al. Live monitoring of brain damage in the rat model of amyotrophic lateral sclerosis. *Gen Physiol Biophys.* (2009) 28:212–8.

46. Angenstein F, Niessen HG, Goldschmidt J, Vielhaber S, Ludolph AC, Scheich H. Age-dependent changes in MRI of motor brain stem nuclei in a mouse model of ALS. *Neuroreport*. (2004) 15:2271–4. doi: 10.1097/00001756-200410050-00026
47. Majchrzak M, Drela K, Andrzejewska A, Rogujski P, Figurska S, Fiedorowicz M, et al. SOD1/Rag2 mice with low copy number of SOD1 gene as a new long-living immunodeficient model of ALS. *Sci Rep*. (2019) 9:799. doi: 10.1038/s41598-018-37235-w
48. Bucher S, Braunstein KE, Niessen HG, Kaulisch T, Neumaier M, Boeckers TM, et al. Vacuolization correlates with spin–spin relaxation time in motor brainstem nuclei and behavioural tests in the transgenic G93A–SOD1 mouse model of ALS. *Eur J Neurosci*. (2007) 26:1895–901. doi: 10.1111/j.1460-9568.2007.05831.x
49. Caron I, Micotti E, Paladini A, Merlino G, Plebani L, Forloni G, et al. Comparative magnetic resonance imaging and histopathological correlates in Two SOD1 transgenic mouse models of amyotrophic lateral sclerosis. *PLoS ONE*. (2015) 10:e0132159. doi: 10.1371/journal.pone.0132159
50. Cowin GJ, Butler TJ, Kurniawan ND, Watson C, Wallace RH. Magnetic resonance microimaging of the spinal cord in the SOD1 mouse model of amyotrophic lateral sclerosis detects motor nerve root degeneration. *Neuroimage*. (2011) 58:69–74. doi: 10.1016/j.neuroimage.2011.06.003
51. Niessen HG, Angenstein F, Sander K, Kunz WS, Teuchert M, Ludolph AC, et al. In vivo quantification of spinal and bulbar motor neuron degeneration in the G93A–SOD1 transgenic mouse model of ALS by T2 relaxation time and apparent diffusion coefficient. *Exp Neurol*. (2006) 201:293–300. doi: 10.1016/j.expneurol.2006.04.007
52. Bataveljić D, Stamenković S, Bačić G, Andjus P. Imaging cellular markers of neuroinflammation in the brain of the rat model of amyotrophic lateral sclerosis. *Acta Physiol Hung*. (2011) 98:27–31. doi: 10.1556/APhysiol.98.2011.1.4
53. Verstraete E, Veldink JH, Hendrikse J, Schelhaas HJ, Van Den Heuvel MP, et al. Structural MRI reveals cortical thinning in amyotrophic lateral sclerosis. *J Neurol Neurosurg Psychiatry*. (2012) 83:383–8. doi: 10.1136/jnnp-2011-300909
54. Menke RA, Proudfoot M, Talbot K, Turner MR. The two-year progression of structural and functional cerebral MRI in amyotrophic lateral sclerosis. *NeuroImage Clin*. (2018) 17:953–61. doi: 10.1016/j.nicl.2017.12.025
55. Butman JA, Floeter MK. Decreased thickness of primary motor cortex in primary lateral sclerosis. *Ajnr: Am J Neuroradiol*. (2007) 28:87–91.
56. Schuster C, Kasper E, Machts J, Bittner D, Kaufmann J, Benecke R, et al. Longitudinal course of cortical thickness decline in amyotrophic lateral sclerosis. *J Neurol*. (2014) 261:1871–80. doi: 10.1007/s00415-014-7426-4
57. Cosottini M, Pesaresi I, Piazza S, Diciotti S, Cecchi P, Fabbri S, et al. Structural and functional evaluation of cortical motor areas in Amyotrophic Lateral Sclerosis. *Exp Neurol*. (2012) 234:169–80. doi: 10.1016/j.expneurol.2011.12.024
58. Acosta–Cabronero J, Machts J, Schreiber S, Abdulla S, Kollwe K, Petri S, et al. Quantitative susceptibility MRI to detect brain iron in amyotrophic lateral sclerosis. *Radiology*. (2018) 289:195–203. doi: 10.1148/radiol.2018180112
59. Agosta F, Spinelli EG, Riva N, Fontana A, Basaia S, Canu E, et al. Survival prediction models in motor neuron disease. *Eur J Neurol*. (2019) 26:1143–52. doi: 10.1111/ene.13957
60. Cardenas–Blanco A, Machts J, Acosta–Cabronero J, Kaufmann J, Abdulla S, Kollwe K, et al. Structural and diffusion imaging versus clinical assessment to monitor amyotrophic lateral sclerosis. *NeuroImage Clin*. (2016) 11:408–414. doi: 10.1016/j.nicl.2016.03.011
61. Duning T, Schiffbauer H, Warnecke T, Mohammadi S, Floel A, Kolpatzik K, et al. G–CSF prevents the progression of structural disintegration of white matter tracts in amyotrophic lateral sclerosis: a pilot trial. *PLoS ONE*. (2011) 6:e17770. doi: 10.1371/journal.pone.0017770
62. Ellis CM, Suckling J, Amaro Jr E, Bullmore ET, Simmons A, Williams SC, et al. Volumetric analysis reveals corticospinal tract degeneration and extramotor involvement in ALS. *Neurology*. (2001) 57:1571–8. doi: 10.1212/WNL.57.9.1571
63. Piaggio N, Pardini M, Roccatagliata L, Scialò C, Cabona C, Bonzano L, et al. Cord cross-sectional area at foramen magnum as a correlate of disability in amyotrophic lateral sclerosis. *Eur Radiol Exp*. (2018) 2:13. doi: 10.1186/s41747-018-0045-6
64. Thorns J, Jansma H, Peschel T, Grosskreutz J, Mohammadi B, Dengler R, et al. Extent of cortical involvement in amyotrophic lateral sclerosis—an analysis based on cortical thickness. *BMC Neurol*. (2013) 13:148. doi: 10.1186/1471-2377-13-148
65. Buhour MS, Doidy F, Mondou A, Pélerin A, Carlier L, Eustache F, et al. Voxel-based mapping of grey matter volume and glucose metabolism profiles in amyotrophic lateral sclerosis. *EJNMMI Res*. (2017) 7:21. doi: 10.1186/s13550-017-0267-2
66. Agosta F, Basaia S, Trojsi F, Riva N, Cividini C, Femiano C, et al. Structural and functional organization of the brain connectome in patients with different motor neuron disease: a multicenter study. *Neurology*. (2019) 92:3.
67. Bocchetta M, Gordon E, Cardoso MJ, Modat M, Ourselin S, Warren JD, et al. Thalamic atrophy in frontotemporal dementia — Not just a C9orf72 problem. *NeuroImage: Clinical*. (2018) 18:675–81. doi: 10.1016/j.nicl.2018.02.019
68. Pallebage–Gamarrallage M, Foxley S, Menke RA, Huszar IN, Jenkinson M, Tendler BC, et al. Dissecting the pathobiology of altered MRI signal in amyotrophic lateral sclerosis: A post mortem whole brain sampling strategy for the integration of ultra-high-field MRI and quantitative neuropathology. *BMC Neurosci*. (2018) 19:11. doi: 10.1186/s12868-018-0416-1
69. Menke RA, Körner S, Filippini N, Douaud G, Knight S, Talbot K, et al. Widespread grey matter pathology dominates the longitudinal cerebral MRI and clinical landscape of amyotrophic lateral sclerosis. *Brain*. (2014) 137:2546–55. doi: 10.1093/brain/awu162
70. Senda J, Kato S, Kaga T, Ito M, Atsuta N, Nakamura T, et al. Progressive and widespread brain damage in ALS: MRI voxel-based morphometry and diffusion tensor imaging study. *Amyotrophic Lat Scler*. (2011) 12:59–69. doi: 10.3109/17482968.2010.517850
71. Müller HP, Dreyhaupt J, Roselli F, Schlecht M, Ludolph AC, Huppertz HJ, et al. Focal alterations of the callosal area III in primary lateral sclerosis: an MRI planimetry and texture analysis. *NeuroImage Clin*. (2020) 26:102223. doi: 10.1016/j.nicl.2020.102223
72. Mahoney CJ, Downey LE, Ridgway GR, Beck J, Clegg S, Blair M, et al. Longitudinal neuroimaging and neuropsychological profiles of frontotemporal dementia with C9orf72 expansions. *Alzheimer's Res Therapy*. (2012) 4:41. doi: 10.1186/alzrt144
73. Agosta F, Ferraro PM, Riva N, Spinelli EG, Domi T, Carrera P, et al. Structural and functional brain signatures of C9orf72 in motor neuron disease. *Neurobiol Aging*. (2017) 57:206–19. doi: 10.1016/j.neurobiolaging.2017.05.024
74. Mahoney CJ, Beck J, Rohrer JD, Lashley T, Mok K, Shakespeare T, et al. Frontotemporal dementia with the C9orf72 hexanucleotide repeat expansion: clinical, neuroanatomical and neuropathological features. *Brain*. (2012) 135:736–50. doi: 10.1093/brain/awr361
75. Consonni M, Dalla Bella E, Nigri A, Pinardi C, Demicheli G, Porcu L, et al. Cognitive syndromes and C9orf72 mutation are not related to cerebellar degeneration in amyotrophic lateral sclerosis. *Front Neurosci*. (2019) 13:25. doi: 10.3389/fnins.2019.00440
76. El Mendili MM, Cohen–Adad J, Pelegrini–Issac M, Rossignol S, Morizot–Koutlidis R, Marchand–Pauvert V, et al. Multi-parametric spinal cord MRI as potential progression marker in amyotrophic lateral sclerosis. *PLoS ONE*. (2014) 9:e95516. doi: 10.1371/journal.pone.0095516
77. Fabes J, Matthews L, Filippini N, Talbot K, Jenkinson M, Turner MR. Quantitative FLAIR MRI in amyotrophic lateral sclerosis. *Acad Radiol*. (2017) 24:1187–94. doi: 10.1016/j.acra.2017.04.008
78. Goodin DS, Rowley HA, Olney RK. Magnetic resonance imaging in amyotrophic lateral sclerosis. *Ann Neurol*. (1988) 23:418–20. doi: 10.1002/ana.410230424
79. Boll MC, Meléndez OR, Rios C, Zenil JM, de Alba Y. Is the hypointensity in motor cortex the hallmark of amyotrophic lateral sclerosis? *Can J Neurol Sci*. (2019) 46:166–73. doi: 10.1017/cjn.2018.382
80. Hecht MJ, Fellner C, Schmid A, Neundörfer B, Fellner FA. Cortical T2 signal shortening in amyotrophic lateral sclerosis is not due to iron deposits. *Neuroradiology*. (2005) 47:805–8. doi: 10.1007/s00234-005-1421-5
81. Goodin DS, Rowley HA, Olney RK. Magnetic resonance imaging in amyotrophic lateral sclerosis. *Acta Neurol Scand*. (2002) 105:395–9. doi: 10.1034/j.1600-0404.2002.01321.x
82. Graham JM, Papadakis N, Evans J, Widjaja E, Romanowski CA, Paley MN, et al. Diffusion tensor imaging for the assessment of upper motor neuron integrity in ALS. *Neurology*. (2004) 63:2111–9. doi: 10.1212/01.WNL.0000145766.03057.E7
83. De Reuck JL, Deramecourt V, Auger F, Durieux N, Cordonnier C, Devos D, et al. Iron deposits in post-mortem brains of patients with neurodegenerative and cerebrovascular diseases: a semi-quantitative 70 T magnetic resonance imaging study. *Eur J Neurol*. (2014) 21:1026–31. doi: 10.1111/ene.12432
84. Rajagopalan V, Pioro EP. Disparate voxel based morphometry. (VBM) results between SPM and FSL softwares in ALS patients with frontotemporal dementia: which VBM results to consider? *BMC Neurol*. (2015) 15:1–7. doi: 10.1186/s12883-015-0274-8
85. Sastre–Garriga J, Pareto D, Battaglini M, Rocca MA, Ciccarelli O, Enzinger C, et al. MAGNIMS consensus recommendations on the use of brain and spinal cord atrophy measures in clinical practice. *Nature reviews. Neurology*. (2020) 16:171–182. doi: 10.1038/s41582-020-0314-x
86. J Kwan JY, Jeong SY, Van Gelderen P, Deng HX, Quezado MM, Danielian LE, et al. Iron accumulation in deep cortical layers accounts for MRI signal abnormalities in ALS: correlating 7 tesla MRI and pathology. *PLoS ONE*. (2012) 7:e35241. doi: 10.1371/journal.pone.0035241
87. Sweeney MD, Sagare AP, Zlokovic BV. Blood–brain barrier breakdown in Alzheimer disease and other neurodegenerative disorders. *Nat Rev Neurol*. (2018) 14:133. doi: 10.1038/nrneuro.2017.188
88. Zhong Z, Deane R, Ali Z, Parisi M, Shapovalov Y, O'Banion MK, et al. ALS-causing SOD1 mutants generate vascular changes prior to motor neuron degeneration. *Nat Neurosci*. (2008) 11:420–2. doi: 10.1038/nn.2073
89. Lewandowski SA, Nilsson I, Fredriksson L, Lönnerberg P, Muhl L, Zeitelhofer M, et al. Presymptomatic activation of the PDGF–CC pathway accelerates onset of ALS neurodegeneration. *Acta Neuropathol*. (2016) 131:453–64. doi: 10.1007/s00401-015-1520-2
90. Lassmann H, Bradl M. Multiple sclerosis: experimental models and reality. *Acta Neuropathol*. (2016) 3:14. doi: 10.1007/s00401-016-1631-4



OPEN ACCESS

EDITED BY

Antoni Dalmau,
Institute of Agrifood Research and Technology
(IRTA), Spain

REVIEWED BY

Bettina Bert,
Freie Universität Berlin, Germany
Megan Renee LaFollette,
Independent Researcher,
St. Louis, MO, United States
Pandora Pound,
Safer Medicines Trust, United Kingdom

*CORRESPONDENCE

Herwig Grimm

✉ Herwig.Grimm@vetmeduni.ac.at

†These authors share last authorship

RECEIVED 13 March 2023

ACCEPTED 12 May 2023

PUBLISHED 15 June 2023

CITATION

Grimm H, Biller-Andorno N, Buch T,
Dahlhoff M, Davies G, Cederroth CR,
Maissen O, Lukas W, Passini E, Törnqvist E,
Olsson IAS and Sandström J (2023) Advancing
the 3Rs: innovation, implementation, ethics
and society.
Front. Vet. Sci. 10:1185706.
doi: 10.3389/fvets.2023.1185706

COPYRIGHT

© 2023 Grimm, Biller-Andorno, Buch,
Dahlhoff, Davies, Cederroth, Maissen, Lukas,
Passini, Törnqvist, Olsson and Sandström. This
is an open-access article distributed under the
terms of the [Creative Commons Attribution
License \(CC BY\)](#). The use, distribution or
reproduction in other forums is permitted,
provided the original author(s) and the
copyright owner(s) are credited and that the
original publication in this journal is cited, in
accordance with accepted academic practice.
No use, distribution or reproduction is
permitted which does not comply with these
terms.

Advancing the 3Rs: innovation, implementation, ethics and society

Herwig Grimm^{1*}, Nikola Biller-Andorno², Thorsten Buch³,
Maik Dahlhoff⁴, Gail Davies⁵, Christopher R. Cederroth⁶,
Otto Maissen⁷, Wilma Lukas⁸, Elisa Passini⁹, Elin Törnqvist^{10,11},
I. Anna S. Olsson^{12†} and Jenny Sandström^{6†}

¹Messerli Research Institute, University of Veterinary Medicine Vienna, Medical University of Vienna, University of Vienna, Vienna, Austria, ²Institute of Biomedical Ethics and History of Medicine, University of Zurich, Zurich, Switzerland, ³Institute of Laboratory Animal Science, University of Zurich, Zurich, Switzerland, ⁴Institute of in vivo and in vitro Models, Department of Biomedical Sciences, University of Veterinary Medicine Vienna, Vienna, Austria, ⁵Department of Geography, University of Exeter, Exeter, United Kingdom, ⁶Swiss 3Rs Competence Centre, Bern, Switzerland, ⁷Federal Food Safety and Veterinary Office, Animal Welfare Division, Bern, Switzerland, ⁸Innosuisse - Swiss Innovation Agency, Bern, Switzerland, ⁹National Centre for the Replacement, Refinement and Reduction of Animals in Research (NC3Rs), London, United Kingdom, ¹⁰Department of Animal Health and Antimicrobial Strategies, Swedish National Veterinary Institute (SVA), Uppsala, Sweden, ¹¹Institute of Environmental Medicine, Karolinska Institutet, Solna, Sweden, ¹²Laboratory Animal Science, i3S-Instituto de Investigação e Inovação em Saúde, Universidade do Porto, Porto, Portugal

The 3Rs principle of replacing, reducing and refining the use of animals in science has been gaining widespread support in the international research community and appears in transnational legislation such as the European Directive 2010/63/EU, a number of national legislative frameworks like in Switzerland and the UK, and other rules and guidance in place in countries around the world. At the same time, progress in technical and biomedical research, along with the changing status of animals in many societies, challenges the view of the 3Rs principle as a sufficient and effective approach to the moral challenges set by animal use in research. Given this growing awareness of our moral responsibilities to animals, the aim of this paper is to address the question: Can the 3Rs, as a policy instrument for science and research, still guide the morally acceptable use of animals for scientific purposes, and if so, how? The fact that the increased availability of alternatives to animal models has not correlated inversely with a decrease in the number of animals used in research has led to public and political calls for more radical action. However, a focus on the simple measure of total animal numbers distracts from the need for a more nuanced understanding of how the 3Rs principle can have a genuine influence as a guiding instrument in research and testing. Hence, we focus on three core dimensions of the 3Rs in contemporary research: (1) What scientific *innovations* are needed to advance the goals of the 3Rs? (2) What can be done to facilitate the *implementation* of existing and new 3R methods? (3) Do the 3Rs still offer an adequate ethical framework given the increasing *social awareness* of animal needs and human moral responsibilities? By answering these questions, we will identify core perspectives in the debate over the advancement of the 3Rs.

KEYWORDS

animal research, 3Rs, innovation, implementation, ethics

1. Introduction

The 3Rs principle is recognized in many different places where animals are used in research (1). Since their original formulation in 1959 in *The Principles of Humane Experimental Technique*, the 3Rs have become widely accepted as a prerequisite of responsible, high-quality science in which adequate ethical consideration is given to the human use of animals (2). However, it was not until the 1990s that they were translated into policies that could be used to regulate the practice of using animal models in research (2, 3). The 3Rs are now incorporated as legal requirements in transnational legislation such as the European Directive 2010/63/EU (4) as well as in a number of pieces of national legislation, including some in Switzerland and the UK.

The European Directive 2010/63/EU (4) (henceforth: the Directive) on the use of animals for scientific purposes is arguably internationally the most far-reaching piece of laboratory animal experimentation legislation in the world. While the USA, China and Japan use more animals than the European Union (EU) (5), their national legislation protecting animals used in research is more limited. However, legislation that resembles the Directive in large parts and detail can also be found in non-member states like Switzerland [(6), pp. 305–325].

The use of animals for scientific purposes is lawful in EU Member States if all the conditions – including the 3Rs principle – set out in the Directive and the corresponding national acts are met. The Directive also contains more overarching goals, like respecting the intrinsic value of animals and promoting public awareness of our ethical responsibilities to them (Directive, recital 12), and it speaks of the need to work toward full replacement of live animals in experiments (Directive, recital 10). Hence, it navigates between protecting animals, on the one hand, and allowing their use in research, on the other. In this respect, the 3Rs principle, together with harm-benefit analysis (Art. 38 Directive), provide a nexus for the different values embodied in the Directive: the principle and analysis hold things together that are otherwise in tension – namely, the value intrinsic to animals and the value of scientific benefits such as knowledge gain, safety and education.

It is not surprising that advocates at both ends of the spectrum – i.e. those against animal use in research and those in favor of it – challenge the 3Rs principle: if replacement is possible, why do we still use animals, and is the 3Rs principle not stabilizing the status quo (7, 8)? Indeed, does the 3Rs principle really have the potential to lead the way to animal-free research at all? Such questions have also reached the political arena. To name a few: In 2015 the European Citizens' Initiative *Stop Vivisection* gathered the necessary support to present the demand to the European Parliament to phase out animal research (9). In 2021, the European Citizens' Initiative *Save Cruelty Free Cosmetics* was issued and supported by more than 1.2mio signatories (10). In 2022, the *FDA Modernization Act 2.0* was signed by President Biden that allows for alternatives to animal testing for purposes of drug and biological product applications (11). In early 2022, 2.4 million Swiss citizens voted on a proposal to ban animal (and human) research in Switzerland. The plebiscite resulted in 21% in favor and 79% against the proposition (12). Although neither of these initiatives and legal changes led to a ban of animal use for scientific purposes, they indicate that its acceptance cannot be taken for granted.

In contrast to positions that view animal-free research as an urgent priority, others have argued that we risk losing relevant and important gains in knowledge by refraining from using animals in research (13–15). Debates range widely across ethical positions, whereas the legal context is clear: animals can lawfully be used in research if the conditions of the Directive and implemental legislation in Member States are met, and this requires compliance with the 3Rs principle [Directive, Art. 38 (2) b].

Nevertheless, commentary and debate continue to revolve around how far the 3Rs operate in ways that are sufficient to manage the ethical complexities of animal use in research (16, 17) at the forefront of scientific fields (18) and as social priorities diversify and change [(19); recital 12 Directive]. These debates are increasingly informed by work from the social sciences and humanities looking in detail at the intersection of the social, scientific and ethical processes through which the 3Rs emerged and are applied today (20, 21). Hence, the aim of this paper is to reflect on the structure of this complex arena in an effort to show more clearly where the principle of the 3Rs has potential and limits as regards its innovation and implementation. Furthermore, we will touch upon the complexities of related normative questions and the issue of whether the 3Rs principle remains timely and appropriate as an ethical framework, given the increasing social awareness of animal needs and human moral responsibilities.

This brief introduction may already teach us some critical things about the debate on animal use in research and the 3Rs. First, the 3Rs principle offers guidance in a system of regulation in which animal research is legally permitted but must be justified. Second, observance of the 3Rs principle is an important element of responsible research practice within the given legal framework, but it is not a way to change the existing legal foundation. Hence, third, there is discord between the view that the 3Rs principle allows only for minimal change and may even sustain the status quo rather than leading to desirable, more radical, change.

Here, we address the 3Rs principle's potential, limitations and complexity as a policy instrument in the service of advancing science and knowledge as well as protecting animals. Hence, we will describe successes and challenges of the 3Rs by looking into the past, but we will also consider developments in the innovation, implementation (in the sense of changing practice) and understanding of the 3Rs. Finally, we will contextualize the 3Rs principle in the broader societal debate and sketch some of its limits and short comings as an ethical framework.

2. The (missing) 3R effect: who is missing what?

At the same time as the 3Rs principle has been gaining influence via its integration into legislative frameworks across the world, its effectiveness is coming under growing scrutiny by various stakeholder groups (22). In particular, the discussion of why implementation of the principle has not progressed further is on the table, as is debate over why its implementation has not had a “stronger” impact on, for example, the number of animals still being used in research [(23–27); Expectations concerning measurable effects of the 3Rs principle are high, both from political and from public perspectives. The fact that there has been no substantial and consistent decrease in the absolute number of animals being used in experiments [e.g., (28); for difficulties

of comparing the numbers of animals used in the EU see: (29)] is perceived as a “missing” 3Rs effect. However, to understand how the 3Rs principle can have a genuine influence as a guiding instrument we need to look beyond the simple measure of total numbers. As we will see later in this article, quantifying the effect of any one of the 3Rs is a challenging task in itself. Of course, the scarcity of measurement tools need not prevent us from working toward ensuring the principle has a greater impact. This article will give some selected examples of successful advances in the application of the 3Rs, as well as pointing to some areas where the authors see ways to drive 3Rs implementation further.

We propose that there are three core dimensions where more knowledge and understanding is needed to increase the impact of the 3Rs principle: What scientific *innovations* are on the horizon that will contribute to the goals of the 3Rs? How can existing and new 3R methods be *implemented* to greater effect? Linking the principle back to the societal debate: In what ways does the 3Rs principle embrace *societal expectations* about our moral responsibilities to animals? From this angle, improved effects of the 3Rs might be found not only on the scientific level, in terms of method development and implementation, but also on the institutional, legal, societal and ethical levels, in terms of reconsidering and developing the moral ideals contained in the 3Rs principle and corresponding practice. These three dimensions (roughly speaking: innovation, implementation, ethics/societal matters) are naturally interdependent. They anchor the perspectives laid out below and guided the development of the Swiss National Research Programme 79 “Advancing 3R – Animals, Research and Society” that has been launched in 2021 by the Swiss National Science Foundation (SNSF) (Figure 1).

3. Advancing 3Rs innovation

3.1. Successes and developments in innovation

Innovation is key to ensuring that the effects of the 3Rs become stronger by providing new research methods. Innovation in the replacement of animals in research, either entirely or at least partly, enjoys a special status from an ethics perspective in that it addresses the key problem that animals are instrumentalised: they are used to gain knowledge at the cost of their suffering (30). Historically, most of the 3R research funding, by some distance, has supported innovation in replacement, largely as part of the effort to move toward animal-free toxicology and safety testing (referred to as New Approach Methodologies, NAMs) [e.g., (31, 32)].

Innovative replacement tools and methods that allow the scientific objective to be achieved without animal use include novel cell culture approaches (e.g., tissue culture, organoids, organs-on-chip and microphysiological systems), micro-dosing, non-sentient animals, *in silico* modeling and many other techniques. Yet, innovation is equally important for reduction and refinement, by facilitating research that relies on fewer animals and causes less harm to those that are used. Three examples of successful 3Rs innovation are: the development and validation of *in vitro* methods of hazard and safety testing of cosmetics, replacing the existing animal tests (33, 34); imaging techniques making it possible to follow change in tumor size or bacterial load within the same animal over a period of time (instead of euthanising

and dissecting a cohort of animals for each timepoint) as a means of animal use reduction (35); and the introduction of tunnel handling of mice as a refinement technique (36).

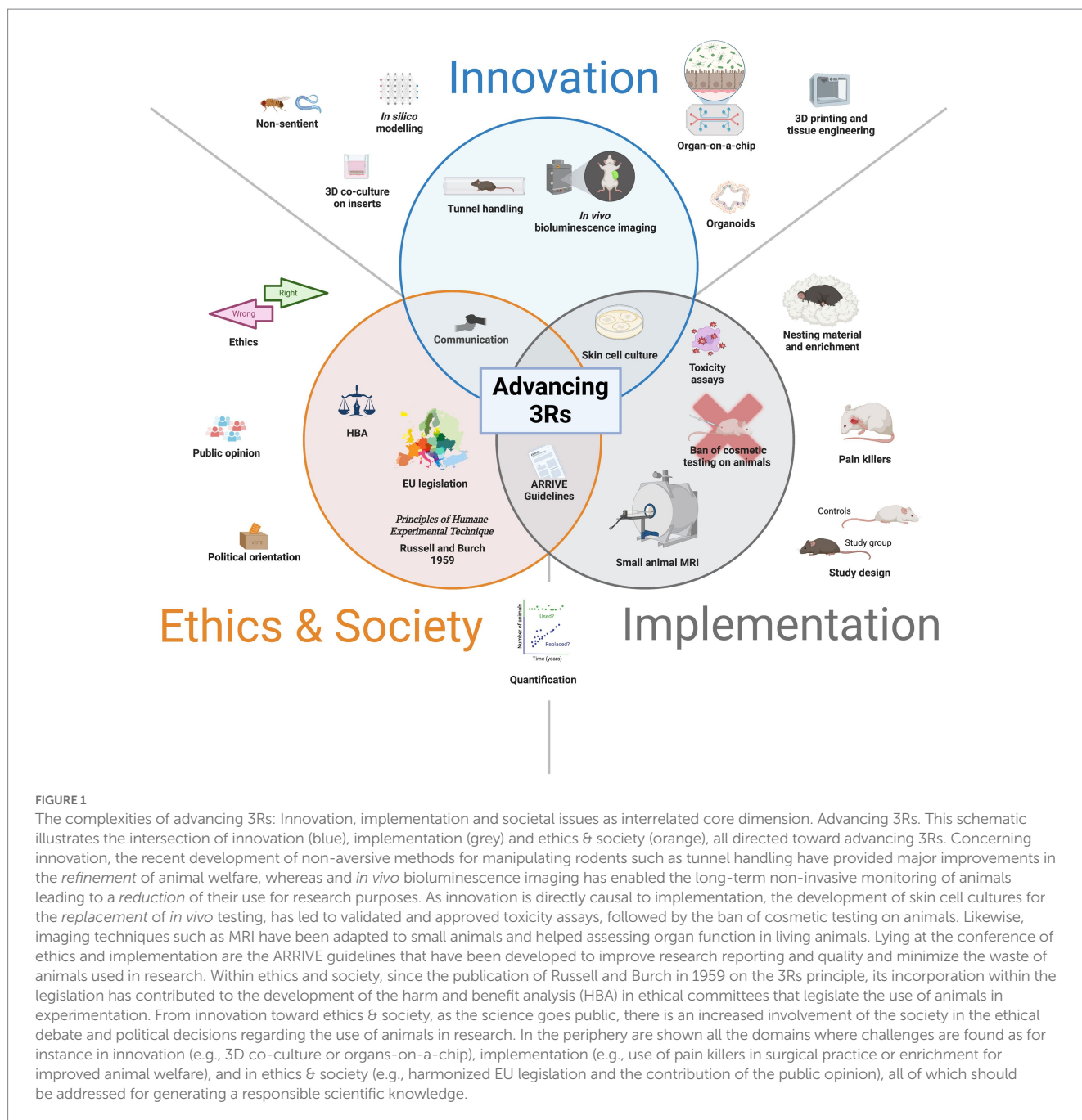
To understand how to strengthen the effect of the 3Rs it is worth considering how the contexts in which these innovations have emerged differ. While the driver of the development of alternatives to animal-based testing of cosmetics was largely political, innovation developed in bioengineering was necessary for the successful replacement of the traditional tests. Deep understanding of the mechanisms of skin sensitisation laid the foundation for a remarkable technical development in *in vitro* approaches (37) that has presented us with unparalleled opportunities to assess human health outcomes without using animals. The political decision, in the early 1990s, to ban cosmetics testing on animals in the EU was further accompanied by investment in research into alternatives. That was important because the ban was conditional upon there being validated alternatives that could be implemented. This can be described as a top-down approach, because policy decisions drove innovation.

In contrast, the new handling methods for mice are an example of innovation changing established practice from the bottom upwards. The first paper on tunnel and cup handling methods by Hurst and West (36) built on research partly funded by the UK's National Centre for the Replacement, Refinement and Reduction of Animal Research (38) through a response mode funding call. The paper reported strong and convincing results showing that tail handling (until recently the predominant method) resulted in more anxious mice – mice that never habituated to the handling method – in comparison with the less aversive and innovative tunnel and cup handling methods. The results attracted great interest in the laboratory animal science community and were especially important for animal technicians who were handling mice in their daily activities. Their dissemination has also been facilitated by the NC3Rs. But the starting point was the innovation, in a bottom-up approach where it was the grant proponent's particular research interest that motivated the choice of topic. Of course, a dynamic combination of top-down and bottom-up approaches is often at work, and industry development may also play a key role, as happened in the adaptation of already existing biomedical imaging techniques for use in small laboratory rodents.

3.2. Complexities: testing required by regulation vs. hypothesis-driven research

Innovation in replacing animal methods in *testing required by regulation* stands out in several ways that are relevant in the discussion. Safety and hazard testing contrast starkly with investigative research: there is a high level of standardization when testing is a strictly regulated process with clearly defined internationally approved guidelines introduced by the Organization for Economic Co-operation and Development (OECD). This makes it comparatively easy to determine clear innovation needs in safety testing (e.g., to identify a particular test that needs to be replaced) and above all to determine when the needs have been met.

Whereas in context of the OECD test guideline program non-animal methods can observably replace previous animal use, this contrasts with, for example, biomedical and disease research, where there is no standardization of the approaches, where the process may be distributed over many laboratories in many institutions, and where



researchers' work is driven by many different research interests. Experimental biomedical research is conducted using a combination of methods, including *in silico*, less complex *in vitro* (e.g., 2D cell cultures) and more complex *in vitro* (e.g., organoids, organ-on-a-chip) techniques, plus animal experiments. In scientific research, the same method can be used for many different purposes, and the same purpose can be achieved by many different methods. Hence, alternative methods are not necessarily seen by researchers as replacement methods, but rather as new-approach methods (NAMs). In this regard, a terminological clarification is in order: "New-approach methods" is not the same as "non-animal methods." Non-animal methods, if used as alternatives to animal models, are "non-animal alternatives," in which case they indeed function as replacement. However, NAMs are often not developed with a direct replacement in

mind; instead, they are rather a different way to approach a research question. Hence, they may not be developed primarily with the intention of replacing a specific animal model. This means that innovations around alternatives in biomedical research are often highly specific; furthermore, the detailed information on methods, materials and data that would help evaluate their use in other situations is not always reported (39).

3.3. Refinement: replacement's "poor cousin"?

Although in principle all the 3Rs have the same status, in practice refinement often comes across as the "poor cousin" of the other Rs. In

comparison with replacement that goes hand in hand with the potential to reduce the number of animals used in many instances, both funding and the positioning of the research field are constraints. For many years, there was little to no public investment in any 3Rs research with the exception of targeted funding for replacement in animal testing. The first public funding to be available for all of the 3Rs was provided in Switzerland in 1987. Judging by the 146 projects funded over the 35-year period since, there has been a clear tendency to fund replacement-focused projects rather than refinement projects (40). Substantial funding for refinement research was arguably not provided by any funding agency until the establishment of the NC3Rs in the UK in 2004, then with an annual budget of £700,000 to be distributed across all of the three Rs (41). For comparison, the year before, the European Commission (42) reported that it had already spent €63 million on research into non-animal alternatives.

To date, much of the innovation in replacement has involved tissue engineering and other advances in cell culture techniques, research topics that are centrally positioned in both biomedical and bioengineering research. Refinement straddles veterinary medicine and the specific biomedical research discipline in question, and for both disciplines, refinement-related research questions tend to be peripheral. In veterinary medicine, laboratory animal science is a small field, sometimes seen as a low-priority research area. Likewise, biomedical refinement research, and other methodology-related research, is generally considered secondary in the research community where animals are used. The problem is exacerbated by the fact that successful refinement research often requires collaboration between experts in animal welfare and highly specialized scientists in a biomedical discipline. For example, better pain control would refine many animal experiments, but whether a pain treatment affects the results of an experiment can only be properly assessed by the specialised scientists (43). Generally speaking, that target can only be achieved with systematic research of species-specific, model-specific and non-model-specific refinement needs. Otherwise, attempts to implement refinement will be limited to best veterinary practice and collective practical wisdom, often relying on scientifically unproven assumptions. Funding schemes addressing refinement play a crucial role in providing context and support for the kind of collaborative research that is required to develop and validate innovative refinement measures. Hence, when substantial funding for refinement research is put in place, biomedical researchers will be more interested in, and likely to pursue, this kind of research and then feed new knowledge into a culture of care.

In short, refinement is seen as a non-instrumental part of the process of generating data, and therefore the innovative refinement of experimental approaches – e.g. creating less invasive ways of administering substances (44) or earlier and less severe endpoints (45) – will rarely be driven by research groups that use animals in experimental settings. Often, this is not a kind of research that is considered suitable for the main journals in a given field of research, and this very fact will act as an obstacle for young biomedical researchers when considering where to focus their early-career effort. This means that the group of researchers from which successful bottom-up proposals (e.g., picking mice up using refined methods (36)) can be expected will be very small, unless refinement research is given greater priority and higher status.

Innovation in refinement has suffered from this situation (with the possible exception of refinement innovation in industry, where

many pharmaceutical companies set aside budgeting and time for smaller refinement projects), and there are clear gaps that need addressing. Moreover, although refinement comes across as the poor cousin of the other Rs in funding, on the practical level of project evaluation for authorization of experiments with animals, refinement seems to be attended to at the expense of in particular replacement; a problem identified already 20 years ago in the Swedish context (46). Replacement requests from an ethics committee require highly specialized expertise in the research field in question, which the committee is unlikely to have. This might shift the focus of the committee work on refinement, which again highlights the need for reliable methods to quantify animal welfare. Hence, the development of knowledge about the interaction of animal welfare and biomedical research is crucial for reducing the negative impact of research and committee work.

A recent systematic review shows the considerable heterogeneity of measures to assess animal welfare in response to environmental enrichment, noting that this heterogeneity makes it impossible to perform reliable meta-analyses (47). Recent tools in fish, relying on an automated monitoring of behavior (48), have been able to capture the impact of post-operative analgesia after fin-clipping on behavioral patterns, thus allowing inferences to be made on the benefits on animal welfare (49). Similar technologies of home cage monitoring for mice have been able to detect the benefits of environmental enrichment against aggression, thus overall improving welfare (50). Such tools may allow indirect objective assessment of animal welfare in a general manner, offering greater applicability such as for assessing pain in animals or evaluating the animal welfare impact of different euthanasia methods.

3.4. Conclusions on advancing 3Rs' innovation

To summarize, innovation has contributed to the impact of 3Rs in the past and will continue to be crucial. Cosmetics testing is an example of how far innovation can take us when it is based on already established biological knowledge (e.g., key events that indicate likelihood of skin sensitization being provoked by a given substance) and technical advances (e.g., biologically non-reactive materials for cell cultures) that allow the innovation to be translated into an effective method of replacement in cosmetic testing and the testing of industrial chemicals. While they are an impressive achievement, the *in vitro* systems for cosmetics testing are comparatively simple, in that they represent a single type of a mainly two-dimensional organ. Current innovations in replacement focus on more complex systems with a more pronounced three-dimensional structure (organoids and spheroids) and organ-organ interactions (on-a-chip systems).

4. Advancing the 3Rs' implementation

4.1. Successes and developments in implementation

To gain further insights into the effective implementation of the 3Rs, we need to know to what extent animal models are being replaced, animal numbers reduced, and procedures on animals

refined. Hence, we need to be able to measure the impact and effects of the 3Rs in some way. Although it is often questioned whether there really are widespread, measurable effects of 3Rs implementation, there has been considerable progress here. Perhaps the most well-known example of a successfully implemented replacement approach is in the integrated testing strategies for assessing the hazard and potency of the skin sensitization in cosmetics discussed above. This effectively allowed animal testing for cosmetics to be banned. What sets this example apart, in terms of implementation, is not only the fact that the biological and technical knowledge was advanced enough to permit the development of the required tests, but also the defined tests themselves (51). Together, these have ensured there is wide acceptance of the relevant regulations allowing for the effective implementation of a political decision.

Replacement strategies can effectively reduce animal numbers – as is very clearly evidenced in the case of cosmetics testing. Similarly, over the past decade, technical developments in *in vivo* small animal imaging have opened up new and improved avenues toward substantial reductions in animal use, while simultaneously allowing more data to be obtained from animals through scientific investigation (52, 53). Other effective reduction approaches have combined several aspects: improved study design, developments in method, and study coordination have together reduced animal use in pharmaceutical toxicity testing (54). The Törnqvist et al. (54) study describes significant animal reductions in both regulatory and investigative safety studies. It concludes that, when they are coordinated at a strategic level, combinations of *in silico*, *in vitro* and *in vivo* methods effectively contribute to reduction.

Regarding refinement, some measures, such as the use of anesthesia in potentially painful procedures (54, 55) and the provision of nesting material to laboratory rodents, are now standard (and legally required) in the EU. These measures have far-reaching consequences, as indicated in a recent systematic review and meta-analysis in which Cait et al. (56) demonstrate lower rates of morbidity and mortality across a number of animal disease models. However, larger scale attempts to quantify both the implementation and the impact of refinement are generally lacking. For quantitative measures of the implementation of refinement we have to turn to research studies such as systematic reviews of the way refinement is reported in research papers (57, 58) and surveys of researchers and technicians asking about their refinement practice (59, 60).

4.2. Complexities of implementation: overcoming barriers

All examples of successful implementation of new 3Rs approaches show that the success is dependent on innovation. Challenges to implementation itself include scientific barriers, such as the limitations of a given method; legal barriers, such as the “gold standard” of animal use in regulatory testing; economic barriers, such as the financial costs and time resources for implementing new approaches; cultural and institutional obstacles, such as difficulties establishing evaluation criteria for academic success that reward 3Rs implementation; and difficulties changing the established mindset. Ongoing efforts to address these issues [e.g., (61–64)] are being made, but the examples are still rare. There are also barriers at the individual and laboratory level, where animal research is sometimes still seen as the nimbus of

“serious research.” All of this together creates a rather inert system in which change is difficult.

Hence, the application of the 3Rs principle may be seen as a tiered approach to the choice of method that is linked to research projects generally conceptualized as being primarily driven by hypothesis testing. Here, the model and methods are chosen with reference to the question to be addressed. This points to a disparity in applications of the 3Rs principle to meet legal requirements imposed by animal welfare legislation in EU Member States and European countries like Switzerland. The 3Rs principle need only be considered when a research project applies for a license in a country where that principle is part of the legal framework. Compliance with the 3Rs throughout the research process, from hypothesis to publication, via an experimental planning and analytic phase, is voluntary and depends on awareness of the 3Rs at an organizational as well as individual level (65).

4.3. Assessing 3Rs implementation and hurdles

To assess the effectiveness of the 3Rs principle as a policy instrument for advancing humane animal experimentation, appropriate parameters for measuring the effects of the 3Rs are still needed. This becomes evident when we are trying to understand the extent to which, for example, replacement methods have been genuinely implemented. To illustrate this point, we would like to highlight two sides to the problem of assessing replacement's implementation. First, the metrics track the numbers of animals used rather than those replaced, and second, most replacement approaches are not recognized as such. Thus, assessing the current impact of already implemented replacement methods is highly complex (as it is in toxicology) and may be impossible, as things stand, in some research fields. Similar observations can be made about the assessment of impacts of the implementation of reduction and refinement.

Besides these fundamental challenges in understanding the impact of active utilization of 3R measures, there are practical hurdles to 3Rs implementation. Establishing and validating new methods may be technically very demanding and time-consuming, creating real problems for researchers seeking to implement new techniques in their laboratories. Comparisons with historical data may require the continued use of established methods, and this too may hamper the switch from established *in vivo* methods to new methods. Moreover, to obtain funding researchers might need to prove they have previous experience and skills in the methods chosen for the project, which may further hinder progression in the implementation of alternative approaches.

Moreover, new methods very often (and perhaps most frequently) serve as measures of reduction, by replacing or omitting steps, or elements, of an existing investigative approach. Therefore, the relevance and reproducibility of these new methods can raise further issues when the capacity of a given model to reduce animal use is determined by its *in vitro*-to-*in vivo* translational value. Hence, other scientists or reviewers might ask for the biological relevance to be proven *in vivo* in confirmative studies, which limits the primary reduction effect of replacement methods in such cases.

Rigorous experimental planning that preserves internal and external validity (66–68) – qualities determined by how rigorously a

study is performed, and how reliably its results can be applied to other situations (69) – will facilitate strategies reducing or even eliminating the need for confirmatory animal studies. Integrated strategies deploying multiple alternative approaches in combination – as happened in the previously mentioned strategy for skin sensitisation testing of cosmetic products – will be required if we are to extend the implementation of replacement.

Turning to the implementation of refinement approaches, there may be gaps here in researchers' and license review committees' awareness of suitable new approaches. Equally obstructive may be a lack, or shortage, of the competencies needed to apply such methods. Applying new methods of experimentation may also jeopardize the academic success of a project, or its productivity, ensuring there is only a modest incentive for the researchers to alter their approach. This applies equally to the implementation of replacement approaches where the required techniques need to be established in a laboratory currently lacking mastery of them. Again, the way in which refinement methods were implemented may not be described in the methodology of scientific articles, which creates difficulties not only in quantifying to what extent such methods have been applied, but also in measuring their potential impact on animal welfare. Therefore, we are again faced with the point that to measure the 3Rs' effectiveness it is necessary to establish better outcome parameters and their measurements. Given all these complexities, the animal welfare representatives in research facilities can play a crucial role. With their direct contact with the animals and the facility, they are well placed to identify refinement needs and to measure impacts on the animals. If they are provided with appropriate support, they can take a key role in the implementation of measures – e.g. by giving advice on the care and use of the animals, and developing and disseminating local animal welfare policies and standards.

Aside from the challenges inherent in the implementation of effective 3Rs methods in the research process, a number of external factors, both positive and negative, may be exerting influence. For instance, within certain domains, such as pharmaceutical safety testing and regulatory risk assessment, the validation process is established and accepted. Standard *in vivo* tests remain within the legal guidelines and thus determine regulatory acceptance of newly established methods (70). An equivalent formal process of validation is not presently used in academic research and disease models. Moreover, academic success is measured mostly in publications in high-impact journals, and these journals make increasing demands regarding the comprehensiveness of the data, which means that *in vitro* studies alone will often not be considered sufficient (71). Thus, *in vivo* studies can be required as a complement to alternative approaches to improve the validity of the results. More generally, the ever-increasing amounts of data required for a single study may make it even more complex and difficult to implement the 3Rs without impacting knowledge gain or publication success. Challenges to this paradigm in the fields of preclinical research and toxicity/safety testing have recently appeared in the literature (72, 73). "The question is raised, whether continuing to require results of animal testing for publications or grant funding still makes scientific or ethical sense and if more physiologically relevant human Organ Chip models might better serve this purpose" (72). This even opens new avenues leading to the questioning of animal studies as the gold standard in other fields as well.

4.4. Conclusions on advancing 3Rs' implementation

In summary, if 3R measures are not implemented, there can be no 3R effects. Additionally, assessing the effects of successfully implemented approaches is far from straightforward given that appropriate outcome parameters and measurement tools are largely missing for replacement, reduction and refinement alike. The only easily accessible parameter of progress in the implementation of the 3Rs we have is one recording those methods that have satisfied regulatory requirements or have been included in national or international regulation: examples are validated alternative tests that replace specific toxicity/safety tests and requirements in environmental enrichment. The total number of animals used in research is often referred to as an outcome measure, but this is highly problematic. At a national level, total numbers depend on many factors, including research activity, the level of investment into research and development, coherent data collection, and so on. Also, they are often presented without correction for the number of biomedical researchers in the respective country at any given time point. Further, changes in reporting and, for example, (severity) classification are usually not reflected in these statistics.

For a nuanced understanding of the effect of the 3Rs it is necessary to generate suitable information through, for example, systematic reviews or questionnaire studies – a kind of 3R "meta-research" that itself needs adequate funding. Hurdles to 3Rs implementation lie at various levels, moreover. They include difficulties in changing established practices, institutional obstacles, and limited awareness and resources, to mention just some. Although the complexity is immense, pragmatic solutions to overcome these hurdles are within reach if the relevant incentives are put in place.

5. Advancing 3Rs: ethics and society

5.1. The 3Rs' development and translation in theory and practice

In the course of scientific developments and changes in human-animal relations in societies, the 3Rs principle has proved adaptive in various respects. One way to respond to new demands in the debate on the use of animals in research was to add complementary Rs, such as a fourth R for Responsibility (74–76), or Rs designed to enhance scientific value by adding, for example, Robustness, Registration or Reporting (77). Further Rs can be found in the literature, including Replication, Reproducibility and Rigor. There has even been talk of a "Rhumba of Rs" (77, 78). Such additions can be read as a reaction to developments and new issues in science and society that challenge both the breadth of applicability and sufficiency of the original 3Rs principle.

We propose that ongoing ethical and social challenges around the 3Rs can be understood by looking at four ways in which the 3Rs have come into widespread use via a set of active and often local translations. First, the moral foundation of the 3Rs has been the subject of academic debate for the past few decades (79). This foundation merits ongoing scrutiny, as the normative and empirical premises underwriting the moral status of animals and their relationship to humans continue to evolve. Considering this, animal

research ethics has developed into a recognized subfield of applied ethics (80, 81). Second, there is the translation from ethical principles into practical recommendations. Russell and Burch (82) first articulated this in the late 1950s, but questions remain, in interdisciplinary debates, around who should define the 3Rs: in societies, professional bodies, campaigning organizations and academic communities today (22, 83, 84). Third, there is the translation of recommendations into national research regulations. Proposals on how to translate the 3Rs into regulations reflect ideas about the proper role of the state in limiting academic freedom and promoting research innovation, as well as in governing scientific procedures and protecting animals (85). Finally, there is the translation of regulatory requirements built upon the 3Rs into everyday policy and scientific practice – from animal technicians seeking to refine procedures (86), to scientists imagining public attitudes when deciding which species to use (87), or institutions creating barriers to the use of replacements (88). There is also the translation of the whole 3Rs endeavor into the public sphere in order to raise awareness and gain support through transparent communication (89). For Russell and Burch, writing within the academic culture of 1950s Oxford, this translation into the public sphere was imagined as something that would come at the end of the process. Today, moves toward openness and transparency in science, together with the growing agenda of responsible innovation (90), mean that the vantage points from which the public may challenge animal research have multiplied. This implies a need for ongoing review around how far the 3Rs principle meets its intended ethical purpose.

The 3Rs principle is not a strategy for phasing out animal use in research. In this respect, the 3Rs principle seems to be in line with the general public's majority view. For instance, in a Danish empirical survey (91) 30–35% of people questioned approved of animal research quite strongly, and 15–20% opposed animal research, whereas the remaining 50% were reserved in their views. In a Swedish survey (92) just over half (55%) of respondents considered that animal experiments are acceptable in medical research. Acceptance increased to 82% when it was stipulated that the animals were being treated well and not exposed to unnecessary suffering (92). In the UK, overall, the public (i.e., British adults aged 15+) is supportive of the use of animals in scientific research: 68% agreed in 2014 that it is acceptable “so long as it is for medical research purposes and there is no alternative,” but there is also widespread agreement (76%) that more work should be done to find alternatives to using animals in such research [(93); for the UK, see also Ipsos Mori (94) and for the U.S. Gallup (95)]. A recent qualitative study conducted in Austria (96) also indicates that strict disapproval is not the rule.

As the above-mentioned surveys show as well, very few people do not care about animals, and most think that animals should only be harmed if sufficient benefits are on the horizon. This is reflected in the Directive, which makes harm-benefit analysis one aspect of project evaluation [Directive, Art. 38 (2) d; (68, 80, 97–101)]. With this, the Directive adds an important aspect, asking whether the research aim outweighs the harm (if there is any) on the animal side. This goes well beyond the 3Rs principle, which focuses on how to achieve a given research aim with the least possible animal harm (including no harm at all, in the case of replacement). Hence, in pragmatic terms, current legal requirements (at least in EU Member States) already go beyond the 3Rs principle. That raises questions about whether the principle should be extended, or complemented, and how it feeds into this new

responsibility to balance harms and benefits. In any case, the successful interplay of the 3Rs principle and the harm-benefit analysis is in need of a clear methodological understanding of both. Problems of the former have been dealt with in this text; methodological challenges and practical hurdles for carrying out the harm-benefit analysis in a clear and transparent manner have been extensively addressed elsewhere [e.g., (97, 101–104)].

5.2. Rethinking replacement strategies

The idea of replacement is typically understood so that animal use is to be avoided if, and only if, the same scientific goal can be achieved with the same quality with alternative methods. Thus, if animals are not *instrumentally necessary* to reach a given research objective, they are replaced by other methods. The correlative question is whether the proposed project, and its use of animals, is appropriate and necessary to achieve a given research objective. However, looking at the idea of replacement more broadly, it can also be asked whether the research objective itself is sufficiently important to justify the harms caused to the animals. This question addresses the *goal-related necessity* of a project – a focus mirrored in the idea of harm-benefit analysis – and opens up a more substantial debate over whether the promised benefits can be reached through means other than the research in question.

These two perspectives – instrumental and goal-related necessity – have been distinguished and elaborated by the Swiss Academy of Science (105). Following the ideas they present, we might say that, to avoid animal use, replacement can also be applied to the way we are trying to obtain prospective benefits. Sometimes non-research alternatives enabling us to obtain benefits without research at all may exist. An example would be reducing the prevalence of a disease by preventive measures rather than the development of treatments. For instance, at least in theory, metabolic syndrome and some cardiovascular problems can be addressed effectively in many patients by dietary changes and exercise. Also in other areas, like production-related diseases in animal farming where animals are kept densely and in big numbers, alternatives might be considered. Rather than finding solutions in new treatment options with the use of biomedical research, changing the production system might efficiently mitigate the problem.

In fact, as a recent qualitative study indicates, the justificatory basis for solving “self-created” problems via animal use in research is weak (96). The study suggests that it is not only the “weight” of benefits that is to be factored into harm-benefit analysis, but also the quality and nature of those benefits. In this regard, the question emerges: What sorts of benefits can actually generate weight on the scales, and what sorts of benefits *cannot* outweigh animal harms and would therefore need to be achieved through means other than research or not at all? Presently, this debate oscillates around the question of benefits achieved in basic research versus those obtained in applied and translational research [for Switzerland cf. (106)], but the core of the issue reaches far deeper.

Generally speaking, focusing on research goals allows for debate about what would perhaps be even more efficient, and then non-animal and/or non-research-driven strategies might come into the discussion [e.g., (69)]. This goal-oriented view departs from the original thinking behind the 3Rs, since it questions whether the

replacement of research (as a strategy to obtain benefits) is an adequate solution to a given problem. Hence, replacement is not only to be understood in terms of replacing animals in research; it can also be understood as taking ethical considerations into account more broadly by asking whether alternative routes bring about comparable benefits with different, and fewer, costs. However, such debates are at an early stage. To ensure they are effective systematic guidance on participation and exchange might be important. For instance, the accessibility and availability of the alternative routes is linked to the different roles that citizens are allocated in discussions of the harms and benefits of animal research, whether as members of the public, participants in research, or potential patients (107).

5.3. Approaching reduction and refinement from a different perspective

In the light of ethical considerations, the reduction of animal use can also be reframed. Whereas we should avoid using animals as far as possible – for we are indeed legally bound to do so – there seem to be cases in which animal experiments are still the rule. Sometimes they are even legally required, as they are, for example, in regulatory testing in many – but not all [e.g., U.S. (11)] – countries, as we have seen above. As a matter of fact, the term *reduction* itself (making something *less* in amount or number) already implies the mindset of legitimate animal use for scientific purposes under particular circumstances (e.g., the 3Rs), which conflicts with the idea that animal research should be the exception, rather than the rule [recital 12 Directive; (19)]. Turning this “Yes, but...” into a strict “No, but...” position when we are thinking about possible research aims might help here. This means a shift toward considering animal use in research as an option only in exceptional circumstances, and a corresponding shift of the onus of justification: only if abstaining from the use of animals would produce highly undesirable, unbearable costs, is using them an option. However, the very concept of reduction implies use animals in the first place, and reducing their numbers and the harm done to them to a minimum when designing an experiment – a mindset implicit in the 3Rs principle.

Refinement, and its focus on ameliorating the negative subjective experiences of animals (pain, suffering, distress), has been and might be further reconsidered as well. The centring of refinement strategies on negative subjective experience introduces a risk that we will ignore factors contributing to positive welfare. As far as we know, it is not only pain and suffering that make a difference to an animal's life. Taking, for example, newer research on cognitive abilities in animals into account, phenomena like the desire to care for conspecifics (108), the preference for stimulating and changing environments (where neophile animals are concerned) with exploratory possibilities (109), certain emotional states, and so on, might enrich the debate and have a bearing on our responsibilities as regards refinement (110, 111). Again, as in the case of replacement and reduction, thinking through the limitations and possible advances here might broaden the debate and allow 3Rs research in the humanities, legal studies and social sciences to be linked with the public debate, and to reflect the issues addressed in a systematic manner. This is particularly important, since all of these ways of broadening our views would occur in an environment where the human-animal relationship is developing.

5.4. Conclusions on advancing 3Rs and ethics and society

Where advancement of the 3Rs is concerned, research and insights into the ethical issues, as currently conceived, undertaken in social science, history, law, philosophy, and so forth, can lead to an improved and better-informed understanding of the directions in which we should be moving in the future. Gaining empirical insights into changes of opinion in societies and/or research practices, and reflecting these insights, might allow for more thorough-going development of animal research policies. For instance, comparatively little is known about researchers' views and opinions. Hence, investigating the epistemology of labs – an epistemology that is often tacit and inherited from one generation to the next – in sociology and anthropology of science [e.g., (112, 113)], could inform the debate substantially. Ideally, the investigation will identify (mental) hurdles linked to attitudes, traditions and management culture [e.g., (61–63, 114, 115)]. Making such matters explicit through systematic investigation might help us to find ways to tackle them. Thus, the humanities and social sciences could offer a richer and fuller picture of the problems that arise when animals are used in research, and in that way support public debate and dialog [e.g., (94, 116, 117)]. It could also take researchers' views more seriously and treat them indeed as a cornerstone of future efforts to increase our understanding, and improve our use, of the 3Rs. Whether or not this is going to speak in favor of greater efforts being made to protect animals used in research is an open question. In societies where animals are still kept and slaughtered in their billions for food, owned for amusement, hunted and used in sports, it remains unclear which way democratic societies will go.

Looking at the debate on advancing 3Rs from this angle, the humanities and social sciences are not the fifth wheel: they are as important as natural science and biomedicine in the project of advancing implementation of the 3Rs and developing the 3Rs themselves. The proposition that developing humane experimental techniques is both a sociological and scientific problem was present in Russell and Burch's work in the 1950s, still it fell out of favor as the cultures of science and the humanities diverged. The Swiss National Research Programme “Advancing 3R” (NRP 79) is innovative in its focus on questions about how interdisciplinary research might recover these connections. Research in sociological and scientific disciplines might help to close the gap between science and society. It is to be hoped that it will foster reflective debate on what we can reasonably expect from animal research, and what we are willing to sacrifice for the benefits we hope to gain.

6. General discussion and conclusion

The normative principles governing the use of animals are subject to continuous societal negotiation and development. One of the effects of this is that the relationship between us, human beings, and animals can no longer be assumed to be one in which human supremacy reigns. In particular, we can no longer think simply in terms of the instrumental value that animals have for us. To do so, would be to disregard animals' intrinsic value – a value that is acknowledged in legal documents as well as in common morality. Hence, it is not only

in the food production industry, the world of fashion, zoos, our private ownership of pets, and so on, but also in research, that responsible actors have to deal with changing responsibilities and expectations. Given societal change, then, the 3Rs cannot be used as a self-explanatory reference. They need to be continuously re-examined with a view to their normative foundations, their interpretation, their implementation, and their innovation. To give just one illustration of change, we are now much more willing to recognize features such as cognitive and emotional capacities, and prosocial behavior, in non-human species, and to accept the moral responsibilities that follow from such recognition (108, 118–120).

There is a persistent perception that there is a “missing effect” of the implementation of the 3Rs. However, as has been explained in the sections above, proper outcome measures for replacement, reduction and refinement alike are largely undeveloped, and therefore one is entitled to question whether the effect really is missing, or whether instead we are simply unable to properly measure it on a wider, global scale. Total numbers of animals used in research are often the reference point for the public, and for politicians when they point to the supposed missing 3Rs effect. However, when these numbers are not placed in their wider context, what information on the effectiveness of the 3Rs do they provide? A better understanding of the relations between trends and movements in research, in connection with animal use, will not only create an improved understanding of the effects of the 3Rs, but also point to important gaps. So, it is important not only to remove hurdles so as to facilitate 3Rs implementation to the greatest degree possible, but also to develop appropriate outcome measures and understand more fully the environment in which the 3Rs are implemented.

The aims of this paper have been to sketch the potentials, and some success stories, of the 3Rs; to examine the challenges and difficulties of implementing the 3Rs principle; and to identify possible advances in the way the 3Rs are applied and understood. We see a number of ways in which the 3Rs’ effect can be enhanced in the future. First, new or improved tools and methods that increase the probability of successful 3R implementation as well as validation, and broader acceptance of existing tools and methods, will together help to make the 3Rs more effective. Second, strategies to bridge gaps in implementation are of great importance. Third, as we have seen, research on the 3Rs, and particularly on their validation and implementation, generally struggles to find recognition in the funding and publication system. This status problem, as perceived by many scientists, against a background of limited funding incentives, represents an important gap that needs to be filled if we are to encourage greater 3Rs ambition. Hence, fourth, the 3Rs may have more effect if incentives, in the form of reward systems that acknowledge 3R improvements and contribute to career benefits, are put in place. Fifth, to substantiate and develop this further in a bottom-up manner, the inclusion of the 3Rs in training programs and academic curricula is crucial. It will strengthen awareness and knowledge of the 3Rs among scientists. Top-down strategies involving further engagement by regulatory bodies and policy makers in the use of the 3Rs principle as a steering instrument may also encourage the research stakeholder community to advance implementation. Sixth, innovative tools are needed: not just alternative research methods, but tools to raise societal awareness; to promote greater transparency in the research community about animal use; and to encourage dialogue between researchers and ordinary citizens about normative issues raised by the use of animals in research.

In conclusion, the principle of the 3Rs, as an instrument of guidance, is not perfect. Nor is it a comprehensive solution to all of the issues presented by our continuing dependence on animal use in research. To remain useful, the 3Rs therefore need to be both continually advanced at the scientific level and challenged at the normative level. In this way, the goal of responsible scientific knowledge production might be achieved through research involving animals in exceptional cases only.

Data availability statement

The original contributions presented in the study are included in the article/supplementary material, further inquiries can be directed to the corresponding author.

Author contributions

HG: conceptualization. HG, IO, JS, and GD: writing—original draft preparation. HG, IO, JS, NB-A, TB, MD, GD, CC, OM, WL, EP, and ET: writing—review and editing. HG, IO, JS, and CC: review and editing final version. All authors have read and agreed to the published version of the manuscript.

Acknowledgments

The authors would like to thank the SNSF Management team of NRP 79, Marjory Hunt, Irina Sille, Arno Repond, and Adrian Heuss, for their support and Konstantin Deininger (Messerli Research Institute, Vienna) for his work on the lay out and references. EP’s position at the NC3Rs is funded by the Association of the British Pharmaceutical Industry. GD would like to thank her colleagues on the Animal Research Nexus Programme, funded by the Wellcome Trust (Grant no: 205393), for formative and ongoing conversations on the social and historical aspects of animal research.

Conflict of interest

While the paper reports on the scientific concept of NRP 79, the opinions and views presented are the authors’ own and do not necessarily represent the position of SNE, the NRP 79 Steering Committee or the authors’ respective institutional affiliations. This paper was developed as an initiative of the Steering Committee of NRP 79. The following members are remunerated for their time invested in NRP 79: NB-A, TB, MD, GD, HG (as president of the SCC), ET, EP, and IO but not for the preparation of this manuscript. The following authors do not receive any remuneration for their engagement in NRP 79 nor in this paper: JS, WL, and OM. This paper reflects the programmatic development of NRP 79 and did not affect project selection.

The remaining author declares that the research was conducted in the absence of any commercial or financial relationships that could be construed as a potential conflict of interest.

Publisher's note

All claims expressed in this article are solely those of the authors and do not necessarily represent those of their affiliated

References

- Bayne K, Ramachandra GS, Rivera EA, Wang J. The evolution of animal welfare and the 3Rs in Brazil, China, and India. *J Am Assoc Lab Anim Sci.* (2015) 54:181–91.
- Kirk RGW. Recovering the principles of humane experimental technique: the 3Rs and the human essence of animal research. *Sci Technol Hum Values.* (2018) 43:622–48. doi: 10.1177/0162243917726579
- Friese C, Nuyts N. From the principles to the animals (scientific procedures) act: a commentary on how and why the 3Rs became central to laboratory animal governance in the UK. *Sci Technol Hum Values.* (2018) 43:742–7. doi: 10.1177/0162243917743792
- Directive 2010/63/EU. (2010). On the protection of animals used for scientific purpose. European Parliament and Council. Available at: <https://eur-lex.europa.eu/legal-content/EN/TXT/PDF/?uri=CELEX:32010L0063> (Accessed February 16, 2023).
- Statista (2023). Available at: <https://www.statista.com/statistics/639954/animals-used-in-research-experiments-worldwide/> (Accessed January 24, 2023).
- Hehemann L. Die Genehmigung von Tierversuchen im Spannungsfeld von Tierschutz und Forschungsfreiheit. Ein Rechtsvergleich zwischen Deutschland, Österreich und der Schweiz: Arbeiten aus dem Juristischen Seminar der Universität Freiburg Schweiz. Nr (2019). 397 p.
- Blattner CE. Rethinking the 3Rs: from whitewashing to rights In: K Herrmann and K Jayne, editors. *Animal experimentation: working towards a paradigm change*. Leiden: Brill (2019). 168–93.
- Herrmann K. Refinement on the way towards replacement: are we doing what we can? In: K Herrmann and K Jayne, editors. *Animal experimentation: Working towards a paradigm change*. Leiden: Brill (2019). 3–64.
- European Commission. (2015). Available at: https://ec.europa.eu/commission/presscorner/detail/en/IP_15_5094 (Accessed February 16, 2023).
- European Initiative. (2021). Available at: https://europa.eu/citizens-initiative/initiatives/details/2021/000006_en (Accessed April 14, 2023).
- Han JJ. FDA modernization act 2.0 allows for alternatives to animal testing. *Artif Organs.* (2023) 47:449–50. doi: 10.1111/aor.14503
- Bundesrat (2022). Available at: <https://www.bk.admin.ch/ch/d/pore/va/20220213/can651.html> (Accessed February 16, 2023).
- Alliance for Biomedical Research in Europe. (2015). BioMed Alliance welcomes European Commission reply to “Stop Vivisection” European Citizens’ Initiative (ECI). Available at: http://www.biomedalliance.org/images/animal-research/BioMed_Alliance_welcomes_European_Commission_reply_to_Stop_Vivisection.pdf (Accessed February 16, 2023).
- ALLEA. (2015). ALLEA welcomes the European Commission’s response to the “Stop Vivisection” ECI on the use of animals for scientific purposes. Available at: <https://allea.org/allea-welcomes-the-european-commissions-response-to-the-stop-vivisection-eci-on-the-use-of-animals-for-scientific-purposes/> (Accessed February 16, 2023).
- European Animal Research Association. (2017). ‘Stop Vivisection’ petition unsuccessful. Available at: <https://www.eara.eu/post/stop-vivisection-petition-unsuccessful> (Accessed February 16, 2023).
- Pereira S, Tettamanti M. Ahimsa and alternatives—the concept of the 4th R. the CPCSEA in India. *ALTEX.* (2005) 22:3–6.
- Niemi SM, Davies GF. Animal research, the 3Rs, and the “internet of things”: opportunities and oversight in international pharmaceutical development. *ILAR J.* (2016) 57:246–53. doi: 10.1093/ilar/ilw033
- Palmer A, Greenhough B. Out of the laboratory, into the field: perspectives on social, ethical and regulatory challenges in UK wildlife research. *Philos Trans R Soc B.* (2021) 376:20200226. doi: 10.1098/rstb.2020.0226
- European Parliament. (2021). Resolution of 16 September 2021 on plans and actions to accelerate the transition to innovation without the use of animals in research, regulatory testing and education. Available at: https://www.europarl.europa.eu/doceo/document/TA-9-2021-0387_EN.html (Accessed February 16, 2023).
- Davies G, Greenhough B, Hobson-West P, Kirk RGW. Science, culture, and care in laboratory animal research: interdisciplinary perspectives on the history and future of the 3Rs. *Sci Technol Hum Values.* (2018) 43:603–21. doi: 10.1177/0162243918757034
- Davies G, Gorman R, Greenhough B, Hobson-West P, Kirk RGW, Message R, et al. Animal research nexus: a new approach to the connections between science, health and animal welfare. *Med Humanit.* (2020) 46:499–511. doi: 10.1136/medhum-2019-011778
- Davies GF, Greenhough BJ, Hobson-West P, Kirk RGW, Applebee K, Bellingan LC, et al. Developing a collaborative agenda for humanities and social scientific research on laboratory animal science and welfare. *PLoS One.* (2016) 11:7. doi: 10.1371/journal.pone.0158791
- Bailoo JD, Reichlin TS, Würbel H. Refinement of experimental design and conduct in laboratory animal research. *ILAR J.* (2014) 55:383–91. doi: 10.1093/ilar/ilu037
- Beken S, Kasper P, van der Laan JW. Regulatory acceptance of alternative methods in the development and approval of pharmaceuticals. *Adv Exp Med Biol.* (2016) 856:33–64. doi: 10.1007/978-3-319-33826-2_3
- Jirkof P, Rudeck J, Lewejohann L. Assessing affective state in laboratory rodents to promote animal welfare—what is the progress in applied refinement research? *Animals.* (2019) 9:12. doi: 10.3390/ani9121026
- Wange RL, Brown PC, Davis-Bruno KL. Implementation of the principles of the 3Rs of animal testing at CDER: past, present and future. *Regul Toxicol Pharmacol.* (2021) 123:104953. doi: 10.1016/j.yrtph.2021.104953
- Biller-Andorno N, Grimm H, Walker RL. Professionalism and ethics in animal research. *Nat Biotechnol.* (2015) 33:1027–8. doi: 10.1038/nbt.3363
- FSVO (Swiss Federal Food Safety Office). (2021). Available at: <https://www.tv-statistik.ch/de/statistik/> (Accessed January 24, 2023).
- Busquet F, Kleensang A, Rovida C, Herrmann K, Leist M, Hartung T. New European Union statistics on laboratory animal use – what really counts! *ALTEX.* (2020) 37:167–86. doi: 10.14573/altex.2003241
- Herrmann K, Pistollato F, Stephens ML. Beyond the 3Rs: expanding the use of human-relevant replacement methods in biomedical research. *ALTEX.* (2019) 36:343–52. doi: 10.14573/altex.1907031
- EPA (2021). United States Environmental Protection agency. New Approach Methods Work Plan. EPA 600/X-21/209. Available at: https://www.epa.gov/system/files/documents/2021-11/nams-work-plan_11_15_21_508-tagged.pdf (Accessed February 10, 2023).
- Stucki AO, Barton-Maclaren TS, Bhuller Yadvinder HJE, Henry Tala R, Hirn C, Miller-Holt J, et al. Use of new approach methodologies (NAMs) to meet regulatory requirements for the assessment of industrial chemicals and pesticides for effects on human health. *Front Toxicol.* (2022) 4:964553. doi: 10.3389/ftox.2022.964553
- Casati S, Aschberger K, Barroso J, Casey W, Delgado I, Kim TS, et al. Standardisation of defined approaches for skin sensitization testing to support regulatory use and international adoption: position of the International Cooperation on Alternative Test Methods. *Arch Toxicol.* (2018) 92:611–7. doi: 10.1007/s00204-017-2097-4
- Daniel AB, Strickland J, Allen D, Casati S, Zuang V, Barroso J, et al. International regulatory requirements for skin sensitization testing. *Regul Toxicol Pharmacol.* (2018) 95:52–65. doi: 10.1016/j.yrtph.2018.03.003
- Franc BL, Acton PD, Mari C, Hasegawa BH. Small-animal SPECT and SPECT/CT: important tools for preclinical investigation. *J Nucl Med.* (2008) 49:1651–63. doi: 10.2967/jnumed.108.055442
- Hurst JL, West RS. Taming anxiety in laboratory mice. *Nat Methods.* (2010) 7:825–6. doi: 10.1038/nmeth.1500
- Basketter DA, Gerberick GF. Skin sensitization testing: the ascendancy of non-animal methods. *Cosmetics.* (2022) 9:2. doi: 10.3390/cosmetics9020038
- NC3Rs. (2022). Mouse handling. Available at: <https://www.nc3rs.org.uk/3rs-resources/mouse-handling> (Accessed February 16, 2023).
- Sander T, Ghanawi J, Wilson E, Muhammad S, Macleod M, Dietrich Kahlert U. Meta-analysis on reporting practices as a source of heterogeneity in in vitro cancer research. *bioRxiv.* (2021). doi: 10.1101/2021.10.05.463182
- Forschung 3R (2022). Available at: <https://www.forschung3r.ch/en/projects/index.html> (Accessed February 16, 2023).
- NC3Rs. (2013). Annual Report. Available at: <https://nc3rs.org.uk/sites/default/files/2021-09/NC3Rs%20Annual%20Report%202013%20final.pdf> (Accessed February 16, 2023).
- European Commission. (2003). EU project develops alternative to animal experiments. Available at: <https://cordis.europa.eu/article/id/20235-eu-project-develops-alternative-to-animal-experiments> (Accessed February 16, 2023).
- Stumpf F, Algül H, Thoeringer CK, Schmid RM, Wolf E, Schneider MR, et al. Metamizol relieves pain without interfering with cerulein-induced acute pancreatitis in mice. *Pancreas.* (2016) 45:572–8. doi: 10.1097/MPA.0000000000000483
- Scarborough J, Mueller F, Arban R, Dorner-Ciossek C, Weber-Stadlbauer U, Rosenbrock H, et al. Preclinical validation of the micropipette-guided drug

- administration (MDA) method in the maternal immune activation model of neurodevelopmental disorders. *Brain Behav Immun.* (2020) 88:461–70. doi: 10.1016/j.bbi.2020.04.015
45. Mead RJ, Bennett EJ, Kennerley AJ, Sharp P, Sunyach C, Kasher P, et al. Optimised and rapid pre-clinical screening in the SOD1(G93A) transgenic mouse model of amyotrophic lateral sclerosis (ALS). *PLoS One.* (2011) 6:8. doi: 10.1371/journal.pone.0023244
46. Hagelin J, Hau J, Carlsson HE. The refining influence of ethics committees on animal experimentation in Sweden. *Lab Anim.* (2003) 37:10–8. doi: 10.1258/002367703762226656
47. Mieske P, Hobbiesiefken U, Fischer-Tenhagen C, Heinel C, Hohlbaum K, Kahnau P, et al. Bored at home? A systematic review on the effect of environmental enrichment on the welfare of laboratory rats and mice. *Front Vet Sci.* (2022) 9:899219. doi: 10.3389/fvets.2022.899219
48. Thomson JS, Al-Temeemy AA, Isted H, Spencer JW, Sneddon LU. Assessment of behaviour in groups of zebrafish (*Danio rerio*) using an intelligent software monitoring tool, the chromatic fish analyser. *J Neurosci Methods.* (2019) 328:108433. doi: 10.1016/j.jneumeth.2019.108433
49. Thomson JS, Deakin AG, Cossins AR, Spencer JW, Young IS, Sneddon LU. Acute and chronic stress prevents responses to pain in zebrafish: evidence for stress-induced analgesia. *J Exp Biol.* (2020) 223:jeb.224527. doi: 10.1242/jeb.224527
50. Giles JM, Whitaker JW, Moy SS, Fletcher CA. Effect of environmental enrichment on aggression in BALB/c and BALB/cByJ mice monitored by using an automated system. *J Am Assoc Lab Anim Sci.* (2018) 57:236–43. doi: 10.30802/AALAS-JAALAS-17-000122
51. OECD. *Guideline no. 497: defined approaches on skin sensitisation*. Paris: OECD Publishing (2021).
52. Campbell BR, Gonzalez Trotter D, Hines CDG, Li W, Patel M, Zhang W, et al. In vivo imaging in pharmaceutical development and its impact on the 3Rs. *ILAR J.* (2017) 57:212–20. doi: 10.1093/ilar/ilw019
53. Lauber DT, Fülöp A, Kovács T, Szigeti K, Máthé D, Szijártó A. State of the art in vivo imaging techniques for laboratory animals. *Lab Anim.* (2017) 51:465–78. doi: 10.1177/0023677217695852
54. Törnqvist E, Annas A, Granath B, Jalkestén E, Cotgreave I, Öberg M. Strategic focus on 3R principles reveals major reductions in the use of animals in pharmaceutical toxicity testing. *PLoS One.* (2014) 9:7. doi: 10.1371/journal.pone.0101638
55. Flecknell P. *Laboratory animal anaesthesia*. 4th ed. London: Academic Press (2016).
56. Cait J, Cait A, Scott RW, Winder CB, Mason GJ. Conventional laboratory housing increases morbidity and mortality in research rodents: results of a meta-analysis. *BMC Biol.* (2022) 20:15. doi: 10.1186/s12915-021-01184-0
57. Franco NH, Correia-Neves M, Olsson IA. Animal welfare in studies on murine tuberculosis: assessing progress over a 12-year period and the need for further improvement. *PLoS One.* (2012) 7:10. doi: 10.1371/journal.pone.0047723
58. Herrmann K, Flecknell P. Retrospective review of anesthetic and analgesic regimens used in animal research proposals. *ALTEX.* (2019) 36:65–80. doi: 10.14573/altex.1804011
59. Henderson LJ, Smulders TV, Roughan JV. Identifying obstacles preventing the uptake of tunnel handling methods for laboratory mice: an international thematic survey. *PLoS One.* (2020) 15:e0231454. doi: 10.1371/journal.pone.0231454
60. LaFollette MR, Cloutier S, Brady C, Gaskill BN, O'Haire ME. Laboratory animal welfare and human attitudes: a cross-sectional survey on heterospecific play or “rat tickling”. *PLoS One.* (2019) 14:e0220580. doi: 10.1371/journal.pone.0220580
61. Gouveia K, Hurst JL. Improving the practicality of using non-aversive handling methods to reduce background stress and anxiety in laboratory mice. *Sci Rep.* (2019) 9:20305. doi: 10.1038/s41598-019-56860-7
62. LaFollette MR, O'Haire ME, Cloutier S, Gaskill BN. Practical rat tickling: determining an efficient and effective dosage of heterospecific play. *Appl Anim Behav Sci.* (2018) 208:82–91. doi: 10.1016/j.applanim.2018.08.005
63. LaFollette MR, Cloutier S, Brady CM, O'Haire ME, Gaskill BN. Changing human behavior to improve animal welfare: a longitudinal investigation of training laboratory animal personnel about play or “rat tickling”. *Animals.* (2020) 10:1435. doi: 10.3390/ani10081435
64. NC3Rs (2023). 3Rs self-assessment tools. Helping you build a clearer picture of your 3Rs culture. Available at: <https://3rsselfassessment.nc3rs.org.uk> (Accessed January 24, 2023).
65. Brönstad A, Berg A-GT. The role of organizational culture in compliance with the principles of the 3Rs. *Lab Anim.* (2011) 40:22–6. doi: 10.1038/labani11-22
66. Pound P, Ritskes-Hoitinga M. Is it possible to overcome issues of external validity in preclinical animal research? Why most animal models are bound to fail. *J Transl Med.* (2018) 16:304. doi: 10.1186/s12967-018-1678-1
67. Würbel H. More than 3Rs: the importance of scientific validity for harm-benefit analysis of animal research. *Lab Anim.* (2017) 46:164–6. doi: 10.1038/labani.1220
68. Würbel H, Eggel M. Internal consistency and compatibility of the 3Rs and 3Vs principles for project evaluation of animal research. *Lab Anim.* (2020) 55:233–43. doi: 10.1177/0023677220968583
69. Ritskes-Hoitinga M, Pound P. The role of systematic reviews in identifying the limitations of preclinical animal research, 2000–2022: part 2. *J R Soc Med.* (2022) 115:231–5. doi: 10.1177/01410768221100970
70. Schiffelers MJ, Blaauw BJ, Fentener van Vlissingen JM, Kuil J, Remie R, Thuring JW, et al. Factors stimulating or obstructing the implementation of the 3Rs in the regulatory process. *ALTEX.* (2007) 24:271–8. doi: 10.14573/altex.2007.4.271
71. Krebs CE, Lam A, McCarthy J, Constantino H, Sullivan K. A survey to assess animal methods bias in scientific publishing. *bioRxiv preprint.* (2022). doi: 10.1101/2022.03.24.485684
72. Ingber DE. Is it time for reviewer 3 to request human organ chip experiments instead of animal validation studies? *Adv Sci.* (2020) 7:22. doi: 10.1002/adv.202002030
73. Marx U, Akabane T, Andersson TB, Baker E, Beilmann M, Beken S, et al. Biology-inspired microphysiological systems to advance patient benefit and animal welfare in drug development. *ALTEX.* (2020) 37:365–94. doi: 10.14573/altex.2001241
74. Anon. *White paper: Tierversuche in der max-Planck-Gesellschaft; animal research in the MaxPlanck society*. Munich: Max-Planck-Gesellschaft (2016).
75. Binder R, Grimm H. Was heißt es, Verantwortung zu übernehmen? In: R Binder, N Alzmann and H Grimm, editors. *Wissenschaftliche Verantwortung im Tierversuch: Ein Handbuch für die Praxis*. Baden-Baden: Nomos (2013). 9–19.
76. Blakemore C., Boesch C., Glover A., Goldberg M., Kaufmann S., Kerr J., et al. (2016). *White Paper Tierversuche in der Max-Planck-Gesellschaft/Animal research in the Max Planck Society*. Available at: https://www.mpg.de/10882%20259/MPG_Whitepaper.pdf (Accessed February 16, 2023).
77. Strech D, Dirnagl U. 3Rs missing: animal research without scientific value is unethical. *BMJ Open Sci.* (2019) 3:1. doi: 10.1136/bmjopen-2018-000048
78. Steward O. A rhumba of “Rs”: replication, reproducibility, rigor, robustness: what does a failure to replicate mean? *eNeuro.* (2016) 3:4. doi: 10.1523/ENEURO.0072-16.2016
79. Biller-Andorno N. Can they reason? Can they talk? Can we do without moral price tags in animal ethics? In: JP Gluck, T DiPasquale and FB Orlans, editors. *Applied ethics in animal research: philosophy, regulation, and laboratory applications*. West Lafayette, IN: Purdue University Press (2001). 25–54.
80. Beauchamp TL, DeGrazia D. *Principles of animal research ethics*. Oxford: Oxford University Press (2020).
81. Röcklinsberg H, Gjerris M, Olsson AIS. *Animal ethics in animal research*. Cambridge: Cambridge University Press (2017).
82. Russell W, Burch R. *The principles of humane experimental technique*. Essex: Methuen (1959).
83. Balls M, Parascandola J. The emergence and early fate of the Three Rs Concept. *Altern Lab Anim.* (2019) 47:214–20. doi: 10.1177/0261192919896352
84. Tannenbaum J, Bennett BT. Russell and Burch's 3Rs then and now: the need for clarity in definition and purpose. *J Am Assoc Lab Anim Sci.* (2015) 54:120–32.
85. Davies G. Locating the 'culture wars' in laboratory animal research: national constitutions and global competition. *Stud Hist Phil Sci.* (2021) 89:177–87. doi: 10.1016/j.shpsa.2021.08.010
86. Greenhough B, Roe E. Exploring the role of animal technologists in implementing the 3Rs: an ethnographic investigation of the UK University sector. *Sci Technol Hum Values.* (2018) 43:694–722. doi: 10.1177/0162243917718066
87. Hobson-West P, Davies A. Societal sentence: constructions of the public in animal research policy and practice. *Sci Technol Hum Values.* (2018) 43:671–93. doi: 10.1177/0162243917736138
88. Lohse S. Scientific inertia in animal-based research in biomedicine. *Stud Hist Phil Sci.* (2021) 89:41–51. doi: 10.1016/j.shpsa.2021.06.016
89. von Aulock S, Busquet F, Locke P, Herrmann K, Hartung T. Engagement of scientists with the public and policymakers to promote alternative methods. *ALTEX.* (2022) 39:543–59. doi: 10.14573/altex.2209261
90. McLeod C, Hartley S. Responsibility and laboratory animal research governance. *Sci Technol Hum Values.* (2018) 43:723–41. doi: 10.1177/0162243917727866
91. Lund TB, Mørkbak MR, Lassen J, Sandøe P. Painful dilemmas: a study of the way the public's assessment of animal research balances costs to animals against human benefits. *Public Underst Sci.* (2014) 23:428–44. doi: 10.1177/0963662512451402
92. Swedish Research Council (SRC) (2019). Allmänhetens syn på djurförsök: Vetenskapsrådets undersökning om allmänhetens attityd till djurförsök 2018. Available at: <https://www.vr.se/analys/rapporter/vara-rapporter/2019-04-23-allmanhetens-syn-pa-djurforsok.html> (Accessed February 16, 2023).
93. Leaman J., Latter J., Clemence M. (2014). *Attitudes to animal research in 2014. A report by Ipsos MORI for the Department for Business, Innovation & Skills*. Available at: https://www.ipsos.com/sites/default/files/migrations/en-uk/files/Assets/Docs/Polls/sri_BISanimalresearch_NONTRENDreport.pdf (Accessed February 16, 2023).
94. Mori Ipsos. (2018). Available at: https://www.ipsos.com/sites/default/files/ct/news/documents/2019-05/18-040753-01_ols_public_attitudes_to_animal_research_report_v3_191118_public.pdf (Accessed April 16, 2023).

95. Gallup (2023). Gallup. Moral Issues 2023. Available at: <https://news.gallup.com/poll/1681/moral-issues.aspx> (Accessed April 16, 2023).
96. Enzinger S, Dürnberger C. "It's not good for the animals, but I think it should be done"-using focus group interviews to explore adolescent views on animal experimentation. *Animals*. (2022) 12:17. doi: 10.3390/ani12172233
97. Alzmann N. *Zur Beurteilung der ethischen Vertretbarkeit von Tierversuchen*. Tübingen: Narr Francke Attempto (2016).
98. Brønstad A, Newcomer CE, Decelle T, Everitt JJ, Guillen J, Laber K. Current concepts of harm-benefit analysis of animal experiments - report from the AALAS-FELASA working group on harm-benefit analysis - part 1. *Lab Anim*. (2016) 50:-20. doi: 10.1177/0023677216642398
99. Cojocaru M-D, van Gall P. Beyond plausibility checks: a case for moral doubt in review processes of animal experimentation In: K Herrmann and K Jayne, editors. *Animal experimentation: working towards a paradigm change*. Leiden: Brill (2019). 289–304.
100. Grimm H, Eggel M, Deplazes-Zemp A, Biller-Andorno N. The road to hell is paved with good intentions: why harm-benefit analysis and its emphasis on practical benefit jeopardizes the credibility of research. *Animals*. (2017) 7:9. doi: 10.3390/ani7090070
101. Grimm H, Olsson IAS, Sandøe P. Harm-benefit analysis – what is the added value? A review of alternative strategies for weighing harms and benefits as part of the assessment of animal research. *Lab Anim*. (2019) 53:17–27. doi: 10.1177/0023677218783004
102. Gutfreund Y. Harm-benefit analysis may not be the best approach to ensure minimal harms and maximal benefits of animal research-alternatives should be explored. *Animals*. (2020) 10:291. doi: 10.3390/ani10020291
103. Jörgensen S, Lindsjö J, Weber EM, Röcklinsberg H. Reviewing the review: a pilot study of the ethical review process of animal research in Sweden. *Animals*. (2021) 11:708. doi: 10.3390/ani11030708
104. Pound P, Nicol CJ. Retrospective harm benefit analysis of pre-clinical animal research for six treatment interventions. *PLoS One*. (2018) 13:e0193758. doi: 10.1371/journal.pone.0193758
105. SAC (2017). Ethical Commission for Scientific Animal Experiments of the SAMS and the SCNAT. Ethical assessment of conflicting issues in animal experimentation: Guide for self-assessment. Available at: <http://tki.samw.ch/> (Accessed January 24, 2023).
106. VB (2021). Verwaltungsgericht Zürich, VB.2021.00276.
107. Davies G, Gorman R, McGlacken R, Peres S. The social aspects of genome editing: publics as stakeholders, populations and participants in animal research. *Lab Anim*. (2022) 56:88–96. doi: 10.1177/0023677221993157
108. Wrage B. Caring animals and care ethics. *Biol. Philos.* (2022) 37:18. doi: 10.1007/s10539-022-09857-y
109. Bailoo JD, Murphy E, Boada-Saña M, Varholick JA, Hintze S, Baussière C, et al. Effects of cage enrichment on behavior, welfare and outcome variability in female mice. *Front Behav Neurosci*. (2018) 12:232. doi: 10.3389/fnbeh.2018.00232
110. Makowska IJ, Weary DM. A good life for laboratory rodents? *ILAR J*. (2019) 60:373–88. doi: 10.1093/ilar/ilaa001
111. NC3Rs. (2020). Rat tickling. Available at: <https://nc3rs.org.uk/3rs-resources/rat-tickling> (Accessed February 16, 2023).
112. Knorr-Cetina KD. *The manufacture of knowledge: An essay on the constructivist and contextual nature of science*. Oxford: Pergamon (1981).
113. Knorr-Cetina KD. *Epistemic cultures: How the sciences make knowledge*. Cambridge, MA: Harvard University Press (1999).
114. Cressey D. Animal research: battle scars. *Nature*. (2011, 2011) 470:452–3. doi: 10.1038/470452a
115. Franco NH, Sandøe P, Olsson IAS. Researchers' attitudes to the 3Rs—an upturned hierarchy? *PLoS One*. (2018) 13:e0200895. doi: 10.1371/journal.pone.0200895
116. Andersen ML, Floeter-Winter LM, Tufik S. Initial survey on the use of animals in scientific research and teaching reveals divided opinion of the Brazilian population. *Einstein*. (2020) 18:eAO5451. doi: 10.31744/einstein_journal/2020AO5451
117. Pew Research Center, (2018). Most Americans Accept Genetic Engineering of Animals That Benefits Human Health, but Many Oppose Other Uses. Available at: https://www.pewinternet.org/wp-content/uploads/sites/9/2018/08/PS_2018.08.16_biotech-animals_FINAL.pdf (Accessed May 9, 2023).
118. Bartal IB-A, Decety J, Mason P. Helping a cagemate in need: Empathy and pro-social behavior in rats. *Science*. (2011) 334:1427–30. doi: 10.1126/science.1210789
119. Huber L. *Das rationale Tier: Eine kognitionsbiologische Spurensuche*. Berlin: Suhrkamp (2021).
120. Monsó S, Wrage B. Tactful animals: how the study of touch can inform the animal morality debate. *Philos Psychol*. (2020) 34:1–27. doi: 10.1080/09515089.2020.1859100



OPEN ACCESS

EDITED BY

Christopher R. Cederroth,
Swiss 3R Competence Centre, Switzerland

REVIEWED BY

Stéphanie Claudinot,
Centre Hospitalier Universitaire Vaudois (CHUV),
Switzerland
Gabrielle Christine Musk,
University of Western Australia, Australia

*CORRESPONDENCE

Sabine J. Bischoff
✉ sabine.bischoff@med.uni-jena.de

RECEIVED 01 February 2023

ACCEPTED 25 May 2023

PUBLISHED 21 June 2023

CITATION

Enkelmann A and Bischoff SJ (2023) CIRS-LAS – a novel approach to increase transparency in laboratory animal science for improving animal welfare by reducing laboratory animal distress. *Front. Vet. Sci.* 10:1155249. doi: 10.3389/fvets.2023.1155249

COPYRIGHT

© 2023 Enkelmann and Bischoff. This is an open-access article distributed under the terms of the [Creative Commons Attribution License \(CC BY\)](#). The use, distribution or reproduction in other forums is permitted, provided the original author(s) and the copyright owner(s) are credited and that the original publication in this journal is cited, in accordance with accepted academic practice. No use, distribution or reproduction is permitted which does not comply with these terms.

CIRS-LAS – a novel approach to increase transparency in laboratory animal science for improving animal welfare by reducing laboratory animal distress

Astrid Enkelmann and Sabine J. Bischoff*

Animal Welfare Office, University Hospital Jena, Friedrich-Schiller University, Jena, Germany

The 3Rs principle is highly topical in animal-based research. These include, above all, new scientific methods for conducting experiments without an animal model, by using non-animal models (Replace), reducing the number of laboratory animals (Reduction) or taking measures to keep the stress on the laboratory animal as low as possible (Refinement). Despite numerous modern alternative approaches, the complete replacement of animal experiments is not yet possible.

The exchange in the team about the daily work with laboratory animals, about open questions and problems, contributes to a reflection of one's own work and to a better understanding of the work of the others. CIRS-LAS (Critical Incident Reporting System in Laboratory Animal Science) represents a reporting system for incidents in laboratory animal science. It is urgently needed because the lack of transparency about incidents leads to the repetition of failed experiments. Negative experiences from animal-based experiments are often not mentioned in publications, and the fear of hostility is still very high. Therefore, a constructive approach to errors is not a matter of course. To overcome this barrier, CIRS-LAS was created as a web-based database. It addresses the areas of reduction and refinement of the 3Rs principle by providing a platform to collect and analyze incidents. CIRS-LAS is open to all individuals working with laboratory animals worldwide and currently exists with 303 registered members, 52 reports, and an average of 71 visitors per month.

The development of CIRS-LAS shows, that an open and constructive error culture is difficult to establish. Nevertheless, the upload of a case report or the search in the database leads to an active reflection of critical occurrences. Thus, it is an important step towards more transparency in laboratory animal science. As expected, the collected events in the database concern different categories and animal species and are primarily reported by persons involved in an experiment. However, reliable conclusions about observed effects require further analysis and continuous collection of case reports. Looking at the development of CIRS-LAS, its high potential is shown in considering the 3Rs principle in daily scientific work.

KEYWORDS

critical incident reporting system, 3R principle, transparency, laboratory animal science, incidents

1. Introduction

What are the similarities between animal testing and flight safety, military operations, or production in mechanical engineering? All of these areas benefit from a constructive error culture to optimize processes and prevent the repetition of failed procedures (1). However, an important difference between animal experimentation and these other areas are the possible consequences of failures. In animal experiments, the focus is on the welfare of laboratory animals, which is potentially affected by failures. Despite the development of numerous modern and promising alternative models, animal testing cannot be completely replaced from today's perspective. In 2021, 2.5 million laboratory animals were used for experimental studies or teaching in Germany (10.6 million in the EU in 2019) (2, 3). Since the EU Directive EU 2010/63 (4) came into force the 3Rs principle (Replace, Reduce, Refine) which had been published long before has been given a legal basis (5).

In Germany as in all other European states the EU Directive EU 2010/63 is applied within the legal regulations for laboratory animal science by the Animal Welfare Act (TierSchG) and the Animal Welfare Ordinance (TierSchVersV) (6, 7). Both legislative texts were extended by the 3Rs principle (3Rs) in 2013. They form the basis of good scientific practice in animal experimentation. According to the 3Rs, all animal experiments should be designed to minimize the number of animals used for experimental purposes (Reduce) and to improve the conditions for the experimental animals (Refine). Whenever possible, alternative approaches must be used if the experimental purpose can also be achieved in this way (Replace). There is a growing awareness not only of working according to the 3Rs principle, but also of the impact of animal welfare on the reproducibility, reliability, and implementation of data obtained from animal experiments (8, 9).

Since 2016 the focus of initiatives and actions was mainly on animal welfare. In the 2020s, the perspective has changed and the wellbeing of people working with laboratory animals is also coming to the fore. The concept of what is known as Culture of Care (CoC) describes good communication as an essential tool to achieve appreciation of laboratory animals and the people who work with them daily (10, 11). Communication in animal experimental research plays an important role at all levels - on the one hand, internally - from the animal caretaker to the management level - and on the other hand, it should be directed externally. External communication primarily involves exchanges with the public about animal experiments and their acceptance. This acceptance is mainly achieved by supplying all the necessary information about animal testing in general (12) and transparency about the exact goal of an animal test (13). Acceptance is further promoted by the support of the European Animal Research Association EARA (14). EARA offers training for researchers toward open communication on animal testing. Institutions from 20 different European countries are member of EARA to work according to the basic principle of transparency in scientific work.

In addition to the information about animal testing available on several Internet platforms mentioned above, scientific institutions around the world are increasingly changing their communication strategy toward greater transparency about specific scientific results obtained in-house with animal testing (15). The internal communication already mentioned above includes both the worldwide exchange with the entire scientific community of people in the field of

animal experimentation and the exchange within a scientific institution. The discussion in the team about the daily work with laboratory animals, difficulties and problems, contributes significantly to the reflection of one's own work and to a better awareness of possible sources of failures (16). However, issues such as the occurrence of an incident or a failure during an experiment, or even the unexpected death of an animal, are often not adequately discussed or even addressed.

For this reason, the desire for a higher level of transparency has come to the fore in recent years. The transparent handling of animal experiments and especially of unexpected incidents is demanded more and more. However, this demand is confronted with mistrust, fear of consequences, and insufficient error awareness in laboratory animal science (LAS). To overcome this mistrust, a confidence base must be established by means of open and constructive communication. At the same time, the advantages of transparency and an open approach to handle errors or incidents must be made clear.

Recognizing errors, discussing the reasons and thinking about possible improvement measures in exchange with others leads to a changed awareness of failures. Mistakes occur, and it is important to accept them and learn from them. In LAS, this means that improvement measures lead to improved animal welfare by avoiding the repetition of unsuccessful experiments. At the same time, dealing openly and constructively with incidents and mistakes is important for building public trust (17). This breaks the cycle of failure and fear of consequences.

Addressing failures constructively goes back to the so-called Swiss cheese model, originally described by the British psychologist James Reason (18). The model represents how latent and active human errors contribute to the breakdown of complex processes and describes the concatenation of error causes. The model compares safety systems with cheese slices placed one behind the other. The holes in the cheese represent the imperfection of safety measures in processes. An unfavorable combination of individual multifactorial defects may cause damage, accidents, or serious consequences. Nowadays, the Swiss cheese model is used worldwide in various disciplines for the analysis of accident causes, in risk analysis, and in risk management. So-called CIRS (critical incident reporting systems) already exist in numerous technical application areas outside medicine, highlighting the importance and suitability of constructive error culture systems (1).

The development towards a better understanding of errors and the rising awareness of the positive impact of revealing and verbalizing errors and pinpointing their causes took place in human medicine as early as the 1980s. This subsequently led to the introduction of error reporting systems in hospitals in 2013 (19). Since the amendment of the German Patient's Rights Act in 2016 (20), every hospital must implement a CIRS to minimize risks to patient well-being (21, 22).

Based on the experiences of CIRS from human medicine, CIRS was established for LAS in 2015 (23). Several reports on the need for transparent and constructive error management have been published in LAS (24–26). Researchers are increasingly encouraged to mention adverse effects of animal experiments in publications to increase reproducibility (27). However, the use of concrete error management systems is not common in LAS. The few existing systems focus on local error management within a facility, usually as part of a quality management system (24, 28). In these local failure management systems, the focus is primarily on

organizational or constructive incidents that are facility-related and confined to one research institution and are therefore very valuable in evaluation. Therefore, the main approach of the reporting system named here, CIRS-LAS, was to create a supra-regional, web-based error management system that is easily accessible for all those involved in animal research. It should not be limited to a single institution, but rather make incidents available to the entire scientific community. The goal of CIRS-LAS was to develop a global approach to network critical incident reports that subsequently could be implemented on an individual research setting.

At,¹ anyone involved in LAS can enter a critical incident using the case report form without prior registration. Furthermore, the visitors of the website can inform themselves about the project. Research within the case report database is possible after registration at² with name and institution. Registered users can leave comments and suggestions for improvement regarding other reported cases, or read about one's own registered cases.

The entry of a critical event and thus the provision of information represents a transparent handling of errors and incidents in animal science. Addressing refinement activities through open dialog is important, as it consequently contributes to improved animal welfare. At the same time, it allows for improving the quality of results of scientific studies by minimizing sources of bias such as unexpected events, interference from suffering animals, or other circumstances.

The benefits of CIRS-LAS are sustainable but develop slowly, since it depends heavily on the acceptance of the project within the scientific community. Investing time in this voluntary work for animal welfare draws on the limited time available to scientists and therefore might negatively affect the compliance to report.

CIRS-LAS supports work according to the 3Rs 'Reduce' and 'Refine' in several ways. It serves as a platform for analyzing the causes of an incident, which is only possible if the critical incident is the subject of discussion and transparent reflection. It also provides the means to share insights with other scientists, and thus can encourage everyone's willingness to learn from mistakes in animal experiments. Each individual can contribute to reduce the number of laboratory animals by searching the CIRS-LAS database for review reports of similar critical incidents or problems and possible resolution strategies to prevent recurrence. Evaluating critical events in animal experiments, facilitates developing potential solution strategies and refinement methods for one's own planned experiments.

The goal of CIRS-LAS is to sustainably improve quality and transparency in all daily work with laboratory animals. This daily work includes not only experimental setups, but also animal husbandry and breeding, as well as daily routine of animal handling and teaching of experimental techniques.

2. Development of CIRS-LAS

The homepage³ was launched in 2015 and contains a database for critical incidents in LAS. A critical incident includes all processes in

which an unanticipated event occurs. This event can be the unforeseen death of an animal, but also an unexpected injury or in general, a result that was not expected in this way. Such a critical incident can occur in any field of LAS: in husbandry, breeding or during an animal experiment.

CIRS-LAS started as a project for scientists working with laboratory animals and was soon extended to all people involved in animal experiments, e.g., animal caretakers, technicians or animal welfare officers. The homepage is divided into two parts - an interface visible to all visitors and a user-restricted area visible only to registered users. The open access interface provides the case report form and general information about the project. The user-restricted area allows for case research and includes commenting options. The web-based application and its availability in English, French and German allows access to CIRS-LAS worldwide. Any person without registration can report a critical incident anonymously on the homepage. The case report form requests 4 important contents (see attachment): (1) Assignment of a title and keywords for later search, (2) details of the animal (s) involved, (3) details of the critical incident itself (subject area, background information, description of the critical incident, possible reasons and suggestions for improvement) and (4) details of the reporter (scientist, employee). All entered data will be used for the later statistical analysis.

In the third part of the case report form (details of the critical incidents itself) the incident is categorized. The categories are based on the German legislation on the number of animals used in scientific approaches (29) and, in addition, some categories have been added to cover the whole field of LAS. These include, for example, anesthesia, musculoskeletal system, genetics and breeding, regulatory and non-regulatory purposes, animal husbandry/hygiene/nutrition, or new animal facility construction. Information about the content of the planned experiment is important for understanding the case report and helps to place it in one's own work. The exact description of the incident shows the deviation from the planned intention. Negative experiences or negative results of an experiment can be specified. The more detailed the background and the incident are described, the easier it is for other registered users to suggest possible improvement measures.

Furthermore, the degree of distress to the animal, if applicable and estimable, is inquired to capture the impact of the critical incident on the animal. The final question on the reported case includes the factors that may have contributed to the incident. Multiple entries are possible, as there are often multiple factors involved (see also Swiss Cheese Model) (18). Here, contributing factors such as organizational problems within the institution itself or equipment and technical failures but also personal factors such as lack of communication, human error, or problems with a special medication as well as factors related to the animal itself can be mentioned.

The complete case report will be checked for anonymity and plausibility by the project administrators before it is published in the user-restricted area of CIRS-LAS. Named keywords are entered into the database (and modified or added if necessary) to facilitate later searches corresponding to an area of interest. To access the restricted database area, registration with a professional e-mail address is required. The CIRS-LAS administrator team manually checks the assignment to the specified institution of the registering persons. The registration will be activated if the institution is conducting animal experiments or if the person can prove a professional interest in

1 www.cirs-las.org/report_incident

2 www.cirs-las.org/register

3 www.CIRS-LAS.org

LAS. After login, registered users can read their own reports or cases reported by others in the restricted user area of the database. They can also make comments on case reports, which are checked for plausibility and content by the project administrators before being published.

All collected data from registered case reports are statistically evaluated regarding frequency of an animal species, a category, an influencing factor, a reporting group of persons or the influence of an incident on the further course of the experiment or on the severity of an injury. Statistical analyses are performed in Excel due to the number of case reports and the research question.

The desire and willingness for more transparency in dealing with animal experiments and critical incidents has increased greatly in recent years. The increased interest in transparency shows, that there is an urgent need to introduce an incident reporting system. Nevertheless, after the introduction of CIRS-LAS in 2015, the willingness to use the database to report a critical incident was initially low, comparable to the similarly delayed acceptance of CIRS in human medicine.

2.1. Increasing acceptance of CIRS-LAS

At the beginning of 2015, the trend towards more transparency in LAS was far from being evident and the project was only known in the local area where the project originated. There was still enormous reluctance to use CIRS-LAS as means to handle critical incidents transparently in animal-based research. As a result, the number of people registered increased slowly and required much discussion and persuasion (Figure 1). However, presentations at universities and research institutions, and discussions with people involved in animal research led to an increase in registrations, which are no longer just local, but also national and international. These presentations provided an opportunity to critically discuss CIRS-LAS with researchers, students, technical assistants, and others who work with laboratory animals. Questions about anonymity, benefits, the reporting process, and how to deal with authorities as well as

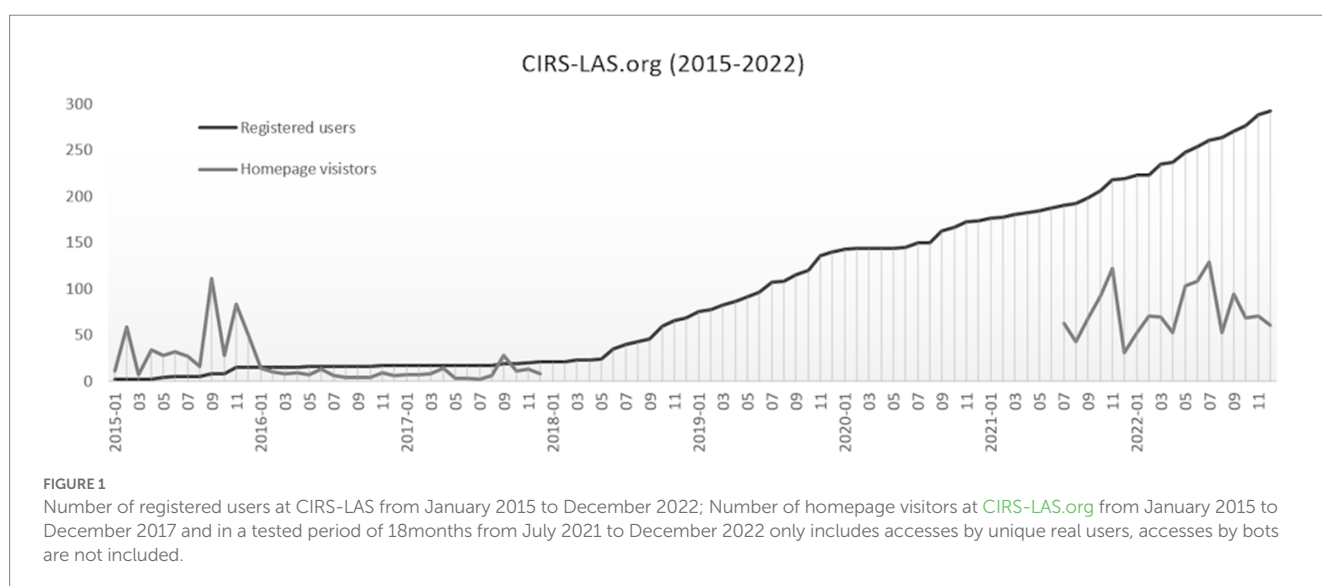
opponents of animal experimentation were answered and discussed. Concerns about anonymity, consequences and even penalties were often dispelled. The intention was to awaken fundamentally their understanding of the need for more transparency in the daily scientific work.

Compared to the beginning, the number of homepage visitors decreased, while more registered users were counted (Figure 1). This may be the result of a more targeted visit to register on [see foot note text 3](#). On the one hand, possible reasons for the initially very hesitant application of CIRS-LAS can be seen in the fact that the trend towards more transparency in animal research developed more strongly only later. On the other hand, the acceptance of CIRS in human medicine developed similarly slowly, since an open-minded error culture had not yet been fully established. Consequently, in the critical discipline of animal-based research, the new approach toward more transparency took even longer.

2.2. Analyses of case reports

The number of case reports ($n=52$) and the fact that each reporting person filled in almost all required fields allowed a statistical validation regarding different aspects of a critical incident report (Figure 2).

Noticeable is the high number of farm animals like sheep and pigs in the reported incidents, followed by rodents (mice, rats) which make up more than 80% of all laboratory animals (Figure 2A). Regarding the incident discipline and the context, most cases were reported in the musculoskeletal field and in laboratory animal husbandry, including the hygiene and nutrition field (Figure 2B). The high number of reported cases concerning farm animals could be based on several possible explanations. First, farm animals are usually not commercially bred homogeneous animals, which is why they are usually not comparable with standardized commercially bred laboratory rodents. Farm animals, usually originated from farm animal environment and thus might be associated with irregular hygienic status. In contrast to laboratory rodents purchased from highly



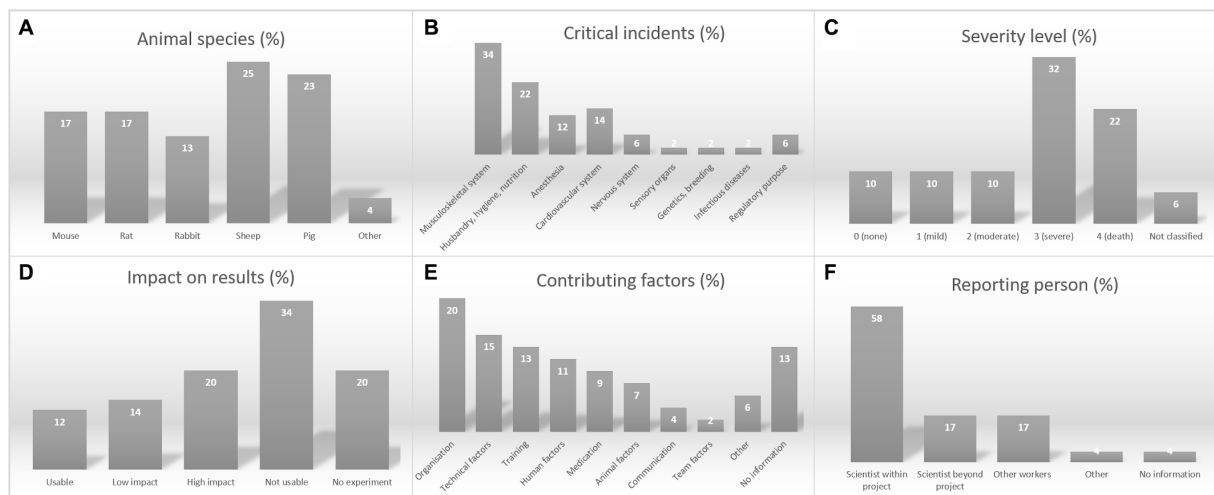


FIGURE 2

Analysis of the reported incidents in the CIRS-LAS database ($n=52$); (A) Animal species, (B) Number of critical incidents in the different disciplines, (C) Severity level, (D) Impact of the incidents on experimental results, (E) Contributing factors, and (F) Reporting person; the percentage of cases and the linked information refer to the period of project launch in January 2015 to December 2022.

standardized and strictly monitored commercial breeding facilities, their hygienic status is oftentimes not even fundamentally analyzed. Subclinical infections might lead to increased biological variability as well as higher risk of occurring side effects under experimental conditions (30, 31). Secondly, farm animals are used as models for particularly challenging complex models, e.g., in musculoskeletal research to determine critical size effects in bone healing or as models for heart failure (32, 33). Considering these risk factors (farm animal species and difficult research areas) in conjunction suggests a higher risk for incidents here.

The so-called expected severity level (Figure 2C) is determined when applying for an animal experiment permit, i.e., before the experiment begins. The maximum severity level to which an animal is expected to be exposed in the planned experiment is defined in 4 severity levels according to EU Directive 2010/63 (4): low, moderate, severe, non-recovery. The severity of the reports in the CIRS-LAS database was primarily severe, and a high number of critical incidents also resulted in the death of laboratory animals (Figure 2C). The reason for the high number of dead animals and severe courses due to an incident may also be related to the high number of reports with large animals as described in the previous section. In addition to the disciplines of musculoskeletal system and husbandry/hygiene/nutrition already mentioned above in connection with farm animals, anaesthesia and cardiovascular interventions also carry very high risks (Figure 2B). Incidents in these disciplines can more quickly lead to a severe severity level. This is also reflected in the proportion of high impact of an incident on the experiment since most frequently, results could not be used for evaluation or experiments could no longer be used continued (Figure 2D).

It can also be assumed that a large proportion of incidents are not reported. It is clear however, that reported incidents can have a significant impact on an experiment and, especially when considered on the scope of an entire research facility, can help to

avoid a significant number of unsuccessful experiments. Based on the evaluation of CIRS-LAS, it becomes clear that the impact of an efficient error management must not be neglected. Not only the number of laboratory animals that are needed for the repetition of a failed experiment must be taken into consideration, but also the resulting costs and the additional time invested. All these things are precious goods at universities and research institutions.

The reporting persons were also asked for the factors that led to the critical incident. The most frequently stated factor was the organization (Figure 2E) which refers not only to the organization of the experiments, but also to the organizational structure of the facility. This mentioned factor can stand for a lot of different causes and could also be a result of the cumulative effect of several influences, like it is described in the Swiss cheese model (18). Technical factors such as equipment failure or technical malfunctions also led to many reported critical incidents. Several failures occurred in training situations or were caused by human factors such as inattention, fatigue, or lack of motivation, to name a few examples.

The statistical analysis of the reporting persons clearly shows that mostly the scientists involved in a project, and less often external scientists or technical staff, reported the incidents (Figure 2F). Project related scientists are mainly responsible for the wellbeing of laboratory animals used for their experimental purposes. That might be a reason why they reflect and evaluate every critical incident. Their aim is to provide good laboratory science, which is why they often critically question themselves, and their work, and search for transparent published data. The trend towards good laboratory practice has been in place for several years, which has led to increased publication of possibilities for ensuring the reproducibility of experiments.

Regarding other measures to improve the reproducibility of animal experiments, such as the ARRIVE guidelines (34), one study found that in the more than 230 examined publications, none of them fulfilled 100% of the requirements of these guidelines. Five years after the ARRIVE guidelines were published, the quality of the information

provided in publications on animal experiments was still not improved across the board (35).

3. Discussion

In an era of transparency initiatives and rising interest from the public in animal experimentation and the wise use of public research funds for basic medical research, every institution should think about how it handles incidents and errors in laboratory animal science and should use CIRS-LAS to do so. To successfully improve transparency in animal experiments in all areas, the use of a CIRS must clearly be supported by the management level. Only then, it is possible to give all employees sufficient security and confidence to talk about incidents without fear of sanctions.

The results clearly show that the majority of reported critical incidents occur in the domains of very complex animal models as musculoskeletal experiments as well as in laboratory animal husbandry. The outcome of incidents with respect to severity assessment was mainly named as severe. However, that conclusion can only be regarded as a presumption based on the number of critical incidents referred to the CIRS-LAS database. Compared to evaluation of use of CIRS in human medicine, the majority of reported critical incidents in hospitals occurred in emergency units, intensive care units, and post anaesthesia care units, which suggests that the probability of a critical incident to occur can be associated with high-risk domains in general.

In the case of critical incidents in LAS, the causes can be traced back to human factors and the surrounding organizational structure in the laboratory or institution. A second consideration involves the difficulty of admitting personal failures. Therefore, it might be possible that contributing organizational factors also include personal failure. Reflecting on one's own work and the mistakes made in the process is still the biggest obstacle, along with the fear of sanctions from colleagues or management. One consequence of this is an unwillingness to enter critical incidents into the CIRS-LAS database. This is also the weakness of CIRS-LAS, which can only be countered by constantly reminding of the goals of an error culture: the improvement of animal welfare and to increase transparency. Both should be in focus of every person who performs animal experiments.

Regarding the question of a local or a global acting reporting system, it should be clear that few incidents are to be expected in a single facility and the exchange about possible reasons and improvement measures is limited. Furthermore, depending on the type of laboratory animals used, not every animal species or category can be mapped. For this reason, CIRS-LAS was designed as a web-based, globally usable system. Only a comprehensive database, representing as far as possible all categories of laboratory animal science, can lead to learning from the mistakes of others. A database with continuously expanding number of cases increases the probability of researching incidents about failed attempts, problems, and possibilities for improvement that affect one's own field of activity. CIRS-LAS is a platform for anyone who is willing to work transparently and to establish a positive error culture in laboratory animal science. Furthermore, this should provide an opportunity for constructive exchange, because ultimately, animal welfare and the reduction of laboratory animals must come first.

From today's perspective, it can be concluded that advantages of using CIRS-LAS to improve quality within animal experiments and to reduce numbers of used animals are proved and undeniable. The active implementation of a constructive failure culture is fundamental to scientific progress while maintaining the highest standards of animal welfare. Recognition of the need for transparent communication in the sense of a positive 'Culture of Care' will ensure public confidence in laboratory animal science.

Data availability statement

The raw data supporting the conclusions of this article will be made available by the authors, without undue reservation.

Author contributions

SB and AE: conceptualization, writing—original draft preparation, review, editing, and validation. SB: methodology, investigation, supervision, project administration, and funding acquisition. AE: formal analysis and visualization. All authors have read and agreed to the published version of the manuscript.

Funding

This research was funded by the German Federal Ministry of Education and Research (BMBF) under grant numbers 031L130 and 031L230. During the second funding period, there was a change in the funding number due to the change of the funding body: 161L0230. The funders had no role in study design, data collection, and analysis, decision to publish, or preparation of the manuscript.

Acknowledgments

Christoph Henniger and David Trietschel were thanked for the administrative and technical support regarding the website and statistical recording. Isabel Jank was thanked for the revision of the manuscript.

Conflict of interest

The authors declare that the research was conducted in the absence of any commercial or financial relationships that could be construed as a potential conflict of interest.

Publisher's note

All claims expressed in this article are solely those of the authors and do not necessarily represent those of their affiliated organizations, or those of the publisher, the editors and the reviewers. Any product that may be evaluated in this article, or claim that may be made by its manufacturer, is not guaranteed or endorsed by the publisher.

References

- Barach P, Small SD. Reporting and preventing medical mishaps: lessons from non-medical near miss reporting systems. *BMJ*. (2000) 320:759–63. doi: 10.1136/bmj.320.7237.759
- Summary report on the statistics on the use of animals for scientific purposes in the member states of the European Union and Norway in 2019. (2022).
- Bf3R Verwendung von Versuchstieren im Jahr 2021. (2022) Available at: https://www.bf3r.de/de/verwendung_von_versuchstieren_im_jahr_2021-309160.html.
- Directive 2010/63/EU of the European parliament and of the council of 22 September 2010 on the protection of animals used for scientific purposes, (2010).
- Russell WMS, Burch RL. Principles of humane experimental-technique. *Roy Soc Health J*. (1959) 79:700.
- BMJV. TierSchG "Tierschutzgesetz in der Fassung der Bekanntmachung vom 18. Mai 2006 (BGBl. I S. 1206, 1313), das zuletzt durch Artikel 280 der Verordnung vom 19. Juni 2020 (BGBl. I S. 1328) geändert worden ist". Bundesministerium der Justiz und für Verbraucherschutz/Federal Ministry of Justice and Consumer Protection; (2020).
- BMJV. Verordnung zum Schutz von zu Versuchszwecken oder zu anderen wissenschaftlichen Zwecken verwendeten Tieren (Tierschutz-Versuchstierverordnung - TierSchVersV). Bundesministerium der Justiz und für Verbraucherschutz/Federal Ministry of Justice and Consumer Protection, (2015).
- Lewis DI. Animal experimentation: implementation and application of the 3Rs. *Emerg Top Life Sci*. (2019) 3:675–9. doi: 10.1042/ETLS20190061
- Turner PV, Pekow C, Clark JM, Vergara P, Payne K, White WJ, et al. Roles of the International Council for Laboratory Animal Science (ICLAS) and International Association of Colleges of laboratory animal medicine (IACLAM) in the global organization and support of 3Rs advances in laboratory animal science. *J Am Assoc Lab Anim Sci*. (2015) 54:174–80.
- Ferrara F, Hiebl B, Kunzmann P, Hutter F, Afkham F, LaFollette M, et al. Culture of care in animal research – expanding the 3Rs to include people. *Lab Anim*. (2022) 56:511–8. doi: 10.1177/00236772221102238
- Williams A. Caring for those who care: towards a more expansive understanding of 'cultures of care' in laboratory animal facilities. *Soc Cult Geogr*. (2021) 24:31–48. doi: 10.1080/14649365.2021.1939123
- Tierversuche verstehen (2022) Available at: <https://www.tierversuche-verstehen.de/>.
- AnimalTestInfo (2022) Available at: <https://animaltestinfo.de/>.
- EARA. European animal research association (2014) Available at: <https://www.eara.eu/>.
- Bertelsen T, Øvlsen K. Assessment of the culture of care working with laboratory animals by using a comprehensive survey tool. *Lab Anim*. (2021) 55:453–62. doi: 10.1177/00236772211014433
- Hubertus J, Pihlmeier W, Heinrich M. Communicating the improvements developed from critical incident reports is an essential part of CIRS. *Klin Padiatr*. (2016) 228:270–4. doi: 10.1055/s-0042-113311
- Mendez JC, Perry BAL, Heppenstall RJ, Mason S, Mitchell AS. Openness about animal research increases public support. *Nat Neurosci*. (2022) 25:401–3. doi: 10.1038/s41593-022-01039-z
- Reason J. Human error: models and management. *BMJ*. (2000) 320:768–70. doi: 10.1136/bmj.320.7237.768
- Bundesanzeiger. Gesetz zur Verbesserung der Rechte von Patientinnen und Patienten. (2013).
- BMJV. Sozialgesetzbuch Fünftes Buch, § 135a Verpflichtung der Leistungserbringer zur Qualitätssicherung. Bundesministerium der Justiz und für Verbraucherschutz/Federal Ministry of Justice and Consumer Protection; (2016).
- Hohenstein C, Hempel D, Schultheis K, Lotter O, Fleischmann T. Critical incident reporting in emergency medicine: results of the prehospital reports. *Emerg Med J*. (2014) 31:415–8. doi: 10.1136/emered-2012-201871
- Neuhaus C, Holzschuh M, Lichtenstern C, St PM. Findings from 10 years of CIRS-AINS: an analysis of usepatterns and insights into new challenges. *Anaesthesist*. (2020) 69:793–802. doi: 10.1007/s00101-020-00829-z
- Bischoff S, Trietschel D, Enkelmann A, Schiffner R, Estrade P, Kobold M. Learning from negative results – critical incident reporting system in laboratory animal science (CIRS-LAS.de). *J Anim Res Vet Sci*. (2018) 2:1–7. doi: 10.24966/ARVS-3751/100009
- Dirnagl U, Przesdzin I, Kurreck C, Major S. A laboratory critical incident and error reporting system for experimental biomedicine. *PLoS Biol*. (2016) 14:e2000705. doi: 10.1371/journal.pbio.2000705
- Ritskes-Hoitinga M, Wever K. Improving the conduct, reporting, and appraisal of animal research. *BMJ*. (2018) 360:j4935. doi: 10.1136/bmj.j4935
- Percie du Sert N, Hurst V, Ahluwalia A, Alam S, Avey MT, Baker M, et al. The ARRIVE guidelines 2.0: updated guidelines for reporting animal research. *Exp Physiol*. (2020) 105:1459–66. doi: 10.1113/EP088870
- Enkelmann A, Bischoff S. How to get more transparency in animal experiments – participation in CIRS-LAS. *AJBSR*. (2020) 10:425–6. doi: 10.34297/AJBSR.2020.10.001546
- Robinson S, White W, Wilkes J, Wilkinson C. Improving culture of care through maximising learning from observations and events: addressing what is at fault. *Lab Anim*. (2022) 56:135–46. doi: 10.1177/00236772211037177
- BMJV. Verordnung über die Meldung zu Versuchszwecken verwendeter Wirbeltiere oder Kopffüßer oder zu bestimmten anderen Zwecken verwendeter Wirbeltiere (Versuchstiermeldeverordnung). Bundesministerium der Justiz und für Verbraucherschutz/Federal Ministry of Justice and Consumer Protection; (2013).
- Rehbinder C, Baneux P, Forbes D, van Herck H, Nicklas W, Rugaya Z, et al. FELASA recommendations for the health monitoring of breeding colonies and experimental units of cats, dogs and pigs. Report of the Federation of European Laboratory Animal Science Associations (FELASA) working group on animal health. *Lab Anim*. (1998) 32:1–17. doi: 10.1258/002367798780559428
- Berset Convenor FWGOFACMCaristo ME, Ferrara F, Hardy P, Oropeza-Moe M, Waters R. Federation of European Laboratory Animal Science Associations recommendations of best practices for the health management of ruminants and pigs used for scientific and educational purposes. *Lab Anim*. (2021) 55:117–28. doi: 10.1177/0023677220944461
- Hettwer W, Horstmann PF, Bischoff S, Gullmar D, Reichenbach JR, Poh PSP, et al. Establishment and effects of allograft and synthetic bone graft substitute treatment of a critical size metaphyseal bone defect model in the sheep femur. *APMIS*. (2019) 127:53–63. doi: 10.1111/apm.12918
- Silva KAS, Emter CA. Large animal models of heart failure: a translational bridge to clinical success. *JACC Basic Transl Sci*. (2020) 5:840–56. doi: 10.1016/j.jacbs.2020.04.011
- Group NCRGW. Animal research: reporting in vivo experiments: the ARRIVE guidelines. *J Physiol*. (2010) 588:2519–21. doi: 10.1113/jphysiol.2010.192278
- Leung V, Rousseau-Blass F, Beauchamp G, Pang DSJ. ARRIVE has not ARRIVED: support for the ARRIVE (animal research: reporting of in vivo experiments) guidelines does not improve the reporting quality of papers in animal welfare, analgesia or anesthesia. *PLoS One*. (2018) 13:e0197882. doi: 10.1371/journal.pone.0197882



OPEN ACCESS

EDITED BY

Luc Zimmer,
Université Claude Bernard Lyon 1, France

REVIEWED BY

Beat M. Jucker,
GlaxoSmithKline, United States
Xuyi Yue,
Nemours Children's Hospital, Delaware,
United States

*CORRESPONDENCE

Nicolau Beckmann,
✉ nicolau.beckmann@novartis.com

[†]These authors have contributed equally
to this work

RECEIVED 21 March 2023

ACCEPTED 16 June 2023

PUBLISHED 28 June 2023

CITATION

Obrecht M, Zurbrugg S, Accart N,
Lambert C, Doelemeyer A, Ledermann B
and Beckmann N (2023), Magnetic
resonance imaging and ultrasound
elastography in the context of preclinical
pharmacological research: significance
for the 3R principles.
Front. Pharmacol. 14:1177421.
doi: 10.3389/fphar.2023.1177421

COPYRIGHT

© 2023 Obrecht, Zurbrugg, Accart,
Lambert, Doelemeyer, Ledermann and
Beckmann. This is an open-access article
distributed under the terms of the
[Creative Commons Attribution License](#)
(CC BY). The use, distribution or
reproduction in other forums is
permitted, provided the original author(s)
and the copyright owner(s) are credited
and that the original publication in this
journal is cited, in accordance with
accepted academic practice. No use,
distribution or reproduction is permitted
which does not comply with these terms.

Magnetic resonance imaging and ultrasound elastography in the context of preclinical pharmacological research: significance for the 3R principles

Michael Obrecht^{1†}, Stefan Zurbrugg^{2†}, Nathalie Accart¹,
Christian Lambert¹, Arno Doelemeyer¹, Birgit Ledermann³ and
Nicolau Beckmann^{1*}

¹Diseases of Aging and Regenerative Medicines, Novartis Institutes for BioMedical Research, Basel, Switzerland, ²Neurosciences Department, Novartis Institutes for BioMedical Research, Basel, Switzerland, ³3Rs Leader, Novartis Institutes for BioMedical Research, Basel, Switzerland

The 3Rs principles—reduction, refinement, replacement—are at the core of preclinical research within drug discovery, which still relies to a great extent on the availability of models of disease in animals. Minimizing their distress, reducing their number as well as searching for means to replace them in experimental studies are constant objectives in this area. Due to its non-invasive character *in vivo* imaging supports these efforts by enabling repeated longitudinal assessments in each animal which serves as its own control, thereby enabling to reduce considerably the animal utilization in the experiments. The repetitive monitoring of pathology progression and the effects of therapy becomes feasible by assessment of quantitative biomarkers. Moreover, imaging has translational prospects by facilitating the comparison of studies performed in small rodents and humans. Also, learnings from the clinic may be potentially back-translated to preclinical settings and therefore contribute to refining animal investigations. By concentrating on activities around the application of magnetic resonance imaging (MRI) and ultrasound elastography to small rodent models of disease, we aim to illustrate how *in vivo* imaging contributes primarily to reduction and refinement in the context of pharmacological research.

KEYWORDS

magnetic resonance imaging, ultrasound elastography, small rodent, pharmacology, translational research, preclinical research, *in vivo* imaging, 3R principles

Introduction

The 3R concept (replacement, reduction, and refinement) concerning the humane treatment of experimental animals was introduced in 1959 by Russell and Burch in the book *The Principles of Humane Experimental Technique* (Russell and Burch, 1959). The development and use of methods that improve the animal welfare by minimizing eventual stress, discomfort and/or pain during experimentation, as well as by reducing the number of animals are central for achieving ethical, scientific and even economic benefits. Moreover, despite ongoing efforts to substitute animal experiments by *in vitro* or *in silico* methods, significant challenges arise in the study of complex regulatory processes of the

cardiovascular, metabolic, respiratory or nervous systems, for instance, or in the investigation of pathology, especially when the disease mechanisms are poorly understood. Thus, animal experimentation remains central to examine disease as well as in the context of drug discovery. Traditional experiments rely heavily on invasive techniques necessitating to sacrifice animals during the course of a study in order to perform, e.g., histopathological analyses. Often such invasive approaches are limited when it comes to identify crucial steps about disease progression or compound effects.

Non-invasive *in vivo* imaging provides potential to quantify with minimal distress anatomical, functional, metabolic or molecular alterations within the animal's body. Imaging allows monitoring temporally and spatially animal models of diseases and the response to therapy (Rudin and Weissleder, 2003; Beckmann, 2006; Ripoll et al., 2008; Beckmann and Garrido, 2013). Through examples primarily from our own experience in adopting imaging in the context of pharmacological studies in small rodent disease models, we aim at illustrating the win-win situation between animal welfare and the relevance of data obtained from animal studies. Non-invasive imaging enables to reduce significantly the number of animals used for experimentation. Repeated measurements allow each animal to serve as its own control, thereby benefitting statistical analyses and resulting in an estimated reduction of more than 80%, depending on the application and the study protocol. For instance, in a rat model of prolactinoma in which pituitary hyperplasia was induced by chronic stimulation with estradiol, a large variability in pituitary volume was observed, which translated into a coefficient of variation of 80% (Rudin et al., 1988). Thus, in order to detect a statistically significant ($p = 0.05$) 50% volume decrease upon treatment, group sizes of at least 35 animals would be required if weighting the pituitary would be the endpoint. However, monitoring the pituitary volume by imaging resulted in a coefficient of variation of 12% and a sample size of $n = 4$ rats were sufficient to reach the same level of statistical significance (Rudin et al., 1988). By repeated examinations of individual mice, animal numbers could be reduced from 96 to 16 mice in a stroke model by incorporating various imaging modalities (Barca et al., 2021). Also, 12 rats were sufficient to longitudinally quantify lung inflammation in an ovalbumin model and to detect compound effects (Tigani et al., 2003). When adopting the traditional terminal method of bronchoalveolar lavage (BAL) fluid analysis, 96 rats would have been necessary. Moreover, the early resolution of edematous signals quantified by imaging upon anti-inflammatory drugs did not involve general suppression of the inflammatory response monitored by traditional BAL fluid analysis (Tigani et al., 2003). In other words, the effect of the compounds on the influx of inflammatory cells in the airways as quantified in BAL was delayed with respect to the effect at the tissue level, as revealed by MRI.

A distinct advantage of imaging is the ability to go back and reanalyze images. Thus, when there are new biological questions/insights there is the option to avoid re-running animal experiments by first re-probing old images. Moreover, there is the possibility to generate information not accessible to *ex vivo* or *post-mortem* approaches, especially regarding functional assessments. This experimental refinement is enabled by the fact that imaging analyzes the organ *in situ* in the intact organism. All these

features bear great relevance in the framework of *in vivo* pharmacology, in particular when addressing therapeutic effects of compounds. Indeed, testing compounds upon established pathology rather than under preventative conditions is of paramount importance. In the case of preclinical experimentation with disease models, it can be expected that every animal reacts differently to a pathological stimulus. Imaging provides the opportunity to non-invasively quantify the pathology just before initiation of treatment. This has an important practical implication as animals can then be randomized into the different treatment groups to have equivalent mean pathology distribution just before initiation of compound or vehicle dosing. Alternatively, the pathology status pre- and post-administration of compound or vehicle can be easily compared in each animal. *Post-mortem* analyses do not allow such direct comparison.

Various imaging techniques including “micro” X-ray computed tomography (micro-CT), position emission tomography (PET), single photon emission computed tomography (SPECT), bioluminescence, fluorescence imaging, magnetic resonance imaging (MRI) and ultrasound, have been used to study biology in small rodent models of diseases (Rudin and Weissleder, 2003; Beckmann et al., 2007; Cunha et al., 2014; Tremoleda and Sosabowski, 2015; Lauber et al., 2017). Within pharmacological research, optical imaging (bioluminescence, near infrared fluorescence imaging) and nuclear medicine techniques (PET, SPECT) are used to address questions related to target engagement, compound distribution and pharmacokinetics (Ripoll et al., 2008; Gomes et al., 2011; Fernandes et al., 2012; Razansky et al., 2012; Jang, 2013; Sharma, 2017). Moreover, the development of radiotheranostic probes enable diagnosis and treatment to be performed with the same agent, particularly in the cancer field (Colombo et al., 2017). Micro-CT, MRI and ultrasound on the other hand provide information on pharmacodynamic effects of compounds on structure and function. Here, attention is going to be limited to applications of MRI or ultrasound shear wave elastography (SWE) (Taljanovic et al., 2017) to pharmacological research in several disease areas incorporating the use of small rodent disease models to highlight the value of imaging in the context of animal welfare. In addition to reduction, these translational techniques enable to apply learnings from the clinics to refine and improve the animal models. Indeed, we aim to illustrate the importance of keeping the clinical picture in mind when performing preclinical pharmacological assessments in small rodents.

In vivo imaging: A few considerations

In most of the *in vivo* imaging applications, animals are anesthetized during the acquisitions. Potential effects of anesthesia need to be attentively considered, as they may not only impact functional acquisitions but also interfere with pharmacological studies. For the majority of the examples discussed in this article, animals were anesthetized with isoflurane, the most widely adopted anaesthetic for laboratory animal imaging (Tremoleda et al., 2012), in air or O₂ administered via a nose cone. Healthy small rodents easily recover from gas anesthesia in a few minutes, but additional

burden may occur in diseased animals. It is important to carefully conceive the studies by considering the number of times an animal is anesthetized and the minimum interval between sequential imaging sessions. As guidance, imaging sessions with a duration under 30 min including positioning of the animals and a minimum interval of 3 h between sequential anesthetics are recommended. No special animal preparation is necessary for MRI or SWE examinations, a minor but important contribution towards refinement. Intravenous administration of a contrast agent is required only occasionally, for instance to verify the leakiness of the blood-brain-barrier. In this case, contrast material approved for clinical use is utilized.

In the past few years, efforts were pursued to reduce the acquisition times by employing image denoising strategies based on filtering or convoluted neural networks. For instance, denoising has been demonstrated to improve small rodent MRI of the heart (Delattre et al., 2012; Tricot et al., 2017), the kidney (de Senneville et al., 2020; Starke et al., 2021) and the central nervous system (Wells et al., 2010; Kim et al., 2016; Wang et al., 2019) as well as spectroscopic analyses (Simões et al., 2022). Even functional connectivity assessments may profit from denoising, as shown in a rat model of sporadic Alzheimer's disease (Diao et al., 2021). Alternative acquisition protocols have been devised to reduce the acquisition times, allowing, e.g., displacements to be detected with temporal resolutions down to 5.5 ms which may benefit cardiac MRI (Lee et al., 2021) and to accelerate the acquisition of anatomical brain images (Spencer Noakes et al., 2017) as well as of diffusion (Lu L. et al., 2012a) or perfusion data (Gao et al., 2014). Another means to reduce the total acquisition time is to combine acquisitions, for instance for assessing two relaxation times simultaneously (Thomas et al., 2002; Liu et al., 2010). More details can be found in specialized reviews (Deshmane et al., 2012; Setsompop et al., 2016; Curtis and Cheng, 2022). Moreover, advancements in data reconstruction, particularly on weighted Compressive Sensing (Kumar et al., 2021) and on model-based or data-driven deep learning tools (Johnson et al., 2020; Wang et al., 2021; Pal and Rath, 2022; Potočník et al., 2023) further reduce aliasing artifact problems and improve signal-to-noise, therefore impacting acquisition times. Of note, many of these developments have been or are being realized on clinical systems. Their adaptation, validation and stability on small animal scanners still needs to be properly addressed.

Prior to being useful for pharmacological studies, *in vivo* imaging readouts need to be carefully validated against standard measures, in general obtained through terminal examinations. Well validated readouts are more relevant, ultimately impacting animal welfare. When histology serves as reference, the importance of having quantitative parameters based on image analysis rather than relying on qualitative scores needs to be stressed. Tissue histopathology slides stored in digital image format are assessable to computerized image analysis tools and machine learning techniques (Komura and Ishikawa, 2018; Hoefling et al., 2021).

Advances in genomic, transcriptomic, proteomic and metabolomic sciences are enabling research into complex diseases. This development is paving the way for the atomic resolution of diseases. Important insights into the genetic basis of human disease are being brought by genome-wide association analyses, while systems biology approaches enhance the

understanding of disease mechanisms by addressing networks, pathways and targets (Yan et al., 2018). Combining imaging providing detailed anatomical and functional information of tissues and organs of the body with -omics approaches provides potential for improved diagnostics and better understanding disease progression, as shown recently in the context of oncology (Zhu et al., 2015; Borgheresi et al., 2022; Fathi Kazerooni et al., 2022), multiple sclerosis (Herman et al., 2018) as well as mild cognitive impairment and Alzheimer's disease (Saykin et al., 2015) to name a few. Pursuing integration of imaging and -omics techniques in small rodents (Chakraborty et al., 2017) opens the door for an improved characterization of models of disease without the necessity of increasing animal usage.

Complex questions can be better addressed through open collaboration between groups at several institutions rather than individually. Exchange of information and experience can improve output quality through, e.g., understanding the factors leading to successful acquisitions, enhanced protocols, and/or data analysis. Such collective efforts may on the long run potentiate future data collection, improve standards, comparability and reproducibility, and ultimately contribute to a reduction of animal use by a diminution of discards. Examples are efforts around standardization of resting state functional MRI (rs-fMRI) in mice (Grandjean et al., 2020) and rats (Grandjean et al., 2023) involving multiple groups around the world mentioned below.

In the next sections, applications of MRI or SWE to quantify pathology in the musculoskeletal system, brain, lung, and liver in the context of small rodent disease models for pharmacological research are discussed keeping the animal welfare in mind. Also safety analyses using imaging are presented.

Musculoskeletal system

Osteoarthritis

Osteoarthritis (OA) is a main cause of disability in older adults. Pain, loss of function and decreased quality of life are among the consequences of this long-term disease frequently affecting knee joints (Hunter et al., 2014). Traditionally OA was considered as a “wear and tear” condition, with articular cartilage damage, inflammation, stiffness, swelling, and loss of mobility resulting from a chronic overload and impaired biomechanics of the joint. Now it is known that OA involves a much more complex process orchestrated by inflammatory and metabolic factors in which the entire joint is affected, most notably the cartilage but also the synovium, joint ligaments, menisci and subchondral bone (Loeser et al., 2012; Martel-Pelletier et al., 2016).

In the absence of disease-modifying compounds, symptomatic treatments and, ultimately, joint replacement are currently the only therapeutic options available for knee OA. Small rodent models play an important role when testing new therapies (Kuyinu et al., 2016). Injury induced in rats by surgery leads to fast cartilage degenerative changes involving chondrocyte/proteoglycan loss and fibrillation as well as osteophyte formation. MRI has been applied in conjunction with such models to evaluate treatments (Huang et al., 2010; Huang et al., 2021; Gu et al., 2015; Mohan et al., 2016). The basis for the use of MRI is the quantification of degenerative cartilage compositional changes by T₂ mapping, which is sensitive to abnormalities of the

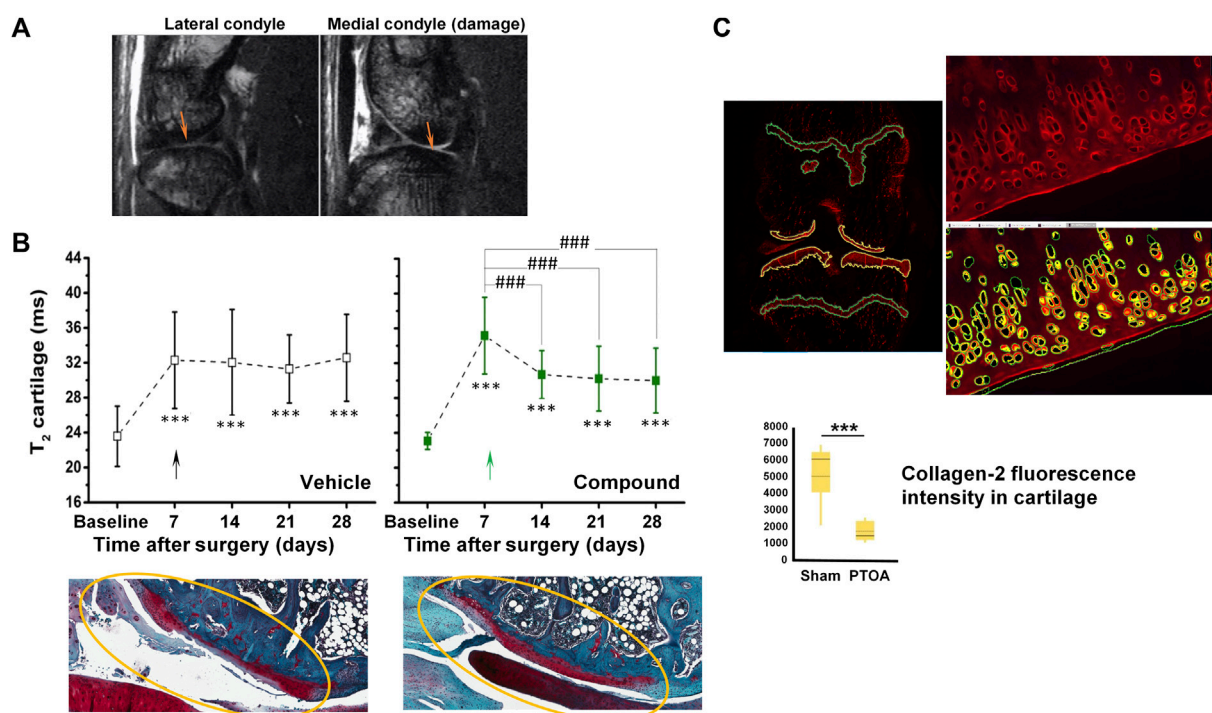


FIGURE 1

MRI in a post-traumatic OA (PTOA) rat surgical model of cartilage injury. (A) Spin-echo images acquired at 7 T from the same joint, 7 days after surgery. Damaged cartilage in the medial condyle displayed higher signal intensity than in the lateral condyle (arrows). (B) Higher signal intensity translated into increased T_2 relaxation times in damaged cartilage. A reduction of T_2 was observed upon intra-articular administration 1 week after injury onset of a compound aiming to promote cartilage regeneration. Representative safranin-O stained histological images confirmed the beneficial effect of the compound. (C) Quantification of fluorescence applying machine learning tools to immunohistochemistry for collagen-2. See Accart et al. (2022) for details on image acquisition and quantification. ©The Authors 2022.

cartilage extracellular matrix including collagen fiber orientation (Joseph et al., 2018). Early phases of cartilage degeneration occurring prior to macroscopic cartilage defects and thinning are detectable, increases in T_2 being associated with cartilage abnormalities (Pan et al., 2011).

Figure 1A shows images acquired in 8.5 min at 7 T from a rat knee joint after meniscal tear and medial collateral ligament transection. Cartilage appears brighter in the injured condyle, consistent with increased relaxation time T_2 upon cartilage damage as illustrated in Figure 1B. Of note, the T_2 of healthy cartilage of ~20 ms in rats is consistent with values reported for hyaline cartilage in humans at the same field strength, ranging between 19 and 24 ms (Juras et al., 2016). Treatment with a compound administered intra-articularly at week 1 after surgery, aiming to promote cartilage regeneration, led to significant decrease of T_2 , suggesting beneficial effects on cartilage confirmed by histology at the end of the study (Figure 1B). Quantitative histological analysis supported the validation of T_2 as non-invasive marker of cartilage damage in this surgical model (Figure 1C).

Modulation of cartilage T_2 upon experimental treatment has also been reported in the clinic for knee OA patients. In a phase I–II trial T_2 reductions upon intra-articular administration of *ex vivo* expanded autologous mesenchymal stromal cells indicated cartilage

regeneration (Soler et al., 2016). Three recent studies demonstrated T_2 reductions after implanting a biomaterial scaffold seeded with chondrocytes (Li et al., 2021; Xu et al., 2021; Janacova et al., 2022). In two of the studies early efficacy suggesting cartilage repair translated into cartilage T_2 reductions within 3–6 months of implantation, accompanied by improvements in functionality and pain levels (Li et al., 2021; Xu et al., 2021). Texture analysis of T_2 quantitative maps has also been introduced to study cartilage repair (Janacova et al., 2022).

The investigation by MRI of the knee joint as an organ with several tissues in focus was pursued in a rat study examining the effects of repeated intra-articular injections of monosodium urate (MSU) crystals with inflammasome priming by lipopolysaccharide (LPS) with the aim to simulate recurrent bouts of gout (Accart et al., 2022). Gout is a common form of arthritis, involving recurrent episodes of painful acute inflammatory flares in response to MSU crystals depositing mainly in peripheral joints (Kuo et al., 2015). The longstanding accumulation of MSU crystals can then elicit damage in the joints. Gout and osteoarthritis (OA) often occur in conjunction. Nonetheless, despite the positive correlation between the uric acid amount in the synovial fluid and OA (Denoble et al., 2011), currently it remains unknown whether gout and OA are pathologically linked (Jarraya et al., 2022). Repeated intra-articular administration of MSU/LPS to rats resulted in joint swelling,

synovial membrane thickening, fibrosis of the infrapatellar fat pad, tidemark breaching, and incursion of inflammatory cells to cartilage (Accart et al., 2022). In comparison to saline administration, animals receiving MSU/LPS displayed higher pain sensitivity to van Frey filament stimulation of the hind-paws. In the joints of rats challenged with MSU/LPS, MRI showed an increase of synovial fluid volume related to inflammation, changes in the infrapatellar fat pad consistent with a progressive decrease of fat volume and fibrosis development, and a progressively increased T_2 in femoral cartilage, in agreement with a reduced proteoglycan content in the same area. MRI displayed as well cyst formation in the tibia, femur remodeling, and T_2 reductions in extensor muscles, the latter consistent with fibrosis generation in this tissue (Accart et al., 2022).

From the 3R's perspective, benefits of including MRI in longitudinal preclinical OA studies are many fold: 1) A reduction by at least 80% in animal usage is estimated; 2) multiple tissues of the knee joint can be analyzed in an acquisition time of 8.5 min; 3) as injury may be heterogeneous, especially in the surgical models, randomizing animals into groups just before initiation of treatment using, e.g., cartilage T_2 as measure contributes to reduce variability in pharmacological studies; and 4) the demonstration that cartilage T_2 can be modulated by therapy both in preclinical animal studies and in OA patients strengthens the translational potential of the readout. Also interesting is the positive correlation between the relaxation time T_2 in the infrapatellar fat pad and the latency time in the von Frey stimulation as a surrogate of pain sensitivity for the repeated intra-articular injections of MSU/LPS in rats (Accart et al., 2022). The infrapatellar fat pad is richly innervated (Lehner et al., 2008) and may be a source of pain in OA (Belluzzi et al., 2019). Trauma can lead to inflammation and eventually fibrotic lesions, both being sources of pain at the level of the infrapatellar fat pad (Eymard and Chevalier, 2016). Despite the positive correlation mentioned before, additional research is necessary to draw conclusions about the value of infrapatellar fat pad T_2 as a surrogate marker of increased pain sensitivity in the MSU/LPS-induced knee joint injury or in other OA models.

Tendon injury

Tendons composed primarily of highly structure collagen fibers connect and transmit forces from the muscle to bone (Docheva et al., 2015). The stiffness of the tendon is critical for such an interaction. Achilles tendon rupture is often accompanied by substantial morbidity, mobility impairment, and increased absence from work. The recovery process of tendon stiffness following an injury is poorly understood, and the decision to return to full weightbearing for normalizing daily activities and practicing sports is solely based on clinical features.

Shear wave elastography (SWE) and wearable insoles evaluating tendon stiffness and foot plantar pressure, respectively, were examined with the aim to verify the feasibility of deriving objective quantitative measures after Achilles tendon rupture to ultimately facilitate decision making (Laurent et al., 2020). Over the 12-week duration of the study, the tendon stiffness in contralateral healthy tendons remained stable. In contrast, at week-2 post-injury the stiffness of the injured tendon was significantly decreased, most prominently in regions close to the rupture. Near complete stiffness recovery was detected at week 8 in distal regions to the rupture.

However, at week 12 the stiffness in the proximal region of the injured Achilles was still significantly below that of the contralateral tendon. Despite the fact that the injured leg reached full weight-bearing capacity at week 12 after the injury, the plantar pressure distribution during walking showed slight sub-optimal function of the affected foot at this time point. Significant correlations between tendon shear wave velocity, insole variables and distinct activities indicated the clinical relevance of SWE and foot plantar pressure assessments (Laurent et al., 2020).

With translational research in mind, a validation preclinical study involving a rat model of tenotomy compared *in vivo* tendon stiffness measurements by SWE with *ex vivo* assessments of the Young's modulus. A strong correlation ($R^2 = 0.87$, $p = 5 \times 10^{-12}$) was found between the tendon shear wave velocity measured *in vivo* and the *ex vivo* values of the Young's modulus determined using biomechanics assays (Laurent et al., 2020). The 3R value of this experiment resides in a refinement, attesting to the adequacy of SWE for the quantification of tendon stiffness.

Ultrasound imaging and MRI were also integral part of a recent study describing enhanced tendon healing by a tough hydrogel with an adhesive side and a high drug-loading capacity (Freedman et al., 2022). Tissue adherent respectively gliding properties on opposing surfaces were displayed by this so-called Janus tough adhesive (JTA), which enabled drug delivery to the tendon tissue. A dual interpenetrating hydrogel network combining an alginate hydrogel and a highly elastic covalently cross-linked acrylamide hydrogel yielded the high JTA mechanical toughness (Sun et al., 2012). Tissue adhesion resulted from the unilateral coupling of the dissipative alginate acrylamide hydrogel to the amine rich bridging polymer chitosan (Li et al., 2017). The ability of the JTA to simultaneously support mechanical tissue integrity and spatially as well as temporally control drug delivery was demonstrated in rat models of tendon injury (Freedman et al., 2022).

Peripheral nerve injury

Peripheral nerve injury constitutes a major clinical and public health problem, often resulting in significant functional impairment, permanent disability and/or chronic pain (Modrak et al., 2020). Despite existing in varying severities, trauma to connective tissue, myelin, and axons is present in most forms of nerve injury. Microsurgery is currently the treatment of choice, but functional recovery following nerve repair is often unsatisfactory. Thus, new therapeutic strategies are necessary to increase functional recovery following injury.

Nerve crush is commonly used as experimental model to study recovery to peripheral nerve injury in small rodents (Bridge et al., 1994). Magnetization transfer ratio (MTR) reflecting myelin content in tissue (van der Weijden et al., 2021) as assessed non-invasively by MRI was adopted when investigating a model of nerve injury in which the sciatic nerve of mice was crushed using a forceps applied gently for 15 s. At baseline, before the injury onset, MTR in the sciatic nerve was significantly smaller in old compared to young animals. In healthy humans, MTR of lower extremity nerves has been found as well to decrease with age (Kollmer et al., 2018). Nerve demyelination elicited by the crush was reflected by reduced MTR in the first week after the crush in several areas along the nerve, with a partial recovery at later time points (Giorgetti et al., 2019) (Figure 2A). For young mice, at week 6 MTR in the nerve region

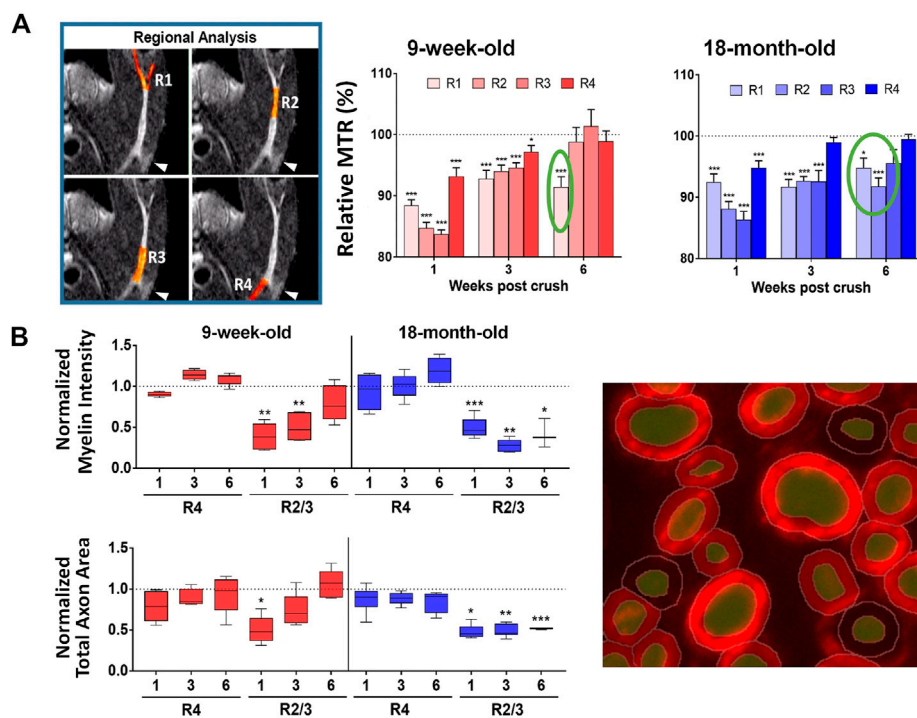


FIGURE 2

Sciatic nerve crush in mice. (A) Significantly lower MTR at different regions of the sciatic nerve were determined 1 week post-injury suggesting demyelination. At week 6, MTR was still below baseline after the nerve bifurcation in young mice, while for old mice the region displaying MTR below baseline was larger. (B) Quantitative histological analyses using machine learning tools of myelin basic protein fluorescence signal confirmed lower myelin content in the sciatic nerve as a function of time after the crush. See Giorgetti et al. (2019) for details. ©The Authors 2019.

after the bifurcation was still significantly below baseline. For old mice, the region displaying MTR below baseline was larger. Histology confirmed a larger area of demyelinated nerve in old compared to young mice at week 6 after the crush (Figure 2B). In other words, *in vivo* MRI and histology revealed an age-related impairment of nerve regeneration after crush (Giorgetti et al., 2019). Of note, electrophysiological recordings for young mice were back to baseline values at week 6. Also, muscle atrophy was more pronounced on aged muscles and did not fully recover at 6 weeks post sciatic nerve crush. Of note, at day 6 after crush, when no change in muscle volume was yet detected by MRI, a significant increase of T_2 could be seen in the calf muscle, consistent with increased extracellular space due to type IIb fiber atrophy as revealed by histology (Giorgetti et al., 2019).

For consistency, the approach was applied to another demyelination model, in which lysolecithin was injected upon the sciatic nerve of rats. The same spatial pattern of MTR reduction observed for the nerve crush was reproduced, with the most pronounced MTR changes occurring at the bifurcation of the sciatic nerve. The reduced MTR was accompanied by reductions in luxol fast blue staining detected histologically (Giorgetti et al., 2019).

Although so far only used to phenotype the models, it remains to be demonstrated that MRI will be useful when assessing therapies. The fact that MTR was sensitive to detect effects of compounds aiming to improve myelination in the brain (Beckmann et al., 2018; Dietrich et al., 2022; see below) indicates that this might also be possible in the

peripheral nervous system. In comparison to electrophysiological assessments, MRI has the advantage of providing spatial information. Moreover, the temporal evolution of nerve conduction and MTR assessments are not necessarily the same, as mentioned for old mice in the nerve crush experiment. In addition to peripheral nerves, MRI can also analyze the central nervous system of the animals. Besides MTR, diffusion tensor imaging (DTI) providing metrics such as fractional anisotropy, axial diffusivity, radial diffusivity, and mean diffusivity, is also an alternative to analyze peripheral nerve dysfunction and repair (Kim et al., 2019; Cheah et al., 2021). However, the demanding technical nature of DTI requiring specialized expertise and long measurement times (12 h were reported for excised rat nerves; Boyer et al., 2015) might be challenges for its routine application to preclinical pharmacological examinations in small rodents. Finally, MTR has been established in the clinic as reliable and reproducible (Preisner et al., 2021; Chen et al., 2023) and provides a means to examine peripheral nerve injury and neuropathies (Dortch et al., 2014; Kollmer et al., 2020; Roth et al., 2022), thereby enhancing the translational potential of the activities described here for small rodents.

Brain

Neurodegeneration in multiple sclerosis

Multiple sclerosis (MS) is the most common non-traumatic disabling disease affecting young adults (Browne et al., 2014).

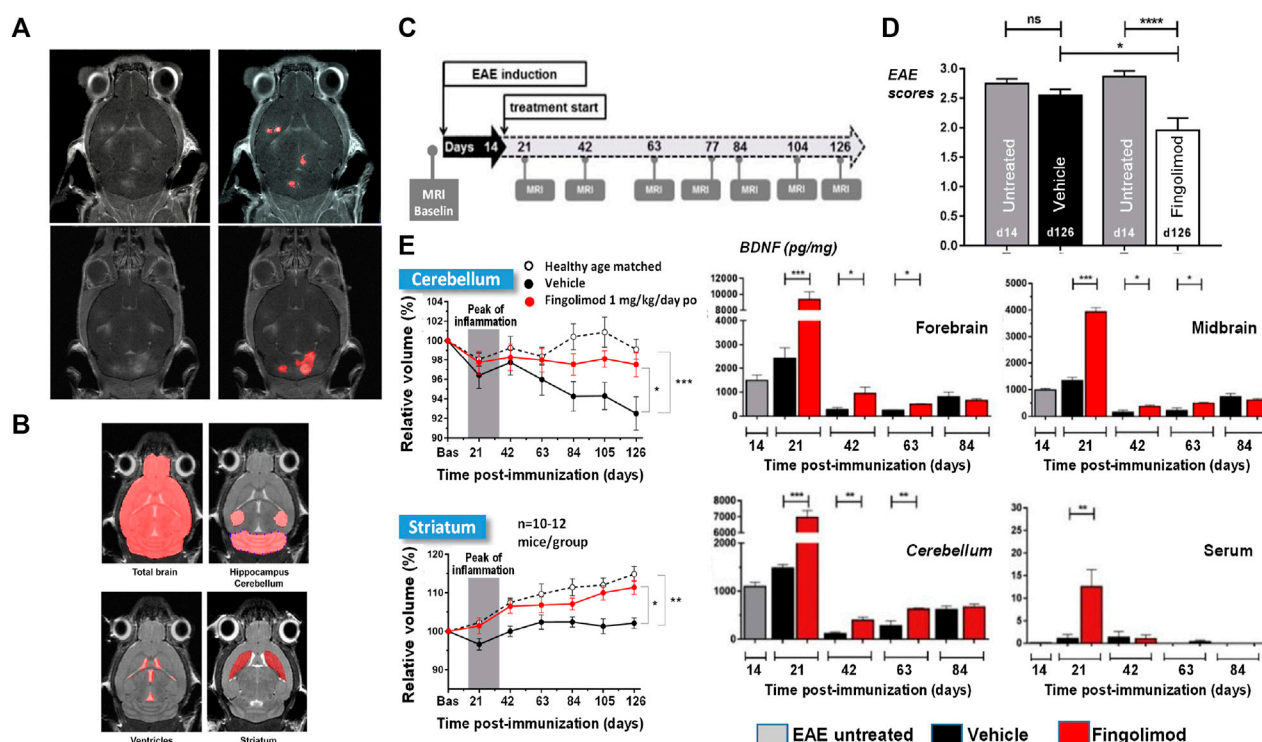


FIGURE 3

MRI for the analysis of EAE mice modeling MS: Lesion detection and neurodegeneration. (A) T_1 -weighted images acquired at the peak of disease from two EAE animals following intravenous injection of the clinically approved contrast agent Dotarem (Gd-DOTA) as a bolus. Lesions corresponding to leakage of the contrast agent in areas of impaired blood-brain barrier are clearly visible. (B) For volumetric analyses of the whole brain and subareas thereof T_2 -weighted images acquired in 12.5 min without administration of contrast material provided sufficient contrast for segmentation. (C) Scheme of study protocol for assessing neurodegeneration in the model. Treatment started at the peak of disease on day 14 after EAE induction. (D) EAE mice treated with fingolimod had improved clinical scores compared to animals receiving vehicle. (E) Neurodegeneration was consistently quantified by MRI in the striatum and cerebellum of EAE mice receiving vehicle but not in those treated with fingolimod. Increased brain derived neurotrophic factor (BDNF) levels were detected in several brain areas and in the serum of fingolimod-treated EAE mice. More details can be found in Smith et al. (2018). © 2018 Elsevier B.V.

Although historically considered as an organ-specific T-cell mediated autoimmune disease, recently the involvement of also B-cells in MS became clearly evident (Greenfield and Hauser, 2018). The disease is viewed as having two stages, comprising early inflammation responsible for a relapsing–remitting pattern and delayed neurodegeneration causing non-relapsing progression in secondary and primary progressive MS (Leray et al., 2010; Thompson et al., 2018). Therapies for MS are required to reduce the number of relapses and to lead to less disability as well as brain lesions detected by gadolinium-MRI (Figure 3A). Moreover, slowing brain atrophy has become a key clinical efficacy readout (Guevara et al., 2019).

Described for several species, experimental autoimmune encephalomyelitis (EAE) is a common animal model in preclinical MS research (Baker and Amor, 2014). In mice, it involves the subcutaneous administration of myelin oligodendrocyte glycoprotein in complete Freund adjuvant, boosted the intraperitoneal injection of pertussis toxin. Brain inflammation, demyelination and neurodegeneration are observed.

Although important for molecular characterization and target validation studies in this model, histology has its limitations when it comes to pharmacological studies. Besides necessitating large

number of animals and not being applicable in the clinic, it is very time consuming especially for deriving volumetric information, and it is prone to sampling errors, as brain volume changes (shrinkage) may occur at autopsy. The feasibility of detecting brain volumetric changes of less than 10% in EAE mice by MRI, using a field strength of 7 T and a conventional radiofrequency coil, has been demonstrated (MacKenzie-Graham et al., 2012). However, acquisition times of the order of 1 h or longer were necessary.

Knowing that EAE mice are very susceptible to their environment, we aimed at having a short measurement time. Following optimization the whole brain was imaged with sufficient contrast for quantifying subareas in a reasonable measurement time of 12.5 min without administration of contrast material (Smith et al., 2018) (Figure 3B). In two separate preparatory studies it was verified whether repeated use of the 12.5 min protocol impacted the disease development, assessed through scores of limb paralysis. Only when we showed that no impact occurred, did pharmacological testing start.

A compound tested in the model was the sphingosine 1-phosphate (S1P) receptor agonist, fingolimod (Smith et al., 2018). Treatment started at the peak of the disease, at day 14 after EAE induction, and went until the end of the study, on day 126

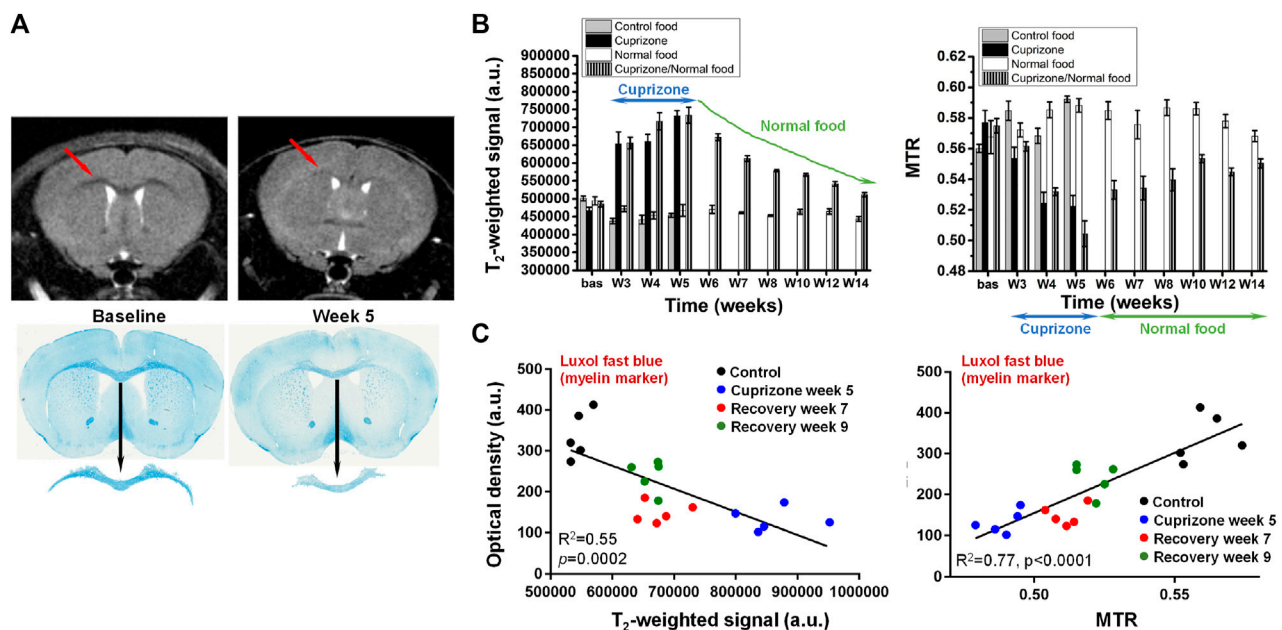


FIGURE 4

Cuprizone-induced demyelination in the brain of mice. (A) Representative T₂-weighted images from the same mouse acquired before (baseline) and after 5 weeks of cuprizone intoxication. A clear contrast change occurred at the level of the corpus callosum (arrows). Luxol fast blue histology revealed demyelination in the same brain area. (B) Cuprizone induced significant signal increase in T₂-weighted images respectively decrease of magnetization transfer ratio (MTR) in the corpus callosum. (C) Comparison between the MRI signal/MTR parameters and the quantitative histology analysis of luxol fast blue. More details can be found in Beckmann et al. (2018). © The Authors. 2018 Open Access.

(Figure 3C). MRI was performed at baseline and at different time points after EAE induction. Fingolimod improved the clinical scores of the EAE animals (Figure 3D). MRI revealed that the cerebellum volume decreased with time in EAE mice receiving vehicle. Moreover, both the cerebellum and the striatum volumes in vehicle-treated EAE mice were significantly lower compared to those in normal mice which served as controls. These observations were consistent with neurodegeneration occurring in the model. Moreover, the longitudinal development of the cerebellum and striatum volumes of fingolimod-treated EAE mice followed the same pattern as that observed for normal mice, showing that the compound protected against neurodegeneration in EAE mice (Figure 3E). Studies performed on other cohorts showed that brain derived neurotrophic factor (BDNF) was increased in several brain areas at least until day 63, as well as in plasma in the initial phase (Figure 3E), providing a possible mechanism for the neuroprotective effects of fingolimod.

In the clinic, several studies showed that fingolimod slowed down neurodegeneration in MS patients as assessed by MRI (Kappos et al., 2015; Zivadinov et al., 2018). Moreover, increased BDNF secretion from circulating T-cells was detected in MS patients receiving the compound (Golan et al., 2019).

MRI opens the avenue for performing neurodegeneration studies in the EAE model. From the 3Rs perspective, besides an impressive reduction of animal numbers (estimated reduction 88%), using a clinically relevant imaging approach improves the translational validity of the MS animal model for compound testing.

Demyelination in the central nervous system: Cuprizone model

Various disorders of the central nervous system, including leukodystrophies and genetic disorders as hematoidosis, Niemann-Pick's disease and aminoacidopathies, are characterized by either demyelination or the destruction of a previously intact myelin sheath. However, MS is the most frequent neurological disease involving myelin pathology. Therapies targeting remyelination have a great potential to delay, prevent or even reverse disability in MS patients.

The cuprizone model, involving toxin-induced demyelination followed by endogenous remyelination after cessation of the intoxication, is largely used to test the efficacy of novel compounds *in vivo* (Torkildsen et al., 2008). It has also contributed substantially to the understanding of important aspects of the MS disease. MRI is an ideal tool to follow longitudinally and non-invasively the pathology in this mechanistic model. Contrast changes in T₂-weighted images became clearly apparent in the corpus callosum of mice receiving the copper chelator in food pellets for 5 weeks, which were then reverted after the interruption of cuprizone administration (Figure 4A). Histology of the myelin marker, luxol fast blue, clearly demonstrated less myelin in the corpus callosum at week 5. A summary of the T₂-weighted signal in this brain area is provided in Figure 4B. For the same animals, a reduction of MTR occurred during the cuprizone intoxication phase. Upon interruption of cuprizone, MTR slowly increased towards baseline values. Signal intensity correlated negatively, while MTR correlated positively with

histology, either with luxol fast blue, a myelin marker, or with myelin oligodendrocyte glycoprotein (Figure 4C).

In pharmacological studies involving the colony-stimulating factor-1 inhibitor, BLZ945, administered preventively, before and during the cuprizone intoxication, both T₂-weighted signal and MTR suggested that the compound had some protective effects against demyelination in the corpus callosum, but less in the external capsule (Beckmann et al., 2018). This was confirmed by luxol fast blue histological analysis. Mice receiving BLZ945 and cuprizone treatment for 5 weeks displayed in the corpus callosum a substantial amount of remaining myelin, and a reduction of Iba1-positive microglia. When BLZ945 was administered therapeutically, namely, starting at week 5 of cuprizone intoxication, T₂-weighted signal in the cortex and striatum was normalized, suggesting increased remyelination in these brain areas. However, no effect of the compound was detected in the corpus callosum. Histology confirmed the *in vivo* MRI observations (Beckmann et al., 2018).

In secondary progressive MS patients, siponimod, a selective S1P receptor 1 and 5 modulator, significantly reduced disability progression, cognitive decline, and total brain volume loss compared to placebo treatment (Kappos et al., 2018; Regner-Nelke et al., 2022). Some of these protective effects might be modulated by the induction of remyelination. Evaluations of MTR and T₂-weighted signals revealed indeed increased remyelination in the cuprizone model for mice treated with siponimod (Dietrich et al., 2022).

Microglia, osteoclasts, dendritic cells and macrophages express the cell-surface immunoreceptor TREM2 (triggering receptor expressed on myeloid cells 2) (Jay et al., 2017). Myelin/neuronal loss and neuroinflammation in neurodegenerative diseases like Alzheimer's disease and frontotemporal dementia have been associated with heterozygous loss-of-function TREM2 mutations, most notably those enhancing cell-surface shedding (Jay et al., 2017; Yeh et al., 2017). The role of soluble and cleavage-reduced TREM2 on myelination processes in the brain has been investigated in TREM2 cleavage-reduced, TREM2 soluble-only, TREM2 knock-out and wildtype mice analyzing MRI readouts within the cuprizone model (Beckmann et al., 2023). Upon cuprizone challenge sustained microglia activation led to increased remyelination, whereas microglia with only soluble TREM2 had reduced phagocytic activity despite displaying an efficient lysosomal function, resulting in a dysfunctional phenotype comprising impaired myelin debris removal capacity, lack of remyelination and axonal pathology.

Although most cuprizone studies define the corpus callosum as main region of interest for evaluations, demyelination also occurs in other white and gray matter areas (Goldberg et al., 2015). MRI provides the opportunity to analyze simultaneously several brain areas, which is certainly an advantage in pharmacological studies using the model. Since some variability can be expected in response to cuprizone, for therapeutic treatment starting after some weeks of intoxication, randomization of animals into different groups based on MRI just before initiation of compound dosing becomes of paramount importance. Acquisition of T₂-weighted and MTR images for every animal enabled to also derive information on myelin debris (Beckmann et al., 2018; 2023), an important aspect when testing compounds as the presence of debris may impair remyelination (Lubetzki et al., 2020). Moreover, there is

translational potential of the MRI readouts. Hyperintense lesions on T₂-weighted images of MS patients are considered as a sign of demyelination in the central nervous system (Thompson et al., 2018) and MTR has been demonstrated to be sensitive to cortical demyelination in MS patients (Chen et al., 2013).

Brain function

The power of functional MRI (fMRI) to study brain disease and pharmacology has been reviewed extensively elsewhere (Bifone and Gozzi, 2012; Jenkins, 2012; Jonckers et al., 2015; Carmichael et al., 2018). Functional experiments can be classified into: 1) Task-based fMRI employing sensory or cognitive stimuli to induce responses in brain regions or circuits; 2) resting-state fMRI (rs-fMRI) used to investigate functional connectivities in the absence of any stimulus; 3) pharmacological MRI (phMRI) dealing with fMRI signals after the administration of pharmacological agents, with the aim to localize the target area in the brain containing the appropriate receptors for the neuromodulatory agents. Upon neural activation, changes in local cerebral blood flow and volume as well as in the cerebral metabolic rate of oxygen lead to a locally increased ratio of oxygenated over deoxygenated hemoglobin. These mechanisms provide the basis for fMRI, which relies primarily on the acquisition of images that are sensitive to the blood level dependent (BOLD) contrast based on the differential magnetic properties of oxygenated (diamagnetic) and deoxygenated (paramagnetic) hemoglobin or to perfusion as assessed using, e.g., arterial spin labeling techniques. Increased ratios of oxygenated over deoxygenated hemoglobin with neural activation results in contrast changes, for instance in a local signal enhancement in T₂*-weighted images. Despite providing only an indirect measure of neuronal activity, fMRI is a powerful tool to examine brain function, as attested by the large number of clinical trials using fMRI as an outcome measure (Sadraee et al., 2021).

The translational character of fMRI between rodents and humans has been carefully addressed by several groups. For instance, robust responses upon ketamine dosing were detected in the cingulate, frontal cortex, and hippocampus (Bifone and Gozzi, 2012) and acute ketamine challenge increased the resting state prefrontal-hippocampal connectivity in both humans and rats (Grimm et al., 2015), a phenotype that is often disrupted in pathological conditions related to psychiatric disorders and their onset. A good agreement between phMRI signatures in rodents and humans was also shown for acute remifentanyl administration, with activation present in the striatum, thalamus, hippocampus, and cingulate cortex (Leppä et al., 2006; Liu et al., 2007). Amphetamine as well induced correlated responses in the reward circuitry in both species (Völm et al., 2004; Schwarz et al., 2007). The default-mode network, initially observed in humans (Raichle et al., 2001) and nonhuman primates (Vincent et al., 2007), has likewise been measured using rs-fMRI techniques in the rat and mouse brain (Lu H. et al., 2012b; Stafford et al., 2014; Gozzi and Schwarz, 2016). Other networks, such as the striatal system, were detected in the rodent brain as well (Becerra et al., 2011; Jonckers et al., 2011; Bajic et al., 2017; Grandjean et al., 2017).

As mentioned previously, fMRI covers multiple paradigms, each of which may differ in implementation details and performance characteristics. Recommendations and good practices for fMRI studies were summarized by different groups (Schwarz et al.,

2011a; Schwarz et al., 2011b; Mandeville et al., 2014; Khalili-Mahani et al., 2017). Performing brain fMRI studies in small rodents poses additional challenges, related not only to data acquisition and analysis but also to anesthesia (Pan et al., 2015; Chuang and Nasrallah, 2017; Sumiyoshi et al., 2019; Huang et al., 2022). Although patterns of resting-state functional connectivity have been shown to be present in humans under anesthesia (Greicius et al., 2008) or during the early stages of sleep (Larson-Prior et al., 2009), great care needs to be taken when performing brain functional in anesthetized small rodents. Multiple anesthesia regimens were tested (see, e.g., Bukhari et al., 2017; Wu et al., 2017). The use of low doses of isoflurane or medetomidine has been reported in small rodent fMRI studies. By combining both agents vasodilatory effects of isoflurane, resulting in a dose-dependent increase of cerebral blood flow that influences neurovascular interactions detected by fMRI, may thus be counteracted by medetomidine, which is known to dose-dependently cause vasoconstriction (Nakai et al., 1986). For fMRI studies in mice, intubation, artificial ventilation and even paralysis with pancuronium bromide has been sometimes adopted (Bukhari et al., 2017; Wu et al., 2017; Pagani et al., 2021). Of note, mechanical ventilation may sometimes inadvertently cause lung injury (Walder et al., 2005; Nickles et al., 2014), especially if applied repeatedly. Awake animal imaging is also an alternative, as demonstrated by the robust and reproducible detection of brain networks in conscious rats and mice (Becerra et al., 2011; Liang et al., 2011; Liu et al., 2020; Fadel et al., 2022; Gutierrez-Barragan et al., 2022), but has its own constraints related to motion, stress and habituation.

Given the complexity of brain fMRI studies, collaborative work of various groups aiming at standardizing acquisition/analysis protocols is promoting the dissemination and reuse of clinical data (Alfaro-Almagro et al., 2018; Esteban et al., 2019; Notter et al., 2022). In the preclinical area, acquisitions in animals have been reported using a multitude of protocols comprising differences in strains, anesthesia conditions, coil designs, magnetic fields and data analysis pipelines, to name a few distinctive features. In analogy to the clinics, collaboration between several labs around the globe were also reported recently for fMRI acquisitions in animals (Mandino et al., 2020; Grandjean et al., 2020; Grandjean et al., 2023). Dissemination and comparison of learnings/experience through such consortia might lead to optimized consensus protocols that could substantially facilitate future experimental work in this area.

Lung

A short overview of imaging techniques of interest for pharmacological research in pulmonary diseases has been provided elsewhere (van Echteld and Beckmann, 2011; Beckmann and Crémillieux, 2016). Here, we illustrate how MRI can be used to refine models of pulmonary fibrosis and cancer in small rodents.

Bleomycin-induced lung injury

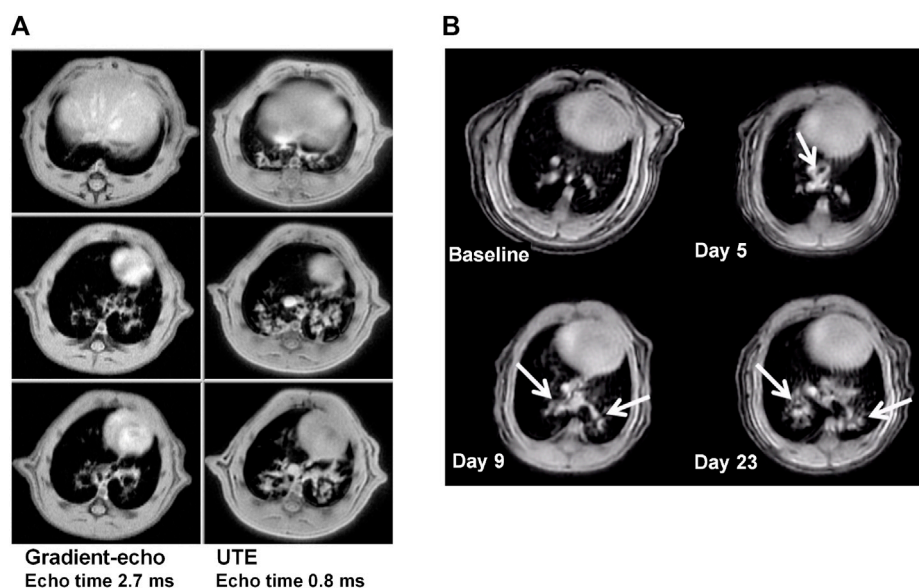
Pulmonary fibrosis is characterized by the accumulation of inflammatory cells, excessive fibroblast proliferation, increase in collagen content, and deposition of extracellular matrix in the

lungs (Strieter and Mehrad, 2009; King Jr et al., 2011). The local administration of bleomycin into the lungs is commonly used to model pulmonary fibrosis in small rodents, resulting in a phenotype that mimics in many respects the human disease (Jenkins et al., 2017). MRI provided the opportunity to non-invasively follow the course of bleomycin-induced lung injury in mice (Babin et al., 2012; Egger et al., 2013) and rats (Karmouty-Quintana et al., 2007; Jacob et al., 2010; Babin et al., 2011; Egger et al., 2013), with acquisitions performed in spontaneously breathing animals without respiratory gating. Micro-CT has also been adopted to detect fibrosis-related lesions in bleomycin models (Ask et al., 2008; De Langhe, et al., 2012). Considering that the lung tissue is particularly sensitive to cumulative doses of ionizing radiation (Plathow et al., 2004; Graves et al., 2010; Tang et al., 2020), it needs to be kept in the mind that radiotoxicity may play a role for repeated micro-CT scanning. The excellent agreement found between *in vivo* MRI, *in vivo* micro-CT and standard histological measures of lung fibrosis in mice (Velde et al., 2014) provides clear evidence in favor of MRI as imaging readout in the bleomycin model.

While gradient-echo MRI was initially employed for the quantification of bleomycin-induced injury (Karmouty-Quintana et al., 2007; Babin et al., 2011; Babin et al., 2012), introduction of ultrashort echo time (UTE) acquisitions improved the sensitivity for detecting lesions (Figure 5A). This increased sensitivity had the beneficial consequence of a reduction in measurement times by factors of 3–5, with two-dimensional UTE acquisitions declining respectively to 7.3 min and 4 min for rats and mice (Egger et al., 2013) (Figure 5B). Three-dimensional UTE with an echo time of 20 μ s enabled images of the lungs to be acquired at higher spatial resolution in 11.6 min and 6.9 min for rats and mice, respectively (Egger et al., 2014). Also, the bleomycin dose could be reduced, providing another experimental refinement.

Fibrotic process can lead to an impairment of lung function reflected in changes in tidal volume and breathing cycle times as shown for mice challenged with bleomycin (Milton et al., 2012). Also, increased lung elastance and reduced compliance occur in pulmonary fibrosis models (Ask et al., 2008; Manali et al., 2011). An increase of total lung volume, consistent with increased post-mortem dry and wet lung weights, hydroxyproline content as well as collagen level, was determined *in vivo* by MRI in bleomycin animals (Egger et al., 2014). Respiration-gated MRI demonstrated an increased lung volume at both inspiration and expiration, as well as a transient decrease of the tidal volume for bleomycin-treated rats. Terminal lung function analyses performed in tracheotomized and mechanically ventilated bleomycin rats using a flexyVent® system revealed decreased dynamic lung compliance (Egger et al., 2014). In summary, the increase of lung volume quantified by MRI after bleomycin administration was in agreement with tissue remodeling accounting for a reduced lung elasticity. Therapeutic treatment of bleomycin rats with the somatostatin analogue, SOM230, resulted in a decrease of lesion and total lung volume, the latter observation suggesting an improvement of lung function in the diseased animals (Egger et al., 2014).

From the standpoint of animal welfare, many factors contribute to a refinement of the fibrosis experiments introduced by MRI: measurements performed in spontaneously respiring animals; high sensitivity to detect

**FIGURE 5**

MRI at 4.7 T in the bleomycin model, for animals under spontaneous respiration. **(A)** Comparison between two-dimensional gradient-echo and UTE images acquired in 22 and 7.4 min, respectively, from one Sprague Dawley rat in the same imaging session at day 15 after bleomycin challenge (4 mg/kg intra-tracheal). The three slices for each acquisition method correspond to the same anatomical location. Note the increase in sensitivity for lesion detection by using ultrashort echo time technique. **(B)** Detection of bleomycin-induced lung injury by UTE-MRI in a BALB/c mouse. Comparable slices from two-dimensional UTE images (4 min acquisition time, echo time 0.5 ms) before and at different timepoints after oropharyngeal bleomycin administration (1.0 mg/kg/day on 6 consecutive days). Bleomycin-elicited lesions are indicated by the arrows. See Egger et al. (2013), Egger et al. (2014) for more details. © 2013 Egger et al. and © 2014. The American Physiological Society.

lesions using UTE enable fast acquisitions and/or a reduction of bleomycin dose; quantification of changes in total lung volume allow functional information reflecting reduced lung elasticity due to fibrosis development to be derived; MRI constitutes an imaging alternative free from ionizing radiation for assessing fibrosis in small rodent models. These features are of relevance in pharmacological studies, particularly when considering therapeutic effects of compounds administered when fibrosis is already established in the lungs. MRI has indeed been incorporated into several preclinical drug investigations and in the *in vivo* validation of pharmacological targets involving the bleomycin model (Babin et al., 2011; Babin et al., 2012; Egger et al., 2014; Egger et al., 2015a; Egger et al., 2017).

Lung tumor resistance

In recent years, the generation of animal models has been facilitated by CRISPR as well as developments around *in vivo* gene delivery technologies, including viral vectors, electroporation, and lipid nanoparticles (Ciampricotti et al., 2021; Lima and Maddalo, 2021). The combination of specific delivery methods optimized to the organ of interest with the CRISPR/Cas9 system has enabled consistent genome editing of somatic cells at the target organ (Maddalo et al., 2014). Complex genetically engineered mouse models could thus be generated relying on the versatility of CRISPR/Cas9 (Maddalo et al., 2014). Moreover, a substantial reduction in animal numbers were achieved because in the generation of these so-called somatically engineered mouse models, germline engineering and animal breeding steps are skipped.

This section exemplifies studies around tumor resistance in a CRISPR-induced mouse model of anaplastic lymphoma kinase (Alk) positive non-small cell lung cancer (NSCLC), for which adenoviral particles expressing the CRE recombinase and the CRISPR/Cas9 system were administered intra-tracheally. The study protocol is summarized in Figure 6A: 4 months after the infection, MRI was performed to quantify the tumors in the lungs. A first 3-week-cycle of treatment with an Alk inhibitor followed. MRI was performed again to verify the effect of the first cycle of treatment. The next 3 weeks were of treatment free, and at the end of this period MRI was again performed. This was repeated twice. MRI images for one representative mouse are shown in Figure 6B. The MRI baseline at 4 months after infection showed that the lung was full of lesions. Following treatment with the Alk inhibitor, these lesions were wiped off. However, the cancer lesions reappeared after the treatment was interrupted. A second cycle of treatment reduced the lesions, but this time, some of them persisted. Following treatment interruption, the lung was again full of lesions. A third round of Alk inhibitor treatment was definitely much less efficient compared to the previous ones, suggesting resistance of the lung cancer to treatment. This is summarized for a number of mice in Figure 6C.

In the present example, an estimated reduction of animal usage by 90% was achieved by using CRISPR, and this number increased to 98% by the incorporation of MRI in the experiment. Although micro-CT could also have been used as imaging modality, the effects of repeated exposure to ionising radiation in particular in tumor models needs to be taken into account. Recently, MRI and CT were shown to be equivalent to monitor lung cancer-bearing mice, but

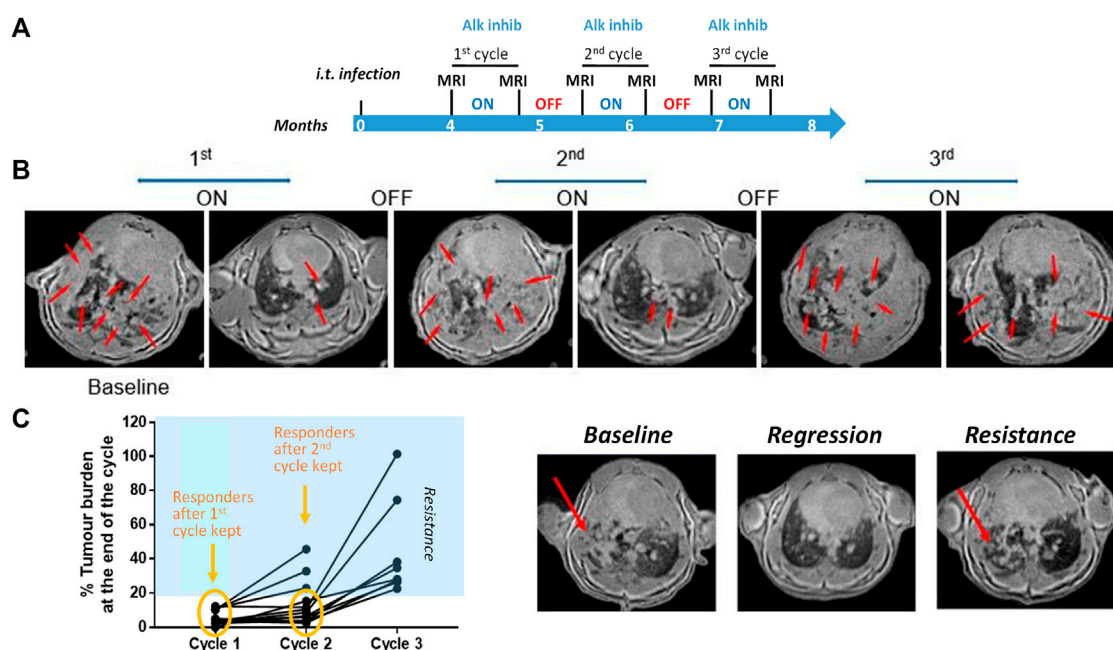


FIGURE 6

Imaging in a mouse lung tumor model. **(A)** Study protocol scheme. **(B)** MRI images from one representative mouse at different time points of the treatment phases. Tumor lesions are indicated by the red arrows. **(C)** Summary of tumor burden based on the quantification of lung lesions in the images. Images from one mouse acquired at baseline (left), at the end of the first (middle) and third cycle of treatment (right). See Egger et al. (2013) for details on image acquisition and lesion quantification. © 2013 Egger et al.

non-ionising MRI was considered particularly well suited for longitudinal studies (Spiro et al., 2020; Baier et al., 2020; Baier et al., 2023). Finally, chromosomal rearrangements of Alk are detected in 3%–7% of NSCLCs (Soda et al., 2007) and lung cancers displaying Alk rearrangements are highly sensitive to Alk tyrosine kinase inhibition. However, despite a high response rate of 60% in Alk-rearranged NSCLC, resistance to therapy based on Alk inhibition was shown to develop typically within one to 2 years (Friboulet et al., 2014; Mizuta et al., 2021). The model discussed here may be helpful when testing new therapies to overcome resistance.

Liver

Liver regeneration

The ability of the liver to regenerate itself upon loss of hepatic tissue has been known for a long time. However, reduced regenerative capacity exists under various circumstances, for instance in chronic liver disease, acute liver failure or liver resection encompassing tumor surgery. Methods that enhance the intrinsic regeneration potential of the liver are therefore required. Hepatic cell line-based *in vitro* systems Molecular mechanisms of liver cell growth can be studied in hepatic cell line-based *in vitro* systems. On the other hand, complex processes such as liver development or regeneration need to be studied *in vivo*. For this purpose, partial hepatectomy performed in small rodents, consisting of the surgical removal of three of the five liver lobes, is often adopted. Cells of the remaining two lobes proliferate and a complete recovery with the liver regaining its original size is achieved within

approximately 8 days after surgery (Mitchell and Willenbring, 2008).

Taking animal welfare into account, noninvasive imaging has a role to play when it comes to assess liver regeneration longitudinally. Two important parameters can be quantified by imaging, namely, the pre-surgery liver volume and the amount of actually excised tissue. For instance, Miyazaki et al. (2011) employed x-ray micro-CT to assess the regenerating direction and the shape of the regenerated remnant liver in hepatectomized rats (Miyazaki et al., 2011). Radiation dose may be a limiting factor in view of repeated scans within a relatively short time interval when CT-based liver volumetry is applied to small rodents. Such concerns obviously do not exist for MRI, which has also been demonstrated to allow precise liver volume determination before and following partial hepatectomy in mice (Garbow et al., 2004; Inderbitzin et al., 2004) or rats (Hockings et al., 2002) without or with application of contrast material. To reduce movement artifacts, respiration gating was used, and acquisition times ranged from 7 to 42 min.

MRI volumetry has also been established as a primary end point of liver regeneration in a murine model of partial hepatectomy with the scope of performing pharmacologic experiments (Orsini et al., 2016). Acquisitions of 14.5 min duration performed on anesthetized, spontaneously respiring animals, without gating and administration of contrast agent resulted in a highly significant correlation ($R = 0.98$, $p = 1.5 \times 10^{-14}$) between the MRI-derived liver volumes and the post-mortem liver weights in hepatectomized, untreated mice. 1,4-bis [2-(3, 5-dichloropyridyloxy)] benzene (TCPOBOP), a synthetic agonist of the mouse constitutive androstane receptor and a potent activator of cytochrome

P450 monooxygenase activity (Halwachs et al., 2007) shown earlier to induce hepatocyte proliferation and hepatomegaly (Ledda-Columbano et al., 2000), was then evaluated as test compound in the model. An enhanced liver regrowth capacity upon TCPOBOP treatment was revealed *in vivo* by MRI and confirmed by *post mortem* comparative hepatocyte proliferation assays (Ki67 expression) and liver weight analysis (Orsini et al., 2016). The feasibility of using imaging in pharmacologic studies in the context of liver regeneration has thus been demonstrated. In comparison to terminal procedures, the number of hepatectomized mice needed to derive a liver (re)growth curve was reduced by a factor of 6. Following this validation step, imaging was also included in studies demonstrating that the RSPO-LGR4/5-ZNRF3/RNF43 module controls metabolic liver zonation and constitutes a hepatic growth/size rheostat during development, homeostasis and regeneration (Planas-Paz et al., 2016).

In the clinic, liver volumetry is important in the context of liver resection and transplant surgery. Partial hepatectomy has become an important approach to address many primary and secondary hepatic tumors (Orcutt and Anaya, 2018; Riddiough et al., 2021). However, the percentage of functional liver parenchyma remaining after major hepatic resection is crucial to predict surgical success (Kishi et al., 2009). Imaging-based liver volumetry demonstrated that measurable changes in remnant liver volume begin approximately 5 days following surgery (Simpson et al., 2014). Also, imaging is important in the domain of living donor liver transplantation, both for the preoperative evaluation of the donor liver (Kim et al., 2018) and for the assessment of remnant liver regeneration in the follow-up of donors (Klink et al., 2014). Deep learning applied to MRI data is gaining attention due to the precision achieved in segmental volume assessments (Mojtahed et al., 2022).

Nonalcoholic steatohepatitis (NASH)

Non-alcoholic fatty liver disease (NAFLD) is one of the most common liver disorders, in which hepatic steatosis occurs in the absence of secondary causes like medications, excessive alcohol consumption, or heritable conditions (Byrne and Targher, 2015; Friedman et al., 2018). Around 25% of the world population is estimated to have NAFLD, and 25% of NAFLD patients are thought to have nonalcoholic steatohepatitis (NASH) (Younossi et al., 2018), characterized by excessive liver fat accumulation, hepatic inflammation and fibrosis (Diehl and Day, 2017; Sheka et al., 2020). Often clinically silent, with time NASH can progress to cirrhosis, end-stage liver disease, and ultimately the need for an organ transplant.

Changes of dietary habits and exercise aiming to reduce weight constitute the basis of NASH treatment, and no specific therapies do exist. Early detection is a prerequisite to control the impact of the condition, the challenge being the frequently asymptomatic nature of NASH, as mentioned before. Patients presenting high body mass index ($>25 \text{ kg/m}^2$) and type 2 diabetes mellitus features comprising hyperglycemia and insulin resistance are recommended to test for fatty liver disease (Friedman et al., 2018). Although elevation of the liver enzymes alanine transaminase (ALT) and aspartate aminotransferase (AST) in the blood plasma generally provides a first line of evidence (Wong et al., 2018), analysis of a liver biopsy is the gold standard for assessing the presence and severity of NASH.

Since biopsies entail a small risk of complications such as bleeding and represent only a small fraction of the liver volume, often resulting in an underestimation of disease severity, imaging alternatives are of need. Indeed, MRI and ultrasound can be applied for the noninvasive assessment of fat and fibrosis in the liver (Ajmera and Loomba, 2021). For instance, MRI-derived proton density fat fraction (MRI-PDFF) provides an accurate measure of liver fat content and has been adopted in early-phase NASH trials (Caussy et al., 2018). Ultrasound relying on the assessment of parameters such as the attenuation, backscatter coefficient, and speed/wavelength of the ultrasonic wave can be used as well for the quantification of hepatic steatosis (Han et al., 2020). Elastography based on MRI or shear wave ultrasound provides liver stiffness measurements as a surrogate quantitative biomarker for fibrosis (Xiao et al., 2017; Ozturk et al., 2022).

Currently established animal models of NASH are broadly divided into three main categories: dietary-induced, diet-toxin-induced, and diet-genetically mutated models (Farrell et al., 2019; Peng et al., 2020). Dietary regimens comprise high fat diet, methionine deficient diet, choline deficient diet, methionine choline deficient diet, amylin NASH diet, or high fat diet containing cholesterol supplemented by high fructose and sucrose. Toxins such as streptozotocin, diethylnitrosamine or carbon tetrachloride (CCl_4) can be added to the diet to increase the severity of liver injury. Genetic models include leptin-receptor-deficient mice, apolipoprotein E knock out mice, 148 isoleucine to methionine protein variant (I148 M) of patatin-like phospholipase domain-containing protein 3 (PNPLA3) knock-in mice, or mice overexpressing urokinase plasminogen activator introduced into hepatocytes via adeno-associated virus.

Imaging techniques have also been applied to animal models (Figure 7). Mice exposed to a high fat/NASH diet had elevated serum AST and ALT levels accompanied by increased liver fat quantified by MRI (Gapp et al., 2019). Imaging demonstrated that the total liver fat progressively increased during the first 8 weeks of high fat/NASH feeding and subsequently plateaued. The MRI data were consistent with biochemical analyses of liver lipids, which were elevated at all measured time points in NASH mice, and with histology demonstrating the presence of microvesicular and macrovesicular steatosis (Gapp et al., 2019). The therapeutic efficacy of GS-0976, an acetyl-coenzyme A carboxylase inhibitor, and LJP305, a close analogue of the farnesoid X receptor agonist tropifexor, was then studied in the model. Following a high fat/NASH diet for 20 weeks, mice were treated with either GS-0976 or LJP305 while continuing to be fed the high fat/NASH diet. LJP305 and GS-0976 treatments reversed fatty liver by markedly decreasing liver fat content, as measured by MRI. However, a rebound in liver fat was observed during the last 4 weeks of treatment with GS-0976. Both drugs significantly resolved microvesicular steatosis, but macrovesicular steatosis was solely improved by LJP305 (Gapp et al., 2019). Of note, macrovesicular steatosis is primarily related to liver fat in NAFLD and microvesicular steatosis has been connected with more advanced fibrosis (Tandra et al., 2011).

Fibrosis grade was significantly related to shear-wave velocity in rats receiving CCl_4 (Sugimoto et al., 2018). Texture analysis of SWE images further improved the diagnostic accuracy for severe fibrosis (Gu et al., 2021). In a CCl_4 mouse model, magnetic resonance elastography and atomic force microscopy demonstrated a

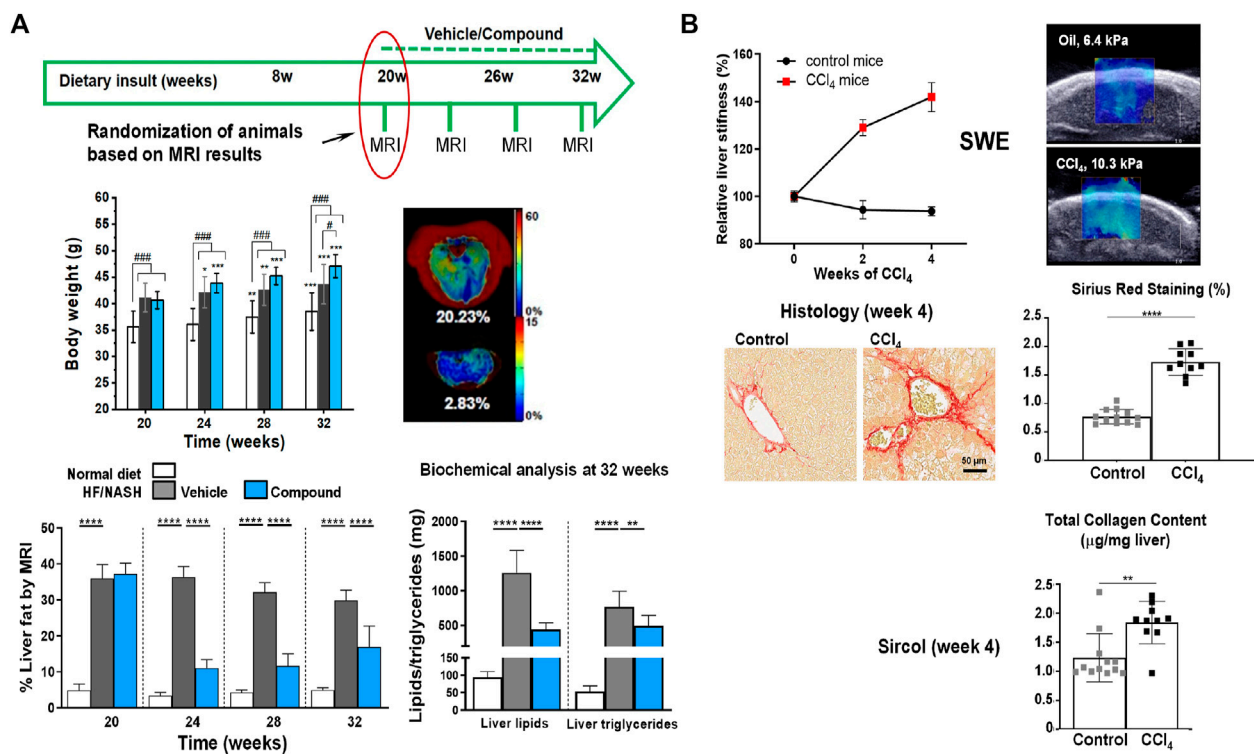


FIGURE 7

Imaging analysis of liver injury in mouse models. (A) Longitudinal non-invasive liver fat quantification by MRI. Livers of mice receiving a NASH diet for 20 weeks had an approximately 9x higher fat content than livers of control animals receiving a normal diet. Treatment with a compound (comp) led to significant reduction of liver fat as assessed by MRI, despite continuation of the NASH diet. Biochemical analyses at the end of the study confirmed reduced lipids and triglycerides in NASH animals treated with comp. Of note, despite reducing liver fat, comp had no impact on body weight, pointing to the importance of having a non-invasive readout for liver fat. (B) Liver stiffness assessed by shear wave elastography (SWE). Mice receiving CCl₄ (0.75 μL/g intraperitoneal injection 3x per week) developed significantly higher liver stiffness compared to control animals, which was consistent with biochemical and histological analyses demonstrating higher collagen content and picrosirius red (PSR) staining in the livers of CCl₄-challenged animals. See Gapp et al. (2019) for more details. © 2019 The Authors.

heterogeneous distribution of liver stiffness at macroscopic and microscopic levels, respectively, with high stiffness being attributed to areas of dense extracellular matrix (Kostallari et al., 2022). In another study, ultrasound measurements of echogenicity and stiffness in the liver were strongly correlated with macrovesicular steatosis and fibrosis, respectively, for mice submitted to a choline-deficient, L-amino acid-defined, high-fat diet to induce NASH features (Czernuszewicz et al., 2022). Also, SWE demonstrated the predisposition of mice with hepatic epithelial cell-specific deletion of leucine-rich repeat-containing G-protein-coupled receptors 4 and 5 (Lgr4/5dLKO) to liver fibrosis. These and additional data supported the concept that mice with decreased Wnt/β-catenin signaling on Lgr4/5dLKO deletion were susceptible to develop a NASH-like phenotype including fibrosis (Saponara et al., 2023).

From the 3R's perspective, there are multiple advantages of incorporating imaging into preclinical NASH studies: enhancement of the translational power of activities by applying the same imaging techniques preclinically in the animal models and clinically in patients; the non-invasive nature of imaging supports longitudinal studies by allowing repeated assessments in the same animal, thereby contributing to the reduction (>80%) of animal usage in the experiments; imaging strongly supports therapeutic

studies, by allowing randomization of animals before treatment begin.

Safety

Besides efficacy, *in vivo* toxicology may largely profit from imaging (Reid, 2006; Wang and Yan, 2008; Hockings and Powell, 2013; Hockings and Beckmann, 2022). Indeed, non-invasive small rodent imaging is in line with the concept and strategy of toxicity testing in the 21st century developed by the National Academy of Sciences in the United States (Krewski et al., 2010). A few examples on the use of imaging for assessment of safety, a fundamental aspect of pharmaceutical research, are discussed next.

Brain microbleeds in Alzheimer's disease

The deposition of amyloid-β (Aβ) as plaques in brain parenchyma and in vessels, this known as cerebral amyloid angiopathy (CAA), is an important pathological feature of Alzheimer's disease. Lowering amyloid has thus been a therapeutic strategy in the past decades. Unfortunately, microbleeds comprising spots of attenuated signal due to the presence of hemosiderin (ferric iron, Fe³⁺) deposits were detected

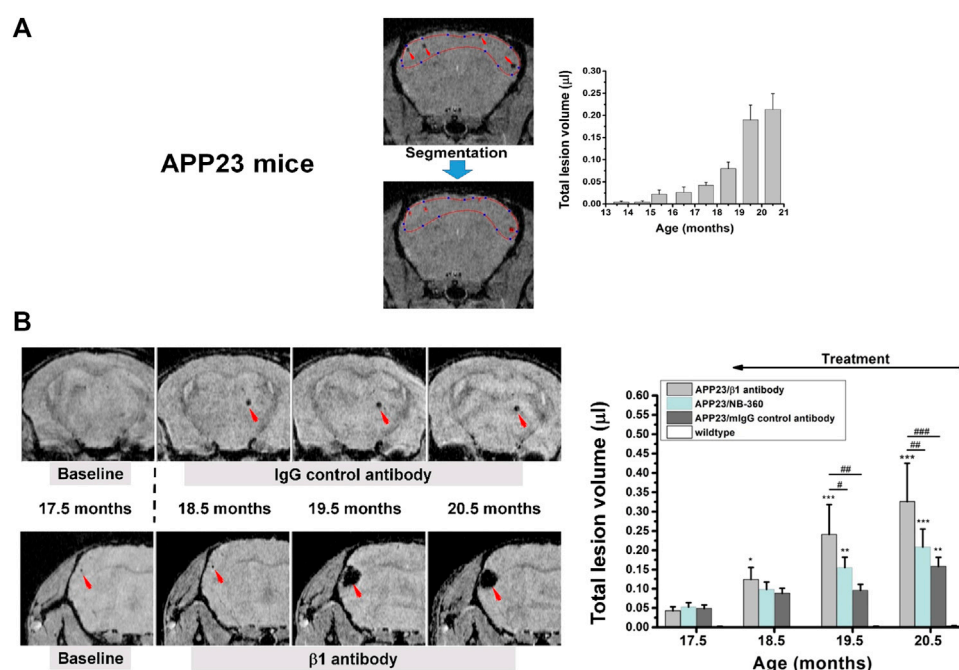


FIGURE 8

Microbleeds in the brain of APP23 mice modeling Alzheimer's disease. (A) Gradient-echo MRI was sensitive to detect microbleeds from an age of 15.5 months onward. Lesion volume was quantified by segmenting the regions displaying signal attenuation. (B) Longitudinal images from two APP23 mice at approximately the same anatomical location for each animal. Treatment started immediately after the acquisition of baseline images at 17.5 months of age. The lesion volume over the three-month-period of treatment is summarized on the right. More details can be found in Beckmann et al. (2016). © 2016 The Authors.

by MRI in the brain of Alzheimer's patients receiving bapineuzumab, a monoclonal antibody against Aβ (Sperling et al., 2012). It was hypothesized that such microbleeds could result from altered vascular permeability due to mobilization of parenchymal or vascular Aβ (Sperling et al., 2011). The term amyloid-related imaging abnormalities (ARIA) describes MRI findings including sulcal effusion and parenchymal edema (ARIA-E) as well as hemosiderin deposition (ARIA-H), the latter referring specifically to hypointense spots on gradient-echo images (Sperling et al., 2011). In view of safety, ARIA-H has become an integral part of animal (Beckmann et al., 2011; Marinescu et al., 2017; Neumann et al., 2018) and clinical studies (Sperling et al., 2012; Arrighi et al., 2016; Lowe et al., 2021) of compounds aiming to lower Aβ deposition in the brain. Assessment of cerebral microbleeds has even been introduced as biomarker for assessing therapy effect (Chiu et al., 2020).

In a back-translational effort, MRI was included in preclinical safety studies for the BACE-inhibitor NB-360 in APP23 mice (Beckmann et al., 2016), which in addition to parenchymal amyloid plaques also develop CAA (Winkler et al., 2001). Prior to the safety studies, the ability of gradient-echo MRI to quantify microbleeds in these mice was verified in a longitudinal characterization. Indeed, microbleeds started to develop at 15 months of age and increased significantly at later ages (Figure 8A). Based on this initial assessment, safety analyses were performed in a consecutive 3-month study on APP23 mice starting at 17.5 months of age. For the safety study, mice at age

17.5 months were examined at baseline by gradient-echo MRI, randomized in groups for microbleed volume, and then treatment followed for 3 months with a β1-antibody known to exacerbate microbleeds (Beckmann et al., 2011), a control antibody, and NB-360. The microbleed load in the brains of APP23 mice receiving the β1 antibody increased significantly, while APP23 mice receiving the control antibody or the BACE inhibitor displayed a microbleed development similar to that of untreated APP23 animals (Figure 8B). These data pointed to the safety of NB-360 in the model and supported the transition of the BACE-inhibitor to clinical studies (Neumann et al., 2018).

Kidney function in a renal safety assessment

Nucleos(t)ide analogues administered orally and primarily excreted through the kidney are commonly used for the treatment of hepatitis B and HIV (Fontana, 2009). Unfortunately, renal toxicity has been reported for some of such antiretroviral drugs (Izzedine et al., 2005; Fontana, 2009). The next example addresses a comparative renal safety assessment of four hepatitis B compounds in healthy rats: Adefovir, Tenofovir, Telbivudine, and Entecavir (Uteng et al., 2017). To this end, a functional assessment was performed with MRI: images from the kidney were sequentially acquired with a temporal resolution of 3 s/image. Following the acquisition of a number of baseline images, a contrast agent named Dotarem (Gd-DOTA) was injected intravenously during 1 s as a bolus. Dotarem, which is clinically approved, is cleared through the

kidney. After the bolus injection, contrast changes due to Dotarem occurred first in the cortex and then in the medulla. Such signal profiles were then be used to estimate the time of arrival (or time-to-peak, TTP) and the amount of Dotarem in each kidney compartment. Rats were treated during 28 days with a low dose (10x the human equivalent dose) or a high dose (ranging between 25x and 40x the human equivalent dose, depending on the compound). For Adefovir, the temporal profiles of the contrast agent for the renal cortex changed considerably during the course of the study—at day 28, a significantly increased TTP as well as Dotarem amount was detected in the cortex for the higher dose of Adefovir, suggesting an impaired kidney ability to clear the agent. In other words, a toxic effect of Adefovir. Pathology examination at the end of the study revealed morphological kidney alterations affecting mainly the proximal tubules, consistent with the functional deficits detected by MRI in the renal cortex. Neither functional alterations nor significant pathological changes were detected for the other three compounds (Uteng et al., 2017).

Interestingly, nephrotoxicity was reported for Adefovir in post-marketing studies (Izzedine et al., 2005; Fontana, 2009). Overall, in this functional study MRI led not only to a reduction of animals but had also the sensitivity to quantify functional alterations that remained undetectable by standard glomerular filtration rate assessments (Uteng et al., 2017). A similar approach has also been used to study adriamycin-induced nephropathy in rats (Egger et al., 2015b).

Vascular leakage in the lung

A balanced signaling at the level of S1P receptors on the endothelium contributes to the functioning of vascular barriers (Marsolais and Rosen, 2009). Tight junctions between cells are stabilized by tonic S1P1 signaling, which activates endothelial nitric oxide (NO) synthase resulting in NO production and activation of the soluble guanylate cyclase, thus contributing to maintain the patency of vessels (Wilkerson et al., 2012). On the other hand, a disruption of adherent junctions and an increase in paracellular permeability are associated to S1P2 and/or S1P3 signaling (McVerry and Garcia, 2005).

Using the potent and selective S1P1 antagonist, NIBR-0213, Bigaud et al. (2016) examined potential acute and long term impact of S1P1 competitive antagonism on vascular barriers. NIBR-0213 had previously demonstrated good oral efficacy and tolerability in a mouse model of autoimmune disease but also a leakage effect in the lung (Quancard et al., 2012). Rats were treated orally during 4 days with the compound and examined repeatedly by MRI at baseline and at different time points during the course of the treatment. At 6 h, fluid signals were detected in the lungs and the pleura (Bigaud et al., 2016). Fluid volumes were reduced by 30%–40% at 24 h and could no longer be detected after 72 h, despite continuation of NIBR-0213 treatment. In other words, longitudinal MRI demonstrated an acute and transient fluid leakage induced by NIBR-0213 in the rat lungs (Bigaud et al., 2016). From the 3R perspective, inclusion of imaging as readout enabled to generate the data with 5x less animals in comparison to terminal assessments based on, e.g., Evans blue dye leakage.

Final remarks

Besides significant reduction in animal numbers, the main asset of *in vivo* imaging within of preclinical pharmacological research lies in its ability to support translational research: applying the same technique in animal models and in the clinic enhances the confidence about the usefulness of a therapeutic agent. Moreover, back-translating learnings from the clinic contributes to refining the animal models and to enhancing the relevance of preclinical studies, since these can be guided by clinical requirements and questions as illustrated here through several examples discussed. Assessment of pharmacodynamic effects of compounds on established pathology with stratification of animals into groups based on imaging measures occurring just before treatment initiation becomes feasible.

There are important points to take into account when adopting anatomy-based imaging techniques like MRI and SWE in small rodent models: 1) The non-specific nature of the readouts. This means that, for every new application, a validation of the assessed parameters is necessary in order to verify their appropriateness and to make the link to histological or molecular analyses. In the context of pharmacology, the validation ideally comprises two steps, namely, the biological validation in which the ability of imaging to detect pathological changes is verified, followed by pharmacological validation involving testing a reference compound known to work in the model in order to analyze the sensitivity of the readout to map compound effects. Only after such extensive validation can imaging be utilized in routine pharmacological testing. In the absence of a reference compound, things become more complicated, on the other hand there is the opportunity to truly test a new therapy in an application for which earlier attempts failed; 2) the macroscopic character of the *in vivo* imaging techniques. Despite providing good spatial resolution in reasonable measurement times consistent with animal welfare, MRI and SWE are far from the microscopic world of histology, and comparisons between images obtained at different scales are in many cases challenging. SWE has in addition limited depth of penetration into the body; 3) absolute quantification of MRI parameters often comprises extensive calibration and comparison to measurements on phantoms. For instance, Na²³-MRI may provide a measure of sodium concentration in tissue, but a complex calibration of radiofrequency inhomogeneity with a procedure not well established beyond research is necessary (Lommen et al., 2016) and the limited sensitivity make it very demanding for use in small rodents. Arterial spin labeling (ASL) enabling the quantification of tissue perfusion without administration of a contrast agent is very useful for research and clinical studies, particularly in those involving multiple longitudinal measurements. However, ASL has been confronted with a number of challenges, including relatively low signal-to-noise ratio and temporal resolution, as well as a large number of sequence variants (Jezzard et al., 2018), hampering its uptake by clinical and preclinical practice. Despite the challenges with absolute quantification, in preclinical routine relative numbers, involving for instance comparisons between assessments performed pre- and post-compound dosing, are largely sufficient in the vast majority of applications.

By law experimenters involved in *in vivo* research are required to abide to rules that take full account of the 3Rs principles. Protocols regulating experimental procedures are constantly revised and reviewed by authorities. The examples discussed previously clearly illustrate that the main benefit of *in vivo* imaging for the 3Rs lies in reducing the animal numbers followed by the potential to refine experimental procedures. Despite the fact that the replacement of animals is a constant consideration throughout the design and conduct of research programs, it needs to be shown how imaging can contribute to it. Promising alternative methods comprise organoids (*in vitro* growing human cells that form a 3D structure, allowing to study their interactions), organs-on-a-chip (human 3D microfluidic cell culture integrated chips simulating, e.g., mechanical and physiological responses of an organ or organ system) or *in silico* models (computer models without living tissue of, e.g., physiological processes) (Zhou et al., 2021; Zietek et al., 2021; Kreutzer et al., 2022; Nolan et al., 2023). Confocal, super-resolution confocal, multiphoton or light-sheet microscopy can be used for high-resolution 3D examination of cleared organoids containing fluorescence reporters and after immunolabeling (Dekkers et al., 2019). However, the complexity of human physiology involving innumerable interactions between countless, often unknown and insufficiently understood molecules or cell types remains an obstacle for a widespread replacement of animal studies by such alternative techniques at the present stage. Nevertheless, the possibility to employ learnings and data obtained *in vivo* to optimize organs-on-a-chip or *in silico* models might be a small but constructive contribution of imaging to replacement. A dialogue between *in vitro* and *in vivo* researchers in view of 3Rs is thus very important.

The ultimate goal of pharmacological research is to test new therapies in humans. Animals allow not only to gain knowledge on basic mechanisms but ensure that tests in humans are as safe as possible. Preclinical research intends to reduce the experimentation in humans, by selecting the safest and potentially most efficacious compounds to enter clinical testing. Since imaging is also an integral part of clinical compound development, imaging biomarkers/readouts may be investigated in small rodents and validated through histology before adopting them in humans. Overall, it remains the responsibility of the investigators to conceive the experiments in a way that the 3Rs principles are respected in every biomedical activity involving the use of *in vivo* imaging—a reduction of unnecessary procedures in both animals and humans in the framework of pharmacological research and development needs always to be kept in mind.

Author contributions

MO and SZ performed *in vivo* imaging experiments, NA and CL performed histology, AD was responsible for image analyses. BL contributed with animal welfare expertise. NB, head of the imaging/histology group, was the main author and conceived the manuscript. All authors contributed to the article and approved the submitted version.

Funding

Some of the work reported here was funded through annual research budget from Novartis Pharma AG, Basel, Switzerland. However, the company had no role in study design, data collection and analysis, decision to publish, or preparation of the manuscript.

Acknowledgments

We are gratefully thankful to a large number of persons within and outside Novartis, mentors and colleagues, who over the years believed in the value of imaging for pharmacological research and therefore supported our efforts: Peter Allegrini, Michael Bidinosti, Marc Bigaud, Geoffrey Bodenhausen (Univ. of Lausanne), Christian Bruns, Catherine Cannet, Emilie Chapeau, Yannick Crémillieux (Univ. of Bordeaux), Henry Danahay, Janet Dawson, Ricardo Dolmetsch, Richard Ernst (ETH Zurich), Stephane Ferretti, John Fozard, Benjamin Freedman (Harvard Univ.), Christophe Freyre, Nelly Frossard (Univ. of Strasbourg), Fabrizio Gasparini, Nicole Gerwin, Elisa Giorgetti, Joanes Grandjean (Radboud Univ.), Hiroto Hatabu (Harvard Univ.), Shinji Hatakeyama, Paul Herrling, Robert Hof, Gabor Jarai, Elisabeth Jarman, Michaela Kneissel, Rainer Kneuer, Ina Kramer, Thomas Krucker (Scripps), Iwona Ksiazek, Didier Laurent, Jianping Li, Amanda Littlewood-Evans, Danilo Maddalo, Peter Maier (Univ. of Zurich), Rudolf Markstein, Lazzaro Mazzoni, Christina Merz-Stöckle, Anis Mir, Frédéric Morvan, Mark Nash, Ulf Neumann, Barbara Nüsslein, Clive Page (King's College London), Horácio Panepucci (Univ. of São Paulo), Alessandro Piaia, Peter Richards, Markus Rudin (ETH Zurich), Herbert Schmid, Joachim Seelig (Univ. of Basel), Valérie Salazar, Henk Schurman, Derya Shimshek, Paul Smith, Matthias Staufenbiel, Serge Summermatter, Thomas Suply, Jan Tchorz, Dietmar Thal (Univ. of Leuven), Bruno Tigani, Ulrike Trendelenburg, Alexandre Trifilieff, Marianne Uteng, Saurabh Vaishampayan (ETH Zurich), Eckhard Weber, Karl Welzenbach, Hans Widmer, Grazyna Wiecek.

Conflict of interest

The authors are employed by Novartis Pharma AG, Basel, Switzerland. All authors declare no other competing interests and that the research was conducted in the absence of any commercial or financial relationships that could be construed as a potential conflict of interest.

Publisher's note

All claims expressed in this article are solely those of the authors and do not necessarily represent those of their affiliated organizations, or those of the publisher, the editors and the reviewers. Any product that may be evaluated in this article, or claim that may be made by its manufacturer, is not guaranteed or endorsed by the publisher.

References

- Accart, N., Dawson, J., Obrecht, M., Lambert, C., Flueckiger, M., Kreider, J., et al. (2022). Degenerative joint disease induced by repeated intra-articular injections of monosodium urate crystals in rats as investigated by translational imaging. *Sci. Rep.* 12, 157. doi:10.1038/s41598-021-04125-7
- Ajmera, V., and Loomba, R. (2021). Imaging biomarkers of NAFLD, NASH, and fibrosis. *Mol. Metab.* 50, 101167. doi:10.1016/j.molmet.2021.101167
- Alfaro-Almagro, F., Jenkinson, M., Bangerter, N. K., Andersson, J. L. R., Griffanti, L., Douaud, G., et al. (2018). Image processing and Quality Control for the first 10,000 brain imaging datasets from UK Biobank. *Neuroimage* 166, 400–424. doi:10.1016/j.neuroimage.2017.10.034
- Arrighi, H. M., Barakos, J., Barkhof, F., Tampieri, D., Jack, C., Jr, Melançon, D., et al. (2016). Amyloid-related imaging abnormalities-haemosiderin (ARIA-H) in patients with Alzheimer's disease treated with bapineuzumab: A historical, prospective secondary analysis. *J. Neurol. Neurosurg. Psychiatry* 87, 106–112. doi:10.1136/jnnp-2014-309493
- Ask, K., Labiris, R., Farkas, L., Moeller, A., Froese, A., Farncombe, T., et al. (2008). Comparison between conventional and "clinical" assessment of experimental lung fibrosis. *J. Transl. Med.* 6, 16. doi:10.1186/1479-5876-6-16
- Babin, A. L., Cannet, C., Gérard, C., Saint-Mezard, P., Page, C. P., Sparrer, H., et al. (2012). Bleomycin-induced lung injury in mice investigated by MRI: Model assessment for target analysis. *Magn. Reson. Med.* 67, 499–509. doi:10.1002/mrm.23009
- Babin, A. L., Cannet, C., Gérard, C., Wyss, D., Page, C. P., and Beckmann, N. (2011). Noninvasive assessment of bleomycin-induced lung injury and the effects of short-term glucocorticosteroid treatment in rats using MRI. *J. Magn. Reson. Imaging* 33, 603–614. doi:10.1002/jmri.22476
- Baier, J., Rix, A., Darguzyte, M., Girbig, R. M., May, J. N., Palme, R., et al. (2023). Repeated contrast-enhanced micro-CT examinations decrease animal welfare and influence tumor physiology. *Invest. Radiol.* 58, 327–336. doi:10.1097/RLI.0000000000000936
- Baier, J., Rix, A., Drude, N. I., Darguzyte, M., Baues, M., May, J. N., et al. (2020). Influence of MRI examinations on animal welfare and study results. *Invest. Radiol.* 55, 507–514. doi:10.1097/RLI.0000000000000669
- Bajic, D., Craig, M. M., Mongerson, C. R. L., Borsook, D., and Becerra, L. (2017). Identifying rodent resting-state brain networks with independent component analysis. *Front. Neurosci.* 11, 685. doi:10.3389/fnins.2017.00685
- Baker, D., and Amor, S. (2014). Experimental autoimmune encephalomyelitis is a good model of multiple sclerosis if used wisely. *Mult. Scler. Relat. Disord.* 3, 555–564. doi:10.1016/j.msard.2014.05.002
- Barca, C., Wiesmann, M., Calahorra, J., Wachsmuth, L., Döring, C., Foray, C., et al. (2021). Impact of hydroxytyrosol on stroke: Tracking therapy response on neuroinflammation and cerebrovascular parameters using pet-mr imaging and on functional outcomes. *Theranostics* 11, 4030–4049. doi:10.7150/thno.48110
- Becerra, L., Pendse, G., Chang, P. C., Bishop, J., and Borsook, D. (2011). Robust reproducible resting state networks in the awake rodent brain. *PLoS One* 6, e25701. doi:10.1371/journal.pone.0025701
- N. Beckmann (Editor) (2006). *Vivo MR techniques in drug discovery and development* (New York: Taylor and Francis).
- Beckmann, N., and Crémillieux, Y. (2016). "Magnetic resonance imaging in animal models of respiratory diseases," in *MRI of the lung*. Editors H. U. Kauczor and M. O. Welpütz (Cham, Switzerland: Springer), 433–452. Medical Radiology. doi:10.1007/174_2016_85
- Beckmann, N., Doelemeyer, A., Zurbrugg, S., Bigot, K., Theil, D., Friauff, W., et al. (2016). Longitudinal noninvasive magnetic resonance imaging of brain microhemorrhages in BACE inhibitor-treated APP transgenic mice. *Neurobiol. Aging* 45, 50–60. doi:10.1016/j.neurobiolaging.2016.05.009
- Beckmann, N., and Garrido, L. (2013). *New applications of NMR in drug discovery and development*. Cambridge, UK: Royal Society of Chemistry.
- Beckmann, N., Gérard, C., Abramowski, D., Cannet, C., and Staufenbiel, M. (2011). Noninvasive magnetic resonance imaging detection of cerebral amyloid angiopathy-related microvascular alterations using superparamagnetic iron oxide particles in APP transgenic mouse models of Alzheimer's disease: Application to passive abeta immunotherapy. *J. Neurosci.* 31, 1023–1031. doi:10.1523/JNEUROSCI.4936-10.2011
- Beckmann, N., Giorgetti, E., Neuhaus, A., Zurbrugg, S., Accart, N., Smith, P., et al. (2018). Brain region-specific enhancement of remyelination and prevention of demyelination by the CSFIR kinase inhibitor BLZ945. *Acta Neuropathol. Commun.* 6, 9. doi:10.1186/s40478-018-0510-8
- Beckmann, N., Kneuer, R., Gremlich, H. U., Karmouty-Quintana, H., Blé, F. X., and Müller, M. (2007). *In vivo* mouse imaging and spectroscopy in drug discovery. *NMR Biomed.* 20, 154–185. doi:10.1002/nbm.1153
- Beckmann, N., Neuhaus, A., Zurbrugg, S., Volkmer, P., Patino, C., Joller, S., et al. (2023). Genetic models of cleavage-reduced and soluble TREM2 reveal distinct effects on myelination and microglia function in the cuprizone model. *J. Neuroinflammation* 20, 29. doi:10.1186/s12974-022-02671-z
- Belluzzi, E., Stocco, E., Pozzuoli, A., Granzotto, M., Porzionato, A., Vettor, R., et al. (2019). Contribution of infrapatellar fat pad and synovial membrane to knee osteoarthritis pain. *Biomed. Res. Int.* 2019, 6390182. doi:10.1155/2019/6390182
- Bifone, A., and Gozzi, A. (2012). Neuromapping techniques in drug discovery: Pharmacological MRI for the assessment of novel antipsychotics. *Expert Opin. Drug Discov.* 7, 1071–1082. doi:10.1517/17460441.2012.724057
- Bigaud, M., Dincer, Z., Bollbuck, B., Dawson, J., Beckmann, N., Beerli, C., et al. (2016). Pathophysiological consequences of a break in S1P1-dependent homeostasis of vascular permeability revealed by S1P1 competitive antagonism. *PLoS One* 11, e0168252. doi:10.1371/journal.pone.0168252
- Borgheresi, R., Barucci, A., Colantonio, S., Aghakhanyan, G., Assante, M., Bertelli, E., et al. (2022). Navigator: An Italian regional imaging biobank to promote precision medicine for oncologic patients. *Eur. Radiol. Exp.* 6, 53. doi:10.1186/s41747-022-00306-9
- Boyer, R. B., Kelm, N. D., Riley, D. C., Sexton, K. W., Pollins, A. C., Shack, R. B., et al. (2015). 4.7-T diffusion tensor imaging of acute traumatic peripheral nerve injury. *Neurosurg. Focus* 39, E9. doi:10.3171/2015.6.FOCUS1590
- Bridge, P. M., Ball, D. J., Mackinnon, S. E., Nakao, Y., Brandt, K., Hunter, D. A., et al. (1994). Nerve crush injuries - a model for axotomy. *Exp. Neurol.* 127, 284–290. doi:10.1006/exnr.1994.1104
- Browne, P., Chandraratna, D., Angood, C., Tremlett, H., Baker, C., Taylor, B. V., et al. (2014). Atlas of multiple sclerosis 2013: A growing global problem with widespread inequity. *Neurology* 83, 1022–1024. doi:10.1212/WNL.0000000000000768
- Bukhari, Q., Schroeter, A., Cole, D. M., and Rudin, M. (2017). Resting state fMRI in mice reveals anesthesia specific signatures of brain functional networks and their interactions. *Front. Neural Circuits* 11, 5. doi:10.3389/fncir.2017.00005
- Byrne, C. D., and Targher, G. (2015). Nafld: A multisystem disease. *J. Hepatol.* 62 (1), S47–S64. doi:10.1016/j.jhep.2014.12.012
- Carmichael, O., Schwarz, A. J., Chatham, C. H., Scott, D., Turner, J. A., Upadhyay, J., et al. (2018). The role of fMRI in drug development. *Drug Discov. Today* 23, 333–348. doi:10.1016/j.drudis.2017.11.012
- Caussy, C., Reeder, S. B., Sirlin, C. B., and Loomba, R. (2018). Noninvasive, quantitative assessment of liver fat by MRI-PDFF as an endpoint in NASH trials. *Hepatology* 68, 763–772. doi:10.1002/hep.29797
- Chakraborty, N., Meyerhoff, J., Jett, M., and Hammamieh, R. (2017). Genome to phenotype: A systems biology approach to ptsd using an animal model. *Methods Mol. Biol.* 1598, 117–154. doi:10.1007/978-1-4939-6952-4_6
- Cheah, P. L., Krisnan, T., Wong, J. H. D., Rozalli, F. I., Fadzli, F., Rahmat, K., et al. (2021). Microstructural integrity of peripheral nerves in charcot-marie-tooth disease: An MRI evaluation study. *J. Magn. Reson. Imaging* 53, 437–444. doi:10.1002/jmri.27354
- Chen, J. T., Easley, K., Schneider, C., Nakamura, K., Kidd, G. J., Chang, A., et al. (2013). Clinically feasible MTR is sensitive to cortical demyelination in MS. *Neurology* 80, 246–252. doi:10.1212/WNL.0b013e31827deb99
- Chen, Y., Baraz, J., Xuan, S. Y., Yang, X., Castoro, R., Xuan, Y., et al. (2023). Multiparametric quantitative MRI of peripheral nerves in the leg: A reliability study. *J. Magn. Reson. Imaging*. in press. doi:10.1002/jmri.28778
- Chiu, W. T., Lee, T. Y., Chan, L., Wu, D., Huang, L. K., Chen, D. Y., et al. (2020). Deep cerebral microbleeds are associated with poor cholinesterase inhibitor treatment response in people with Alzheimer disease. *Clin. Neurol. Neurosurg.* 195, 105959. doi:10.1016/j.clineuro.2020.105959
- Chuang, K. H., and Nasrallah, F. A. (2017). Functional networks and network perturbations in rodents. *Neuroimage* 163, 419–436. doi:10.1016/j.neuroimage.2017.09.038
- Ciampricotti, M., Karakousi, T., Richards, A. L., Quintanal-Villalonga, A., Karatza, A., Caesar, R., et al. (2021). Rlf-mycl gene fusion drives tumorigenesis and metastasis in a mouse model of small cell lung cancer. *Cancer Discov.* 11, 3214–3229. doi:10.1158/2159-8290.CD-21-0441
- Colombo, I., Overchuk, M., Chen, J., Reilly, R. M., Zheng, G., and Lheureux, S. (2017). Molecular imaging in drug development: Update and challenges for radiolabeled antibodies and nanotechnology. *Methods* 130, 23–35. doi:10.1016/j.jymeth.2017.07.018
- Cunha, L., Horvath, I., Ferreira, S., Lemos, J., Costa, P., Vieira, D., et al. (2014). Preclinical imaging: An essential ally in modern biosciences. *Mol. Diagn. Ther.* 18, 153–173. doi:10.1007/s40291-013-0062-3
- Curtis, A. D., and Cheng, H. M. (2022). Primer and historical review on rapid cardiac CINE MRI. *J. Magn. Reson. Imaging* 55, 373–388. doi:10.1002/jmri.27436
- Czernuszewicz, T. J., Aji, A. M., Moore, C. J., Montgomery, S. A., Velasco, B., Torres, G., et al. (2022). Development of a robotic shear wave elastography system for noninvasive staging of liver disease in murine models. *Hepatol. Commun.* 6, 1827–1839. doi:10.1002/hep4.1912
- De Langhe, E., Vande Velde, G., Hostens, J., Himmelreich, U., Nemery, B., Luyten, F. P., et al. (2012). Quantification of lung fibrosis and emphysema in mice using automated micro-computed tomography. *PLoS ONE* 7, e43123. doi:10.1371/journal.pone.0043123

- de Senneville, B. D., Cardiet, C. R., Trotier, A. J., Ribot, E. J., Lafitte, L., Facq, L., et al. (2020). Optimizing 4D abdominal MRI: Image denoising using an iterative back-projection approach. *Phys. Med. Biol.* 65, 015003. doi:10.1088/1361-6560/ab563e
- Dekkers, J. F., Alieva, M., Wellens, L. M., Ariesse, H. C. R., Jamieson, P. R., Vonk, A. M., et al. (2019). High-resolution 3D imaging of fixed and cleared organoids. *Nat. Protoc.* 14 (6), 1756–1771. doi:10.1038/s41596-019-0160-8
- Delattre, B. M., Van De Ville, D., Brauersreuther, V., Pellieux, C., Hyacinthe, J. N., Lerch, R., et al. (2012). High time-resolved cardiac functional imaging using temporal regularization for small animal on a clinical 3T scanner. *IEEE Trans. Biomed. Eng.* 59, 929–935. doi:10.1109/TBME.2011.2174363
- Denoble, A. E., Huffman, K. M., Stabler, T. V., Kelly, S. J., Hershfield, M. S., McDaniel, G. E., et al. (2011). Uric acid is a danger signal of increasing risk for osteoarthritis through inflammasome activation. *Proc. Natl. Acad. Sci. U. S. A.* 108, 2088–2093. doi:10.1073/pnas.1012743108
- Deshmane, A., Gulani, V., Griswold, M. A., and Seiberlich, N. (2012). Parallel MR imaging. *J. Magn. Reson. Imaging* 36, 55–72. doi:10.1002/jmri.23639
- Diao, Y., Yin, T., Gruetter, R., and Jolescu, I. O. (2021). Piracy: An optimized pipeline for functional connectivity analysis in the rat brain. *Front. Neurosci.* 15, 602170. doi:10.3389/fnins.2021.602170
- Diehl, A. M., and Day, C. (2017). Cause, pathogenesis, and treatment of nonalcoholic steatohepatitis. *N. Engl. J. Med.* 377, 2063–2072. doi:10.1056/nejma1503519
- Dietrich, M., Hecker, C., Martin, E., Langui, D., Gliem, M., Stankoff, B., et al. (2022). Increased remyelination and progenitor microglia under sponimod therapy in mechanistic models. *Neurol. Neuroimmunol. Neuroinflamm* 9, e1161. doi:10.1212/NXI.0000000000001161
- Docheva, D., Müller, S. A., Majewski, M., and Evans, C. H. (2015). Biologics for tendon repair. *Adv. Drug Deliv. Rev.* 84, 222–239. doi:10.1016/j.addr.2014.11.015
- Dortch, R. D., Dethrage, L. M., Gore, J. C., Smith, S. A., and Li, J. (2014). Proximal nerve magnetization transfer MRI relates to disability in Charcot-Marie-Tooth diseases. *Neurology* 83, 1545–1553. doi:10.1212/WNL.0000000000000919
- Egger, C., Cannet, C., Gérard, C., Debon, C., Stohler, N., Dunbar, A., et al. (2015b). Adriamycin-induced nephropathy in rats: Functional and cellular effects characterized by MRI. *J. Magn. Reson. Imaging* 41, 829–840. doi:10.1002/jmri.24603
- Egger, C., Cannet, C., Gérard, C., Dunbar, A., Tigani, B., and Beckmann, N. (2015a). Hyaluronidase modulates bleomycin-induced lung injury detected non-invasively in small rodents by radial proton MRI. *J. Magn. Reson. Imaging* 41, 755–764. doi:10.1002/jmri.24612
- Egger, C., Cannet, C., Gérard, C., Jarman, E., Jarai, G., Feige, A., et al. (2013). Administration of bleomycin via the oropharyngeal aspiration route leads to sustained lung fibrosis in mice and rats as quantified by UTE-MRI and histology. *PLoS ONE* 8, e63432. doi:10.1371/journal.pone.0063432
- Egger, C., Cannet, C., Gérard, C., Suply, T., Ksiazek, I., Jarman, E., et al. (2017). Effects of the fibroblast activation protein inhibitor, PT100, in a murine model of pulmonary fibrosis. *Eur. J. Pharmacol.* 809, 64–72. doi:10.1016/j.ejphar.2017.05.022
- Egger, C., Gérard, C., Vidotto, N., Accart, N., Cannet, C., Dunbar, A., et al. (2014). Lung volume quantified by MRI reflects extracellular-matrix deposition and altered pulmonary function in bleomycin models of fibrosis: Effects of SOM230. *Am. J. Physiol. Lung Cell. Mol. Physiol.* 306, L1064–L1077. doi:10.1152/ajplung.00027.2014
- Esteban, O., Markiewicz, C. J., Blair, R. W., Moodie, C. A., Isik, A. I., Erramuzpe, A., et al. (2019). fMRIprep: a robust preprocessing pipeline for functional MRI. *Nat. Methods* 16, 111–116. doi:10.1038/s41592-018-0235-4
- Eymard, F., and Chevalier, X. (2016). Inflammation of the infrapatellar fat pad. *Jt. Bone Spine* 83, 389–393. doi:10.1016/j.jbspin.2016.02.016
- Fadel, L. C., Patel, I. V., Romero, J., Tan, I. C., Kesler, S. R., Rao, V., et al. (2022). A mouse holder for awake functional imaging in unanesthetized mice: Applications in 31P spectroscopy, manganese-enhanced magnetic resonance imaging studies, and resting-state functional magnetic resonance imaging. *Biosens. (Basel)* 12, 616. doi:10.3390/bios12080616
- Farrell, G., Schattenberg, J. M., Leclercq, I., Yeh, M. M., Goldin, R., Teoh, N., et al. (2019). Mouse models of nonalcoholic steatohepatitis: Toward optimization of their relevance to human nonalcoholic steatohepatitis. *Hepatology* 69, 2241–2257. doi:10.1002/hep.30333
- Fathi Kazerooni, A., Saxena, S., Toorens, E., Tu, D., Bashyam, V., Akbari, H., et al. (2022). Clinical measures, radiomics, and genomics offer synergistic value in AI-based prediction of overall survival in patients with glioblastoma. *Sci. Rep.* 12, 8784. doi:10.1038/s41598-022-12699-z
- Fernandes, E., Barbosa, Z., Clemente, G., Alves, F., and Abrunhosa, A. J. (2012). Positron emitting tracers in pre-clinical drug development. *Curr. Radiopharm.* 5 (2), 90–98. doi:10.2174/1874471011205020090
- Fontana, R. J. (2009). Side effects of long-term oral antiviral therapy for Hepatitis B. *Hepatology* 49 (5), S185–S195. doi:10.1002/hep.22885
- Freedman, B. R., Kuttler, A., Beckmann, N., Nam, S., Kent, D., Schuleit, M., et al. (2022). Enhanced tendon healing by a tough hydrogel with an adhesive side and high drug-loading capacity. *Nat. Biomed. Eng.* 6, 1167–1179. doi:10.1038/s41551-021-00810-0
- Friboulet, L., Li, N., Katayama, R., Lee, C. C., Gainor, J. F., Crystal, A. S., et al. (2014). The ALK inhibitor ceritinib overcomes crizotinib resistance in non-small cell lung cancer. *Cancer Discov.* 4, 662–673. doi:10.1158/2159-8290.CD-13-0846
- Friedman, S. L., Neuschwander-Tetri, B. A., Rinella, M., and Sanyal, A. J. (2018). Mechanisms of NAFLD development and therapeutic strategies. *Nat. Med.* 24, 908–922. doi:10.1038/s41591-018-0104-9
- Gao, Y., Goodnough, C. L., Erokwu, B. O., Farr, G. W., Darrah, R., Lu, L., et al. (2014). Arterial spin labeling-fast imaging with steady-state free precession (ASL-FISP): A rapid and quantitative perfusion technique for high-field MRI. *NMR Biomed.* 27, 996–1004. doi:10.1002/nbm.3143
- Gapp, B., Jourdain, M., Bringer, P., Kueng, B., Weber, D., Osmont, A., et al. (2019). Farnesoid X receptor agonism, acetyl-coenzyme A carboxylase inhibition, and back translation of clinically observed endpoints of *de novo* lipogenesis in a murine NASH model. *Hepatology* 4, 109–125. doi:10.1002/hep4.1443
- Garbow, J. R., Kataoka, M., and Flye, M. W. (2004). MRI measurement of liver regeneration in mice following partial hepatectomy. *Magn. Reson. Med.* 52, 177–180. doi:10.1002/mrm.20107
- Giorgetti, E., Obrecht, M., Ronco, M., Panesar, M., Lambert, C., Accart, N., et al. (2019). Magnetic Resonance Imaging as a Biomarker in Rodent Peripheral Nerve Injury Models Reveals an Age-Related Impairment of Nerve Regeneration. *Sci. Rep.* 9, 13508. doi:10.1038/s41598-019-49850-2
- Golan, M., Mausner-Fainberg, K., Ibrahim, B., Benhamou, M., Wilf-Yarkoni, A., Kolb, H., et al. (2019). Fingolimod increases brain-derived neurotrophic factor level secretion from circulating T cells of patients with multiple sclerosis. *CNS Drugs* 33, 1229–1237. doi:10.1007/s40263-019-00675-7
- Goldberg, J., Clarner, T., Beyer, C., and Kipp, M. (2015). Anatomical distribution of cuprizone-induced lesions in C57BL6 mice. *J. Mol. Neurosci.* 57, 166–175. doi:10.1007/s12031-015-0595-5
- Gomes, C. M., Abrunhosa, A. J., Ramos, P., and Pauwels, E. K. (2011). Molecular imaging with SPECT as a tool for drug development. *Adv. Drug Deliv. Rev.* 63 (7), 547–554. doi:10.1016/j.addr.2010.09.015
- Gozzi, A., and Schwarz, A. J. (2016). Large-scale functional connectivity networks in the rodent brain. *Neuroimage* 127, 496–509. doi:10.1016/j.neuroimage.2015.12.017
- Grandjean, J., Canella, C., Anckaerts, C., Ayranci, G., Bougacha, S., Bienert, T., et al. (2020). Common functional networks in the mouse brain revealed by multi-centre resting-state fMRI analysis. *Neuroimage* 205, 116278. doi:10.1016/j.neuroimage.2019.116278
- Grandjean, J., Desrosiers-Gregoire, G., Anckaerts, C., Angeles-Valdez, D., Ayad, F., Barrière, D. A., et al. (2023). A consensus protocol for functional connectivity analysis in the rat brain. *Nat. Neurosci.* 26, 673–681. in press. doi:10.1038/s41593-023-01286-8
- Grandjean, J., Zerbi, V., Balsters, J. H., Wenderoth, N., and Rudin, M. (2017). Structural basis of large-scale functional connectivity in the mouse. *J. Neurosci.* 37, 8092–8101. doi:10.1523/JNEUROSCI.0438-17.2017
- Graves, P. R., Siddiqui, F., Anscher, M. S., and Movsas, B. (2010). Radiation pulmonary toxicity: From mechanisms to management. *Semin. Radiat. Oncol.* 20, 201–207. doi:10.1016/j.semdonc.2010.01.010
- Greenfield, A. L., and Hauser, S. L. (2018). B-Cell therapy for multiple sclerosis: Entering an era. *Ann. Neurol.* 83, 13–26. doi:10.1002/ana.25119
- Greicius, M. D., Kiviniemi, V., Tervonen, O., Vainionpää, V., Alahuhta, S., Reiss, A. L., et al. (2008). Persistent default-mode network connectivity during light sedation. *Hum. Brain Mapp.* 29, 839–847. doi:10.1002/hbm.20537
- Grimm, O., Gass, N., Weber-Fahr, W., Sartorius, A., Schenker, E., Spedding, M., et al. (2015). Acute ketamine challenge increases resting state prefrontal-hippocampal connectivity in both humans and rats. *Psychopharmacol. (Berl.)* 232, 4231–4241. doi:10.1007/s00213-015-4022-y
- Gu, L. H., Gu, G. X., Wan, P., Li, F. H., and Xia, Q. (2021). The utility of two-dimensional shear wave elastography and texture analysis for monitoring liver fibrosis in rat model. *Hepatobiliary Pancreat. Dis. Int.* 20, 46–52. doi:10.1016/j.hbpd.2020.05.008
- Gu, Q., Li, D., Wei, B., Guo, Y., Yan, J., Mao, F., et al. (2015). Effects of nicotine on a rat model of early stage osteoarthritis. *Int. J. Clin. Exp. Pathol.* 8, 3602–3612. PMC4466929.
- Guevara, C., Garrido, C., Martinez, M., Farias, G. A., Orellana, P., Soruco, W., et al. (2019). Prospective assessment of No evidence of disease activity-4 status in early disease stages of multiple sclerosis in routine clinical practice. *Front. Neurol.* 10, 788. doi:10.3389/fneur.2019.00788
- Gutierrez-Barragan, D., Singh, N. A., Alvino, F. G., Coletta, L., Rocchi, F., de Guzman, E., et al. (2022). Unique spatiotemporal fMRI dynamics in the awake mouse brain. *Curr. Biol.* 32, 631–644.e6. doi:10.1016/j.cub.2021.12.015
- Halwachs, S., Kneuer, C., and Honscha, W. (2007). Downregulation of the reduced folate carrier transport activity by phenobarbital-type cytochrome P450 inducers and protein kinase C activators. *Biochim. Biophys. Acta* 1768, 1671–1679. doi:10.1016/j.bbame.2007.03.023

- Han, A., Zhang, Y. N., Boehringer, A. S., Montes, V., Andre, M. P., Erdman, J. W., Jr, et al. (2020). Assessment of hepatic steatosis in nonalcoholic fatty liver disease by using quantitative US. *Radiology* 295, 106–113. doi:10.1148/radiol.2020191152
- Herman, S., Khoonsari, P. E., Tolf, A., Steinmetz, J., Zetterberg, H., Åkerfeldt, T., et al. (2018). Integration of magnetic resonance imaging and protein and metabolite CSF measurements to enable early diagnosis of secondary progressive multiple sclerosis. *Theranostics* 8, 4477–4490. doi:10.7150/thno.26249
- Hockings, P. D., and Beckmann, N. (2022). “Magnetic resonance imaging in pharmaceutical safety assessment,” in *Drug discovery and evaluation: Safety and pharmacokinetic assays*. Editors F. J. Hock, M. R. Gralinski, and M. K. Pugsley (Cham, Switzerland: Springer). doi:10.1007/978-3-030-73317-9
- Hockings, P. D., and Powell, H. (2013). “Vivo MRI/S for the safety evaluation of pharmaceuticals,” in *New applications of NMR in drug discovery and development*. Editors L. Garrido and N. Beckmann (Cambridge, UK: Royal Society of Chemistry Publishing). 361–375.
- Hockings, P. D., Roberts, T., Campbell, S. P., Reid, D. G., Greenhill, R. W., Polley, S. R., et al. (2002). Longitudinal magnetic resonance imaging quantitation of rat liver regeneration after partial hepatectomy. *Toxicol. Pathol.* 30, 606–610. doi:10.1080/01926230290105811
- Hoefling, H., Sing, T., Hossain, I., Boisclair, J., Doelemeyer, A., Flandre, T., et al. (2021). HistoNet: A deep learning-based model of normal histology. *Toxicol. Pathol.* 49, 784–797. doi:10.1177/0192623321993425
- Huang, G. S., Lee, H. S., Chou, M. C., Shih, Y.-Y. I., Tsai, P. H., Lin, M. H., et al. (2010). Quantitative MR T2 measurement of articular cartilage to assess the treatment effect of intra-articular hyaluronic acid injection on experimental osteoarthritis induced by ACLX. *Osteoarthritis. Cartil.* 18, 54–60. doi:10.1016/j.joca.2009.08.014
- Huang, G. S., Peng, Y. J., Hwang, D. W., Lee, H. S., Chang, Y. C., Chiang, S. W., et al. (2021). Assessment of the efficacy of intra-articular platelet rich plasma treatment in an ACLT experimental model by dynamic contrast enhancement MRI of knee subchondral bone marrow and MRI T2* measurement of articular cartilage. *Osteoarthritis. Cartil.* 29, 718–727. doi:10.1016/j.joca.2021.02.001
- Huang, J., Zhang, Y., Zhang, Q., Wei, L., Zhang, X., Jin, C., et al. (2022). The current status and trend of the functional magnetic resonance combined with stimulation in animals. *Front. Neurosci.* 16, 963175. doi:10.3389/fnins.2022.963175
- Hunter, D. J., Schofield, D., and Callander, E. (2014). The individual and socioeconomic impact of osteoarthritis. *Nat. Rev. Rheumatol.* 10, 437–441. doi:10.1038/nrrheum.2014.44
- Inderbitzin, D., Gass, M., Beldi, G., Ayouni, E., Nordin, A., Sidler, D., et al. (2004). Magnetic resonance imaging provides accurate and precise volume determination of the regenerating mouse liver. *J. Gastrointest. Surg.* 8, 806–811. doi:10.1016/j.gassur.2004.07.013
- Izzedine, H., Launay-Vacher, V., and Deray, G. (2005). Antiviral drug-induced nephrotoxicity. *Am. J. Kidney Dis.* 45, 804–817. doi:10.1053/j.ajkd.2005.02.010
- Jacob, R. E., Amidan, B. G., Soelberg, J., and Minard, K. R. (2010). *In vivo* MRI of altered proton signal intensity and T2 relaxation in a bleomycin model of pulmonary inflammation and fibrosis. *J. Magn. Reson. Imaging* 31, 1091–1099. doi:10.1002/jmri.22166
- Janacova, V., Szomolanyi, P., Kirner, A., Trattig, S., and Juras, V. (2022). Adjacent cartilage tissue structure after successful transplantation: A quantitative MRI study using T2 mapping and texture analysis. *Eur. Radiol.* 32, 8364–8375. doi:10.1007/s00330-022-08897-y
- Jang, B. S. (2013). MicroSPECT and MicroPET imaging of small animals for drug development. *Toxicol. Res.* 29 (1), 1–6. doi:10.5487/TR.2013.29.1.001
- Jarraya, M., Roemer, F., Kwok, C. K., and Guermazi, A. (2022). Crystal arthropathies and osteoarthritis-where is the link? *Skelet. Radiol.* in press. doi:10.1007/s00256-022-04246-8
- Jay, T. R., von Saucken, V. E., and Landreth, G. E. (2017). TREM2 in neurodegenerative diseases. *Mol. Neurodegener.* 12, 56. doi:10.1186/s13024-017-0197-5
- Jenkins, B. G. (2012). Pharmacologic magnetic resonance imaging (phMRI): Imaging drug action in the brain. *Neuroimage* 62, 1072–1085. doi:10.1016/j.neuroimage.2012.03.075
- Jenkins, R. G., Moore, B. B., Chambers, R. C., Eickelberg, O., Königshoff, M., Kolb, M., et al. (2017). An official American thoracic society workshop report: Use of animal models for the preclinical assessment of potential therapies for pulmonary fibrosis. *Am. J. Respir. Cell. Mol. Biol.* 56, 667–679. doi:10.1165/rcmb.2017-0096ST
- Jeppard, P., Chappell, M. A., and Okell, T. W. (2018). Arterial spin labeling for the measurement of cerebral perfusion and angiography. *J. Cereb. Blood Flow. Metab.* 38, 603–626. doi:10.1177/0271678X17743240
- Johnson, P. M., Recht, M. P., and Knoll, F. (2020). Improving the speed of MRI with artificial intelligence. *Semin. Musculoskelet. Radiol.* 24, 12–20. doi:10.1055/s-0039-3400265
- Jonckers, E., Shah, D., Hamaide, J., Verhoye, M., and Van der Linden, A. (2015). The power of using functional fMRI on small rodents to study brain pharmacology and disease. *Front. Pharmacol.* 6, 231. doi:10.3389/fphar.2015.00231
- Jonckers, E., van Audekerke, J., de Visscher, G., van der Linden, A., and Verhoye, M. (2011). Functional connectivity fMRI of the rodent brain: Comparison of functional connectivity networks in rat and mouse. *PLoS One* 6, e18876. doi:10.1371/journal.pone.0018876
- Joseph, G. B., Nevitt, M. C., McCulloch, C. E., Neumann, J., Lynch, J. A., Heilmeier, U., et al. (2018). Associations between molecular biomarkers and MR-based cartilage composition and knee joint morphology: Data from the osteoarthritis initiative. *Osteoarthritis. Cartil.* 26, 1070–1077. doi:10.1016/j.joca.2018.04.019
- Juras, V., Zbýň, S., Mlynarik, V., Szomolanyi, P., Hager, B., Baer, P., et al. (2016). The compositional difference between ankle and knee cartilage demonstrated by T2 mapping at 7 Tesla MR. *Eur. J. Radiol.* 85, 771–777. doi:10.1016/j.ejrad.2016.01.021
- Kappos, L., Bar-Or, A., Cree, B. A. C., Fox, R. J., Giovannoni, G., Gold, R., et al. (2018). Siponimod versus placebo in secondary progressive multiple sclerosis (EXPAND): A double-blind, randomised, phase 3 study. *Lancet* 391, 1263–1273. doi:10.1016/S0140-6736(18)30475-6
- Kappos, L., O'Connor, P., Radue, E. W., Polman, C., Hohlfeld, R., Selmaj, K., et al. (2015). Long-term effects of fingolimod in multiple sclerosis: The randomized FREEDOMS extension trial. *Neurology* 84, 1582–1591. doi:10.1212/WNL.0000000000001462
- Karmouty-Quintana, H., Cannet, C., Zurbrugg, S., Blé, F. X., Fozard, J. R., Page, C. P., et al. (2007). Bleomycin-induced lung injury assessed noninvasively and in spontaneously breathing rats by proton MRI. *J. Magn. Reson. Imaging* 26, 941–949. doi:10.1002/jmri.21100
- Khalili-Mahani, N., Rombouts, S. A., van Osch, M. J., Duff, E. P., Carbonell, F., Nickerson, L. D., et al. (2017). Biomarkers, designs, and interpretations of resting-state fMRI in translational pharmacological research: A review of state-of-the-Art, challenges, and opportunities for studying brain chemistry. *Hum. Brain Mapp.* 38, 2276–2325. doi:10.1002/hbm.23516
- Kim, B., Kim, S. Y., Kim, K. W., Jang, H. Y., Jang, J. K., Song, G. W., et al. (2018). MRI in donor candidates for living donor liver transplant: Technical and practical considerations. *J. Magn. Reson. Imaging* 48, 1453–1467. doi:10.1002/jmri.26257
- Kim, H. S., Yoon, Y. C., Choi, B. O., Jin, W., Cha, J. G., and Kim, J. H. (2019). Diffusion tensor imaging of the sciatic nerve in charcot-marie-tooth disease type I patients: A prospective case-control study. *Eur. Radiol.* 29, 3241–3252. doi:10.1007/s00330-018-5958-1
- Kim, J. H., Song, S. K., and Haldar, J. P. (2016). Signal-to-noise ratio-enhancing joint reconstruction for improved diffusion imaging of mouse spinal cord white matter injury. *Magn. Reson. Med.* 75, 852–858. doi:10.1002/mrm.25691
- King, T. E., Jr, Pardo, A., and Selman, M. (2011). Idiopathic pulmonary fibrosis. *Lancet* 378, 1949–1961. doi:10.1016/S0140-6736(11)60052-4
- Kishi, Y., Abdalla, E. K., Chun, Y. S., Zorzi, D., Madoff, D. C., Wallace, M. J., et al. (2009). Three hundred and one consecutive extended right hepatectomies: Evaluation of outcome based on systematic liver volumetry. *Ann. Surg.* 250, 540–548. doi:10.1097/SLA.0b013e3181b674df
- Klink, T., Simon, P., Knopp, C., Ittrich, H., Fischer, L., Adam, G., et al. (2014). Liver remnant regeneration in donors after living donor liver transplantation: Long-term follow-up using CT and MR imaging. *Rofo* 186, 598–605. doi:10.1055/s-0033-1355894
- Kollmer, J., Hegenbart, U., Kimmich, C., Hund, E., Purrucker, J. C., Hayes, J. M., et al. (2020). Magnetization transfer ratio quantifies polyneuropathy in hereditary transthyretin amyloidosis. *Ann. Clin. Transl. Neurol.* 7, 799–807. doi:10.1002/acn3.51049
- Kollmer, J., Kästel, T., Jende, J. M. E., Bendszus, M., and Heiland, S. (2018). Magnetization transfer ratio in peripheral nerve tissue: Does it depend on age or location? *Invest. Radiol.* 53, 397–402. doi:10.1097/RLI.0000000000000455
- Komura, D., and Ishikawa, S. (2018). Machine learning methods for histopathological image analysis. *Comput. Struct. Biotechnol. J.* 16, 34–42. doi:10.1016/j.csbj.2018.01.001
- Kostallari, E., Wei, B., Sicard, D., Li, J., Cooper, S. A., Gao, J., et al. (2022). Stiffness is associated with hepatic stellate cell heterogeneity during liver fibrosis. *Am. J. Physiol. Gastrointest. Liver Physiol.* 322, G234–G246. doi:10.1152/ajpgi.00254.2021
- Kreutzer, F. P., Meinecke, A., Schmidt, K., Fiedler, J., and Thum, T. (2022). Alternative strategies in cardiac preclinical research and new clinical trial formats. *Cardiovasc Res.* 118 (3), 746–762. doi:10.1093/cvr/cvab075
- Krewski, D., Acosta, D., Jr, Andersen, M., Anderson, H., Bailar, J. C., 3rd, Boekelheide, K., et al. (2010). Toxicity testing in the 21st century: A vision and a strategy. *J. Toxicol. Environ. Health B Crit. Rev.* 13, 51–138. doi:10.1080/10937404.2010.483176
- Kumar, P. A., Gunasundari, R., and Aarthi, R. (2021). Systematic analysis and review of magnetic resonance imaging (MRI) reconstruction techniques. *Curr. Med. Imaging* 17, 943–955. doi:10.2174/1573405616666210105125542
- Kuo, C. F., Grainge, M. J., Zhang, W., and Doherty, M. (2015). Global epidemiology of gout: Prevalence, incidence and risk factors. *Nat. Rev. Rheumatol.* 11, 649–662. doi:10.1038/nrrheum.2015.91
- Kuyinu, E. L., Narayanan, G., Nair, L. S., and Laurencin, C. T. (2016). Animal models of osteoarthritis: Classification, update, and measurement of outcomes. *J. Orthop. Surg. Res.* 11, 19. doi:10.1186/s13018-016-0346-5

- Larson-Prior, L. J., Zempel, J. M., Nolan, T. S., Prior, F. W., Snyder, A. Z., and Raichle, M. E. (2009). Cortical network functional connectivity in the descent to sleep. *Proc. Natl. Acad. Sci. U. S. A.* 106, 4489–4494. doi:10.1073/pnas.0900924106
- Lauber, D. T., Fülöp, A., Kovács, T., Szigeti, K., Máthé, D., and Szijártó, A. (2017). State of the art *in vivo* imaging techniques for laboratory animals. *Lab. Anim.* 51, 465–478. doi:10.1177/0023677217695852
- Laurent, D., Walsh, L., Muaremi, A., Beckmann, N., Weber, E., Chaperon, F., et al. (2020). Relationship between tendon structure, stiffness, gait patterns and patient reported outcomes during the early stages of recovery after an Achilles tendon rupture. *Sci. Rep.* 10, 20757. doi:10.1038/s41598-020-77691-x
- Ledda-Columbano, G. M., Pibiri, M., Loi, R., Perra, A., Shinozuka, H., and Columbano, A. (2000). Early increase in cyclin-D1 expression and accelerated entry of mouse hepatocytes into S phase after administration of the mitogen 1, 4-bis[2-(3,5-dichloropyridyloxy)] benzene. *Am. J. Pathol.* 156, 91–97. doi:10.1016/S0002-9440(10)64709-8
- Lee, H., Lee, J., Park, J. Y., and Lee, S. K. (2021). Line scan-based rapid magnetic resonance imaging of repetitive motion. *Sci. Rep.* 11 (1), 4505. doi:10.1038/s41598-021-83954-y
- Lehner, B., Koeck, F. X., Capellino, S., Schubert, T. E., Hofbauer, R., and Straub, R. H. (2008). Preponderance of sensory versus sympathetic nerve fibers and increased cellularity in the infrapatellar fat pad in anterior knee pain patients after primary arthroplasty. *J. Orthop. Res.* 26, 342–350. doi:10.1002/jor.20498
- Leppä, M., Korvenoja, A., Carlson, S., Timonen, P., Martinkauppi, S., Ahonen, J., et al. (2006). Acute opioid effects on human brain as revealed by functional magnetic resonance imaging. *Neuroimage* 31, 661–669. doi:10.1016/j.neuroimage.2005.12.019
- Leray, E., Yaouanq, J., Le Page, E., Coustans, M., Laplaud, D., Oger, J., et al. (2010). Evidence for a two-stage disability progression in multiple sclerosis. *Brain* 133, 1900–1913. doi:10.1093/brain/awq076
- Li, J., Celiz, A. D., Yang, J., Yang, Q., Wamala, I., Whyte, W., et al. (2017). Tough adhesives for diverse wet surfaces. *Science* 357, 378–381. doi:10.1126/science.aah6362
- Li, X., Li, S., Qian, J., Chen, Y., Zhou, Y., and Fu, P. (2021). Early efficacy of type I collagen-based matrix-assisted autologous chondrocyte transplantation for the treatment of articular cartilage lesions. *Front. Bioeng. Biotechnol.* 9, 760179. doi:10.3389/fbioe.2021.760179
- Liang, Z., King, J., and Zhang, N. (2011). Uncovering intrinsic connectional architecture of functional networks in awake rat brain. *J. Neurosci.* 31, 3776–3783. doi:10.1523/JNEUROSCI.4557-10.2011
- Lima, A., and Maddalo, D. (2021). SEMMs: Somatically engineered mouse models. A new tool for *in vivo* disease modeling for basic and translational research. *Front. Oncol.* 11, 667189. doi:10.3389/fonc.2021.667189
- Liu, C. H., Greve, D. N., Dai, G., Marota, J. J., and Mandeville, J. B. (2007). Remifentanyl administration reveals biphasic pHMRI temporal responses in rat consistent with dynamic receptor regulation. *Neuroimage* 34, 1042–1053. doi:10.1016/j.neuroimage.2006.10.028
- Liu, X., Feng, Y., Lu, Z. R., Morrell, G., and Jeong, E. K. (2010). Rapid simultaneous acquisition of T1 and T2 mapping images using multishot double spin-echo EPI and automated variations of TR and TE (ms-DSEPI-T12). *NMR Biomed.* 23, 97–104. doi:10.1002/nbm.1440
- Liu, Y., Perez, P. D., Ma, Z., Ma, Z., Dopfel, D., Cramer, S., et al. (2020). An open database of resting-state fMRI in awake rats. *Neuroimage* 220, 117094. doi:10.1016/j.neuroimage.2020.117094
- Loeser, R. F., Goldring, S. R., Scanzello, C. R., and Goldring, M. B. (2012). Osteoarthritis: A disease of the joint as an organ. *Arthritis Rheum.* 64, 1697–1707. doi:10.1002/art.34453
- Lommen, J., Konstandin, S., Krämer, P., and Schad, L. R. (2016). Enhancing the quantification of tissue sodium content by MRI: Time-efficient sodium B1 mapping at clinical field strengths. *NMR Biomed.* 29, 129–136. doi:10.1002/nbm.3292
- Lowe, S. L., Duggan-Evans, C., Shcherbinin, S., Cheng, Y.-J., Willis, B. A., Gueorgieva, I., et al. (2021). Donanemab (LY3002813) phase 1b study in Alzheimer's disease: Rapid and sustained reduction of brain amyloid measured by florbetapir F18 imaging. *J. Prev. Alzheimers Dis.* 8, 414–424. doi:10.14283/jpad.2021.56
- Lu, H., Zou, Q., Gu, H., Raichle, M. E., Stein, E. A., and Yang, Y. (2012b). Rat brains also have a default mode network. *Proc. Natl. Acad. Sci. U. S. A.* 109, 3979–3984. doi:10.1073/pnas.1200506109
- Lu, L., Erokku, B., Lee, G., Gulani, V., Griswold, M. A., Dell, K. M., et al. (2012a). Diffusion-prepared fast imaging with steady-state free precession (DP-FISP): A rapid diffusion MRI technique at 7 T. *Magn. Reson. Med.* 68 (3), 868–873. doi:10.1002/mrm.23287
- Lubetzki, C., Zalc, B., Williams, A., Stadelmann, C., and Stankoff, B. (2020). Remyelination in multiple sclerosis: From basic science to clinical translation. *Lancet Neurol.* 19, 678–688. doi:10.1016/S1474-4422(20)30140-X
- MacKenzie-Graham, A., Rinek, G. A., Avedisian, A., Gold, S. M., Frew, A. J., Aguilar, C., et al. (2012). Cortical atrophy in experimental autoimmune encephalomyelitis: *In vivo* imaging. *NeuroImage* 60, 95–104. doi:10.1016/j.neuroimage.2011.11.099
- Maddalo, D., Manchado, E., Concepcion, C. P., Bonetti, C., Vidigal, J. A., Han, Y. C., et al. (2014). *In vivo* engineering of oncogenic chromosomal rearrangements with the CRISPR/Cas9 system. *Nature* 516, 423–427. doi:10.1038/nature13902
- Manali, E. D., Moschos, C., Triantafyllidou, C., Kotanidou, A., Psallidas, I., Karabela, S. P., et al. (2011). Static and dynamic mechanics of the murine lung after intratracheal bleomycin. *BMC Pulm. Med.* 11, 33. doi:10.1186/1471-2466-11-33
- Mandeville, J. B., Liu, C. H., Vanduffel, W., Marota, J. J., and Jenkins, B. G. (2014). Data collection and analysis strategies for pHMRI. *Neuropharmacology* 84, 65–78. doi:10.1016/j.neuropharm.2014.02.018
- Mandino, F., Cerri, D. H., Garin, C. M., Straathof, M., van Tilborg, G. A. F., Chakravarty, M. M., et al. (2020). Animal functional magnetic resonance imaging: Trends and path toward standardization. *Front. Neuroinform.* 13, 78. doi:10.3389/fninf.2019.00078
- Marinescu, M., Sun, L., Fatar, M., Neubauer, A., Schad, L., van Ryn, J., et al. (2017). Cerebral microbleeds in murine amyloid angiopathy: Natural course and anticoagulant effects. *Stroke* 48, 2248–2254. doi:10.1161/STROKEAHA.117.017994
- Marsola, D., and Rosen, H. (2009). Chemical modulators of sphingosine 1-phosphate receptors as barrier oriented therapeutic molecules. *Nat. Rev. Drug Discov.* 8, 297–307. doi:10.1038/nrd2356
- Martel-Pelletier, J., Barr, A. J., Cicuttini, F. M., Conaghan, P. G., Cooper, C., Goldring, M. B., et al. (2016). Osteoarthritis. *Nat. Rev. Dis. Prim.* 2, 16072. doi:10.1038/nrdp.2016.72
- McVerry, B. J., and Garcia, J. G. (2005). *In vitro* and *in vivo* modulation of vascular barrier integrity by sphingosine 1-phosphate: Mechanistic insights. *Cell. Signal* 17, 131–139. doi:10.1016/j.cellsig.2004.08.006
- Milton, P. L., Dickinson, H., Jenkin, G., and Lim, R. (2012). Assessment of respiratory physiology of C57BL/6 mice following bleomycin administration using barometric plethysmography. *Respiration* 83, 253–266. doi:10.1159/000330586
- Mitchell, C., and Willenbring, H. (2008). A reproducible and well-tolerated method for 2/3 partial hepatectomy in mice. *Nat. Protoc.* 3, 1167–1170. doi:10.1038/nprot.2008.80
- Miyazaki, K., Eguchi, S., Tomonaga, T., Inokuma, T., Hamasaki, K., Yamanouchi, K., et al. (2011). The impact of the intraabdominal space on liver regeneration after a partial hepatectomy in rats. *J. Surg. Res.* 171, 259–265. doi:10.1016/j.jss.2010.01.012
- Mizuta, H., Okada, K., Araki, M., Adachi, J., Takemoto, A., Kutkowska, J., et al. (2021). Gilteritinib overcomes lorlatinib resistance in ALK-rearranged cancer. *Nat. Commun.* 12, 1261. doi:10.1038/s41467-021-21396-w
- Modrak, M., Hassan-Talukder, M. A., Gurgenshvil, K., Noble, M., and Elfar, J. C. (2020). Peripheral nerve injury and myelination: Potential therapeutic strategies. *J. Neurosci.* 38, 780–795. doi:10.1002/jnr.24538
- Mohan, G., Magnitsky, S., Melkus, G., Subburaj, K., Kazakia, G., Burghardt, A. J., et al. (2016). Kartogenin treatment prevented joint degeneration in a rodent model of osteoarthritis: A pilot study. *J. Orthop. Res.* 34, 1780–1789. doi:10.1002/jor.23197
- Mojtahed, A., Núñez, L., Connell, J., Fichera, A., Nicholls, R., Barone, A., et al. (2022). Repeatability and reproducibility of deep-learning-based liver volume and Couinaud segment volume measurement tool. *Abdom. Radiol. (NY)* 47, 143–151. doi:10.1007/s00261-021-03262-x
- Nakai, M., Yamamoto, J., and Matsui, Y. (1986). Acute systemic and regional hemodynamic effects of alpha 1-adrenoceptor blockade in conscious spontaneously hypertensive rats. *Clin. Exp. Hypertens.* A 8, 981–996. doi:10.3109/10641968609044081
- Neumann, U., Ufer, M., Jacobson, L. H., Rouzade-Dominguez, M. L., Huledal, G., Kolly, C., et al. (2018). The BACE-1 inhibitor CNP520 for prevention trials in Alzheimer's disease. *EMBO Mol. Med.* 10, e9316. doi:10.15252/emmm.201809316
- Nickles, H. T., Sumkauskaitė, M., Wang, X., Wegner, I., Puderbach, M., and Kuebler, W. M. (2014). Mechanical ventilation causes airway distension with proinflammatory sequelae in mice. *Am. J. Physiol. Lung Cell. Metab.* 307, L27–L37. doi:10.1152/ajplung.00288.2013
- Nolan, J., Pearce, O. M. T., Screen, H. R. C., Knight, M. M., and Verbruggen, S. W. (2023). Organ-on-a-Chip and microfluidic platforms for oncology in the UK. *Cancers (Basel)* 15 (3), 635. doi:10.3390/cancers15030635
- Notter, M. P., Herholz, P., da Costa, S., Gulban, O. F., Isik, A. I., Gaglianese, A., et al. (2022). fMRIflows: A consortium of fully automatic univariate and multivariate fMRI processing pipelines. *Brain Topogr.* 36, 172–191. in press. doi:10.1007/s10548-022-00935-8
- Orcutt, S. T., and Anaya, D. A. (2018). Liver resection and surgical strategies for management of primary liver cancer. *Cancer control.* 25, 1073274817744621. doi:10.1177/1073274817744621
- Orsini, V., Zurbuegg, S., Pikiólek, M., Tchorz, J. S., and Beckmann, N. (2016). MRI as primary end point for pharmacologic experiments of liver regeneration in a murine model of partial hepatectomy. *Acad. Radiol.* 23, 1446–1453. doi:10.1016/j.acra.2016.07.008
- Ozturk, A., Olson, M. C., Samir, A. E., and Venkatesh, S. K. (2022). Liver fibrosis assessment: MR and US elastography. *Abdom. Radiol. (NY)* 47, 3037–3050. doi:10.1007/s00261-021-03269-4

- Pagani, M., Barsotti, N., Bertero, A., Trakoshis, S., Ulysse, L., Locarno, A., et al. (2021). mTOR-related synaptic pathology causes autism spectrum disorder-associated functional hyperconnectivity. *Nat. Commun.* 12, 6084. doi:10.1038/s41467-021-26131-z
- Pal, A., and Rathi, Y. (2022). A review and experimental evaluation of deep learning methods for MRI reconstruction. *J. Mach. Learn. Biomed. Imaging* 1, 001. PMID: 35722657. doi:10.59275/j.melba.2022-3g12
- Pan, J., Pialat, J. B., Joseph, T., Kuo, D., Joseph, G. B., Nevitt, M. C., et al. (2011). Knee cartilage T2 characteristics and evolution in relation to morphologic abnormalities detected at 3-T MR imaging: A longitudinal study of the normal control cohort from the osteoarthritis initiative. *Radiology* 261, 507–515. doi:10.1148/radiol.11102234
- Pan, W. J., Billings, J. C., Grooms, J. K., Shakil, S., and Keilholz, S. D. (2015). Considerations for resting state functional MRI and functional connectivity studies in rodents. *Front. Neurosci.* 9, 269. doi:10.3389/fnins.2015.00269
- Peng, C., Stewart, A. G., Woodman, O. L., Ritchie, R. H., and Qin, C. X. (2020). Non-alcoholic steatohepatitis: A review of its mechanism, models and medical treatments. *Front. Pharmacol.* 11, 603926. doi:10.3389/fphar.2020.603926
- Planas-Paz, L., Orsini, V., Boulter, L., Calabrese, D., Pikiólek, M., Nigsch, F., et al. (2016). The RSPO-LGR4/5-ZNRF3/RNF43 module controls liver zonation and size. *Nat. Cell. Biol.* 18, 467–479. doi:10.1038/ncb3337
- Plathow, C., Li, M., Gong, P., Zieher, H., Kiessling, F., Peschke, P., et al. (2004). Computed tomography monitoring of radiation induced lung fibrosis in mice. *Invest. Radiol.* 39, 600–609. doi:10.1097/01.rli.0000138134.89050.a5
- Potočník, J., Foley, S., and Thomas, E. (2023). Current and potential applications of artificial intelligence in medical imaging practice: A narrative review. *J. Med. Imaging Radiat. Sci.* 54, 376–385. doi:10.1016/j.jmir.2023.03.033
- Preisner, F., Behnisch, R., Foesleitner, O., Schwarz, D., Wehrstein, M., Meredig, H., et al. (2021). Reliability and reproducibility of sciatic nerve magnetization transfer imaging and T2 relaxometry. *Eur. Radiol.* 31, 9120–9130. doi:10.1007/s00330-021-08072-9
- Quancard, J., Bollbuck, B., Janser, P., Angst, D., Berst, F., Buehlmaier, P., et al. (2012). A potent and selective S1P(1) antagonist with efficacy in experimental autoimmune encephalomyelitis. *Chem. Biol.* 19, 1142–1151. doi:10.1016/j.chembiol.2012.07.016
- Raichle, M. E., MacLeod, A. M., Snyder, A. Z., Powers, W. J., Gusnard, D. A. D. A., and Shulman, G. L. (2001). A default mode of brain function. *Proc. Natl. Acad. Sci. U. S. A.* 98, 676–682. doi:10.1073/pnas.98.2.676
- Razansky, D., Deliolanis, N. C., Vinegoni, C., and Ntziachristos, V. (2012). Deep tissue optical and optoacoustic molecular imaging technologies for pre-clinical research and drug discovery. *Curr. Pharm. Biotechnol.* 13 (4), 504–522. doi:10.2174/138920112799436258
- Regner-Nelke, L., Pawlitzki, M., Willison, A., Rolfes, L., Oezalp, S. H., Nelke, C., et al. (2022). Real-world evidence on siponimod treatment in patients with secondary progressive multiple sclerosis. *Neurol. Res. Pract.* 4, 55. doi:10.1186/s42466-022-00219-3
- Reid, D. (2006). “MRI in pharmaceutical safety assessment,” in *In vivo MR techniques in drug discovery and development*. editor N. Beckmann (New York: Taylor and Francis). 537–554.
- Riddiough, G. E., Jalal, Q., Perini, M. V., and Majeed, A. W. (2021). Liver regeneration and liver metastasis. *Semin. Cancer Biol.* 71, 86–97. doi:10.1016/j.semcancer.2020.05.012
- Ripoll, J., Ntziachristos, V., Cannet, C., Babin, A. L., Kneuer, R., Gremlich, H. U., et al. (2008). Investigating pharmacology *in vivo* using magnetic resonance and optical imaging. *Drugs R. D.* 9, 277–306. doi:10.2165/00126839-200809050-00001
- Roth, A. R., Li, J., and Dortch, R. D. (2022). Candidate imaging biomarkers for PMP22-related inherited neuropathies. *Ann. Clin. Transl. Neurol.* 9, 925–935. doi:10.1002/actn.3.51561
- Rudin, M., Briner, U., and Doepfner, W. (1988). Quantitative magnetic resonance imaging of estradiol-induced pituitary hyperplasia in rats. *Magn. Reson. Med.* 7, 285–291. doi:10.1002/mrm.1910070305
- Rudin, M., and Weissleder, R. (2003). Molecular imaging in drug discovery and development. *Nat. Rev. Drug Discov.* 2, 123–131. doi:10.1038/nrd1007
- Russell, W. M. S., and Burch, R. L. (1959). *The principles of humane experimental technique*. London: Methuen.
- Sadræe, A., Paulus, M., and Ekhtiari, H. (2021). fMRI as an outcome measure in clinical trials: A systematic review in clinicaltrials.gov. *Brain Behav.* 11, e02089. doi:10.1002/brb3.2089
- Saponara, E., Penno, C., Orsini, V., Wang, Z. Y., Fischer, A., Aebi, A., et al. (2023). Loss of hepatic leucine-rich repeat-containing G-protein-coupled receptors 4 and 5 promotes nonalcoholic fatty liver disease. *Am. J. Pathol.* 193, 161–181. doi:10.1016/j.ajpath.2022.10.008
- Saykin, A. J., Shen, L., Yao, X., Kim, S., Nho, K., Risacher, S. L., et al. (2015). Genetic studies of quantitative MCI and AD phenotypes in ADNI: Progress, opportunities, and plans. *Alzheimers Dement.* 11, 792–814. doi:10.1016/j.jalz.2015.05.009
- Schwarz, A. J., Becerra, L., Upadhyay, J., Anderson, J., Baumgartner, R., Coimbra, A., et al. (2011a). A procedural framework for good imaging practice in pharmacological fMRI studies applied to drug development #1: Processes and requirements. *Drug Discov. Today* 16, 583–593. doi:10.1016/j.drudis.2011.05.006
- Schwarz, A. J., Becerra, L., Upadhyay, J., Anderson, J., Baumgartner, R., Coimbra, A., et al. (2011b). A procedural framework for good imaging practice in pharmacological fMRI studies applied to drug development #2: Protocol optimization and best practices. *Drug Discov. Today* 16, 671–682. doi:10.1016/j.drudis.2011.03.011
- Schwarz, A. J., Gozzi, A., Reese, T., Heidbreder, C. A., and Bifone, A. (2007). Pharmacological modulation of functional connectivity: The correlation structure underlying the phMRI response to d-amphetamine modified by selective dopamine D3 receptor antagonist SB277011A. *Magn. Reson. Imaging* 25, 811–820. doi:10.1016/j.mri.2007.02.017
- Setsompop, K., Feinberg, D. A., and Polimeni, J. R. (2016). Rapid brain MRI acquisition techniques at ultra-high fields. *NMR Biomed.* 29, 1198–1221. doi:10.1002/nbm.3478
- Sharma, S. (2017). Translational multimodality neuroimaging. *Curr. Drug Targets* 18 (9), 1039–1050. doi:10.2174/1389450118666170315111542
- Sheka, A. C., Adeyi, O., Thompson, J., Hameed, B., Crawford, P. A., and Ikramuddin, S. (2020). Nonalcoholic steatohepatitis: A review. *JAMA* 323, 1175–1183. doi:10.1001/jama.2020.2298
- Simões, R. V., Henriques, R. N., Cardoso, B. M., Fernandes, F. F., Carvalho, T., and Shemesh, N. (2022). Glucose fluxes in glycolytic and oxidative pathways detected *in vivo* by deuterium magnetic resonance spectroscopy reflect proliferation in mouse glioblastoma. *Neuroimage Clin.* 33, 102932. doi:10.1016/j.nicl.2021.102932
- Simpson, A. L., Geller, D. A., Hemming, A. W., Jarnagin, W. R., Clements, L. W., D’Angelica, M. I., et al. (2014). Liver planning software accurately predicts postoperative liver volume and measures early regeneration. *J. Am. Coll. Surg.* 219, 199–207. doi:10.1016/j.jamcollsurg.2014.02.027
- Smith, P. A., Schmid, C., Zurbrugg, S., Jivkov, M., Doelemeyer, A., Theil, D., et al. (2018). Fingolimod inhibits brain atrophy and promotes brain-derived neurotrophic factor in an animal model of multiple sclerosis. *J. Neuroimmunol.* 318, 103–113. doi:10.1016/j.jneuroim.2018.02.016
- Soda, M., Choi, Y. L., Enomoto, M., Takada, S., Yamashita, Y., Ishikawa, S., et al. (2007). Identification of the transforming EML4-ALK fusion gene in non-small-cell lung cancer. *Nature* 448, 561–566. doi:10.1038/nature05945
- Soler, R., Orozco, L., Munar, A., Huguet, M., López, R., Vives, J., et al. (2016). Final results of a phase I-II trial using *ex vivo* expanded autologous Mesenchymal Stromal Cells for the treatment of osteoarthritis of the knee confirming safety and suggesting cartilage regeneration. *Knee* 23, 647–654. doi:10.1016/j.knee.2015.08.013
- Spencer Noakes, T. L., Henkelman, R. M., and Nieman, B. J. (2017). Partitioning k-space for cylindrical three-dimensional rapid acquisition with relaxation enhancement imaging in the mouse brain. *NMR Biomed.* 30 (11), e3802. doi:10.1002/nbm.3802
- Sperling, R. A., Jack, C. R., Jr, Black, S. E., Frosch, M. P., Greenberg, S. M., Hyman, B. T., et al. (2011). Amyloid-related imaging abnormalities in amyloid-modifying therapeutic trials: Recommendations from the Alzheimer’s association research roundtable workgroup. *Alzheimers Dement.* 7, 367–385. doi:10.1016/j.jalz.2011.05.2351
- Sperling, R. A., Salloway, S., Brooks, D. J., Tampieri, D., Barakos, J., Fox, N. C., et al. (2012). Amyloid-related imaging abnormalities in patients with Alzheimer’s disease treated with bapineuzumab: A retrospective analysis. *Lancet Neurol.* 11, 241–249. doi:10.1016/S1474-4422(12)70015-7
- Spiro, J. E., Rinneburger, M., Hedderich, D. M., Jokic, M., Reinhardt, H. C., Maintz, D., et al. (2020). Monitoring treatment effects in lung cancer-bearing mice: Clinical CT and clinical MRI compared to micro-CT. *Eur. Radiol. Exp.* 4, 31. doi:10.1186/s41747-020-00160-7
- Stafford, J. M., Jarrett, B. R., Miranda-Dominguez, O., Mills, B. D., Cain, N., Mihalas, S., et al. (2014). Large-scale topology and the default mode network in the mouse connectome. *Proc. Natl. Acad. Sci. U. S. A.* 111, 18745–18750. doi:10.1073/pnas.1404346111
- Starke, L., Tabelow, K., Niendorf, T., and Pohlmann, A. (2021). Denoising for improved parametric MRI of the kidney: Protocol for nonlocal means filtering. *Methods Mol. Biol.* 2216, 565–576. doi:10.1007/978-1-0716-0978-1_34
- Strieter, R. M., and Mehrad, B. (2009). New mechanisms of pulmonary fibrosis. *Chest* 136, 1364–1370. doi:10.1378/chest.09-0510
- Sugimoto, K., Moriyasu, F., Oshiro, H., Takeuchi, H., Yoshimasu, Y., Kasai, Y., et al. (2018). Viscoelasticity measurement in rat livers using shear-wave US elastography. *Ultrasound Med. Biol.* 44, 2018–2024. doi:10.1016/j.ultrasmedbio.2018.05.008
- Sumiyoshi, A., Keeley, R. J., and Lu, H. (2019). Physiological considerations of functional magnetic resonance imaging in animal models. *Biol. Psychiatry Cogn. Neurosci. Neuroimaging* 4, 522–532. doi:10.1016/j.bpsc.2018.08.002
- Sun, J. Y., Zhao, X., Illeperuma, W. R., Chaudhuri, O., Oh, K. H., Mooney, D. J., et al. (2012). Highly stretchable and tough hydrogels. *Nature* 489, 133–136. doi:10.1038/nature11409
- Taljanovic, M. S., Gimber, L. H., Becker, G. W., Latt, L. D., Klausner, A. S., Melville, D. M., et al. (2017). Shear-wave elastography: Basic physics and musculoskeletal applications. *Radiographics* 37, 855–870. doi:10.1148/rg.2017160116
- Tandra, S., Yeh, M. M., Brunt, E. M., Vuppalanchi, R., Cummings, O. W., Unalp-Arida, A., et al. (2011). Presence and significance of microvesicular steatosis in nonalcoholic fatty liver disease. *J. Hepatol.* 55, 654–659. doi:10.1016/j.jhep.2010.11.021

- Tang, B., Xi, Y., Cui, F., Gao, J., Chen, H., Yu, W., et al. (2020). Ionizing radiation induces epithelial-mesenchymal transition in human bronchial epithelial cells. *Biosci. Rep.* 40, BSR20200453. doi:10.1042/BSR20200453
- Thomas, D. L., Lythgoe, M. F., Gadian, D. G., and Ordidge, R. J. (2002). Rapid simultaneous mapping of T2 and T2* by multiple acquisition of spin and gradient echoes using interleaved echo planar imaging (MASAGE-IEPI). *Neuroimage* 15, 992–1002. doi:10.1006/nimg.2001.1042
- Thompson, A. J., Banwell, B. L., Barkhof, F., Carrol, W. M., Coetzee, T., Comi, G., et al. (2018). Diagnosis of multiple sclerosis: 2017 revisions of the McDonald criteria. *Lancet Neurol.* 17, 162–173. doi:10.1016/S1474-4422(17)30470-2
- Tigani, B., Cannel, C., Zurbrugg, S., Schaeublin, E., Mazzoni, L., Fozard, J. R., et al. (2003). Resolution of the oedema associated with allergic pulmonary inflammation in rats assessed noninvasively by magnetic resonance imaging. *Br. J. Pharmacol.* 140, 239–246. doi:10.1038/sj.bjp.0705429
- Torkildsen, O., Brunborg, L. A., Myhr, K. M., and Bø, L. (2008). The cuprizone model for demyelination. *Acta Neurol. Scand. Suppl.* 188, 72–76. doi:10.1111/j.1600-0404.2008.01036.x
- Tremoleda, J. L., Kerton, A., and Gsell, W. (2012). Anaesthesia and physiological monitoring during *in vivo* imaging of laboratory rodents: Considerations on experimental outcomes and animal welfare. *EJNMMI Res.* 2, 44. doi:10.1186/2191-219X-2-44
- Tremoleda, J. L., and Sosabowski, J. (2015). Imaging technologies and basic considerations for welfare of laboratory rodents. *Lab. Anim. (NY)* 44, 97–105. doi:10.1038/labani.665
- Tricot, B., Descoteaux, M., Dumont, M., Chagnon, F., Tremblay, L., Carpentier, A., et al. (2017). Improving the evaluation of cardiac function in rats at 7T with denoising filters: A comparison study. *BMC Med. Imaging* 17, 62. doi:10.1186/s12880-017-0236-2
- Uteng, M., Mahl, A., Beckmann, N., Piaia, A., Ledieu, D., Dubost, V., et al. (2017). Editor's highlight: Comparative renal safety assessment of the hepatitis B drugs, Adefovir, Tenofovir, telbivudine and Entecavir in rats. *Toxicol. Sci.* 155, 283–297. doi:10.1093/toxsci/kfw208
- van der Weijden, C. W., Vázquez-García, D., Borra, R. J. H., Thurner, P., Meilof, J. F., van Laar, P. J., et al. (2021). Myelin quantification with MRI: A systematic review of accuracy and reproducibility. *Neuroimage* 226, 117561. doi:10.1016/j.neuroimage.2020.117561
- van Echteld, C. J. A., and Beckmann, N. (2011). A view on imaging in drug research and development for respiratory diseases. *J. Pharmacol. Exp. Ther.* 337, 335–349. doi:10.1124/jpet.110.172635
- Velde, G. V., De Langhe, E., Poelmans, J., Dresselaers, T., Lories, R. J., and Himmelreich, U. (2014). Magnetic resonance imaging for noninvasive assessment of lung fibrosis onset and progression: Cross-validation and comparison of different magnetic resonance imaging protocols with micro-computed tomography and histology in the bleomycin-induced mouse model. *Invest. Radiol.* 49, 691–698. doi:10.1097/RLI.0000000000000071
- Vincent, J. L., Patel, G. H., Fox, M. D., Snyder, A. Z., Baker, J. T., van Essen, D. C., et al. (2007). Intrinsic functional architecture in the anesthetized monkey brain. *Nature* 447, 83–86. doi:10.1038/nature05758
- Völlm, B. A., de Araujo, I. E., Cowen, P. J., Rolls, E. T., Kringelbach, M. L., Smith, K. A., et al. (2004). Methamphetamine activates reward circuitry in drug naïve human subjects. *Neuropsychopharmacology* 29, 1715–1722. doi:10.1038/sj.npp.1300481
- Walder, B., Fontao, E., Totsch, M., and Morel, D. R. (2005). Time and tidal volume-dependent ventilator-induced lung injury in healthy rats. *Eur. J. Anaesthesiol.* 10, 785–794. doi:10.1017/s0265021505001304
- Wang, H., Zheng, R., Dai, F., Wang, Q., and Wang, C. (2019). High-field mr diffusion-weighted image denoising using a joint denoising convolutional neural network. *J. Magn. Reson. Imaging* 50, 1937–1947. doi:10.1002/jmri.26761
- Wang, S., Cao, G., Wang, Y., Liao, S., Wang, Q., Shi, J., et al. (2021). Review and prospect: Artificial intelligence in advanced medical imaging. *Front. Radiol.* 1, 781868. doi:10.3389/fradi.2021.781868
- Wang, Y. X., and Yan, S. X. (2008). Biomedical imaging in the safety evaluation of new drugs. *Lab. Anim.* 42, 433–441. doi:10.1258/la.2007.007022
- Wells, J. A., Thomas, D. L., King, M. D., Connelly, A., Lythgoe, M. F., and Calamante, F. (2010). Reduction of errors in ASL cerebral perfusion and arterial transit time maps using image de-noising. *Magn. Reson. Med.* 64, 715–724. doi:10.1002/mrm.22319
- Wilkinson, B. A., Grass, G. D., Wing, S. B., Argraves, W. S., and Argraves, K. M. (2012). Sphingosine-1-phosphate (S1P) carrier-dependent regulation of endothelial barrier: High density lipoprotein (HDL)-S1P prolongs endothelial barrier enhancement as compared with albumin-S1P via effects on levels, trafficking, and signaling of S1P1. *J. Biol. Chem.* 287, 44645–44653. doi:10.1074/jbc.M112.423426
- Winkler, D. T., Bondolfi, L., Herzig, M. C., Jann, L., Calhoun, M. E., Wiederhold, K. H., et al. (2001). Spontaneous hemorrhagic stroke in a mouse model of cerebral amyloid angiopathy. *J. Neurosci.* 21, 1619–1627. doi:10.1523/JNEUROSCI.21-05-01619.2001
- Wong, V. W., Adams, L. A., de Lédinghen, V., Wong, G. L., and Sookoian, S. (2018). Noninvasive biomarkers in NAFLD and NASH - current progress and future promise. *Nat. Rev. Gastroenterol. Hepatol.* 15, 461–478. doi:10.1038/s41575-018-0014-9
- Wu, T., Grandjean, J., Bosshard, S. C., Rudin, M., Reutens, D., and Jiang, T. (2017). Altered regional connectivity reflecting effects of different anaesthesia protocols in the mouse brain. *Neuroimage* 149, 190–199. doi:10.1016/j.neuroimage.2017.01.074
- Xiao, G., Zhu, S., Xiao, X., Yan, L., Yang, J., and Wu, G. (2017). Comparison of laboratory tests, ultrasound, or magnetic resonance elastography to detect fibrosis in patients with nonalcoholic fatty liver disease: A meta-analysis. *Hepatology* 66, 1486–1501. doi:10.1002/hep.29302
- Xu, X., Gao, J., Liu, S., Chen, L., Chen, M., Yu, X., et al. (2021). Magnetic resonance imaging for non-invasive clinical evaluation of normal and regenerated cartilage. *Regen. Biomater.* 8, rbab038. doi:10.1093/rb/rbab038
- Yan, J., Risacher, S. L., Shen, L., and Saykin, A. J. (2018). Network approaches to systems biology analysis of complex disease: Integrative methods for multi-omics data. *Brief. Bioinform.* 19, 1370–1381. doi:10.1093/bib/bbx066
- Yeh, F. L., Hansen, D. V., and Sheng, M. (2017). TREM2, microglia, and neurodegenerative diseases. *Trends Mol. Med.* 23, 512–533. doi:10.1016/j.molmed.2017.03.008
- Younossi, Z., Anstee, Q. M., Marietti, M., Hardy, T., Henry, L., Eslam, M., et al. (2018). Global burden of NAFLD and NASH: Trends, predictions, risk factors and prevention. *Nat. Rev. Gastroenterol. Hepatol.* 15, 11–20. doi:10.1038/nrgastro.2017.109
- Zhou, Z., Zhu, J., Jiang, M., Sang, L., Hao, K., and He, H. (2021). The combination of cell cultured technology and in silico model to inform the drug development. *Pharmaceutics* 13 (5), 704. doi:10.3390/pharmaceutics13050704
- Zhu, Y., Li, H., Guo, W., Drukker, K., Lan, L., Giger, M. L., et al. (2015). Deciphering genomic underpinnings of quantitative MRI-based radiomic phenotypes of invasive breast carcinoma. *Sci. Rep.* 5, 17787. doi:10.1038/srep17787
- Zietek, T., Boomgaarden, W. A. D., and Rath, E. (2021). Drug screening, oral bioavailability and regulatory aspects: A need for human organoids. *Pharmaceutics* 13 (8), 1280. doi:10.3390/pharmaceutics13081280
- Zivadinov, R., Medin, J., Khan, N., Korn, J. R., Bergsland, N., Dwyer, M. G., et al. (2018). Fingolimod's impact on MRI brain volume measures in multiple sclerosis: Results from MS-MRIUS. *J. Neuroimaging* 28, 399–405. doi:10.1111/jon.12518

Glossary

Aβ	Amyloid-β
Alk	Anaplastic lymphoma kinase
ALT	Alanine aminotransferase
ARIA	Amyloid-related imaging abnormalities
ASL	Arterial spin labeling
AST	Aspartate aminotransferase
BDNF	Brain derived neurotrophic factor
CAA	Cerebral amyloid angiopathy
CCl ₄	Carbon tetrachloride
CMT	Charcot-Marie-Tooth
COV	Coefficient of variation
CRISPR	Clustered regularly interspaced short palindromic repeats
CT	Computed tomography
DTI	Diffusion tensor imaging
EAE	Experimental autoimmune encephalomyelitis
ECM	Extracellular matrix
fMRI	Functional MRI
JTA	Janus Tough Adhesive
LPS	Lipopolysaccharide
MRI	Magnetic resonance imaging
MRI-PDFF	MRI-derived proton density fat fraction
MS	Multiple sclerosis
MSU	Monosodium urate
MTR	Magnetization transfer ratio
NO	Nitric oxide
NSCLC	Non-small cell lung cancer
OA	Osteoarthritis
OARSI	Osteoarthritis Research Society International
phMRI	Pharmacological MRI
PMP22	Peripheral myelin protein-22
rs-fMRI	Resting state functional MRI
S1P	Sphingosine-1-phosphate
SD	Standard deviation
SPECT	Single photon emission computed tomography
TCPOBOP	1, 4-bis [2-(3, 5-dichloropyridyloxy)] benzene
TREM2	Triggering receptor expressed on myeloid cells 2
TTP	Time-to-peak
US	United States
UTE	Ultrashort echo time



OPEN ACCESS

EDITED BY

Annemarie Lang,
University of Pennsylvania, United States

REVIEWED BY

Melody Li,
University of Melbourne, Australia
Thomas Marissal,
INSERM U901 Institut de Neurobiologie de la
Méditerranée, France

*CORRESPONDENCE

Gentzane Sanchez-Elexpuru
✉ gentzane.sanchez@zeclinics.com
Vincenzo Di Donato
✉ vincenzo.didonato@zeclinics.com

†These authors have contributed equally to this work and share last authorship

RECEIVED 04 May 2023

ACCEPTED 14 August 2023

PUBLISHED 31 August 2023

CITATION

Miguel Sanz C, Martinez Navarro M, Caballero Diaz D, Sanchez-Elexpuru G and Di Donato V (2023) Toward the use of novel alternative methods in epilepsy modeling and drug discovery.
Front. Neurol. 14:1213969.
doi: 10.3389/fneur.2023.1213969

COPYRIGHT

© 2023 Miguel Sanz, Martinez Navarro, Caballero Diaz, Sanchez-Elexpuru and Di Donato. This is an open-access article distributed under the terms of the [Creative Commons Attribution License \(CC BY\)](#). The use, distribution or reproduction in other forums is permitted, provided the original author(s) and the copyright owner(s) are credited and that the original publication in this journal is cited, in accordance with accepted academic practice. No use, distribution or reproduction is permitted which does not comply with these terms.

Toward the use of novel alternative methods in epilepsy modeling and drug discovery

Claudia Miguel Sanz, Miriam Martinez Navarro,
Daniel Caballero Diaz, Gentzane Sanchez-Elexpuru*† and
Vincenzo Di Donato*†

ZeClinics SL, IGTP (Germans Trias I Pujol Research Institute), Badalona, Spain

Epilepsy is a chronic brain disease and, considering the amount of people affected of all ages worldwide, one of the most common neurological disorders. Over 20 novel antiseizure medications (ASMs) have been released since 1993, yet despite substantial advancements in our understanding of the molecular mechanisms behind epileptogenesis, over one-third of patients continue to be resistant to available therapies. This is partially explained by the fact that the majority of existing medicines only address seizure suppression rather than underlying processes. Understanding the origin of this neurological illness requires conducting human neurological and genetic studies. However, the limitation of sample sizes, ethical concerns, and the requirement for appropriate controls (many patients have already had anti-epileptic medication exposure) in human clinical trials underscore the requirement for supplemental models. So far, mammalian models of epilepsy have helped to shed light on the underlying causes of the condition, but the high costs related to breeding of the animals, low throughput, and regulatory restrictions on their research limit their usefulness in drug screening. Here, we present an overview of the state of art in epilepsy modeling describing gold standard animal models used up to date and review the possible alternatives for this research field. Our focus will be mainly on *ex vivo*, *in vitro*, and *in vivo* larval zebrafish models contributing to the 3R in epilepsy modeling and drug screening. We provide a description of pharmacological and genetic methods currently available but also on the possibilities offered by the continued development in gene editing methodologies, especially CRISPR/Cas9-based, for high-throughput disease modeling and anti-epileptic drugs testing.

KEYWORDS

epilepsy, genetic models, Dravet syndrome, zebrafish, alternative methods, anti-epileptic drug screening, 3Rs

1. Introduction to causes of epilepsy and available treatments

Epilepsy, one of the most common neurological disorders, affects around 50 million people according to the World Health Organization (WHO). It is a severe neurological disorder characterized by recurrent seizures (1). A seizure is defined as “a transient occurrence of signs and/or symptoms due to abnormal excessive or synchronous neuronal activity in the brain” (2). In 2017, International League Against Epilepsy (ILAE) approved and published an updated

classification of seizure types (3, 4). This classification was generated for practical use in the clinical setting, but it can also be used by researchers with specific purposes. Depending on their onset, seizures can be classified into focal (originated in localized parts of the brain), general (originated from extensive regions in both hemispheres of the brain) and unknown. Focal seizures can be further classified based on the level of awareness, understood as the person's awareness of self and environment during the seizure. In addition, both focal and generalized seizures can be divided into motor (e.g., tonic or clonic) and non-motor (e.g., sensorial signs as absence) seizures, and subdivided into different categories described in detail by Devinsky et al. (5) and Fisher et al. (6).

Epilepsy is considered a spectrum disorder with highly diverse etiology, comprising structural, genetic, metabolic, autoimmune and infection-related causes. Structural causes (5, 7) refers to abnormal structural brain defects that are known to substantially increase the risk of seizures. These structural abnormalities can be congenital or acquired, like brain tumors, strokes or head trauma (8). The epileptic syndromes are defined by the ILAE as "a characteristic cluster of clinical and electroencephalographic (EEG) features, often supported by specific etiological findings." The correct diagnosis of an epileptic syndrome is crucial since it usually has important implications in the prognosis and treatment (9).

1.1. Genetic basis of epileptic syndromes

Genetic causes of epilepsy usually involve single-gene mutations affecting ion channels, synaptic support proteins, mTOR pathway regulators chromatin remodeling and transcription regulators (10). These types of epilepsies are very diverse and in most cases the underlying genes have not been identified yet (8). Some of the identified single gene mutations causing epilepsy are in the SCN1A (11), SCN8A and HCN1 genes for Dravet Syndrome (DS) (12), in the GABRA1 gene (A322D mutation) for Juvenile myoclonic epilepsy (13), in the LIS1 gene for Classical Lissencephaly (14), in the STXBP1, DNMT1, DEPDC5 and GRIN2B genes for Epileptic Encephalopathy (15), in the CHD2 (16) and GABRB3 (17) genes for Lennox–Gastaut syndrome and PCDH19 genes for PCDH19 female epilepsy (18). Over the last years, thanks to the constant improvements in sequencing technologies, a growing number of novel variants have been discovered by analyzing large cohorts of patients within the framework of several international collaborations. Among those, the Epi4k consortium, composed by more 60 researchers in USA, Australia and United Kingdom, aims to unravel, by sequencing and analyzing over 4,000 genomes, genetic causes of under studied forms of epilepsy (Infantile Spasms and Lennox–Gastaut Syndrome) and identify novel *de novo* or rare pathogenic variants (19, 20). A similar example of an inter-institutional effort is the Epi25 collaborative established in 2014 with the aim to perform exome sequencing of 25,000 epilepsy patients and correlate the data sequencing results with phenotypic data in order to reach a better patient stratification and genotype/phenotype spectrum correlation. The work of the collaborative led to a very recent publication releasing data from the largest analysis of copy number variants as risk factor for epilepsy performed to date, including discovery of novel variants and definition of phenotypic signatures for almost 20 clinical categories (21). On the same line, the International League Against Epilepsy (ILAE) Consortium on

Complex Epilepsies run a genome-wide analysis of nearly 45,000 people which led to the identification of 16 genetic loci associated with generalized epilepsy (11 of which newly identified) and, within these loci, 21 genes coding for ion-channel subunits (SCN1A, SCN2A, SCN3A, GABRA2, KCNN2, KCNAB1, and GRIK1), transcription factors (ZEB2, STAT4, and BCL11A), synaptic transmission regulators (STX1B), etc. (22).

Despite the aforementioned efforts to untangle the complexity of the genetics underlying epileptic phenotypic heterogeneity is high. Indeed, *de novo* or familial mutations in epilepsy-related genes are characterized by a variable expressivity, thus an extremely variable phenotyping spectrum ranging from generalized epilepsies to severe encephalopathies (23, 24). The causes for these very diverse phenotypic outcomes linked to gene modification are hotly debated in the genetics community. Among other causes, can be found the probable involvement of modifier loci, somatic mosaicism, repeated expansion and significant environmental variables. Genetic modifiers, which interact with the primary mutation and modulate the disease severity, have been identified for the SCN1a gene in mice (25) and human patients (26). In other cases, post-zygotically acquired mutations can be accumulated in a tissue specific manner affecting subpopulations in a variable number of neuronal cells in different brain regions (27). For example, variants of the GLI3 gene in the germline give rise to Pallister Hall, a syndrome that includes congenital anomalies as Hypothalamic hamartoma (HH), while variants limited to (or enriched in) the hypothalamus can lead to isolated HH (28).

Other cases where genomic instability plays a role in the severity or age of onset of epileptic symptoms in human patients have caught the interest of clinicians and researchers in the field during the last years. Importantly, until the advent of the advanced sequencing technologies, the search for pathogenic variants was mainly focused in the coding regions of the identified genes and those could not justify the incomplete penetrance and variable expressivity of the pathogenesis nor the high percentages of individuals affected even not being carriers of the mutations. Indeed, genetic linkage analysis, where the use of several molecular markers is employed to identify the location of a disease-causing variant, have provided the groundbreaking discovery that non-coding regions of defined genetic loci contribute to the etiology of forms of epilepsy. In particular, repeat expansions in non-coding regions of different genetic loci cause autosomal dominant forms of Familial adult onset myoclonus epilepsy (FAME) (29, 30). Intriguingly, the length of the repeats, which shows generational instability, correlates with the age of onset and severity of the detected phenotypes (31).

If on one hand the genetic complexity of epilepsy is a burden for understanding the pathophysiology, on the other hand the novel discoveries on somatic mosaicism and repeated expansion open an opportunity for better patient stratification and enhance the possibilities of diagnostic detection of the disease.

1.2. Environmental factors and comorbidities

In addition to genetic causes environmental causes have been identified for pathogenesis (8). A common risk factor for seizures and acquired epilepsy are infections. Epilepsies with infectious etiology are the ones in which seizures are the main symptom as a

direct consequence of an infection. Seizures can be the only symptom, or can represent one symptom among other dysfunctions of the central nervous system (32). Epilepsies can also be a result of a metabolic disorder, although in most of the cases they will also have a genetic basis, or can also be a consequence of an immune disorder. Moreover, there are still some epilepsies of unknown etiology (8).

Moreover, it is important to note the significant negative impact of comorbidities in epilepsy. Comorbidity was defined by Feinstein as “any distinct additional entity that has existed or may occur during the clinical course of a patient who has the index disease under study” (33). Patients with epilepsy are affected by several diseases such as depression, anxiety, dementia, migraine, heart disease, peptic ulcers, and arthritis up to eight times more than the general population (34). In addition, some conditions such as psychiatric, endocrine/metabolic, and respiratory disorders are associated with worse seizure outcomes in the long-term (35). Various models have been generated to account for the relation between comorbid disorders. These models are not mutually exclusive and even within a single person, the same comorbid disease may be linked to epilepsy for a variety of reasons. It is particularly interesting the role of genetics in epilepsy and its comorbidities. Genetic mutations can be a shared risk factor, like for example in the SCN1A gene, where mutations predispose individuals to the development of epilepsy, but also a gait disorder. Genetic factors can also act as modifiers, impacting the relation between cause and effect, like for example the higher risk of epilepsy in carriers of the APOE4 allele after traumatic brain injury. The contribution of comorbidities to mortality in epilepsy is quite significant, underlying the relevance of the study of the causal mechanisms (34).

1.3. Overview on anti-seizure medications

Currently there is no effective treatment for epilepsy and most of the drugs used in the treatment of epilepsy are directed to treat the symptoms or seizures rather than treating the underlying disease. Therefore, although historically they have been named anti-epileptic drugs (AEDs), the term anti-seizure medications (ASMs) is nowadays more widely accepted. By definition, ASMs prevent or suppress the generation, propagation, and severity of epileptic seizures. The majority of ASMs work by altering voltage-gated ion channels, enhancing gamma aminobutyric acid (GABA)-mediated inhibition, interacting with synaptic release machinery, blocking ionotropic glutamate receptors, or a combination of these mechanisms (36). Some patients achieve seizure control with the use of one medication, however in many cases a combination of multiple medications is necessary. There are other types of approaches for the treatment of epilepsies, including surgery, neuromodulation devices or diet (5). Even with the currently available ASMs and other types of therapies, about one third of the patients do not achieve seizure control. This is partly due to the drug resistance that many patients with different types of epilepsy develop. In addition to resistance mechanisms, a critical issue contributing to the slow pace of novel ASM discovery is reliability of evaluation of compound efficacy in human patients starting from data generated with rodent models or NAMs. Performing the ADME (administration, distribution, metabolism and excretion) profiling of a molecule and assessing its capacity to cross the blood brain barrier (BBB) are challenging tasks and the

results might not accurately predict the outcomes in patients, also considering inter individual susceptibility and differential response based on age to compound administration (37). Regarding ADME in *in vivo* models, it has to be taken into account that rodents eliminate drugs at a quicker rate than humans, making the generation of dose–response efficacy curves complicated. Nevertheless, longitudinal studies with rat or mouse models with multi-injections regimes followed by blood serum concentration analysis allow to study the pharmacodynamics of the administered molecules (38). Thereafter, the evaluation of the concentration of the compound reaching the CNS is estimated with the brain–blood or brain–plasma ratio, a model that correlates the brain-targeting ability of therapeutics with the CNS pharmacokinetics (39). This tool is more straightforward than other time consuming and invasive techniques such as microdialysis and *in situ* brain perfusion (40). Indeed, over the last years, *in silico* predictions based on available *in vivo* and *in vitro* data and molecular descriptors of the compounds of interest have been optimized to infer the BBB permeability of neurotherapeutics (41, 42). In *in vitro* models ADME studies cannot be directly performed, however cost effective assays can be used as indicators of the ADME fate of compounds *in vivo*. Among other parameters, it is possible to calculate the physicochemical properties as lipophilicity, solubility as well as its metabolic fate via hepatic microsome stability and plasma stability assays (43). In addition to these, multiple cell culture models derived from a variety of species have been developed to mimic the BBB and study molecule transport through this structure (44). With regard to whole embryo non animal studies, as the ones performed with the zebrafish model, it is possible to extrapolate relevant Absorption, Metabolism and Excretion values since zebrafish can adsorb and metabolize toxicants in a similar manner to that of mammals. In this case, zebrafish embryos are treated with selected compounds by waterborne exposure and collected at different exposure times for LC-HRMS analysis (45). This method allows the evaluation of the stability and toxicokinetic profile of novel molecules. Also in the zebrafish model, the brain-to-plasma concentration can be calculated and, interestingly, it has been shown that there is a correlation between the partition coefficient (K_p , brain) values obtained from the zebrafish and mice, indicating that zebrafish can be an alternative to rodent models to predict drug penetration in humans (46).

Taking into account all the previous considerations, there is an essential need for a better understanding of the basic mechanisms of the processes leading to epilepsy, the biological mechanisms of pharmacoresistance and the development of disease-modifying therapies. To achieve these goals, well established models of epilepsy are the most important prerequisite.

2. Current state of art in epilepsy models

Over the years different animal models have been developed to study epilepsy (Figure 1). A very classic and widely used group of epilepsy models are the ones with an induction of seizures in wild-type animals. This induction can be electrical or chemical and in both cases it can be an acute or a chronic induction (47, 48).

Among the electrically induced acute seizures, the best-validated preclinical test is the maximal electroshock seizure (MES) test, in

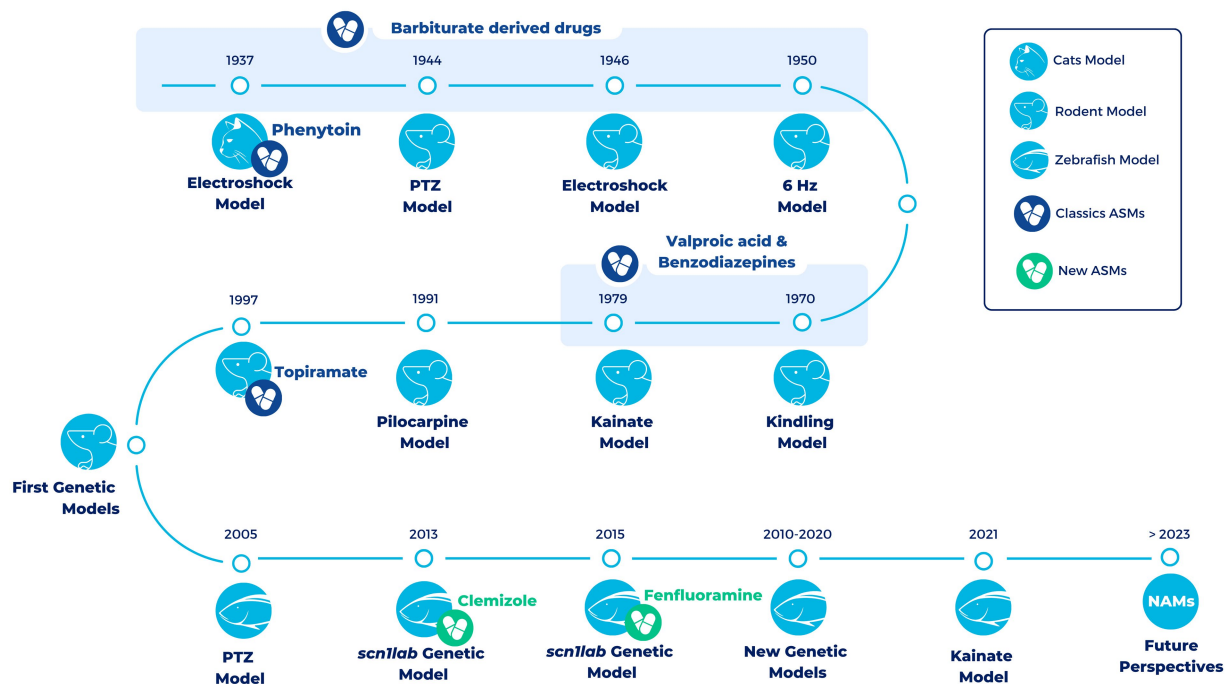


FIGURE 1

Timeline of the most representative vertebrate animal models in epilepsy over the last century. All models (exception of the electroshock models in cats) are still being used in the development of new treatments for epilepsy. During the first half of the twentieth century and up to the late 1990s, a large number of compounds with antiepileptic properties were discovered in these models (Classics ASMs). However, most of these compounds were discovered in pharmacoresistant models of epilepsy. The development of the first genetic models has allowed progress to be scored in the search for novel antiseizure medications that are able to overcome drug resistance. In the last decade, the use of zebrafish has led to the development of Fenfluramine (FDA-approved drug) and Clemizole (in DS clinical phases). In the future, it is hoped that new approach methodologies (NAMs), such as zebrafish, organoids and induced Pluripotent Stem Cells (iPSCs), will facilitate the discovery of new drugs useful for different types of epilepsy (new ASMs).

which an acute seizure is electrically induced in a normal non-epileptic animal. This test is very effective in identifying drugs against generalized tonic-clonic seizures (49). Another example of electrically induced acute seizures is the 6-Hz psychomotor seizure model of partial epilepsy, a model of pharmacoresistant epilepsy. This model, in which an electrical stimulation by low-frequency (6-Hz) is delivered through corneal electrodes, has been used both with mice and rats (50, 51). Repeated 6 Hz corneal stimulation in mice has also been used to successfully establish a kindling model showing resistance to ASMs (52). Kindling models are the models in which repeated non-convulsive stimuli are applied progressively producing a change in seizure response and finally reaching a fully kindled state with a stable seizure response to each stimulation (53). These models belong to electrically induced chronic seizures, and the best established model among them is the amygdala kindling rat model of temporal lobe epilepsy (TLE). In this model, there is a repeated application of electrical stimuli through a depth electrode in the basolateral amygdala of rats and this induces a permanent enhancement of seizure susceptibility together with other brain alterations that are similar to the ones occurring in human TLE. It was the first proposed model of pharmacoresistant partial epilepsy (48, 54).

On the other hand, there are chemically induced seizures. One of the most commonly used models of acute chemically induced seizures is the pentylenetetrazole (PTZ) test, which has been crucial for the identification of many ASMs that are clinically used today. PTZ is an antagonist of the type A receptor of γ -aminobutyric acid (GABA).

The administration of low doses of PTZ (sub-convulsive) in animal models can result in absence seizures (55), whereas higher doses (convulsive) produce generalized tonic-clonic seizures (56). PTZ has also been used to generate a chemically induced kindling model by the repeated administration of sub-convulsive doses (57). Although PTZ use is very extended in mice and rats, it is also routinely used in other models such as zebrafish (58).

Another important group of chronic models of epilepsy are models in which after inducing status epilepticus by chemical or electrical stimulation spontaneous recurrent seizures develop (48). Status epilepticus is defined by the ILAE as “a condition resulting either from the failure of the mechanisms responsible for seizure termination or from the initiation of mechanisms, which lead to abnormally prolonged seizures” (59). Although these models can be induced by electrical stimulus, the most extended models are the ones generated by either pilocarpine, cholinergic muscarinic agonist pilocarpine, or kainate, a cyclic analog of L-glutamate and an agonist of the ionotropic kainate receptors. Both pilocarpine and kainate represent post-status epilepticus models of TLE (48, 60).

The other main group of epilepsy models is the genetic animals models. With the description of more single gene mutations causing epilepsy, and the advancements in gene-editing techniques, more genetic animal models have been developed and validated (61). The generation of these models contributes to a better understanding of the mechanisms of epileptogenesis. A good example of this are the mouse models of lissencephalies (14, 62). In humans, heterozygous

mutation or deletion of the lissencephaly gene (LIS1) leads to classical or type I Lissencephaly, causing cognitive deficits, severe seizures, and a serious disruption of cortical and hippocampal lamination. Before the generation of mouse models, how neurons communicate in Lis1-deficient brain was not well understood. The generation of a Type I Lissencephaly mouse model permitted the description of alterations in synaptic inhibition that may contribute to seizures and altered cognitive function, which can potentially lead to advances in novel therapeutic strategies (62). Moreover, the models of lissencephalies have been crucial for understanding the function of LIS1 and the pathways associated with it during brain development (14). Furthermore, genetic animal models have been fundamental for the advancement of therapeutic interventions. This is for example the case of the mouse models that have been generated for DS, which have also been extensively characterized (63–65). In one of these models, for example, treatment with low-dose clonazepam, a positive allosteric modulator of GABAA receptors, completely rescued the abnormal social behaviors and deficits in fear memory of these mice (66). In a more recent study, Hawkins et al. also demonstrated that treatment with soticlestat, a novel potent and highly selective brain-specific inhibitor of the CH24H enzyme, significantly improved Dravet-like phenotypes of Scn1a Dravet mouse models (67). In summary, the development of genetic animal models has been of relevance not only to expand the knowledge of the mechanisms of epileptogenesis, but also to move forward in the discovery of new potential therapies.

Despite the large number of models that have been established for the development of new therapies in epilepsy, 30% of the patients do not response to classic ASMs and consequently more research and new models are needed. The discovery of new ASMs requires the screening of large number of compounds and, therefore, the models need to be not only predictive of clinical activity, but also easy to perform and time and cost efficient.

3. Alternative models: toward the 3R in epilepsy model generation and drug screening

The high impact of epilepsy on patients and their communities highlights the urgent need to improve the understanding of its pathophysiology and develop efficient treatments for seizure regulation. However, the use of conventional *in vivo* and *in vitro* models based on rodents display substantial limitations and ethical concerns. Although rodent models may be particularly useful for predicting treatment responses in humans due to the greater similarities between the nervous systems of different mammalian species, variation in the genetic background of rodent strains can also result in opposing or contradictory results. Rodent models are also more expensive and require complicated, invasive procedures to study the role of genes in seizure mechanisms (68). Additionally, growing awareness of the sentience of animals and their experience of pain has led to the adoption of the 3Rs principle (replace, reduce, and refine) by all the ethical committees and whenever possible, novel alternative models to animal experimentation are recommended (69).

Multiple alternative methods have arisen in order to provide relevant insights into the epileptic pathology and accelerate treatment innovation (Figure 2). Among them, organotypic brain slice cultures (OSCs), Induced pluripotent Stem Cells (iPSC) and organoids appear as relevant models for new antiseizure drug candidates screening. On another hand,

several models not classified as animals larval stage of *Danio rerio* (70) or non-vertebrates *C. elegans* (71, 72) and *Drosophila melanogaster* (73), traditionally used in basic research on embryonic development, have proven valuable in epilepsy research. This is because these models allow for high-throughput pharmacological screening, enabling the simultaneous evaluation of a large number of samples, the automated analysis of different phenotypes in short times, and the generation of avatars of human patients for the testing of new therapies. Among these, we will focus on the most widely used vertebrate zebrafish model.

3.1. *Ex vivo* and *in vitro* models

To identify new ASMs, it is key to employ a wide range of appropriate experimental approaches, including alternatives models. Thus, the establishment of these models/platforms ensures improved validity and relevance for their clinical use. Several alternatives to classical animal models based on *ex vivo* and *in vitro* models are currently available and being developed in the field of epilepsy.

3.1.1. Organotypic brain slice cultures

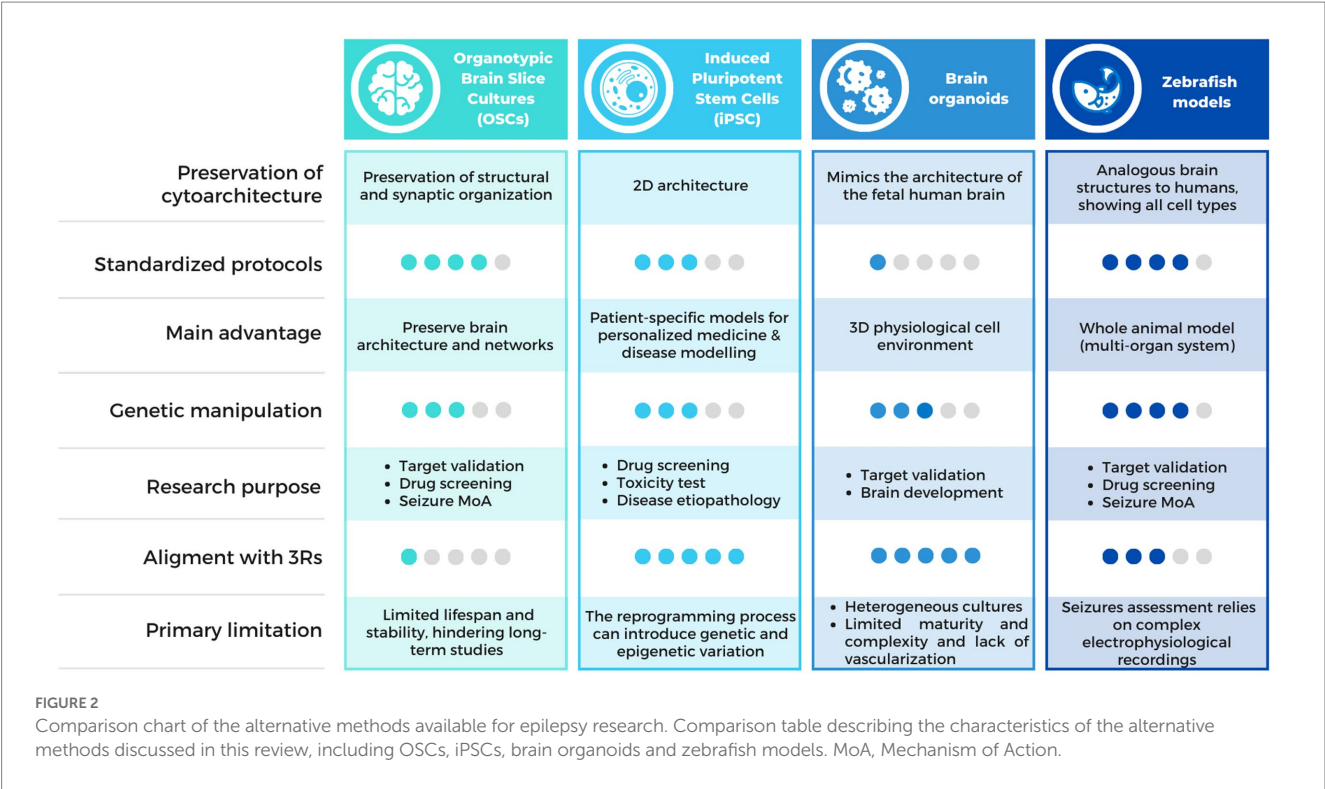
Unlike conventional primary cell cultures, that allow the study of single cell populations, OSCs enable the simultaneous analysis of different cell types in a three-dimensional model, with preservation of some structural and synaptic organization features of the original tissue (74, 75).

In addition, OSCs allow the assessment of many aspects of relevance for the study of epilepsy and ASMs. Neurodegeneration, a possible consequence of seizures (76), can be evaluated through propidium iodide or other stainings, or even by measuring the levels of lactate dehydrogenase released to the medium (77). OSCs can be very useful to perform procedures that, although possible, are normally more challenging to carry out *in vivo*, including long-term live imaging (75), or electrophysiology (78). Recombinant adeno-associated viruses, commonly used to generate disease models *in vivo* (79, 80) can also be used to generate disease models in OSCs (78) and different compounds can be added into the culture medium to study them (81). As previously mentioned, they can support all the cell types found in the CNS, and therefore changes in cell types other than neurons, like glia and vascular cells, can also be studied.

Moreover, the use of OSCs significantly decreases the number of animal experiments that are considered severe, thereby promoting the principles of the 3Rs—reduce, refine, and replace (74).

However, many aspects of brain slice preparation can affect their viability and might influence neuronal connections. These aspects have been previously reviewed in detail by the ILAE (82). Briefly, the survival of the neurons depends on a variety of factors, including the species and age of the animal, the brain area selected, the medium composition and thinning of the slice. Nevertheless, contrary to what is observed in acute slices, where projection fibers are severed during the preparation, in OSCs the extended maintenance of the slices in an incubator with access to a cultured medium can produce a relatively stable cell viability, resulting in a long lifespan. Additionally, there is a significant synaptic rearrangement during the regrowth after slicing-induced deafferentation, but the properties of synaptic transmission are overall maintained (82).

Many brain areas have been used for OSCs, such as hippocampus, cortex, cerebellum and brainstem structures. In particular, organotypic hippocampal slice cultures have been broadly used to study epilepsy,



because they allow for thorough and controlled investigation of the mechanisms behind epileptogenesis, while keeping the network phenotypic characteristics of epilepsy, especially the development of spontaneous seizures (83, 84). The most commonly used method for the preparation of organotypic hippocampal slice cultures was first described by Stoppini et al. (85) and later detailed by De Simoni and Yu (86).

Brain preparations derived from a variety of mammalian species, including rabbits, guinea pigs, rats, mice, and humans, have been shown to induce *in vitro* epileptiform activity (82). Most OSCs are generated from mice or rats before postnatal day 12, since at this developmental stage, the brain's cytoarchitecture is well-established. Furthermore, the larger size of the brain at this stage makes it easier to handle, which allows neuronal cells to survive explantation. Additionally, explanted neuronal cells at this age exhibit greater plasticity, making them more resistant to the mechanical trauma that can occur when cutting neuronal processes (86).

Although most of the OSCs are generated from mice or rats, they have also been successfully established from tissue of adult patients. This represents a very good alternative to animal models since it allows to perform basic functional and mechanistic studies in a completely homologous model. Moreover, human OSCs preserve the complex neuronal cytoarchitecture and electrophysiological properties of human pyramidal neurons (87). However, it requires the availability of human tissue obtained from neurosurgery for refractory epilepsy (88). An example is the model of temporal lobe epilepsy in which the characteristic morphology and pathological activities are preserved, and epileptiform activities can be modulated by the addition of glutamatergic and GABAergic receptor antagonists (83).

3.1.2. Induced pluripotent stem cells

iPSC technology has considerable potential for toxicity and efficacy drug screening and disease modeling, allowing the generation, growth, and study of human cells without the need for invasive isolation procedures or extensive ethical approval (89). Somatic cells obtained from patients can be reprogrammed to a pluripotent stem cell state which can then be differentiated into a broad range of different cell types, including neurons and glia (90, 91). iPSCs can be produced in about a month, and therefore, it is possible to rapidly generate a model with patient specific mutations with a lower cost than a mouse model. This is particularly relevant in epilepsy due to the heterogeneous nature of genetic epilepsies, with more than 500 loci listed as potentially causative when mutated and in some cases, such as in SCN1A-related epilepsies, over 1,250 distinct mutations identified in patients (92).

Several functional and molecular approaches can be used for the phenotyping of patient iPSC-derived neurons. Most of them are directed to study neuronal excitability, such as patch-clamp recording, which provides direct single cell measurements of electrical activity, multielectrode arrays (MEAs), for the measurement of electrical activity of a network of cultured neurons for extended periods, fluorescent assays of intracellular calcium or membrane voltage, and all-optical electrophysiology methods that allow high throughput studies. Other approaches for the phenotyping of iPSCs-derived neurons in the context of epilepsy include live cell imaging and omics studies (93).

Despite being a good model to study epilepsy, they also present some limitations. iPSC lines can have variable expression profiles and differentiation potential (92). In addition, it is very challenging to recapitulate the complexity of the brain and, despite the efforts to create brain circuits in 2D culture using iPSC-derived neural cells, the

circuitry is still very different from the complex brain neuronal network. This is now improving thanks to the development of brain organoids made using 3D culturing technology (94).

Multiple patient-specific iPSCs derived disease models exist, generated from patient's cells carrying specific mutations (95). These models have shown altered neuronal morphology, including soma size, neurite outgrowth, formation of synapse, and length of dendritic spine (92). The first *in vitro* model from a Dravet patient with a mutation in the SCN1A locus demonstrated how the primary cause of epileptogenesis seems to be the loss of function in GABAergic inhibition (96). After that, different studies have been published studying different mutations in the gene SCN1A (97, 98). Other diseases have also been successfully modeled using patient iPSCs, including Rett syndrome (99, 100) and Angelman syndrome (101) among others (92). These advancements have broadened the understanding of the disease etiology and pathology and set an extraordinary basis for the application of personalized medicine by developing targeted therapeutic strategies (102). In parallel to the development of iPSC, great advances in gene editing technologies have been made. This coincidence has considerably contributed to a fast expansion in the understanding of neurological disorders (103). CRISPR/Cas9 in iPSCs can be used to generate new models of various disorders, such as Alzheimer's (104) and to generate isogenic pairs, which differ only by a single genetic modification, and are powerful tools to understand gene function. Furthermore, genome-wide CRISPR screens enable high-throughput investigation for genetic modifiers, opening up new pathways and revealing potential therapeutic targets (103).

CRISPR/Cas9 in human iPSCs was first used in epilepsy to generate a loss of function SCN1A mutation in order to gain more knowledge on DS. In this study, they fluorescently labeled GABAergic iPSC-derived neurons using CRISPR/Cas9 and studied their electrophysiology and the postsynaptic activity of inhibitory and excitatory neurons. They described a reduction in the amplitudes and an enhancement of the thresholds of action potential in patient-derived GABAergic neurons, together with a change in the postsynaptic activity from inhibitory to excitatory. These results further contributed to the previous knowledge on the physiological basis underlying epileptogenesis caused by SCN1A loss-of-function mutation (105). This strategy has been thereafter applied in several other studies, including more on the SCN1A gene (106), but also in other models of epilepsy, like in a model of KCNQ2 encephalopathy (95, 107). In this last study, they used patient iPSC-derived neurons and generated an isogenic mutation-corrected control line using CRISPR/Cas9, so that they could link phenotypic changes to the disease associated variant. They discover a functional enhancement of Ca^{2+} -activated K^{+} channels, a rapid action potential repolarization and a larger post-burst afterhyperpolarization in the patient-derived neurons in comparison to the isogenic control ones. Once again, the combination of CRISPR/cas9 technology and iPSCs resulted in new findings that add to the previous knowledge on the disease mechanisms.

3.1.3. Brain organoids

Brain organoids are organized structures composed of progenitor, neuronal, and glial cell types that closely resemble the architecture of the fetal human brain. Reprogrammed human iPSCs could undergo a self-organization process (108). To induce the formation of neural rosette structures, 3D aggregation of pluripotent stem cells, including

both human iPSCs and ESCs, is facilitated in the presence of neural induction molecules, crucial step in the generation of brain organoids (109). Under optimal conditions, these cellular aggregates undergo self-organization, leading to the development of more complex and differentiated structures known as cerebral or brain organoids (110, 111).

Brain organoids replicate the human brain's tissue structure and developmental pathway, in addition to its cellular composition, making them distinct from conventional two-dimensional (2D) cell cultures. As a result, they offer a unique opportunity to model human brain development and function, which may not be directly testable in direct experimentation (112). As with iPSCs, recent advances in genome editing, high-throughput single cell transcriptomics and epigenetics, have significantly advanced the use of brain organoids as a tool to study the development, evolution, and diseases of the human brain. This has resulted in a revolutionary expansion of our investigative capabilities (112).

In recent years, a novel approach has emerged as a second generation of brain organoids, known as brain assembloids, which offer a promising strategy for modeling human brain development and disease. Assembloids provide a solution by integrating multiple organoids or combining organoids with missing cell types or primary tissue explants (113). These assembloids use self-organization enabling complex cell–cell interactions, circuit formation, and maturation in long-term culture, distinguishing them from approaches that mix cell lineages in 2D cultures or use engineered microchips (114, 115). The successful growth and functional properties observed in assembloids composed of cortical, hippocampal, and thalamic organoids with active neuronal migration and interaction demonstrate the potential of these flexible, scalable, and controlled microfluidic systems for broad applications in neurological and biomedical research. It is anticipated that these innovative approaches will prove invaluable in unraveling human-specific aspects of neural circuit assembly and in modeling neurodevelopmental disorders using patient-derived cells. The integration of brain assembloids into the scientific landscape holds great promise for advancing our understanding of the human brain and developing targeted therapeutic strategies for neurological disorders as epilepsy (114).

Organoids have proven to be a valuable tool for exploring cellular phenotypes related to epilepsy. Nevertheless, the development of seizures and the replication of the electrophysiological properties of the brain in organoids, which are essential components of epilepsy research, are still active areas of investigation (116).

3.1.3.1. Epilepsy progressive myoclonus 1

Di Matteo laboratory performed experiments using cerebral organoids derived from both Epilepsy Progressive Myoclonus 1 (EPM1) patients and healthy individuals (117). EPM1, an autosomal recessive disorder, is the most common form of progressive myoclonus epilepsy and associated with mutations in the cystatin B (*CSTB*) gene and its promoter. They found that *CSTB* overexpression in control organoids increases cell proliferation, whereas overexpression of a mutant form of *CSTB* led to its inhibition. Additionally, control organoids exposed to media from mutated organoids (from EPM1 patients) showed a decrease in cell proliferation, whereas media from control organoids rescued the proliferation deficit in EPM1 organoids. Low levels of functional *CSTB* result in an alteration of progenitor's proliferation, premature differentiation, and changes in interneurons

migration. This research manifested that the use of derived cerebral organoids provided valuable insights into the cellular and molecular mechanisms underlying this disorder.

3.1.3.2. Developmental epileptic encephalopathies

Developmental epileptic encephalopathies are severe disorders characterized by intractable epileptic seizures and developmental delay where UDP-glucose-6-dehydrogenase (UGDH) gene has been implicated as a critical component, responsible for the conversion of UDP-glucose to UDP-glucuronic acid. Hengel et al. have recently generated cerebral organoids from patients with different mutations in the *UGDH* gene (118). Mutant organoids were significantly reduced in size and showed decreased expression of neuronal progenitor markers and proliferative cells. This study using cerebral organoids provides valuable insights into the molecular mechanisms underlying developmental epileptic encephalopathies and suggests potential therapeutic avenues, focusing on nutritional supplements and regulatory interventions. Remarkably, a similar experiment was performed with zebrafish, but *UGDH* mutant zebrafish did not show the same defects, indicating different responses between the organoid and zebrafish models. This fact underscores the importance of studying different models of the disease to gain comprehensive insights, as each model contributes unique aspects to our understanding and contributes to a more holistic understanding of the disease.

3.1.3.3. Additional disorders

Recently some advances in this field have been made, with the successful establishment of brain organoid models of Angelman syndrome showing among other features hyperactive neuronal firing (119), and Rett syndrome, with susceptibility to hyperexcitability and recurring epileptiform spikes. This last model was also used to test valproic acid (VPA) and the TP53 inhibitor pifithrin- α (PFT) as possible treatments for this syndrome (120). Furthermore, another study succeeded in the development of a brain organoid model of developmental and epileptic encephalopathies (DEE), demonstrating not only the presence of epileptiform activity, but also showing the utility of this model for the molecular study of epilepsy (121). Although more studies are needed to enhance the accuracy of these disease models, they are promising tools for the evaluation of future treatments in epilepsy.

3.1.3.4. Therapeutics testing with brain organoids

Brain organoids provide a unique and valuable platform for gaining insight into complex neurological diseases. However, the current state of organoids is characterized by their simplicity and as a consequence of being *in vitro* models, the knowledge derived from them may carry intrinsic limitations. While brain organoids are valuable models, they have certain limitations in recapitulating the complex tissue structure and functions of the human brain, particularly with respect to the choroid plexus (ChP). The ChP plays an important role in cerebrospinal fluid (CSF) secretion and the formation of the blood-CSF barrier. To overcome this limitation, researchers have made efforts to establish human ChP organoids capable of simulating selective barrier properties and CSF-like fluid secretion within self-contained compartments. An exciting feature of these ChP-CSF organoids is that they exhibit similar small molecule selectivity as observed *in vivo* (122). This property makes them

valuable tools for predicting the CNS permeability of new compounds. Given the growing demand for more effective CNS drugs, it is critical to avoid the shortcomings of drug candidates that enter clinical trials only to fail due to lack of efficacy, limited CNS penetration, or translatability issues from animal models.

Further technological development is required to advance the field and increase the utility of brain organoids as reliable models. Efforts toward accelerating functional maturation to more closely resemble the *in vivo* state, as well as incorporating additional cell and tissue types, should be directed toward creating more comprehensive and faithful representations of the human brain. These advances will contribute significantly to the reliability and relevance of brain organoids in the study of neurological disorders (112).

3.2. The zebrafish model

While the zebrafish model has been extensively used in classic developmental studies for many years, in particular in neurodevelopment (123), in the last two decades it is being exploited for target validation and drug screening (124, 125).

Zebrafish provides a large variety of possibilities in order to explore the underlying principles of seizure generation in multiple epilepsy models (126). With their small size, high breeding rate, rapid development and relatively low maintenance costs, in addition to their ability to take up compounds from the water surrounding them, zebrafish larvae are particularly suited to perform high-throughput phenotype-based drug screening (127). In addition, zebrafish exhibit genetic similarities with humans and present numerous advantages for genetic manipulation. Advanced and efficient genome manipulation techniques have facilitated the creation of models for various genetic epilepsies and disorders where seizures are a primary symptom (58, 127). Moreover, zebrafish larvae possess analogous brain structures to those present in mammals and exhibit a diverse range of complex behaviors, which can be susceptible to seizures, within just a few days post-fertilization (128).

Cortical and subcortical structures of zebrafish larvae are conserved and maintained in relation to their characteristic cellular features and main connections. The main sections in which zebrafish brain is subdivided include forebrain, midbrain and hindbrain/spinal cord. During early development, further subdivisions occur, giving rise to specialized structures in the adult brain which can also be found in rodent models and humans: pallium, subpallium, thalamus, and cerebellum (70). Moreover, some structures are highly homologous between humans and zebrafish, including the habenula (129), striatum, basal ganglia (130, 131), and cerebellum (132).

The similarities between zebrafish and mammalian (human and rodent) models are remarkable, both in terms of general brain organization and cellular morphology (128). In particular, the zebrafish amygdala and habenula are involved in affection-related behaviors, mirroring human data on these brain structures. The habenula, a group of nuclei in the epithalamus, plays a role in regulating the release of serotonin and dopamine (133), making it an experimentally feasible system for dissecting vertebrate brain circuits (134). This conservation allows for the study of brain substrates in zebrafish and their translational value for the study of pathological behavior, as habenular hyperactivity has been observed in humans with depression and in rodent models of this disorder (135).

In terms of brain neurochemistry, zebrafish share a highly conserved profile with humans and rodents. They possess all major neuromediator systems, including neurotransmitter receptors, transporters, and enzymes involved in synthesis and metabolism (136–138).

Zebrafish also have well-developed functional neuroendocrine systems, analogous to those found in mammals. The neuroendocrine system remains conserved in zebrafish (ZF) and for hypothalamus development, the same genes as in mammals are employed. Additionally, the majority of neuropeptidergic systems and neurotransmitters exist in this model (139, 140). Stress responses in zebrafish, similar to humans, are mediated by cortisol, which is activated by hypothalamic–pituitary hormones and acts through glucocorticoid receptors (141, 142). Zebrafish cortisol responses closely resemble behavioral indicators of stress and can be genetically and pharmacologically modulated (141–143). These similarities make zebrafish a valuable model for studying CNS disorders.

In order to study epilepsy, zebrafish allow the performance of multiple bioassays. Notable advantages include the capacity to perform *in vivo* brain imaging through activity-dependent fluorescent/bioluminescent reporters, EEG recordings in both larval and adult fish, and high-throughput behavioral analysis by means of automated video tracking systems (58, 144). Regarding seizure evaluation, zebrafish has the ability to mimic motor behaviors observed in humans, including changes in swimming patterns and body shaking (58).

Overall, taking into account all these characteristics, the zebrafish model is suitable for investigating the source of these disorders as well as the series of events leading to their onset. Additionally, it serves as a high-throughput *in vivo* drug screening platform for compounds with anti-seizure potential (58).

3.2.1. Pharmacological models (PTZ and kainic acid)

3.2.1.1. Pentylenetetrazole model

The PTZ model was first described in zebrafish in the early 2000 (145). Consecutive studies then concluded that zebrafish larvae at 7 days post fertilization (dpf) exhibit electrophysiological, behavioral and molecular changes similar to the rodent PTZ models (58, 146). In rodents, the dose of PTZ required to induce seizures may vary depending on factors such as strain, sex, age, and route of administration (primarily intraperitoneal injection). PTZ is primarily used as a screening tool for ASDs in rodents rather than to study the pathophysiology of epilepsy. Different types of seizures are reproduced at different doses of PTZ, with low doses inducing absence seizures and higher doses inducing generalized tonic–clonic seizures. Commonly used protocols for PTZ administration in mice during antiseizure drug screening aim to induce clonic seizures lasting at least 5 s in at least 97% of animals within 30 min (147, 148). Similar to rodents, PTZ in the ZF is considered a model for generalized seizures, particularly absence and generalized tonic–clonic seizures.

Zebrafish larvae are capable of eliciting seizure-like behavior when immersed in a volume containing PTZ. This compound is absorbed by the gills, gut or skin and eventually reaches the brain (58). Within seconds or minutes, switches in locomotor activity are detected. These movements are characterized by a series of events, starting from Stage

I, consisting of accelerated movements around the periphery of the behavioral chamber. During stage 2, ZF larvae perform “whirlpool-like” movements. The epileptic behavior concludes with stage 3, which takes place in case of high PTZ concentrations. ZF larvae experience loss of posture, rapid and uncontrolled movements, intermittent pauses and occasional stiffening of the body (145). The locomotor behavior induced by PTZ displays a correlation with the electrical activity of the brain determined by EEG. This behavior is characterized by spontaneous epileptiform discharges, which manifest variations in frequency, amplitude and duration depending on the timing of PTZ exposure (145).

This model has enabled the standardization of simple locomotion assessments (tracked using software analysis) and electrophysiological tests for quantifying and monitoring seizures in zebrafish larvae (146). Subsequently, the zebrafish PTZ model has gained popularity in laboratories worldwide and has demonstrated consistency with the rodent PTZ models in validating antiepileptic drug candidates. This emphasizes the importance of zebrafish as a fast and robust model for ASMs screening (149).

Multiple ASMs with known effect in the rodent PTZ model, have been tested in zebrafish. During the study performed by Gupta et al., ZF were exposed for 15 min to a 6 mM PTZ solution co incubated with standard ASMs in order to monitor their anti-seizure activity (150). These compounds were valproic acid, carbamazepine, diazepam, gabapentin, carbamazepine, pregabalin and lacosamide. Lacosamide, valproic acid, gabapentin, carbamazepine and diazepam presented a concentration dependent increase in latency during all stages of seizures. For lacosamide it was significant at 100 μ M to 3 mM, for valproic acid at 300 μ M to 10 mM, for gabapentin at 1–10 mM, carbamazepine at 10–100 μ M and diazepam 30–100 μ M (150). Pregabalin by contrast, did not increase seizure latency compared to the vehicle control (PTZ 6 mM).

Efficacy data of ASMs obtained from the zebrafish model compares to the rodent one. Carbamazepine at 20 mg/kg, sodium valproate at 300 mg/kg, diazepam at 1 mg/kg were tested in this rodent model and showed protection from clonic seizures (151). Pregabalin tested at 200 mg/kg did not cause a significant reduction of clonic seizures compared to the vehicle control, as described in the PTZ zebrafish model (150).

3.2.1.2. Kainic acid, novel model by pericardial injection

Kainic acid (KA) is defined as a potent agonist of AMPA/KA glutamatergic receptors. It induces network reorganization, excitotoxicity and neuronal death in different brain regions. Since it produces acute seizures in rodents through systemic injections and recurrent seizures mimicking a chronic model of temporal lobe epilepsy by intracerebral injections, it is a widely utilized proconvulsant drug (48, 58).

KA is considered a model in adult ZF that is reported to reproduce seizures, similar to its use in rodents (152). In ZF, the majority of KA studies have been conducted in adult animals. In these studies, KA is administered intraperitoneally to induce seizure-like behavior, resulting in clonic convulsions observed in all ZF treated at a dose of 6–8 mg/kg (152). It is noteworthy that these doses are comparable to those commonly used in rodent models (6–15 mg/kg) (153).

Previous efforts in order to trigger seizures in zebrafish larvae by incubating them in KA solution failed to produce the desired seizure phenotype. According to the study performed by Kim et al. (154), KA

perfusion by means of artificial cerebrospinal fluid immediately led to local electrographic brain discharges. Additionally, Alfaro et al. (152) observed that adult zebrafish intraperitoneally injected with KA presented convulsions mimicking clonus. The results of these studies imply that the high hydrophilicity of KA prevents ZF larvae from efficiently absorbing it when dissolved in tank water (155).

In 2021, a novel KA model was introduced in zebrafish larvae (155). This KA-induced zebrafish epilepsy model is achieved by intrapericardial injection of KA in 3dpf zebrafish larvae. Due to a shift in balance between GABAergic inhibition and glutamatergic excitation, larvae show whole brain abnormalities and involuntary seizure-like movement patterns shortly after injection. After the latency phase, larvae also experience epileptiform brain discharges (155). Following treatment with commonly used ASMs, as topiramate 100 μ M, tiagabine 100 μ M and carbamazepine 100 μ M, a reduction in epileptiform discharges was observed while none of the compounds tested decreased seizure-like behavior (155). Multiple ASMs were also tested in the kainate mouse model of mesial temporal lobe epilepsy obtained by unilateral injection of kainate into the dorsal hippocampus (156). All the compounds tested: valproate (300 mg/kg), lamotrigine (90 mg/kg), carbamazepine (75 mg/kg), levetiracetam (600 mg/kg), pregabalin (50 mg/kg), phenobarbital (20 mg/kg), diazepam (1 mg/kg), tiagabine (0.3 mg/kg), and vigabatrin (50 mg/kg) acutely reduced the occurrence of hippocampal paroxysmal discharges (156).

The kainic model described above, provides useful insights into the mechanisms of seizures and epileptogenic processes and could possibly be applicable in the future for the discovery of novel therapeutics including disease-modifying strategies in the fight against drug-resistant epilepsies (155).

3.2.2. Genetic models

Another common approach for epilepsy studies is based on the modulation of epilepsy-associated genes. The rodent brain has a long maturation time, which makes it challenging to determine the optimal timing for pharmaceutical intervention in epilepsy studies, even with various rodent genetic models available. In contrast, using zebrafish epilepsy models could be more useful in researching the epileptogenic pathway related to genetic abnormalities. Also, since most genetic epilepsy syndromes occur in childhood, studying larval zebrafish can be an effective method to monitor brain development.

Given the rather recent inclusion of the zebrafish in epilepsy research, in most cases the widespread antisense morpholino strategy has been used for disease in early days. Through this methodology the knockdown of several genes such as *kcnj10* (157, 158), *kcnq3* (159), *stx1b* (160), *chd2* (16, 161) has been reported to induce severe behavioral alterations (epileptic discharges, poly-spikes, paroxysmal discharges). Nevertheless, given the variable results that might be obtained comparing studies in mutants and morphants (162) mostly due to genetic compensation mechanisms induced by loss-of-function mutations and mutant mRNA degradation (163, 164) the gold standard model for zebrafish epilepsy research is a mutant line carrying a loss-of-function mutation in domain III of the voltage-gated sodium channel *scn1Lab* (165). The zebrafish gene, *scn1Lab*, is highly homologous to the human gene SCN1A, with 77% of DNA identity. In the developing zebrafish brain, *scn1Lab* is expressed widely, especially in the forebrain, optic tectum, and cerebellum. Frameshift or missense mutation in this gene can lead to the onset of

DS, a severe form of genetic pediatric epilepsy that causes developmental disabilities and persistent drug-resistant seizures. *scn1Lab* gene disruption in zebrafish is able to recapitulate human epileptic phenotypes. Specifically, zebrafish with a mutated *scn1Lab* gene show spontaneous seizures detected through electrophysiological recordings, similar to epilepsy in humans. When challenged with a light dark (LD) transition assay, mutant zebrafish exhibit abnormal locomotor patterns, with consistently higher activity levels (hyperlocomotion) compared to their wild-type siblings. In the pioneer study where the mutant was characterized (165), the model was challenged with over 300 compounds in a phenotype-based screening. As a result, Clemizole (EPX-100), an FDA-approved compound with anti-histaminic properties, was found to be effective in inhibiting seizures in the mutant fish and has passed through phase I clinical trials as an “add-on treatment” for DS. Starting from this success case, other drug repurposing screening have been conducted using the *scn1Lab* mutant and identified several drugs like fenfluramine (144) (now FDA-approved as Fintepla®), synthetic cannabinoids (166) (similar to the FDA-approved cannabidiol Epidiolex®), trazodone (Desyrel®), and lorcaserin (Belviq®) (167), which have also shown promise in treating DS in zebrafish experiments. These findings demonstrate how quickly discoveries in zebrafish can lead to potential clinical treatments for DS.

Although the aforementioned repurposing studies are based on the use of the same genetic mutant background, the advent of CRISPR/Cas9 and the continuous refinement of the technologies based on this system offer now the possibility of inducing mutations with high efficiency in human epilepsy-associated genes. Along this line, in a recent study (168) a range of loss-of-function single gene mutations identified through genome wide association (GWAS) represented the starting point for the generation of 37 mutant zebrafish lines carrying deletions in the selected loci. Among these, 8 lines (homozygous mutant for *arxa*, *eef1a2*, *gabrb3*, *pnpo*, *scn1lab*, *strada*, and *stxbp1b* and heterozygous for *grin1b*) result in recurrent electrographic seizures, thus opening new avenues for the study of the pathophysiology of rare disease and at the same time expanding the portfolio of lines that can be used for high-throughput screenings of ASMs.

Despite the fact that the generation of isogenic lines is crucial for the assessment of loss of function phenotypes, the time required for the obtention of mutant lines, including husbandry of fish, crossing for two generations and genotyping does not meet the current needs of personalized therapy based on genetic background of the affected individuals. Indeed, new genetic targets and genomic variants involved in epilepsy pathophysiology are being identified quickly through large-scale exome sequencing studies of cohorts of patients. This requires the development of high-throughput methods for timely generation of animal disease models to test the efficacy of compounds modulating these targets. To reduce the generation time for genetic target validation and the characterization of loss-of-function alleles in zebrafish, a variety of CRISPR/Cas9-based methods have been improved. The continuous refinement of single guide RNA (sgRNA) and Cas9 synthesis for the targeting of genes of interest has reached such efficiency that it is possible to induce gene loss-of-function already in the F0 generation. This is achieved by induction of high rates of open reading frame disruption mutations in microinjected zebrafish embryos, which are somatic mutants or CRISPANTs (169,

170). This transient approach makes it possible to directly identify and analyze mutant phenotypes and shortens the time and expense needed to achieve homozygosis in the F2 generation.

CRISPANTs models have been generated for human indications (9), epilepsy being one of them. Indeed, in a recent report (171), the behavioral fingerprint, intended as multiparametric analysis of larval behavior derived by tracking the animals over time, of *scn1lab* zebrafish homozygous mutant and F0 CRISPANTs for the same gene have been compared. Interestingly, the F0 knockouts phenotypes highly correlated with the mutant phenotype, being the behavioral fingerprint of both groups significantly different from their wildtype counterpart.

The use of CRISPANTs could be crucial for the high-throughput generation of novel zebrafish epilepsy mutants and allow antiepileptic drug screening already in F0 larvae, enabling fast-track personalized treatment design.

At the same time, a wide array of strategies has been developed, in order to precisely insert human mutations into the zebrafish genome. The gold standard technique for precise gene modification is based on Homologous directed repair (HDR), which involves the use of template DNA carrying the desired sequence change to substitute the sequence at the target locus following a double-strand break (DSB) by the CRISPR/Cas9 system (172). HDR-genome editing, however, is linked to significant amounts of off-target mutations and insertions/deletions byproducts. To overcome these issues, base editing, which uses a DNA C or A deaminase enzyme coupled to the Cas9 nickase protein to install precise modifications without the need for donor DNA or DSBs (173), was firstly developed and it has shown a great efficiency even in F0 in zebrafish larvae (174). Finally, a key breakthrough in the field of genome editing is the Prime editing (175). This technique is based on the fusion of a Cas9 nickase to a Reverse Transcriptase. In this case, the sequence of interest is copied into the target locus by reverse transcription of an RNA template sequence, thus avoiding double strand break and drastically reducing unintended DNA mutations at the target locus. The implementation of Prime editor proteins in zebrafish has led to promising results, with relatively high percentages (up to 30%) of correct edits in F0 embryos (176).

All these strategies are being employed at a fast pace and already allowing the development of humanized zebrafish in a short time frame, thus paving the ground for future customized high-throughput drug screenings.

4. Discussion and future perspectives on the use of alternative models

More than 20 years have passed since the signing of the Bologna declaration in 1999, at the third World Congress on Alternatives to the Use of Animals in the Life Sciences. The proclamation established the requirement to abolish cruelty in science before it could be applied to humans, encouraging the strict implementation of the 3Rs (replace, reduce, and refine) in processes involving laboratory animals. Since then, there have been many changes that have occurred in the regulation of animal experimentation and advances in the search for and validation of alternative models.

Here, we have presented some of the alternatives to current methods applied to epilepsy research. Although the classic models greatly contributed to the development of multiple drugs to treat

epilepsy, there is still a high percentage of patients with no seizure control, partly due to the development of drug resistance, but also to the lack of accurate models to study the mechanisms underlying epileptogenesis. The continuous advances in the development of NAMs (new approach methodologies) has the potential to fill this gap in epilepsy research, while contributing to the implementation of the 3Rs. Moreover, the success in the use of Clemizole in a zebrafish model of DS and other drug repurposing screenings (144, 165, 166), has proved the benefit of the use of novel model to translate the results into potential clinical treatments.

Nevertheless, a consistent change in animal experimentation pushing forward the 3R principle in neurological disorders and other human indications can be achieved only with a strong coordinated effort led by governmental agencies, international institutions, pharmaceutical and chemical industry, academia and animal welfare organizations.

4.1. Advancements in regulation of use of NAMs in research

Importantly, the use of NAMs such as *in vitro* and non-animal models, some of which we have presented in this overview, is gradually gaining momentum in novel policies adopted by regulatory agencies worldwide. For example, since 2011, the European Medicines Agency (EMA) has supported Directive 2010/63/EU in a number of ways (177). One of them is the establishment of the “3Rs Working Party” (3RsWP), which encourages the adoption of alternative techniques and supports drug developers who are dedicated to minimizing the use of animals during the regulatory process. Organization for Economic Cooperation and Development (OECD) guidelines have been established to assist businesses in creating alternate techniques for determining if chemicals are safe enough to register with the European Chemicals Agency (ECHA). In the USA, the FDA (Food and Drug Administration)’s NCTR (National Center for Toxicological Research) (178) division works to develop and validate alternative (*in vitro* and *in silico*) toxicity evaluation techniques. The last step forward on this matter is the FDA Modernization 2.0 Act (179), signed by Joe Biden, president of the United States, at the end of 2022. This mandate is groundbreaking since it ends a 1938 federal mandate according to which experimental drugs had to be tested on animals before being used in human clinical trials. Today, the alternative methods accepted by U.S. agencies to reduce or replace experimental animals is as high as 128 (180).

4.2. A combinatorial approach for discovery and testing of new ASMs

All these initiatives that suggest an important change in global drug discovery pipelines not restricted to the epilepsy field, raise the questions of how NAMs can eventually completely replace animal experimentation, providing safe treatments for patients in a more ethical and sustainable manner. Here, we have extensively reviewed alternative models for the discovery of novel therapeutics in epilepsy, with their relative advantages and limitations and we do believe that the answer to the aforementioned question relies on a comprehensive approach that integrates data from different methods. A relatively

novel concept in toxicity assessment of chemicals for regulatory purposes is based on the IATA, Integrated approaches for testing and assessment (181). IATA rely on the combination of a variety of information sources to infer hazard for chemical risk assessment. A similar strategy could be used to evaluate the potential efficacy of novel ASM compounds. Following a IATA framework, the first step would be to collect all available information through a literature review on generated data about the compound of interest, if a repurposing approach is used, or the chemical class, in the case of a newly synthesized molecule. Additional testing using the multiple models presented would help inform on the effect of a compound at different levels of complexity (e.g., molecule, cell, organ, tissue, organism). The individual outcomes deriving from the presented *in vitro*, *ex vivo* or whole organism would be integrated and decision frameworks can be established for the analyzed chemicals. If results are concordant in orthogonal assays with NAMs, the compounds would progress to physiologically based kinetic (PBK) modeling for *In-Vitro-to-In-Vivo-Extrapolation* (IVIVE) (182, 183). IVIVE uses physiologically based kinetic (PBK) models to estimate a human equivalent dose that can be compared with estimated human exposures (reverse dosimetry) or estimate internal doses (blood, tissue levels) based on a specified exposure for comparison with *in vitro* bioactive concentrations (forward dosimetry). In this case there would be no need for further animal experiments. When discordant results are obtained, additional tests with NAMs or rodent models, in this case in a much reduced number since extensive information has been generated with previous steps, might be required to take a decision on the tested chemical.

Overall, applying an integrated strategy with data proceeding from multiple sources would greatly reduce and eventually replace animal testing.

It could be expected that the integration of results obtained with experiments in NAMs coupled with the advancements in high-throughput disease modeling via genome editing will enable development of personalized treatment approaches not only in epilepsy but also for other human indications.

Throughout the review, we have mentioned a few strategies to tackle the genetic variability underlying phenotypic heterogeneity of epilepsy among which stable and somatic Knockout generation for loss-of-function alleles, base editing and prime editing for accurate insertion of single nucleotide polymorphisms (SNPs). These methodologies can be either used for disease modeling or for disease-associated mutation corrections for SNPs or even more complex scenarios as repeated expansions. For example, a recent study reported successful excision of hexanucleotide repeat expansions in

patient-derived iPSC neurons, brain organoid and mouse models of ALS amyotrophic lateral sclerosis (ALS) and frontotemporal dementia (FTD) (184). These tools can be virtually applied in any model of interest for a selected indication, broadening the possibilities to discover novel therapeutics.

To conclude, all these initiatives confirm that we are in a change of era in biomedical research and drug discovery. Over the next 5 years, it is likely that the use of cell based models or larval models as zebrafish will continue to grow in research as scientists seek to reduce reliance on traditional animal models and develop more efficient and ethical methods of disease modeling, drug discovery and toxicology testing.

Author contributions

CM, MM, DC, GS-E, and VD conceptualized the study and reviewed and edited the manuscript. CM and MM performed bibliographic research. DC conceptualized and prepared the supporting figures. GS-E and VD prepared the original draft. All authors have read and agreed to the published version of the manuscript.

Acknowledgments

We would like to acknowledge Valentina Schiavone for help and critical discussion on the manuscript.

Conflict of interest

All authors are employees of ZeClinics SL, a contract research organization using the zebrafish model for research in disease modeling, target validation and drug screening.

Publisher's note

All claims expressed in this article are solely those of the authors and do not necessarily represent those of their affiliated organizations, or those of the publisher, the editors and the reviewers. Any product that may be evaluated in this article, or claim that may be made by its manufacturer, is not guaranteed or endorsed by the publisher.

References

1. WHO (2023). *Epilepsy, epilepsy - World Health Organization*. Available at: <https://www.who.int/news-room/fact-sheets/detail/epilepsy> (Accessed April 27, 2023).
2. Fisher RS, Boas WE, Blume W, Elger C, Genton P, Lee P, et al. Epileptic seizures and epilepsy: definitions proposed by the international league against epilepsy (ILAE) and the International Bureau for Epilepsy (IBE). *Epilepsia*. (2005) 46:470–2. doi: 10.1111/j.0013-9580.2005.66104.x
3. Fisher RS, Cross JH, D'Souza C, French JA, Haut SR, Higurashi N, et al. Instruction manual for the ILAE 2017 operational classification of seizure types. *Epilepsia*. (2017) 58:531–42. doi: 10.1111/epi.13671
4. Fisher RS, Cross JH, French JA, Higurashi N, Hirsch E, Jansen FE, et al. Operational classification of seizure types by the international league against epilepsy: position paper of the ILAE commission for classification and terminology. *Epilepsia*. (2017) 58:522–30. doi: 10.1111/epi.13670
5. Devinsky O, Vezzani A, O'Brien TJ, Jette N, Scheffer IE, de Curtis M, et al. Epilepsy. *Nat Rev Dis Primers*. (2018) 4:18024. doi: 10.1038/nrdp.2018.24
6. Fisher RS, Cross H, D'Souza C, French JA, Haut S, Higurashi N, et al. 2017 international league against epilepsy classifications of seizures and epilepsy are steps in the right direction. *Epilepsia*. (2019) 60:1040–4. doi: 10.1111/epi.15052
7. Bhalla D, Godet B, Druet-Cabanac M, Preux PM. Etiologies of epilepsy: a comprehensive review. *Expert Rev Neurother*. (2011) 11:861–76. doi: 10.1586/ern.11.51
8. Scheffer IE, Berkovic S, Capovilla G, Connolly MB, French J, Guilhoto L, et al. ILAE classification of the epilepsies: position paper of the ILAE commission for classification and terminology. *Epilepsia*. (2017) 58:512–21. doi: 10.1111/epi.13709
9. Winter MJ, Ono Y, Ball JS, Walentinsson A, Michaelsson E, Tochwin A, et al. A combined human in silico and CRISPR/Cas9-mediated *in vivo* zebrafish based approach

- to provide phenotypic data for supporting early target validation. *Front Pharmacol.* (2022) 13:827686. doi: 10.3389/fphar.2022.827686
10. Ellis CA, Petrovski S, Berkovic SF. Epilepsy genetics: clinical impacts and biological insights, the lancet. *Neurology.* (2020) 19:93–100. doi: 10.1016/S1474-4422(19)30269-8
11. Ding J, Li X, Tian H, Wang L, Guo B, Wang Y, et al. SCN1A mutation-beyond Dravet syndrome: a systematic review and narrative synthesis. *Front Neurol.* (2021) 12:743726. doi: 10.3389/fneur.2021.743726
12. Steel D, Symonds JD, Zuberi SM, Brunklaus A. Dravet syndrome and its mimics: beyond SCN1A. *Epilepsia.* (2017) 58:1807–16. doi: 10.1111/epi.13889
13. Hirose S. Mutant GABA(A) receptor subunits in genetic (idiopathic) epilepsy. *Prog Brain Res.* (2014) 213:55–85. doi: 10.1016/B978-0-444-63326-2.00003-X
14. Wynshaw-Boris A, Pramparo T, Youn YH, Hirotsune S. Lissencephaly: mechanistic insights from animal models and potential therapeutic strategies. *Semin Cell Dev Biol.* (2010) 21:823–30. doi: 10.1016/j.semcdb.2010.07.008
15. Perucca P, Bahlo M, Berkovic SF. The genetics of epilepsy. *Annu Rev Genomics Hum Genet.* (2020) 21:205–30. doi: 10.1146/annurev-genom-120219-074937
16. Galizia EC, Myers CT, Leu C, de Kovel CG, Afrikanova T, Cordero-Maldonado ML, et al. CHD2 variants are a risk factor for photosensitivity in epilepsy. *Brain.* (2015) 138:1198–207. doi: 10.1093/brain/awv052
17. Mastrangelo M. Lennox-Gastaut syndrome: a state of the art review. *Neuropediatrics.* (2017) 48:143–51. doi: 10.1055/s-0037-1601324
18. Samanta D. PCDH19-related epilepsy syndrome: a comprehensive clinical review. *Pediatr Neurol.* (2020) 105:3–9. doi: 10.1016/j.pediatrneurol.2019.10.009
19. Epi4K Consortium. De novo mutations in SLC1A2 and CACNA1A are important causes of epileptic encephalopathies. *Am J Hum Genet.* (2016) 99:287–98. doi: 10.1016/j.ajhg.2016.06.003
20. EpiPM Consortium. A roadmap for precision medicine in the epilepsies. *Lancet Neurol.* (2015) 14:1219–28. doi: 10.1016/S1474-4422(15)00199-4
21. Montanucci L, Lewis-Smith D, Collins RL, Niestroj LM, Parthasarathy S, Xian J, et al. Genome-wide identification and phenotypic characterization of seizure-associated copy number variations in 741,075 individuals. *Nat Commun.* (2023) 14:4392. doi: 10.1038/s41467-023-39539-6
22. The International League Against Epilepsy Consortium on Complex Epilepsies. Abou-Khalil B, Auce P, Avbersek A, Bahlo M, Balding DJ, et al. Genome-wide mega-analysis identifies 16 loci and highlights diverse biological mechanisms in the common epilepsies. *Nat Commun.* (2018) 9:5269. doi: 10.1038/s41467-018-07524-z
23. Hewson S, Puka K, Mercimek-Mahmutoglu S. Variable expressivity of a likely pathogenic variant in KCNQ2 in a three-generation pedigree presenting with intellectual disability with childhood onset seizures. *Am J Med Genet A.* (2017) 173:2226–30. doi: 10.1002/ajmg.a.38281
24. Marini C, Porro A, Rastetter A, Dalle C, Rivolta I, Bauer D, et al. HCN1 mutation spectrum: from neonatal epileptic encephalopathy to benign generalized epilepsy and beyond. *Brain.* (2018) 141:3160–78. doi: 10.1093/brain/awy263
25. Hawkins NA, Zachwieja NJ, Miller AR, Anderson LL, Kearney JA. Fine mapping of a Dravet syndrome modifier locus on mouse chromosome 5 and candidate gene analysis by RNA-Seq. *PLoS Genet.* (2016) 12:e1006398. doi: 10.1371/journal.pgen.1006398
26. de Lange IM, Mulder F, van 't Slot R, Sonsma ACM, van Kempen M, Nijman JJ, et al. Modifier genes in SCN1A-related epilepsy syndromes. *Mol Genet Genomic Med.* (2020) 8:e1103. doi: 10.1002/mgg3.1103
27. Heinzen EL. Somatic variants in epilepsy - advancing gene discovery and disease mechanisms. *Curr Opin Genet Dev.* (2020) 65:1–7. doi: 10.1016/j.gde.2020.04.004
28. Kang S, Graham JM Jr, Olney AH, Biesecker LG. GLI3 frameshift mutations cause autosomal dominant Pallister-hall syndrome. *Nat Genet.* (1997) 15:266–8. doi: 10.1038/ng0397-266
29. Corbett MA, Depienne C, Veneziano L, Klein KM, Brancati F, Guerrini R, et al. Genetics of familial adult myoclonus epilepsy: from linkage studies to noncoding repeat expansions. *Epilepsia.* (2023) 64 Suppl 1:S14–21. doi: 10.1111/epi.17610
30. Plaster NM, Uyama E, Uchino M, Ikeda T, Flanagan KM, Kondo I, et al. Genetic localization of the familial adult myoclonic epilepsy (FAME) gene to chromosome 8q24. *Neurology.* (1999) 53:1180–3. doi: 10.1212/wnl.53.6.1180
31. Ishiura H, Doi K, Mitsui J, Yoshimura J, Matsukawa MK, Fujiyama A, et al. Expansions of intronic TTCA and TTTTA repeats in benign adult familial myoclonic epilepsy. *Nat Genet.* (2018) 50:581–90. doi: 10.1038/s41588-018-0067-2
32. Vezzani A, Fujinami RS, White HS, Preux PM, Blümcke I, Sander JW, et al. Infections, inflammation and epilepsy. *Acta Neuropathol.* (2016) 131:211–34. doi: 10.1007/s00401-015-1481-5
33. Feinstein AR. The pre-therapeutic classification of co-morbidity in chronic disease. *J Chronic Dis.* (1970) 23:455–68. doi: 10.1016/0021-9681(70)90054-8
34. Keezer MR, Sisodiya SM, Sander JW. Comorbidities of epilepsy: current concepts and future perspectives, the lancet. *Neurology.* (2016) 15:106–15. doi: 10.1016/S1474-4422(15)00225-2
35. Giussani G, Bianchi E, Beretta S, Carone D, DiFrancesco JC, Stabile A, et al. Comorbidities in patients with epilepsy: frequency, mechanisms and effects on long-term outcome. *Epilepsia.* (2021) 62:2395–404. doi: 10.1111/epi.17022
36. Löscher W, Klein P. The pharmacology and clinical efficacy of Antiepileptic medications: from bromide salts to Cenobamate and beyond. *CNS Drugs.* (2021) 35:935–63. doi: 10.1007/s40263-021-00827-8
37. Gilman JT, Duchowny M, Campo AE. Pharmacokinetic considerations in the treatment of childhood epilepsy. *Paediatr Drugs.* (2003) 5:267–77. doi: 10.2165/00128072-200305040-00005
38. Markowitz GJ, Kadam SD, Boothe DM, Irving ND, Comi AM. The pharmacokinetics of commonly used antiepileptic drugs in immature CD1 mice. *Neuroreport.* (2010) 21:452–6. doi: 10.1097/wnr.0b013e328338ba18
39. Kulkarni AD, Patel HM, Surana SJ, Belgamwar VS, Pardeshi CV. Brain-blood ratio: implications in brain drug delivery. *Expert Opin Drug Deliv.* (2016) 13:85–92. doi: 10.1517/17425247.2016.1092519
40. Stangler LA, Kouzani A, Bennet KE, Dumeé L, Berk M, Worrell GA, et al. Microdialysis and microperfusion electrodes in neurological disease monitoring. *Fluids Barriers CNS.* (2021) 18:52. doi: 10.1186/s12987-021-00292-x
41. Bagchi S, Chhibber T, Lahooti B, Verma A, Borse V, Jayant RD. In-vitro blood-brain barrier models for drug screening and permeation studies: an overview. *Drug Dev Deliv Ther.* (2019) 13:3591–605. doi: 10.2147/DDDT.S218708
42. Tong X, Wang D, Ding X, Tan X, Ren Q, Chen G, et al. Blood-brain barrier penetration prediction enhanced by uncertainty estimation. *J Chem.* (2022) 14:44. doi: 10.1186/s13321-022-00619-2
43. Chung T.D.Y., Terry D.B., Smith L.H. (2004) *In vitro* and *in vivo* assessment of ADME and PK properties during lead selection and lead optimization – guidelines, benchmarks and rules of thumb, in S. Markossian et al. (eds) *Assay guidance manual*. Bethesda, MD: Eli Lilly & Company and the National Center for Advancing Translational Sciences. Available at: <http://www.ncbi.nlm.nih.gov/books/NBK326710/> (Accessed July 27, 2023).
44. Helms HC, Abbott NJ, Burek M, Cecchelli R, Couraud PO, Deli MA, et al. *In vitro* models of the blood-brain barrier: an overview of commonly used brain endothelial cell culture models and guidelines for their use. *J Cereb Blood Flow Metab.* (2016) 36:862–90. doi: 10.1177/0271678X16630991
45. Achenbach JC, Hui JPM, Berrue F, Woodland C, Ellis LD. Evaluation of the Uptake, Metabolism, and Secretion of Toxicants by Zebrafish Larvae. *Toxicol Sci.* (2022) 190:133–145. doi: 10.1093/toxsci/kfac102
46. Kim SS, Im SH, Yang JY, Lee YR, Kim GR, Chae JS, et al. Zebrafish as a screening model for testing the permeability of blood-brain barrier to small molecules. *Zebrafish.* (2017) 14:322–30. doi: 10.1089/zeb.2016.1392
47. Löscher W. Critical review of current animal models of seizures and epilepsy used in the discovery and development of new antiepileptic drugs. *Seizure.* (2011) 20:359–68. doi: 10.1016/j.seizure.2011.01.003
48. Löscher W. Animal models of seizures and epilepsy: past, present, and future role for the discovery of antiepileptic drugs. *Neurochem Res.* (2017) 42:1873–88. doi: 10.1007/s11064-017-2222-z
49. Castel-Branco MM, Alves GL, Figueiredo IV, Falcao AC, Caramona MM. The maximal electroshock seizure (MES) model in the preclinical assessment of potential new antiepileptic drugs. *Methods Find Exp Clin Pharmacol.* (2009) 31:101–6. doi: 10.1358/mf.2009.31.2.1338414
50. Barton ME, Klein BD, Wolf HH, Steve White H. Pharmacological characterization of the 6 Hz psychomotor seizure model of partial epilepsy. *Epilepsy Res.* (2001) 47:217–27. doi: 10.1016/s0920-1211(01)00302-3
51. Metcalf CS, West PJ, Thomson KE, Edwards SF, Smith MD, White HS, et al. Development and pharmacologic characterization of the rat 6 Hz model of partial seizures. *Epilepsia.* (2017) 58:1073–84. doi: 10.1111/epi.13764
52. Leclercq K, Matagne A, Kaminski RM. Low potency and limited efficacy of antiepileptic drugs in the mouse 6 Hz corneal kindling model. *Epilepsy Res.* (2014) 108:675–83. doi: 10.1016/j.eplepsyres.2014.02.013
53. Goddard GV, McIntyre DC, Leech CK. A permanent change in brain function resulting from daily electrical stimulation. *Exp Neurol.* (1969) 25:295–330. doi: 10.1016/0014-4886(69)90128-9
54. Löscher W, Jäckel R, Czuczwar SJ. Is amygdala kindling in rats a model for drug-resistant partial epilepsy? *Exp Neurol.* (1986) 93:211–26. doi: 10.1016/0014-4886(86)90160-3
55. Snead OC, Banerjee PK, Burnham MI, Hampson D. Modulation of absence seizures by the GABA(A) receptor: a critical role for metabotropic glutamate receptor 4 (mGluR4), the journal of neuroscience: the official journal of the society for. *Neuroscience.* (2000) 20:6218–24. doi: 10.1523/JNEUROSCI.20-16-06218.2000
56. André V, Pineau N, Motte JE, Marescaux C, Nehlig A. Mapping of neuronal networks underlying generalized seizures induced by increasing doses of pentylenetetrazol in the immature and adult rat: a c-Fos immunohistochemical study. *Eur J Neurosci.* (1998) 10:2094–106. doi: 10.1046/j.1460-9568.1998.00223.x
57. Dhir A. Pentylenetetrazol (PTZ) kindling model of epilepsy. *Curr Prot Neurosci.* (2012) 9:Unit9.37. doi: 10.1002/0471142301.ns0937s58
58. Gawel K, Langlois M, Martins T, van der Ent W, Tiraboschi E, Jacmin M, et al. Seizing the moment: zebrafish epilepsy models. *Neurosci Biobehav Rev.* (2020) 116:1–20. doi: 10.1016/j.neubiorev.2020.06.010
59. Trinka E, Cock H, Hesdorffer D, Rossetti AO, Scheffer IE, Shinnar S, et al. A definition and classification of status epilepticus—report of the ILAE task force on classification of status epilepticus. *Epilepsia.* (2015) 56:1515–23. doi: 10.1111/epi.13121

60. Leite JP, Garcia-Cairasco N, Cavalheiro EA. New insights from the use of pilocarpine and kainate models. *Epilepsy Res.* (2002) 50:93–103. doi: 10.1016/S0920-1211(02)00072-4
61. Marshall GF, Gonzalez-Sulser A, Abbott CM. Modelling epilepsy in the mouse: challenges and solutions. *Dis Model Mech.* (2021) 14:dmm047449. doi: 10.1242/dmm.047449
62. Jones DL, Baraban SC. Characterization of inhibitory circuits in the malformed hippocampus of *Lis1* mutant mice. *J Neurophysiol.* (2007) 98:2737–46. doi: 10.1152/jn.00938.2007
63. Griffin A, Hamling KR, Hong SG, Anvar M, Lee LP, Baraban SC. Preclinical animal models for Dravet syndrome: seizure phenotypes, comorbidities and drug screening. *Front Pharmacol.* (2018) 9:573. doi: 10.3389/fphar.2018.00573
64. Kalume F, Yu FH, Westenbroek RE, Scheuer T, Catterall WA. Reduced sodium current in Purkinje neurons from *Nav1.1* mutant mice: implications for ataxia in severe myoclonic epilepsy in infancy. *J Neurosci Off J Soc Neurosci.* (2007) 27:11065–74. doi: 10.1523/JNEUROSCI.2162-07.2007
65. Yu FH, Mantegazza M, Westenbroek RE, Robbins CA, Kalume F, Burton KA, et al. Reduced sodium current in GABAergic interneurons in a mouse model of severe myoclonic epilepsy in infancy. *Nat Neurosci.* (2006) 9:1142–9. doi: 10.1038/nn1754
66. Han S, Tai C, Westenbroek RE, Yu FH, Cheah CS, Potter GB, et al. Autistic-like behaviour in *Scn1a*+/- mice and rescue by enhanced GABA-mediated neurotransmission. *Nature.* (2012) 489:385–90. doi: 10.1038/nature11356
67. Hawkins NA, Jurado M, Thaxton TT, Duarte SE, Barse L, Tatsukawa T, et al. Soticlestat, a novel cholesterol 24-hydroxylase inhibitor, reduces seizures and premature death in Dravet syndrome mice. *Epilepsia.* (2021) 62:2845–57. doi: 10.1111/epi.17062
68. Cunliffe VT, Baines RA, Giachello CNG, Lin WH, Morgan A, Reuber M, et al. Epilepsy research methods update: understanding the causes of epileptic seizures and identifying new treatments using non-mammalian model organisms. *Seizure.* (2015) 24:44–51. doi: 10.1016/j.seizure.2014.09.018
69. Kiani AK, Pheby D, Henahan G, Brown R, Sieving P, Sykora P, et al. Ethical considerations regarding animal experimentation. *J Prev Med Hyg.* (2022) 63:E255–66. doi: 10.15167/2421-4248/jpmh2022.63.2S3.2768
70. DAmora M, Galgani A, Marchese M, Tantussi F, Faraguna U, de Angelis F, et al. Zebrafish as an innovative tool for epilepsy modeling: state of the art and potential future directions. *Int J Mol Sci.* (2023) 24:7702. doi: 10.3390/ijms24097702
71. Riskey MG, Kelly SP, Jia K, Grill B, Dawson-Scully K. Modulating behavior in *C. elegans* using electroshock and antiepileptic drugs. *PLoS One.* (2016) 11:e0163786. doi: 10.1371/journal.pone.0163786
72. Wong SQ, Jones A, Dodd S, Grimes D, Barclay JW, Marson AG, et al. A *Caenorhabditis elegans* assay of seizure-like activity optimised for identifying antiepileptic drugs and their mechanisms of action. *J Neurosci Methods.* (2018) 309:132–42. doi: 10.1016/j.jneumeth.2018.09.004
73. Fischer FP, Karge RA, Weber YG, Koch H, Wolking S, Voigt A. *Drosophila melanogaster* as a versatile model organism to study genetic epilepsies: an overview. *Front Mol Neurosci.* (2023) 16:1116000. doi: 10.3389/fnmol.2023.1116000
74. Humpel C. Organotypic brain slice cultures: a review. *Neuroscience.* (2015) 305:86–98. doi: 10.1016/j.neuroscience.2015.07.086
75. Linsley JW, Tripathi A, Epstein I, Schmunk G, Mount E, Campioni M, et al. Automated four-dimensional long term imaging enables single cell tracking within organotypic brain slices to study neurodevelopment and degeneration. *Commun Bio.* (2019) 2:155. doi: 10.1038/s42003-019-0411-9
76. Farrell JS, Colangeli R, Wolff MD, Wall AK, Phillips TJ, George A, et al. Postictal hypoperfusion/hypoxia provides the foundation for a unified theory of seizure-induced brain abnormalities and behavioral dysfunction. *Epilepsia.* (2017) 58:1493–1501. doi: 10.1111/epi.13827
77. Noraberg J, Kristensen BW, Zimmer J. Markers for neuronal degeneration in organotypic slice cultures, brain research. *Brain Res Protocol.* (1999) 3:278–90. doi: 10.1016/S1385-299X(98)00050-6
78. Croft CL, Futch HS, Moore BD, Golde TE. Organotypic brain slice cultures to model neurodegenerative proteinopathies. *Mol Neurodegener.* (2019) 14:45. doi: 10.1186/s13024-019-0346-0
79. Jansen NA, Dehghani A, Breukel C, Tolner EA, van den Maagdenberg A. Focal and generalized seizure activity after local hippocampal or cortical ablation of *NaV 1.1* channels in mice. *Epilepsia.* (2020) 61:e30–6. doi: 10.1111/epi.16482
80. Spratt PWE, Ben-Shalom R, Keeshen CM, Burke KJ Jr, Clarkson RL, Sanders SJ, et al. The autism-associated gene *Scn2a* contributes to dendritic excitability and synaptic function in the prefrontal cortex. *Neuron.* (2019) 103:673–685.e5. doi: 10.1016/j.neuron.2019.05.037
81. Croft CL, Kurbatskaya K, Hanger DP, Noble W. Inhibition of glycogen synthase kinase-3 by BTA-EG4 reduces tau abnormalities in an organotypic brain slice culture model of Alzheimer's disease. *Sci Rep.* (2017) 7:7434. doi: 10.1038/s41598-017-07906-1
82. Raimondo JV, Heinemann U, de Curtis M, Goodkin HP, Dulla CG, Janigro D, et al. Methodological standards for *in vitro* models of epilepsy and epileptic seizures. A TASK1-WG4 report of the AES/LAE translational TASK force of the ILAE. *Epilepsia.* (2017) 58 Suppl 4:40–52. doi: 10.1111/epi.13901
83. Albus K, Heinemann U, Kovács R. Network activity in hippocampal slice cultures revealed by long-term *in vitro* recordings. *J Neurosci Methods.* (2013) 217:1–8. doi: 10.1016/j.jneumeth.2013.04.014
84. Magalhães DM, Pereira N, Rombo DM, Beltrão-Cavacas C, Sebastião AM, Valente CA. Ex vivo model of epilepsy in organotypic slices—a new tool for drug screening. *J Neuroinflammation.* (2018) 15:203. doi: 10.1186/s12974-018-1225-2
85. Stoppini L, Buchs PA, Muller D. A simple method for organotypic cultures of nervous tissue. *J Neurosci Methods.* (1991) 37:173–82. doi: 10.1016/0165-0270(91)90128-m
86. De Simoni A, Yu LMY. Preparation of organotypic hippocampal slice cultures: interface method. *Nat Protoc.* (2006) 1:1439–45. doi: 10.1038/nprot.2006.228
87. Schwarz N, Uysal B, Welzer M, Bahr JC, Layer N, Löffler H, et al. Long-term adult human brain slice cultures as a model system to study human CNS circuitry and disease. *eLife.* (2019) 8:e48417. doi: 10.7554/eLife.48417
88. Jones RSG, da Silva AB, Whittaker RG, Woodhall GL, Cunningham MO. Human brain slices for epilepsy research: pitfalls, solutions and future challenges. *J Neurosci Methods.* (2016) 260:221–32. doi: 10.1016/j.jneumeth.2015.09.021
89. Shi Y, Inoue H, Wu JC, Yamanaka S. Induced pluripotent stem cell technology: a decade of progress. *Nat Rev Drug Discov.* (2017) 16:115–30. doi: 10.1038/nrd.2016.245
90. Bassett AR. Editing the genome of hiPSC with CRISPR/Cas9: disease models. *Mamm Genome.* (2017) 28:348–64. doi: 10.1007/s00335-017-9684-9
91. Srikanth P, Young-Pearse TL. Stem cells on the brain: modeling neurodevelopmental and neurodegenerative diseases using human induced pluripotent stem cells. *J Neurogenet.* (2014) 28:5–29. doi: 10.1007/01677063.2014.881358
92. Tidball AM, Parent JM. Concise review: exciting cells: modeling genetic epilepsies with patient-derived induced pluripotent stem cells. *Stem Cells.* (2016) 34:27–33. doi: 10.1002/stem.2203
93. Simkin D, Ambrosi C, Marshall KA, Williams LA, Eisenberg J, Gharib M, et al. Channeling therapeutic discovery for epileptic encephalopathy through iPSC technologies. *Trends Pharmacol Sci.* (2022) 43:392–405. doi: 10.1016/j.tips.2022.03.001
94. Hirose S, Tanaka Y, Shibata M, Kimura Y, Ishikawa M, Higurashi N, et al. Application of induced pluripotent stem cells in epilepsy. *Mol Cell Neurosci.* (2020) 108:103535. doi: 10.1016/j.mcn.2020.103535
95. Javadi MS, Tan T, Dvir N, Anderson A, O'Brien TJ, Kwan P, et al. Human *in vitro* models of epilepsy using embryonic and induced pluripotent stem cells. *Cells.* (2022) 11:3957. doi: 10.3390/cells11243957
96. Higurashi N, Uchida T, Lossin C, Misumi Y, Okada Y, Akamatsu W, et al. A human Dravet syndrome model from patient induced pluripotent stem cells, molecular. *Brain.* (2013) 6:19. doi: 10.1186/1756-6606-6-19
97. Jiao J, Yang Y, Shi Y, Chen J, Gao R, Fan Y, et al. Modeling Dravet syndrome using induced pluripotent stem cells (iPSCs) and directly converted neurons. *Hum Mol Genet.* (2013) 22:4241–52. doi: 10.1093/hmg/ddt275
98. Liu Y, Lopez-Santiago LF, Yuan Y, Jones JM, Zhang H, O'Malley HA, et al. Dravet syndrome patient-derived neurons suggest a novel epilepsy mechanism. *Ann Neurol.* (2013) 74:128–39. doi: 10.1002/ana.23897
99. Cheung AYL, Horvath LM, Grafodatskaya D, Pasceri P, Weksberg R, Hotta A, et al. Isolation of MECP2-null Rett syndrome patient hiPS cells and isogenic controls through X-chromosome inactivation. *Hum Mol Genet.* (2011) 20:2103–15. doi: 10.1093/hmg/ddr093
100. Marchetto MCN, Carronmeu C, Acab A, Yu D, Yeo GW, Mu Y, et al. A model for neural development and treatment of Rett syndrome using human induced pluripotent stem cells. *Cells.* (2010) 143:527–39. doi: 10.1016/j.cell.2010.10.016
101. Chamberlain SJ, Chen PF, Ng KY, Bourgois-Rocha F, Lemtiri-Chlieh F, Levine ES, et al. Induced pluripotent stem cell models of the genomic imprinting disorders Angelman and Prader-Willi syndromes. *Proc Natl Acad Sci U S A.* (2010) 107:17668–73. doi: 10.1073/pnas.1004487107
102. Simkin D, Kiskinis E. Modeling pediatric epilepsy through iPSC-based technologies, epilepsy. *Currents.* (2018) 18:240–5. doi: 10.5698/1535-7597.18.4.240
103. McTague A, Rossignoli G, Ferrini A, Barral S, Kurian MA. Genome editing in iPSC-based neural systems: from disease models to future therapeutic strategies. *Front Genome Edit.* (2021) 3:630600. doi: 10.3389/fgeed.2021.630600
104. Kwart D, Gregg A, Sheckel C, Murphy EA, Paquet D, Duffield M, et al. A large panel of isogenic APP and PSEN1 mutant human iPSC neurons reveals shared endosomal abnormalities mediated by APP β -CTFs, not A β . *Neuron.* (2019) 104:256–270.e5. doi: 10.1016/j.neuron.2019.07.010
105. Liu J, Gao C, Chen W, Ma W, Li X, Shi Y, et al. CRISPR/Cas9 facilitates investigation of neural circuit disease using human iPSCs: mechanism of epilepsy caused by an SCN1A loss-of-function mutation, translational. *Transl Psychiatry.* (2016) 6:e703. doi: 10.1038/tp.2015.203
106. Xie Y, Ng NN, Safrina OS, Ramos CM, Ess KC, Schwartz PH, et al. Comparisons of dual isogenic human iPSC pairs identify functional alterations directly caused by an epilepsy associated SCN1A mutation. *Neurobiol Dis.* (2020) 134:104627. doi: 10.1016/j.nbd.2019.104627

107. Simkin D, Marshall KA, Vanoye CG, Desai RR, Bustos BI, Piyevsky BN, et al. Dyshomeostatic modulation of Ca^{2+} -activated K^+ channels in a human neuronal model of KCNQ2 encephalopathy. *eLife*. (2021) 10:e64434. doi: 10.7554/eLife.64434
108. Lancaster MA, Renner M, Martin CA, Wenzel D, Bicknell LS, Hurler ME, et al. Cerebral organoids model human brain development and microcephaly. *Nature*. (2013) 501:373–9. doi: 10.1038/nature12517
109. Li W, Sun W, Zhang Y, Wei W, Ambasudhan R, Xia P, et al. Rapid induction and long-term self-renewal of primitive neural precursors from human embryonic stem cells by small molecule inhibitors. *Proc Natl Acad Sci U S A*. (2011) 108:8299–304. doi: 10.1073/pnas.1014041108
110. Benito-Kwiecinski S, Lancaster MA. Brain organoids: human neurodevelopment in a dish. *Cold Spring Harb Perspect Biol*. (2020) 12:a035709. doi: 10.1101/cshperspect.a035709
111. Di Lullo E, Kriegstein AR. The use of brain organoids to investigate neural development and disease. *Nat Rev Neurosci*. (2017) 18:573–84. doi: 10.1038/nrn.2017.107
112. Qian X, Song H, Ming G-L. Brain organoids: advances, applications and challenges. *Development*. (2019) 146:dev166074. doi: 10.1242/dev.166074
113. Kanton S, Pasca SP. Human assembloids. *Development*. (2022) 149:dev201120. doi: 10.1242/dev.201120
114. Miura Y, Li MY, Revah O, Yoon SJ, Narazaki G, Pasca SP. Engineering brain assembloids to interrogate human neural circuits. *Nat Protoc*. (2022) 17:15–35. doi: 10.1038/s41596-021-00632-z
115. Zhu Y, Zhang X, Sun L, Wang Y, Zhao Y. Engineering human brain assembloids by microfluidics. *Adv Mater*. (2023) 35:e2210083. doi: 10.1002/adma.202210083
116. Nieto-Estévez V, Hsieh J. Human brain organoid models of developmental epilepsies, epilepsy. *Currents*. (2020) 20:282–90. doi: 10.1177/1535759720949254
117. di Matteo F, Picicelli F, Kyroutsi C, Tovecci I, Penna E, Crispino M, et al. Cystatin B is essential for proliferation and interneuron migration in individuals with EPM1 epilepsy. *EMBO Mol Med*. (2020) 12:e11419. doi: 10.15252/emmm.201911419
118. Hengel H, Bosso-Lefèvre C, Grady G, Szenker-Ravi E, Li H, Pierce S, et al. Loss-of-function mutations in UDP-glucose 6-dehydrogenase cause recessive developmental epileptic encephalopathy. *Nat Commun*. (2020) 11:595. doi: 10.1038/s41467-020-14360-7
119. Sun AX, Yuan Q, Fukuda M, Yu W, Yan H, Lim GGY, et al. Potassium channel dysfunction in human neuronal models of Angelman syndrome. *Science*. (2019) 366:1486–92. doi: 10.1126/science.aav5386
120. Samarasinghe RA, Miranda OA, Buth JE, Mitchell S, Ferando I, Watanabe M, et al. Identification of neural oscillations and epileptiform changes in human brain organoids. *Nat Neurosci*. (2021) 24:1488–500. doi: 10.1038/s41593-021-00906-5
121. Steinberg DJ, Repudi S, Saleem A, Kustanovich I, Viukov S, Abudiah B, et al. Modeling genetic epileptic encephalopathies using brain organoids. *EMBO Mol Med*. (2021) 13:e13610. doi: 10.15252/emmm.202013610
122. Pellegrini L, Bonfio C, Chadwick J, Begum F, Skehel M, Lancaster MA. Human CNS barrier-forming organoids with cerebrospinal fluid production. *Science*. (2020) 369:eaaz5626. doi: 10.1126/science.aaz5626
123. Sakai C, Ijaz S, Hoffman EJ. Zebrafish models of neurodevelopmental disorders: past, present, and future. *Front Mol Neurosci*. (2018) 11:294. doi: 10.3389/fnmol.2018.00294
124. Cornet C, Di Donato V, Terriente J. Combining zebrafish and CRISPR/Cas9: toward a more efficient drug discovery pipeline. *Front Pharmacol*. (2018) 9:703. doi: 10.3389/fphar.2018.00703
125. Rubbini D, Cornet C, Terriente J, di Donato V. CRISPR meets zebrafish: accelerating the discovery of new therapeutic targets. *SLAS Discov*. (2020) 25:552–67. doi: 10.1177/2472555220926920
126. Yakis E, Jamali A, Diaz Verdugo C, Jurisch-Yaksi N. Past, present and future of zebrafish in epilepsy research. *FEBS J*. (2021) 288:7243–7255. doi: 10.1111/febs.15694
127. Kundap UP, Kumari Y YK, Othman I IO, Shaikh MF MFS. Zebrafish as a model for epilepsy-induced cognitive dysfunction: a pharmacological, biochemical and behavioral approach. *Front Pharmacol*. (2017) 8:515. doi: 10.3389/fphar.2017.00515
128. Kalueff AV, Stewart AM, Gerlai R. Zebrafish as an emerging model for studying complex brain disorders. *Trends Pharmacol Sci*. (2014) 35:63–75. doi: 10.1016/j.tips.2013.12.002
129. Amo R, Aizawa H, Takahoko M, Kobayashi M, Takahashi R, Aoki T, et al. Identification of the zebrafish ventral habenula as a homolog of the mammalian lateral habenula. *J Neurosci Off J Soc Neurosci*. (2010) 30:1566–74. doi: 10.1523/JNEUROSCI.3690-09.2010
130. Mueller T, Vernier P, Wullmann MF. The adult central nervous cholinergic system of a neurogenetic model animal, the zebrafish *Danio rerio*. *Brain Res*. (2004) 1011:156–69. doi: 10.1016/j.brainres.2004.02.073
131. Rink E, Wullmann MF. Development of the catecholaminergic system in the early zebrafish brain: an immunohistochemical study. *Brain Res Dev Brain Res*. (2002) 137:89–100. doi: 10.1016/s0165-3806(02)00354-1
132. Köster RW, Fraser SE. FGF signaling mediates regeneration of the differentiating cerebellum through repatterning of the anterior hindbrain and reinitiation of neuronal migration, the journal of neuroscience: the official journal of the society for Neuroscience. (2006) 26:7293–304. doi: 10.1523/JNEUROSCI.0095-06.2006
133. Mathuru AS, Jesuthasan S. The medial habenula as a regulator of anxiety in adult zebrafish. *Front Neural Circ*. (2013) 7:99. doi: 10.3389/fncir.2013.00099
134. Beretta CA, Dross N, Guitierrez-Triana JA, Ryu S, Carl M. Habenula circuit development: past, present, and future. *Front Neurosci*. (2012) 6:51. doi: 10.3389/fnins.2012.00051
135. Welberg L. Psychiatric disorders: reining in the habenula? *Nat Rev Neurosci*. (2013) 14:668–9. doi: 10.1038/nrn3602
136. Anichtchik O, Sallinen V, Peitsaro N, Panula P. Distinct structure and activity of monoamine oxidase in the brain of zebrafish (*Danio rerio*). *J Comp Neurol*. (2006) 498:593–610. doi: 10.1002/cne.21057
137. Chen Y-C, Priyadarshini M, Panula P. Complementary developmental expression of the two tyrosine hydroxylase transcripts in zebrafish. *Histochem Cell Biol*. (2009) 132:375–81. doi: 10.1007/s00418-009-0619-8
138. Panula P, Sallinen V, Sundvik M, Kolehmainen J, Torkko V, Tiittula A, et al. Modulatory neurotransmitter systems and behavior: towards zebrafish models of neurodegenerative diseases. *Zebrafish*. (2006) 3:235–47. doi: 10.1089/zeb.2006.3.235
139. Becker TS, Rinkwitz S. Zebrafish as a genomics model for human neurological and polygenic disorders. *Dev Neurobiol*. (2012) 72:415–28. doi: 10.1002/dneu.20888
140. Panula P, Chen YC, Priyadarshini M, Kudo H, Semenova S, Sundvik M, et al. The comparative neuroanatomy and neurochemistry of zebrafish CNS systems of relevance to human neuropsychiatric diseases. *Neurobiol Dis*. (2010) 40:46–57. doi: 10.1016/j.nbd.2010.05.010
141. Griffiths BB, Schoonheim PJ, Ziv L, Voelker L, Baier H, Gahtan E. A zebrafish model of glucocorticoid resistance shows serotonergic modulation of the stress response. *Front Behav Neurosci*. (2012) 6:68. doi: 10.3389/fnbeh.2012.00068
142. Ziv L, Muto A, Schoonheim PJ, Meising SH, Strasser D, Ingraham HA, et al. An affective disorder in zebrafish with mutation of the glucocorticoid receptor. *Mol Psychiatry*. (2013) 18:681–91. doi: 10.1038/mp.2012.64
143. Egan RJ, Bergner CL, Hart PC, Cachat JM, Canavello PR, Elegante MF, et al. Understanding behavioral and physiological phenotypes of stress and anxiety in zebrafish. *Behav Brain Res*. (2009) 205:38–44. doi: 10.1016/j.bbr.2009.06.022
144. Dinday MT, Baraban SC. Large-scale phenotype-based antiepileptic drug screening in a zebrafish model of Dravet syndrome. *eNeuro*. (2015) 2:ENEURO.0068-15.2015. doi: 10.1523/ENEURO.0068-15.2015
145. Baraban SC, Taylor MR, Castro PA, Baier H. Pentylene tetrazole induced changes in zebrafish behavior, neural activity and c-fos expression. *Neuroscience*. (2005) 131:759–68. doi: 10.1016/j.neuroscience.2004.11.031
146. Afrikanova T, Serruys ASK, Buenafe OEM, Clinckers R, Smolders I, de Witte PAM, et al. Validation of the zebrafish pentylenetetrazol seizure model: locomotor versus electrophysiological responses to antiepileptic drugs. *PLoS One*. (2013) 8:e54166. doi: 10.1371/journal.pone.0054166
147. Krall RL, Penry JK, White BG, Kupferberg HJ, Swinyard EA. Antiepileptic drug development: II. Anticonvulsant drug screening. *Epilepsia*. (1978) 19:409–28. doi: 10.1111/j.1528-1157.1978.tb04507.x
148. Velišek L. CHAPTER 11 - models of chemically-induced acute seizures In: A Pitkänen, PA Schwartzkroin and SL Moshé, editors. *Models of seizures and epilepsy*. Burlington: Academic Press (2006). 127–52.
149. Bertoncello KT, Bonan CD. Zebrafish as a tool for the discovery of anticonvulsant compounds from botanical constituents. *Eur J Pharmacol*. (2021) 908:174342. doi: 10.1016/j.ejphar.2021.174342
150. Gupta P, Khobragade SB, Shingatgeri VM. Effect of various antiepileptic drugs in zebrafish PTZ-seizure model. *Indian J Pharm Sci*. (2014) 76:157–63.
151. Mandhane SN, Aavula K, Rajamannar T. Timed pentylenetetrazol infusion test: a comparative analysis with s.c.PTZ and MES models of anticonvulsant screening in mice. *Seizure*. (2007) 16:636–44. doi: 10.1016/j.seizure.2007.05.005
152. Alfaro JM, Ripoll-Gómez J, Burgos JS. Kainate administered to adult zebrafish causes seizures similar to those in rodent models. *Eur J Neurosci*. (2011) 33:1252–5. doi: 10.1111/j.1460-9568.2011.07622.x
153. Lévesque M, Avoli M. The kainic acid model of temporal lobe epilepsy. *Neurosci Biobehav Rev*. (2013) 37:2887–99. doi: 10.1016/j.neubiorev.2013.10.011
154. Kim Y-H, Lee Y, Lee K, Lee T, Kim YJ, Lee CJ. Reduced neuronal proliferation by proconvulsant drugs in the developing zebrafish brain. *Neurotoxicol Teratol*. (2010) 32:551–7. doi: 10.1016/j.ntt.2010.04.054
155. Heylen L, Pham DH, de Meulemeester AS, Samarut É, Skiba A, Copmans D, et al. Pericardial injection of Kainic acid induces a chronic epileptic state in larval zebrafish. *Front Mol Neurosci*. (2021) 14:753936. doi: 10.3389/fnmol.2021.753936
156. Duveau V, Pouyatos B, Bressand K, Bouyssières C, Chabrol T, Roche Y, et al. Differential effects of antiepileptic drugs on focal seizures in the Intrahippocampal Kainate mouse model of mesial temporal lobe epilepsy. *CNS Neurosci Ther*. (2016) 22:497–506. doi: 10.1111/cns.12523
157. Mahmood F, Mozere M, Zdebek AA, Stanescu HC, Tobin J, Beales PL, et al. Generation and validation of a zebrafish model of EAST (epilepsy, ataxia, sensorineural

deafness and tubulopathy) syndrome. *Dis Model Mech.* (2013) 6:652–60. doi: 10.1242/dmm.009480

158. Zdebek AA, Mahmood F, Stanescu HC, Kleta R, Bockenhauer D, Russell C. Epilepsy in *kcnj10* morphant zebrafish assessed with a novel method for long-term EEG recordings. *PLoS One.* (2013) 8:e79765. doi: 10.1371/journal.pone.0079765

159. Chege SW, Hortopan GA, Dinday MT, Baraban SC. Expression and function of KCNQ channels in larval zebrafish. *Dev Neurobiol.* (2012) 72:186–98. doi: 10.1002/dneu.20937

160. Schubert J, Siekierska A, Langlois M, May P, Huneau C, Becker F, et al. Mutations in STX1B, encoding a presynaptic protein, cause fever-associated epilepsy syndromes. *Nat Genet.* (2014) 46:1327–32. doi: 10.1038/ng.3130

161. Suls A, Jaehn JA, Kecskés A, Weber Y, Weckhuysen S, Craiu DC, et al. De novo loss-of-function mutations in CHD2 cause a fever-sensitive myoclonic epileptic encephalopathy sharing features with Dravet syndrome. *Am J Hum Genet.* (2013) 93:967–75. doi: 10.1016/j.ajhg.2013.09.017

162. Kok FO, Shin M, Ni CW, Gupta A, Grosse AS, van Impel A, et al. Reverse genetic screening reveals poor correlation between morpholino-induced and mutant phenotypes in zebrafish. *Dev Cell.* (2015) 32:97–108. doi: 10.1016/j.devcel.2014.11.018

163. el-Brolosy MA, Kontarakis Z, Rossi A, Kuenne C, Günther S, Fukuda N, et al. Genetic compensation triggered by mutant mRNA degradation. *Nature.* (2019) 568:193–7. doi: 10.1038/s41586-019-1064-z

164. Rossi A, Kontarakis Z, Gerri C, Nolte H, Hölper S, Krüger M, et al. Genetic compensation induced by deleterious mutations but not gene knockdowns. *Nature.* (2015) 524:230–3. doi: 10.1038/nature14580

165. Baraban SC, Dinday MT, Hortopan GA. Drug screening in *Scn1a* zebrafish mutant identifies clemizole as a potential Dravet syndrome treatment, nature. *Communications.* (2013) 4:2410. doi: 10.1038/ncomms3410

166. Griffin A, Anvar M, Hamling K, Baraban SC. Phenotype-based screening of synthetic cannabinoids in a Dravet syndrome zebrafish model. *Front Pharmacol.* (2020) 11:464. doi: 10.3389/fphar.2020.00464

167. Griffin A, Hamling KR, Knupp K, Hong S, Lee LP, Baraban SC. Clemizole and modulators of serotonin signalling suppress seizures in Dravet syndrome. *Brain.* (2017) 140:669–83. doi: 10.1093/brain/aww342

168. Griffin A, Carpenter C, Liu J, Paterno R, Grone B, Hamling K, et al. Phenotypic analysis of catastrophic childhood epilepsy genes. *Commun Biol.* (2021) 4:680. doi: 10.1038/s42003-021-02221-y

169. Burger A, Lindsay H, Felker A, Hess C, Anders C, Chiavacci E, et al. Maximizing mutagenesis with solubilized CRISPR-Cas9 ribonucleoprotein complexes. *Development.* (2016) 143:2025–37. doi: 10.1242/dev.134809

170. Shah AN, Moens CB, Miller AC. Targeted candidate gene screens using CRISPR/Cas9 technology. *Methods Cell Biol.* (2016) 135:89–106. doi: 10.1016/bs.mcb.2016.01.008

171. Kroll F, Powell GT, Ghosh M, Gestri G, Antinucci P, Hearn TJ, et al. A simple and effective F0 knockout method for rapid screening of behaviour and other complex phenotypes. *eLife.* (2021) 10:e59683. doi: 10.7554/eLife.59683

172. Bak RO, Gomez-Ospina N, Porteus MH. Gene editing on center stage. *Trends Genet.* (2018) 34:600–11. doi: 10.1016/j.tig.2018.05.004

173. Porto EM, Komor AC, Slaymaker IM, Yeo GW. Base editing: advances and therapeutic opportunities. *Nat Rev Drug Discov.* (2020) 19:839–59. doi: 10.1038/s41573-020-0084-6

174. Rosello M, Serafini M, Mignani L, Finazzi D, Giovannangeli C, Mione MC, et al. Disease modeling by efficient genome editing using a near PAM-less base editor *in vivo*. *Nat Commun.* (2022) 13:3435. doi: 10.1038/s41467-022-31172-z

175. Anzalone AV, Randolph PB, Davis JR, Sousa AA, Koblan LW, Levy JM, et al. Search-and-replace genome editing without double-strand breaks or donor DNA. *Nature.* (2019) 576:149–57. doi: 10.1038/s41586-019-1711-4

176. Petri K, Zhang W, Ma J, Schmidts A, Lee H, Horng JE, et al. CRISPR prime editing with ribonucleoprotein complexes in zebrafish and primary human cells. *Nat Biotechnol.* (2022) 40:189–93. doi: 10.1038/s41587-021-00901-y

177. European Medicines Agency (EMA) (2011) *Statement of the EMA position on the application of the 3Rs (replacement, reduction and refinement) in the regulatory testing of human and veterinary medicinal products*. Available at: https://www.ema.europa.eu/en/documents/other/statement-european-medicines-agency-position-application-3rs-replacement-reduction-refinement_en.pdf.

178. Food and Drug Administration (FDA) (2023) *National Center for toxicological research, FDA*. Available at: <https://www.fda.gov/about-fda/office-chief-scientist/national-center-toxicological-research>.

179. Congress Gov (2022) *FDA modernization 2.0 act*. Available at: <https://www.congress.gov/bills/117th-congress/senate-bill/5002/text>.

180. National Toxicology Program (NTP) (2023). *Alternative methods accepted by US agencies*. Available at: <https://ntp.niehs.nih.gov/whatwestudy/niceatm/accept-methods/index.html>.

181. Integrated Approaches to Testing and Assessment (IATA) - OECD (n.d.). Available at: <https://www.oecd.org/chemicalsafety/risk-assessment/iata/> (Accessed July 28, 2023).

182. Chang X, Tan YM, Allen DG, Bell S, Brown PC, Browning L, et al. IVIVE: facilitating the use of *in vitro* toxicity data in risk assessment and decision making. *Toxics.* (2022) 10:232. doi: 10.3390/toxics10050232

183. Paini A, Tan YM, Sachana M, Worth A. Gaining acceptance in next generation PBK modelling approaches for regulatory assessments - an OECD international effort. *Comput Toxicol.* (2021) 18:100163:18. doi: 10.1016/j.comtox.2021.100163

184. Meijboom KE, Abdallah A, Fordham NP, Nagase H, Rodriguez T, Kraus C, et al. CRISPR/Cas9-mediated excision of ALS/FTD-causing hexanucleotide repeat expansion in C9ORF72 rescues major disease mechanisms *in vivo* and *in vitro*. *Nat Commun.* (2022) 13:6286. doi: 10.1038/s41467-022-33332-7



OPEN ACCESS

EDITED BY

Christopher R. Cederroth,
Swiss 3R Competence Centre, Switzerland

REVIEWED BY

Anthony John Hannan,
University of Melbourne, Australia
Ruth Catriona Newberry,
Norwegian University of Life Sciences, Norway

*CORRESPONDENCE

Lena Bohn

✉ lena.bohn@uni-muenster.de

S. Helene Richter

✉ richterh@uni-muenster.de

RECEIVED 17 April 2023

ACCEPTED 14 September 2023

PUBLISHED 29 September 2023

CITATION

Bohn L, Bierbaum L, Kästner N, von
Kortzfleisch VT, Kaiser S, Sachser N and
Richter SH (2023) Structural enrichment for
laboratory mice: exploring the effects of
novelty and complexity.

Front. Vet. Sci. 10:1207332.

doi: 10.3389/fvets.2023.1207332

COPYRIGHT

© 2023 Bohn, Bierbaum, Kästner, von
Kortzfleisch, Kaiser, Sachser and Richter. This is
an open-access article distributed under the
terms of the [Creative Commons Attribution
License \(CC BY\)](#). The use, distribution or
reproduction in other forums is permitted,
provided the original author(s) and the
copyright owner(s) are credited and that the
original publication in this journal is cited, in
accordance with accepted academic practice.
No use, distribution or reproduction is
permitted which does not comply with these
terms.

Structural enrichment for laboratory mice: exploring the effects of novelty and complexity

Lena Bohn^{1,2*}, Louisa Bierbaum^{1,2}, Niklas Kästner^{1,2},
Vanessa Tabea von Kortzfleisch¹, Sylvia Kaiser^{1,2},
Norbert Sachser^{1,2} and S. Helene Richter^{1,2*}

¹Department of Behavioural Biology, Institute of Neuro- and Behavioural Biology, University of Münster, Münster, Germany, ²Münster Graduate School of Evolution, University of Münster, Münster, Germany

Providing structural enrichment is a widespread refinement method for laboratory rodents and other animals in captivity. So far, animal welfare research has mostly focused on the effect of increased complexity either by accumulating or combining different enrichment items. However, increasing complexity is not the only possibility to refine housing conditions. Another refinement option is to increase novelty by regularly exchanging known enrichment items with new ones. In the present study, we used pair-housed non-breeding female C57BL/6J and DBA/2N mice to investigate the effect of novelty when applying structural enrichment. We used a double cage system, in which one cage served as home cage and the other as extra cage. While the home cage was furnished in the same way for all mice, in the extra cage we either provided only space with no additional enrichment items (space), a fixed set of enrichment items (complexity), or a changing set of enrichment items (novelty). Over 5 weeks, we assessed spontaneous behaviors, body weight, and extra cage usage as indicators of welfare and preference. Our main results showed that mice with access to structurally enriched extra cages (complexity and novelty) spent more time in their extra cages and complexity mice had lower latencies to enter their extra cages than mice with access to the extra cages without any structural enrichment (space). This indicates that the mice preferred the structurally enriched extra cages over the structurally non-enriched space cages. We found only one statistically significant difference between the novelty and complexity condition: during week 3, novelty mice spent more time in their extra cages than complexity mice. Although we did not detect any other significant differences between the novelty and complexity condition in the present study, more research is required to further explore the potential benefits of novelty beyond complexity.

KEYWORDS

refinement, enrichment, animal welfare, housing condition, complexity, novelty

Introduction

Environmental enrichment is a major tool to refine housing conditions for captive animals. Since the benefits of environmental enrichment have been first described (1), the effects of different types of sensory, social, and structural enrichment have been investigated, covering a variety of different species living in laboratories, in zoos, and on farms [e.g., (2–9)]. Still, the

main body of research on environmental enrichment has been conducted using laboratory rodents (10, 11).

While the results between the studies sometimes vary depending on the strain, sex, age, and differences in exposure to environmental enrichment (12–15), they support the general notion that environmental enrichment can increase the animals' welfare. The wide range of reported beneficial effects through environmental enrichment include (but are not limited to): increased neurogenesis, learning and memory performance (16–19); promotion of species-specific behaviors and preventing the occurrence of behavioral disturbances like stereotypies (10, 20–24); facilitation of development of individual variation (25–27); as well as the reduction and mediation of anxiety, depression, and stress (17, 28–31). Together with the already mentioned factors, preference can likewise be used to assess welfare (32–34), and indeed, rodents show a preference for increased complexity and are even willing to work for access to additional enrichment (35).

Yet, given that laboratory rodents adapt very quickly to new conditions and environments, an initially beneficial impact of increased complexity might cease over time. One simple way of providing not only complexity but also novelty is to regularly exchange enrichment items, for example as part of the cage-changing routine. Indeed, researchers conducting enrichment studies have used novelty as part of their enrichment. However, it is impossible to disentangle whether reported welfare effects or preferences were due to the increased complexity or the novelty. That is because novelty was not systematically applied as a distinct enrichment strategy. Rather, novelty was used as part of the complex housing condition to further increase the contrast between the enriched and unenriched environments [see e.g., (11, 25, 36–38)].

So far, only a few studies have focused specifically on the effect of novelty on the welfare of laboratory rodents. For example, Abou-Ismaïl and Mendl (39) housed rats under two conditions, labeled complexity and novelty. In the novelty condition, the rats were provided five copies of the very same enrichment item, e.g., five ladders, which were exchanged weekly for five copies of another enrichment item, e.g., five shelters. In contrast, the rats from the complexity condition were offered five different items at a time which were not exchanged over the course of the 5 weeks. They found the complexity condition preferable over the novelty condition. Notably, their novelty condition did not always offer shelter or nesting material. Because nesting material has been identified as a major enrichment item for laboratory rodents (10, 40), their novelty housing condition without nesting material can arguably be considered impoverished compared to their complexity condition which always offered nesting material. In another experiment performed with mice, Gross et al. (41) did not find beneficial effects of novelty either. In their study, the shelters remained inside the cages for the duration of the experiment in the complexity housing condition, but in the novelty housing condition the shelters were replaced with a different kind of shelter every week (41). However, it has previously been argued that novel objects, especially when introduced into the home cage, might be perceived as a threat (42). Hence, to avoid potential adverse effects of novelty, it would be more cautious to avoid applying novel objects to the home cage but find ways to provide novelty outside the home cage (e.g., in an accessible extra cage or a play chamber).

With the present study, we aimed to further explore the potential benefits of novelty when providing structural enrichment.

We compared the effects of three different enrichment conditions on mice, the most commonly used model species (43, 44). In contrast to the aforementioned studies, we used a double cage system (45), in which one cage served as home cage and the second one was used as extra cage. This system allowed us to provide the mice constant access to nesting material and shelter in their home cage, and additionally, to offer novelty in a voluntarily accessible extra cage outside the familiar home cage. To systematically compare the effects of novelty and complexity on the mice, the extra cages either provided a weekly changing set of enrichment items (novelty), a fixed set of enrichment items (complexity), or no additional enrichment items (space). To gain insights regarding the effects of enrichment condition on the mice's welfare and their preferences, we monitored the mice's spontaneous behavior, body weight, and extra cage usage. More specifically, if for example, novelty were superior to complexity, we would expect to see more behaviors indicative of good welfare, e.g., more play, and fewer signs of poor welfare, e.g., fewer stereotypies, in the novelty mice (32, 46, 47), and if for example, novelty were more attractive to the mice than mere complexity, we would expect that novelty mice enter the extra cages faster when access is provided and spend more time in the extra cage, as well as interacting more with the enrichment therein.

Methods

Animals and housing condition

We purchased 18 female C57BL/6J and 18 female DBA/2N mice from a professional breeder (Charles River Laboratories, Germany GmbH, Sulzfeld, Germany) at the age of post-natal day (PND) 28.

After arrival and prior to the present study, the mice participated in another experiment (45). In brief, the mice's previous experience included different housing conditions as well as behavioral tests. Upon arrival, the mice were pair-housed in either same-strain or mixed-strain pairs in Makrolon type III cages (39 × 23 × 15 cm³). The cage floor was covered with wood shavings (Tierwohl, Wilhelm Reckhorn GmbH & Co. KG, Warendorf, Germany). Food (Altromin 1,324, Altromin Spezialfutter GmbH & Co. KG, Lage, Germany) and water were provided *ad libitum*. The cages were furnished with a paper towel, a wooden gnawing stick, a red transparent plastic house (Mouse House™, Tecniplast Deutschland GmbH, Hohenpeißenberg, Germany), and a red transparent plastic tunnel (Mouse Tunnel Red, Plexx B.V., Elst, Netherlands), which was attached to the cage lid via wire hangers (Stainless Steel wire Hanger for Mouse Tunnel, Plexx B.V., Elst, Netherlands). On PNDs 76–92, the mice were tested on the elevated plus maze, in the dark–light test, the open field test, the free exploration test, and in a labyrinth. On PND 97, always two pairs were merged to form quartets (two C57BL/6J mice and two DBA/2N mice) and were transferred into a double cage system. The double cage system consisted of two Makrolon type III cages, which were furnished as described above and were connected via a transparent tunnel (length: 8.4 cm, diameter: 3.9 cm). The tunnel was closable using a gray PVC platelet (height: 4.9 cm, width: 3.4 cm). On PND 157, the groups were divided into mixed-strain pairs and transferred to single Makrolon Type III cages.

At the beginning of the present study on PND 167, the mixed-strain pairs were transferred from single Makrolon type III cages

into double cage systems. One of the two cages served as home cage and was furnished as described above minus the red mouse house, the second cage served as extra cage and will be described in detail below. Enrichment and bedding were changed weekly (paper tissue, bedding) or biweekly (tunnel, wooden gnawing stick). We decided to pair-house one C57BL/6J and one DBA/2N mouse because results from previous studies suggested that the effects of environmental enrichment can be strain-specific (44, 48, 49) and the use of more than one strain allows for a greater generalization of the results (12, 50). We decided on these two strains in particular because they are widely used in research (44, 48), their different coats allow for individual recognition during the behavioral observations, and previous studies showed that these two strains can be housed together harmoniously (51). All experiments and observations were carried out in the dark phase of the inverted 12 h/12 h dark–light cycle. Room temperature and humidity were kept around 22°C and 50%, respectively. The 18 double cage systems were distributed over three racks in a balanced way to account for systematic differences within the housing rooms, especially regarding light conditions and human traffic.

Experimental design

To explore the effect of enrichment novelty on the mice, we assigned the 18 cages to either of three enrichment conditions: space, complexity, or novelty (Figure 1A). In the space enrichment condition, the extra cage was empty apart from the bedding material. In the complexity and novelty enrichment conditions, the extra cage was furnished with three different enrichment items. While for the complexity enrichment condition the set of enrichment items remained the same and the items were merely replaced by clean ones, mice in the novelty enrichment condition were presented with a different set of items every week.

We used enrichment items of three categories: shelter, climbing, and nesting. For each category, we used three different enrichment items (Figure 1B). In category shelter, we used the following items: red transparent plastic houses (s1; 11.1 × 11.1 × 5.5 cm³; Tecniplast Deutschland GmbH, Hohenpeißenberg, Germany), cardboard houses (s2; 13 × 9 × 6 cm³; ZOONLAB GmbH, Castrop-Rauxel, Germany), and opaque gray PVC tunnels (s3; 3.5 × 10 cm; Bauhaus AG, Belp, Schweiz). In category climbing, we used: wooden scaffolds (c1; 11 × 14 × 22 cm), nylon mouse swings (c2; PLEXX B.V., Elst, Netherlands), and hemp rope (c3). In category nesting, we used: nestlets (n1; 5 × 5 cm²; ZOONLAB GmbH, Castrop-Rauxel, Germany), cocoons (n2; 3.6 × 1.2 cm; ZOONLAB GmbH, Castrop-Rauxel, Germany), and nest packs (n3; 100 g; ZOONLAB GmbH, Castrop-Rauxel, Germany). The extra cage enrichment was replaced during the regular cage-changing routine on the first day of the week (day 1) during the morning (Figure 1C). For the present study, we used 6 different combinations of enrichment items. Each of the six cages assigned to the complexity enrichment condition had one of the six combinations in their extra cage throughout the experiment. The six extra cages of the novelty enrichment condition each started with a different one of the six possible combinations. In the following weeks, the combination of enrichment items in the novelty extra cages was changed.

Over the course of 5 weeks, we assessed body weight, extra cage usage, and spontaneous behaviors (Figure 1C). We measured the mice's weight once a week during the cage-changing routine on Day 1, using a digital scale (CM 150-1 N, Kern, Ballingen, Germany; weighing capacity: 150 g, resolution: 0.1 g). To assess extra cage usage, we measured the mice's latency to enter the extra cage, the relative time they spent in the extra cage, as well as enrichment item interaction frequency in the extra cage (only for the complexity and novelty enrichment condition). We measured the latency nine times per week: once in the afternoon of day 1 and twice per day on the following weekdays. We measured the latencies for both mice at the same time, immediately after we opened the connection tunnel, using stopwatches, for a maximal latency of 180 s. Five times per week, we conducted behavioral observations after all the latencies had been taken: Once on day 1 and twice on days 3 and 5. During each behavioral observation, we recorded the spontaneous behaviors (Table 1A) and enrichment item interactions in the extra cage by counting the number of events (Table 1B), and by measuring the time the mice spent in the extra cage using stopwatches. The mice of one cage were observed separately but immediately after one another before moving on to the next cage, alternating with the starting mouse between observation sessions. Each observation lasted for 60 s, except on the very first day when observations lasted for 90 s (the data have been corrected accordingly in the analysis). To have a more balanced observation, we split the 60 s (or 90 s) observations in two intervals: After the first 30 s (or 45 s) for each of the two mice in one cage, we moved on to the next cage until all mice of all cages were observed once before we returned to the first cage to observe the mice for the second interval. The observations started either with cage 1 and finished with cage 18 going forward through the rows, started with cage 18 and finished with cage 1 going backwards, or started in the middle and continued forwards.

For the behavioral observations we used continuous recording except for inactivity, for which we used one-zero sampling (53). After the second observation interval, the observations for a given cage were over, the mice were gently guided back into their home cage and the connection tunnels were closed again. This design led to slightly different extra cage access times, as they were depending on the latencies of the other mice. The mice had access to the extra cages twice a day (except for Day 1 of the week, where they had access once in the afternoon) for roughly 90 min each time, starting with the opening of the tunnels before the latency measurement until the closing of the tunnel at the end of the second observation interval.

All observations were performed by the same observer. Due to the nature and design of the experiment, it was not possible to blind the observer to the enrichment condition.

Statistical analysis

To statistically analyze our data, we fitted linear mixed-effect models (LMMs) or used non-parametric tests, depending on our outcome measures.

We fitted two LMMs with three fixed factors to analyze the effect of enrichment condition (factor with three levels: space, complexity, and novelty), strain (factor with two levels: C57BL/6J and DBA/2N), and week (numeric factor) on latency to enter the extra cage and on

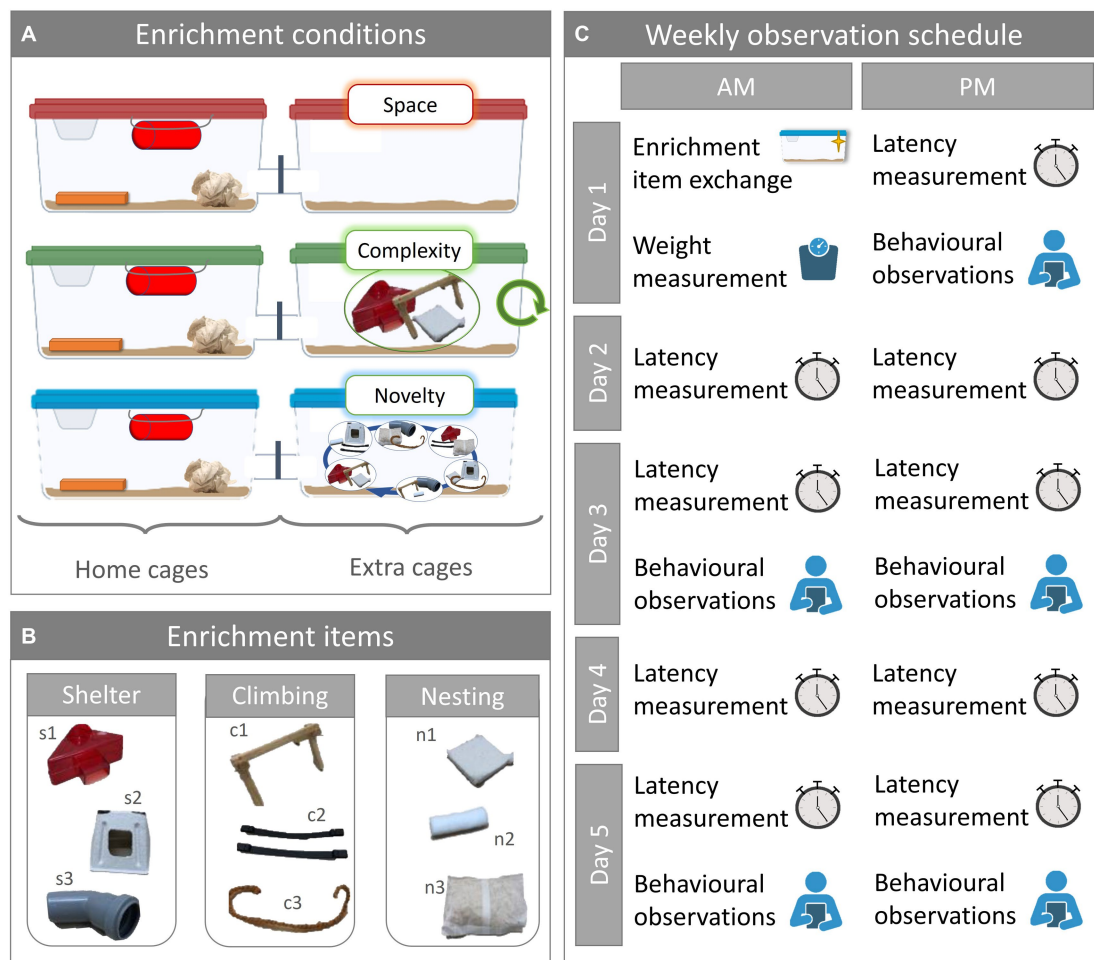


FIGURE 1

Experimental design. **(A)** Enrichment conditions. Mice were housed in mixed strain pairs in double cage systems and were assigned to one of three enrichment conditions designated as space, complexity, or novelty. One of the cages served as home cage and was furnished the same way for all enrichment conditions. The second cage served as extra cage and was furnished depending on the enrichment condition: extra cage space did not contain any additional enrichment; extra cage complexity offered a fixed set of additional three enrichment items; extra cage novelty offered a changing set of three additional enrichment items. Total sample size was $N = 36$, with $n = 6$ per group ($N_{C57BL/6J, space} = N_{C57BL/6J, complexity} = N_{C57BL/6J, novelty} = N_{DBA/2N, space} = N_{DBA/2N, complexity} = N_{DBA/2N, novelty} = 6$). **(B)** Enrichment items. The enrichment items used in the extra cages can be grouped into three categories: shelter, climbing, and nesting. For shelter, we used red transparent plastic houses (s1), cardboard houses (s2), and gray opaque PVC tubes (s3). For climbing we used wooden scaffolds (c1), mouse swings (c2), and hemp rope (c3). For nesting we used nestlets (n1), cocoons (n2), and nest packs (n3). **(C)** Weekly observation schedule. Once a week on Day 1, enrichment items were exchanged, and the mice were weighed. In the afternoon of Day 1 and twice on every other weekday, latency to enter the extra cage was measured. On five occasions, the latency measurement was followed by behavioral observation sessions.

relative body weight. Relative body weight captures individual weight changes better than absolute body weights; therefore, we set the first measurement (week 1) as the baseline value and divided the following measurements (week 2 onwards) by the baseline value. In addition to the main effects, the models included two interactions, namely enrichment condition*strain and enrichment condition*week, as well as animal ID as random factor. As reference levels for our fixed factors enrichment condition and strain, we used space enrichment condition and C57BL/6J, respectively. In case of significant results from the ANOVA of the fitted model, we conducted Tukey-adjusted pairwise comparisons as *post hoc* analysis.

Our other outcome measures, namely relative time spent in the extra cage, extra cage enrichment item interaction frequency, inactivity, and spontaneous behaviors could not be fitted by LMMs without violating model assumptions, even after transformation of

the raw data. Relative time spent in the extra cage was calculated by dividing the time the mice spent in the extra cage by the time the mice were observed. This was done to account for differences in observation durations (90s or 60s). To analyze the effect of enrichment condition on our outcome measures, we used Kruskal-Wallis rank sum tests. However, for the extra cage enrichment item interaction frequency, we used Mann-Whitney-U tests because we only had the novelty and complexity enrichment condition to compare (the space enrichment condition did not offer any enrichment items in the extra cage). We tested for an overall enrichment condition effect by comparing mouse means from both strains across all 5 weeks, as well as testing for each week separately.

Even though this was not in the focus of the present study, we also tested for strain and week effects, to better match the non-parametric

TABLE 1 Ethogram.

(A) Spontaneous behaviors		
Lid climbing		The mouse grabs the grid of the cage lid with at least two paws without touching the ground or the mouse house and moves along it.
Digging		The mouse shoves bedding material under its body using its forepaws in alternating movement. The hind paws may push the bedding material behind the mouse. Alternatively, it pushes the bedding material in front of its body showing a forward locomotion.
Bar-mouthing		The mouse holds a bar of the cage lid in its mouth for at least 3 s without an interruption longer than 1 s. Biting movements may be seen.
Inactivity		The mouse does not move for the whole length of the observed interval except for breathing or tiny ear or whisker movements.
Play (14)	Hopping	The mouse suddenly (without identifiable reason) jumps vertically. The behavior is often accompanied by head shaking.
	Jumping	The mouse suddenly (without identifiable reason) jumps horizontally, not shorter than the length of a mouse.
Agonistic behavior (52)	Chasing	The mouse approaches another mouse which then runs away while being followed by the focal mouse.
	Mounting	The mouse lays its upper body on the back of another mouse. The front paws grab the sides of the body of the recipient mouse. The mouse may show pelvic thrusts.
	Fighting	The mouse bites, kicks, and wrestles another mouse in fast movements. The recipient mouse may produce squeaking noises.
Stereotypic behavior	Route-tracing	The mouse moves along an identical path on the cage lid or bottom for at least three times in a row. Circular paths are excluded.
	Circling	The mouse moves along an identical circular path for at least three times in a row.
(B) Extra cage enrichment item interaction		
Shelter	In	The mouse moves into the shelter or stays within. The whole body is under the roof of the shelter, only the tail may be outside.
	On	The mouse is sitting, standing, or moving along the top of the shelter. At least two paws need to touch it without touching the bottom or different objects.
	Gnawing	The mouse touches the shelter with its mouth for at least 2 s. A slight movement of the head is visible.
Climbing item	On	The mouse is sitting, standing, or moving along the top of the climbing item. At least two paws touch it without touching the bottom or different objects.
	Gnawing	The mouse touches the shelter with its mouth for at least 2 s. A slight movement of the head is visible.
Nesting material	Carrying	The mouse holds the nesting material in its mouth and is moving around the cage.
	Manipulating	The mouse touches the nesting material with its mouth and pushes or tears it apart without showing locomotion.

On five live observations per week, we recorded the mice's spontaneous behavior (A) and enrichment interaction in the extra cage (B) by counting the events.

analysis with the LMMs described above. To analyze the effect of strain on our outcome measures, we used Mann–Whitney-U tests. To analyze the effect of week on our outcome measures, we used Friedman rank sum tests.

To account for multiple hypothesis testing in analysis, we used sequential Bonferroni-Holm correction (54) to adjust the *p*-values from the Kruskal-Wallis, Mann–Whitney-U, and Friedmann tests as well as the *p*-values from the *post hoc* pairwise comparisons.

Due to the two different approaches in the analysis (LMMs and non-parametric tests), there are differences in the way the results are reported and displayed. In our analysis, week is a numeric factor in the LMMs but a five-level factor in our non-parametric Friedman rank sum tests. Hence, we needed to

conduct *post hoc* pairwise comparisons for a significant effect of week following the Friedman ranks sum tests, while this was not necessary for the LMMs. Likewise, in our plots, we display the values which we used for the analysis. As we used every single value for the analysis of latency to enter the extra cage and relative body weight, we also used all the values when creating the plot. For the non-parametric tests, on the other hand, we used individual means, hence the plots display individual means rather than every value for each individual.

Across all three enrichment conditions, some mice did not enter the extra cage during the observation time. This was accounted for in the analysis as follows: for latency to enter the extra cage, observations in which the mice did not enter the extra cage were excluded from the analysis; for time spent in the extra cage, observations in which the

mice did not enter the extra cages scored 0; for enrichment item interaction frequency in the extra cage, observations in which mice did not enter the extra cage were excluded from the analysis, as we divided the number of extra cage enrichment item interactions by the time the mice spent in the extra cage (and division by 0 is an invalid operation).

All statistical analyses were performed in R version 4.1.2 (55). To fit the LMMs, we used the lme4 (56) and lmerTest packages (57). For the *post hoc* analysis, we used the emmeans package (58) and the dunn.test package (59). To test model assumptions like normal distribution of model residuals, we used the packages nortest (60) and performance (61). For the Tukey transformation of the latency data, we used the rcompanion package (62). We used the packages ggplot2 (63) and ggpubr (64) to create the figures. We considered a value of $p < 0.05$ as an indicator of statistically significant differences. For easier reading, we simply referred to “differences” instead of “statistically significant differences” in the results section.

In addition to our statistical analysis in R, we also conducted a sensitivity analysis using the software G*Power (65), with an α error probability = 0.05 and β error probability = 0.2, to determine the detectable effect sizes for the LMMs. Our sensitivity analysis revealed that the detectable effect size for enrichment condition was Cohen's $f = 0.542$, which is above what is considered to be the threshold for a large effect size (for more details, please see Supplementary Table S8) (66, 67).

Results

To test whether enrichment condition influenced the mice's spontaneous behavior, body weight, and usage of the extra cage, we conducted behavioral observations and monitored the mice's weight over the course of 5 weeks. We indeed found that enrichment condition influenced some of our outcome measures, namely relative time the mice spent in the extra cage, latency to enter the extra cage, and relative body weight.

Regarding relative time spent in the extra cage, we see that across all 5 weeks, mice from the complexity and novelty enrichment condition spent more time in their extra cages than mice from the space enrichment condition (Kruskal-Wallis test for Weeks 1–5: $\chi^2 = 16.294$, $p < 0.001$; *post hoc* pairwise comparison for Weeks 1–5, complexity-space: $Z = 2.519$, $p_{\text{adjusted}} = 0.012$, novelty-space: $Z = 3.991$, $p_{\text{adjusted}} < 0.001$; Supplementary Table S1 and Figure 2A). This effect of enrichment condition on relative time spent in the extra cage, with mice spending more time in the structurally enriched extra cages compared to the structurally non-enriched extra cages from the space enrichment condition, can also be seen for all individually analyzed weeks, except during week 4 (for details please see Supplementary Table S1 and Figure 2A). The only time we detected a difference between the novelty and complexity enrichment condition was during week 3 (Kruskal-Wallis test for Week 3: $\chi^2 = 14.114$, $p_{\text{adjusted}} = 0.005$; *post hoc* pairwise comparison complexity-novelty: $Z = -2.558$, $p_{\text{adjusted}} = 0.011$, Supplementary Table S1 and Figure 2A), showing that mice from the novelty enrichment condition spent more time in the extra cage than mice from the complexity enrichment condition.

Regarding latency to enter the extra cage, we found a statistically significant interaction between enrichment condition and week (LMM: $F_{2,1429.553} = 4.828$, $p = 0.008$, Supplementary Table S2 and Figure 2B). *Post hoc* analysis indicated that over the weeks, the latency to enter the extra cage decreased significantly faster for mice from the complexity enrichment condition compared to mice from the space enrichment condition (*post hoc* pairwise comparison, space-complexity: $b = -0.012 \pm 0.004$, $t_{1429.334} = 2.956$, $p_{\text{adjusted}} = 0.009$, space-novelty: $b = 0.010 \pm 0.004$, $t_{1429.702} = -2.345$, $p_{\text{adjusted}} = 0.050$, Supplementary Table S3 and Figure 2B).

Regarding relative body weight, we also found a statistically significant interaction between enrichment condition and week (LMM: $F_{2,105} = 4.04$, $p = 0.020$, Supplementary Table S2 and Figure 2C). Here, *post hoc* analysis revealed differences in the slopes for the week effect on mice from the space enrichment condition and mice from the novelty enrichment condition, indicating a decrease in relative body weight over the weeks in space mice compared to mice from the novelty enrichment condition (*post hoc* pairwise comparison: $b = -1.290 \pm 0.491$, $t_{105} = -2.625$, $p_{\text{adjusted}} = 0.027$, Supplementary Table S3 and Figure 2C). We also found a statistically significant effect of enrichment condition on relative body weight (LMM: $F_{2,134.1} = 3.37$, $p = 0.037$, Supplementary Table S2 and Figure 2C), but *post hoc* analysis revealed no statistically significant effect after correcting for multiple comparisons (for details please see Supplementary Table S3 and Figure 2C). For all other outcome measures, we did not find statistically significant effects of enrichment condition on our outcome measures (for more details please see Supplementary Table S1 and Supplementary Figure S1).

Albeit not the focus of this study, we also analyzed the effect of strain and week on our outcome measures. We found that week influenced latency to enter the extra cage. Apart from the interactive effect of week with enrichment condition described above, week had a statistically significant main effect on latency to enter the home cage (LMM: $F_{1,1429.553} = 1004.212$, $p < 0.0001$, Supplementary Table S2 and Figure 2B), showing that the latency to enter the extra cage decreased over the weeks. For all other outcome measures, we did not find statistically significant effects of week or strain after *post hoc* pairwise comparisons and correcting for multiple comparisons (for more details please see Supplementary Tables S4–S6 and Supplementary Figure S1).

Because of their rare occurrence, some spontaneous behaviors were only descriptively analyzed, namely agonistic behavior, stereotypic behaviors, and bar mouthing. Upon visual inspection of the data, we did not detect an effect of enrichment condition (for more details, please see Supplementary Table S7 and Supplementary Figure S2).

Discussion

The present study aimed to explore whether novelty of environmental enrichment may offer beneficial effects beyond that of structural complexity alone. To this end, we allowed mice of two strains access to an extra cage offering either novelty, complexity, or space. Over the course of 5 weeks, we recorded spontaneous behaviors and body weight, as well as extra cage usage as indicators of welfare. With one exception during week 3, in which mice from the novelty

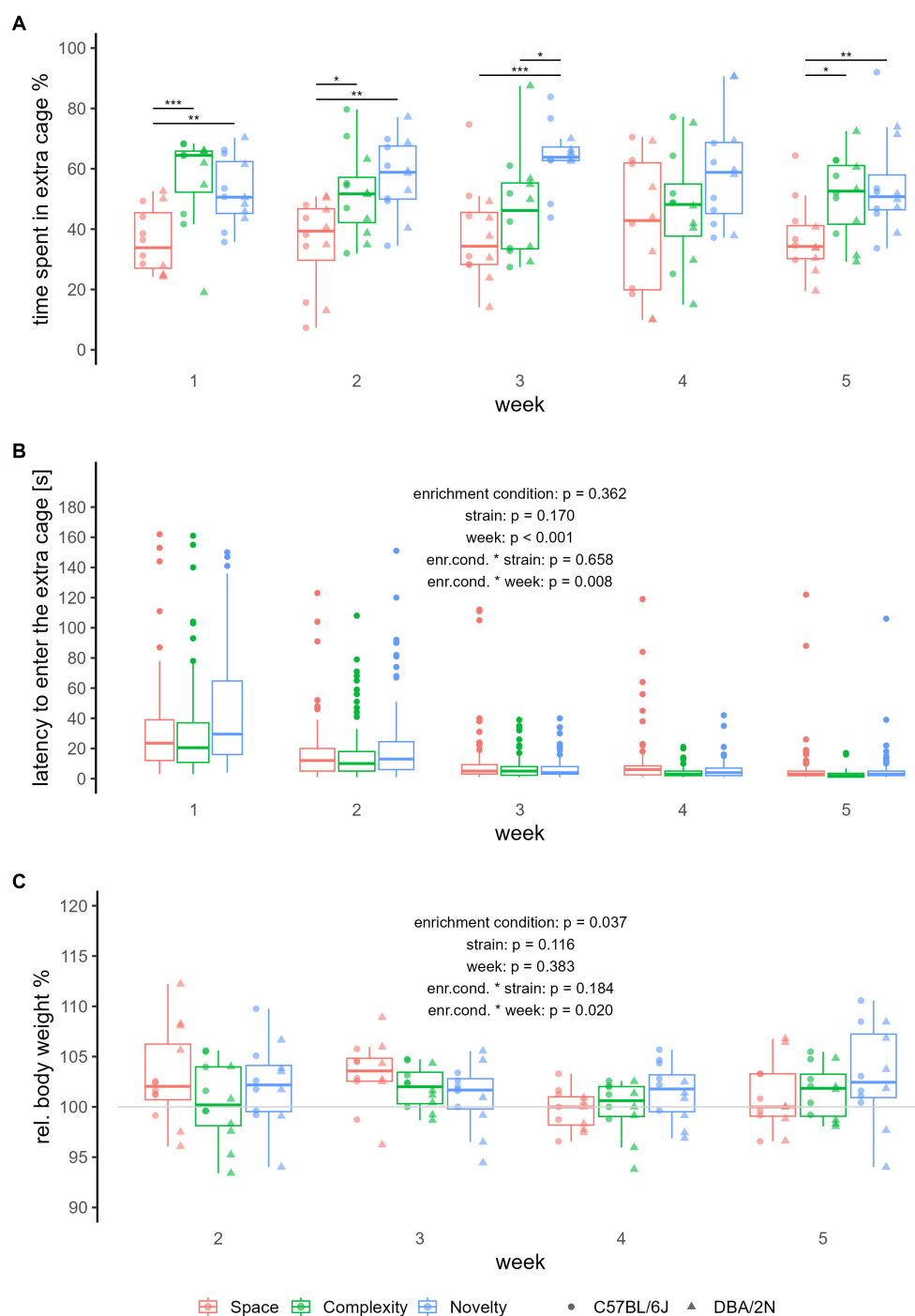


FIGURE 2

Relative time spent in the extra cage, latency to enter the extra cage, and relative body weight. The boxplots show the median, upper and lower quartile of the respective group. The colours refer to enrichment condition (red = space, green = complexity, blue = novelty), the dot shapes in (A,C) refer to strains (round = C57BL/6J, triangular = DBA/2N). We used $N_{C57BL/6J, space} = N_{C57BL/6J, complexity} = N_{C57BL/6J, novelty} = N_{DBA/2N, space} = N_{DBA/2N, complexity} = N_{DBA/2N, novelty} = 6$ individuals per group, all non-breeding females. Where no p -values are given, significance levels are indicated as follows: $*p_{adjusted} \leq 0.05$, $**p_{adjusted} \leq 0.01$, $***p_{adjusted} \leq 0.001$. (A) Each dot represents the average time spent in the extra cage of one individual each week, with 10 measurements per individual and week. Indicated are the statistically significant differences between the groups after the Kruskal-Wallis *post hoc* pairwise comparison using Dunn tests with Bonferroni-Holm adjustment. For the analysis of latency to enter the extra cage (B) and relative body weight (C), we fitted linear mixed-effect models. Hence, (B,C) represent all measurements per individual, (B) with a max of 60 measurements per enrichment condition and week (measurements of >180 s were omitted), and (C) with a total of 12 measurements per enrichment condition and week. The weight measure of Week 1 was taken as the baseline value (horizontal line).

condition spent statistically significant more time in their extra cages than mice from the complexity condition, we did not find distinct differences between the complexity and novelty conditions. However, we saw that mice spent more time in the structurally enriched extra cages (complexity and novelty) compared to the structurally non-enriched extra cages (space) and that mice from the complexity enrichment condition reduced their latency to enter the extra cage faster than mice from the structurally non-enriched condition (space).

This is in line with the study by Gross et al. (41), who investigated the effects of different housing conditions on stereotypic and anxiety-related behaviors in mice. They, too, did not find systematic differences between the novelty and complexity condition. In contrast, Abou-Ismaïl and Mendl (39) found that their complexity housing condition was superior to their novelty housing condition. This discrepancy between the study by Abou-Ismaïl and Mendl (39) on one hand and the present study on the other could be due to species-specific differences between mice and rats. However, we think that their findings are more likely related to the study's experimental design. As already mentioned in the introduction, a plausible explanation is their non-permanent provision of nesting material in their novelty housing condition compared to their complexity condition, where nesting material was always available to the rats. The findings of the two studies led us to use a double cage system, in which we could provide constant access to nesting material in the mice's home cages while offering different levels of enrichment in a voluntarily accessible extra cage rather than the home cage itself.

Our other results indicate a preference for the structurally enriched conditions (complexity and novelty) over the structurally non-enriched space condition, a preference which has been reported previously (35, 68). As it has been argued that preferences can be used to give welfare insights (32–34), a preference for the enriched extra cages over the structurally non-enriched space extra cage might indicate that additional space alone is less beneficial for the mice than increased complexity and novelty. Apart from the differences in preferences, relative body weight was the only other outcome measure affected by enrichment condition. However, we advise caution when interpreting this result. *Post hoc* pairwise comparisons did not reveal any statistically significant differences between the groups. Furthermore, our mice were all non-breeding, healthy, adult females, and unlike young or breeding mice, our mice did not need to gain weight, and their body weight fluctuations were mild and within the normal range.

Apart from a preference for the structurally enriched extra cages (complexity and novelty) over the structurally non-enriched extra cages (space) and the differences in body weight, our results did not reveal further effects of enrichment condition. Albeit not the focus of our study, as the rationale for including different mouse strains was to be better able to generalize our findings, we also tested for strain differences. In the literature, behavioral differences between C57BL/6J and DBA/2N mice have been reported (69). There are also studies showing that the effects of environmental enrichment can be strain-specific (29, 49, 70) and that the presence of the other strain can have an influence as well (45). In our study, however, we did not detect statistically significant differences between the strains. Even so,

we cannot conclude that there were no strain differences, as our sensitivity analysis indicated that we could only detect strain effects of large effect sizes (Cohen's $f \geq 0.481$).

Overall, the spontaneous behaviors either did not show differences between the groups or the behaviors happened too rarely to be statistically analyzed. Nonetheless, the behavioral data we gathered gave some insights. For instance, the occurrence of bar mouthing, stereotypic and agonistic behavior was very low, and we saw play behavior in all three housing conditions despite the mice's relatively advanced age (PND 167–202), albeit rarely. Play behavior has been reported to be a reliable indicator of good welfare, whereas weight loss, inactivity, and the presence of stereotypic and agonistic behavior are considered signs of impaired welfare (32, 46, 47). Together with the mice's relatively stable weight, our observations indicated that the furnishing we offered in the home cages was already of a relatively high standard and provided the mice with good welfare, even though definite claims cannot be made here, as in addition to the provided enrichment in the home cages, all mice had regular access to at least extra space. As the authors of previous studies already pointed out, the provision of nesting material is already sufficient to improve the welfare of laboratory mice greatly (10, 41). Likewise, it has been argued that providing enrichment diversity, i.e., complexity, is probably more important for the animals' welfare than providing novelty without diversity (39).

In conclusion, our study showed that additional structural enrichment was more attractive to mice than extra space alone. However, with only one result indicating that novelty was preferred over complexity, the present study does not allow us to determine whether or not enrichment novelty increased mouse welfare beyond the effects of enrichment complexity. We did not detect differences between the two enrichment conditions in mice, but it is still conceivable that there are effects of novelty beyond complexity, especially regarding extended periods and with a wider range of variables assessed. To answer this question is of great interest not only for mice and other lab animals. Rather, this concern regards all captive animals, be it in zoos, on farms, or in our own homes. Further research is needed to explore whether additional novelty may be more refining than environmental complexity alone.

Data availability statement

The raw data supporting the conclusions of this article will be made available by the authors, without undue reservation.

Ethics statement

The animal study was approved by the local (Amt für Gesundheit, Veterinär- und Lebensmittelangelegenheiten, Münster, Nordrhein-Westfalen, reference number: 39.32.7.1) and federal authorities (Landesamt für Natur, Umwelt und Verbraucherschutz Nordrhein-Westfalen "LANUV NRW"). The study was conducted in accordance with the local legislation and institutional requirements.

Author contributions

SK, SR, and NS conceived the study. LBi, NK, SK, SR, and NS designed the experiments. LBi carried out the experimental procedures. LBo and VK analyzed the data. LBo prepared the manuscript. All authors reviewed and approved the final version of the manuscript.

Funding

This research was funded by the German Research Foundation (DFG) as part of the SFB TRR 212 (NC³), project numbers 316099922 and 396776123, responsible PIs: SR and NS.

Acknowledgments

Figure 1 used the following templates by BioRender.com (2022), retrieved from <https://app.biorender.com/biorender-templates>: “Rodent cage,” “Weight scale,” “Person reading a letter,” “Clock (no hands),” and “Hourglass.”

References

- Hebb DO. The effects of early experience on problem-solving at maturity. *Am Psychol.* (1947) 2:306–7.
- Arechavala-Lopez P, Cabrera-Álvarez MJ, Maia CM, Saraiva JL. Environmental enrichment in fish aquaculture: a review of fundamental and practical aspects. *Rev Aquac.* (2022) 14:704–28. doi: 10.1111/raq.12620
- Fernandez EJ, Martin AL. Animal training, environmental enrichment, and animal welfare: a history of behavior analysis in zoos. *J Zool Bot Gard.* (2021) 2:531–43. doi: 10.3390/jzbg2040038
- Mandel R, Whay HR, Klement E, Nicol CJ. Invited review: environmental enrichment of dairy cows and calves in indoor housing. *J Dairy Sci.* (2016) 99:1695–715. doi: 10.3168/jds.2015-9875
- Newberry RC. Environmental enrichment: increasing the biological relevance of captive environments. *Appl Anim Behav Sci.* (1995) 44:229–43. doi: 10.1016/0168-1591(95)00616-Z
- Orihuela A, Mota-Rojas D, Velarde A, Strappini-Asteggiano A, La Vega LT, Borderas-Tordesillas F, et al. Environmental enrichment to improve behaviour in farm animals. *CABI Rev.* (2018) 2018:1–25. doi: 10.1079/PAVSNNR201813059
- Swaigood R, Shepherdson D. Environmental enrichment as a strategy for mitigating stereotypies in zoo animals: a literature review and meta-analysis In: G Mason, editor. *Stereotypic animal behaviour: fundamentals and applications to welfare*. Wallingford: CABI (2006). 256–85.
- van de Weerd H, Ison S. Providing effective environmental enrichment to pigs: how far have we come? *Animals.* (2019) 9:254. doi: 10.3390/ani9050254
- Young RJ. *Environmental enrichment for captive animals*. New York, NY: John Wiley & Sons (2013).
- Olsson IAS, Dahlborn K. Improving housing conditions for laboratory mice: a review of environmental enrichment. *Lab Anim.* (2002) 36:243–70. doi: 10.1258/002367702320162379
- Ratuski AS, Weary DM. Environmental enrichment for rats and mice housed in laboratories: a meta-review. *Animals.* (2022) 12:414. doi: 10.3390/ani12040414
- Bayne K. Environmental enrichment and mouse models: current perspectives. *Anim Model Exp Med.* (2018) 1:82–90. doi: 10.1002/ame2.12015
- Marashi V, Barnekow A, Ossendorf E, Sachser N. Effects of different forms of environmental enrichment on behavioral, endocrinological, and immunological parameters in male mice. *Horm Behav.* (2003) 43:281–92. doi: 10.1016/S0018-506X(03)00002-3
- Marashi V, Barnekow A, Sachser N. Effects of environmental enrichment on males of a docile inbred strain of mice. *Physiol Behav.* (2004) 82:765–76. doi: 10.1016/j.physbeh.2004.05.009
- Mo C, Renoir T, Hannan AJ. What's wrong with my mouse cage? Methodological considerations for modeling lifestyle factors and gene-environment interactions in mice. *J Neurosci Methods.* (2016) 265:99–108. doi: 10.1016/j.jneumeth.2015.08.008
- Kozorovitskiy Y, Gross CG, Kopil C, Battaglia L, McBreen M, Stranahan AM, et al. Experience induces structural and biochemical changes in the adult primate brain. *Proc Natl Acad Sci U S A.* (2005) 102:17478–82. doi: 10.1073/pnas.0508817102
- Macartney EL, Lagisz M, Nakagawa S. The relative benefits of environmental enrichment on learning and memory are greater when stressed: a meta-analysis of interactions in rodents. *Neurosci Biobehav Rev.* (2022) 135:104554. doi: 10.1016/j.neubiorev.2022.104554
- Mohammed AH, Zhu SW, Darmopil S, Hjerling-Leffler J, Ernfors P, Winblad B, et al. Environmental enrichment and the brain. *Prog Brain Res.* (2002) 138:109–33. doi: 10.1016/S0079-6123(02)38074-9
- van Praag H, Kempermann G, Gage FH. Neural consequences of environmental enrichment. *Nat Rev Neurosci.* (2000) 1:191–8. doi: 10.1038/35044558
- Bailoo JD, Murphy E, Boada-Saña M, Varholick JA, Hintze S, Baussière C, et al. Effects of cage enrichment on behavior, welfare and outcome variability in female mice. *Front Behav Neurosci.* (2018) 12:232. doi: 10.3389/fnbeh.2018.00232
- Fraser D, Weary D, Pajor E, Milligan B. A scientific conception of animal welfare that reflects ethical concerns. *Anim Welf.* (1997) 6:187–205. doi: 10.1017/S0962728600019795
- Jennings M, Batchelor GR, Brain PF, Dick A, Elliott H, Francis RJ, et al. Refining rodent husbandry: the mouse: report of the rodent refinement working party. *Lab Anim.* (1998) 32:233–59. doi: 10.1258/002367798780559301
- van de Weerd HA, van Loo P, van Zutphen L, Koolhaas JM, Baumans V. Nesting material as environmental enrichment has no adverse effects on behavior and physiology of laboratory mice. *Physiol Behav.* (1997) 62:1019–28. doi: 10.1016/S0031-9384(97)00232-1
- Würbel H, Chapman R, Rutland C. Effect of feed and environmental enrichment on development of stereotypic wire-gnawing in laboratory mice. *Appl Anim Behav Sci.* (1998) 60:69–81. doi: 10.1016/S0168-1591(98)00150-6
- Kempermann G, Lopes JB, Zocher S, Schilling S, Ehret F, Garthe A, et al. The individuality paradigm: automated longitudinal activity tracking of large cohorts of genetically identical mice in an enriched environment. *Neurobiol Dis.* (2022) 175:105916. doi: 10.1016/j.nbd.2022.105916
- Körholz JC, Zocher S, Grzyb AN, Morisse B, Poetzsch A, Ehret F, et al. Selective increases in inter-individual variability in response to environmental enrichment in female mice. *eLife.* (2018) 7:e35690. doi: 10.7554/eLife.35690

Conflict of interest

The authors declare that the research was conducted in the absence of any commercial or financial relationships that could be construed as a potential conflict of interest.

Publisher's note

All claims expressed in this article are solely those of the authors and do not necessarily represent those of their affiliated organizations, or those of the publisher, the editors and the reviewers. Any product that may be evaluated in this article, or claim that may be made by its manufacturer, is not guaranteed or endorsed by the publisher.

Supplementary material

The Supplementary material for this article can be found online at: <https://www.frontiersin.org/articles/10.3389/fvets.2023.1207332/full#supplementary-material>

27. Zocher S, Schilling S, Grzyb AN, Adusumilli VS, Bogado Lopes J, Günther S, et al. Early-life environmental enrichment generates persistent individualized behavior in mice. *Sci Adv.* (2020) 6:eabb1478. doi: 10.1126/sciadv.abb1478
28. Benaroya-Milshtein N, Hollander N, Apter A, Kukulansky T, Raz N, Wilf A, et al. Environmental enrichment in mice decreases anxiety, attenuates stress responses and enhances natural killer cell activity. *Eur J Neurosci.* (2004) 20:1341–7. doi: 10.1111/j.1460-9568.2004.03587.x
29. Chapillon P, Manneché C, Belzung C, Caston J. Rearing environmental enrichment in two inbred strains of mice: 1. Effects on emotional reactivity. *Behav Genet.* (1999) 29:41–6. doi: 10.1023/A:1021437905913
30. Girbovan C, Plamondon H. Environmental enrichment in female rodents: considerations in the effects on behavior and biochemical markers. *Behav Brain Res.* (2013) 253:178–90. doi: 10.1016/j.bbr.2013.07.018
31. Prior H, Sachser N. Effects of enriched housing environment on the behaviour of young male and female mice in four exploratory tasks. *J Exp Anim Sci.* (1995) 37:57–68.
32. Baumans V. Science-based assessment of animal welfare: laboratory animals. *Rev Sci Tech Off Int Epiz.* (2005) 24:503–14. doi: 10.1017/9781316678329.003
33. Fraser D, Matthews LR. *Animal welfare: preference and motivation testing*. New York, NY: CAB International (1997).
34. Kirkden RD, Pajor EA. Using preference, motivation and aversion tests to ask scientific questions about animals' feelings. *Appl Anim Behav Sci.* (2006) 100:29–47. doi: 10.1016/j.applanim.2006.04.009
35. Lewejohann L, Sachser N. Präferenztests zur Beurteilung unterschiedlicher Haltungsbedingungen von männlichen Labormäusen. *KTBL-Schrift.* (1999) 391:170–7.
36. Ambrée O, Leimer U, Herring A, Görtz N, Sachser N, Heneka MT, et al. Reduction of amyloid angiopathy and Abeta plaque burden after enriched housing in TgCRND8 mice: involvement of multiple pathways. *Am J Clin Pathol.* (2006) 169:544–52. doi: 10.2353/ajpath.2006.051107
37. Friske JE, Gammie SC. Environmental enrichment alters plus maze, but not maternal defense performance in mice. *Physiol Behav.* (2005) 85:187–94. doi: 10.1016/j.physbeh.2005.03.022
38. Hendershott TR, Cronin ME, Langella S, McGuinness PS, Basu AC. Effects of environmental enrichment on anxiety-like behavior, sociability, sensory gating, and spatial learning in male and female C57BL/6J mice. *Behav Brain Res.* (2016) 314:215–25. doi: 10.1016/j.bbr.2016.08.004
39. Abou-Ismaïl UA, Mendi MT. The effects of enrichment novelty versus complexity in cages of group-housed rats (*Rattus norvegicus*). *Appl Anim Behav Sci.* (2016) 180:130–9. doi: 10.1016/j.applanim.2016.04.014
40. Hutchinson E, Avery A, Vandewoude S. Environmental enrichment for laboratory rodents. *ILAR J.* (2005) 46:148–61. doi: 10.1093/ilar.46.2.148
41. Gross AN-M, Engel AKJ, Würbel H. Simply a nest? Effects of different enrichments on stereotypic and anxiety-related behaviour in mice. *Appl Anim Behav Sci.* (2011) 134:239–45. doi: 10.1016/j.applanim.2011.06.020
42. Misslin R, Ropartz P. Responses in mice to a novel object. *Behaviour.* (1981) 78:169–77. doi: 10.1163/156853981X00301
43. Hedrich HJ, Bullock G eds. *The laboratory mouse*. Amsterdam: Elsevier Academic Press (2010).
44. Hickman DL, Johnson J, Vemulapalli TH, Crisler JR, Shepherd R. *Principles of animal research for graduate and undergraduate students: commonly used animal models*. San Diego, CA, United States: Elsevier (2017). doi: 10.1016/B978-0-12-802151-4.00007-4
45. Bodden C, Wewer M, Kästner N, Palme R, Kaiser S, Sachser N, et al. Not all mice are alike: mixed-strain housing alters social behaviour. *Physiol Behav.* (2021) 228:113220. doi: 10.1016/j.physbeh.2020.113220
46. Ahloy-Dallaire J, Espinosa J, Mason G. Play and optimal welfare: does play indicate the presence of positive affective states? *Behav Process.* (2018) 156:3–15. doi: 10.1016/j.beproc.2017.11.011
47. Broom DM, Johnson KG. *Stress and animal welfare*. London: Chapman & Hall (1993).
48. Tam WY, Cheung K-K. Phenotypic characteristics of commonly used inbred mouse strains. *J Mol Med.* (2020) 98:1215–34. doi: 10.1007/s00109-020-01953-4
49. van de Weerd HA, Baumans V, Koolhaas JM, van Zutphen LF. Strain specific behavioural response to environmental enrichment in the mouse. *J Exp Anim Sci.* (1994) 36:117–27.
50. Walker M, Fureix C, Palme R, Newman JA, Ahloy Dallaire J, Mason G. Mixed-strain housing for female C57BL/6, DBA/2, and BALB/c mice: validating a split-plot design that promotes refinement and reduction. *BMC Med Res Methodol.* (2016) 16:11–3. doi: 10.1186/s12874-016-0113-7
51. Walker M, Fureix C, Palme R, Mason G. Co-housing rodents with different coat colours as a simple, non-invasive means of individual identification: validating mixed-strain housing for C57BL/6 and DBA/2 mice. *PLoS One.* (2013) 8:1–12. doi: 10.1371/journal.pone.0077541
52. Nip E, Adcock A, Nazal B, MacLellan A, Niel L, Choleris E, et al. Why are enriched mice nice? Investigating how environmental enrichment reduces agonism in female C57BL/6, DBA/2, and BALB/c mice. *Appl Anim Behav Sci.* (2019) 217:73–82. doi: 10.1016/j.applanim.2019.05.002
53. Bateson P, Martin P. *Measuring behaviour: an introductory guide*. United Kingdom: Cambridge University Press (2021).
54. Holm S. A simple sequentially rejective multiple test procedure. *Scand J Stat.* (1979) 6:65–70.
55. R Core Team. *R: a language and environment for statistical computing*. Vienna: R Foundation for Statistical Computing (2020).
56. Bates D, Maechler M, Bolker B, Walker S. *Linear mixed-effects models using Eigen and S4 [R package lme4 version 1.1-27.1]*. (2021). Available at: <https://cran.r-project.org/web/packages/lme4/index.html>
57. Kuznetsova A, Brockhoff PB, Christensen RHB. lmerTest package: tests in linear mixed effects models. *J Stat Softw.* (2017) 82:1–26. doi: 10.18637/jss.v082.i13
58. Lenth R. (2023). *emmeans: estimated marginal means, aka least-squares means*. Available at: <https://CRAN.R-project.org/package=emmeans>
59. Dinno A. (2017). *dunn.test: Dunn's test of multiple comparisons using rank sums*. Available at: <https://cran.r-project.org/web/packages/dunn.test/dunn.test.pdf> (Accessed July 11, 2022).
60. Gross J, Ligges U. (2015). *nortest: tests for normality*. Available at: <https://CRAN.R-project.org/package=nortest>
61. Lüdtke D, Ben-Shachar M, Patil I, Waggoner P, Makowski D. Performance: an R package for assessment, comparison and testing of statistical models. *JOSS.* (2021) 6:3139. doi: 10.21105/joss.03139
62. Mangiafico S. (2022). *rcompanion: functions to support extension education program evaluation*. Available at: <https://CRAN.R-project.org/package=rcompanion>
63. Wickham H. ggplot2: elegant graphics for data analysis. *J Stat Softw.* (1992) 35:1–3.
64. Kassambara A. (2020). *ggpubr: 'ggplot2' based publication ready plots*. Available at: <https://CRAN.R-project.org/package=ggpubr>
65. Faul F, Erdfelder E, Buchner A, Lang A-G. Statistical power analyses using G*power 3.1: tests for correlation and regression analyses. *Behav Res Methods.* (2009) 41:1149–60. doi: 10.3758/BRM.41.4.1149
66. Cohen J. Statistical power analysis. *Curr Dir Psychol Sci.* (1992) 1:98–101. doi: 10.1111/1467-8721.ep10768783
67. Sawilowsky SS. New effect size rules of thumb. *J Mod Appl Stat Methods.* (2009) 8:597–9. doi: 10.22237/jmasm/1257035100
68. Chamove AS. Cage design reduces emotionality in mice. *Lab Anim.* (1989) 23:215–9. doi: 10.1258/002367789780810608
69. Bodden C., Kortzfleisch V. T. Von, Karwinkel F., Kaiser S., Sachser N., Richter S. H. (2019). Heterogenising study samples across testing time improves reproducibility of behavioural data. *Sci Rep* 9, 8247–8249. doi: 10.1038/s41598-019-44705-2
70. Nicol CJ, Brocklebank S, Mendl M, Sherwin CM. A targeted approach to developing environmental enrichment for two strains of laboratory mice. *Appl Anim Behav Sci.* (2008) 110:341–53. doi: 10.1016/j.applanim.2007.05.006

Frontiers in Veterinary Science

Transforms how we investigate and improve
animal health

The third most-cited veterinary science journal,
bridging animal and human health with a
comparative approach to medical challenges. It
explores innovative biotechnology and therapy for
improved health outcomes.

Discover the latest Research Topics

[See more →](#)

Frontiers

Avenue du Tribunal-Fédéral 34
1005 Lausanne, Switzerland
frontiersin.org

Contact us

+41 (0)21 510 17 00
frontiersin.org/about/contact

